Florida Institute of Technology
High Tech with a Human Touch™

Improving the Properties of Reclaimed Asphalt Pavement for Roadway Base Applications

Final Report

FDOT Contract Number: BDK81 977-02

Date Prepared: August 2012
Submitted to
The Florida Department of Transportation
Research Center
605 Suwannee St., MS 30
Tallahassee, FL 32399
c/o David Horhota, Ph.D., P.E.

Submitted by
Paul J. Cosentino, Ph.D., P.E.
Florida Institute of Technology
Department of Civil Engineering
150 West University Boulevard
Melbourne, FL 32901-6975
(321) 674-7555
Email: cosentin@fit.edu

EN-448-612

Disclaimer

The opinions, findings, and conclusions expressed in this publication are those of the authors and not necessarily those of the State of Florida Department of Transportation.

Metric Conversion Table

Symbol		Multiply By	To Find	Symbol
LENGTH				
in	inches	25.4	millimeters	mm
ft	feet	0.305	meters	m
AREA				
in^2	square inches	645.2	square millimeters	mm^2
ft^2	square feet	0.093	square meters	m^2
yd^2	square yards	0.836	square meters	m^2
VOLUME				
ft^3	cubic feet	0.028	cubic meters	m^3
MASS				
oz	ounces	28.35	grams	g
lb	pounds	0.454	kilograms	kg
T	short tons (2000lb)	0.907	megagrams ("metric ton")	Mg (or "t")
UNIT WEIGHT				
pcf	lbf/ft^3	16.02	kilograms/ cubic meter	kg/m^3
TEMPERATURE (exact degrees)				
°F	fahrenheit	5 (F-32)/9 or (F-32)/1.8	celsius	°C
FORCE and PRESSURE or STRESS				
lbf	pound force	4.45	newtons	N
kip	1,000 lbf	4.45	kilonewtons	kN
lbf/in^2	pound force/ square inch	6.89	kilopascals	kPa
ksi	kips / square inch	6.89	megapascals	mPa

Technical Report Documentation Page

1. Report No. FL/DOT/BDK81 97702	2. Government Accession No.	3. Recipient's Catalog No.
4. Title and Subtitle Improving the Properties of Reclaimed Asphalt Pavement for Roadway Base Applications		5. Report Date August 2012
		6. Performing Organization Code Index 201368 201369
7. Author(s) P. J. Cosentino, E. H. Kalajian, A. M. Bleakley, B. S. Diouf, T. J. Misilo, A. J. Petersen, R. E. Krajcik, A.M. Sajjadi		8. Performing Organization Report No.
9. Performing Organization Name and Address Florida Institute of Technology (321) 674-7555 Civil Engineering Department 150 West University Blvd. Melbourne, FL 32901-6975		10. Work Unit No. (TRAIS) 11. Contract or Grant No. Contract Number BDK81 977-02
12. Sponsoring Agency Name and Address Florida Department of Transportation 605 Suwannee Street Tallahassee, Florida 32399-0450		13. Type of Report and Period Covered Final Report October 2009 to August 2012 14. Sponsoring Agency Code 99700-7601-119
15. Supplementary Notes		

16. Abstract

The objective of this study was to improve Reclaimed Asphalt Pavement's (RAP) strength in base course applications while reducing creep to an acceptable level using compaction techniques, fractionating, blending with high quality base course aggregate, and/or by chemical stabilization with asphalt emulsion, Portland cement, or lime. RAP/limerock blends with and without chemical stabilization were compacted by modified Proctor, Marshall, or gyratory methods, cured, and tested for strength and creep. Strength tests included limerock bearing ratio (LBR), unconfined compression, Marshall compression, and indirect tensile tests. Strength specimens were tested dry and soaked to evaluate retained strength. Seven-day one-dimensional creep testing was performed. Gyratory compaction produced higher densities than modified Proctor or Marshall compaction. At the same density, gyratory compaction improved RAP's strength by a factor of two to three over modified Proctor but had less effect on creep. Modified Proctor moisture-density plots followed an S-shape without a clear optimum; modified Proctor may not be the best method to predict RAP compaction behavior. Fractionating RAP did not improve strength or creep unless RAP was remixed to match a maximum density curve. Fractionating did not produce acceptable LBRs or creep. RAP blended with limerock, cemented coquina, or reclaimed concrete aggregates showed improved LBR and creep performance. RAP/aggregate blends have the potential to be used as Florida base course. As the amount of aggregate blended with RAP increased, LBR increased and creep decreased. Creep behavior of blends with 75% aggregate was similar to 100% aggregate. Unstabilized blends with 50% aggregate did not produce LBR values over 100. Blends of 50% RAP/50% limerock stabilized with 1% of either asphalt emulsion or cement attained soaked LBRs over 100 and acceptable creep. Blends of RAP with 75% limerock attained soaked LBRs close to 100 and low creep without any chemical stabilizer. Adding RAP to limerock blends generally increased the soaked retained strength and improved permeability compared to 100% limerock.

17. Key Word Recycled Asphalt Pavement, Base, Subbase, Subgrade	18. Distribution Statement Document is available to the U.S. public through the National Technical Information Service, Springfield, Virginia 22161		
19. Security Classif. (of this report) Unclassified	20. Security Classif. (of this page) Unclassified	21. No. of Pages 603	22. Price

Form DOT F 1700.7 (8-72) Reproduction of completed page authorized

Acknowledgements

This work was completed under FDOT contract number BDK81 977-02. The authors would like to acknowledge the following people for their invaluable guidance and help in the completion of this study.

The support of Dr. David Horhota, P.E., Mr. John Shoucair, P.E., and James Musselman, P.E., of the Florida Department of Transportation State Materials Office; throughout the project was critical to its successful completion. The hard work and assistance of Dan Pitocchi, David Webb, Susan Andrews, Greg Sholar, and Dr. Sungho Kim at the FDOT State Materials Office is most appreciated.

The authors also wish to acknowledge the valuable contributions of the following individuals and companies: Kevin Hardin, Mariani Asphalt, for providing asphalt emulsion samples and Marshall molds for use during the study and for advice on mix design using the modified Marshall method; Kevin McGlumphy, P.E., Road Science LLC, for providing asphalt emulsion samples and advice on mix design using the gyratory compactor; Terri Duncan, Universal Engineering for performing confirmatory Marshall compression tests; Barry McKeon and Robert Bistor, Hubbard Construction for their presentation on full-depth reclamation and case studies on the use of RAP as a base course; Larry Mudd, V.E. Whitehurst for providing RAP and A-3 sand samples; Patrick Boylan and Mark Hopkins, APAC, S.E. Melbourne plant for providing RAP samples; Paul Coffman, APAC, SE, Jacksonville for providing RAP samples and for the loan of a gyratory compaction machine; Jeremy Baumgarten and Rich Crump, Cemex, for providing limerock samples; Stewart Mining Industries for providing cemented coquina samples; and Woodruff and Sons, Inc. for providing crushed concrete samples.

The following Florida Institute of Technology undergraduate students who tirelessly helped with retrieving samples from across the state and performing numerous laboratory tests: Stephen Craig, Bradley Hahn, Raymond Sy, and Etienne Wolmarans.

Executive Summary

by

Paul J. Cosentino, Ph.D., P.E.

Edward H. Kalajian Ph.D., P.E.

Albert M. Bleakley, P.E.

Babacar S. Diouf

Ryan E. Krajcik

Thaddeus J. Misilo

Andrew J. Petersen

Amir M. Sajjadi

The United States has over two million miles of paved roads. Over 90 percent of these roads are surfaced with asphalt pavement (Asphalt Pavement Alliance, 2012). These roads must be periodically resurfaced by milling and replacing all or part of the asphalt pavement. Reclaimed Asphalt Pavement (RAP) is produced by this milling process. A portion of this RAP can be recycled directly as a component of new hot-mix asphalt pavement; however this is generally limited to approximately 25% of the new material. The remaining RAP is available for other uses.

RAP has both positive and negative engineering characteristics. On the positive side, RAP is a granular material with good drainage characteristics and adequate shear strength. On the negative side, RAP has low bearing strength and exhibits creep deformation over time due to the asphalt material coating the aggregates (Cosentino and Kalajian, 2001, Cosentino et al., 2003, and 2008). Previous research at the Florida Institute of Technology (FIT) showed that blends of RAP and AASHTO A-3 sand had increased bearing strength and decreased creep compared to 100% RAP. This research also showed that the lower total asphalt content of the blend correlated to decreased creep (Cosentino et al., 2008).

Because of RAP's limitations, FDOT currently limits RAP to use as a base course material on paved shoulders, bike paths, or other non-traffic applications (FDOT Standard Specifications for Road and Bridge Construction, Section 283). Further research using blends

with other higher quality aggregate materials may increase bearing strength and decrease creep enough to make RAP an acceptable base course component.

The objective of this research was to develop methods to improve the strength of RAP or RAP/aggregate blends, while reducing creep, to acceptable levels in the base course. A literature search was conducted, and states that currently allow RAP usage in higher traffic areas were contacted to determine methods that allowed successful RAP use as a base course material.

The research team developed a testing program that focused on improving the limerock bearing ratio (LBR) and reducing creep. The complete testing program is described in Chapter 3. Methods investigated included:

1) modifying RAP gradation by fractionating or re-blending
2) blending RAP with high quality limerock, cemented coquina, or reclaimed concrete aggregates
3) adjusting asphalt content by blending with virgin aggregates
4) mechanical stabilization by different compaction methods
5) chemical stabilization with asphalt emulsion, Portland cement, or lime.

RAP/aggregate blends have the potential to be used successfully as a base course material. Blends of RAP with 50% limerock base material could attain a soaked LBR strength of 100 and acceptable levels of creep with the addition of 1% of either asphalt emulsion or Portland cement. Blends of RAP with 75% or more limerock could attain a soaked LBR of 100 and low levels of creep without any chemical stabilizer. In general adding RAP to limerock blends increased the retained strength when soaked and improved permeability compared to 100% limerock. Blends of RAP with cemented coquina or crushed concrete did not consistently reach soaked LBR values of 100 even at 75% aggregate.

Fractionating RAP by using only the material either above or below a selected sieve size did not improve the LBR or creep properties of pure RAP. Vibratory compaction of RAP gave very low densities and strengths. Gyratory compaction achieved higher densities than modified Proctor compaction. Gyratory compaction improved RAP's LBR strength by a factor of two to three compared to modified Proctor compaction at the same density. This indicates that compaction specifications for RAP which use modified Proctor optimum densities are not

achieving the potential of the material. Additional field testing is required to determine whether it is feasible to reproduce the gyratory compaction effort on an actual construction site.

Significant variability was noted between results with different aggregates, compaction methods, and stabilizing agents. Site-specific performance testing should be conducted to establish the viability of blending RAP into a base or subbase.

Contents

List of Figures

List of Tables

List of Abbreviations

AASHTO - American Association of State Highway and Transportation Officials

AC - Asphalt Content

AJC - RAP Sample from APAC-Florida Jacksonville, Crushed

AMC - RAP Sample from APAC-Florida Melbourne, Crushed

AMM - RAP Sample from APAC-Florida Melbourne, Milled

ASTM - American Society for Testing and Materials

CBR - California Bearing Ratio

CSR - Creep Strain Rate

FDOT - Florida Department of Transportation

FHWA - Federal Highway Administration

FIT - Florida Institute of Technology

HMA - Hot-Mix Asphalt

HMAC - Hot-Mix Asphalt Concrete

LR - Limerock Base Material

LBR - Limerock Bearing Ratio

MRAP - Milled RAP

RAP - Reclaimed Asphalt Pavement, Recycled Asphalt Pavement

SGC - SuperPave Gyratory Compactor

SMO - FDOT State Materials Office

WHM - RAP Sample from V.E. Whitehurst Gainesville, Milled

1. Introduction

The United States has over two million miles of paved roads. Construction and maintenance of these roads is a multi-billion dollar a year industry. Over 90 percent of these roads are surfaced with asphalt pavement (Asphalt Pavement Alliance, 2012). These roads must be periodically resurfaced by milling and replacing part or the entire asphalt pavement. Reclaimed Asphalt Pavement (RAP) is produced by this milling process. A portion of this RAP can be recycled directly as a component of new hot-mix asphalt pavement; however this is generally limited to approximately 25% of the new material. The remaining RAP is available for other uses.

Historically, Florida has relied on in-state production of aggregates for road base course construction. Finding innovative ways to more broadly incorporate RAP into highway base course applications will provide both environmental and economic benefits.

1.1. Background

Extensive research on RAP has shown that it possesses both positive and negative engineering behavior. On the positive side, RAP is a granular material with good drainage characteristics and adequate shear strength. On the negative side, RAP has low bearing strength and exhibits creep deformation over time (Cosentino and Kalajian, 2001, Cosentino et al., 2003 and 2008). These undesirable engineering properties result from the properties of the asphalt binder surrounding the aggregates.

RAP throughout Florida has relatively consistent properties with the exception of materials with high shell contents typically found in Southwestern Florida (Collier County) (Cosentino et al., 2008). Previous research at FIT showed that blends of RAP and AASHTO A-3 sand showed increased bearing strength and decreased creep compared to 100% RAP. This research also showed that decreasing the asphalt content decreased the amount of creep (Cosentino et al., 2008). Research showed that the majority of deformation occurred within the first few hours of laboratory testing followed by deformation at a constant rate (creep) (Cosentino et al, 2008).

Because of RAP's limitations, the Florida Department of Transportation (FDOT) currently limits RAP to use as a base course material on paved shoulders, bike paths, or other non-traffic applications (FDOT Standard Specifications for Road and Bridge Construction, Section 283). American Association of State Highway and Transportation officials (AASHTO) A-3 sand has average strength and stiffness engineering properties. Further research using blends with other higher quality aggregate materials may increase bearing strength and decrease creep enough to make RAP a an acceptable base course component. The FDOT bearing strength is measured using the Limerock Bearing Ratio (LBR).

1.2. Objective

The objective of this research is to develop engineering methods that will improve density and bearing ratios of RAP or RAP/aggregate blends while reducing creep, leading to increased applications for RAP as a roadway base course.

1.3. Approach

The project objective was achieved by accomplishing the following tasks.

1.3.1. Task 1 – Literature Review

The existing literature base was updated and a summary of the information was created. States that currently allow RAP usage in higher traffic areas were contacted and discussions were focused on determining methods that allowed successful RAP use as a base course material.

1.3.2. Task 2 – Testing Program Development

The research team developed a testing program that focused on improving density, bearing ratio and reducing creep. The complete testing program is described in Chapter 3. It included methods or techniques for:

1) gradation modification by evaluating certain sizes or fractions,
2) blending with high quality limerock, cemented coquina, or crushed concrete
3) asphalt content modifications
4) performance improvements using mechanical stabilization
5) performance improvements using chemical stabilization

1.3.3. Task 3 – Gradation Modification Testing, Data Reduction and Analysis

Modifications in RAP gradation were evaluated by performing the tests outlined in Task 2 on various grain size fractions. A review of industry practices indicated that contractors were separating materials using sieves to help with quality control. The Unified Soils Classification System (USCS) uses the #4, #40 and #200 sieves, while the AASHTO classification system uses the #10, #40 and #200 sieves. Based on these and pertinent literature findings, RAP gradation was modified into various sizes, tested in its original form and finally tested using an optimum density blend. Following the testing, data reduction and analysis was completed.

1.3.4. Task 4 – Blending RAP with High Quality Materials Testing, Data Reduction and Analysis

Previous research on RAP-soil blends only included low to medium quality embankment and subgrade materials. In this study, blends with high quality base course materials (limerock, cemented coquina and crushed concrete) were investigated. Blends of 25%, 50% and 75% RAP to the control base materials were tested, reduced and analyzed.

1.3.5. Task 5 – Asphalt Content Improvements Testing, Data Reduction and Analysis

The objective for this task was to refine the basic asphalt content versus creep behavior of RAP blends. To date this relationship was based on RAP-Sand blends. This refinement was accomplished by evaluating blends of RAP with cemented coquina, limerock and waste concrete from FDOT approved sources such that the percent asphalt in the blends varied between approximately 1% and 5.5%. Blended RAP samples with varying asphalt contents were tested as outlined in Task 2. Following the testing, data reduction and analysis was completed.

1.3.6. Task 6 – Compaction Improvements Using Mechanical Energy and/or Chemical Admixtures Testing, Data Reduction and Analysis

Various compaction techniques were evaluated to determine how they affected the compaction characteristics of RAP and RAP Blends. This evaluation included varying the Proctor, gyratory, and vibratory compaction energies. The analysis component of this work included a coordinated discussion with several contractors to help determine the practicality of

applying these research results to construction. The compacted samples were evaluated using both LBR and creep testing. In conjunction with the mechanical energy work, various chemical admixtures were investigated, to determine if they can be mixed with RAP to improve its engineering performance. Chemically stabilized blends were prepared using modified Proctor, Marshall, or gyratory compaction, cured, and tested for creep, LBR, Marshall compression, unconfined compression, and indirect tensile performance.

2. Literature Review

Large quantities of RAP are produced during highway maintenance and construction. While some can be used in new hot mix asphalt concrete (HMA), surplus RAP is frequently available. If this material could be reused on site as a subbase or base material it would reduce the environmental impact, reduce the waste stream, and reduce the materials transportation costs associated with road maintenance and construction.

Approximately ¼ of other U.S. states allow the use of RAP in pavement base or subbase. Previous studies (Cosentino and Kalajian, 2001; Cosentino et al., 2003 and 2008) have identified two major problems with RAP: LBR strength below the FDOT specification requirement of 100 for base material or 40 for subbase material, and creep deformation over time. RAP may also fail to meet the FDOT gradation specification for graded aggregate base (Section 204). This study focused on improving the properties of RAP through a variety of methods as discussed in Section 1.3 including improved compaction methods, fractionating RAP, and blending RAP with virgin aggregate materials.

This study also included an investigation of the addition of chemical stabilizing agents to improve the properties of RAP and RAP/aggregate blends. In order for contractors to use chemically stabilized blends they would use procedures typically used when conducting Full Depth Reclamation (FDR) during pavement rehabilitations. FDR with asphalt pavement surfaces are a specialized blending of RAP that typically blends the asphalt pavement surface into the existing base and possibly subbase on low volume roads.

2.1. Characteristics of RAP

2.1.1. Variability

RAP has generally consistent asphalt content, aggregate constituents and gradation throughout the State of Florida (Cosentino et al., 2008). A summary of general Florida RAP properties is shown in Table 2-1. Average gradation curves are shown in Figure 2-1 and gradation parameters are summarized in Table 2-2. The primary aggregate used in Florida for HMAC has been limerock and therefore this is the primary aggregate found in Florida RAP. Asphalt contents of various sources of RAP have generally been consistent with a statewide

average of 6.2%. Most contractors throughout the state stockpile both unprocessed (milled) and processed (crushed) RAP available (Sandin, 2008).

Table 2-1: Summary of RAP Variability (Sandin, 2008)

Property	Average	Range
Asphalt Content	6.2 %	4.5% - 8.5%
Maximum Density (pcf)	114	106 - 126
LBR	17	7 - 44

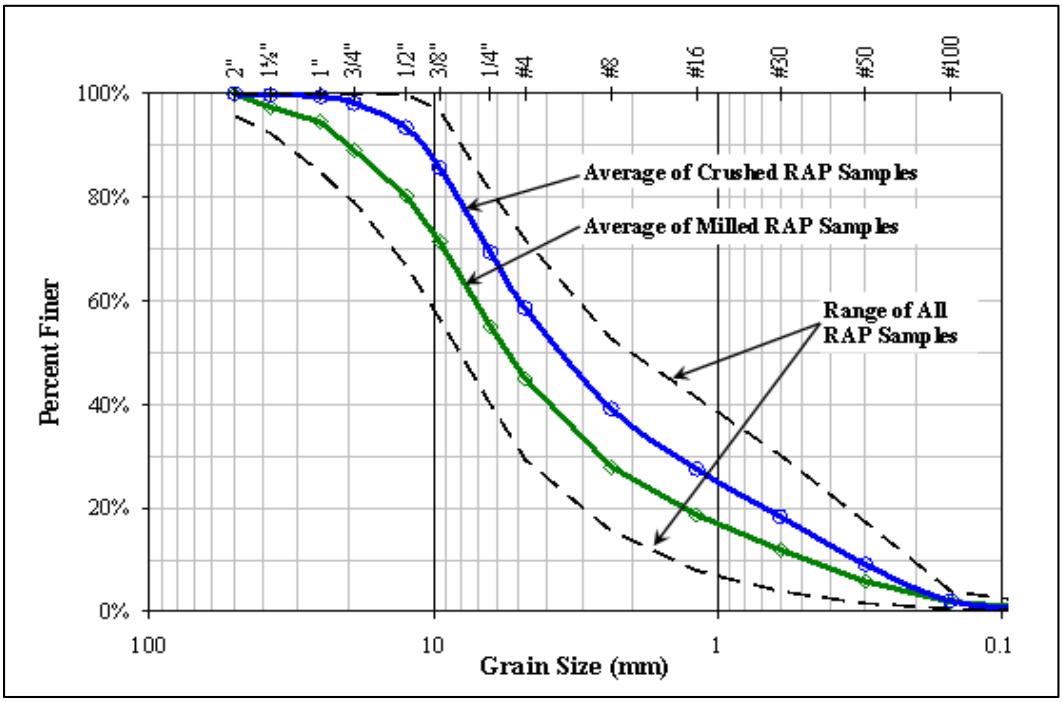

Figure 2-1: Florida RAP Average Grain Size Distribution Curves (Sandin, 2008)

There is no current standard for processing and crushing RAP. Two types of crushing have been identified, hammermill and tubgrinder. Generally, the engineering properties of RAP crushed by either method did not vary significantly (Sandin, 2008).

Table 2-2: Statewide Average RAP Gradation Parameters (Sandin, 2008)

	Milled			Crushed		
	Average	Min.	Max.	Average	Min.	Max.
Number of Samples Tested	52	-	-	43	-	-
Nominal Maximum Particle Size, D_{nom} (mm)	23.6	12.5	37.5	12.9	9.5	25.0
Percent Passing #4	45%	29%	64%	59%	30%	72%
Percent Passing #30	12%	4%	19%	19%	4%	30%
Percent Passing #200	0.6%	0.2%	1.6%	0.5%	0.1%	1.8%
D_{10} (mm)	0.58	0.29	1.43	0.40	0.21	1.90
C_U	13	5	23	13	4	22
C_C	1.8	0.7	4.2	1.2	0.4	2.9

2.1.2. Evaluation of RAP in Bases and Subbases

Taha et al., (1999) conducted laboratory evaluations of RAP and RAP/virgin aggregate blends used as both road base and subbase in the Sultanate of Oman. Gradation, compaction, and bearing strength tests were performed on RAP/aggregate blends of 0%, 20%, 40%, 60%, 80% and 100% RAP. The virgin aggregate was a mix of well graded sand and gravelly sand with little or no fines. RAP was obtained through milling and contained 5.5% asphalt content. RAP was classified as well graded with 100% of the particles passing 1½ inch sieve and 0.5% fines. Moisture-density testing for the six materials resulted in a series of relatively flat curves, as shown in Figure 2-2, with 100% RAP positioned at the bottom and achieving a maximum modified Proctor unit weight of 117.3 lb/ft^3 at 7.3% optimum moisture content. The 100% RAP produced the lowest bearing strength, with a California Bearing Ratio (CBR) of 11 (LBR of 13.8).

Taha et al., (1999) recommended that blends with 60% or less RAP were suitable for road subbase construction. For base construction, however, only mixes containing 10% RAP or less were recommended.

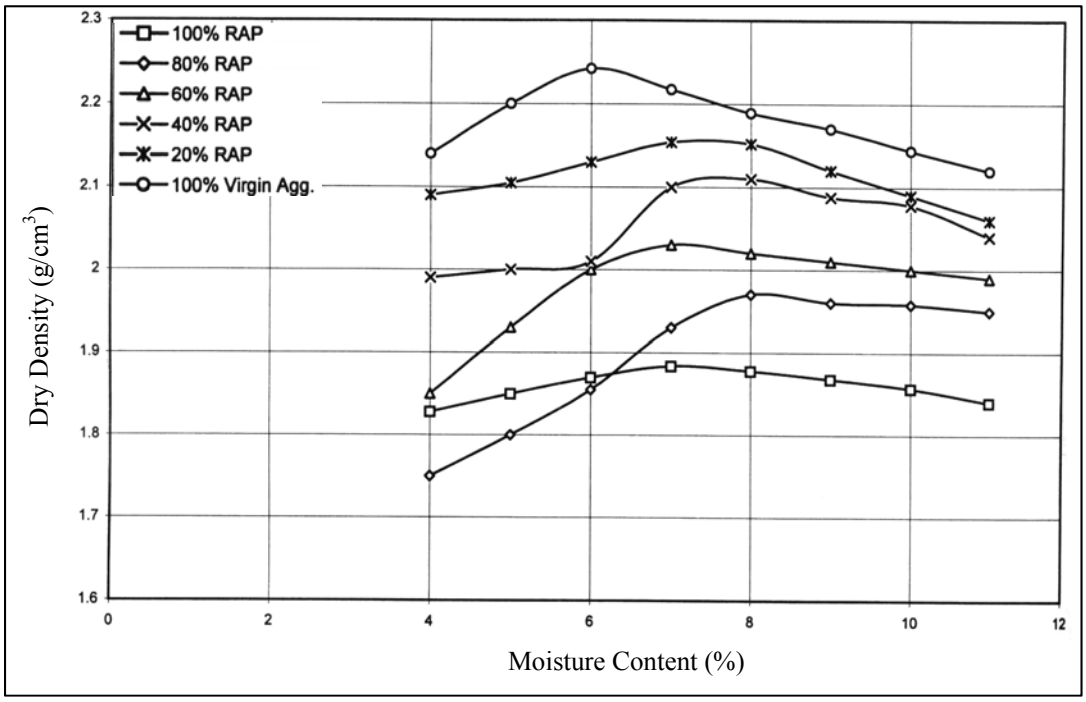

Figure 2-2: Moisture Density Curves for Various RAP-Aggregate Blends (Taha et al., 1999)

2.1.3. RAP and RAP Blend Properties

McGarrah (2007) surveyed U.S. states and summarized current RAP practices in the WSDOT report WA-RD 713.1. The literature findings on RAP and RAP blends included data on density, moisture, permeability, CBR, and resilient modulus. In general the density, optimum moisture content and CBR decrease with the addition of RAP while the resilient modulus increases with the addition of RAP (Table 2-3). McGarrah (2007) referenced several reports regarding hydraulic conductivity of RAP/aggregate blends and determined that the permeability of the material must be determined on a case by case basis due to the large variations in RAP and aggregate properties.

Table 2-3: Literature Summary (McGarrah, 2007)

Reference	Blended[1]	Dry Density[2]	Moisture Content[3]	Permeability[4]	CBR[5]	Resilient Modulus[6]
Cooley (2005)	Yes	Decreased	Decreased	---	Decreased	---
Garg and Thompson (1996)	No	Decreased	Increased	---	Decreased	---
MacGregor et al.(1999)	Yes	---	---	No Change	---	Increased
Bennert and Maher (2005)	Yes	Decreased	Decreased	Decreased	---	Increased
Papp (1998)	Yes	Decreased	Decreased	---	---	Increased
Sayed (1993)	No	---	Decreased	---	Decreased	---
Taha et al. (1999)	Yes	Decreased	No Change	Increased	Decreased	---
Trzebiatowski and Benson (2005)	No	Decreased	---	Increased	---	---

1. Details whether the RAP was blended with virgin aggregate.
2. Effect on the dry density of the material as the percent RAP increased.
3. Effect on the optimum moisture content as the percent RAP increased.
4. Effect on the permeability as the percent RAP increased.
5. Effect on the CBR as the percent RAP increased.
6. Effect on the resilient modulus as the percent RAP increased

The literature findings developed by Cosentino et al., (2008) (phase three of this FDOT research sequence) are in Table 2-4. RAP applications include base, subbase and subgrade work. Various processing methods have been used. Six of the 10 works cited used milled RAP. The top size was 1.5 inch with generally less than 2% passing the #200 sieve. The USCS classification was well graded sand or gravel (i.e., SW or GW) in nearly all cases. The AASHTO classification was A-1-a. Optimum moisture ranged between 5.4% and 8.5% which is typical of granular material. Low densities were obtained for 100 % RAP; blends and special compaction procedures produced higher values. All 100 % RAP specimens produced LBR values below 100. The asphalt content ranged from 5.2% to 6.7% which matches the range found in the statewide variability testing by Sandin (2008).

Table 2-4: Summary of RAP Engineering Properties from Literature Review (Cosentino et al., 2008)

Study	Author	Year	RAP Application	Process	Gradation		Soil Classification		Compaction			LBR	Asphalt Content
					Passing 1.5 in sieve	Passing #200 sieve	USCS	AASHTO	Optimum Moisture (%)	Mod Proctor Max Dry Density (lb/ft^3)	Standard Proctor Max Dry Density (lb/ft^3)		
100% RAP													
SR 500 Holopaw FL	Sayed et al.	1993	Shoulder and base	Milled	97%	4%	GW/SW	A-1-a	6.2%	122.9		25- 38	5.6%
Lincoln Avenue IL	Garg and Thompson	1996	Base course	Crushed	100%	4%	GW/GP	A-1-a 7.2%		125.2	81		
US Route 1 NJ	Maher et al.	1997	Base and subbase		93%	0%	GW	A-1-a	5.5%		113	11- 21	
SH 395 CA	Bejarano et al.	2003	Pulverized base		98%	2%	GW	A-1-a	5.5%	145.6[1]			
Florida Tech Research	Montemayor	1998	Base and subbase		100%	0.5%	GW/SW	A-1-a	7/8.5%	112	104	16-43	6.7%
Florida Tech Research	Gomez	2003	Base and subbase	Crushed	98%	0%	GW	A-1-a	80%	117.8		40	
Florida Tech Research	Cleary	2005	Backfill	Crushed	100%	1%	GW/SW	A-1-a	7.0%	116.8	114.3		5.2%
RAP-Soil Mixtures													
Kuwait[2]	Aljassar et al.	2005	Subgrade	Milled	100%	6.5%	GW	A-1-a	8.5%	127.5		110	
University of Montana	Mokwa and Peebles	2005	Base & Subbase	Milled	96%	1%	GW	A-1-a	5.4%	131 .3[3]			
Oman	Taha et al.	1999	Base & Subbase	Milled	100%	0.5%	GW	A-1-a	7.3%	117.3		14	

2.1.4. Reclaimed Asphalt Pavement Field Studies

An eight-week field testing program was carried out at the Florida Institute of Technology to measure the strength-deformation behavior of RAP (Cosentino et al., 2003). Field CBR values, Clegg Impact hammer stiffness and Initial Stiffness Moduli (ISM) from Falling Weight Deflectometer (FWD) data indicated that RAP experienced a 50 percent strength gain over 8 weeks while the Soil Stiffness Gauge (SSG) stiffness results indicated that the strength gain was 15 percent. The Clegg, FWD and SSG testing also indicated that RAP had stiffness similar to limerock. Based on field CBR tests conducted, RAP did not meet the FDOT minimum LBR of 100 for base course material. RAP did achieve a minimum CBR of 32 (LBR of 40) for approximately 80% of the tests and therefore has potential to be utilized as a subbase and/or subgrade.

Limerock strength-deformation characteristics decreased significantly when the test site was saturated by rain, but the RAP base test section retained strength better when wet than the limerock base test section. Limerock was used as a control material for this work.

Garg and Thompson (1996) evaluated the Lincoln Avenue demonstration project in Urbana, Illinois by conducting laboratory and field FWD tests. The project pavement consisted of a 12-inch lime modified subgrade, an 8-inch RAP base course, and a 3-inch asphalt concrete surface course. The study was that RAP can be successfully used as a conventional flexible pavement base material based on FWD deflection data.

2.1.5. Reclaimed Asphalt Pavement Base Applications

2.1.5.1. Overview of RAP Practices (Chesner et al., 1998)

According to Chesner et al., (1998) at least 13 state agencies (Arizona, Illinois, Louisiana, Maine, Nebraska, New Hampshire, North Dakota, Oregon, Rhode Island, South Dakota, Texas, Virginia, and Wisconsin) have used RAP as aggregate in roadway base course, four state agencies (Alaska, New York, Ohio, and Utah) have used RAP as unbound aggregate in subbase, and two states (California and Vermont) have experience with RAP use in stabilized base course.

Chesner et al., (1998) found that RAP that has been properly processed and in most cases blended with conventional aggregates has demonstrated satisfactory performance as granular road base for more than 30 years. The report includes a case study of an early application of RAP in base course, the FHWA Demonstration Project 39 Asphalt Recycling: Tamworth Cold Recycling Project in New Hampshire (FHWA 1981). The project included construction of a stabilized base course consisting of the existing bituminous surface and an approximately equal amount of gravel base (from the existing base course) and/or added gravel. During construction the pavement was broken up with a grader mounted ripper and crushed in-place with a vehicle mounted rotating hammer mill. The mobile mill crushed the material so that all of the crushed RAP/gravel blend passed the 2.5 inch sieve. The crushed blend was stockpiled, then dumped by trucks, milled, and graded to the required depth. Compaction was performed with a vibratory single drum roller. The mechanically stabilized base appeared to be in excellent condition as a temporary riding surface with heavy traffic flowing at moderate speeds between 30 and 40 mph. RAP showed good performance on this project as a base course aggregate. This report also recommended investigating the addition of an asphalt emulsion as a binding agent.

2.1.5.2. Pavement Rehab Using RAP Base (Foye, 2011)

Foye (2011) evaluated RAP used as a pavement base course for the asphalt parking lot rehabilitation at Fort Snelling, MN. Work was completed under the direction of the U.S. Army Corps of Engineers (USACE) Kansas City and St. Paul Districts. The existing, distressed asphalt pavement was milled and stockpiled for reuse in the new pavement base course. The RAP base course was compacted with vibratory rollers. Field observation was that RAP drained rapidly, hampering compaction. Compaction was much more effective with the frequent addition of water, achieving a firm base in fewer compactor passes, passing dynamic cone penetrometer testing, and exhibiting no rutting or deflection under proof rolling.

The main observation from the project is the drainage and compaction behavior of RAP. In the field, RAP drains rapidly. Agglomeration effects, where residual asphalt binder within RAP causes finer particles to adhere to each other, tend to reduce the amount of fines available to hold water. Frequent addition of water was required for effective compaction. The technical performance and economy of the RAP base were viewed as a success in this application.

2.1.6. Permeability of RAP and RAP Blends

2.1.6.1. Permeability of RAP Blends (Bennert and Maher, 2005)

Bennert and Maher (2005) conducted a study to develop performance specifications for granular base and subbase materials. The study included permeability tests on 100% RAP and RAP/aggregate blends. RAP was blended with two highly permeable materials, Dense Graded Aggregate Base Course (DGABC) material and I-3 material (NJDOT Standard Specifications for Road and Bridge Construction, 2007 Section 901.11-1 Standard Soil Aggregate Gradation).

Permeability results are summarized in Table 2-5. In general, as RAP content increased, permeability decreased. RAP permeability was in the 10^{-3} cm/s range and the aggregates had permeabilities in the 10^{-2} cm/s range. The virgin aggregates were generally one order of magnitude more permeable than RAP.

Table 2-5: Permeability of RAP and RAP Blends after Bennert and Maher (2005)

Blend Percentage	Constant Head				Falling Head			
	DGABC		I-3		DGABC		I-3	
	ft/day	cm/s	ft/day	cm/s	ft/day	cm/s	ft/day	cm/s
0% RAP	172.7	0.0609	55.8	0.0197	121.1	0.0427	43.2	0.0152
25% RAP	121.4	0.0428	2.2	0.0008	27.8	0.0098	2.4	0.0008
50% RAP	113.7	0.0401	8.3	0.0029	39.0	0.0138	7.7	0.0027
75% RAP	1.7	0.0006	3.0	0.0011	2.1	0.0007	3.3	0.0012
100% RAP	16.9	0.0060	16.9	0.0060	13.9	0.0049	13.9	0.0049

2.1.6.2. Permeability of RAP Blends (MacGregor et al., 1999)

MacGregor et al., (1999) performed tests on reclaimed asphalt pavement base and subbase course mixes to determine structural numbers for use in highway design. As part of the study, the researchers also determined the hydraulic conductivity of 100% RAP and RAP/aggregate blends. This study, along with results from Bennert and Maher (2005), provides data to compare to tests

conducted during the current research. A summary of their permeability data is presented in Table 2-6. Permeabilities decreased as the RAP content increased, indicating that the crushed stone base was more permeable than the RAP used. This trend matched the trend produced by Bennert and Maher (2005).

Table 2-6: Hydraulic Conductivity Results of RAP and RAP Blends after MacGregor et al., (1999)

RAP/Dense Graded Crushed Stone Base Mixture				
% RAP	Density		Avg. Hydraulic Conductivity	
	lbs/ft^3	Mg/m^3	ft/s	cm/s
0	114.2	1.83	0.0240	0.73
0	118.6	1.9	0.0105	0.32
10	116.7	1.87	0.0105	0.32
10	124.9	2.0	0.0033	0.1
30	118.6	1.9	0.0043	0.13
50	112.4	1.8	0.0079	0.24

2.1.6.3. Permeability Summary of RAP and RAP Blends

The data from Table 2-5 and Table 2-6 was assembled into a plot (Figure 2-3) which shows that as RAP percentage decreases, the overall permeability of RAP and RAP blended with dense graded aggregates increases.

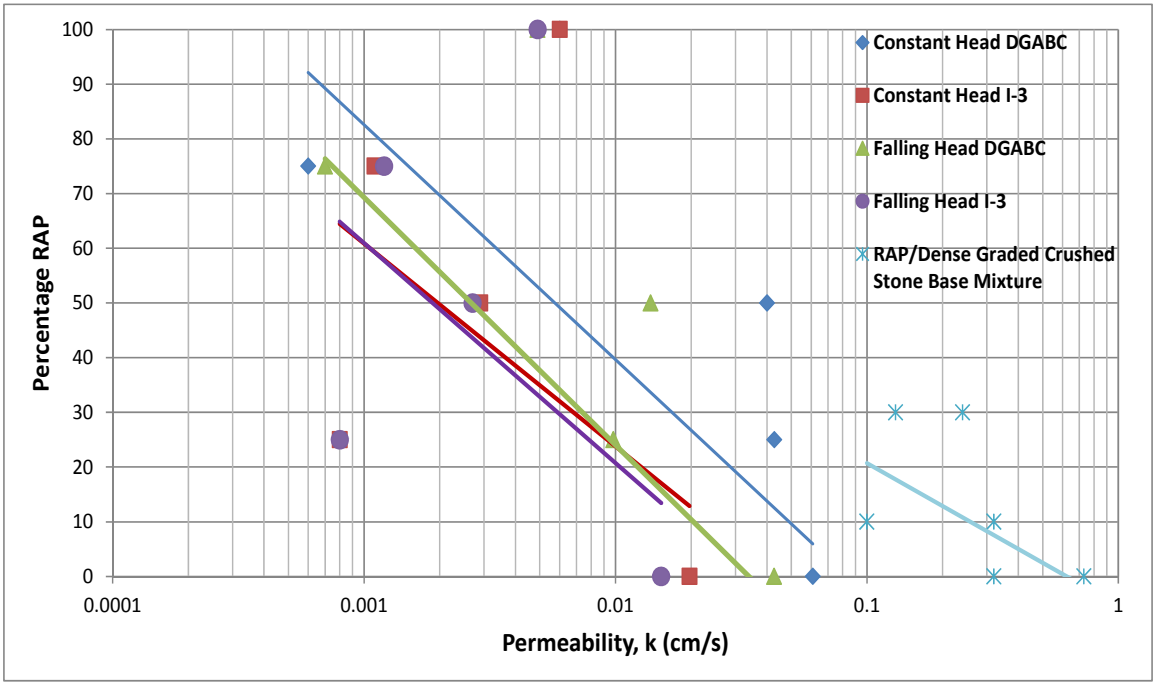

Figure 2-3: Summary of Literature Permeability versus RAP Percent (Bennert and Maher, 2005; MacGregor et al., 1999)

2.1.7. Freeze Thaw and Moisture Effects (Alam et al., 2010)

Alam et al. conducted an investigation of the effect of freeze-thaw cycles and severe moisture conditions on the structural capacity of base layers containing RAP. This study was incorporated into Minnesota DOT Report MN/RC 2009-05 by Attia et al. (2009). RAP was used as a replacement for virgin aggregates in base courses of new road construction. The samples studied were taken from various highways in the state of Minnesota and were comprised of 100% RAP, Minnesota Class 5 virgin aggregate, and three Class 7 mixtures of RAP and virgin aggregate. The 100% RAP samples were then combined with virgin aggregate to create 50% and 75% RAP/virgin aggregate blends.

Testing included gradation, asphalt content, moisture density, RAP resistance to abrasion and degradation, RAP structural capacity, dry densities, shear strength, and the effect of freeze-thaw on the resilient modulus and the shear strength of RAP. The moisture-density relationships were found using both standard Proctor and Superpave gyratory compaction procedures.

RAP had a higher resilient modulus and equivalent shear strength compared to Minnesota Department of Transportation (MnDOT) Class 5 virgin aggregate and the effect of freeze-thaw

cycles was negligible. The Proctor and Gyratory compaction methods produced different optimum moisture contents.

2.1.8. RAP as a Base Course Material (Locander, 2009)

The Colorado Department of Transportation (CDOT) allows RAP to be substituted for unbound aggregate base course (ABC). Locander (2009) performed a comprehensive testing program to develop pavement design guidelines for using RAP in a base course. The testing program included grain size, Atterberg limits, permeability, moisture-density, asphalt content, resilient modulus, and Hveem resistance values.

The results indicated that RAP should have a top-size of 2 inches, a plasticity index (PI) below 6 and liquid limit (LL) below 30. The author recommended a structural number ranging from 0.15 to 0.19 depending upon how the RAP is used. Finally, it was concluded that RAP has good to excellent drainage characteristics based on the FHWA drainage guidelines (Carpenter et al., 1981).

2.2. Current RAP Specifications

2.2.1. Florida Department of Transportation Specifications (2010)

The FDOT Standard Specifications for Road and Bridge Construction, 2010, Section 283 governs the use of RAP as a pavement base and Section 914-3.2 governs the use of RAP as a stabilizer, to be mixed with existing materials, to create a stabilized subgrade. FDOT also published a Memorandum "Use of RAP in Roadway Embankment Construction" in an FDOT August 2005, Materials Bulletin (No. 08-05). This memorandum outlines that RAP can be used for subgrade stabilization (per Section 914-3.2) or base material (Section 283) but not as backfill for mechanically stabilized earth (MSE) walls.

Section 283 limits the use of RAP as base course to paved shoulders, bike paths, or other non-traffic applications. Section 283 requires the asphalt content of RAP to be greater than 4% whenever the material does not originate from FDOT projects and its source is unknown. Section 914 allows RAP as a stabilizer for subgrade stabilization use provided that a minimum LBR of 40 can be achieved, the material does not cause excessive deformations, and it improves the bearing capacity of the stabilized material.

In 2007 FDOT published a Memorandum prohibiting the use of RAP or RAP/soil mixtures use as MSE wall backfill material (Horhota et al., 2007) based on research conducted under Contract BDB09 (Cosentino et al., 2008) which found that RAP or RAP/soil blends had excessive creep settlement.

2.2.2. Survey of State Highway Agencies (Collins and Ciesielski, 1994)

Collins and Ciesielski (1994) published a book on recycling and waste products in highway construction. As part of that effort the authors surveyed state highway agencies and found that at that time, 16 states allowed the use of RAP as an unbound aggregate base or subbase under some conditions.

2.2.3. Summary of State Practices (McGarrah, 2007)

McGarrah (2007) conducted an evaluation of current RAP practices for the Washington State DOT (WSDOT). McGarrah found that 9 states currently allowed RAP as an unbound aggregate base or subbase. Table 2-7 is a summary of McGarrah's findings on states that allow RAP as a base course material. This table indicates that the majority of states that allow RAP in base courses limit the RAP content to a maximum of approximately 50% by weight. Two states limit RAP content based on the overall asphalt binder content of the blend with an upper limit for asphalt content of blends at 3%. This 3% asphalt content for the blend corresponds to approximately 50% RAP by weight based on a Florida statewide RAP average asphalt content of 6.2% (Cosentino et al., 2008).

Table 2-7: State DOT Survey after McGarrah (2007)

State	RAP Allowed[1]	Max %[2]	Processed[3]	Testing[4]
Florida	No	---	---	---
Illinois	No	---	---	---
Montana	Yes	50-60%	No	Corrected Nuclear Gauge
New Jersey	Yes	50%[5]	Yes Gradation	Corrected Nuclear Gauge + Sample
Minnesota	Yes	3%[6]	Yes Gradation	Dynamic Cone Penetrometer
Colorado	Yes	50%[5]	Yes Max Agg. Size	Roller Compaction Strip
Utah	Yes	2%[6]	Yes Gradation	Nuclear Gauge or Breakdown Curve
Texas[7]	Yes	20%	Unknown	Various (Including Nuclear Gauge)
California[7]	Yes	50%	Unknown	No special testing procedure listed
New Mexico[7]	Yes	Unknown	Unknown	Corrected Nuclear Gauge
Rhode Island[7]	Yes	Unknown	Yes Gradation	Unknown
South Dakota[7]	No	---	---	---

1. Describes whether or not state allows RAP as a base course material.
2. The maximum percentage or RAP (by weight) allowed.
3. Describes whether the listed state requires the RAP blend to be processed prior to placement and what requirements must be met.
4. Describes the type of QA testing required
5. Modified values. Current values are 100%, but the DOT is modifying them.
6. Maximum AC content allowed in blends.
7. These states were not contacted and the information listed in the table is from the state's current standard specification.

McGarrah also included excerpts comparing state specifications for RAP or RAP/aggregate blend gradation. Table 2-8 shows the gradation requirement from New Jersey

DOT (NJODT) for using RAP as a base course. At the time of the McGarrah publication NJDOT was in the process of changing their specifications from allowing 100% RAP to allowing a maximum of 50% RAP in base courses. Utah DOT (UDOT) limits the asphalt content of RAP used in base courses to 2% and specifies the gradation listed in Table 2-9.

Table 2-8: NJDOT Base Course Gradation for RAP after McGarrah (2007)

Sieve Size	% Passing
2 in (50.0 mm)	100
1-1/2 in (38.1 mm)	85-100
3/4 in (19.0 mm)	55-90
#4 (4.76 mm)	23-60
#50 (0.297 mm)	3-25
#200 (0.074 mm)	0-10

Table 2-9: Utah Base Course Gradation after McGarrah (2007)

Gradation Limits – Single Value Job – Mix Formula			
Sieve Size	Percent Passing of Total Aggregate (Dry Weight)		
	1-1/2 in (38.1 mm)	1 in (25.4 mm)	3/4 in (19.0 mm)
1-1/2 in (38.1 mm)	100	---	---
1 in (25.4 mm)	---	1000	---
3/4 in (19.0 mm)	81-91	---	100
1/2 in (12.7 mm)	67-77	79-91	---
3/8 in (9.51 mm)	---	---	78-92
#4 (4.75 mm)	43-53	49-61	55-67
#16 (1.19 mm)	23-29	27-35	28-38
#200 (0.074 mm)	6-10	7-11	7-11

2.2.4. Draft RAP Base Specification Arizona Department of Transportation (ADOT)

Draft Arizona DOT standard specifications Section 303 Aggregate Subbases and Bases Class 2 include requirements for virgin aggregates and for blends of virgin aggregates with up to 50% RAP. There are separate requirements for milled and crushed RAP, with the major difference being the removal of all material passing the ½ inch sieve prior to crushing for crushed RAP. Both virgin aggregates and RAP/aggregate blends are required to meet the same gradation requirements.

2.3. Summarized Theory of Compaction

The most common method of densification in roadway construction is compaction by mechanical compactors. Typical field compaction equipment includes smooth steel wheel rollers, pneumatic tire rollers, and textured steel wheel rollers (e.g., sheepsfoot and padfoot). Compaction equipment may be static pressure or vibratory. Steel-wheeled rollers are often used for proof rolling subgrades and HMA surfaces. Textured drum rollers are effective in compacting soils in deeper lifts, but due to the projections on each wheel do not produce a smooth surface. Vibratory rollers are effective in compacting granular, cohesionless soil. Pneumatic rubber tired rollers produce a combination of pressure and kneading action (Das, 2004). The vibration function is built-in to many compactors. Like most materials, as compactive energy increases RAP dry density increases (Montemayor, 1998). Montemayor (1998) found that LBR values for RAP specimens increased as dry density increases as shown in Figure 2-4.

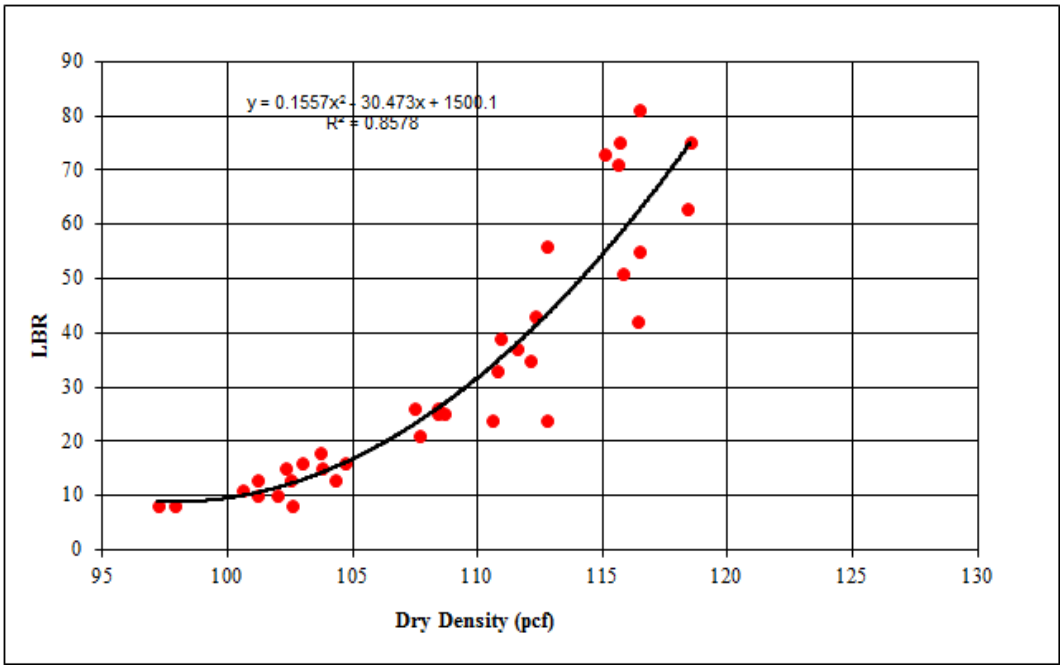

Figure 2-4: RAP LBR versus Dry Density (Montemayor, 1998)

2.4. Gradation Modification or Control

2.4.1. Graded Aggregate Base Material Specifications

Florida graded aggregate is used as a base or subbase for asphalt paving or for structural applications. FDOT requires that Graded Aggregate Base have an LBR strength of not less than 100 and meet the gradation of Table 2-10 (FDOT Standard Specifications for Road and Bridge Construction, Section 204-2).

Table 2-10: Gradation Requirements for Graded Aggregate Base

Sieve Size	Percent Passing
2 inch	100
1 1/2 inch	95 to 100
3/4 inch	65 to 90
3/8 inch	45 to 75
No. 4	35 to 60
No. 10	25 to 45
No. 50	5 to 25

No. 200	0 to 10

The material retained on the No. 10 sieve should be 45% of Group 1 aggregates (limestone, marble, or dolomite) or 65% of Group 2 aggregates (granite, gneiss, or quartzite). For Group 1 aggregates, the fraction passing the #40 sieve should have a Plasticity Index less than 4.0, a Liquid Limit less than 25, and less than 67% passing the # 200 sieve. For Group 2 aggregates, the fraction passing # 10 sieve should have a sand equivalent (ASTM D 2419) value of not less than 28. Sand equivalent indicates the relative proportions of fine dust or clay-like materials in granular soils or fine aggregates.

2.4.2. Gradation Modification Techniques

The simplest way to modify the gradation of RAP is to sieve it into +/- fractions at one or more screen sizes. Some of the industry firms contacted during this study had experience with fractionating. One of the asphalt plants used as a RAP source in this study currently fractionates their crushed RAP.

Whitehurst and Sons Asphalt Company, Gainesville, FL, fractionates RAP into two stockpiles into plus and minus #4 sieve materials. The company developed that system to control the gradation of RAP used in HMA mixes. Bechtol Engineering and Testing, Inc. Deland, FL, also recommends fractionating RAP to separate it into coarser and finer fractions. They report that fractionating allows for greater gradation and volumetric adjustability and control during hot mix production when the fractionated RAP is combined with the virgin aggregates. The fractionated RAP allows a more homogeneous blend during hot mix production.

No references to fractionating RAP for use in a base course were found in the literature or during interviews with industry. Hubbard Construction has performed Full Depth Reclamation of secondary roads in Florida. During discussions, company representatives said that they sometimes incorporate select sized aggregate during the milling/blending process to alter the gradation of FDR mix.

There has been research on adjusting gradation to achieve maximum density in compacted aggregate, HMA, or concrete mixes. Initially, Fuller and Thompson (1907) presented approach that required engineers to plot the grain size data with percent passing versus the particle diameter raised to a power near the square root (i.e., 0.5). This power type axis is to be used

instead of the conventional logarithm axis for the particle diameters. A second very similar approach known as the Talbot and Richart Curve method (Talbot and Richart, 1923) was developed mainly for concrete mixtures. Both methods can be used to determine how much of each aggregate to use in a mix to provide the maximum density or minimum voids. Talbot and Richart developed the well-known equation:

$$P = [d/D_{max}]^m \qquad \text{Equation 2-1}$$

P = percent, by weight, of the particles with diameter less than d

D_{max} = maximum particle diameter in the mixture

m = exponent governing the distribution of sizes with a maximum density.

Based on this work, the Federal Highway Administration (FHWA, 1988) recommends an optimum density gradation based on Equation 2-1 using a 0.45 power formulation (m = 0.45) for highway materials (Mamlouk and Zaniewski, 2011).There is some debate as to whether the maximum particle diameter in the mixture (D_{max}), should be the maximum aggregate size, nominal maximum aggregate size or somewhere in between, however the most commonly accepted practice is to consider the maximum aggregate size (the smallest sieve through which 100 percent of the aggregate sample particles pass). This gradation is referred to as the FHWA or Talbot curve in the body of this report.

2.4.3. Impact of Gradation on Base Material (Gandara et al., 2003)

Gandara et al., (2003) evaluated the engineering properties and performance of base material with a focus on the gradation. This study focused on the percentage of fines (passing the #200 sieve). The properties of the material were analyzed through a series of tests including sieve analysis, moisture-density curves, Atterberg limits, triaxial tests, moisture susceptibility, permanent deformation, and resilient modulus. The material used in the research was a typical blended base course material from the El Paso District in Texas. Three types of materials were blended. The gradation of each is shown in Figure 2-5.

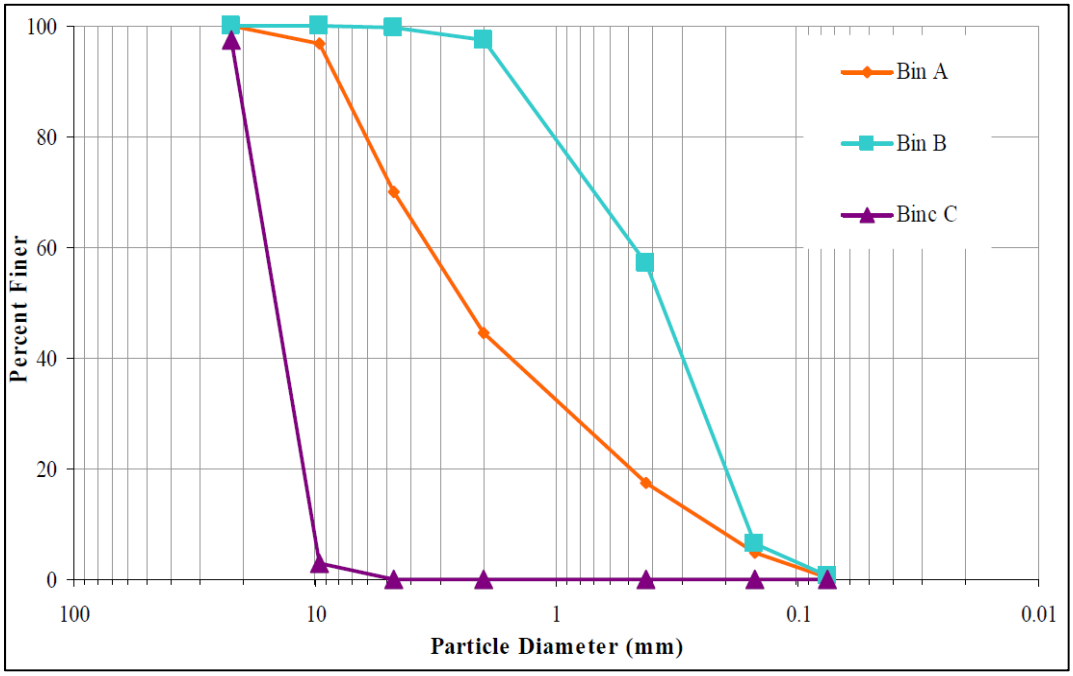

Figure 2-5: Gradations of Bin A, Bin B, and Bin C (Gandara et al., 2003)

Seven different specimens were blended and tested.

Equation 2-2 shows the relationship developed by Cooper et al., (1985) to ensure the densest state of each blend for a predetermined fine content, F.

$$P = \frac{(100 - F)(d^n - 0.075^n)}{(D^n - 0.075^n)} + F \qquad \text{Equation 2-2}$$

P = percentage passing a sieve of size d in mm

F = percentage of material passing through a 0.075 mm sieve (fines)

d = sieve size (mm)

D = maximum particle size (mm)

n = power relationship (typically 0.45)

Of these seven specimens, three contained different percentages of low-plasticity fines naturally mixed with the material. The second set of three specimens were similar to the first three in gradation, however, the low-plasticity fines were replaced with high plasticity clay. The seventh specimen contained no clay or fines and was used as a control mix. The mixes had a fines content F = 0%, 5%, 10%, and 20%. The blended gradations are presented in Figure 2-6

along with the Texas Department of Transportation (TxDOT) Items 245 and 247 base course material gradation limits.

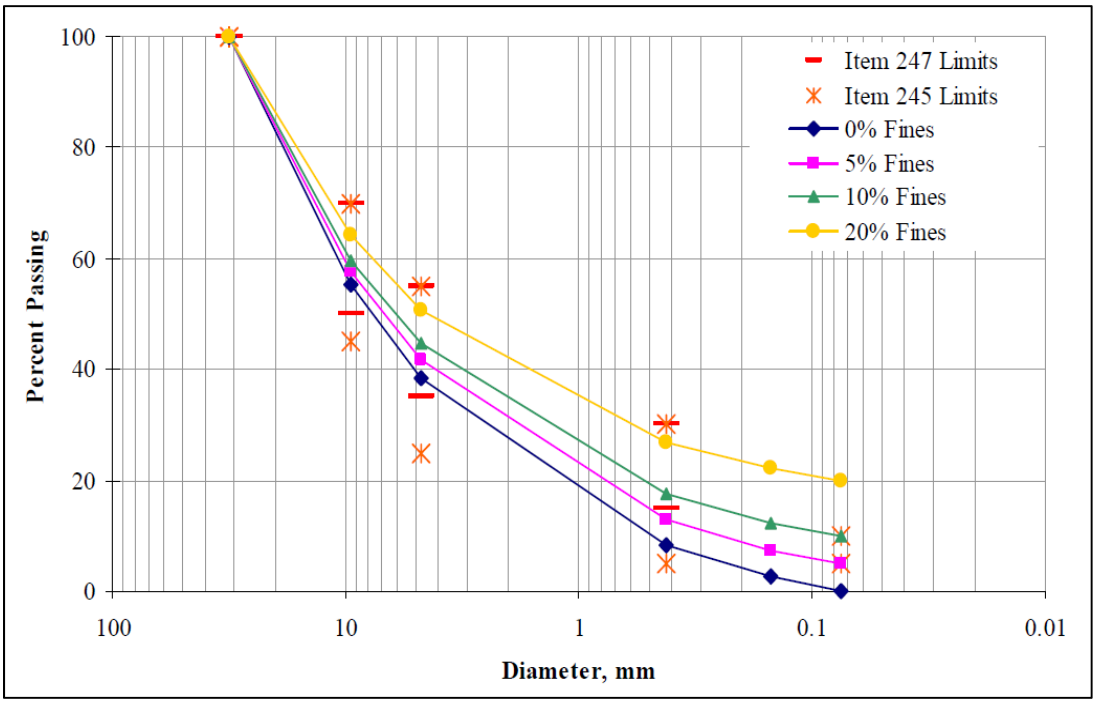

Figure 2-6: Gradation of Control Blend and Selected Mixtures (with TxDOT Specification for Items 247 and 245)

The maximum dry density and optimum moisture content were determined for each of the seven mixtures by test method Tex-113-E. The specimens used to determine the moisture-density relationship were also used to determine the seismic modulus with the Free Resonant Column (FFRC) device according to test method Tex-145-E adapted for base and subgrade materials through hardware and software modifications.

In FFRC tests, an impulse load is applied to the specimen and energy travels over a large range of frequencies. The energy associated with one or more frequencies is trapped and magnified (resonates), depending on the dimensions and stiffness of the specimen. The specimen dimensions and resonant frequencies were used to determine the specimen modulus. Table 2-11 shows a summary of the results.

Table 2-11: Maximum Dry Densities and Seismic Moduli of the Blends from FFRC Testing

Percent Fines in Blend	Moisture Density		Moisture & Modulus		
	Optimum Moisture Content (%)	Maximum Dry Unit Weight (pcf)	Modulus at Optimum Moisture Content (ksi)	Moisture Content at Maximum Modulus (%)	Maximum Modulus (ksi)
0%	3.6	139.1	40.1	4.0	40.8
5%	4.3	143.2	40.8	3.8	41.4
10%	6.0	144.0	37.0	3.2	43.6
20%	5.4	143.8	44.7	2.6	55.3
5% Clay	4.9	144.8	37.2	3.5	37.4
10% Clay	5.1	145.6	46.8	4.0	48.7
20% Clay	4.6	143.0	53.3	3.6	55.1

Specimens were exposed to both extreme wet and dry conditions through placement in a water bath and oven. Each specimen was weighed and tested daily for seismic modulus. For both low and high plasticity fines, the maximum dry densities of all specimens containing fines were approximately 3% higher than the control mix (with no fines). For the current study, it appears that adding fines to RAP or RAP blends will improve dry density.

Texas Triaxial testing was used to determine the shear strength of the soil at several confining pressures. TxDOT currently has two procedures to obtain the shear strength of soils: Tex-143-E and Tex-117-E, the results from Tex-143-E being more representative of the field conditions of the base course, and those from Tex-117-E corresponding to the long-term behavior of the material.

All of the blends were tested both ways. Each specimen nominally measured six inches in diameter and eight inches in height. All specimens were moistened, mixed, molded, and finished so that their properties would be as uniform as possible. All specimens were then encased in a rubber membrane and allowed to mature for at least 24 hours prior to testing. Tex-117-E specimens were subjected to ten days of capillary wetting and exposed to a constant pressure of 1.0 psi and loaded with a surcharge load before shear testing. Tex-143-E specimens were tested at confining pressures of 3.0, 7.0, or 10.0 psi, with an increasing load of 1.0% strain per minute. Under Tex-117-E, they were tested at confining pressures of 0.0 psi, 5.0 psi, 10.0 psi and 15.0 psi with an increasing load set at 2.0% strain per minute. The load and deformation of the

material were recorded up to failure. Mohr's circle diagrams were constructed, and the failure envelope determined. Table 2-12 shows results from the two test methods.

Table 2-12: Triaxial Results of Blends with Low and High Plasticity Fines (Gandara et al., 2003)

a) According to Tex-143-E

Percent Fines in Blend	Angle of Internal Friction (degrees)	Cohesion (psi)	Strength at 10 psi Confining Pressure (psi)
0%	41.4	10.2	40.9
5%	53.3	6.3	60.3
10%	54.1	9.1	71.2
20%	57.6	1.2	61.5
5% Clay	54.2	3.4	56.8
10% Clay	53.2	7.8	62.0
20% Clay	49.1	9.2	54.6

b) According to Tex-117-E

Percent Fines in Blend	Internal Angle of Friction	Cohesion (psi)	Strength at 10 psi Confining Pressure (psi)
0%	51.8	5.6	55.3
5%	52.2	8.8	64.7
10%	54.5	12.2	78.2
20%	33.2	20.8	50.6
5% Clay	52.7	7.6	61.1
10% Clay	51.0	12.8	73.2
20% Clay	42.5	12.3	52.4

The angles of internal friction from all blends were over 50 degrees except for the 0.0% fines control and the 20% high plasticity fines blend. Cohesion was variable ranging from 3.4 psi to 20.8 psi. The strength at a confining pressure of 10.0 psi increased for both high and low plasticity fines when adding fines up to 10% and then decreased at 20%. In general the data from Tex-117-E, corresponding more to the long-term behavior of the material, displayed greater strength.

The resilient properties of the base materials were determined using a repeated load triaxial test (resilient modulus testing). The resilient modulus and permanent deformation relate to field performance. Permanent deformation can be predicted through static creep tests as well as repeated load tests. Brown et al., (2001) found that repeated load tests correlate with in-service pavement rutting measurements better than static creep test results. To relate static creep and repeated loading, rutting potential was correlated to the cumulative permanent deformation as a function of the number of load cycles. For static loading, rutting potential was correlated to the measured permanent deformation after unloading.

Gandara et al., (2003) carried out the resilient modulus tests on six inch diameter, 12-inch-high specimens compacted at the optimum moisture content in six layers. After compaction specimens were extruded from the mold and encased in a rubber membrane and allowed to mature for 24 hours prior to testing. A thin layer of grout was placed on the top and bottom of the specimens. The specimen was then encased in a second rubber membrane to ensure no moisture loss or air leakage occurs during testing. Finally, the membranes were secured to the platens by sealing them with vacuum grease and placing O-rings over the membranes.

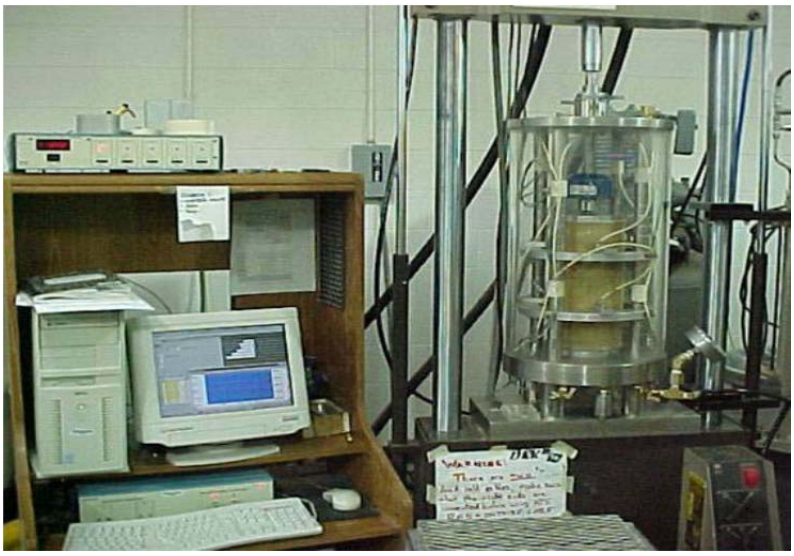

Figure 2-7: Resilient Modulus and Permanent Deformation Test Set-up (Gandara et al., 2003)

Resilient moduli were determined at a confining pressure of 5 psi and a deviator stress of 15 psi using the Feliberti (1991) equation for granular material:

$$M_r = k_1 \, x \, \sigma_c^{k_2} \, x \, \sigma_c^{k_3}$$ Equation 2-3

M_r = resilient modulus
k_i = regression constants
σ_c = confining pressure
σ_d = deviatoric stress

Resilient modulus results are reported in Table 2-13. In general, as fines content increased, M_r decreased. There was a slight increase in M_r at 20% fines, but the increase still produced values lower than the control. Gandara et al., (2003) concluded that adding fines to base course materials adversely affects their resilient moduli.

Table 2-13: Resilient Modulus Results from Low and High Plasticity Fines Blends (Gandara et al., 2003)

Percent Fines in Blend	Model Parameters			R^2	Resilient Modulus ksi
	k_1	k_2	k_3		
0%	22	0.42	-0.03	0.98	39.9
5%	25	0.36	-0.03	0.97	41.1
10%	22	0.44	-0.22	0.96	24.6
20%	15	0.54	-0.08	0.97	28.8
5% Clay	23	0.46	-0.07	0.98	39.9
10% Clay	18	0.27	-0.06	0.94	23.6
20% Clay	20	0.38	-0.09	0.97	28.9

The permanent deformation properties materials were also determined. The resilient moduli tests were conducted at a confining pressure (σ_c) of 15.0 psi and a deviator stress (σ_d) of 13.5 psi. The results are shown in Figure 2-8. The blend containing no fines exhibited minimal permanent deformation. According to Gandara et al., (2003), this trend was anticipated because of grain-to-grain contact between the aggregates with low fines content. According to the author, the blends with both low-plasticity and high-plasticity 10% fines performed well. However, for higher load cycle repetitions that are not presented on the figure, they exhibit large tertiary deformations, indicative of poor performance. The two blends that contained 20% fines exhibited

large initial permanent deformations, but became stable after 1,000 cycles. Blends with high plasticity fines displayed more rutting than blends with low plasticity fines.

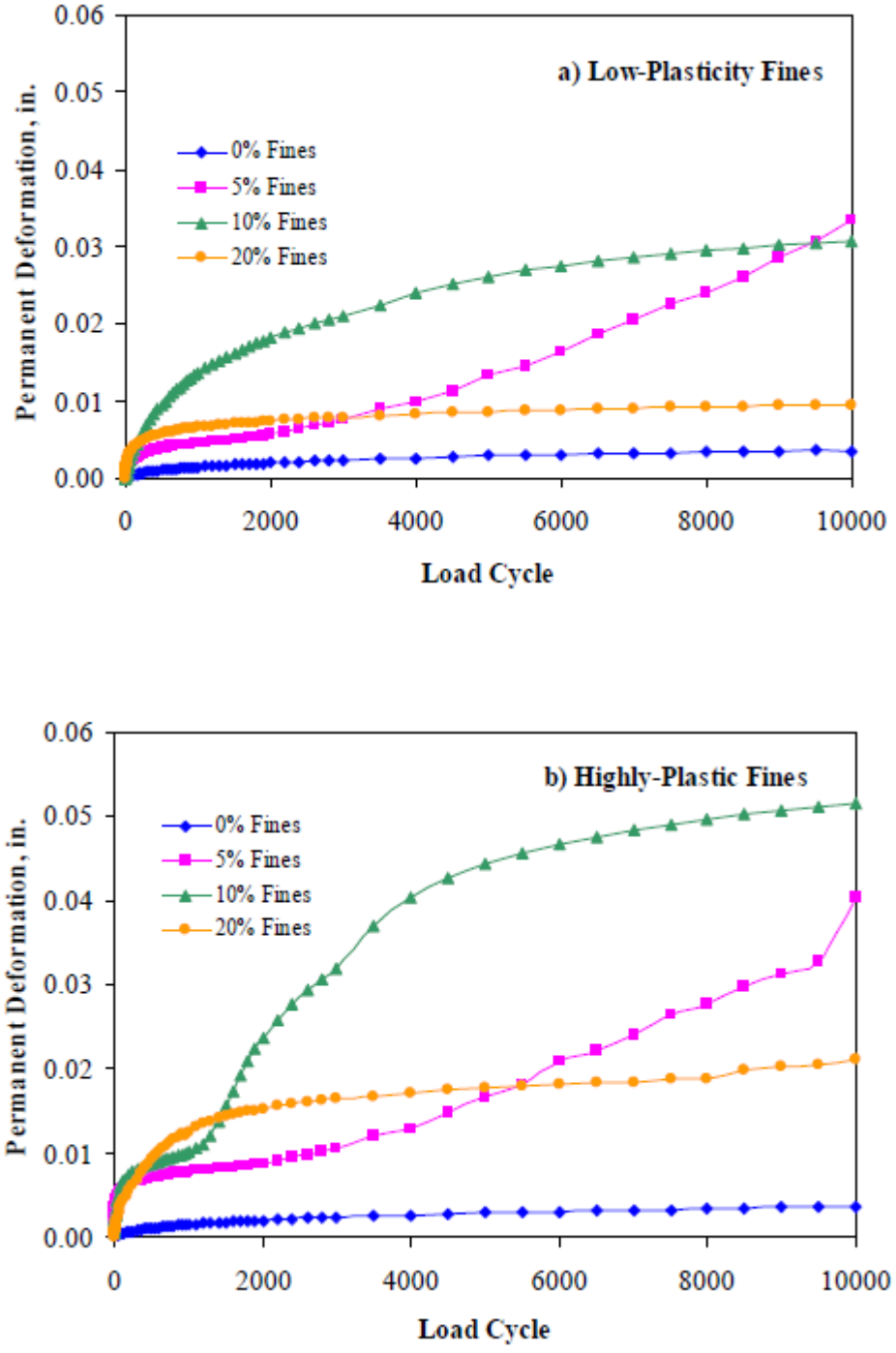

Figure 2-8: Permanent Deformation Results for Different Blends (Gandara et al., 2003)

Gandara et al., (2003) concluded that the addition of fines affected the properties of the base material. Adding up to 10% fines resulted in an increase in density. Density decreased with 20% fines. All specimens with 10% fines reached Class 1, the highest rating under Texas specifications. Materials with low-plasticity fines were typically better than those with high-plasticity fines. Increases in both high and low plasticity fines content resulted in higher permanent deformation and lower resilient moduli. The specimens containing 0%, 5% and 10% fines exhibited increases in the permanent deformation with the increase in fines. Specimens with 5% fines exhibited the most deformation. The specimens with 20% fines content in both cases deformed the least. The optimum fines content appeared to be between 10% and 20%.

2.5. Blending RAP with High Quality Materials

2.5.1. Structural Capacity of RAP Blends (Alam et al., 2010)

Alam et al., (2010) investigated the structural capacity of base courses consisting of RAP blended with varying amounts of aggregates. Capacity was evaluated by resilient modulus (M_r) testing. Tests were conducted with RAP and RAP/aggregate blends at varying moisture contents and densities. RAP content varied between 100% RAP, 30%, 50% and 70% RAP/Class 6 (CL6) material and 50% RAP/taconite. Moisture content varied between 7.0% and 8.0%. Dry densities varied between 125 pcf (2.00 Mg/m^3), 130 pcf (2.08 Mg/m^3) and 135 pcf (2.16 Mg/m^3).

Figure 2-9 shows typical Resilient Modulus (M_r) plots. For fine-grained material axial deviator stress has the most significant effect on M_r but for granular material both confining pressure and the deviator stress have significant effects on M_r (Yoder and Witczak, 1975). Note that M_r and E are used interchangeably in these figures. The M_r versus log deviator stress plot, typically used for fine grained soils, produces a straight line like the one shown. Constants k_3 is M_r at a deviator stress of one; k_4 is the slope of the line. The M_r versus log bulk stress (sum of the principal stress or first stress invariant) is typically used for coarse grained soils because it accounts for the combined effects of all principal stresses. Constant k_1 is M_r at a bulk stress of 1; k_2 is the slope of the line.

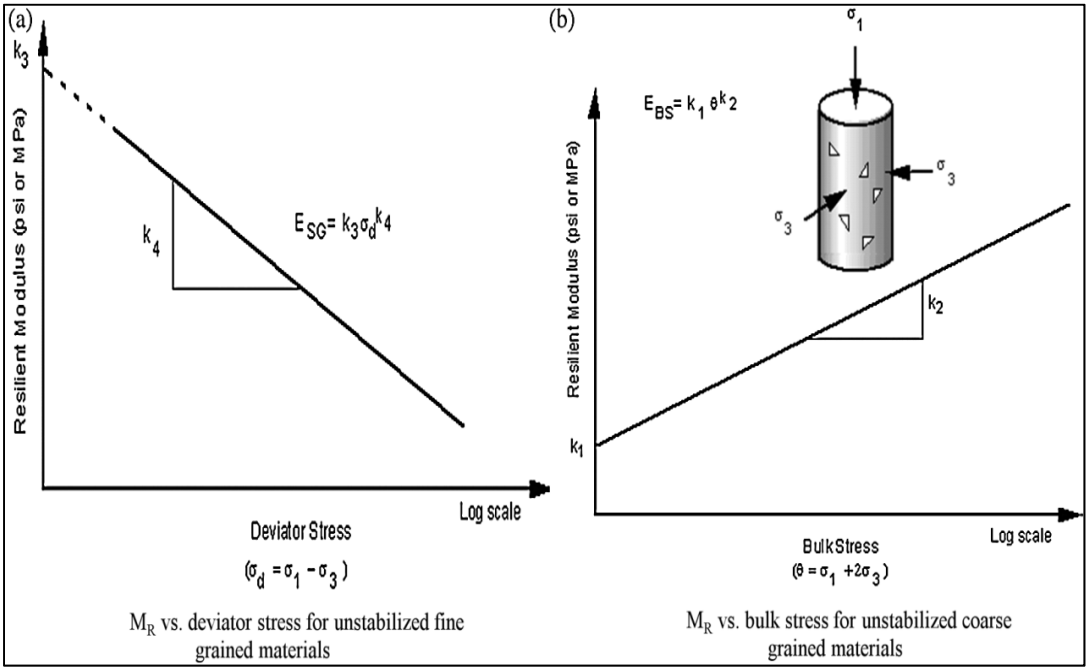

Figure 2-9: Typical M_r versus Stress Graph for Fine and Coarse Aggregates (Kim et al., 2005)

Tests of specimens with varying RAP content showed that M_r increases with RAP content. This indicates that RAP improves resistance to cyclic loading which is a critical property for a base course material. Increased RAP content and dry density correlated to increased M_r. Moisture content did not affect M_r.

Alam et al., (2010) used the resilient modulus results as inputs for *The AASHTO Guide for Mechanistic-Empirical Design of New and Rehabilitated Pavement Structures*, 2002 (MEPDG, National Cooperative Highway Research Program (NCHRP) 1-37A 2011) to predict the effect of RAP content on pavement performance. The computer trials were based on inputs of RAP and RAP blends of 0%, 30%, 50%, 70% and 100% for the granular subbase. For the 0% RAP trial, the pavement structure consisted of 6 inches of HMA on 15 inches of AASHTO A-1-b material. Results showed that as RAP content increased, the predicted alligator or fatigue cracking of the HMA decreased and that high RAP contents yielded lower fatigue. RAP content had a minimal effect on the predicted rutting in the subbase. The difference between 0% and 100% RAP blends was less than 0.05 inch (1.4 mm) of rutting.

2.5.2. Engineering Characteristics of RAP/Aggregate Blends (Mokwa and Peebles, 2005)

Mokwa and Peebles (2005) evaluated the changes in engineering properties of granular soils from various sources in Montana after blending them with RAP. The research focused on primary engineering properties including compaction, gradation, strength, stiffness, permeability, and resistance to degradation. Milled RAP was mechanically mixed at percentages of 20%, 50% and 75% by weight with four aggregates – three of them mechanically processed materials meeting the crushed base course specifications, and the fourth being a natural gravel material.

The grain-size distributions for the unblended materials showed that they were well-graded. RAP displayed a well graded curve with 96% passing 1½ inch sieve and 1% fines. For all four aggregates tested, the addition of RAP to the virgin materials resulted in an increase in the amount of particles passing the larger opening sieves and a decrease in the percentage of particles passing the smaller opening sieves. The smaller particles reduction was believed to be due to adhesion with the asphalt and the milling process used to produce the RAP material.

The modified Proctor compaction tests on the four materials showed that adding RAP caused the compaction curves to decrease and shift to the left. The curves for one of the aggregates used, pit run gravel, are presented in Figure 2-10. The curves in the figure displayed a relatively small decrease of the maximum unit weight of 3.3% at 75% RAP content, still suggesting that the blends were comparable to the virgin aggregate. It was believed that the decrease was caused by the lower specific gravity of RAP. For the same pit run gravel the gradation changes due to compaction were analyzed and found to be minimal. The particles between the #4 and #16 sieve were slightly affected with changes of less 5%. These changes were attributed to the presence of water, the viscosity of RAP, and the dynamic impact of the compaction equipment.

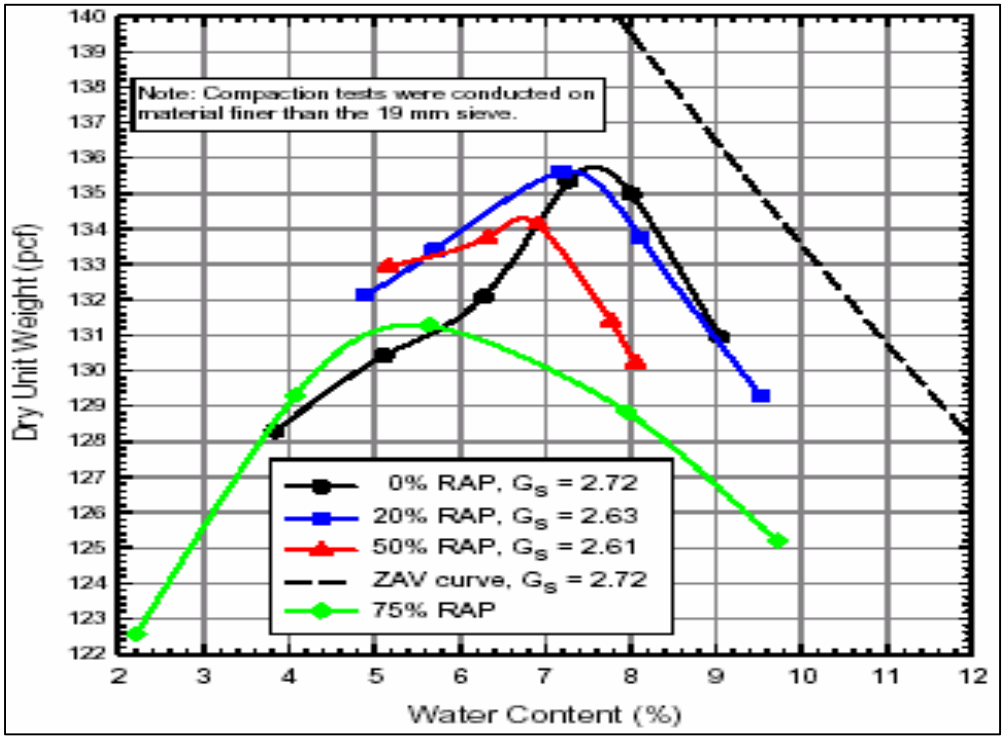

Figure 2-10: Moisture-Density Curves for Blends of Pit Run Gravel with RAP (Mokwa and Peebles, 2005)

Results from direct shear tests conducted on blends of crushed base course aggregate and RAP indicated that at a given normal stress, the soil shear strength decreased as the quantity of RAP in a sample increased. This effect was more pronounced as the normal stress increased. Overall the shear strength decrease was not significant enough for the exclusion of RAP as a blending alternative.

Permeability increased with higher RAP percentage which was attributed to the more uniform gradation of the material occurring after adding RAP. In general, the conclusion from this study was that blending RAP with conventional base aggregates results in only minor changes to the engineering properties of the original material. It was recommended, however, that future studies on the long-term field performance of blends are necessary to determine the maximum amount of RAP allowed in the blend.

2.6. Asphalt Content Improvements

Cosentino et al. (2008) showed that the Florida statewide variability of asphalt content by weight ranges from about 4.4% to 8.6%. One dimensional creep testing showed that creep

decreased as asphalt content by weight decreased. Figure 2-11 shows that this improvement was most prevalent at RAP contents below 60% which corresponds to asphalt contents below 3.5%.

Creep results were based on blends of RAP and A-3 sands with the asphalt contents varying from 0 to 5.8% as the RAP content varied between 0 and 100%. The overall project findings included a recommendation that a portion of the FDOT specification on RAP (Section 283) be changed to limit the asphalt content of RAP materials which are used for fill rather than require a minimum asphalt content.

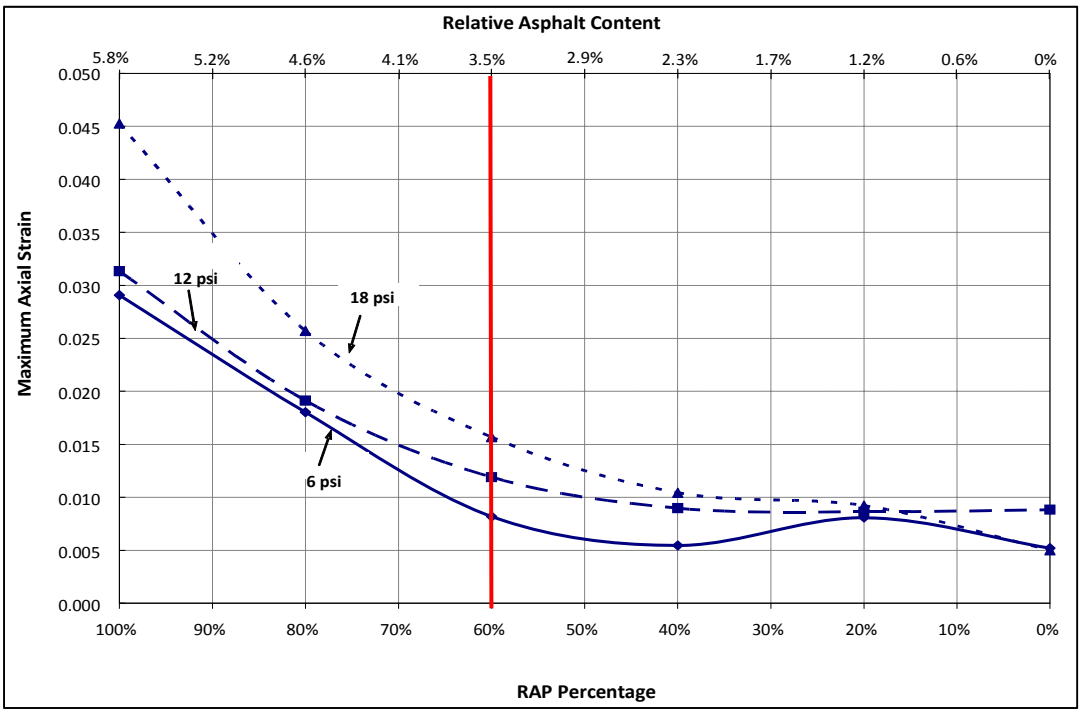

Figure 2-11: Maximum Axial Strain of RAP, RAP-Soil Mixtures, and A-3 Soil During Creep at Stress Levels of 6, 12 and 18 psi (Cosentino et al., 2008)

2.7. Compaction Improvements

2.7.1. Impact Compaction of RAP (Montemayor, 1998)

FDOT specifies the modified Proctor method for determining optimum moisture content and density of subbase and base course materials. The Proctor methods rely on impact from a series of blows from a dropped hammer to compact samples. Impact compaction of free draining, cohesionless soils, does not produce a well-defined optimum moisture content or maximum

density (Ping et al., 2003). Montemayor (1998) conducted Proctor compaction tests on RAP and found that this did not produce well defined maximum density curves (Figure 2-12). These studies indicate that specifying density as a percentage of the modified Proctor optimum may not be the best method for RAP.

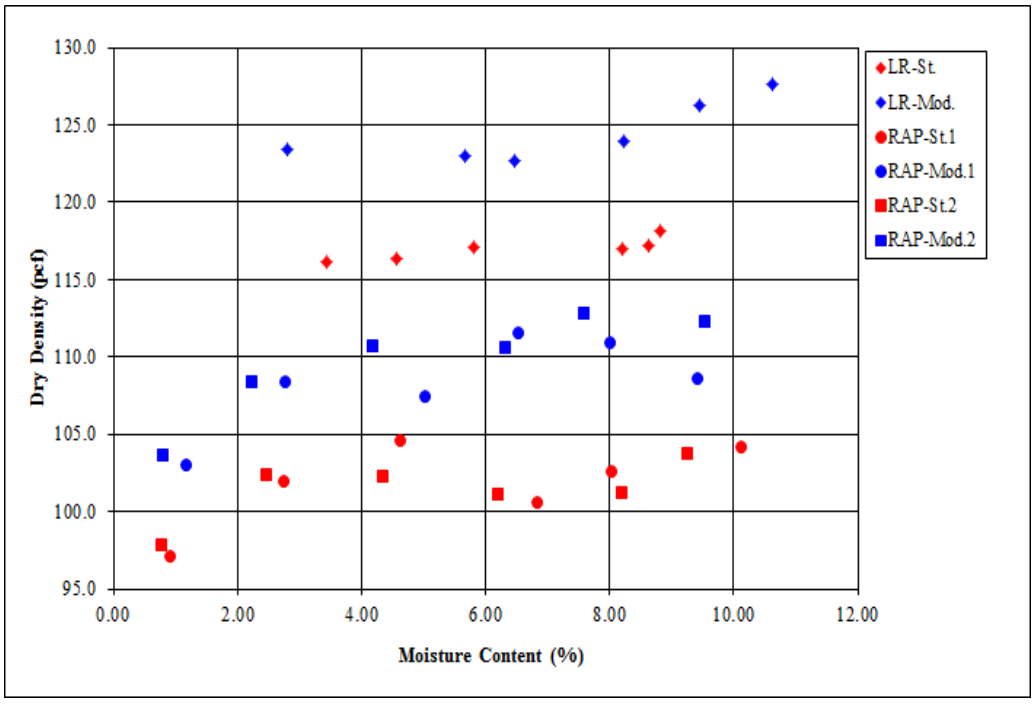

Figure 2-12: Dry Density versus Moisture Content for RAP and Limerock Compacted by Standard and Modified Proctor Methods (Montemayor, 1998)

2.7.2. Static Compaction of RAP (Cosentino and Kalajian, 2001)

RAP was placed into a universal testing machine and a compressive force was applied until a predetermined surface stress was achieved. The density and LBR results were then reported. The static pressures included 212, 400, 700, and 1000 psi. Densities increased approximately 4% at each loading interval while LBR values increased significantly with each load interval (Figure 2-13). This study demonstrates that it is possible to compact RAP to higher densities and higher LBR strength than those achieved by the normal modified Proctor method.

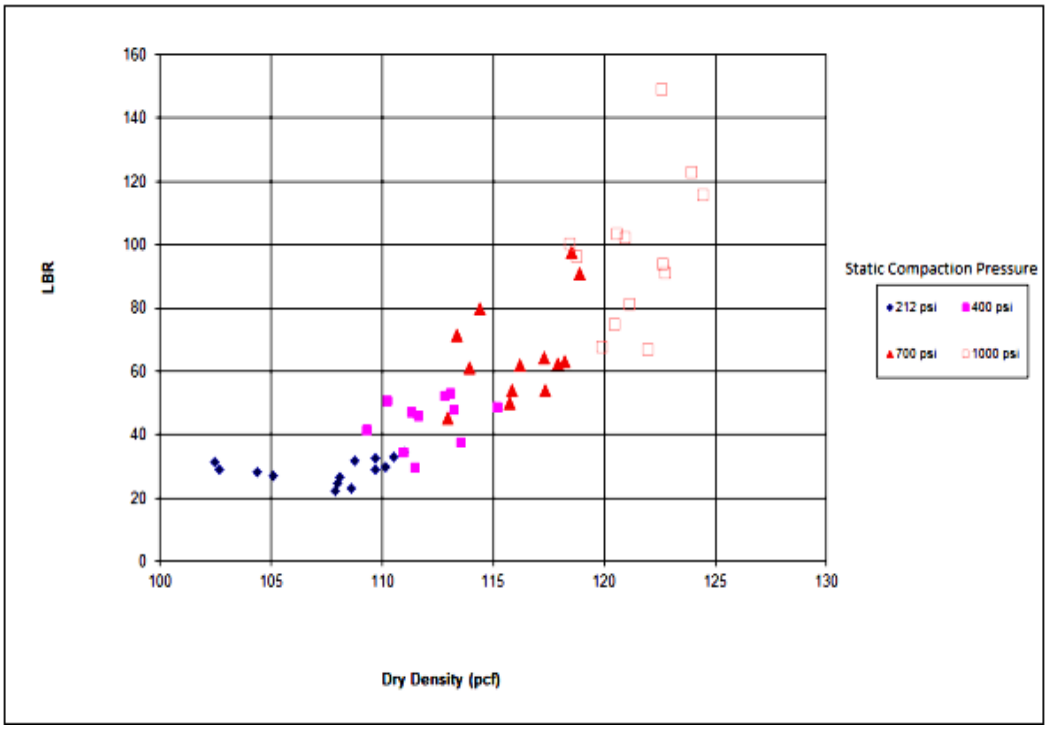

Figure 2-13: LBR versus Dry Density for Static Compaction Method (Cosentino and Kalajian, 2001)

2.7.3. Vibratory Compaction (Ping et al., 2003a & 2003b)

Compaction using a vibratory roller is often used in roadway construction in both base course applications and rolling of HMA. Laboratory testing for determining the maximum index density and unit weight of soil using a vibratory table is specified in ASTM D4253. Soil is placed in a mold, a surcharge weight is placed on top, and the sample is vibrated on the table for 8 minutes. After the time has elapsed, the density (maximum index density) is determined. The minimum index density as specified in ASTM D4254 is determined by loosely filling the vibratory mold to capacity, measuring the weight then dividing by the volume.

As shown in Figure 2-14, laboratory vibratory compaction of A-3 soil is less indicative of measured field compaction than the modified Proctor compaction method (Ping et al., 2003a&b). Vibratory compaction of RAP resulted in lower dry densities than the modified Proctor method at the same moisture content ranges.

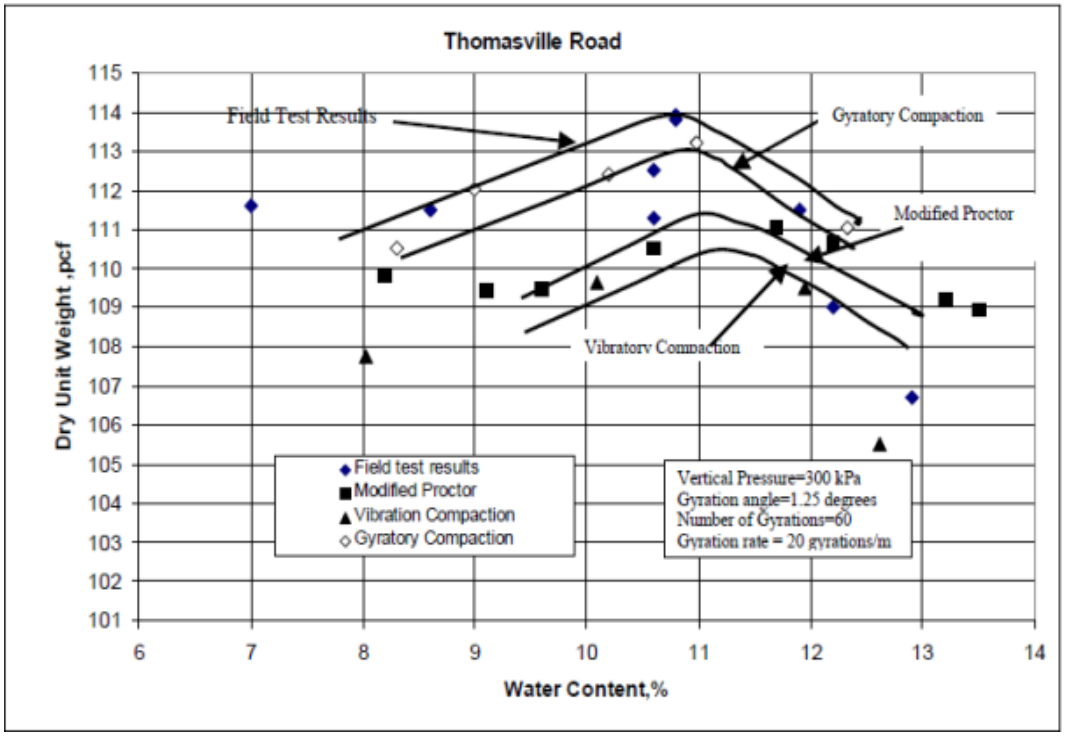

Figure 2-14: Comparison of Compaction Methods for an A-3 Soil (Ping et al., 2003a & b)

2.7.4. Gyratory Compaction of Soil (Ping et al., 2003a &2003b; Zhang, 2010)

Gyratory Compaction (ASTM D6925) is used in Superpave HMA design. HMA is poured into a 6-inch (150 mm) diameter mold (Figure 2-15) which is subjected to a constant compressive force of 88 psi (600 kPa) while the bottom of the mold is angled, typically at 1.25 degrees, from the top of the mold and the mold is gyrated. The sample height is measured and recorded after each gyration. The compacted density (unit weight) is determined based on the weight of material placed into the mold and the sample height after compaction. The Superpave gyratory compactor is intended to simulate the kneading action and shear forces induced by a pneumatic rubber tire roller moving along the pavement (Womack et al., 1969).

Figure 2-15: Gyratory Mold Assembly

No literature was found for gyratory compaction of RAP. Gyratory compaction has been used on varying types of soils and asphalt mixes. Gyratory compaction has been used on clay soils to measure shear strength since the kneading action induces shear stresses in the specimen (Zhang, 2010). Gyratory compaction has also been used on base and subbase soils in Florida in an effort to evaluate a better laboratory analogue to field compaction techniques than impact compaction methods. As previously shown in Figure 2-14 gyratory compaction produced dry unit weight results which were are closer to field compaction results than either modified Proctor or vibratory laboratory results. Gyratory compaction results are sensitive to the number of gyrations (Ping et al., 2003a & 2003b; and Zhang, 2010) but less sensitive to the gyration rate (speed at which the machine turns the sample). The angle of gyration did not affect dry density (unit weight) results (Ping et al., 2003a & 2003b).

2.7.5. FDOT Concurrent Lab and Field Compaction Studies (Ping et al., 2003 a & 2003b)

These combined studies produced two FDOT reports with one report number: FL/DOT/RMC/BB-890(F). The Phase I report summarized lab simulations of field compaction and the Phase II report expanded evaluations of the lab compaction and field testing techniques. The main finding from Phase I was that gyratory compaction on AASHTO Classified A-3 and A-2-4 soils better simulates field compaction than Proctor impact compaction. The gyratory compaction procedures used on the samples were varied to show the effects of number of gyrations, the tilt angle during compaction and the compaction pressure.

Field compaction was accomplished using four passes of the sheepsfoot roller followed by four passes with the smooth drum roller. One pass is defined as both the forward and backward motion of the roller. In general, gyratory compaction at 29 psi (200 kPa), with 90 gyrations at 1.25 degrees tilt, produced moisture density results similar to field densities as shown in Figure 2-16. Compaction specifications for base or subbase material are based on modified Proctor densities and optimum moisture content so there is currently no application for these results. Gyratory equipment is required for Superpave and would typically be available at asphalt plants where RAP would be stockpiled. Gyratory equipment is not commonly available at testing labs that do not routinely test HMA.

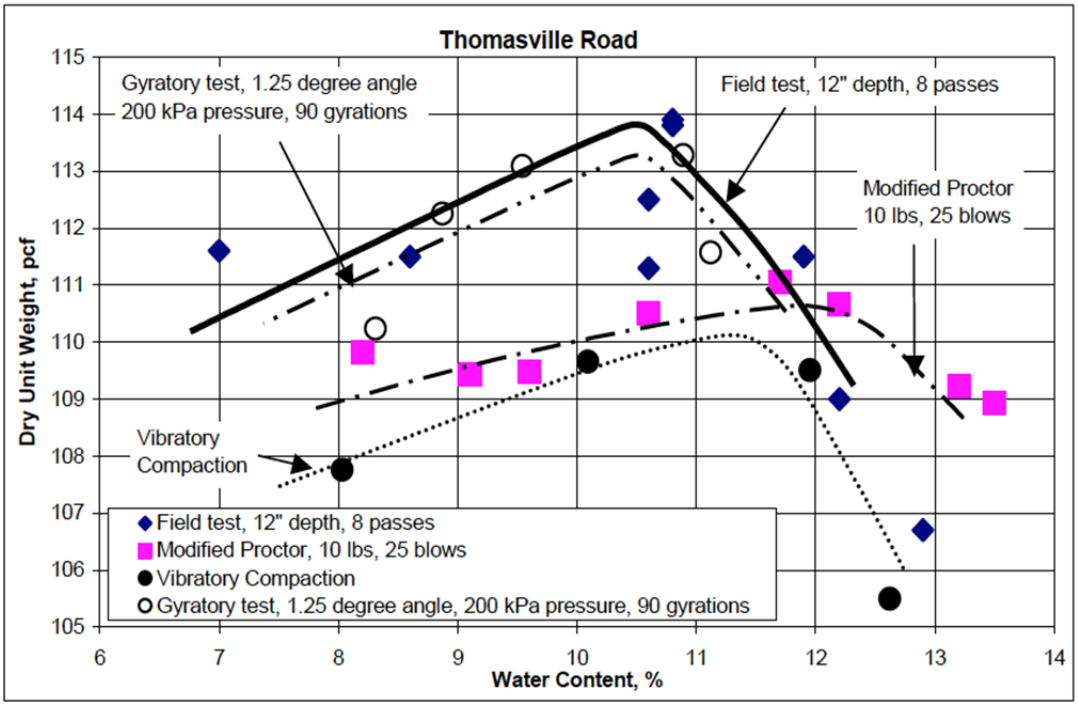

Figure 2-16: Correlations Between field and Laboratory Compaction Testing from the FDOT Thomasville Road Project (Ping et al., 2003b)

2.8. Chemical Stabilizing Agent Additives

A variety of chemical stabilizing agents exist for both coarse and fine soils. The literature search focused on stabilizing agents that have been used successfully with RAP or RAP/aggregate blends. Some contractors have reported that using a small amount of detergent in compaction water improved field compaction of RAP. Previous laboratory testing at the Florida Institute of Technology and FDOT evaluated the effect of detergent on density and strength of compacted RAP. These tests found no improvement in density or strength, so it was determined that no further investigation of detergent as an additive was warranted. Polymers are commonly added to HMA, but the literature review did not uncover any polymers intended for blending with RAP. Therefore, this line of investigation was also eliminated.

2.8.1. Cement, Hydrated Lime CIR Blending, Niazi and Jalili (2009)

Niazi and Jalili (2009) investigated cement, hydrated lime, and lime slurry as additives for Cold In-place Recycling (CIR) of asphalt pavement. All three additives improved Marshall

Stability and several other properties. The authors did not test creep. The authors recommended cement as the most effective additive.

2.8.2. RAP and Fly Ash Subgrade Stabilization (Rupnow, 2002)

Construction site soils with high moisture exhibit severe rutting and deformation, which make it difficult to move construction machinery. Rupnow (2002) conducted an investigation on the soil-stabilizing potential of fly ash and RAP to see if these two materials can decrease rutting and deformation within the subgrade during the movement of construction machinery. RAP, fly ash, and subgrade soil were mixed in-place using a reclaimer machine and then compacted to a smooth surface to prevent water infiltration from rain and to provide a suitable paving platform to test rutting.

Dynamic Cone Penetrometer (DCP) tests were used to measure the in situ stability versus depth. For each fly ash application, a DCP test was taken immediately after compaction, and 1 hour, 24 hours, 3 days, 7 days, and 28 days after compaction. Testing stability at these time intervals was done to determine when paving operations could start. Once the soil, RAP, and fly ash were mixed, several samples were taken to conduct unconfined compression testing.

Proctor tests on unconfined compression strength specimens of 50% RAP/50% soil by dry weight were conducted to determine the optimum moisture content. Once the optimum moisture contents were determined, unconfined compressive strength specimens were produced at varying moisture contents to determine strength and then compared to field samples. Rupnow (2002) found that specimens compacted dry of optimum moisture showed substantial strength loss when soaked prior to unconfined compression testing. Samples compacted wet of optimum showed significantly less soaked strength loss when soaked. Gradation analysis was conducted on field samples to see what effect the addition of RAP had on the grain size distribution of the subgrade blend.

Based on the results from these tests Rupnow (2002) concluded that the addition of fly ash to soil RAP mixtures produced a DCP penetration resistance stiffness gain and that the addition of RAP to soil shifted the grain size distribution curve and stabilized the soil. Overall, the addition of RAP and fly ash to the subgrade soil proved to be very effective at soil stabilization.

2.8.3. RAP Foamed Asphalt, Soil Cement and Fly Ash Blends (Tao et al., 2008)

Tao et al., (2008) investigated the use of several recycled materials as base course: foamed asphalt (FA), soil cement (SC), fly-ash-stabilized blended calcium sulfate (BCS), and BCS stabilized with the 120 grade ground granulated blast furnace slag (BCS-GCBFS). Multiple blend combinations were tested: 100% FA-RAP, 50% FA-RAP/50% SC, BCS-fly ash, BCS-GCBFS, and crushed limestone.

Full scale testing was performed to determine structural numbers by both Dynaflect and Falling Weight Deflectometer. Both the RAP/SC blend and 100% RAP produced higher structural numbers than virgin crushed limestone.

2.8.4. Cement-Treated Base Design Mix, (ODOT, 2009)

Oklahoma Department of Transportation (ODOT) test method OHD L-53 describes compaction and unconfined compressive strength testing of cement stabilized base course blends. The OHD L-53 is conducted with 6-inch diameter by 6-inch high molds and Proctor compaction. Unlike the regular Proctor method, OHD-L53 allows up to 1.5 inch diameter material to be used without precrushing or sieving. The method discusses blending to include recommended adjustment of moisture content by 0.25% per 1.0%, variation in cement content. Curing techniques and extraction from the molds are discussed. The method discusses but does not require conditioning (soaking) prior to unconfined compression testing. The method specifies a target unsoaked unconfined strength of 700 psi with an acceptable range of 600 psi to 1,200 psi. These procedures were used in the development of the cement stabilization and 6-inch diameter unconfined compression testing protocols for the current research.

2.8.5. Engineering Behavior of Chemically Stabilized Soils (Parsons and Milburn, 2002)

Parsons and Milburn (2002) conducted an investigation to determine which stabilizing agent or combination of agents performed best with fine grained soils. The primary objective of the research was to evaluate and compare the performance of soils treated with a variety of traditional additive products. A second objective of this research was to observe changes in the

modulus during the curing period using the SSG to monitor the level of ongoing reactions within stabilized soils.

Lime, cement, Class C fly ash and enzymatic stabilizers were mixed with a total of seven soils of types CH, CL, ML, and SM. Each soil/additive combination was evaluated by freeze-thaw, wet-dry, leaching, free swell, and Atterberg limits tests. Specimens were prepared over a range of moisture contents and moist cured for 28 days. The stiffness was measured using the SSG at intervals of 10 minutes, 4 hours, and 1, 7, 14, and 28 days after compaction to measure changes in the soil stiffness and modulus and as a potential indicator of chemical activity within the samples during curing.

The results showed that all treated soils increased in stiffness immediately after compaction. Significant strength improvements were observed for soils treated with lime, fly ash, and cement while enzyme treated soils showed modest strength gains. The cement treated soils had the least loss in freeze-thaw testing; fly ash had lower soil losses in freeze-thaw testing than lime. Lime generally performed better on fine grained materials and cement on coarse grained materials during the wet-dry cycles, and fly ash performed well only on the SM soil for a limited time. Lime and cement treated soils maintained higher strengths and lower plasticity values than fly ash after leaching. The enzymatic stabilizer did not substantially improve soil performance in this study.

2.8.6. Emulsion Polymers for Soil Stabilization (Newman and Tingle, 2004)

Newman and Tingle (2004) tested the effect of six polymer emulsion chemical stabilizing agents on silty sand (SM) material. An emulsion content of 2.75% by weight was used for all six agents. Results were compared to control specimens stabilized with 2.75%, 6%, and 9% Portland cement. The 4 inch (102 mm) diameter 5.98 inch (152 mm) high specimens were prepared using a Gyratory compactor. All specimens were compacted for 90 gyrations with a RAM pressure of 125 psi (870 kPa) at an angle of gyration of 1.25°. Following compaction, specimens were ejected from the mold and cured for 1 day, 7 days, or 28 days at 23°C and 50% relative humidity for varying time period depending on the stabilizing agent. Six specimens were prepared for each stabilizing agent and curing time combination.

After curing, three specimens were partially soaked by laying them on their sides in 1 inch (25.4 mm) of water for 15 minutes to determine moisture sensitivity. After soaking, specimens were drained for five minutes then subjected to unconfined compression testing along with the three unsoaked specimens. Compressive load was applied as a constant rate of 0.0165 in/min (0.42 mm/min) until the specimen failed or reached 8.0% strain. In addition to failure stress, the researchers evaluated the toughness of the material by calculating the area under the stress-strain curve prior to failure.

All of the stabilized soils gained strength with longer curing times. This was more pronounced with the emulsions. The authors hypothesized that the emulsions continued to break (separation of polymer and water) as the specimens dried during curing. The most pronounced effect of all of the stabilizing agents was a large reduction in moisture susceptibility. The 28 day retained strength (wet strength/dry strength) improved from approximately 20% for the unstabilized control specimen to approximately 60% for the stabilized specimens. The 28 day retained toughness followed a similar pattern (Figure 2-17).

These results were used in the development of the emulsion curing procedures for the current study. In this current study emulsion stabilized specimens were oven cured to accelerate the breaking process. Based on the large improvement in retained (soaked/unsoaked) strength seen by Newman and Tingle (2004), specimens in this study were tested in both dry and soaked condition to evaluate the effect of stabilizing agents on retained strength.

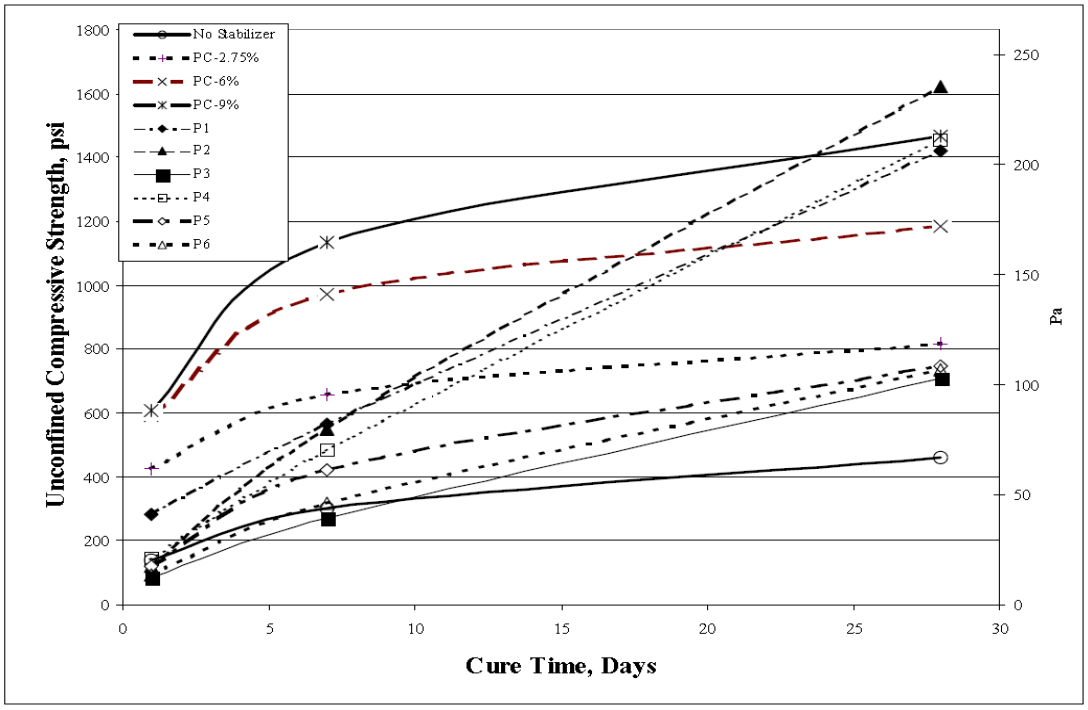

Figure 2-17: Effect of Cure Time on Unconfined Compressive Strength (Newman and Tingle, 2004)

2.9. Evaluation of Creep in RAP

2.9.1. Creep Behavior of Soils (Augustesen et al., 2004)

Augustesen et al. (2004) compiled a review of time dependent soil behavior. Observations from both triaxial compression and one-dimensional oedometer tests were evaluated considering different time related effects including creep, relaxation and rate dependency. The characteristic behavior of cohesionless and cohesive materials was analyzed separately. The author's defined creep, discussed its stages, discussed reference time, and analyzed behavioral specifics of cohesive and cohesionless soils. Creep tests in the current study were all uniaxial so this literature review is focused on uniaxial creep of granular soils.

Augustesen et al., (2004) described three stages in typical oedometer tests: primary, secondary, and tertiary compression (Figure 2-18). The primary stage was attributed to void reduction or excess pore pressure dissipation. This initial consolidation under load is typical of all soils. Cosentino et al., (2008) found that course grained A-3 sand goes through a primary consolidation but then stops compressing if the pressure is held constant. RAP, on the other

hand, continues to deform under constant pressure. Augusten et al., (2004) called this continued deformation secondary creep. In this region the relationship between strain and logarithm of time is linear. If the load and secondary deformation are large enough, the specimen begins to fail. This tertiary stage is characterized by a nonlinear increasing strain rate leading to failure.

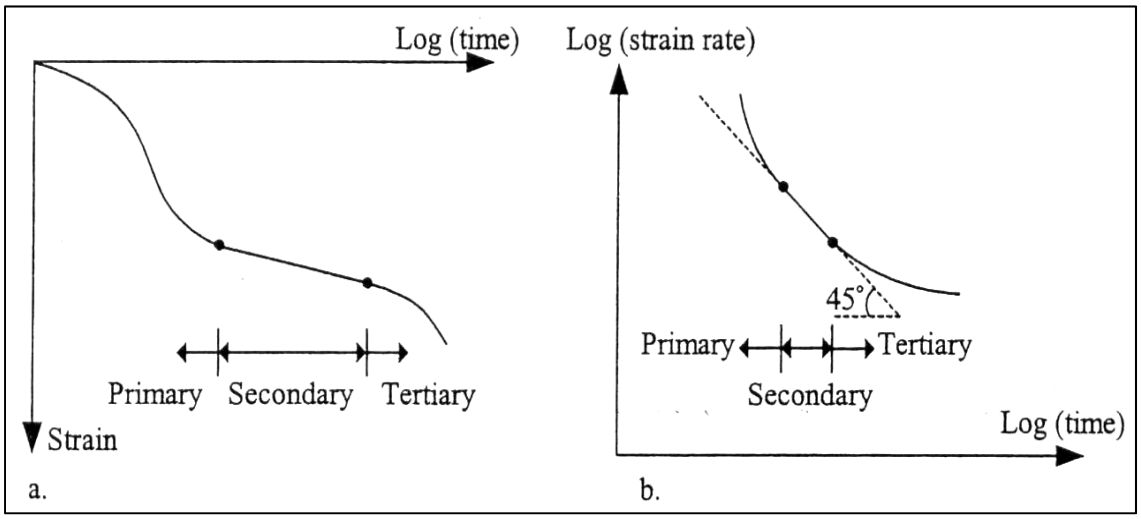

Figure 2-18: Primary, Secondary, and Tertiary Compression for Oedometer Testing: (a) Strain vs. Log(time) and (b) Log Strain Rate vs.Log(time) (Augustesen et al., 2004)

Augustesen et al., (2004) defined reference time as the end of primary consolidation (EOP). For granular soils a logarithmic function can be used to model the specimen's vertical strain versus time performance following the EOP time.

Granular soils deform by either rearranging the soil skeleton due to sliding at relatively low stress, or by deformation/crushing of the individual grains at high stress. The stress dividing the two behavior modes was dependent on the nature of the material and was termed "critical pressure". For example, a sample of calcareous sand produced a critical pressure at 116 psi, while siliceous sand produced a critical pressure at 726 psi. For road base courses with low confining stresses and relatively low load stresses deformation is primarily due to the first sub critical mode.

As discussed earlier, coarse soils under load reach equilibrium quickly and then stop consolidating. Creep typically occurs in highly plastic cohesive soils such as clays and silts. Although RAP is primarily composed of coarse aggregates, these aggregates are coated with

asphalt binder. The binder is a viscoelastic material which allows the aggregates to continue to reposition by sliding over one another resulting in continuing deformation.

Cleary (2005) and Dikova (2006) documented the creep of RAP and RAP-sand mixtures. Cleary's study modeled the creep compliance using Maxwell and Voigt models as described in Huang (2004) to predict settlements based on the rate process theory from Singh and Mitchell (1968). The Cleary (2005) and Dikova (2006) works are also summarized by Cosentino et al., (2008).

Cleary (2005) used two consolidometers and one pneumatic loading device (PLD) to measure the creep of RAP and RAP-sand mixtures. The samples were compacted using standard and modified Proctor compaction tests. RAP proportions of 100%, 80%, 60% and 0% were mixed with an AASHTO classified A-3 sand. The materials were evaluated under constant stress for 6 to 12 days.

Dikova's (2006) built on Cleary's study by conducting a series of creep tests of RAP and RAP/A-3 sand blends at varying pressures. Blends of 100%, 80%, 60%, 40%, 20% and 0% RAP and A-3 sand were subjected to vertical stresses of 6, 12 and 18 psi. Dikova showed that that asphalt content or blend percentages could be used to characterize creep behavior.

Both studies found consistent results: decreasing RAP content resulted in decreased creep. Blending as little as 20% A-3 sand with RAP reduced creep deformation by approximately 30%. The greatest incremental improvement occurred in the 80% RAP/20% A-3 blend. Figure 2-19 shows creep compliance (strain divided by stress) versus linear time curves for RAP and RAP blends compacted using the modified Proctor. While the difference in total deformation is significant, the reduction in secondary creep following the initial consolidation is even more pronounced. Figure 2-20 shows creep compliance versus log(time). A material with no creep such as A-3 sand will have a slope of zero (horizontal). Materials that creep such as RAP or RAP/A-3 blends have a positive slope. As the slope increases the creep increases.

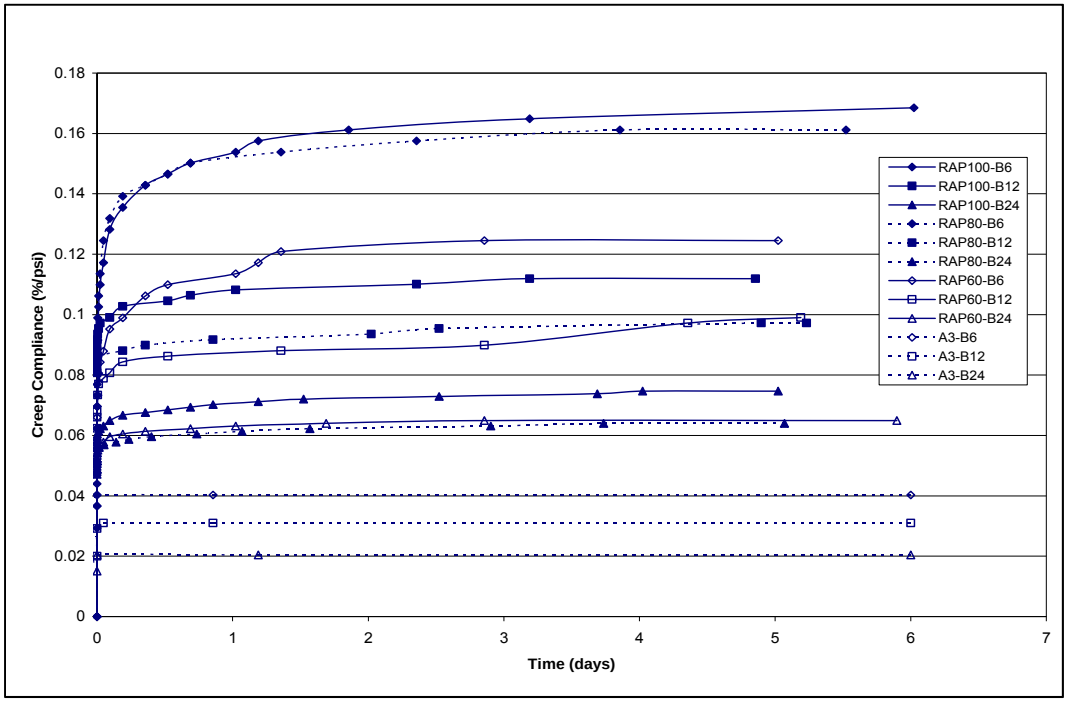

Figure 2-19: Creep Compliance vs. Linear Time of RAP Mixtures and A-3 Control Material at 6, 12, and 24 psi Creep Pressure (Cleary, 2005)

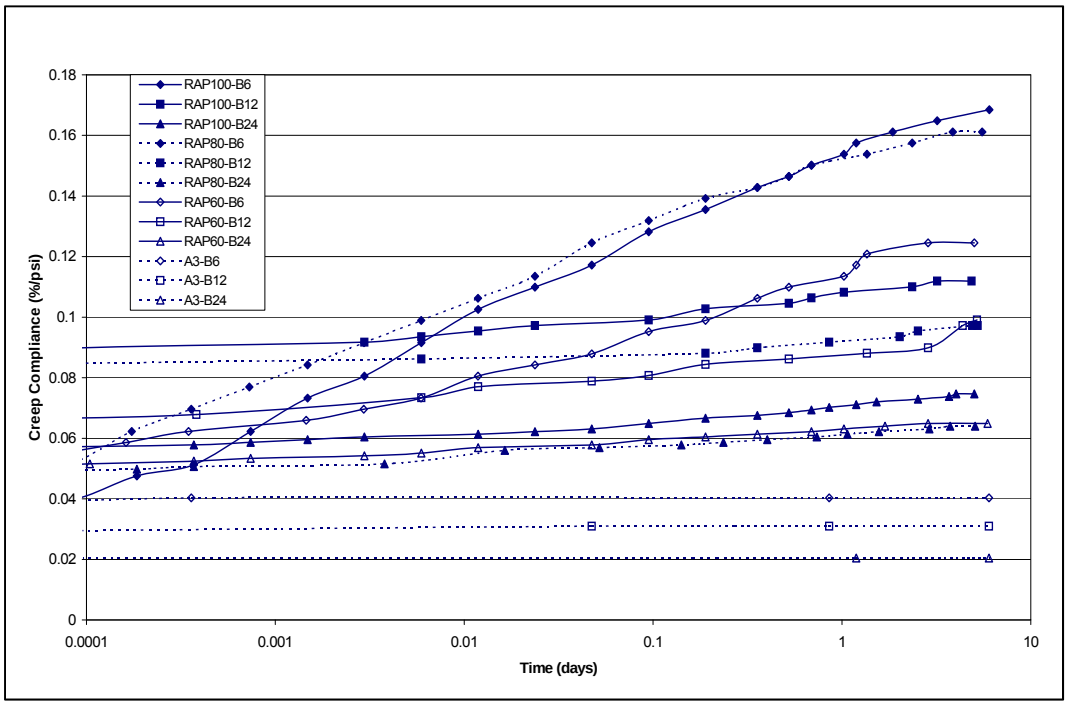

Figure 2-20: Creep Compliance vs. Log(Time) of RAP Mixtures and A-3 Control Material at 6, 12, and 24 psi Creep Pressure (Cleary, 2005)

2.10. Rate Process Theory (Creep)

2.10.1. Development of Rate Process Theory

Singh and Mitchell (1968) developed a simple equation describing the creep relationships between strain and time and strain rate and time. The authors found that this relationship was applicable to a reasonable range of stresses, a variety of soil types.

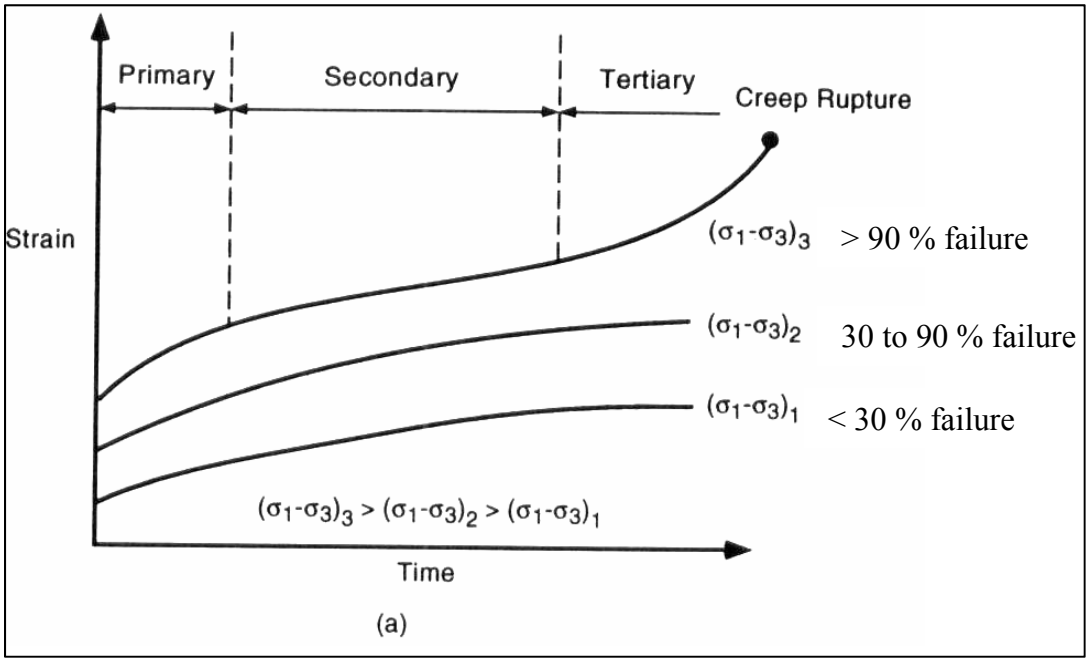

Figure 2-21: Creep under Constant Stress (Mitchell, 1993)

Figure 2-21 shows the general creep behavior of soils under a constant deviator stress (σ1-σ3). The stress level was defined as the creep stress divided by the failure strength determined in a conventional strength test. The stress level affects the shape of the strain-time curves. At relatively low deviator stresses the creep deflections were small and cease after some time period. Higher stress levels (30% to 90% of the strength) resulted in prolonged or infinite creep but not rupture. Deviator stresses over 90% of failure stress results in a secondary creep followed by a tertiary stage leading to rupture.

Mitchell (1993) discovered that if the same data was plotted on a log of strain rate versus log of time graph, the resulting function was always linear. The line slopes proved to be independent of the creep stress intensity and the only effect from stress increase was a shift of the lines upwards and to the right.

Singh and Mitchell (1968) represented the creep stress and creep magnitude relationship with a strain-rate variation dependent on a hyperbolic sine function of stress. For a variety of soils, it was found that within the midrange of stresses, a nearly linear relationship existed between the log of strain rate and stress.

The relationship between strain rate and time can be expressed by Equation 2-4 (Singh and Mitchell, 1968).

$$\ln \frac{\dot{\varepsilon}}{\dot{\varepsilon}(t_1, D)} = -m \ln\left(\frac{t_1}{t}\right) \qquad \text{Equation 2-4}$$

where: $\dot{\varepsilon}$ = strain rate at any time t;
D = deviator stress;
t = any time;
t_1 = unit time;
m = slope of log strain versus log time straight line.

$$\ln\left(\frac{\dot{\varepsilon}}{\dot{\varepsilon}(t, D_0)}\right) = \alpha D \qquad \text{Equation 2-5}$$

where: $\dot{\varepsilon}_{(t,D_0)}$ = strain rate after start of creep at $D = 0$;
α = slope of the linear portion of the logarithm strain versus deviator-stress plot.

Combining Equations 2-4 and 2-5 produces a three-parameter relationship that adequately characterizes the creep rate of a variety of soils:

$$\dot{\varepsilon} = A e^{\alpha D}\left(\frac{t_1}{t}\right)^m \qquad \text{Equation 2-6}$$

where: $A = \dot{\varepsilon}_{(t_1, D_0)}$, the strain rate obtained by projecting the straight line portion of the relationship between log strain rate and deviator stress at unit time to a value of $D = 0$.

For Singh and Mitchell's development of Equation 2-6, the stress intensity, D, was taken as the deviator stress (σ_1-σ_3) from a triaxial creep test. In a later study, Mitchell (1993) stated that

applied uniaxial stress level from an oedometer test could also be used. In order to establish the parameters A, α, and m, a minimum of two creep tests are needed. Testing identical specimens at different creep stress intensities, a plot of log strain rate versus log time would yield the value of m, and a plot of log strain rate versus stress for different time intervals would produce α and A from the slope and intercept, respectively.

2.10.2. Triaxial Creep of RAP (Viyanant et al., 2007)

Viyanant et al., (2007) evaluated RAP with a series of constant stress, drained triaxial creep tests. Drained conditions were selected because of RAP's high hydraulic conductivity. Each of the specimens was gradually loaded using the equipment shown in Figure 2-22. After the target deviator stress was reached, which usually occurred within the first two minutes, the deviator stress was maintained at a constant rate for the duration of the test. Although asphalt performance is related to the temperature, all of these tests were performed at a constant room temperature of 72°F. During tests, an external Linear Variable Displacement Transducer (LVDT) and external load cell produced the axial deformations and deviator stress. Creep tests were performed for approximately 10,000 minutes (7 days).

The testing program consisted of creep tests using confining stresses of 20 psi and 40 psi while varying the deviator stress level from 0.4 to approximately 0.8, or 80% of the ultimate strength producing tests at deviator stresses between 5 and 50 psi. Plots were developed based on arithmetic, semi-log, and log-log data.

Arithmetic plots of deviator stress level as a percent of the ultimate strength versus time for the various confining levels showed how the specimens were loaded. A typical stress level versus time plot for a confining stress of 20 psi is shown in Figure 2-23, with stress levels (D) from 0.4 to 0.8 of the ultimate strength.

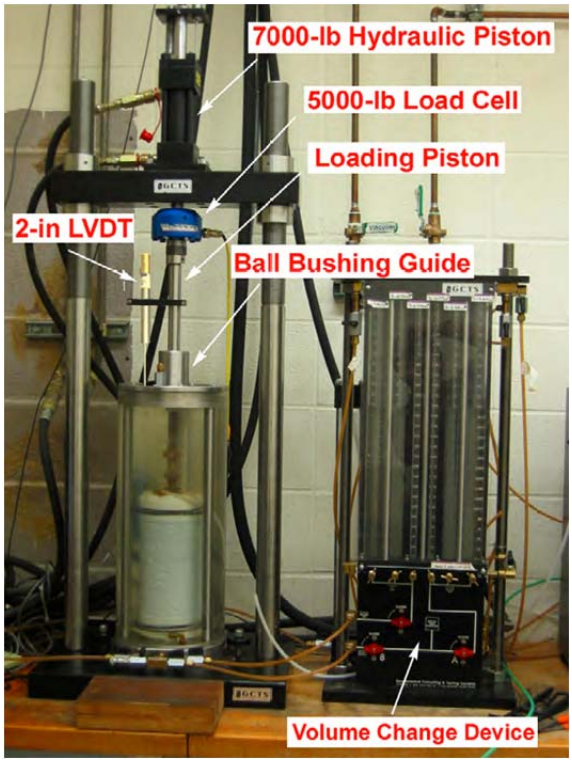

Figure 2-22: Triaxial Cell and Loading Components Used for Creep Testing (Viyanant et al., 2007)

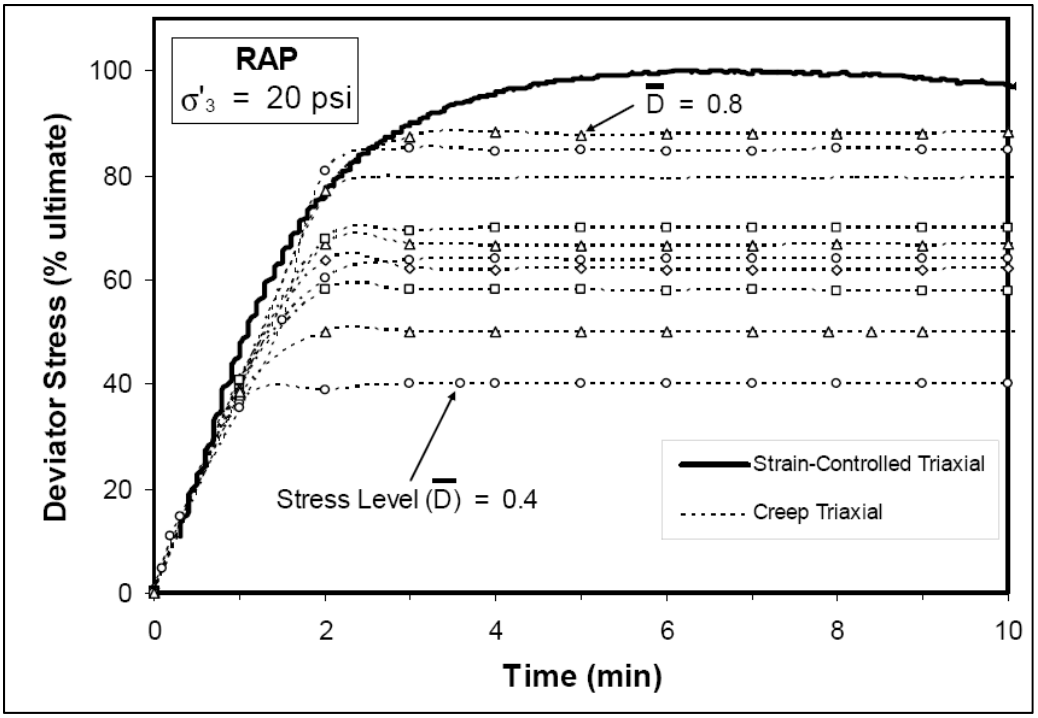

Figure 2-23: Typical Deviator Stress Level versus Time Plot for RAP (Viyanant et al., 2007)

To show the effects that stress level has on axial strain, semi-log plots of axial strain versus time were developed. A typical plot, again at a confining stress of 20 psi, is shown in

Figure 2-24. As the stress levels increase from 0.4 to 0.88, the time to failure (i.e., when the axial strain increase is nearly vertical) decreases to 15 minutes. This plot indicates that the lower stress levels do not produce failure within 10,000 minutes.

Log-log plots of axial strain rate verus time were developed to expand and examine the data in the early portion of the curves. The plots were used to determine an average slope (m_{ave}) from the linear region and produced data such as that shown in Figure 2-25 for the 40 psi confining level. The 20 psi average slope was 0.7 while the 40 psi slope was 0.9, as shown.

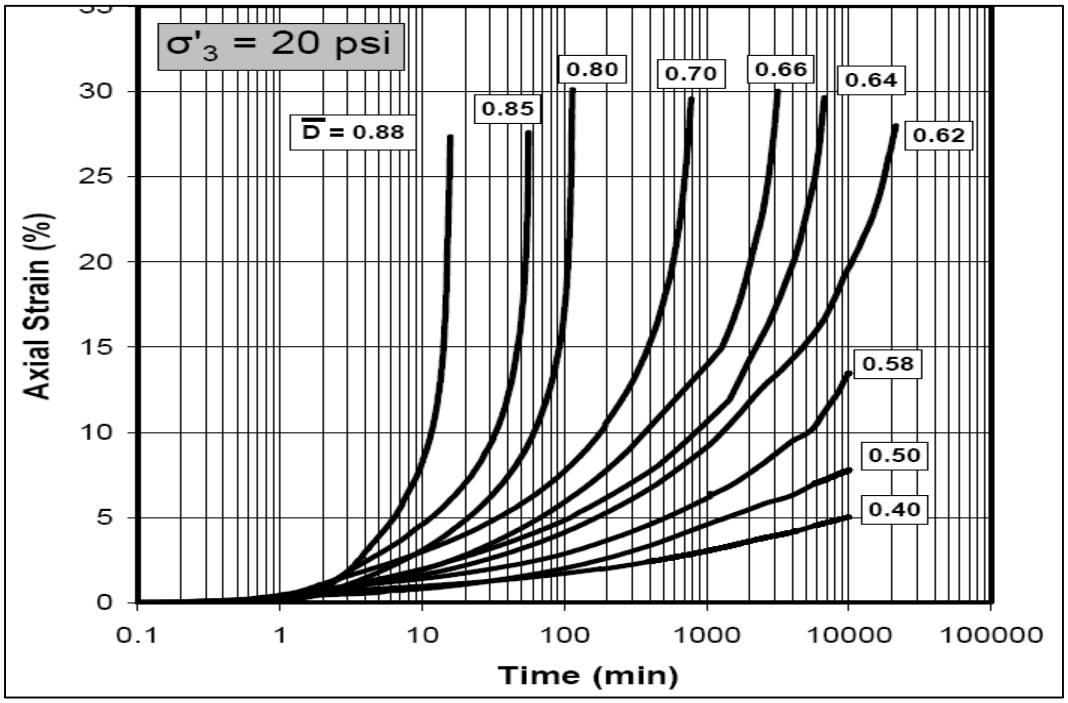

Figure 2-24: Typical Axial Strain Versus Time Plot for RAP on Semi-log Scale (Viyanant et al., 2007)

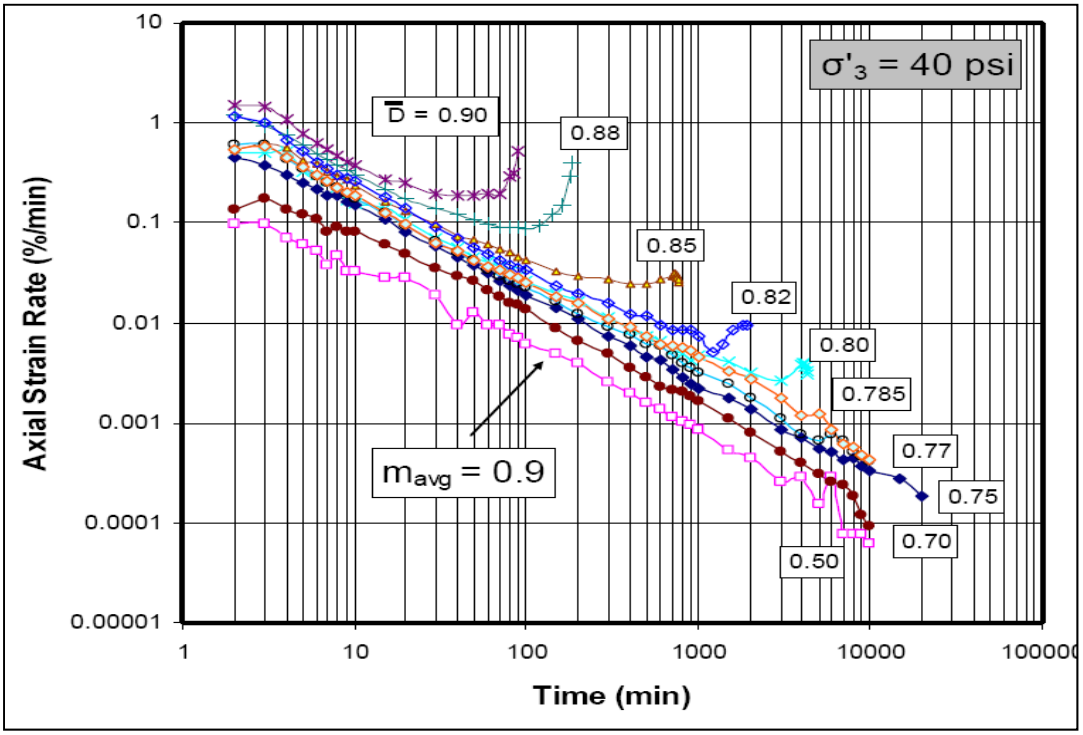

Figure 2-25: Typical Log Axial Strain Rate versus Log Time Plot for RAP (Viyanant et al., 2007)

It is also possible to determine the time to failure from the log-log plot, as the time where this linear portion ends or there is acceleration in the strain rate. This data is presented in Figure 2-26, along with the data from undrained creep tests on Haney clay reported by Vaid and Campanella (1977). The Haney clay data only followed a linear trend at stress levels greater than 0.8, therefore, Vaid and Campanella (1977) include an upper yield line above this stress level. However, data from RAP testing was linear throughout the range of stress levels; therefore, Rathje et al. (2007) do not recommend the use of this upper yield line for RAP.

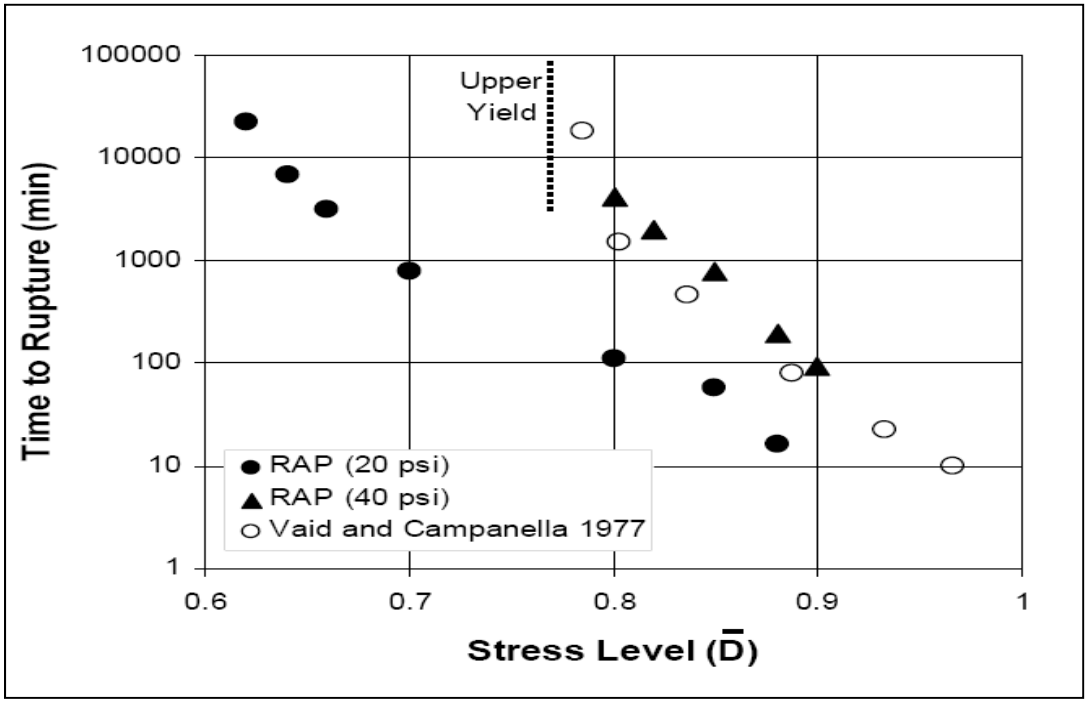

Figure 2-26: Time to Rupture versus Stress Level for RAP (Viyanant et al., 2007)

2.11. Full-Depth Reclamation Field Studies

2.11.1. Structural Evaluation of FDR Pavements in Virginia (Apeagyei and Diefenderfer, 2009)

Apeagyei and Diefenderfer (2009) conducted an investigation involving the use of recycled pavement to extend the service life of pavement. The study team performed structural testing of foamed asphalt and asphalt emulsion-based FDR materials on an existing two-lane rural highway in Virginia. The FDR sites were chosen because they showed structural distresses including longitudinal cracking and alligator cracking.

There are two methods of in situ pavement restoration: Cold In-Place Recycling (CIR) or Full-Depth Reclamation (FDR). In CIR all or a portion of the existing HMA layers are pulverized and mixed with a rejuvenating agent. In FDR the existing HMA layers are milled along with all or a portion of the unbound base layers and a binding agent (such as foamed or emulsified asphalt binder, Portland cement, or fly ash). The mixture is compacted and serves as a structural base which is surfaced with a new HMA layer. When applied, this reclaimed material was shaped by using a motor grader and compacted with a pad foot and pneumatic tire roller.

The samples mixed with emulsions had a relative compaction of 102% of the modified Proctor target density of 128 pcf.

These samples were then tested by applying loads of 40-kN (9000-lbf) while deflection vs. time (months) graphs were prepared from the results. The results show that deflection values for the emulsified section were higher than pre-construction levels for the total time tested, 7 months. On the other hand, the foamed asphalt had lower deflection values for the same given time. Based on this deflection testing there was a definite increase in structural capacity.

2.11.2. MoDOT CIR Evaluations (2009)

Cold In-place Recycled Asphalt Pavement (CIR) has been used as a cost effective means for road rehabilitation for years and often extend the pavement's service life. When applied to the roadways with the use of a mixer and pavers, heavy rollers are used to compact the CIR.

The Missouri Department of Transportation (2009) performed CIR testing on two low volume rural roads in 2008. Milling depth ranged from 2 to 3 inches. Cost per lane-mile ranged from $41,000 to $46,000. Performance was good for approximately six months, but significant rutting and fatigue cracking began to occur after six months. Approximately 15 months after the initial CIR (October 2009) MoDOT placed a 1 1/4 in (31.75 mm) hot mix overlay on the CIR. The Staff Summary document was published in December 2009 so there was no information about long-term durability of the new pavement.

Sample areas included sections of Missouri highways where rutting and fatigue cracking were found. Six months after the application of CIR to cover this rutting and cracking, there was no evidence of rutting and only a small amount of low severity fatigue cracking found. One year after the CIR was applied the rutting was the same as it was prior to the initial CIR placement. Conversely, fatigue cracking was not as severe after one year as it was prior to the construction but was increasing dramatically. Following this, CIR repairs became more frequent to the point that it was recommended that a 1 ¼ in layer of HMA be placed over the CIR.

2.12. Summary of Literature

The two major shortcomings of RAP as a base course material are its low bearing strength and its tendency to creep under constant load. Many states allow the use of RAP or RAP/aggregate blends in base course applications. RAP is typically limited to a maximum of

approximately 50% in base course blends. Blends generally have higher strength than 100% RAP and have higher permeability than 100% conventional base materials. Full depth reclamation projects essentially entail producing a roughly 50% RAP/50% aggregate blend which is strengthened with a chemical stabilizing agent. The literature indicates that blending RAP with select aggregate materials and using chemical stabilizing agents both have the potential to improve the strength of base courses containing RAP. Although there is no direct literature on the gyratory compaction of RAP, there have been some studies indicating that laboratory gyratory compaction provides a better indication of in-place densities and strength than the normal modified Proctor method.

None of the states investigated have a direct method to evaluate the creep potential of base courses containing RAP. Creep of RAP in an embankment or retaining wall application has been evaluated in Texas and Florida. These states recognize creep as a potential factor in the use of RAP. Creep testing has been successfully conducted using either one-dimensional oedometer type equipment or three-dimensional, triaxial testing equipment. Most tests are conducted for 10,000 seconds or 7 days. One-dimensional creep testing provides a relatively simple way to evaluate primary and secondary creep characteristics which can be modeled using the Singh and Mitchell (1968) approach to predict creep over the lifetime of a pavement project.

3. Methodology

The testing program was developed to investigate improving the performance of RAP by improving LBR strength to meet FDOT base or subbase specifications and decreasing creep deformation to an acceptable level. Five different approaches to achieve these properties were investigated: gradation modification (Task 3); blending RAP with high quality materials (Task 4); asphalt content improvements (Task 5); compaction improvements (Task 6a); and chemical additives (Task 6b). The testing program for each task is described in Section 3.1. Sample source selection is discussed in Section 3.2. Sample processing is discussed in Section 3.3. Index and mechanical tests are described in Section 3.4.

3.1. Test Programs

3.1.1. Gradation Modification

For this task both milled and crushed RAP was fractionated at varying sieve sizes. All fractionated specimens were 100% RAP. Preliminary tests including grain-size, asphalt content and specific gravity were performed on unfractionated RAP and on each fraction. The results of these initial tests were used to understand the behavior of each fraction and to select fractions for further testing. For the preliminary tests, fractionating consisted of sieving RAP and collecting the fractions retained and passed by each sieve. To support the overall objectives of this study, the LBR strength and creep behavior of each fraction were evaluated.

There are no standard tests for creep of a granular material such as RAP. The pneumatic loading device oedometer creep testing method developed by Cosentino et al. (2008) as part of previous phases of RAP research conducted at FIT for the FDOT was used in this study. The creep behavior of unfractionated RAP and each fraction was investigated by uniaxial compression in a one-dimensional oedometer at a pressure of 12 psi. Post creep unsoaked LBR tests were then performed to evaluate strength. Unsoaked specimens were evaluated for comparative purposes. Because all the specimens tested in this part of the study were 100% RAP, trends observed for unsoaked specimens should be indicative of trends in soaked specimens. Other portions of this study which blended RAP and aggregates or added chemical stabilizers evaluated soaked LBR strengths.

3.1.1.1. Preliminary Tests

Virgin non-cohesive aggregates do not creep (Cosentino et al., 2008). RAP, a blend of aggregates and asphalt binder, does creep. Asphalt content tests were performed on unfractionated RAP samples to evaluate the relationship between asphalt content and LBR and creep. RAP was also fractionated at each sieve size in the FDOT graded aggregate base specifications (Section 204-2): 1.5 inch, 3/4 inch, 3/8 inch, No. 4, No. 10, No. 50, and No. 200.

3.1.1.2. Selection of RAP Fractions for Further Testing

Classification systems, base course specifications, and literature findings were used to choose particles sizes for the fractionating analysis. AASHTO classifies material retained on the #10 sieve as gravel, material between the #10 and #40 sieves as coarse sand, and material between the #40 and #200 as fine sand. The USCS classifies material larger than the #4 sieve as gravel and material between the #4 and #200 sieves as sand. Fines are defined in both systems as material passing the #200 sieve. FDOT Standard Specifications for Road and Bridge Construction 2010 uses the amount of material passing the #4 sieve as a gradation test for shell base material (Section 913). Material passing the #40 sieve is used in the Atterberg limits test to characterize the plasticity of a soil.

For this study RAP was fractionated at the #4 sieve to evaluate the effect of the coarsest material (gravel) and at the #40 sieve to evaluate the effect of the finer materials. RAP was also fractionated at the #8 sieve because previous studies noted differences in the gradations of milled and crushed RAP starting at this sieve size. Material retained on the #8 sieve is classified as coarse sand under the USCS but as gravel under the AASHTO classification system. In this second phase of the testing program, fractionating consisted of splitting the material in two fractions above and below (+/-) the chosen sieve sizes. Samples of unfractionated RAP were tested as a control material. Specimens of RAP were also blended following the FHWA maximum density (FHWA T 5060.27 1988) gradation formula to achieve optimum density. These optimum density specimens were used to evaluate the effect of density on strength and creep. Figure 3-1 shows a graphical depiction of the Gradation Modification test program.

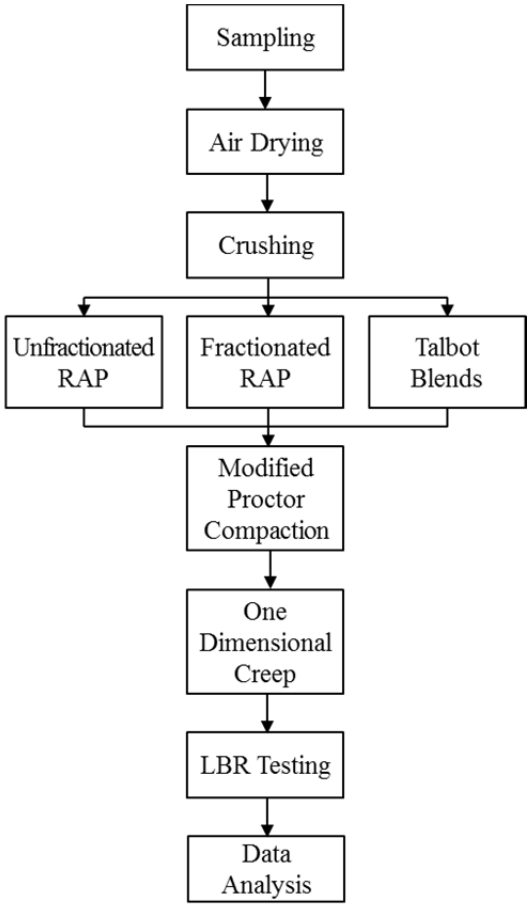

Figure 3-1: Task 3: Gradation Modification Test Program Flowchart

3.1.2. Blending RAP with High Quality Materials

The Gradation Modification task described above examined the effect of modifying pure RAP. Previous studies at FIT found that blending A-3 sand with RAP improved the LBR and decreased the creep of the blends. These blends, however, did not show the potential to achieve a soaked LBR strength of 100 (Dikova, 2006). FDOT specifications (Section 230) allow construction of a base course composed of roadbed soil stabilized with limerock. This task examined the effect of blending high quality (FDOT approved) base course materials with RAP in varying proportions on LBR strength and creep.

3.1.2.1. Selection of RAP and aggregates

Three commonly available base materials were selected from FDOT approved sources: limerock, cemented coquina, and crushed concrete. The sources selected for these materials are discussed in Section 3.2, Sample Selection.

3.1.2.2. Test Program

The same one dimensional creep and LBR strength tests performed in the Gradation Modification task were performed in this portion of the study. A graphical depiction of the test program is shown in Figure 3-2.

3.1.2.3. Creep

Blends of 0%, 25%, 50%, 75%, and 100% RAP and either limerock, cemented coquina, or crushed concrete were subjected to creep tests at 12, 25, 50, and 100 psi to assess the creep response at different loading conditions in the pavement system.

3.1.2.4. LBR

Following creep testing, specimens were tested for unsoaked LBR strength to determine which blends had the potential to reach the required soaked LBR strength of 40 for subbase or 100 for base material. Blends which reached an unsoaked LBR of at least 150 were evaluated further; those that did not were eliminated. The best performing blends were tested for soaked LBR strength in accordance with FM 5-515.

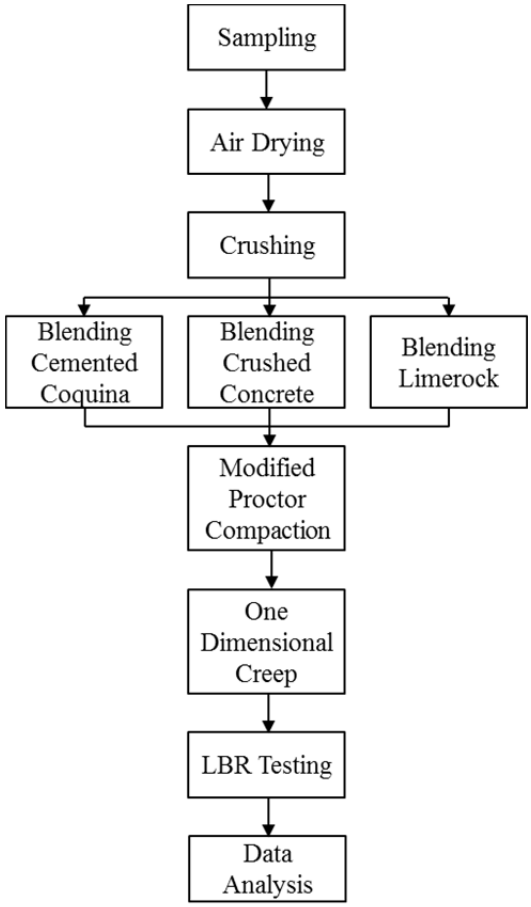

Figure 3-2: Task 4: Blending RAP Test Program Flowchart

3.1.3. Asphalt Content Modification

Previous studies at FIT found a correlation between the asphalt content of RAP or RAP/aggregates and creep (Dikova, 2006, Sandin, 2008). Based on the previous Florida statewide RAP variability study conducted by Sandin (2008) the range of asphalt content is relatively narrow. After attempting to adjust asphalt content by using several RAP sources it was concluded that this approach was not practical.

It was therefore determined that it would be possible to achieve larger variations in asphalt content by blending RAP with aggregate materials. This approach allowed the evaluation of RAP or RAP/aggregate blends with approximately 5%, 2.5%, 1.25% and 0% asphalt content. This blending allowed to the relationship between asphalt content and several strength tests as well as creep to be evaluated.

3.1.3.1. Selection of RAP and Aggregates

A single RAP source, APAC Melbourne Milled RAP with an asphalt content of 5.42%, was chosen to eliminate variations caused by RAP aggregate type or gradation differences. The same three aggregate sources used in the Blending RAP portion of the study (Section 3.1.2) were used in this portion. This allowed direct comparison with results in other portions of the study.

3.1.3.2. Test Program

A suite of mechanical performance tests, performed in other sections of this study, were used for this task. A graphical depiction of the test program is shown in Figure 3-3.

3.1.3.2.1. Creep (One Dimensional)

These creep tests were directly comparable to those conducted in other parts of this study and to previous research. This procedure is described in Section 3.4.3.2.1.

3.1.3.2.2. Creep (Unconfined)

Unconfined creep tests (Section 3.4.3.2.2) were conducted on a limited number of specimens in order to directly compare modified Proctor and gyratory compacted specimens. Gyratory molds have a different geometry from the modified Proctor molds used in the one dimensional creep test. Ejected specimens were tested to eliminate this mold geometry factor.

3.1.3.2.3. LBR

LBR tests (Section 3.4.3.1) were conducted the same way as those described in previous sections. Unsoaked LBR tests were conducted after one dimensional creep tests or as standalone tests.

3.1.3.2.4. Marshall

Marshall testing (Section 3.4.3.4) was conducted because it includes both a strength (Marshall Stability) and deflection (Marshall Flow) component. FDOT has adopted the Superpave Gyratory method for HMA design rather than the Marshall method. The Asphalt Institute modified Marshall mix design method has been used by several laboratories in Florida to design emulsion stabilized Full Depth Reclamation base materials.

3.1.3.2.5. Unconfined Compression

The LBR test is conducted with the specimen in the mold under partially confined conditions. Unconfined compression testing (Section 3.4.3.5) was added to the test suite because it is commonly used to evaluate chemically stabilized soils.

3.1.3.2.6. Indirect Tensile Test (IDT)

All of the other tests primarily evaluate the compressive strength of a soil. Indirect tensile testing (Section 3.4.3.3) was included to evaluate the effect of asphalt content on the tensile strength of RAP or RAP/aggregate blends. In HMA the asphalt binder provides tensile strength. IDT's are used in some states to evaluate stabilized Full Depth Reclamation mixes.

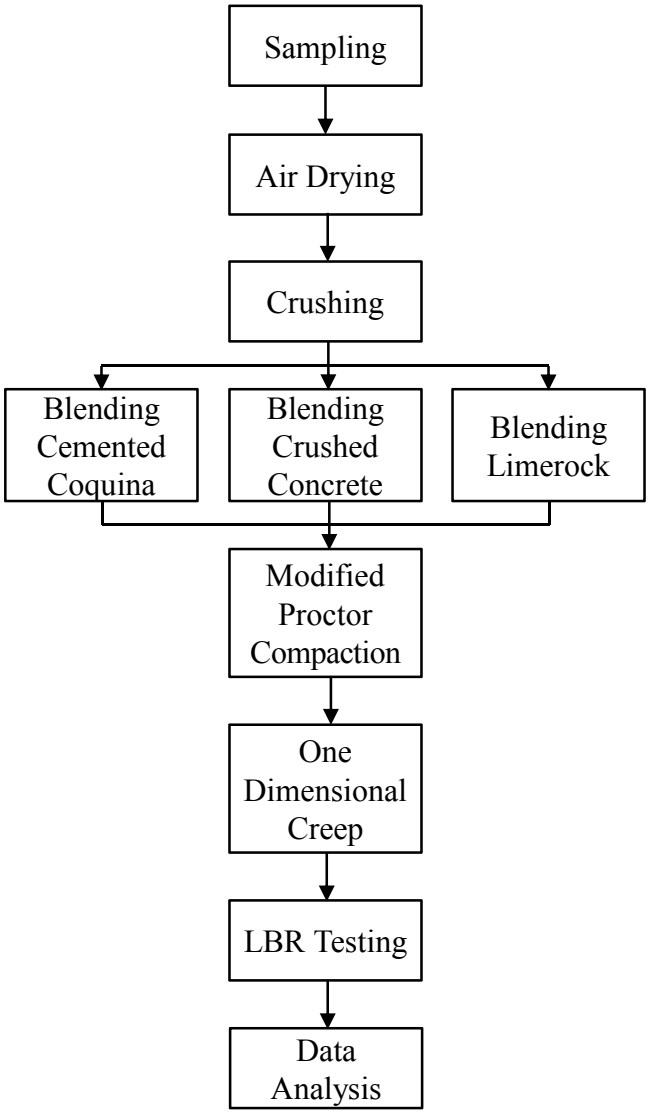

Figure 3-3: Task 5: Asphalt Content Modification Test Program Flowchart

3.1.4. Compaction improvements

The literature indicates that by compacting RAP to higher densities, strength increases. The objective of this research project task was to document the effects that various compaction methods would have on compressive and tensile strength of 100% RAP.

3.1.4.1. Selection of RAP and Aggregate

All four milled and crushed RAP samples listed in Section 3.2 were tested in this phase of the project. Testing was primarily done with 100% RAP samples. Samples of 100% limerock,

cemented coquina, and clayey sand were selected to investigate the effect of modified Proctor and Gyratory compaction on materials containing no asphalt binder. 100% limerock, 50% RAP/50% limerock blends, and 100% RAP were tested to examine the creep performance of modified Proctor and Gyratory compacted specimens of the same material. See Section 3.2 for a complete description of the RAP and aggregates selected for this study.

3.1.4.2. Compaction Methods

Compaction methods included Modified Proctor (Section 3.4.2.1), vibratory using the relative density apparatus (Section 3.4.2.5), and gyratory compaction using a Superpave Gyratory Compactor (Section 3.4.2.3). Within the physical limitations of the tests, compaction effort (energy/volume) was constant for each method. The gyratory compaction machine can be set for either a level of compactive effort (number of gyrations) or a density (sample height). The modified Proctor and vibratory methods do not have this flexibility. For this reason, modified Proctor specimens were made first and then gyratory specimens were made to match the density. No attempt was made to match vibratory specimen densities because of the low densities achieved.

3.1.4.3. Test Program

A suite of mechanical performance tests performed in other sections of this study was used for this task. A graphical depiction of the test program is shown in Figure 3-4.

3.1.4.3.1. LBR

LBR tests (Section 3.4.3.1) were conducted because this is the FDOT standard for base and subbase material. Specimens were tested in their respective molds. Specimens were not soaked because the gyratory and vibratory molds are not designed for this purpose.

3.1.4.3.2. Unconfined Compression

Unconfined compression tests (Section 3.4.3.5) were conducted on ejected modified Proctor and gyratory specimens to eliminate mold geometry effects.

3.1.4.3.3. IDT

IDT's (Section 3.4.3.3) were conducted on ejected modified Proctor and gyratory specimens to eliminate mold geometry effects.

3.1.4.3.4. Unconfined Creep

Unconfined creep tests (Section 3.4.3.2.2) were performed to investigate the creep of ejected modified Proctor and gyratory specimens. Due to the geometry of the vibratory mold, it was not possible to eject or test vibratory specimens.

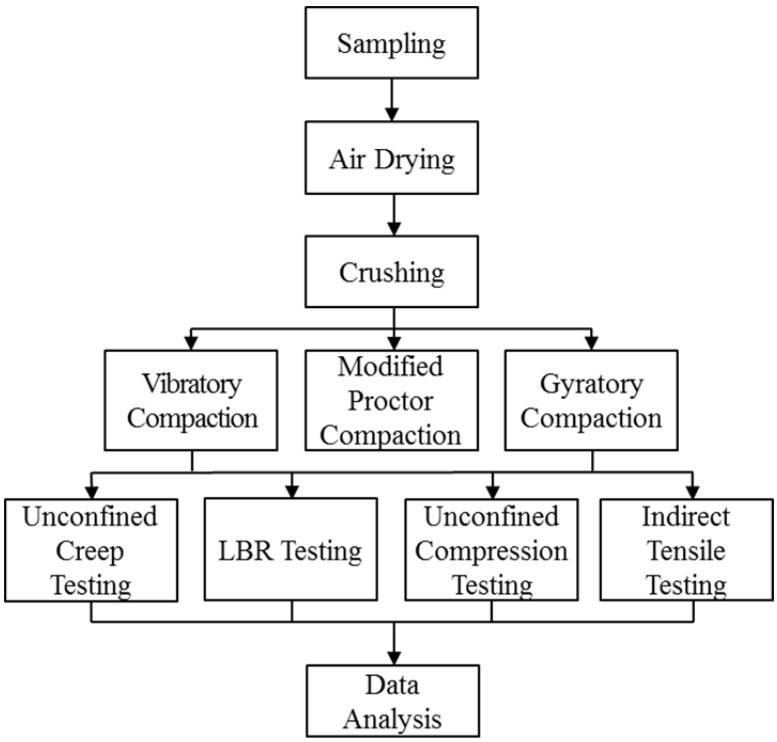

Figure 3-4: Task 6a: Compaction Improvement Test Program Flowchart

3.1.5. Chemical Stabilizing Agents

3.1.5.1. Selection of RAP and Aggregate

Earlier studies at FIT had some success blending RAP and A-3 sand (Cosentino et al., 2003, 2008). RAP/aggregate blends with chemical stabilizing agents were tested to evaluate whether any combination of blend proportions and chemical stabilizers had the potential to achieve a soaked LBR of 100 for base course or 40 for subbase. The FDOT base and subbase

specifications use the FM 5-515 Limerock Bearing Ratio test as a basis for material selection. Chemical stabilizing agent blends were all tested with a single source of RAP (APAC Melbourne Milled RAP) and virgin aggregate (limerock base) in order to isolate the effect of the stabilizing agent.

3.1.5.2. Selection of Stabilizing Agents

Based on previous research, initial testing of chemically stabilized blends was performed using 100% RAP and 80% RAP /20% A-3 sand blends. The specimens were chemically stabilized with 2% CSS-1H asphalt emulsion. The objective of these initial trials was to obtain baseline data and to evaluate curing and testing techniques for chemically stabilized specimens. Initial testing only achieved unsoaked LBR results of around 50. Since the specification for base course requires an LBR of 100. Limerock base material was used as a blending material for the remainder of the research.

Some literature references assert that anionic asphalt emulsion more readily bonds with limestone because of the chemical nature of the rock (Mamlouk and Zaniewski, 2011). Both an anionic slow-setting (SS-1H) and a cationic slow-setting (CSS-1H) emulsion were chosen to investigate whether the chemistry of the emulsion had an effect. Emulsion samples were obtained from two different sources (i.e., Mariani Asphalt, and Road Science LLC).

The literature review produced several studies which used Portland cement and/or lime as a chemical stabilizing agent for RAP/aggregate blends (primarily for Full Depth Reclamation). In all cases Portland cement performed better than lime so a full suite of tests was done using Portland cement stabilization.

Lime stabilization is common for soils, particularly clayey soils. A limited suite of tests with lime stabilization of soaked and unsoaked modified Marshall and soaked and unsoaked unconfined compression tests were conducted. Specimens were prepared with 50% RAP/50% limerock blends with 1%, 2%, and 3% lime for comparison with the same blend stabilized with Portland cement. The results of this testing are shown in Chapter 4.

3.1.5.3. Selection of Test Series

The overall objective of this study was to improve the properties of RAP so that it can be used as a component of a highway base course. As previously discussed, the two principal deficiencies of RAP are its relatively low LBR strength and its tendency to creep under constant stress. Figure 3-5 shows a graphical depiction of the test program.

The chemical stabilization portion of this study evaluated LBR, unconfined compression, and indirect tensile strength of RAP and RAP/limerock blends stabilized with the chemical stabilizing agents discussed in the previous section.

Creep testing is not commonly conducted on base course materials. This study primarily used one dimensional creep testing as described in section 3.4.3.2.1 to compare total deformation and creep strain rate of RAP and RAP/limerock blends. Unconfined creep testing as described in section 3.4.3.2.2 was performed on a subset of the same blends primarily to compare modified Proctor and gyratory specimens.

The Marshall method of HMA design has been supplanted by the Superpave gyratory method, however the Asphalt Institute recommends using a modified Marshall method for mix design of emulsion stabilized base materials. Two Florida laboratories contacted during the literature review have used this modified Marshall method to design Full Depth Reclamation mixes for county or municipal customers. FDR involves chemical stabilization of crushed/blended RAP and underlying base material so it is very similar to the stabilized RAP/aggregate blending process used in this study. The Marshall method produces two results, a Marshall stability number (compressive strength), and a Marshall flow number (deformation at peak strength). Of particular interest was whether the Marshall stability correlated to LBR and others strength tests and whether the Marshall flow correlated to creep strain rate or total deformation.

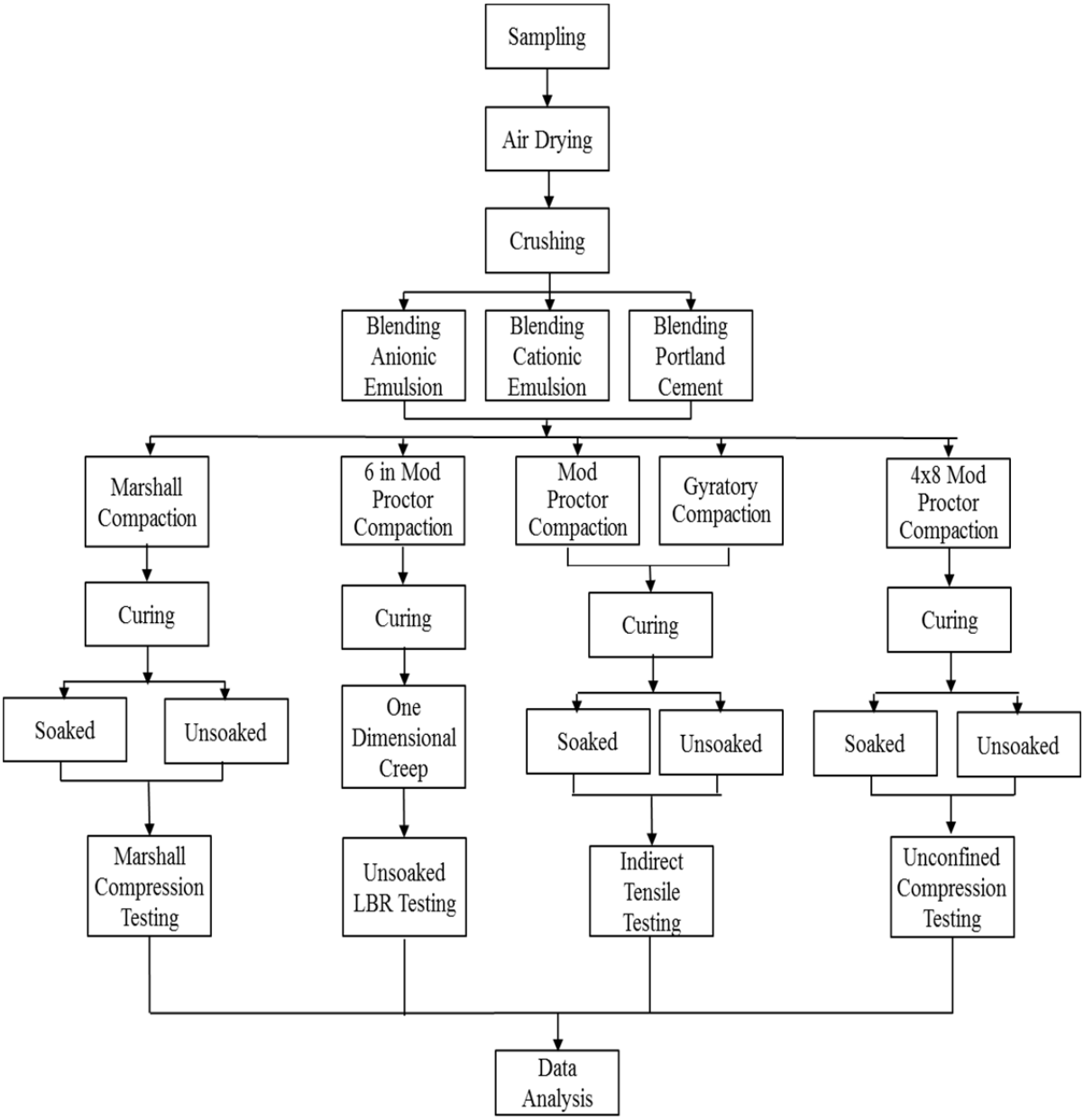

Figure 3-5: Task 6b: Chemical Stabilizing Agents Test Program Flowchart

3.2. Sample Selection

3.2.1. RAP Samples

3.2.1.1. Milled RAP

Two sources of unprocessed milled RAP were used in this study. Based on previous research on RAP variability (Sandin, 2008) both sources are typical of Florida milled RAP.

Approximately 3,000 pounds of milled RAP was sampled from the primary source, the APAC-Southeast asphalt plant in Melbourne Florida. This RAP contained primarily limestone aggregate with trace amounts of granite aggregate. This source was selected because it was close to the researchers so that they could obtain additional material as needed without causing delay on scheduling trips to obtain material.

Approximately 1,000 pounds of milled RAP was sampled from the secondary source, the Whitehurst and Sons asphalt plant in Gainesville, Florida. This RAP contained limestone aggregate with granite. This source was selected because both RAP and A-3 sand were available at this site.

Unprocessed milled RAP that was predominantly composed of granite was not readily available at the APAC-Southeast asphalt Plant #1 in Jacksonville Florida because the milled stockpile included plant waste.

3.2.1.2. Crushed RAP

Two sources of crushed RAP were used in this study. One source was typical of limestone based RAP. The other source was chosen because it was primarily granite based RAP.

Approximately 1,500 pounds of crushed RAP was sampled from the primary source, the APAC-Southeast asphalt plant in Melbourne Florida. This source was selected because it was close to the researchers so that they could obtain additional material as needed without causing delay on scheduling trips to obtain material. Based on previous research on RAP variability this source is typical of Florida crushed RAP (Sandin, 2008). This material was used to compare milled and crushed RAP properties and performance.

Approximately 1,000 pounds of crushed RAP was sampled from the secondary source, the APAC-Southeast asphalt Plant #1 in Jacksonville Florida. This source was selected because the aggregate was predominantly granite rather than limestone which is more common in most of Florida (Sandin, 2008). Granite aggregates are common in Florida asphalt because of granites strength and lower asphalt absorption. This material allowed testing to determine whether aggregate type had an effect on RAP performance.

Crushed RAP from the Whitehurst and Sons plant in Gainesville, Florida was not used because their crushed RAP was fractionated into separate plus #4 and minus #4 stockpiles as part of the crushing operation. This made it impossible to sample crushed RAP with its original gradation.

3.2.2. Select Base Course Materials

Three FDOT approved sources of select base course materials were used in this project to compare the properties of RAP, conventional base course aggregate materials and RAP/aggregate blends.

3.2.2.1. Limerock Base

Approximately 4,000 pounds of limerock base (FDOT Standard Specification for Road and Bridge Construction 2010 Section 911) for this project was acquired from the CEMEX City Point plant in Cocoa, FL. This facility was selected because it is an FDOT approved source (Mine ID: 87090, Material ID: B01).

3.2.2.2. Cemented Coquina

Approximately 1,000 pounds of cemented coquina (FDOT Standard Specification for Road and Bridge Construction, 2010 Section 915) for this project was sourced from Stewart Mining Industries, Fort Pierce, FL. This facility was selected because it is an FDOT approved source (Mine ID: 94488, Material ID: B03).

3.2.2.3. Reclaimed Portland Cement Concrete

For this project, approximately 750 pounds (340.2 kg) of reclaimed concrete aggregate (RCA) (FDOT Standard Specification for Road and Bridge Construction, 2010 Section 901-5)

was sourced from Woodruff and Sons, Inc., Bradenton, FL. This facility was selected because it is an FDOT approved source (Mine ID: 13700, Material ID: B12).

3.2.3. Other Study Materials

3.2.3.1. A-3 Sand

Approximately 1,000 pounds of A-3 sand was sampled from the Whitehurst and Sons plant in Gainesville, FL. This source was selected because it was used in previous studies at FIT. This allowed for direct comparison to previous research (Cosentino et al., 2008).

3.2.3.2. Clayey – Sand

Approximately 200 pounds of clayey sand (SC) material was sampled from the stockpile used to maintain Florida Tech baseball infields. This material was used to compare modified Proctor and gyratory compaction of a cohesive soil.

3.3. Sample Preparation

3.3.1. Sampling

All materials were sampled following FM 1-T 002, *Sampling Course and Fine Aggregate* and AASHTO T-2. For consistency, base materials for all mechanical performance tests were processed the same way.

3.3.2. Drying

The sampled materials were transported to the Florida Tech Transportation Lab where they were air dried on canvas sheets at ambient temperature (approximately 75^0F (23.8^0C)) and then stored in buckets.

3.3.3. Sample Reduction

Material was initially reduced by the quartering method of FM-1 T 248, *Reducing Field Samples of Aggregate to Testing Size*. A Gilson Versa-Splitter model #SP-2.5 was used to evenly split the material for individual test specimens.

3.3.4. Oversize Material Crushing

Crushed RAP, A-3 sand, and clayey sand samples did not contain any particles larger than ¾-inch so no additional processing was required. The limerock, cemented coquina, and crushed concrete used in this study did contain aggregate particles larger than ¾-inch. Although RAP does not normally contain individual aggregate particles larger than ¾-inch, milled RAP samples did include agglomerations of aggregate and asphalt binder larger than this size.

The procedure for base course sample preparation in FM 5-515, *Limerock Bearing Ratio*, was followed to crush material over ¾ inch (19 mm) prior to compaction. Oversized material was processed with a Wiley model 2 crushing machine to reduce all particles to pass the ¾-inch sieve. The crushed material was recombined with the rest of the sample. This method differs from the ASTM Modified Proctor procedure in which material over ¾ inch diameter is discarded and replaced. For consistency, the FM 5-515 method was followed for these compaction tests.

3.3.5. Gradation Modification

3.3.5.1. Gradation Analysis

Task 3 of this study involved modifying RAP gradation. Samples were fractionated at the #4, #8 and #10 sieves, or were modified to produce a theoretical optimum density blend. A ¾-inch (19 mm) top size was chosen for the optimum blend because that is the maximum size allowed in the LBR modified Proctor test. For this part of the study, all specimens were comprised of 100% RAP to isolate the effect of gradation on RAP strength and creep.

Since this study was considering RAP as a potential base course material, gradation analysis was based on the sieve sizes in the FDOT graded aggregate base specification (FDOT, 2010 204-2). The resulting samples were sent to the FDOT state materials lab for asphalt content testing. Table 3-1 shows the gradations tested for asphalt content.

Table 3-1: Gradations used for Asphalt Content Testing of RAP Fractions

d > 1-1/2-inch (38.1 mm)
1-1/2-inch (38.1 mm) ≤ d > ¾-inch (19.0 mm)

¾-inch (19.0 mm) ≤ d > #4 (4.75 mm)
#4 (4.75 mm) ≤ d > #10 (2.00 mm)
#10 (2.0 mm) ≤ d > #50 (0.300 mm)
#50 (0.300 mm) ≤ d > #200 (0.075 mm)
#200 (0.075 mm) ≤ d

Based on the results of the of asphalt contents, the #4, #8 and #40 sieves were chosen to determine the effects of gradation on creep. Table 3-2 shows the selected modifications to RAP gradation that were chosen. Tests were conducted on both milled and crushed RAP samples.

Table 3-2: Selected RAP Gradation Modifications

Unmodified	No Modification
+#4	d > #4 (4.75 mm)
-#4	d ≤ #4 (4.75 mm)
+#8	d > #8 (2.38 mm)
-#8	d ≤ #8 (2.38 mm)
+#40	d > #40 (0.425 mm)
-#40	d ≤ #40 (0.425 mm)
Talbot Gradation	Gradation to Match Talbot D_{max}

3.3.5.2. Theoretical Maximum Density Gradation

Fractions of RAP were assembled to achieve a maximum density following the FHWA maximum density gradation formula (Equation 2-1). Depending on the source, this equation is referred to as the Talbot, FHWA, or Fuller-Thompson equation.

D_{max} was ¾ inch since this is the maximum size aggregate used in LBR testing (FM 5-515). The percentages of each fraction were calculated using the FHWA maximum density gradation formula (Table 3-3). Knowing the percentages of each fraction in the original RAP,

specimens identified as Talbot or FHWA blends of RAP were obtained by increasing or reducing the quantity of material at each sieve size to match the theoretical optimum gradation.

Table 3-3: Grain Size Distribution for Maximum Density Using the FHWA Maximum Density Gradation Formula with m=0.45 (FHWA)

Sieve Size	Particle Size (mm)	% Passing
D_{max}=3/4 inch	19.0	P = (19.0/19.0)0.45 = 100%
3/8 inch	9.5	P = (9.5/19.0)0.45 = 73.2%
#4	4.75	P = (4.75/19.0)0.45 = 53.6%
#10	2.0	P = (2/19.0)0.45 = 36.3%
#50	0.3	P = (0.3/19.0)0.45 = 15.5%
#100	0.149	P = (0.149/19.0)0.45 = 11.3%

3.3.6. Blending RAP with High Quality Materials

Several parts of this study evaluated the effect of blending RAP and high quality conventional aggregates. Oversized RAP and the aggregate were separately reduced to < ¾ inch (19 mm) size prior to blending. Blends were then produced based on percent by weight of RAP.

3.3.6.1. RAP/A-3 Sand blends

Previous research (Dikova, 2006) indicated that blends of 80% RAP /20% A-3 Sand had higher LBR strength and significantly less creep than 100% RAP specimens. Initial tests in this study investigated 80% RAP/20% A-3 sand blends and blends with chemical stabilizing agents. The objective of these initial trials was to obtain baseline data and to evaluate curing and testing techniques for chemically stabilized specimens. Initial testing indicated that achieving a soaked LBR of 100 was unlikely using RAP/A-3 sand blends. Since the objective for base course is a soaked LBR of 100, limerock base material was selected for all other blends.

3.3.6.2. RAP/Limerock, Cemented Coquina, or Crushed Concrete Blends

Other than the A-3 sand blends, all blends in this study were prepared at 0%, 25%, 50%, 75%, and 100% RAP by weight. 0% RAP samples were controls of pure aggregate; 100% RAP samples were controls of pure RAP.

3.3.7. Chemically Stabilized Sample Conditioning

As explained earlier, all chemically stabilized blends were prepared using Melbourne Milled RAP and limerock to isolate the effect of the stabilizing agent.

3.3.7.1. Blends with Asphalt Emulsion

All specimens were prepared in 6-inch Proctor molds and initially oven cured at 60°C for 24 hours, followed by 24 hours of room temperature air curing. At higher emulsion contents the specimens still contained significant moisture after 24 hours. To ensure that the emulsified asphalt broke (water and asphalt fully separated), samples were weighed after 24 hours and placed back in the oven until the sample moisture content stabilized. Based on this experience, future asphalt emulsion specimens were uniformly cured for 48 hours in the oven.

Blended RAP/limerock specimens with 25%, 50%, and 75% RAP were chemically stabilized with cationic slow set emulsion (CSS-1H) at concentrations of 1%, 2%, and 3%. The same blends were chemically stabilized with anionic slow set emulsion (SS-1H) at concentrations of 1%, 2%, and 3% by weight. The residual asphalt content of both emulsions averaged 62.5% according to the manufacturer. 100% limerock and 100% RAP specimens were prepared with the same emulsion concentrations. The samples were oven cured in the mold for 48 hours at 60°C, then cured at ambient temperature for an additional 24 hours prior to creep testing. Specimens were tested for LBR strength following the 7-day creep test.

For selected trials, the emulsion stabilized specimens were split into two groups with one group tested unsoaked and the other group tested soaked by immersion in water to evaluate retained strength. Both the unsoaked and soaked samples were tested after the 48 hour soaking period so that they would be the same age at test time.

3.3.7.2. Blends with Portland Type I Cement

Blends of RAP/limerock were prepared with 0%, 25%, 50%, 75%, and 100% milled Melbourne RAP. Each blend was tested with 1%, 2% and 3% Portland type I cement by weight. Unlike the emulsion stabilized specimens, cement stabilized specimens were not oven cured since drying the specimens would have inhibited cement hydration. The samples were cured in the mold for 7 days prior to placing them in the creep test devices. The samples were wrapped in plastic to retain moisture during curing but no water was added. LBR tests were performed after the 7 day creep tests, so the results represent 14 day strength.

For selected trials the cement stabilized specimens were split into two groups with one group tested unsoaked and the other group tested soaked for LBR strength to evaluate retained strength. Both the unsoaked and soaked samples were tested after the 48 hour soaking period so that they would be the same age at test time.

3.3.7.3. Blends with Lime

Soaked and unsoaked modified Marshall and unconfined compression tests were conducted on 50% RAP/50% limerock blends with 1%, 2%, and 3% lime for comparison with the same blends stabilized with Portland cement and asphalt emulsions.

3.4. Materials Properties Testing

3.4.1. Index Tests

3.4.1.1. Grain Size Analysis

Grain size analysis was performed by dry sieving following FM 1-T 027, *Sieve Analysis of Fine and Coarse Aggregate*. As discussed in Section 3.3.5, analysis was performed with eight inch diameter U.S. standard sieves: 1.5-inch (38.1 mm), 1.0-inch (25.4 mm), ¾-inch (19.0 mm), 3/8-inch (9.51 mm), #4 (4.75 mm), #10 (2.00 mm), #50 (0.300 mm), and #200 (0.075 mm).These sieves coincide with the FDOT specification for graded aggregate base. A motorized sieve shaker was used (Figure 3-6). Individual batches weighed approximately 3.0 lbs (1.36 kg) each to limit the quantity of material on a given sieve. Three samples were tested to find an average gradation for each source material. The results of these tests were used to classify the

materials by to the USCS and the AASHTO system. Evaluation included the overall material gradation and calculated properties such as fineness modulus and coefficients of curvature, C_c and uniformity, C_u.

Figure 3-6: Sieve Analysis Shaker with Sieves

3.4.1.2. Asphalt Content

Asphalt content tests were carried out on unprocessed and fractionated milled and crushed RAP to determine their asphalt content because asphalt content has been correlated to creep in RAP (Cosentino et al., 2008).

Samples for testing were sealed in plastic bags and transported to the FDOT Bituminous Laboratory in Gainesville, FL. The asphalt content of RAP samples was determined following FM 5-524, *Reflux Extraction of Bitumen from Bituminous Paving Mixtures* (Figure 3-7). This method was selected rather than the ignition method, FM 5-563 (ASTM D 6307), because the high temperature used in the ignition method may cause breakdown of limestone aggregates resulting in overstating the asphalt content. Asphalt content results, conducted according to FM 5-563 (ASTM D 6307) for the APAC Jacksonville RAP sample, were provided by the APAC Jacksonville Division, Materials Testing Laboratory.

As discussed in Section 3.3.5, a first round of testing was conducted on crushed and milled APAC Melbourne RAP fractions retained by the following sieves: 1.5-inch, 1-inch, ¾-inch, 3/8-inch, #4, #10 #50, and #200. 100% crushed and milled APAC Melbourne RAP was also tested to serve as control material. A second round of tests was performed on fractions of + #40 and - #40, +#4 and -#4, and +#8 and -#8 crushed and milled APAC Melbourne RAP and on unfractionated RAP from all sources.

Figure 3-7: Rotavapor Apparatus for Reflux Extraction Test (FM 5-524)

3.4.1.3. Specific Gravity

The bulk specific gravity of RAP and fractionated RAP samples were determined by performing the *Theoretical Maximum Specific Gravity Test* (FM 1-T 209, Rice test FDOT, 1994). Fractions of +40, -#40, +#4, -#4, +#8, -#8 crushed and milled APAC Melbourne RAP, were tested at the FDOT SMO. All types of unfractionated RAP were also tested. This testing required two specimens of 2.3 lbs (1050 g) at each fraction.

3.4.1.4. Permeability

The permeability of selected samples was determined according to FM 1-T 215, *Permeability of Granular Soils (Constant Head)*. The tests were run using APAC Melbourne milled RAP, Jacksonville crushed RAP and Whitehurst milled RAP. Other blending materials tested were limerock, cemented coquina, and RCA. The RAP was mixed with the virgin

aggregates and the RCA to determine the permeability of these blends. The blend proportions chosen for this test were 50% RAP/50% aggregate or 25% RAP/75% aggregate. The 75% RAP/25% aggregate blends were not tested since these blends did not have the potential to reach a soaked LBR of 100.

3.4.1.5. Moisture Content

The moisture content of all samples was determined according to FM 1-T 265 *Laboratory Determination of Moisture Content of Soils.*

3.4.2. Compaction Methods

3.4.2.1. Modified Proctor

Modified Proctor compaction was used for all specimens except for the gyratory, vibratory, and Marshall specimens. Modified Proctor compaction was performed following FM 5 521 *Moisture Density Relation of Soils Using a 10 lb. (4.5 kg) Rammer and an 18 in (457 mm) Drop* Method. A total compactive effort of 56,000 ft-lb/ft^3 was used for all impact compacted specimens. All specimens were prepared using a modified Proctor compaction machine as shown in Figure 3-8.

Specimens for optimum moisture, LBR, Indirect Tensile, one dimensional creep (in mold), and 6 inch diameter unconfined compression tests were prepared following Method C, which uses a 6 inch diameter mold with a volume of 0.075 ft³.

Unconfined Creep tests specimens to compare Modified Proctor and Gyratory compaction were prepared following Method B which uses a 4 inch diameter mold with a volume of 0.0333 ft³. The 4 inch diameter mold was used to be comparable to the 100 mm (3.94 in) diameter Gyratory specimens.

Unconfined Compression specimens were also compacted using the modified Proctor total compactive effort equal to 56,000 ft-lb/ft^3. The preparation of these specimens is discussed in section 3.4.2.2.

Figure 3-8: Modified Proctor Compaction Machine

3.4.2.2. Unconfined Compression Samples

Unconfined Compression tests (AASHTO T 208, *Standard Test Method for Unconfined Compressive Strength of Cohesive Soil*) were used to compare chemically stabilized RAP/aggregate blends. Modified Proctor Method B was modified for these specimens to account for the additional volume of the mold. The 4-inch diameter x 8.35-inch high molds with a volume of 0.0607 ft^3 were manufactured at FIT to achieve a 2:1 height to diameter ratio to eliminate end effects during testing. Samples were prepared using a manual modified Proctor hammer. Compaction was accomplished in 5 equal layers using 44 blows/layer to achieve the 56,000 ft-lb/ ft^3 compactive effort specified for the modified Proctor. Samples were ejected from the mold using a hydraulic jack (Figure 3-9), cured for 48 hours in a 60°C oven (Figure 3-10), and then cured 24 hours at ambient temperature prior to testing.

For selected trials, half of the specimens were tested dry after curing, the other half were conditioned by immersing in water for 48 hours (Figure 3-11), then removed and drained for 15 minutes prior to testing to determine moisture susceptibility. For trials with soaked specimens,

both the soaked and dry specimens were tested after the 48 hour soaking period so that they were the same age.

Figure 3-9: Extracting a 4 in x 8 in Unconfined Compression Sample from Mold

Figure 3-10: Unconfined Compression and Marshall Samples in Curing Oven

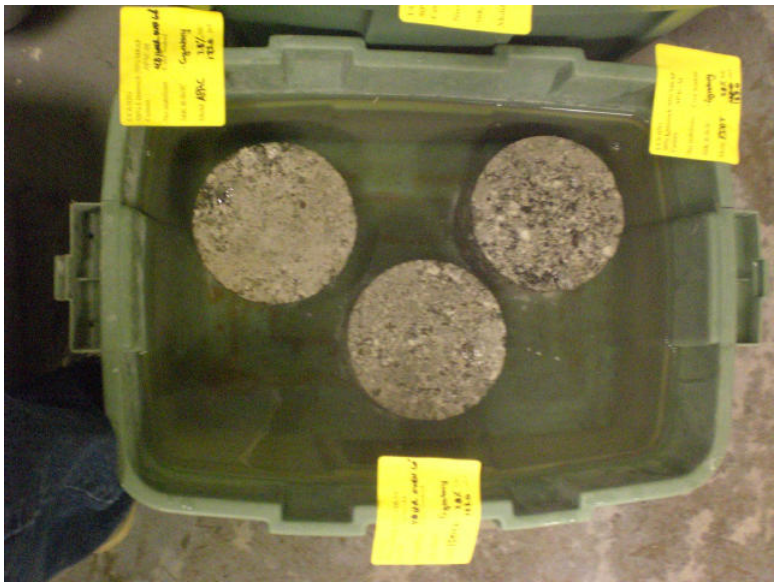

Figure 3-11: Unconfined Compression Samples Conditioned by 48-hour Soaking

3.4.2.3. Gyratory Compaction

There is currently no specification for compacting soil in the gyratory compactor. The procedure for compacting HMA in ASTM D6925 was used with the exception that the specimen and molds were not heated. Specimens were prepared at approximately 75^0F (23.8^0C), ambient temperature in the laboratory. Samples were mixed with water to achieve target moisture contents of 3%, 6%, and 9%, and then compacted for 75 gyrations. To determine the effect of additional compactive effort, other specimens were mixed to achieve a target moisture content of 3% and compacted for 100 and 150 gyrations. Figure 3-12 shows the Troxler Model 4140 gyratory compaction machine with the front access panels removed. Neither the angle of gyration nor the gyration rate was varied. After compaction was completed the specimens were subjected to the LBR test while still in the gyratory mold or extruded from the mold for the unconfined compression, indirect tensile splitting, or unconfined creep tests.

Figure 3-12: Troxler® Model 4140 Gyratory Compaction Machine

3.4.2.4. Modified Marshall Compaction

During our discussions with industry, two Florida laboratories were interviewed that had performed mix designs for county or municipal FDR projects. Both labs generally followed the modified Marshall mix design procedure in the Asphalt Institute Manual Series No. 14 (1997) and No. 19 (2008). Modified Marshall tests were used in this study for comparison with other compaction methods. During the literature search, an alternative mix design was identified using the Superpave gyratory compaction machine and asphalt binder characteristics outlined in the South Carolina Department of Transportation's FDR mix design method (SC-T-99, 2008). This mix design procedure was not used for this study; however several strength and creep comparisons were made between gyratory and other specimens.

3.4.2.4.1. Modifications to Standard Marshall Method

Modified Marshall compaction in this study was conducted at approximately 23.8^{0}C (75^{0}F) rather than at 60° C as specified in Marshall hot mix design (AASHTO T 245). Specimens were compacted with 37 blows per side to achieve the same 56,000 ft-lb/ft^3

compactive effort used in the modified Proctor and all other impact compaction methods in this study.

3.4.2.4.2. Anionic Emulsion (SS-1H) Stabilized Blends

Modified Marshall testing was conducted using the same RAP/limerock blends used in other tests: 0%, 25%, 50%, 75%, and 100% RAP with 0%, 1%, 2%, and 3% emulsion.

3.4.2.4.3. Cationic Emulsion (CSS-1H) Stabilized Blends

Modified Marshall testing was conducted using the same RAP/limerock blends used in the SS-1H tests.

3.4.2.4.4. Portland Cement Stabilized Blends

Modified Marshall testing was conducted using the same RAP/limerock blends used in the SS-1H tests.

3.4.2.4.5. Hydrated Lime Stabilization Blends

Hydrated lime tests were only conducted with 50% RAP/50% limerock blends. Based on relatively poor performance, no additional lime stabilized blends were tested.

3.4.2.5. Vibratory Compaction (Relative Density)

For this study, the specimens were compacted using the Relative Density procedure in ASTM D 4253 (there is no Florida Method for this test), then were subjected to LBR testing. A vibration meter was used to determine the peak to peak double amplitude of the vibration apparatus. Vibration time was extended from the standard 8 minutes to 12 and 16 minute periods for additional compactive effort. Samples were also tested at different moisture contents to determine the effect of moisture content on vibratory compaction of RAP. The vibratory table, mold and surcharge weight are shown in Figure 3-13.

A digital vibration meter was used to accurately measure the vibration of the apparatus. The meter uses a small accelerometer to measure peak acceleration during vibration. Since acceleration is the second derivative of displacement, the acceleration needed to achieve the specified 0.013 inch amplitude was calculated. It was assumed that since the alternating current

electricity follows a sine wave, the vibration of the electromagnet was also a sine wave. The basic equation of a sine wave is $y(t) = A \times \sin(\omega t + \varphi)$ where A is the amplitude in inches, ω is the angular frequency in radians per second, and φ is the phase offset. The angular frequency $\omega = 2 \pi f$, where f is the frequency in Hertz.

By substituting in the specified amplitude and frequency values, the displacement function becomes

$$y(t) = 0.013 \times \sin(2\pi\ 60\ t + 0)\ \text{in} \qquad \text{Equation 3-1}$$

The velocity function can be obtained by taking the first derivative of the displacement function. The result is:

$$v(t) = 0.013 \times 120\ \pi \times \cos(120\ \pi\ t)\ \text{in/s} \qquad \text{Equation 3-2}$$

The second derivative of the displacement function will result in the acceleration function:

$$a(t) = -\ 0.013 \times 120^2\ \pi^2 \times \sin(120\ \pi\ t)\ \ \text{in/s}^2 \qquad \text{Equation 3-3}$$

Converting to S.I. units, the acceleration function is:

$$a(t) = 46.93 \times \sin(120\ \pi\ t)\ \text{m/s}^2 \qquad \text{Equation 3-4}$$

Since the vibration meter samples once per second, it only reads the maximum value, when $\sin (2\ \pi\ 60\ t) = 0$, therefore the maximum acceleration will be 1.848 in/s^2 (46.93 m/s^2). When the meter reads 1.848 in/s^2 (46.93 m/s^2) the displacement will be 0.013 inches or 0.3302 mm.

To calibrate the relative density apparatus, a sample of material was placed into the mold along with the guide sleeve and surcharge weight. The rheostat was adjusted until the vibration

meter readout was 46.93 m/s². A computer with a data acquisition system recorded the vibration meter's readout during the length of the test and averaged the results. The amplitude of the displacement function was varied with the rheostat until the acceleration matched the average acceleration from the meter.

Figure 3-13: Relative Density Apparatus with 0.1 ft^3 Mold (left) and 56.5 lb Surcharge Weight (right)

3.4.3. Mechanical Performance Tests

3.4.3.1. Limerock Bearing Ratio

The LBR test, FM 5-515, is a variation on the California Bearing Ratio test, ASTM D1883 and AASHTO T-193. In FM 5-515, 6-inch diameter specimens are compacted using the modified Proctor method. The actual test measures force required for penetration of a 3-in^2 piston driven at a constant strain rate using the test machine shown in Figure 3-14. The LBR value is determined by the stress at a deflection of 0.1-inches. LBR test results are given as a ratio of measured stress to a reference standard of 800 psi. FM 5-515 requires specimens to be conditioned by soaking in water for 48 hours prior to testing. The majority, of these tests in this

study, was performed following creep testing or was performed on samples prepared by gyratory or vibratory compaction without creep.

A modified LBR test was performed on gyratory and vibratory compaction samples to compare compaction methods. Gyratory and vibratory specimens were compacted and tested in their respective molds. Due to the design of the molds, it was not possible to invert the specimens for penetration as specified in FM 5-515. These molds also were not designed to be immersed in water, so the penetration test was performed without soaking. To ensure comparability of results, LBR tests on modified Proctor specimens were also performed without soaking.

Creep specimens were prepared following FM 5-515 and inverted prior to the 7-day creep test. The LBR test was performed on these specimens following the creep tests. As discussed in the previous paragraph, these specimens were not soaked.

Unsoaked results are not directly comparable to soaked results; these results should only be used for comparison with other similarly prepared unsoaked specimens. Unless specifically noted as "soaked," tests in this study were conducted without soaking or "unsoaked." During the final phase of this research, soaked LBR testing was conducted on RAP/aggregate blends with and without chemical stabilization which showed potential for reaching a soaked LBR of 100. These test results are designated "soaked LBR" to differentiate them from the unsoaked results.

Figure 3-14: LBR Test in Progress

3.4.3.2. Creep

Creep is the tendency of a solid material to slowly move or deform under constant stress. FIT researchers have developed a one dimensional creep test method that monitors the three basic factors involved with creep: stress, deformation, and time. This creep test was first experimented by Cleary (2005). Dikova (2006) further developed this method during the investigation of RAP as a backfill material for retaining walls. The six test devices used by Dikova (2006) were capable of applying static pressure up to 18 psi to model earth pressures at the base of a 30 foot high retaining wall. For this current study, six additional testing units were built with higher capacity pneumatic pistons that raised the applied pressures up to 100 psi (689.5 kPa) to study the effect of changes in stress levels on creep. 100 psi (698.5 kPa) was chosen as a conservative worst-case pressure at the top of a highway base course. The six higher pressure devices and the data acquisition computer are shown in Figure 3-15.

The loading apparatus for this test consists of two aluminum beams joined by two threaded rods. A pneumatic piston is mounted to the top beam that applies a load to the top of

the sample. The force of the piston is transferred through a 1.0-inch diameter ball bearing to a 0.5-inch thick aluminum plate resting on the surface of the sample. This ball bearing allows for the transfer of the load without the effects of any irregularities of the surface of the sample.

The test monitors the deflection of the sample with respect to time under a constant applied pressure. Deflections are recorded by a custom Labview® program every second for the first two minutes of testing. The sampling interval then doubles for each sample (2 sec, 4 sec, 8 sec, etc.) until the interval reaches 4 hours. Samples are then recorded at 4 hour intervals until the completion of the test. This sampling pattern is similar to that of a soil consolidation test. Creep tests for this project were conducted for a minimum of 7 days. Sample preparation varied depending on the type of materials and stabilizing agents being evaluated.

Figure 3-15: Six Creep Test Devices and Data Acquisition Computer

3.4.3.2.1. One Dimensional Creep

A minimum of two samples of each material or blend were compacted according to the specification for LBR Testing (FM 5-515). After compaction chemically stabilized specimens were cured. Non-stabilized specimens were tested immediately. Specimens in this research were tested for seven days at a constant stress. This study selected loading pressures of 12 psi (82.7 kPa), 25 psi (172.4 kPa), 50 psi (344.7 kPa), and 100 psi (689.5 kPa) to better understand the creep behavior under different loading conditions that could be encountered in the pavement system.

3.4.3.2.2. Unconfined Creep

Unconfined creep tests were conducted on gyratory and modified Proctor-compacted specimens to directly compare with the creep response. Ejected specimens were tested to eliminate any effects resulting from the different geometries of the Proctor and gyratory molds. The modified Proctor samples were prepared following FM 5-521 Method B. Modified Proctor specimens were 4 inch (101.6 mm) diameter with a height of 4.584 inches (116.4 mm). The modified Proctor specimens were prepared first. The gyratory mold diameter was 3.94 inches (100 mm). Gyratory specimens were prepared with a height of 4.72 inches (120 mm) to produce the same volume of material as the modified Proctor specimens. The same volume of material was then compacted using the "Gyrate to height" setting on the machine to match the density of the modified Proctor specimens. Tests were conducted on 100% limerock, 100% Melbourne Milled RAP, and 50%/50% blends of the two materials. Unconfined creep samples were conducted at a stress level of 12 psi (82.7 kPa).

3.4.3.3. IDT

The Indirect Tensile Splitting Test, ASTM D3967, was used to compare tensile strength of gyratory and modified Proctor-compacted specimens, and to compare tensile strength of chemically stabilized specimens. After compaction, the samples were extruded from their molds and placed on their sides into a compression testing machine as shown in Figure 3-16. A rigid bar was placed on top of the sample to apply a line load along its length. The tensile stress, σ_t, was calculated from Equation 1 in ASTM D3967.

$$\sigma_t = \frac{2P}{\pi LD} \qquad \text{Equation 3-5}$$

P = load, L = thickness, and D = diameter.

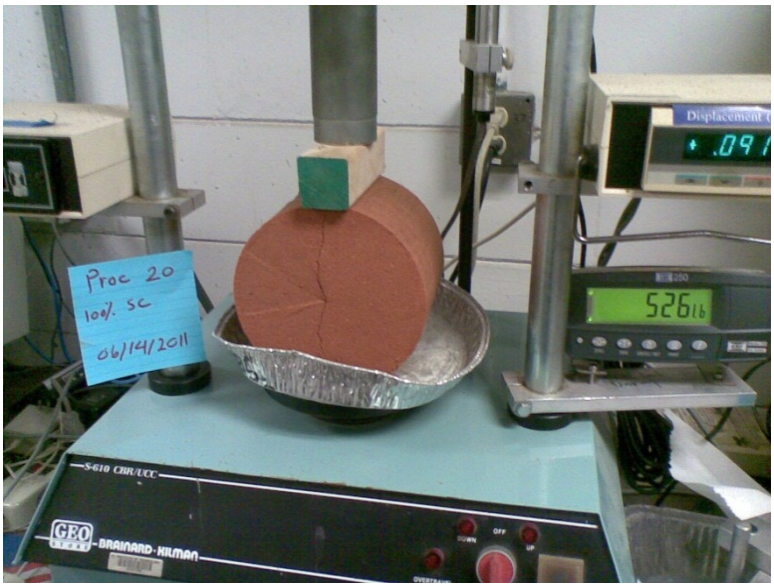

Figure 3-16: Indirect Tensile Splitting Test in Progress

3.4.3.4. Marshall Compression Test

Marshall compressive strength (Marshall Stability) and deformation (Marshall Flow) are recorded during a Marshall compression test (AASHTO T 245). Figure 3-17 shows a Marshall compression test in progress.

The Marshall method was modified to test at ambient temperature in our laboratory to match the conditions for our other types of tests. Modified Marshall testing in this study was conducted at approximately 23.8° C (75° F) rather than at 60° C as specified in Marshall hot mix design. Modified Marshall results are not directly comparable to standard Marshall results. The modified Marshall method in the Asphalt Institute Manual Series No. 14 and No. 19 specifies testing of both dry and saturated (conditioned) samples to establish retained strength when wet. Normal Marshall testing is done at a strain controlled loading rate of 2 in/min. This study used a lower strain rate of 0.05 in/min to be consistent with the loading rate for the LBR and unconfined compression tests.

One set of specimens was prepared to compare Marshall number and Marshall flow from tests on the Florida Tech test machine at 0.05 in/min with the results for specimens tested on a standard Marshall test machine at 2.0 in/min. The comparison tests were run at the Universal Engineering Sciences commercial laboratory in Rockledge, FL.

Figure 3-17: Marshall Compaction Test in Progress

3.4.3.5. Modified Unconfined Compression 6-inch Diameter

Unconfined compression tests were performed to compare the strength of Gyratory and Modified Proctor-compacted samples. After compaction, the samples were extruded from their molds and placed into a compression testing machine as shown in Figure 3-18. Normally unconfined compression samples are proportioned with a 2:1 or greater height to diameter ratio to eliminate end effects from the compression plates. It was not possible to prepare samples with these proportions in the gyratory test machine. ASTM allows cutting or trimming of samples to achieve the 2:1 ratio but the coarse aggregates in RAP specimens cannot be trimmed without significant sample disturbance. The method was modified to test untrimmed 3.94-inch x 4.72-inch gyratory specimens and 6-inch x 4.584-inch modified Proctor specimens. While this is not in exact compliance with the test specifications stated in ASTM D2166, it provided a comparison of the two different compaction methods. The 6-inch unconfined compressive strengths in this report are not comparable to standard unconfined compression unless a correction is applied for the geometry of the specimens.

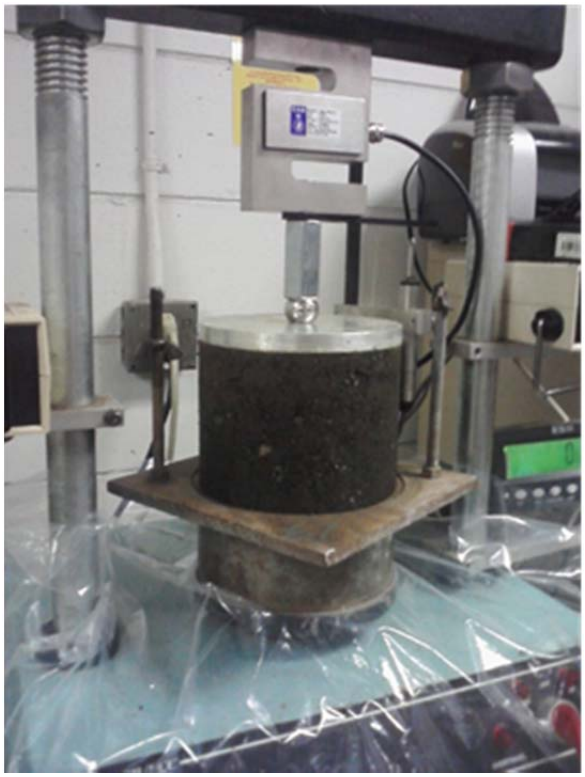

Figure 3-18: 6-inch x 4.584-inch Unconfined Compression Test

3.4.3.6. Unconfined Compression 4-inch Diameter

Unconfined compression tests generally following *Standard Test Method for Unconfined Compressive Strength of Cohesive Soil* (AASHTO T 208, ASTM D2166). After compaction and curing, ejected samples were tested as shown in Figure 3-19. Stiff rubber seating plates were placed on both ends of the specimen to distribute load uniformly over surface irregularities. A rigid aluminum plate was placed on top of the specimen. A 1.0-inch diameter ball bearing was seated in a machined indentation at the center of the plate. This arrangement allowed the top plate to adjust to apply uniform pressure to the top of the specimen. The specimen was loaded at a constant rate of 0.05 in/min, the same rate used for all other compression testing.

Figure 3-19: 4-inch x 8-inch Unconfined Compression Test

4. Findings

RAP, limerock, cemented coquina and crushed concrete samples were obtained from the various sources throughout the 24-month project. The results from the index testing are based on typical samples from the sources. The limerock, cemented coquina and crushed concrete were obtained from FDOT approved sources.

4.1. Index Properties of 100 % RAP

The engineering properties presented are representative of RAP used throughout the study. The basic index properties from sieve analyses, asphalt content and specific gravity tests were used to categorize the engineering properties of RAP.

4.1.1. Classification

Table 4-1 summarizes the index properties of the RAP including soil classifications and asphalt content. The engineering properties of the RAP from all sources were similar. The major variation occurred with the APAC Jacksonville crushed RAP which has more fines.

All four RAP sources were classified as sand under the Unified Soil Classification System (USCS). The Melbourne milled RAP had a coefficient of uniformity, C_u greater than six and a coefficient of curvature, C_c between 1 and 3 classifying it as well graded sand, SW. The other three RAP samples had coefficients of uniformities, C_u, greater than 6 but coefficients of curvature, C_c, less than one classifying them as poorly graded sand, SP. The APAC Melbourne crushed and Whitehurst Gainesville milled RAP C_c coefficients were slightly below 1, while the Jacksonville crushed RAP C_c was less than 0.5. This result is slightly different from the Sandin (2008) variability study which found that the majority of Florida RAP sampled was well graded. Under the AASHTO classification system all of the RAP samples were classified as an A-1-a soil except for the Jacksonville crushed RAP which classified as an A-1-b soil. In the AASHTO classification system, an A-1-a soil is preferred for highway construction while an A-1-b soil is the second preferred soil.

Table 4-1: General Properties of RAP

Property	Sample Source			
	APAC Melbourne Crushed	APAC Melbourne Milled	Whitehurst Gainesville Milled	APAC Jacksonville Crushed
C_c	0.9	1.9	0.8	0.4
C_u	10.7	9.6	11.2	26.2
% Fines	0.6	0.5	0.4	6.8
AASHTO	A-1-a	A-1-a	A-1-a	A-1-b
USCS	SP	SW	SP	SP
AC	4.4%	5.4%	4.2%	4.0%

4.1.2. Sieve Analysis

The grain size distribution curves from the sieve analyses are presented in Figure 4-1. The sieves used to determine the gradations are those specified for use for FDOT Graded Aggregate Base under Section 204 of the Road and Bridge Construction Specifications (FDOT, 2010). The maximum particle size ranged from about ½-inch to 1 ½-inch. APAC Melbourne milled RAP contained higher percentages of large diameter materials than the other sources. APAC Jacksonville crushed RAP contained the highest amount of material passing the #10 and finer sieves. Melbourne and Jacksonville crushed RAP followed a very similar gradation for material larger than the #4 sieve but diverged at smaller sizes indicating that the crushing processes may have been different. APAC Melbourne milled and the Whitehurst Gainesville milled RAP followed similar gradation curves with the exception of the amount of material passing the #10 sieve.

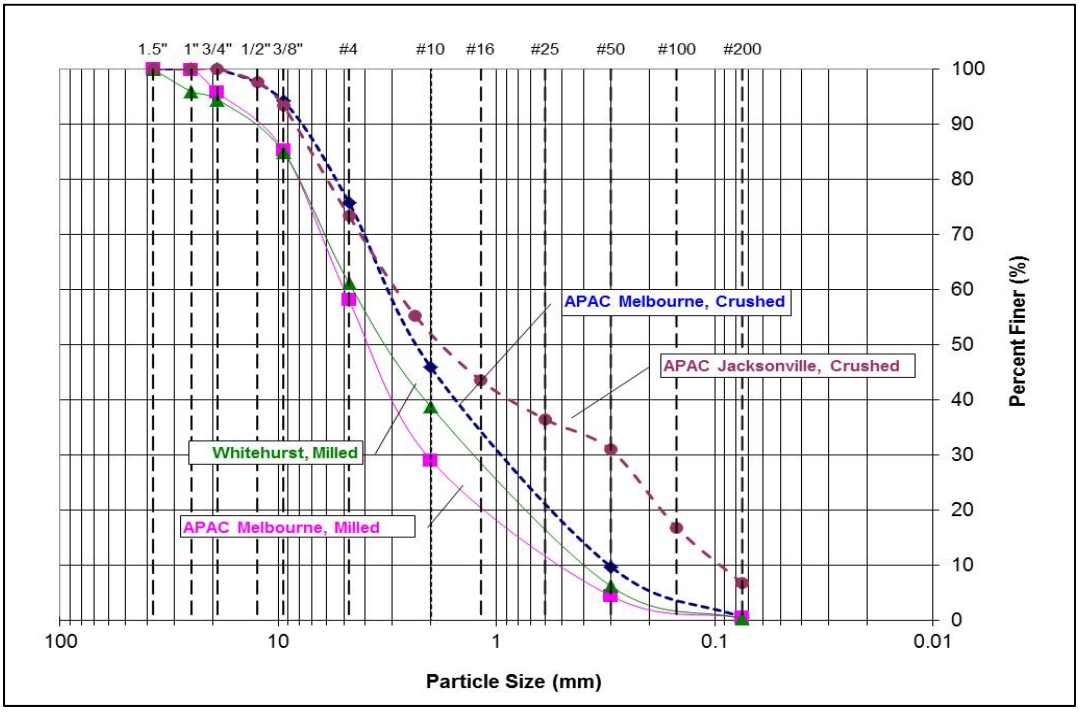

Figure 4-1: Grain Size Distribution of RAP Samples Used for Compaction Improvement

Fuller and Thompson (1907) and Talbot and Richart (1923) developed formulas for theoretical maximum density gradation of aggregate. Based on this work, the Federal Highway Administration (FHWA T 5040.27, 1988) recommends an optimum density gradation based on a 0.45 power curve. This gradation is referred to as the FHWA or Talbot curve in the body of this report. A top aggregate size of ¾-inch was chosen to calculate the optimum gradation because it matched the top size of the processed RAP samples used in this study. The FHWA gradation curve is a straight line when plotted on a 0.45 power scale as shown by the dashed line in Figure 4.2. RAP gradation curves from all four sources are shown on the plot. The large deviations from the dashed line indicate that RAP does not have enough large aggregates or fines to produce the maximum density. It appears that the fines (mineral dust) remain bound to the asphalt during the milling or crushing process so they do not appear as fines in the RAP gradation analysis.

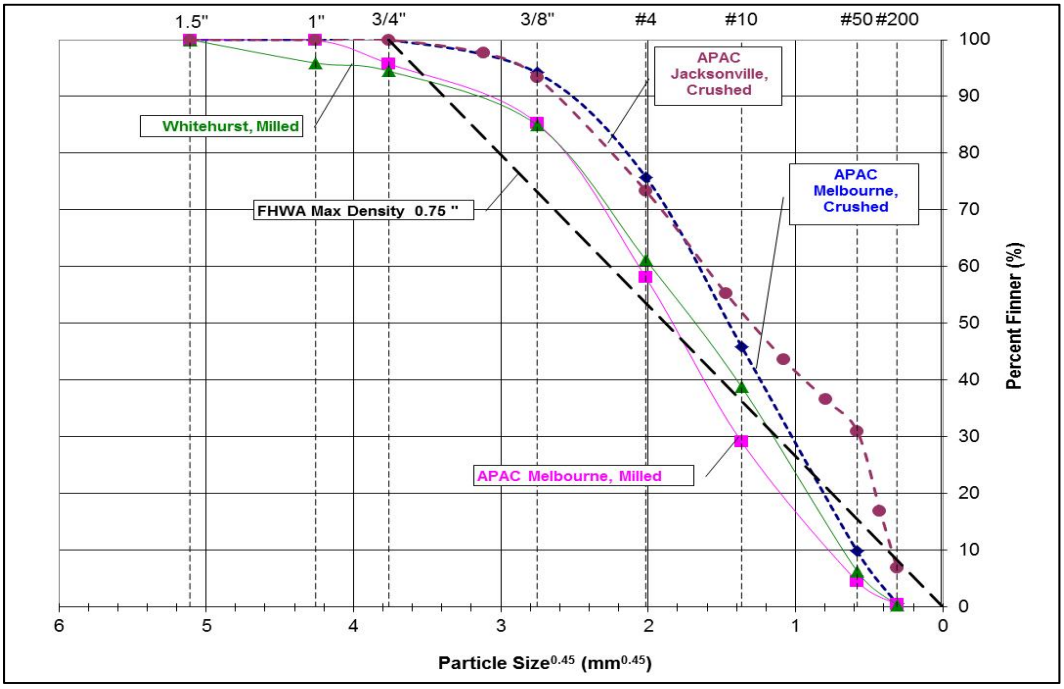

Figure 4-2: RAP Grain Size Distribution Compared to FHWA Maximum Density

4.1.3. Asphalt Content

As shown in Table 4-1 the Melbourne milled RAP asphalt content was 5.4 % while the Melbourne crushed RAP had an asphalt content of 4.4 %.This lower asphalt content in crushed RAP is consistent with the results of Sandin's (2008) statewide variability study of RAP which found statewide mean asphalt contents of 6.6% for milled RAP and 5.8% for crushed RAP.

As part of the gradation modification research completed under Task 4, a separate set of asphalt content tests were carried out on samples of 100% crushed and milled APAC Melbourne RAP plus the portions of RAP retained between the 1.5-inch, ¾-inch, 3/8-inch, No. 4, No. 10, No. 50, and No. 200 sieves. Two samples were tested per sieve.

The results presented in Figure 4-3 and Figure 4-4 show the asphalt content for the material between successive sieves. The largest aggregates, from APAC Melbourne crushed RAP passed the ¾-inch sieve, and were retained by the 3/8-inch sieve. The largest aggregates for APAC Melbourne Milled RAP passed the 1.5-inch sieve and were retained on the 1-inch sieve.

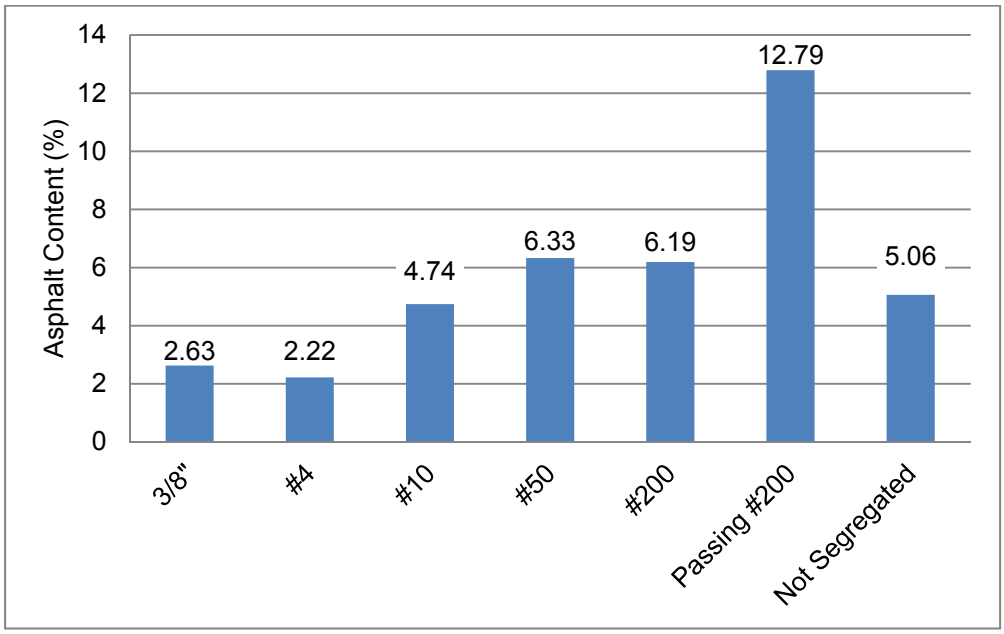

Figure 4-3: Average Asphalt Content of Retained Material for APAC Melbourne Crushed RAP (2 samples per fraction)

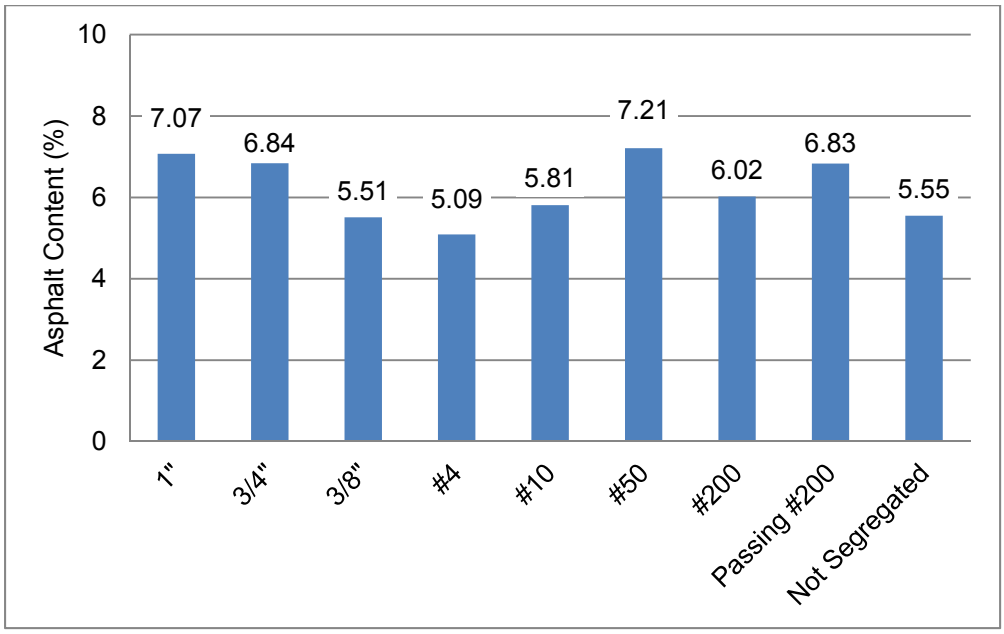

Figure 4-4: Average Asphalt Content of Retained Material for APAC Melbourne Milled RAP (2 samples per fraction)

In this round of testing, the average asphalt content of the APAC milled RAP (5.55%) and crushed RAP (5.06%) were slightly higher than those from the first test round reported in

Table 4-1. The values are still within the range reported by Sandin (2008) and are consistent with the trend that milled RAP had higher asphalt contents than crushed RAP.

Figure 4-3 shows that for APAC crushed RAP, the asphalt content significantly increased for the material passing the # 200 sieve. The fraction passing 3/8-inch sieve has an asphalt content of 2.63%, while the fraction passing the #200 sieve has an asphalt content of 12.79%. This particular asphalt content is misleading because it represents less than 2% of the total material. Figure 4-4 shows that the asphalt content was more evenly distributed in APAC Melbourne milled RAP. The asphalt content for the fractions varied between 5.09% for the fraction passing #4 and 7.21% for fraction passing #50. Fractions from the 1-inch to the 3/8-inch sieve are mostly agglomerates of aged asphalt binder and aggregates that have enough strength to resist crumbling during the sieve shaking process

Figure 4-5 and Figure 4-6 show the distribution of the weighted asphalt content at each fraction size. This value is the product of the asphalt content percentage at a given fraction multiplied by the weight of material at that fraction. It was calculated to produce a better picture of the total asphalt binder at a given fraction. For example, the passing #200 fraction of APAC crushed RAP had a very high asphalt content of over 12%, however there was a very small quantity of this material. The corresponding weighted value shown in Figure 4.6 is below 5% of the total asphalt content by weight. The majority of the asphalt binder is contained in fractions retained by the # 10 and #50 sieves. For both milled and crushed APAC RAP, asphalt content increases up to #50 sieve and then decreases.

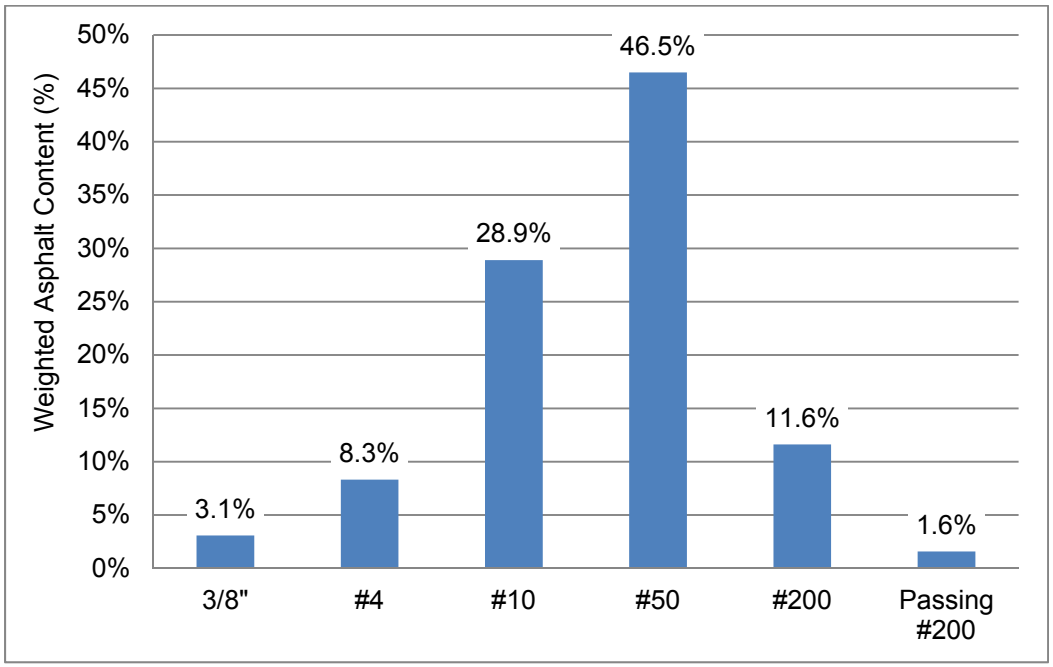

Figure 4-5 Distribution of Weighted Asphalt Content by Grain Sizes for APAC Melbourne Crushed RAP

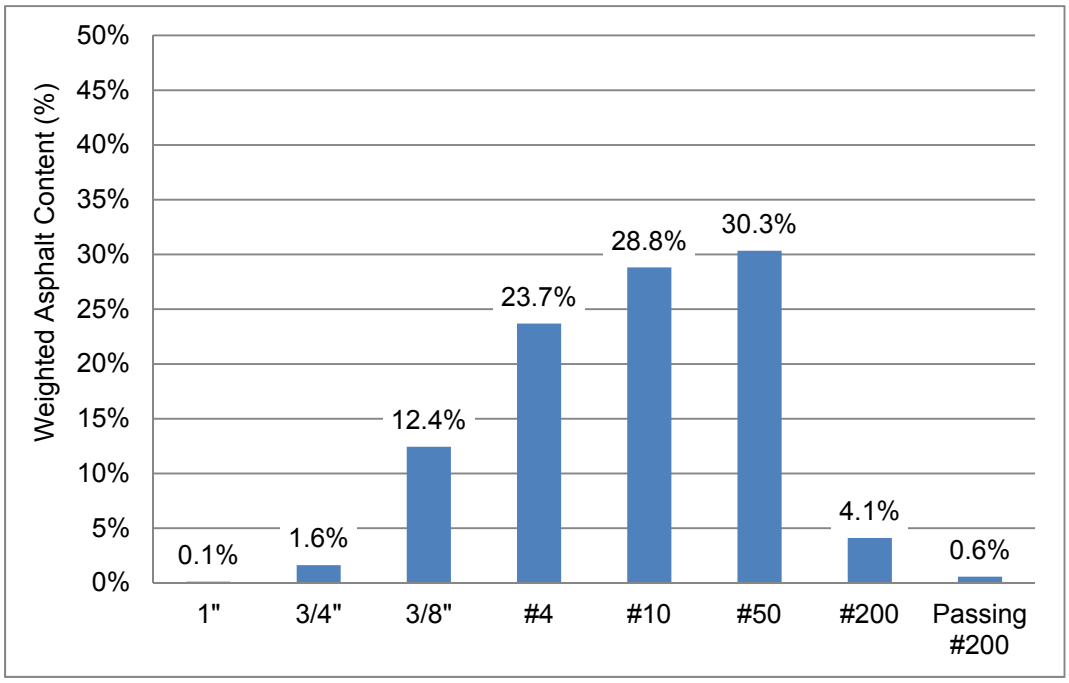

Figure 4-6: Distribution of Weighted Asphalt Content by Grain Sizes for APAC Melbourne Milled RAP

4.1.4. Specific Gravity

Specific gravity results for the four RAP sources used in this study are shown in Table 4-2. Specific gravity of fractionated RAP is shown in Section 4.2.1.3. The higher specific gravities of the Whitehurst RAP (2.576) and Jacksonville RAP (2.604) are similar to those of RAP containing granite aggregate (Das, 2002). According to Lee et al., (1990) granite aggregate absorbs less asphalt binder than limestone aggregates. The lower asphalt contents of the Whitehurst RAP and Jacksonville RAP may be attributed to the lower absorption of asphalt binder of the granite aggregate in these samples which allows producers to add less binder to granite based HMA mixes. Both milled and crushed RAP from APAC Melbourne had specific gravities similar to RAP containing limestone aggregate.

Table 4-2: Summary of Bulk Specific Gravity by FM 1 – T209 Rice Method

RAP Source	Bulk Specific Gravity
APAC Crushed Jacksonville	2.604
Whitehurst Milled	2.576
APAC Milled Melbourne	2.524
APAC Crushed Melbourne	2.508

4.1.5. Permeability of RAP and RAP Aggregate Blends

Table 4-3 shows the permeability for the RAP, aggregate, and RAP/ aggregate blends. APAC Melbourne crushed RAP is not included in the table because it was not used as a blend material in this study. Crushed concrete was only blended with Melbourne milled RAP. The range of these values lies between the 10^{-6} and 10^{-3} cm/s. The permeabilities of the APAC Melbourne and Whitehurst Gainesville milled RAP samples fall near the higher end of this spectrum indicating that they possess good drainage characteristics.

These results indicate that the RAP crushing process decreases permeability. The APAC Jacksonville RAP has much lower permeability with a magnitude on the order of 10^{-5} cm/s. This lower permeability is most likely due to the higher percentage of finer materials than the other RAP used in this study as shown in Figure 4-1. APAC Melbourne crushed RAP also had permeability in the 10^{-5} cm/s range. The limerock, cemented coquina and crushed concrete all

had permeabilities in the 10^{-5} to 10^{-6} cm/s range. The virgin aggregates are one to two orders of magnitude lower in permeability than 50% RAP/50% aggregate blends indicating that they will not drain as well as the blends.

Table 4-3: Permeability of RAP/Aggregate Blends

	Permeability (cm/s)						
% RAP	Milled Melb. RAP/ Limerock	Milled Melb. RAP/ Cemented Coquina	Milled Melb. RAP/ Crushed Concrete	Crushed Jax. RAP/ Limerock	Crushed Jax. RAP/ Cemented Coquina	Milled W.H. RAP/ Limerock	Milled W.H. RAP/ Cemented Coquina
100	3.1×10^{-3}	3.1×10^{-3}	3.1×10^{-3}	1.8×10^{-5}	1.8×10^{-5}	1.3×10^{-4}	1.3×10^{-4}
50	3.2×10^{-4}	1.8×10^{-5}	1.2×10^{-4}	2.1×10^{-5}	5.5×10^{-5}	8.3×10^{-5}	3.6×10^{-5}
25	3.2×10^{-5}	5.9×10^{-6}	1.4×10^{-4}	4.2×10^{-6}	5.4×10^{-4}	1.2×10^{-6}	2.7×10^{-4}
0	1.2×10^{-6}	3.0×10^{-6}	2.9×10^{-5}	1.2×10^{-6}	3.0×10^{-6}	1.2×10^{-6}	3.0×10^{-6}

Figure 4-7 is a plot of the permeability of each RAP/aggregate blend versus the percentage of RAP in the blend. The regression coefficients for each are shown. The lowest regression coefficient corresponds to the blend of APAC Jacksonville crushed RAP/cemented coquina; the second lowest corresponds to the Whitehurst RAP/cemented coquina blends. With the exception of these two sets of data the regression coefficients, developed from a logarithmic regression line, all indicated relatively strong correlations between permeability and percent RAP.

In conclusion, for the blends tested, increasing the amount of RAP increased the permeability. From these tests it appears that blending RAP with Florida's most common base course materials would improve the drainage of the base materials.

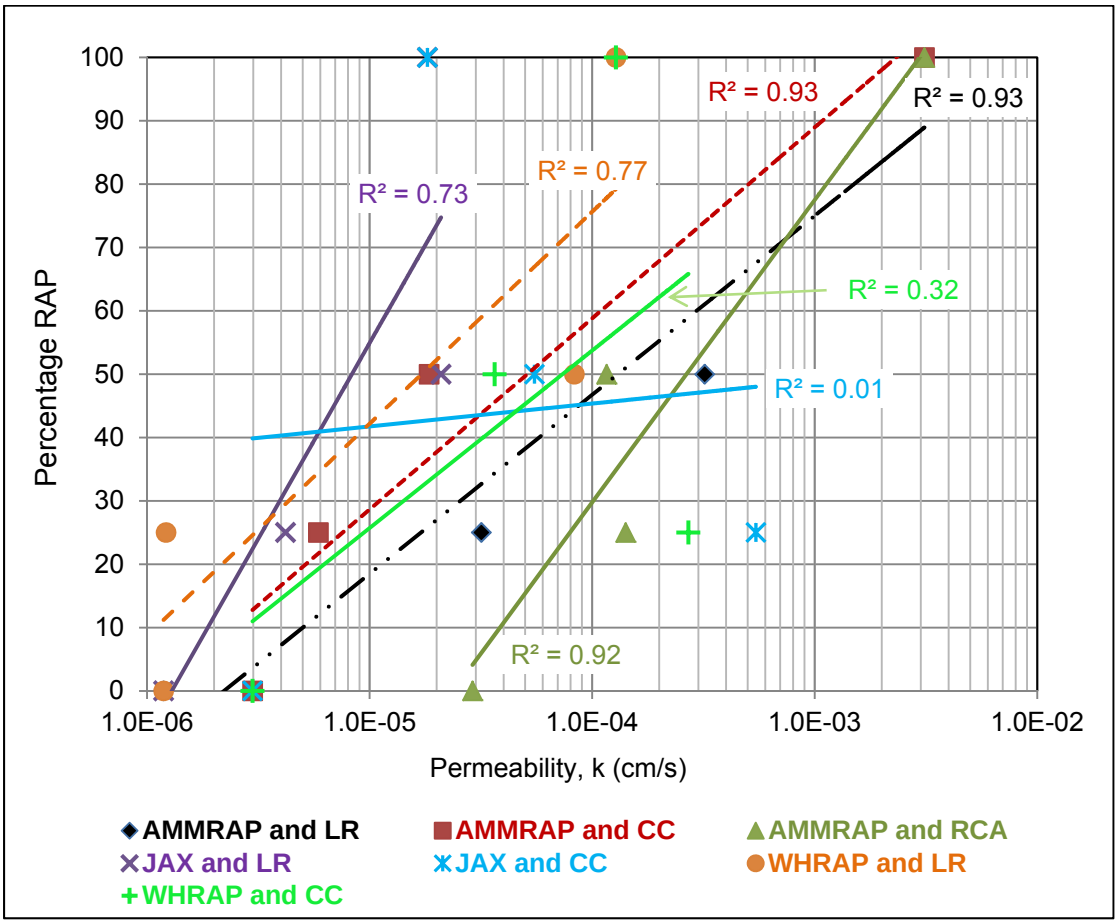

Figure 4-7: Permeability of RAP/Aggregate Blends

4.2. Gradation Modifications or Fractionating 100% RAP

RAP from the various sources was fractioned or split above and below designated sieves to evaluate their engineering properties. The results presented in this section are based on averages from at least two tests per source for a total of at least eight tests per type of experiment conducted. Consequently, the linear regression graphs showing correlations with four points, which are averages from the four RAP sources, are in reality results of at least eight tests.

The results were limited to this number of tests because the creep testing program was the central concern of the research program and the number of tests along with the duration of each test limited the total number of tests that could be conducted. Additional testing is recommended to substantiate these trends.

4.2.1. Engineering Properties of Fractions

4.2.1.1. Grain Size Distribution of Fractions

Table 4-4 shows the percent passing for the sieves used to evaluate the RAP fractions. The # 4 and #8 sieves have the largest percent passing; samples based on these sieves required the least amount of effort and time. Preparing samples for the percent passing the #40 sieve required more effort while a major effort was required to prepare samples of the material passing the #200 sieve because there was so little of this material in the unprocessed RAP.

Table 4-4: Percent Passing for Designated Fractioning Sieves

Properties	APAC Melbourne Milled	APAC Melbourne Crushed	Whitehurst Milled	APAC Jacksonville Crushed	Average
Passing #4 (%)	58.1	75.8	46.0	73.4	63.3
Passing #8 (%)	32.8	50.0	42.0	55.3	32.5
Passing #40 (%)	7.7	14.3	11.0	33.3	16.6
Passing #200 (%)	0.5	0.6	0.3	6.8	2.1

4.2.1.2. Asphalt Content of Fractions

Asphalt content tests were carried out on the +#4 and -#4, +#8 and -#8, +#40 and -#40, and 100% RAP fractions. To create a fraction, a sample of RAP was split using the corresponding sieves. A minimum of two samples were tested for each fraction. The results for crushed and milled APAC Melbourne RAP are presented in Figure 4-8 and Figure 4-9.

For each sieve shown in the figures, higher asphalt contents were observed on the percent passing than on the percent retained fraction. This trend was most likely caused by the larger surface area coated with asphalt to volume ratio of the finer grain sizes. The largest range observed for the fractions of APAC Melbourne crushed RAP is on sieve #4: 4.3% for the

fraction retained to 5.8% for the fraction passing. The asphalt content of the fractions of APAC Melbourne milled RAP had the largest variation on the #40 sieve: 5.2% versus 6.2%.

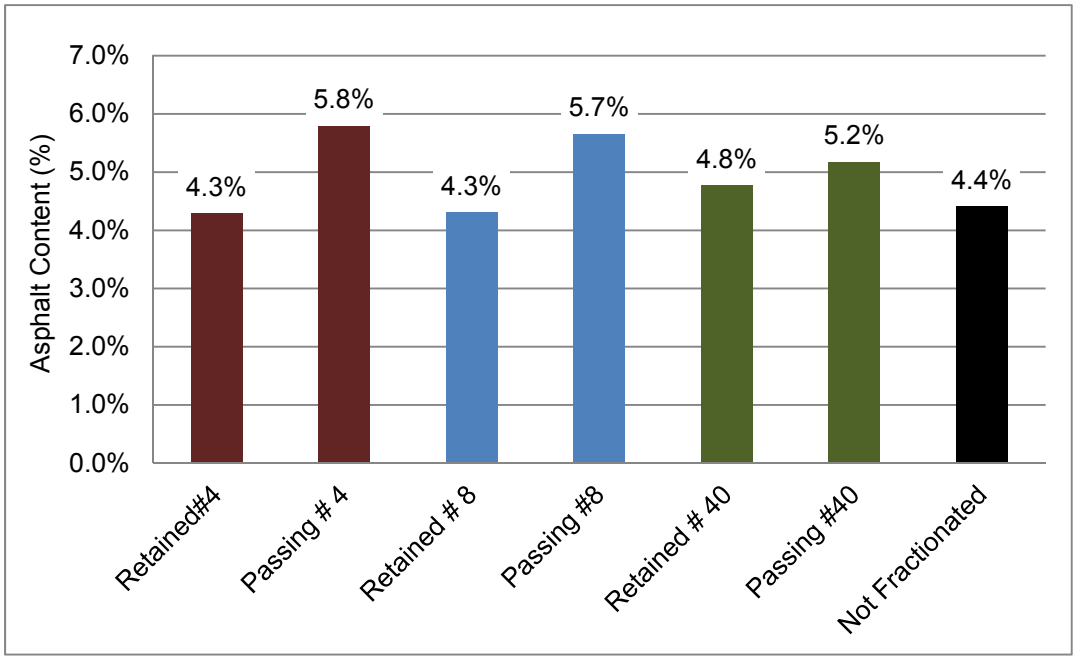

Figure 4-8 Asphalt Content by Fraction of APAC Melbourne Crushed RAP

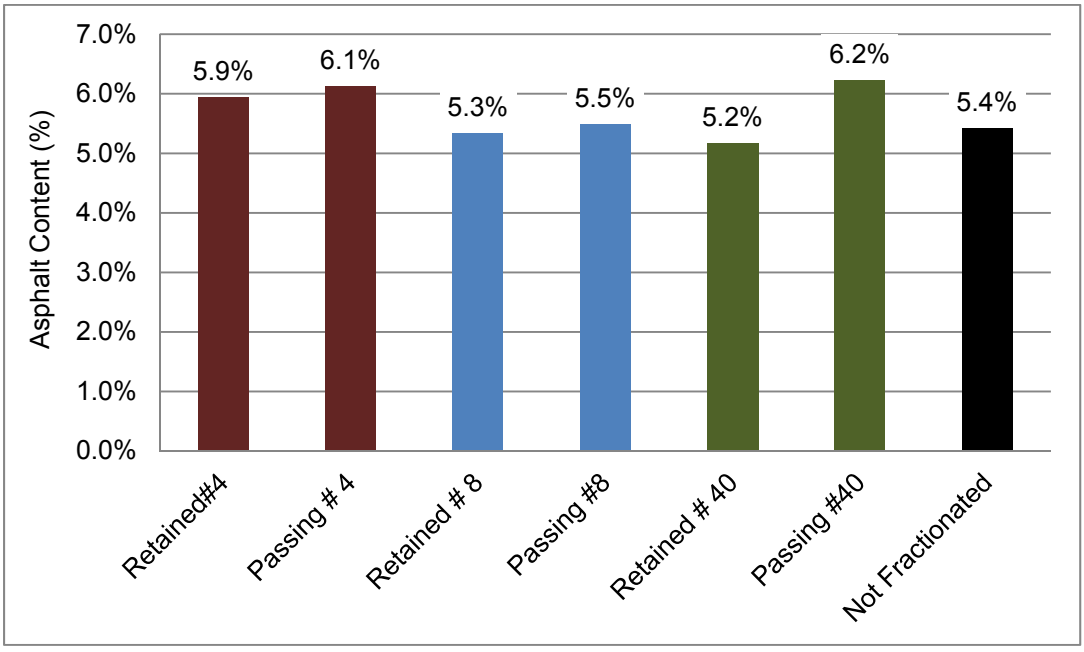

Figure 4-9: Asphalt Content by Fraction of APAC Melbourne Milled RAP

The same trends were observed for Whitehurst milled RAP (Figure 4-10) and APAC Jacksonville crushed RAP (Figure 4-11). In all cases the fraction passing a given sieve had a higher asphalt content than the fraction retained.

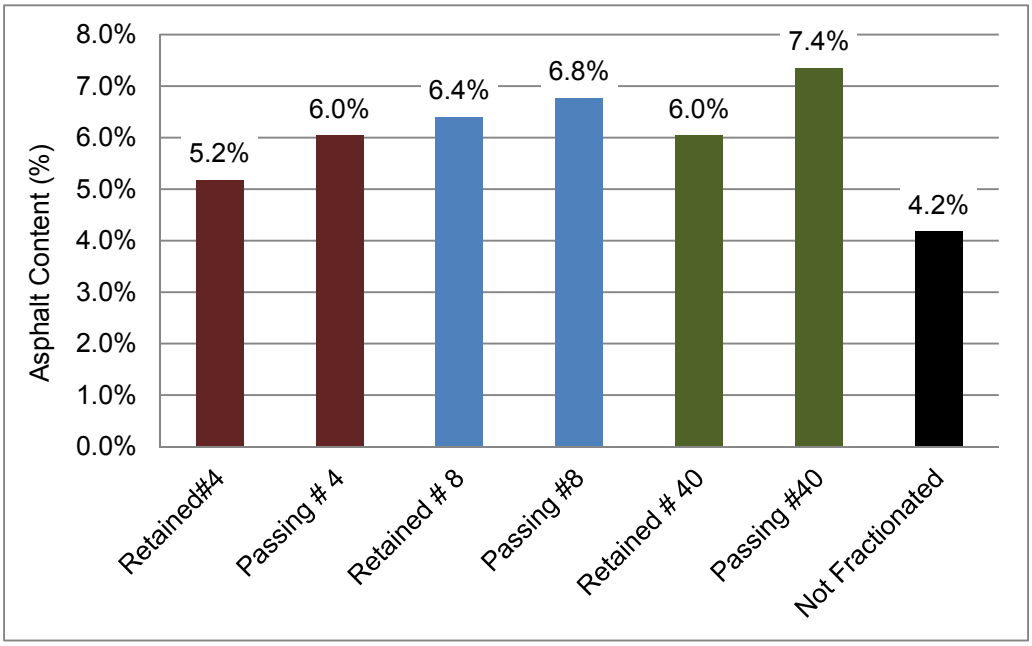

Figure 4-10 Asphalt Content by Fraction of Whitehurst Milled RAP

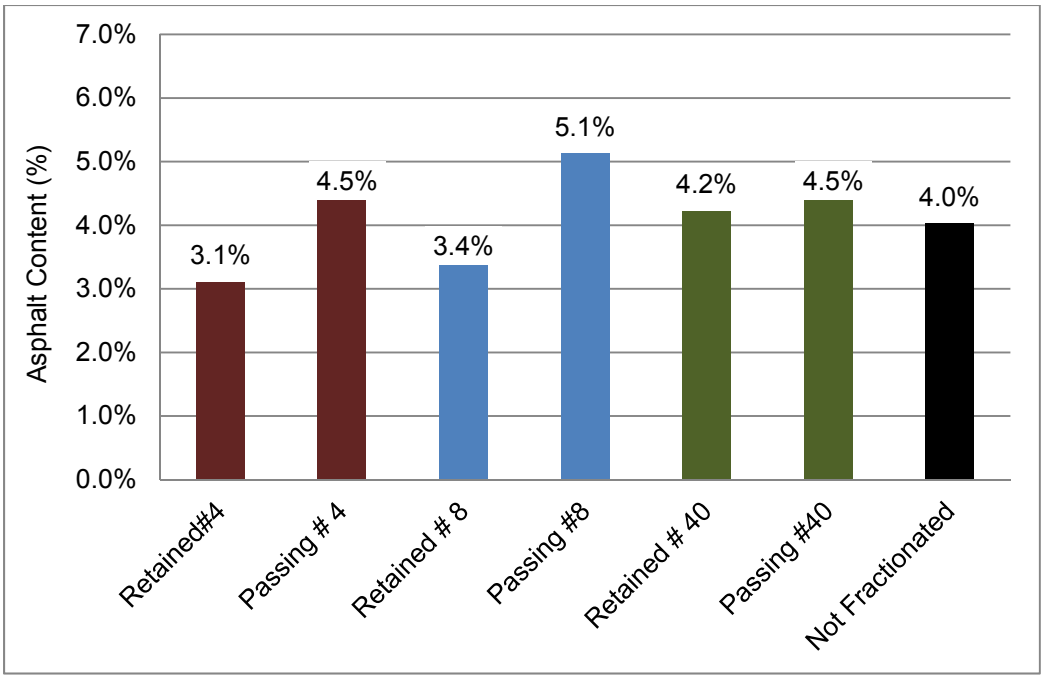

Figure 4-11: Asphalt Content by Fraction of APAC Jacksonville Crushed RAP

4.2.1.3. Specific Gravity of RAP Fractions

Results of the Bulk Specific Gravity test (FM 1-T209, Rice test) for milled and crushed APAC Melbourne RAP are presented in Figure 4-12 and Figure 4-13. Data from all sources is in Appendix J. For each sieve, the fractions passing had lower specific gravity than the fractions retained. This is expected since the specific gravity of asphalt binder, typically around 1.03, is lower than the aggregate specific gravity which is 2.65 (Sandin, 2008). The specific gravity of RAP fractions ranges from 2.46 to 2.56 for crushed RAP and from 2.50 to 2.56 for milled RAP.

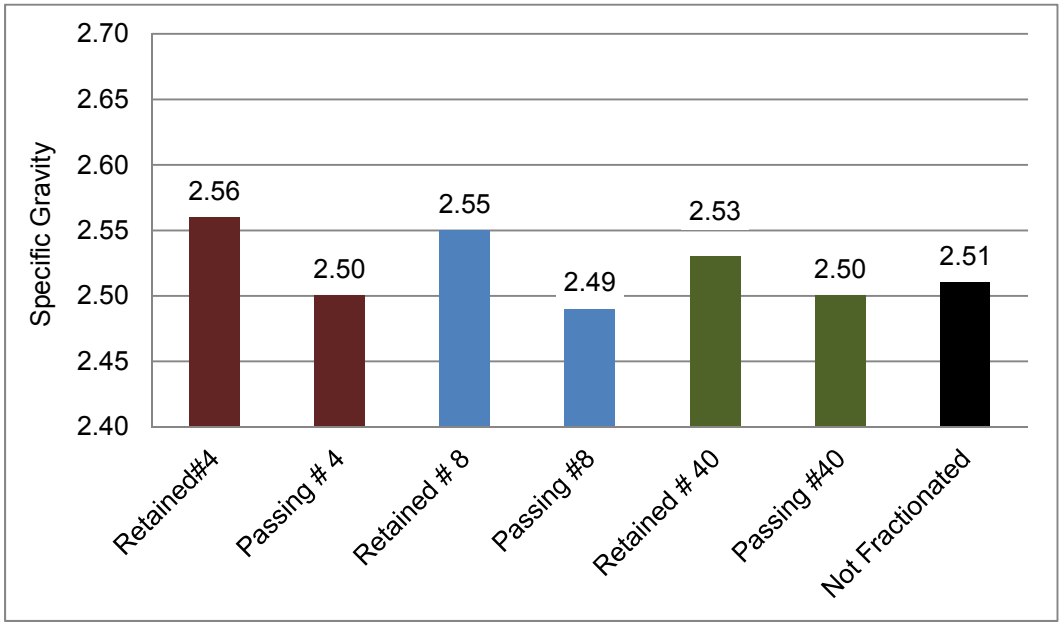

Figure 4-12: Specific Gravity by Fraction of APAC Melbourne Crushed RAP

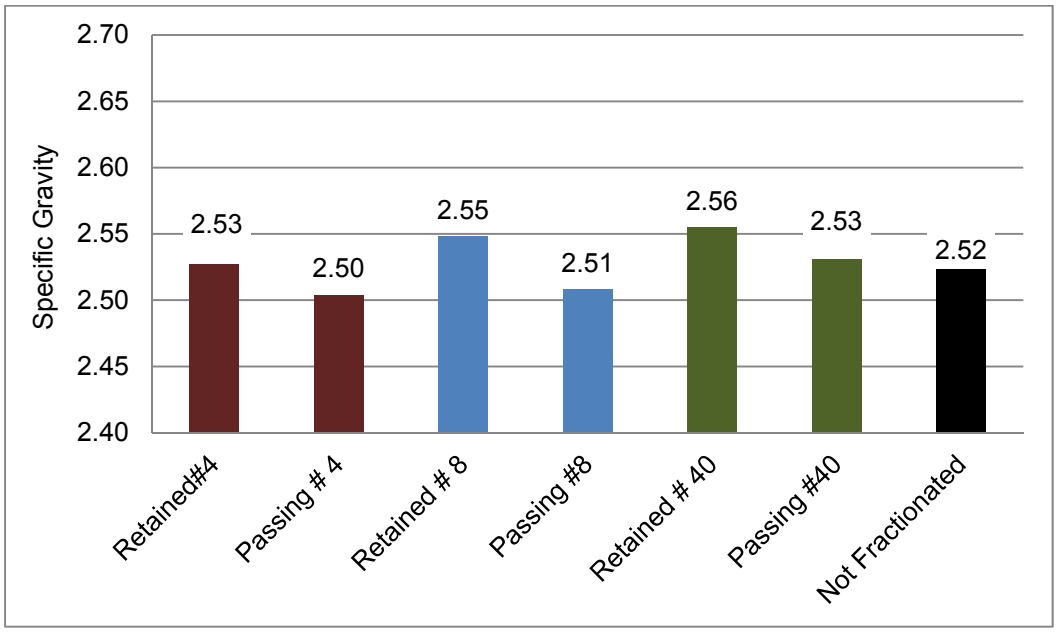

Figure 4-13: Specific Gravity by Fraction of APAC Melbourne Milled RAP

Unprocessed APAC Jacksonville crushed RAP (Figure 4-14) had an average specific gravity of 2.60 compared to 2.58 for Whitehurst Gainesville milled RAP (Figure 4-15), 2.52 for APAC Melbourne milled RAP and 2.51 for APAC Melbourne crushed RAP. Based on visual observation, APAC Jacksonville crushed RAP and Whitehurst milled RAP contained a higher percentage of granite aggregate while the APAC Melbourne RAP contained mostly limestone aggregate.

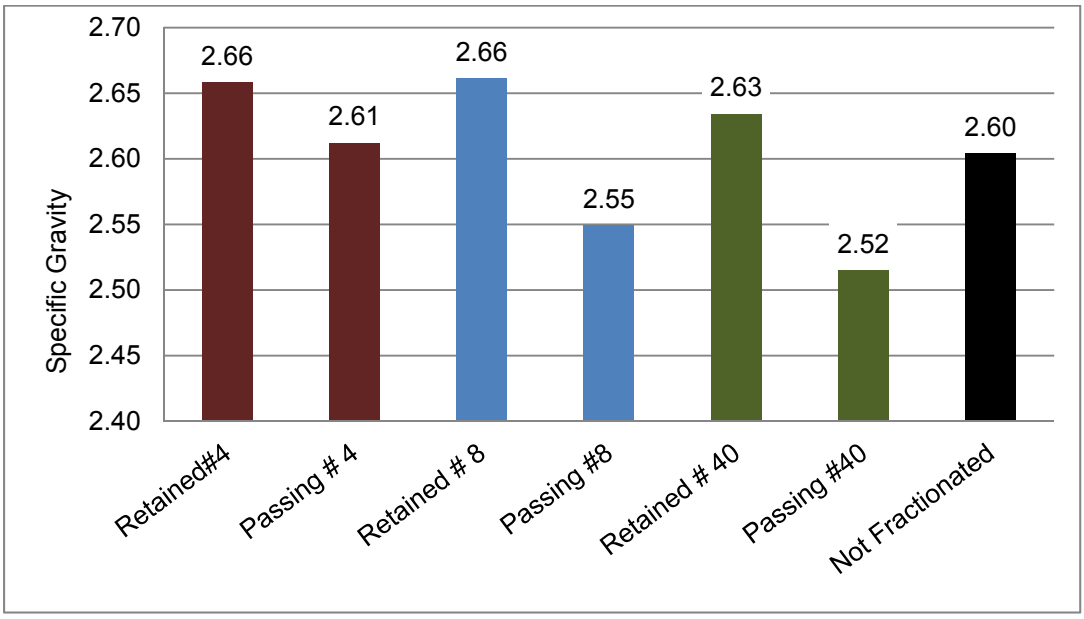

Figure 4-14: Specific Gravity by Fraction of APAC Jacksonville Crushed RAP

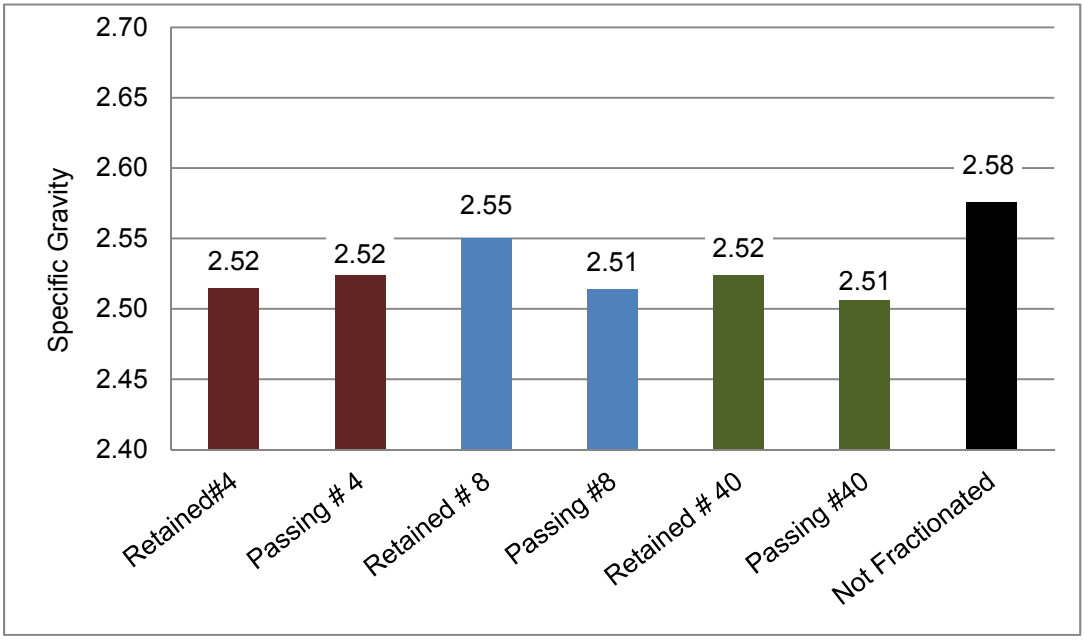

Figure 4-15: Specific Gravity by Fraction of Whitehurst Gainesville Milled RAP

4.2.2. Creep Behavior of Fractions

Creep performance was evaluated for the +/- #4, #8, and #40 fractions of RAP, unprocessed RAP, and for blends of 100% RAP with its gradation modified to match the FHWA curve.

4.2.2.1. Creep Terminology

Creep response of fine grained soils progresses through primary, secondary and tertiary creep stages. Stage one, the primary portion, includes the initial deformation or primary settlement due to the application of the load. Conventional base aggregates exhibit this initial settlement when loaded but then stop deforming. RAP exhibits this first stage large deformation but the deformations do not stop under constant stress.

In stages two and three RAP deforms (creeps) under the constant stress. According to Mitchell (1993) the secondary stage of creep primarily results from rearranging the soil skeleton as particles slide. If the tertiary stage occurs, the material fails. RAP subjected to one-dimensional loading in a mold displayed only primary and secondary creep deformations (Cleary, 2005 and Dikova, 2006). The fractionating portion of this investigation focused on the secondary creep to determine the deformation rate over time under a constant pressure. Viyanant et al., (2007) performed creep tests of RAP in a triaxial device with varying confining stresses. They found that the onset of creep rupture occurred at around 3% axial strain under low confining stress. Tertiary creep was observed in this study during unconfined creep testing at an axial strain of 0.4%; these results are discussed in Section 4.5.4.2. Since base course is partially confined, the onset of tertiary creep would occur between these two values.

Figure 4-16 shows typical results of the one-dimensional creep tests. On the left is a graph of deformation (in) versus linear time (days) with the specimen displaying primary (stage 1) and secondary (stage 2) creep. Tests on materials that exhibit insignificant creep, such as limerock, would yield a flat curve during the secondary creep stage. In this example, the curve clearly shows an increasing deformation with respect to time. Deformation (in) versus log (time) is displayed on the right. When plotted on a log (time) axis, the secondary stage creep is nearly linear. A logarithmic trend line can be fitted to the secondary creep curve resulting in a trendline of the form $\delta = m \log(t) + b$. In this research the deformations were divided by the sample height to produce strains. The slope (m) of this line, referred to in this study as the creep strain rate (CSR), was used to compare creep. A higher CSR indicates a steeper slope resulting in greater creep deformation over time. CSR has units of in/in/log time (days). In addition to providing a

way to compare the creep of different specimens, the CSR equation also provides a way to project creep deflection over the life of a project.

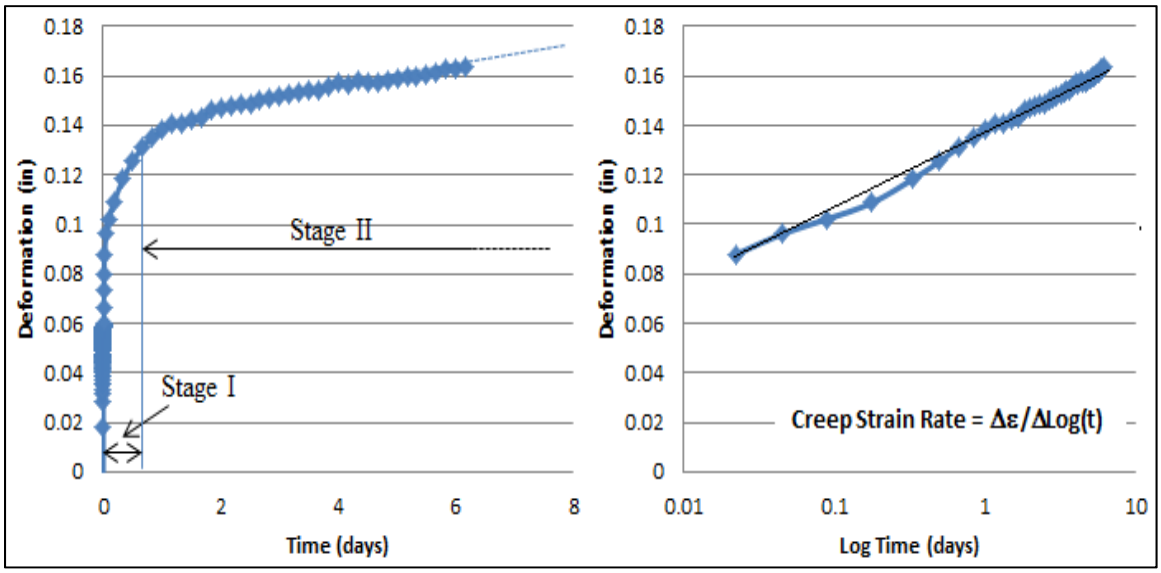

Figure 4-16: Typical RAP Creep Results on Arithmetic and Log Time Plots

4.2.2.2. Creep Results for Fractions

Individual deformations vs. time and log time plots, from the fractionating tests are in Appendix C. The secondary stage CSR's observed are presented in Figure 4-17 through Figure 4-20 . The FHWA maximum density is shown as the Talbot blend while 100% represents the non-fractionated RAP.

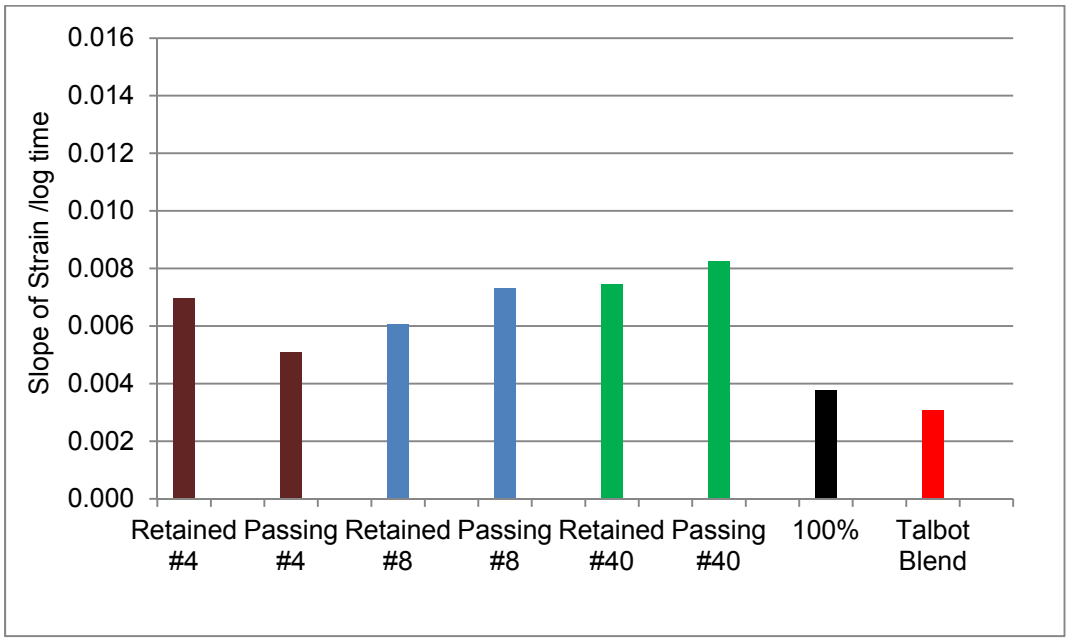

Figure 4-17: Creep Results of APAC Melbourne Crushed RAP

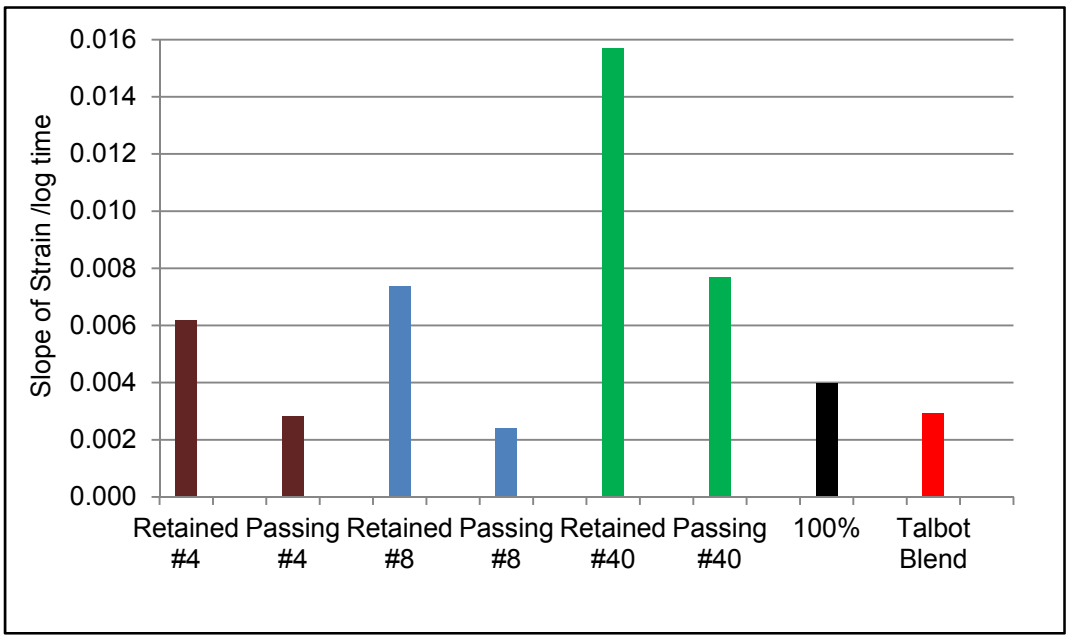

Figure 4-18: Creep Results of APAC Melbourne Milled RAP

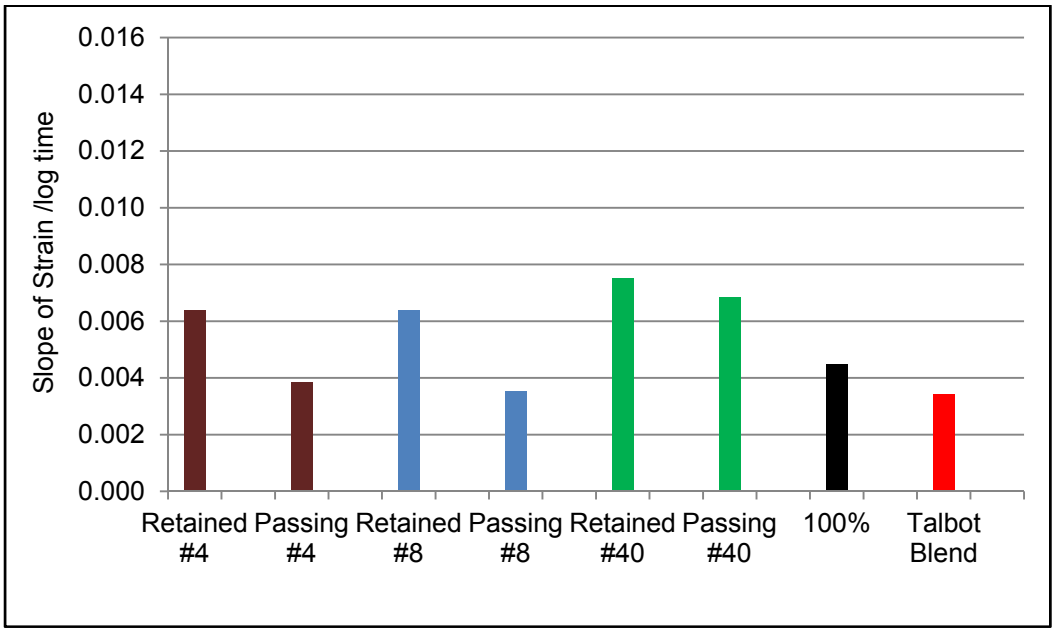

Figure 4-19: Creep Results of Crushed APAC Jacksonville RAP

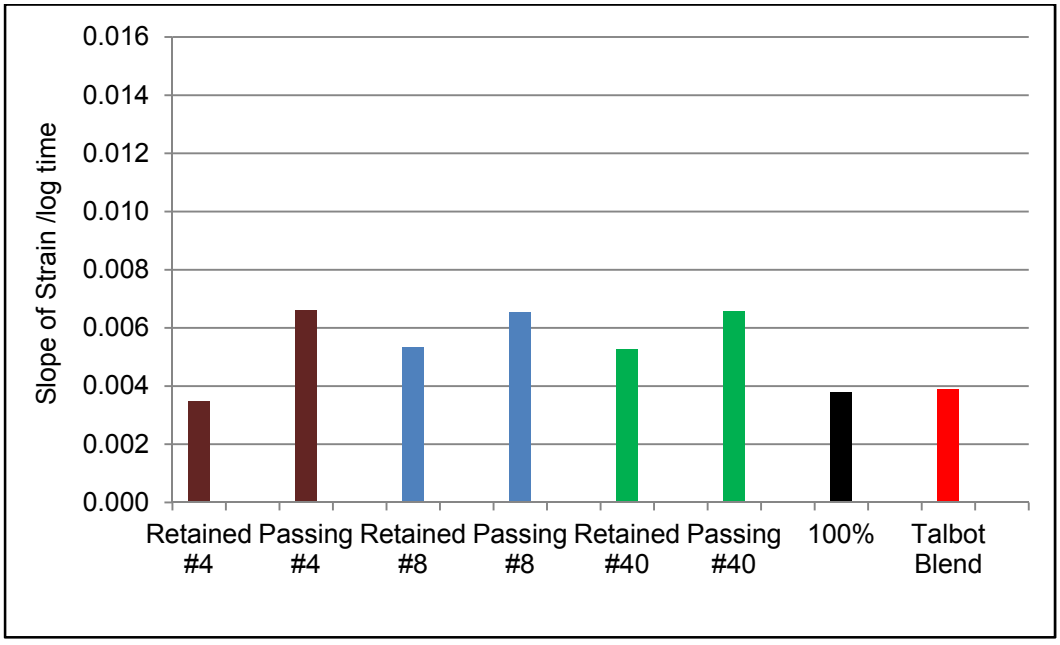

Figure 4-20: Creep Results of Milled Whitehurst Gainesville RAP

Fractionating generally did not improve the creep characteristics of RAP but matching the FHWA maximum density gradation did improve the creep characteristics. 68% (19 of 28 excluding the Talbot Blend) of the fractions of RAP exhibited more creep than the 100% RAP.

93% (26 of 28 excluding the 100% RAP) of the fractions produced more creep than the Talbot blends.

4.2.2.3. CSR and Density Comparisons for Fractions

A best fit linear regression trend line was drawn for each fraction to examine the relationship between the creep and density. At least eight tests were used to develop the correlations. A summary of the linear regression coefficients (m and b) and correlation coefficients (R^2) is shown in Table 4-5. Table 4-6 was used to evaluate the results of the R^2 values (Buda and Jarynowski, 2010).

Table 4-5: Summary of Linear Regression Coefficients for Density vs. CSR

	R^2	m ((in/in)/day)	b (pcf)
Retained #4	0.04	1223.4	102.52
Passing #4	0.26	-1629.5	127.57
Retained #8	0.29	-2668.2	124.49
Passing #8	0.11	-745.4	109.44
Retained #40	0.54	-1018.0	121.21
Passing #40	0.29	1839.4	81.05
100%	0.83	13761.0	62.48
Talbot Blend	0.32	-1421.4	125.53

The 100% RAP specimens displayed the highest R^2 of 0.83 which is in the middle of the strong correlation range. The second highest was the retained on #40 data, with an R^2 of 0.57 which is at the lower end of the strong correlations. All of the other fractions produced small or weak correlations.

The slopes were inconsistent varying between positive and negative values. Negative slopes imply that an increasing density reduces the CSR, while positive slopes imply that increasing density increases the strain rate. The logical conclusion would be that negative slopes

should be produced, however only five of the eight sets (62.5%) of data produced negative slopes. Fractions retained on the #4, passing the #40, and the 100% RAP displayed positive slopes. Fractions passing the #4, retained on and passing the #8, passing the #40, and the Talbot or FHWA T5040.27 (1988) blend displayed negative slopes.

Table 4-6: Interpretation of Correlation Coefficients (Buda and Jarynowski, 2010)

Correlation	Negative	Positive
None	−0.09 to 0.0	0.0 to 0.09
Small	−0.3 to −0.1	0.1 to 0.3
Medium	−0.5 to −0.3	0.3 to 0.5
Large (strong)	−1.0 to −0.5	0.5 to 1.0

The intercept indicates the density at which no creep would be expected. They are very low when positive slopes were produced, which is not logical, and in the 125 pcf range when negative slopes were produced, which is logical. The higher densities should correlate to less creep, however none of the regression coefficients for the fractions are very strong.

Based on the low correlations, plus the inconsistency of the intercepts and slopes, it was concluded that developing correlations between density and creep for fractions of RAP is not useful.

4.2.2.4. Asphalt Content vs. CSR

Correlations were made between asphalt content and CSR. Table 4-7 shows that there were very weak correlations between asphalt content and CSR. The slopes did not indicate a clear trend between the two parameters with both positive and negative correlations. Positive slopes were expected indicating more creep as the asphalt content increased, however this occurred in only three of the seven cases.

The intercepts varied between 4.49 and 9.76 %. The intercept is the asphalt content that should produce no creep. The higher asphalt contents are associated with data which produced negative slopes for this correlation as would be expected.

Based on the low correlations and inconsistency of the intercepts and slopes there was not a clear relationship between asphalt content and creep. it was concluded that asphalt content was not useful in predicting creep behavior.

Table 4-7: Summary of Linear Regression Coefficients for Asphalt Content vs. CSR

	R^2	m (%AC/day)	b (%)
Retained #4	0.13	-2.87	6.28%
Passing #4	0.05	0.99	5.18%
Retained #8	0.09	-4.59	7.75%
Passing #8	0.35	1.77	4.88%
Retained #40	0.19	0.92	4.49%
Passing #40	0.11	-5.39	9.76%
100%	0.07	-5.10	6.55%

4.2.2.5. Specific Gravity vs. CSR

Correlations were made between CSR and specific gravity. Table 4-8 shows that there were very weak correlations between specific gravity and CSR. The slopes did not indicate a clear trend between the two parameters.

Previous studies (Cosentino et al., 2008) have shown that creep increased with increasing asphalt content in RAP/sand blends. Since the fractions used in this part of the study are from a single RAP source, lower specific gravity indicates that there is more asphalt in the fraction. Based on these previous findings, the expectation was that more creep should correlate to lower specific gravity.

The data was plotted with CSR on the x-axis and specific gravity on the y-axis. The slopes varied between positive and negative values. Negative slopes would indicate that higher specific gravities correlate to less creep while positive slopes would indicate that higher specific gravities correlate to more creep. Negative slopes only occurred in three of the seven cases.

The intercepts varied between specific gravities of 2.17 and 2.56; however most of the values were near the upper limit. The intercept is the specific gravity that should produce no

creep. Higher specific gravities were associated with data which produced both positive and negative slopes.

Based on the low correlations and inconsistency of the intercepts and slopes there was not a clear relationship between specific gravity and creep. It was concluded that specific gravity is not a reliable indicator of creep in RAP fractions.

Table 4-8: Summary of Linear Regression Coefficients for Specific Gravity vs. CSR

	R^2	m (%AC/day)	b (%)
Retained #4	0.25	21.06	2.44
Passing #4	0.03	-5.19	2.56
Retained #8	0.01	4.73	2.55
Passing #8	0.27	-5.33	2.54
Retained #40	0.00	0.65	2.55
Passing #40	0.01	-1.75	2.53
100%	0.49	95.76	2.17

4.2.3. Post-Creep LBR of Fractions

LBR was used to evaluate and compare the strength of the chosen fractions of RAP and of blends of 100% RAP modified to achieve maximum density. Unsoaked LBR tests were carried out on specimens following 7-day creep tests at a constant load of 12 psi. This combination of creep followed by unsoaked LBR produces higher LBR values than normal soaked tests. These LBR results should only be used for comparison of the fractions and not for design.

4.2.3.1. Post-Creep LBR results

FM 5-515 specifies that surcharge weights be used during LBR testing of stabilized subgrade and embankment specimens but no surcharge be used for base materials. Since this project was investigating RAP as a base material, no surcharge was applied to the specimen during testing. According to Breytenbach et al., (2010), the CBR test has poor reproducibility and repeatability. Because the LBR and CBR testing procedures are nearly identical, an attempt to reduce the inherent variability associated with LBR test was made by keeping the procedure

standard and averaging the results of at least two tests depending on the difference in results. ASTM's specified CBR single operator variability limit of 22% from the mean was used as the maximum allowable difference between test results. Specimens outside of this range were rejected and redone. Summaries of the results from post-creep LBR tests on the different RAP fractions from the four sources are presented in Figures 4.19, 4.20, 4.21, and 4.22.

Overall, Talbot blends produced the highest LBR values followed by 100% RAP. In general, the post-creep LBR values from the fractions were below 40. All but one fraction tested had a lower LBR than unfractionated RAP. Specimens at the Talbot maximum density in some cases exhibited double the LBR of unfractionated RAP. The largest LBR of 93 was achieved with a Talbot gradation of APAC Melbourne milled RAP; the largest improvement to the LBR due to the increasing density (121%) also occurred with APAC Melbourne milled RAP (Figure 4-22).

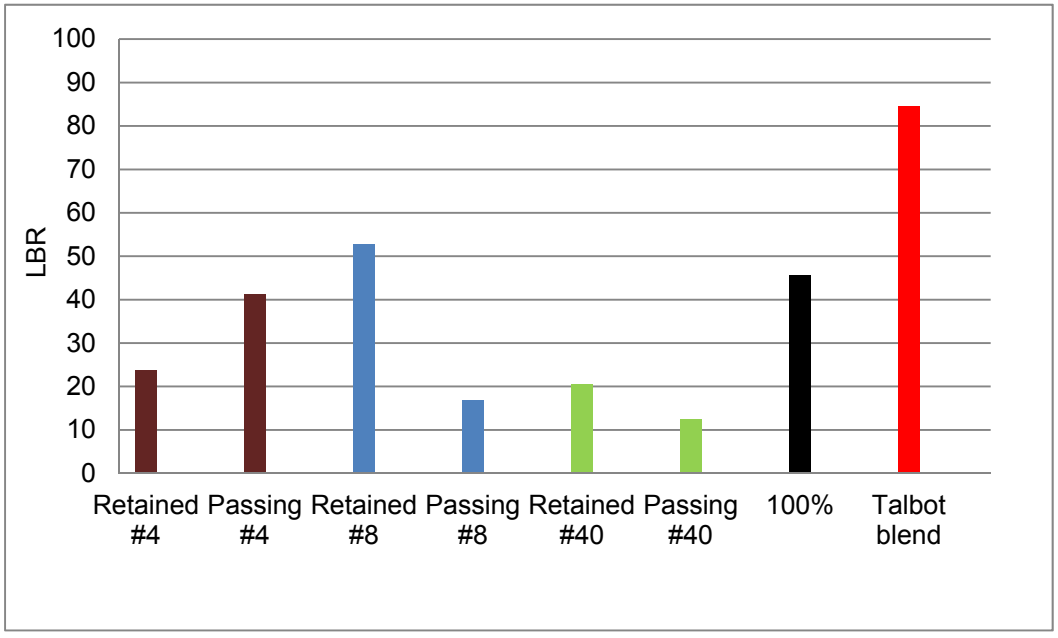

Figure 4-21: Post-Creep LBR Results of APAC Melbourne Crushed RAP

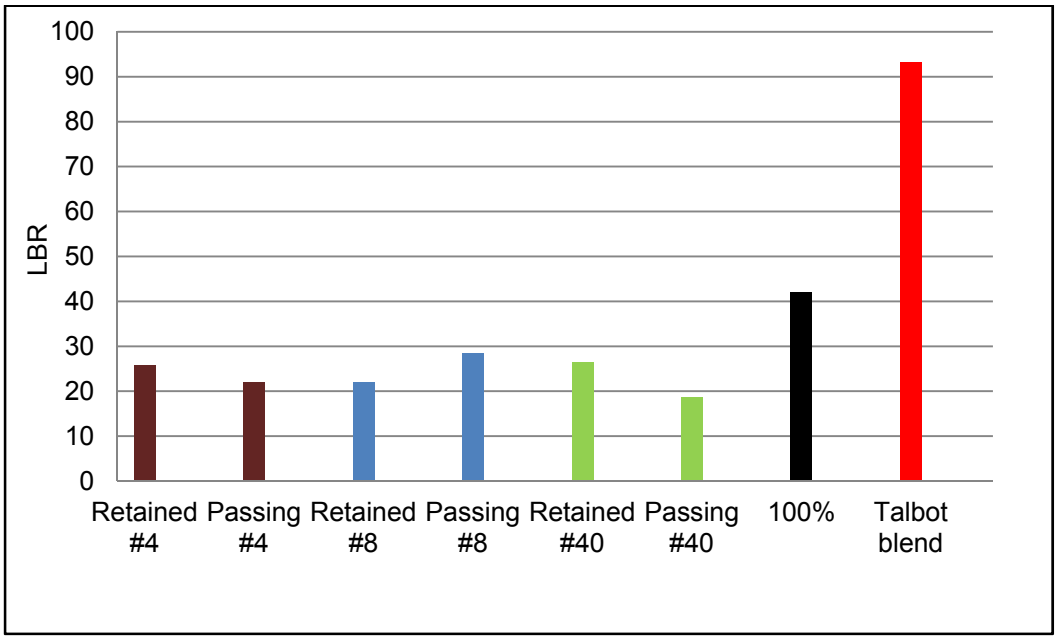

Figure 4-22: Post-creep LBR Results of APAC Melbourne Milled RAP

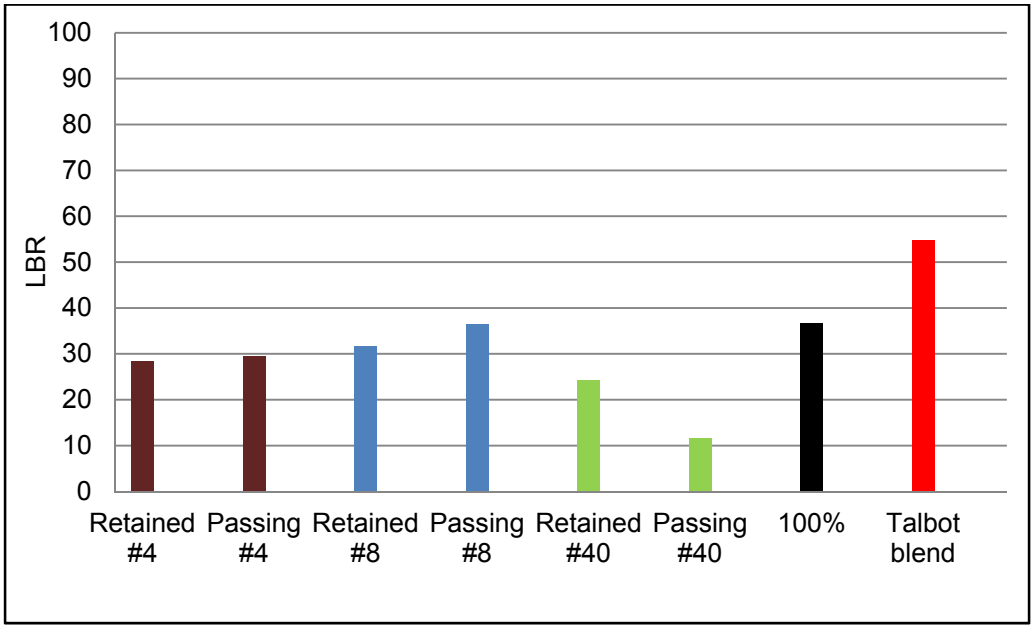

Figure 4-23: Post-creep LBR Results of APAC Jacksonville Crushed RAP

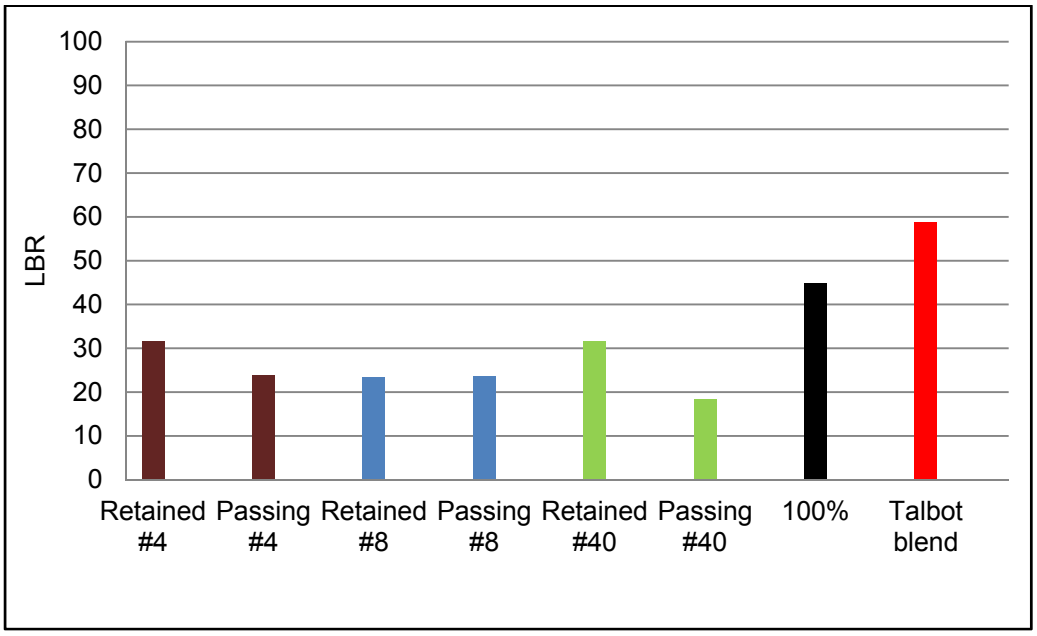

Figure 4-24: Post Creep LBR Results of Whitehurst Gainesville Milled RAP

Figure 4-25 shows the percent change in LBR of each fraction of RAP and Talbot blend compared to 100% RAP. With the exception of the APAC Melbourne crushed fraction retained on the # 8 sieve, all the fractions produced lower LBR values than unfractionated RAP. Only the LBR values from the Talbot blends were higher than 100% RAP with a minimum improvement of 31% for Whitehurst milled RAP and a maximum of 122% for APAC milled RAP.

The overall conclusions from the LBR fractionating and blending process are that RAP fractions have lower LBR strength than unfractionated RAP while Talbot maximum density blends have higher LBR than unfractionated RAP. Even the highest Talbot blend unsoaked LBR was below the FDOT specified soaked LBR of 100 for base course materials. Fractionating or gradation modified 100% RAP will not produce sufficient improvements to meet base course specifications.

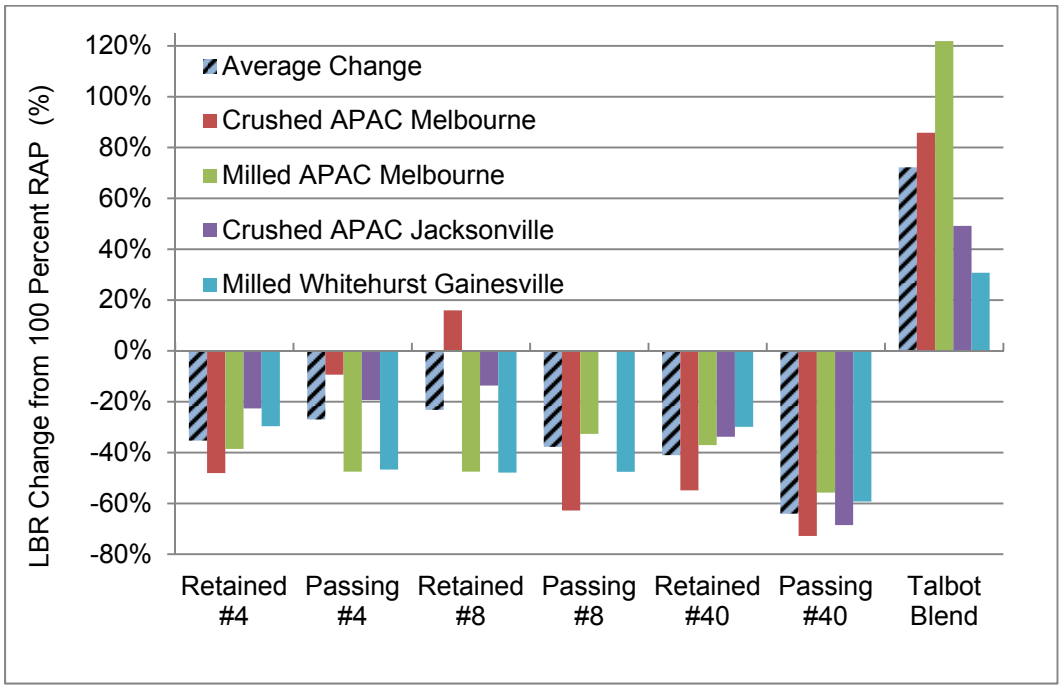

Figure 4-25: Post-Creep LBR Change Versus 100% RAP LBR for RAP Fractions and Talbot Blends

4.2.3.2. LBR and Density

Table 4-9 shows a summary of the regression coefficients and R^2 values from the linear regressions between LBR and density. The retained #4, retained and passing #40, and the Talbot blend, displayed very weak correlations. The other fractions showed strong correlations. Because the slopes (m) are all positive, they indicate that higher density will produce higher LBR values. This trend was expected.

The intercepts would be the density associated with an LBR of zero, and therefore, should be relatively low. Evaluations of the LBR versus density data from the Talbot testing shows inconsistent results near the LBR of 60, which produced the intercept value of 120.6. Had the one point been excluded a lower intercept would have resulted, however, it was not excluded because it was the average from two tests.

In conclusion, the consistently positive slopes plus low intercepts indicate that there is a relationship between LBR and density for various fractions of RAP. This finding is consistent

with similar trends reported for 100 % RAP and density by Cosentino et al. (2011) and Cosentino and Kalajain (2001).

Table 4-9: Summary of Linear Regression Coefficients for Density vs. LBR

	R^2	M (density/LBR)	b (pcf)
Retained #4	0.07	0.72	89.95
Passing #4	0.57	0.54	98.36
Retained #8	0.86	0.27	98.84
Passing #8	0.68	0.54	91.53
Retained #40	0.06	0.35	103.00
Passing #40	0.21	0.33	89.62
100%	0.63	0.97	76.36
Talbot Blend	0.00	0.003	120.60

4.2.3.3. Asphalt Content versus LBR of Fractions

Linear correlations were made between asphalt content and LBR. Table 4-10 shows a summary of results from the linear regression. The regression coefficients were all below the strong correlation level except for the 0.82 for the passing # 40 testing. This trend suggests that asphalt content of fractions is not a good predictor of LBR.

Positive slopes indicate that the LBR increased as asphalt content increased and negative slopes indicate that LBR increased as asphalt content decreased. From previous research, negative slopes were expected. Three of the seven slopes were negative; however the magnitude of the positive and negative slopes is so small that there was no real trend observed.

The intercepts varied between 1.2% and 6.9%. The intercept would be the asphalt content associated with an LBR of zero and logically it should be a very high value. The highest asphalt contents were associated with the negative slopes but these occur in only three of seven cases.

Based on the low correlations, inconsistency of the intercepts and slopes it was concluded that developing correlations between LBR and asphalt content was not useful in predicting the performance of RAP fractions.

Table 4-10: Summary of Linear Regression Coefficients for Asphalt Content vs. LBR

	R^2	m (%AC/LBR)	b (%AC)
Retained #4	0.00	0.0000	4.7%
Passing #4	0.00	-0.0001	5.8%
Retained #8	0.28	-0.0005	6.4%
Passing #8	0.25	-0.0004	6.9%
Retained #40	0.48	0.0002	1.5%
Passing #40	0.82	0.0031	1.2%
100%	0.03	0.0003	3.4%

4.2.3.4. Specific Gravity vs. LBR

Linear correlations were made between specific gravity and LBR. LBR was plotted on the x-axis and specific gravity was plotted on the y-axis. Based on previous research, higher specific gravities were expected to result in higher densities and hence higher LBR values. Table 4-11 shows a summary of results from the linear regression.

The regression coefficients were all below the strong correlation level except for the 0.87 for the passing # 8 data. This trend suggests that specific gravity of fractions is not a good predictor of LBR.

Positive slopes, indicating that LBR increased as specific gravity increased, occurred in only two of seven cases. The magnitudes of the positive and negative slopes are so small that no clear trend was observed.

The intercepts varied between 2.44 and 2.87. The intercept would be the specific gravity associated with an LBR of zero, and logically it should be a very low value. The lowest values are associated with the passing # 8 and # 40 data, and both slopes, although very small, are positive.

Based on the low correlations, inconsistency of the intercepts, and slopes, it was concluded that developing correlations between specific gravity and LBR was not useful in predicting the performance of RAP fractions.

Table 4-11: Summary of Linear Regression Coefficients for Specific Gravity vs. LBR

	R^2	m	b
Retained #4	0.00	-0.0012	2.60
Passing #4	0.08	-0.0021	2.60
Retained #8	0.00	-0.0003	2.59
Passing #8	0.87	0.0028	2.44
Retained #40	0.04	-0.0023	2.62
Passing #40	0.23	0.0018	2.49
100%	0.45	-0.0074	2.87

4.2.4. Correlating CSR to Post-Creep LBR

Correlation analyses were done using the fraction and creep testing data, to examine the relationship between the CSR and LBR. Results of the linear regression, based on a total of 32 tests, are shown in Figure 4-26. The general trend observed for CSR vs. LBR is an increasing LBR for a decreasing CSR. The trend was expected. The negative slope from the trendline also shows a statistical reduction of the CSR with an increasing LBR. The regression coefficient of 0.43 indicates a medium correlation.

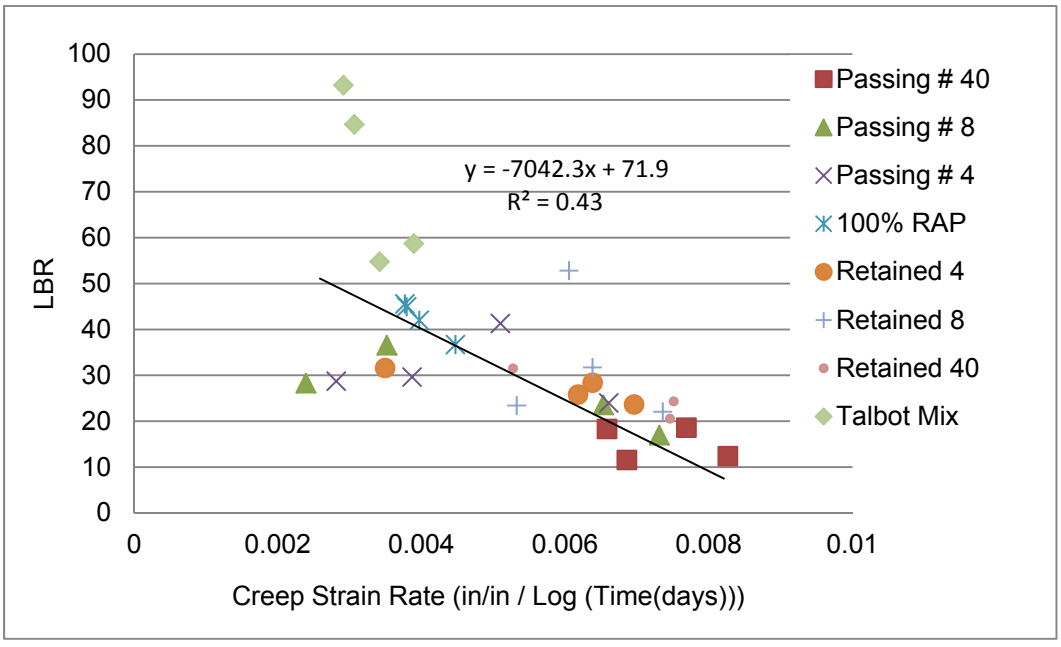

Figure 4-26: Linear Regression for CSR vs. LBR

The same trend was observed for each fraction as shown in Table 4-12. Strong correlations exist between CSR and LBR for 100% RAP, Talbot blends and fractions of RAP with the exception of passing #4, retained #8 and passing #40. The passing #4, retained #8 and passing #40 fractions showed weak correlations. The negative slopes for all correlations suggest that decreasing CSR is correlated to increasing LBR. The intercept, which is the LBR associated with zero creep, generally lies below the FDOT specified value of 100 for base materials. This suggests that the specification will not be achieved with any fraction or blend of RAP. The exception to this conclusion is the maximum density or Talbot blend but creating a Talbot blend purely out of RAP is not practical in the field.

Table 4-12: Summary of Linear Regression Coefficients for LBR vs. CSR

	R^2	m	b
Retained #4	0.79	-1970.40	38.70
Passing #4	0.01	-483.72	33.11
Retained #8	0.04	-3399.00	53.83
Passing #8	0.63	-2770.90	40.02
Retained #40	0.87	-4074.80	52.95
Passing #40	0.05	-1122.80	23.46
100%	0.99	-12266.00	91.36
Talbot blend	0.73	-37187.00	196.36

4.2.5. LBR and Gradation

Figure 4-27 shows the gradation curves by RAP source with the LBR value of each. The Talbot curve is also included. Generally, LBR increased as the finer sieve sizes approached the theoretical maximum density curve. To examine this trend, the variations or differences between the percentage passing for each sieve and the percentage from the FHWA curve were plotted versus LBR (Appendix N). Figure 4-28 and Figure 4-29 show LBR vs. percent passing difference between the FHWA curve and the passing #30 and #50 sieve sizes respectively which displayed the highest R^2 values. Each data point is the average of two specimens.

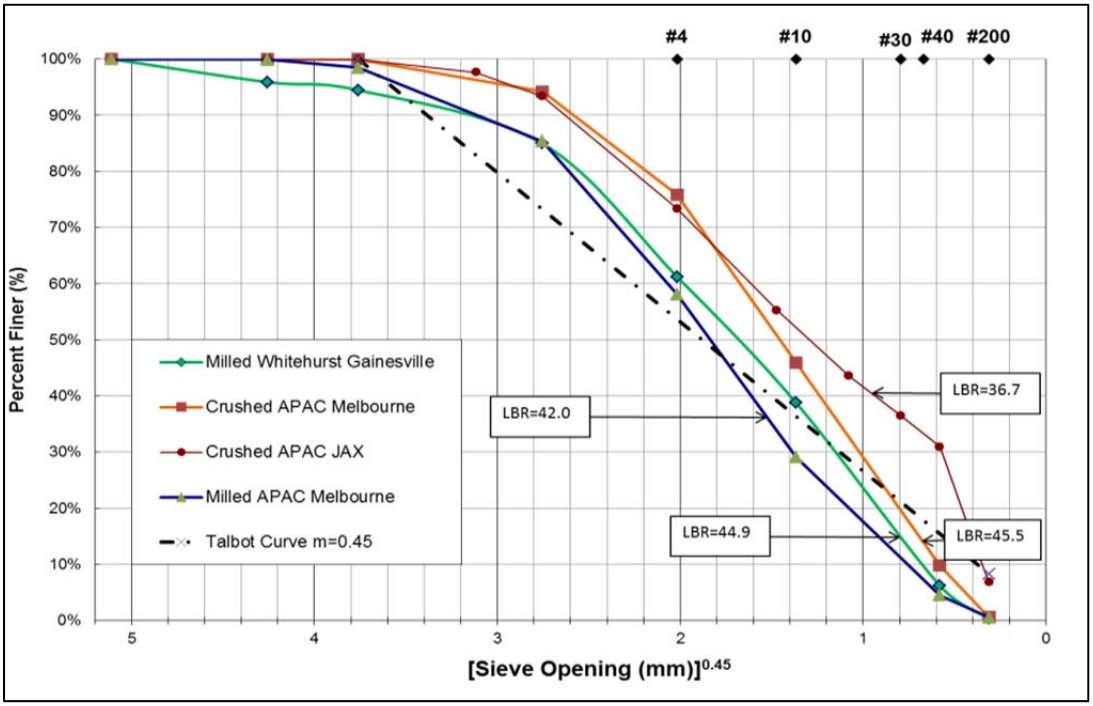

Figure 4-27: 0.45 Power Gradation Graphs of RAP with LBR and FHWA Curve

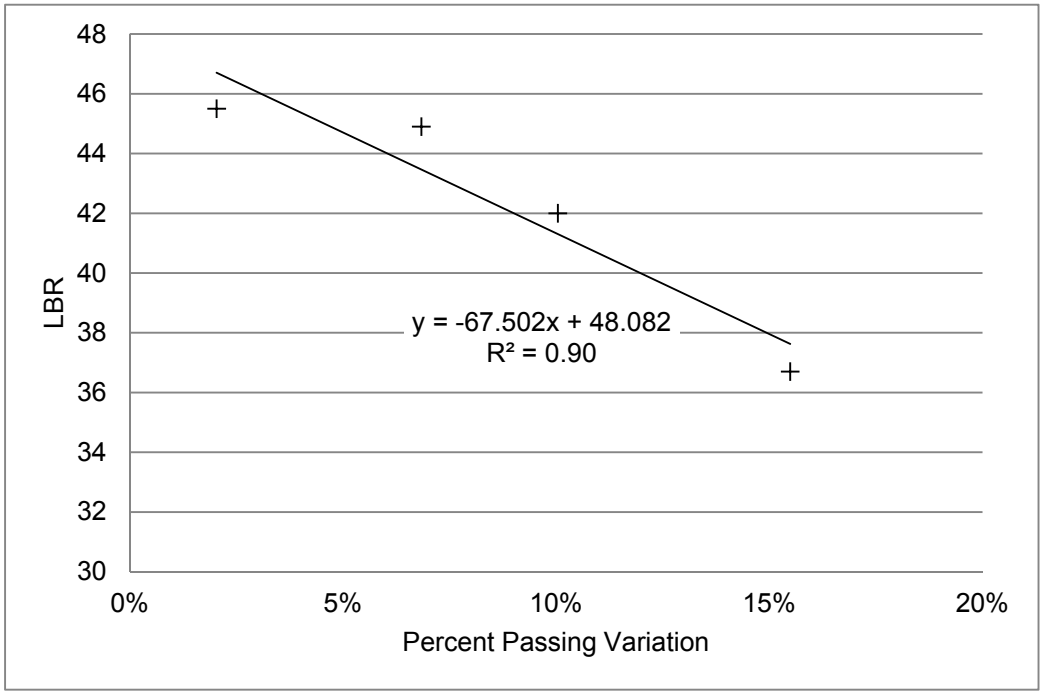

Figure 4-28: LBR vs. Percent Passing Difference between FHWA Curve and Gradation Curve at #30 Sieve

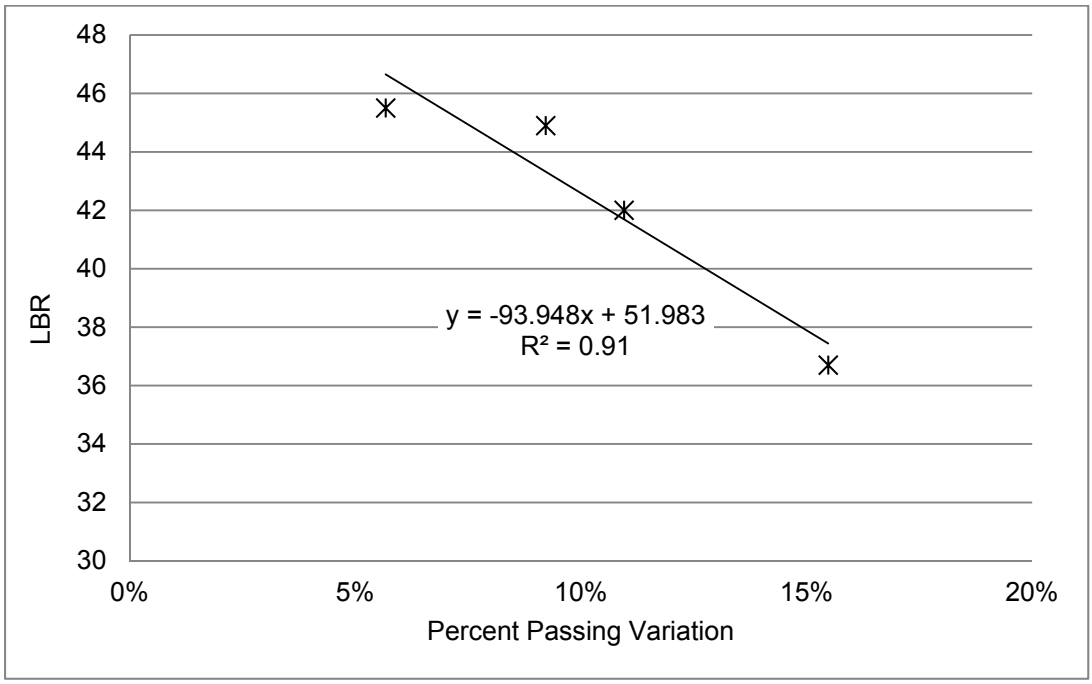

Figure 4-29: LBR vs. Percent Passing Difference between the FHWA Curve and Gradation Curve at #50 Sieve

These figures show that the smaller the difference between the FHWA curve and the gradation curves at the #30 and #50 sieves, the larger the LBR: the closer a gradation curve is to the FHWA curve at #30 and #50 sieve, the higher its LBR will be. The #30 and #50 sieves showed the strongest correlations.

The linear regression results for the different sieve sizes are presented in Table 4-13. Negative slopes imply that the closer the gradation is to the Talbot curve the higher the LBR, which is desirable. Strong correlations with negative slopes were observed for the #10, #30, and #50 sieves suggesting that adding materials in these ranges would improve the LBR. A strong correlation was also observed at the #200 sieve but with a positive slope, implying that for material passing the #200 sieve, the closer a RAP gradation curve is to the Talbot curve, the smaller the LBR, which is not desirable. The intercept from this data corresponds to the LBR when the gradation matches the Talbot curve. This value should be the maximum possible based on gradation. Since they are all well below the FDOT specified 100 LBR for base materials it was concluded that adjusting the gradation of RAP is unlikely to produce LBR values that meet FDOT base requirements.

Table 4-13: Summary of Linear Regression Coefficients for LBR vs. Percent Passing Difference between FHWA Curve and Gradation Curve

Sieve	R^2	m (LBR/% Variation)	b (LBR)
3/4"	0.20	68.60	41.1
3/8"	0.08	-22.75	46.0
#4	0.04	8.58	43.4
#10	0.63	-56.15	47.2
#30	0.90	-67.50	48.1
#50	0.91	-93.95	52.0
#200	0.86	117.73	35.0

4.2.6. CSR and Gradation

Figure 4-30 shows the gradation curves and CSR for each RAP. The FHWA (Talbot) curve is also included. The process conducted for the LBR gradation comparison was repeated using CSR and gradation. Obtaining the lowest possible CSR is desirable. Inspection of the data in Figure 4-30 indicated that lower CSR may be associated with the proximity of the gradation curve and the maximum density curve.

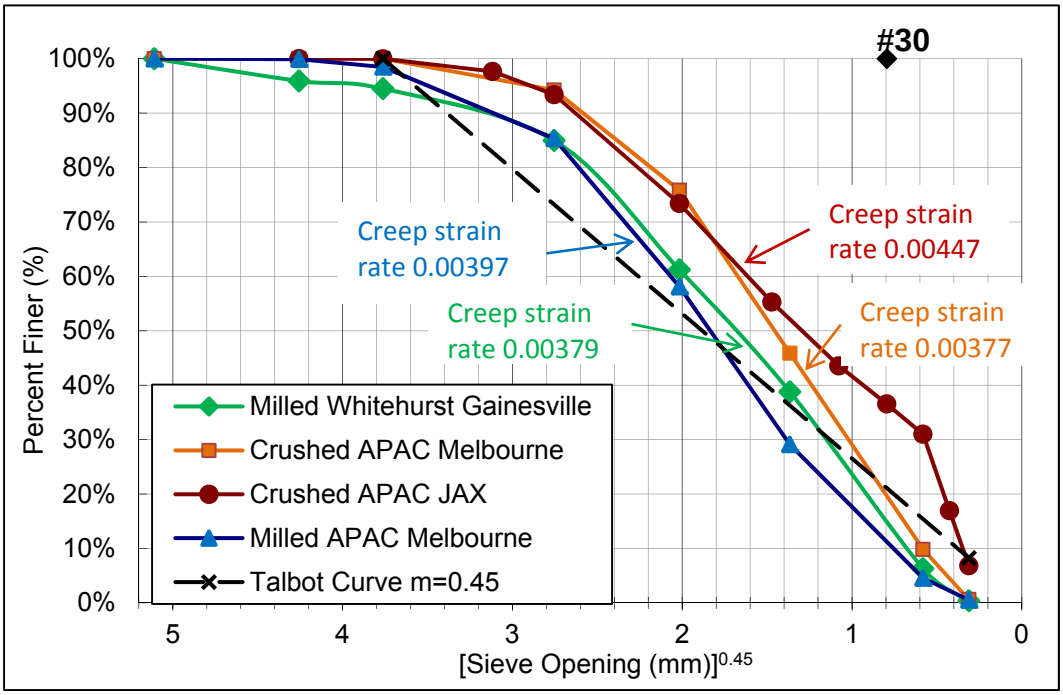

Figure 4-30: 0.45 Power Gradation Graphs of RAP with CSR and FHWA Curve

At the #30 sieve, the closer the gradation curves are to the FHWA curve, the lower the CSR. The APAC Melbourne crushed RAP gradation curve is closest to the FHWA curve for material passing the #30 sieve; it displayed the lowest CSR.

Figure 4-31and Figure 4-32 show CSR vs. percent passing difference between FHWA curve and the gradation curves respectively at #30 sieve and #50 sieve. These figures show that the smaller the difference between the FHWA curve and the RAP gradation curves at the #30 and #50 sieves, the smaller the creep.

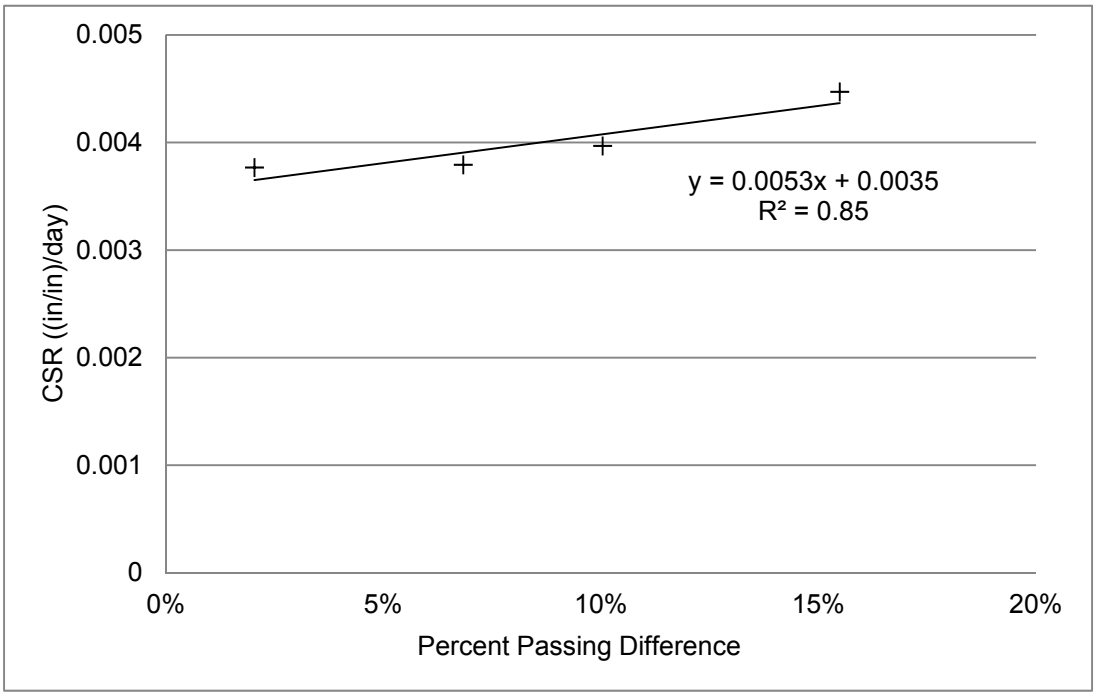

Figure 4-31: CSR vs. Percent Passing Difference between FHWA Curve and Gradation Curve at the #30 Sieve

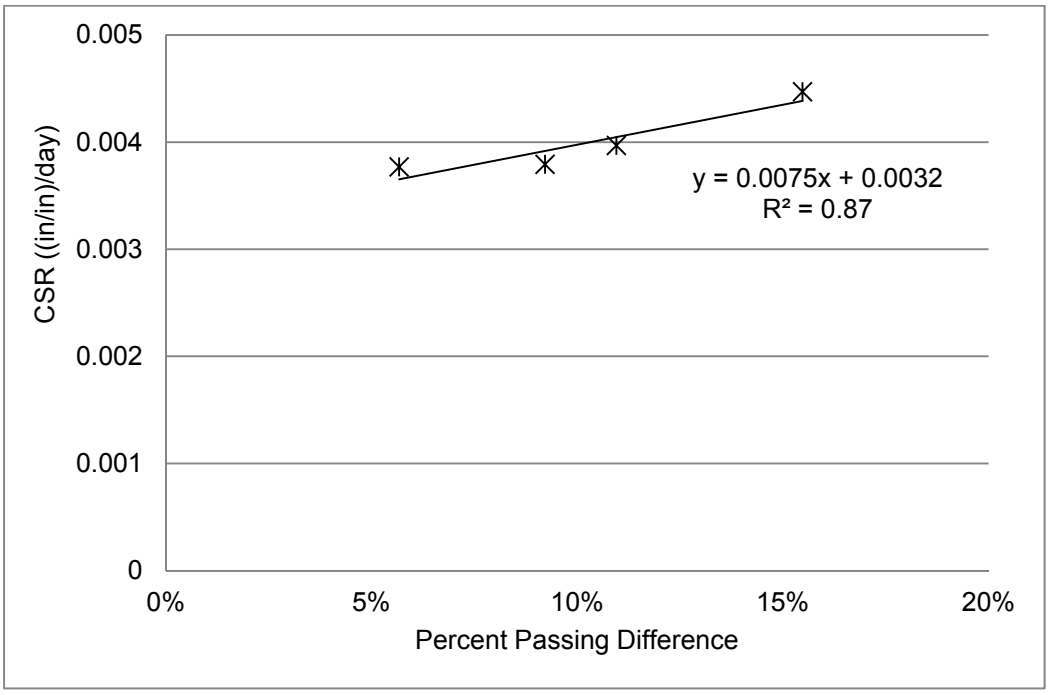

Figure 4-32: CSR vs. Percent Passing Difference between FHWA Curve and Gradation Curve at the #50 Sieve

Table 4-14 shows the linear regression coefficient at the sieve sizes used to develop Figure 4-30. Strong correlations were observed at the #'s 10, 30, 50 and 200 sieves. In this analysis it is desirable to have a positive slope so that as the grain size approaches the maximum density gradation there is less creep. Negative slopes exit for the ¾" sieve and the # 200 sieve; the high regression coefficient for the # 200 sieve does not imply a useful correlation. However, the positive slopes for the #10, #30, and #50 sieves implies that there is a useful relationship between the closeness of the percent passing at these sieves and the maximum density curve. The regression coefficients increase as the sieve sizes decrease implying that adding finer material would help decrease the CSR.

Table 4-14: Summary of Linear Regression Coefficients for CSR vs. Percent Passing Difference between FHWA Curve and Gradation Curve

Sieve	R^2	m (CSR/%)	b (CSR)
3/4"	0.21	-0.006	0.004
3/8"	0.13	0.002	0.004
#4	0.08	0.001	0.004
#10	0.69	0.005	0.004
#30	0.85	0.005	0.004
#50	0.87	0.008	0.003
#200	0.93	-0.010	0.005

Based on these regression values it was concluded that adding fines to the grain size distribution of RAP would decrease the CSR. Previous research did achieve improvements in LBR and creep of RAP/sand blends but this approach was not able to achieve an LBR close to 100 (Cosentino et al., 2003).

A plot of CSR change from unfractionated RAP was developed. This plot, shown in Figure 4-33, indicates that CSR for the Maximum Density Blends generally decrease. It also shows that the CSR decreases for both the Melbourne milled RAP and APAC crushed Jacksonville RAP for the Passing # 4 and Retained # 8 fractions. Based on this comparison graph, it was concluded that producing the maximum density blend of RAP would decrease the CSR.

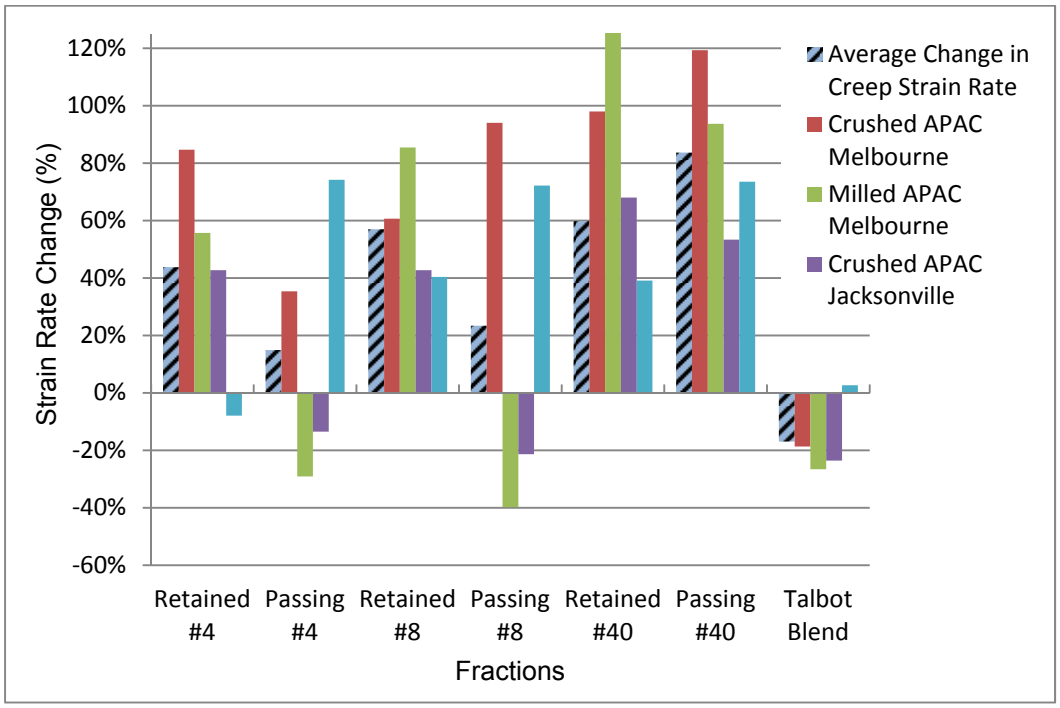

Figure 4-33: Strain Rate Change Compared to Unfractionated RAP

4.3. Blending RAP with High Quality Materials

The objective of this task was to determine whether blends of RAP with high quality FDOT approved base materials will meet the required soaked LBR strength of 40 for subbase or of 100 for base course while reducing creep to an acceptable level.

4.3.1. Gradation Analysis of Blends

Gradations of blends were mathematically computed from the experimental sieve analyses of each of the four different RAP and three different aggregate materials used in this study. The FDOT 2010 specification for graded aggregate base (Section 204-2) has upper and lower limits by screen size. The limerock base specification (Section 911-5.2) does not have specific sieve targets but requires that the material is "uniformly (well) graded." Figure 4-34 shows typical experimental gradation curves of limerock base and Melbourne Milled RAP along with the calculated 25%/75%, 50%/50%, and 75%/25% RAP/ limerock blends.

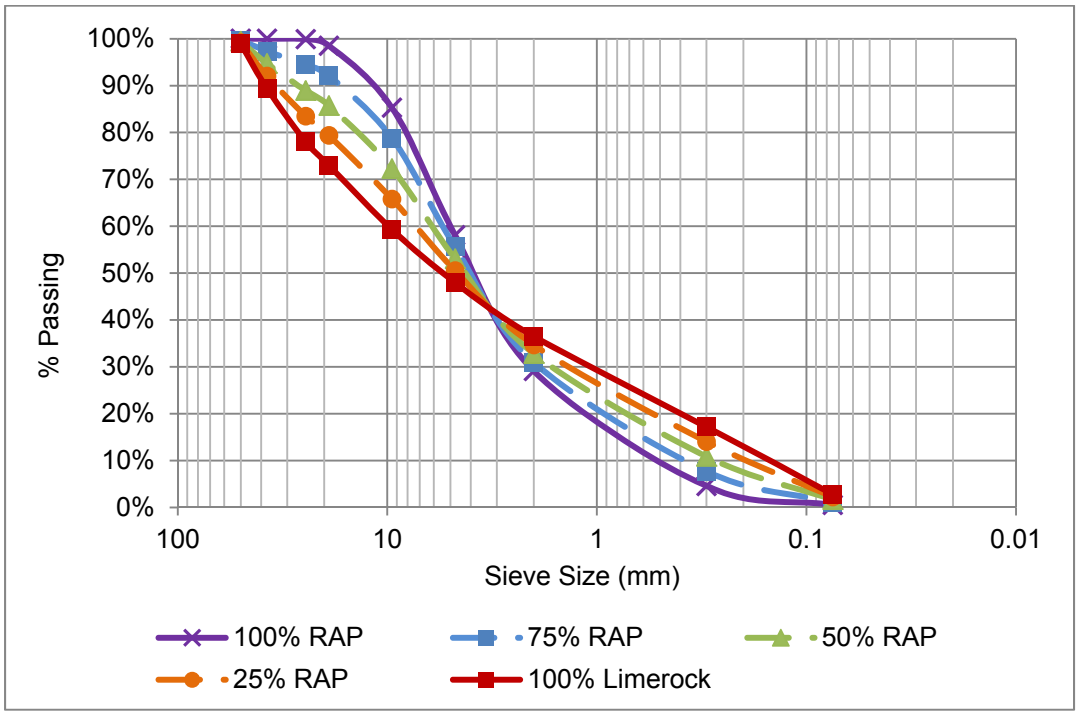

Figure 4-34: Gradation Curves for Limerock and Melbourne Milled RAP Calculated Blends

4.3.2. Milled Melbourne RAP

4.3.2.1. Moisture Density Unsoaked LBR Results

100% MRAP was compacted by the modified Proctor method (FM 5-521) at six target moisture contents from 2% to 12% at 2% intervals. This moisture-density test information is summarized in Figure 4-35. The actual moisture content of the compacted samples ranged from 2.9% to 11.2%. Dry densities ranged from 112.6 to 118.6 lb/ft^3 and the unsoaked LBR's ranged from 24.5 to 31.4.

As shown in Figure 4-35, there was no discernible peak in either the dry density or the unsoaked LBR. Both the 11% and 6% moisture contests produced peaks in density and unsoaked LBR; 6% was chosen for additional testing. Although there is an additional peak in dry density at around 11% moisture, water drained out of the mold during compaction indicating that all of the water was not absorbed by the sample so this moisture content was not considered. None of the 100% milled RAP specimens met the 100 soaked LBR specified for base material.

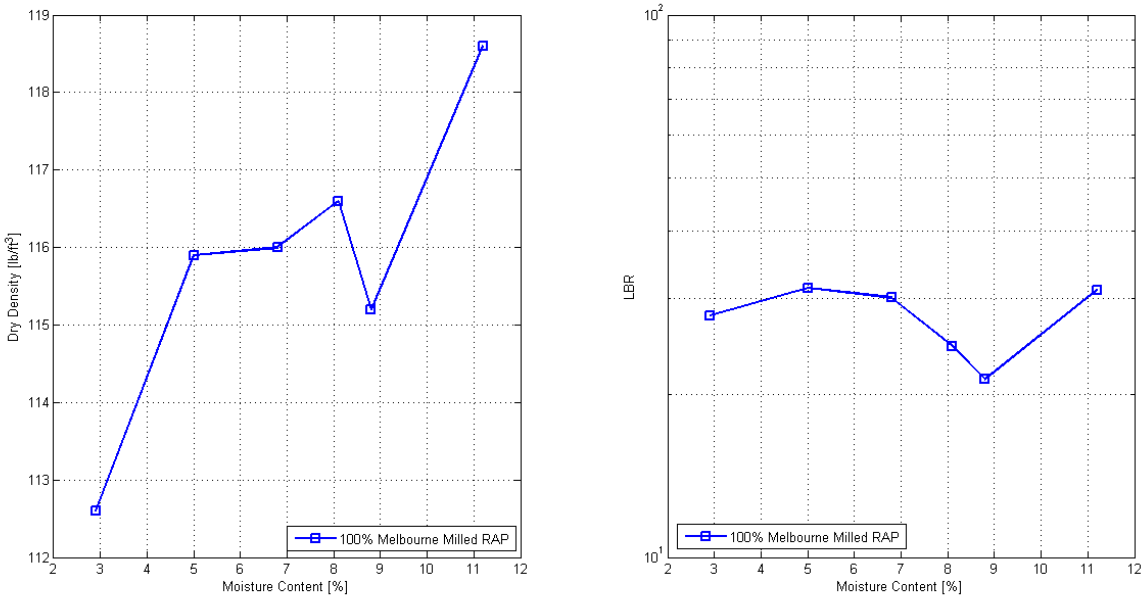

Figure 4-35: 100% Milled Melbourne RAP Optimum Moisture Content and Unsoaked LBR Plot

4.3.2.2. Confined Creep Testing

Six samples of 100% MRAP were compacted at a target moisture content of 6%. The samples actual moisture contents ranged from 5.4% to 7.2%, and the dry densities ranged from 115.2 to 123.2 lb/ft^3. Samples were grouped together into three two-specimen groups based on the dry densities. Each group was loaded to a different loading pressure, 25 psi, 50 psi, and 100 psi for a minimum of seven-days. The data was plotted as deflection versus time, deflection versus log(time), and creep compliance (ε/σ) versus log time. A linear trendline was applied to the semi-log plot of the creep compliance versus $\log_{10}$ of time. The slope of this line is the change of creep compliance per day. This slope is referred to as the Creep Compliance Rate ($\Delta D/\Delta \log(t)$) (CCR) and it ranged from 8.11×10^{-5} to 2.72×10^{-4} in/in/psi/day. CCR for each plot was calculated by computing the slope between the creep compliance at t=0.1 days and t=7 days divided by the log of Δt. After creep testing each sample was subjected to an unsoaked LBR test. The results are summarized in Table 4-15. CCR and LBR's for each pressure are similar, indicating that both vary with applied creep pressures. Figure 4-36 shows CCR$\times 10^{-5}$ and post-creep unsoaked LBR versus creep pressure. CCR decreases non-linearly while the unsoaked LBR increases linearly with creep pressure.

Table 4-15: Results of Confined Creep Tests on 100% MRAP

Target Moisture Content (%)	Actual Moisture Content (%)	Dry Density (lb/ft^3)	Loading Pressure (psi)	CCR (in/in/ psi/day)	Post-Creep Unsoaked LBR
6.0	5.6	115.2	25	$2.72x10^{-4}$	55
6.0	5.7	116.4	25	$2.58x10^{-4}$	50
Average		115.8	25	$2.65x10^{-4}$	53
6.0	6.0	117.8	50	$1.43x10^{-4}$	75
6.0	6.9	118.7	50	$1.28x10^{-4}$	72
Average		118.3	50	$1.36x10^{-4}$	74
6.0	7.2	118.8	100	$8.54x10^{-5}$	97
6.0	5.4	123.2	100	$8.11x10^{-5}$	99
Average		128.6	100	$8.33x10^{-5}$	98

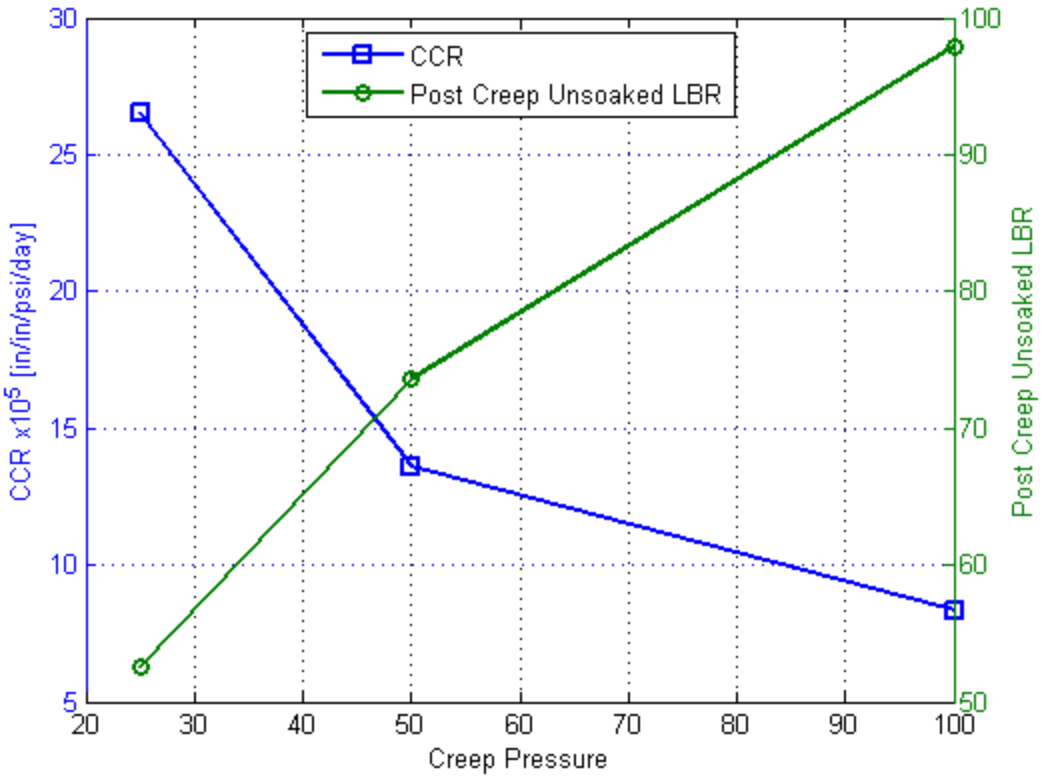

Figure 4-36: CCR and Post-Creep Unsoaked LBR vs. Creep Pressure for 100% MRAP

4.3.3. Limerock Blends

4.3.3.1. Moisture Density Unsoaked LBR Results

Limerock MRAP blends were prepared with 100% limerock, 25% MRAP/75% LR, 50% MRAP/50% LR, and 75% MRAP/25% LR. Batches of six samples were compacted for each blend. Samples were compacted based on modified Proctor energy at target moisture contents varying from 2% to 12% in 2% intervals and then subjected to unsoaked LBR tests. The results of these tests are presented in Figure 4-37.

A well-defined Proctor peak was evident for the 100% limerock and the 25% MRAP/75% limerock blends. For the other blends an S-shaped curve was produced. This type of curve was described by Lambe and Whitman (1969) as typical of cohesionless soils. For these blends no true optimum moisture content is achieved. Moisture contents were chosen by considering both moisture-density and LBR-density plots.

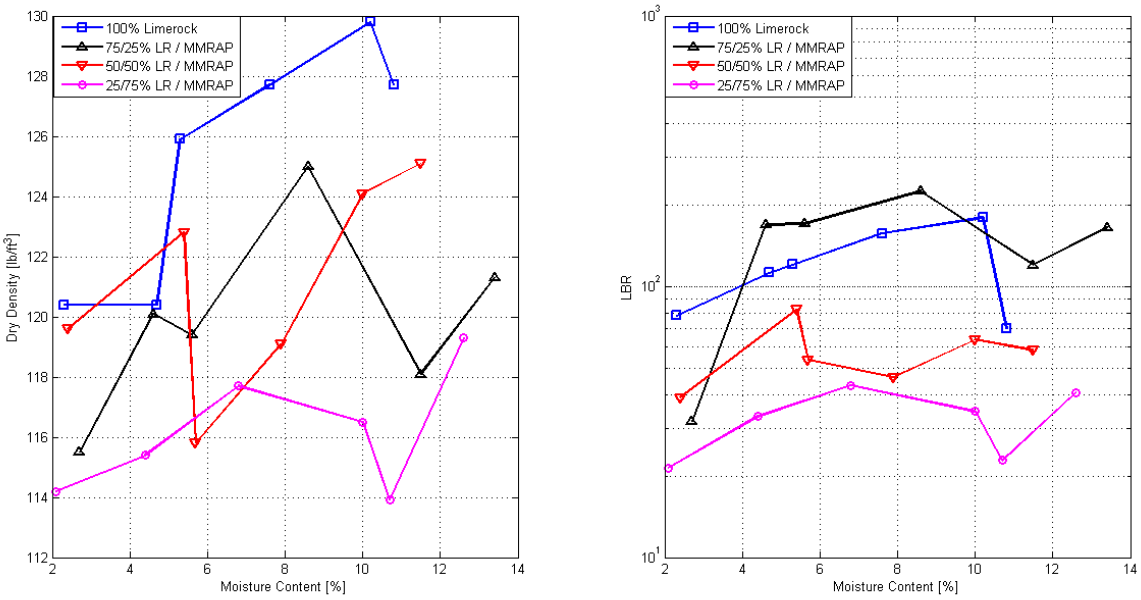

Figure 4-37: Moisture Density and Unsoaked LBR vs. Moisture Content of Limerock Blends

The optimum moisture content for 100% limerock was 10% at a dry density of 128.8 lb/ft^3 and an unsoaked LBR of 180. The 25% MRAP/ 75% LR had an optimum moisture content of 8.5% at a dry density of 125.0 lb/ft^3 and an unsoaked LBR of 225. The increased unsoaked

LBR over that of 100% limerock is attributed to the variation of the LBR test. The 50%/50% blend moisture-density plot S-shaped curve had an initial peak near 6% moisture and second peak above 10% moisture. This second peak produced a lower LBR, and samples had water draining from the molds during compaction and subsequent testing. 6% moisture content was chosen as optimum for future testing. The 50%/50% blend had an optimum moisture content of 6.0%, a dry density of 122.8 lb/ft^3, and an unsoaked LBR of 82. This same S-shaped double peak curve was produced for the 75% MRAP/25% limerock blend. The lower peak density moisture content of 7% was chosen for future testing. The 75% MRAP blend had an optimum moisture content of 7.0% a dry density of 117.7 lb/ft^3, and an unsoaked LBR of 43. A summary of MRAP/limerock blends is presented in Table 4-16. These moisture contents were used to compact creep samples and additional testing samples. These results show that a 25% MRAP/75% limerock blend had potential to meet the 100 soaked LBR specified for base course. Soaked LBR tests were conducted on this blend.

4.3.3.2. Confined Creep Testing

Results of confined creep testing conducted on the varying blends are summarized in Table 4-16 and Figure 4-38. The CCR decreased with increased applied pressure and increased with increasing amounts of RAP in the blend. The log-log linear relationship seen in Figure 4-38 can be used to estimate the CCR for different loading pressures.

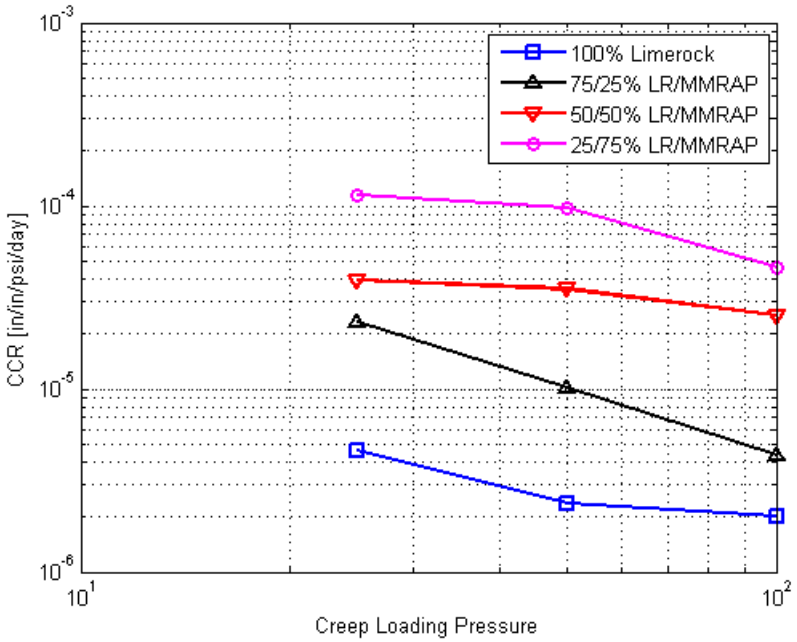

Figure 4-38: Limerock Blends CCR vs. Creep Loading Pressure (log – log plot)

Table 4-16: Summary of Optimum Moisture Contents for Blends of Limerock

Blend	Optimum Moisture Content (%)	Un-soaked LBR	Dry Density (lb/ft^3)	Creep Loading Pressure (psi)	Average CCR (in/in/ psi/day)	Average Post-Creep Unsoaked LBR
100% Limerock	10.0	179.7	128.8	N/A	N/A	N/A
			128.6	25	4.62×10^{-6}	140.7
			129.3	50	2.36×10^{-6}	153.8
			130.9	100	2.02×10^{-6}	166.1
25% MRAP/ 75% LR	8.5	225.3	125.0	N/A	N/A	N/A
			122.8	25	2.32×10^{-5}	162.8
			125.1	50	1.01×10^{-5}	183.5
			127.6	100	4.34×10^{-6}	206.8
50% MRAP/ 50% LR	6.0	82.4	122.8	N/A	N/A	N/A
			114.3	25	3.92×10^{-5}	84.0
			120.1	50	3.53×10^{-5}	136.6
			122.0	100	2.51×10^{-5}	158.5
75% MRAP/ 25% LR	7.0	43.2	117.7	N/A	N/A	N/A
			112.7	25	1.15×10^{-4}	78.4
			115.2	50	9.75×10^{-4}	93.5
			119.5	100	4.46×10^{-5}	131.6

As shown in Figure 4-39 adding milled RAP to limerock generally decreased the unsoaked LBR. Applying higher pressure increased the unsoaked LBR in an approximately linear fashion.

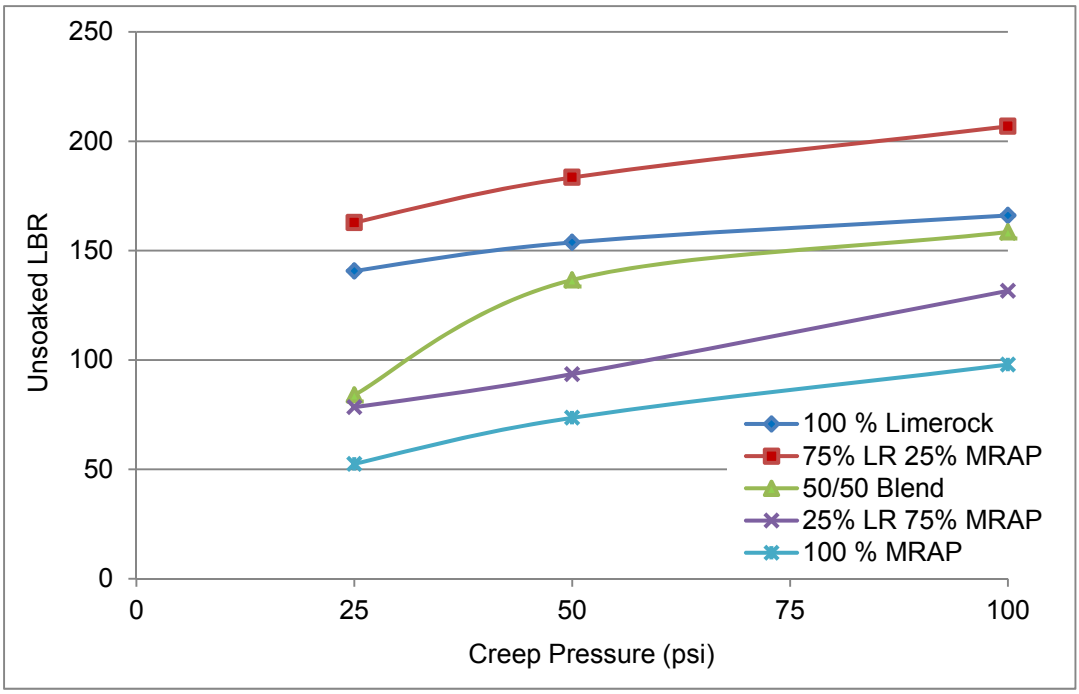

Figure 4-39: Limerock Blends Unsoaked LBR vs. Creep Loading Pressure

4.3.4. Cemented Coquina Base (CCB) Blends

4.3.4.1. Moisture Density Unsoaked LBR Results

CCB/MRAP blends were prepared with of 25, 50, 75 and 100% cemented coquina. Batches of six samples were compacted for each blend. Samples were prepared based on modified Proctor energy at target moisture contents varying from 2% to 12% in 2% intervals and then subjected to unsoaked LBR tests. The results of these tests are presented in Figure 4-40.

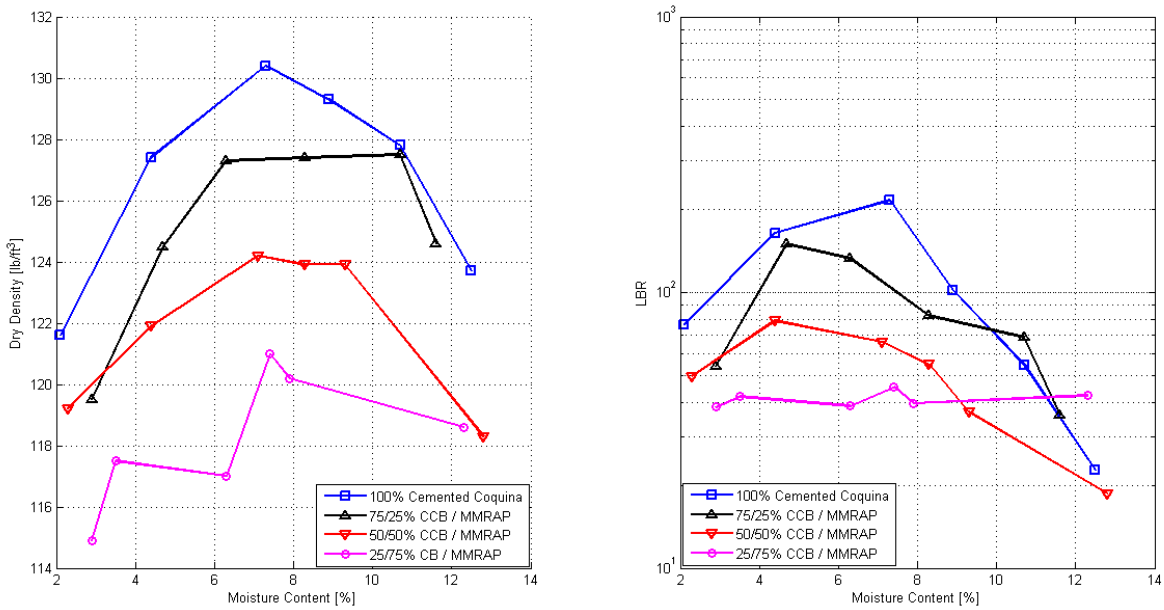

Figure 4-40: Dry Density and Unsoaked LBR vs. Moisture Content of Cemented Coquina Blends

Proctor moisture-density curves with well-defined peaks were produced for three of the four cemented coquina blends. The 75% MRAP/25% cemented coquina blend produced an S-shaped curve with a slight peak near 4% and a more pronounced peak near 8% moisture content. The more pronounced peak was used for the remaining testing. The optimum moisture content for 100% cemented coquina was 7.0% with a dry density of 130.4 lb/ft^3, and an unsoaked LBR of 216. The 25% MRAP/75% cemented coquina blend had an optimum moisture content of approximately 5.5%, a dry density of 124.5 lb/ft^3, and an unsoaked LBR of 150. The 50%/50% CCB/MRAP blend had an optimum moisture content of 7.0%, the dry density was 121.5 lb/ft^3, and the unsoaked LBR was 79. The blend of 75% MRAP/25% CCB had an optimum moisture content of 7.5%, a dry density of 120.2 lb/ft^3, and an unsoaked LBR 40. These optimum moisture contents were used to compact creep sample and additional testing samples. CCB/MRAP results are summarized in Table 4-17. The unsoaked LBR of 150 for the 25% MRAP/75% CCB blend indicates that it has potential to meet the base course specification. Soaked LBR tests were done on this blend.

Table 4-17: Summary of Optimum Moisture Contents for Blends of Cemented Coquina

Blend	Optimum Moisture Content (%)	Un soaked LBR	Dry Density (lb/ft^3)	Creep Loading Pressure (psi)	Average CCR (in/in/ psi/day)	Average Post-Creep Unsoaked LBR
100% Cemented Coquina	7.0	216.0	130.4	N/A	N/A	N/A
			126.3	25	9.09×10^{-6}	196
			127.1	50	2.66×10^{-6}	171
			129.4	100	9.43×10^{-7}	263
25% MRAP/ 75% CCB	5.5	150.0	124.5	N/A	N/A	N/A
			124.2	25	1.94×10^{-5}*	158
			125.7	50	7.44×10^{-6}*	170
			126.3	100	5.65×10^{-6}*	212
50% MRAP/ 50% CCB	7.0	79.0	121.5	N/A	N/A	N/A
			122.1	25	5.13×10^{-5}	99
			123.2	50	3.05×10^{-5}	105
			124.3	100	1.86×10^{-5}	127
75% MRAP/ 25% CCB	7.5	39.7	120.2	N/A	N/A	N/A
			115.8	25	1.99×10^{-4}	57
			118.3	50	1.09×10^{-4}	83
			121.0	100	5.94×10^{-5}	121
* Data calculated from 0.01 days to 6.9 days						

4.3.4.2. Confined Creep Tests

Table 4-17 and Figure 4-41 show the results of confined creep testing of the blends. The cemented coquina blend results follow the same general trends seen with limerock blends. The CCR decreases with increasing loading pressure and the more RAP, the higher the CCR.

As shown in Figure 4-42 adding milled RAP to cemented coquina decreased the unsoaked LBR. Applying higher pressures increased the unsoaked LBR. The 25% MRAP/75% cemented coquina blend produced unsoaked LBR values comparable to 100% cemented coquina.

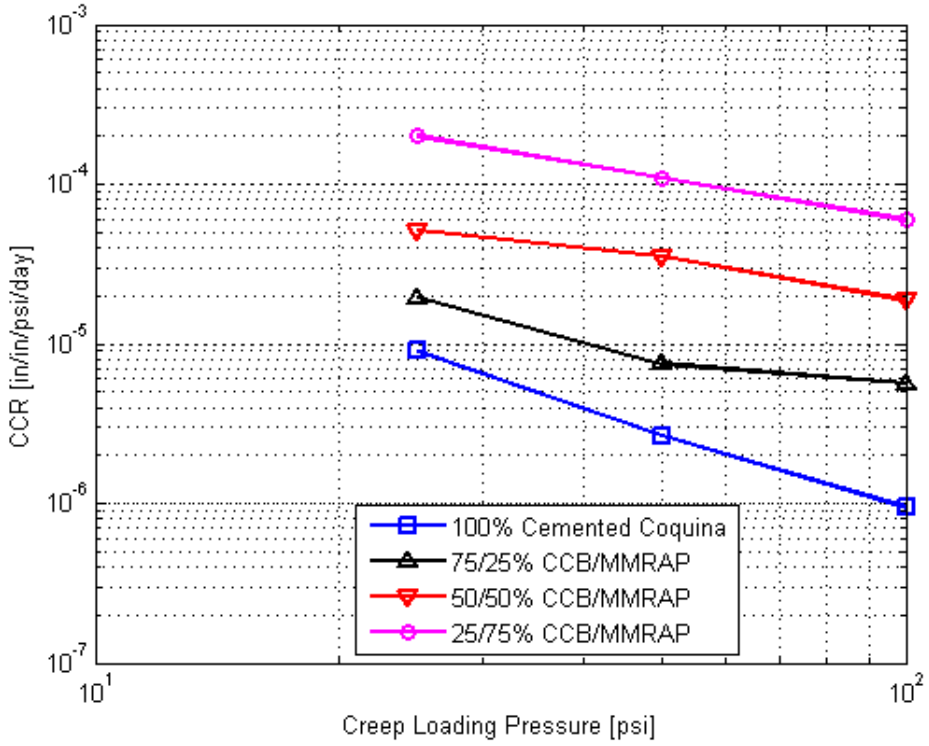

Figure 4-41: Cemented Coquina Blends CCR vs. Creep Loading Pressure (log – log plot)

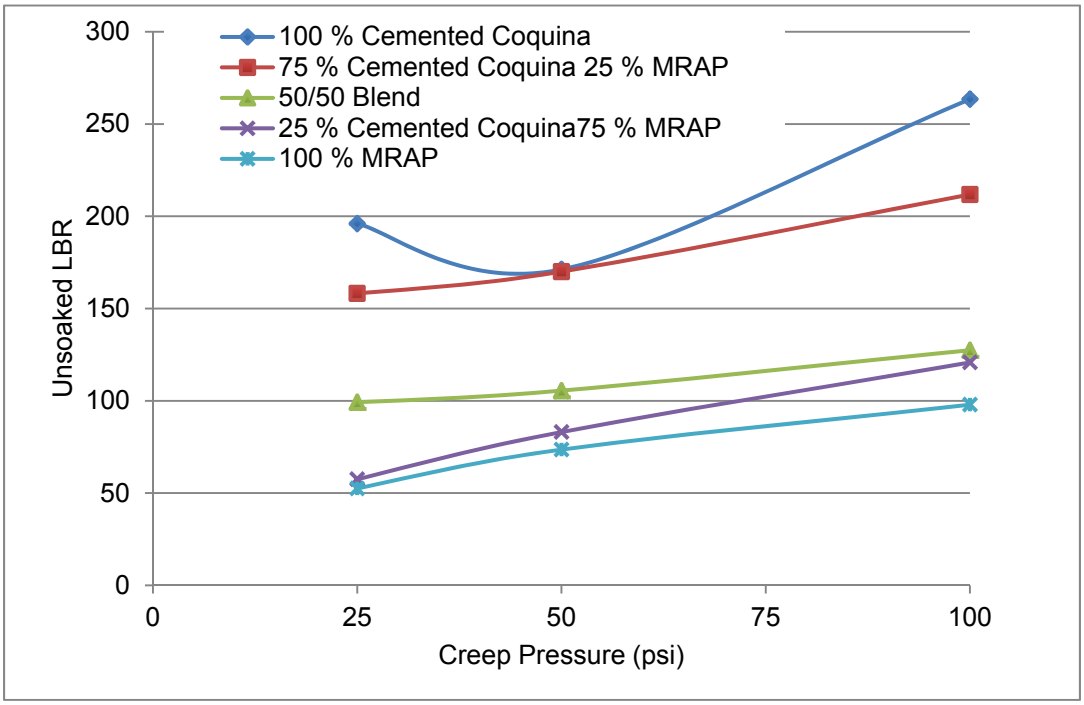

Figure 4-42: Cemented Coquina Blends Unsoaked LBR vs. Creep Loading Pressure

4.3.5. RCA Blends

4.3.5.1. Moisture Density Unsoaked LBR Results

Specimens with 100% reclaimed concrete and blends with 75%, 50%, and 25% MRAP were tested. Batches of six samples were compacted for each blend. Samples were compacted based on modified Proctor energy at target moisture contents in 2% intervals, and then subjected to unsoaked LBR tests. The results of testes tests are presented in Figure 4-43. None of the moisture-density plots from the reclaimed concrete testing produced Proctor curves with well-defined peaks. A substantial increase in density occurred for the 100% reclaimed concrete near 17%. This moisture content did not coincide with the peak LBR; 15% moisture content was selected for additional testing.

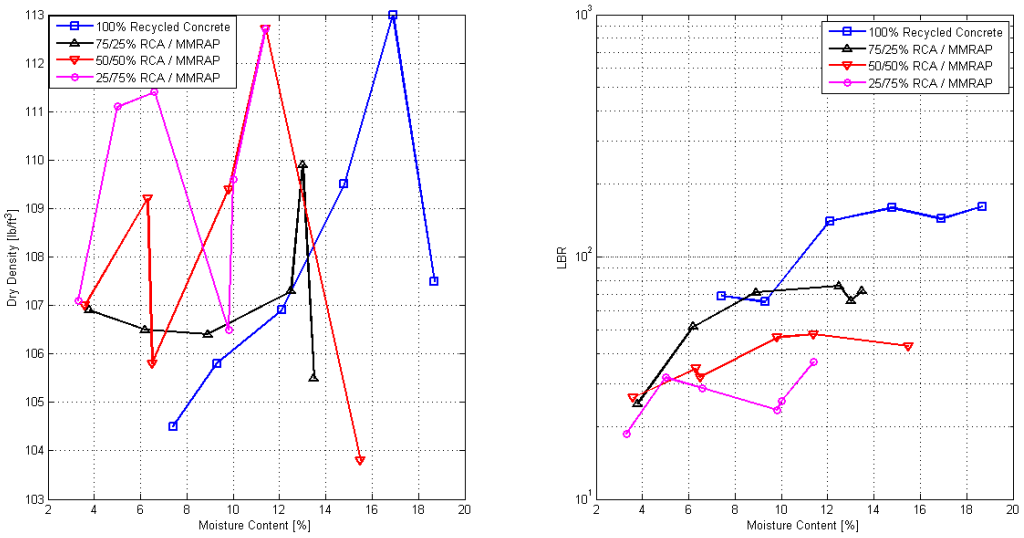

Figure 4-43: Dry Density and Unsoaked LBR vs. Moisture Content of RCA Blends

The testing moisture content for 100% RCA was 15.0% with a dry density of 109.5 lb/ft^3, and an unsoaked LBR of 159. The 25% MRAP/75% RCA blend had a moisture content of 10.0%, a dry density of 107.3 lb/ft^3, and an unsoaked LBR of 76. The 50%/50% MRAP/RCA blend had a moisture content of 10%, a dry density of 109.4 lb/ft^3, an unsoaked LBR of 48. The 75%/25% blend of MRAP/RCA had a moisture content of 5.0%, a dry density of 111.4 lb/ft^3, and an unsoaked LBR of 30. Reclaimed concrete/MRAP blend results are presented in Table

4-18. These testing moisture contents were used to compact creep samples. Test results show that blends of RCA with RAP would not have a high enough strength to be used as a base material as they were unable to achieve an unsoaked LBR greater than 100. No soaked LBR testing was done on these blends.

Table 4-18: Summary of Optimum Moisture Contents for Blends of RCA

Blend	Optimum Moisture Content (%)	Un soaked LBR	Dry Density (lb/ft^3)	Creep Loading Pressure (psi)	Average CCR (in/in/ psi/day)	Average Post-Creep Unsoaked LBR
100% RCA	15.0	159.3	109.5	N/A	N/A	N/A
			107.0	25	7.09×10^{-7}*	197
			109.2	50	7.03×10^{-6}	249
			109.3	100	3.12×10^{-6}	301
25% MRAP/ 75% RCA	10.0	76.0	107.3	N/A	N/A	N/A
			107.6	25	1.38×10^{-5}	117
			106.0	50	9.47×10^{-6}	125
			107.6	100	3.72×10^{-6}	143
50% MRAP/ 50% RCA	10.0	47.9	109.4	N/A	N/A	N/A
			106.3	25	3.28×10^{-5}	58
			110.1	50	2.04×10^{-5}	104
			112.2	100	1.77×10^{-5}	110
75% MRAP/ 25% RCA	5.0	30.2	111.4	N/A	N/A	N/A
			108.2	25	1.73×10^{-4}	49
			109.2	50	1.11×10^{-4}	58
			111.0	100	6.24×10^{-5}	74
* Outlier, not used						

4.3.5.2. Unconfined Creep Testing

The results of the creep tests for RCA are presented in Table 4-18 and Figure 4-44. CCR's of reclaimed concrete produced the same trends seen in limerock and cemented coquina: decreasing with loading pressure, and increasing with RAP content. The data point for 100% reclaimed concrete at 25 psi is lower than the others because it is an average of two slope values, one of which was negative. Eliminating the negative value only increases the CCR to about $1.5x10^{-5}$ which still results in a nonlinear trend. For these reasons, this data point was not used.

The reclaimed concrete had a very flat creep curve and very small difference in deflection between 0.01 days and 7 days.

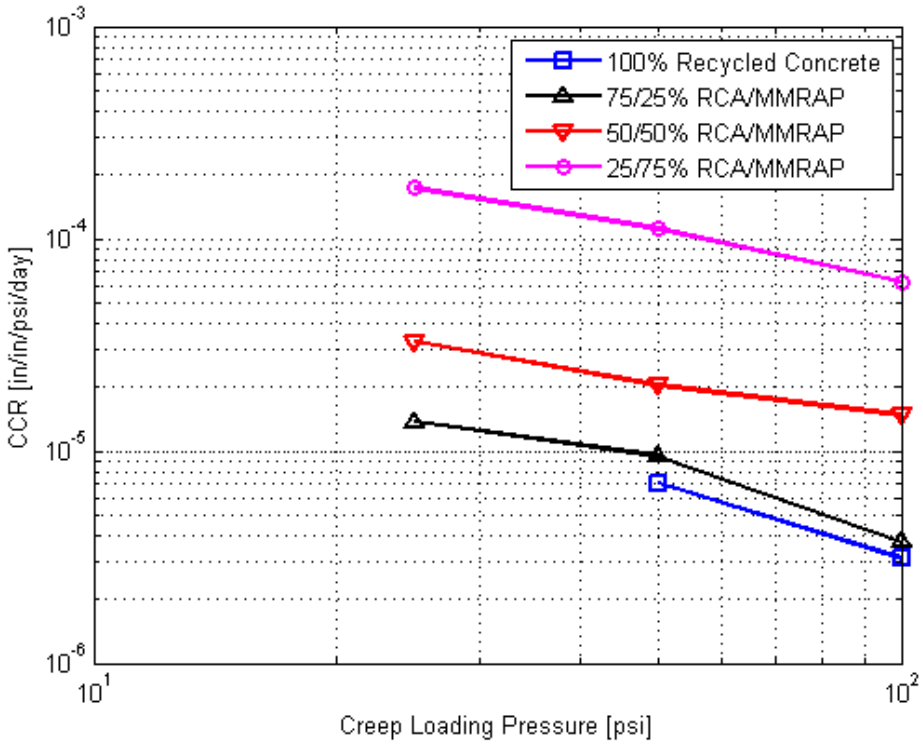

Figure 4-44: RCA Blends CCR vs. Creep Loading

As shown in Figure 4-45 adding milled RAP to RCA reduced the unsoaked LBR. Increasing creep pressure increased the post-creep unsoaked LBR for all blend percentages.

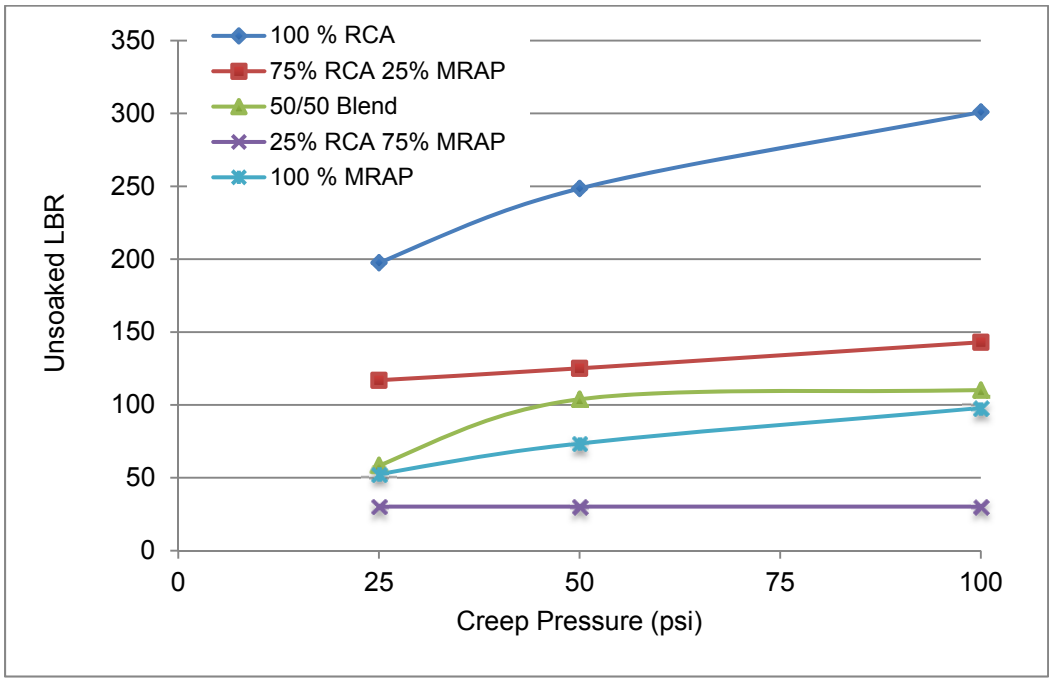

Figure 4-45: RCA Blends Unsoaked LBR vs. Creep Pressure

4.3.6. Summary of Effects of Blending

4.3.6.1. Moisture-Density Summary

The modified Proctor compaction data for the limerock, cemented coquina and reclaimed concrete blends at high RAP contents produced S-shaped plots without clear peak or optimum values. The limerock blends produced the plots for the 50%/50% and 75%/25% MRAP/limerock blends. The cemented coquina blends produced these plots only for the 75% MRAP/25% CCB blends. The reclaimed concrete blends all produced S-shaped results. Modified Proctor may not be an accurate method to evaluate moisture-density for RAP blends with the three base course materials tested.

4.3.6.2. Limerock Bearing Ratio Summary

The addition of milled Melbourne RAP decreased the unsoaked LBR of all of the base materials. Unsoaked LBR values for all three virgin base materials are plotted against RAP content in Figure 4-46. Blends of 25% RAP with limerock and cemented coquina had high enough unsoaked LBR values to indicate that they may exceed a soaked LBR of 100. All tested blends of RAP and reclaimed concrete had unsoaked LBR values below 100 so they will not be

able to achieve the soaked LBR necessary for base course material. Soaked LBR testing was conducted on blends with potential to reach a soaked LBR of 100.

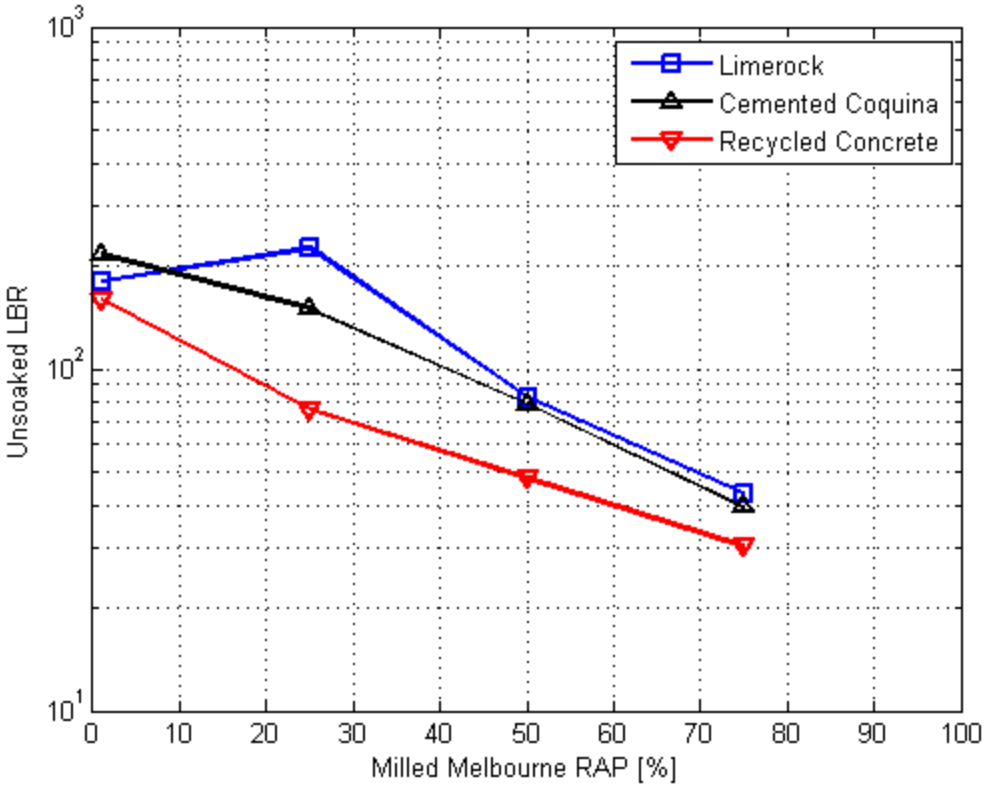

Figure 4-46: Unsoaked LBR vs. Percent Milled Melbourne RAP for Select Base Material

4.3.6.3. Confined Creep Summary and Acceptable Creep Definition

As the loading pressure increases from 25 to 100 psi the average CCR decreases for all materials tested. As RAP content increase from 25% to 75% the average CCR increases indicating that more creep will occur.

Table 4-19 is a summary of the LBR and 30 year projected creep deformations for a 10-inch base course subjected to a creep pressure of 25 psi. Using 3.0 % triaxial creep strain determined by Viyanant et al., (2007) as failure, 30 year deformations were estimated from the creep tests and compared to a maximum allowable deformation of 0.3 inches in the 10-inch base material. Both unsoaked and soaked LBR data is included. If the unsoaked LBR's were below 100 the soaked testing was not conducted.

Table 4-19 shows that LBR's are below 100 for blends with 50 % or more RAP. It also shows that creep may be acceptable for a majority of the blends if the 3 % failure criterion is valid. In conclusion, RAP blends should be limited to a maximum of 25 % RAP with these high quality materials.

Table 4-19: Summary of LBR and Creep Projections for Blending with High Quality Base Materials

Description		Unsoaked LBR	Acceptable	Soaked LBR	Acceptable	10 in base, 25 psi	
						30 Year Deformation	Acceptable
Limerock	**MRAP**						
100	0	180	Yes	162	Yes	0.08	Yes
75	25	225	Yes	99	No	0.12	Yes
50	50	82	No	55	No	0.15	Yes
25	75	43	No	NP	No	0.28	Yes
0	100	31	No	NP	No	0.56	No
Cemented Coquina	**MRAP**						
100	0	216	Yes	63	No	0.07	Yes
75	25	150	Yes	93	No	0.08	Yes
50	50	79	No	NP	No	0.17	Yes
25	75	40	No	NP	No	0.44	No
0	100	31	No	NP	No	0.56	No
Recycled Concrete Aggregate	**MRAP**						
100	0	159	Yes	162	Yes	0.07	Yes
75	25	76	No	NP	No	0.08	Yes
50	50	48	No	NP	No	0.13	Yes
25	75	30	No	NP	No	0.43	No
0	100	31	No	NP	No	0.56	No

NP - Soaked LBR test not performed since Unsoaked LBR was below 100

4.4. Asphalt Content Modification

Figure 4-47 shows the unsoaked LBR of 100% Melbourne milled RAP, 100% limerock, and five different blends of the two materials. Asphalt contents were calculated based on the blend percentages with limerock having zero asphalt content and Melbourne Milled RAP having 5.42% asphalt content. These specimens were produced at optimum moisture content and tested while moist at ambient temperature (air cured) rather than oven cured. These LBR values are expected to be closer to but still higher than soaked LBR values.

Only the 25% MRAP/75% blend produced an unsoaked LBR over 100. There appears to be a large change in unsoaked LBR between a blend with an asphalt content of 1.36% (25% MRAP) and a blend with an asphalt content of 2.17% (40% MRAP).

Figure 4-48 shows similar unsoaked LBR versus asphalt content data for oven-cured specimens. There were no oven-cured 45% and 40% MRAP blends in this round of testing. The same general trends are seen in the oven-cured specimens but the unsoaked LBR values are approximately two times those of the specimens prepared and tested at moist at ambient temperature. These LBR values are approximately 2 to 2.5 times higher than the soaked LBR values for these same materials. Once again the most rapid decrease occurs between the 1.36% asphalt content (25% MRAP) and the 2.72% asphalt content (50% MRAP).

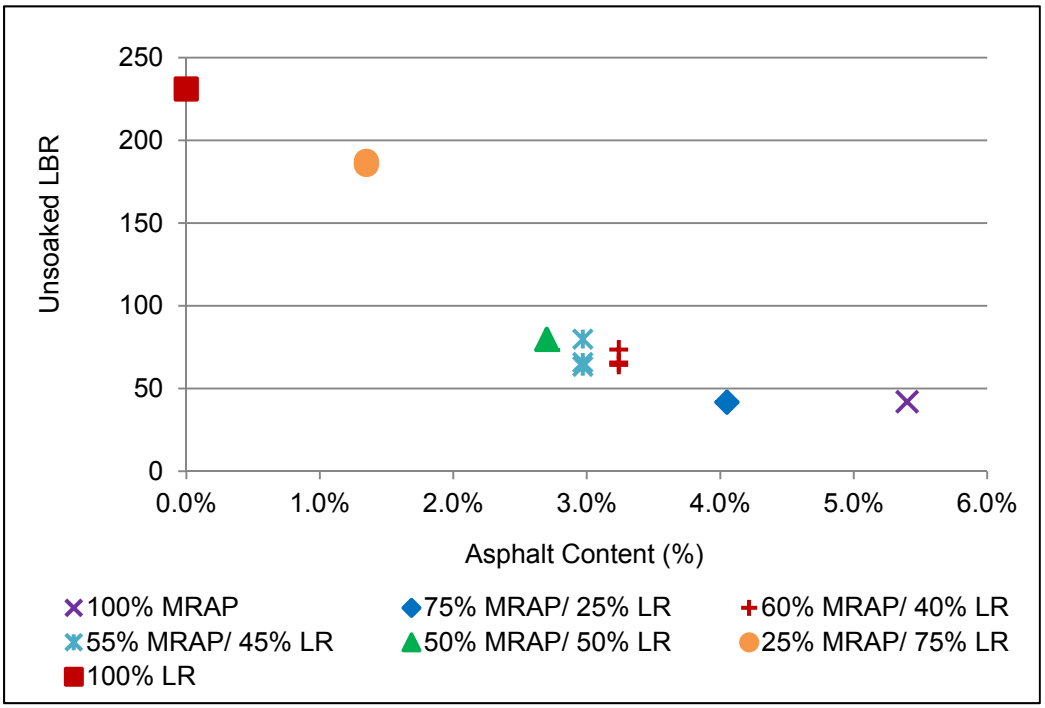

Figure 4-47: Unsoaked LBR versus Asphalt Content for Air Cured Specimens

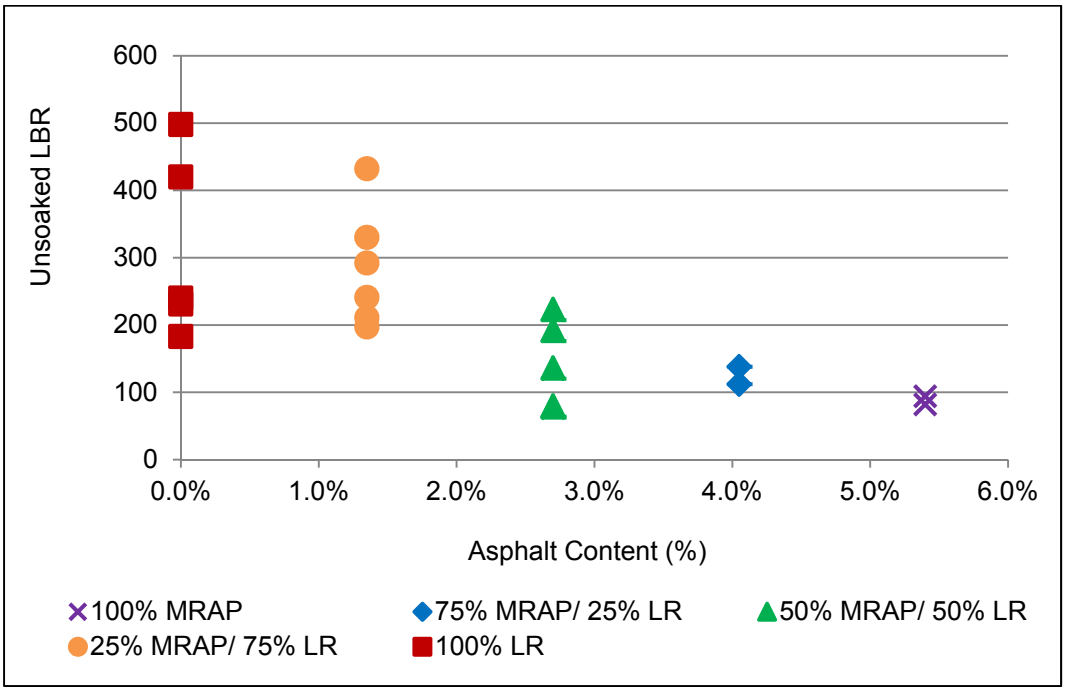

Figure 4-48: Unsoaked LBR versus Asphalt Content for Oven-cured Specimens

As shown in Figure 4-49. RAP blends with high quality aggregates showed similar LBR trends. This figure also shows an increase in variability in LBR near 3 % asphalt. Asphalt contents of 100% RAP throughout Florida typically varied between approximately 5% and 7% (Sandin, 2008).

As shown in Figure 4-50 the projected 30-year creep deformations show increasing variability near 3 % asphalt content. In conclusion, blending RAP with base course material is a more practical way to adjust the asphalt content of a blended RAP base than attempting to finely adjust the asphalt content of the RAP. Therefore, the current FDOT RAP Base 283 specification should be changed to eliminate the requirement for any minimum asphalt content. Section 283-2 currently states that "The average asphalt content of the six stockpile samples must be 4 % or gr3eater with no individual result below 3 ½ %." (FDOT, 2010).

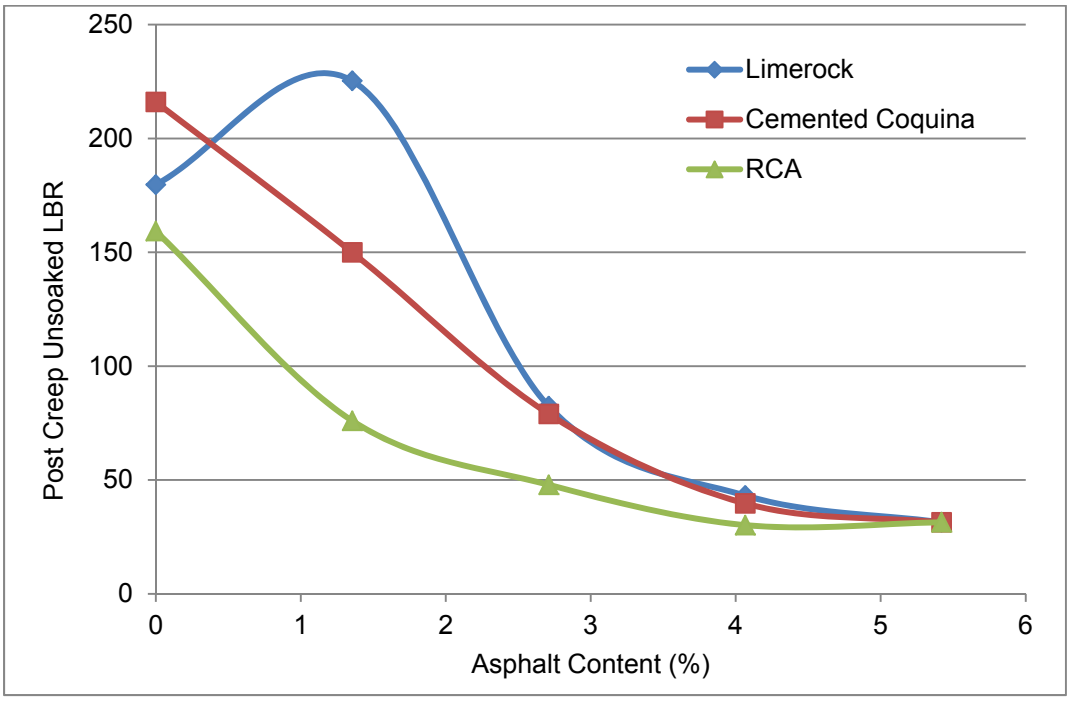

Figure 4-49 Unsoaked Post-Creep LBR versus Asphalt Content for High Quality Base Materials

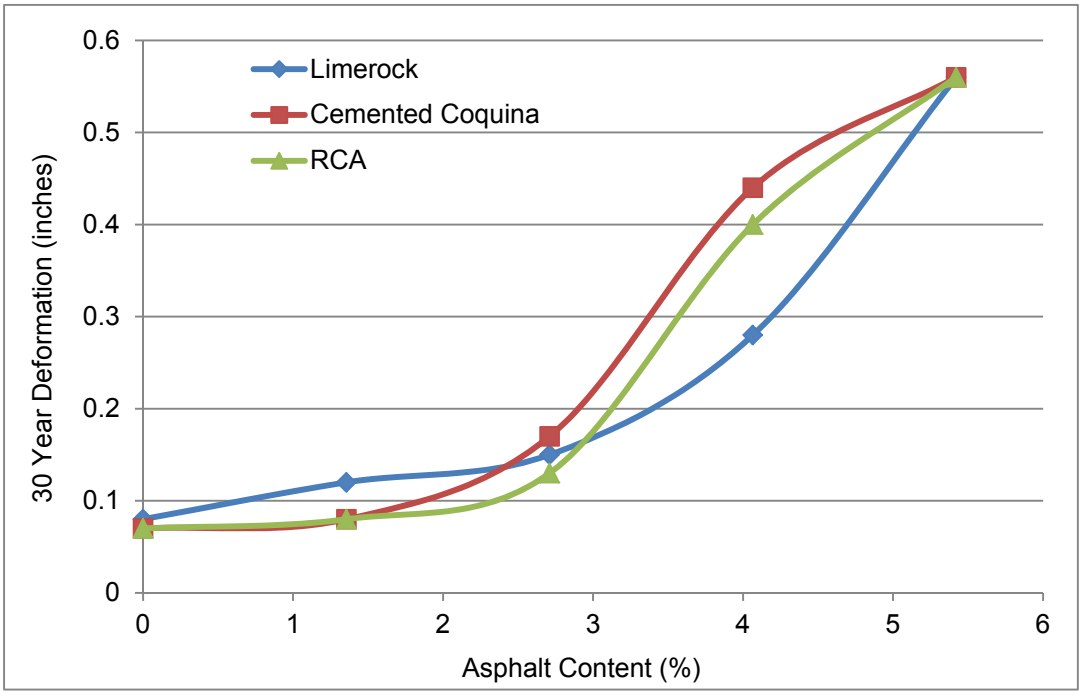

Figure 4-50 Predicted 30-year Deformation of 10-inch Base versus Asphalt Content for High Quality Base Materials

4.5. Compaction Improvements

The compaction evaluation of 100% RAP included modified Proctor, vibratory, and gyratory compaction methods. Specimen density and unsoaked LBR strength were compared. Selected specimens were evaluated using unconfined compressive and IDT's to evaluate strength.

4.5.1. Compaction Results - Density

4.5.1.1. Modified Proctor

The moisture-density relationship for modified Proctor compaction is shown in Figure 4-51. As noted in Chapter 2, RAP generally does not have a well-defined optimum moisture density curve.

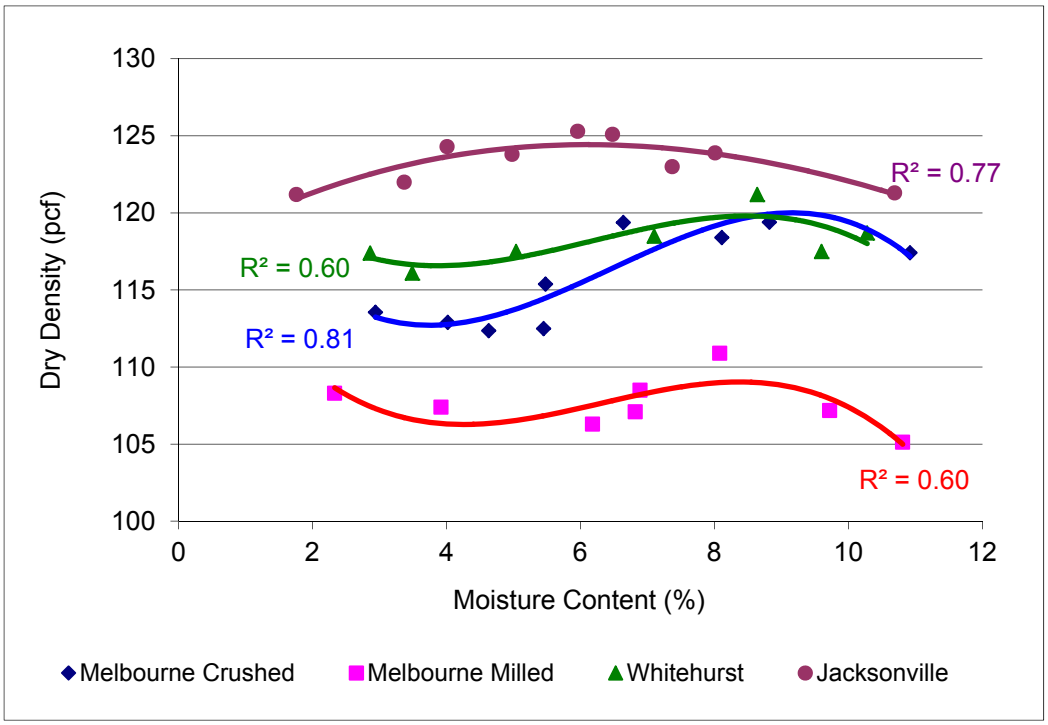

Figure 4-51: Moisture Density Relationship from Modified Proctor Test

Cohesionless granular soils have been shown to follow an 'S-curve' type of moisture-density relationship. Initial high densities at low moisture contents are a result of capillary action causing bulking (Lambe and Whitman, 1969). Three of the four RAP sources produce this 'S-curve'. RAP sampled from APAC Jacksonville does follow the typical moisture density

parabola probably due to the high amount of fine material passing the #200 sieve which may produce cohesive effects.

Visual inspections revealed that APAC Melbourne RAP was primarily composed of limestone aggregate and only minor amounts of granite. APAC Melbourne crushed RAP yielded higher densities than the milled RAP. RAP sampled from Whitehurst contained more granite aggregates mixed with limerock. Whitehurst milled RAP yielded higher densities than APAC Melbourne crushed RAP at lower moisture content, but yielded similar densities at higher moisture contents. RAP from APAC Jacksonville yielded the highest densities of any of the samples tested due to the higher fines content and higher specific gravity of the predominantly granite aggregate.

Table 4-20: Modified Proctor Summary

Source	Dry Density		Optimum Moisture Content (%)	% Fines	Specific Gravity
	Minimum (pcf)	Maximum (pcf)			
APAC Melbourne Crushed RAP	112.4	119.4	n/a	0.60	2.51
APAC Melbourne Milled RAP	105.1	110.9	n/a	0.50	2.52
Whitehusrt Milled RAP	116.1	121.2	n/a	0.38	2.58
APAC Jacksonville Crushed RAP	121.2	125.3	6.1	6.82	2.60
n/a = optimum not available due to “S” shaped moisture-density curves					

Table 4-20 is a summary of the modified Proctor testing from the fours sources, with the percent passing the number 200 sieve and Specific Gravity data included. When comparing whether crushed or milled material would yield higher densities, only comparisons between two similar aggregates can accurately be made. Between the two samples of RAP from Melbourne, which both contain similar aggregate constituents, crushed RAP yielded higher densities than milled RAP. Previous research has indicated that crushed RAP typically yields higher densities than milled RAP from the same source (Sandin, 2008). The specific gravity of the aggregate has a larger effect on dry densities. Whitehurst Milled RAP had a higher specific gravity than APAC

Melbourne Crushed RAP, and yielded higher densities despite being milled rather than crushed. The APAC Jacksonville Crushed RAP has the highest Specific Gravity and produced the highest densities; however, it also has nearly 7 % fines allowing for better compaction.

4.5.1.2. Gyratory Compaction

Based upon previous research involving gyratory compaction on soil, variables that affect density are moisture content, number of gyrations, and consolidation pressure (Ping et al., 2003).

4.5.1.2.1. Gyratory Moisture Density Relationships

Moisture-density relationships for gyratory compaction at 75 gyrations are presented in Figure 4-52 and Table 4-21. RAP samples were tested at target moisture contents of 3, 6, and 9% to determine if moisture content has an effect on gyratory compaction. Moisture contents below 9% were used to prevent excess water from leaking into the gyratory compactor. Based upon the results shown in Figure 4-52, three of the four samples showed a peak dry density, while Whitehurst Milled RAP did not. Melbourne crushed RAP showed a peak density of 121.7 pcf at 5.1 %, and RAP from APAC Jacksonville showed a peak dry density at 4.6%. The large difference in densities of Melbourne milled RAP between 3% and 5.5% moisture content may be the result of sample variability since these materials were obtained at two different times.

Table 4-21: Moisture Density Relationship from Gyratory Compaction at 75 Gyrations

Source	Dry Density (pcf)		Optimum Moisture Content
	Minimum	Maximum	
APAC Melbourne Crushed RAP	115.4	124.8	6%
APAC Melbourne Milled RAP	113.0	121.7	6%
Whitehurst Milled RAP	119.3	125.4	n/a
APAC Jacksonville Crushed RAP	112.9	128.9	4%
n/a = optimum not available due to “S” shaped moisture-density curves			

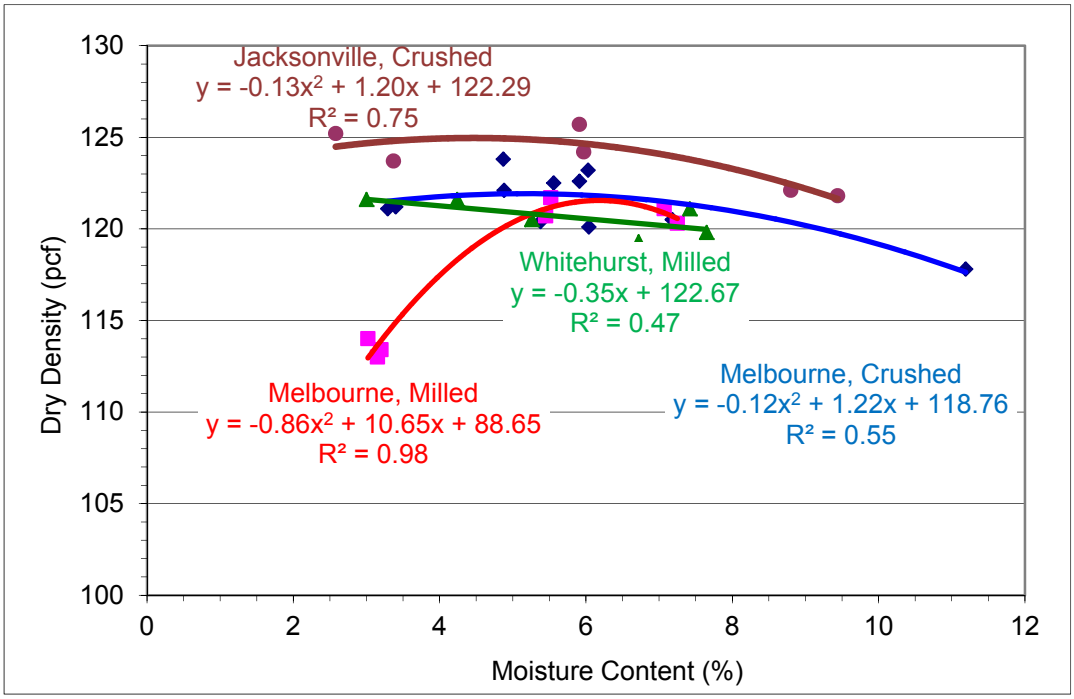

Figure 4-52: Dry Density versus Moisture Content for Gyratory Compaction

4.5.1.2.2. Density versus Number of Gyrations

To determine the effect of additional compactive energy from increased gyrations on dry density, samples from each of the four RAP sources were compacted for 75, 100, and 150 gyrations. A total of 62 samples were tested with 22 tests on Melbourne crushed, 8 on Melbourne milled, 11 on Whitehurst milled, and 21 on Jacksonville crushed. The Gyratory compactor records the height of the sample at the end of each gyration and the cross sectional area of 27.4 in^2 is constant so the change in density after each gyration can be readily determined. Figure 4-53 shows a typical plot of dry density after each gyration. The density increases nonlinearly.

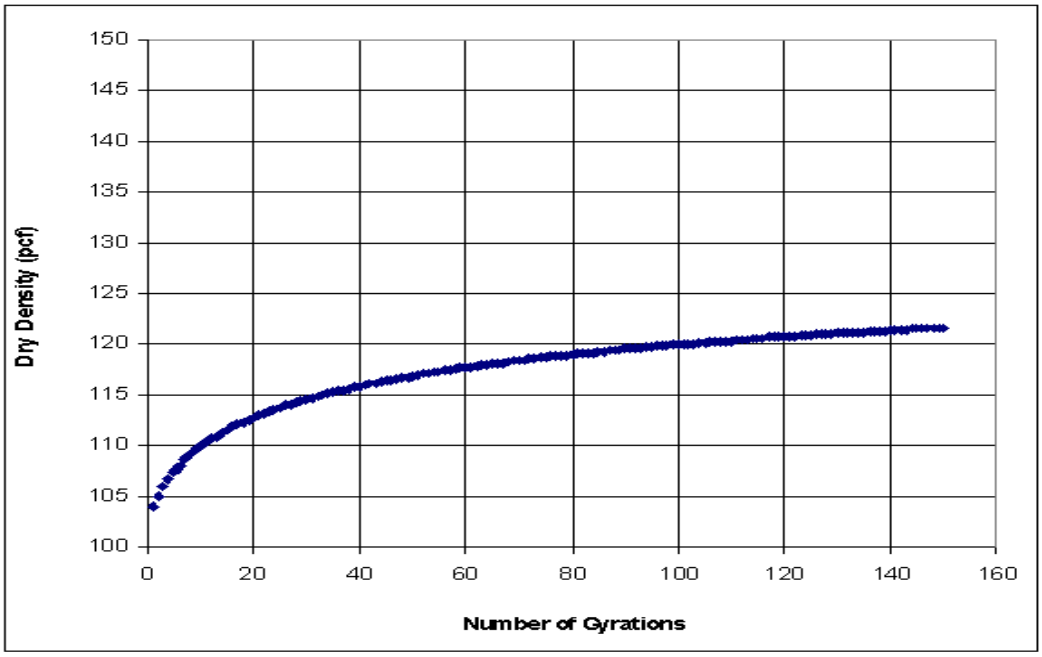

Figure 4-53: Typical Plot of Dry Density after Each Gyration for a Single Test

When plotted on a semi-log graph (Figure 4-54), a linear relationship occurs after about 10 gyrations. For all the tests performed, dry densities increased an average of 12 pcf per 1 log gyration. Dry density versus gyration data for all the tests performed is shown in Appendix M.

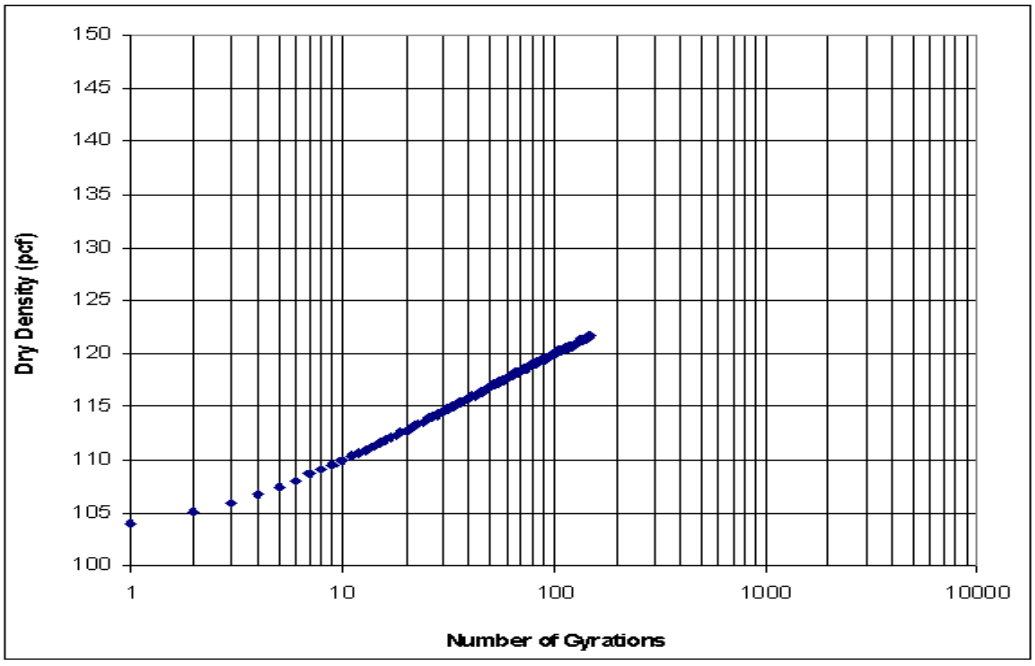

Figure 4-54: Typical Single Test Semi-Log Plot of Dry Density after Each Gyration

Data from all 62 tests with samples compacted at 75, 100, and 150 gyrations were assembled along with specialized tests with the number of gyrations set to a desired density. As shown in Figure 4-55, dry densities increased as the number of gyrations increased. The increase in dry density from 100 to 150 gyrations is less than the increase from 75 to 100 gyrations, which indicates a logarithmic trend. Data points for less than 75 gyrations shown on Figure 4-55 were obtained by matching the maximum densities obtained by modified Proctor compaction.

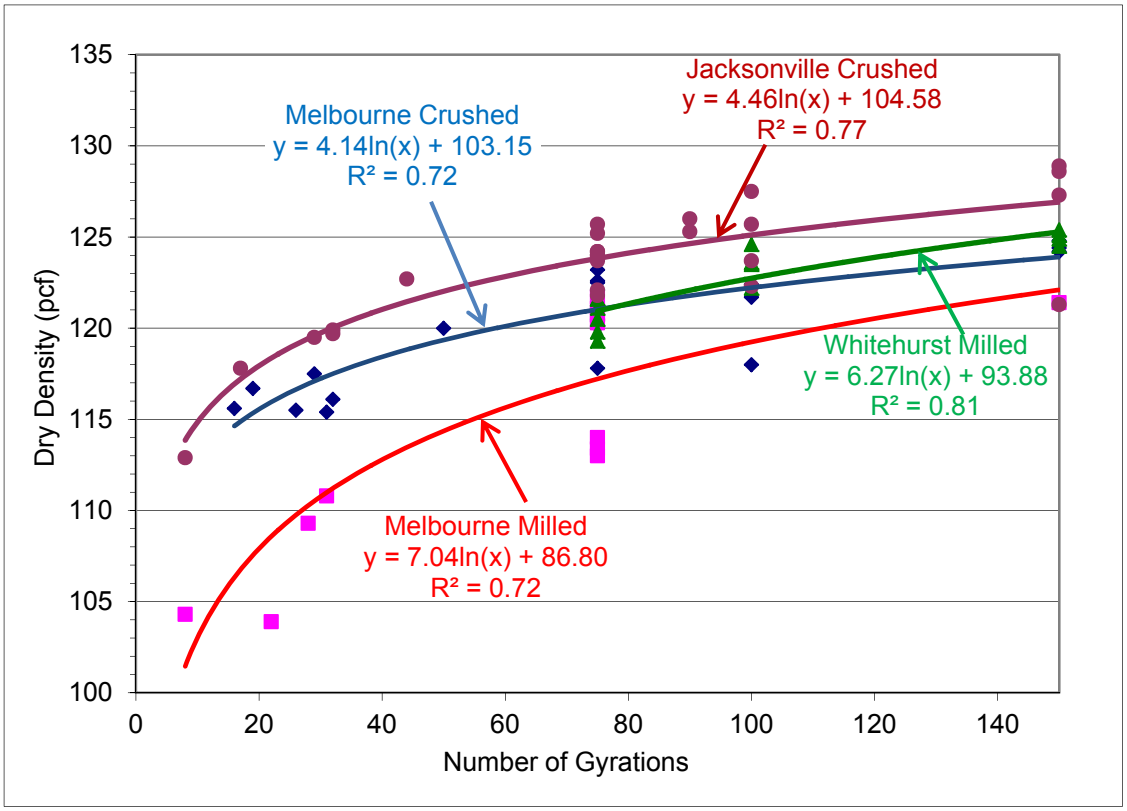

Figure 4-55: Dry Density versus Total Number of Gyrations per Test

4.5.1.2.3. Gyratory Final Density versus Initial Sample Height

While an effort was made to ensure that the same amount of material by weight was placed in the mold for each test, the initial height of each sample was not perfectly consistent. Due to the difficulty in measuring the initial height of material in the mold, for the purpose of this study the initial sample height was defined as the sample height recorded by the gyratory compactor after the first gyration. Results from all 62 tests were used to develop a plot of final dry density versus initial sample height as shown in Figure 4-56.

The highest densities occurred when the initial sample height was near 5.1 inches (130 mm), while the lowest occurred near 5.5 inches (140 mm). Initial heights between 4.88 and 5.28 inches (124 and 134 mm) produced dry densities above 120 pcf, while those outside this range produced dry densities as low as 113 pcf.

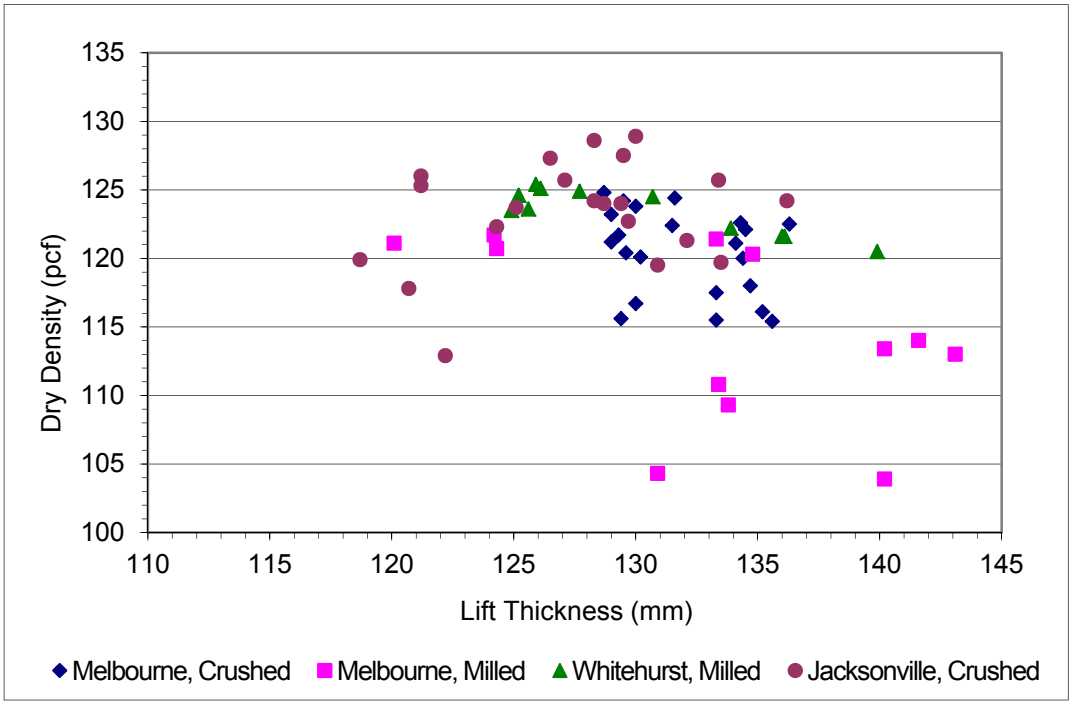

Figure 4-56: Final Dry Density versus Initial Sample Height for all Gyratory Samples

4.5.1.3. Vibratory Moisture Density Relationships

The vibratory compaction tests were initially conducted following the specifications of ASTM D4253 to evaluate different moisture contents. Vibratory compaction typically produced high densities at very low and very high moisture contents. Moisture - density and density - compactive effort plots are presented in Figure 4-57 and Figure 4-58 respectively. Figure 4-57 shows that three of the four materials produced peak densities at very high moisture contents, while the Whitehurst milled RAP produced a curve similar to Proctor curves.

A series of tests were conducted to evaluate the effects of compaction time. The vibration time was varied from the specified 8 minutes to 12 minutes and 16 minutes. Figure 4-57 shows moisture-density relationships for only the 8 minute tests. 12 and 16 minute compaction times yielded similar results. The maximum moisture content was limited during the

testing due to the physical limitations of the relative density apparatus. During the Proctor compaction procedure excess water can to drain through small holes in the bottom of the mold, while the relative density mold bases and sides are solid and prevent drainage. During the pretesting stage, it was observed that excess water floated to the top of the mold during the vibration period and splattered on the equipment.

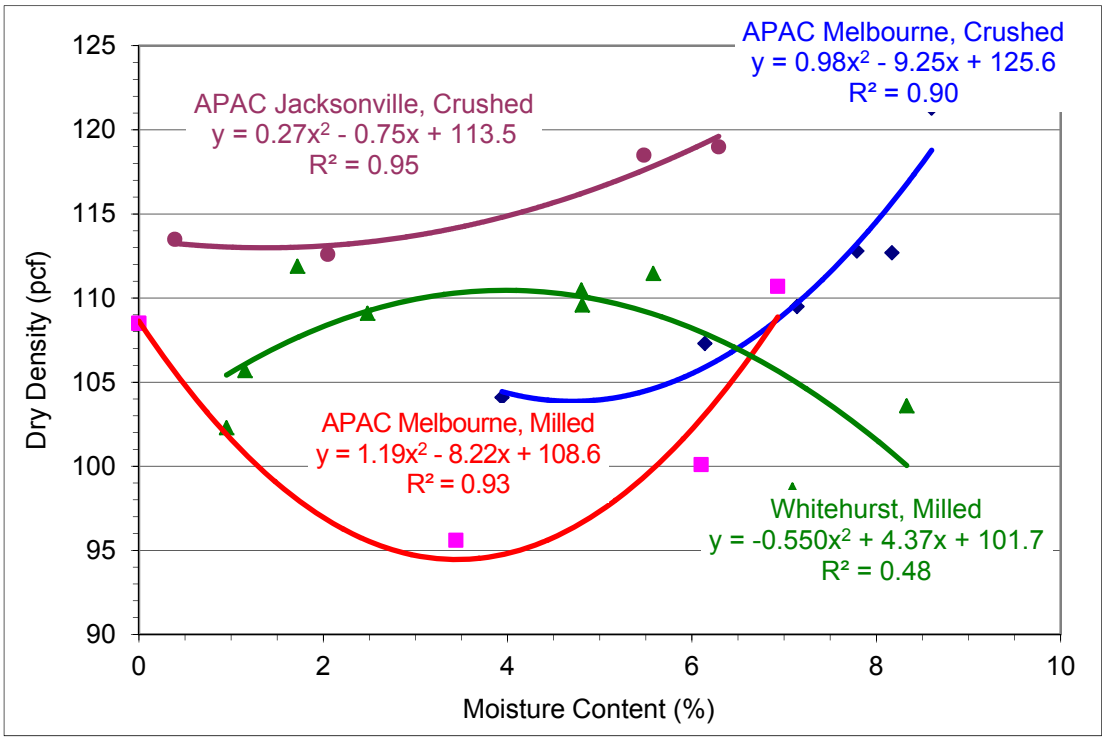

Figure 4-57: Dry Density versus Moisture Content for Vibratory Compaction

As shown in Figure 4-57, correlations between dry-density and moisture content for vibratory compaction were inconclusive and varied by source. Three of four samples appeared to initially decrease in density as moisture content increased, then increased as moisture content increased above 4.0%. The Whitehurst milled RAP appears to show an opposite relationship, where dry density peaked at approximately 111.0 pcf at an optimum moisture content of 4.0%. Polynomial trendlines were used because they yielded the best correlation coefficients of any type of trend lines. There was no major difference between the crushed and milled RAP. Similar to the modified Proctor results, APAC Jacksonville crushed, with the highest % fines and specific gravity, produced the highest densities.

4.5.1.4. Vibratory Density versus Compactive Effort

Compactive effort (compactive energy) was calculated by multiplying the displacement measured by the vibration meter by the vibration time and cycles per second, then dividing by the final sample density. Figure 4-58 shows dry density variations versus compactive effort with moisture contents controlled between 4 and 6% for all three vibration times. As the vibration time increased, the compactive effort and the dry density increased. APAC Jacksonville RAP again had the highest density.

All four RAP types exhibited positive slopes on their correlation curves indicating that increasing compactive effort is correlated to higher dry density. As shown in Figure 4-58, additional compactive energy had minimal effect on dry density for the APAC Jacksonville crushed RAP. The very low correlation coefficient (0.02) indicates no correlation between vibratory compactive effort and dry density for this material. Whitehurst milled RAP showed a slightly higher but still small correlation coefficient (0.16) while APAC Melbourne crushed and milled specimens showed medium correlations between compactive effort and dry density.

Comparing the moisture versus density results (Figure 4-57) to the compactive effort versus density results (Figure 4-58) shows that moisture content has a greater effect on dry density than compactive effort. The variations in dry density as water content increased were more pronounced than the insignificant increases in density as vibratory compactive effort increased (except for Melbourne milled RAP). For Melbourne milled RAP the data point for the highest compactive effort appears to be inconsistent with the other points resulting in an overstated increase in density and skewing the apparent trend. For all four of the RAP samples, vibratory compaction yielded lower dry densities than the modified Proctor method, as shown in Table 4-22.

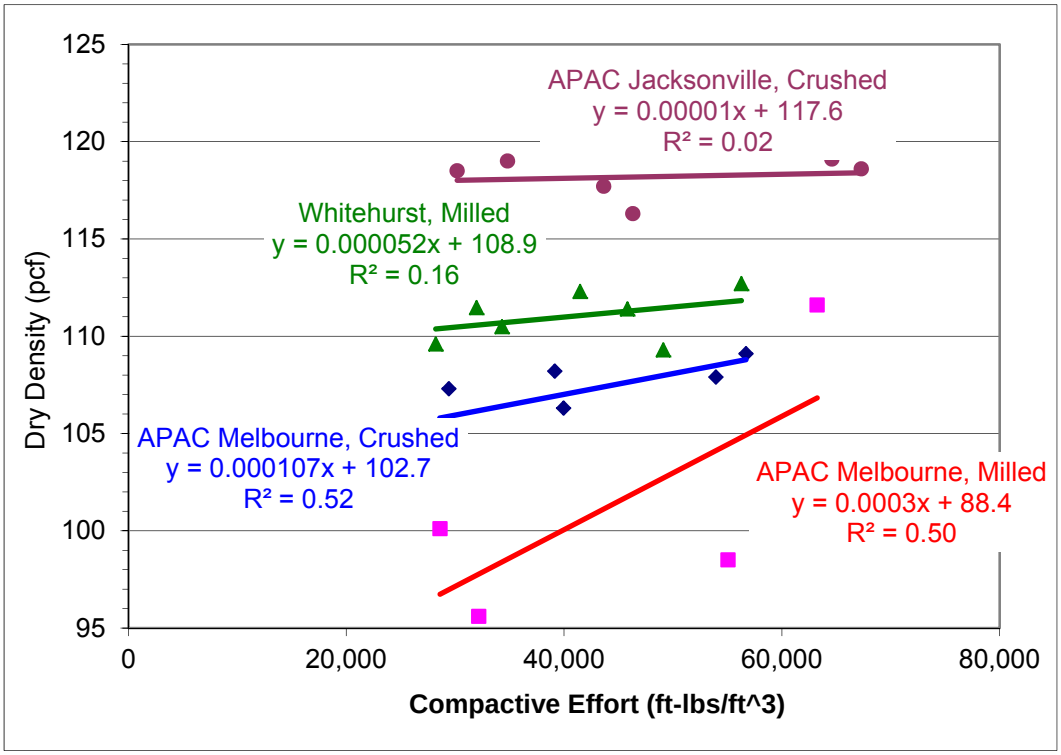

Figure 4-58: Dry Density versus Compactive Effort for Vibratory Compaction

Table 4-22: Comparison of Modified Proctor to Vibratory Compaction

Source	Modified Proctor			Vibratory Compaction		
	Dry Density		Optimum Moisture Content (%)	Dry Density		Optimum Moisture Content (%)
	Min (pcf)	Max (pcf)		Min (pcf)	Max (pcf)	
APAC Melbourne Crushed	112.4	119.4	n/a	104.1	121.3	n/a
APAC Melbourne Milled	105.1	110.9	n/a	95.6	111.6	n/a
Whitehurst Milled	116.1	121.2	n/a	98.6	112.7	3.8
APAC Jacksonville Crushed	121.2	125.3	6.1	112.6	119.1	n/a
n/a = optimum not available due to “S” shape moisture-density curves						

4.5.2. Compaction Improvements Performance Tests

4.5.2.1. Limerock Bearing Ratio

Following modified Proctor, vibratory, and gyratory compaction, unsoaked LBR tests were conducted on 116 samples from the RAP sources. The results are presented in the following sections. These results are not directly comparable to post-creep LBR values shown in other sections of this report because the 7 days of additional creep consolidation generally increased those specimens' LBR values.

4.5.2.2. Modified Proctor Compaction

The unsoaked LBR values obtained from the modified Proctor compaction are presented as LBR versus dry density in Figure 4-59. A total of 32 tests were conducted with 9 from Melbourne crushed, 8 from Melbourne milled, 7 from Whitehurst Milled, and 8 from Jacksonville crushed.

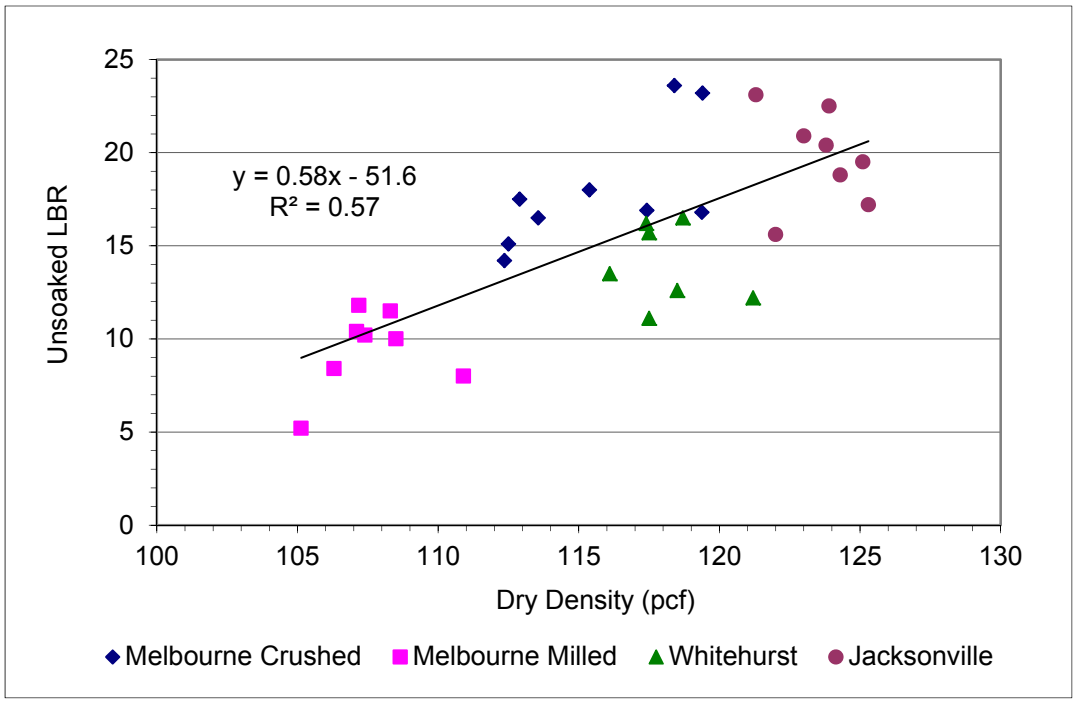

Figure 4-59: Unsoaked LBR vs. Dry Density for All Modified Proctor Compacted Samples Based on the Modified Proctor Densities

Unsoaked LBR values rose as dry density increased. The general trend among all data points indicated a linear relationship which produced a regression coefficient of 0.57. LBR

increased 0.58 per 1 pcf increase in dry density. The highest observed unsoaked LBR of 24 obtained from the modified Proctor method did not achieve the FDOT's specified LBR of 100 for base course or of 40 for subbase material.

4.5.2.3. Vibratory Compaction

The LBR values obtained from vibratory compaction are presented as LBR versus dry density in Figure 4-60. A total of 32 tests were conducted with 10 from Melbourne crushed, 7 from Melbourne milled, 8 from Whitehurst milled, and 7 from Jacksonville crushed. For the vibratory compaction method, LBR values slightly increased as dry density increased. The general trend among all data points indicates a weak linear relationship with a regression coefficient of 0.17. LBR increased 0.24 per 1 pcf increase in dry density, which is less than half the rate obtained from the modified Proctor compaction.

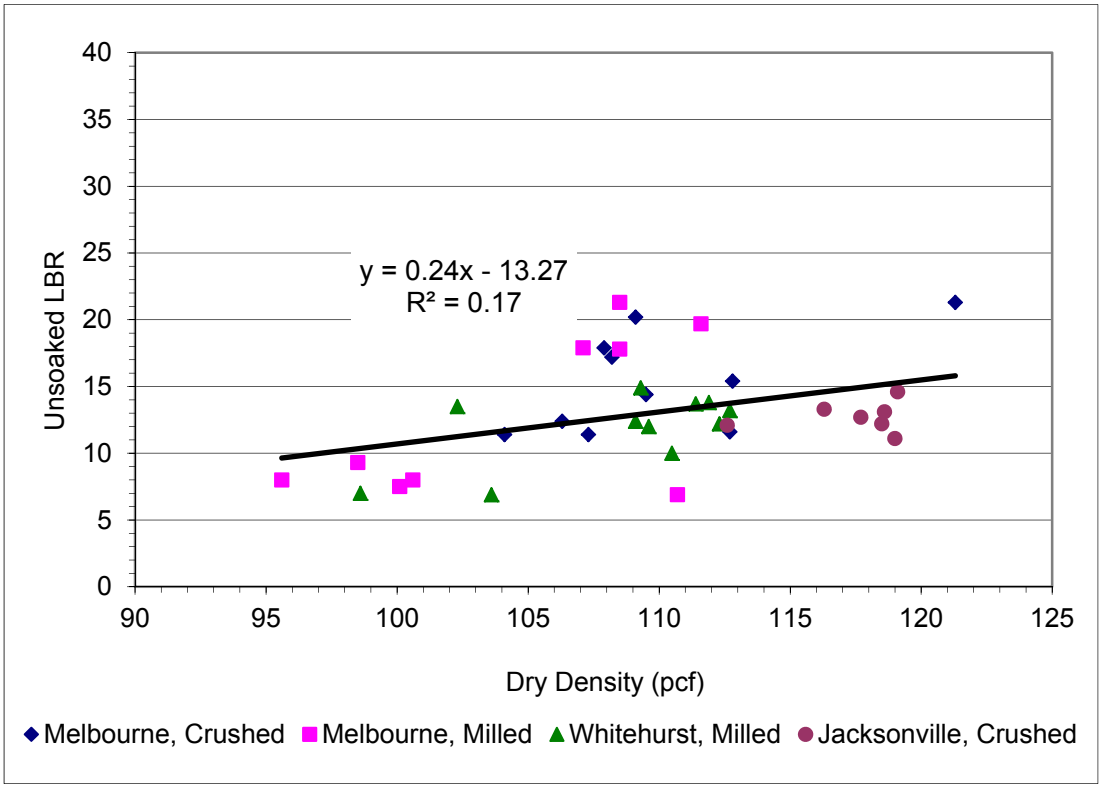

Figure 4-60: LBR vs. Dry Density for Vibratory Compaction

To determine if compactive effort had any influence on the LBR, a graph of the LBR versus Compactive Effort based on all 32 tests is presented in Figure 4-61. The very low

correlation coefficient of 0.076 indicates that changes in LBR values were not correlated to additional vibratory compaction time. The highest LBR achieved with vibratory compaction was 21, far less than the required value of 100 for base or 40 for subbase material.

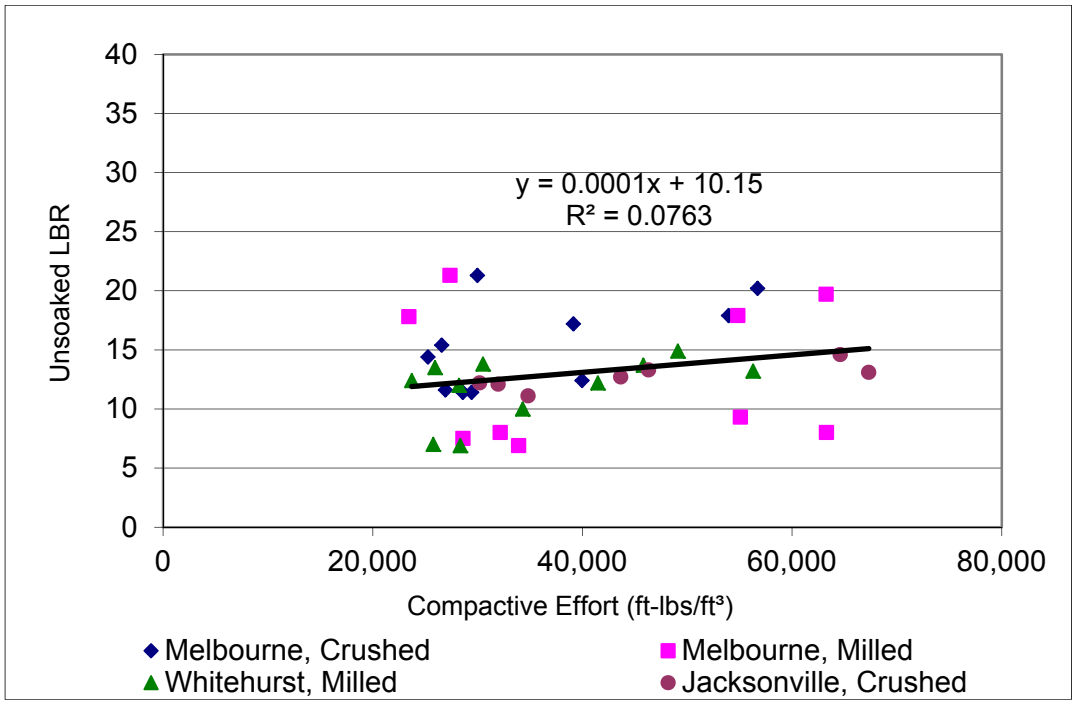

Figure 4-61: Unsoaked LBR vs. Compactive Effort for Vibratory Compaction

4.5.2.4. Gyratory Compaction

The LBR versus dry density results from the gyratory compaction samples are presented in Figure 4-62. A total of 52 tests were conducted with 12 from Melbourne crushed, 8 from Melbourne milled, 14 from Whitehurst milled, and 18 from Jacksonville crushed. The LBR values from gyratory compaction are higher than those achieved with any other compaction methods. Similar to the results of the modified Proctor compaction, LBR values generally increased as dry density increased. As shown in Figure 4-62, LBR increased linearly 2.75 per 1 pcf increase in final dry density. This rate is much higher than the rates associated with either modified Proctor or vibratory compaction. The correlation coefficient of 0.62 indicates a strong linear correlation.

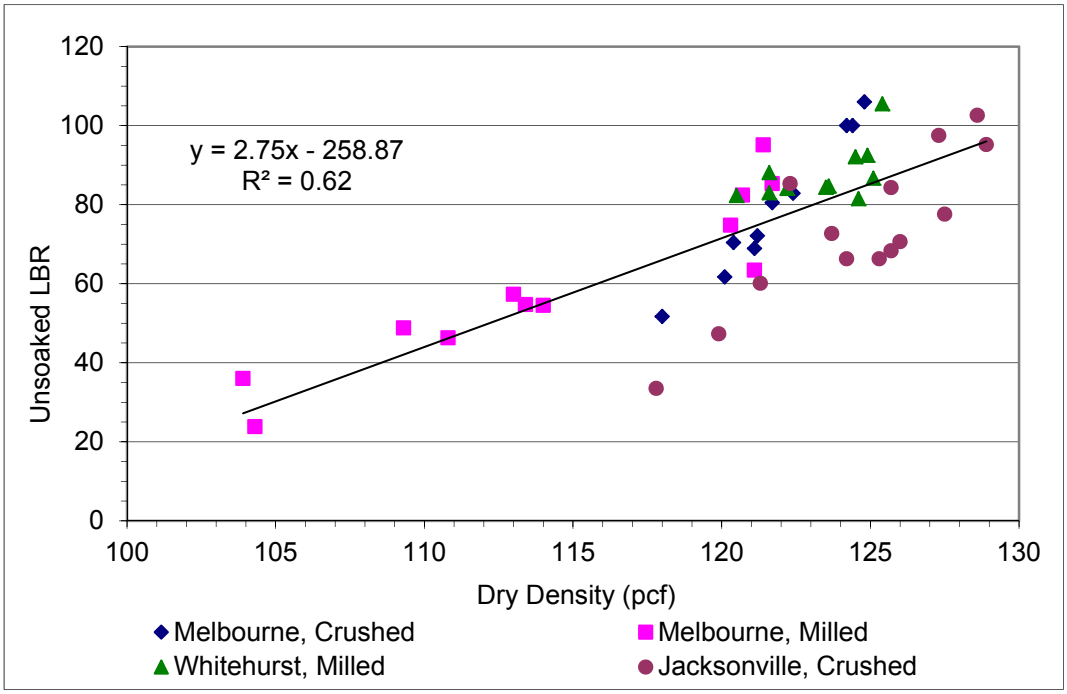

Figure 4-62: LBR vs. Dry Density for Gyratory Compaction of Samples with Approximately 5% Moisture Content

A graph of the LBR versus number of gyrations was prepared to determine whether the extra compactive effort from additional gyrations had any influence on the LBR (Figure 4-63). LBR increased linearly 0.41 per gyration, with a strong correlation coefficient of 0.70. Two outliers, one at 100 gyrations, and one at 150 gyrations, produced LBR values approximately 30 below the trendline. These results may be a result of experimental error in the LBR test. Four specimens compacted for 150 gyrations produced LBR values at or greater than 100. All samples compacted for 75 or more gyrations produced LBR values greater than 40. Only 2 of the 52 samples tested produced LBR below 40, which is approximately 4% of the samples.

Five samples with densities over 125 pcf produced unsoaked LBR values slightly greater than 100 while samples with densities above 116 pcf produced LBR values over 40. Samples compacted for less than 25 gyrations did not achieve the FDOT specified LBR of 40 for subbase applications. In conclusion, gyratory compaction of RAP may produce acceptable unsoaked LBR values

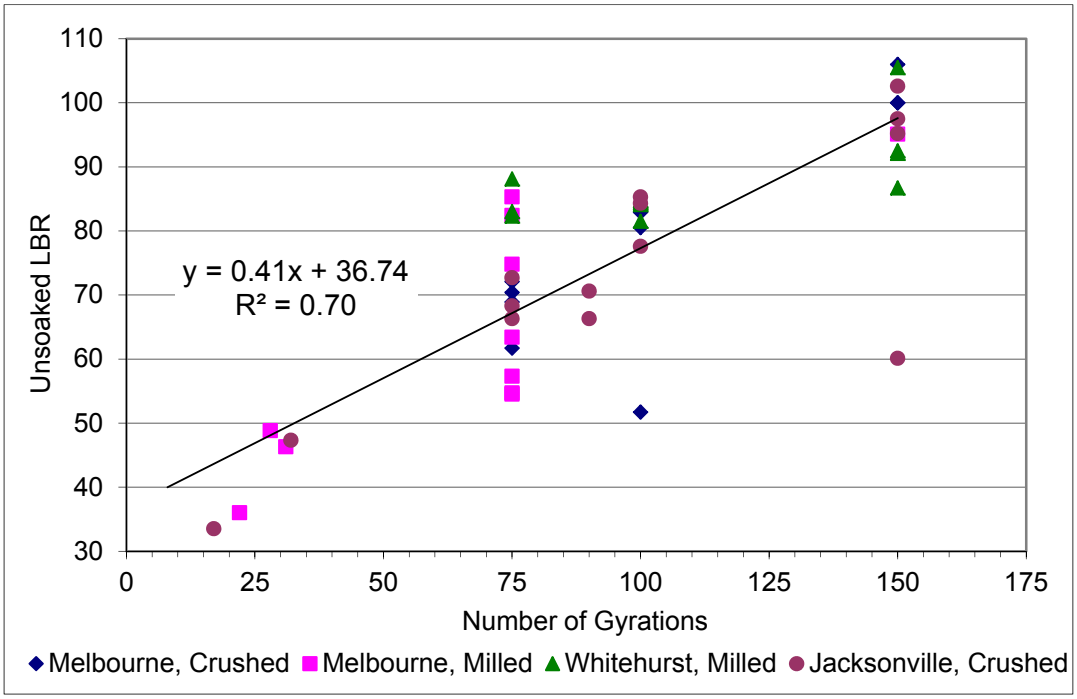

Figure 4-63: Unsoaked LBR vs. Number of Gyrations for Gyratory Compaction of Samples with Approximately 5% Moisture Content

4.5.2.5. Comparison of Gyratory to Modified Proctor Compaction

A direct comparison of modified Proctor and gyratory LBR was performed by holding dry density constant for both compaction methods. The results are presented in the sections that follow.

4.5.2.5.1. Limerock Bearing Ratio

Table 4-23 is a summary of unsoaked LBR values from both modified Proctor and Gyratory compaction. Densities were grouped into 5 pcf increments. The data shows that LBR increases with density; however, they seem to peak near the 125 pcf range for the modified Proctor data. The average values from Gyratory compaction are about four times higher that those from modified Proctor testing.

The LBR values obtained from RAP samples compacted using the gyratory and the modified Proctor methods are shown in Figure 4-64. Both methods showed an increase in LBR with density. Gyratory compaction yielded significantly higher LBR values than the modified Proctor method at similar densities. The FDOT State Materials Office confirmed these results

with tests conducted in their laboratory. FDOT performed LBR tests on two modified Proctor-compacted samples, three samples compacted with 75 gyrations and four gyratory compacted samples which matched the maximum modified Proctor density.

As seen in Figure 4-64, gyratory compaction yielded several times higher LBR values than modified Proctor compaction at similar densities. The linear regression line for the modified Proctor-compacted samples indicated a 0.58 increase in LBR for every 1.0 pcf increase in dry density with a regression coefficient of 0.45 (medium correlation). The linear regression line for the gyratory samples indicated a much larger LBR increase of 2.71 for every 1.0 pcf increase in dry density with a regression coefficient of 0.40 (medium correlation). The slopes and regression coefficients shown in Figure 4-64 differ from those shown in Figure 4-59 and Figure 4-62 due to the additional data provided by FDOT SMO. The lowest LBR gyratory specimen was composed of Jacksonville crushed RAP compacted with only 17 gyrations to match the corresponding modified Proctor dry density of 117.8 pcf. This specimen's LBR of 34 was still greater than any of the modified Proctor compacted samples compacted with the full modified Proctor compactive effort.

Table 4-23: Unsoaked LBR comparison versus Density from Modified Proctor and Gyratory Compaction

Dry Density Range (pcf)	Limerock Bearing Ratio					
	Modified Proctor			Gyratory		
	Min	Avg	Max	Min	Avg	Max
105 - 110	5.2	9.6	11.8	23.8	36.2	48.8
110 - 115	14.2	16.3	18.0	54.5	55.5	57.3
116 - 120	11.1	18.1	26.0	33.5	60.4	75.0
121 - 125	12.2	18.8	23.1	60.1	80.8	106.0
126 - 130	17.2	18.4	19.5	66.3	84.8	105.5

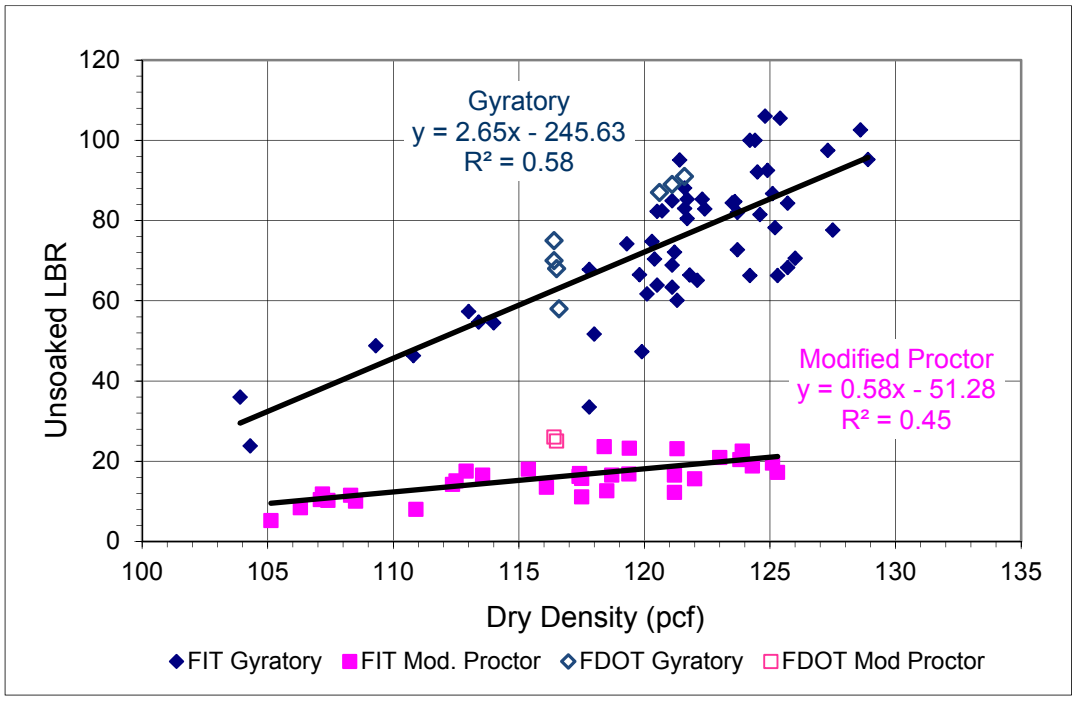

Figure 4-64: Unsoaked LBR Comparison between Modified Proctor and Gyratory Compaction Methods for all RAP Stockpiles

4.5.2.5.2. Modified Unconfined Compression (UCC) Test

Unconfined compression (UCC) tests were performed on samples extruded from modified Proctor and gyratory molds. ASTM standards specify a 2:1 length to diameter ratio to minimize end effects, however the limitation of the gyratory mold geometry made it impossible to create specimens with these proportions. Both the modified Proctor and gyratory samples were approximately 4.5-inches tall by 6-inches in diameter. Since the modified Proctor and gyratory specimens had the same relative proportions, the results are valid for comparison. Correction factors would need to be applied to these results to compare them to standard unconfined compression tests. The data was plotted as stress versus deflection and the peak stress values were used as the unconfined compressive strength.

Five specimens were compacted by the modified Proctor method, four specimens were gyratory compacted at 75 gyrations, and three specimens were gyratory compacted to match the modified Proctor compacted specimen densities. Results from the UCC tests are presented in terms of dry density in Figure 4-65 and

Table 4-24. Similar to the strength variations found from LBR tests, gyratory compacted specimens yielded unconfined compressive strengths 3 to 4 times higher than the modified Proctor specimens. Similar to previous results (see Figure 4-55) of the gyratory compacted specimens, dry density increased as the number of gyrations increased. Figure 4-65 shows the unconfined compressive strength of the gyratory compacted specimens increased linearly from about 25 to 105 psi as density increased while the unconfined compressive strength of the modified Proctor specimens remained constant at about 20 psi.

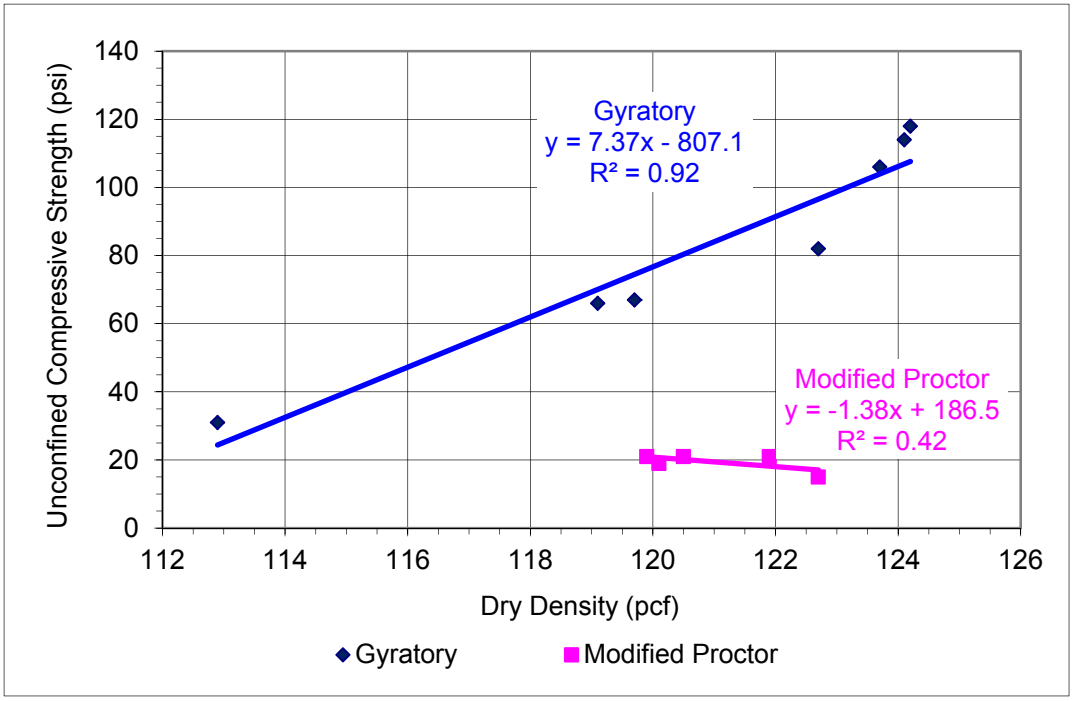

Figure 4-65: Unconfined Compressive Strength Comparison of Modified Proctor and Gyratory Compaction Methods

Table 4-24: Unconfined Compressive Strength Comparison of Modified Proctor to Gyratory Compaction

Dry Density (pcf)	Unconfined Compressive Strength (psi)					
	Modified Proctor			Gyratory		
	Min	Avg	Max	Min	Avg	Max
110 - 115	31.0	31.0	31.0	NDR	NDR	NDR
115 - 120	21.0	21.3	22.0	54.0	61.8	67.0
120 - 125	15.0	20.6	27.0	82.0	106.0	118.0
NDR - No data within this range						

4.5.2.5.3. Indirect Tensile Splitting Test

Indirect tensile splitting (IDT) tests were also performed on specimens extruded from modified Proctor and gyratory molds. IDT results are presented in terms of dry density in Figure 4-66 and Table 4-25. A total of 10 tests were conducted, 4 compacted using modified Proctor, 3 compacted at 75 gyrations, and 3 compacted with the gyratory compactor to match the Modified Proctor densities. Equation 3-5 was used to calculate the tensile strength (stress) from the peak loads recorded during the test. This data was then plotted versus the corresponding dry density as shown in Figure 4-66. As was the case for both the LBR and UCC results, gyratory testing yielded tensile strengths 2 to 3 higher than modified Proctor specimens. Some of the modified Proctor specimens crumbled during extraction from the mold, indicating zero tensile strength, while all of the gyratory compacted specimens remained intact. The tensile strength of the specimens compacted by both methods increased linearly as density increased.

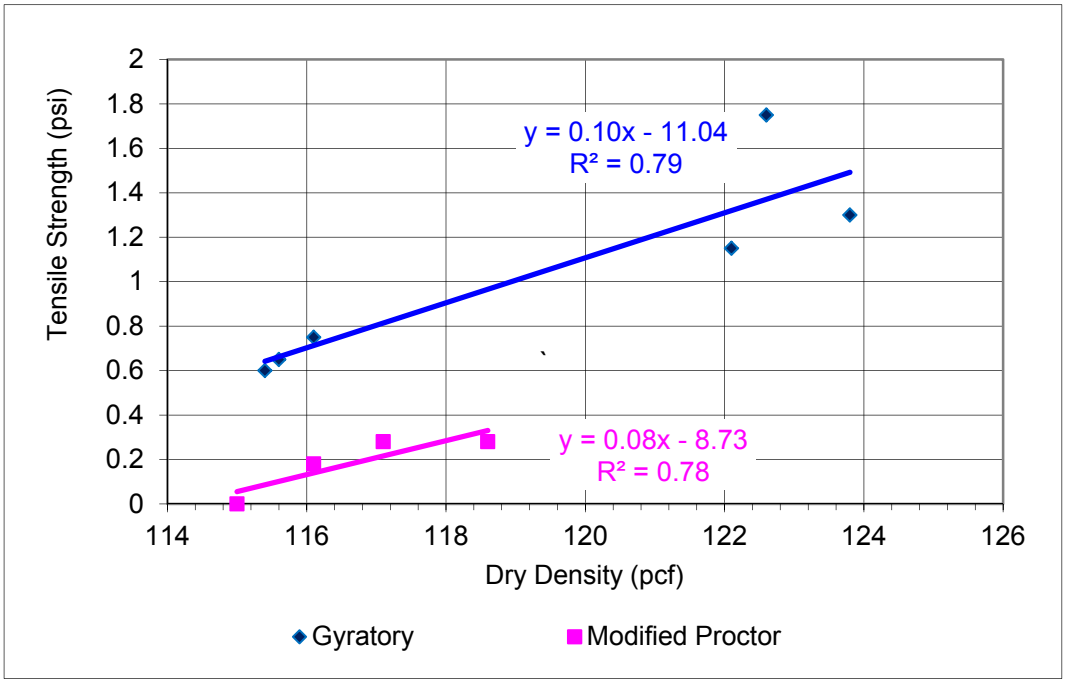

Figure 4-66: Indirect Tensile Splitting Test Comparison of Modified Proctor and Gyratory Compaction Methods

Table 4-25: Indirect Tensile Strength Comparison of Modified Proctor to Gyratory Compaction

Dry Density Range (pcf)	Indirect Tensile Strength (psi)					
	Modified Proctor			Gyratory		
	Min	Avg	Max	Min	Avg	Max
110 - 115	0.00*	0.00*	0.00*	NDR	NDR	NDR
115 - 120	0.18	0.25	0.28	0.6	0.7	0.75
120 - 125	NDR	NDR	NDR	1.15	1.4	1.75
* Samples crumbled during extrusion and therefore have zero IDT strength NDR - No data within this range						

4.5.2.5.4. Summary of Strength Comparison Methods

Table 4-26 is a summary of the compaction methods comparisons for LBR, unconfined compressive strength, and indirect tensile strength categorized by density ranges. Blank spaces in the table are because the compacted samples did not fall within that density range.

Figure 4-67 shows the ratio of strengths between the gyratory compaction and the modified Proctor compaction categorized by density. At lower densities the ratio of LBR values ranged from 3.34 to 3.80. At higher densities the LBR ratio ranged from 4.31 to 4.62. At the lower densities, the unconfined compressive strength ratio was 2.9, while at higher densities it was 5.15. All indirect tensile specimens had densities between 116 to 120 pcf with strength ratio of 2.70. The unweighted average ratio among all three strength tests showed that the gyratory compaction yield approximately 3.55 times the strength of modified Proctor compaction.

Table 4-26: Comparison of Compaction Methods Summary

Dry Density (pcf)	Modified Proctor			Gyratory		
	LBR	UCC (psi)	IDT (psi)	LBR	UCC (psi)	IDT (psi)
105 - 110	9.6	NDR	NDR	36.2	NDR	NDR
110 - 115	16.3	NDR	0.00	55.5	31.0	NDR
116 - 120	18.1	21.3	0.25	60.4	61.8	0.67
121 - 125	18.8	20.6	NDR	80.8	106.0	1.40
126 - 130	18.4	NDR	NDR	84.8	NDR	NDR
Average*	16.0	20.9	0.19	74.4	82.0	1.03
*Unweighted average from raw data NDR - No data within this range						

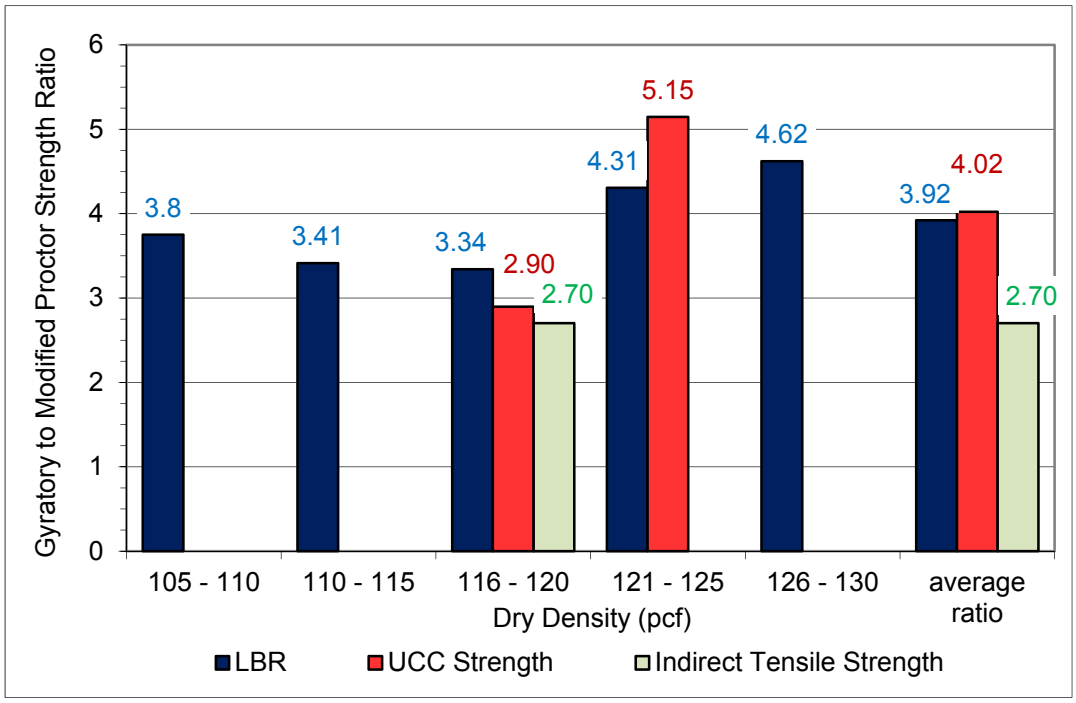

Figure 4-67: Ratio of Gyratory Compaction to Modified Proctor Compaction

4.5.3. Strength Test Comparison of Gyratory and Proctor-Compacted Specimens without Asphalt Binder

The finding of consistently very large differences in both compressive and tensile strength for specimens of the same density was unusual. Compaction specifications assume that strength is dependent only on density. To explain this result, a hypothesis was developed that the strength differences occurred because gyratory compaction restored some of the asphalt binder bonding due to a combination of constant pressure and kneading action. To validate this hypothesis, LBR and IDT's were performed on three materials which contain no asphalt binder. A total of three samples of each material were prepared for each of the three tests:

a. Noncohesive Limerock Base (LR)

b. Noncohesive Cemented Coquina (CC)

c. Cohesive Clayey Sand (CS)

4.5.3.1. Unsoaked LBR Strength of Gyratory and Modified Proctor

Figure 4-68 shows the unsoaked LBR strengths achieved with the two compaction methods. Average strength ratios were determined by dividing the gyratory by the modified

Proctor strength results. These are shown in Table 4-27. These ratios are near 1 indicating that gyratory compaction does not improve strengths of these conventional soils. Based on these results, there was no significant difference between the unsoaked LBR strengths from gyratory and modified Proctor specimens of 100% aggregate.

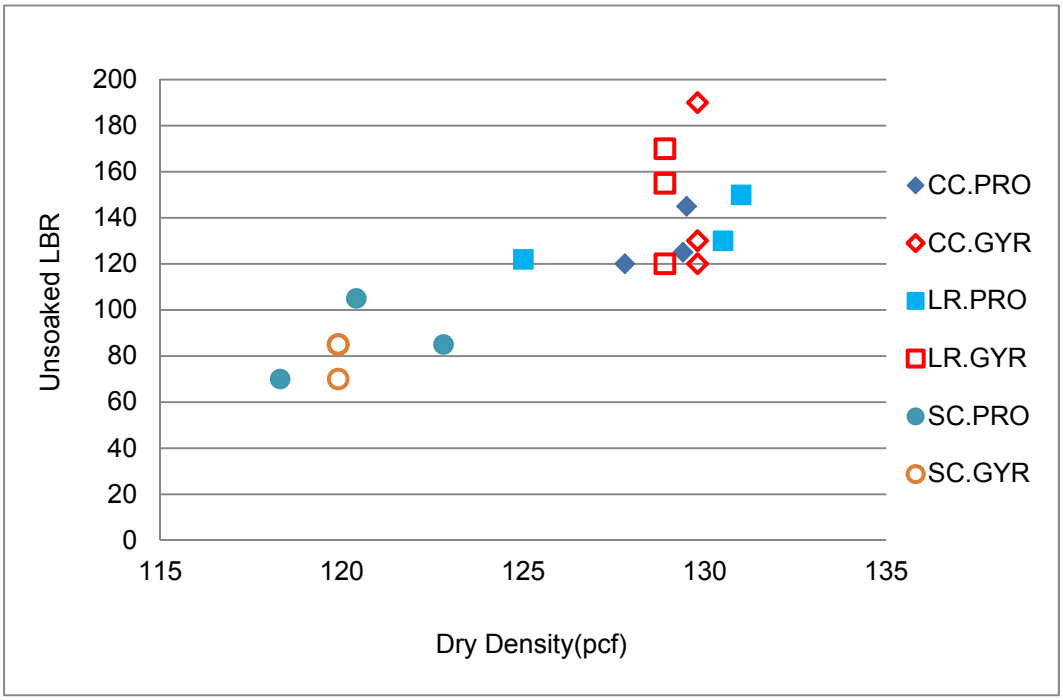

Figure 4-68: LBR Strength of Gyratory (Gyr) and Modified Proctor (Pro) Specimens of 100% Limerock (LR), Cemented Coquina (CC) and Clayey Sand (SC)

Table 4-27: Average Gyratory/Modified Proctor LBR Ratio for 100% Aggregate

	Average LBR ratio
100% Limerock	1.10
100% Cemented Coquina	0.96
100% Clayey Sand	0.92

4.5.3.2. IDT Strength of Gyratory and Modified Proctor Specimens

Figure 4-69 shows the IDT strengths for the two compaction methods. Similar to the LBR results, there was no significant difference between the unsoaked IDT strengths of gyratory and modified Proctor specimens of 100% aggregate. Table 4-28 shows the average strength ratios determined by dividing the gyratory by the modified Proctor IDT strength results. The

apparently high gyratory/modified Proctor strength ratio for 100% limerock shown in Table 4-23 is an artifact of the extremely low IDT strength (< 1.0 psi) measured for both types of specimens.

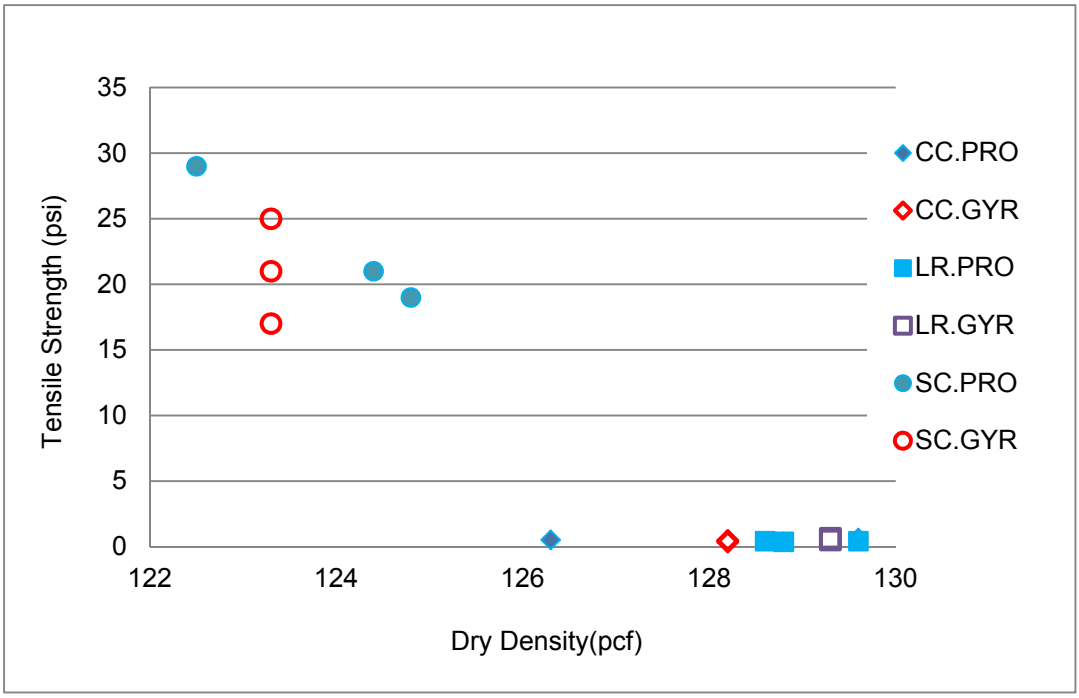

Figure 4-69: IDT Strength of Gyratory and Modified Proctor Specimens of 100% Limerock (LR), Cemented Coquina (CC) and Clayey Sand (SC)

Table 4-28: Average Gyratory/Modified Proctor IDT Ratio for 100% Aggregate

	Average IDT ratio
100% Limerock	1.42
100% Cemented Coquina	0.82
100% Clayey sand	0.91

In summary, gyratory compacted 100% RAP specimens showed large strength increases compared to modified Proctor compacted specimens. Gyratory compacted 100% aggregate specimens did not show significant strength differences compared to modified Proctor compacted specimens. The results to date clearly indicate that gyratory compaction does improve the strength of RAP in a manner not observed in conventional soils/aggregates.

4.5.4. Unconfined Creep Behavior of Gyratory and Modified Proctor-Compacted Specimens

The preceding tests established that gyratory compaction restores some bonding in the asphalt binder, resulting in higher compressive and tensile strength. Unconfined creep tests were conducted on ejected gyratory and Proctor specimens to determine whether gyratory compaction affected creep performance as well as strength. Ejected specimens were tested to eliminate any effects resulting from the different geometry of the Proctor and gyratory molds. The 4-inch (101.6 mm) diameter, 4.584-inch (116.43 mm) high modified Proctor specimens were prepared first. Gyratory specimens with slightly different diameters of 3.94-inches (100 mm) and heights of 4.72=inches (120 mm) were then prepared in order to maintain similar volumes (about 0.15% difference). Tests were conducted on 100% limerock, 100% Melbourne milled RAP, and 50%/50% blends of the two materials.

4.5.4.1. Creep of 100% Limerock Specimens

Confined creep tests of conventional aggregates have shown undetectably low levels of creep. These unconfined specimens showed extremely low but measurable creep. While the modified Proctor and gyratory specimens of 100% limerock produced different initial displacements (Figure 4-70), they had essentially the same CSR (Figure 4-71). The difference in initial displacement was attributed to seating of the specimen in the creep apparatus. CSR is more significant because it demonstrates that the two compaction methods resulted in nearly the same rate of creep. The average CSR of $1.03\times10^{-4}\times\log(\text{time})$ for the gyratory compaction specimens is only slightly lower than the $1.09\times10^{-4}\times\log(\text{time})$ rate for the modified Proctor 100% limestone specimens. This result is consistent with the previous strength testing which found essentially no difference between gyratory and modified Proctor compacted specimens of conventional aggregate. To put these results in perspective, 100 years of creep at this rate would result in an additional 0.002-inch of deformation.

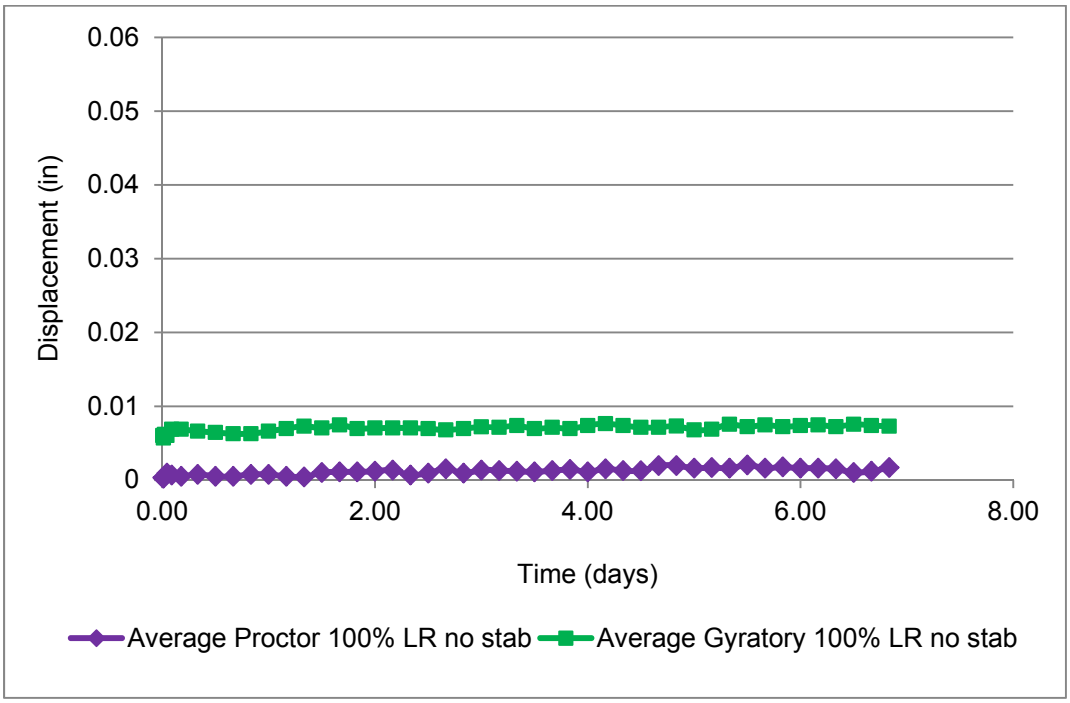

Figure 4-70: Gyratory and Proctor Unconfined Creep: 100% Limerock

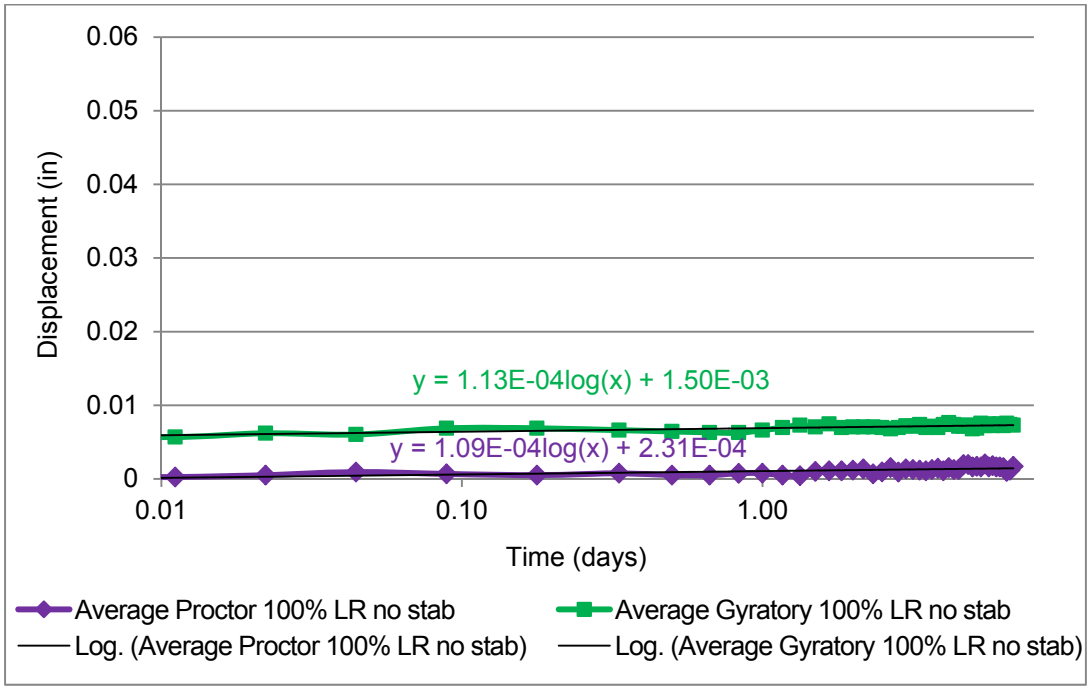

Figure 4-71: Gyratory and Proctor Unconfined Creep: 100% Limerock Log (t)

4.5.4.2. Creep of 100% Melbourne Milled RAP Specimens

The 100% MRAP Proctor and gyratory specimens exhibited nearly identical initial displacements (Figure 4-72) however, the Proctor specimens showed about 50 % more creep deflection at seven days and nearly double the CSR (Figure 4-73). This test was the first instance that tertiary creep (accelerating CSR) was observed. This creep is considered the beginning of failure because the strain rate would continue to increase until rupture. The Proctor and gyratory specimens both exhibited tertiary creep near 0.02-inches of movement. This is not visible in the displacement versus linear time plot but can be clearly seen in the change in slope of the displacement versus log(time) plot at a time of approximately one day. The CSR for the modified Proctor specimen was $4.04\times10^{-3}\times\log(\text{time})$ while the rate for the gyratory specimen was lower at $2.34\times10^{-3}\times\log(\text{time})$. These rates are 20 to 30 times higher than those observed in the 100% limerock specimens.

The onset of tertiary creep at a low 0.4% axial strain (0.02-inch displacement/ 4.584-inch sample thickness) was attributed to the worst-case unconfined loading condition used. Actual base courses have some confinement so creep rates in a roadway application would be less than those observed in these unconfined creep tests but more than those observed in the one-dimensional (in mold) testing in other sections of this report.

The lowest observed failure strain from triaxial testing occurred at 3% strain (Viyanant et al., 2007). These tests were conducted at low confining stresses similar to that found in pavements. Using 3% as an upper limit seems reasonable because many soils subjected to confining stresses between 10 and 30 psi reach failure at between 3 and 5 % strain (Holtz and Kovacs, 1981).

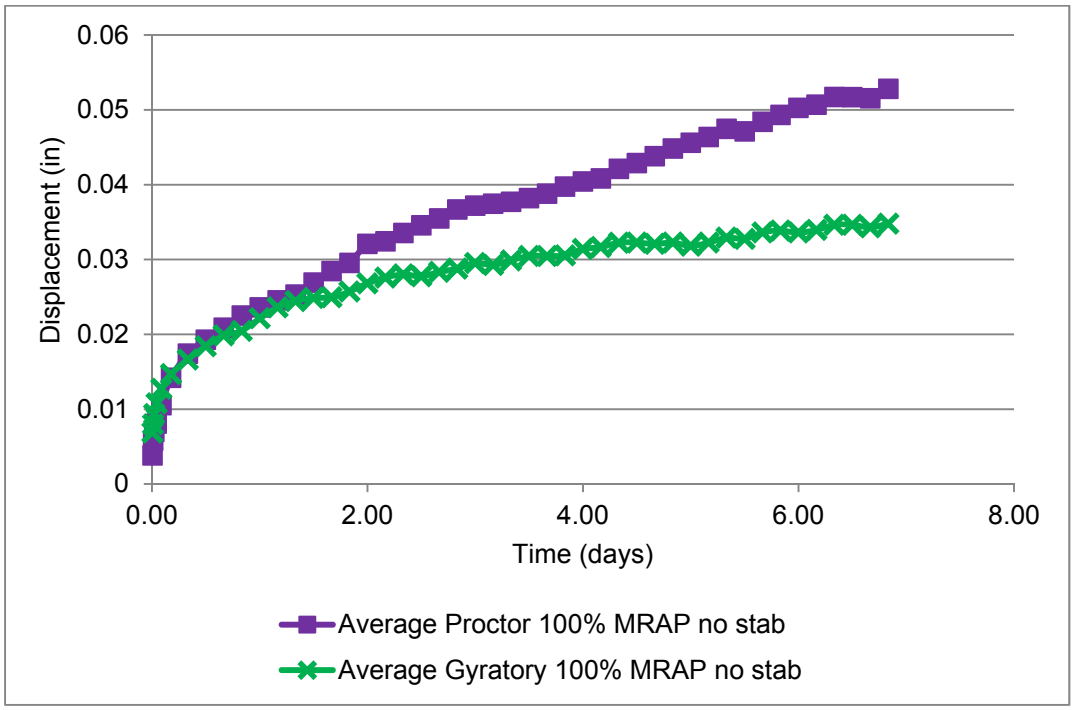

Figure 4-72- Gyratory and Proctor Unconfined Creep: 100% Melbourne Milled RAP

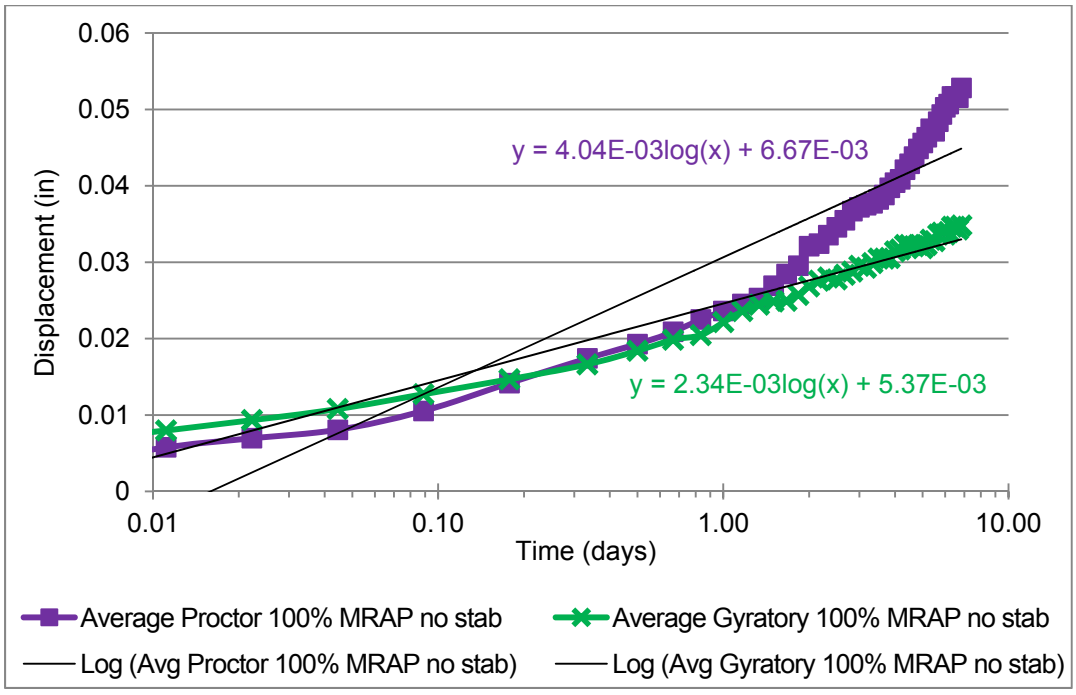

Figure 4-73- Gyratory and Proctor Unconfined Creep:100% MRAP Log (t)

4.5.4.3. Creep of 50% RAP/50% Limerock Specimens

The Proctor and gyratory specimens of blended 50% MRAP/ 50% limerock showed some difference in initial displacements (Figure 4-74) and a difference in CSR (Figure 4-75). CSR for the Proctor specimens (2.53×10^{-4}) was approximately 25% higher than the rate for the gyratory specimens (2.09×10^{-4}). These were approximately two times the rates observed for 100% (2x) limerock but only 4% ($1/25^{th}$) of the rates observed for 100% MRAP. To put these results in perspective, 100 years of creep at the 2.53×10^{-4} log(t) rate would result in an additional 0.0045-inches of deformation.

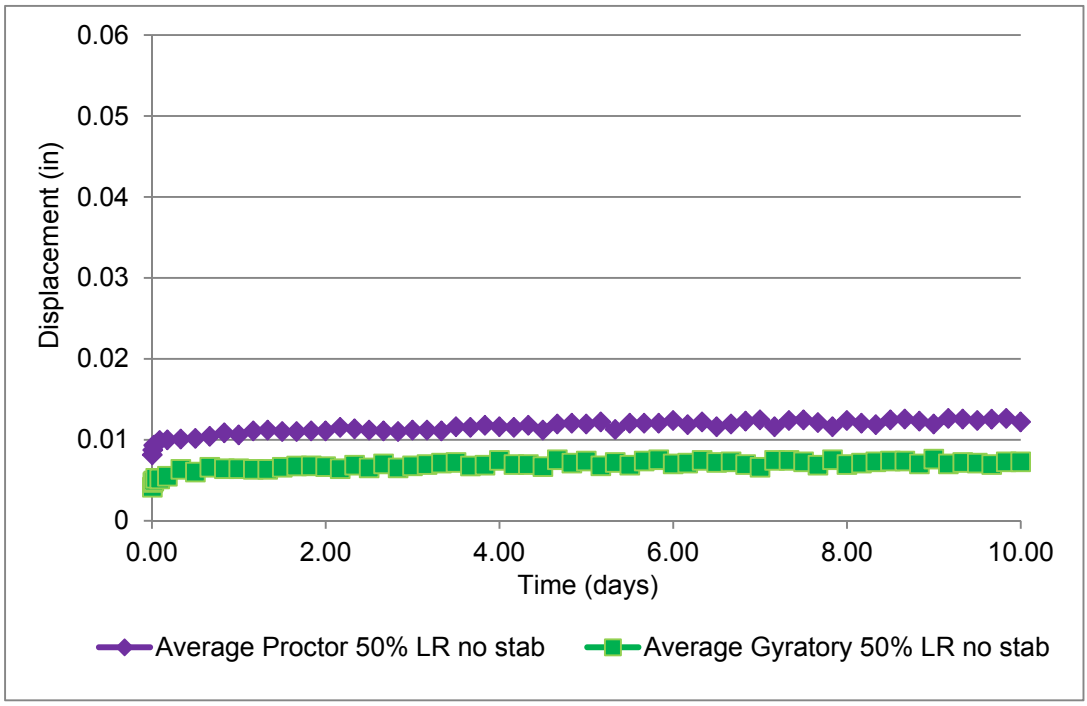

Figure 4-74: Gyratory and Proctor Unconfined Creep: 50% MRAP 50% LR

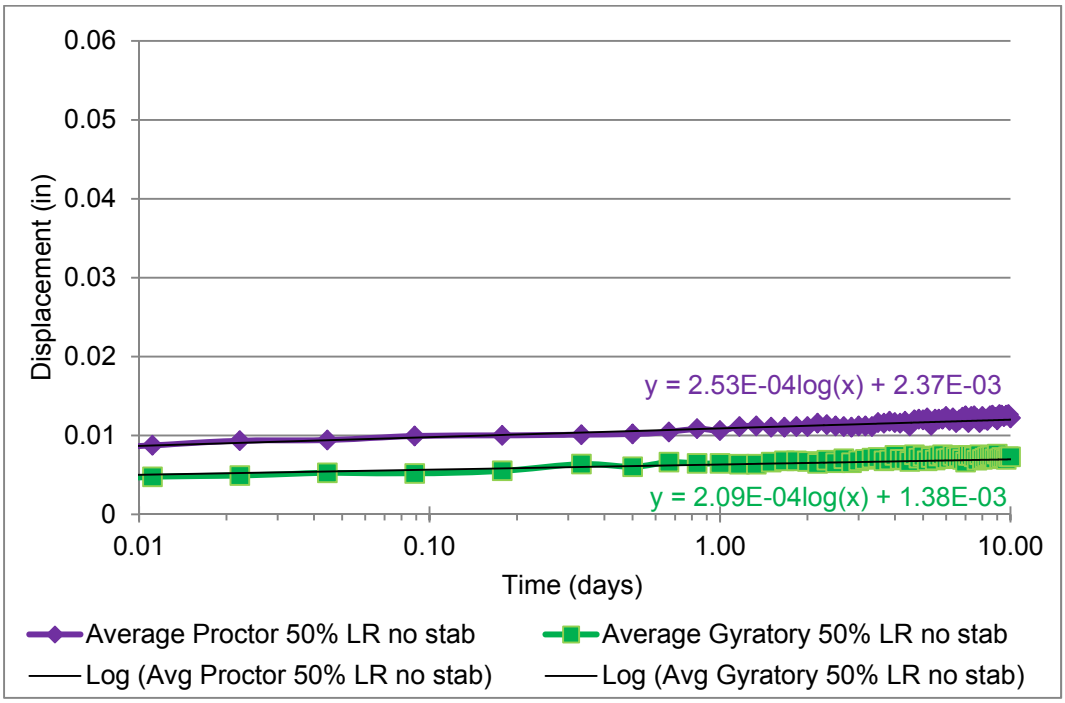

Figure 4-75: Gyratory and Proctor Unconfined Creep: 50% MRAP 50% LR Log (t)

4.5.4.4. Summary of Unconfined Creep

As was the case with the strength tests, gyratory compaction had a larger effect on deflection and CSR for the 100% RAP, a moderate effect on the 50%/50% blend, and no effect on 100% limerock. The differences observed were not as pronounced as those observed in the strength tests. The most significant result of these tests was that blending had a much greater impact on deflection and CSR than the method of compaction. Both the gyratory and modified Proctor 100% RAP specimens entered tertiary creep after approximately one day of unconfined 12 psi stress while the 50%/50% blends were projected to remain in linear secondary creep over any reasonable design life. The improvements in CSR and total deflection from blending are more evident when the three different blends are plotted on the same graph. As Figure 4-76 and Figure 4-77 show, the 50%/50% blend has much less total creep deformation and a CSR very close to 100% limerock for both Proctor and gyratory compaction specimens.

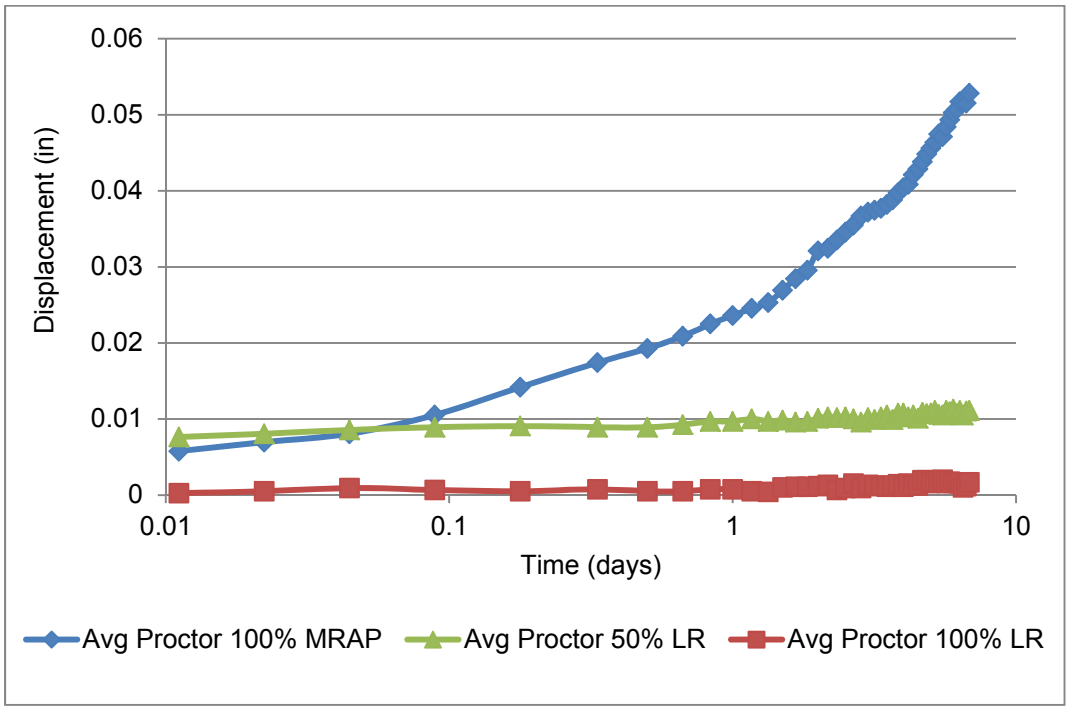

Figure 4-76: Unconfined Creep of Proctor Compacted Specimens Log (t)

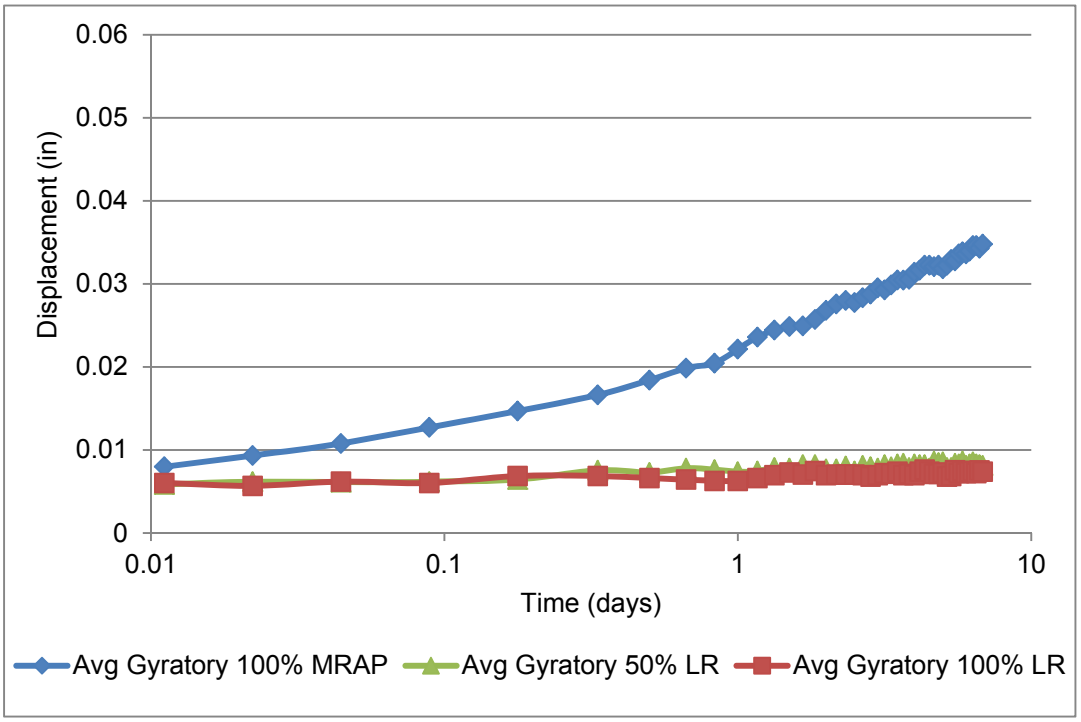

Figure 4-77: Unconfined Creep of Gyratory Compacted Specimens Log (t)

Table 4-29 is a summary of the creep displacements and strain rates obtained from the unconfined creep testing. Both parameters were evaluated in comparison to limerock and the results are shown in terms of ratios between MRAP and Limerock. The creep displacements include the effects of the initial displacement; however, they clearly show significant increases for 100 % MRAP. The 50%/50% blend displacement increases are about 1/5th those for the 100% MRAP. This data also shows that gyratory compaction improves the creep performance.

Table 4-30 is a summary of the ratios between the Modified Proctor and gyratory displacement and CSR between MRAP and Limerock. Comparing the values in this table to Table 4-29 data shows that blending (where the ratios decrease from over 20 to 1) has a greater effect on creep than gyratory compaction (where the ratios decrease from 1.68 to 1).

Table 4-29 Summary of 7-day Creep Displacements and Strain Rates from Unconfined Creep Testing

Sample Description	7-day Creep Displacement (in)	Ratio to 100% Limerock Gyratory	CSR (Strain/Log (t (days))	Ratio to 100% Limerock Gyratory
100 % MRAP Proctor	0.053	31x	.00404	37x
50%/50% Blend Proctor	0.011	6.5x	.000253	2.3x
100 % LR Proctor	0.0017	0.23x	.00011	0.97x
100% MRAP Gyratory	0.035	4.77x	.00234	20.8x
50%/50% Blend Gyratory	0.0082	1.12x	.00021	2.3x
100 % LR Gyratory	0.0073	1.00	.00013	1.00

Table 4-30: Summary of Ratios between Modified Proctor and Gyratory 7-day Creep Displacements and Strain Rates

Sample Description	Displacement Ratio Proctor/gyratory	CSR Ratio Proctor/gyratory
100 % MRAP	1.52	1.73
50%/50% Blend	1.37	1.21
100 % LR	0.23	0.97

4.6. Performance Improvements Using Chemical Stabilizers

This section discusses the effects of adding chemical stabilizing agents to blends of Melbourne milled RAP (MRAP) and high quality virgin aggregates. Dikova (2006) observed improvements in RAP/A-3 sand blends compared to 100% RAP. An initial round of tests was completed in this study using the MRAP and A-3 sand and a chemical stabilizing agent, however the LBR of the blends fell well below 100 (Section 4.6.1.1.). Because of this initial result, a higher strength aggregate was chosen for subsequent blends. The remaining blends in this part of the research program were made using limerock and one of four different chemical stabilizing agents. A single type of RAP and a single high quality base material were used in this section to isolate the effect of the stabilizing agent from the effect of the different aggregates and RAP sources. Unless otherwise noted, all compaction was performed according to the modified Proctor procedure in FM 5-515 (Limerock Bearing Ratio). All LBR values are from unsoaked tests conducted after curing and creep testing which results in higher values than those from soaked tests. The testing was done in this fashion to enable completion of the research in a timely manner. These LBR results are for comparison purposes and not to be associated with design values.

100% MRAP, 100% limerock, and blends of 75%, 50%, and 25% MRAP were tested. The LBR versus dry density results from 20 LBR tests of blends without chemical stabilizing agents are shown in Figure 4-78. Both dry density and unsoaked LBR increased with increasing amounts of limerock in the blend. The 75% MRAP/25% LR specimens had a lower dry density than the 100% MRAP but still had higher LBR values. The largest increases occurred from the

50%/50% to the 25%/75% MRAP/limerock blends. Similar results were already shown throughout this and previous studies (Cosentino and Kalajian, 2001, Cosentino et al., 2011).

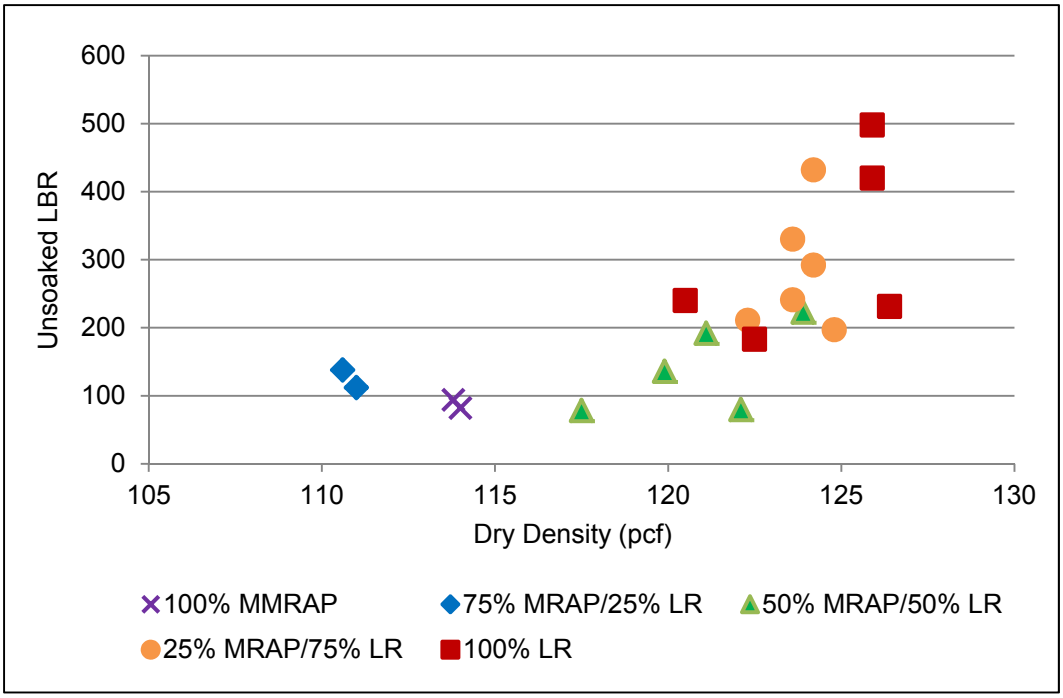

Figure 4-78: Unsoaked LBR versus Dry Density for MRAP/LR Blends

Table 4-31 shows the average unsoaked post-creep LBR for each blend shown in Figure 4-78. This data shows a large rise in average LBR value between the 50% MRAP/50% LR and the 25% MRAP/75% LR blend, doubling from an LBR of 142 to an LBR of 284.

Table 4-31 Average Unsoaked Post-Creep LBR for MRAP/LR Blends with No Chemical Stabilizer

Sample Description	Average Post-Creep Unsoaked LBR
100% MRAP	88
75%/25% MRAP/LR Blend	125
50%/50% MRAP/LR Blend	142
25%/75% MRAP/LR Blend	284
100% LR	314

4.6.1. LBR Results

4.6.1.1. Cationic (CSS-1H) Emulsion Stabilized RAP/A-3 Sand Blends

Dikova (2006) observed that blending varying amounts of A-3 sand with RAP resulted in an increase in LBR and decrease in creep. Dikova (2006) found that blends of 80% RAP/20% A-3 sand gave the highest dry density and LBR. The seven day creep deflection of this blend was 50% less than for 100% RAP.

One round of eight specimens was tested in this study using an 80% RAP/20% A-3 blend and a control of 100% MRAP with 0% and 2% CSS-1H cationic asphalt emulsion. Adding emulsion to MRAP/A-3 blends increased the unsoaked LBR by approximately 40% from an average of 40 to an average of 55 (Figure 4-79). The MRAP/A-3 blends improved strength but did not achieve the required LBR value of 100. The A-3 sand grain size indicates it is uniformly graded with about 90% passing the # 40 sieve and about 8% passing the #100. This increase most likely resulted from the addition of this material passing the # 40 sieve which improved the gradation of the blend.

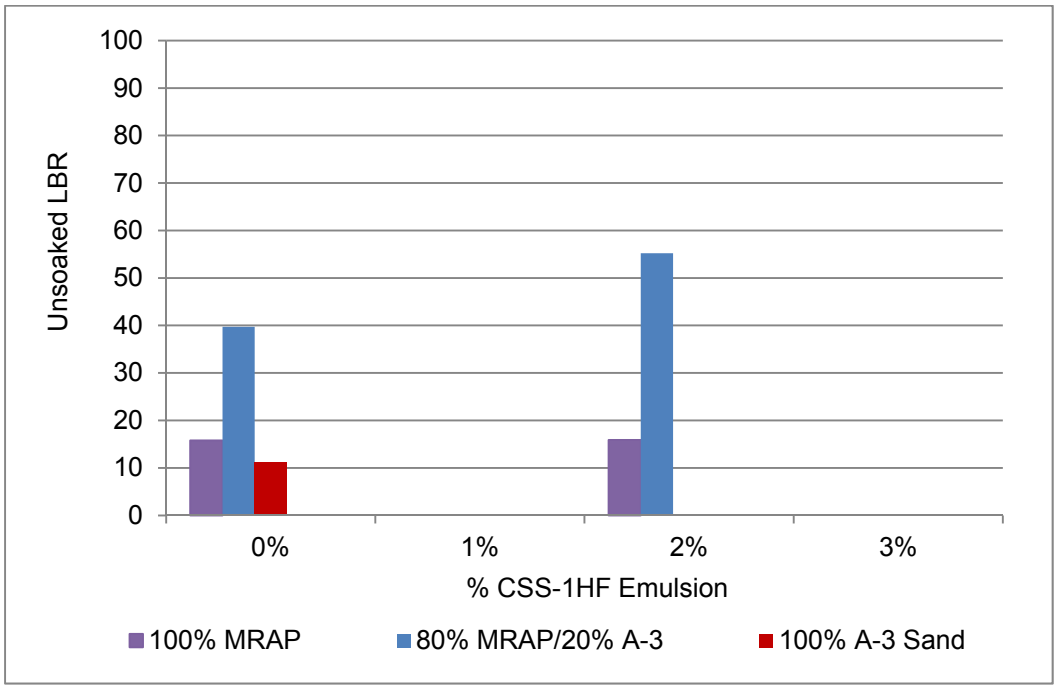

Figure 4-79: Preliminary Post-Creep LBR Results: A-3/RAP Blends

Further testing with A-3 blends was not pursued because the unsoaked LBR values of approximately 50 were inadequate for base course use. These tests were only conducted with 2% CSS-1H so it is not possible to make any conclusions about varying the amount of emulsion. Additional testing with a range of emulsion contents and soaked testing would be required to determine whether MRAP/A-3 blends may achieve the soaked LBR of 40 required for subbase.

4.6.1.2. Cationic (CSS-1H) Stabilized MRAP/Limerock Blends

Adding 2% CSS-1H emulsion to 100% MRAP resulted in an unsoaked LBR of 22 – identical to the unsoaked LBR of 100% MRAP. These specimens were air cured at ambient temperature. Other trials which used oven curing produced higher unsoaked LBRs, however, all LBR values were so far below the required soaked LBR of 100 that no additional emulsion stabilized tests were performed on 100% MRAP specimens.

Unsoaked LBR tests were conducted, with 0%, 1%, 2%, and 3% CSS-1H emulsion added to MRAP/LR blends with 100%, 75%, 50%, 25%, and 0% MRAP. Two specimens were tested for each blend/stabilizer level for a total of 24 specimens. The results are summarized in Figure 4-80. Complete results are shown in Appendix B. The 100% MRAP and 100% limerock

specimens were used in this series of tests as control samples with no emulsion added. Adding 1% CSS-1H emulsion to 50% MRAP/50% LR blends increased LBR by approximately 25%. Adding 2% CSS-1H to the same blend had little effect on LBR. Adding over 2% CSS-1H decreased LBR (Figure 4-80). The same general trend was observed for 75% MRAP/25% LR blends. The 75% MRAP/25% LR blend results were similar. At 2% emulsion the LBR was lower than the reference unstabilized LBR. Since these unsoaked LBR values were below 100, there was no possibility of an acceptable soaked LBR.

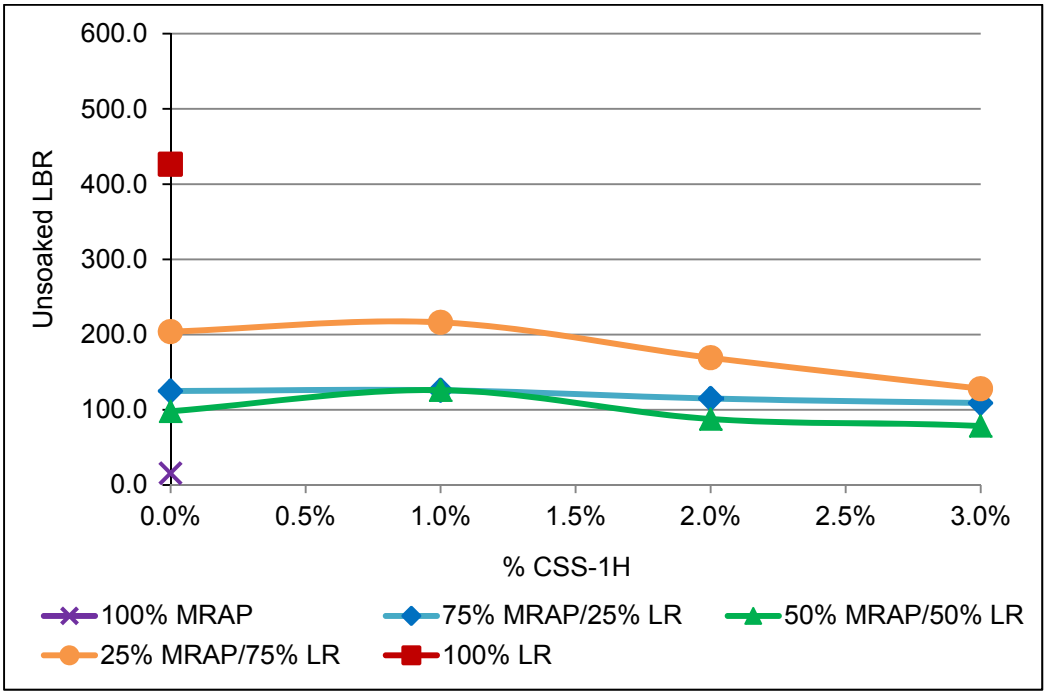

Figure 4-80: Post-Creep LBR vs % CSS-1H Emulsion Limerock/RAP Blends

In summary, the largest improvement in LBR occurred with 1% CSS-1H emulsion. The 25% MRAP/75% LR blend consistently exceeded an LBR of 100 but these values are for unsoaked post-creep tests.

4.6.1.3. Anionic Emulsion (SS-1H) Stabilized MRAP/Limerock Blends

The same MRAP/limerock blends were tested with anionic (SS-1H) emulsion. For this round of testing the limerock specimens were also stabilized with emulsion for comparison purposes. A total of 34 specimens were tested in this round. Complete results are shown in Appendix B. The oven curing period was lengthened to 48 hours due to some instances of

incomplete separation of the emulsified asphalt and water at higher emulsion contents. The longer oven curing period resulted in higher unsoaked LBR values in this round of testing than were observed in the CSS-1H round. Because of the longer oven curing period the SS-1H results are not directly comparable to the CSS-1H results reported above.

As was the case with CSS-1H emulsion, adding 1% SS-1H to 100% MRAP decreased the unsoaked LBR. Since its LBR was under 100, no tests were done at the higher asphalt contents (not shown on chart). Summarized results are shown in Figure 4-81. 100% MRAP and 100% limerock LBR values are shown without stabilizer as control specimens. The 75% MRAP/25% LR specimens decreased in LBR with added SS-1H. On the other hand, adding 1% SS-1H to 50% MRAP/50% LR blends increased LBR by approximately 5%. Adding 2% or 3% SS-1H to the same blend decreased LBR. 75% MRAP/25% LR blends showed a similar increase in unsoaked LBR at 1% emulsion and a decrease with additional emulsion.

The largest improvement in unsoaked LBR in this round of testing was approximately 20% for 1% SS-1H added to the 75% MRAP/25% LR blend. Both the 25%/75% and 50%/50% MRAP/LR blends consistently produced unsoaked post-creep LBR values greater than 100.

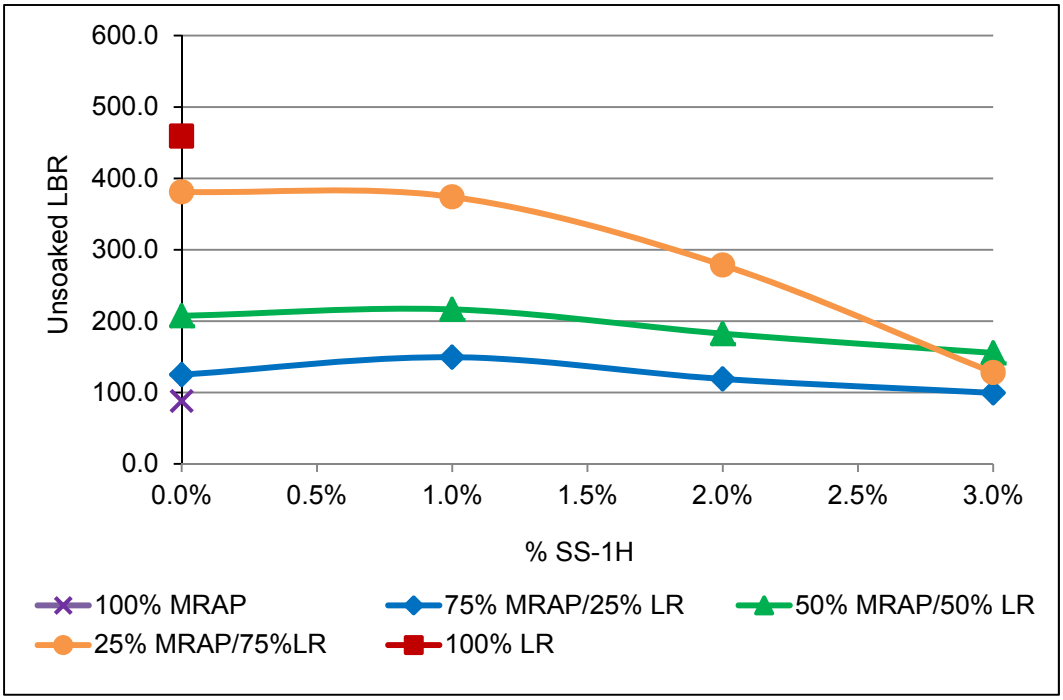

Figure 4-81: Post-Creep LBR vs % SS-1H Emulsion MRAP/Limerock Blends

4.6.1.4. Portland Cement (PC) MRAP/Limerock Stabilized Blends

The same MRAP/limerock blends were tested using Portland cement as a stabilizing agent at 1%, 2% and 3% cement by weight. Cement was only added to the MRAP/LR blends. The unstabilized 100% limerock and 100% MRAP specimens were used as controls for comparison. A total of 28 specimens were tested in this round. Complete results are shown in Appendix B. The specimens were cured in the mold for 7 days at ambient temperature prior to placing them in the creep test devices. Cement stabilized specimens were not oven cured.

The cement stabilized specimens consistently gained unsoaked LBR strength as more cement was added. At 3% cement content the strength exceeded the 10,000 pound capacity of the CBR (LBR) test machine before reaching 0.1-inches of penetration. The maximum capacity of the test machine corresponds to an LBR of approximately 416. LBR values greater than 416 were extrapolated from the load-deflection test data as indicated by a dashed line in Figure 4-82.

The 100% limerock and 100% MRAP specimens were the control samples. Cement stabilization was only performed on blends of MRAP/LR. Adding 1% Portland cement to 75% MRAP/25% LR blends improved unsoaked LBR by over 70% compared to an unstabilized blend. Adding 2% cement improved LBR by nearly 350% and 3% cement improved by nearly 500%. The same general trend was observed for all three blends. Unlike the emulsion stabilized samples which showed an optimum % of stabilizing agent, the cement stabilized samples continued to gain significant strength with increasing cement content (Figure 4-82).

Both the 50% MRAP/50% LR blend with 2% cement and the 25% MRAP/75% LR blend with 1% cement achieved an unsoaked LBR approximately equal to 100% limerock. The largest increase in LBR occurred between the 50%/50% and 25%/75% blends. This trend matches the trends from the emulsions.

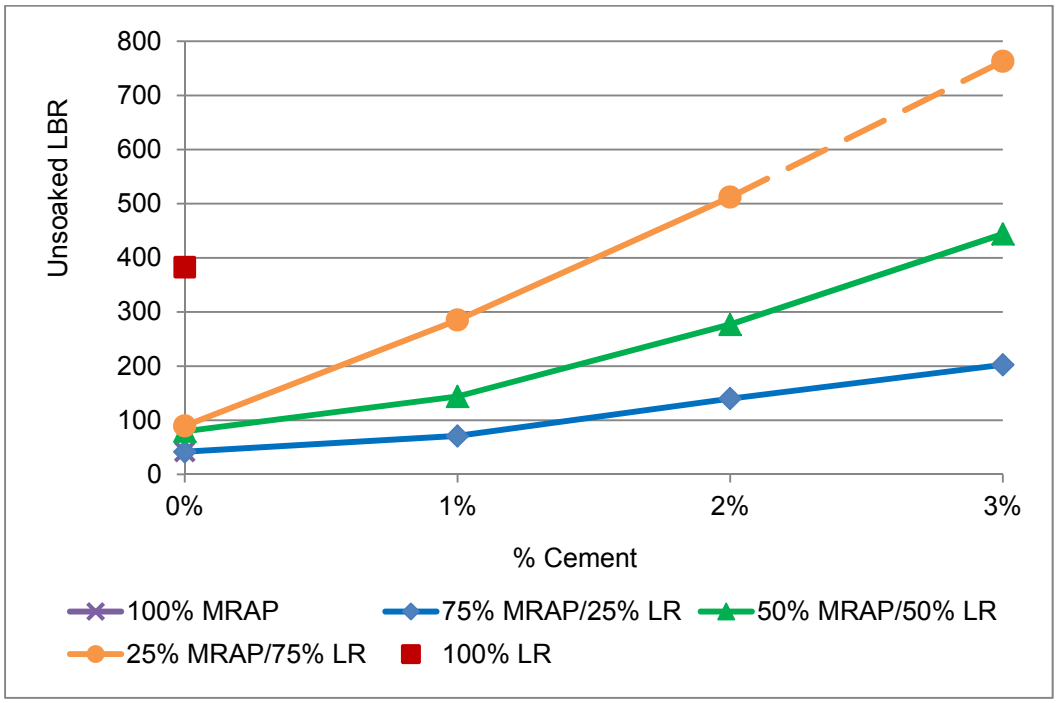

Figure 4-82: Post-Creep LBR vs. % Portland Cement Limerock/RAP Blends

4.6.1.5. Summary of Chemically Stabilized LBR for 50%/50% and 25%/75% MRAP/Limerock Blends

Due to the curing, chemically stabilized MRAP/LR blends with no more than 50% MRAP had unsoaked LBR strengths over 100. 50% MRAP/50% LR blend LBR versus percent stabilizing agent is shown in Figure 4-83.

As discussed earlier in Section 4.6.1.3, the consistently higher LBR values of the SS-1H specimens compared to the CSS-1H specimens are an anomaly. The unsoaked LBR of all three blends would be expected to be the same with no stabilizing agent. The Portland cement stabilized specimens were not oven cured since drying them would have removed the moisture required for cement hydration. The 0% cement stabilized blend and the 0% CSS-1H blend which was oven cured for a 24 hour period show good agreement. The large apparent difference in LBR between the 0% SS-1H and the other two specimens is probably the result of increasing the oven curing time for the SS-1H specimens to 48 hours and not due to the difference between the anionic and cationic emulsions. Soaked LBR testing, which will be discussed in Section 4.6.5, showed much closer consistency between the emulsion types.

Aside from the difference resulting from the curing time, the anionic and cationic emulsions showed nearly identical trends: a small unsoaked post-creep LBR increase at approximately 1% emulsion content followed by a gradual decrease in LBR strength with the addition of 2% and 3% emulsion. Cement, on the other hand, increased LBR of the 50%/50% blends in an almost linear relationship with no observed peak or optimum amount. Aside from the anomalously high SS-1H results, 1% emulsion and 1% cement stabilized specimens had similar unsoaked LBR strengths. At 2% or 3% stabilizer the cement specimens were much stronger than the emulsion stabilized specimens.

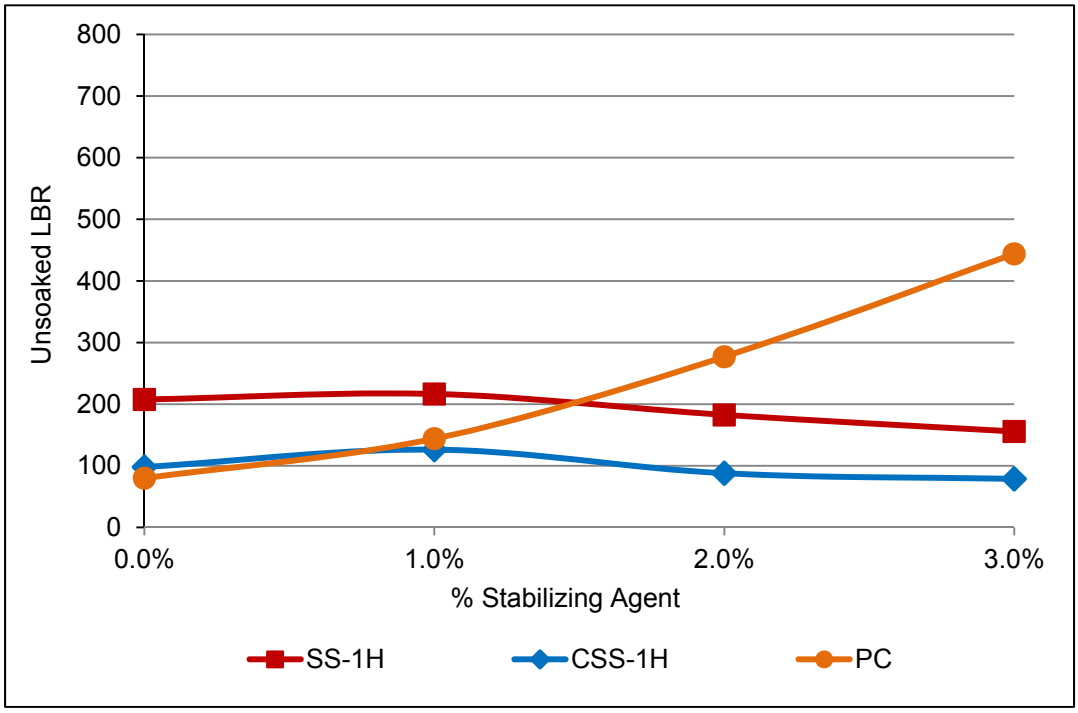

Figure 4-83: Stabilized 50% MRAP/50% LR Blend Unsoaked LBR Summary

Test results for 25% MRAP/75% LR blends are summarized in Figure 4-84. Complete results are shown in Appendix B. Both blends showed very similar trends for all three stabilizing agents.

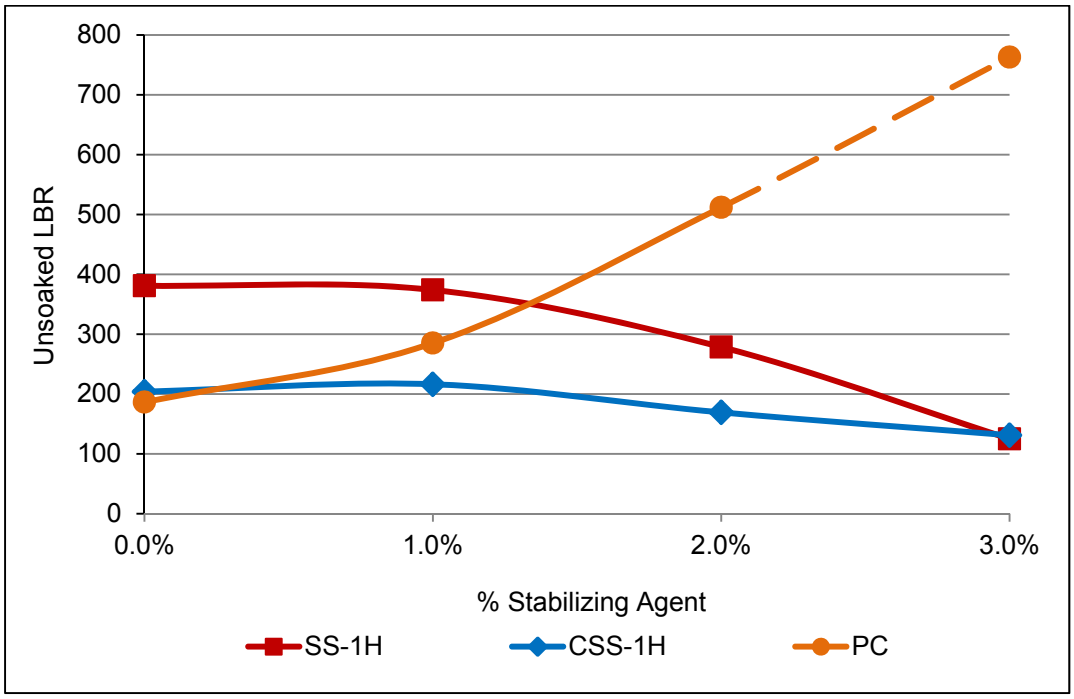

Figure 4-84: Stabilized 25% MRAP/75% LR Blend Unsoaked LBR Summary

In summary, except for the 2% and 3% cement stabilized specimens 75% MRAP/25% LR blends had unsoaked LBR strengths under 100 making them unsuitable for base course applications. The 50% MRAP/50% LR blends produced unsoaked LBR strengths over 100 with 1% emulsion or cement. Additional emulsion lowered the LBR but additional cement raised the LBR. The 25% MRAP/75% LR blends consistently produced unsoaked post-creep LBR values over 200. Soaked LBR testing was used to determine if the FDOT specification of 100 can be achieved with the 50% MRAP/ 50% LR and/or 25% MRAP/75% LR chemically stabilized blends. Soaked results will be discussed in Section 4.6.5.

4.6.2. Creep Test Results

This section presents the creep results for blended chemically stabilized specimens. All creep results in this section were conducted on specimens subjected to a constant stress of 12 psi for seven days. Results were plotted as displacement versus time and displacement versus log(time). Displacement was used instead of strain for several reasons. First, measurements were taken as deformations, second, the one-dimensional (in mold) testing confines the specimens

resulting in varying stress levels, and third, all samples were the same height so plotting strain rather than deformation produced the same trends.

As was previously discussed in Section 4.2.2, logarithmic trendlines were fitted to the secondary creep portion of the log(time) curves starting at time of 0.01 days (14.4 minutes). The 0.01 day time was selected based on experimental results indicating that the large primary stage deformations occur before this time. On the log(time) plot, this produces a line with the equation $\delta = m \log(t) + b$. In this report the slope of the trendline, m, is referred to as the CSR. The y axis intercept, b, is the primary (settlement) deformation that occurs in response to the application of the loading pressure.

This primary settlement has two major and two minor components. Neither of the major components: displacements resulting from surface irregularities/seating or rearrangement of the soil skeleton are indicative of creep under constant load. The two minor components are elastic (recoverable) deformation of the soil skeleton and viscoelastic creep. It is not possible to differentiate between these four stage-one deformation components. It is possible to state that creep deformation is a very small portion of the total stage-one deformation because of the very short time frame.

During stage-two creep (creep) settlement, the seating and soil skeleton deformations have already occurred and add no further to deformation. Elastic deformation remains constant under constant stress. The CSR (slope, m) during the secondary stage deformations under constant stress is an accurate indicator of creep susceptibility because it solely represents viscoelastic deformation under constant stress. For these reasons, CSR is a better indicator in comparing the creep performance of the various chemically stabilized blends rather than total 7-day deformation.

A typical set of displacement versus linear time curves for 100% limerock and 50% MRAP/50% LR with 0%, 1%, and 2% CSS-1H stabilizer is shown in Figure 4-85. Each curve represents a single specimen. The 100% limerock plot is nearly flat (zero slope) while the blend plots have slight slopes. In this figure there is more total deformation in the MRAP/LR blends than in the 100% limerock.

The CSR (slope) differences are more evident in the deformation versus log(time) plot in Figure 4-86. 100% limerock has the lowest CSR (slope), followed by the unstabilized 50%/50% blend, then the 50%/50% blend with 1% emulsion, and finally the 50%/50% blend with 2% emulsion. These results indicate that as the emulsion percentage increases the creep increases. Asphalt emulsion is approximately 67% asphalt binder and 33% water with a small amount of emulsifier. The net effect is that adding emulsion increases the asphalt content of the blend. This trend of higher creep deformation with higher asphalt content of blends agrees with results of earlier research (Dikova, 2006).

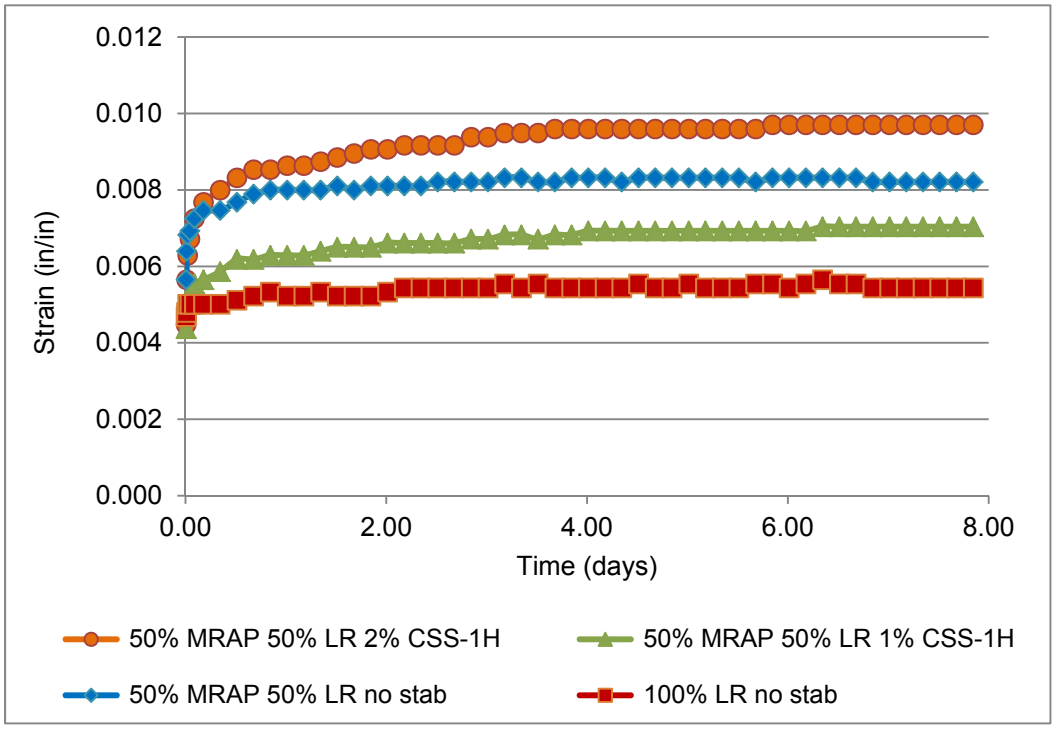

Figure 4-85: Typical Creep of CSS-1H Stabilized Blends – Linear Time

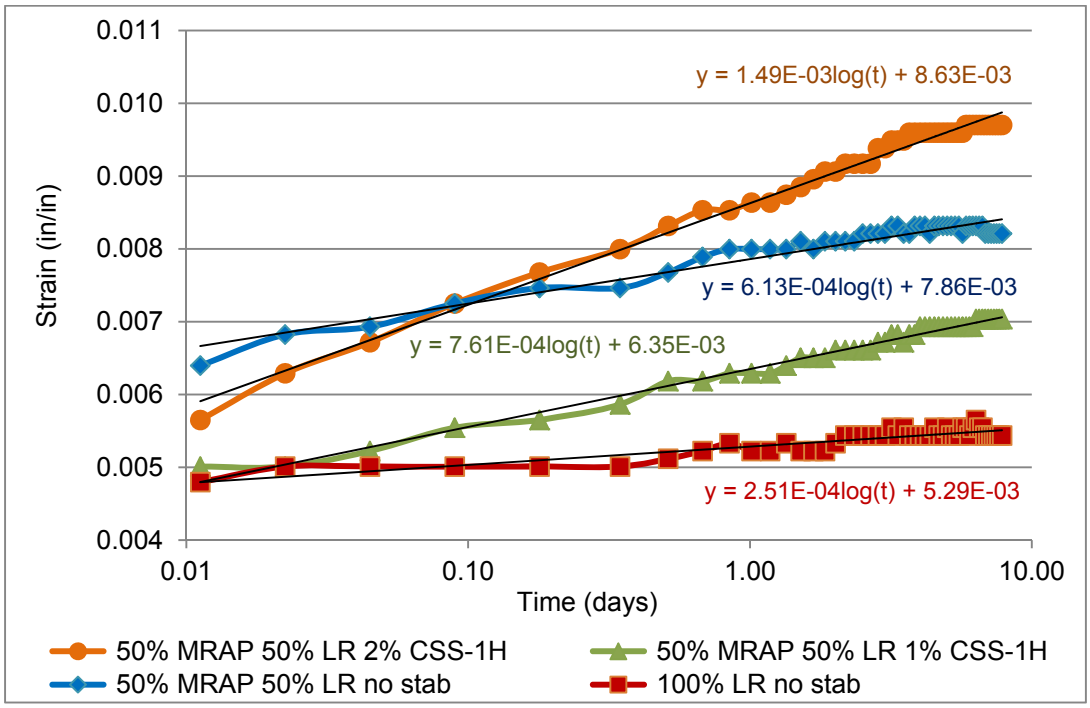

Figure 4-86: Typical Creep of CSS-1H Stabilized Blends – Log (time)

4.6.2.1. Cationic Emulsion (CSS-1H) Stabilized MRAP/A-3 Sand Blends

Dikova (2006) noted decreased creep deformation in RAP/A-3 sand blends. As briefly discussed in the creep test results introduction, an initial round of testing was performed to confirm Dikova's (2006) results using a constant pressure of 12 psi for 7 days. The data from this testing is shown in Figure 4-87. The 100% Melbourne milled RAP produced the most deformation. The 100% A-3 sand exhibited nearly no secondary creep deformation. Specimens of 80% MRAP/20% A-3 sand blends with 2% CSS-1H emulsion produced creep deflections of approximately 0.025-inches, which is about 1/3 that of the 0.073-inches observed in unblended unstabilized RAP. The emulsion stabilized blends had less total deflection after 7 days than the 100% A-3 specimen, most likely because of initial specimen seating.

The 100% A-3 specimen reached 90% of its final deformation after approximately one hour and 98% of its final deformation after one day. Both the 100% MRAP and the MRAP/A-3 sand blends continued to deform (creep) under constant pressure throughout the duration of the test. This trend is clearly shown when deflection is plotted versus log(time) in Figure 4-88.

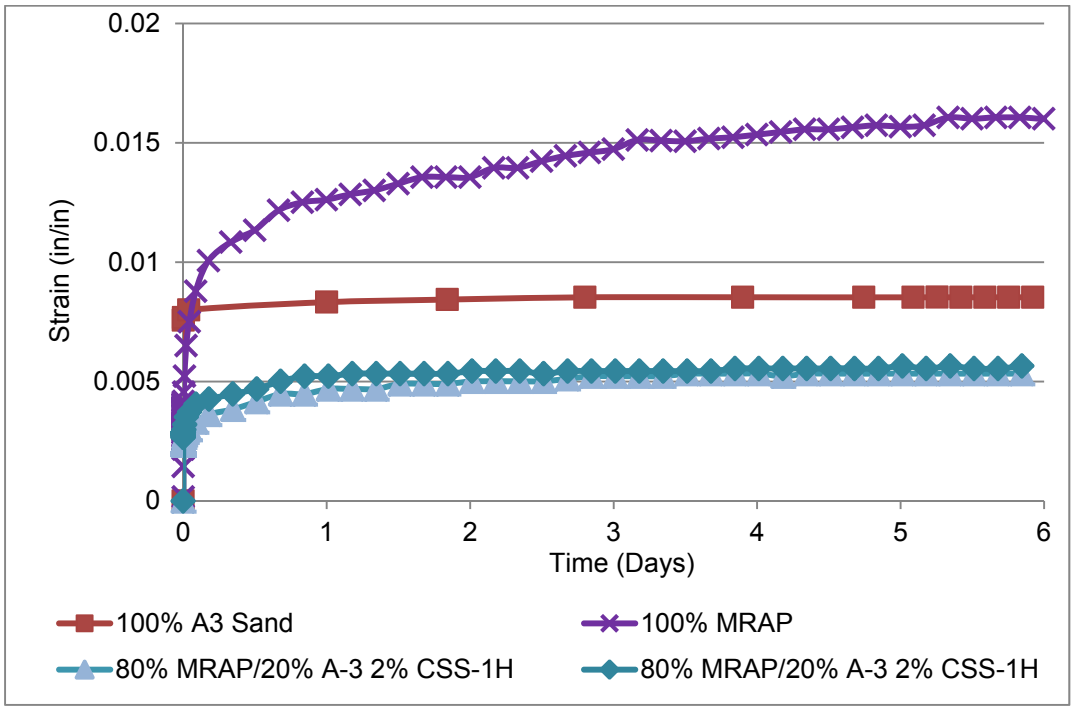

Figure 4-87: Creep of MRAP/A-3 Blends – Linear Time

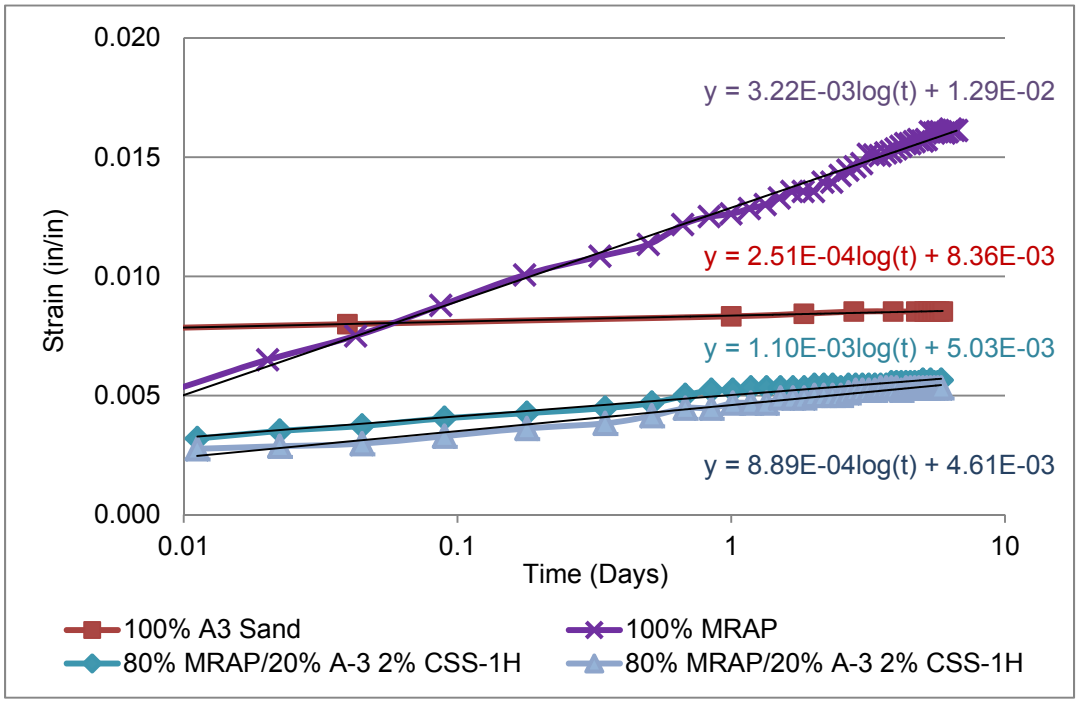

Figure 4-88: Creep of MRAP/A-3 Sand Blends – Log(time)

The CSR of the Melbourne milled RAP and its blends are all higher than that of the A-3 sand. Based on the initial round of testing chemically stabilized RAP/A-3 blends had better creep performance than 100% MRAP. At the observed creep rates, a 10-inch thick base course comprised of 100% RAP would experience 0.29-inches of creep while the stabilized 80% MRAP/20% A-3 blend would experience 0.09-inches of creep (average) after 30 years. A 100% A-3 base course would not creep. While this was a significant improvement in creep performance, as discussed earlier the LBR values of these blends were too low to be used as a base course material. The remaining chemical stabilizing agent tests were conducted with Melbourne milled RAP/limerock blends.

4.6.2.2. Cationic Emulsion (CSS-1H) Stabilized MRAP/Limerock Blends

Twenty two creep tests were conducted and the data reduced to the slope of the displacement versus log (time (days)) and creep rate versus % CSS-1H emulsion. Figure 4-89 shows the creep rate for CSS-1H emulsion stabilized MRAP/limerock blends, plus the 100% limerock, and 100% MRAP. Limerock was used as a control material since it does not creep and 100% RAP was used as a control to evaluate the effect of blending and stabilizing agents on creep.

There is only one data point for 100% limerock which overlaps 0% CSS-1H 25% MRAP/75% LR blend data point. The 50% MRAP/50% LR blend with no emulsion had approximately two times the creep rate of 100% limerock but this was approximately 1/4 of the creep rate of 100% MRAP and 1/3 the creep rate of 75% MRAP/25% LR. The addition of 1% CSS-1H emulsion produced a slight decrease in creep rate for the 50% MRAP/50% LR blend while the addition of 2% or 3% emulsion increased the rate of creep above that of the blend without stabilizer. The 25%MRAP/75%LR blend had the same creep rate as limerock without adding any emulsion. With 1% emulsion the creep rate of the 25% MRAP/75% LR blend was slightly lower than the creep rate of the 100% limerock. Addition of 2% emulsion caused the creep to increase above the original value without stabilizer similar to the 50%/50% blend. Since the 2% emulsion blend already exceeded the unstabilized creep rate, a 3% specimen was not tested.

Adding 2% CSS-1H to 100% MRAP increased the creep rate by approximately 40% over the unstabilized MRAP. No other specimens of 100% MRAP were tested because of their high creep rates. Only one specimen of 75% MRAP/25% CSS-1H was tested because the creep rate without chemical stabilization was over 7 times that of the 100% limerock so there was no likelihood of achieving an acceptable CSR by adding emulsion.

Adding 1% emulsion reduced creep slightly but 2% or higher increased creep. Blending had a much greater effect on creep than adding emulsion. Blends with 50% or less MRAP had creep rates approximately 30% of the creep rate of 100% MRAP (< 0.01 versus 0.03 in/in/log(t)). Stated another way, blending MRAP with at least 50% virgin aggregate reduced the creep rate by over 70% compared to unblended MRAP.

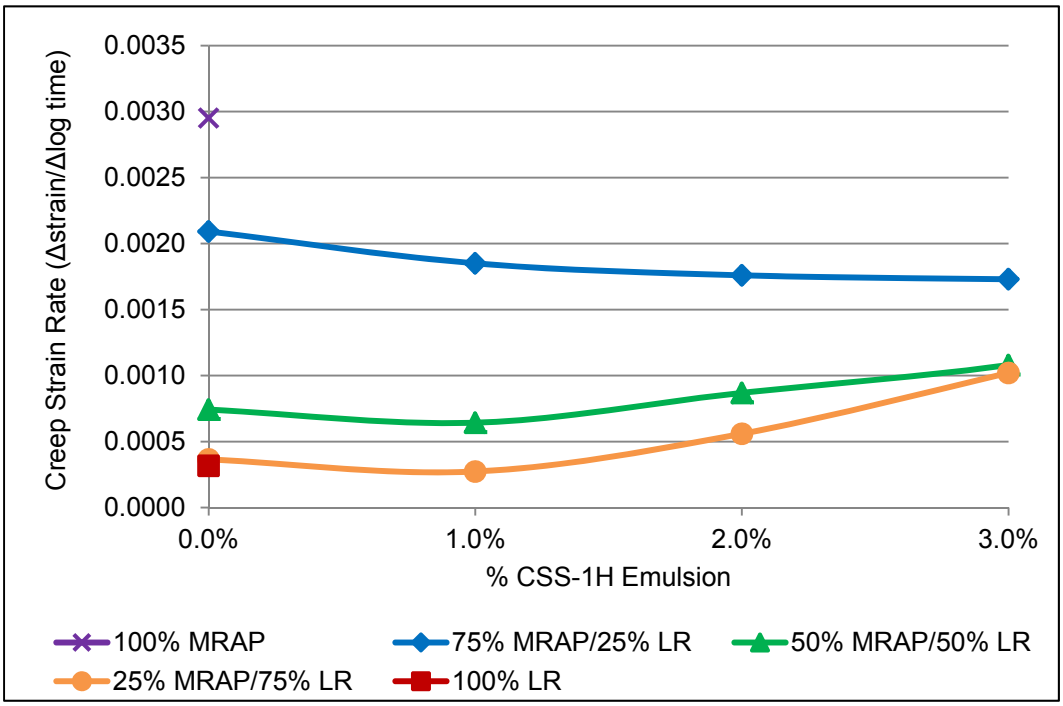

Figure 4-89: Strain Rate in CSS-1H Stabilized Limerock/RAP Blend

4.6.2.3. Anionic Emulsion (SS-1H) Stabilized MRAP/Limerock Blends

Thirty four creep tests were conducted and the data reduced to plot the displacement versus time or log (time (days)). CSR was calculated and plotted versus % SS-1H emulsion. As seen in Figure 4-90, the creep rates for the 50% MRAP/50% LR and 25% MRAP/75% LR blends were similar to 100% limerock throughout the SS-1H testing. Adding 1% SS-1H

emulsion decreased the creep rate slightly for the 75% MRAP/25% LR blend. Adding 2% SS-1H continued to decrease the creep rate but at 3% SS-1H the rate creep rate showed a small increase. These trends are slightly different from the general trends observed with CSS-1H emulsions however the difference may be related to the longer curing times used for the SS-1H emulsion specimens rather than differences in the emulsions themselves.

The addition of SS-1H emulsion to blends containing 50% MRAP resulted in a slight increase in CSR up to 2% emulsion. The 25% MRAP CSR increased slightly with the addition of emulsion. At 50% or higher limerock contents the deflections and hence creep rates are so small that they are close to the accuracy limits of the LVDT used for deflection measurements resulting in some fluctuation in the data.

As was the case for CSS-1H stabilized blends, the 50% MRAP/50% LR and 25% MRAP/75% LR blends had creep rates similar to 100% limerock. The 75% MRAP/25% LR blend had higher creep rates that were closer to 100% MRAP. As discussed earlier, longer curing times (48 hr) were used for the SS-1H emulsion specimens than CSS-1H emulsions (24 hr) which led to significantly higher (approximately doubled) unsoaked LBR values. There were not dramatic differences between the creep displacements or rates for the two emulsions. The SS-1H better reduced creep in the 75% and 100% MRAP specimens; otherwise the CSR's for the two types of specimens were nearly identical.

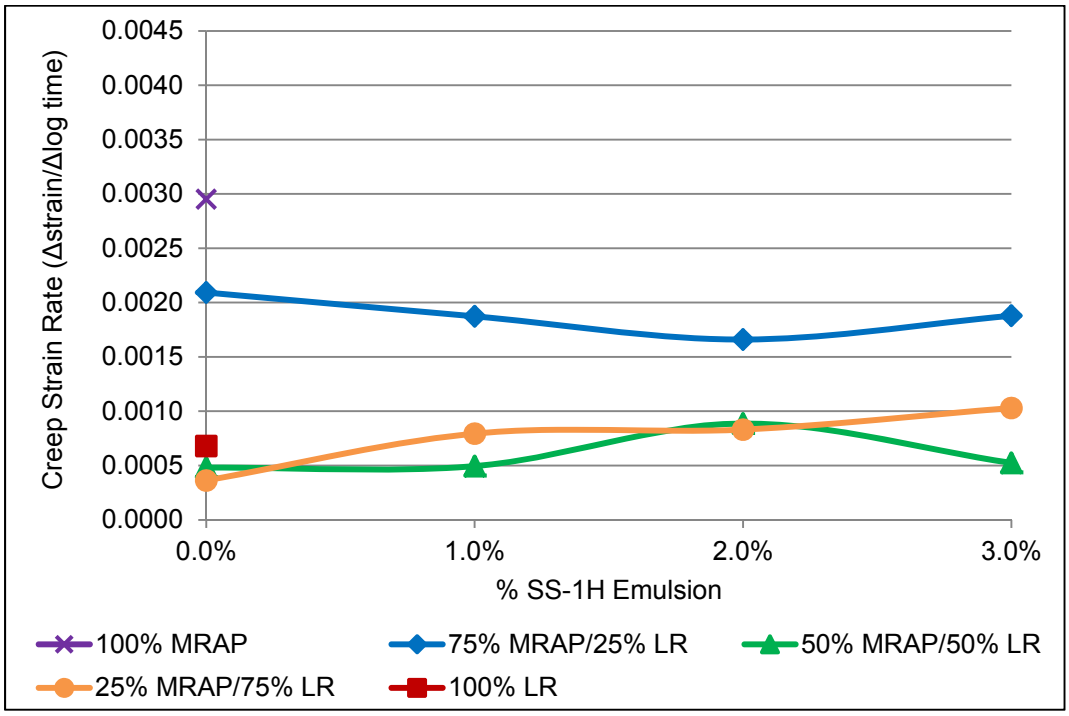

Figure 4-90: CSR in SS-1H Stabilized MRAP/Limerock Blends

4.6.2.4. Portland Cement (PC) Stabilized MRAP/Limerock Blends

Twenty six creep tests were conducted with MRAP/LR blends stabilized with Portland cement. Control specimens of 100% MRAP and 100% limerock were only tested without stabilizer. The results were reduced to plot displacement versus time and log (time (days)) or to plot calculated CSR versus % Portland Cement. As seen in Figure 4-91, the addition of 1% Portland cement drastically reduced creep rate in all blends. This effect was especially pronounced in the 75% MRAP/25% LR blends reducing the creep rate by approximately 75%. Unlike the asphalt emulsions which increased creep at higher concentrations, adding more Portland cement essentially eliminated creep in all of the blended specimens.

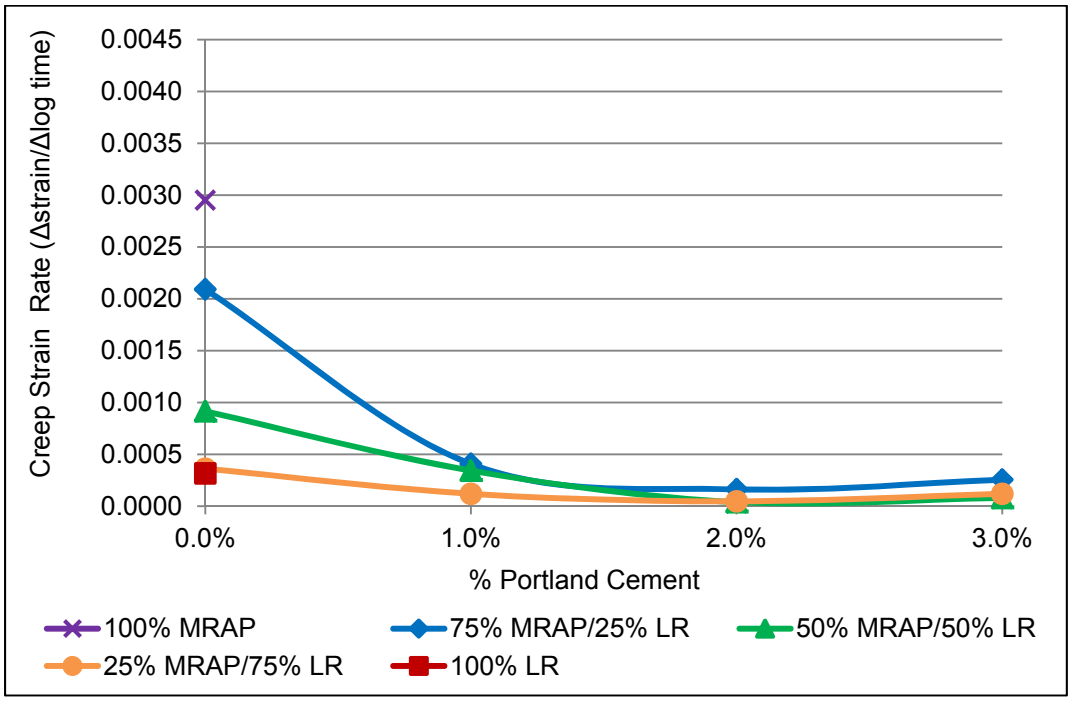

Figure 4-91: CSR in Portland Cement Stabilized MRAP/Limerock Blends

4.6.2.5. Summary of Stabilized MRAP/Limerock Blend Creep Rates

As discussed above, 75% MRAP/25% LR blends exhibited CSR's and trends in rates when stabilized similar to 100% MRAP. In contrast, 50% MRAP/50% LR and 75% MRAP/25% LR blends exhibited CSR's that were close to, or in some cases, lower than 100% LR. This section directly compares the observed CSR's for the 50% MRAP and 25% MRAP blends to more clearly show the effect of the three different stabilizing agents.

A summary comparing the CSR versus percent stabilizing agent for 50% MRAP/50% limerock blends is shown in Figure 4-92. Adding Portland cement nearly eliminates creep in 50%/50% blends especially at the 2 and 3 percent levels. For both anionic and cationic emulsions 1% slightly reduced creep but adding more than 2% generally increased creep. The 3% SS-1H specimens were processed in a separate batch from the 0%, 1%, and 2% specimens. The apparent decrease in creep at 3% SS-1H is probably due to differences in curing.

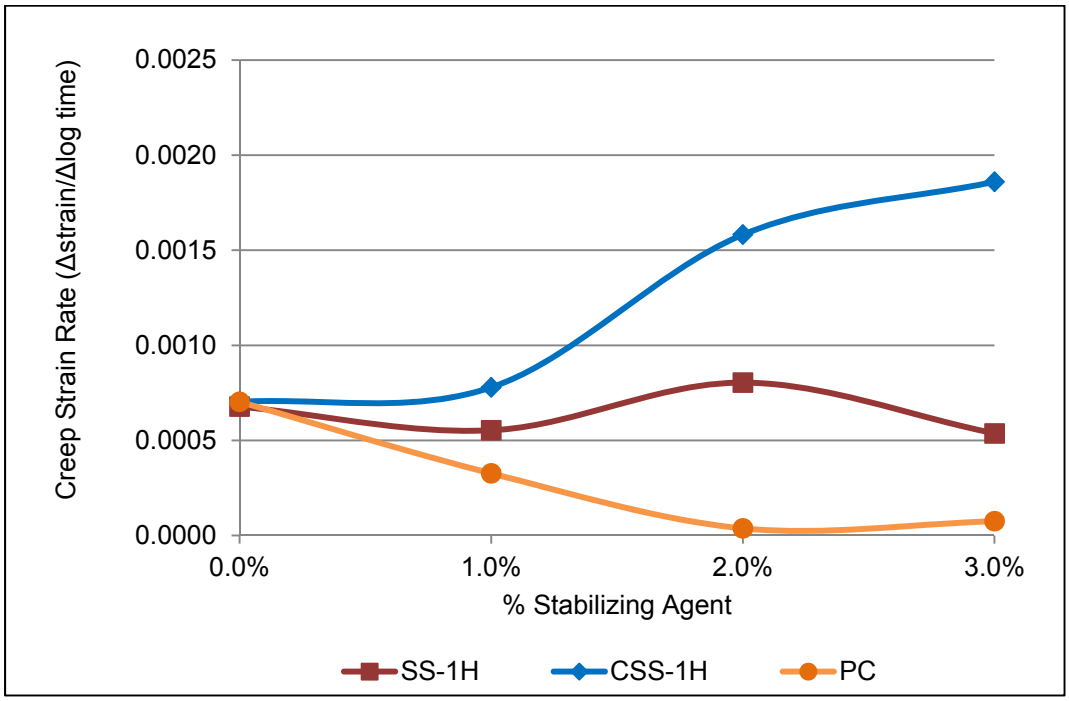

Figure 4-92: Stabilized 50% MRAP/50% LR Blend Creep Rate Summary

A similar summary for 25% MRAP/75% LR blends is shown in Figure 4-93. Cement nearly eliminated creep. The differences between 1%, 2% and 3% cement reflect the limits of the instruments used to measure the creep deformations. CSS-1H slightly increased creep while SS-1H slightly decreased creep compared to the unstabilized blend. Both emulsions increased creep at the 3% stabilizer level.

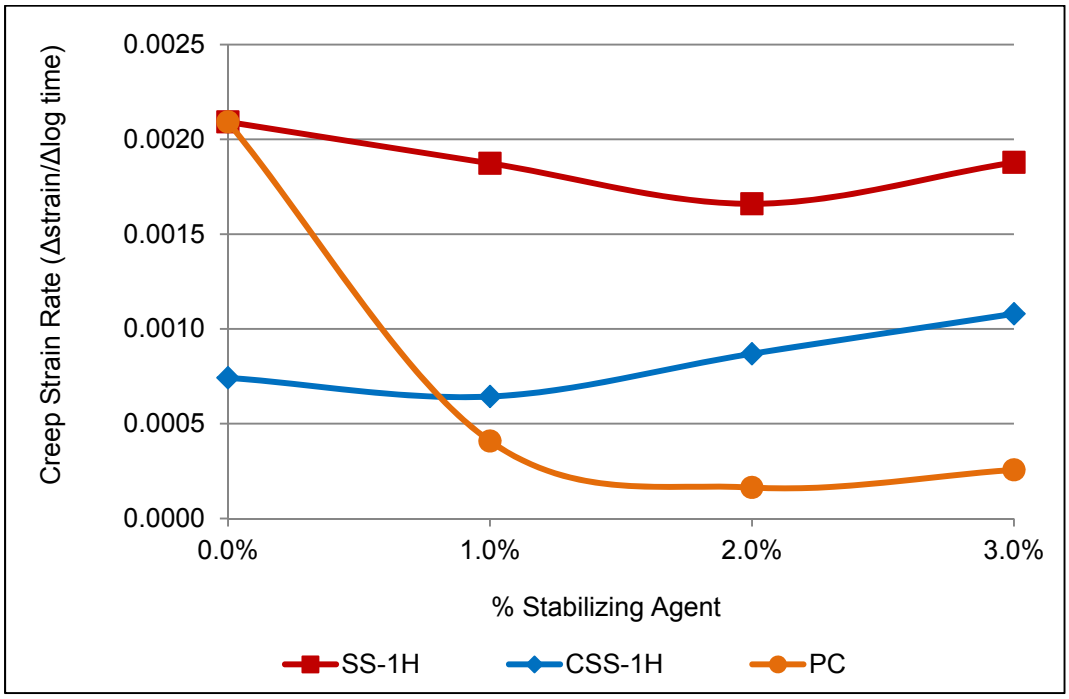

Figure 4-93: Stabilized 25% MRAP/75% LR Blend Creep Rate Summary

4.6.2.6. Effect of Unload-Reload Cycle on Creep Deformation and Strain Rate

The creep tests discussed up to this point have reported the effect of a constant load applied for seven days. Actual loading for pavements and hence base courses is cyclical. A series of unload-reload cycle tests was performed to determine: 1) whether the large stage one deformations are repeated on the reload cycle, 2) whether the creep slope remains constant after unloading/reloading, 3) the response time of the dynamic system to loading and unloading.

As previously discussed in Section 4.5.4, unconfined creep tests exhibited stage 3 tertiary stress while confined (in mold) creep tests have not progressed beyond stage 2 secondary creep. Unconfined creep tests were chosen for the unload-reload cycling to accentuate any trend toward stage 3 instability. These unload-reload tests were performed using three modified Proctor compacted and three gyratory compacted specimens of 50% MRAP/50% limerock with no chemical stabilizer. The specimens were loaded for 12 days, unloaded for 5 days, and reloaded for 5 days. The average displacements for each set of thee specimens are plotted in Figure 4-94 (linear time) and 4-95 (log time).

Both types of specimens exhibited an elastic rebound of between 10% and 20% of total deformation when unloaded that occurs in approximately 0.01 days (14.4 minutes). Also in both cases reloading caused the specimens to recompress to their previous displacement within approximately 0.01 days (14.4 minutes) and then continue to creep at the same rate observed during the initial loading cycle. Creep only occurred during load cycles. Load cycles for a pavement system are much higher in frequency but much shorter in duration than the loads used in this test. Exciting a dynamic system at well above its natural frequency decreases the magnitude of the deformation response so it is conservative to use the CSR observed during constant stress loading to predict worst case deformation over the life of the pavement under short duration cyclical loading.

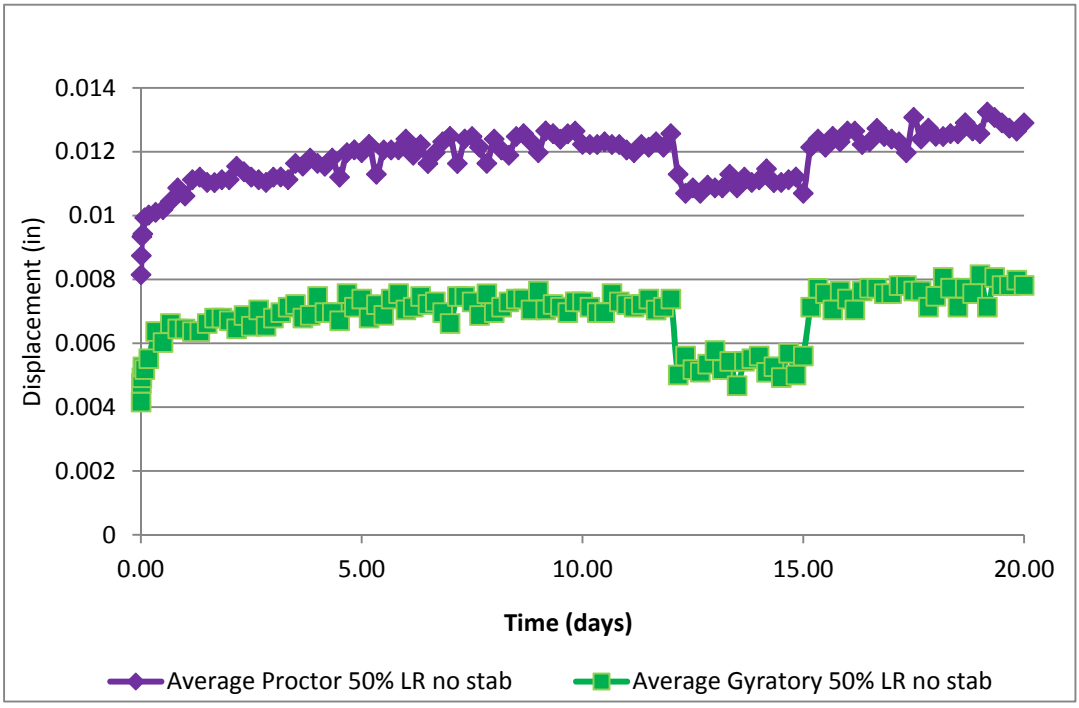

Figure 4-94: Average Unconfined Creep 50% MRAP 50% Limerock Load-Unload-Reload Linear Time

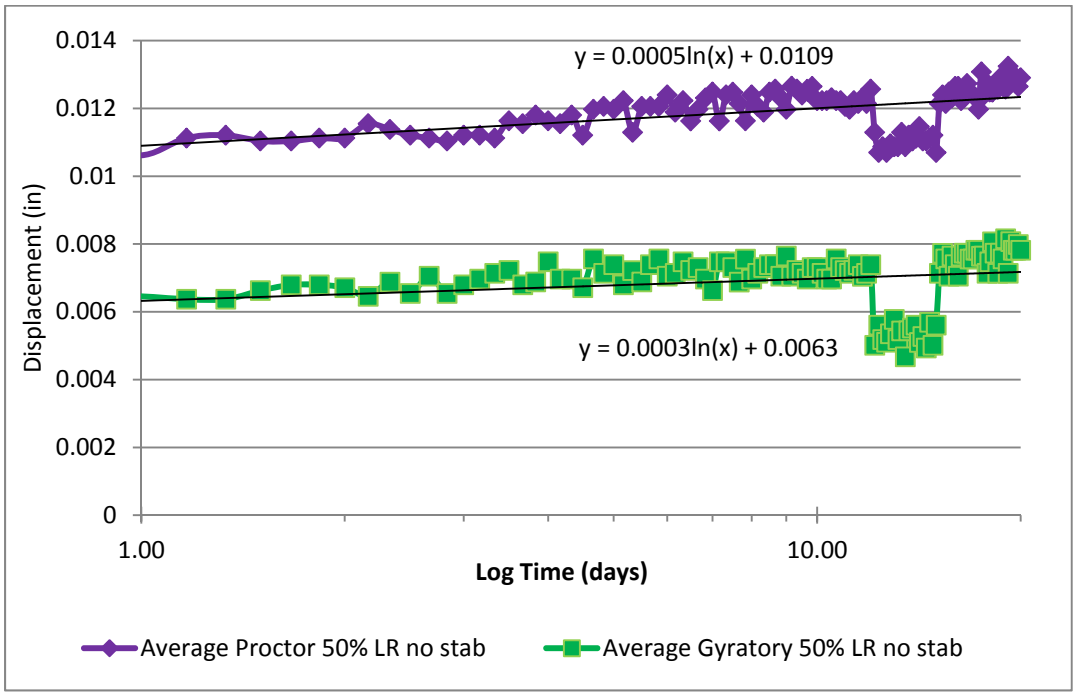

Figure 4-95: Average Unconfined Creep 50% MRAP 50% Limerock Load-Unload-Reload Log(Time)

4.6.3. Unconfined Compression Testing of Stabilized MRAP/Limerock Blends

Many specifications for stabilized soil use unconfined compressive strength testing. Unconfined compression specimens were prepared in 4-inch by-8 inch molds compacted with a modified Proctor hammer using the same compactive effort used in preparing the LBR specimens (56,000 ft-lb/ft^3). After compaction, emulsion stabilized specimens were initially cured in the mold at ambient temperature, ejected, oven cured at 60° C for 48 hours, then cooled prior to testing. Portland cement stabilized samples were initially cured in the mold, ejected, wrapped in plastic to keep them moist, and cured for 14 days prior to testing for comparability to the cement stabilized LBR samples. For all stabilizing agents soaked samples were immersed in water for 48 hours and drained for 15 minutes generally following the LBR method (FM 5-515) for comparability with the LBR samples.

The same Melbourne milled RAP and limerock base materials used in the LBR and creep tests were tested for unconfined compressive tests. Specimens of 100% MRAP, 100% limerock, and MRAP/limerock blends were tested with the same 0%, 1%, 2%, and 3% concentrations of anionic emulsion, cationic emulsion, and Portland cement used for the LBR and creep testing.

Limited testing was also performed with hydrated lime as a stabilizing agent since it is commonly used for soil stabilization.

The unconfined compression test is simple to perform. Unlike the LBR test, no interpretation is required because only the peak unconfined compression strength is measured. All specimens tested exhibited well defined peak strengths. The deflection at the peak strength was recorded for correlations to creep deflection or creep rate.

4.6.3.1. Cationic Emulsion (CSS-1HF) Stabilized Blends

A total of 24 unconfined compression tests were conducted on the MRAP/LR CSS-1HF stabilized blends. Four control specimens of 100% limerock and 100% MRAP with no stabilizing agent were tested. Typical unconfined compression results for 75% MRAP/25% limerock blends stabilized with 1%, 2%, and 3% CSS-1HF emulsion are shown in Figure 4-96. The "F" indicates that this CSS-1H cationic emulsion was from a different supplier. Unsoaked and soaked specimens are shown on the same plot. The soaked strengths were between 60% and 90% of the unsoaked strengths.

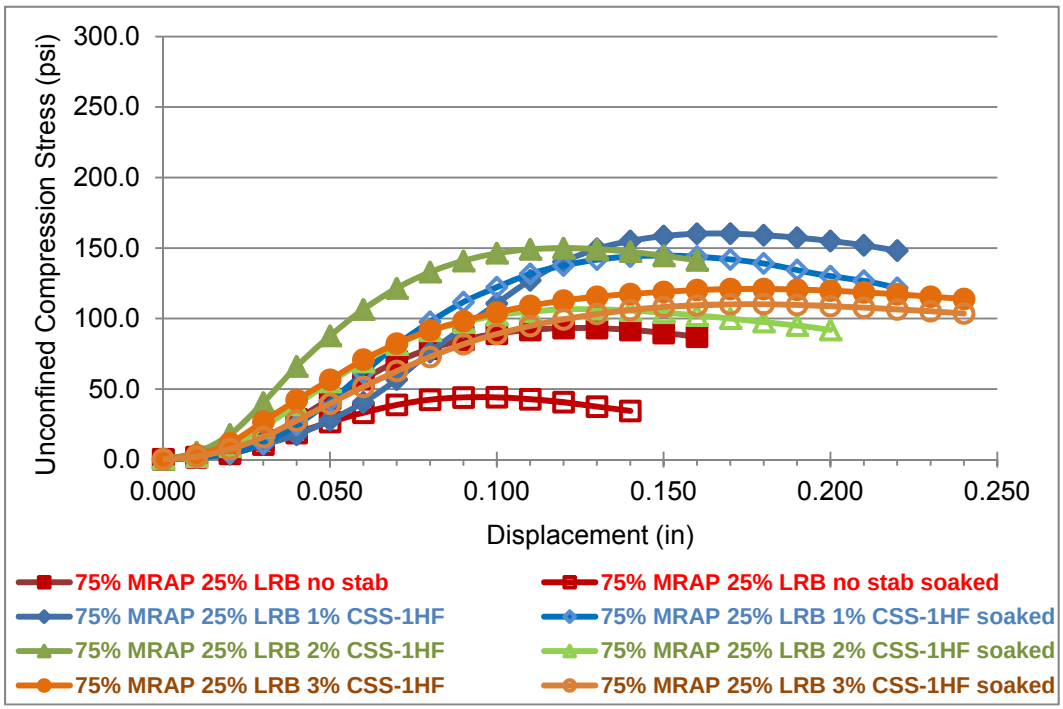

Figure 4-96: CSS-1HF Unconfined Compression on Soaked and Unsoaked 75% MRAP/25% Limerock Specimens

Summaries of unconfined compression results for all blend and emulsion combinations are presented in Figure 4-97 (unsoaked) and Figure 4-98 (soaked). Each data point represents a single test. The data point for the unstabilized 100% MRAP control specimens is partly obscured because it overlaps the unstabilized blend data points. The complete results for these tests are shown in Appendix D.

Similar to the CSS-1H LBR results in Section 4.6.1.2, adding 1% CSS-1HF emulsion increased unconfined compressive strength for all of the MRAP/limerock blends. Also similar to the LBR results there was a slight peak in unconfined compressive strength at 1% CSS-1HF followed by lower strength gains at 2% emulsion for all three blends. The 25% MRAP/75% LR blend had the highest unsoaked compressive strengths. At both 1% and 2% CSS-1HF all three blends exceeded the unconfined compressive strength of the reference 100% limerock specimens. Adding 3% emulsion again resulted in a small decrease in strength for the 75% and 50% MRAP blends but a small increase in strength for the 25% MRAP blend. For all specimens unconfined compressive strength remained higher than the strength of the unstabilized specimens.

Unlike the LBR results, which only showed small strength improvements, unconfined compression results increased by over 70% for the 75% and 50% MRAP and 25% for the 25% MRAP blends. All of the stabilized blends had higher unconfined compressive strength than 100% limerock and more than 300% of the strength of 100% RAP.

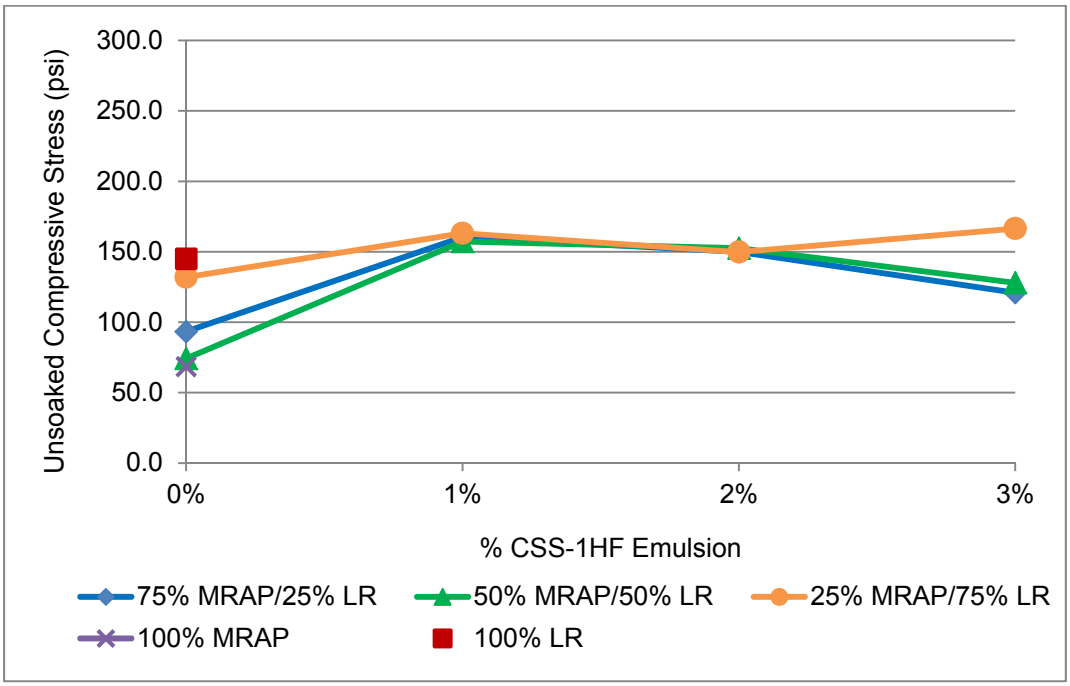

Figure 4-97: Unsoaked CSS-1HF Unconfined Compression Test Summary

Unconfined compression strength gain was more pronounced in the soaked specimens. The 100% limerock specimens disintegrated when soaked. Adding 1% CSS-1HF increased soaked strength by over 20% for the 50% and 75% MRAP blends and by more than 300% for the 25% MRAP blends. Unlike the unsoaked specimens, the soaked specimens' unconfined compressive strength peaked at different emulsion contents. Soaked strength peaked at 1% CSS-1HF for the 25% MRAP blend but continued to increase slightly at 2% and 3% emulsion level for both the 50% MRAP and 75% MRAP blends. In all cases the unconfined compressive strength of the emulsion stabilized specimens remained significantly higher than the unstabilized blends, 100% MRAP, and 100% limerock (which had zero soaked strength). Unlike 100% limerock, all blends and 100% MRAP retained significant strength when soaked even without added stabilizer.

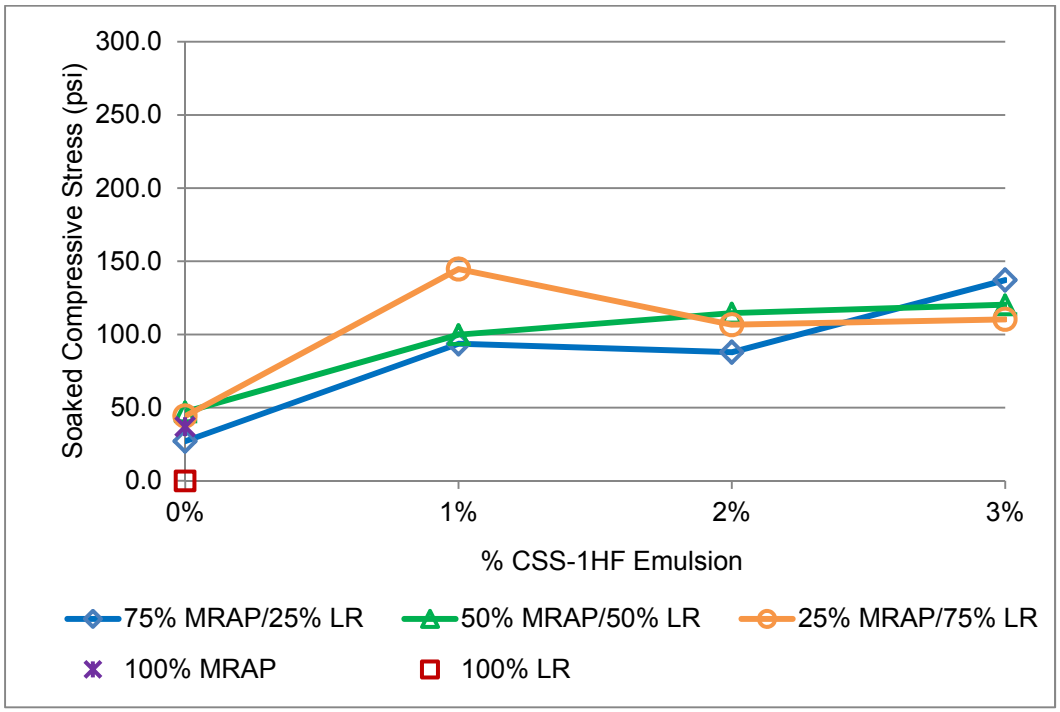

Figure 4-98: Soaked CSS-1HF Unconfined Compression Test Summary

Emulsion stabilization significantly improved soaked strength compared to unstabilized specimens. Figure 4-99 shows the percent of the soaked strength retained during unconfined compression testing. All three stabilized soaked MRAP/limerock blends retained between 80% and 90% of their unsoaked strengths at the 3% emulsion content. For the 1% and 2 % emulsion, the 50% MRAP and 25% MRAP blends retained between 60 and 70% of the unsoaked strength, while the 75% MRAP/25% LR retained 90% of its strength at 1% emulsion. The 100% limerock does not appear on the chart because it had zero strength.

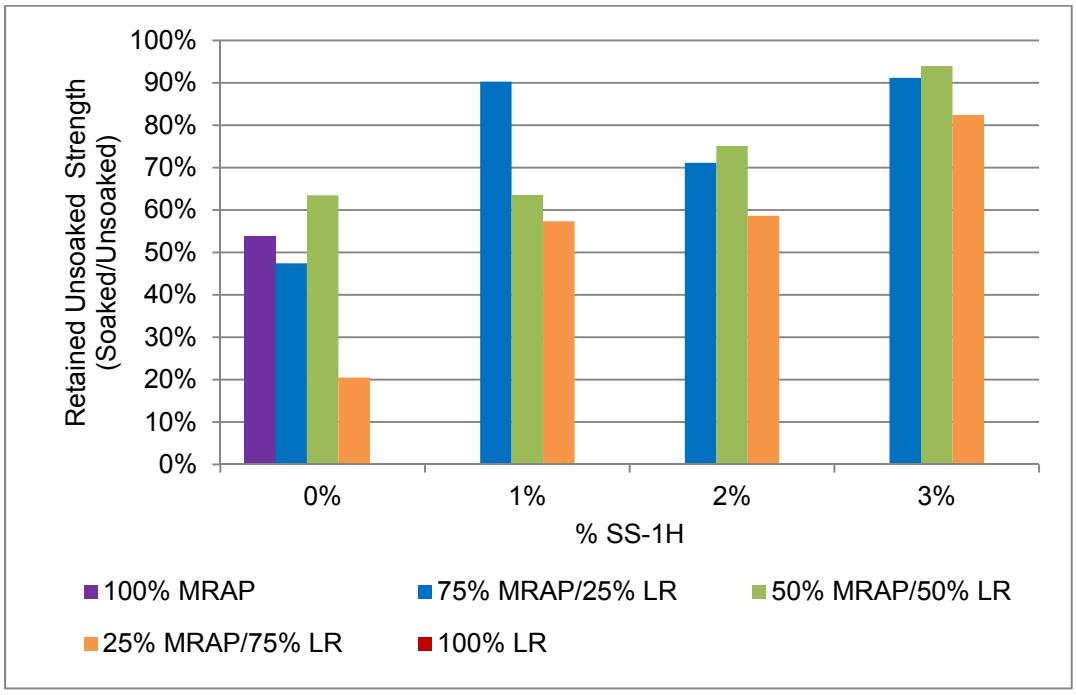

Figure 4-99: Percent of Unsoaked Strength Retained for CSS-1HF Stabilized Blends

Unsoaked and soaked unconfined compressive strengths for all blends with SS-1H emulsions are shown in Figure 4-100 and Figure 4-101. As discussed above, only the 25% MRAP/75% LR blend produced an unsoaked strength greater than limerock. In contrast, Figure 4-100 shows that all three blends had slightly higher unsoaked unconfined compressive strengths than limerock at 1% and 2% SS-1H..

The unconfined compressive strength of unsoaked 100% limerock is shown as a dashed red line for reference. Soaked 75% MRAP blends exceeded the unsoaked limerock strength. Soaked blends of 50% and 25% MRAP had between 80% and 90% of the unsoaked limerock strength.

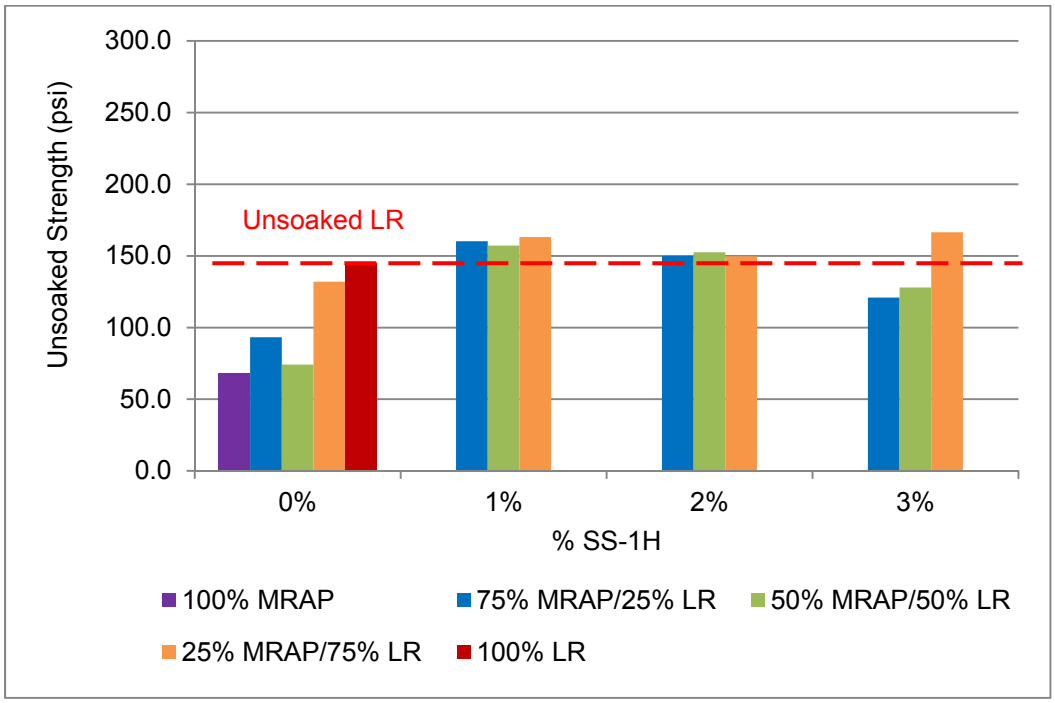

Figure 4-100: Unsoaked CSS-1HF Unconfined Compression Comparison

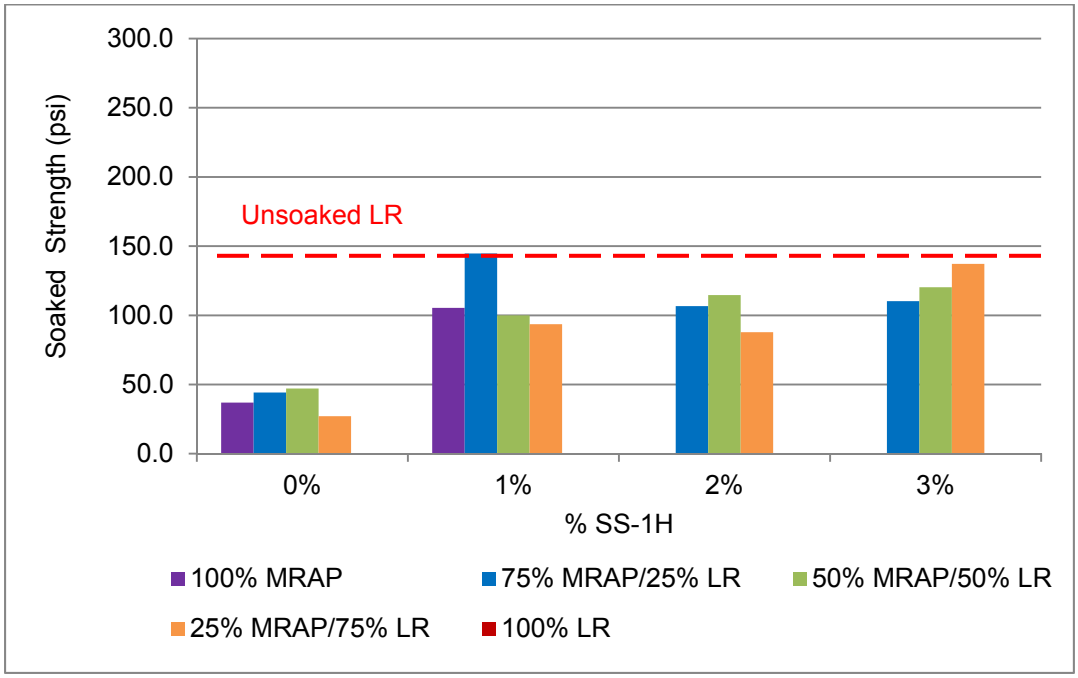

Figure 4-101: Soaked CSS-1HF Unconfined Compression Comparison

The displacements at peak unconfined compressive strength were compared to 7-day creep displacements and CSR's to determine if correlations could be developed. Figure 4-102

shows displacement trends for unsoaked specimens. Peak displacements for 25% and 50% MRAP blends with no stabilizer were approximately equal to the peak displacement for 100% limerock. The 100% MRAP had approximately 35% higher displacement at peak stress than 100% limerock. The 75% MRAP blend peak displacements were in between 100% limerock and 100% MRAP. The peak displacement is directly related to the asphalt content. All three blends showed a clear trend of increasing peak displacements with the increasing emulsion. MRAP blends had peak displacements that were 25% to 125% higher than 100% limerock and 0% to 60% higher than 100% MRAP.

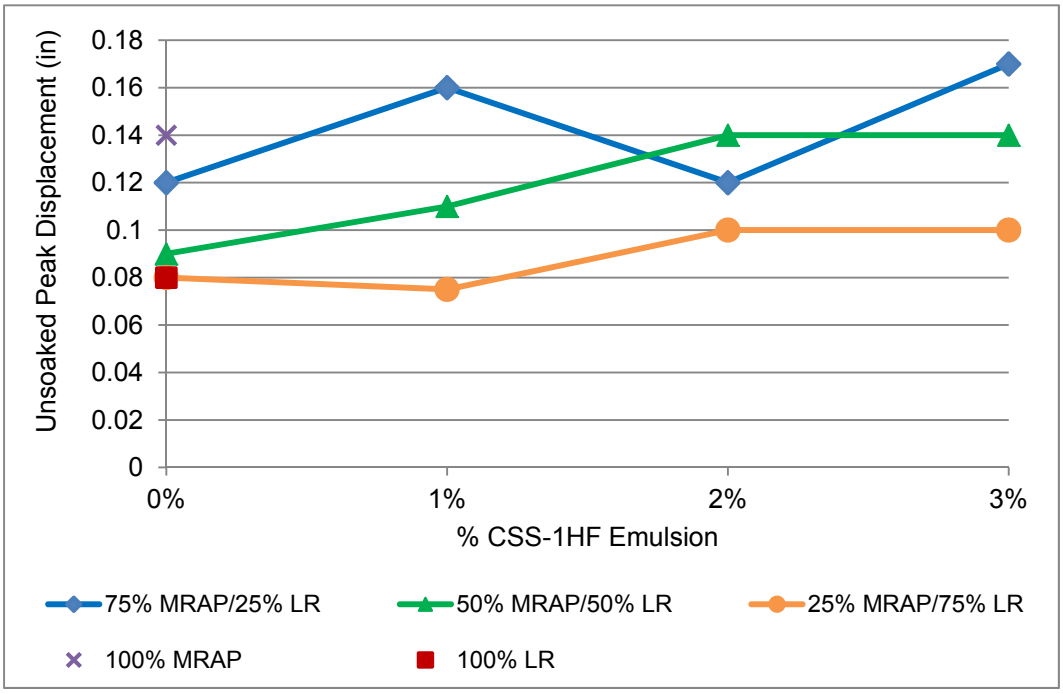

Figure 4-102: Unsoaked CSS-1HF Unconfined Compression Peak Displacements

Figure 4-103 shows the peak displacement trends from soaked unconfined compression testing. The trends are very similar to Figure 4-102, with a general increase in peak displacement with increasing percent emulsion. The smallest increase occurred with the 25%MRAP/75%LR blend while the largest increase occurred with the 75%MRAP/25%LR blend. The 50%/50% blend had a consistent increase which fell between the other two blends.

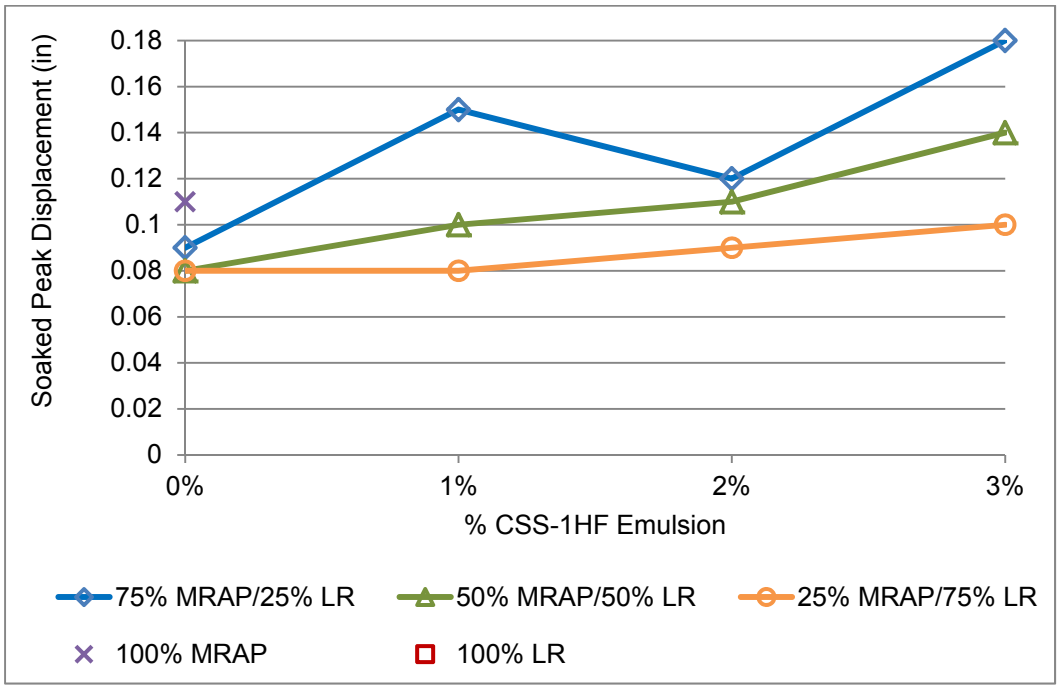

Figure 4-103: Soaked CSS-1HF Unconfined Compression Peak Displacements

4.6.3.2. Anionic Emulsion (SS-1H) Stabilized Blends

A total of 24 unconfined compression tests were conducted on the MRAP/LR SS-1H stabilized blends. Four additional specimens of 100% limerock and 100% MRAP without any stabilizing agent were tested as controls. Typical unconfined compression results for 75% MRAP/25% limerock blends stabilized with 1%, 2%, and 3% SS-1H emulsion are shown in Figure 4-104. Both unsoaked and soaked specimens are shown on the same plot. Soaked specimens retained approximately 60% of the strength of unsoaked samples.

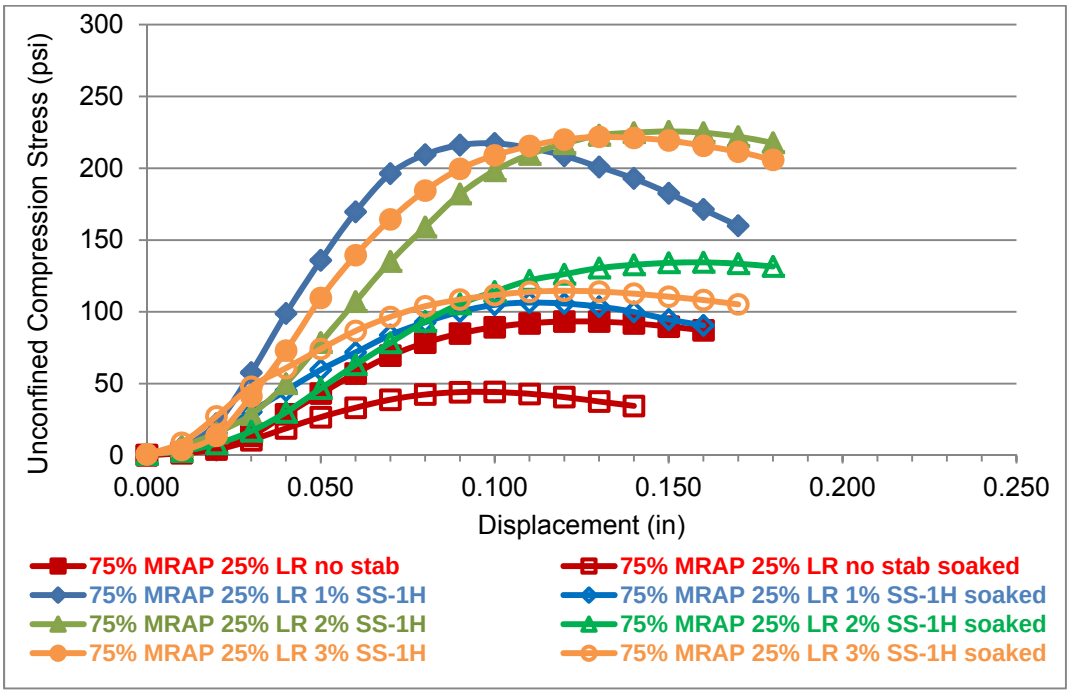

Figure 4-104: SS-1H Unconfined Compression on Soaked and Unsoaked 75% MRAP/25% Limerock

Summary unconfined compression results for all blend and emulsion combinations are shown for the soaked tests in Figure 4-105 and unsoaked tests in Figure 4-106. Each data point represents a single test.

Similar to the CSS-1HF results in the preceding section and LBR results in Section 4.6.1.3, adding 1% SS-1H emulsion increased unconfined compressive strength for all of the MRAP/limerock blends. Unlike the LBR results which only showed small improvements, unconfined compression results increased by approximately 50% with the addition of 1% of SS-1H. All of the stabilized blends had higher unconfined compressive strengths than 100% limerock and more than 300% of the strength of 100% RAP. Blends with 75% MRAP showed a slight decrease in strength with the addition of more emulsion similar to the weak peak at 1% emulsion seen in the LBR tests. Unlike the LBR results, blends with 50% MRAP and 25% MRAP continued to increase in unconfined compressive strength with the addition of up to 3% SS-1H. Blends with 75% MRAP did not show improved strength with increasing emulsion content above 1%.

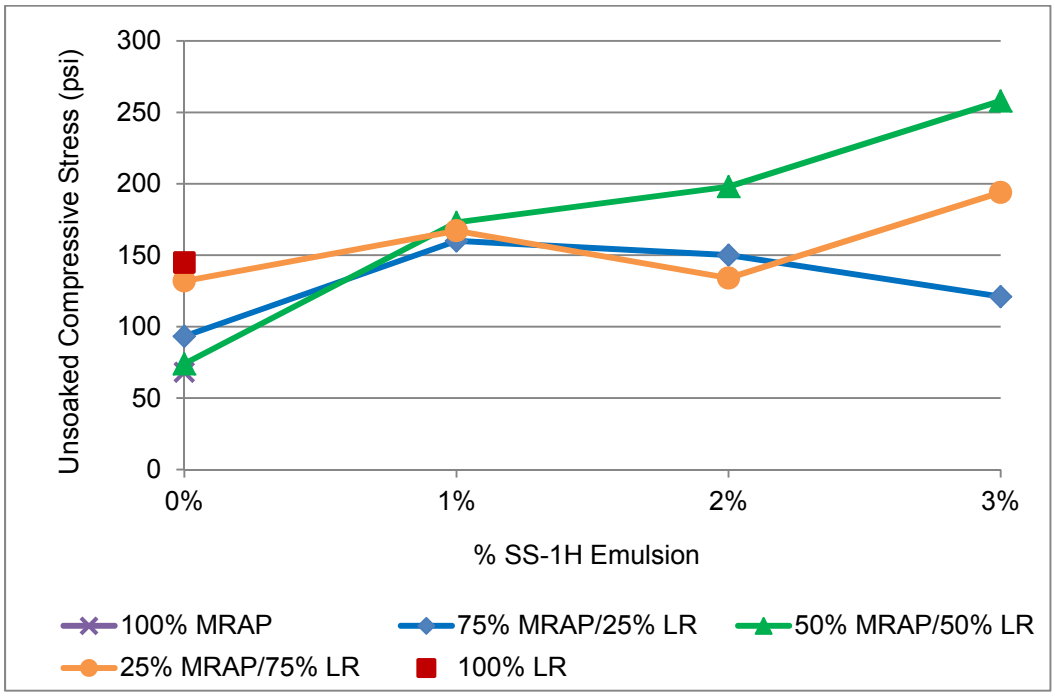

Figure 4-105: Unsoaked SS-1H Unconfined Compression Test Summary

Unconfined compression strength gain was most pronounced in the soaked specimens (Figure 4-106). The 100% limerock specimens disintegrated when soaked. All blends and 100% MRAP retained significant strength when soaked. Adding 1% SS-1H increased soaked strength by nearly 90% for 25% MRAP blends (37 psi to 69 psi) and by over 200% for 50% ((37 psi to 111 psi) and 75% MRAP blends (37 psi to 137 psi). Soaked strength peaked at 1% SS-1H for both 50% and 75% MRAP blends but continued to increase with more emulsion for the 25% MRAP blend. At 1% SS-1H the soaked strength of the 50% (145 psi) and 75% (158 psi) blends were equal to or higher than the unsoaked strength (145 psi) of the 100% limerock control material. There is a clear trend that emulsion stabilization significantly improves soaked strength compared to unstabilized specimens.

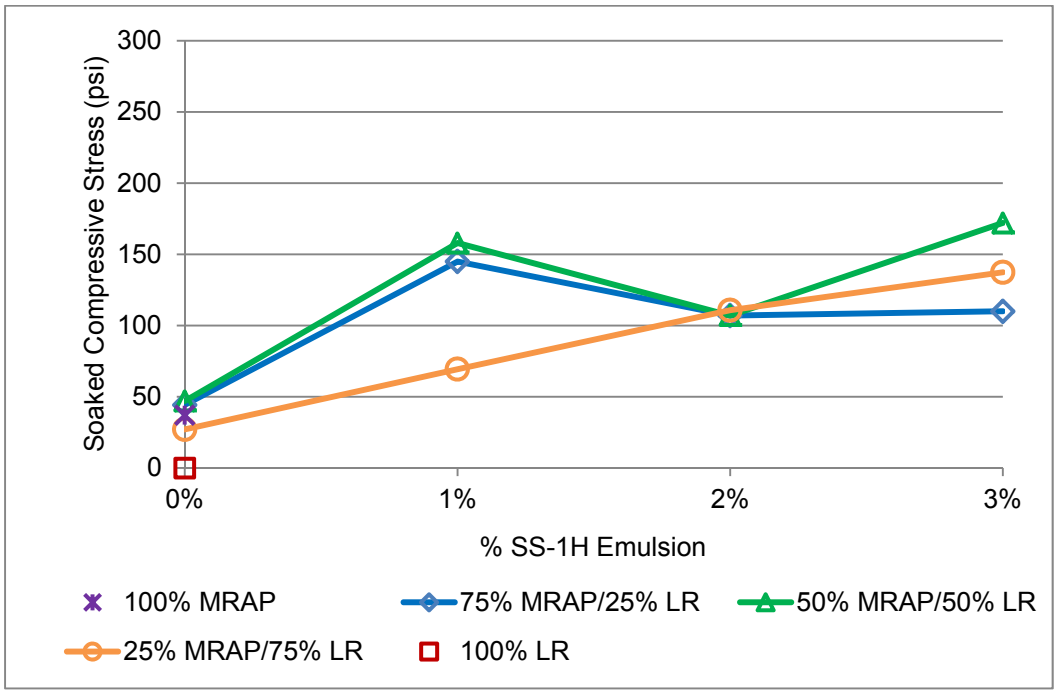

Figure 4-106: Soaked SS-1H Unconfined Compression Test Summary

Figure 4-107 shows the percent of the soaked strength retained during unconfined compression testing. The soaked 75% MRAP and 50% MRAP blends retained between 80% and 90% of their unsoaked strengths. The 25% MRAP blend had the lowest retained strength. The100% limerock does not appear on the chart because it had zero strength. This reduction in limerock's strength when soaked also contributed to the lowest retained strength for the 25% MRAP/75% LR blends.

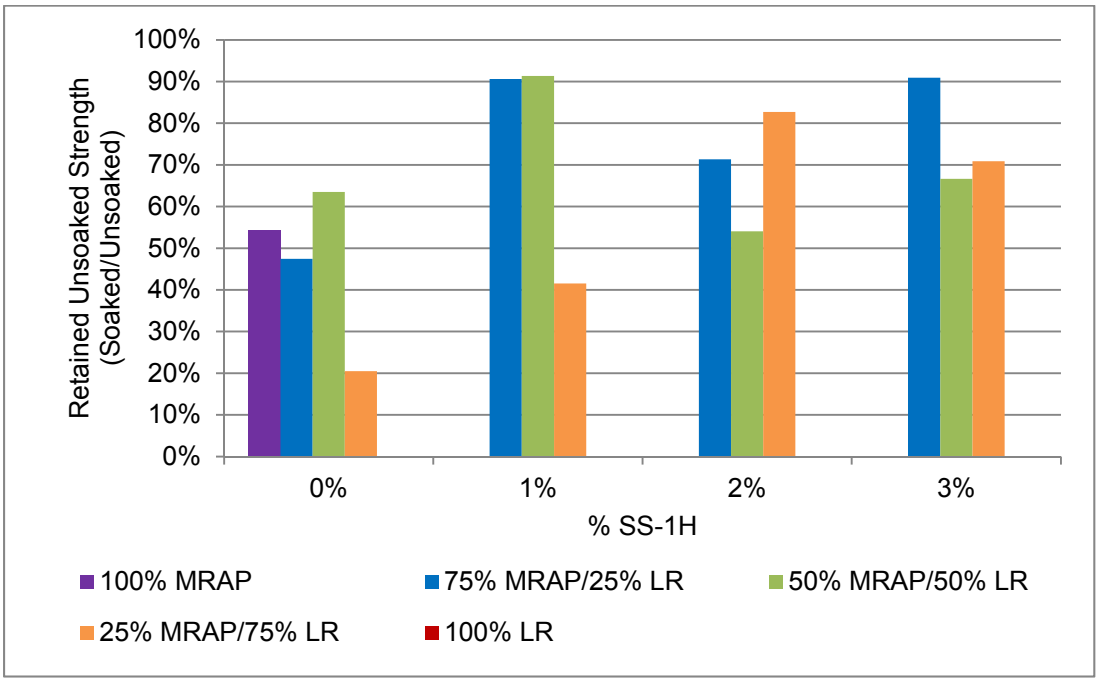

Figure 4-107: Percent of Unsoaked Strength Retained for SS-1H Stabilized Blends

Unsoaked and soaked unconfined compressive strengths for all blends are shown in Figure 4-108 and Figure 4-109 respectively. The unconfined compressive strength of unsoaked 100% limerock is shown as a dashed red line for reference. As noted earlier, all blends with 1% SS-1H exceeded the strength of 100% limerock. Soaked blends of 50% and 75% MRAP 2% emulsion, and 50% and 25% MRAP at 3% emulsion also exceeded the unsoaked 100% limerock strength.

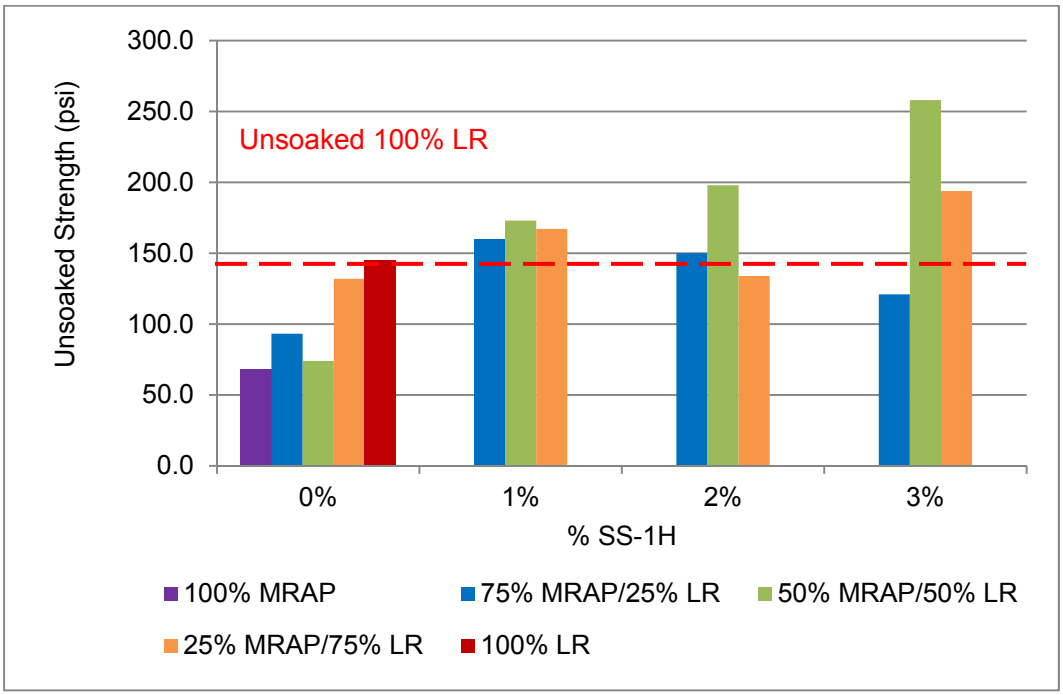

Figure 4-108: SS-1H Unsoaked Unconfined Compression Comparison

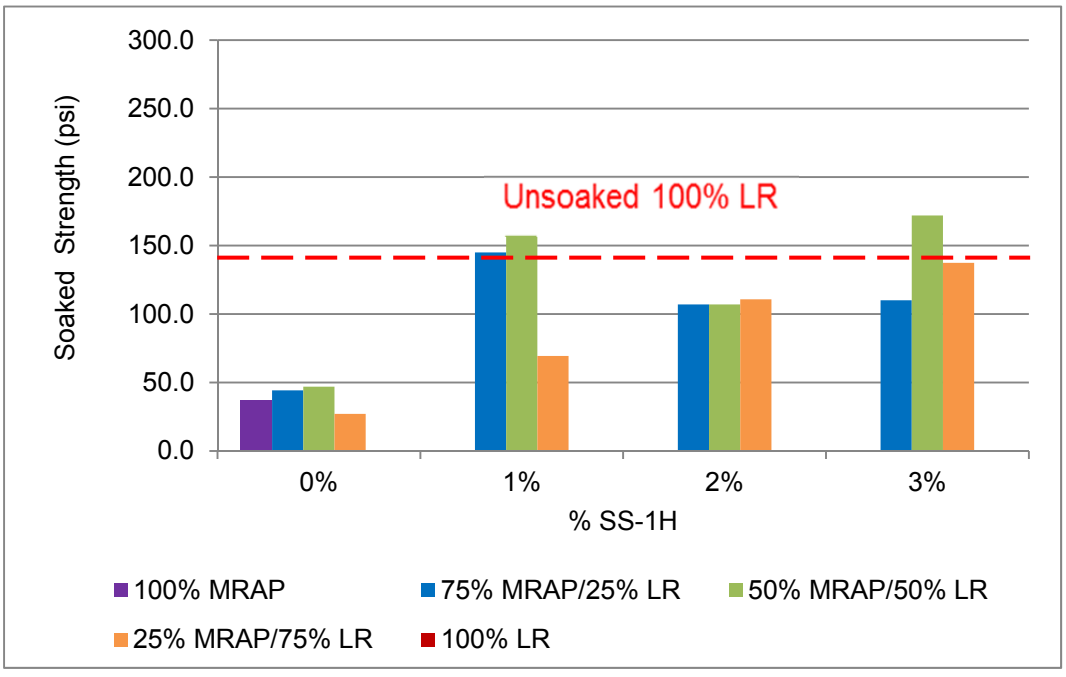

Figure 4-109: SS-1H Soaked Unconfined Compression Comparison

Peak displacement trends for unsoaked specimens are shown in Figure 4-110. Peak displacement for unstabilized 25% and 50% MRAP blends was approximately equal to peak

displacement for 100% limerock. Both the 100% MRAP and 75% MRAP blends had approximately 50% higher displacement at peak stress. The 25% and 50% MRAP SS-1H stabilized blends showed peak displacements approximately 20% to 30% slightly higher (0.1 to 0.11-inches) than unstabilized blends or 100% limerock (0.085-inches). SS-1H stabilized 75% MRAP blends had peak displacements that were 50% to 100% higher (0.16 to 0.17) than 100% limerock and 0% to 30% higher than 100% MRAP (0.12).

Figure 4-111 shows displacement trends for soaked specimens. The general trends were the same for soaked specimens as for unsoaked specimens. It was not possible to compare displacements to soaked 100% limerock because the 100% soaked limerock specimens disintegrated. Soaked stabilized 25% MRAP and 50% MRAP blends had approximately 15% higher peak displacements than their unstabilized counterparts. Conversely, soaked stabilized 75% MRAP had approximately 5% lower peak displacements than their unsoaked counterparts. Soaked unstabilized blends had approximately the same peak displacements (0.18-inches) as unsoaked unstabilized blends with the exception of the 75% MRAP blend which had approximately 25% less displacement.

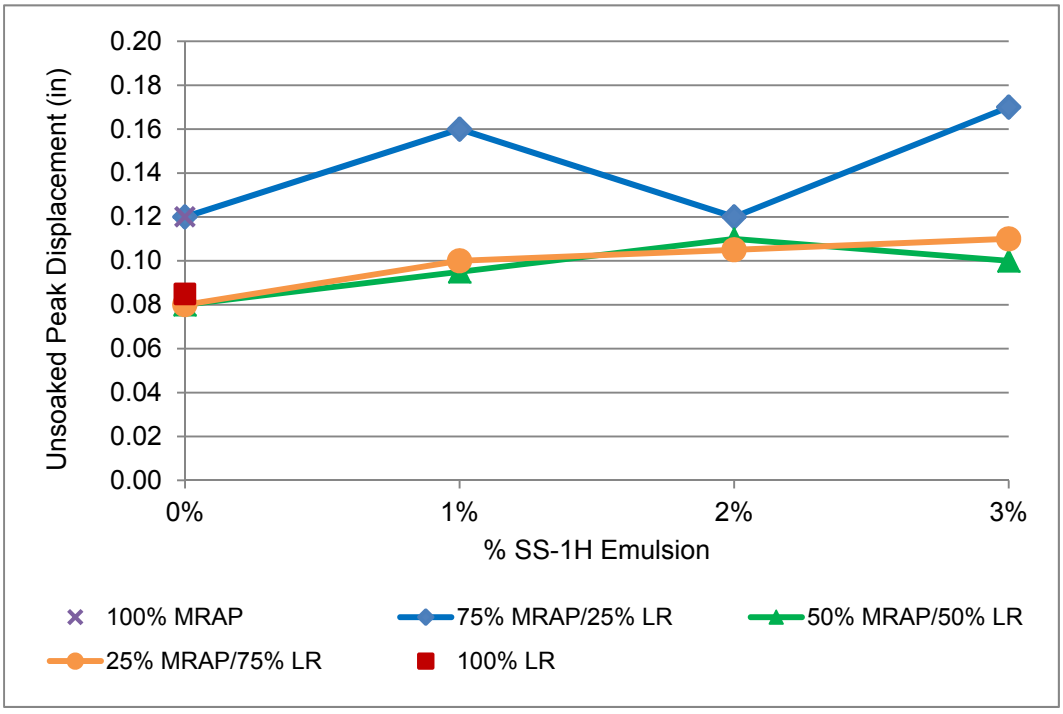

Figure 4-110: SS-1H Unsoaked Unconfined Compression Peak Displacements

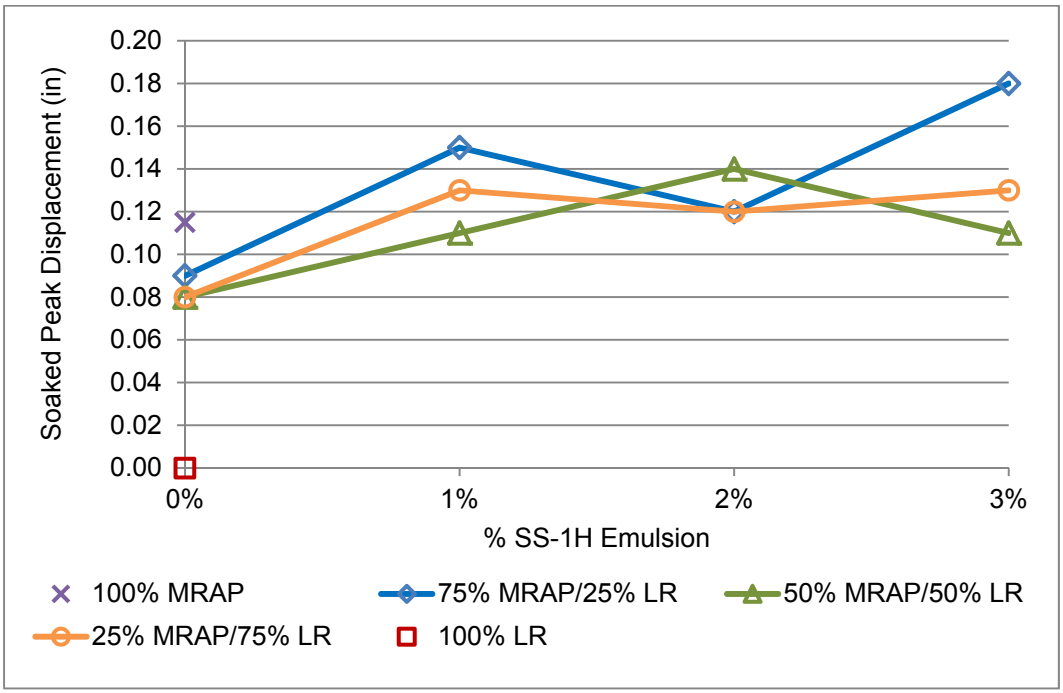

Figure 4-111: SS-1H Soaked Unconfined Compression Peak Displacements

4.6.3.3. Portland Cement (PC) Stabilized Blends

A total of 30 unconfined compression tests were conducted on MRAP/LR Portland cement stabilized specimens. Four additional control specimens of 100% limerock and 100% MRAP were tested without cement. Typical unconfined compression results for both unsoaked and soaked 75% MRAP/25% limerock blends with 1%, 2%, and 3% cement are shown in Figure 4-112.

Soaked specimens retained between 60% and 90% of the strength of unsoaked samples. Unsoaked cement stabilized strengths are not directly comparable to unsoaked emulsion stabilized strengths because the emulsion stabilized specimens were oven cured while the cement stabilized specimens were moist cured at ambient temperature. Because of this the unsoaked cured emulsion stabilized specimens had very low moisture content while the cement stabilized specimens were at approximately the moisture level used for compaction. Soaked strengths are directly comparable because both types of specimens were fully saturated by soaking for 48 hours prior to testing.

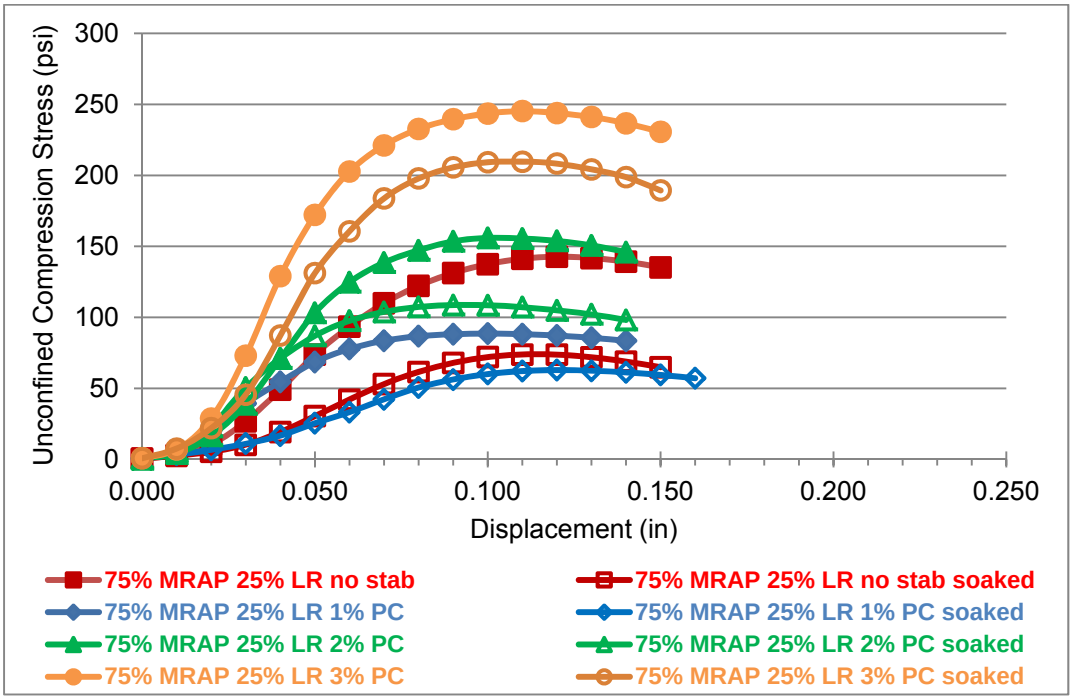

Figure 4-112: Unconfined Compression of Soaked and Unsoaked 50% Limerock/50% MRAP Blends with Portland Cement

Summary unconfined compression results for all blend and cement combinations tested are shown for unsoaked data in Figure 4-113 and soaked data in Figure 4-114. Each data point represents a single test. Complete results are shown in Appendix D.

Similar to the LBR results in Section 4.6.1.4, adding cement increased unsoaked unconfined compressive strength for all of the MRAP/limerock blends. Unlike the emulsion stabilized specimens, which gained significantly more strength in the unconfined compression testing compared to the LBR testing, the cement stabilized unconfined compression results showed strength improvements that were similar in magnitude to those observed in the LBR testing. Unconfined compressive strength gains varied between 25% and 300% depending on the amount of cement added.

At 1% cement the unsoaked 75% and 50% MRAP blends improved in strength but were both approximately 65% as strong as 100% limerock while the 25% MRAP blend was approximately 25% stronger than the 100% limerock control. At 2% and 3% cement all of the stabilized blends had higher unsoaked unconfined compressive strength than 100% limerock and between 200% and 500% of the strength of 100% RAP. Strength improvements were even more

dramatic for the soaked specimens since the 100% limerock specimens disintegrated had zero soaked strength. As was the case with the emulsion stabilized specimens, there was a clear trend that cement stabilization significantly improves soaked strength compared to unstabilized specimens. Unlike the emulsion stabilized specimens, unconfined compressive strength continued to increase approximately linearly with additional cement.

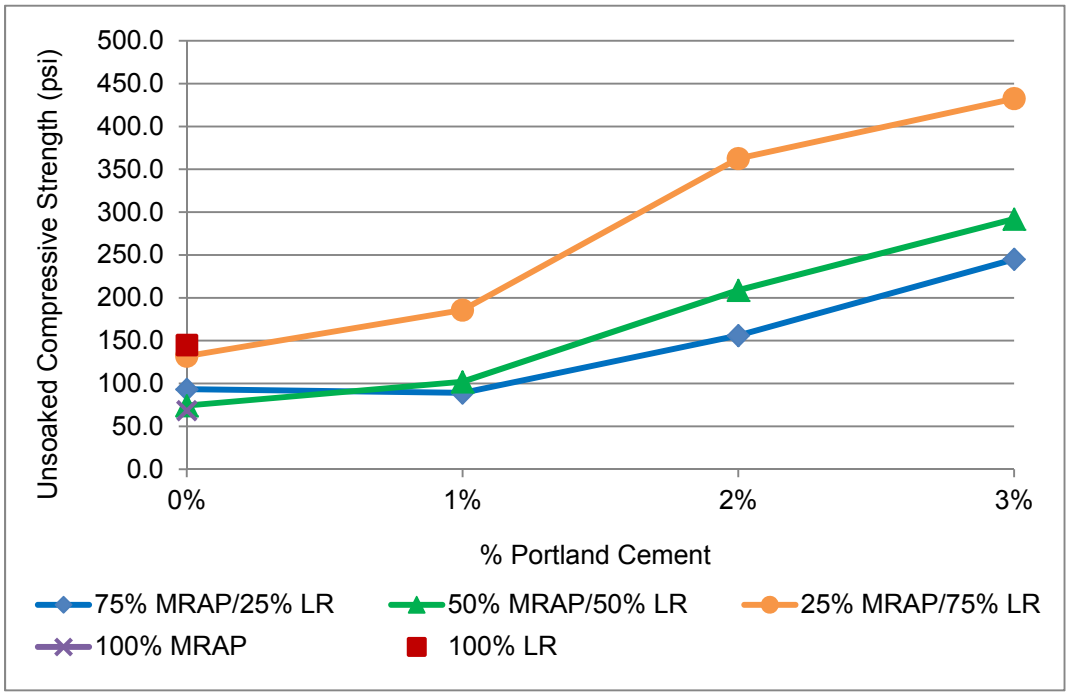

Figure 4-113: Unsoaked PC Unconfined Compression Test Summary

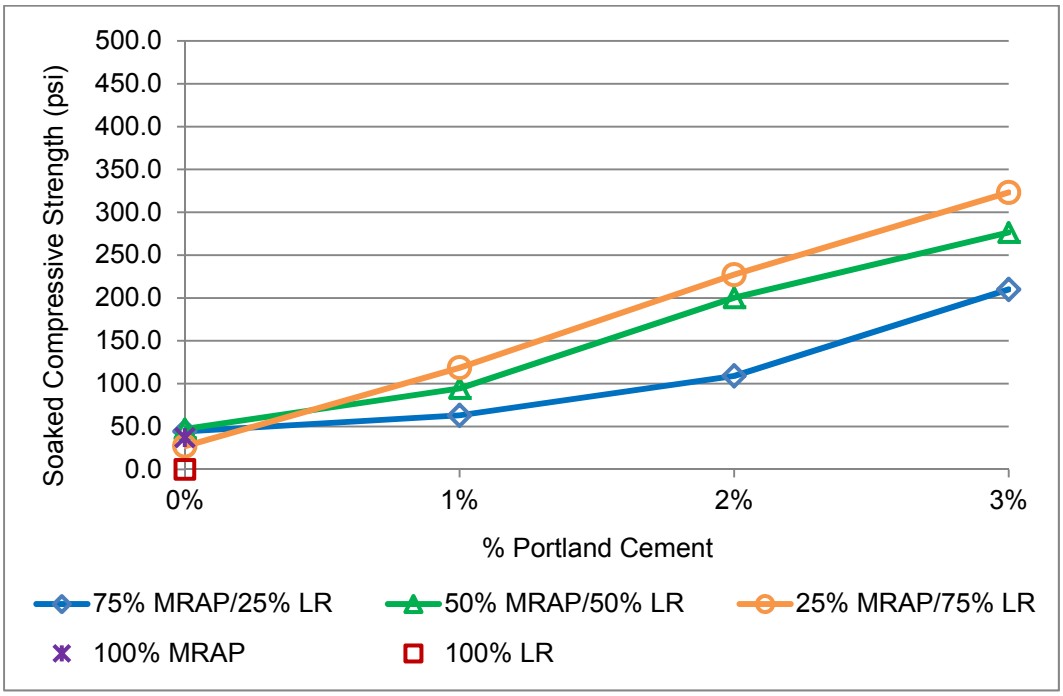

Figure 4-114: Soaked PC Unconfined Compression Test Summary

For comparison, Figure 4-115 shows the soaked unconfined compressive strength retained as a percent of unsoaked strength. The 100% limerock does not appear on the chart because it had zero strength. The retained strength generally increased with increasing cement content. Again the 25% MRAP/75% limerock blend has low retained strength percentages indicating degradation of the limerock strength during soaking. In the best cases soaked MRAP/limerock blends retained between 75% and 95% of their unsoaked strengths. The 50% MRAP blends had consistently high retained strengths at all cement contents tested.

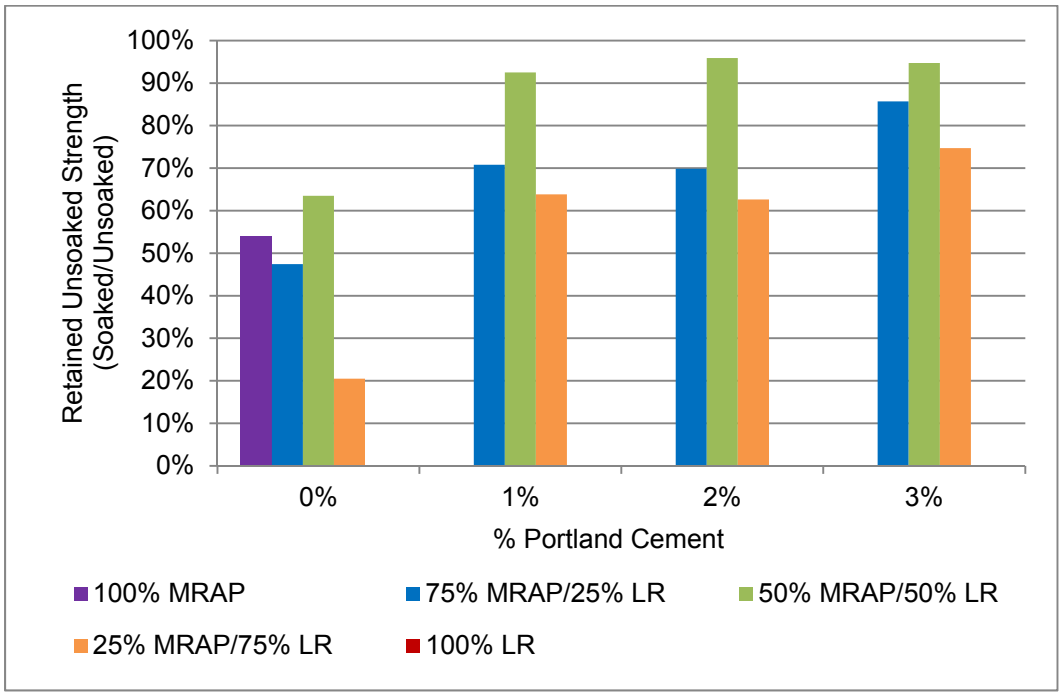

Figure 4-115: Retained Strength of PC Stabilized Blends

Unsoaked and soaked unconfined compressive strengths for all blends are shown in Figure 4-116 and Figure 4-117 respectively. The unconfined compressive strength of unsoaked 100% limerock is shown as a dashed red line for reference. As noted earlier, all unsoaked blends with 2% or 3% cement exceeded the unsoaked strength of 100% limerock. Soaked blends of 25% and 50% MRAP with 2% cement, and all blends with 3% cement exceeded the unsoaked strength of 100% limerock.

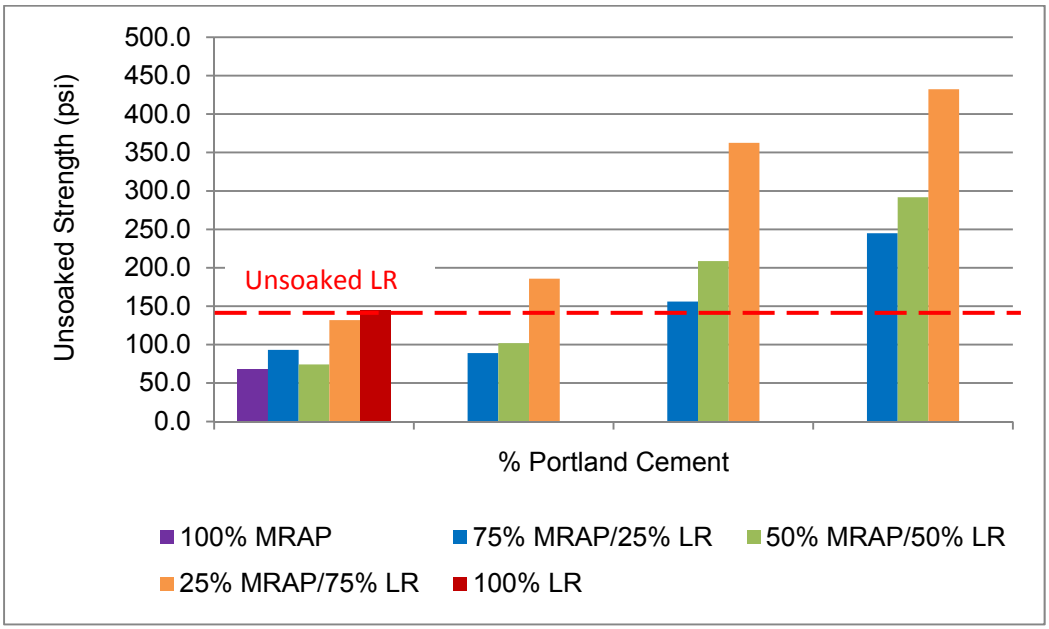

Figure 4-116: Unsoaked PC Unconfined Compression Comparison

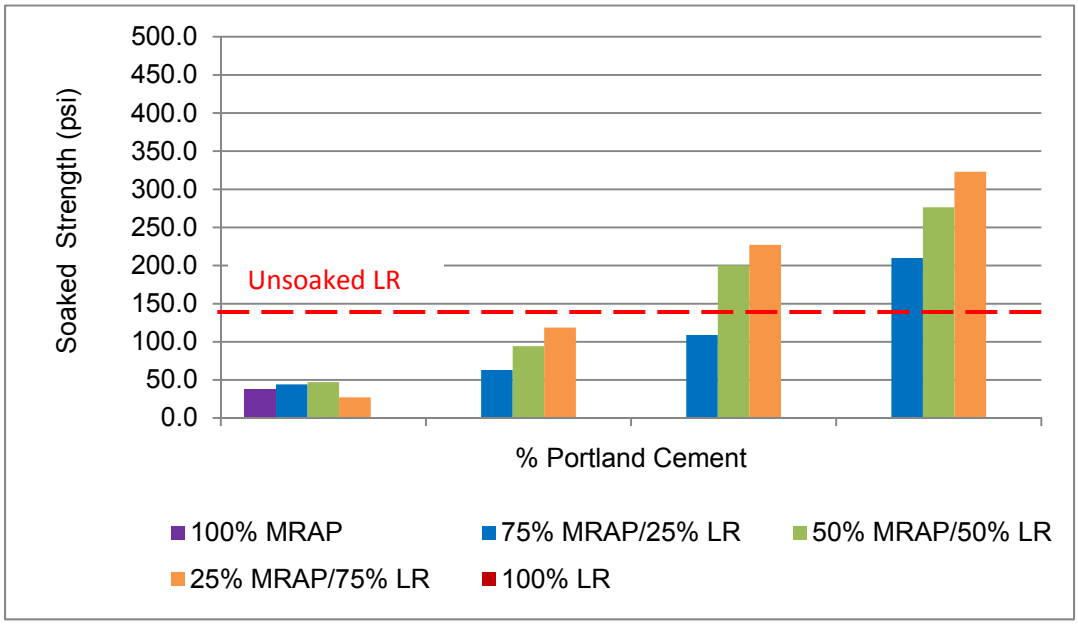

Figure 4-117: Soaked PC Unconfined Compression Comparison

Figure 4-118 shows displacement trends for unsoaked specimens. Peak displacements for all blends were greater than the peak displacements for 100% limerock but lower than those for 100% MRAP. Unlike the emulsion stabilized specimens, peak displacements remained approximately constant at the three different levels of cement.

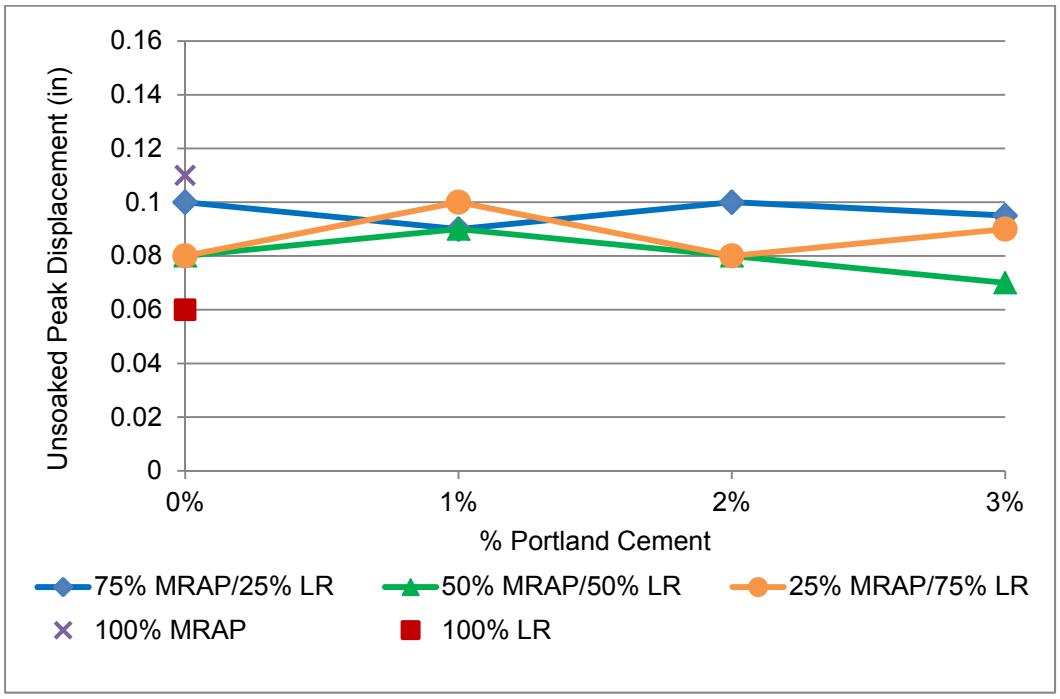

Figure 4-118: Unsoaked PC Unconfined Compression Peak Displacements

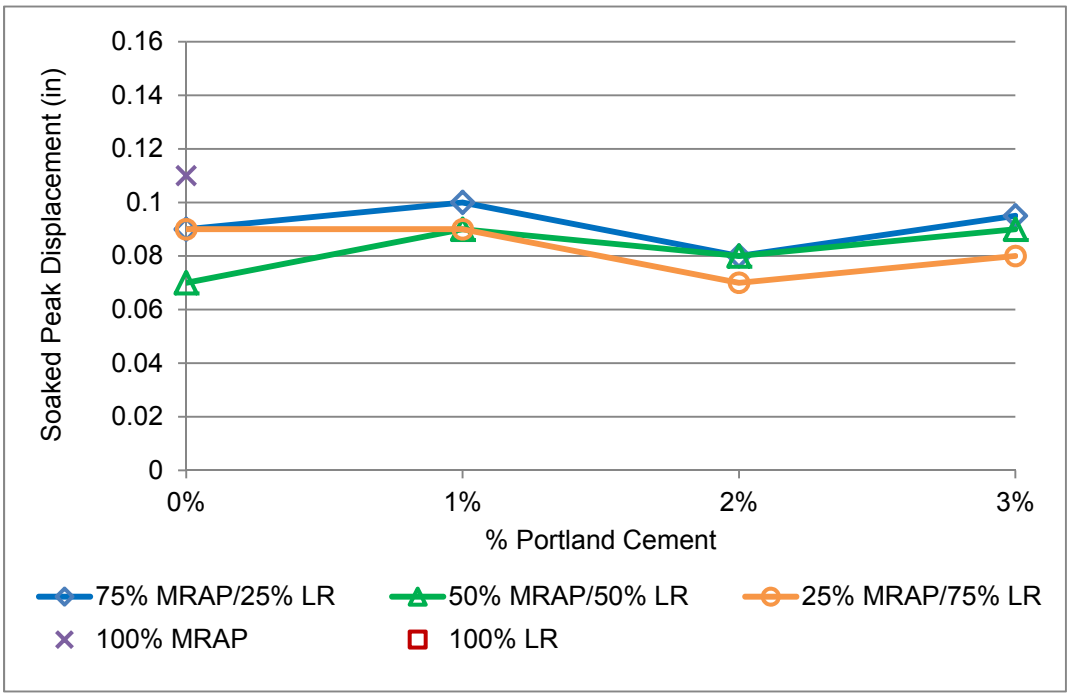

Figure 4-119: Soaked PC Unconfined Compression Peak Displacements

4.6.3.4. Hydrated Lime Stabilized MRAP/Limerock Blends

A total of eight lime stabilized MRAP/limerock specimens were tested. The purpose of this testing was to determine whether to conduct a full round of tests with lime. For this screening investigation, 50% MRAP/50% limerock blends were tested because both emulsions and cement had shown good results with this blend. Both unsoaked and soaked specimens are shown in Figure 4-120. Unsoaked compressive strengths decreased by about 30% while the soaked compressive strengths increased by about 30% with lime stabilization. The 50% MRAP/50% limerock blends showed slightly lower unsoaked strengths at 1%, 2% and 3% lime than unstabilized material (from 127 psi to just below 100 psi). Lime stabilization at these same percentages produced a slight improvement in soaked strength (from 47 psi to between 67 and 84 psi). Based on the inconsistent performance of lime stabilized blends on these tests, lime was eliminated from further testing.

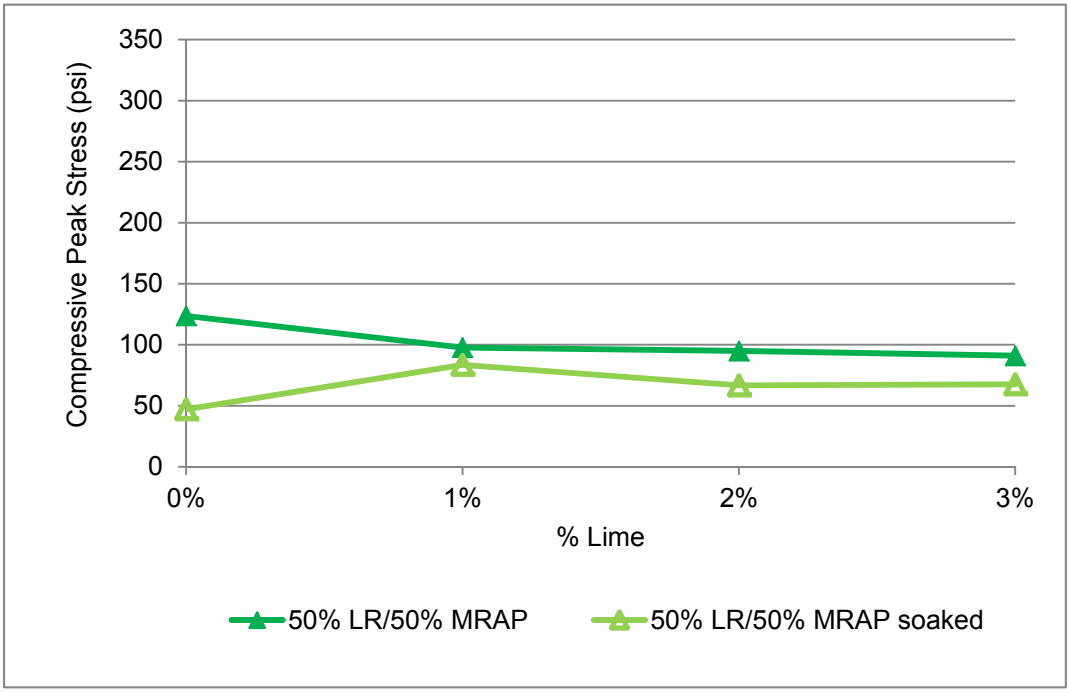

Figure 4-120: Lime Stabilized 50% MRAP/50% Limerock Blend Strength

4.6.3.5. Summary of Chemically Stabilized MRAP/LR Blends

The same general trends seen in unsoaked LBR testing were seen in unconfined compression testing. Chemically stabilized MRAP/LR blends with 50% or less RAP MRAP had significantly higher unconfined compressive strength than specimens with 75% or 100% MRAP.

4.6.3.5.1. Summary of Chemically Stabilized 50% MRAP/50% LR Blends

The preceding sections have separately discussed each chemical stabilizing agent. This section compares the effect of the stabilizing agents on 50% MRAP/50% limerock blends. This blend was selected because initial testing indicated that this blend had the potential to reach the objective soaked LBR of 100. Figure 4-121 shows the unsoaked unconfined compressive strength results for SS-1H, CSS-1HF, Portland cement, and lime stabilized specimens. The unsoaked unconfined compressive strength of 100% limerock is shown as a dashed red line for comparison. General trends were the same as those observed during LBR testing with a peak in emulsion stabilized strength between 1% and 2%, continued increase in cement stabilized strength, and little effect from lime stabilization. The 3% SS-1H specimens were rejected due to overheating in the curing oven.

Unsoaked specimens with 1% of either emulsion and with 2% or more cement exceeded the unsoaked unconfined compressive strength of the 100% limerock control. All stabilized specimens retained strength when soaked. The soaked 1% SS-1H, 2% cement, and 3% cement specimens had a higher unconfined compressive strength than the unsoaked 100% limerock control (Figure 4-122).

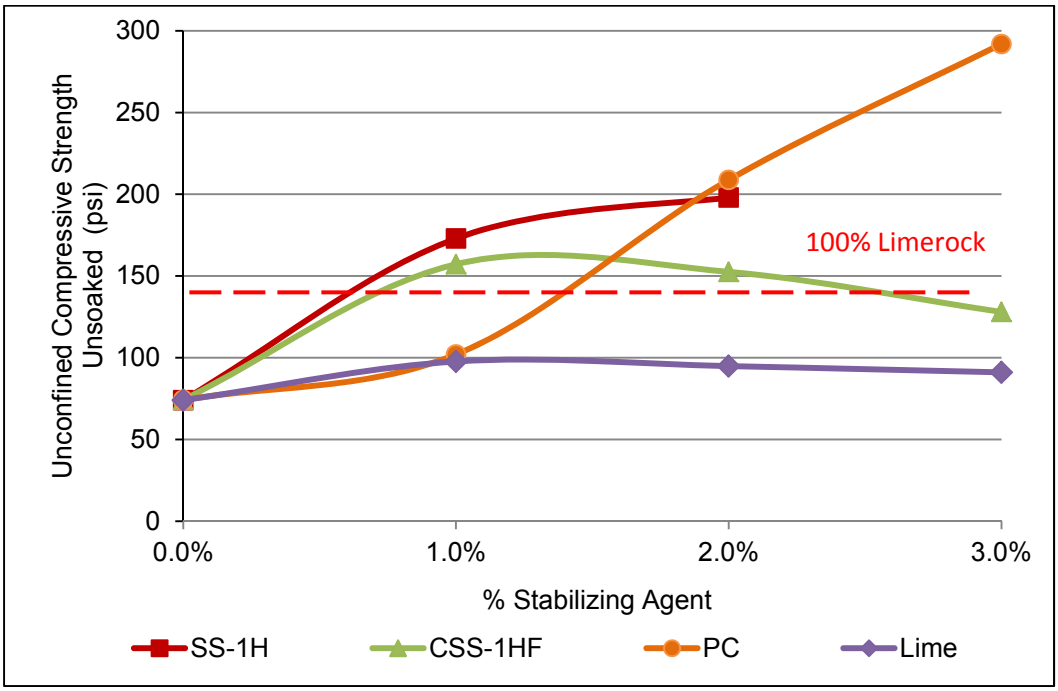

Figure 4-121: Unsoaked Unconfined Compressive Strength Summary of 50% MRAP/50% LR Blend

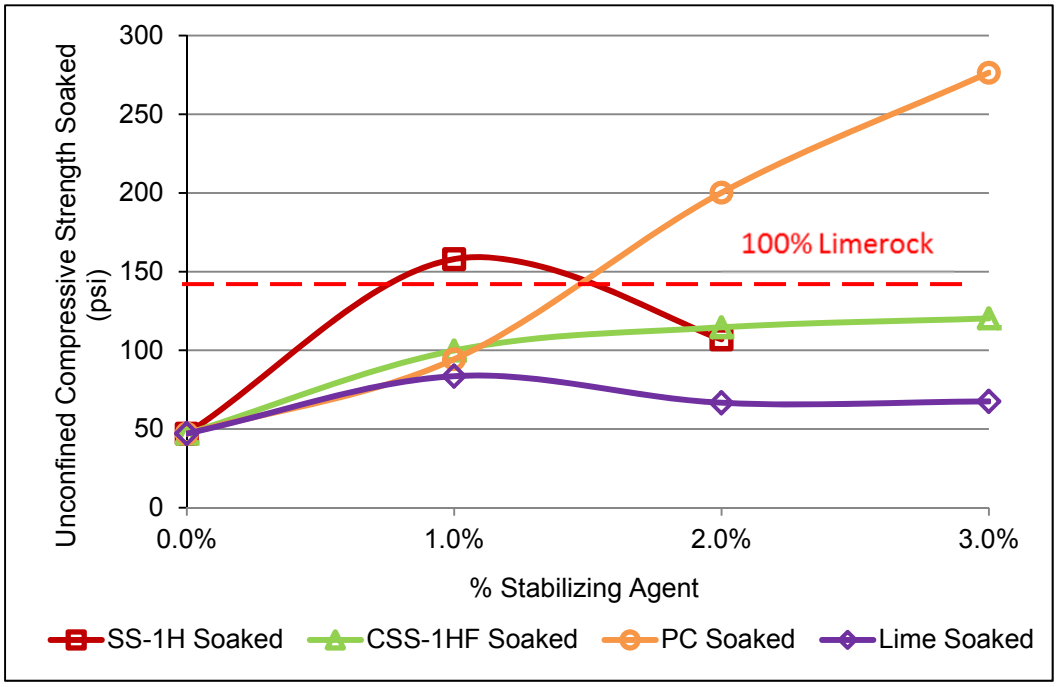

Figure 4-122: Soaked Unconfined Compressive Strength Summary of 50% MRAP/50% LR Blend

Figure 4-123 shows a summary of the retained strength (soaked strength/unsoaked strength) for the four stabilizing agents tested. The retained strength of 100% RAP is shown for reference. Specimens of 100% limerock had zero retained strength. Cement stabilized specimens exhibited over 90% retained strength across all concentrations. SS-1H stabilized specimens showed a peak retained strength of over 90% at 1% emulsion. CSS-1HF showed a peak retained strength over 90% at 3% emulsion. As noted in Section 4.6.3.4, lime stabilization had negligible effect on unconfined compressive strength. Lime stabilized specimen retained strength increased with increasing amounts of lime, peaking at over 80% retained at 1% lime. The improved retained strength performance at higher lime concentrations is misleading because it was due to a decline in the unsoaked lime strengths while the soaked strengths remained approximately constant.

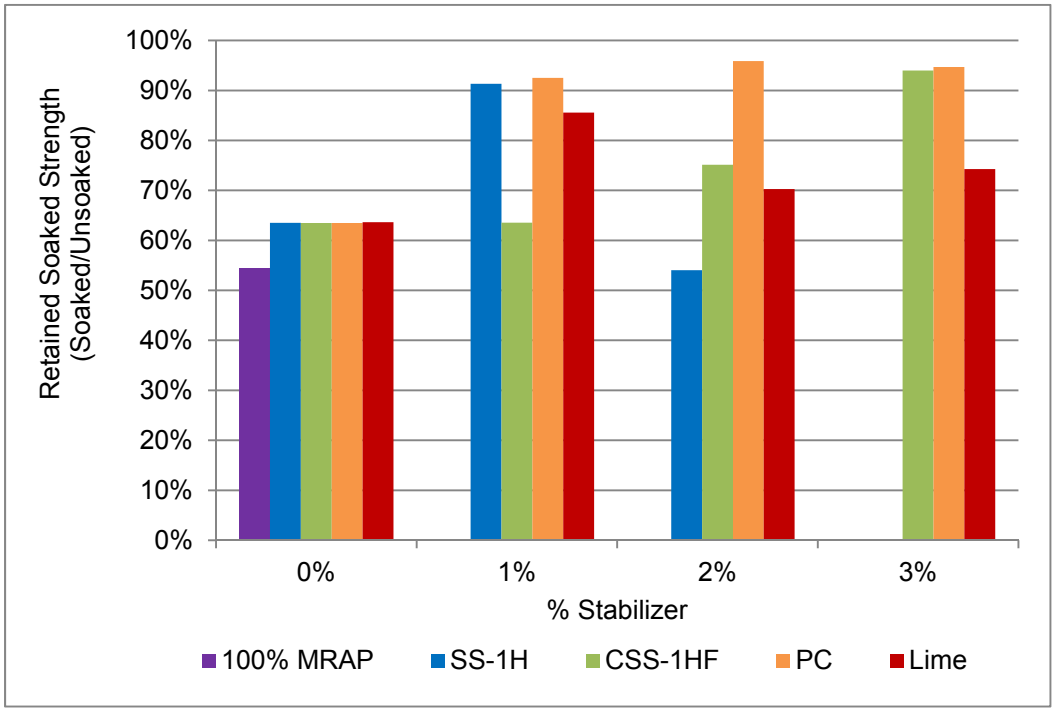

Figure 4-123: Retained Soaked Strength of Stabilized 50% MRAP/50% LR Blends

4.6.3.5.2. Summary of Chemically Stabilized 25% MRAP/75% LR Blends

This section compares the effect of the stabilizing agents on 25% MRAP/75% limerock blends. Like the 50%/50% blend discussed in the previous section, this blend had the potential to reach the objective soaked LBR of 100. Figure 4-124 shows the unsoaked unconfined

compressive strength results for SS-1H, CSS-1HF, and Portland cement. Lime was not used in this test series because of poor performance in the 50%/50% blends. The unsoaked unconfined compressive strength of 100% limerock is shown as a dashed red line for comparison. General trends were the same as those observed during LBR testing with a peak in emulsion stabilized strength between 1% and 2%, continued increase in cement stabilized strength. Unlike the LBR tests or the 50%/50% blend unconfined compression tests the 75%/25% blends increased in strength with the addition of 3% SS-1H.

All unsoaked specimens exceeded the unsoaked unconfined compressive strength of the 100% limerock control with the exception of the 2.0% SS-1H specimen which was slightly lower. All stabilized specimens retained strength when soaked. The soaked 2% cement, and 3% cement, SS-1H, and CSS-1HF specimens had a higher soaked unconfined compressive strength than the unsoaked 100% limerock control (Figure 4-125).

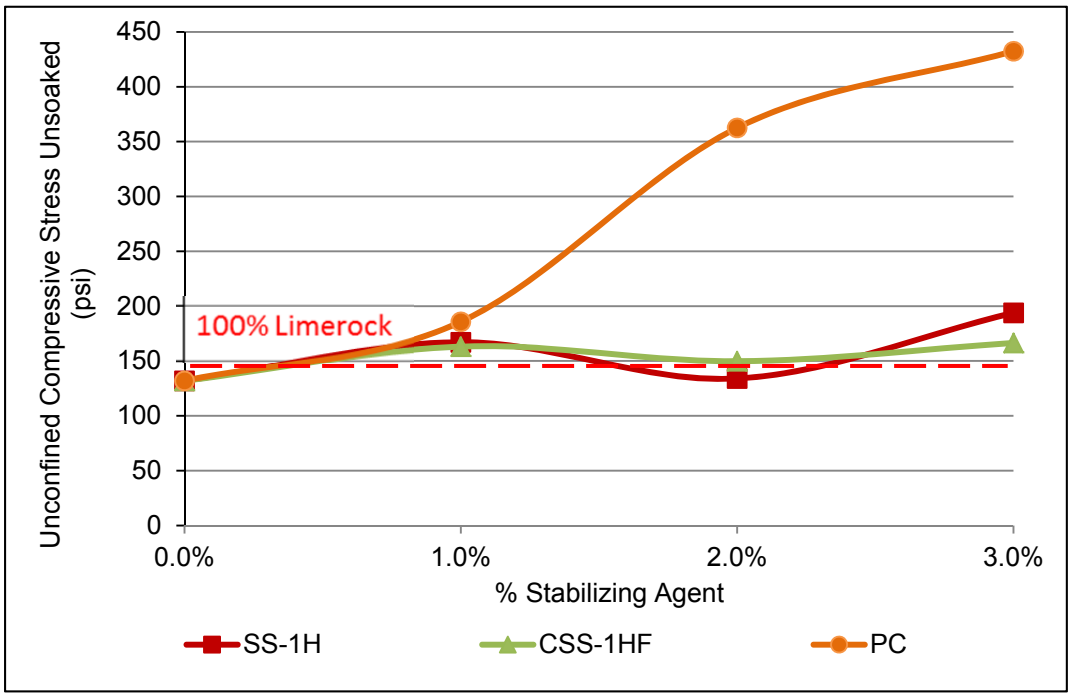

Figure 4-124 Unsoaked Unconfined Compressive Strength Summary of 25% MRAP/75% LR Blend

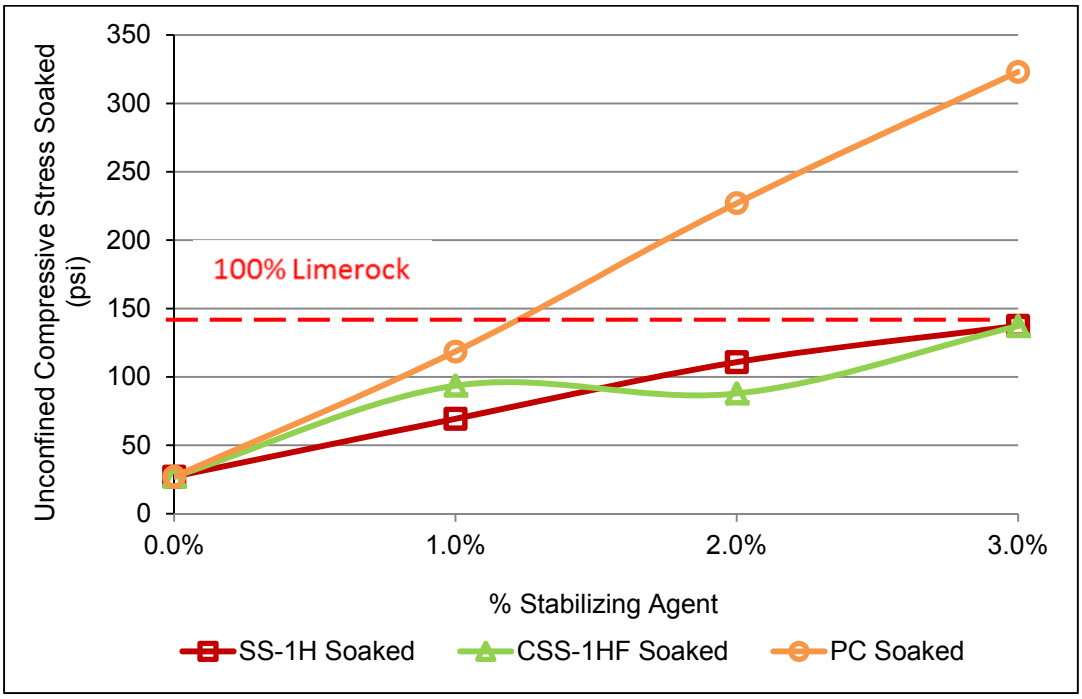

Figure 4-125 Soaked Unconfined Compressive Strength Summary of 25% MRAP/75% LR Blend

Figure 4-126 shows a summary of the retained strength for the three stabilizing agents tested. The retained strength of 100% RAP is shown for reference. Specimens of 100% limerock had zero retained strength. Cement stabilized specimens exhibited over 60% retained strength across all concentrations. SS-1H stabilized specimens showed a peak retained strength of over 80% at 2% emulsion. CSS-1HF showed a peak retained strength over 80% at 3% emulsion. These retained strength percentages are lower than those observed for the 50%/50% blends; however this is primarily because the unsoaked strengths of the 25% MRAP/75% LR blends were higher. The actual soaked strengths of the emulsion stabilized 25% MRAP/75% LR blends are generally comparable to their 50%/50% counterparts. The cement stabilized 25% MRAP/75% LR blends are all about 15% higher than their 50%/50% counterparts.

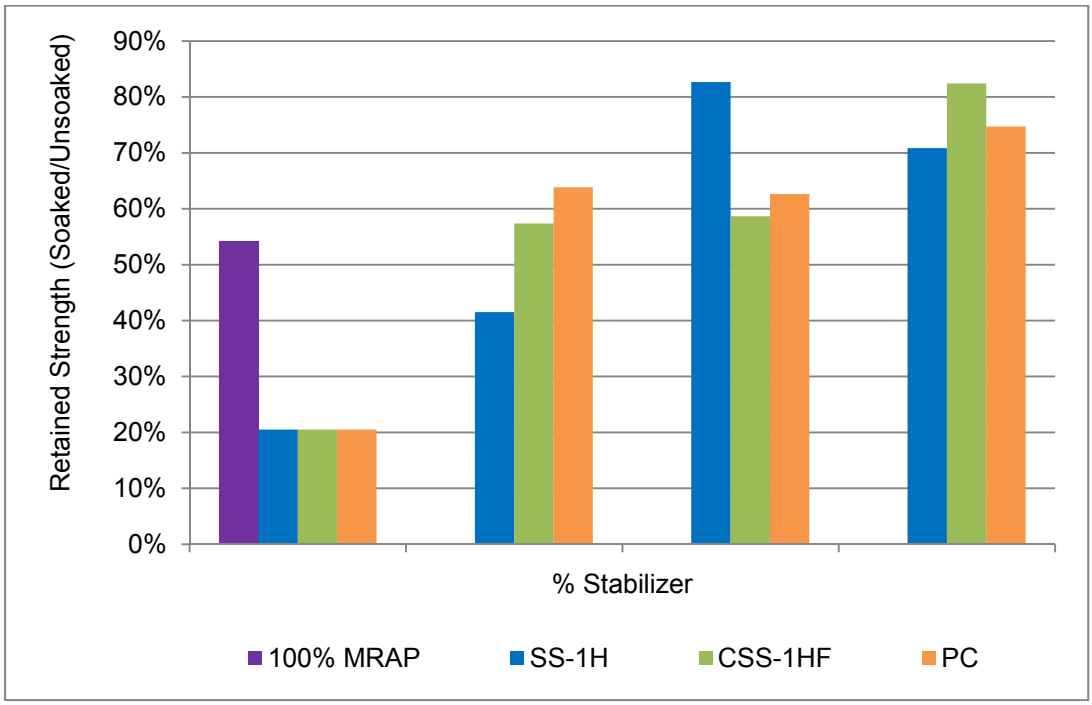

Figure 4-126: Retained Soaked Strength of Stabilized 25% MRAP/75% LR Blends

4.6.4. Modified Marshall Test Results

During discussions with industry, two Florida laboratories were interviewed that had performed mix designs for county or municipal Full Depth Reclamation (FDR) projects. Both labs generally followed the Modified Marshall mix design procedure in the Asphalt Institute Manual Series Number 19 (2008). The Asphalt Institute Modified Marshall method specifies testing of both dry and saturated (conditioned) samples to establish retained strength when wet. Modified Marshall tests were performed for comparison with other mechanical performance results. Some states have adopted a Full Depth Reclamation mix design using the Superpave gyratory compaction machine as outlined in the South Carolina Department of Transportation's FDR mix design method (SC-T-99, 2008) however the gyratory method was not evaluated in this study.

Typical modified Marshall compression test results are shown in Figure 4-127. Each plot is a single specimen. The figure shows a total of three unsoaked (red with solid markers) and three soaked specimens (blue with hollow markers).

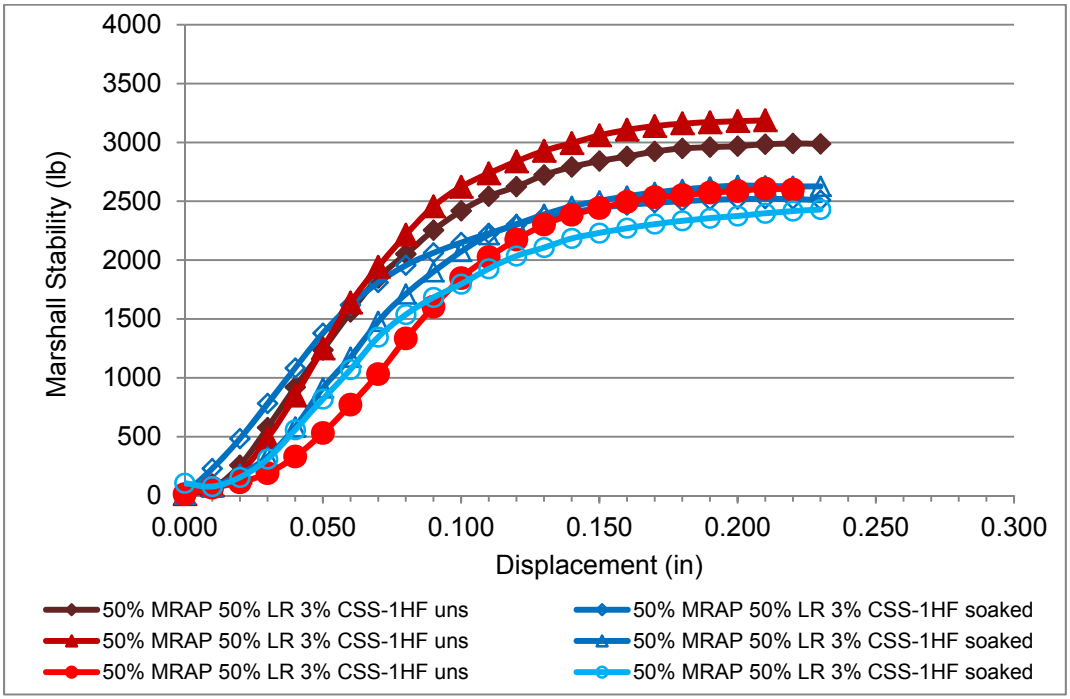

Figure 4-127: Typical Marshall Compression Test Results

In this study modified Marshall compaction was conducted and tested at 25° C rather than testing at the 60° C used in Marshall hot mix design. Compression testing was conducted at ambient laboratory temperature to match the conditions for the other tests. Normal Marshall testing is done at a strain controlled loading rate of 2 in/min. A lower strain rate of 0.05 in/min was used in this study to be consistent with the loading rate for the LBR and unconfined compression tests. Because of the forgoing, modified Marshall results presented here are only for relative comparisons and are not directly comparable to standard Marshall results.

A series of 12 tests was performed to compare specimens tested at 0.05 in/min on the FIT laboratory testing machine and at 2 in/min on a local commercial laboratory's Marshall test machine to determine the effect of the rate change. The 50% MRAP/50% limerock blends were selected for the comparison testing since this blend had potential to reach a soaked LBR of 100. Specimens were tested with no stabilization, 1% SS-1H emulsion, and 1% Portland cement. Only one emulsion type was tested because previous testing had shown similar performance trends for both anionic and cationic emulsion.

The Marshall stability number is the peak load during compression testing with a Marshall test frame. Figure 4-128 shows the average Marshall stability numbers for each pair of specimens at both loading rates. The Marshall stability number was 60% to 100% higher for the 2.0-inch per minute loading. The emulsion stabilized specimens showed the greatest difference. This result is expected since asphalt is a viscoelastic material and hence sensitive to loading rate.

Marshall flow is the deflection of the specimen at peak load given in units of 0.01-inches. A deflection of 0.15-inches would be a Marshall flow of 15. Figure 4-129 shows the average Marshall flow values for the specimens. Unlike the Marshall stability numbers, Marshall flow numbers were essentially unaffected by the difference in loading speeds. This result indicates that the deformation at failure is relatively independent of loading rate or of asphalt content.

Based on these comparisons, the Marshall stability numbers reported are understated compared to Marshall stability numbers, expected using a normal 2.0-inch per minute Marshall test machine at ambient temperature. Marshall flow numbers are approximately the same as those expected on a normal Marshall test machine.

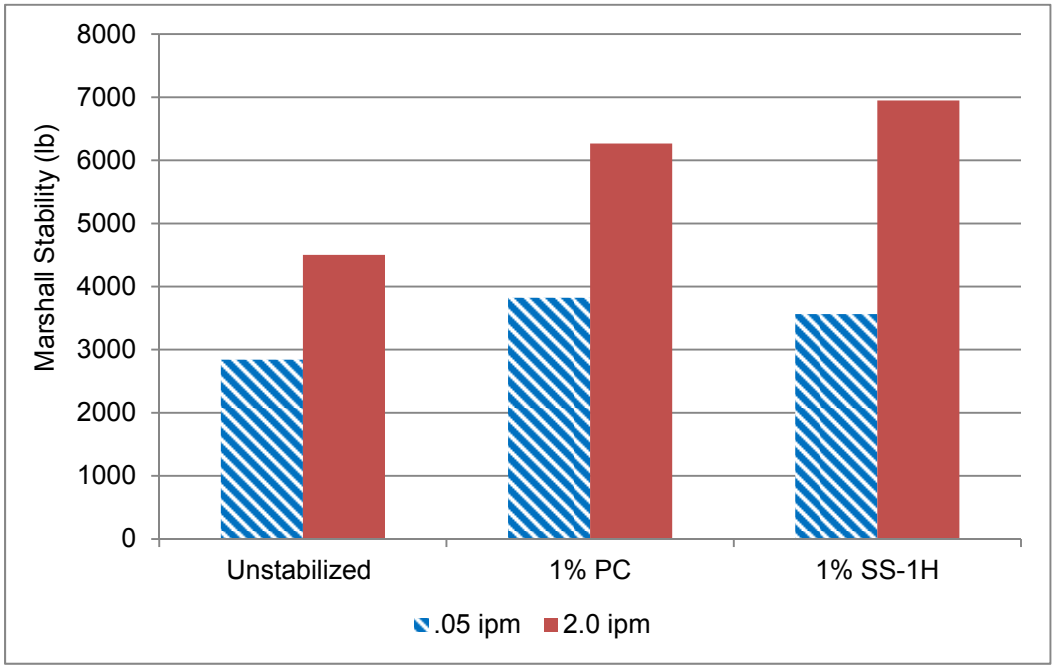

Figure 4-128: Marshall Stability of 50% MRAP/50% LR Specimens at 0.05 in/min and 2.0 in/min

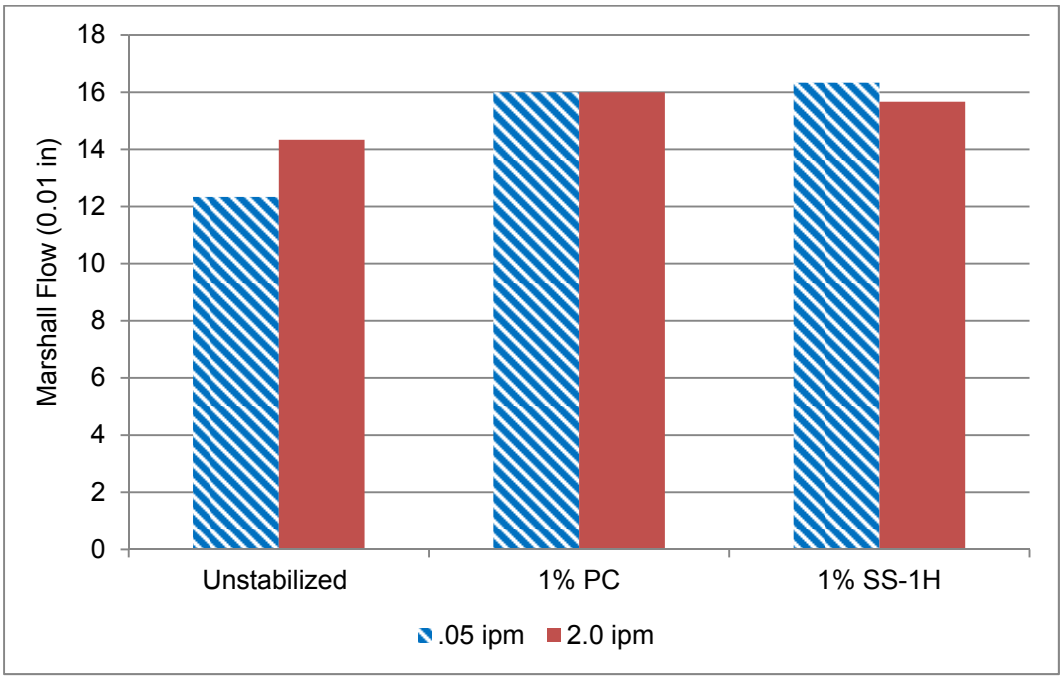

Figure 4-129 Marshall Flow of 50% MRAP/50% LR Specimens at 0.05 in/min and 2.0 in/min

4.6.4.1. Cationic Emulsion (CSS-1HF) Stabilized Blends

120 total specimens were used in this round of testing. Soaked and unsoaked modified Marshall testing was conducted using the same RAP/limerock blends and chemical stabilizing agents used in the previous LBR and unconfined compression tests. Specimens of 100% MRAP and 100% limerock were also stabilized with 1%, 2%, and 3% emulsion to obtain data to specifically compare Marshall flow to CSR's obtained earlier.

The 75% MRAP/25 % LR and 25 % MRAP / 75 % LR blends produced the highest Marshall stability number at 1% CSS-1HF (Figure 4-130). This peak was most pronounced in the 75% RAP/25% limerock blend. The 50/50 blend peaked at 2 %. The 100% limerock specimens showed a decrease in Marshall number with increasing CSS-1HF, while 100% RAP showed the opposite effect with the Marshall number increasing with increasing emulsion content.

Figure 4-131 shows the results for soaked specimens. CSS-1HF emulsion had a large effect on retained strength after soaking. The addition of 1% CSS-1HF more than doubled the soaked Marshall stability number of all specimens. The effect was most pronounced with the

100% and 75% limerock samples. The unstabilized 100% limerock disintegrated while soaking, and the unstabilized 75% limerock without stabilizer heavily eroded.

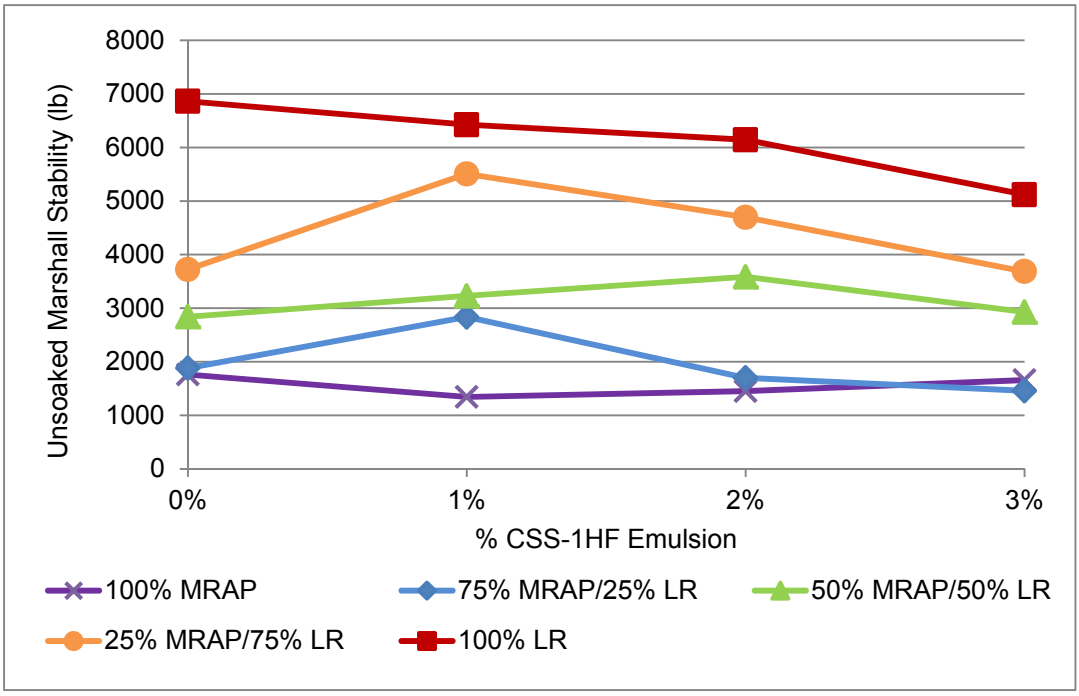

Figure 4-130: CSS-1HF Stabilized Modified Marshall Stability – Unsoaked

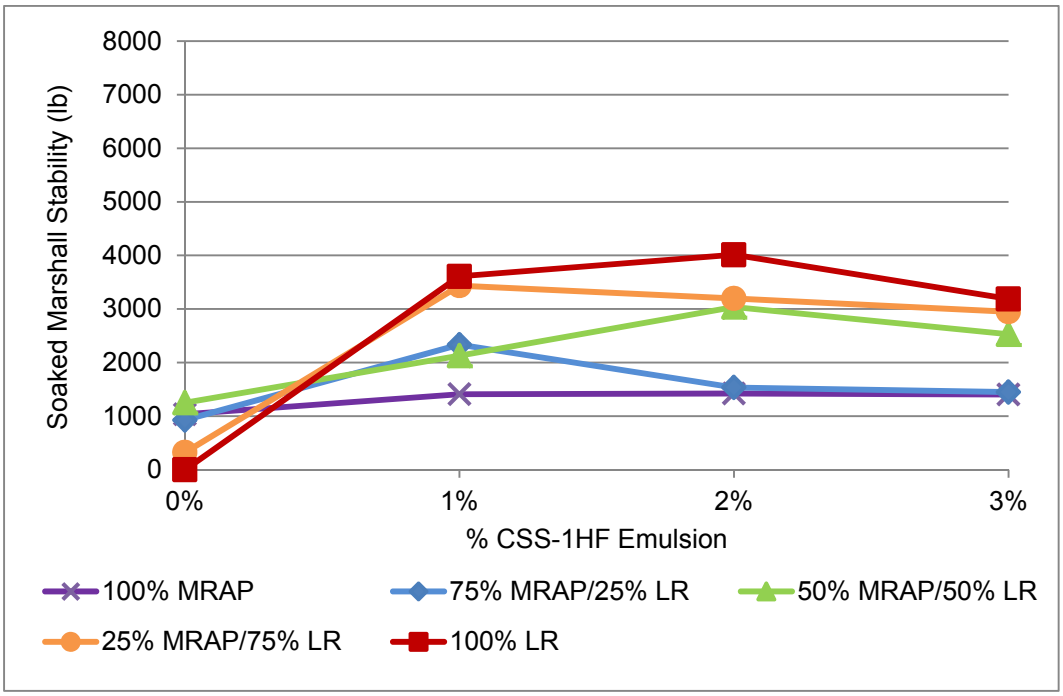

Figure 4-131: CSS-1HF Stabilized Modified Marshall Stability – Soaked

The retained soaked strength as a percentage of the unsoaked Marshall stability is shown in Figure 4-132. All stabilized specimens had higher retained strength with emulsion and adding more emulsion generally increased retained strength. As mentioned above, the most pronounced improvements in retained strength were observed in 100% limerock and 25% MRAP/75% limerock blends. Both materials had close to zero retained strength without emulsion but they retained between 56% and 62% of their unsoaked strength with the addition of 1% CSS-1HF. Additional emulsion improved both blends with the 25% MRAP/75% LR blend reaching 80% retained strength at 3% emulsion. Soaked 100% MRAP specimens retained 100% of their unsoaked strength. Contrary to the result observed with the blends, 100% MRAP showed a peak at 1% emulsion then declined at 2% and 3%. The 75% MRAP results are slightly misleading in that the increase in retained strength is due to a decrease in unsoaked strength at higher emulsion contents while the soaked strength remained essentially constant.

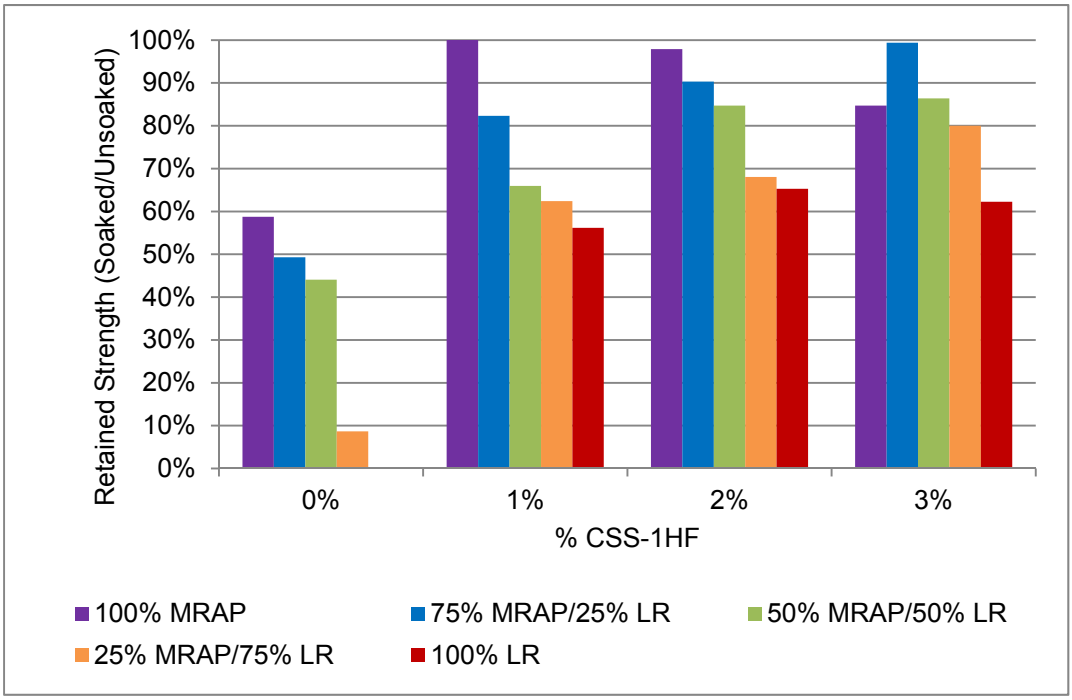

Figure 4-132: Percent of Unsoaked Marshall Stability Retained for CSS-1HF Stabilized Blends

Figure 4-133 summarizes the Marshall flow from the CSS-1HF testing. The Marshall flow for all three unsoaked unstabilized blends was approximately equal to the flow for the 100% limerock control and approximately 30% lower than the 100% MRAP control.

Adding 1% emulsion increased the flow by approximately 10% for the 100% limerock specimen and by approximately 35% for the 100% MRAP specimen. The flow of the blends increased between 10% and 35%. Increasing the emulsion content to 2% or 3% increases the flow of 50% and 25% MRAP specimens but had negligible effect on the other specimens. Soaked flow values for unstabilized specimens were 10% to 20% higher than their unsoaked counterparts. Adding 1% emulsion to the 100% limerock specimens kept them from disintegrating when soaked. More than 1% emulsion had little effect.

Adding emulsion decreased the flow of the soaked 100% MRAP specimens compared to their unsoaked counterparts. Emulsion increased the flows of the blends by approximately 30% at 1% emulsion up to 60% at 3% emulsion.

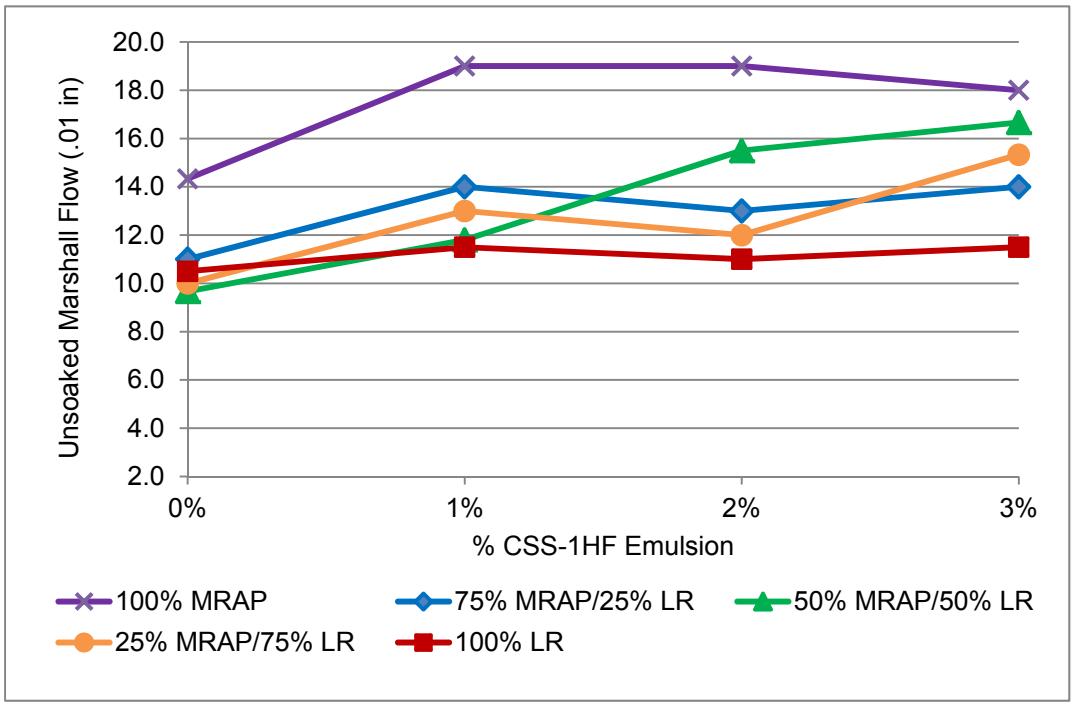

Figure 4-133: CSS-1HF Modified Marshall Flow – Unsoaked

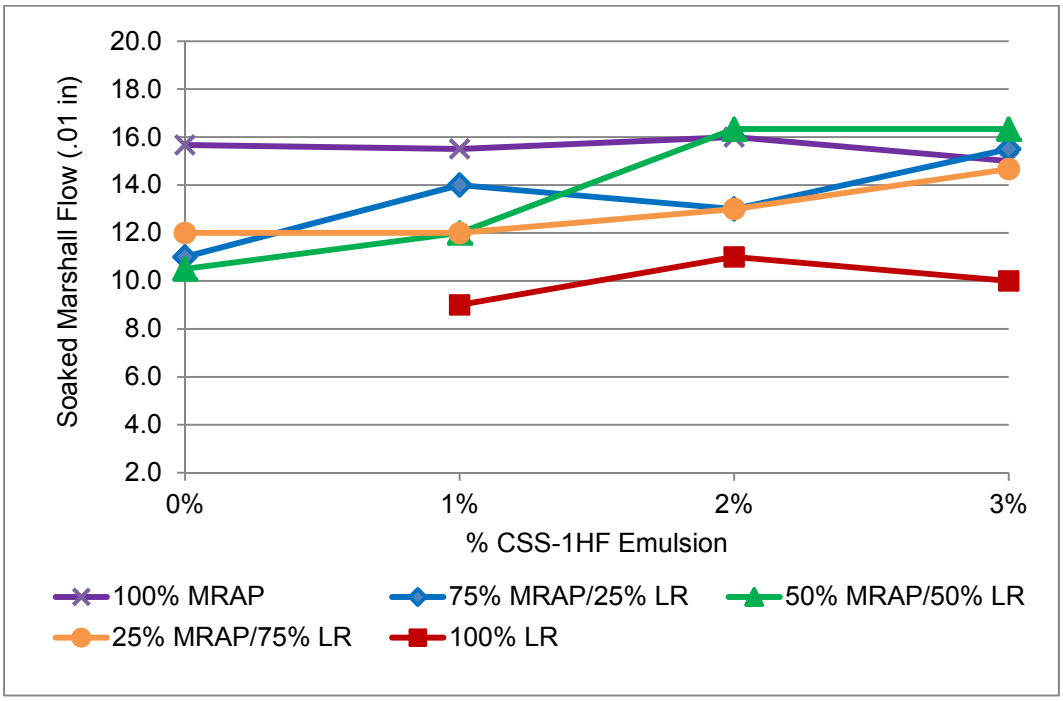

Figure 4-134: CSS-1HF Modified Marshall Flow – Soaked

4.6.4.2. Anionic Emulsion (SS-1H) Stabilized Blend

84 total specimens were used in this round of testing. Soaked and unsoaked modified Marshall testing was conducted using the same RAP/limerock blends and chemical stabilizing agents used in the previous tests. The 100% MRAP and 100% limerock control specimens in this round were only tested without emulsion. Results were similar for the three blends tested. In each case adding 1% SS-1H increased the Marshall stability by between 25% for the 50% MRAP (2841 to 3564) and 60% for the 75% MRAP blend. As was the case with CSS-1HF, these increases are larger than the increases seen in LBR testing. Also, like the CSS-1HF, adding 2% or 3% SS-1H decreased the Marshall stability in 10% increments.

The 25% RAP/75% LR blend consistently showed the highest unsoaked Marshall stability numbers (Figure 4-135). The 50% MRAP blend produced the second highest and the 75% MRAP blend the lowest. Increasing the MRAP percentage consistently decreased the unsoaked Marshal stability.

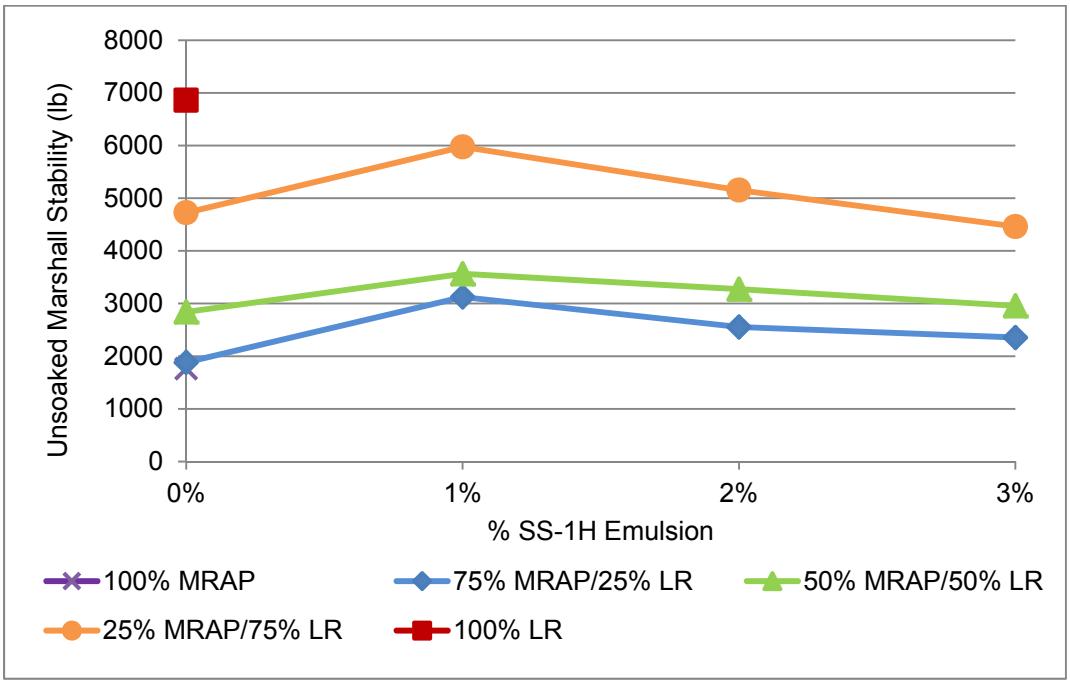

Figure 4-135: SS-1H Emulsion Stabilized Modified Marshall Stability – Unsoaked

Figure 4-136 shows that adding 1% SS-1H dramatically increased the soaked Marshall Stability by between 300% for the 75% blend and by over 1,000% for the 25% MRAP blend. After this large initial gain, the soaked Marshall stability remained relatively constant at 2% and 3% emulsion.

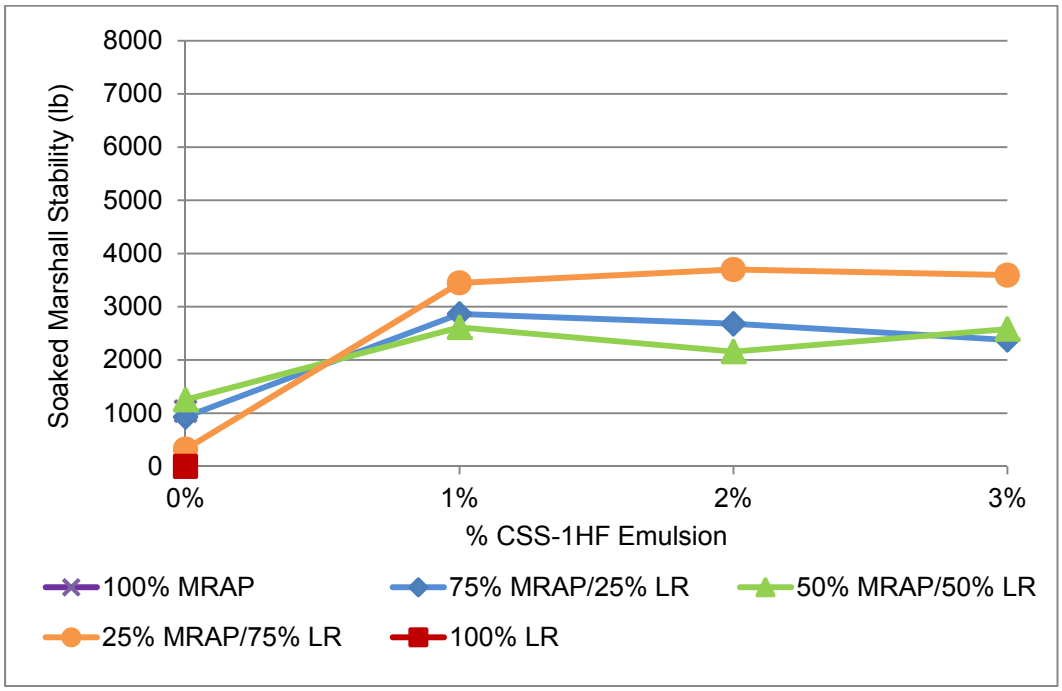

Figure 4-136: SS-1H Emulsion Stabilized Modified Marshall Stability – Soaked

As was the case with the CSS-1HF emulsion, the largest strength gains were noted in the unstabilized 25% MRAP blend due to the severe degradation of the limerock during soaking.

The retained soaked strength as a percentage or the unsoaked Marshall stability is shown in Figure 4-137. Similar to the CSS-1H results, all stabilized specimens had higher retained strength with emulsion. Adding more emulsion generally increased retained strength. As mentioned above, the most pronounced improvements in retained strength were observed in the 25% MRAP/75% limerock blend which had close to zero retained strength without emulsion but retained over 60% of its unsoaked strength with the addition of 1% SS-1H. Additional emulsion improved all blends with the exception of a slight decrease in the retained strength of the 50% MRAP blend at 2% emulsion. As was the case with the CSS-1HF emulsion, the 75% MRAP results are slightly misleading in that the increase in retained strength is due to a decrease in unsoaked strength at higher emulsion contents while the soaked strength remained essentially constant.

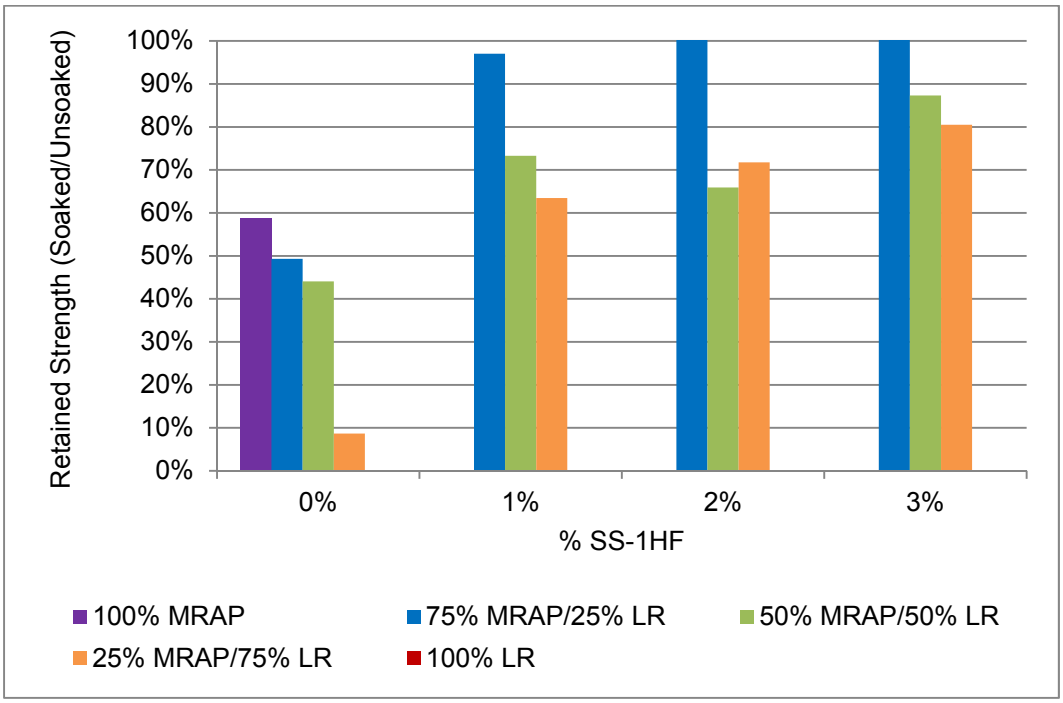

Figure 4-137: Percent of Unsoaked Marshall Stability Retained for SS-1HF Stabilized Blends

Figure 4-138 summarizes the Marshall flow for the unsoaked SS-1H testing. The Marshall flow of all three unstabilized blends was very close to that of 100% LR and approximately 30% lower than the flow of 100% MRAP. Adding 1% emulsion increased the flow for all three blends. Beyond 1% emulsion the 75% and 25% MRAP blends showed increased flow while the 50% MRAP blend showed decreased flow. In all cases the flow of the stabilized specimens remained higher than the flow of the unstabilized specimens.

The flow of soaked specimens (Figure 4-139) was between 10% and 20% higher than their unsoaked counterparts. Soaked specimens showed essentially the same trends as the unsoaked specimens except that there was no decrease in soaked flow for the 25% MRAP blends with 2% emulsion.

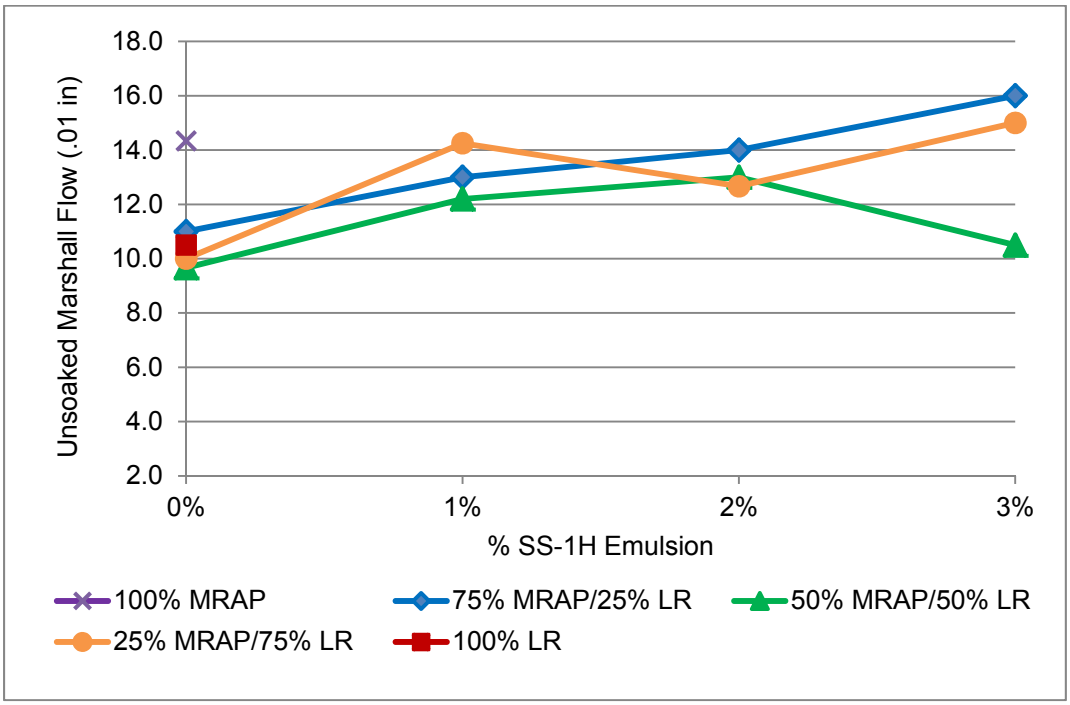

Figure 4-138: SS-1HF Emulsion Stabilized Modified Marshall Flow – Unsoaked

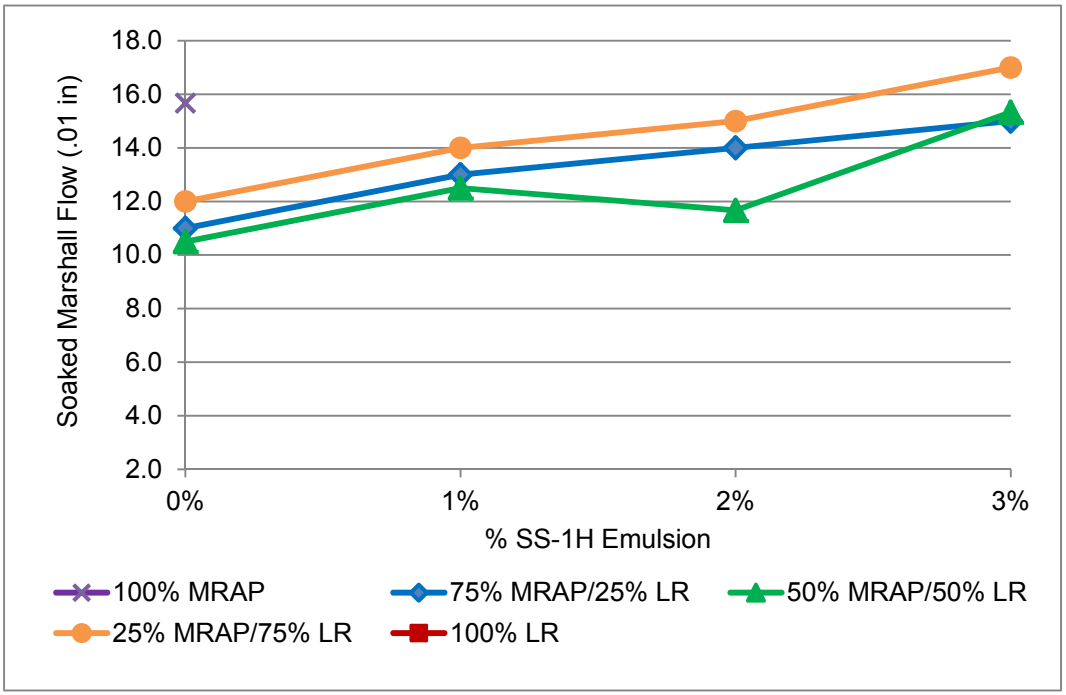

Figure 4-139: SS-1HF Emulsion Stabilized Modified Marshall Flow – Soaked

4.6.4.3. PC Stabilized Blends

120 total specimens were used in this round of testing. Soaked and unsoaked modified Marshall testing was conducted using the same RAP/limerock blends and cement stabilizing agents previously described. Specimens of 100% MRAP and 100% limerock were also stabilized with 1%, 2%, and 3% cement specifically to obtain data to compare Marshall flow to creep deformation and strain rates discussed in Section 4.6.2.4.

Figure 4-140 shows a summary of the effects of Portland cement stabilizing agent. Adding cement generally improved the unsoaked Marshall stability numbers. The largest improvement was seen in the 25% MRAP/75% limerock blend which increased 125% with the addition of 1% cement (from 2841 to 3824). Blends with 50% MRAP, and 100% MRAP with 1% cement showed increases of approximately 35%. For these three blends unsoaked Marshall stability increases were approximately linearly related to the amount of cement stabilizer. Specimens of 100% limerock and 25% MRAP/75% limerock blends with 3% cement exceeded the 10,500 lb capacity of the test machine. Projected values are shown with dashed lines. Trends were different for 100% MRAP and 75% MRAP/25% LR blends which showed inconsistent results and little change in Marshall stability from the addition of cement stabilizer.

The soaked Marshall strengths (Figure 4-141) followed similar trends to those observed in the unsoaked specimens. The 100% limerock and 25% MRAP/75% LR had zero or little soaked strength without stabilizer but had the highest soaked strengths with 1% cement added. The 50% MRAP/50% LR blend also showed increased soaked Marshall stability with 1% cement. All three of these blends showed an approximately linear increase in Marshall stability with increasing cement content. The 75% MRAP 100% RAP specimens showed little variation with increasing cement content.

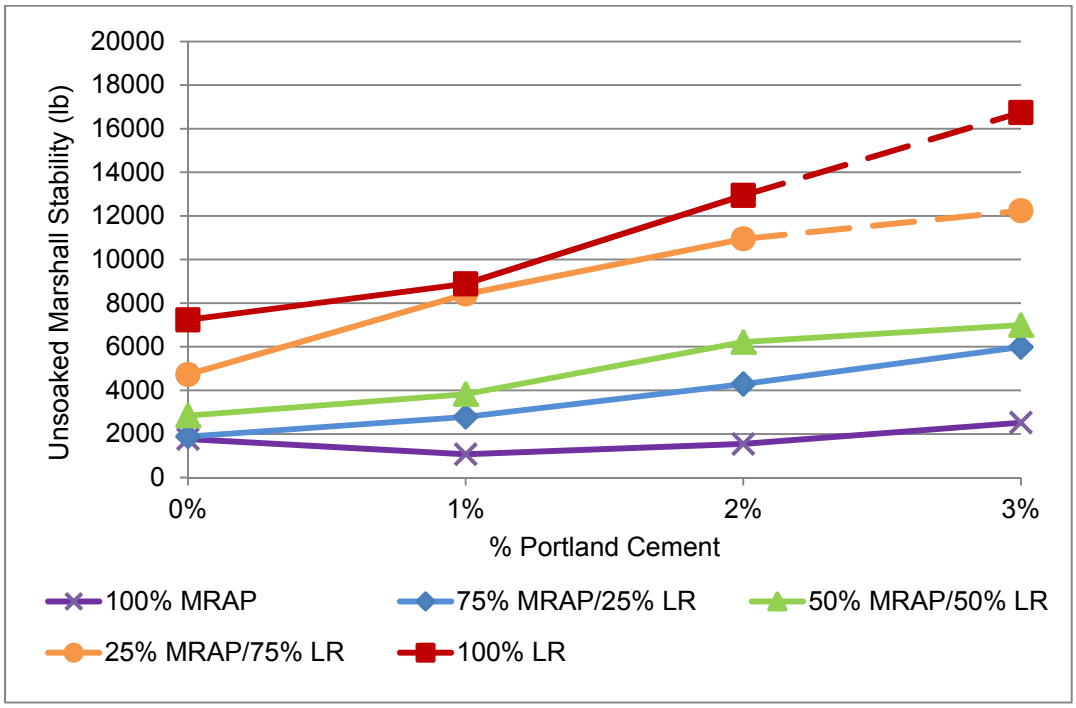

Figure 4-140: Portland Cement Stabilized Modified Marshall Stability – Unsoaked

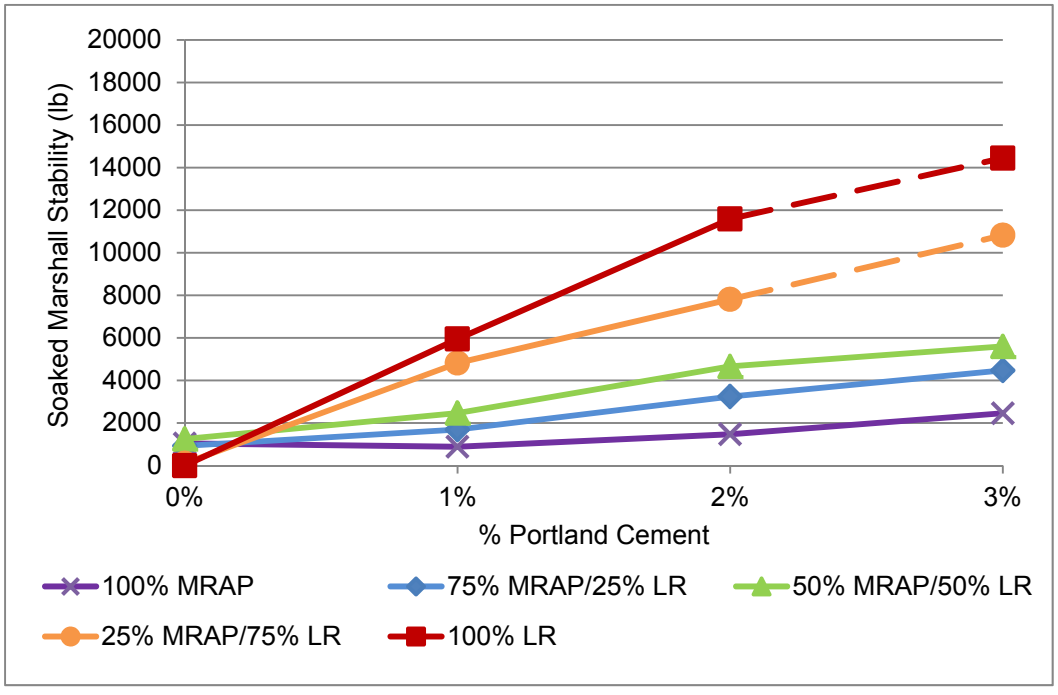

Figure 4-141: Portland Cement Stabilized Modified Marshall Stability – Soaked

The retained soaked strength as a percentage or the unsoaked Marshall stability is shown in Figure 4-142. Similar to both emulsion results, all stabilized specimens had higher retained strength with cement. Adding more cement always increased retained strength. As mentioned above, the most pronounced improvements in retained strength were observed in 100% limerock and 25% MRAP/75% limerock blends. Both materials had close to zero retained strength without cement but they retained between 57% and 67% of their unsoaked strength with the addition of 1% cement. Additional cement improved both blends with the 25% MRAP/75% LR blend reaching 88% retained strength at 3% cement. Soaked 100% MRAP and 75% MRAP specimens retained nearly 100% of their unsoaked strength with 3% cement.

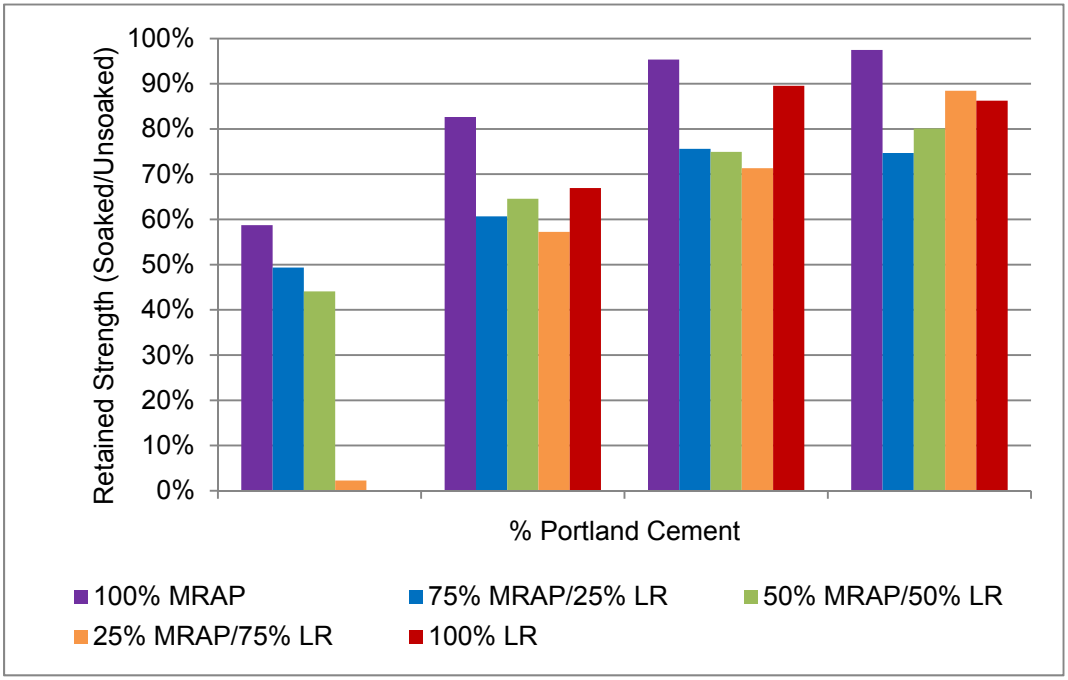

Figure 4-142: Percent of Unsoaked Marshall Stability Retained for Cement Stabilized Blends

Figure 4-143 is a summary of the flow from the unsoaked Marshall tests. 100% MRAP, the 75% MRAP/25% LR and 50% MRAP/50% LR blends show increases in Marshall flow with 1% cement. The 100% limerock and 75% MRAP/25% LR blend show decreasing flow with 1% cement. With one exception (25% MRAP/75% LR), all of the materials show decreasing or constant Marshall flow numbers with 2% or 3% cement. In all but one case (25% MRAP/75% LR with 3% cement), the amount of Marshall flow was approximately proportional to the RAP content of the blend.

Figure 4-144 is a summary of the soaked Marshall flows. The trends are similar to those in the unsoaked testing. As was the case with the emulsion specimens, the soaked Marshall flows were very close to the same values as those obtained in the unsoaked testing, indicating that soaking did not have a major effect on the measured flow. The flow of the stabilized specimens is very nearly proportional to the RAP content of the blend. Except for the 25% MRAP blend, all of the blends had lower Marshall flow at 3% cement content than they had with 0% cement indicating that cement stabilizing agent slightly reduced the amount of strain that the specimen withstood before failure. In other words, cement stabilization made the specimens slightly more brittle. The opposite trend was observed with the emulsions, both of which made the specimens fail at slightly higher strains indicating that the emulsion made the specimens more flexible. Both of these results could be expected from the nature of the cement and asphalt binder.

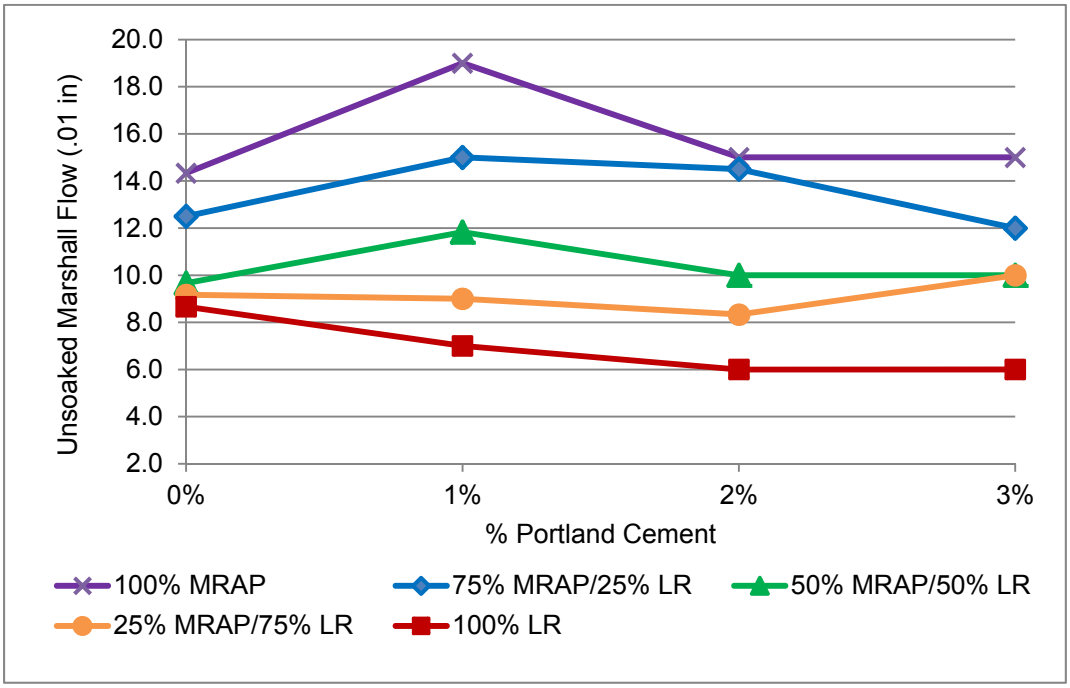

Figure 4-143: Portland Cement Stabilized Modified Marshall Flow – Unsoaked

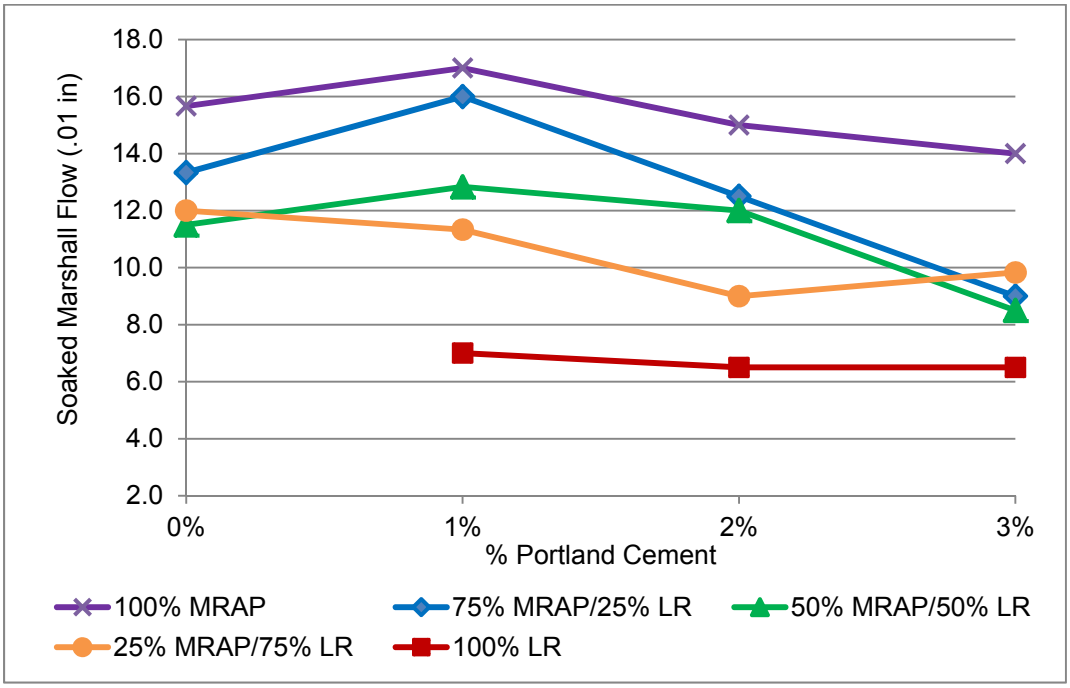

Figure 4-144: Portland Cement Stabilized Modified Marshall Flow – Soaked

4.6.5. Soaked LBR of Stabilized Limerock/RAP Blends

After the initial testing phase, selected specimens were tested using soaked conditions, without being subjected to creep, for direct comparison to standard LBR values. 36 specimens were prepared for this round of testing. Complete results are shown in Appendix G.

Based on the LBR, unconfined compression, and Marshall tests discussed above, 50% RAP/50% limerock was selected as the minimum aggregate blend likely to achieve a soaked LBR of 100 with chemical stabilizer. The 50% limerock/50% RAP blends were prepared with 0%, 1%, 2%, and 3% of each stabilizing agent (SS-1H, CSS-1H, and Portland cement). FM 5-515 was followed except that all emulsion stabilized specimens were oven cured for 48 hours at 60°C and the Portland cement stabilized specimens were covered in plastic wrap and cured for 14 days. Following curing, all specimens were soaked for 48 hours, drained for 15 minutes and tested. Control specimens of 100% limerock, 50% MRAP/50% limerock, and 25% MRAP/75% limerock were tested with no stabilizing agent.

Figure 4-145 shows a summary of the soaked LBR versus percent chemical stabilizer. The 100% limerock specimens had an average soaked LBR of 162. The 25% MRAP/75% LR

specimens had an average soaked LBR of 99. FDOT test data for 21 samples of the same limerock source used in this study showed a minimum LBR of 149, a maximum of 239, and a mean of 184with a standard deviation of 25 (Appendix G). The 100% limerock soaked LBR values found in this round of testing were nearly one standard deviation below the FDOT mean; there is over an 80% probability that limerock from the source selected would test higher than the values obtained in this testing.

The 50% RAP/50% limerock blend without stabilizer achieved a soaked LBR of 53. This is well below the 100 required for base course material. Based on the comparison of compaction methods covered earlier, it is possible that gyratory compaction of this blend might achieve a soaked LBR strength of 100, however gyratory molds are not designed to be immersed in water so this was not tested. The 50% MRAP/50% limerock blend meets the subbase LBR requirement of 40. FM 5-515 specifies a surcharge weight during subbase LBR testing so this material would achieve an LBR higher than the 53 observed with a surcharge.

4.6.5.1. Cationic Emulsion (CSS-1HF) Stabilized Blends

The 50% RAP/50% limerock blends stabilized with 1% CSS-1HF emulsion achieved an LBR of 127, moderately over the 100 required for base material. Blends with 2% and 3% emulsion achieved an LBR of 105 and 107 respectively. Similar to the SS-1H emulsion, the relationship between % CSS-1HF emulsion and LBR shows a peak at 1% and gradual decline with increasing concentrations tested (Figure 4-145).

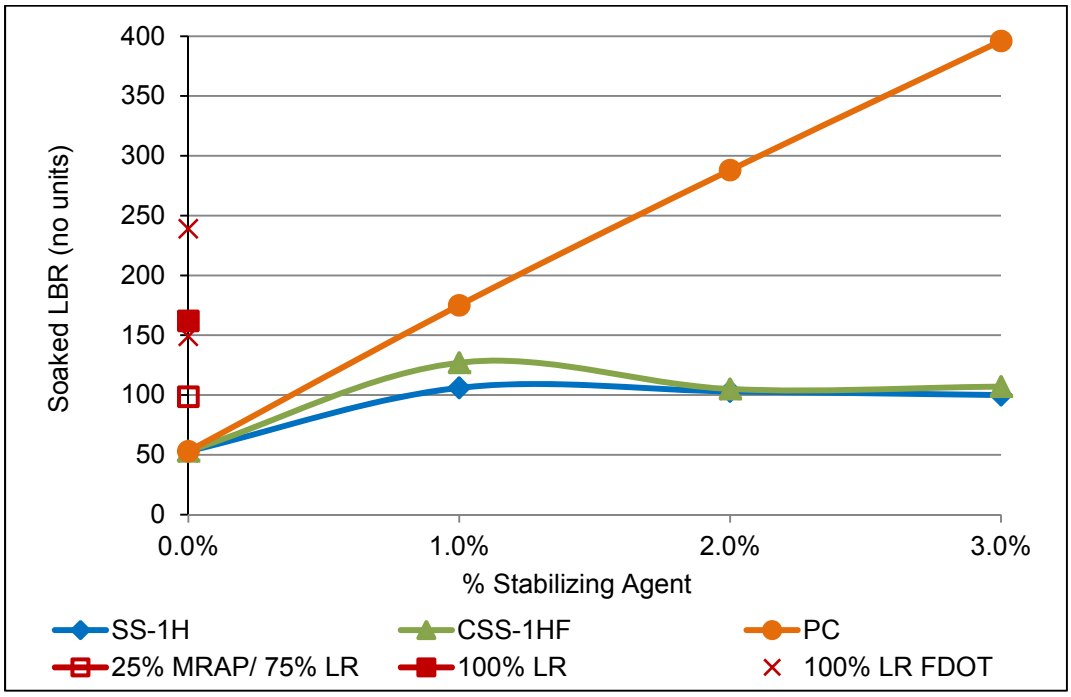

Figure 4-145: Soaked LBR of Stabilized 50% MRAP/50% Limerock Blends

4.6.5.2. Anionic Emulsion (SS-1H) Stabilized Blends

The 50% RAP/50% limerock blends stabilized with 1% SS-1H emulsion achieved an LBR of 106, slightly over the 100 required for base material. Blends with 2% and 3% emulsion achieved an LBR of 103 and 100 respectively. Like the CSS-1HF emulsion, SS-1H emulsion and LBR shows a weak peak soaked LBR at 1% concentration and a gradual decline with increasing concentrations tested (Figure 4-145).

4.6.5.3. Portland Cement Stabilized Blends

The 50% RAP/50% limerock blends stabilized with 1% Portland cement achieved an LBR of 175, well above the 100 required for base material. Blends with 2% and 3% cement achieved an LBR of 288 and 396 respectively. The relationship between % cement and LBR is almost perfectly linear for the four concentrations tested (Figure 4-145).

4.6.5.4. Summary of Soaked LBR of Stabilized MRAP/Limerock Blends

Portland cement is the most predictable of the three chemical stabilizing agents tested. Interpolating from the observed results, blends with 0.5% cement stabilization would still

achieve a soaked LBR over 100. Since these LBR values are based on 14 day strengths, normal hydration of cement will probably increase strength with additional time.

Both SS-1H and CSS-1HF emulsion showed a peak at 1% concentration, then a gradual drop off in strength. For an actual mix design, it would be prudent to test concentrations of 0.5% and 1.5% emulsion to refine the optimum emulsion content. LBR values are based on strengths measured after approximately 5 days (curing and soaking). This research did not include an investigation of whether these strengths will change with additional time.

4.6.6. Overall LBR and Creep Displacement Acceptance

Soaked LBR and 30 year deformation projections for a 10-inch thick base course continuously loaded with a 25 psi average stress are shown in Table 4-32. Soaked LBR values above 100 are characterized as acceptable. Projected 30 year deformation is characterized as acceptable if it is below 0.3-inches (3.0% strain in a 10-inch base layer).

Table 4-32: Stabilized Blends Soaked LBR and 30-year Deformation Projections for a 10-inch Base Course at 25 psi

Description		Stabilizing Agent	Soaked LBR	Accept-able	30-year Defor-mation	Accept-able
Limerock	MRAP					
100%	0%	No Stabilizer	162	Yes	0.08	Yes
75%	25%	No Stabilizer	99	No	0.12	Yes
50%	50%	No Stabilizer	55	No	0.15	Yes
50%	50%	1% Cement	175	Yes	0.09	Yes
50%	50%	1% SS-1H	106	Yes	0.08	Yes
50%	50%	1% CSS-1H	127	Yes	0.20	Yes

4.6.7. IDT Results for Stabilized 50% MRAP/ 50% Limerock Blends

From previously discussed testing, chemical stabilizing agents significantly improved the retained strengths of soaked Marshall, unconfined compression, and LBR specimens. All of these tests are compression tests. Tensile strength is an indicator of resistance to cracking and of

retained strength when saturated. IDT's were conducted on 50% MRAP/50% limerock specimens with 1% of either SS-1H emulsion, CSS-1H emulsion, or Portland cement. Control samples of 50% RAP/50% limerock, 100% RAP and 100% limerock with no chemical stabilization were also tested.

60 total specimens were tested in this phase. Equivalent sets of specimens were prepared with modified Proctor and gyratory compaction to investigate whether the method of compaction had an effect on IDT strength. Half of each set was tested unsoaked and half was tested soaked to determine the retained strength after soaking.

4.6.7.1. IDT Strength Comparison of Modified Proctor and Gyratory Compaction Specimens

4.6.7.1.1. IDT of Specimens with No Chemical Stabilization (Unstabilized)

Unstabilized, unsoaked 50% MRAP/50% LR modified Proctor specimens had an average IDT strength of 11.7 psi while gyratory specimens had an average IDT strength of 20.5 psi (Figure 4-146). This ratio of 1.75 gyratory to modified Proctor strength is consistent with unconfined compression and LBR test results discussed in Section 4.5.3 and Section 4.5.4. The 100% MRAP control specimens showed a much larger difference between the two compaction methods. The unstabilized, unsoaked 100% RAP modified Proctor control specimens showed an average IDT strength of 9.2 psi while gyratory specimens had an average IDT strength of 24.2 psi for a ratio of 2.62. The 100% limerock control specimens showed almost no tensile strength for either compaction method.

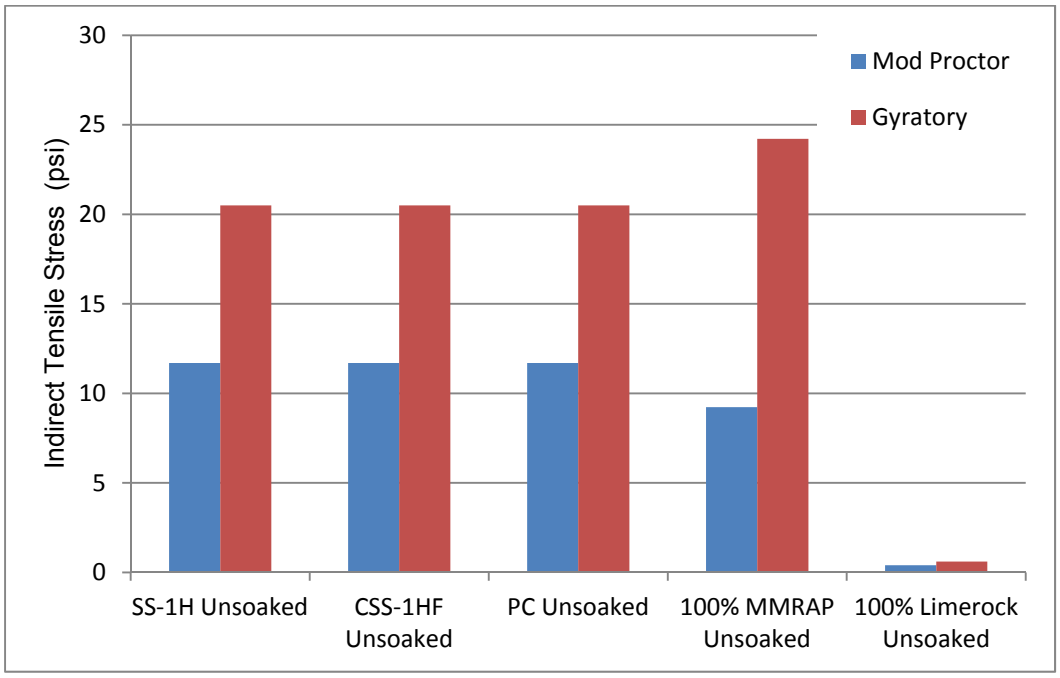

Figure 4-146: 50% MRAP/50% Limerock 0% Stabilizer Unsoaked

Soaked specimens exhibited a similar trend. Unstabilized, soaked 50% MRAP/50% LR modified Proctor specimens had an average IDT strength of 2.2 psi while gyratory specimens had an average IDT strength of 4.1 psi (Figure 4-147).

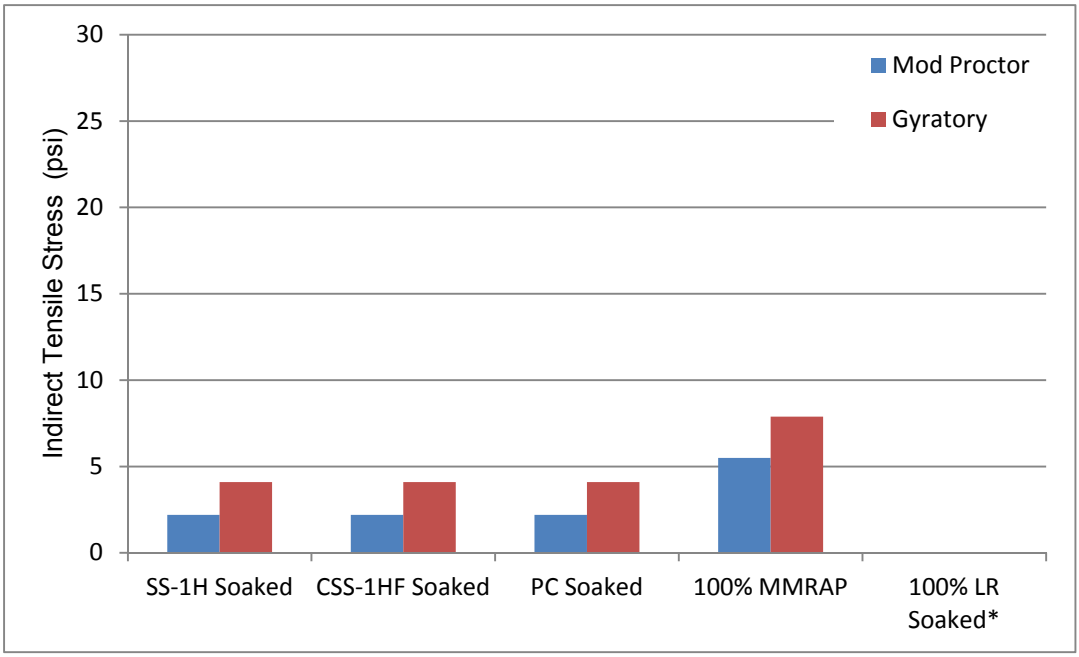

Figure 4-147: 50% MRAP/50% Limerock 0% Stabilizer -- Soaked

This ratio of 1.86 gyratory to modified Proctor strength is consistent with the previously mentioned unconfined compression and LBR test results. The unstabilized, soaked 100% MRAP modified Proctor control specimens showed an average IDT strength of 5.5 psi while gyratory specimens had an average IDT strength of 7.9 psi for a ratio of 1.43. The 100% limerock control specimens disintegrated when soaked so they are shown as zero IDT strength.

4.6.7.1.2. IDT of Specimens with 1% Chemical Stabilization (Stabilized)

Stabilized, unsoaked 50% RAP/50% modified Proctor specimens had an average IDT strength of 13.3 psi while gyratory specimens had an average IDT strength of 20.1 psi (Figure 4-148). This ratio of 1.51 gyratory to modified Proctor strength is consistent with unconfined compression and LBR test results. Specimens of 100% MRAP and 100% limerock were not tested with stabilization. Unstabilized results are shown for comparison to stabilized blends.

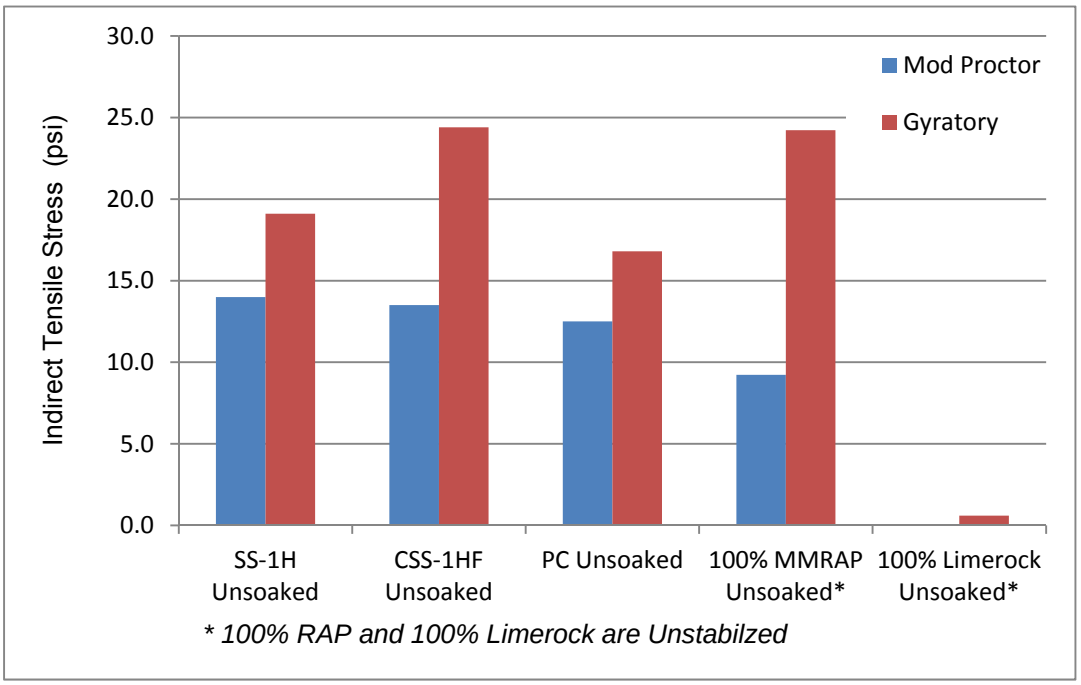

Figure 4-148: 50% MRAP/50% Limerock 1% Stabilizer-- Unsoaked

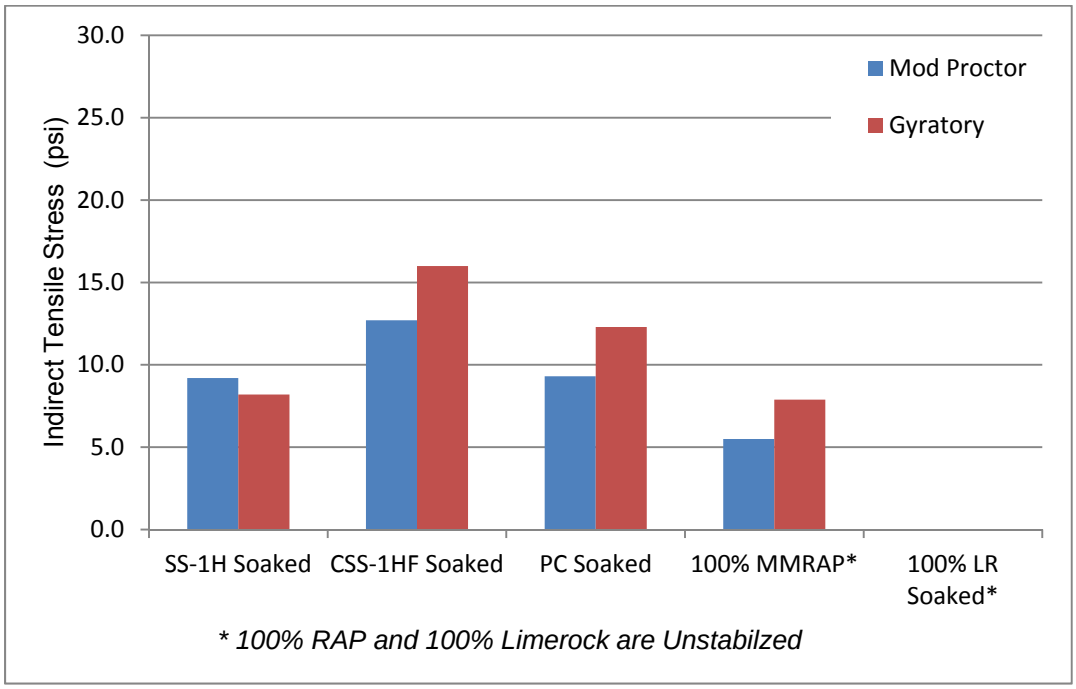

Figure 4-149: 50% RAP/50% Limerock 1% Stabilizer-- Soaked

4.6.7.2. IDT Strength Comparison of Unstabilized and Stabilized Specimens

This section presents the same data covered above but reorganized to show unstabilized and stabilized IDT strengths for unsoaked and soaked specimens organized by compaction type. This change makes the effect of chemical stabilization readily visible, by showing the 0 and 1% stabilizer data in a group. Specimens of 100% RAP and 100% limerock were not tested with stabilization. Unstabilized results are shown for comparison to stabilized blends.

4.6.7.2.1. IDT of Stabilized and Unstabilized Modified Proctor Specimens

Unstabilized unsoaked 50%/50% blends had an IDT strength 1.27 times that of the 100% RAP control, and 29.3 times that of 100% limerock. Unstabilized, unsoaked 50% MRAP/50% LR modified Proctor specimens had an average IDT strength of 11.7 psi while stabilized specimens had an average IDT strength of 13.3 psi (Figure 4-150). This ratio of 1.14 stabilized to unstabilized strength was much lower than the results from the Marshall, unconfined compression and LBR data.

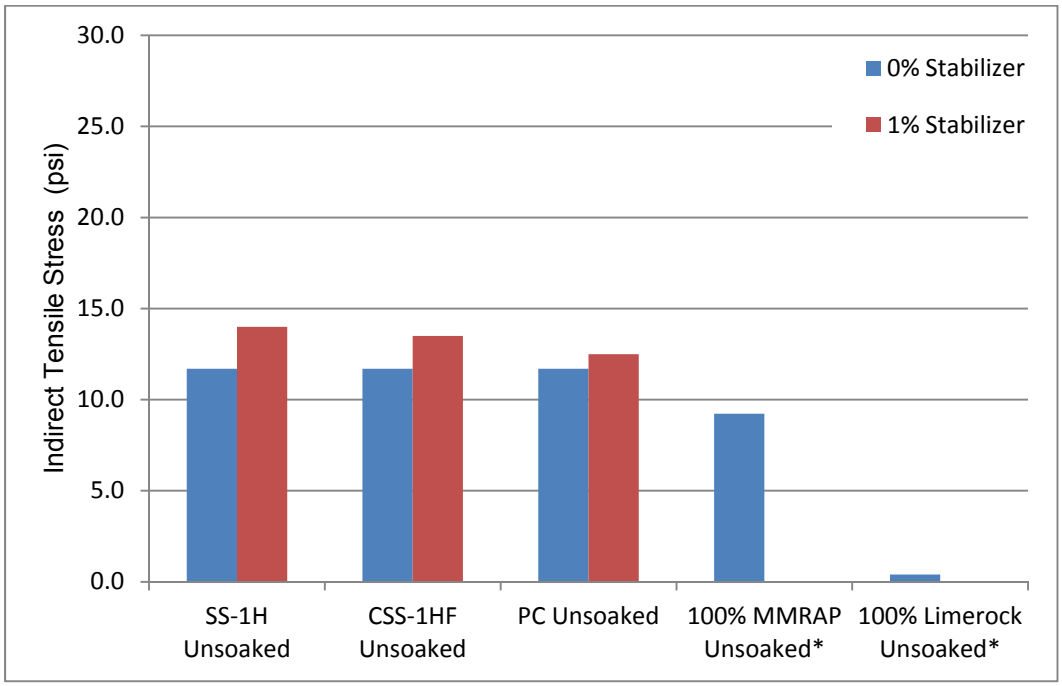

Figure 4-150: 50% RAP/50% Limerock Modified Proctor Compacted Specimens-- Unsoaked

While 1% stabilizer produced relatively small IDT strength gains in unsoaked samples, 1% stabilizer produced dramatic gains in soaked 50%/50% blends. Unstabilized 50%/50% blends had an IDT strength only 40% of that of the 100% RAP control indicating that adding limerock to RAP decreases its soaked IDT strength. On the other hand, 50%/50% blends maintained some IDT strength while the 100% limerock disintegrated indicating that blending RAP with limerock greatly improves limerock's soaked IDT strength. Unstabilized soaked 50% MRAP/50% specimens had an average IDT strength of 2.2 psi while stabilized specimens had an average IDT strength of 10.4 psi (Figure 4-151). This ratio of 4.73 stabilized to unstabilized strength was much higher than the results of the Marshall, unconfined compression and LBR tests. Since soaked limerock disintegrated it is shown with a strength of zero.

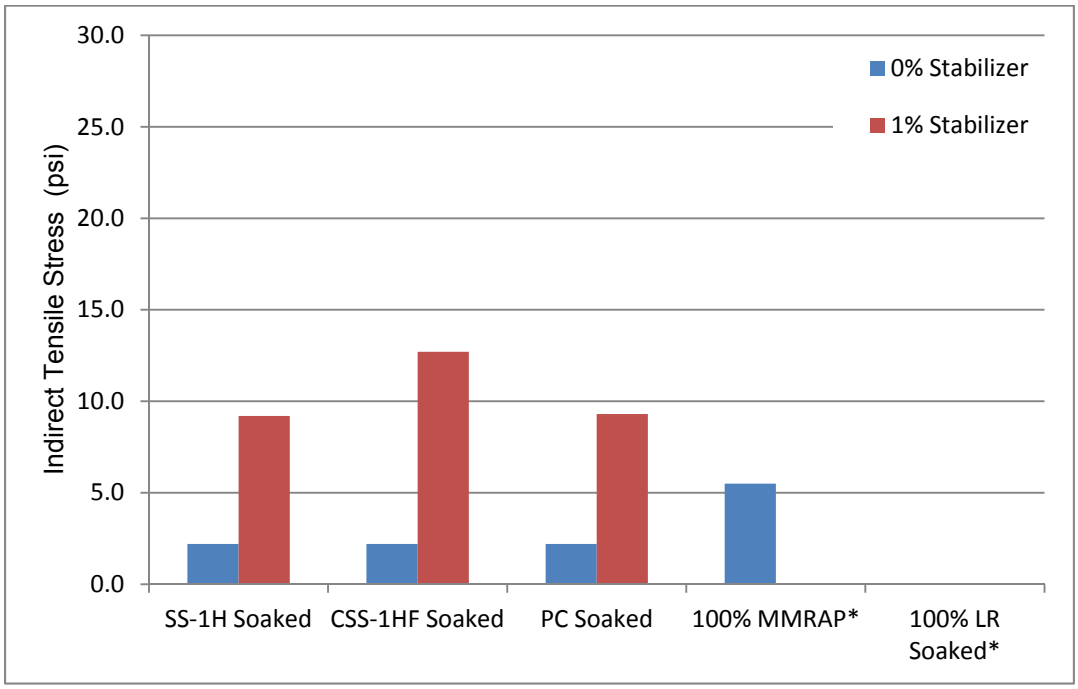

Figure 4-151: 50% RAP/50% Limerock Modified Proctor Compacted Specimens-- Soaked

4.6.7.2.2. IDT of Stabilized and Unstabilized Gyratory Specimens

Unsoaked unstabilized 50%/50% blends had and IDT strength 0.85 times that of the 100% MRAP control, and 34.2 times that of 100% limerock. Unstabilized, unsoaked 50% MRAP/50% LR modified Proctor specimens had an average IDT strength of 20.5 psi while stabilized specimens had an average IDT strength of 20.1 psi (Figure 4-152). This ratio of 0.98 stabilized to unstabilized strength was much lower than the results of the Marshall, unconfined compression and LBR test results. The CSS-1HF emulsion stabilized sample improved to nearly the same IDT strength as 100% RAP while the SS-1H emulsion and Portland cement stabilized specimens decreased slightly in IDT strength. This indicates that the gyratory compaction process itself is effective in creating tensile strength in materials containing RAP so the chemical stabilizing agent has an essentially neutral effect on unsoaked results.

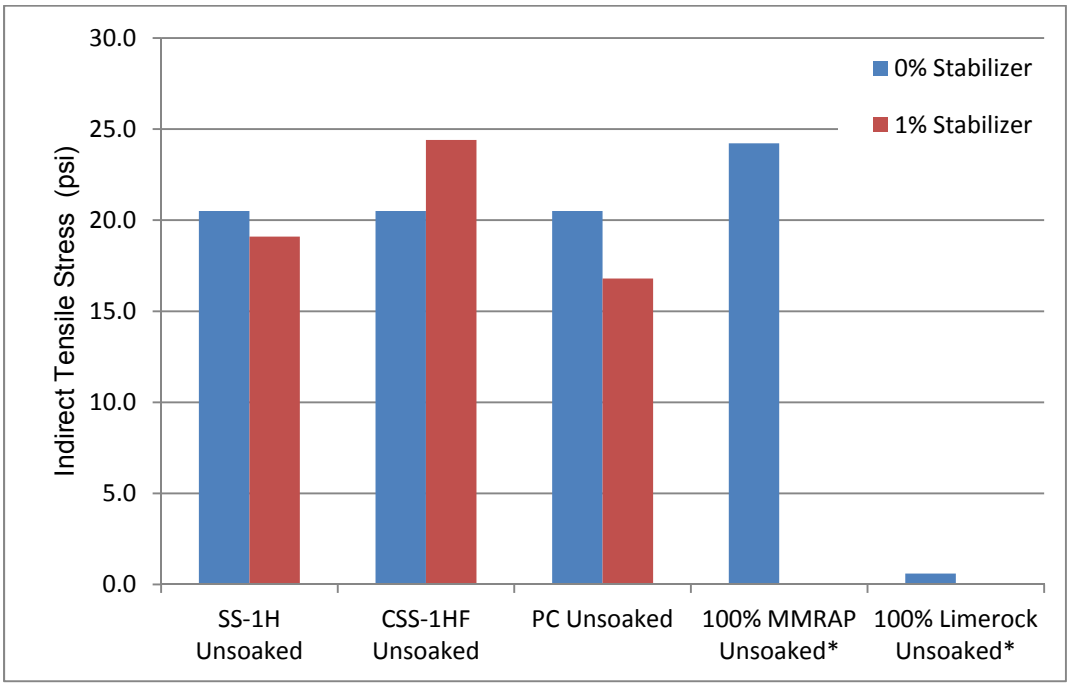

Figure 4-152: 50% RAP/50% Limerock Gyratory Compacted Specimens-- Unsoaked

While 1% stabilizer produced mixed results in IDT strength gains in unsoaked samples, 1% stabilizer produced dramatic gains in soaked 50%/50% blends. Unlike the unsoaked specimens, all of the stabilized specimens had a higher IDT strength than the 100% RAP control. CSS-1H had the highest relative strength of 16.0 psi - approximately double that of 100% RAP. Similar to the unsoaked specimens, soaked unstabilized 50%/50% blends had an IDT strength 0.52 times that of the 100% RAP control indicating that adding limerock to RAP decreases its soaked IDT strength. On the other hand, 50%/50% blends maintained some IDT strength while the 100% limerock disintegrated indicating that blending RAP with limerock greatly improves limerock's soaked IDT strength. Unstabilized soaked 50% MRAP/50% specimens had an average IDT strength of 4.1 psi while stabilized specimens had an average IDT strength of 12.2 psi (Figure 4-153). This ratio of 2.97 stabilized to unstabilized strength was much higher than the results of the Marshall, Unconfined Compression and LBR test results. Since soaked limerock disintegrated it is shown with a strength of zero.

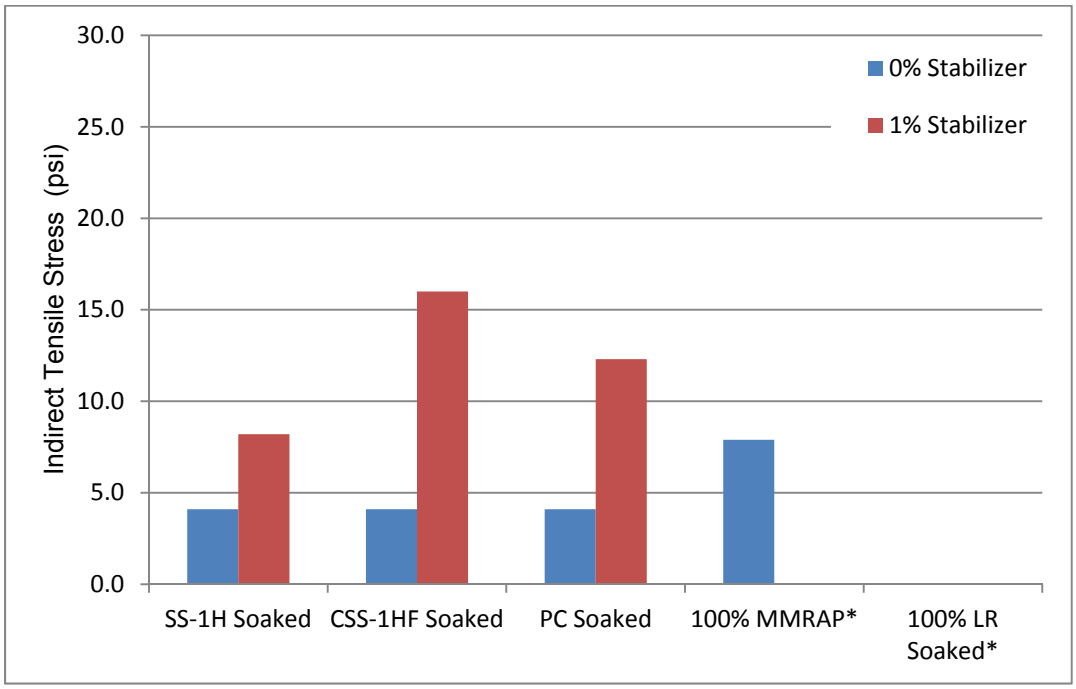

Figure 4-153: 50% RAP/50% Limerock Gyratory Compacted Specimens-- Soaked

4.6.7.3. Summary of IDT Strength Comparisons

Unsoaked unstabilized blends of 50% RAP/50% limerock had approximately 30 times the IDT tensile strength of 100% limerock for both modified Proctor and gyratory compaction. Unsoaked IDT strength relative to 100% RAP depended on the compaction method. Modified Proctor compacted blends averaged 1.3 times the IDT strength of 100% RAP. Gyratory compacted blends had averaged 0.85 times the IDT strength of 100% RAP.

Soaked unstabilized blends retained 78% of their dry strength for modified Proctor and 60.6% of their dry strength for gyratory specimens compared to zero strength for 100% limerock. Specimens of 100% RAP retained 59.6% of its dry strength for modified Proctor and 32.6% for Gyratory compaction. For both compaction methods 100% RAP had a higher soaked IDT strength than the 50%/50% blends.

Like the unstabilized blends, unsoaked stabilized blends also had approximately 30 times the IDT tensile strength of 100% limerock for both compaction methods. Unsoaked IDT strength was higher than 100% RAP for modified Proctor but lower for gyratory compacted specimens.

Soaked stabilized blends retained an average of 78% of their dry strength for modified Proctor and 60.6% of their dry strength for gyratory specimens compared to zero strength for 100% limerock. Specimens of 100% RAP retained 59.6% of their dry strength for modified Proctor and 32.6% for gyratory compaction. Reversing the results of unstabilized soaked samples, stabilized specimens produced by both compaction methods had a higher soaked IDT strength than the unstabilized 100% RAP control.

4.6.8. Correlations between Test Methods

In Section 4.6.1 and Section 4.6.2 strong correlations were noted for MRAP/aggregate blends between RAP content and CSR (positive correlation) and between RAP content and LBR (negative correlation). In this section strength and deformation results from each of the test methods used were analyzed to determine whether there were correlations between test results for each of the three principal stabilizing agents used.

4.6.8.1. Marshall Flow and Stability Correlation to Creep and LBR

Strong correlations were found between unsoaked Marshall stability and unsoaked LBR for MRAP/limerock blends with all three stabilizing agents (Figure 4-154). Portland cement blends showed the strongest correlation with an R^2 value of 0.90. LBR values above 417 and Marshall stabilities above 10,000 (unfilled triangles) are extrapolated. SS-1H blends showed almost as strong a correlation with an R^2 value of 0.84. CSS-1H showed the least strong correlations with an R^2 value of 0.58. All slopes were positive indicating that increasing Marshall stability indicated higher LBR values. The intercepts are the Marshall stability that would correspond to an LBR of zero. Soaked specimen results were not correlated because of the relatively few soaked LBR tests that were performed.

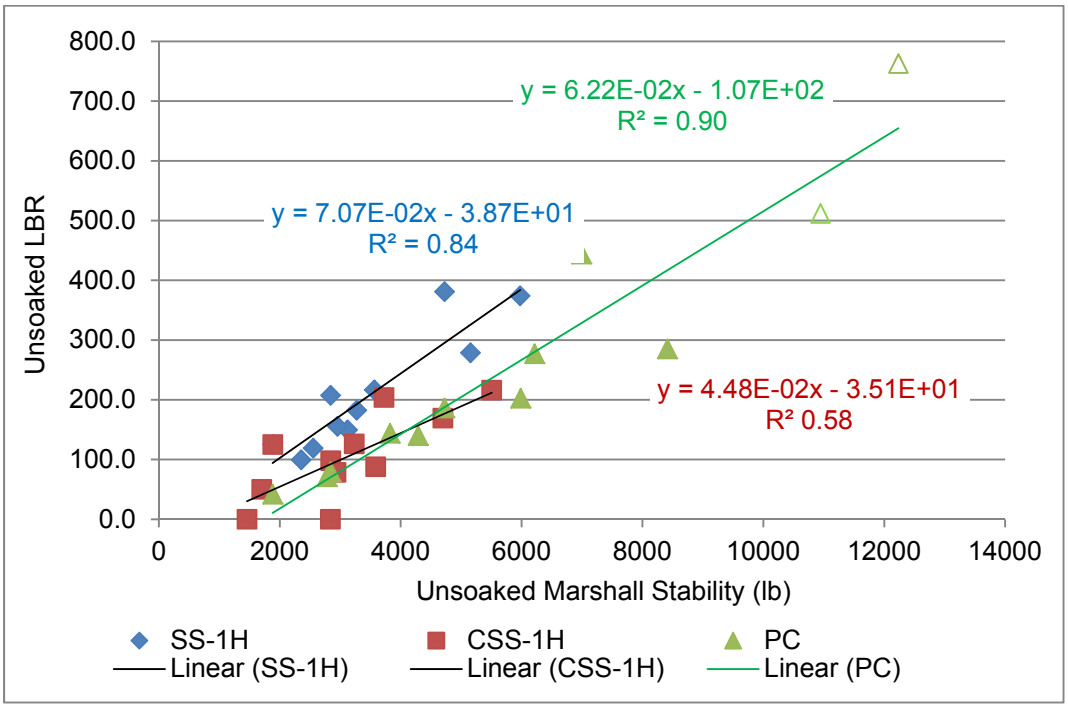

Figure 4-154: Unsoaked LBR - Unsoaked Marshall Stability Correlation

As shown in Figure 4-155, strong correlations were found between unsoaked Marshall flow and CSR for Portland cement (R^2 value of 0.56) and CSS-1H emulsion (R^2 value of 0.64). For both cement and CSS-1H the correlation slopes were positive indicating that increasing Marshall flow is associated with increase CSR. The intercept values indicate that zero flow would correspond to zero creep. SS-1H stabilized specimens showed no correlation to CSR (R^2 value of 0.00007). The slope of the SS-1H correlation curve was also nearly zero indicating no relationship between terms.

Based on these results the Marshall test is a good predictor of both LBR and CSR for stabilized blends of MRAP and limerock. The SS-1H flow/creep strain results indicate that more testing should be conducted with this type of emulsion.

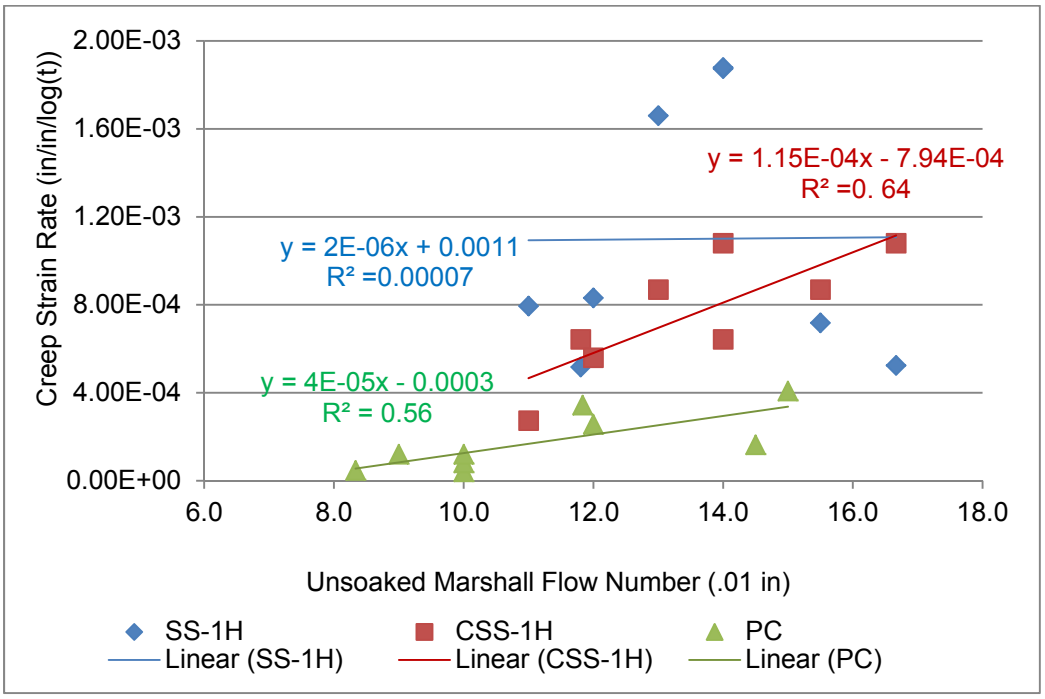

Figure 4-155 CSR - Unsoaked Marshall Flow Correlation

4.6.8.2. Unconfined Compression Peak Displacement and Strength Correlations to Creep and LBR

As shown in Figure 4-156, a strong correlation was found between unsoaked unconfined compression strength and unsoaked LBR for MRAP/limerock blends with cement stabilization (R^2 0.92). LBR values above 417 (unfilled triangles) are extrapolated. The slope was positive indicating that increasing unconfined compressive strength indicated higher LBR values. The intercepts are the unconfined compressive strength that would correspond to an LBR of zero. CSS-1H and SS-1H specimens showed essentially no correlation to LBR.

A strong positive correlation was found between unsoaked unconfined compression peak displacement and CSR for CSS-1H stabilized blends (R^2 0.78) (Figure 4-157). Weak positive correlations were found for the cement (R^2 0.16) and SS-1H (R^2 0.12) stabilized specimens. All of the slopes were positive and all of the intercepts were near zero indicating that a peak displacement of zero would correspond to zero creep.

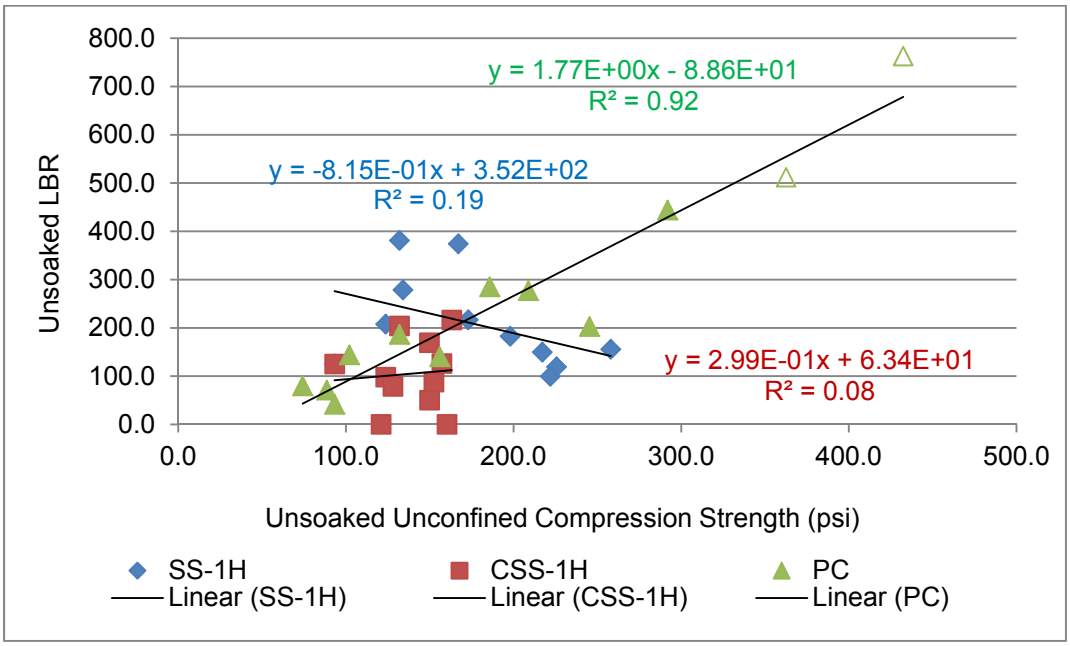

Figure 4-156: Unsoaked LBR - Unsoaked Unconfined Compression Correlation

Based on these results, unconfined compressive strength was not a good indicator of LBR except for the cement stabilized specimens. The unconfined compression test peak deformation was not an indicator of CSR except for the CSS-1H specimens.

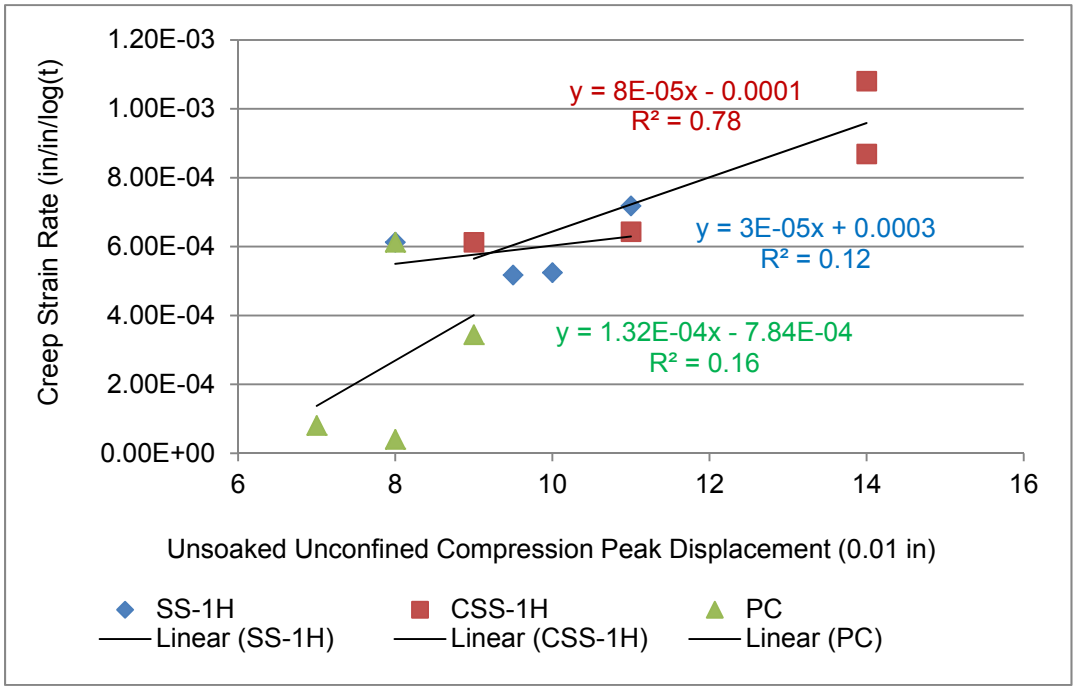

Figure 4-157: CSR - Unsoaked UCC Peak Displacement Correlation

4.6.8.3. IDT Peak Displacement and Strength Correlations to Creep and LBR

IDT's were only performed on a limited group of specimens so it was not possible to perform correlations for each stabilizing agent. IDT tests were performed on 100% MRAP, 100% limerock, and 50% MRAP/50% limerock without stabilizer. IDT tests were also performed on 50% MRAP/50% limerock blends with 1% CSS-1H, 1% SS-1H, and 1% cement. 100% limerock is shown in a separate data series in Figure 4-158 because it had the unusual properties of almost zero tensile strength coupled with very high unsoaked LBR strength. All of these trials were aggregated into a single data series in order to produce enough points for a regression. The aggregate group is denoted as "all other blends" in the figure. For all materials except 100% limerock there was a moderately strong positive correlation between indirect tensile strength and unsoaked LBR. The intercept value indicates that a material with a tensile strength of zero would have a negative LBR which may not have a physical significance in this case.

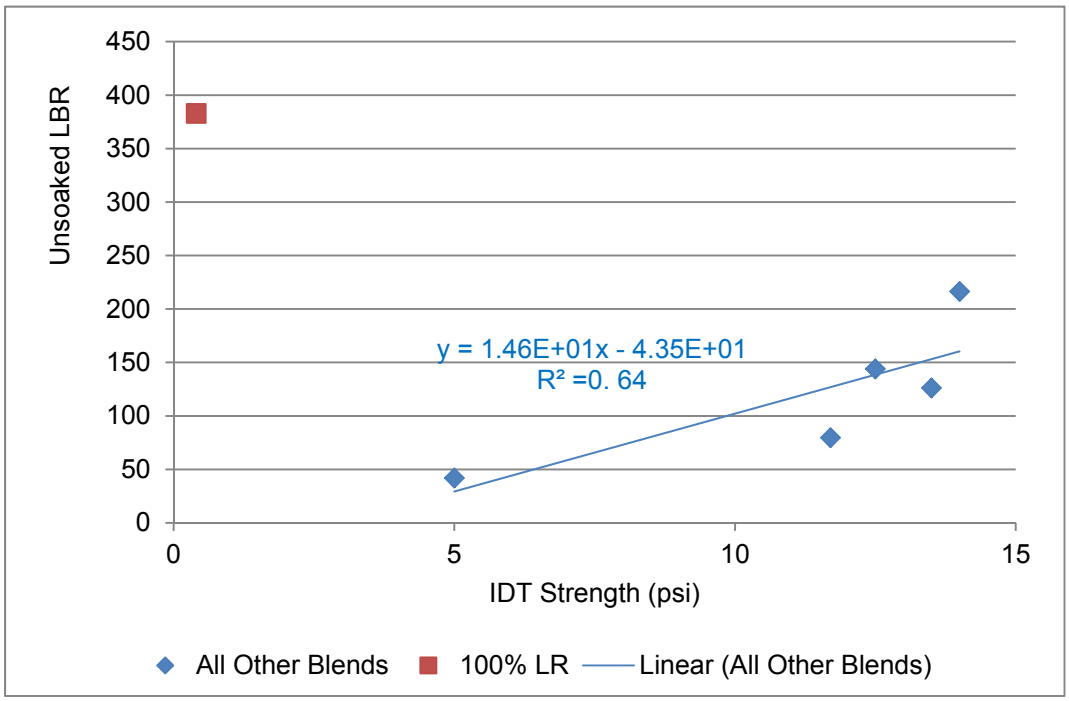

Figure 4-158: Unsoaked LBR - Unsoaked Indirect Tensile Strength Correlation

All data points including the 100% limerock were incorporated into the same series for the CSR versus IDT peak displacement correlation shown in Figure 4-159. There was a moderate positive correlation indicating that increasing IDT peak displacement correlated to increasing

CSR. The intercept value in this case is nearly zero indicating that a material with an IDT peak displacement of zero would have almost zero creep. Additional testing would be required to make any definitive conclusions about the usefulness of the IDT as an indicator of LBR or creep.

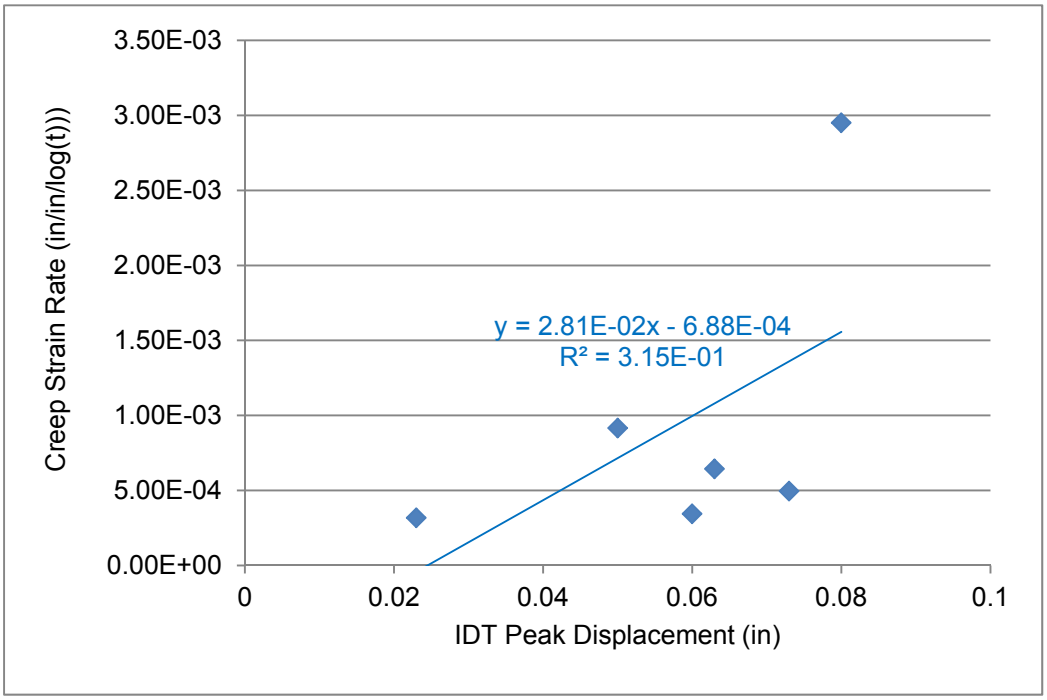

Figure 4-159: CSR - Unsoaked IDT Peak Displacement Correlation

4.7. Creep Models

In Section 4.6.2 the creep of different blends was compared using the CSR (CSR), the slope of the creep curve plotted against log(time). This method was used because it was simpler to calculate that traditional Singh and Mitchell (1968) creep models which require the determination of several parameters at varying deviator stress levels. This section compares Singh and Mitchell (1968) model predictions of creep settlement to the CSR method. Specimens of 100% RAP, 100% limerock, and 50% RAP/50% limerock without stabilizing agent and specimens of 50% RAP/50% limerock with 1% cement were tested at multiple stress levels to develop parameters to create the Singh and Mitchell (1968) models. Projected creep settlements by both models were calculated at the pressures indicated for a 10-inch base course thickness. As discussed earlier, acceptable creep was defined as settlement as less than 3.0% strain over 30 years.

As discussed in Chapter 2, Singh and Mitchell (1968) initially developed this model to represent creep in clay soils. Dikova (2006) found a good comparison between the Singh and Mitchell (1968) model and experimental results for RAP and RAP/A-3 sand blends. The model is an exponential function shown below in Equation 4-1 (previously shown in Equation 2-3). The parameters A, α, and m, were determined by performing two or more creep tests on identical specimens at different creep stress levels. Plotting the log strain rate versus log time defines m. Plotting the log strain rate versus stress for two separate times defines α (slope) and A (intercept). D is the deviator stress. For one dimensional oedometer tests D is taken as the applied stress; the confining stress of the container is assumed as zero.

$$\dot{\varepsilon} = Ae^{\alpha D}\left(\frac{t_1}{t}\right)^m \qquad \text{Equation 4-1}$$

4.7.1. Modeling 100% RAP Specimens

Dikova (2006) performed 100% RAP creep tests at 12 and 18 psi. These results were used to determine the parameters of the 100% RAP Singh and Mitchell (1968) model in the current study. Figure 4-160 shows the average experimental settlements observed during 7 day creep tests at both 12 psi and 18 psi. For each pressure the CSR based on a logarithmic curve fit to the experimental data from 0.01 days to 7 days is shown as a dashed line. The Singh and Mitchell model for each pressure is shown as a solid line with unfilled markers which correspond to the experimental curves which have filled markers. The 18 psi CSR and Singh and Mitchell predicted values are within 3% of the experimental observations (compared at 1, 2, 4, and 7 days). The 12 psi Singh and Mitchell (1968) model shows a +11% average variance from experimental values.

Figure 4-161 shows the 7-day experimental data and CSR and Singh and Mitchell (1968) projected creep settlement over the 30 year planning life for the pavement. At 12 psi the CSR predicted value is 12% lower than the Singh and Mitchell value. At 18 psi the CSR value is 10% lower than the Singh and Mitchell (1968) value. In all cases the predicted creep settlement exceeds the acceptable level of 0.3 inches which is 3.0% strain in a 10 inch base course.

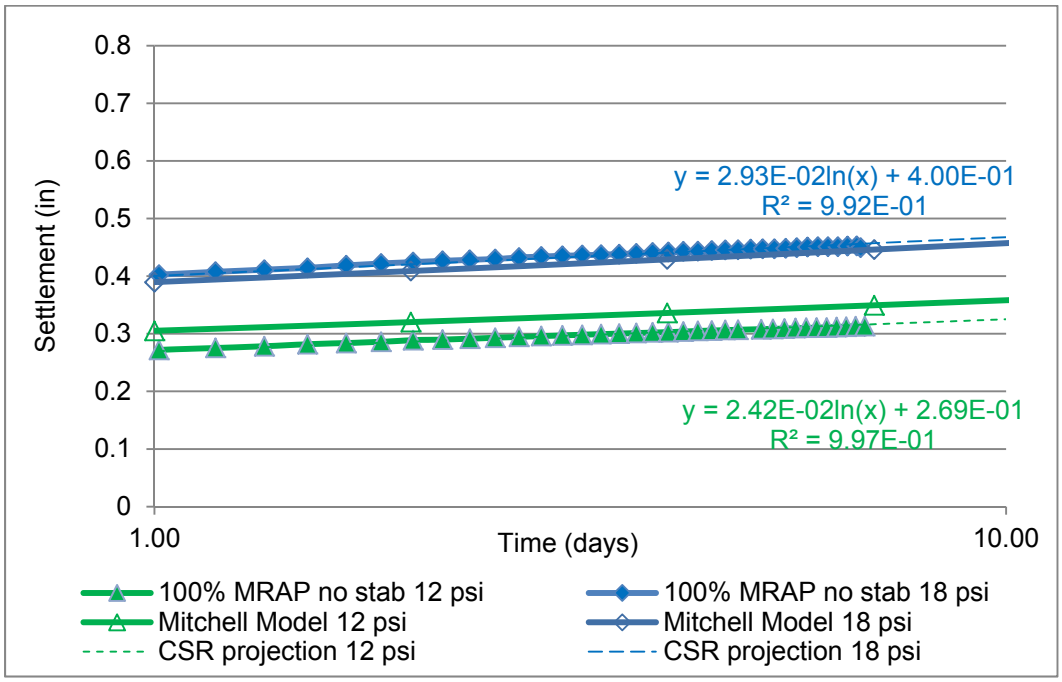

Figure 4-160: 7-day Experimental and Modeled Displacement for 100% MRAP (Dikova, 2006)

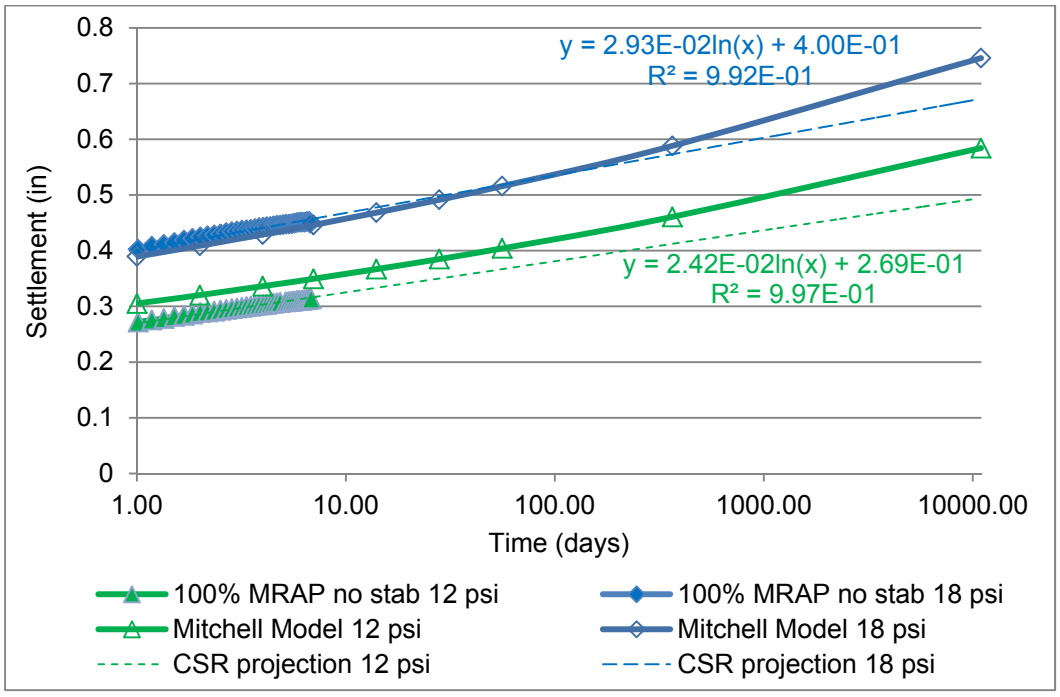

Figure 4-161: 30-year Projected Settlement for 100% MRAP

4.7.2. Modeling 100% Limerock Specimens

Specimens of 100% limerock were tested in this study at 12 and 25 psi to determine the parameters of the Singh and Mitchell (1968) model. Figure 4-162 shows the average experimental settlements observed during 7-day creep tests at both 12 psi and 25 psi. For each pressure the CSR based on a logarithmic curve fit to the experimental data from 0.01 days to 7 days is shown as a dashed line. The Singh and Mitchell (1968) model for each pressure is shown as a solid line with unfilled markers which again correspond to the solid markers on the experimental curves. The 25 psi CSR and Singh and Mitchell (1968) predicted values are within 10% of the experimental observations at 1, 2, 4, and 7 days. The 12 psi Singh and Mitchell (1968) model is within 1% of the experimental values for the same periods.

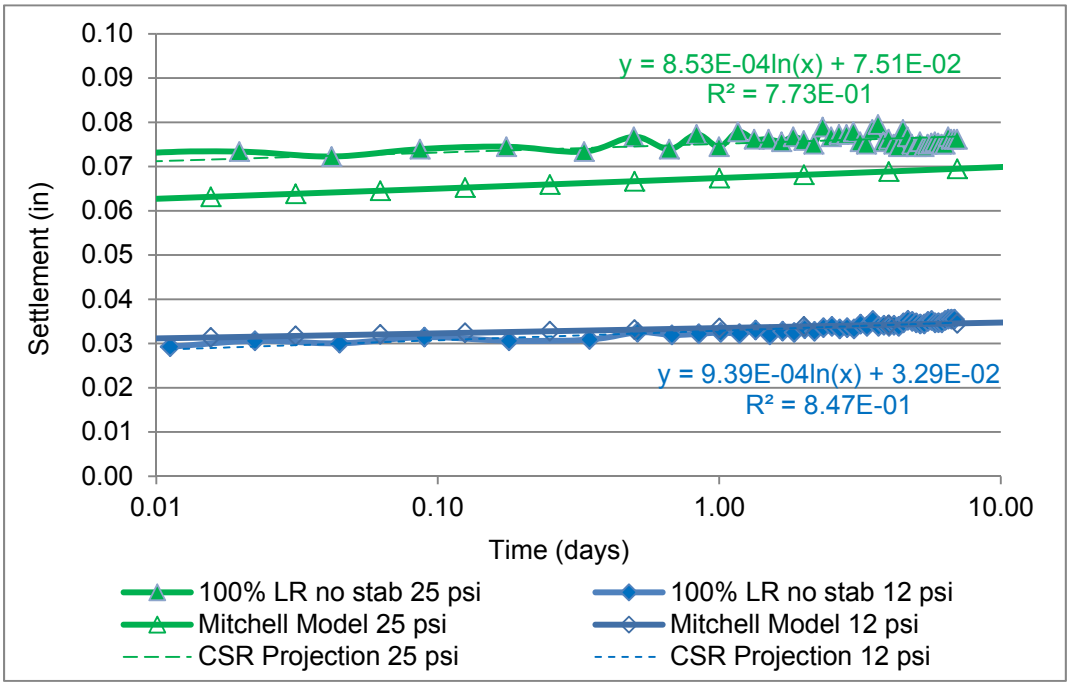

Figure 4-162: 7-day Experimental and Modeled Settlement for 100% Limerock

Figure 4-163 shows the 7-day experimental data and CSR and Singh and Mitchell (1968) projected creep settlement over the 30 year planning life for the pavement. At 12 psi the CSR predicted value is within 1% of the Singh and Mitchell (1968) value. At 25 psi the CSR value is 10% lower than the Singh and Mitchell (1968) value. In all cases the predicted creep settlement is well under the acceptable level of 0.3 inches or 3.0% strain in a 10 inch base course.

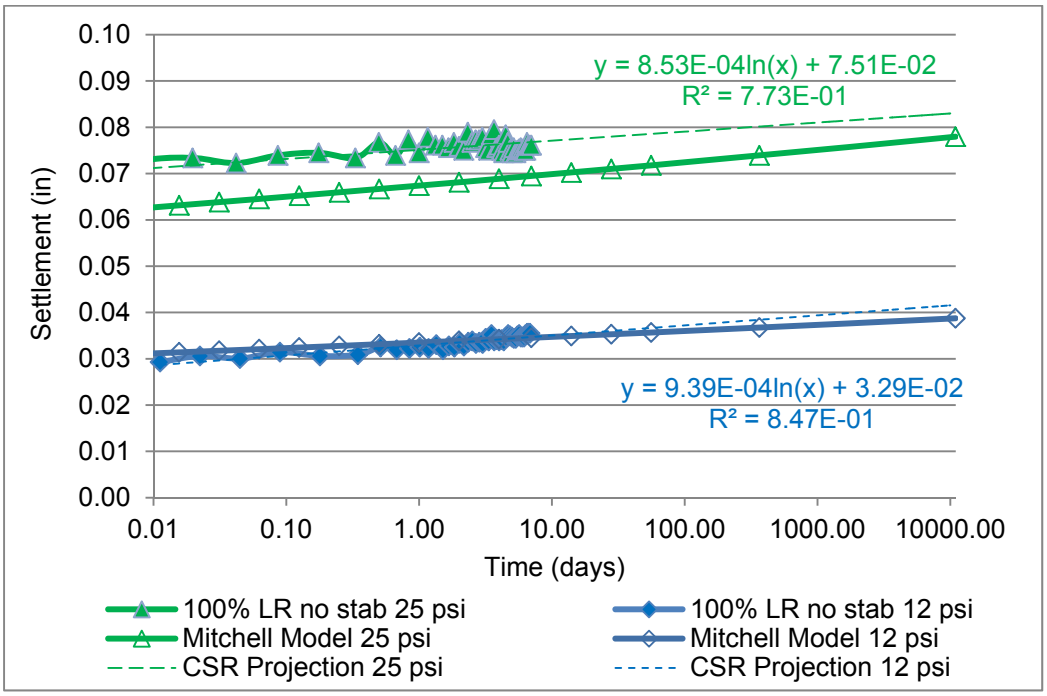

Figure 4-163: 30-year Settlement Projections for 100% Limerock

4.7.3. Modeling 50% MRAP/50% Limerock Specimens without Stabilization

50% limerock specimens were tested in this study at 12 and 25 psi to determine the parameters of the Singh and Mitchell (1968) model. Figure 4-164 shows the average experimental settlements observed during 7-day creep tests at 12 and 25 psi. For each pressure the CSR based on a logarithmic curve fit to the experimental data from 0.01 days to 7 days is shown as a dashed line. The Singh and Mitchell (1968) model for each pressure is shown as a solid line with unfilled markers which correspond to the filled markers on the experimental curves. The 25 psi CSR and Singh and Mitchell (1968) predicted values are within 10% of the experimental observations compared at 1, 2, 4, and 7 days. The 12 psi Singh and Mitchell (1968) model is within 1% of the experimental values for the same periods.

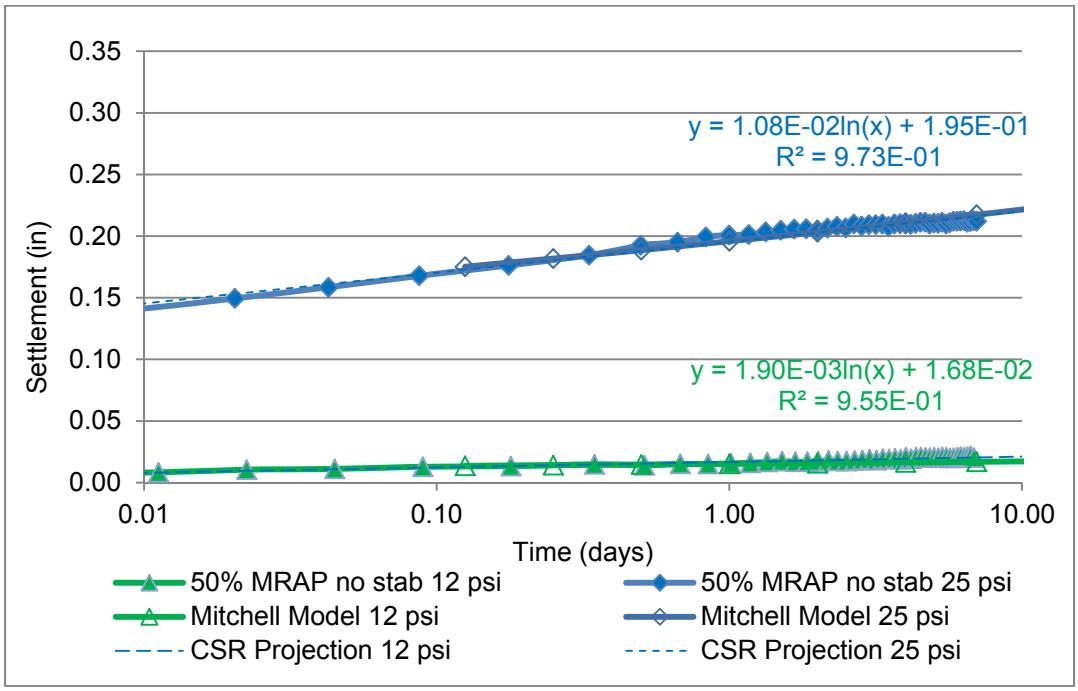

Figure 4-164: 7-day Experimental and Modeled Settlement for 50% MRAP/50% LR without Stabilizer

Figure 4-165 shows the 7-day experimental data and CSR and Singh and Mitchell (1968) projected creep settlement over the 30 year planning life for the pavement. At 12 psi the CSR predicted value is within 38% of the Singh and Mitchell (1968) value. The percent difference is misleading because the magnitudes of the projected settlements are very small, between 0.025 and 0.034 inches. At 25 psi the CSR value is 8% lower than the Singh and Mitchell (1968) value. The 12 psi predicted creep settlement is well under the acceptable level of 0.3 inches (3.0% strain in a 10 inch base course) but both 25 psi projections are close to 0.3 inches indicating that the 50% MRAP/50% limerock blend without stabilizer is marginally acceptable for projected creep.

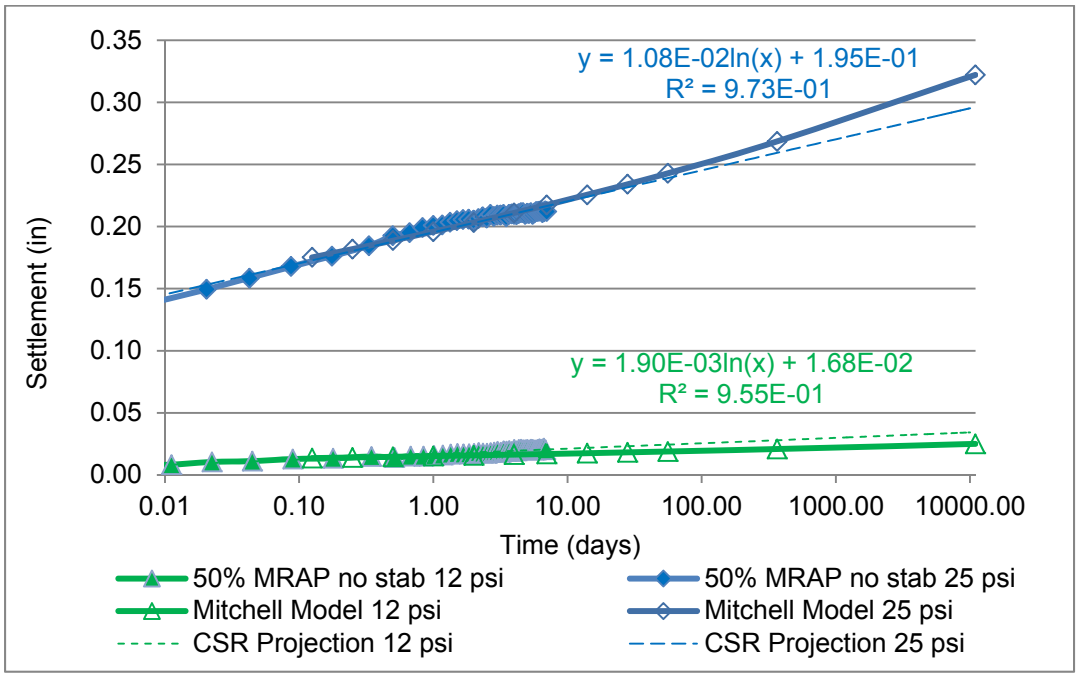

Figure 4-165: 30-year Settlement Projections for 50% MRAP/50% LR without Stabilizer

4.7.4. Modeling 50% MRAP/50% Limerock Specimens with Stabilization

50% MRAP/50% limerock specimens with 1% Portland cement stabilizing agent were tested in this study at 12 and 25 psi to set the parameters of the Singh and Mitchell (1968) model. Figure 4-166 shows the average experimental settlements observed during 7-day creep tests at 12 and 25 psi. For each pressure the CSR is shown as a dashed line. The Singh and Mitchell model for each pressure is shown as a solid line with unfilled markers corresponding to the filled markers on the experimental curves. Both the 12 psi and 25 psi CSR and Singh and Mitchell predicted values are within 4% of the experimental observations compared at 1, 2, 4, and 7 days. There is an anomaly with these results in that the 12 psi specimens had a higher average total settlement than the 25 psi specimens. This is attributed to initial seating in the apparatus. The 25 psi specimens had a higher CSR slope but the difference is very small (0.00173 versus 0.00171).

Figure 4-167 shows the 7-day experimental data and 30-year CSR and Singh and Mitchell (1968) projected creep settlement. At 12 psi the CSR predicted value is within 1% of the Singh and Mitchell (1968) value. At 25 psi the CSR value is 4% higher than the Singh and Mitchell (1968) value. Both the 12 psi and 25 psi predicted creep settlements are well under the acceptable level of 0.3 inches (3.0% strain in a 10 inch base course).

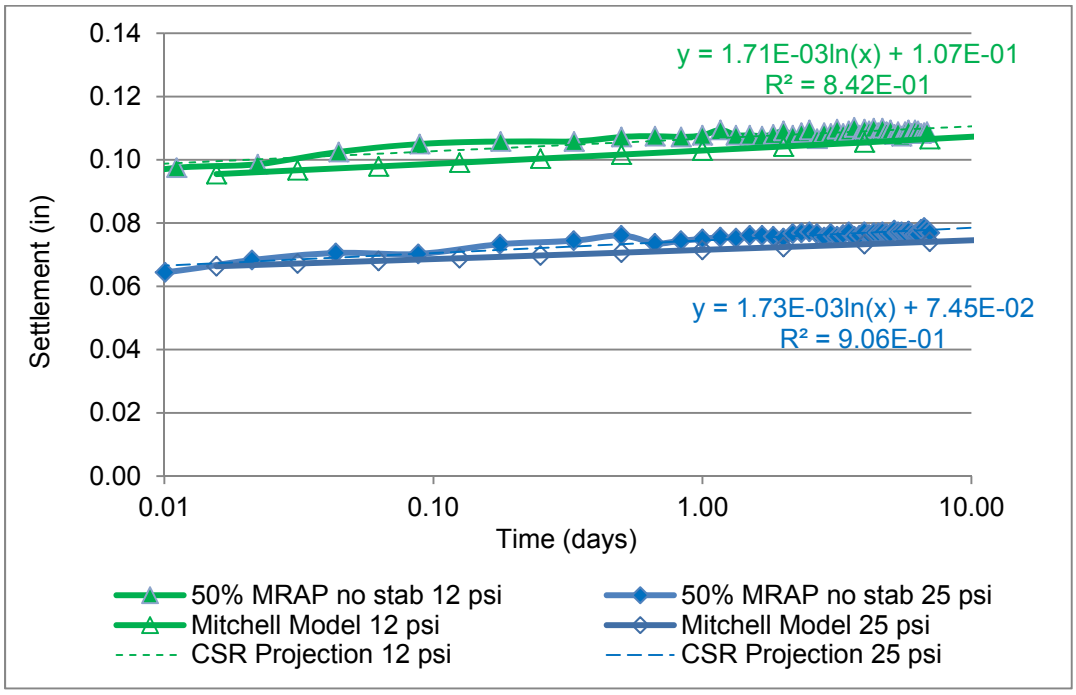

Figure 4-166: 7-day Experimental and Modeled Settlement for 50% MRAP/ 50% LR 1% Cement

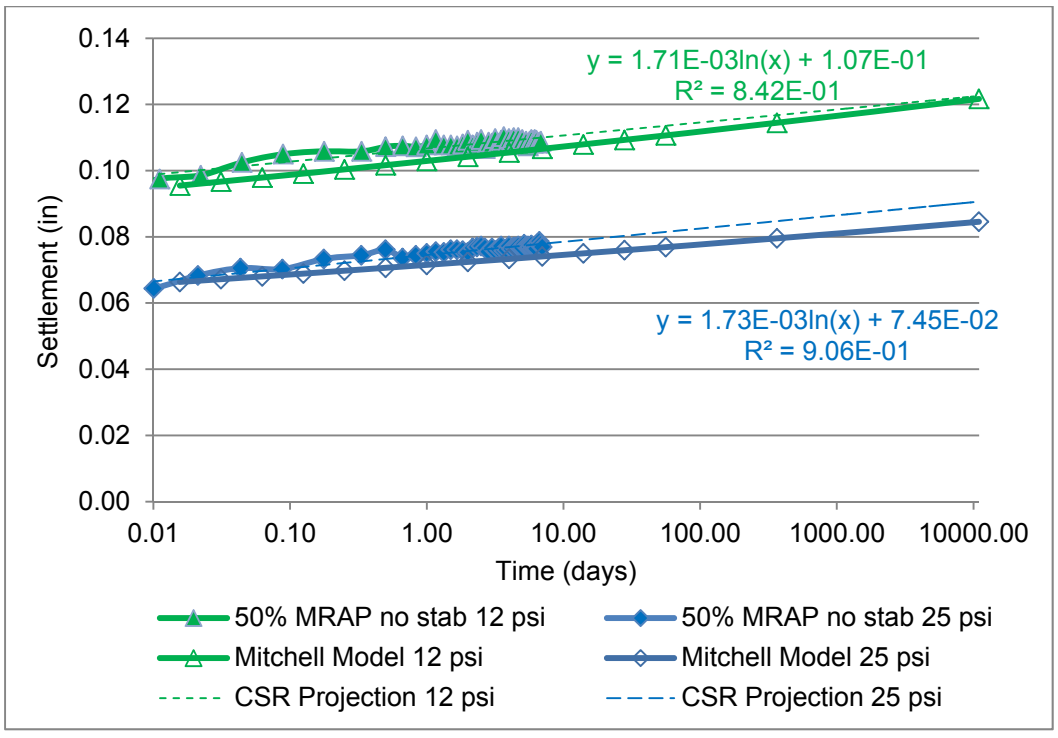

Figure 4-167: 30-year Settlement Projections for 50% MRAP/50% LR 1% Cement

50% MRAP/50% limerock specimens with either 1% SS-1H or 1% CSS-1H asphalt emulsion stabilizing agent were tested at 12 psi. As shown in the previous sections, the CSR projection agreed very closely with the Singh and Mitchell (1968) models. Only the CSR projection was used to predict 30-year creep for the two emulsion stabilized blends. Figure 4-168 shows the 7-day experimental data and CSR projected creep settlement over the 30 year planning life for the pavement. The 12 psi predicted creep settlements for both emulsions are well under the acceptable level of 0.3 inches (3.0% strain in a 10 inch base course). No 25 psi creep tests were conducted with these blends. For comparison purposes, 25 psi creep settlement for these blends was estimated by multiplying the 12 psi settlement projections by the ratio of pressures (25 psi/12psi). Based on the differences observed between other 12 psi and 25 psi creep settlement results this linear extrapolation should overstate the 25 psi settlement and thus be a conservative estimate.

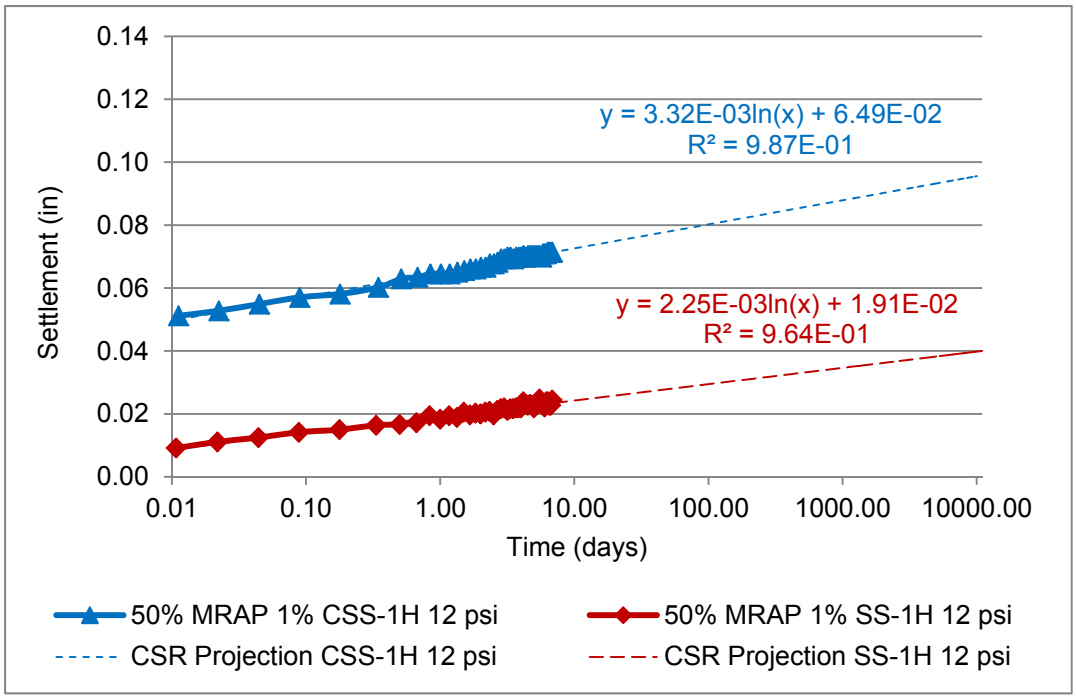

Figure 4-168: 30-year Settlement Projections for 50% MRAP/50% LR 1% Emulsion

4.7.5. Modeling 25% MRAP/75% Limerock Specimens without Stabilization

Specimens of 25% MRAP/75% limerock without stabilizing agent were tested at 12 and 25 psi. Like the emulsion stabilized 50% MRAP/50% limerock specimens, only the CSR

projection was used to predict future creep settlement. For each pressure the experimental data is shown as a solid line and the CSR logarithmic curve fit is shown as a dashed line (Figure 4-169). At both 12 and 25 psi the CSR projected 30-year settlement is well under the acceptable level of 0.3 inches or 3.0% strain in a 10 inch base course.

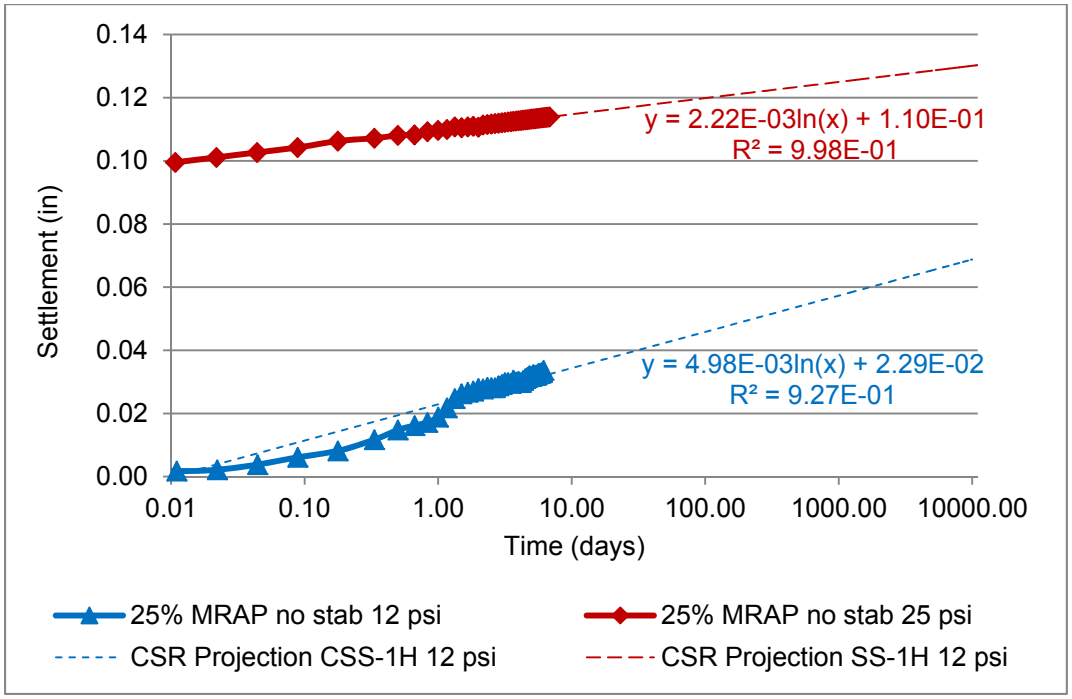

Figure 4-169: 30-year Settlement Projections for 25% MRAP/75% Limerock

4.7.6. Summary of Creep Models

Figure 4-170 shows a comparative summary of the 30-year creep settlement projections for all of the models discussed above. The Singh and Mitchell (1968) models agreed well with experimentally observed 7-day creep settlements. The CSR method of fitting a logarithmic trend line to creep test data between 0.01 days and 7 days produced 30 year creep settlement projections that were generally within 10% of the Singh and Mitchell (1968) model projections. The acceptable 0.3 inch (3.0% strain in a 10 inch base layer) 30-year creep settlement level is shown as a heavy horizontal line on the figure for reference.

The 100% MRAP specimens had projected creep settlements approximately double the acceptable 0.3 inch level. The 50% MRAP/50% limerock blends without stabilizer had less than 50% of the projected creep of 100% RAP at 25 psi and less than 10% of the creep of 100% RAP

at 12 psi. Based on the 25 psi results, the 50%/50% blend had marginally acceptable projected 30-year creep levels of 0.3 inches (3.0% strain). Adding 1% cement or 1% of either SS-1H or CSS-1H asphalt emulsion stabilizer to the 50%/50% blend reduced projected 30-year creep well below the acceptable 0.3 inches. The 25% MRAP/75% limerock blends with no stabilizing agent also had projected 30-year creep settlements well below the acceptable 0.3 inch level at both 12 and 25 psi.

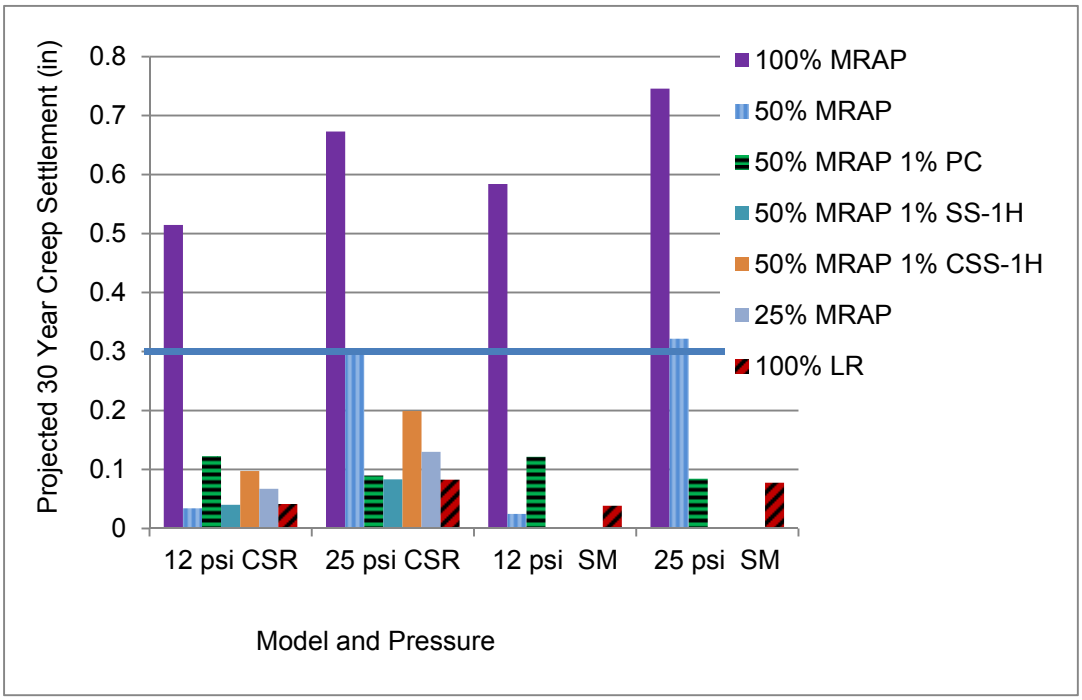

Figure 4-170: 30-year Projected Creep Settlement Model Summary

5. Discussion and Conclusions

The overall project objective of developing engineering methods that improve density and bearing ratios while reducing creep were achieved most consistently by blending RAP with 50% or more virgin aggregate and stabilizing the blends with cement or asphalt emulsions. 50% RAP/50% limerock blends stabilized with 1% cement, SS-1H emulsion, or CSS-1H emulsion all achieved a soaked LBR of at least 100. Blends of 25% RAP/75% limerock with no chemical stabilizer achieved an average soaked LBR of 99.

All blends containing RAP showed some amount of creep. Some creep is acceptable if the base does not enter the tertiary creep stage which would lead to rupture and if the total deformations do not detract from the serviceability of the roadway, by decreasing the long-term pavement performance and necessitating premature pavement rehabilitation. In Section 4.6.5 unconfined specimens entered tertiary creep at approximately 0.4% axial strain. As was discussed in Section 4.2.2.1 Viyanant et al., (2007) found that low confining stress triaxial specimens failed at 3.0% or higher axial strain. Based on these results it is conservative to define acceptable creep as less than 3.0% axial strain in the base layer over a 30 year design life. For a typical 10 inch thick base layer, this would correspond to 0.3 inches. By this definition, all of the blends with 50% or less RAP with or without chemical stabilizer have acceptable projected creep. Adding 1% cement stabilizing agent virtually eliminated creep in these same blends. Adding 1% asphalt emulsion produced acceptable creep deformations and large improvements in retained soaked strength.

5.1. Gradation Modification of 100% RAP

This task focused on RAP gradation modifications or fractionating to determine if splitting or properly blending RAP fractions could produce improvements in strength and/or creep. Samples were first subjected to creep pressures of 12 psi and then unsoaked LBR tests. The results indicate that neither LBR nor creep improved unless RAP was fractioned then blended using the optimum gradation blend. Fractionating also adds processing steps that may not be practical for contractors.

Lower CSR's and higher LBR values were correlated with the proximity of the gradation curve and the FHWA or Talbot maximum density curve at the #30 and #50 sieves. These results are similar to Gomez's (2003) findings that the density and LBR of RAP improved with the addition of material passing the #40 sieve. However, they do not improve to the point where they would meet both LBR and creep requirements.

5.1.1. Asphalt Content of RAP Fractions

Based on results of asphalt content tests on APAC Melbourne milled and crushed RAP fractions at the #4, #8, #40 and #200 sieves, there are larger variations in asphalt content of milled (2.2% to 12.9%) than crushed RAP (5.1% to 7.2%). The milled RAP results showed the largest percent asphalt for the portion passing the number 200 sieve.

5.1.2. Specific Gravity of RAP Fractions

No trends were apparent for the specific gravity of fractions of milled and crushed APAC RAP. Specific gravity values ranged from 2.49 to 2.56 for milled and 2.50 to 2.56 for crushed materials.

5.1.3. Post-Creep Unsoaked LBR of RAP Fractions

Gradation improvements by fractionating alone did not produce an adequate post-creep unsoaked LBR. All but one of the +/- #4, #8, and #200 sieve fractions produced LBR's from fractions lower than LBR values from the unfractionated RAP (only the plus # 8 fraction from APAC Melbourne milled RAP produced a slightly higher LBR than unfractionated RAP).

The unsoaked post-creep LBR of the fractions ranged from approximately 10 to 40. Re-blending RAP with gradations composed of the theoretical maximum density using the 0.45 power data improved the strength of RAP approximately 30 to 120%, however all of these unsoaked LBR's were still below 100.

5.1.4. Creep of Fractionated RAP

The CSR, which was used to evaluate the test results, indicates that re-blending RAP to match the maximum density gradation based on the Talbot curve decreased the CSR nearly 17%

when compared to 100% RAP. The CSR for various fractions increased between 15% and 85% over that for 100% RAP. All of the observed CSR's would result in an unacceptable creep of more than 3.0% strain over a 30 year roadway design life

5.1.5. Parametric Correlations for Fractionated RAP

Extremely weak linear correlations were observed between asphalt content and LBR of fractions. The trendlines were all nearly flat, which imply that there were no major variations in LBR related to the variation in asphalt content.

Inconsistent and extremely weak linear correlations were observed between asphalt content and CSR. The slopes obtained from seven plots varied between positive (i.e., CSR increased with increasing asphalt content) to negative (i.e., CSR decreasing with increasing asphalt content). No consistent conclusion can be drawn concerning the relationship between asphalt content and CSR of RAP fractions. Consistent linear correlations were observed between density and LBR, with increases in density producing increases in LBR.

A linear correlation was observed between CSR and LBR which indicated that higher LBR values produce lower CSR's. Although the correlation was relatively weak, the trendline equations suggest that as the LBR decreases from 60 to 10 the CSR increases by a factor of 4.

5.2. Blending with High Quality Materials

Blending RAP with high quality base materials increased LBR strength and decreased creep. The strength gains from blending milled RAP with all three high quality base materials were similar.

Blends with 25% virgin aggregate had unsoaked LBR's far below 100. These blends exhibited creep deformation and CSR's that were similar to 100% RAP.

Blends with 50% RAP also had LBR's below 100, but the 30 year projected creep deformation was below 3% for a majority of these blends.

LBR's were close to 100 for some blends with 25% RAP. Blends with 25% RAP/75% virgin aggregate exhibited creep behavior similar to 100% aggregate. Creep for the high aggregate blends were reduced by 70% to 90% compared to 100% RAP specimens. For the high quality aggregates tested, RAP blends without stabilizing agents should be limited to a maximum of 25% RAP.

5.2.1. RAP/Limerock Blends

Blends of 50% RAP/50% limerock produced a soaked LBR of 55. This does not meet the required 100 LBR for base course but does meet the required 40 LBR for stabilized subbase. FM 5-515 subbase LBR tests are performed with a surcharge weight so the subbase LBR value of this blend would be higher than the soaked LBR's without surcharge determined in this study.

Projected creep of a 10 inch base course layer of 50% RAP/50% limerock would be 0**.**15 inches over a 30 year design life at a constant pressure of 25 psi. This would be an acceptable amount of creep deformation since it is less than 3.0% strain or 0.3 inches.

Blends of 25% RAP/75% limerock achieved a soaked LBR strength of 99. Final acceptance of this process would need to be made on a source-by-source basis to ensure that the final product meets the required 100 LBR for base course installations.

Projected creep of a 10 inch base course layer of 25% RAP/75% limerock would be 0**.**12 inches over a 30 year design life at a constant pressure of 25 psi. This would be an acceptable amount of creep deformation since it is less than 3.0% strain or 0.3 inches.

5.2.2. Cemented Coquina/RAP Blends

Blends of 50% RAP/50% cemented coquina produced an unsoaked LBR below 80 so soaked LBR tests were not performed. This blend does not meet the required 100 LBR for base course but may meet the requirements for subbases.

Projected creep of a 10 inch base course layer of 50% RAP/50% cemented coquina would be 0**.**17 inches over a 30 year design life at a constant pressure of 25 psi. This would be an acceptable amount of creep deformation since it is less than 3.0% strain or 0.3 inches.

Blends of 25% RAP/75% cemented coquina achieved a soaked LBR strength of 94, which does not meet the required 100 LBR for base course but should meet the subbase course requirement.

Projected creep of a 10 inch base course layer of 25% RAP/75% cemented coquina would be 0.08 inches over a 30 year design life at a constant pressure of 25 psi. This would be an acceptable amount of creep deformation since it is less than 3.0% strain or 0.3 inches.

5.2.3. Crushed Concrete/RAP Blends

Blends of 50% RAP/50% RCA produced an unsoaked LBR of 48 so soaked LBR testing was not performed. Blends with crushed concrete would have to be evaluated to determine whether they would meet the required 40 LBR for stabilized subgrades.

Projected creep of a 10 inch base course layer of 50% RAP/50% RCA would be 0. 13 inches over a 30 year design life at a constant pressure of 25 psi. This would be an acceptable amount of creep deformation since it is less than 3.0% strain or 0.3 inches.

Blends of 25% RAP/75% RCA achieved an unsoaked LBR strength of 76 so soaked LBR testing was not performed. This blend does not meet the required 100 LBR for base course but may meet the subbase LBR requirement.

Projected creep of a 10 inch base course layer of 25% RAP/75% RCA would be 0. 08 inches over a 30 year design life at a constant pressure of 25 psi. This would be an acceptable amount of creep deformation since it is less than 3.0% strain or 0.3 inches.

5.3. Asphalt Content Modifications

In general, it is not practical to obtain RAP samples with varying asphalt contents for LBR and creep testing. To evaluate the effects of asphalt content on these parameters, the quantity of virgin aggregate was adjusted so that the asphalt content of the RAP/Aggregate blend could be evaluated.

5.3.1. Effect of Asphalt Content on LBR

For fractionated RAP from different sources, variations in asphalt content between about 3% and 6% did not correlate to post-creep unsoaked LBR strength.

For blends of RAP with high quality aggregates, decreasing asphalt content of the blend correlated to as increase in LBR. For asphalt contents near 3% an increase in variability occurred.

Blending of RAP/Limerock, RAP and limerock, with 1% asphalt emulsion by weight (approximately 0.5% asphalt binder) increased LBR. Adding 2% - 3% asphalt emulsion (approximately 1.0% - 1.5% asphalt binder) decreased LBR strength from the peak observed at 1% emulsion. The higher levels of asphalt emulsion resulted in higher retained strength for soaked specimens compared to dry specimens. This same pattern was observed in unconfined compression, Marshall compression, and indirect tensile testing.

5.3.2. Effect of Asphalt Content on Creep

For fractionated RAP from different sources, asphalt content did not correlate to creep. For blends of RAP and high quality aggregates, with overall asphalt contents less than or equal to 3 %, the post-creep unsoaked LBR for both cemented coquina and limerock outperformed the RCAs. For asphalt contents greater than or equal to 3 % significant increase in creep occurred, producing unacceptable 30-year creep deformations (i.e. larger than 0.3-inches).

Chemical stabilization of RAP, blends of RAP/Limerock, and limerock, with 1% asphalt emulsion by weight (approximately 0.5% asphalt binder) decreased total creep deformation and decreased CSR. Adding 2% to 3% asphalt emulsion (approximately 1.0% to 1.5% asphalt binder) increased total creep deformation and CSR. Creep tests were only conducted with unsoaked specimens so no conclusions can be made concerning the effect on creep of saturated soils.

5.4. Vibratory, Proctor, and Gyratory Compaction of 100% RAP

Vibratory compaction did not work well with the RAP samples tested. Vibratory compaction consistently produced lower densities and lower strengths than either modified Proctor or gyratory compaction.

Modified Proctor compaction produced higher densities and LBR values than vibratory compaction, but produced lower densities and LBR strength than gyratory compaction. Modified Proctor compaction also produced lower LBR values than gyratory compaction at the same density.

Gyratory compaction of RAP produced much higher strengths than the modified Proctor or vibratory compaction methods. In general, based on the linear correlations developed, the LBR increased 3 to 4 times at the same density for samples compacted using gyratory compaction compared to samples compacted with modified Proctor compaction. Blended specimens, of 50% RAP/50% limerock, showed pronounced but smaller strength increases. No significant LBR differences were observed between modified Proctor and gyratory compacted specimens of limerock, cemented coquina or clayey sand. It was concluded that the constant pressure and kneading action of the gyratory compaction method reestablished some of the adhesion in the asphalt binder.

5.4.1. Limerock Bearing Ratio of 100% RAP

Modified Proctor compaction of 100% RAP yielded unsoaked LBR values less than 40. Gyratory compaction at 75 gyrations consistently produced unsoaked LBR values greater than 40. Compacting RAP with 150 gyrations yielded unsoaked LBR values of 100 or greater.

5.4.2. Unconfined Compressive Strength of 100% RAP

RAP compacted using Gyratory compaction achieved 3 to 4 times the modified unconfined compression Strength than RAP compacted by the modified Proctor method at similar densities.

5.4.3. Indirect Tensile Strength of 100% RAP

Gyratory compacted samples yielded 3 to 4 times the indirect tensile splitting strength compared to modified Proctor compacted samples at similar densities.

5.4.4. Creep of RAP and RAP Blends

Gyratory compacted specimens of RAP and RAP/aggregate blends showed less creep compared to modified Proctor compacted specimens at the same density; however, the difference in CSR was not as pronounced as the differences in strength previously noted.

5.5. Improvements through Chemical Additives

Adding asphalt emulsion or Portland cement chemical stabilizing agents improved 100% RAP to a soaked LBR of 40 but did not improve it to 100. At low concentrations asphalt emulsion reduced CSR's but at higher concentrations CSR's increased. Portland cement significantly reduced CSR at all concentrations. Adding hydrated lime as a stabilizing agent did not have a significant effect on either strength or creep for the RAP/limerock aggregates tested.

The combination of blending 50% RAP/50% limerock aggregate and chemically stabilizing with asphalt emulsion or with Portland cement resulted in soaked LBR strengths exceeding 100. Chemically stabilized blends also had better retained strength after soaking. Adding hydrated lime as a stabilizing agent did not have a significant effect on either strength or creep for the RAP/limerock aggregates tested.

5.5.1. Anionic (SS-1H) and Cationic (CSS-1H) Asphalt Emulsion

Anionic and cationic emulsion gave similar improvements in the strength of RAP and RAP/aggregate blends. Emulsions from two different suppliers were used in this study. Both types of emulsion showed a peak LBR improvement at a concentration of 1% to 2% with a slight decline as emulsion content increased. Lower concentrations of emulsion improved creep performance of the RAP or RAP/aggregate blend but CSR increased with higher emulsion content. Emulsion formulations are proprietary so it is not possible to draw general conclusions about whether an anionic (SS-1H) or cationic (CSS-1H) emulsion will give better results for a given RAP/aggregate blend.

5.5.2. Portland Cement

Portland cement produced better soaked LBR strengths and reduced creep deformations compared to either asphalt emulsion. Unlike the emulsions, the effect of 1%, 2%, and 3% Portland cement was essentially a linear increase in LBR. CSR was significantly reduced with the addition of 1% Portland cement. Addition of 2% or 3% Portland cement nearly eliminated creep deformation in the RAP/ limerock aggregate blends tested. However, there is still an engineering concern that this product might be too brittle, resulting in excessive shrinkage cracking and consequently reflective cracking of overlying HMA.

5.5.3. Test Method Correlations to LBR and Creep

The modified Marshall method was the best indicator of both LBR and creep potential in the chemically stabilized blends. Marshall stability (strength) was strongly correlated to LBR strength for all three chemical stabilizing agents tested. Marshall flow (displacement at peak strength) was strongly correlated to CSR for both cement and CSS-1H stabilized specimens but not for SS-1H specimens. Because of their smaller size, Marshall specimens require less material than LBR or creep specimens and are easier to cure.

Unsoaked unconfined compression strength showed a strong positive correlation to unsoaked LBR strength for cement, but no or weak correlations for the SS-1H and CSS-1H emulsion. Unsoaked unconfined compression peak displacement showed a strong positive correlation to CSR for CSS-1H but weak correlations for cement and SS-1H. Based on these results, the unconfined compression test does not give a consistently good indication of LBR or creep of RAP/limerock blends.

Unsoaked indirect tensile strength showed a strong positive correlation to unsoaked LBR strength for all stabilizing agents. Unsoaked IDT peak displacement showed a moderate positive correlation to CSR for all stabilizing agents. Based on these results, the IDT generally gives a good indication of LBR and a moderate indication of creep of RAP/limerock blends.

6. Recommendations

6.1. Compaction

Based on the increased strengths obtained from gyratory compaction of RAP, additional evaluations should be performed either in a laboratory or field environment. The focus of these evaluations would be to determine how the strength increases observed in the laboratory would relate to actual construction processes and in-place conditions (see Section 6.8).

6.2. Blending with High Quality Aggregates

It is recommended that milled RAP be blended with limerock at a maximum of 25% MRAP to 75% limerock by weight. Soaked LBR testing should be performed on the actual RAP and limerock used. If a 25% MRAP/ 75% cemented Coquina is requested by contractors careful evaluation of soaked LBR results must be included. MRAP/RCA blends are not recommended.

6.3. Gradation Modification

Re-blending or fractionating 100% RAP is not recommended as a method to produce base or subbase material.

6.4. Asphalt Content

The current FDOT RAP specification Section 283 should be changed to eliminate the minimum asphalt content requirement. The change should include wording that specifies a maximum asphalt content of 3 % for non-traffic base applications. For traffic base applications it should also include the requirement to blend RAP with select aggregate material, plus add the option to chemically stabilize RAP blends. Proposed wording for the specification is presented in the following three sections.

6.4.1. RAP Aggregate Blends used in traffic base applications

Unstabilized RAP material must be blended with a minimum of 75% approved base course aggregate material such that the LBR of the blended material meets the LBR strength requirement of Section 911-6. Alternatively, blends may be proportioned such that the asphalt binder content of the total blend does not exceed 1.5% by weight.

6.4.2. RAP aggregate blends stabilized with asphalt emulsion used in traffic base applications

Asphalt emulsion stabilized RAP/aggregate blends must include a minimum of 50% approved base course aggregate. The amount and type of asphalt emulsion shall be determined by a mix design method which results in a blend that meets the LBR strength requirement of Section 911-6. Alternatively, blends may be proportioned such that the asphalt binder content of the total blend including the asphalt emulsion does not exceed 3.5% by weight

6.4.3. RAP aggregate blends stabilized with Portland cement used in traffic base applications

Portland cement stabilized RAP/aggregate blends must include a minimum of 50% approved base coarse aggregate. The amount and type of Portland cement shall be determined by a mix design method which results in a blend which meets the LBR strength requirement of Section 911-6. Portland cement content may not exceed 2% by weight.

6.5. Chemical Stabilization

It is recommended that Portland cement be used in a field trial to evaluate possible shrinkage cracking. Several asphalt emulsions should be used in a field trial to evaluate creep, curing techniques and compaction protocol.

6.6. Evaluate Accumulated Strain from Cyclic Loading and Creep Tests

It is recommended that creep tests should be carried out in a manner to reflect the pavement rutting conditions from cyclic loading. Correlations should be developed between the accumulated strains from cyclic loading to the accumulated strains from constant pressure creep testing. The correlation would allow predictions of pavement life versus traffic loadings.

6.7. Combinations of Chemical Stabilizing Agents

In this study each chemical stabilizing agent was used alone. Contractors who perform Full Depth Reclamation of roads have indicated that they sometimes use a combination of

asphalt emulsion and Portland cement. Therefore, there is a need to evaluate RAP/aggregate blends stabilized with a combination of chemical stabilizing agents.

6.8. Recommended Field Evaluation

To determine the best correlations between lab and field behavior, a field site should be constructed with a control base material, plus different sections of RAP and RAP/aggregate blends, including chemically stabilized blends. The materials should be installed to meet base course specifications.

The site should be of sufficient size to allow a comprehensive field testing program to be conducted over 12-months. The field testing should include density, temperature, Field CBR, dynamic cone penetrometer, and FWD. FWD testing should be conducted such that the effects of cyclic loads can be correlated to rutting. Repetitive FWD loads, of 9 kips, should be applied at specified site locations and rut depth versus loading cycle should be recorded. Deflections could be recorded with proper surveying equipment following each sequence of four, 9 K load applications. A creep pressure that matches the FWD pressure should also be applied to determine rut depths from creep that could be correlated to rut depths from the FWD cyclic testing. The creep loading would require a constant pressure equivalent to the 9 kips on the FWD loading plate (110 in^2) or about 80 psi. This pressure should be attainable using the State Materials Office Cone Truck. Temperature profiles along with ambient temperatures should be recorded.

Field compaction methods (e.g., padfoot, vibratory steel wheel, and pneumatic rubber tired) alone or in combination should be evaluated. Based on the results obtained from gyratory compaction, it is recommended that pneumatic rollers and compaction trains of pneumatic and steel drum be considered. The field density results should be correlated to lab density data, to determine a recommended compaction process. To evaluate the asphalt emulsions, evaluate laboratory curing temperature and time to determine what curing conditions give the best representation of field strength.

7. References

Alam, T. B., Abdelrahman, M., and Schram, S., *Laboratory Characterization of Recycled Asphalt Pavement as a Base Layer,* International Journal of Pavement Engineering. Vol. 11; No. 2, pp. 123-131. 2010.

Aljassar, A.T., Metwali, S., Ali, M.A., and Al-Shammari, F., *Using Reclaimed Asphalt Pavements to Improve Subgrade Soil Properties in Kuwait*. 84th Annual Meeting of Transportation Research Board, TRB, National Research Council, Washington, D.C. 2005.

American Association of State Highway and Transportation Officials., *AASHTO Guide for Mechanistic-Empirical Design of New and Rehabilitated Pavement Structures*. 2002.

Apeagyei, A., and Diefenderfer, B., "Structural Evaluation of FDR Pavements" in *Virginia Bearing Capacity of Roads, Railways and Airfields, Two Volume Set*. Proceedings of the 8th International Conference (BCR2A'09), University of Illinois at Urbana - Champaign, Champaign, Illinois, USA June 29 - July 2 2009.

Asphalt Institute, *MS-19 Basic Asphalt Emulsion Manual*, Fourth Edition, ISBN 978 1934 154 564. 2008.

Asphalt Institute, *MS-14 Asphalt Col Mix Manual*, Third Edition, ISBN 978 1934 154 090. 1997.

Asphalt Pavement Alliance: website http://www.asphaltpavement.org, 2012.

Attia, M., Abdelrahman, M., and Alam, T., *Investigation of Stripping in Minnesota Class 7 (RAP) and Full-Depth Reclamation Base Materials,* MN/RC 2009-05, 2009.

Augustesen, A., Liingaard, M., and Lade, P. V., *Evaluation of Time-Dependent Behavior of Soils*, ASCE International Journal of Geomechanics, Vol. 4, no. 3, pp. 321-338. 2004.

Bejarano, M.O., Harvey, J.T., and Lane, L., *In Situ Recycling Asphalt Concrete as Base Material in California.,* 82nd Annual Meeting of the Transportation Research Board, TRB, National Research Council, Washington, D.C. 2003.

Bennert, T., and Maher, A., *The Development of a Performance Specification for Granular Base and Subbase Material,* FHWA-NJ-2005-003, for NJDOT. 2005.

Breytenbach, I.J., Paige-Green, P., Van Rooy, J.L., *The Relationship between Index Testing and California Bearing Ratio Values for Natural Road Construction Materials in South Africa*. Journal of the South African Institution of Civil Engineering. vol.52; no.2, Oct. 2010.

Brown, E.R., Kandhal, P.S. and Zhang, J., *Performance Testing for Hot Mix Asphalt*. National Center for Asphalt Technology (NCAT). NCAT Report No. 01-05. Auburn, AL. 2001.

Buda, A., and Jarynowski, A., *Life-time Of Correlation and Its Application (volume 1)*, Wydawnictwo Niezalezne, Wroclaw 2010.

Carpenter, S. H., Darter, M. I., and Demsey, B. J., A Pavement Moisture-Accelerated Distress (MAD) Identification System, Vol. I, FHWA/RD-81/079 Vol. II FHWA/RD-81/080, Sept 1981.

Chesner, W. H., Collins, R. J., and MacKay, M. H., User Guidelines for Byproduct and Secondary Use Materials in Pavement Construction FHWA-RD-97-148. 1998.

Cleary, E. D., Long-Term Behavior of RAP-Soil Mixtures for Use as Backfill behind MSE Walls, M.S. Thesis, Florida Institute of Technology, 2005.

Collins, R., and Ciesielski, S., *Recycling and Use of Waste Materials and By-Products in Highway Construction*. Washington, D.C.: National Academy Press.1994.

Cooley, Dane A., Effects of Reclaimed Asphalt Pavement on Mechanical Properties of Base Materials. Brigham Young University. Master Thesis. 2005.

Cooper , K. E., Brown, S. F., and Pooley, G. R., *The Design of Aggregate Grading for Asphalt Base Courses*. Proc., Association of Asphalt Paving Technologists, Technical Session, San Antonio, Tex., 1985.

Cosentino, P. J. and Kalajian E. H., *Developing Specifications for Using Recycled Asphalt Pavement as Base, Subbase, or General Fill Materials*. Final Report. Contract BB-892. State Materials Office, FDOT. 2001.

Cosentino, P. J., Kalajian, E. H., Shieh C. S., Mathurin W. J .K., Gomez, F. A., Cleary E. D., Treerattakoon. A., *Developing Specifications for Using Recycled Asphalt Pavement as Base, Subbase, or General Fill Materials, Phase II. Final Report*. FL/DOT/RMC/06650-7754 BC 819, State Materials Office, FDOT, 2003.

Cosentino, P. J., Kalajian, E. H. Dikova, D., Patel, M., Sandin, C., *Investigating the Statewide Variability and Long Term Strength Deformation Characteristics of RAP and RAP-Soil Mixtures.* Florida Department of Transportation, State Materials Office, Gainesville, Florida. FL/DOT/RMC/06650-7754 BCB 809. 2008.

Cosentino, P. J., Kalajian, E. H., Montemayor, T. A., Doig, B. A., and Horhota, D. J., *Strength-Deformation Properties of Florida's Recycled Asphalt Pavement*, Proceedings of the 26th International Conference on Solid Waste Technology and Management, Philadelphia, PA March 2011.

Das, B. M., *Soil Mechanics Laboratory Manual*. Sixth Edition. New York, NY: Oxford University Press, 2002.

Das, B. M., *Principles of Foundation Engineering*, Fifth Edition. Pacific Grove, California: Brooks/Cole - Thompson Learning, 2004.

Dikova, D., *Creep Behavior of RAP-Soil Mixtures in Earthwork Applications*. M.S. Thesis, Florida Institute of Technology, 2006.

Federal Highway Administration (FHWA)., Demonstration Project 39: Asphalt Recycling: Tamworth Cold Recycling Project. Project FR-024-1(8), May 1981.

Federal Highway Administration (FHWA)., Asphalt Concrete Mix Design and Field Control Technical Advisory T 5040.27, 1988.

Feliberti M., Critical Evaluation of Parameters Affecting Resilient Modulus Tests on Subgrades. MS thesis, University of Texas at El Paso, No. 4081. 1991.

Florida Department of Transportation (FDOT)., Manual of Florida Testing and Sampling Methods (FM). Tallahassee, Florida, 1994.

Florida Department of Transportation (FDOT)., Standard Specifications for Road and Bridge Construction. State Materials Office, Gainesville, Florida, 2010.

Foye, K. C. Use of Reclaimed Asphalt Pavement in Conjunction with Ground Improvement: A Case History. Advances in Civil Engineering. vol. 2011, article number 808561, 2011.

Fuller, W. B., & Thompson, S. E., The Laws of Proportioning Concrete. Proceedings of the American Society of Civil Engineers, March, 1907.

Gandara, J. A., Kancherla, A., Alvarado, G., Nazarian, S., and Scullion, T., Impact of Aggregate Gradation on Base Material Performance. Texas Department of Transportation Research Report TX-0-4358-2, 2003.

Garg, N., and Thompson, M. R., Lincoln Avenue Reclaimed Asphalt Pavement Base Project. Transportation Research Record. No. 1547, pp. 89-95. 1996.

Gomez, F. A., Strength and Drainage Characteristics of RAP-Soil Mixture in Highway Applications. M.S. Thesis, Florida Institute of Technology. 2003.

Holtz, R., & Kovacs, W., *An Introduction to Geotechnical Engineering*. Englewood Cliffs, New Jersey: Prentice Hall. 1981.

Horhota, D. J., Jones L., Putcha, S., Memorandum: *RAP Use as MSE Wall Backfill Material*, Florida Department of Transportation, 2007.

Huang, Y. H., *Pavement Analysis and Design.* Prentice Hall Second Edition ISBN 01314247304, 2004.

Kim, W., Labuz, J. F., and Dai, S., *Resilient Modulus of Base Course Containing Recycled Asphalt Pavement*. Transportation Research Board of the National Academies, 27-35, 2005.

Lee, D-Y., Guinn, J. A., Khandhal, P. S., and Dunning, R. L., *Absorption of Asphalt Into Porous Aggregates*. Strategic Highway Research Program SHRP-A/UIR-90-009, National Research Council, Washington, D.C. 1990.

Locander, R., *Analysis of Using Reclaimed Asphalt Pavement (RAP) as a Base Course Material*, Colorado DOT Report CDOT-2009-5. 2009.

MacGregor, J. A. C., Highter, W. H. and DeGroot, D. J., *Structural Numbers for Reclaimed Asphalt Pavement Base and Subbase Course Mixes*. In Transportation Research Record: Journal of the Transportation Research Board of the National Academies, No 1687, pp. 22-28. 1999.

Maher, M. H., Gucunski, N, and Papp Jr., W. J., *Recycled Asphalt Pavement as a Base and Sub-base Material*. Testing Soil Mixed with Waste or Recycled Materials. ASTM STP 1275 pp. 42-53. 1997.

Mamlouk M. S., and Zaniewski J. P., *Materials for Civil and Construction Engineers* Third Edition, Prentice Hall 2011.

McGarrah, E. J., *Evaluation of Current Practices of Reclaimed Asphalt Pavement/Virgin Aggregate as Base Course Material*. Report No. WA-RD 713.1, Washington State Department of Transportation, Olympia, WA, 2007.

Missouri Department of Transportation (MoDOT), Organizational Results Division, *Analysis of Cold In-place Recycled Asphalt Pavements* December 2009.

Mitchell, J. K., *Fundamentals of Soil Behavior.* John Wiley and Sons, New York. 1993.

Mokwa, R. L., and Peebles, C. S., *Evaluation of the Engineering Characteristics of RAP/Aggregate Blends*, Montana Department of Transportation, FHWA/MT-05-008/8117-24, August 2005.

Montemayor, T. A., *Compaction and Strength-Deformation Characteristics of Reclaimed Asphalt Pavement*. M.S. Thesis, Florida Institute of Technology. 1998.

NCHRP 1-37A, *The Mechanistic-Empirical Pavement Design Guide* (MEPDG) 2011.

Newman, K., and Tingle, J. *Emulsion Polymers for Soil Stabilization*, FAA Worldwide airport Technology Transfer Conference, Atlantic City, New Jersey April 2004.

Niazi, Y., and Jalili M., *Effect of Portland Cement and Lime Additives on Properties of Cold in Place Recycled Mixtures with Asphalt Emulsion*. Construction & Building Materials Vol 23. Issue 3 pp. 1338-43. Elsevier.com. 2009.

Oklahoma Department of Transportation (ODOT)., *Method of Test for Cement-Treated Base Mix Design*. *OHD L-53.* 2009.

Papp, W. J. Jr., Maher, M. H., Bennert, T. A., and Gucunski, N., Behavior of Construction and Demolition Debris in Base and Subbase Applications: Recycled Materials in Geotechnical Applications. Vol. 79 122-136. 1998.

Parsons, R., and Milburn, J., *Engineering Behavior of Stabilized Soils*, TRB 2003 Annual Meeting 2002.

Ping, W. V., Leonard, M., Yang, Z., *Laboratory Simulation of Field Compaction Characteristics (Phase I). Final Report*. State Materials Office, FDOT. Final Report No.: FL/DOT/RMC/BB-890(F), 2003.

Ping, W. V., Leonard, M., Yang, Z., *Evaluation of Laboratory Compaction Techniques for Simulating Field Soil Compaction (Phase II).* Final Report. State Materials Office, FDOT. Final Report No.: FL/DOT/RMC/BB-890(F), 2003.

Rathje, E.M., Rauch, A. F., Trejo, D., Folliard, K. J., Viyanant, C., Esfeller, M., Jain, A., and Ogalla, M., *Evaluation of Crushed Concrete and Recycled Asphalt Pavement as Backfill for Mechanically Stabilized Earth Walls*. Research Report FHWA/TX-06/0-4177-3, Center for Transportation Research, Austin, Tex., March, 176 pp. 2006.

Rupnow, T. D., *Subgrade Stabilization Using Recycled Asphalt Pavement and Fly Ash Mixtures* Iowa State University Internal Publication, 2002.

Sandin, C., *Laboratory Evaluation of the Variability of Florida's RAP Materials for Use in Earthwork Applications*. M.S. Thesis, Florida Institute of Technology. 2008.

Sayed, S.M., Pulsifier, J. M., and Schmitt, R. C., *Construction and Performance of Shoulders Using UNRAP Base*, Journal of Materials in Civil Engineering. Vol 5, no. 3: 321-338. 1993.

South Carolina Department of Transportation SC-T-99, *Standard Method of Test for Full Depth Reclamation Using Asphalt Emulsion – Job Mix Formula Preparation.* SCDOT Designation: SC-T-99. 2008.

Singh, A., and Mitchell, J. K., *General Stress-Strain-Time Function for Soils.* ASCE Journal of the Soil Mechanics and Foundation Division, Vol. 94, No. SM1, pp. 21-47. 1968.

Taha R., Alil G., Basmal, A., Al-Turkl O., *Evaluation of Reclaimed Asphalt Pavement Aggregate in Road Bases and Subbases* Transportation Research Record: Journal of the Transportation Research Board, Volume 1652 , Pages 264-269. 1999.

Talbot, A. N. and Richart, F. E., *The Strength of Concrete and Its Relation to the Cement, Aggregate, and Water*. Bulletin No. 137: 1-116, 1923.

Tao, M., Zhang, Z., and Wu, Z., *Simple Procedure to Assess Performance and Cost Benefits of using Recycled Materials in Pavement Construction*. ASCE Journal of Materials in Civil Engineering, Vol. 20. Issue 11 pp. 718-25. 2008.

Trzebiatowski, B. D., and Benson, C. H., *Saturated Hydraulic Conductivity of Compacted Recycled Asphalt Pavement.* Geotechnical Testing Journal, Vol. 28, No. 5. 2005.

Vaid, Y. P., and Campanella, R. G., Time-Dependent Behavior of an Undisturbed Clay, ASCE, Geotechnical Division JSMFE, Vol. 103. GT 7, July 1977.

Viyanant, C., Rathje E. M., and Rauch A. F., *Creep of Compacted Recycled Asphalt Pavement*. Canadian Geotechnical Journal Vol. 44.No. 6 pp. 687-97. January 2007.

Womack, L.M., Sirr, J. F., and Webster S. L., *Gyratory Compaction of Soil*. Technical Report S-68-6, U.S. Army Engineer Waterways Experiment Station, Vicksburg, MS, November 1969.

Yoder, E. J. and Witczak, M. W., *Principles of Pavement Design, 2nd edition*, John Wiley & Son, Inc, New York, USA, 1975.

Zhang, J., *Evaluation of Mechanistic-Based Compaction Measurements for Earthwork QC/QA*. M.S. Thesis, Iowa State University. 2010.

Appendix A - Grain Size Distribution Data

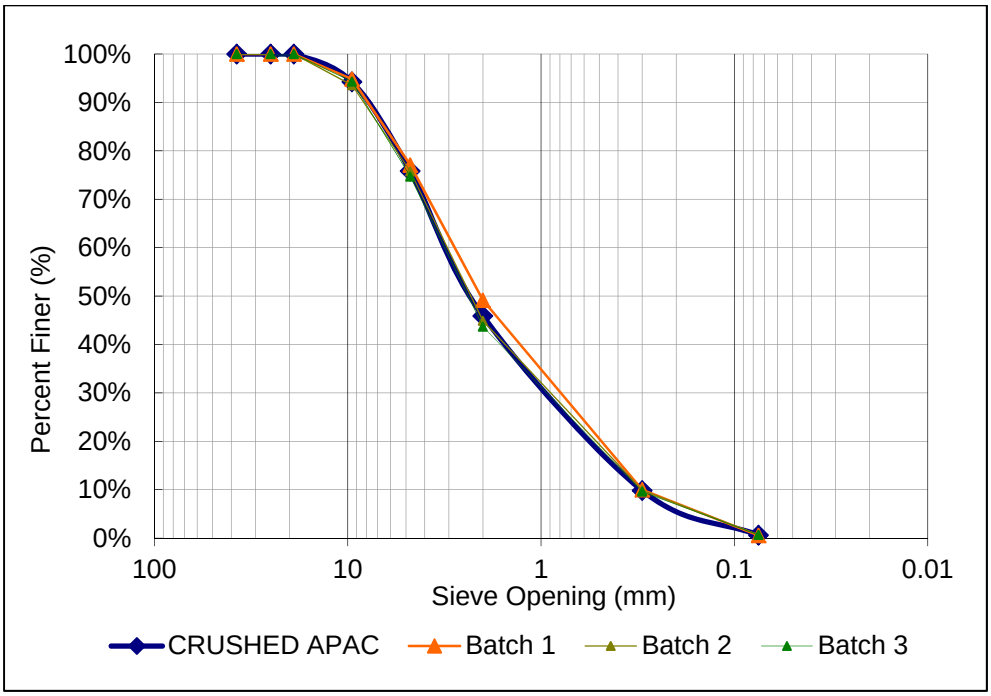

Figure A-1: Sieve Analysis: Crushed Melbourne RAP

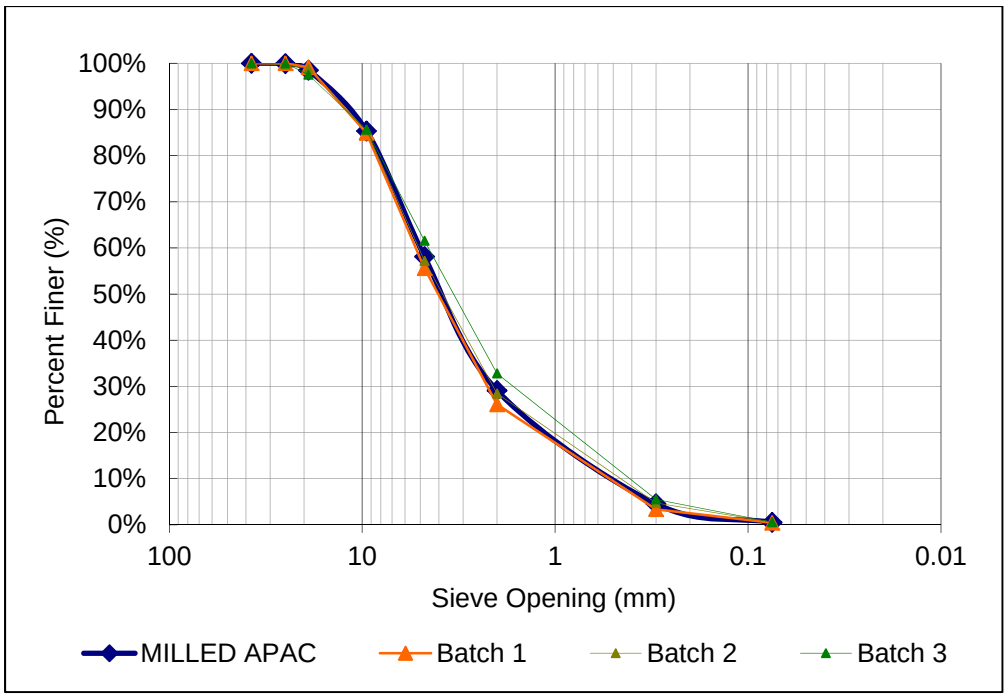

Figure A-2: Sieve Analysis: Milled Melbourne RAP

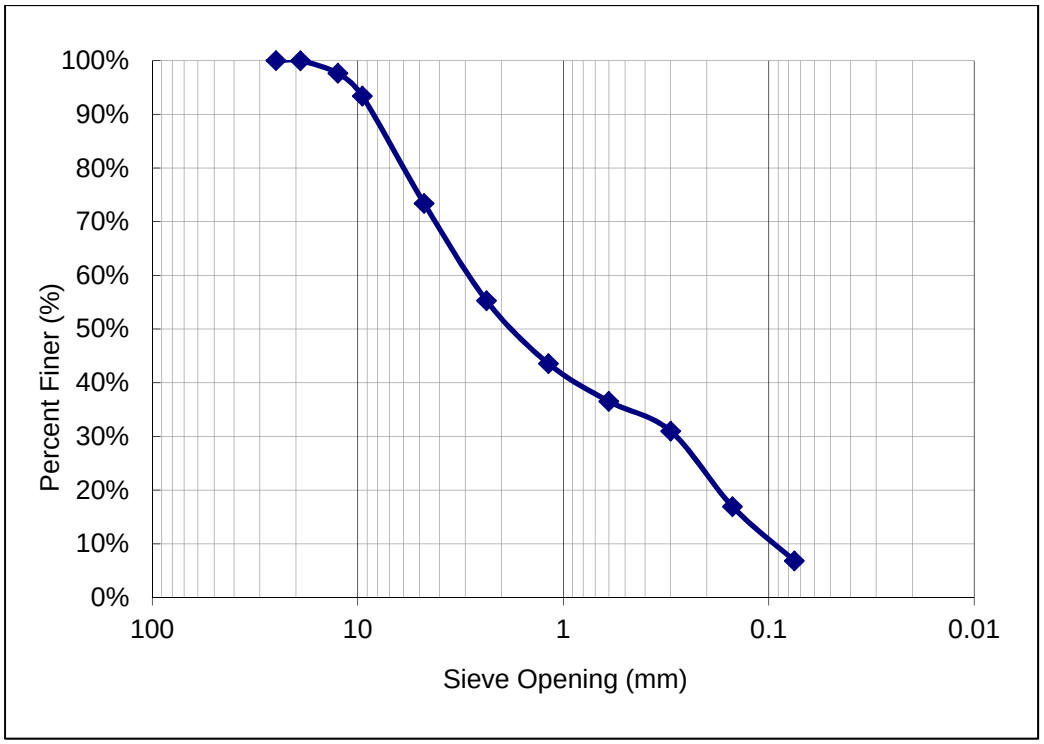

Figure A-3: Sieve Analysis: APAC Jacksonville Crushed RAP

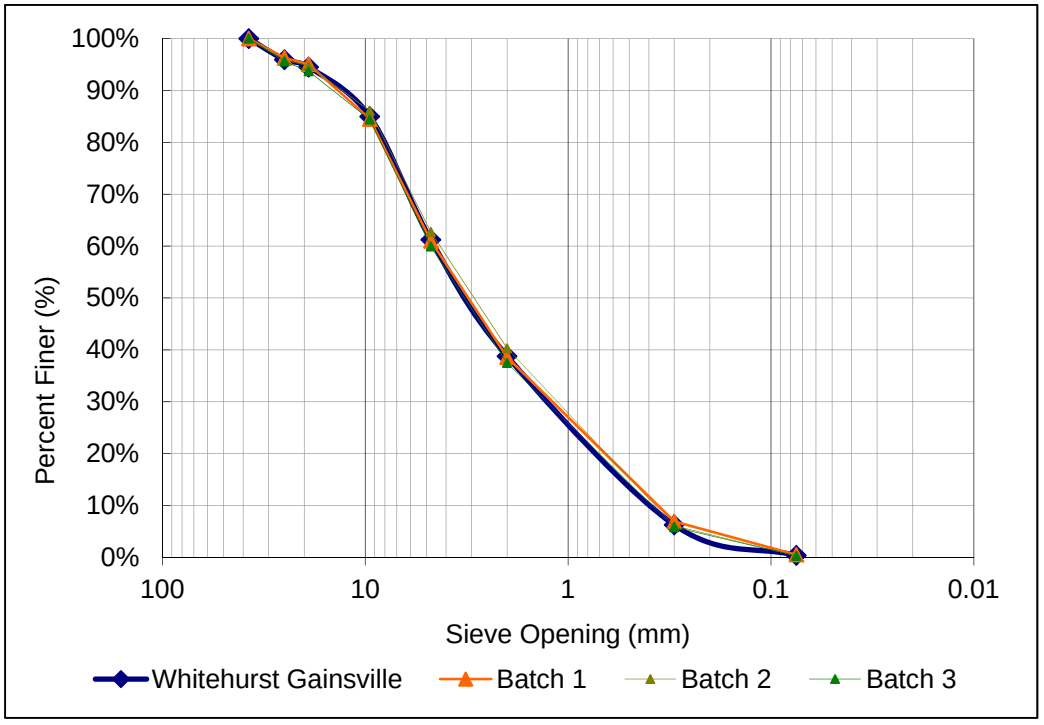

Figure A-4: Sieve Analysis: Whitehurst Gainesville Milled RAP

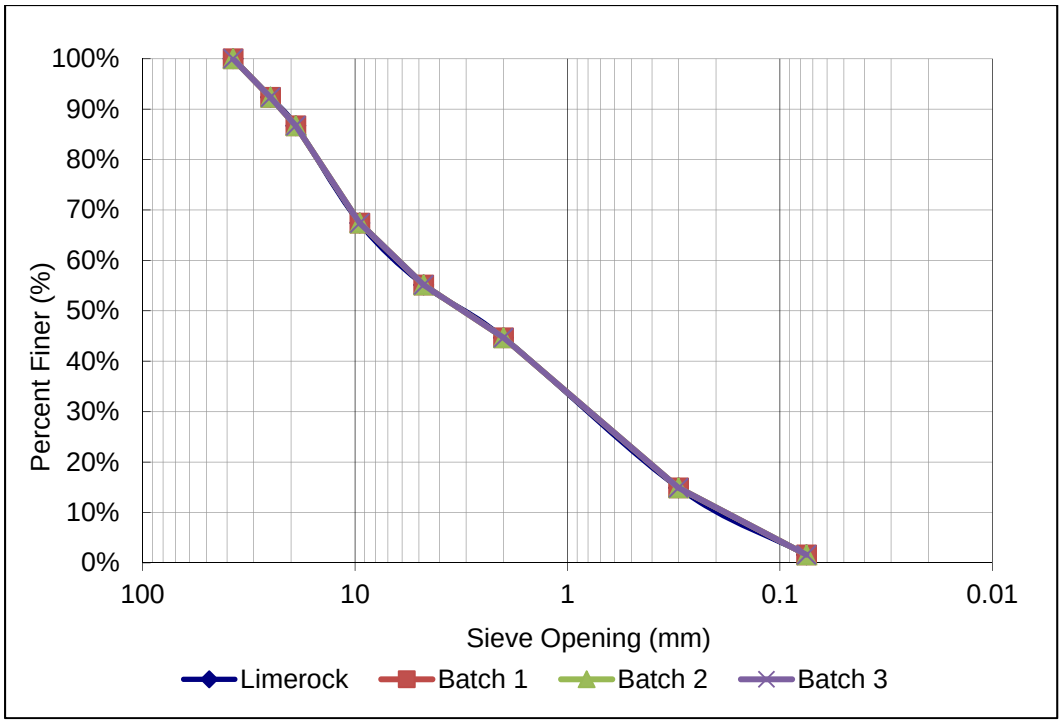

Figure A-5: Sieve Analysis: Limerock Base

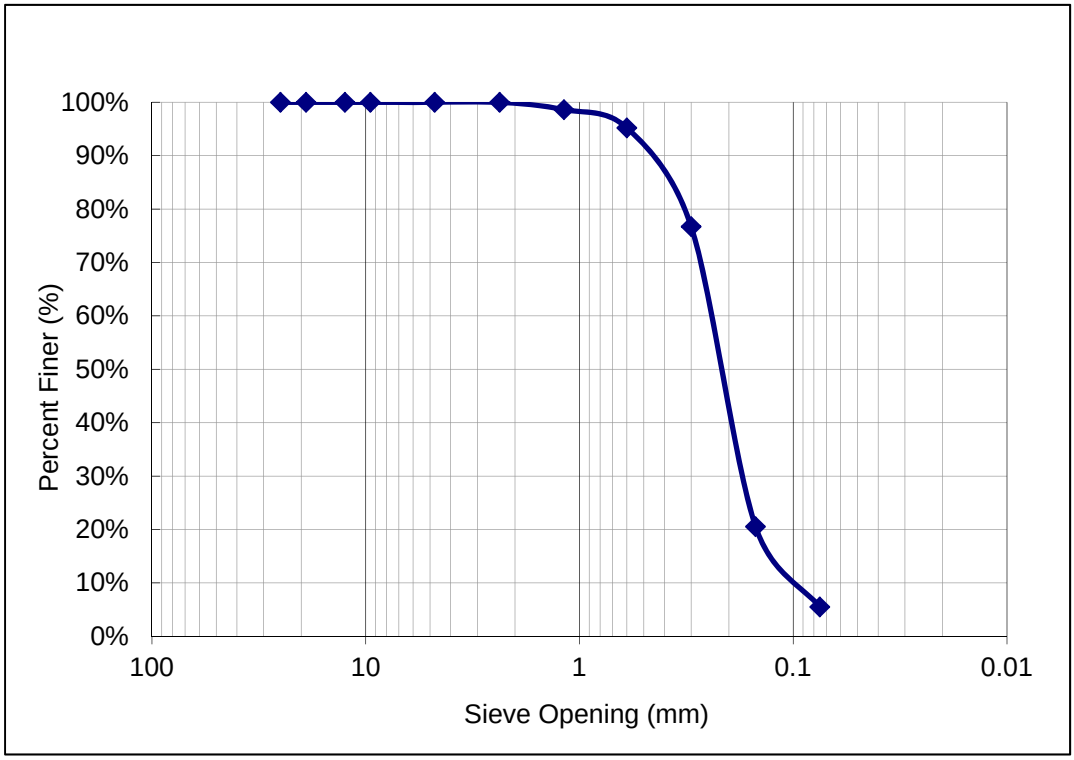

Figure A-6: Sieve Analysis: Clayey Sand

Table A-1: Calculated Grain Size Distributions of MRAP/LR Blends

% MRAP		0%	25%	50%	75%	100%	FDOT Graded Aggregate Base Spec	
% LR		100%	75%	50%	25%	0%		
Sieve #	Sieve (mm)	% Passing					Min	Max
1.5"	37.5	100%	100%	100%	100%	100%	100%	100%
1"	25	92%	94%	96%	98%	100%	95%	100%
3/4"	19	87%	90%	93%	96%	98%	65%	90%
3/8"	9.5	67%	72%	76%	81%	85%	45%	75%
#4	4.75	55%	56%	57%	57%	58%	35%	60%
#10	2	45%	41%	37%	33%	29%	25%	45%
#50	0.3	15%	12%	10%	7%	5%	5%	25%
#200	0.075	2%	1%	1%	1%	1%	0%	10%
Pan	-	0%	0%	0%	0%	0%	-	-

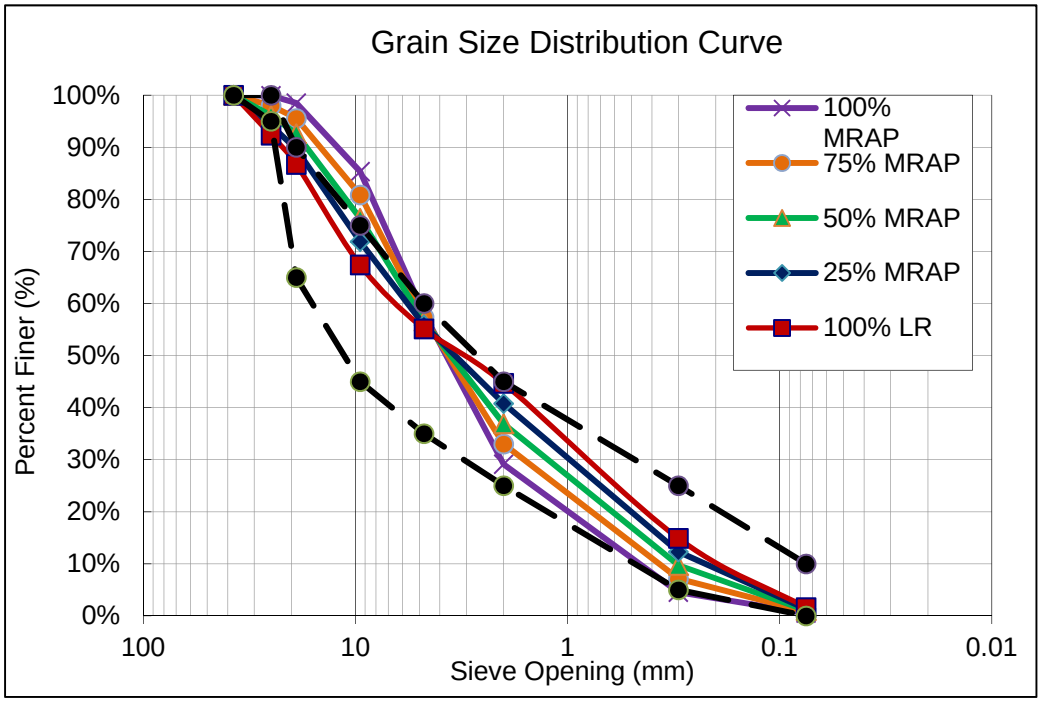

Figure A-7: Calculated Grain Size Distributions Curves for MRAP/LR Blends

Appendix B - Creep and LBR Tabular Data

B.1. Post Creep LBR Tabular Data – Fractions

Table B-1: RAP Fraction LBR

Grain size	Dry Density (pcf)	LBR	Grain size	Dry Density (pcf)	LBR
-#40 crushed APAC Mel S1	91.2	12.2	+#40 crushed APAC Mel S1	109.2	20.9
-#40 crushed APAC Mel S2	97.3	16.6	+#40 crushed APAC Mel S2	108.1	20.2
-#40 Milled APAC Mel S1	94.1	18.5	+#40 Milled APAC Mel S1	105.8	29.9
-#40 Milled APAC Mel S2	94.9	18.7	+#40 Milled APAC Mel S2	104.4	23.0
-#40 crushed JAX S1	93.6	12.1	+#40 crushed JAX S1	124.8	23.8
-#40 crushed JAX S2	92.4	11.0	+#40 crushed JAX S2	113.4	24.8
-#40 Milled W-H S1	91.5	19.2	+#40 Milled W-H S1	115.5	31.6
-#40 Milled W-H S2	93.7	17.4	+#40 Milled W-H S2	115.4	31.4
-#8 crushed APAC Mel S1	100.0	16.3	+#8 crushed APAC Mel S1	113.4	61.1
-#8 crushed APAC Mel S2	104.1	17.6	+#8 crushed APAC Mel S2	112.9	44.5
-#8 Milled APAC Mel S1	112.4	34.7	+#8 Milled APAC Mel S1	102.5	23.3
-#8 Milled APAC Mel S2	92.3	21.9	+#8 Milled APAC Mel S2	103.4	20.8
-#8 crushed JAX S1	114.1	36.8	+#8 crushed JAX S1	107.0	31.8
-#8 crushed JAX S2	113	36.3	+#8 crushed JAX S2	108.8	31.6
-#8 Milled W-H S1	104.9	23.1	+#8 Milled W-H S1	108.0	24.4
-#8 Milled W-H S2	105.1	24.0	+#8 Milled W-H S2	106.0	22.4
-#4 crushed APAC Mel S1	112.2	37.1	+#4 crushed APAC Mel S1	100.6	20.1
-#4 crushed APAC Mel S2	113.3	45.5	+#4 crushed APAC Mel S2	105	27.2
-#4 Milled APAC Mel S1	114.5	32.0	+#4 Milled APAC Mel S1	108.4	31.3

Grain size	Dry Density (pcf)	LBR	Grain size	Dry Density (pcf)	LBR
-#4 Milled APAC Mel S2	113.5	25.4	+#4 Milled APAC Mel S2	105.5	20.3
-#4 crushed JAX S1	119.9	32.1	+#4 crushed JAX S1	111.9	29.2
-#4 crushed JAX S2	118.4	27.1	+#4 crushed JAX S2	110.3	27.6
-#4 Milled W-H S1	108.7	21.2	+#4 Milled W-H S1	106.3	32.6
-#4 Milled W-H S2	107.4	26.7	+#4 Milled W-H S2	108	30.6
100%Crushed APAC Mel S1	107.2	48.5	100% Milled W-H S1	117.8	44.3
100%Crushed APAC Mel S2	119.0	42.6	100% Milled W-H S2	116.8	45.5
100% crushed APAC Mel S1	124.8	41.8	100% Milled APAC Mel S1	115.5	42.4
100% crushed APAC Mel S2	124.1	31.6	100% Milled APAC Mel S2	114.9	41.6
Talbot Crush APAC MEL S1	120.4	77.9	Talbot JAX S1	116.3	32.3
Talbot Crush APAC MEL S2	121.6	91.4	Talbot JAX S2	127.7	77.2
Talbot Milled APAC MEL S1	119.9	84.6	Talbot W-H S1	116.3	52.1
Talbot Milled APAC MEL S2	121.9	101.8	Talbot W-H S2	122.4	65.3

B.2. Creep and Post Creep LBR Tabular Data Blends

Table B-2: RAP/Aggregate Blend Creep and Post Creep LBR

Sample	Material	Pressure (psi)	Moisture Content	Dry Density	Average LBR	Average CSR
1&3	100% MRAP	25	5.7%	115.8	52.5	2.58×10^{-4}
2&4	100% MRAP	50	6.5%	118.3	73.6	1.31×10^{-4}
5&6	100% MRAP	100	6.3%	121.0	97.5	8.08×10^{-5}
1&3	100% LR	25	10.1%	128.6	140.7	7.57×10^{-6}
2&4	100% LR	50	10.4%	129.3	160.4	5.50×10^{-6}
5&6	100% LR	100	10.5%	130.9	172.2	3.00×10^{-6}

Sample	Material	Pressure (psi)	Moisture Content	Dry Density	Average LBR	Average CSR
4&6	100% CCB	25	7.5%	126.3	196.0	8.85×10^{-6}
1&2	100% CCB	50	7.6%	127.1	171.2	4.05×10^{-6}
3&5	100% CCB	100	7.8%	129.4	263.4	1.65×10^{-6}
2&6	100% RCA	25	15.1%	107.0	197.5	3.00×10^{-6}
1&4	100% RCA	50	14.5%	109.2	233.5	5.04×10^{-6}
3&5	100% RCA	100	14.9%	109.3	300.9	2.23×10^{-6}
4&5	25% MRAP/75% LR	25	9.3%	122.8	162.8	1.93×10^{-5}
2&6	25% MRAP/75% LR	50	8.0%	125.1	183.5	9.66×10^{-6}
1&3	25% MRAP/75% LR	100	8.4%	127.6	206.8	5.10×10^{-6}
3&6	50% MRAP/50% LR	25	8.6%	114.3	84.0	4.01×10^{-5}
4&5	50% MRAP/50% LR	50	6.3%	120.1	136.6	3.62×10^{-5}
1&2	50% MRAP/50% LR	100	6.5%	122.0	138.5	2.51×10^{-5}
1&5	75% MRAP/25% LR	25	7.8%	112.7	78.4	1.18×10^{-4}
3&4	75% MRAP/25% LR	50	7.3%	115.2	93.5	9.53×10^{-5}
2&6	75% MRAP/25% LR	100	7.4%	119.5	131.6	4.48×10^{-5}
5&6	25% MRAP/75% CCB	25	7.2%	124.2	158.2	1.84×10^{-5}
3&4	25% MRAP/75% CCB	50	6.2%	125.8	170.0	8.07×10^{-6}
1&2	25% MRAP/75% CCB	100	6.3%	126.3	211.8	5.06×10^{-6}
1&5	50% MRAP/50% CCB	25	6.3%	122.1	99.2	4.66×10^{-5}
3&6	50% MRAP/50% CCB	50	7.5%	123.2	105.5	3.03×10^{-5}
2&4	50% MRAP/50% CCB	100	7.3%	124.3	127.4	1.67×10^{-5}
5&6	75% MRAP/25% CCB	25	5.7%	115.8	57.5	1.96×10^{-4}
1&2	75% MRAP/25% CCB	50	6.5%	118.3	83.1	1.06×10^{-4}
3&4	75% MRAP/25% CCB	100	6.3%	121.0	120.8	5.95×10^{-5}
1&2	25% MRAP/75% RCA	25	8.9%	107.6	116.9	1.33×10^{-5}
4&6	25% MRAP/75% RCA	50	9.9%	106.0	125.1	8.44×10^{-6}

Sample	Material	Pressure (psi)	Moisture Content	Dry Density	Average LBR	Average CSR
3&5	25% MRAP/75% RCA	100	9.1%	107.6	143.0	4.60×10^{-6}
3&4	50% MRAP/50% RCA	25	13.0%	106.3	58.5	2.32×10^{-5}
1&6	50% MRAP/50% RCA	50	12.6%	109.0	103.9	1.54×10^{-5}
2&5	50% MRAP/50% RCA	100	11.6%	112.2	110.2	1.51×10^{-5}
	75% MRAP/25% RCA	25				
	75% MRAP/25% RCA	50				
	75% MRAP/25% RCA	100				

B.3. Creep and Post Creep LBR Tabular Data

Table B-3: CSS-1H Stabilized Blend Creep and Post Creep LBR

Trial Set	Soaked/ Unsoaked	MRAP %	% CSS-1H	Moisture Content	Average Dry Density	Average LBR	Average CSR
15	Unsoaked	100%	0%	6.6%	113.9	88.0	2.95×10^{-3}
12	Unsoaked	75%	0%	7.8%	110.8	125.0	2.09×10^{-3}
21	Unsoaked	75%	1%	7.8%	118.8	126.0	1.85×10^{-3}
21	Unsoaked	75%	2%	7.6%	119.6	115.0	1.76×10^{-3}
21	Unsoaked	75%	3%	7.8%	120.2	109.0	1.73×10^{-3}
04	Unsoaked	50%	0%	7.5%	120.0	98.0	7.42×10^{-4}
05	Unsoaked	50%	1%	9.9%	118.4	126.2	6.43×10^{-4}
04	Unsoaked	50%	2%	7.8%	119.9	87.8	8.69×10^{-4}
04	Unsoaked	50%	3%	7.8%	121.7	78.7	1.08×10^{-3}
S01	Soaked	50%	0%	6.6%	126.6	53.0	N/A
S10	Soaked	50%	1%	7.4%	122.2	127.0	N/A
S11	Soaked	50%	2%	7.4%	122.4	105.0	N/A
S12	Soaked	50%	3%	8.3%	123.0	107.0	N/A
14	Unsoaked	25%	0%	5.6%	123.9	203.9	3.63×10^{-4}
08	Unsoaked	25%	1%	7.0%	124.1	216.3	2.73×10^{-4}
08	Unsoaked	25%	2%	6.7%	124.3	169.2	5.59×10^{-4}
22	Unsoaked	25%	3%	8.7%	128.6	131.0	1.02×10^{-3}
S14	Soaked	25%	0%	7.7%	128.5	98.7	N/A
12	Unsoaked	0%	0%	7.80%	125.4	426.4	3.17×10^{-4}
S13	Soaked	0%	0%	8.6%	130.0	162.0	N/A

Table B-4: SS-1H Stabilized Blend Creep and Post Creep LBR

Trial Set	Soaked/ Unsoaked	% MRAP	% SS-1H	Moisture Content	Average Dry Density	Average LBR	Average CSR
15	Unsoaked	100%	0%	6.6%	113.9	88.0	2.95×10^{-3}
12	Unsoaked	75%	0%	7.8%	110.8	125.0	2.09×10^{-3}
12	Unsoaked	75%	1%	6.3%	114.9	149.5	1.87×10^{-3}
13	Unsoaked	75%	2%	5.8%	116.8	119.0	1.66×10^{-3}
13	Unsoaked	75%	3%	5.7%	117.4	99.5	1.88×10^{-3}
4	Unsoaked	50%	0%	7.5%	117.5	98.0	9.16×10^{-4}
11	Unsoaked	50%	1%	6.7%	122.0	216.5	4.95×10^{-4}
11	Unsoaked	50%	2%	6.0%	121.8	182.5	8.87×10^{-4}
13	Unsoaked	50%	3%	5.7%	118.6	155.5	5.24×10^{-4}
S01	Soaked	50%	0%	6.6%	126.6	53.0	N/A
S06	Soaked	50%	1%	7.3%	123.5	106.0	N/A
S07	Soaked	50%	2%	7.4%	123.0	103.0	N/A
S08	Soaked	50%	3%	7.7%	121.6	100.0	N/A
14	Unsoaked	25%	0%	5.6%	123.9	381.0	3.63×10^{-4}
14	Unsoaked	25%	1%	6.1%	124.1	374.0	7.94×10^{-4}
14	Unsoaked	25%	2%	5.7%	123.0	278.5	8.31×10^{-4}
14	Unsoaked	25%	3%	8.4%	127.1	125.0	1.03×10^{-3}
S14	Soaked	25%	0%	7.7%	128.5	98.7	N/A
12	Unsoaked	0%	0%	7.8%	125.4	459.0	6.81×10^{-4}
S13	Soaked	0%	0%	8.6%	130.0	162.0	N/A

Table B-5: Portland Cement Stabilized Blend Creep and Post Creep LBR

Trial Set	Soaked/ Unsoaked	MRAP %	% PC	Moisture Content	Average Dry Density	Average LBR	Average CSR
15	Unsoaked	100%	0%	6.6%	113.9	42.0	2.95×10^{-3}
12	Unsoaked	75%	0%	7.8%	110.8	41.7	2.09×10^{-3}
17	Unsoaked	75%	1%	8.1%	114.0	71.0	4.08×10^{-4}
17	Unsoaked	75%	2%	7.8%	119.1	140.0	1.63×10^{-4}
17	Unsoaked	75%	3%	8.2%	115.8	202.5	2.56×10^{-4}
4	Unsoaked	50%	0%	7.5%	117.5	79.7	9.16×10^{-4}
16	Unsoaked	50%	1%	7.5%	121.9	144.0	3.44×10^{-4}
16	Unsoaked	50%	2%	7.6%	123.3	277.0	4.03×10^{-5}
16	Unsoaked	50%	3%	7.8%	124.6	444.0	8.06×10^{-5}
S01	Soaked	50%	0%	6.6%	126.6	53.0	N/A
S02	Soaked	50%	1%	8.9%	121.1	175.0	N/A
S03	Soaked	50%	2%	8.1%	121.0	288.0	N/A
S04	Soaked	50%	3%	7.3%	129.3	396.0	N/A
23	Unsoaked	25%	0%	8.5%	124.3	89.5	3.63×10^{-4}
18	Unsoaked	25%	1%	8.1%	128.2	285.0	1.20×10^{-4}
18	Unsoaked	25%	2%	8.8%	128.1	512.0	4.71×10^{-5}
18	Unsoaked	25%	3%	8.2%	129.6	763.0	1.20×10^{-4}
S14	Soaked	25%	0%	7.7%	128.5	98.7	N/A
12	Unsoaked	0%	0%	6.5%	125.4	383.0	3.17×10^{-4}
S13	Soaked	0%	0%	8.6%	130.0	162.0	N/A

Appendix C - Creep Data

C.1. Testing Curves Fractionated RAP

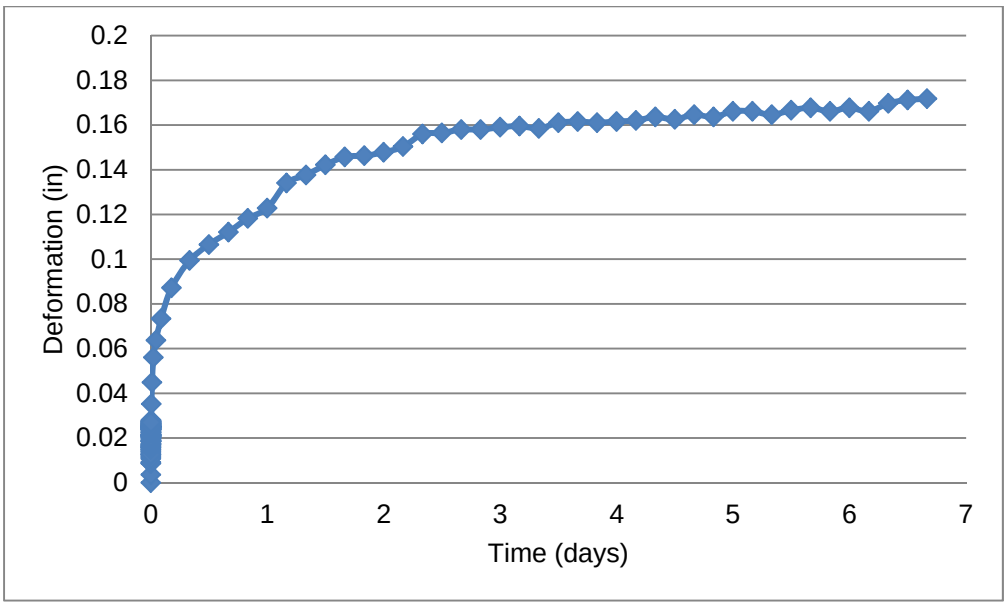

Figure C-1: Creep vs. Time Plot: Plot: Crushed APAC Mel Pass #40 S1

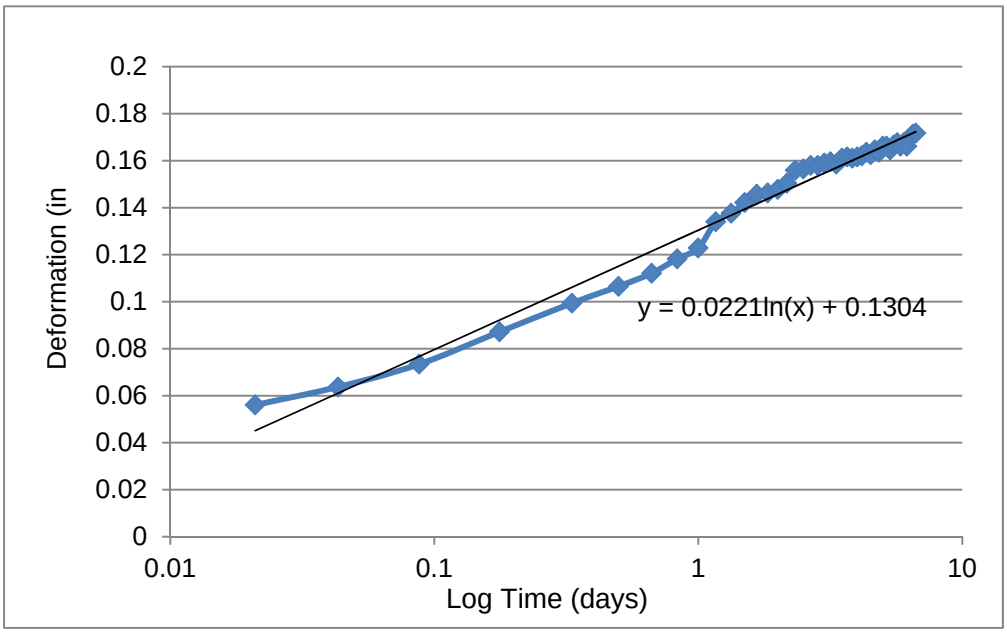

Figure C-2: Creep vs. Log Time Plot: Plot: Crushed APAC Mel Pass #40 S1

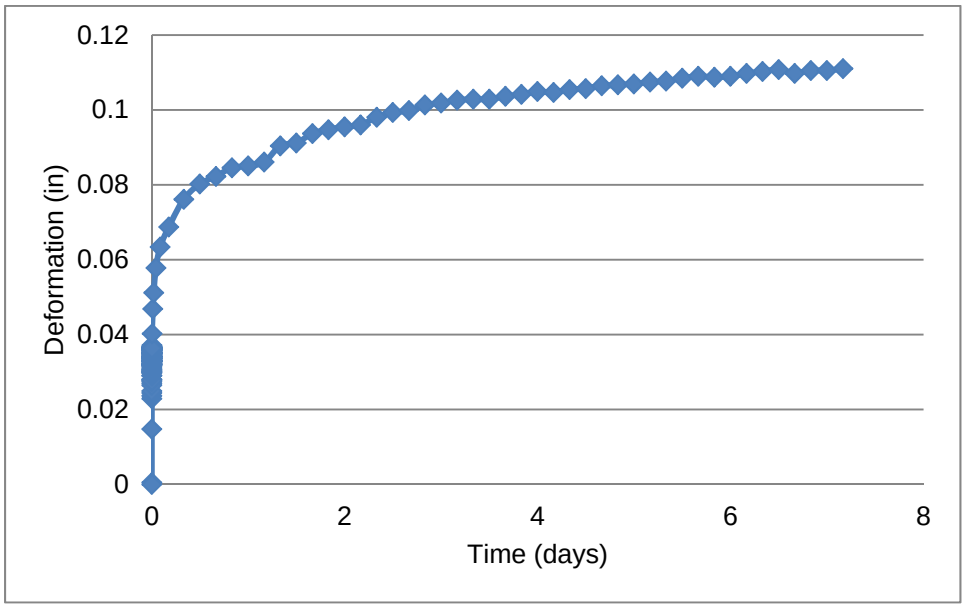

Figure C-3: Creep vs. Time Plot: Crushed APAC Mel Pass #40 S2

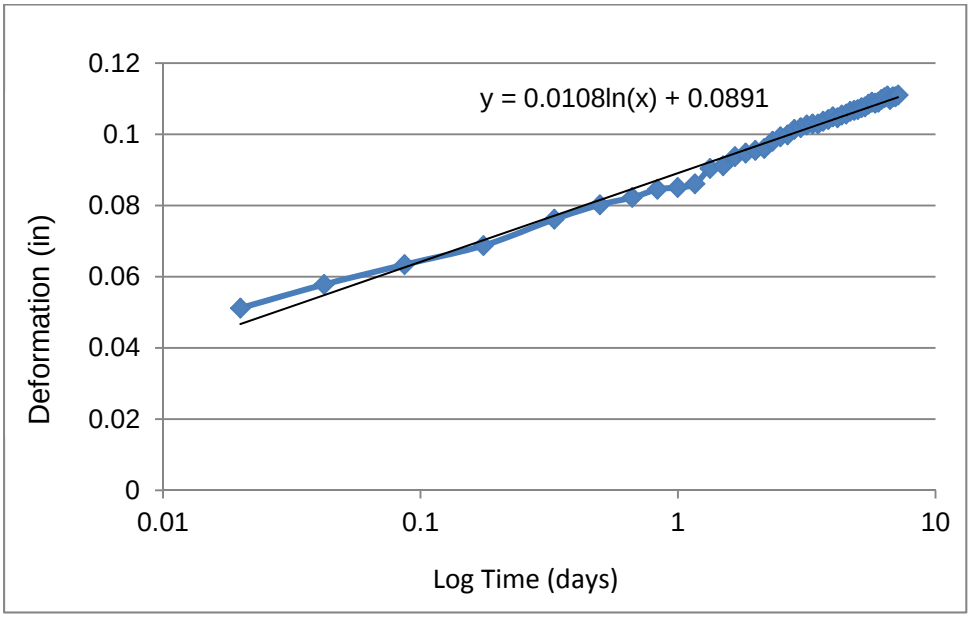

Figure C-4: Creep vs. Log Time Plot: Crushed APAC Mel Pass #40 S2

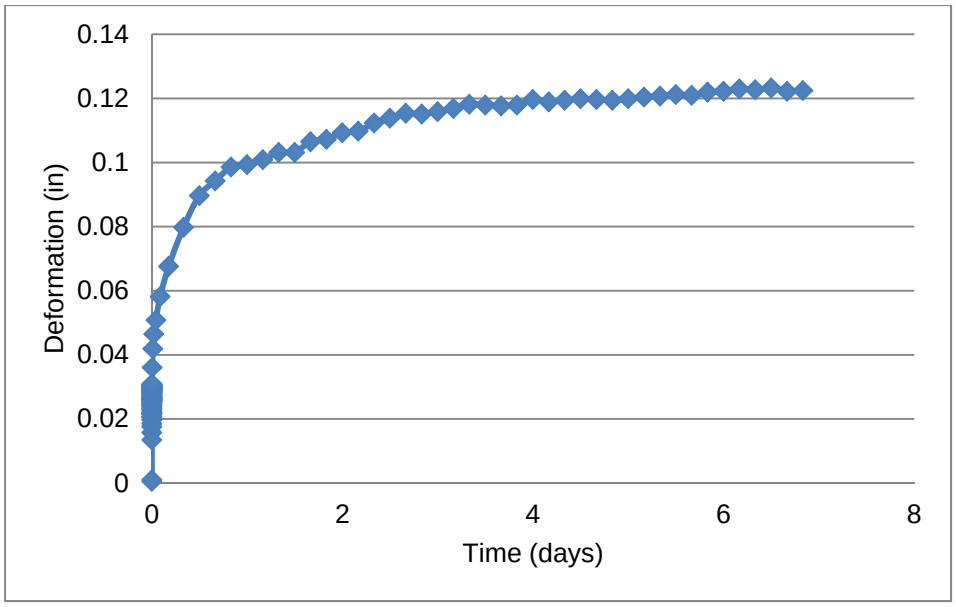

Figure C-5: Creep vs. TIme Plot: Milled APAC Melbourne Pass #40 S1

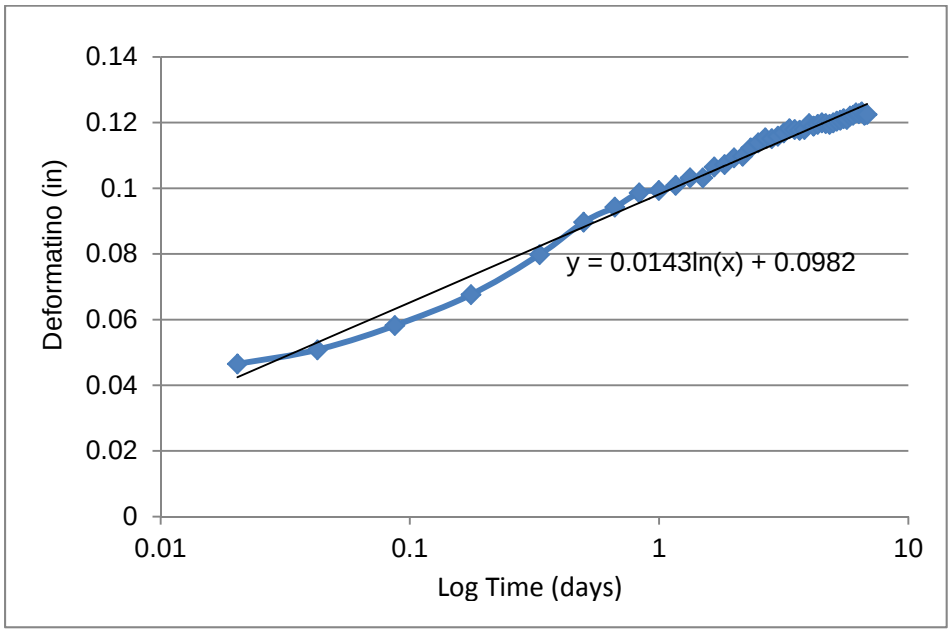

Figure C-6: Creep vs. Log Time Plot: Milled APAC Melbourne Pass # 40 S1

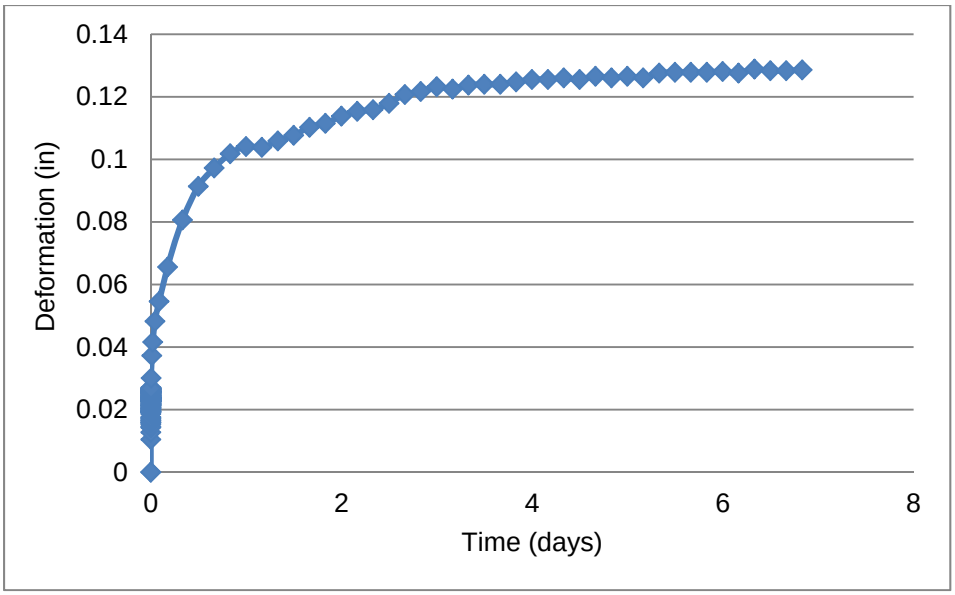

Figure C-7: Creep vs. Time Plot: Milled APAC Melbourne Pass # 40 S2

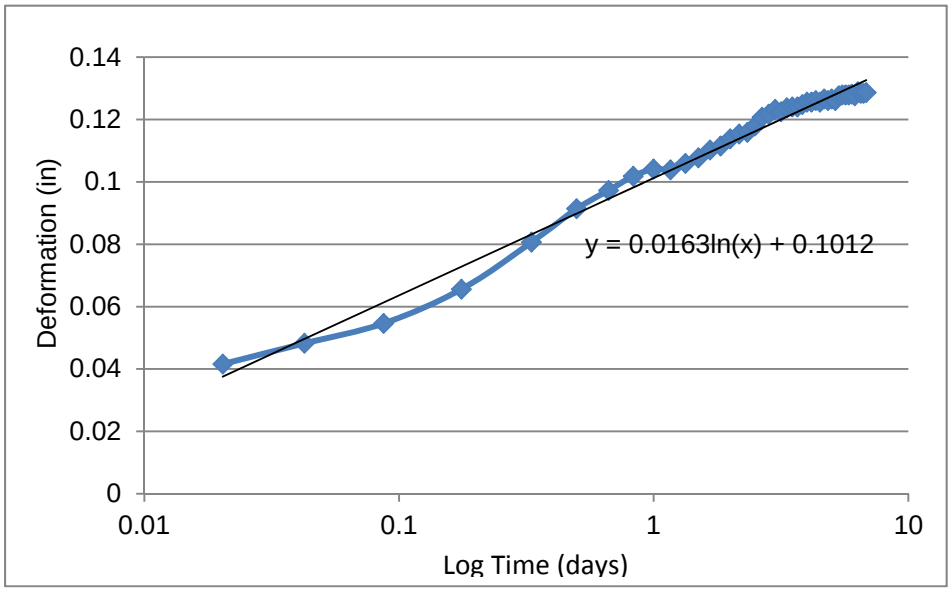

Figure C-8: Creep vs. Log Time Plot: Milled APAC Melbourne Pass # 40 S2

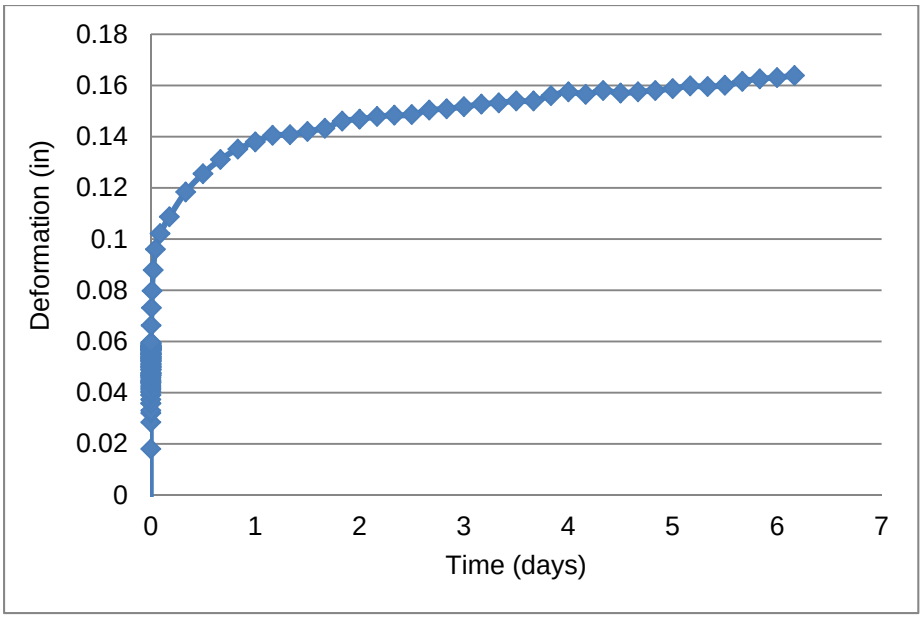

Figure C-9: Creep vs. Time Plot: Crushed APAC Jacksonville Pass #40 S1

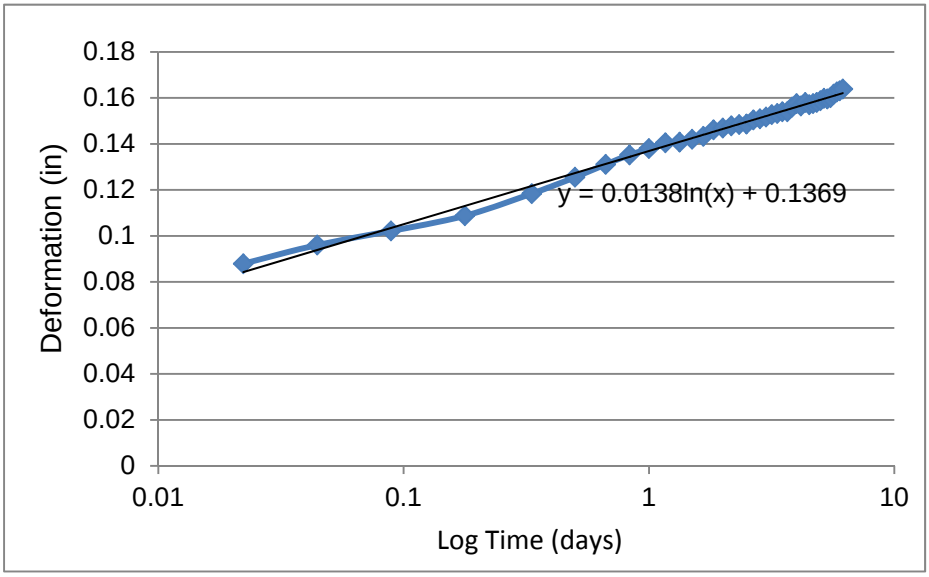

Figure C-10: Creep vs. Log Time Plot: Crushed APAC Jacksonville Pass #40 S1

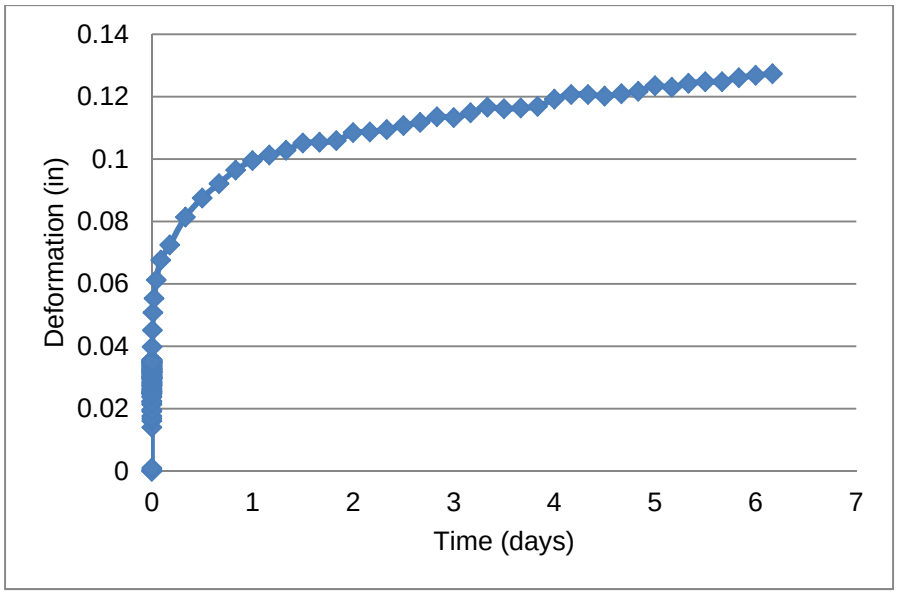

Figure C-11: Creep vs. Time Plot: Crushed APAC Jacksonville Pass #40 S2

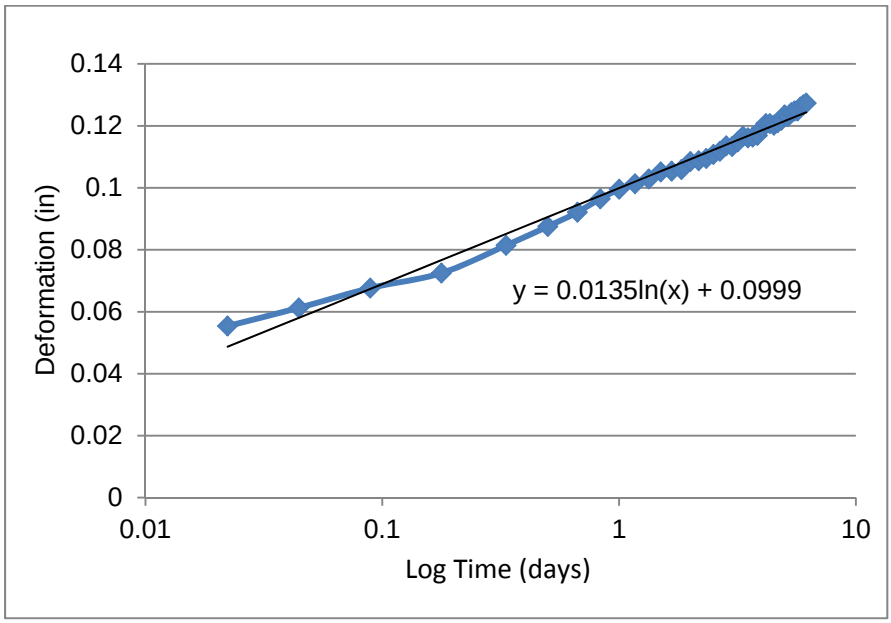

Figure C-12: Creep vs. Log Time Plot: Crushed APAC Jacksonville Pass #40 S2

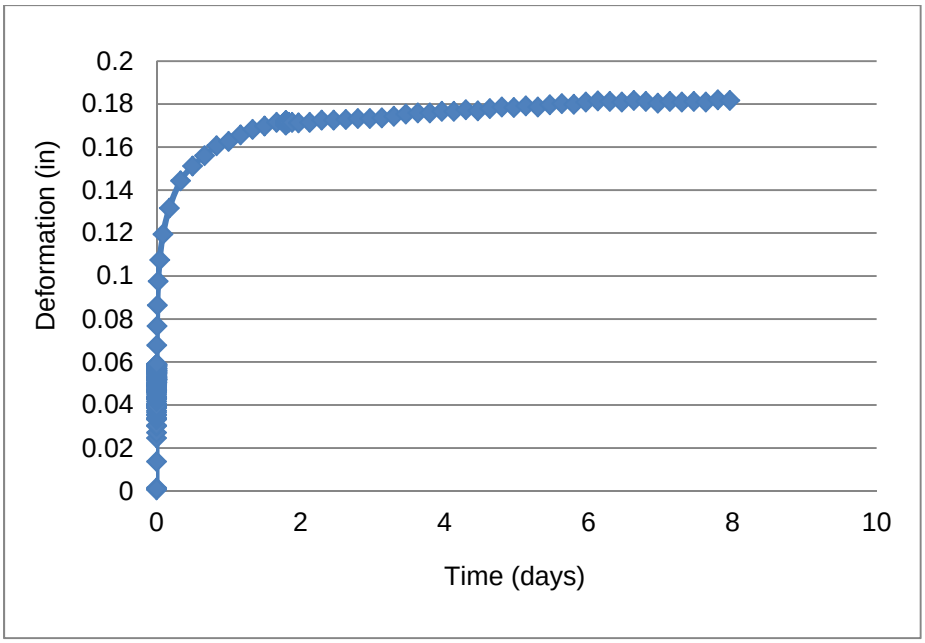

Figure C-13: Creep vs. Time Plot: Milled Whitehurst Pass #40 S1

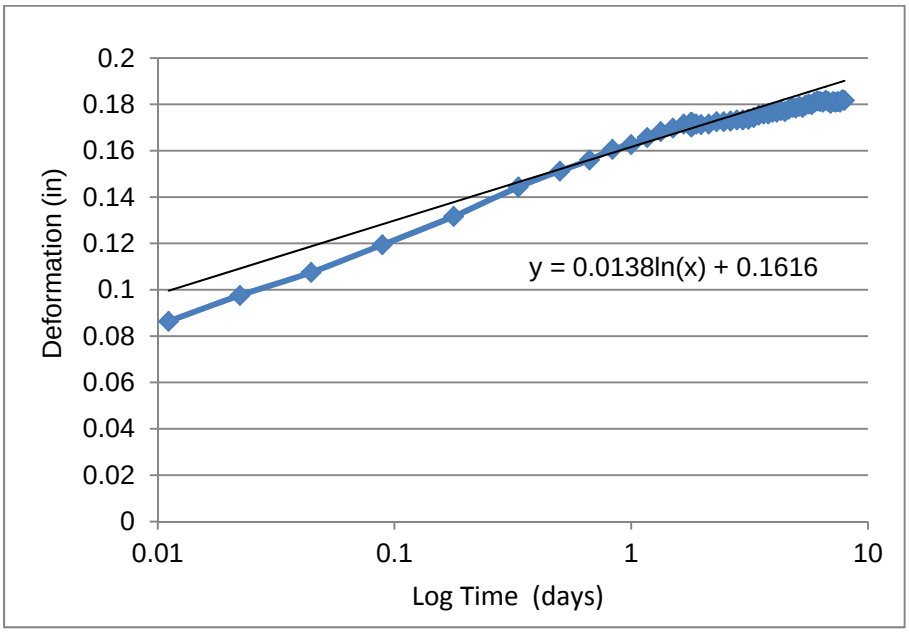

Figure C-14: Creep vs. Log Time Plot: Milled Whitehurst Pass #40 S1

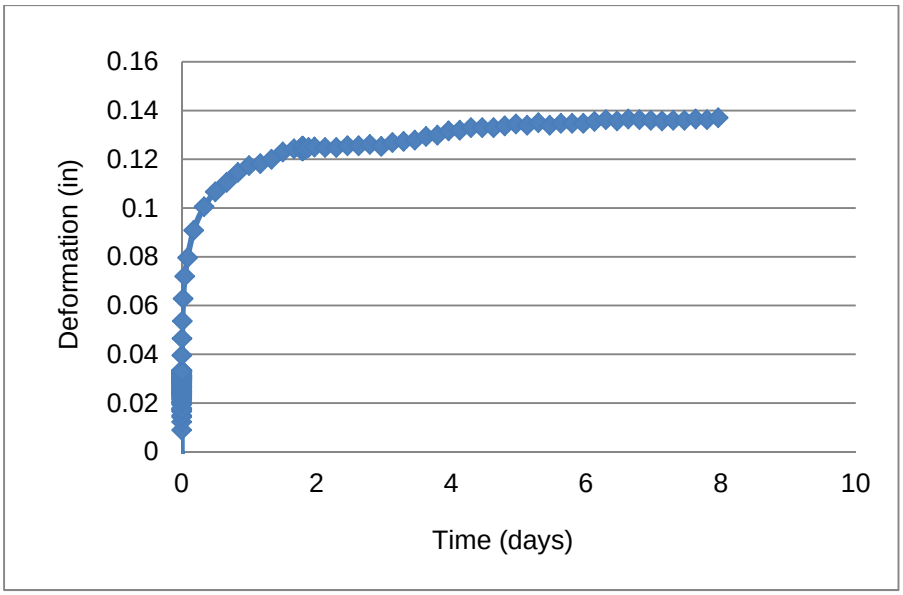

Figure C-15: Creep vs. Time Plot: Milled Whitehurst pass #40 S2

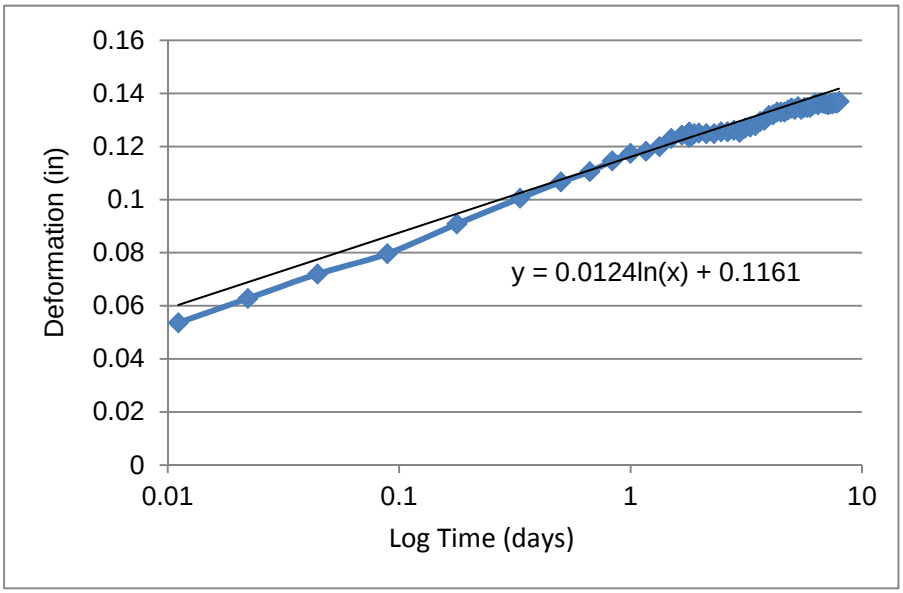

Figure C-16: Creep vs. Log Time Plot: Milled Whitehurst Pass #40 S2

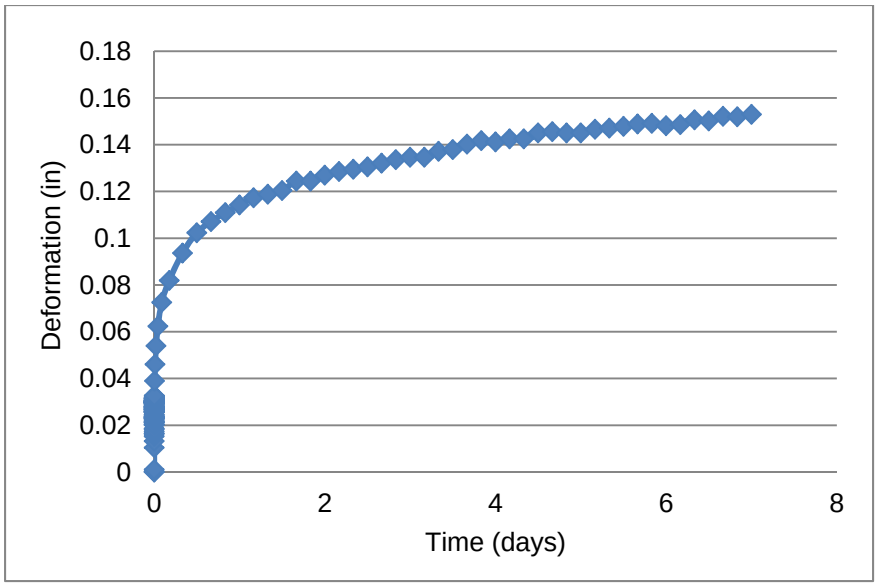

Figure C-17: Creep vs. Time Plot: Crushed APAC Melbourne Pass #8 S1

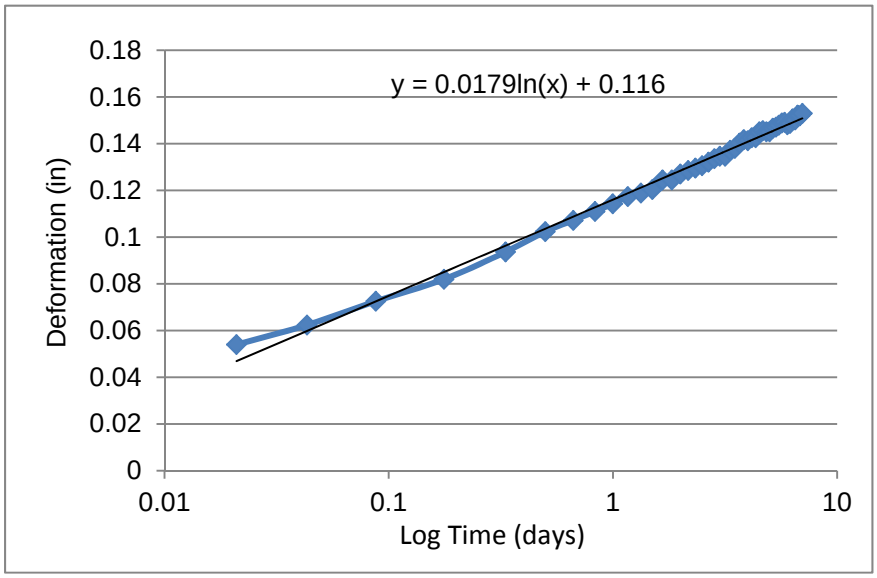

Figure C-18: Creep vs. Log Time Plot: Crushed APAC Melbourne Pass #8 S1

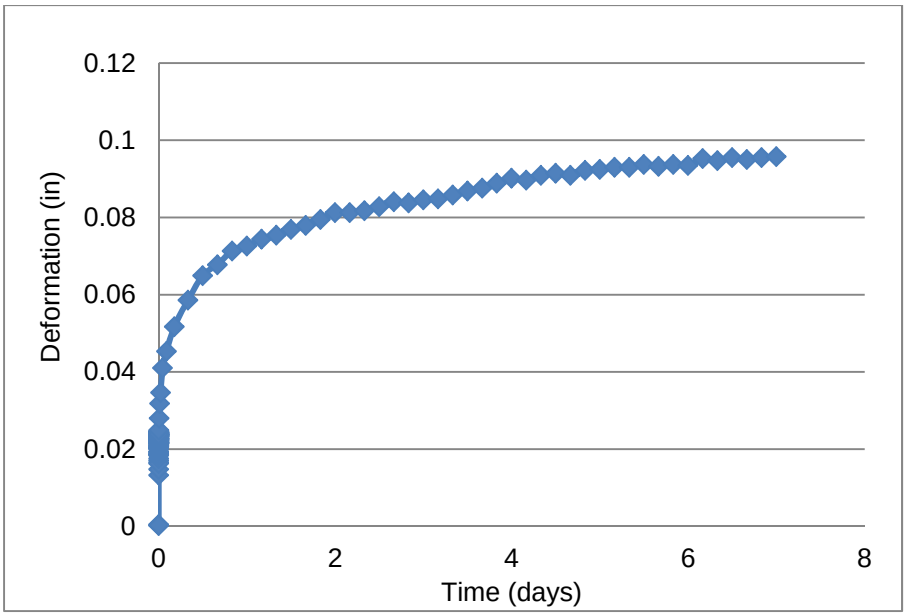

Figure C-19: Creep vs. Time Plot: Crushed APAC Melbourne Pass #8 S2

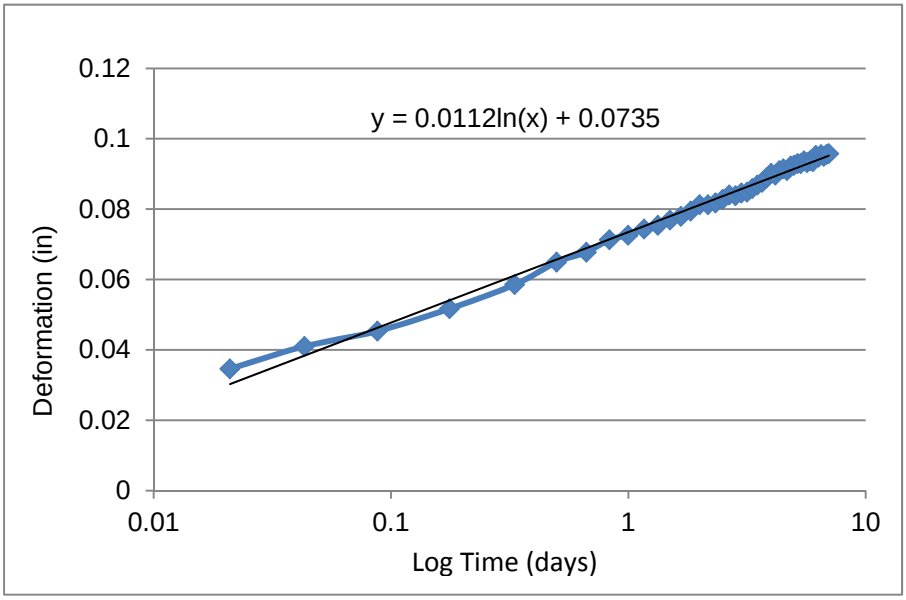

Figure C-20: Creep vs. Log Time Plot: Crushed APAC Melbourne Pass #8 S2

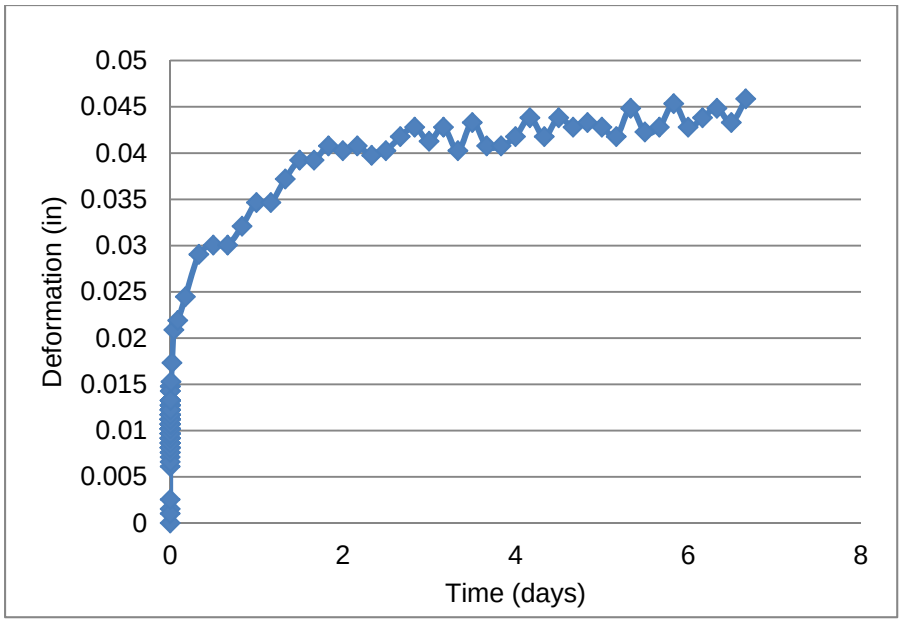

Figure C-21: Creep vs. Time Plot: Milled APAC Melbourne Pass No 8 S1

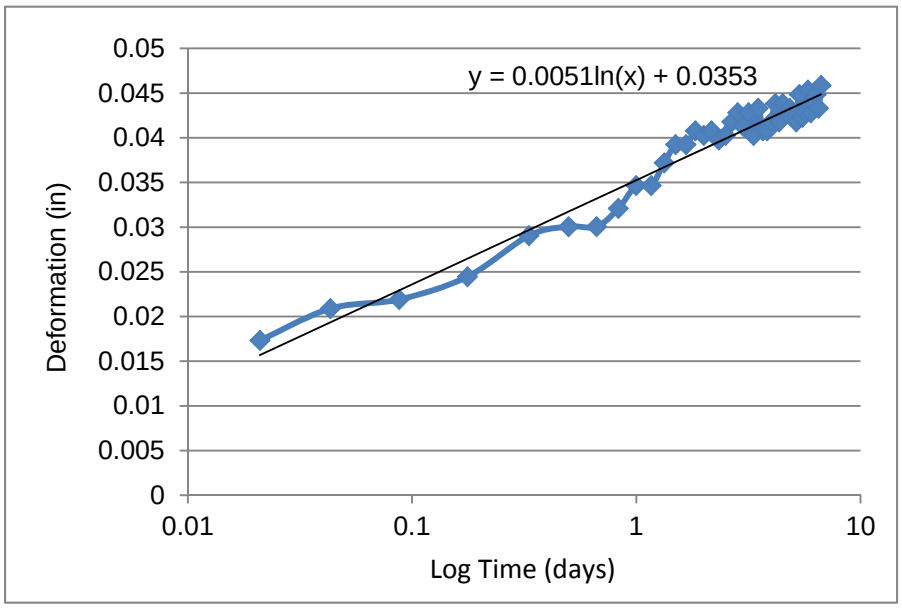

Figure C-22: Creep vs. Log Time Plot: Milled APAC Melbourne Pass No 8 S1

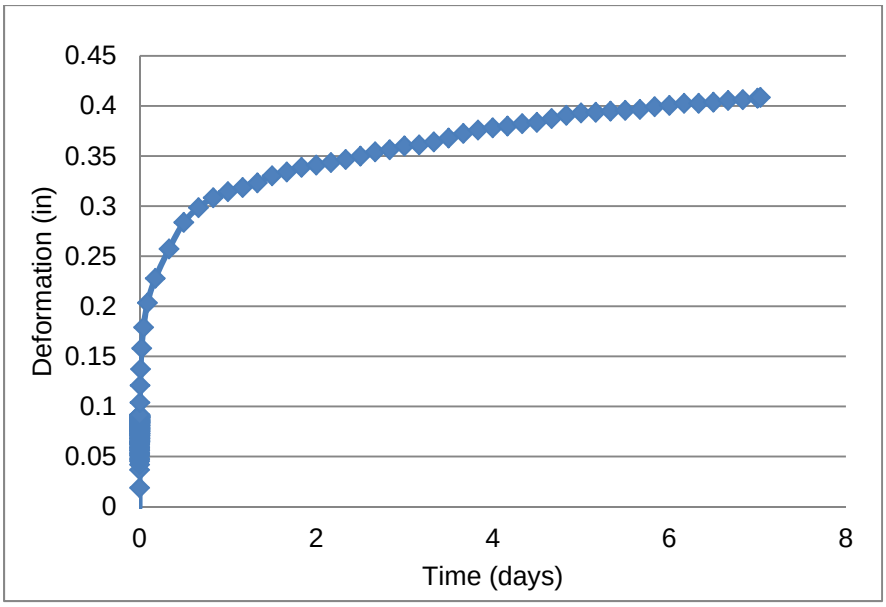

Figure C-23: Creep vs. Time Plot: Milled APAC Melbourne Pass No 8 S2

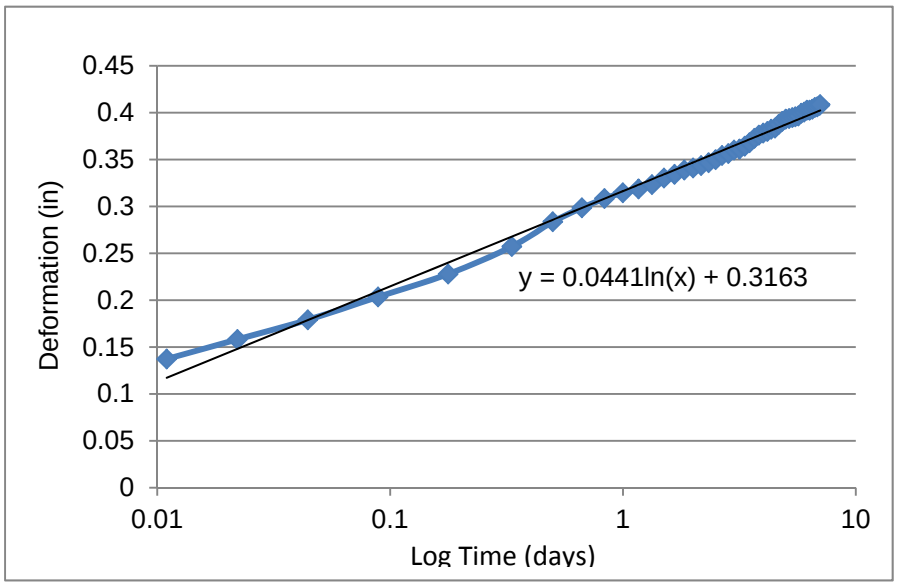

Figure C-24: Creep vs. Log Time Plot: Milled APAC Melbourne Pass No 8 S2

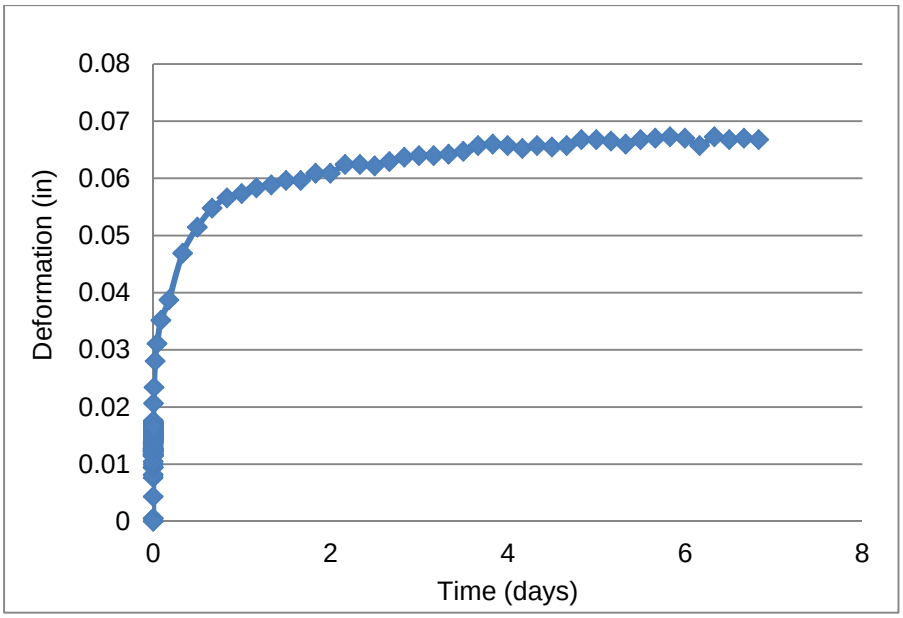

Figure C-25: Creep vs. Time Plot: Crushed Jacksonville Pass #8 S1

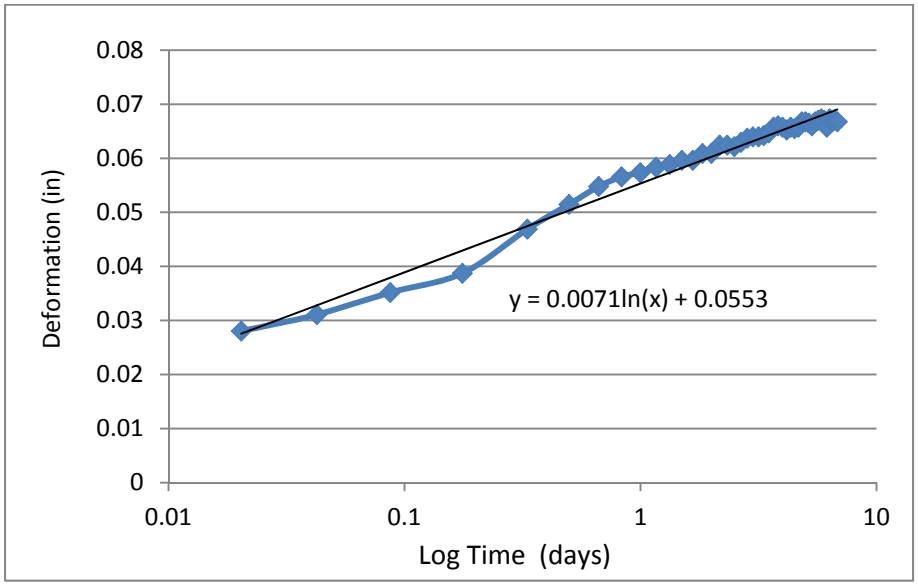

Figure C-26: Creep vs. Log Time Plot: Crushed Jacksonville Pass #8 S1

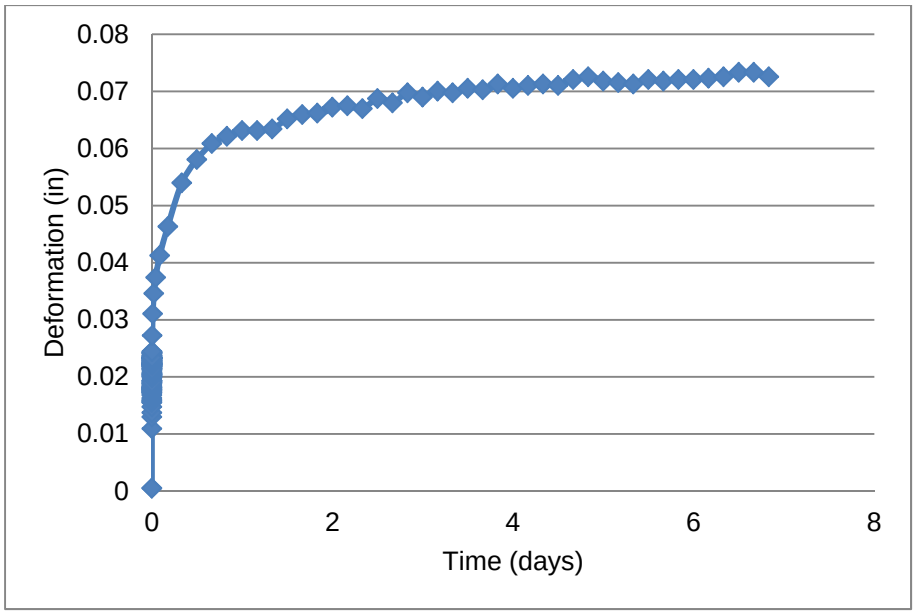

Figure C-27: Creep vs. Time Plot: Crushed Jacksonville Pass #8 S2

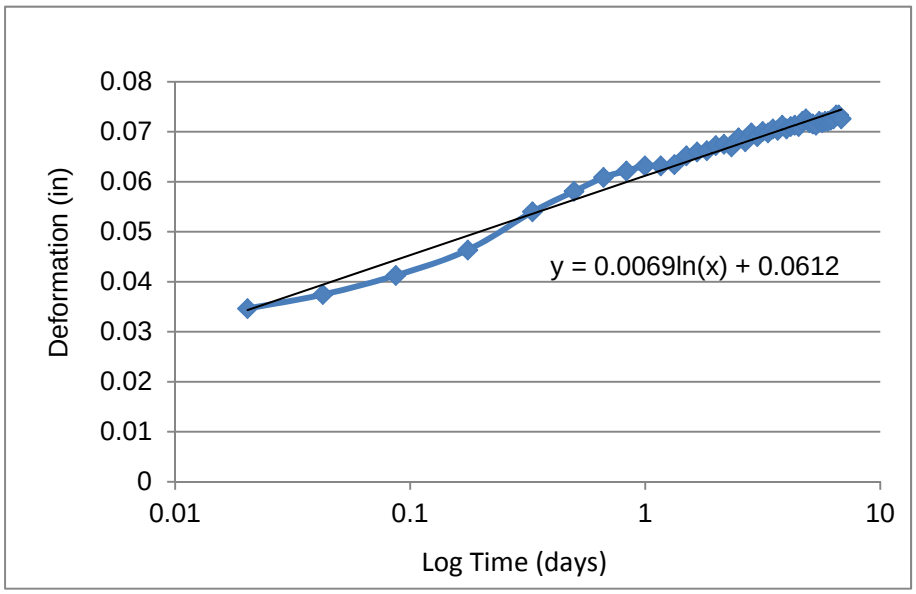

Figure C-28: Creep vs. Log Time Plot: Crushed Jacksonville Pass #8 S2

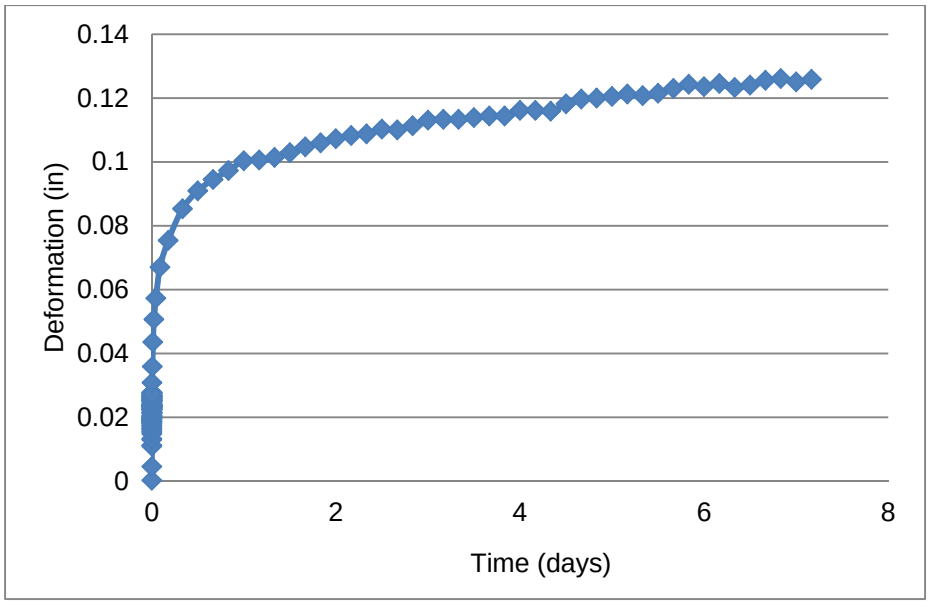

Figure C-29: Creep vs. Time Plot: Whitehurst Milled Passing #8 S1

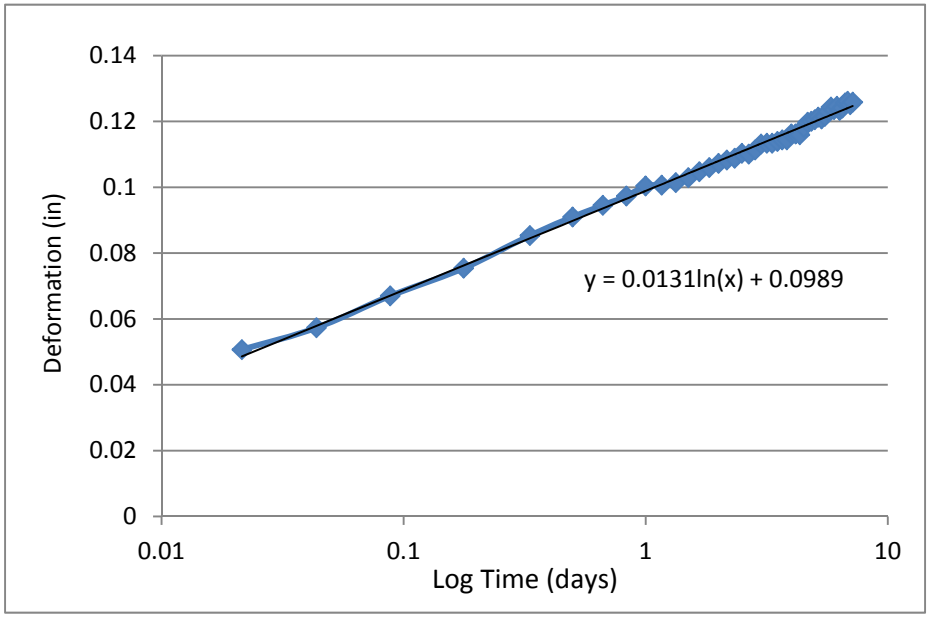

Figure C-30: Creep vs. Log Time Plot: Whitehurst Milled Passing #8 S1

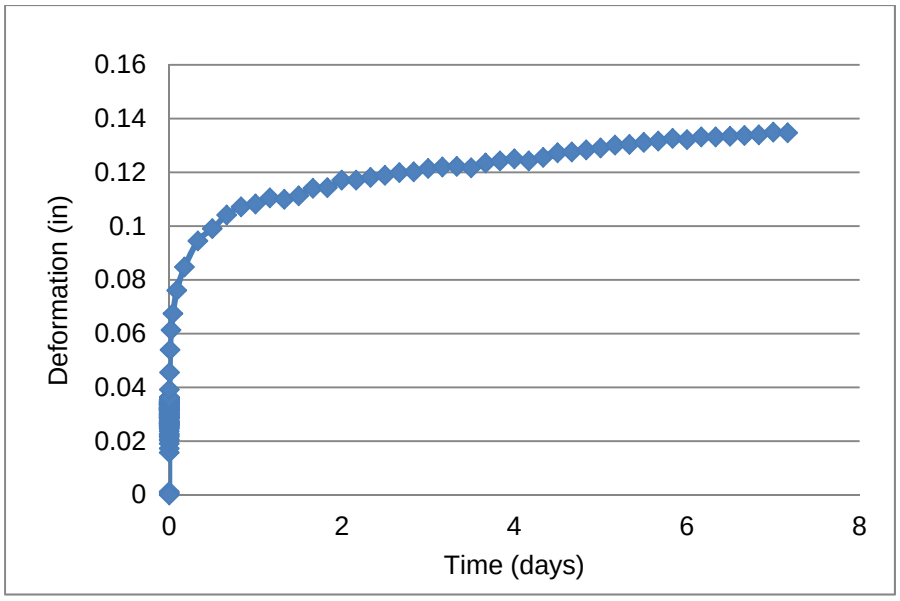

Figure C-31: Creep vs. Time Plot: Whitehurst Milled Passing #8 S2

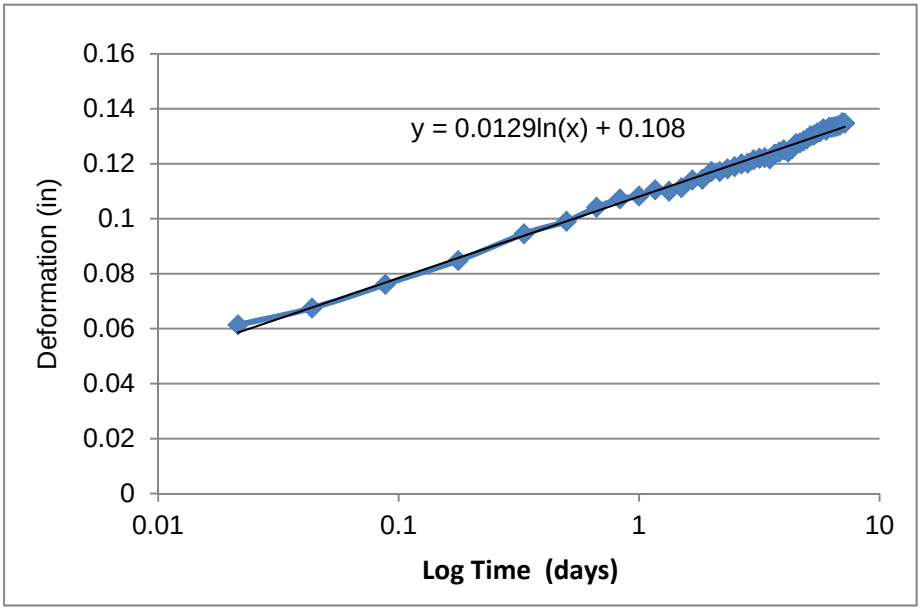

Figure C-32: Creep vs. Log Time Plot: Whitehurst Milled Passing #8 S2

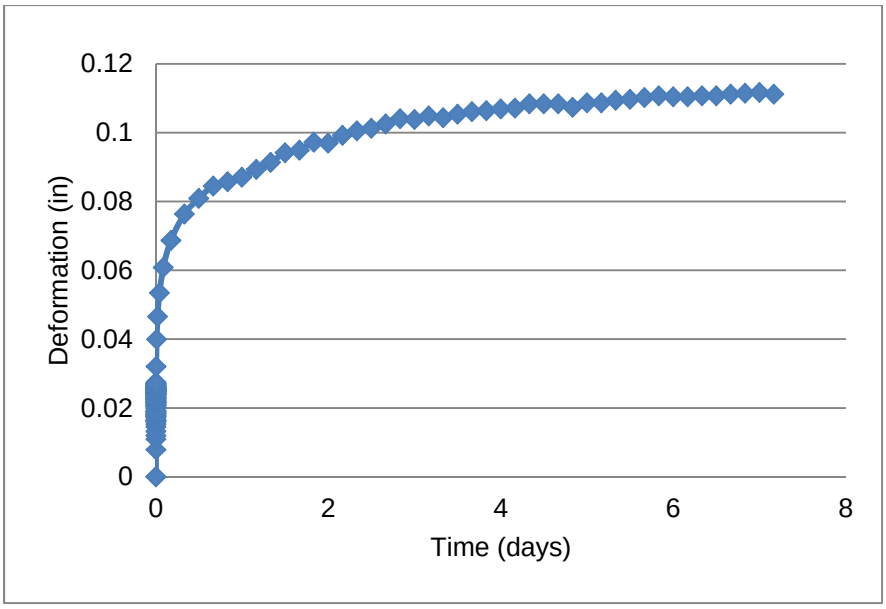

Figure C-33: Creep vs. Time Plot: Crushed APAC Mel Pass #4 S1

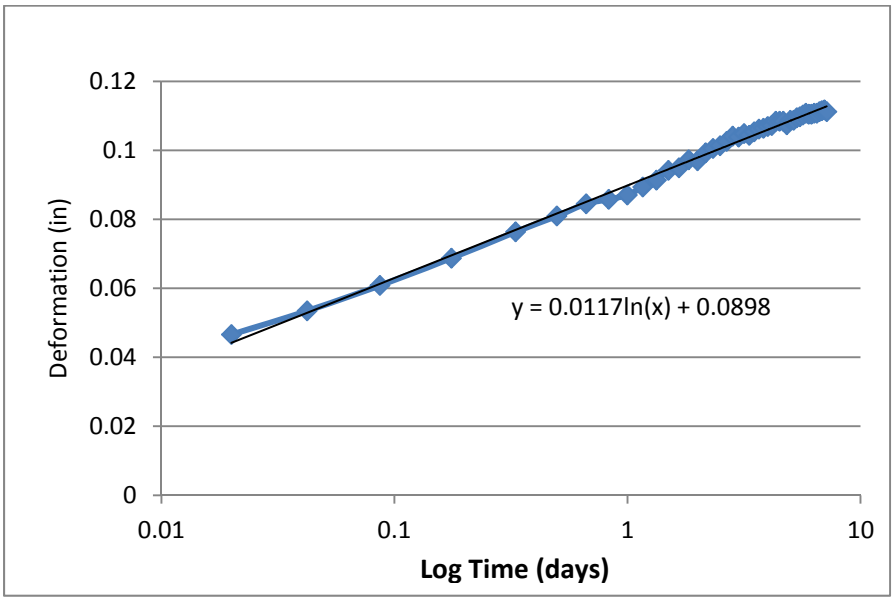

Figure C-34: Creep vs. Log Time Plot: Crushed APAC Mel Pass #4 S1

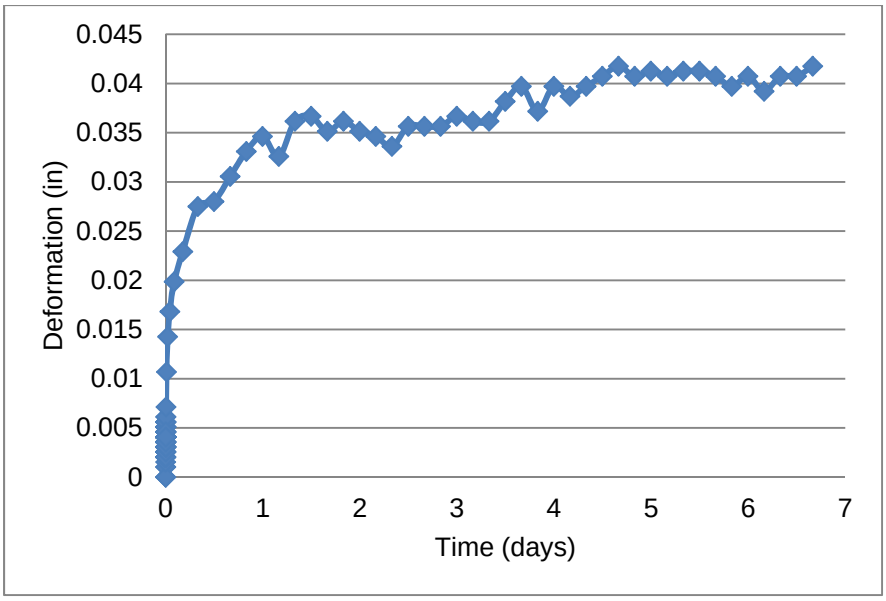

Figure C-35: Creep vs. Time Plot: Milled APAC Mel Pass #4 S1

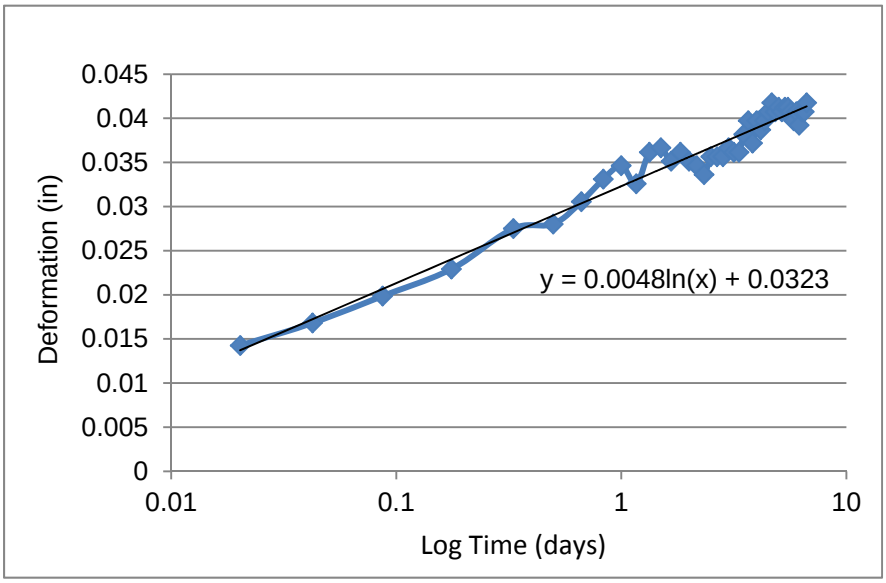

Figure C-36: Creep vs. Log Time Plot: Milled APAC Mel Pass #4 S1

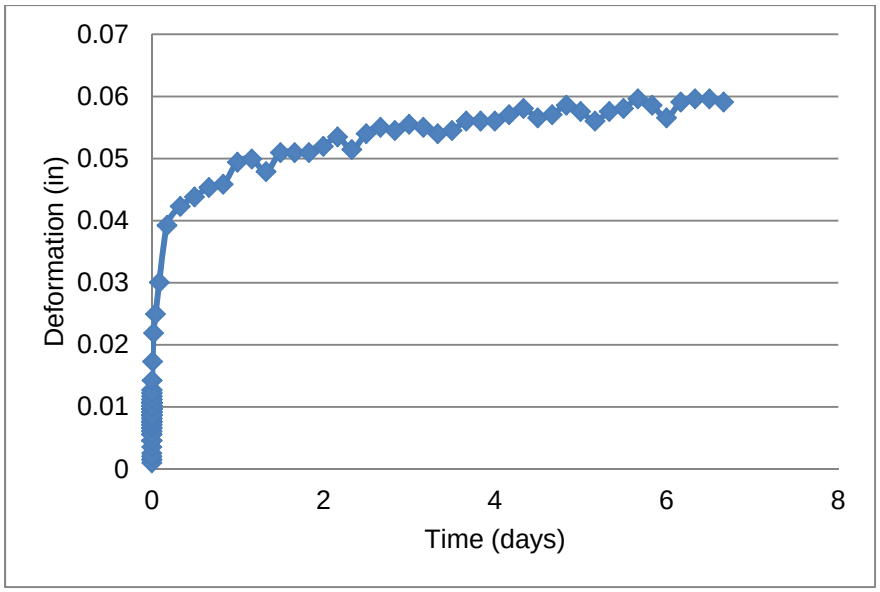

Figure C-37: Creep vs. Time Plot: Milled APAC Mel Pass #4 S2

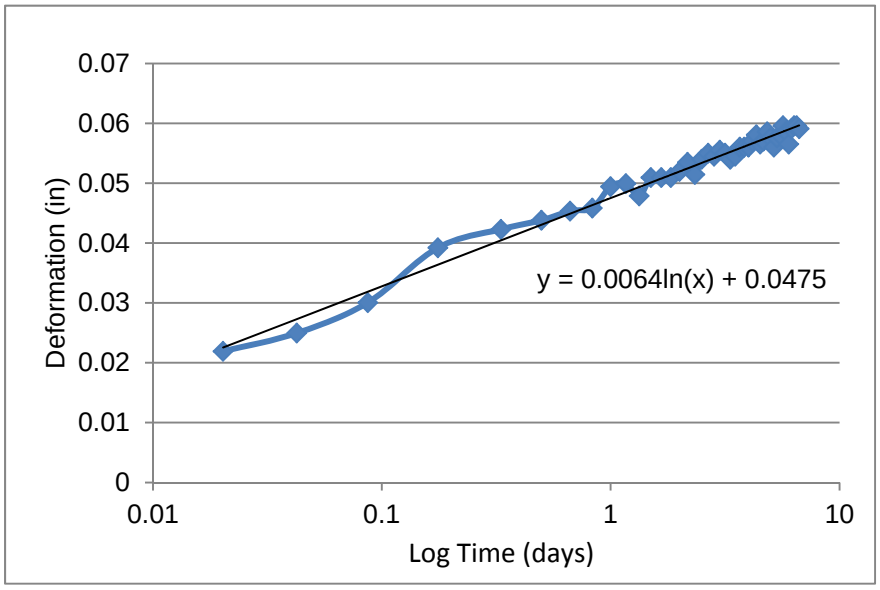

Figure C-38: Creep vs. Log Time Plot: Milled APAC Mel Pass #4 S2

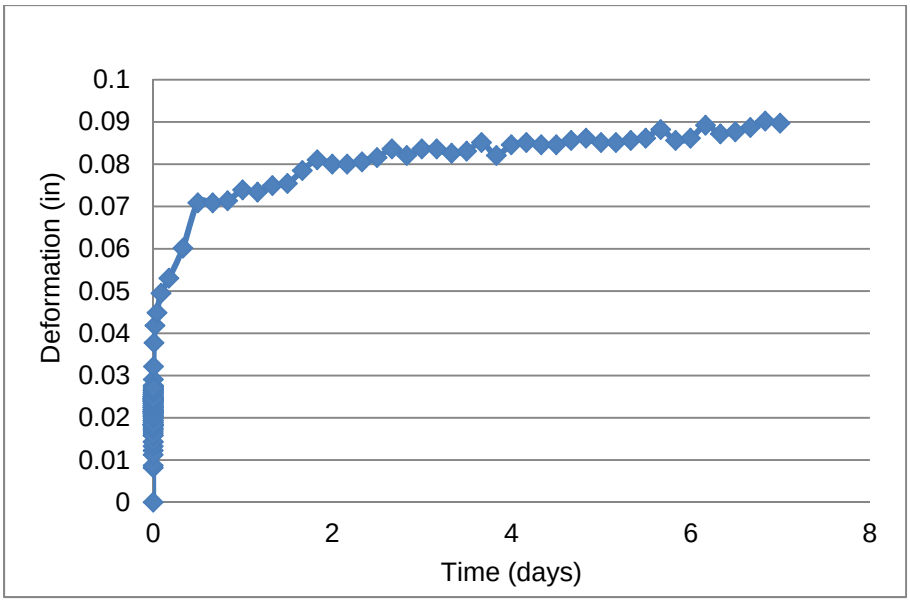

Figure C-39: Creep vs. Time Plot: Crushed APAC Jacksonville Pass #4 S1

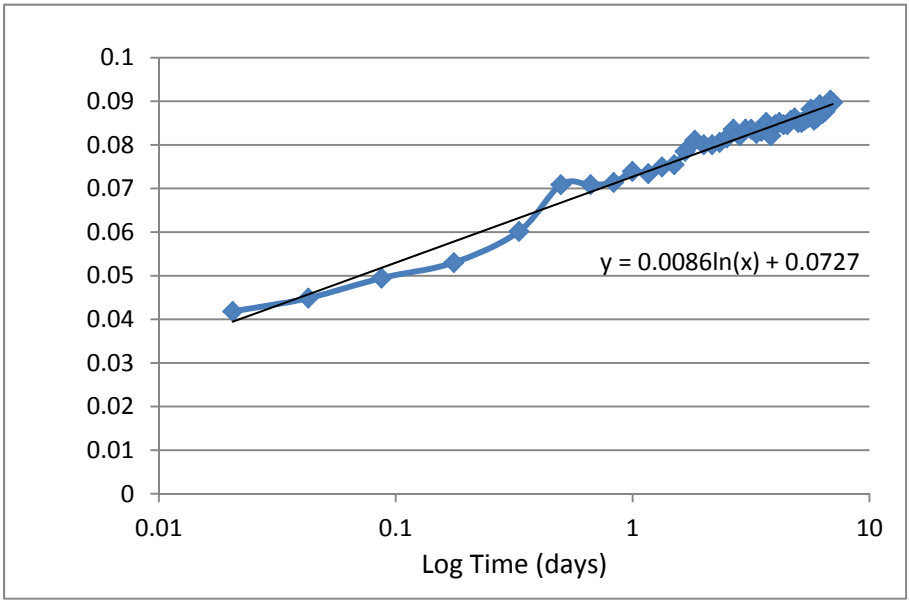

Figure C-40: Creep vs. Log Time Plot: Crushed APAC Jacksonville Pass #4 S1

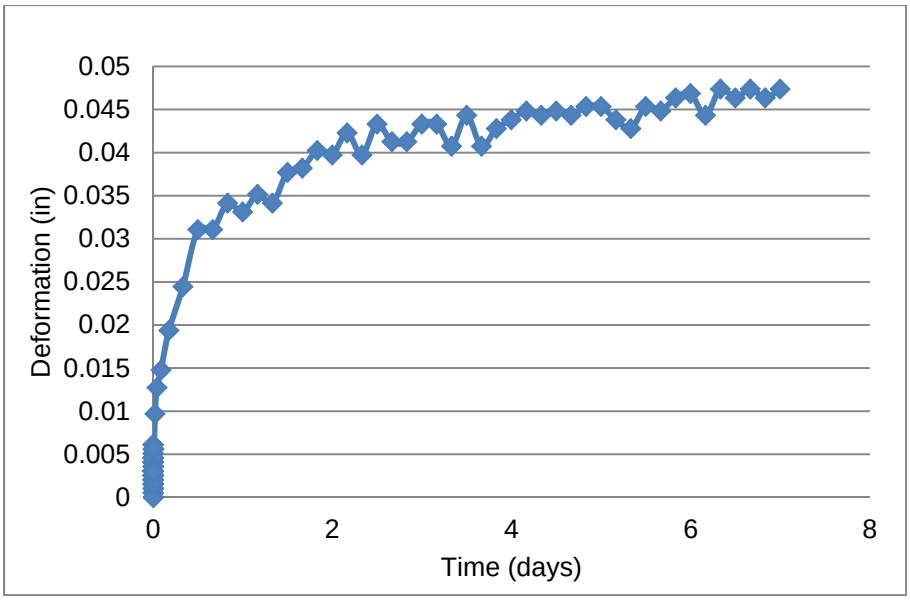

Figure C-41: Creep vs. Time Plot: Crushed APAC Jacksonville Pass #4 S2

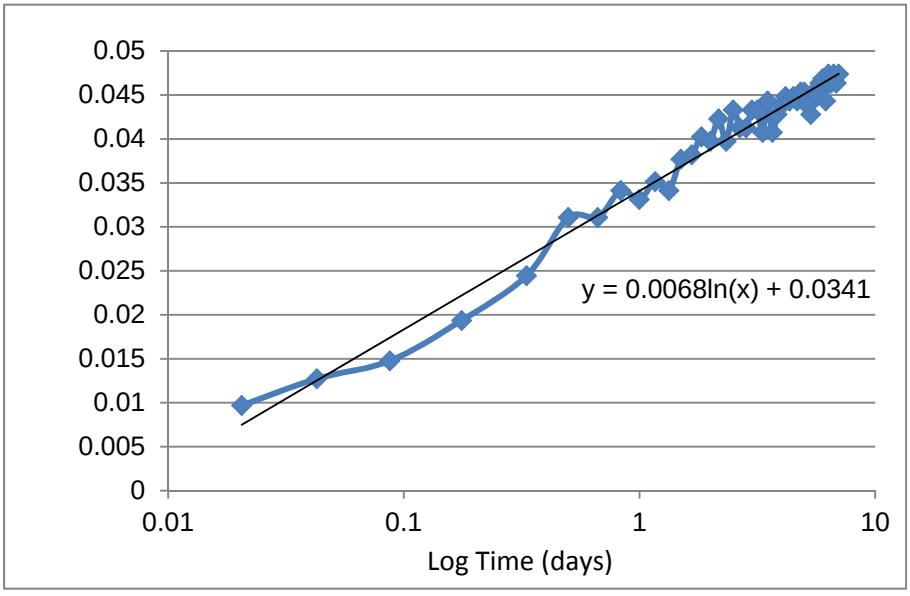

Figure C-42: Creep vs. Log Time Plot: Crushed APAC Jacksonville Pass #4 S2

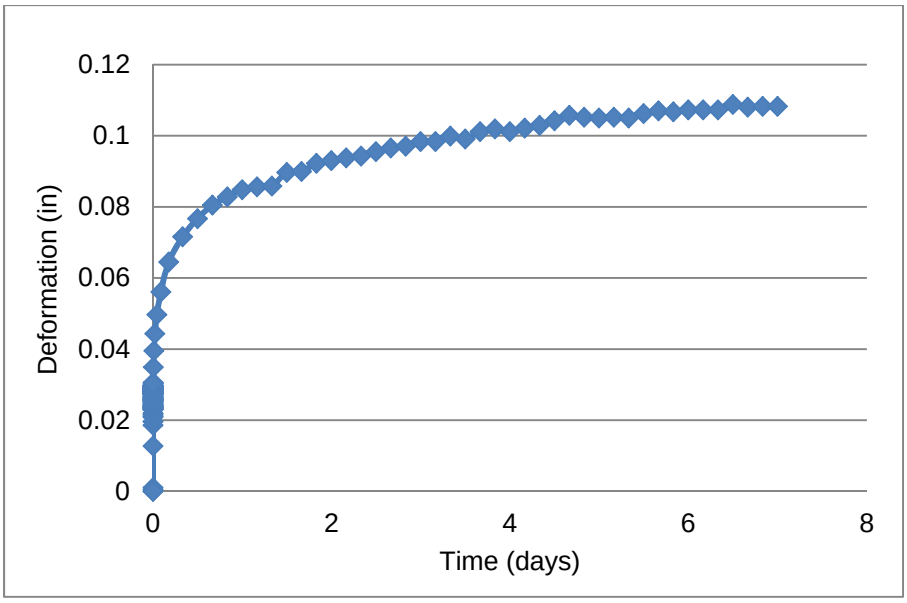

Figure C-43: Creep vs. Time Plot: Milled Whitehurst Pass # 4 S1

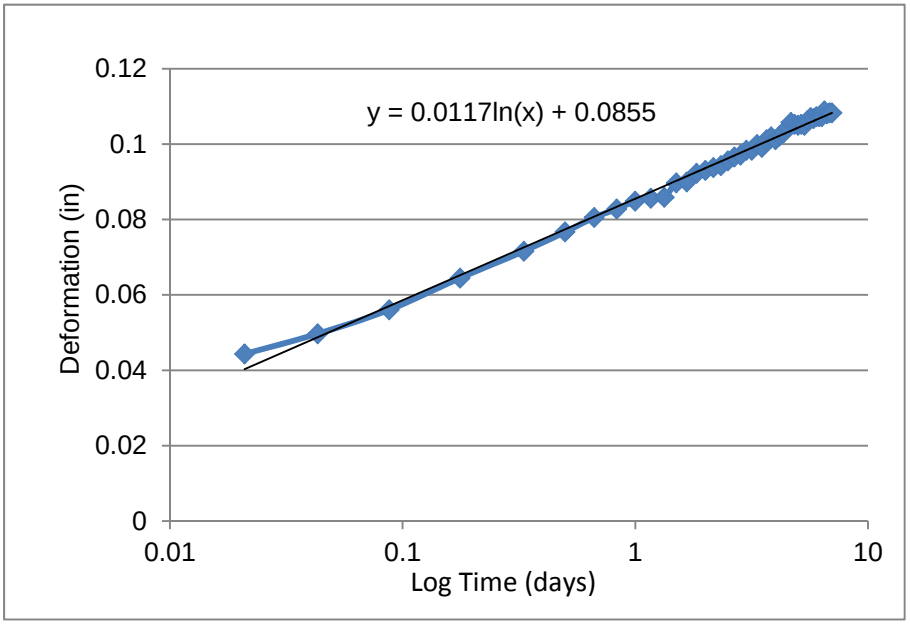

Figure C-44: Creep vs. Log Time Plot: Milled Whitehurst Pass # 4 S1

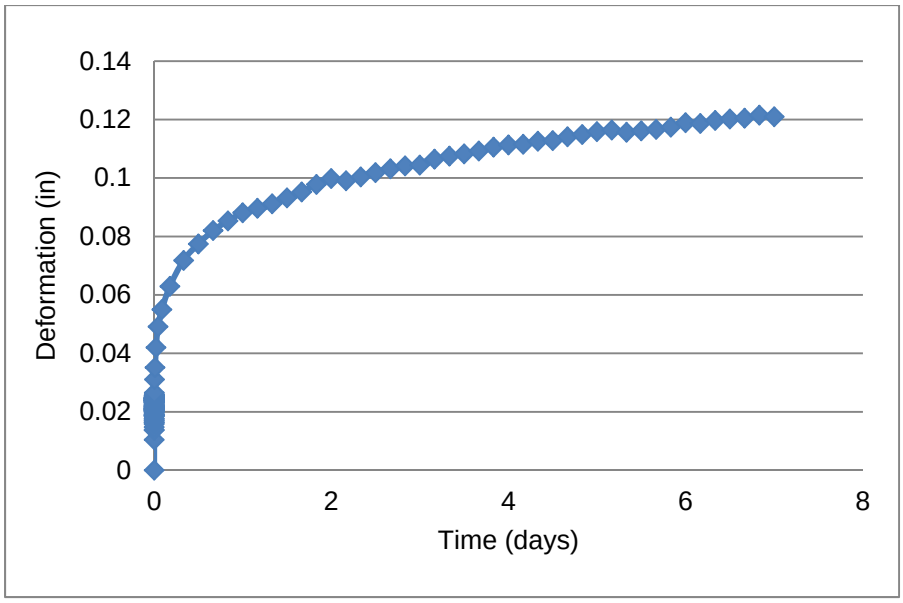

Figure C-45: Creep vs. Time Plot: Milled Whitehurst Pass # 4 S2

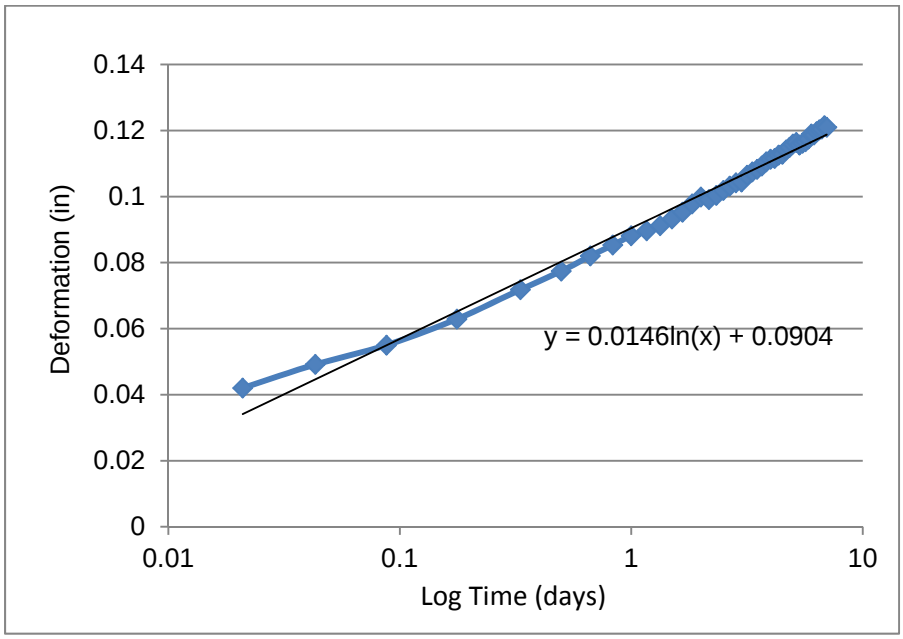

Figure C-46: Creep vs. Log Time Plot: Milled Whitehurst Pass # 4 S2

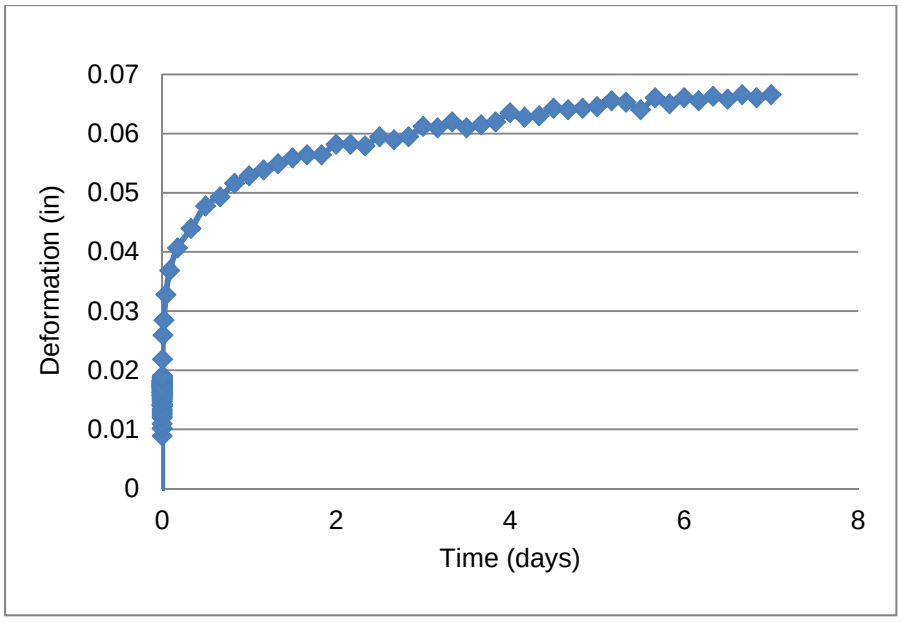

Figure C-47: Creep vs. Time Plot: Crushed APAC Melbourne Non-Segregated S1

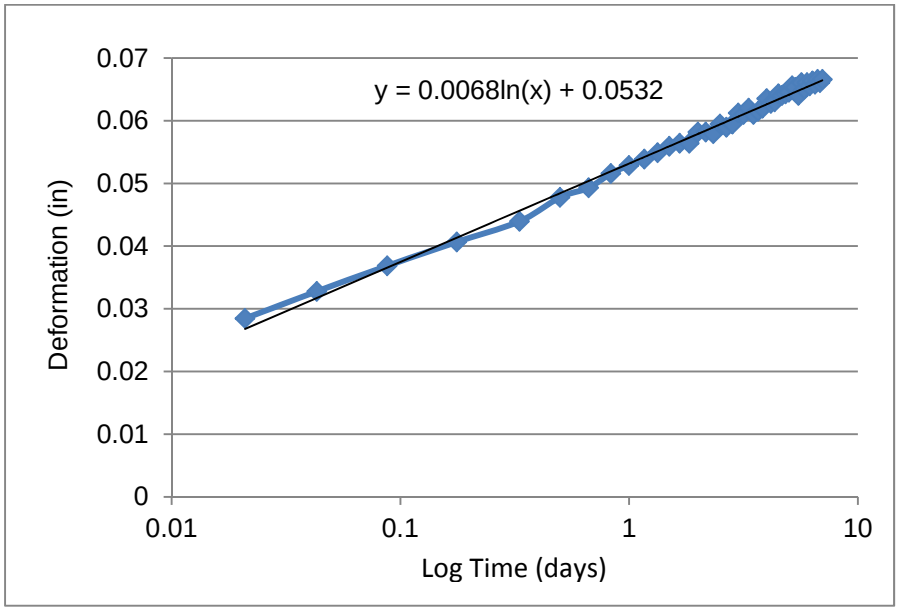

Figure C-48: Creep vs. Log Time Plot: Crushed APAC Melbourne Non-Segregated S1

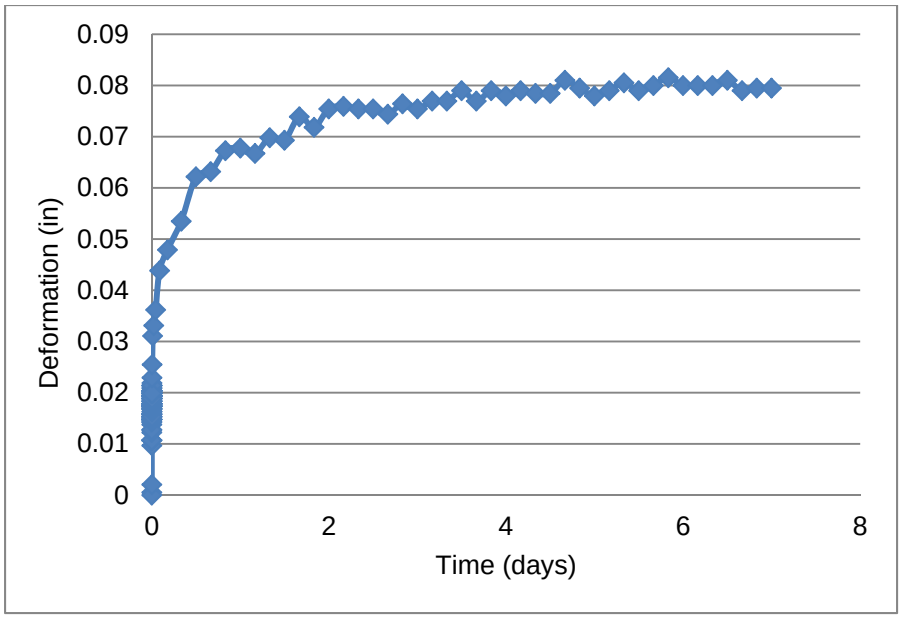

Figure C-49: Creep vs. Time Plot: Crushed APAC Melbourne Non-Segregated S2

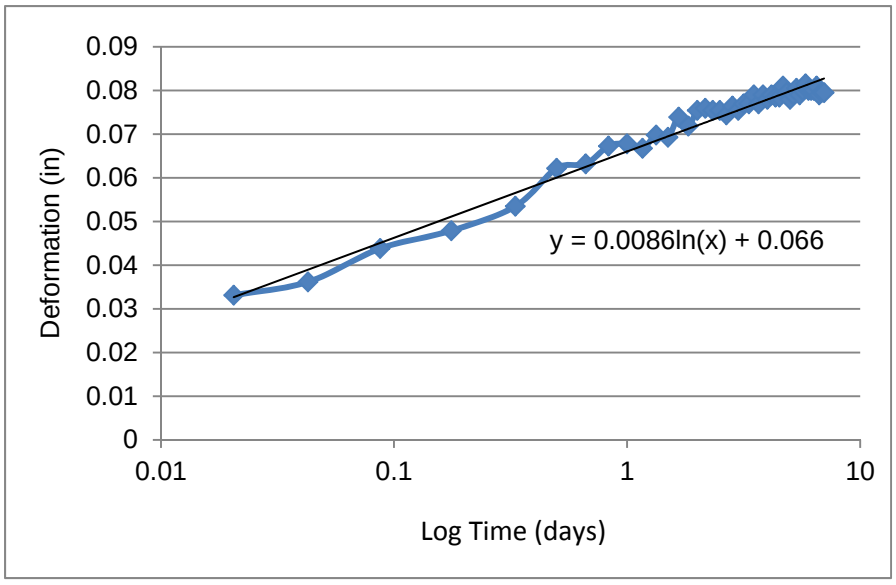

Figure C-50: Creep vs. Log Time Plot: Crushed APAC Melbourne Non-Segregated S2

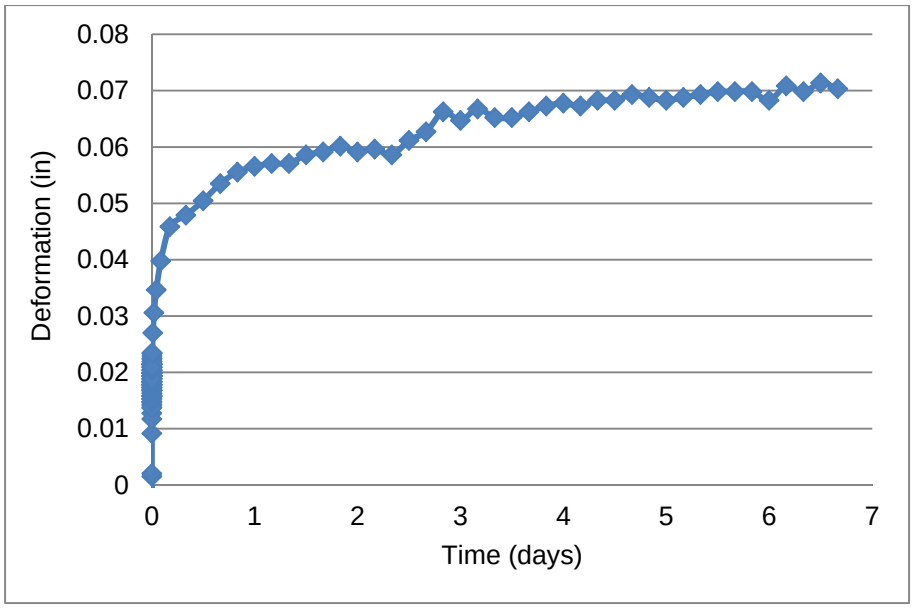

Figure C-51: Creep vs. Time Plot: Milled APAC Melbourne Non-Segregated RAP S1

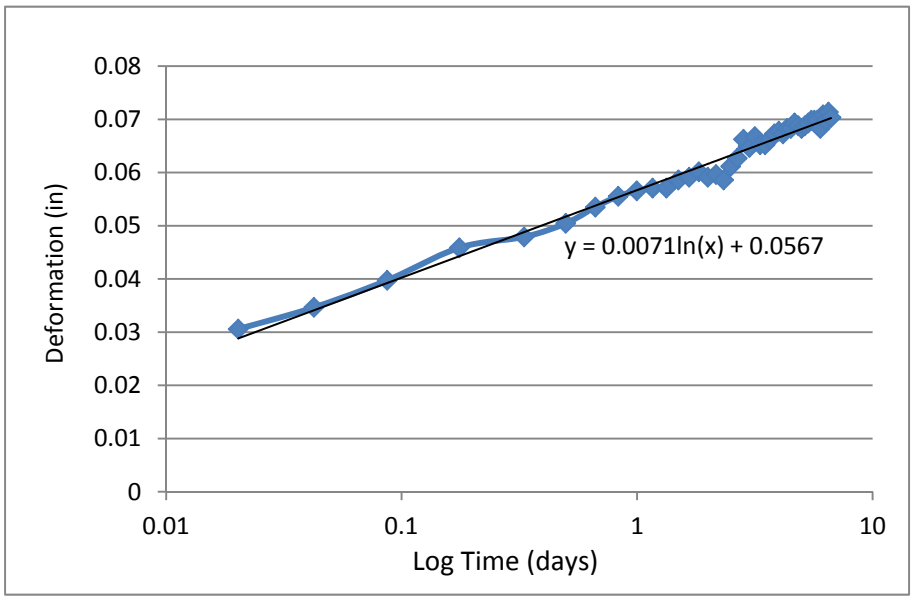

Figure C-52: Creep vs. Log Time Plot: Milled APAC Melbourne Non-Segregated RAP S1

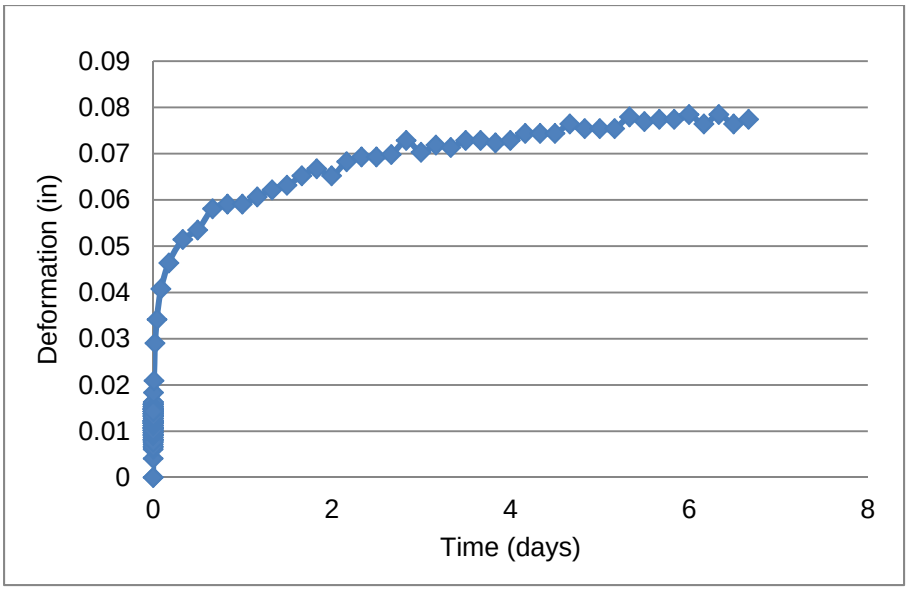

Figure C-53: Creep vs. Time Plot: Milled APAC Melbourne Non-Segregated RAP S2

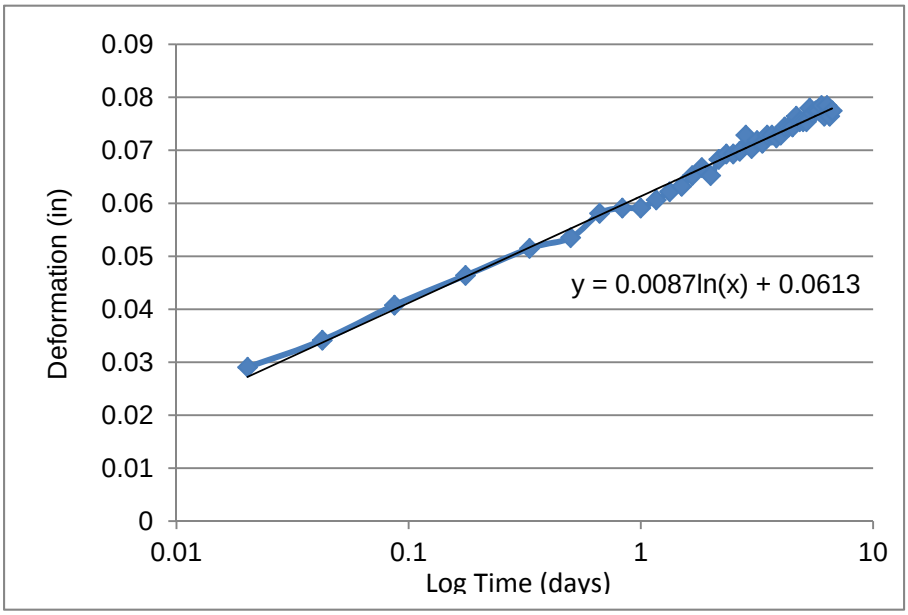

Figure C-54: Creep vs. Log Time Plot: Milled APAC Melbourne Non-Segregated RAP S2

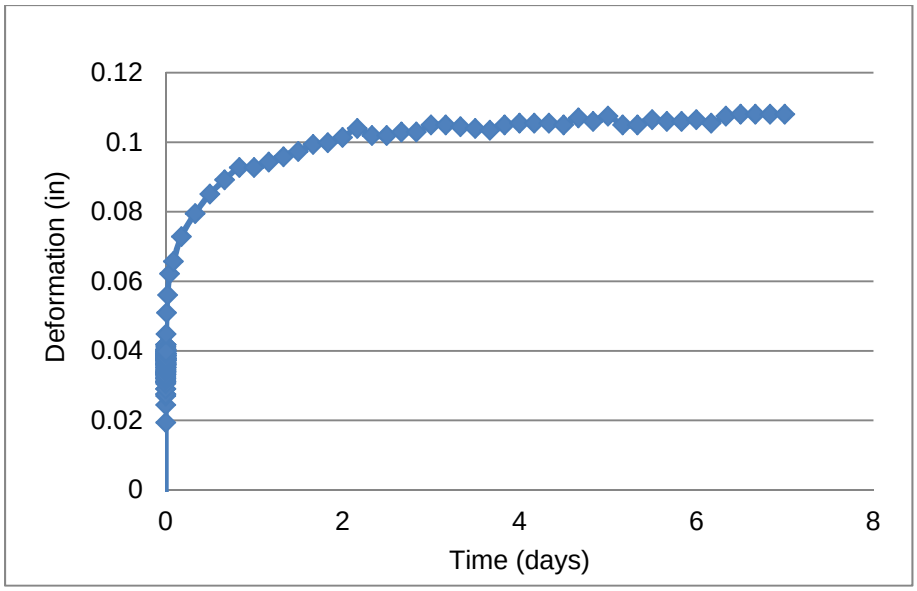

Figure C-55: Creep vs. Time Plot: Crushed APAC Jacksonville non fractionated RAP S1

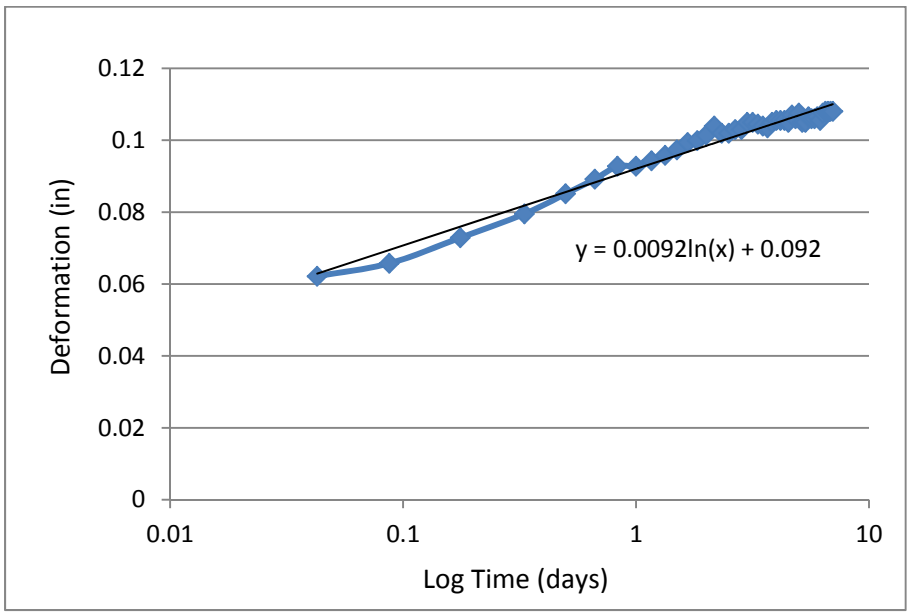

Figure C-56:Creep vs. Log Time Plot: Crushed APAC Jacksonville non fractionated RAP S1

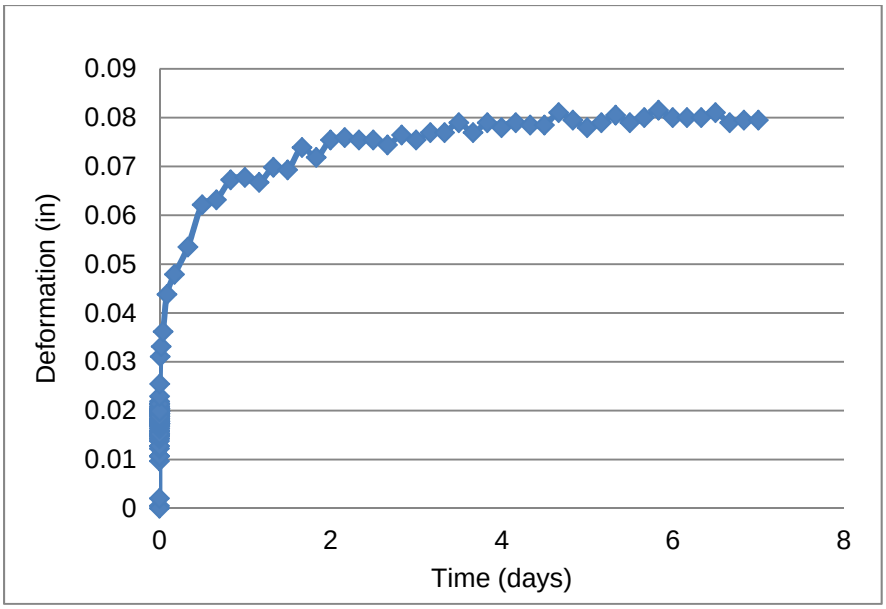

Figure C-57: Creep vs. Time Plot: Crushed APAC Jacksonville non fractionated RAP S2

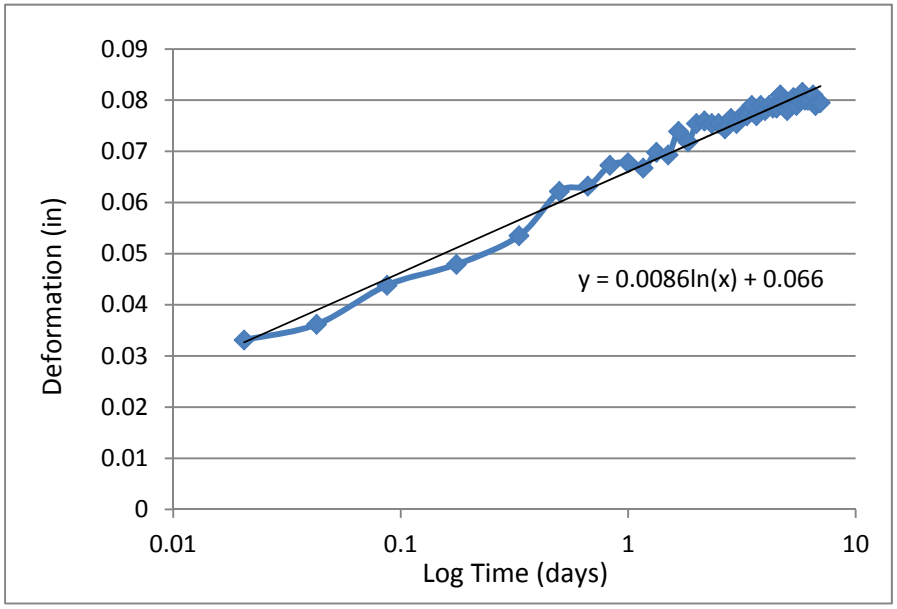

Figure C-58:Creep vs. Log Time Plot: Crushed APAC Jacksonville non fractionated RAP S2

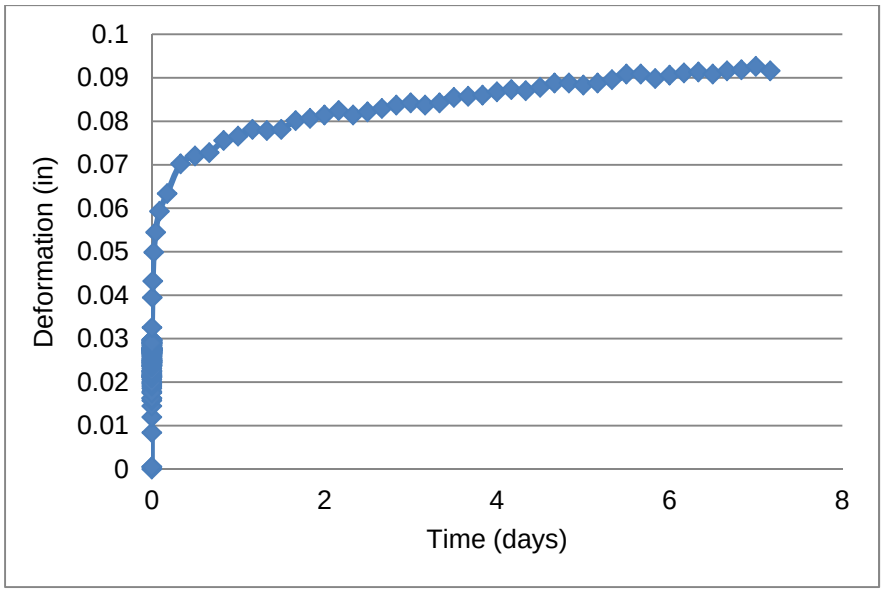

Figure C-59: Creep vs. Time Plot: Milled Non-Segregated Whitehurst S1

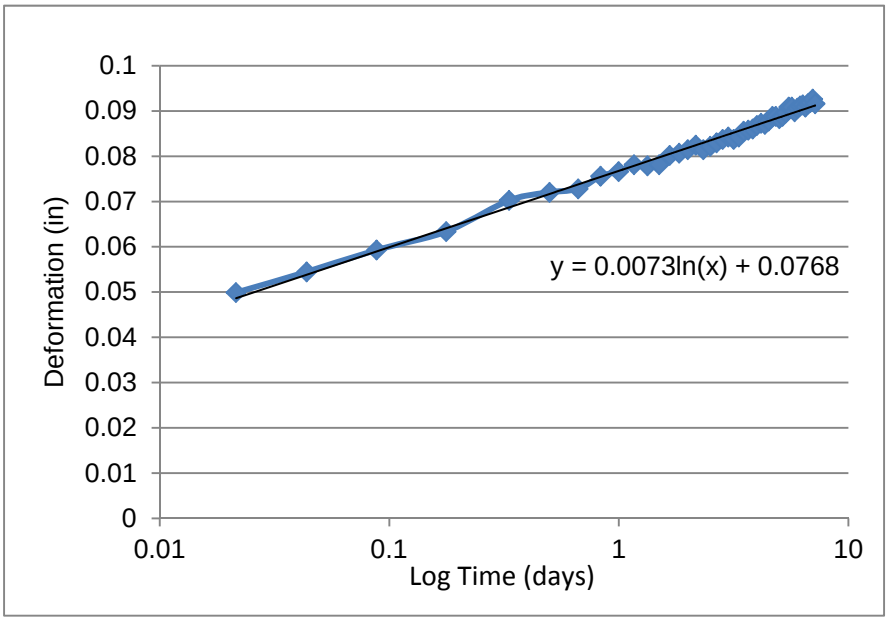

Figure C-60: Creep vs. Log Time Plot: Milled Non-Segregated Whitehurst S1

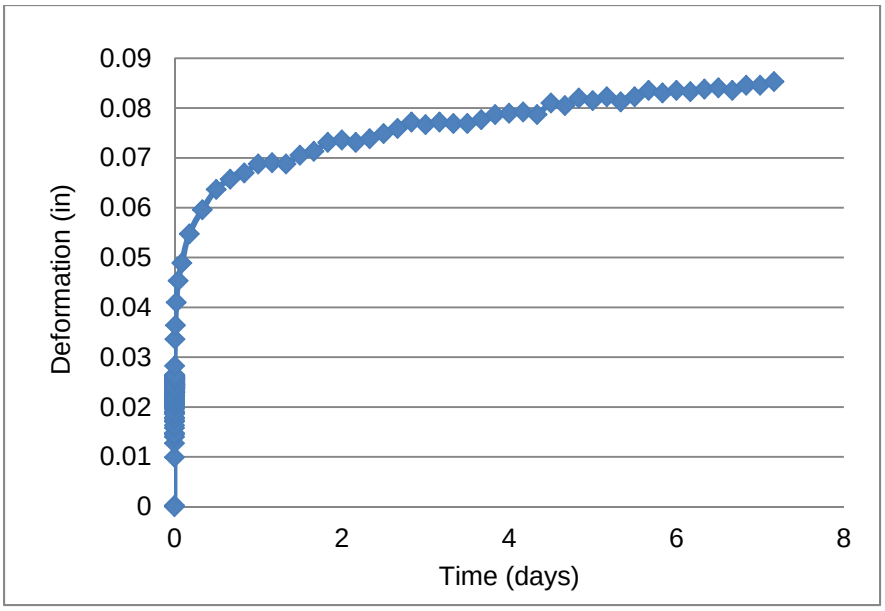

Figure C-61: Creep vs. Time Plot: Milled Non-Segregated Whitehurst S2

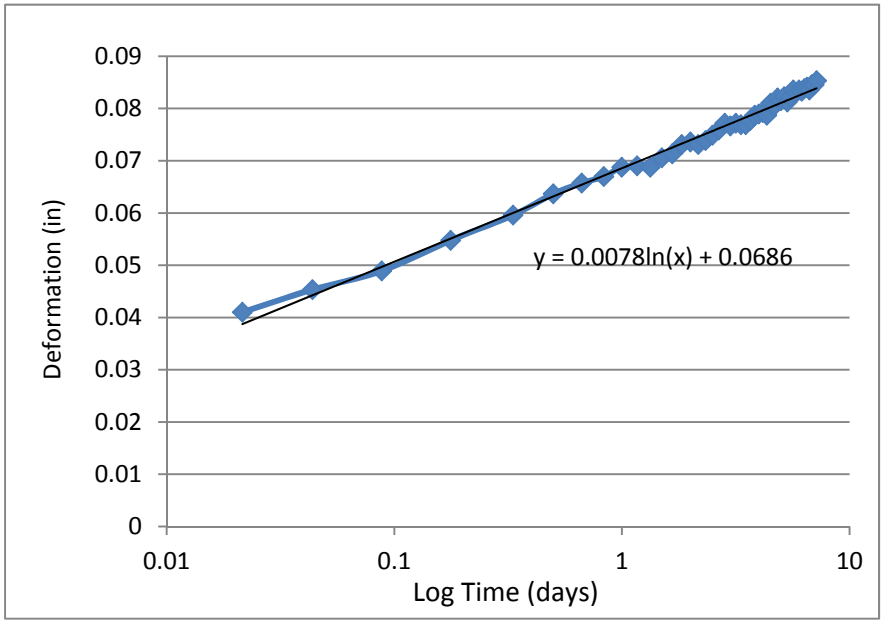

Figure C-62: Creep vs. Log Time Plot: Milled Non-Segregated Whitehurst S2

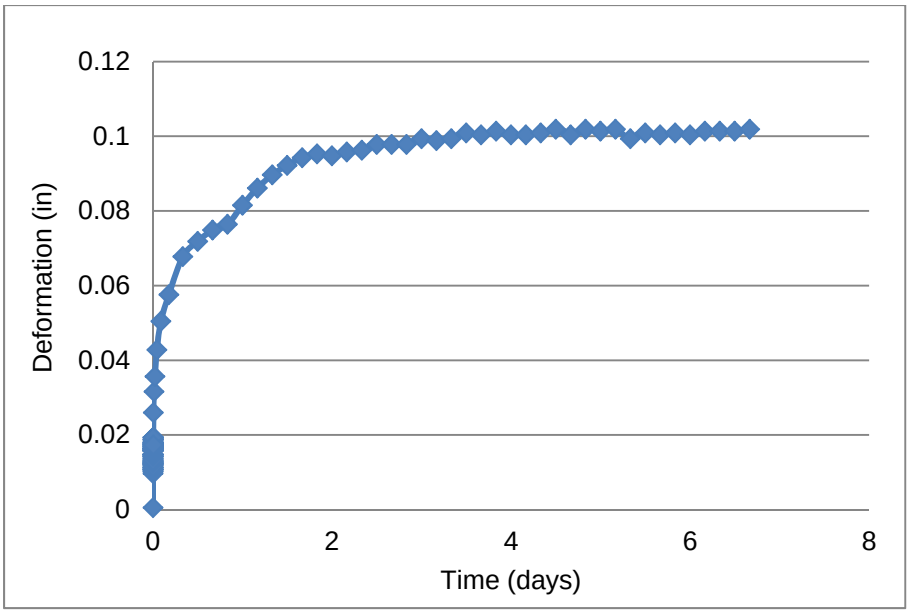

Figure C-63: Creep vs. Time Plot: Crushed APAC Mel Retained #4 S1

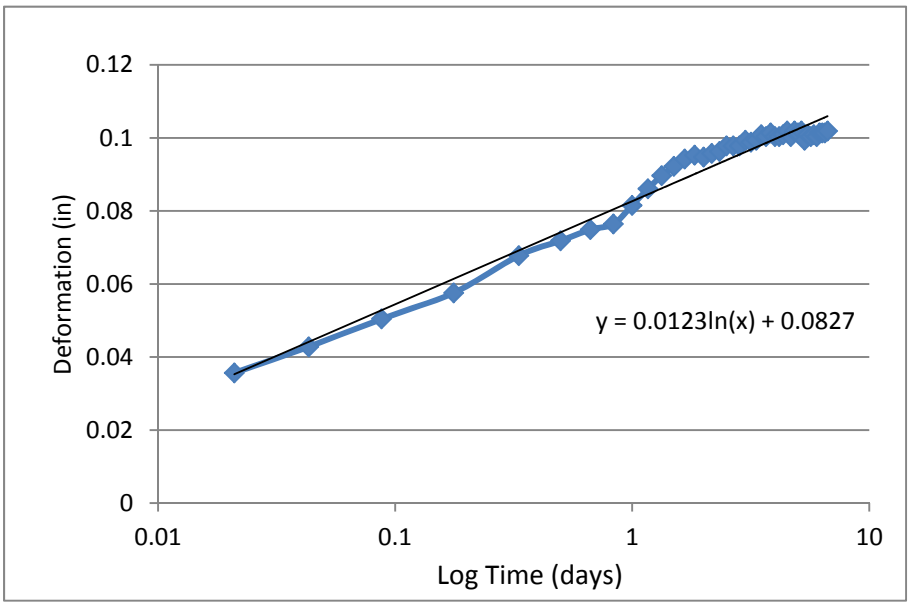

Figure C-64: Creep vs. Log Time Plot: Crushed APAC Mel Retained #4 S1

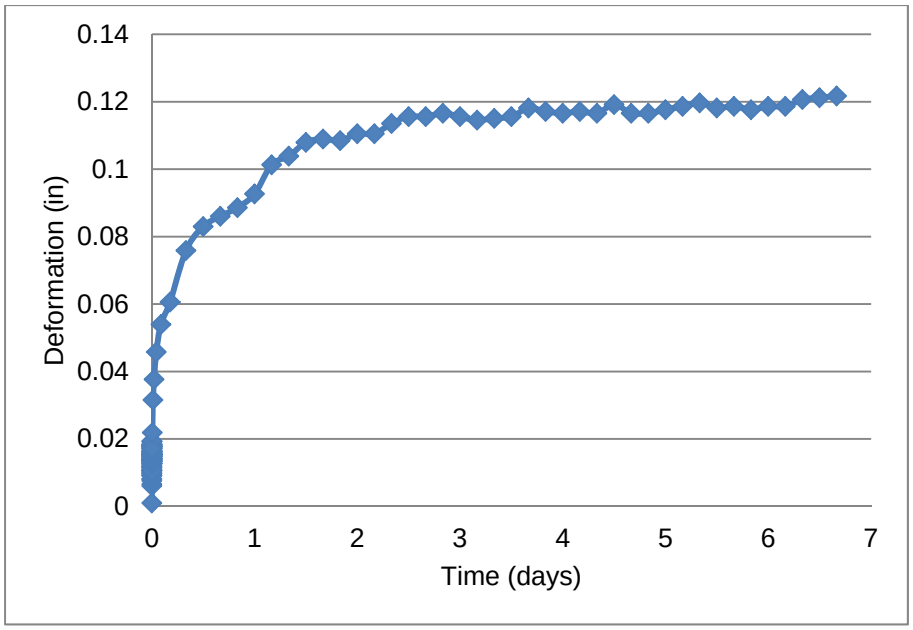

Figure C-65: Creep vs. Time Plot: Crushed APAC Mel Retained #4 S2

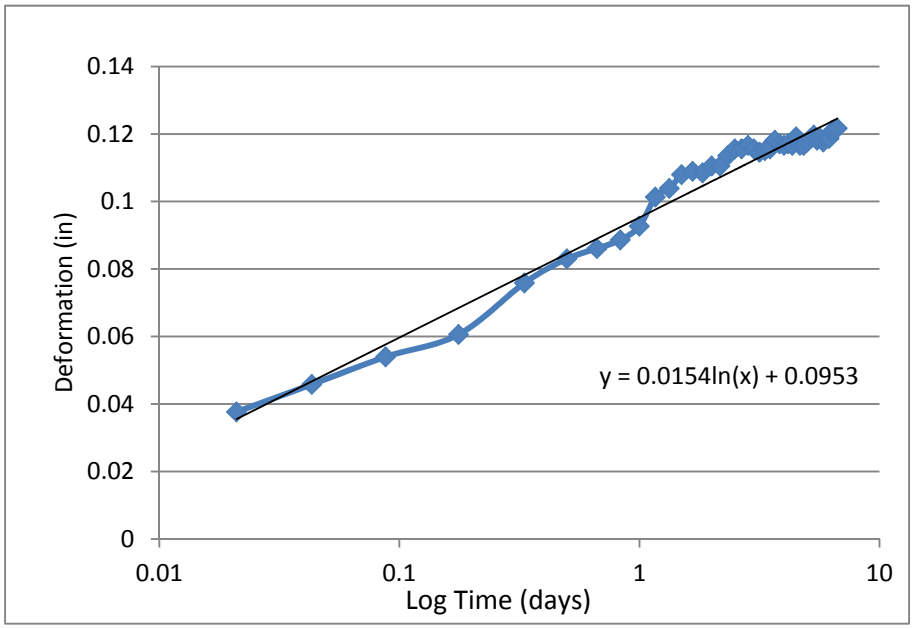

Figure C-66: Creep vs. Log Time Plot: Crushed APAC Mel Retained #4 S2

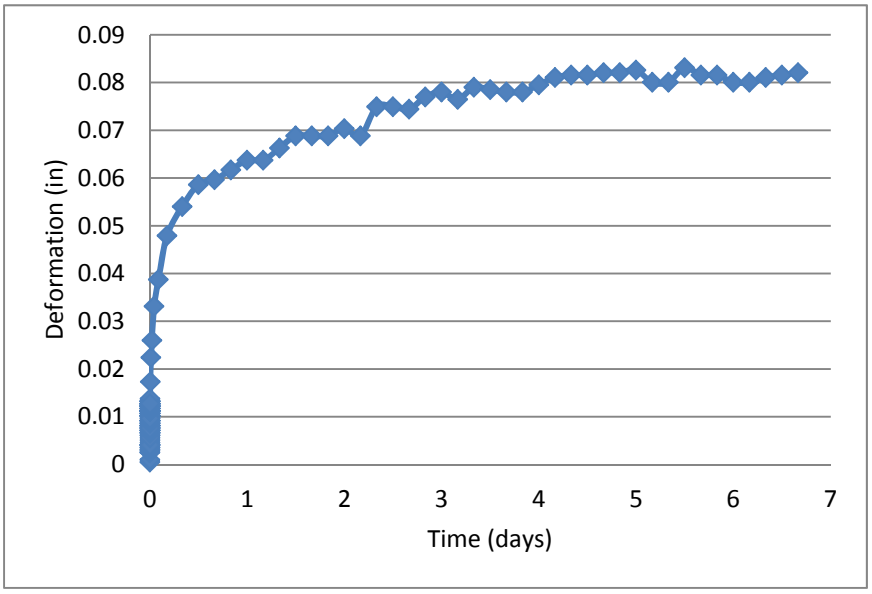

Figure C-67: Creep vs. Time Plot: Milled APAC Mel Retained #4 S1

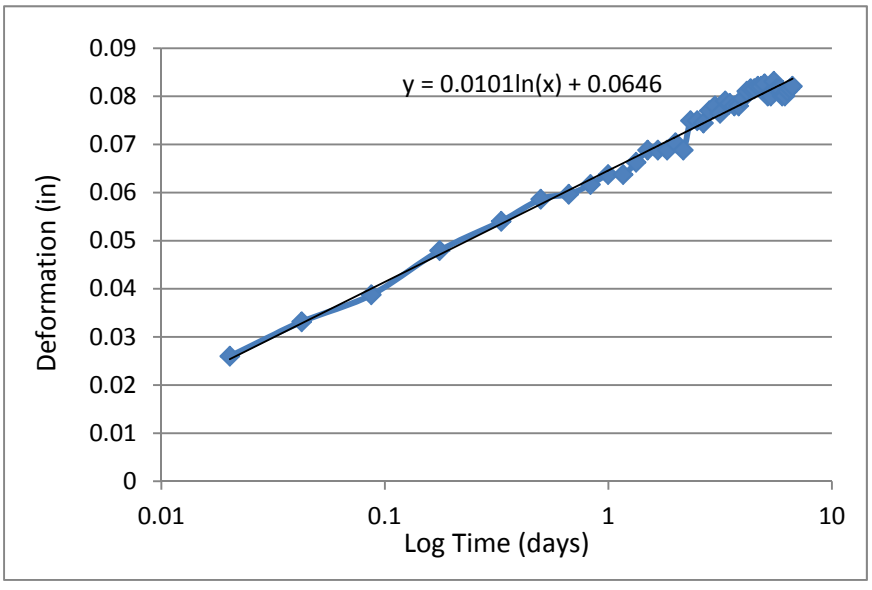

Figure C-68: Creep vs. Log Time Plot: Milled APAC Mel Retained #4 S1

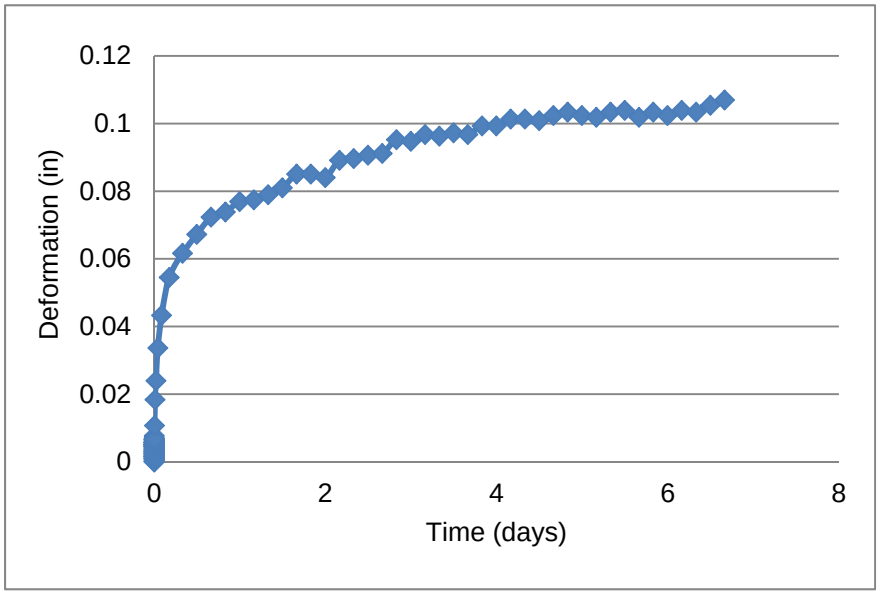

Figure C-69: Creep vs. Time Plot: Milled APAC Mel Retained #4 S2

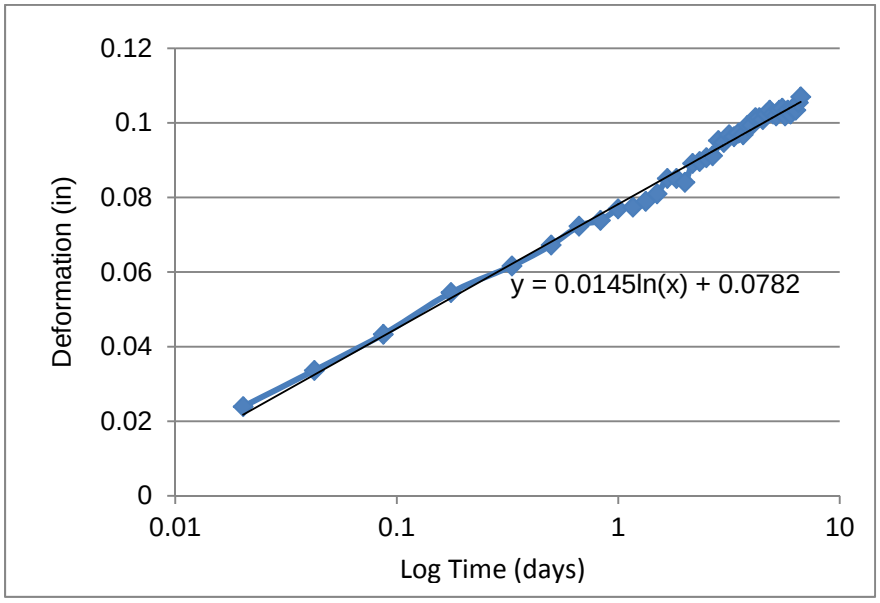

Figure C-70: Creep vs. Log Time Plot: Milled APAC Mel Retained #4 S2

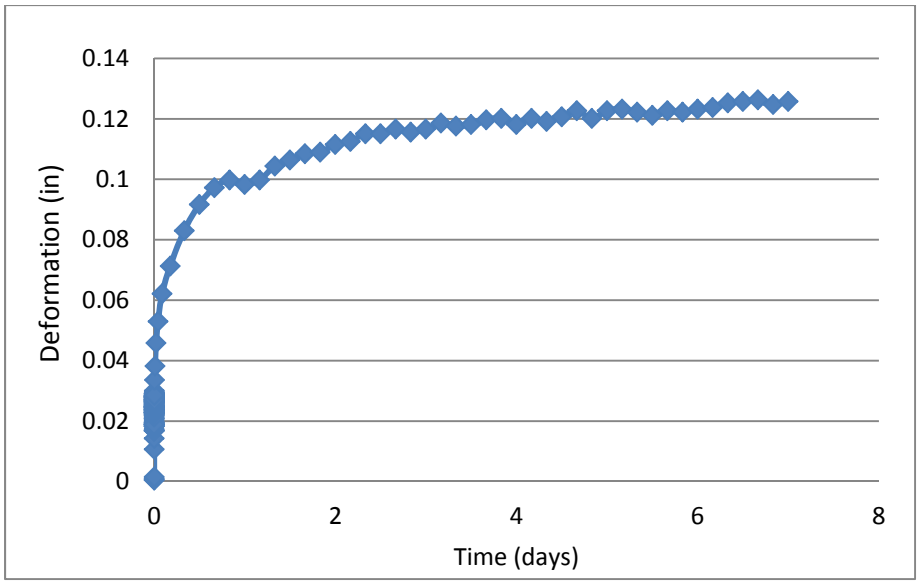

Figure C-71: Creep vs. Time Plot: Crushed APAC Jacksonville Retained #4 S1

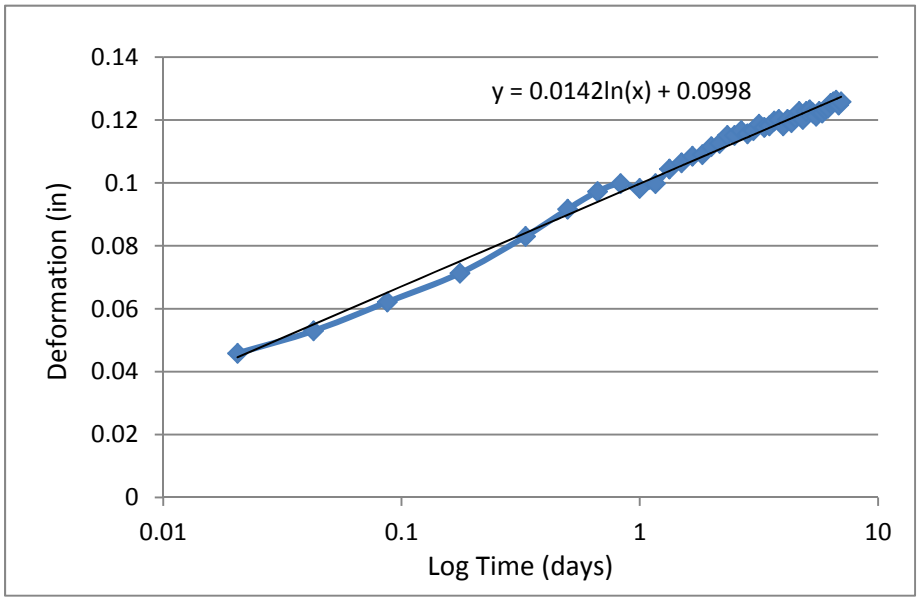

Figure C-72: Creep vs. Log Time Plot: Crushed APAC Jacksonville Retained #4 S1

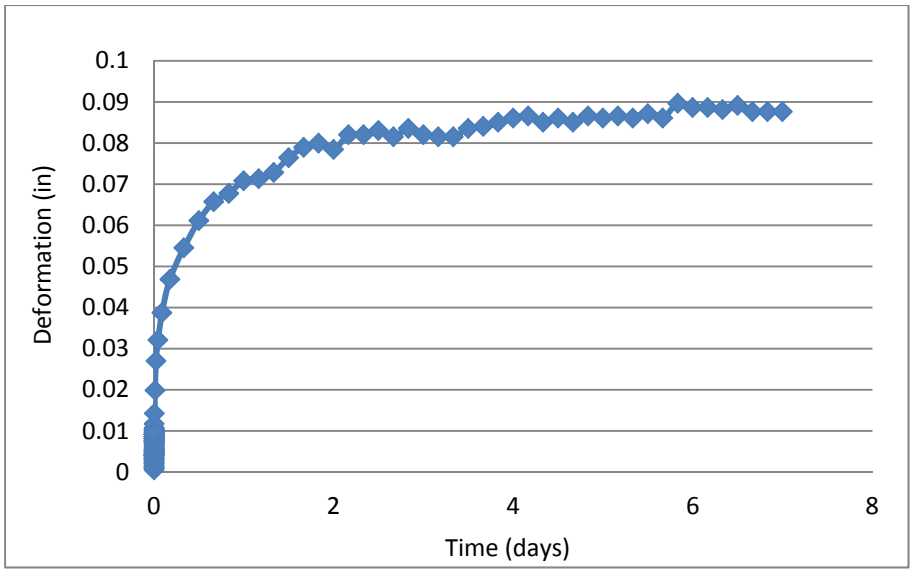

Figure C-73: Creep vs. Time Plot: Crushed APAC Jacksonville Retained #4 S2

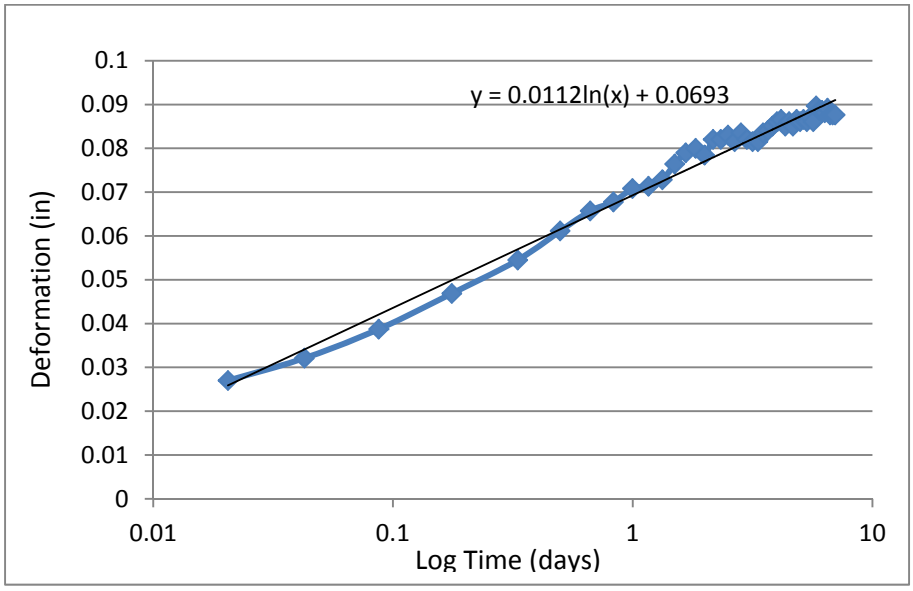

Figure C-74: Creep vs. Log Time Plot: Crushed APAC Jacksonville Retained #4 S2

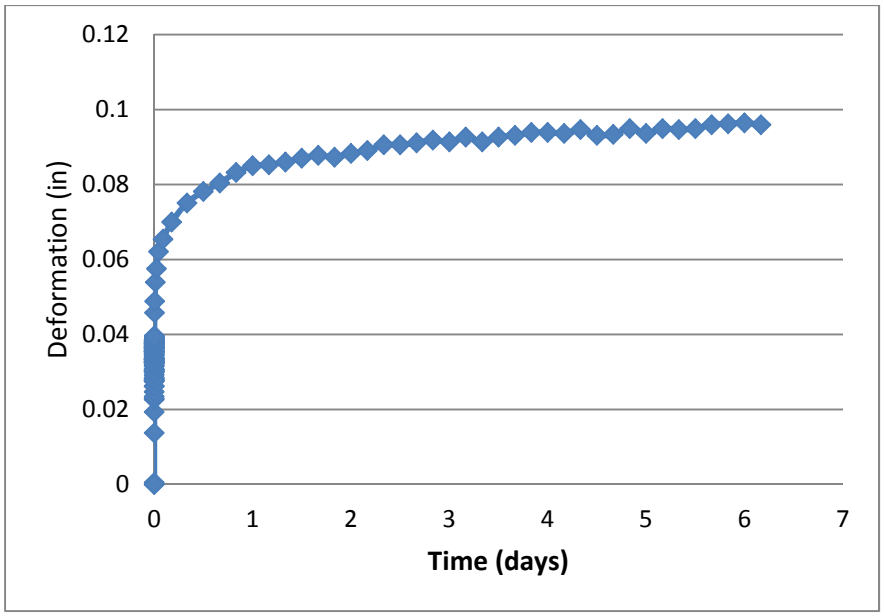

Figure C-75: Creep vs. Time Plot: Whitehurst Milled Retained #4 S1

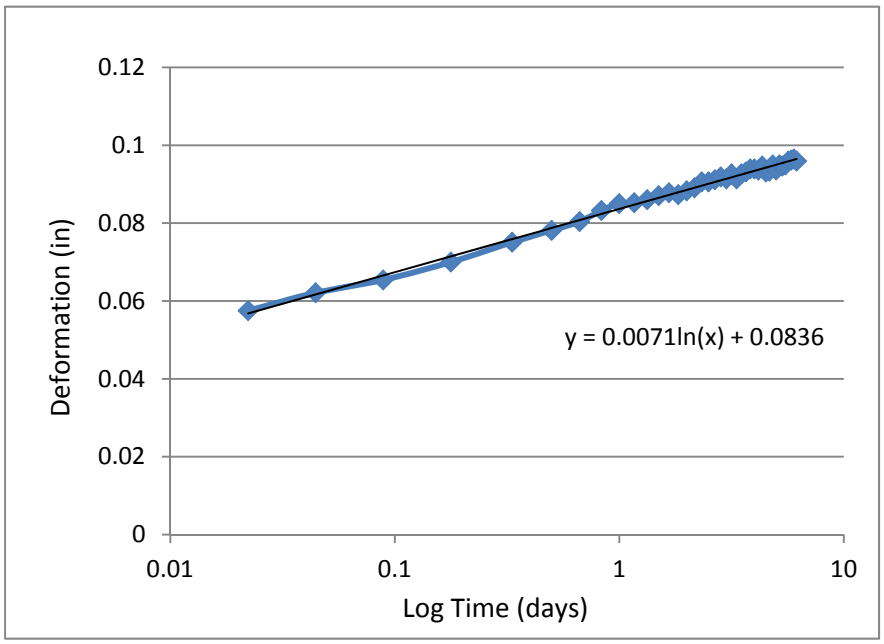

Figure C-76: Creep vs. Log Time Plot: Whitehurst Milled Retained #4 S1

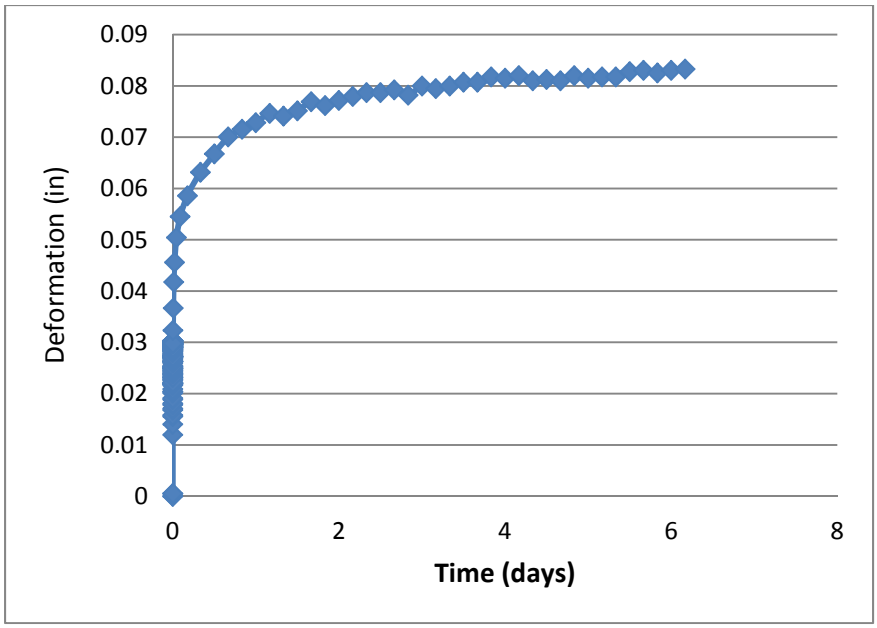

Figure C-77: Creep vs. Time Plot: Whitehurst Milled Retained #4 S2

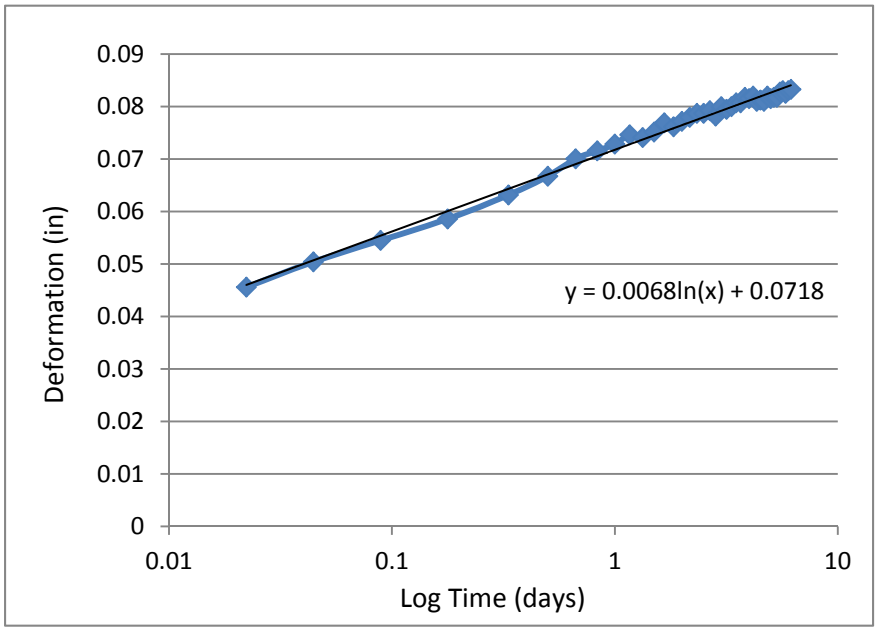

Figure C-78: Creep vs. Log Time Plot: Whitehurst Milled Retained #4 S2

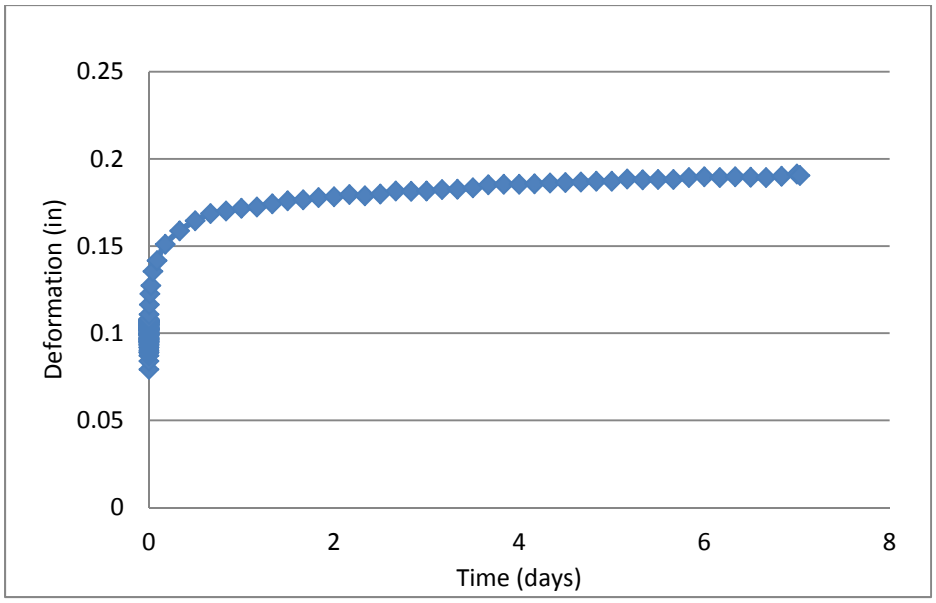

Figure C-79: Creep vs. Time Plot: Crushed APAC Melbourne Retained #8 S1

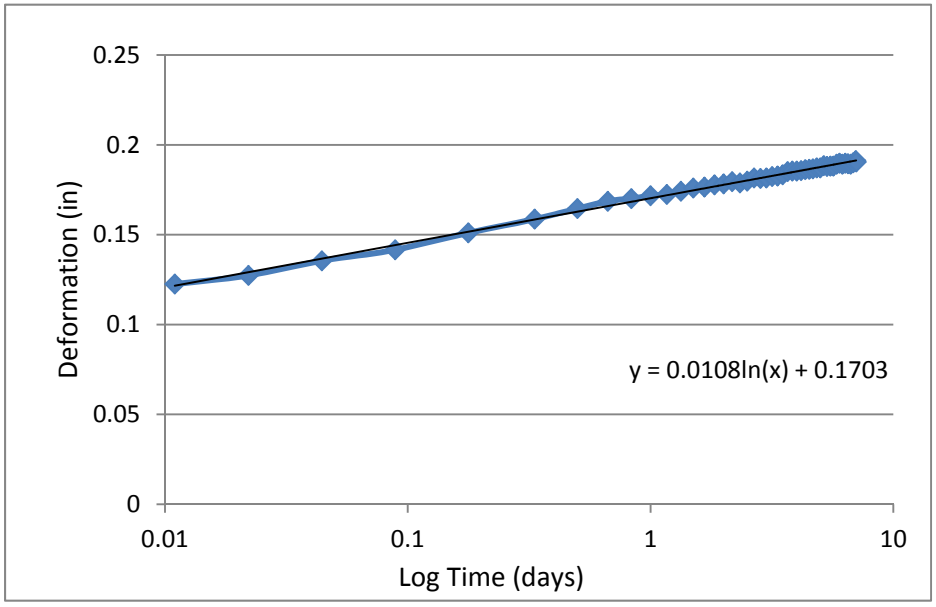

Figure C-80: Creep vs. Log Time Plot: Crushed APAC Melbourne Retained #8 S1

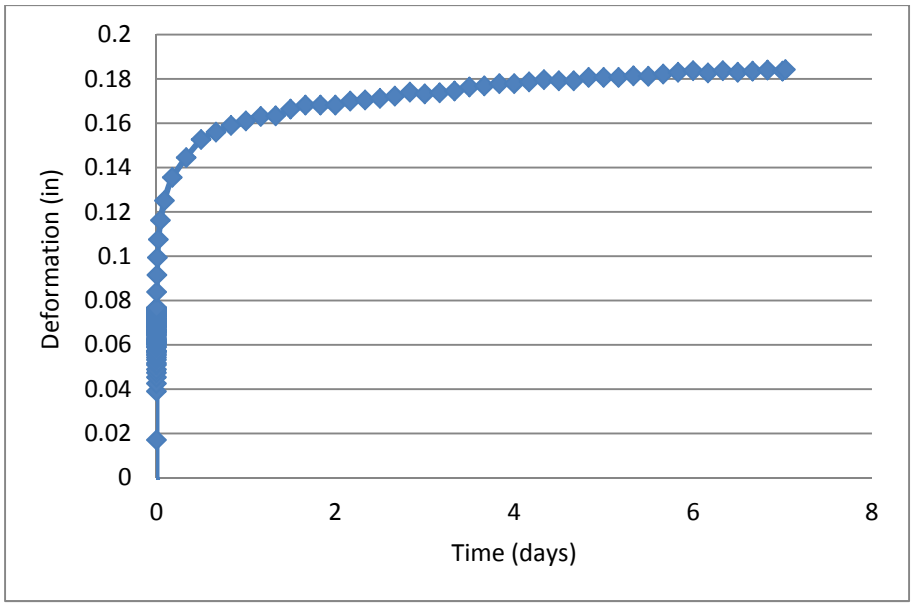

Figure C-81: Creep vs. Time Plot: Crushed APAC Melbourne Retained #8 S2

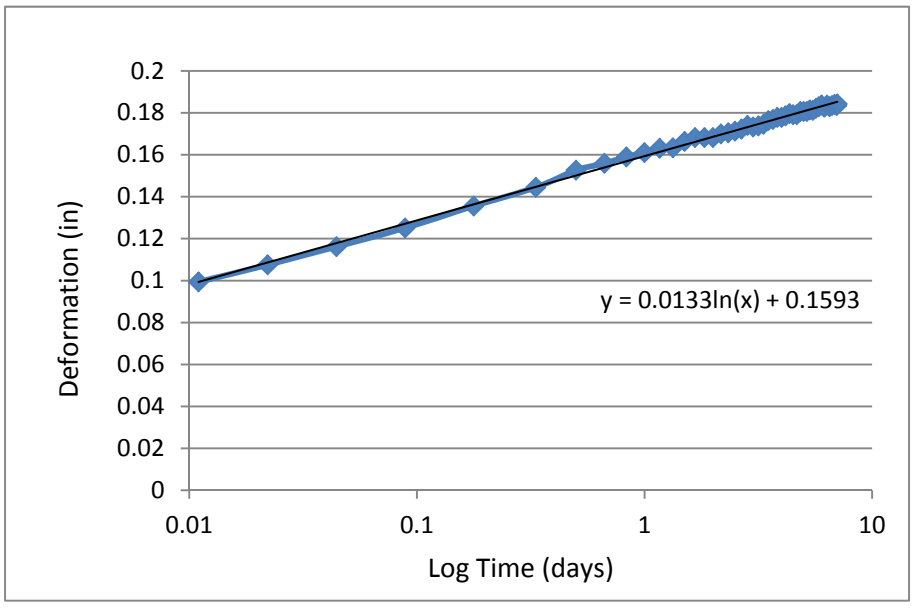

Figure C-82: Creep vs. Log Time Plot: Crushed APAC Melbourne Retained #8 S2

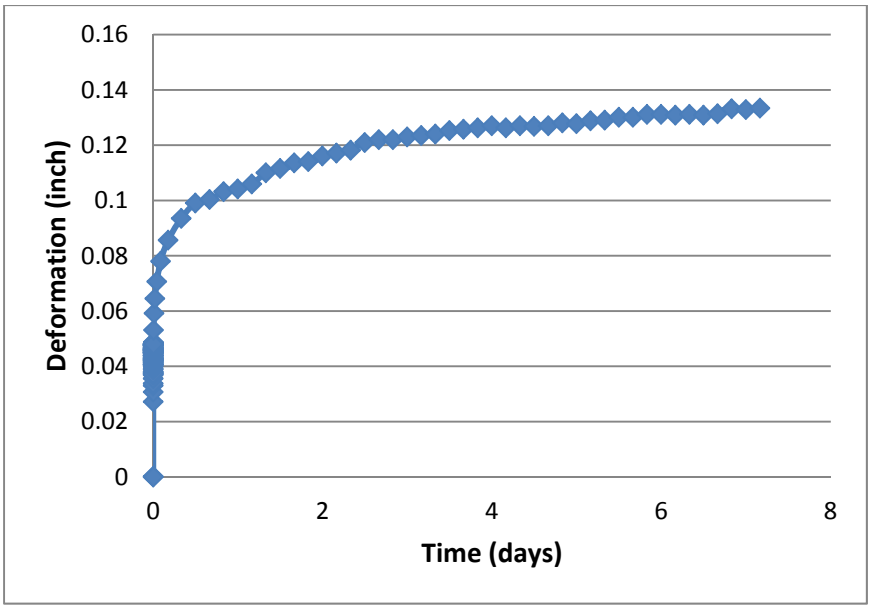

Figure C-83: Creep vs. Time Plot: Milled APAC Mel Retained #8 S1

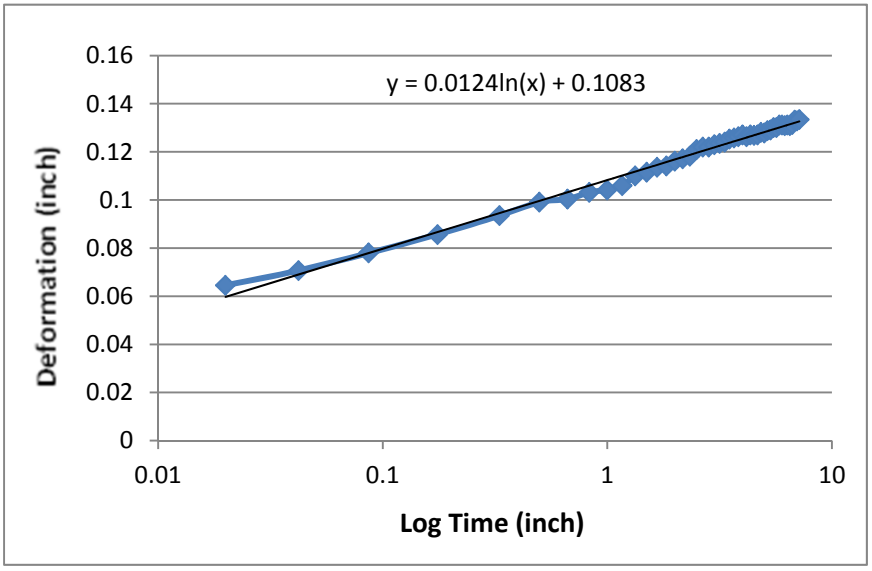

Figure C-84: Creep vs. Log Time Plot: Milled APAC Mel Retained #8 S1

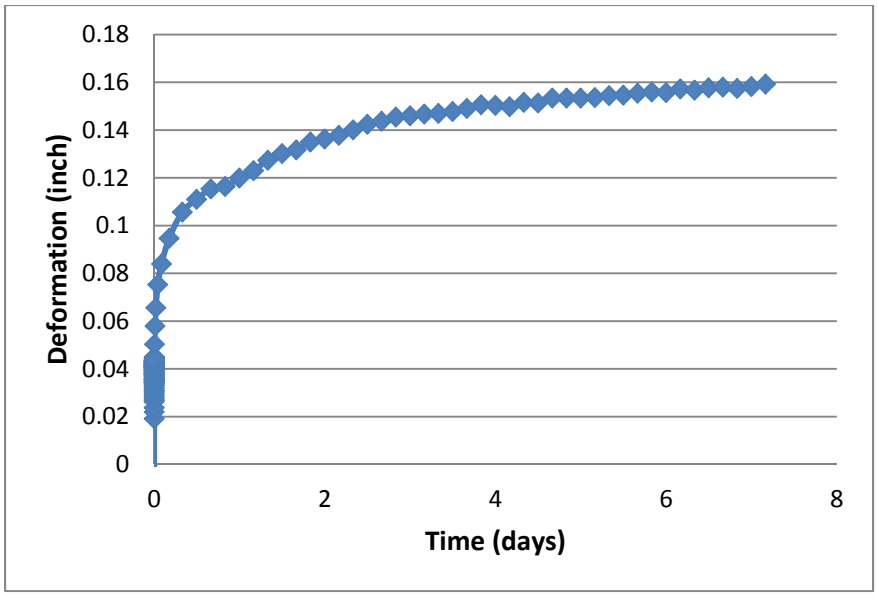

Figure C-85: Creep vs. Time Plot: Milled APAC Mel Retained #8 S2

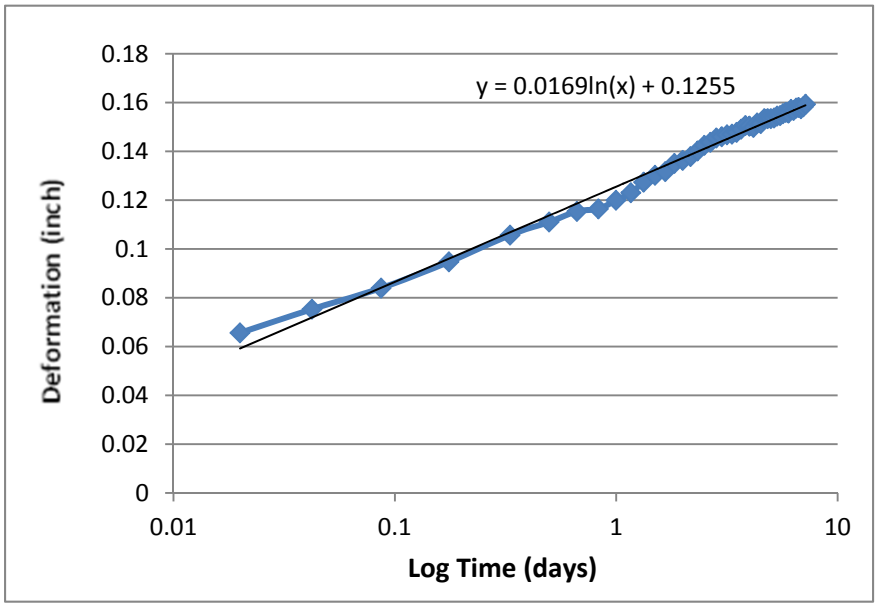

Figure C-86: Creep vs. Log Time Plot: Milled APAC Mel Retained #8 S2

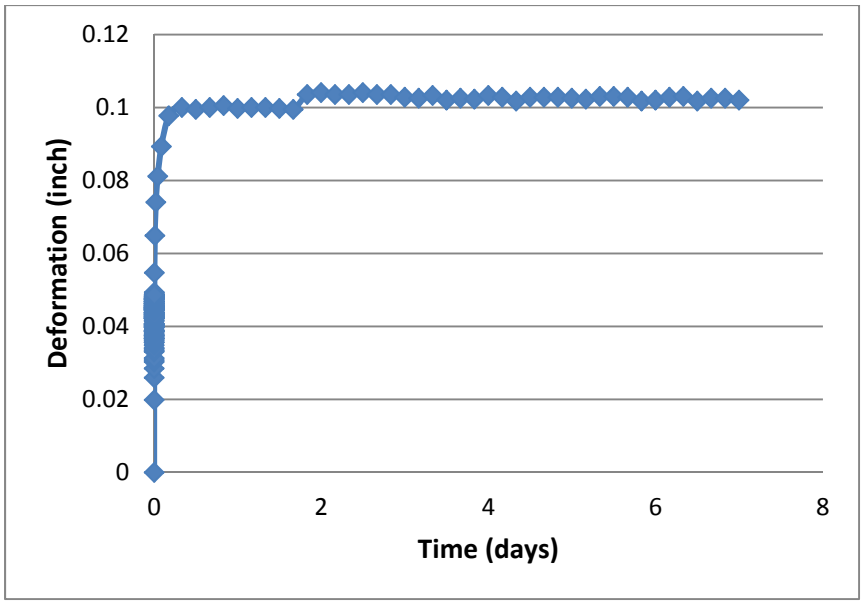

Figure C-87: Creep vs. Time Plot: Crushed APAC Jacksonville Retained # 8 S1

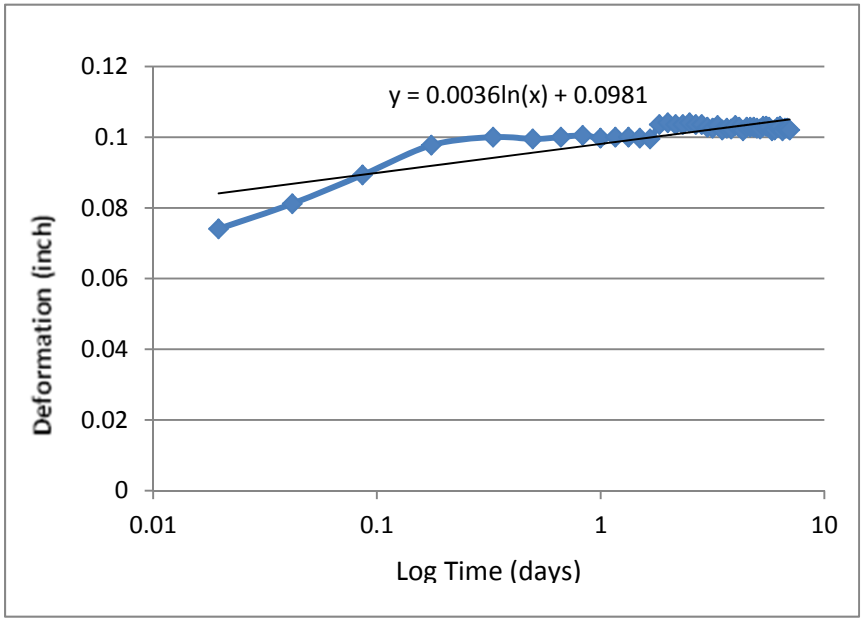

Figure C-88: Creep vs. Log Time Plot: Crushed APAC Jacksonville Retained # 8 S1

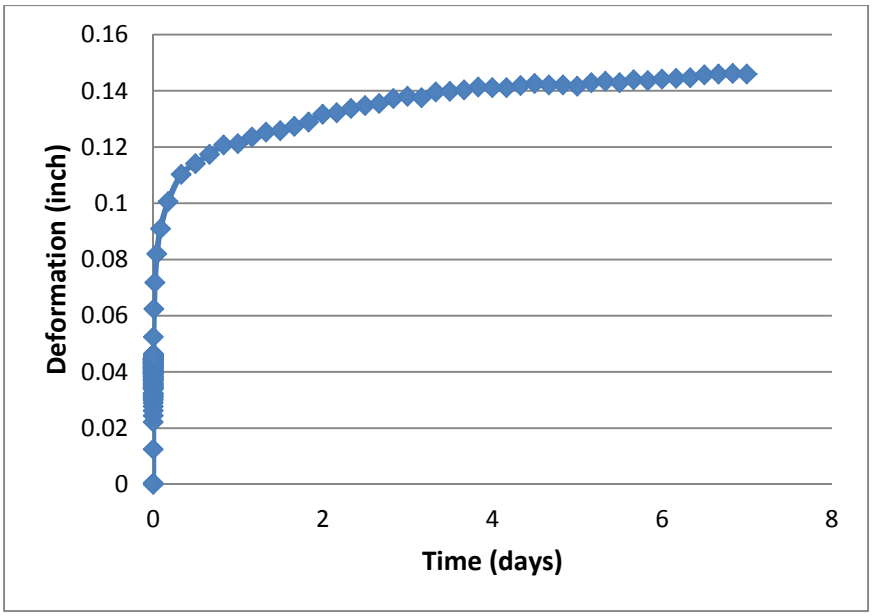

Figure C-89: Creep vs. Time Plot: Crushed APAC Jacksonville Retained # 8 S2

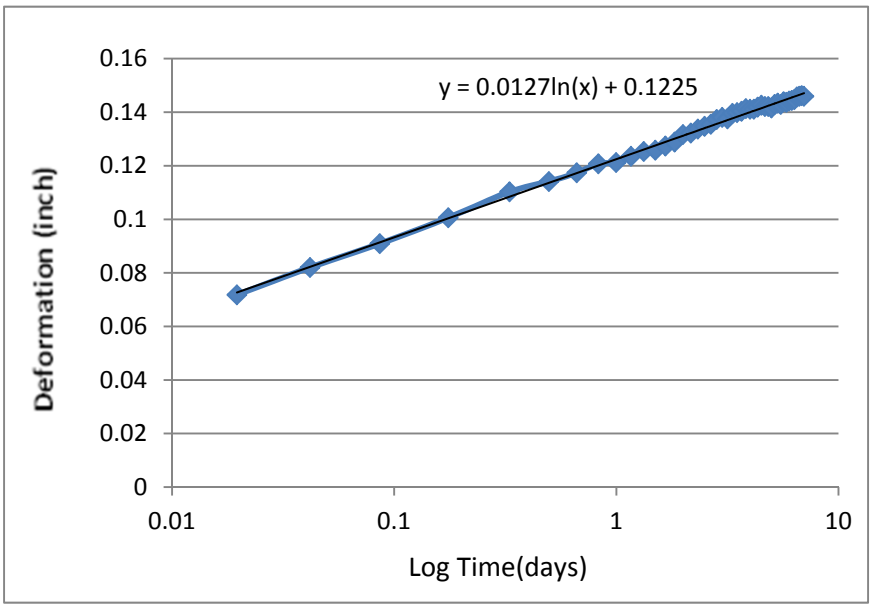

Figure C-90: Creep vs. Log Time Plot: Crushed APAC Jacksonville Retained # 8 S2

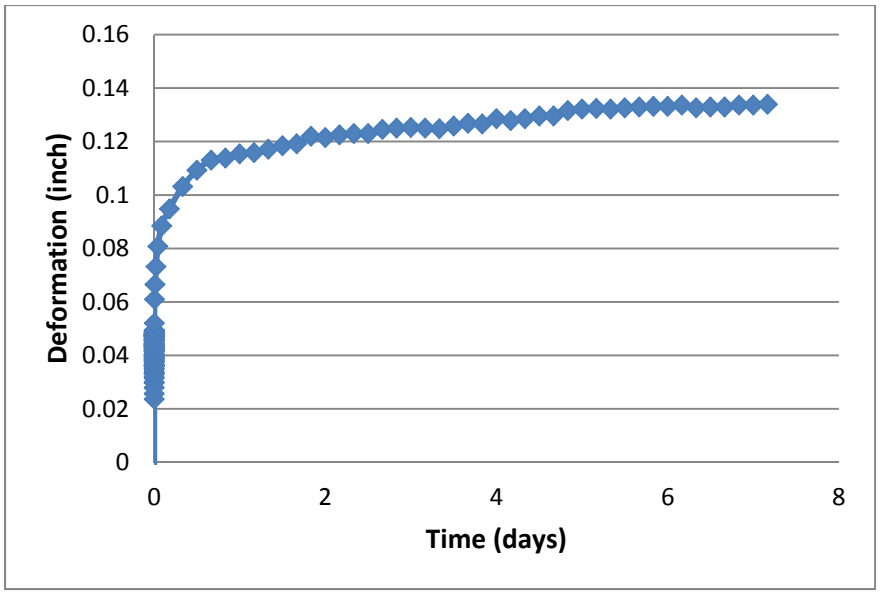

Figure C-91: Creep vs. Time Plot: Whitehurst Milled ret #8 S1

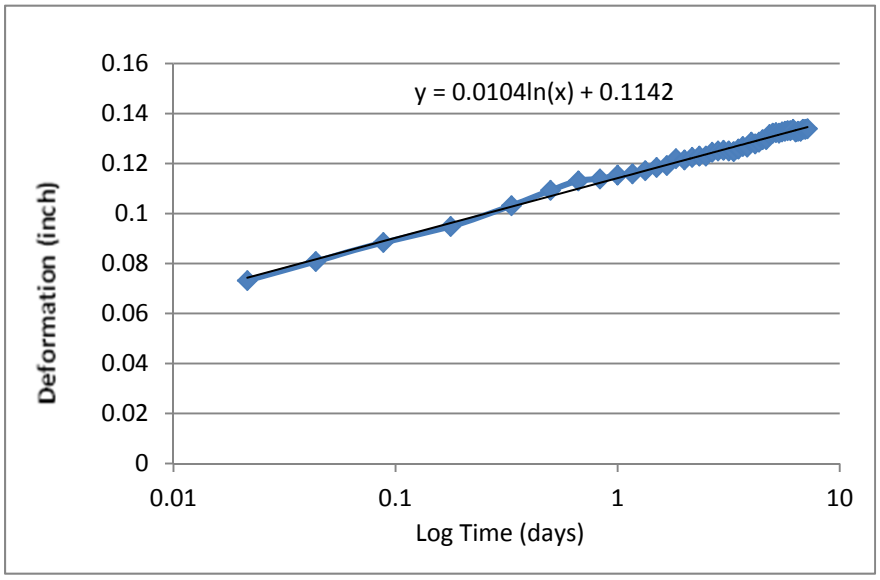

Figure C-92: Creep vs. Log Time Plot: Whitehurst Milled ret #8 S1

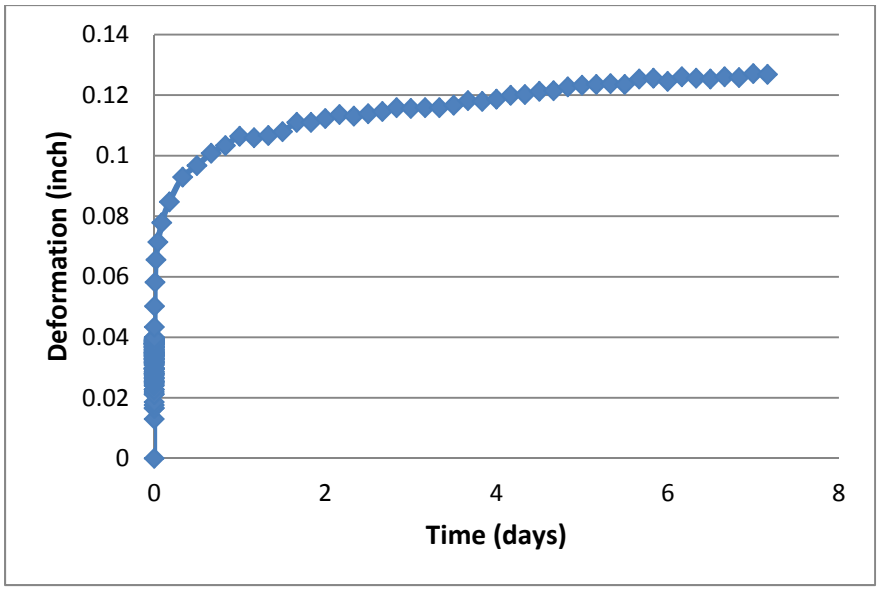

Figure C-93: Creep vs. Time Plot: Whitehurst Milled ret #8 S2

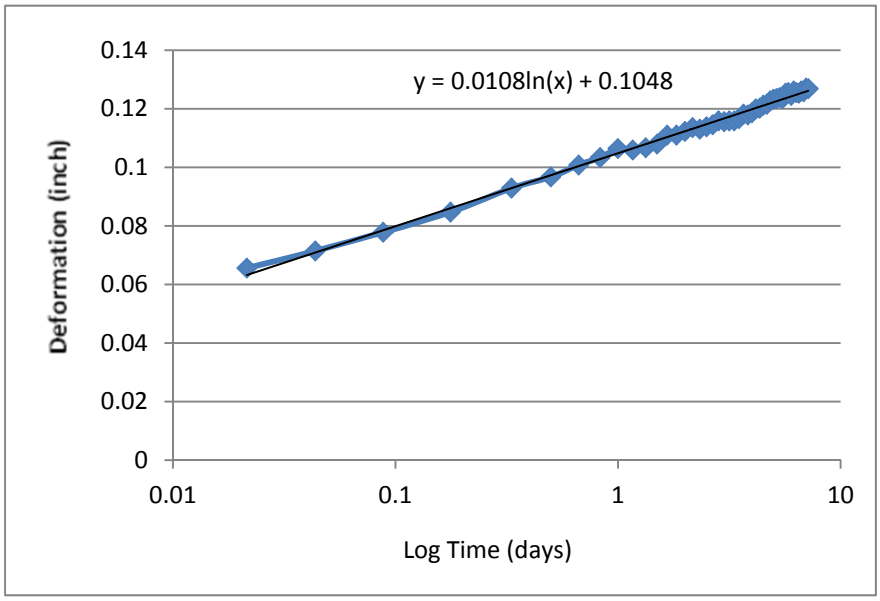

Figure C-94: Creep vs. Log Time Plot: Whitehurst Milled ret #8 S2

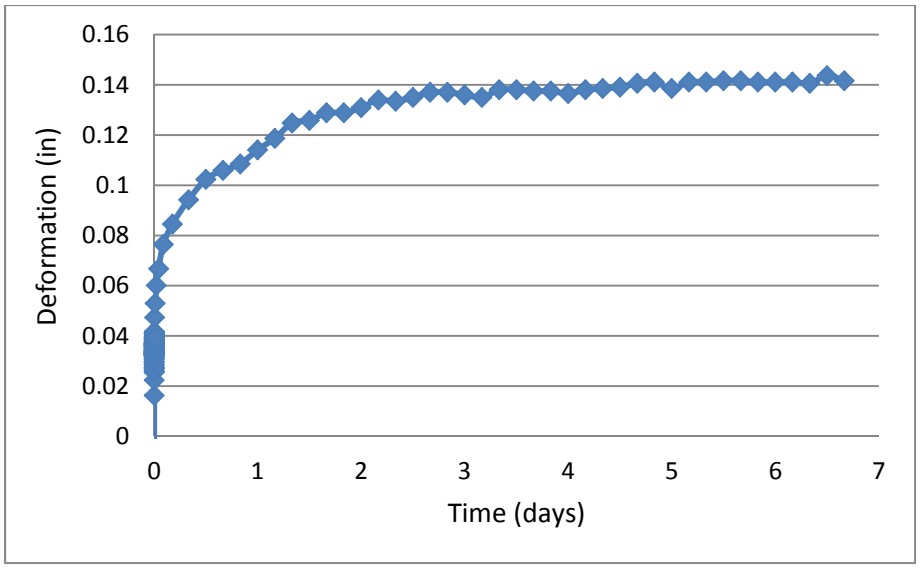

Figure C-95: Creep vs. Time Plot: Crushed APAC Melbourne Retained #40 S1

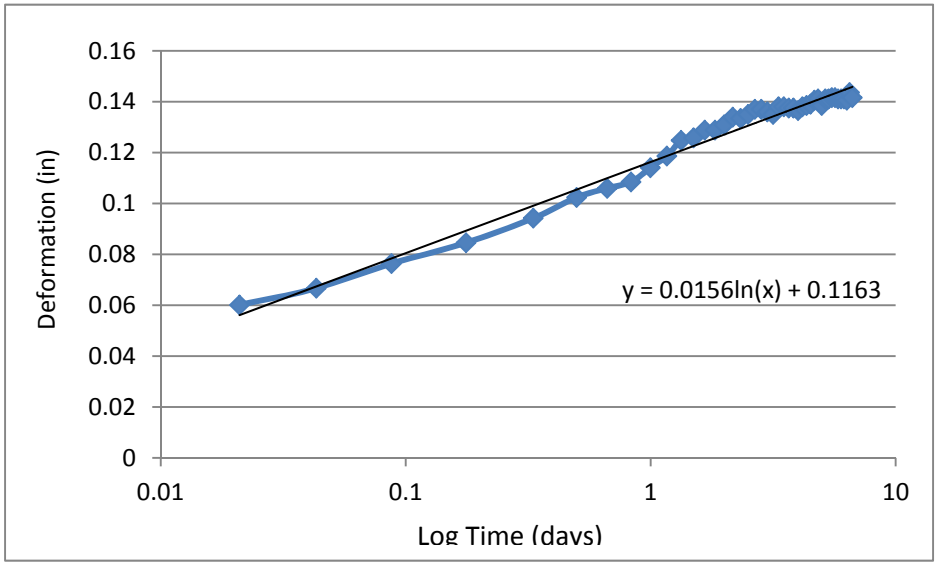

Figure C-96: Creep vs. Log Time Plot: Crushed APAC Melbourne Retained #40 S1

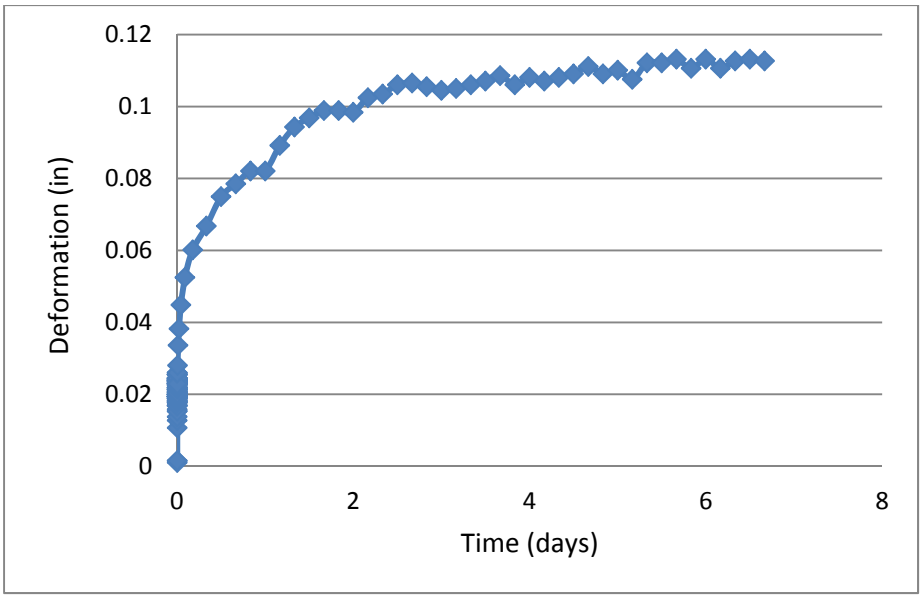

Figure C-97: Creep vs. Time Plot: Crushed APAC Melbourne Retained #40 S2

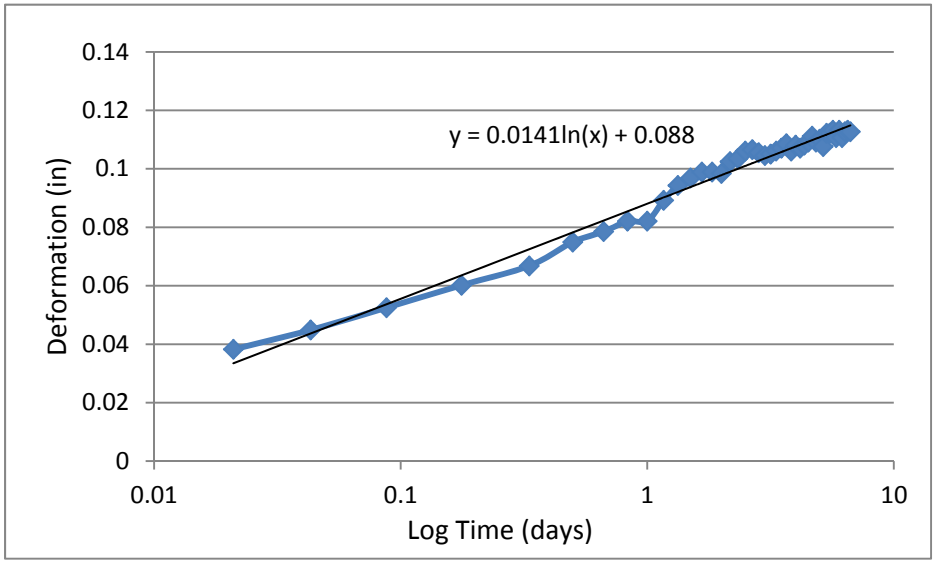

Figure C-98: Creep vs. Log Time Plot: Crushed APAC Melbourne Retained #40 S2

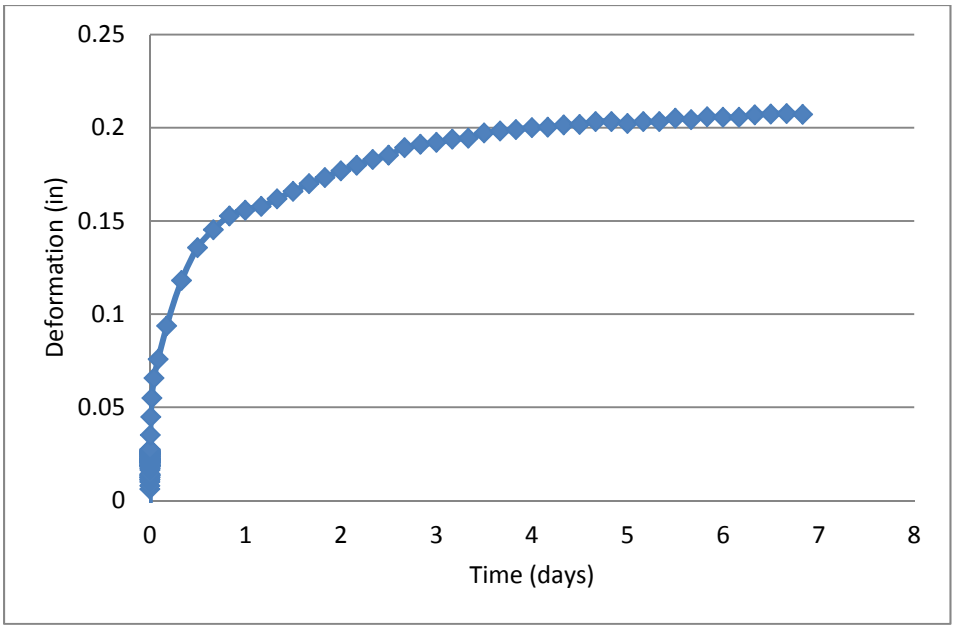

Figure C-99: Creep vs. Time Plot: Milled APAC Melbourne Retained #40 S1

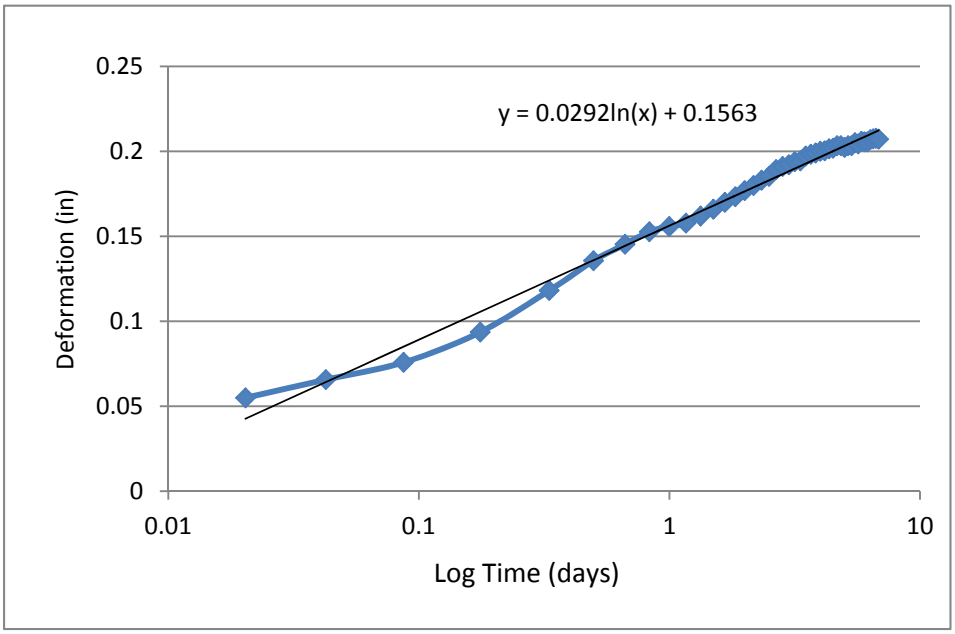

Figure C-100: Creep vs. Log Time Plot: Milled APAC Melbourne Retained #40 S1

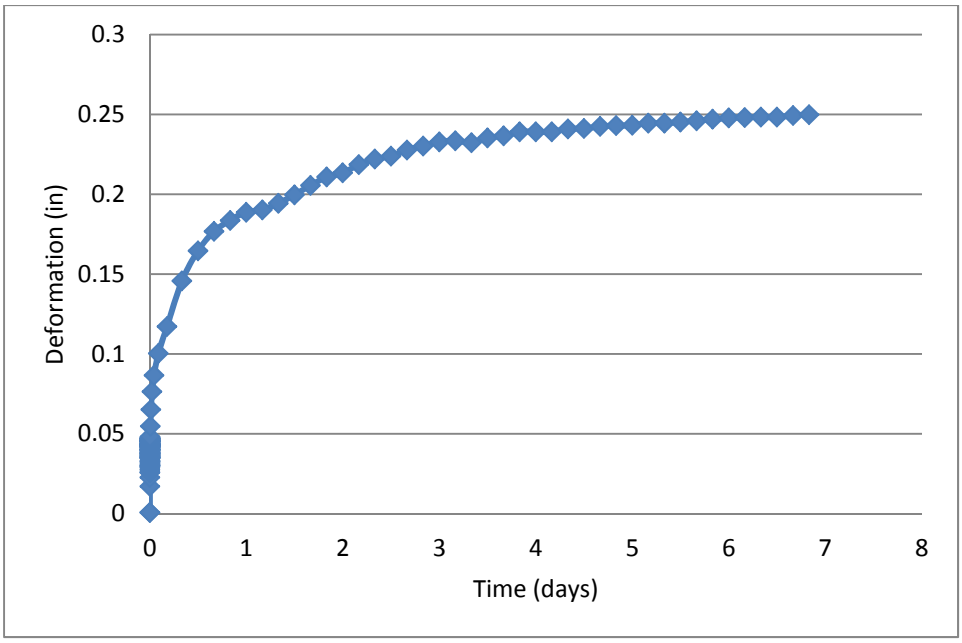

Figure C-101: Creep vs. Time Plot: Milled APAC Melbourne Retained #40 S2

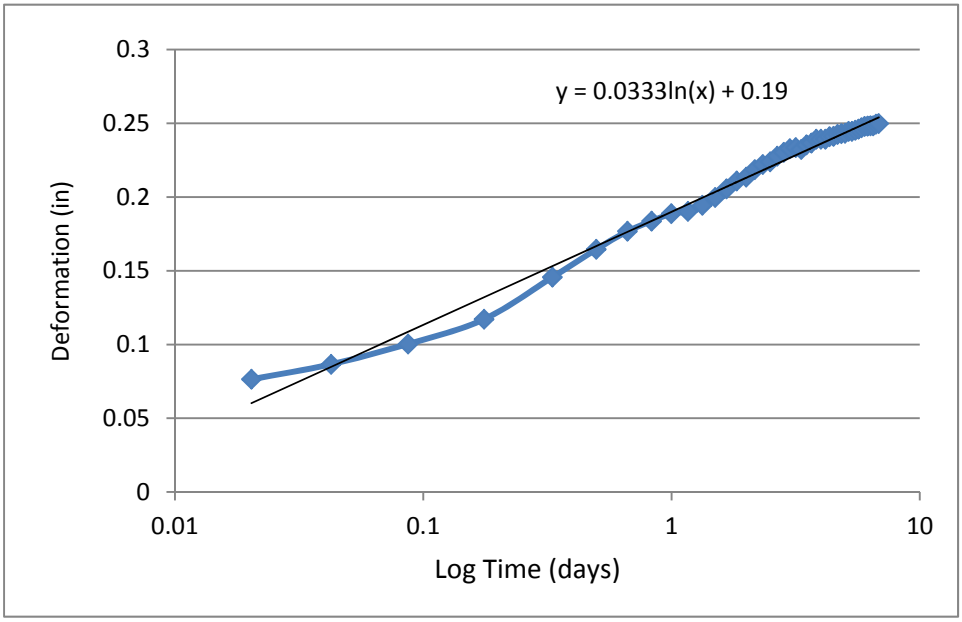

Figure C-102: Creep vs. Log Time Plot: Milled APAC Melbourne Retained #40 S2

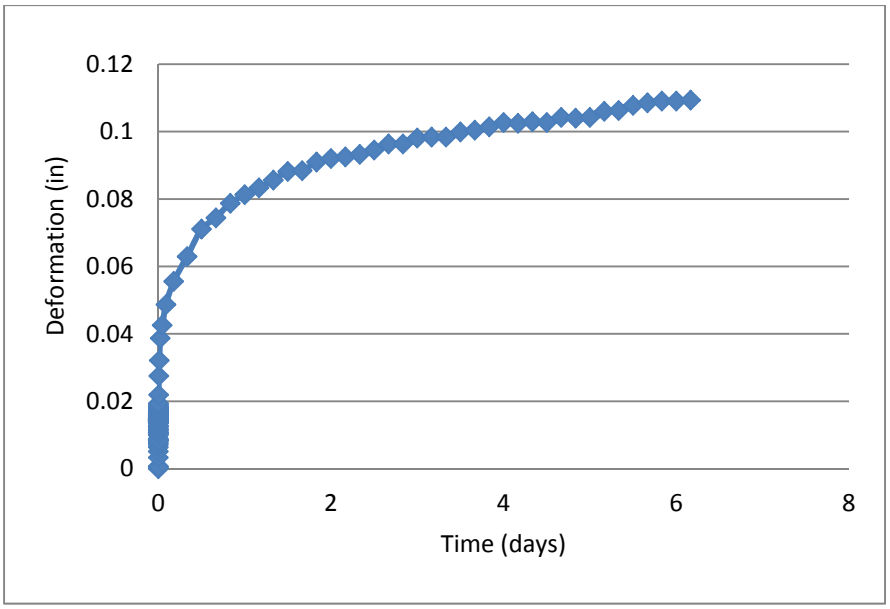

Figure C-103: Creep vs. Time Plot: Crushed APAC Jacksonville Retained #40 S1

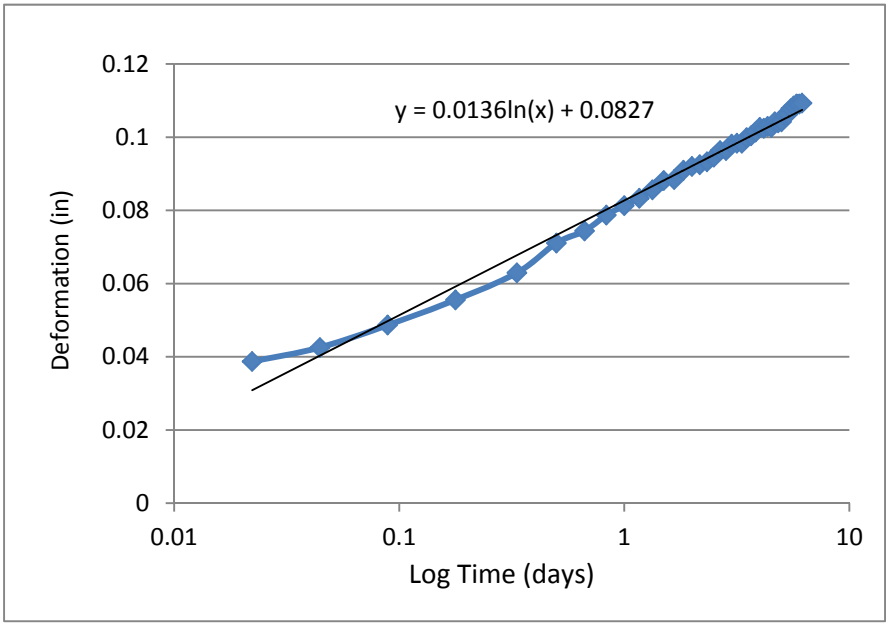

Figure C-104: Creep vs. Log Time Plot: Crushed APAC Jacksonville Retained #40 S1

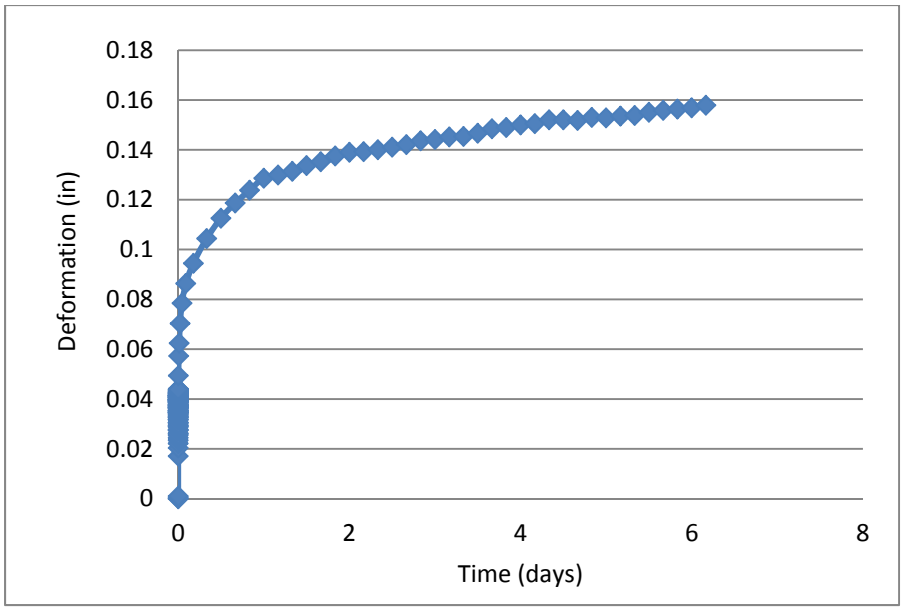

Figure C-105: Creep vs. Time Plot: Crushed APAC Jacksonville Retained #40 S2

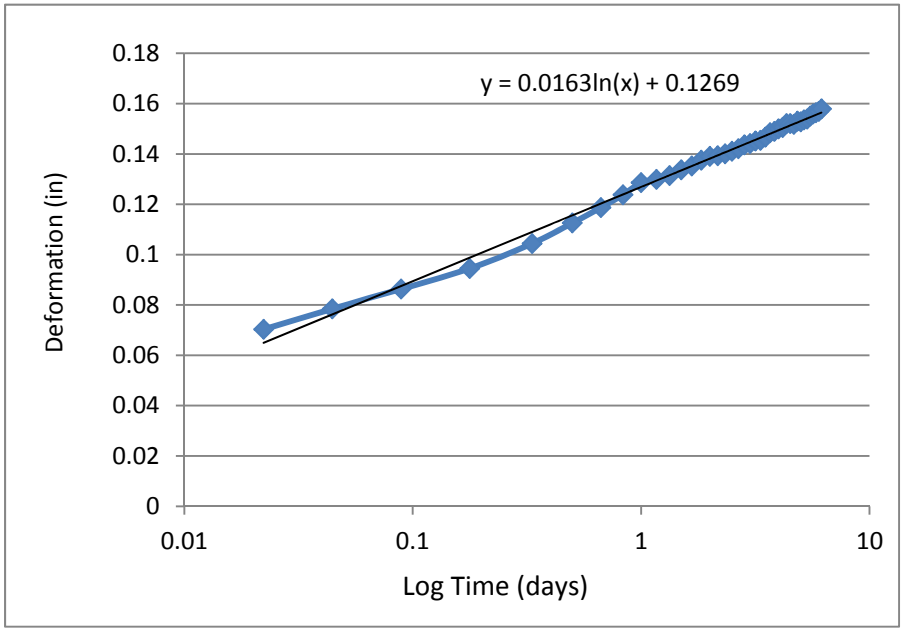

Figure C-106: Creep vs. Log Time Plot: Crushed APAC Jacksonville Retained #40 S2

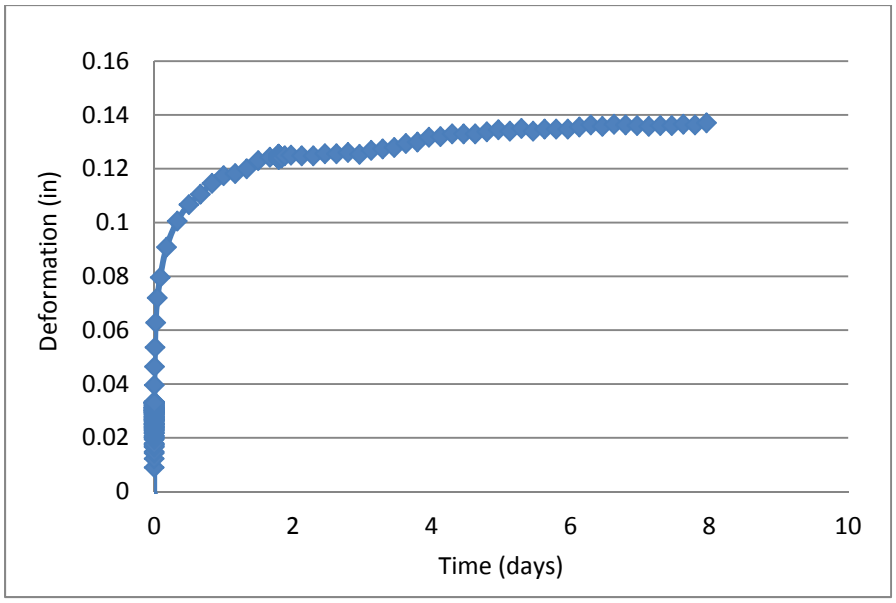

Figure C-107: Creep vs. Time Plot: Milled Whitehurst Retained #40 S1

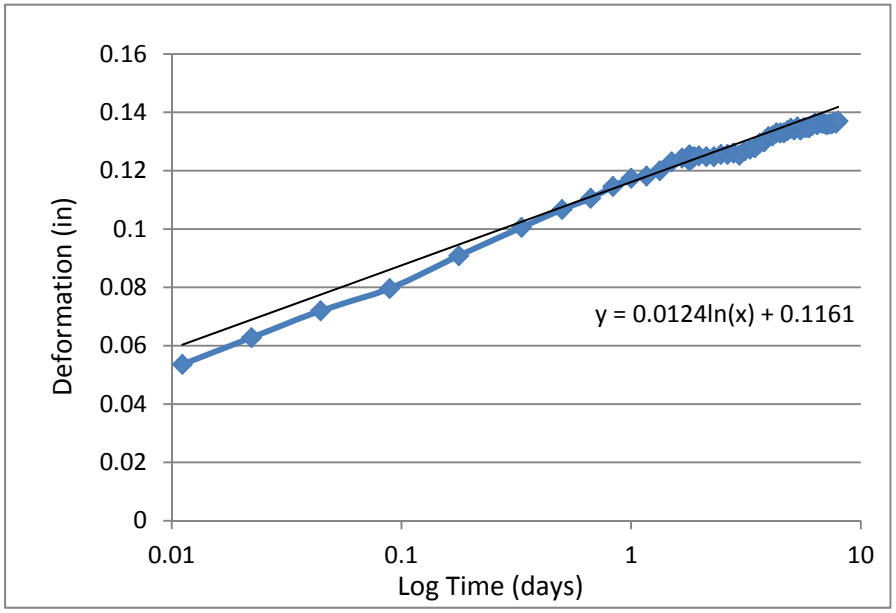

Figure C-108: Creep vs. Log Time Plot: Milled Whitehurst Retained #40 S1

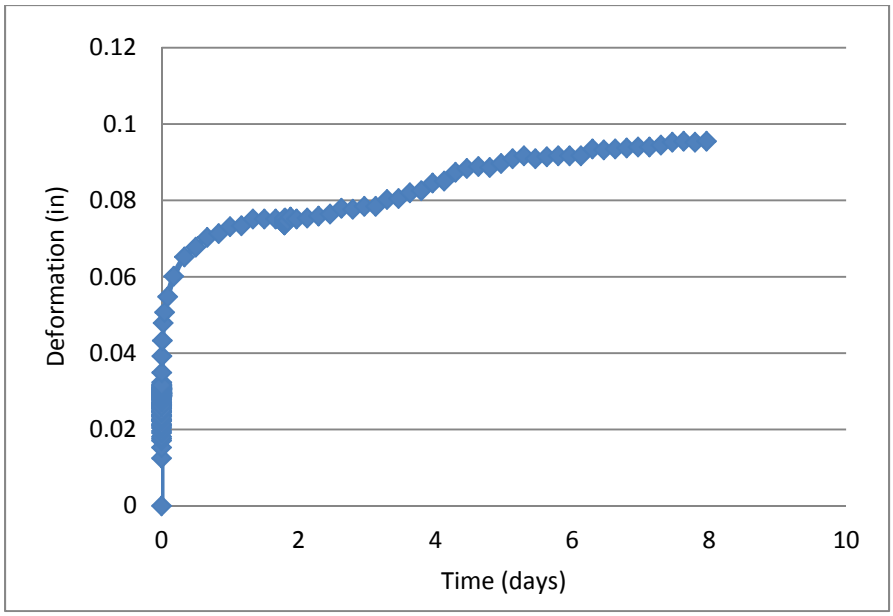

Figure C-109: Creep vs. Time Plot: Milled Whitehurst Retained #40 S2

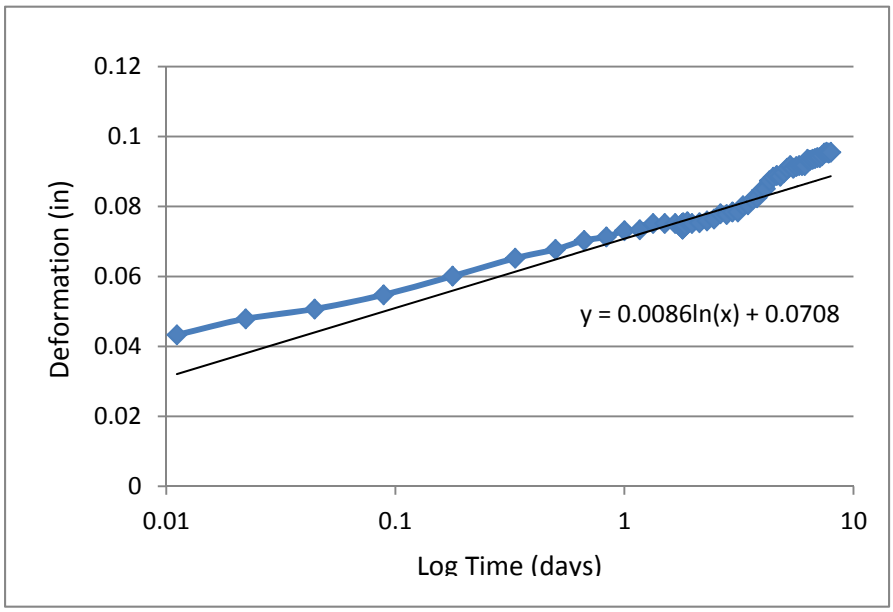

Figure C-110: Creep vs. Log Time Plot: Milled Whitehurst Retained #40 S2

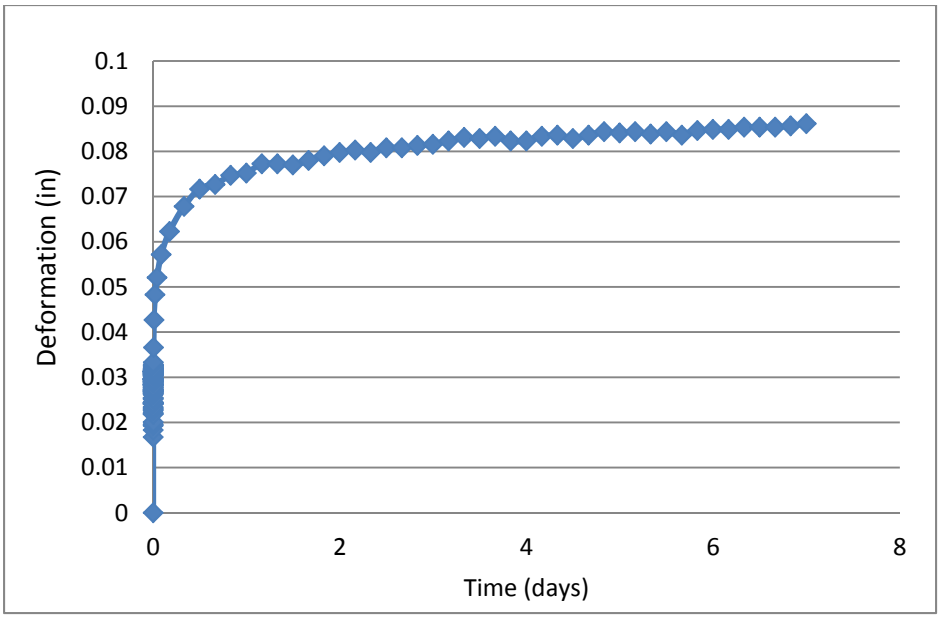

Figure C-111: Creep vs. Time Plot: Crushed APAC Melbourne Talbot S1

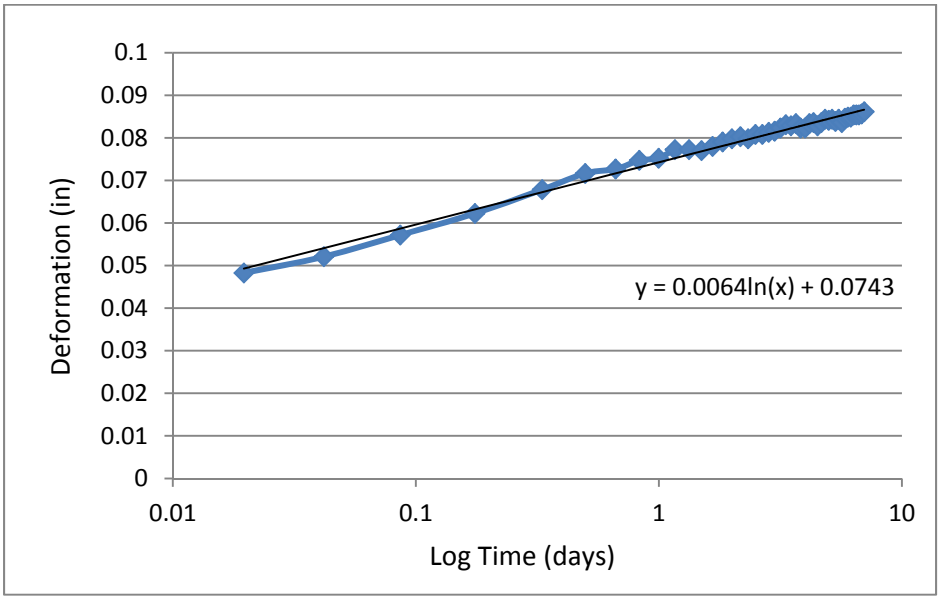

Figure C-112: Creep vs. Log Time Plot: Crushed APAC Melbourne Talbot S1

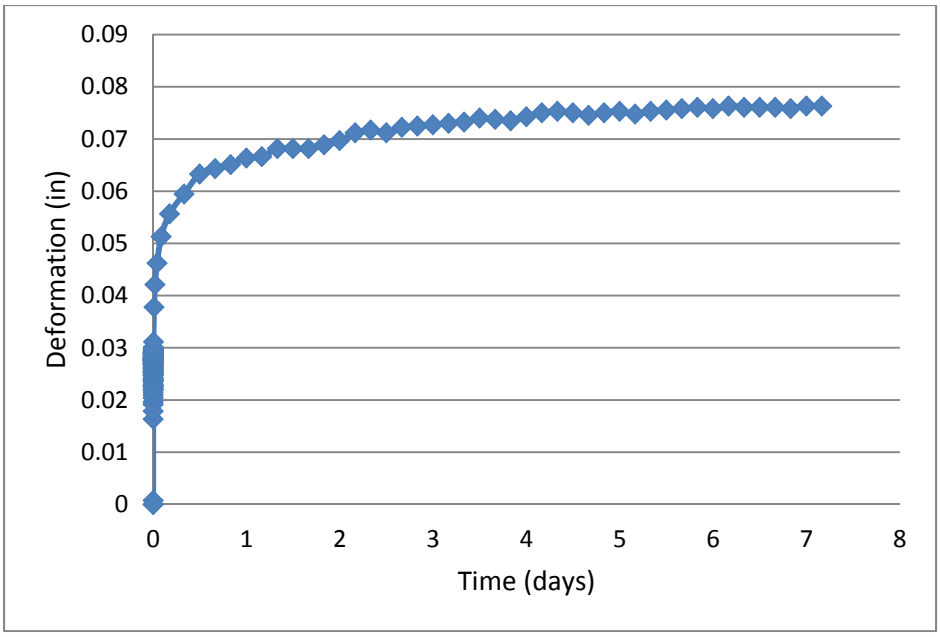

Figure C-113: Creep vs. Time Plot: Crushed APAC Melbourne Talbot S2

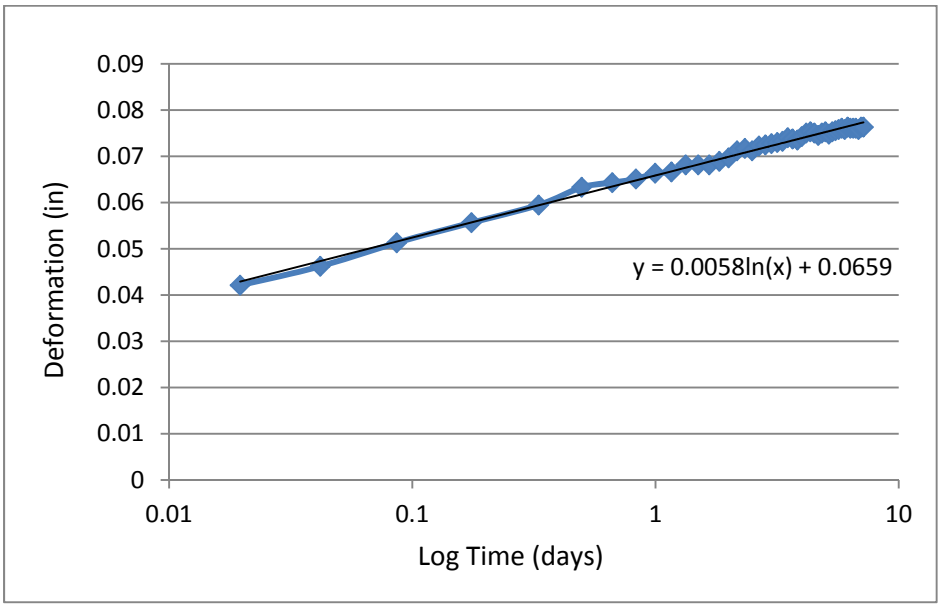

Figure C-114: Creep vs. Log Time Plot: Crushed APAC Melbourne Talbot S2

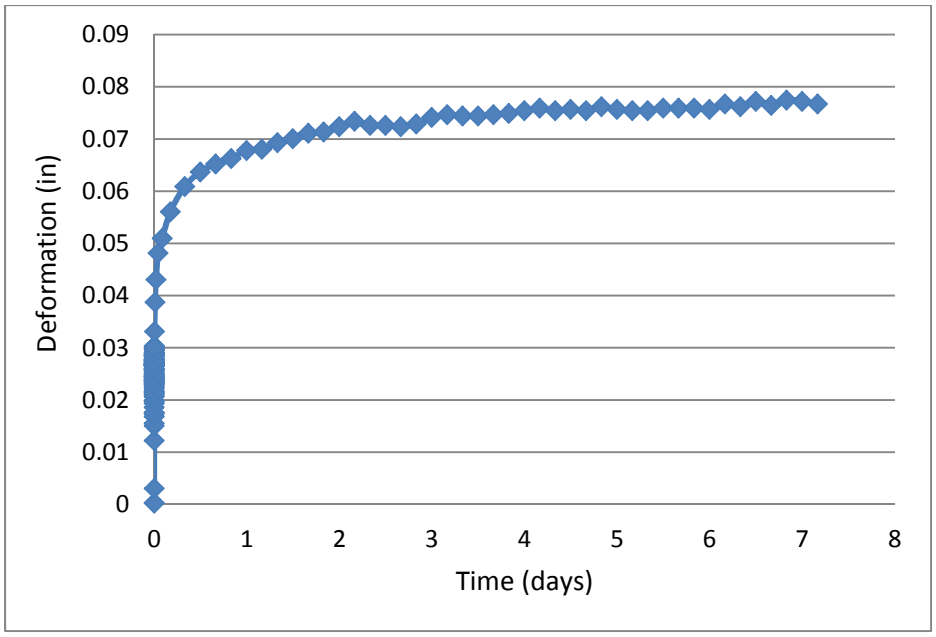

Figure C-115: Creep vs. Time Plot: Milled APAC Melbourne Talbot S1

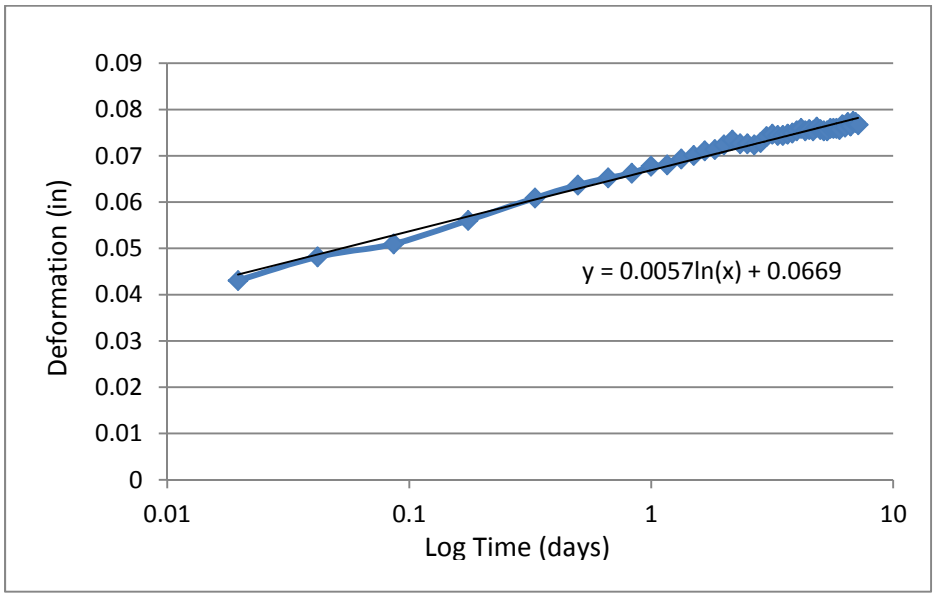

Figure C-116: Creep vs. Log Time Plot: Milled APAC Melbourne Talbot S1

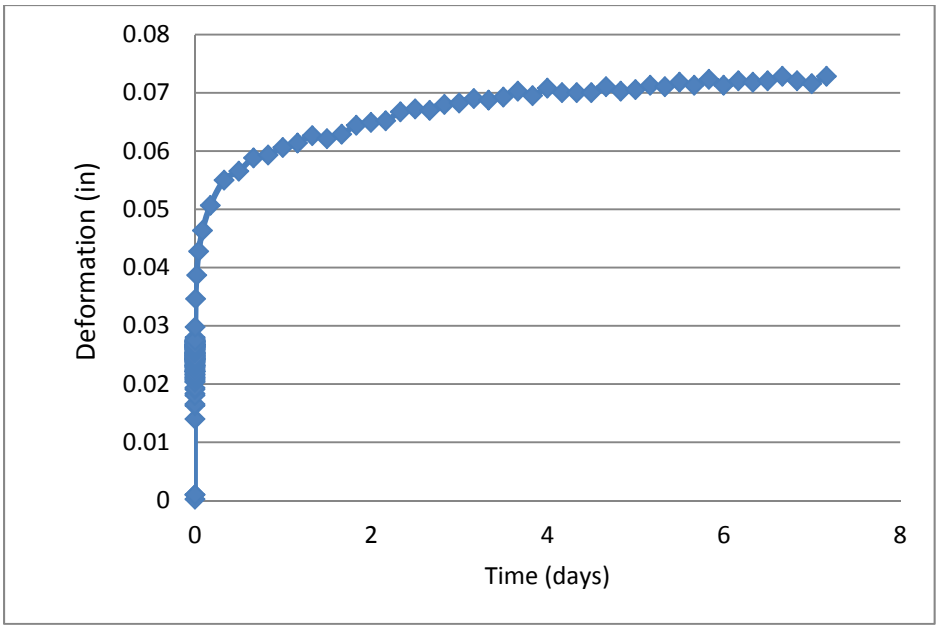

Figure C-117: Creep vs. Time Plot: Milled APAC Melbourne Talbot S2

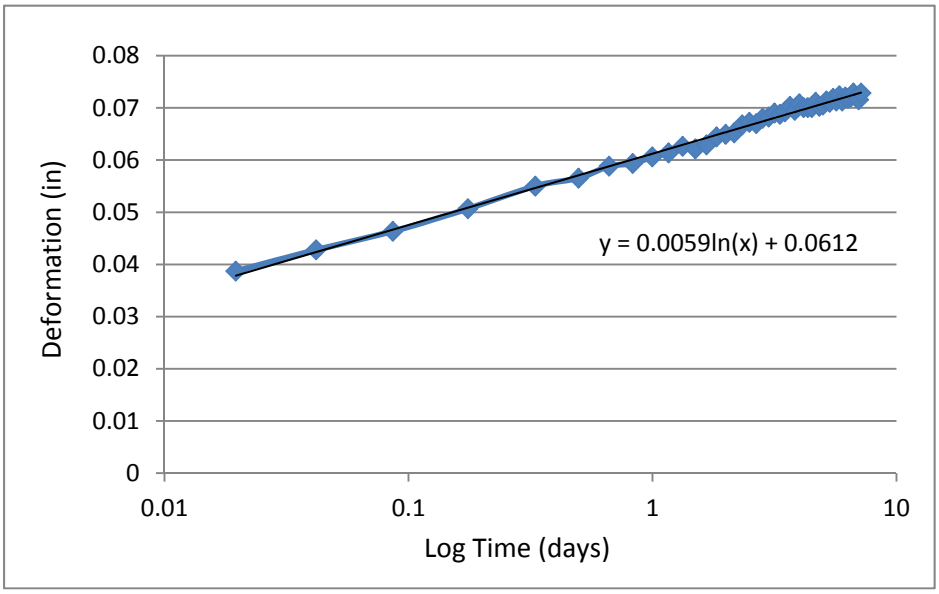

Figure C-118: Creep vs. Log Time Plot: Milled APAC Melbourne Talbot S2

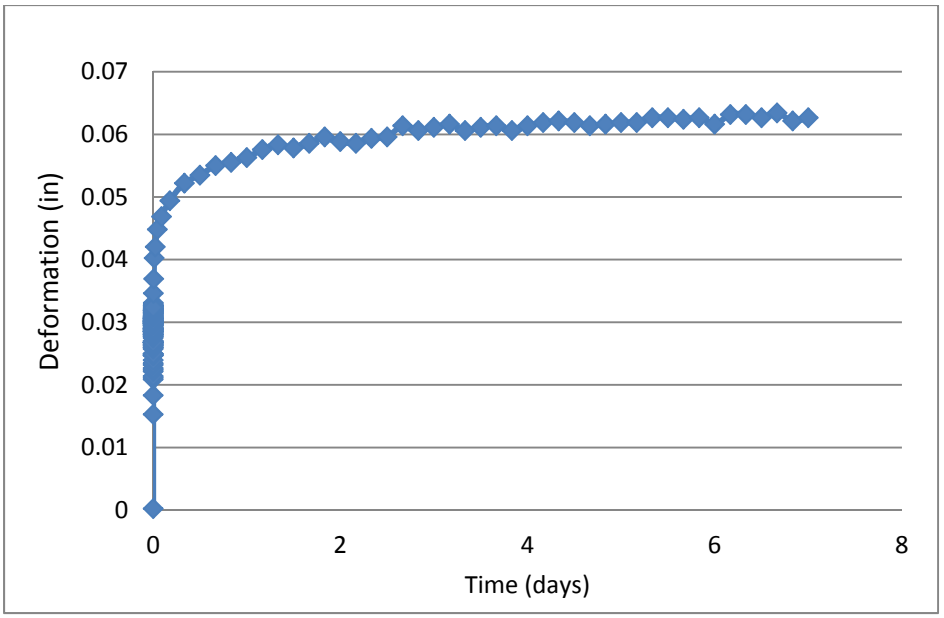

Figure C-119: Creep vs. Time Plot: Crushed APAC Jacksonville Talbot S1

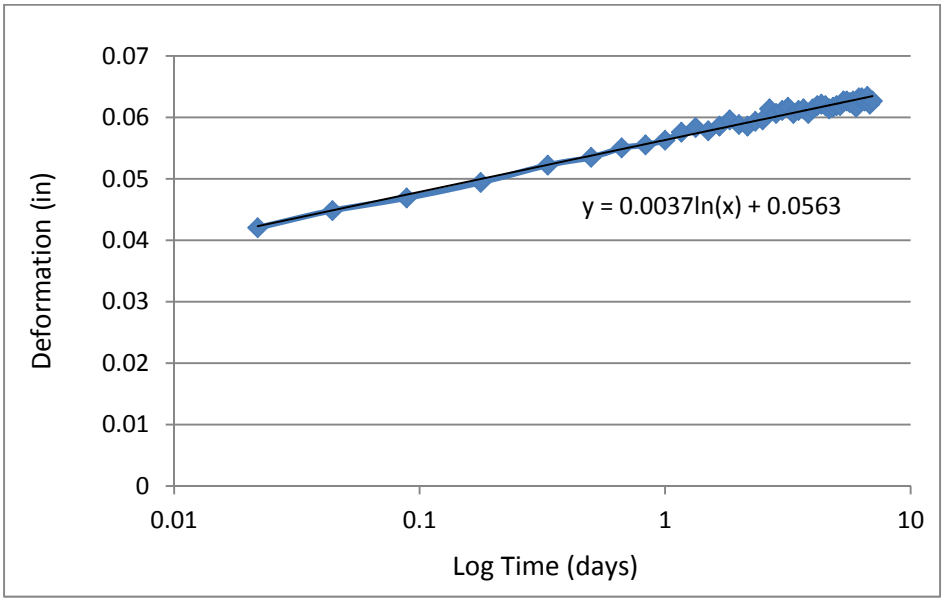

Figure C-120: Creep vs. Log Time Plot: Crushed APAC Jacksonville Talbot S1

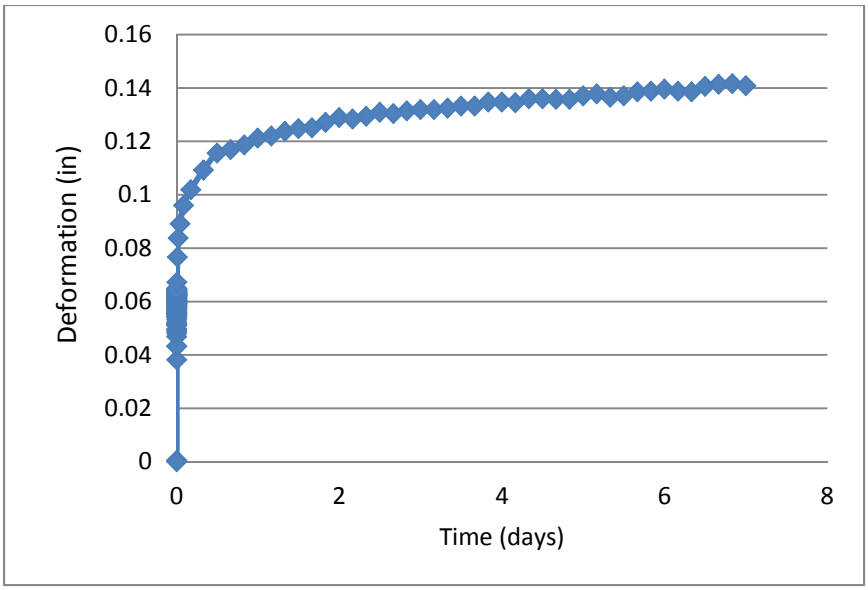

Figure C-121: Creep vs. Time Plot: Crushed APAC Jacksonville Talbot S2

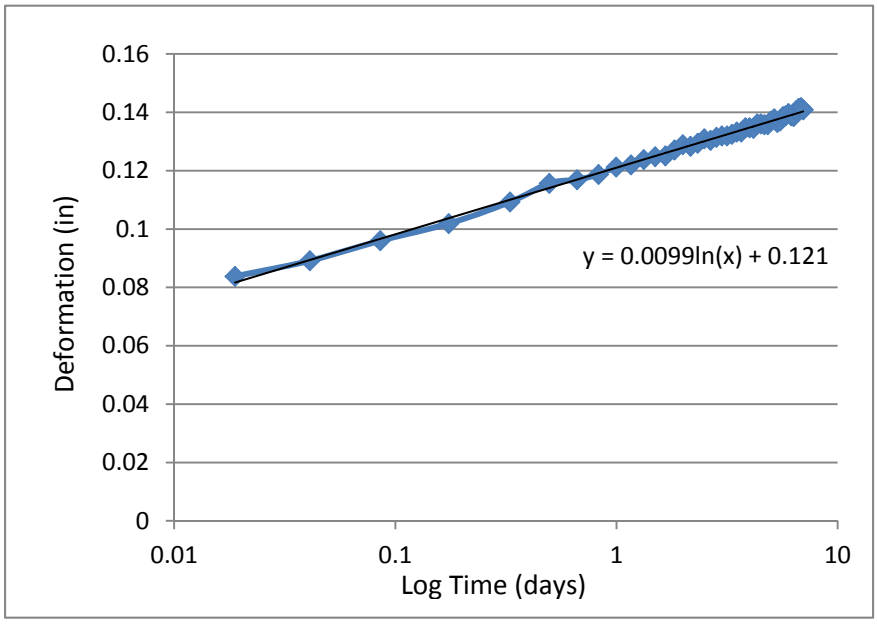

Figure C-122: Creep vs. Log Time Plot: Crushed APAC Jacksonville Talbot S2

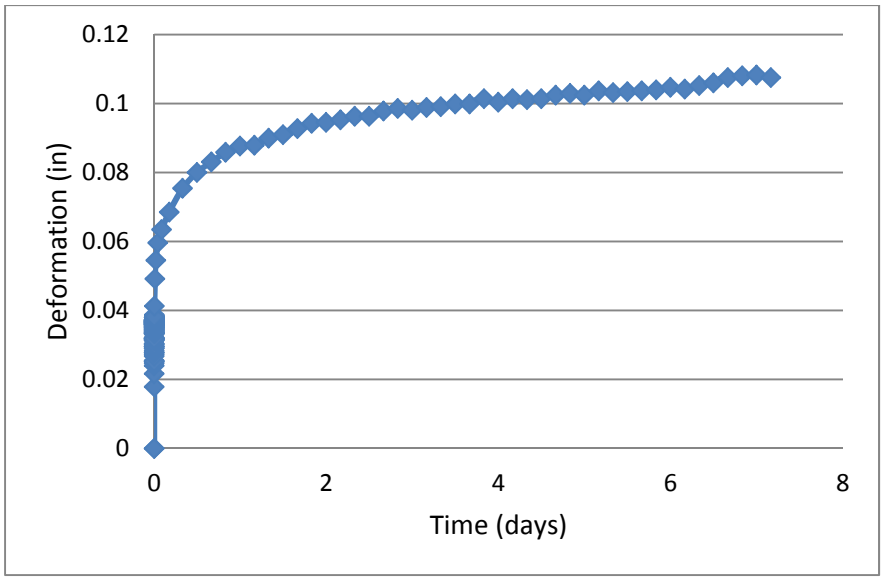

Figure C-123: Creep vs. Time Plot: Milled Whitehurst Talbot S1

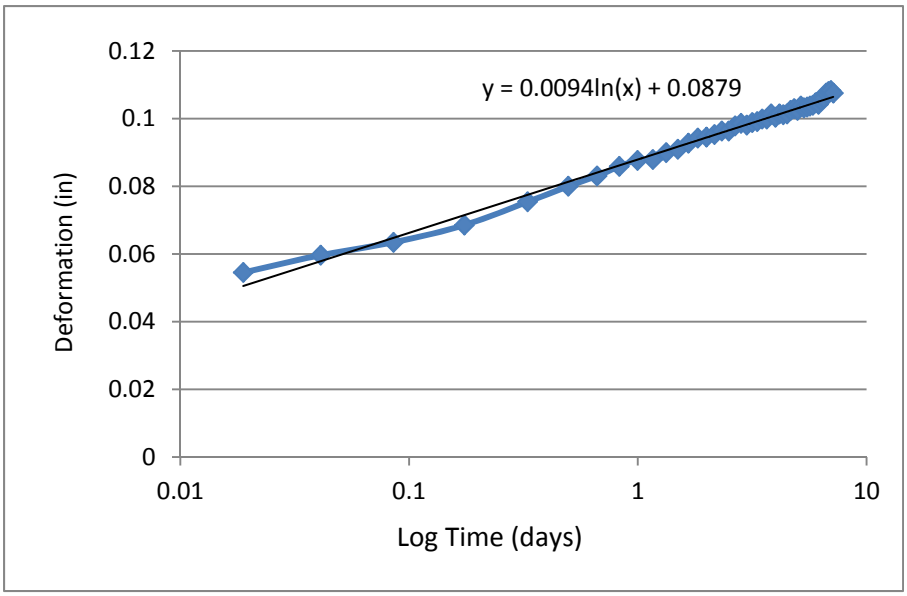

Figure C-124: Creep vs. Log Time Plot: Milled Whitehurst Talbot S1

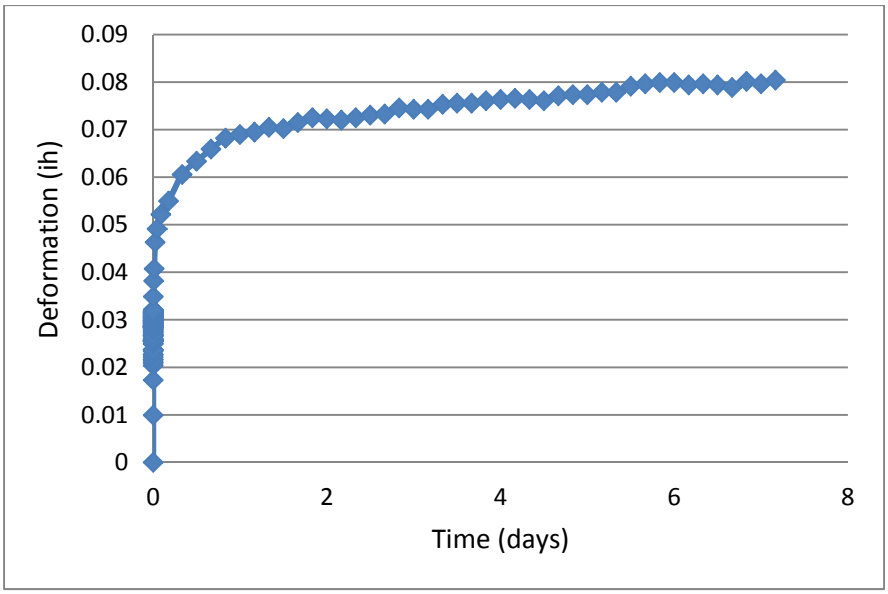

Figure C-125: Creep vs. Time Plot: Milled Whitehurst Talbot S2

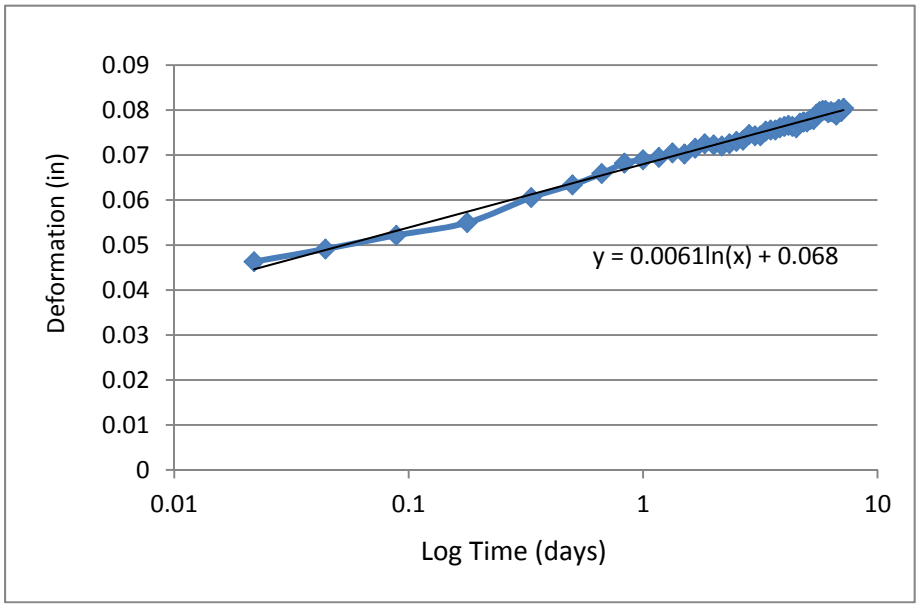

Figure C-126: Creep vs. Log Time Plot: Milled Whitehurst Talbot S2

C.2. Creep Data RAP and Aggregates Unblended

C.2.1. Milled Melbourne RAP

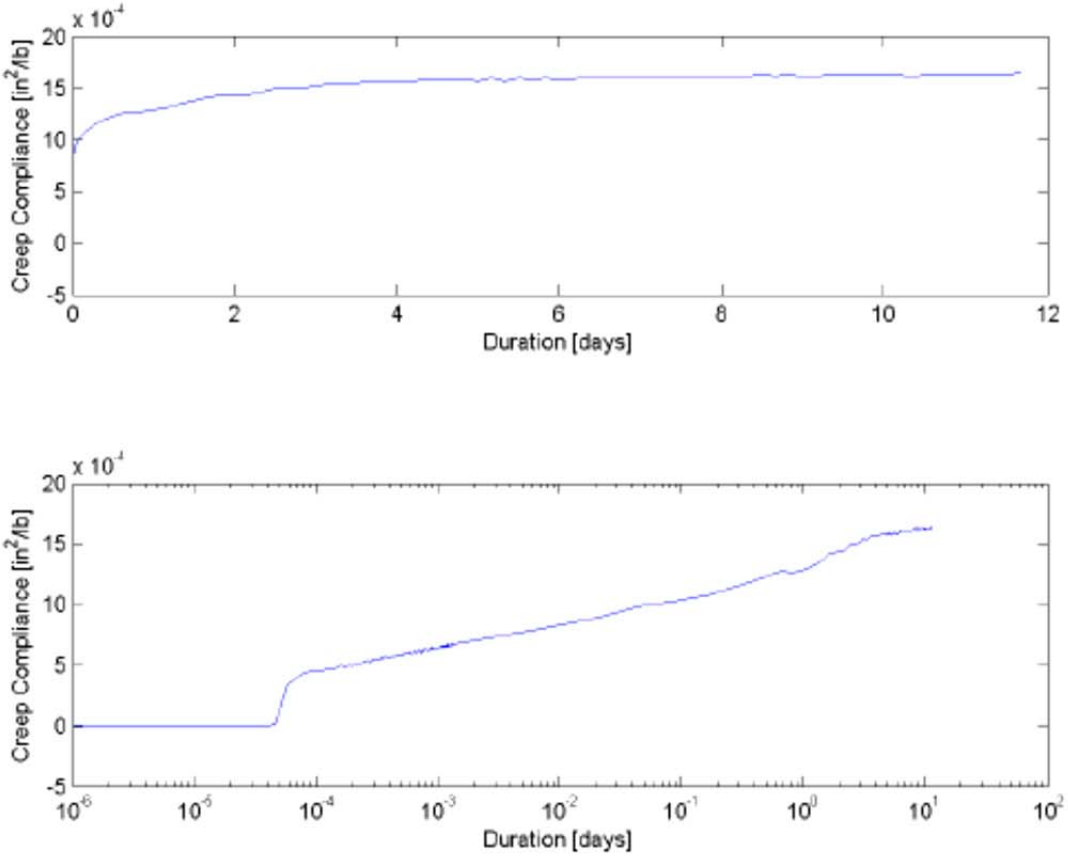

Sample Description:	100% Milled Melbourne RAP
Test Date:	3/2/2011
Mold Number:	32
Sample Number:	1
Loading Pressure:	25.0 [lb/ft^2] (174.65 [kPa])
Dry Density:	115.2 [lb/ft^3] (1845.3 [kg/m^3])
Moisture Content:	5.60%
Limerock Bearing Ratio:	54.9
Test Operator:	TJM
Creep Compliance Curve Fit:	D = 2.66e-004*log10(t)+1.37e-003 [in^2/lb], R^2=0.99
Creep Compliance Rate (0.01d - 7d):	2.72e-004 [in^2/lb/day]
Creep Compliance Rate (0.01d - 4d):	2.85e-004 [in^2/lb/day]

Figure C-127: Creep vs. Time: 100% MRAP 25 psi

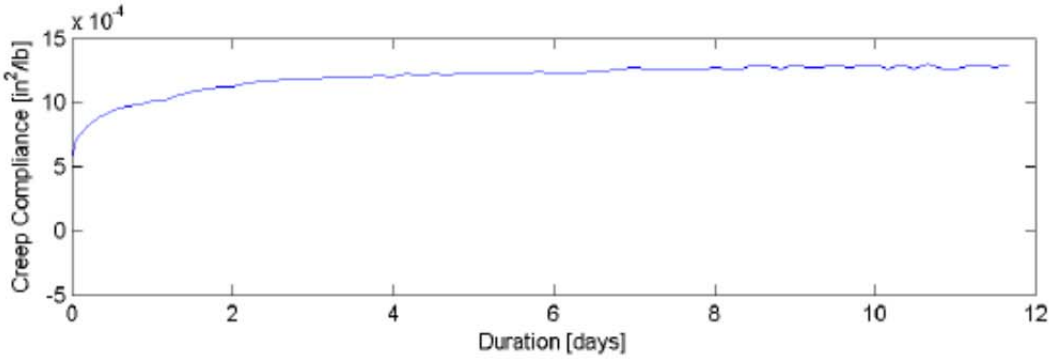

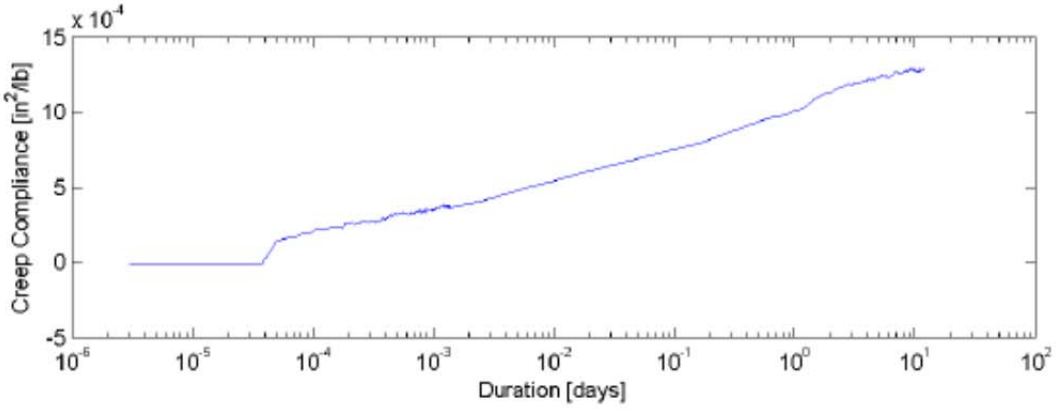

Sample Description:	100% Milled Melbourne RAP
Test Date:	3/2/2011
Mold Number:	38
Sample Number:	3
Loading Pressure:	25.0 [lb/ft^2] (174.65 [kPa])
Dry Density:	116.4 [lb/ft^3] (1864.5 [kg/m^3])
Moisture Content:	5.70%
Limerock Bearing Ratio:	50.0
Test Operator:	TJM
Creep Compliance Curve Fit:	D = 2.50e-004*log10(t)+1.04e-003 [in^2/lb], R^2=0.99
Creep Compliance Rate (0.01d - 7d):	2.58e-004 [in^2/lb/day]
Creep Compliance Rate (0.01d - 4d):	2.56e-004 [in^2/lb/day]

Figure C-128: Creep vs. Time: 100% MRAP 25 psi

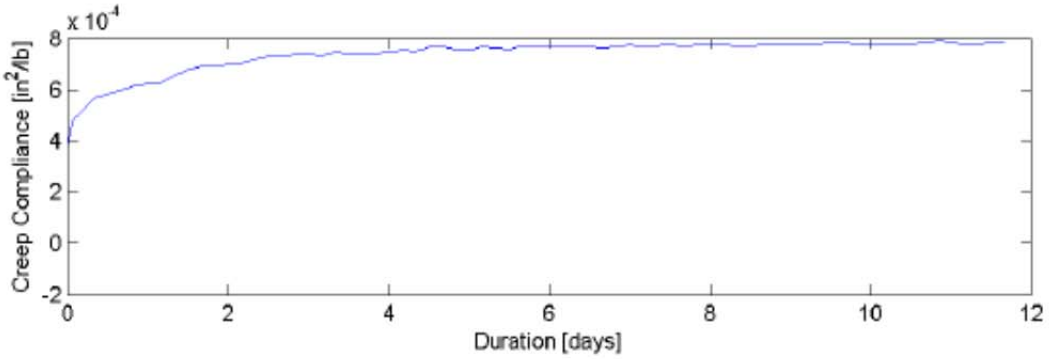

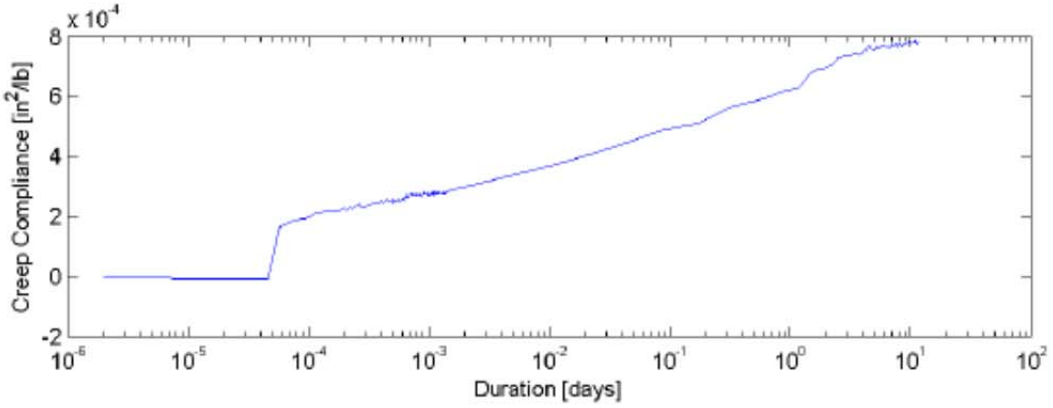

Sample Description:	100% Milled Melbourne RAP
Test Date:	3/2/2011
Mold Number:	36
Sample Number:	2
Loading Pressure:	50.0 [lb/ft²] (349.30 [kPa])
Dry Density:	117.8 [lb/ft³] (1887.0 [kg/m³])
Moisture Content:	6.00%
Limerock Bearing Ratio:	75.5
Test Operator:	TJM
Creep Compliance Curve Fit:	D = 1.38e-004*log10(t)+6.51e-004 [in²/lb], R²=0.99
Creep Compliance Rate (0.01d - 7d):	1.43e-004 [in²/lb/day]
Creep Compliance Rate (0.01d - 4d):	1.45e-004 [in²/lb/day]

Figure C-129: Creep vs. Time: 100% MRAP 50 psi

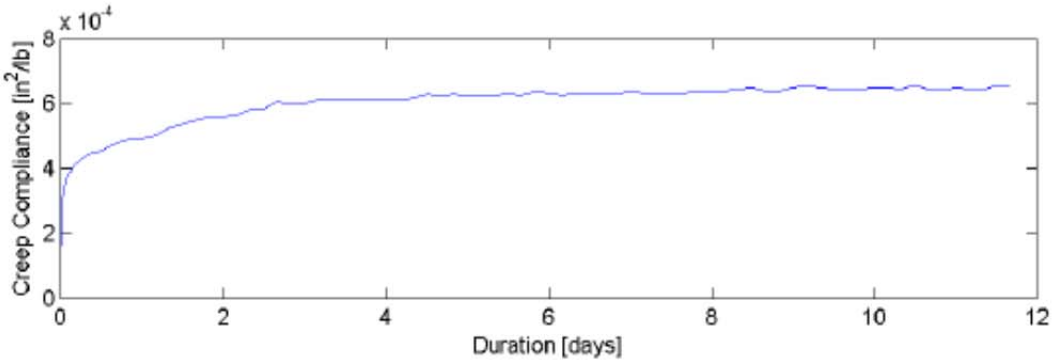

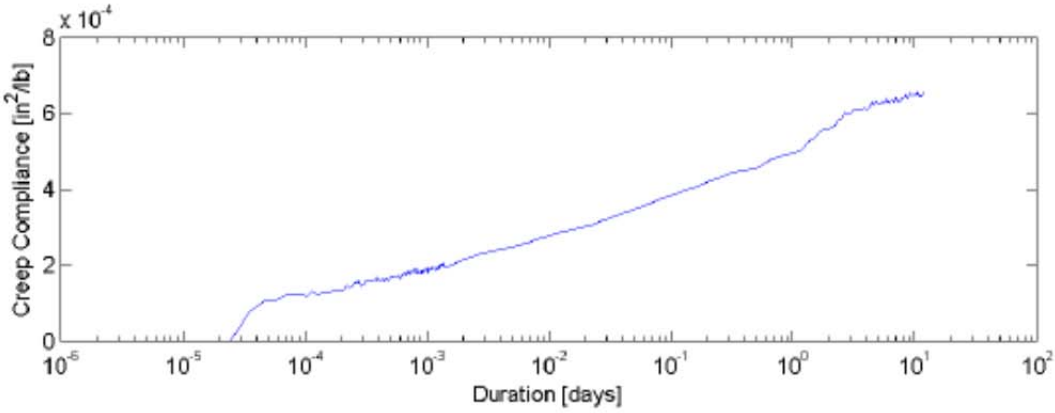

Sample Description:	100% Milled Melbourne RAP
Test Date:	3/2/2011
Mold Number:	52
Sample Number:	4
Loading Pressure:	50.0 [lb/ft^2] (349.30 [kPa])
Dry Density:	118.7 [lb/ft^3] (1901.4 [kg/m^3])
Moisture Content:	6.90%
Limerock Bearing Ratio:	71.6
Test Operator:	TJM
Creep Compliance Curve Fit:	D = 1.24e-004*log10(t)+5.27e-004 [in^2/lb], R^2=0.99
Creep Compliance Rate (0.01d - 7d):	1.28e-004 [in^2/lb/day]
Creep Compliance Rate (0.01d - 4d):	1.29e-004 [in^2/lb/day]

Figure C-130: Creep vs. Time: 100% MRAP 50 psi

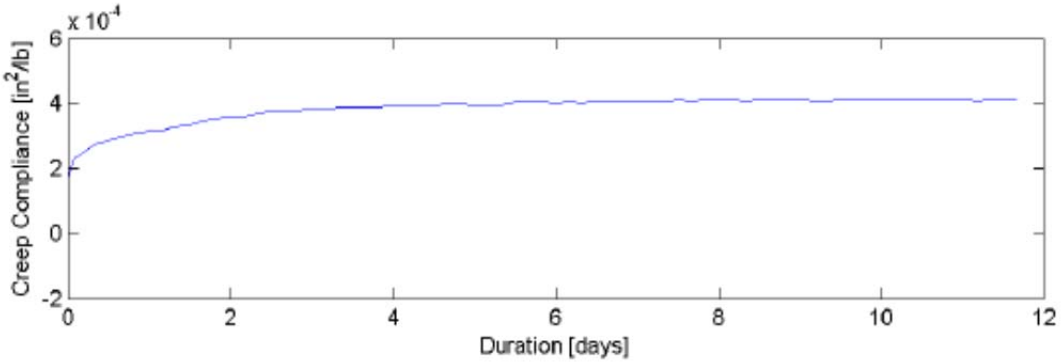

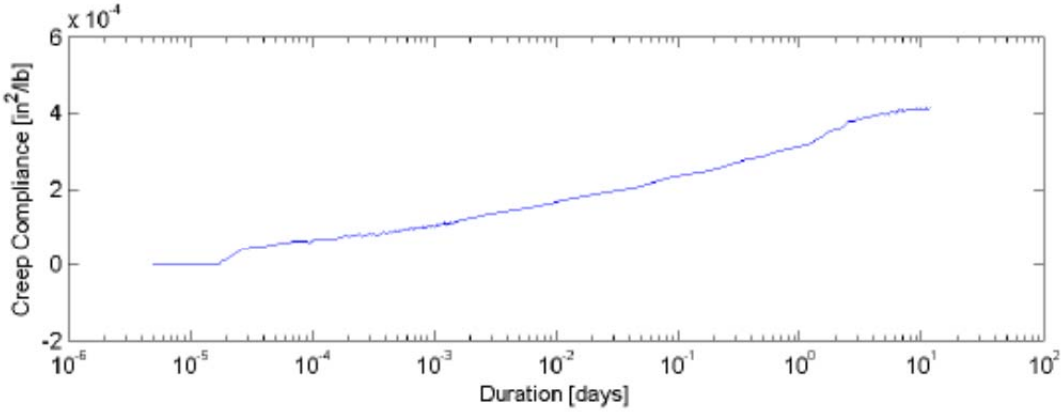

Sample Description:	100% Milled Melbourne RAP
Test Date:	3/2/2011
Mold Number:	53
Sample Number:	5
Loading Pressure:	100.0 [lb/ft²] (698.60 [kPa])
Dry Density:	118.8 [lb/ft³] (1903.0 [kg/m³])
Moisture Content:	7.20%
Limerock Bearing Ratio:	96.8
Test Operator:	TJM
Creep Compliance Curve Fit:	D = 8.36e-005*log10(t)+3.33e-004 [in²/lb], R²=0.99
Creep Compliance Rate (0.01d - 7d):	8.54e-005 [in²/lb/day]
Creep Compliance Rate (0.01d - 4d):	8.82e-005 [in²/lb/day]

Figure C-131: Creep vs. Time: 100% MRAP 100 psi

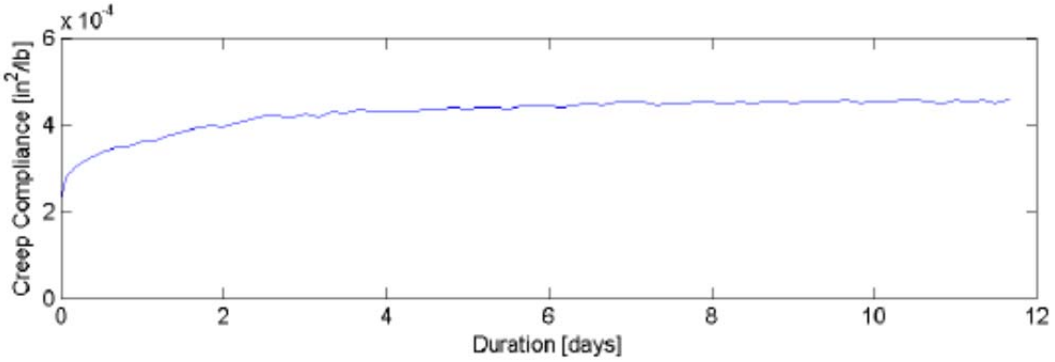

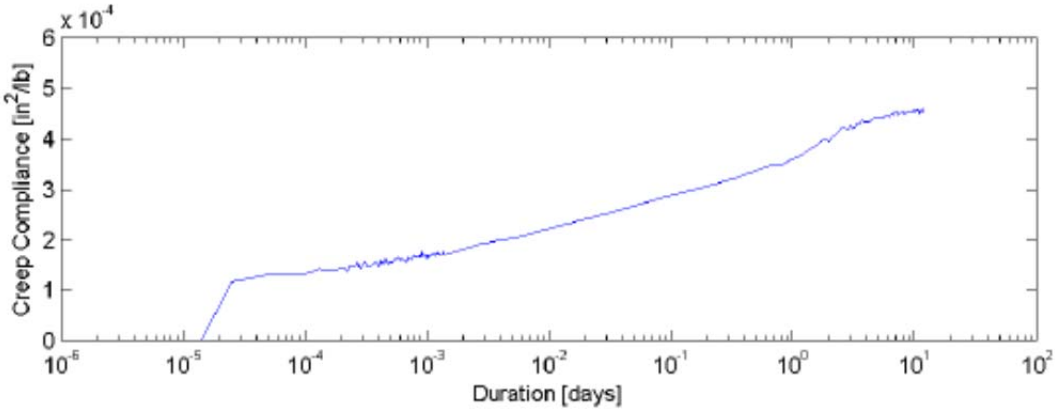

Sample Description:	100% Milled Melbourne RAP
Test Date:	3/2/2011
Mold Number:	55
Sample Number:	6
Loading Pressure:	100.0 [lb/ft^2] (698.60 [kPa])
Dry Density:	123.2 [lb/ft^3] (1973.5 [kg/m^3])
Moisture Content:	5.40%
Limerock Bearing Ratio:	99.0
Test Operator:	TJM
Creep Compliance Curve Fit:	D = 7.80e-005*log10(t)+3.79e-004 [in^2/lb], R^2=0.99
Creep Compliance Rate (0.01d - 7d):	8.11e-005 [in^2/lb/day]
Creep Compliance Rate (0.01d - 4d):	8.18e-005 [in^2/lb/day]

Figure C-132: Creep vs. Time: 100% MRAP 100 psi

C.2.2. Limerock Base

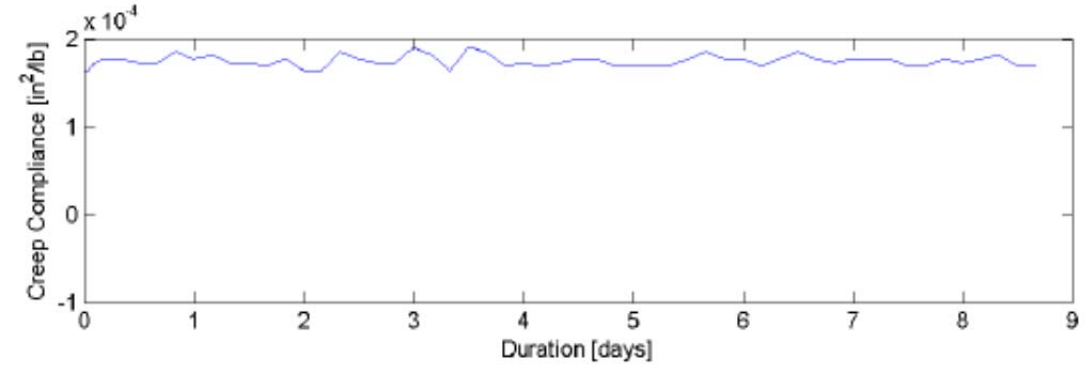

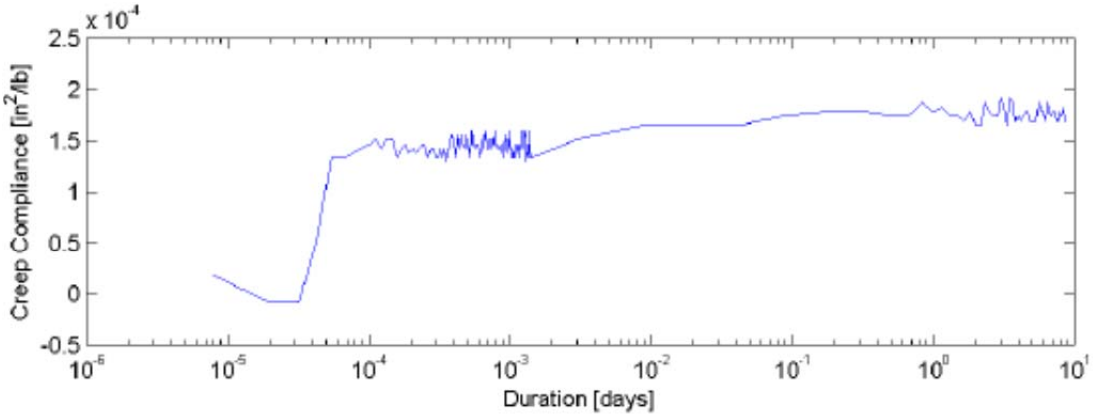

Sample Description:	100% Limerock Base
Test Date:	2/17/2011
Mold Number:	32
Sample Number:	1
Loading Pressure:	25.0 [lb/ft^2] (174.65 [kPa])
Dry Density:	127.1 [lb/ft^3] (2035.9 [kg/m^3])
Moisture Content:	11.40%
Limerock Bearing Ratio:	136.5
Test Operator:	TJM
Creep Compliance Curve Fit:	D = 6.38e-006*log10(t)+1.74e-004 [in^2/lb], R^2=0.58
Creep Compliance Rate (0.01d - 7d):	4.69e-006 [in^2/lb/day]
Creep Compliance Rate (0.01d - 4d):	3.39e-006 [in^2/lb/day]

Figure C-133: Creep vs. Time: 100% Limerock Base 25 psi

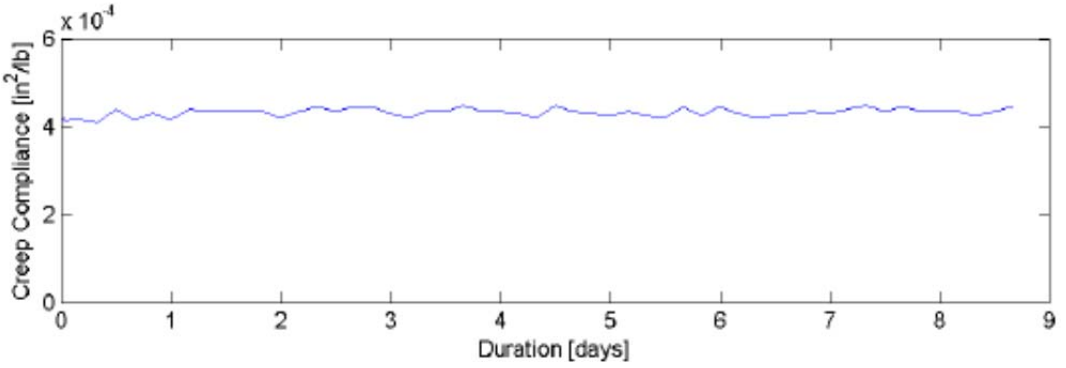

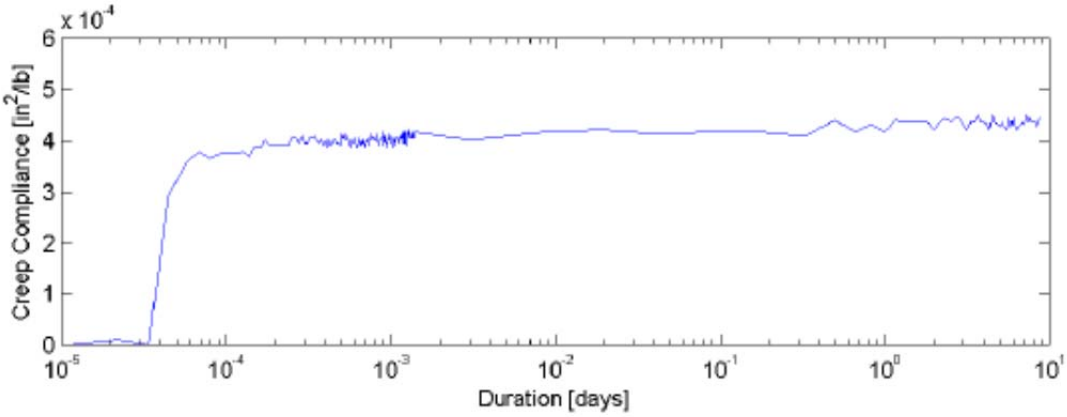

Sample Description:	100% Limerock Base
Test Date:	2/17/2011
Mold Number:	38
Sample Number:	3
Loading Pressure:	25.0 [lb/ft^2] (174.65 [kPa])
Dry Density:	130.1 [lb/ft^3] (2084.0 [kg/m^3])
Moisture Content:	8.80%
Limerock Bearing Ratio:	144.8
Test Operator:	TJM
Creep Compliance Curve Fit:	D = 8.57e-006*log10(t)+4.28e-004 [in^2/lb], R^2=0.66
Creep Compliance Rate (0.01d - 7d):	4.55e-006 [in^2/lb/day]
Creep Compliance Rate (0.01d - 4d):	6.60e-006 [in^2/lb/day]

Figure C-134: Creep vs. Time: 100% Limerock Base 25 psi

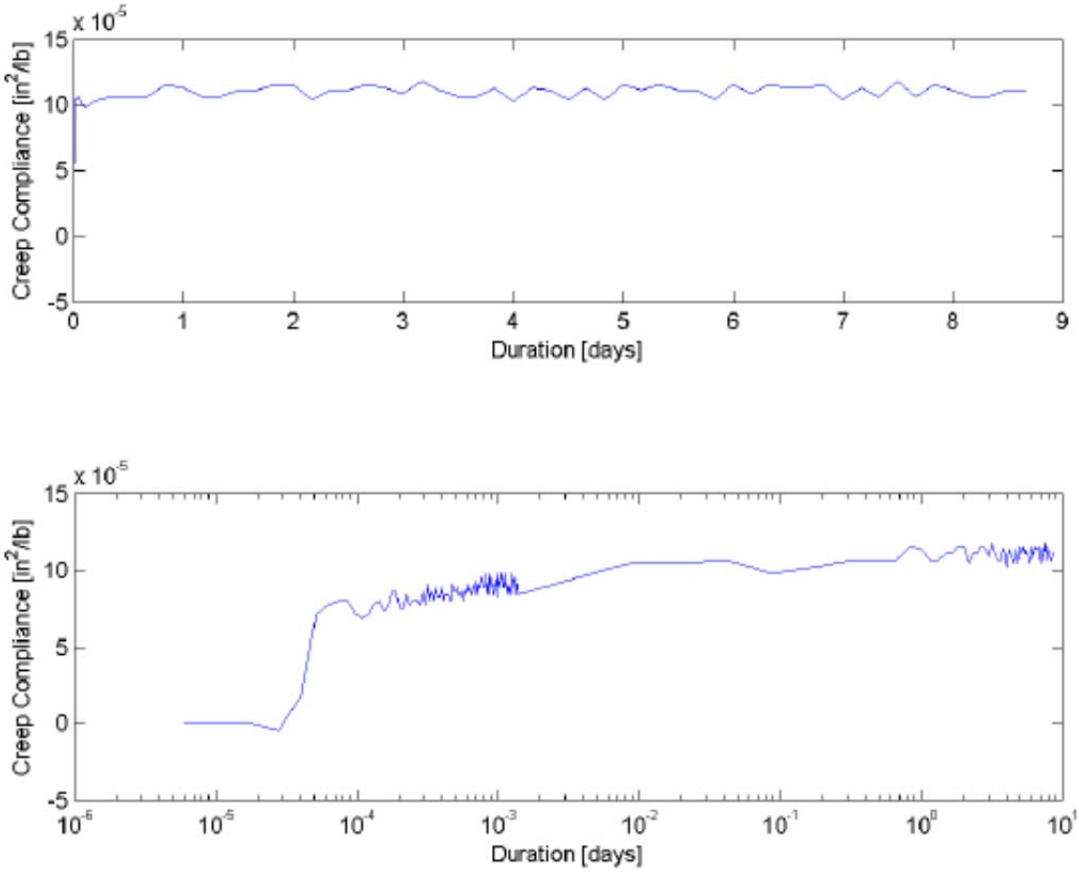

Sample Description:	100% Limerock Base
Test Date:	2/17/2011
Mold Number:	36
Sample Number:	2
Loading Pressure:	50.0 [lb/ft²] (349.30 [kPa])
Dry Density:	128.4 [lb/ft³] (2056.8 [kg/m³])
Moisture Content:	11.20%
Limerock Bearing Ratio:	157.9
Test Operator:	TJM
Creep Compliance Curve Fit:	D = 5.12e-006*log10(t)+1.08e-004 [in²/lb], R^2=0.64
Creep Compliance Rate (0.01d - 7d):	5.36e-008 [in²/lb/day]
Creep Compliance Rate (0.01d - 4d):	-7.86e-007 [in²/lb/day]

Figure C-135: Creep vs. Time: 100% Limerock Base 50 psi

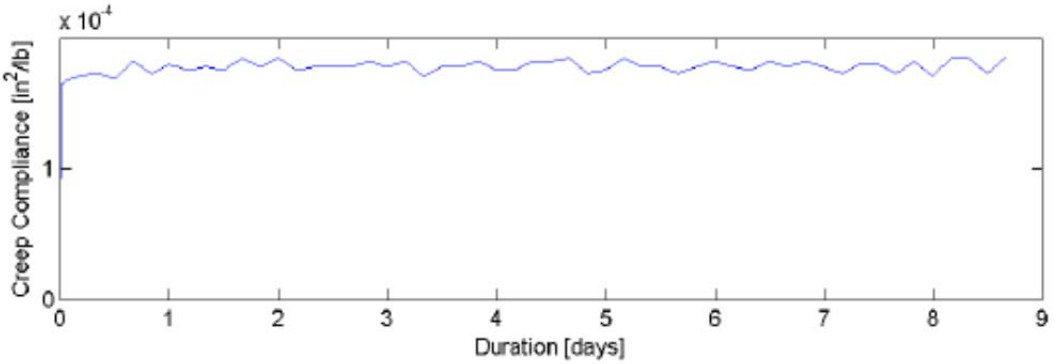

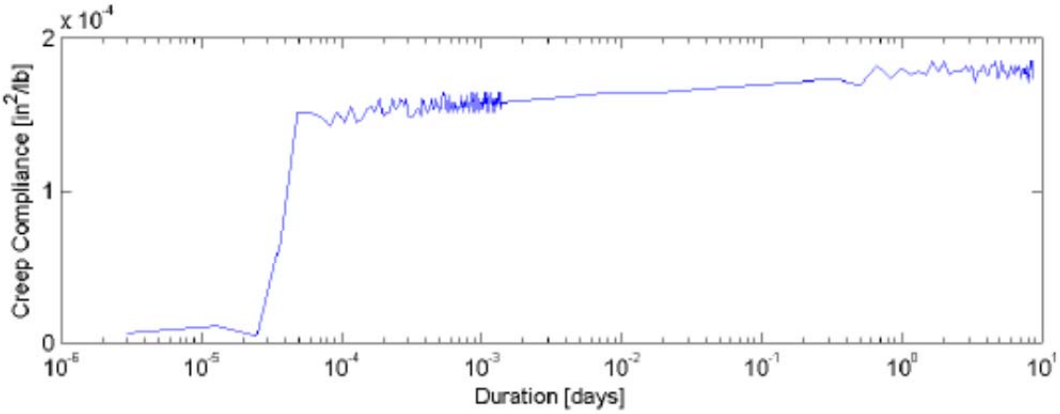

Sample Description:	100% Limerock Base
Test Date:	2/17/2011
Mold Number:	52
Sample Number:	4
Loading Pressure:	50.0 [lb/ft^2] (349.30 [kPa])
Dry Density:	130.2 [lb/ft^3] (2085.6 [kg/m^3])
Moisture Content:	9.60%
Limerock Bearing Ratio:	162.9
Test Operator:	TJM
Creep Compliance Curve Fit:	D = 5.63e-006*log10(t)+1.75e-004 [in^2/lb], R^2=0.83
Creep Compliance Rate (0.01d - 7d):	4.67e-006 [in^2/lb/day]
Creep Compliance Rate (0.01d - 4d):	4.28e-006 [in^2/lb/day]

Figure C-136: Creep vs. Time: 100% Limerock Base 50 psi

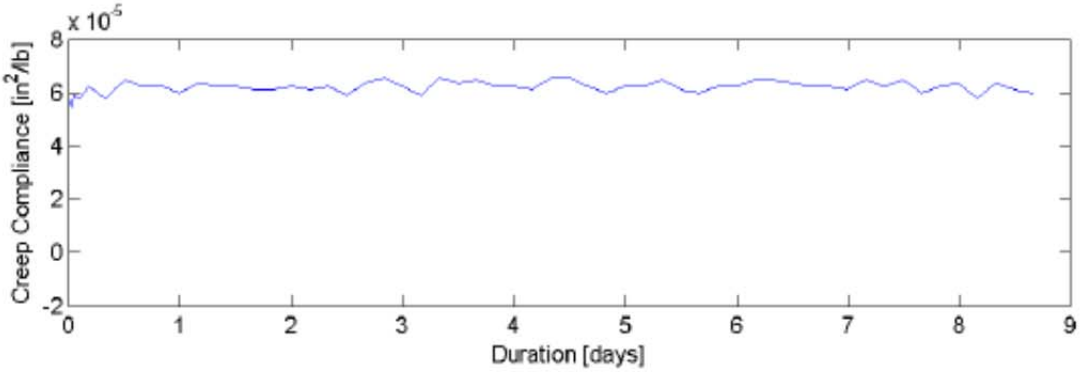

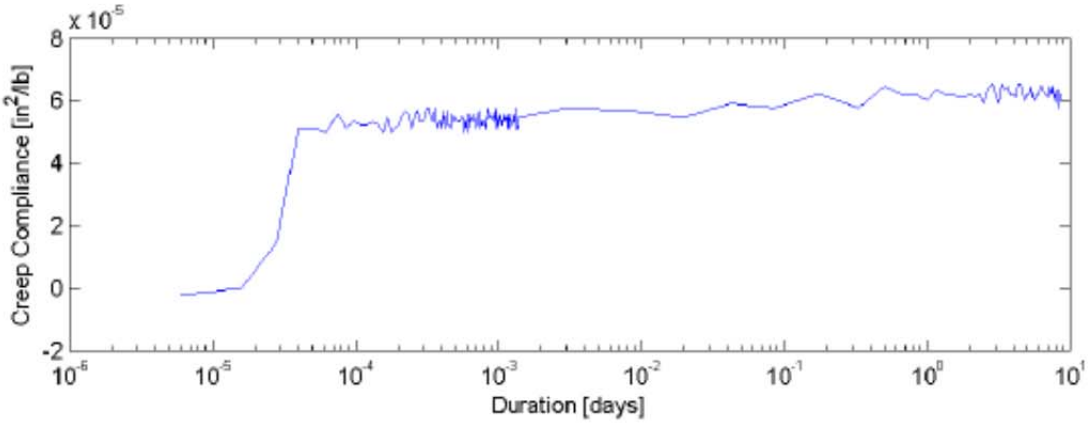

Sample Description:	100% Limerock Base
Test Date:	2/17/2011
Mold Number:	53
Sample Number:	5
Loading Pressure:	100.0 [lb/ft²] (698.60 [kPa])
Dry Density:	130.2 [lb/ft³] (2085.6 [kg/m³])
Moisture Content:	11.20%
Limerock Bearing Ratio:	138.3
Test Operator:	TJM
Creep Compliance Curve Fit:	D = 2.05e-006*log10(t)+6.12e-005 [in²/lb], R²=0.73
Creep Compliance Rate (0.01d - 7d):	1.68e-006 [in²/lb/day]
Creep Compliance Rate (0.01d - 4d):	2.24e-006 [in²/lb/day]

Figure C-137: Creep vs. Time: 100% Limerock Base 100 psi

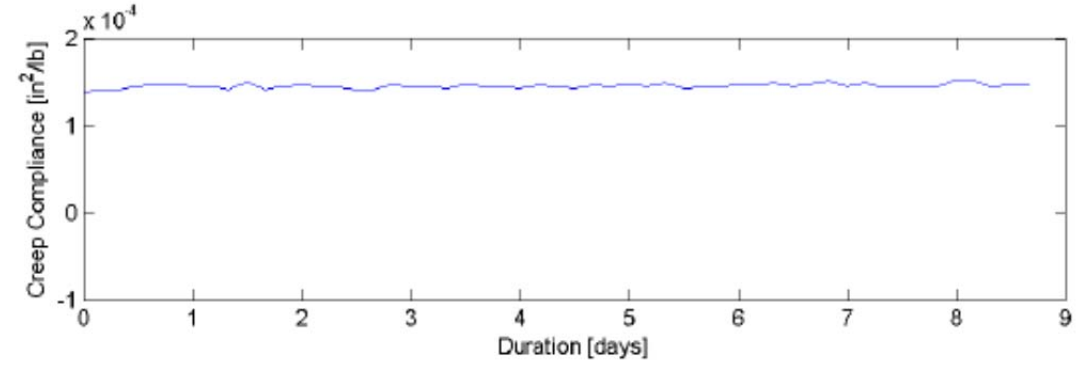

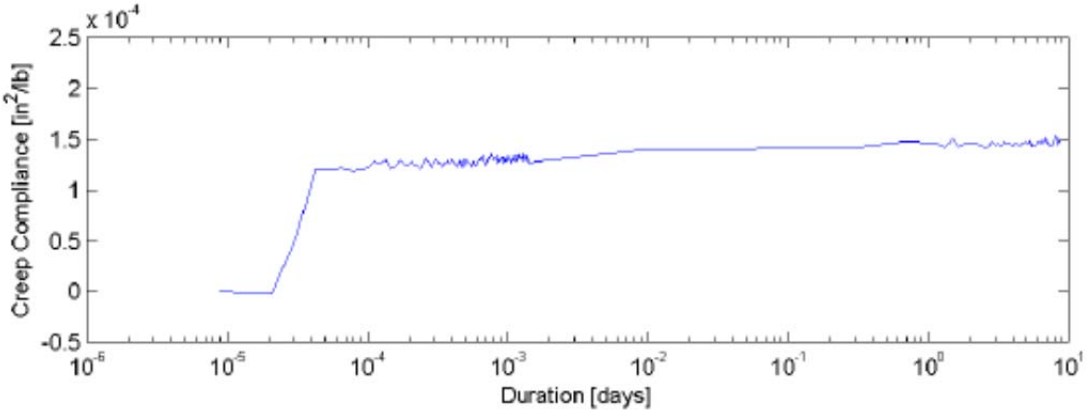

Sample Description:	100% Limerock Base
Test Date:	2/17/2011
Mold Number:	55
Sample Number:	6
Loading Pressure:	100.0 [lb/ft^2] (698.60 [kPa])
Dry Density:	131.6 [lb/ft^3] (2108.0 [kg/m^3])
Moisture Content:	9.80%
Limerock Bearing Ratio:	206.1
Test Operator:	TJM
Creep Compliance Curve Fit:	D = 3.94e-006*log10(t)+1.44e-004 [in^2/lb], R^2=0.78
Creep Compliance Rate (0.01d - 7d):	2.37e-006 [in^2/lb/day]
Creep Compliance Rate (0.01d - 4d):	1.73e-006 [in^2/lb/day]

Figure C-138: Creep vs. Time: 100% Limerock Base 100 psi

C.2.3. Cemented Coquina Base

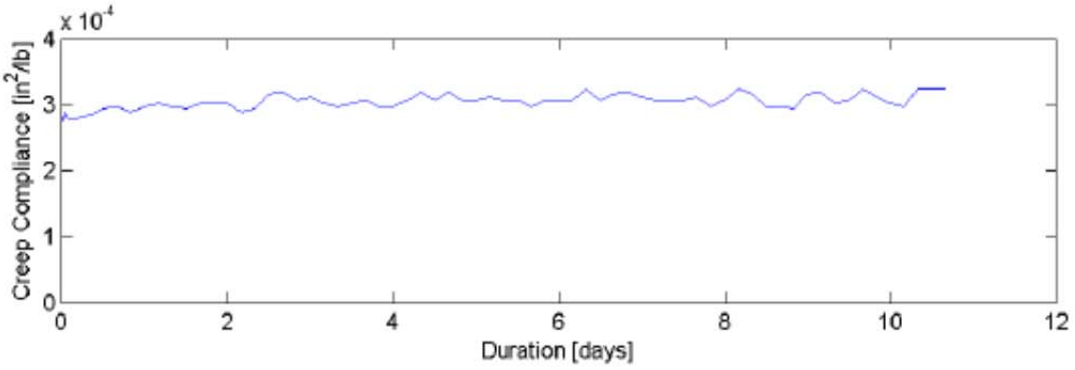

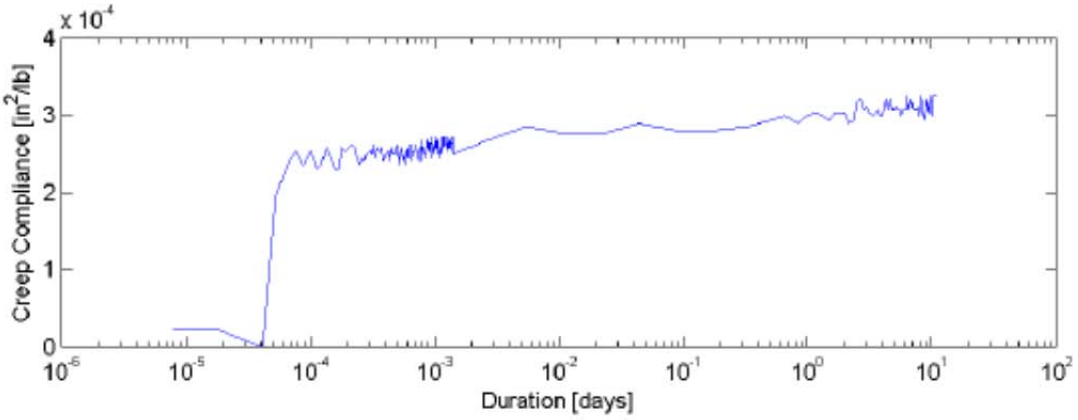

Sample Description:	100% Cemented Coquinia Base
Test Date:	4/1/2011
Mold Number:	52
Sample Number:	4
Loading Pressure:	25.0 [lb/ft^2] (174.65 [kPa])
Dry Density:	126.1 [lb/ft^3] (2019.9 [kg/m^3])
Moisture Content:	7.60%
Limerock Bearing Ratio:	200.5
Test Operator:	TJM
Creep Compliance Curve Fit:	D = 1.10e-005*log10(t)+2.98e-004 [in^2/lb], R^2=0.85
Creep Compliance Rate (0.01d - 7d):	1.19e-005 [in^2/lb/day]
Creep Compliance Rate (0.01d - 4d):	7.94e-006 [in^2/lb/day]

Figure C-139: Creep vs. Time: 100% Cemented Coquina 25 psi

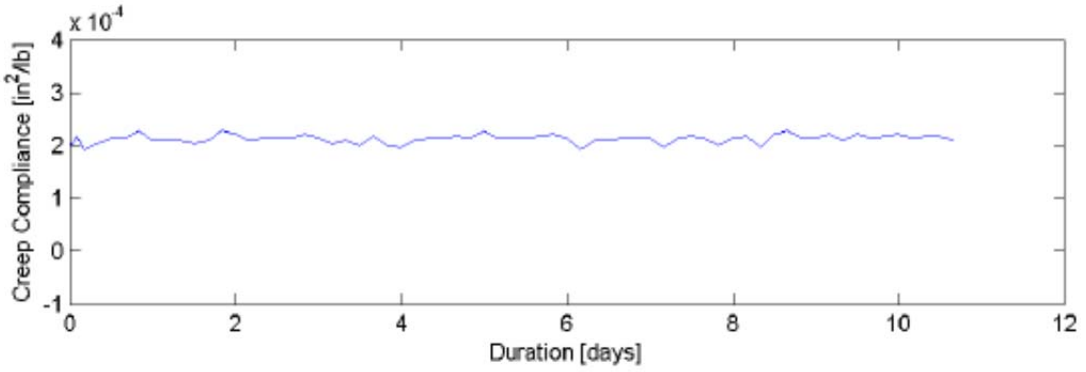

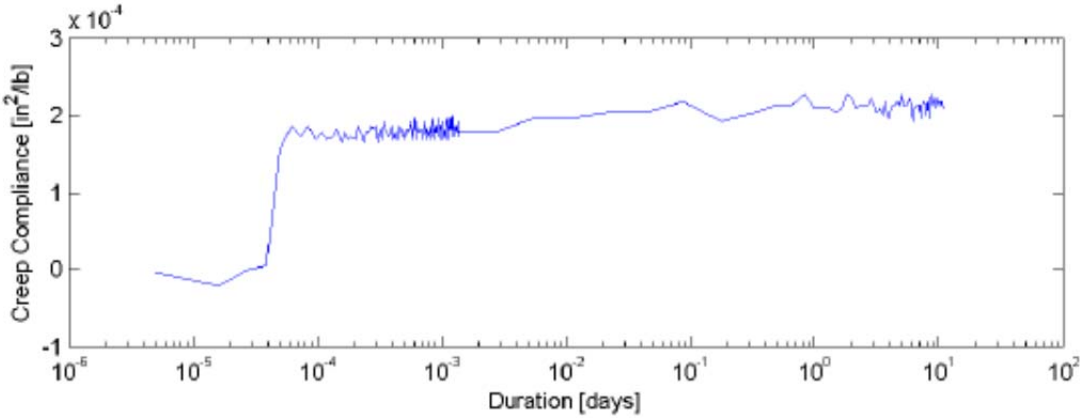

Sample Description:	100% Cemented Coquinia Base
Test Date:	4/1/2011
Mold Number:	55
Sample Number:	6
Loading Pressure:	25.0 [lb/ft²] (174.65 [kPa])
Dry Density:	126.4 [lb/ft³] (2024.7 [kg/m³])
Moisture Content:	7.40%
Limerock Bearing Ratio:	191.4
Test Operator:	TJM
Creep Compliance Curve Fit:	D = 6.70e-006*log10(t)+2.09e-004 [in²/lb], R²=0.56
Creep Compliance Rate (0.01d - 7d):	6.23e-006 [in²/lb/day]
Creep Compliance Rate (0.01d - 4d):	1.41e-008 [in²/lb/day]

Figure C-140: Creep vs. Time: 100% Cemented Coquina 25 psi

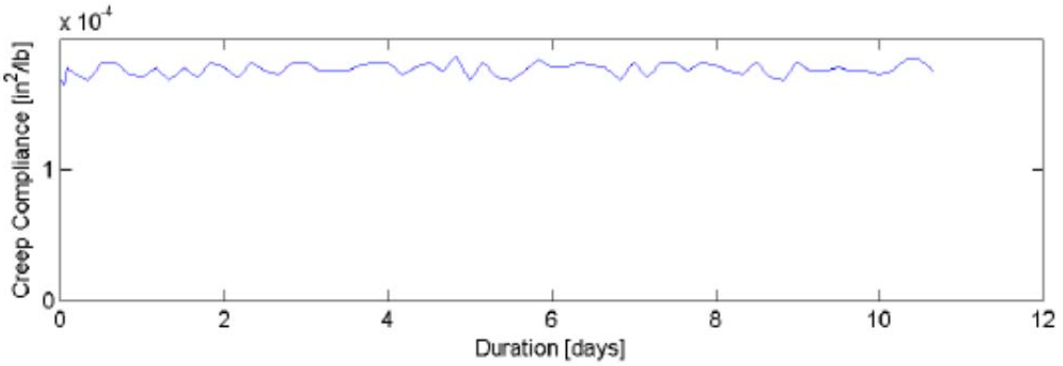

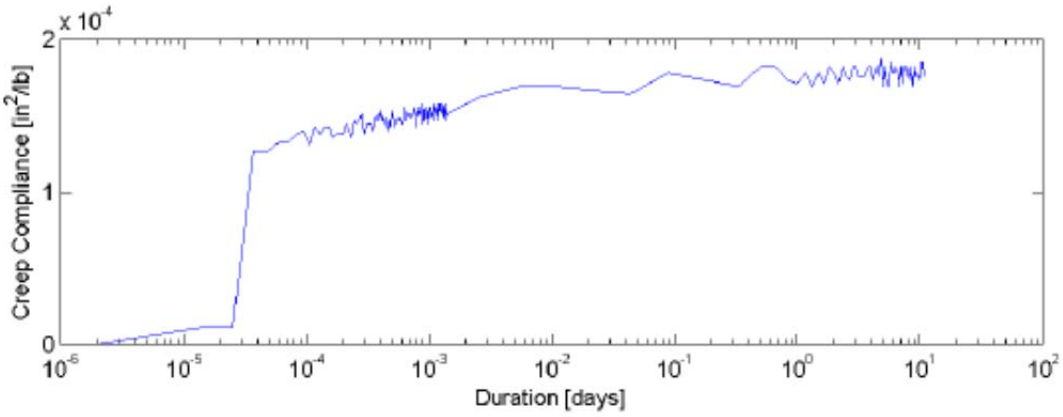

Sample Description:	100% Cemented Coquinia Base
Test Date:	4/1/2011
Mold Number:	32
Sample Number:	1
Loading Pressure:	50.0 [lb/ft^2] (349.30 [kPa])
Dry Density:	126.9 [lb/ft^3] (2032.7 [kg/m^3])
Moisture Content:	7.60%
Limerock Bearing Ratio:	183.2
Test Operator:	TJM
Creep Compliance Curve Fit:	D = 5.08e-006*log10(t)+1.75e-004 [in^2/lb], R^2=0.62
Creep Compliance Rate (0.01d - 7d):	4.68e-006 [in^2/lb/day]
Creep Compliance Rate (0.01d - 4d):	5.12e-006 [in^2/lb/day]

Figure C-141: Creep vs. Time: 100% Cemented Coquina 50 psi

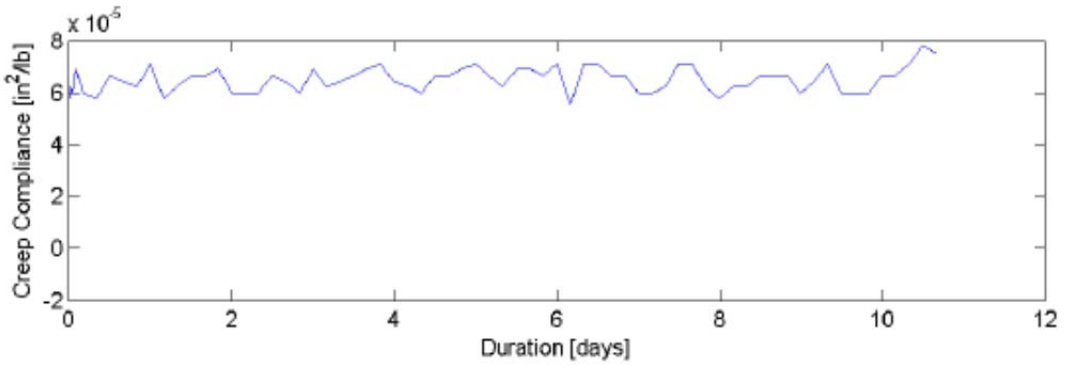

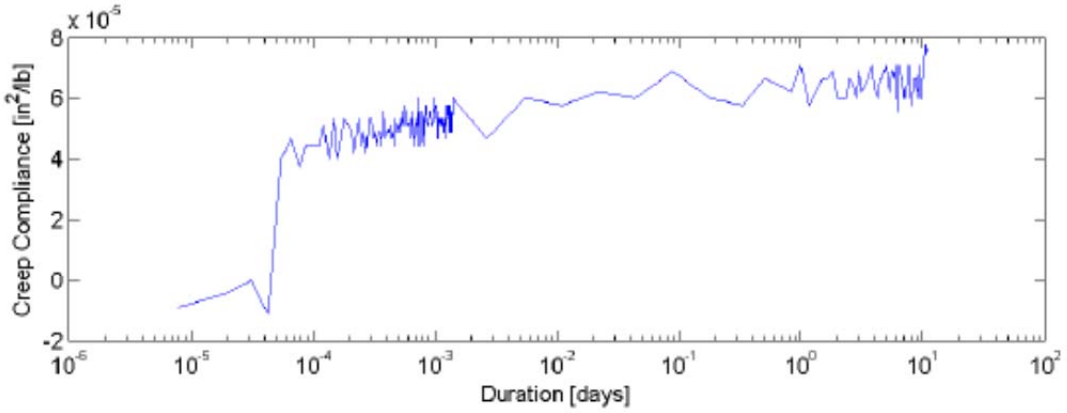

Sample Description:	100% Cemented Coquinia Base
Test Date:	4/1/2011
Mold Number:	36
Sample Number:	2
Loading Pressure:	50.0 [lb/ft²] (349.30 [kPa])
Dry Density:	127.3 [lb/ft³] (2039.2 [kg/m³])
Moisture Content:	7.60%
Limerock Bearing Ratio:	159.1
Test Operator:	TJM
Creep Compliance Curve Fit:	D = 3.01e-006*log10(t)+6.45e-005 [in²/lb], R²=0.41
Creep Compliance Rate (0.01d - 7d):	6.41e-007 [in²/lb/day]
Creep Compliance Rate (0.01d - 4d):	2.39e-006 [in²/lb/day]

Figure C-142: Creep vs. Time: 100% Cemented Coquina 50 psi

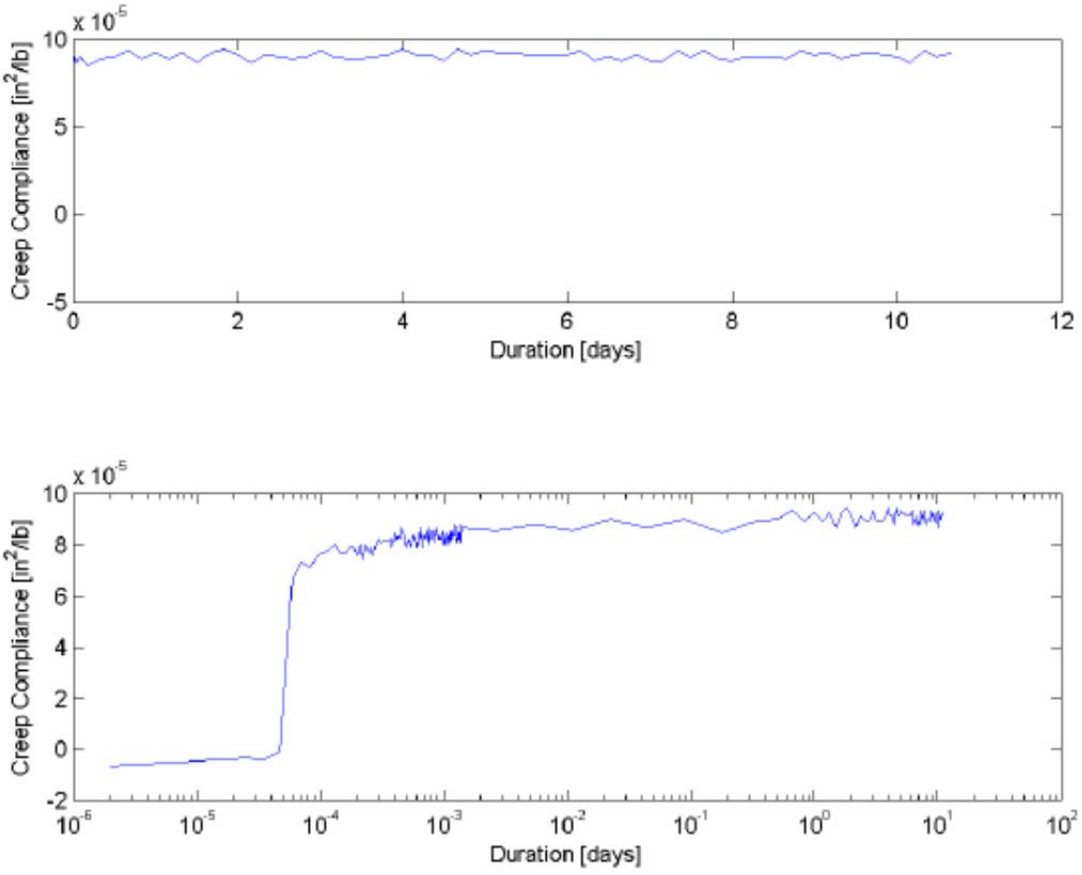

Sample Description:	100% Cemented Coquinia Base
Test Date:	4/1/2011
Mold Number:	38
Sample Number:	3
Loading Pressure:	100.0 [lb/ft^2] (698.60 [kPa])
Dry Density:	128.8 [lb/ft^3] (2063.2 [kg/m^3])
Moisture Content:	7.60%
Limerock Bearing Ratio:	260.7
Test Operator:	TJM
Creep Compliance Curve Fit:	D = 1.57e-006*log10(t)+8.95e-005 [in^2/lb], R^2=0.47
Creep Compliance Rate (0.01d - 7d):	6.40e-007 [in^2/lb/day]
Creep Compliance Rate (0.01d - 4d):	3.26e-006 [in^2/lb/day]

Figure C-143: Creep vs. Time: 100% Cemented Coquina 100 psi

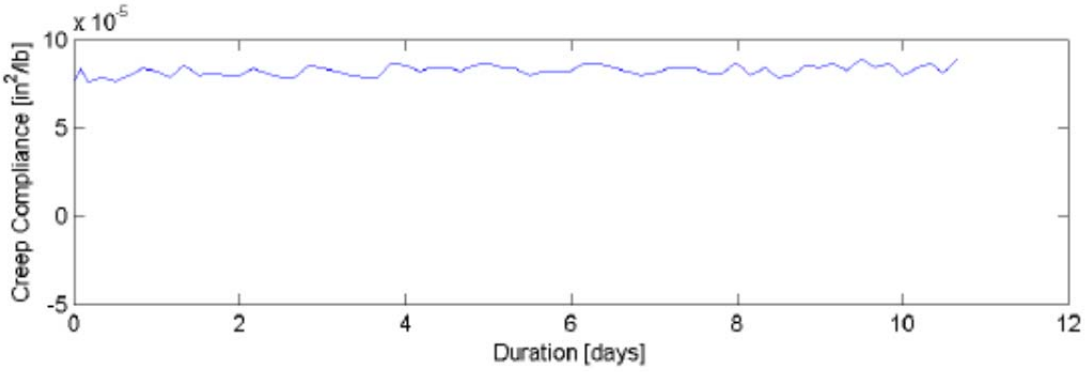

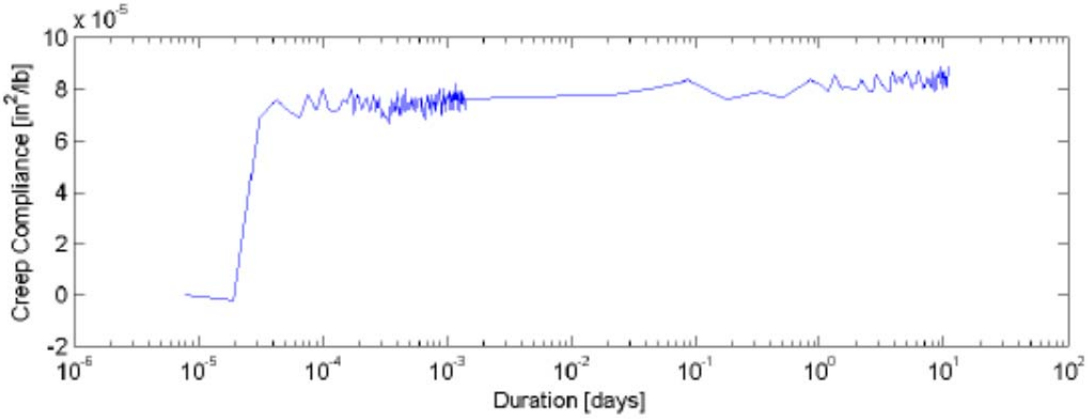

Sample Description:	100% Cemented Coquinia Base
Test Date:	4/1/2011
Mold Number:	53
Sample Number:	5
Loading Pressure:	100.0 [lb/ft²] (698.60 [kPa])
Dry Density:	129.9 [lb/ft³] (2080.8 [kg/m³])
Moisture Content:	8.00%
Limerock Bearing Ratio:	266.1
Test Operator:	TJM
Creep Compliance Curve Fit:	D = 1.72e-006*log10(t)+8.11e-005 [in²/lb], R²=0.44
Creep Compliance Rate (0.01d - 7d):	1.25e-006 [in²/lb/day]
Creep Compliance Rate (0.01d - 4d):	3.06e-006 [in²/lb/day]

Figure C-144: Creep vs. Time: 100% Cemented Coquina 100 psi

C.2.4. Recycled Concrete Aggregate

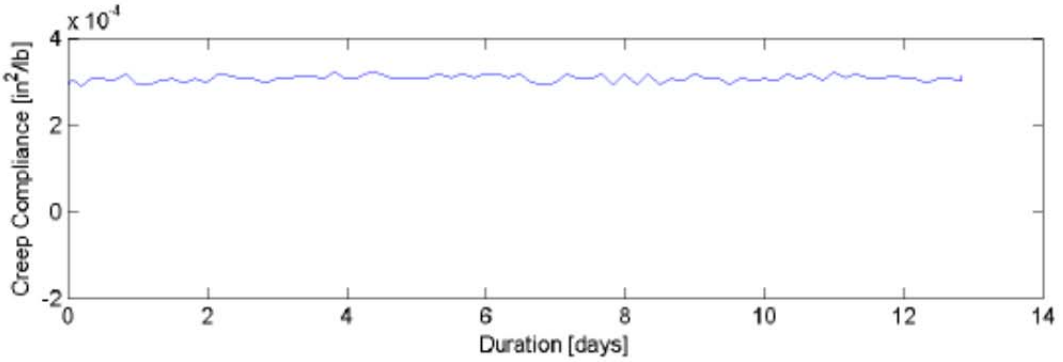

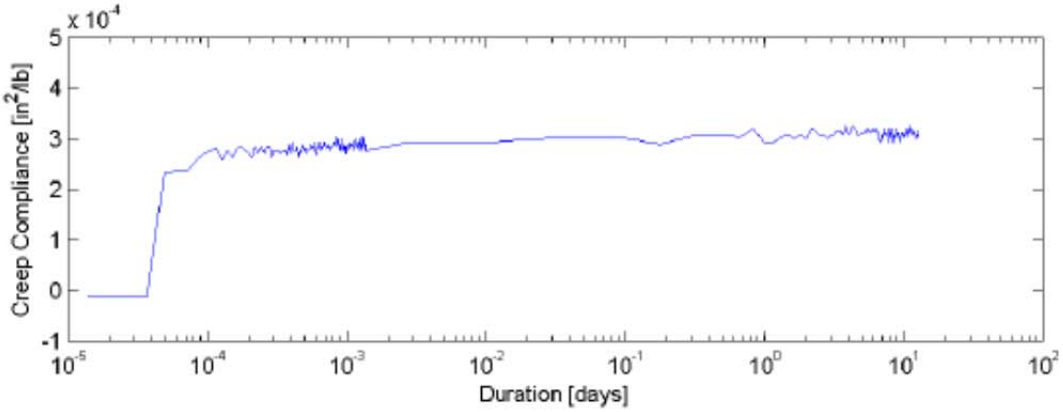

Sample Description:	100% Recycled Concrete Aggragrate
Test Date:	9/6/2011
Mold Number:	52
Sample Number:	2
Loading Pressure:	25.0 [lb/ft²] (174.65 [kPa])
Dry Density:	106.6 [lb/ft³] (1707.6 [kg/m³])
Moisture Content:	15.20%
Limerock Bearing Ratio:	198.3
Test Operator:	TJM
Creep Compliance Curve Fit:	D = 5.96e-006*log10(t)+3.06e-004 [in²/lb], R²=0.50
Creep Compliance Rate (0.01d - 7d):	1.58e-006 [in²/lb/day]
Creep Compliance Rate (0.01d - 4d):	5.13e-006 [in²/lb/day]

Figure C-145: Creep vs. Time: 100% Recycled Concrete Aggregate 25 psi

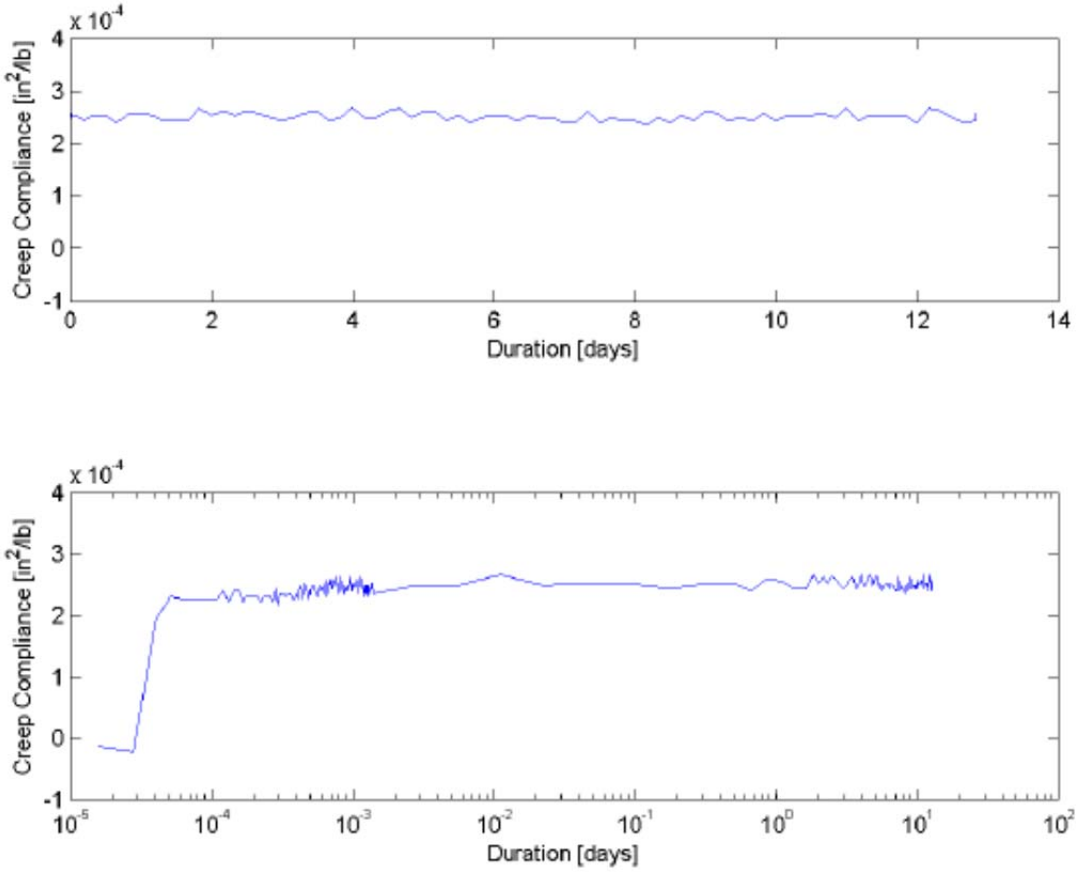

Sample Description:	100% Recycled Concrete Aggragrate
Test Date:	9/6/2011
Mold Number:	69
Sample Number:	6
Loading Pressure:	25.0 [lb/ft²] (174.65 [kPa])
Dry Density:	107.3 [lb/ft³] (1718.8 [kg/m³])
Moisture Content:	14.90%
Limerock Bearing Ratio:	196.7
Test Operator:	TJM
Creep Compliance Curve Fit:	D = 3.96e-008*log10(t)+2.53e-004 [in²/lb], R²=0.00
Creep Compliance Rate (0.01d - 7d):	-8.08e-006 [in²/lb/day]
Creep Compliance Rate (0.01d - 4d):	1.38e-006 [in²/lb/day]

Figure C-146: Creep vs. Time: 100% Recycled Concrete Aggregate 25 psi

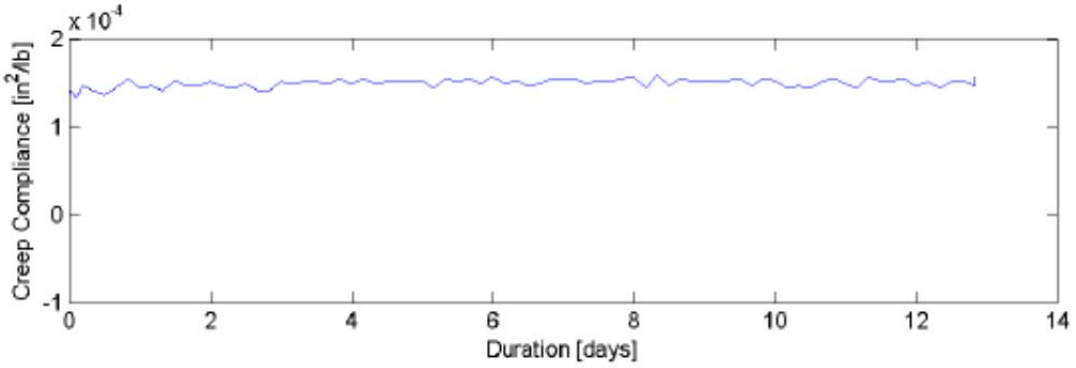

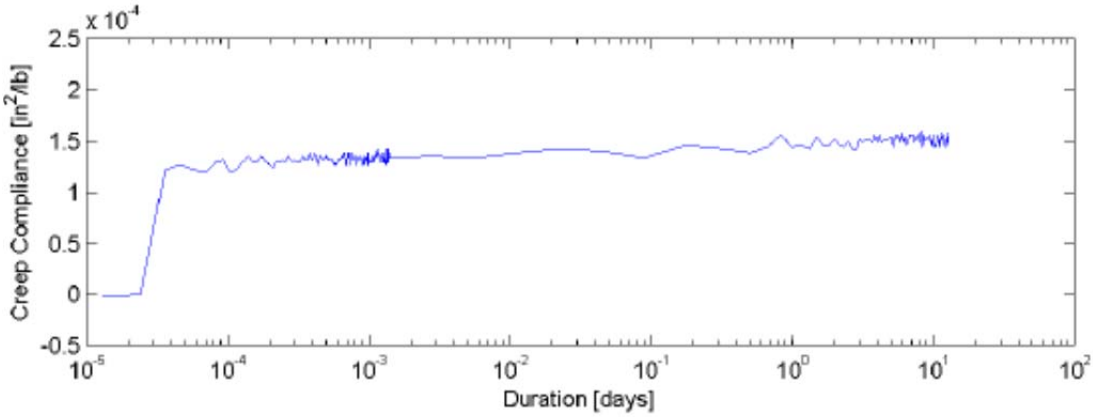

Sample Description:	100% Recycled Concrete Aggragrate
Test Date:	9/6/2011
Mold Number:	55
Sample Number:	4
Loading Pressure:	50.0 [lb/ft²] (349.30 [kPa])
Dry Density:	109.3 [lb/ft³] (1750.8 [kg/m³])
Moisture Content:	14.40%
Limerock Bearing Ratio:	241.9
Test Operator:	TJM
Creep Compliance Curve Fit:	D = 5.64e-006*log10(t)+1.47e-004 [in²/lb], R²=0.78
Creep Compliance Rate (0.01d - 7d):	6.56e-006 [in²/lb/day]
Creep Compliance Rate (0.01d - 4d):	4.61e-006 [in²/lb/day]

Figure C-147: Creep vs. Time: 100% Recycled Concrete Aggregate 50 psi

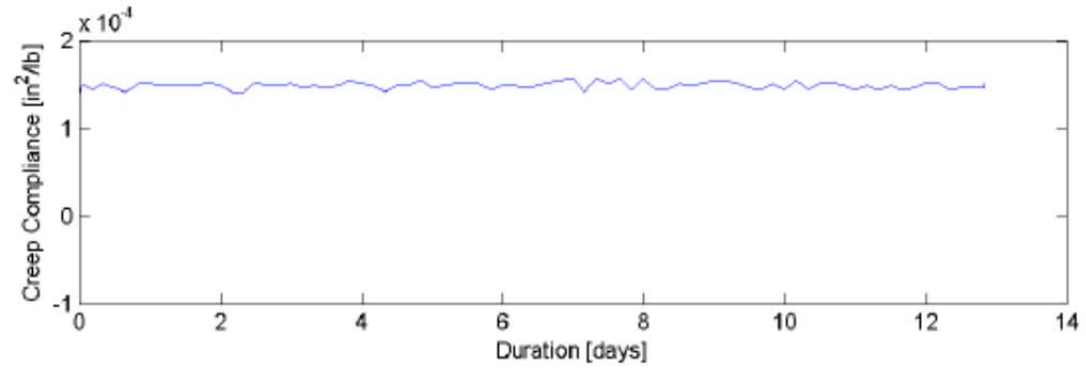

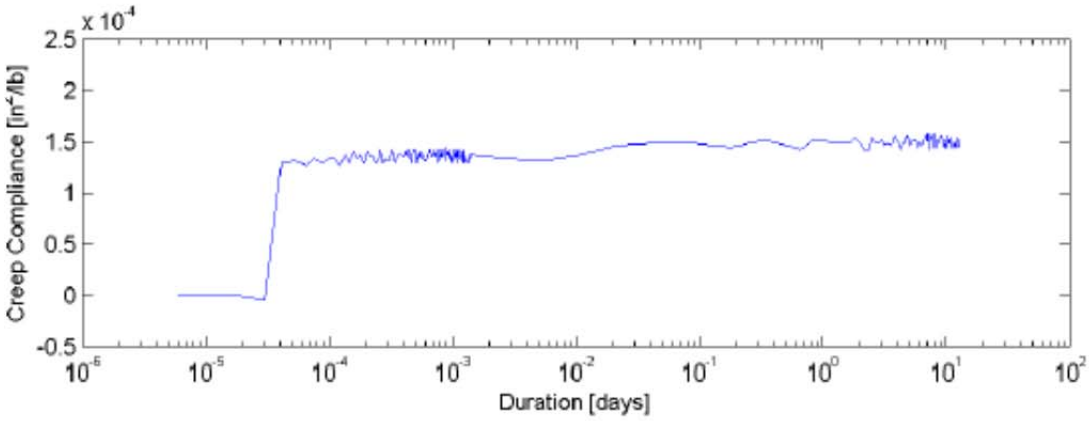

Sample Description:	100% Recycled Concrete Aggragrate
Test Date:	9/6/2011
Mold Number:	26
Sample Number:	1
Loading Pressure:	50.0 [lb/ft^2] (349.30 [kPa])
Dry Density:	109.1 [lb/ft^3] (1747.6 [kg/m^3])
Moisture Content:	14.50%
Limerock Bearing Ratio:	225.0
Test Operator:	TJM
Creep Compliance Curve Fit:	D = 4.44e-006*log10(t)+1.48e-004 [in^2/lb], R^2=0.63
Creep Compliance Rate (0.01d - 7d):	7.50e-006 [in^2/lb/day]
Creep Compliance Rate (0.01d - 4d):	5.64e-006 [in^2/lb/day]

Figure C-148: Creep vs. Time: 100% Recycled Concrete Aggregate 50 psi

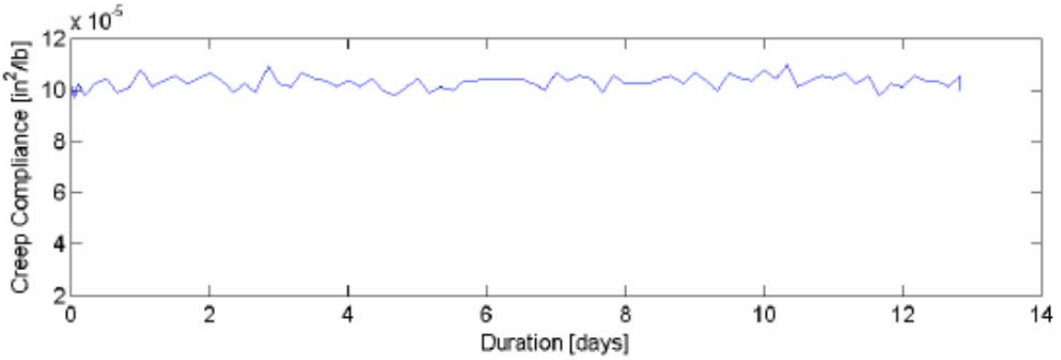

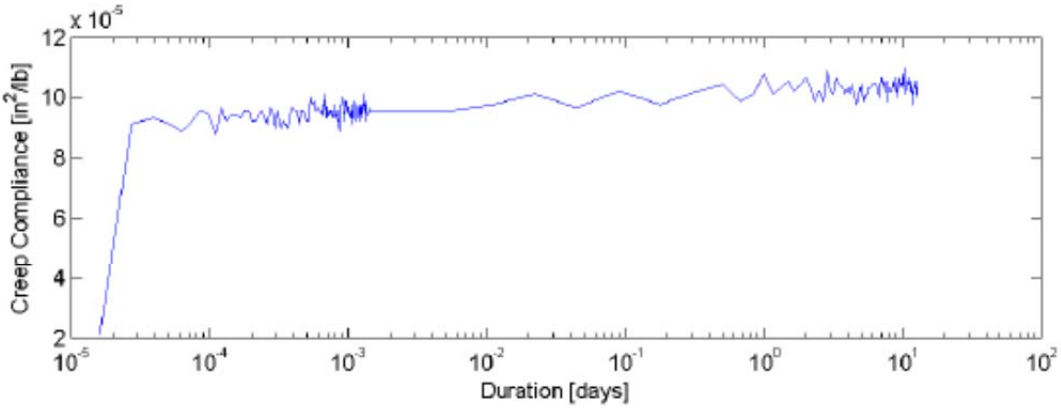

Sample Description:	100% Recycled Concrete Aggragrate
Test Date:	9/6/2011
Mold Number:	65
Sample Number:	5
Loading Pressure:	100.0 [lb/ft^2] (698.60 [kPa])
Dry Density:	108.9 [lb/ft^3] (1744.4 [kg/m^3])
Moisture Content:	14.90%
Limerock Bearing Ratio:	285.1
Test Operator:	TJM
Creep Compliance Curve Fit:	D = 2.43e-006*log10(t)+1.02e-004 [in^2/lb], R^2=0.63
Creep Compliance Rate (0.01d - 7d):	3.28e-006 [in^2/lb/day]
Creep Compliance Rate (0.01d - 4d):	2.30e-006 [in^2/lb/day]

Figure C-149: Creep vs. Time: 100% Recycled Concrete Aggregate 100 psi

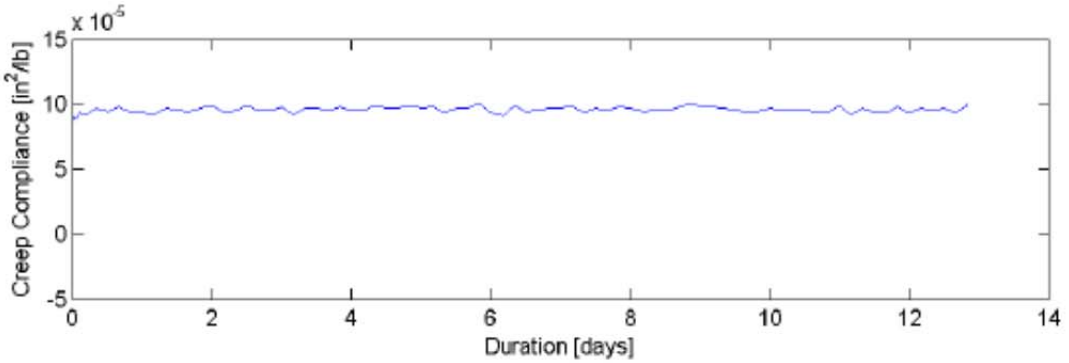

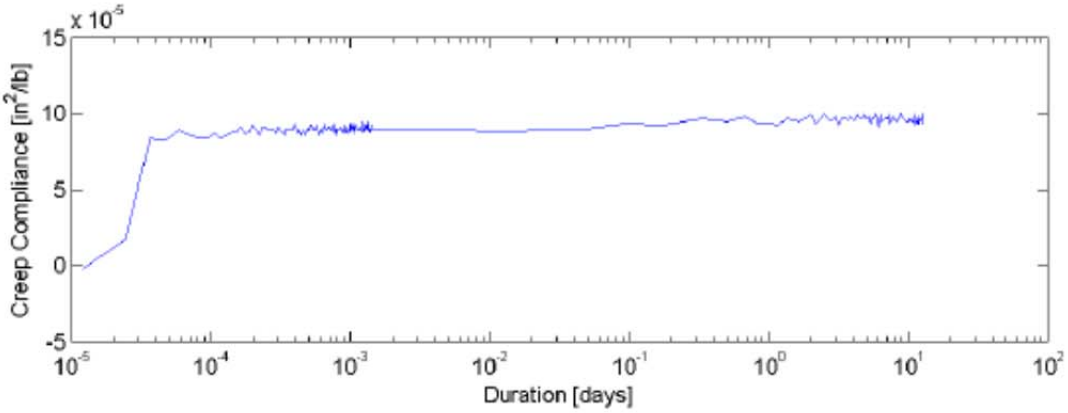

Sample Description:	100% Recycled Concrete Aggragrate
Test Date:	9/6/2011
Mold Number:	53
Sample Number:	3
Loading Pressure:	100.0 [lb/ft²] (698.60 [kPa])
Dry Density:	109.6 [lb/ft³] (1755.6 [kg/m³])
Moisture Content:	14.80%
Limerock Bearing Ratio:	316.7
Test Operator:	TJM
Creep Compliance Curve Fit:	D = 2.02e-006*log10(t)+9.50e-005 [in²/lb], R²=0.61
Creep Compliance Rate (0.01d - 7d):	2.97e-006 [in²/lb/day]
Creep Compliance Rate (0.01d - 4d):	2.82e-006 [in²/lb/day]

Figure C-150: Creep vs. Time: 100% Recycled Concrete Aggregate 100 psi

C.3. Creep Data MRAP/Aggregate Blends

C.3.1. MRAP/Limerock Blends

C.3.1.1. 25% MRAP/75% Limerock Blends

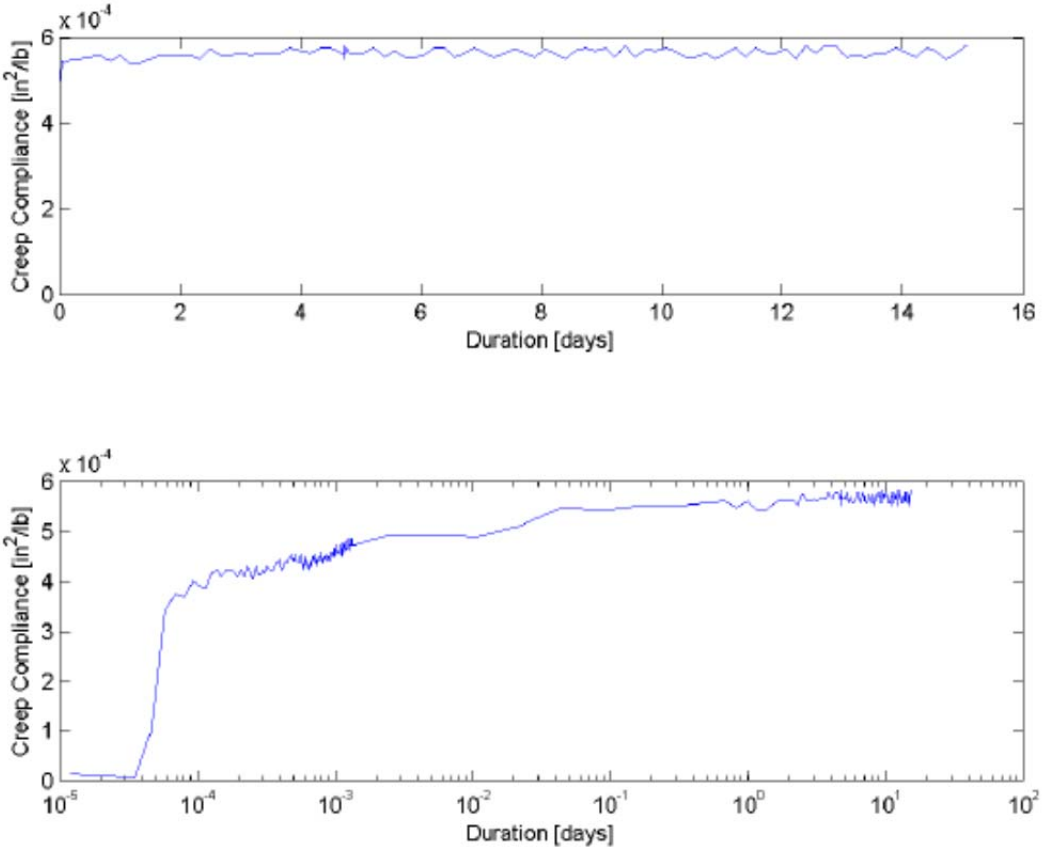

Sample Description:	75%/25% Limerock / Melbourne Milled RAP
Test Date:	8/6/2011
Mold Number:	41
Sample Number:	4
Loading Pressure:	25.0 [lb/ft²] (174.65 [kPa])
Dry Density:	124.2 [lb/ft³] (1989.5 [kg/m³])
Moisture Content:	9.10%
Limerock Bearing Ratio:	197.2
Test Operator:	TJM
Creep Compliance Curve Fit:	D = 2.26e-005*log10(t)+5.51e-004 [in²/lb], R²=0.88
Creep Compliance Rate (0.01d - 7d):	2.80e-005 [in²/lb/day]
Creep Compliance Rate (0.01d - 4d):	3.05e-005 [in²/lb/day]

Figure C-151: Creep vs. Time: 25% MRAP/75% LR Blend 25 psi

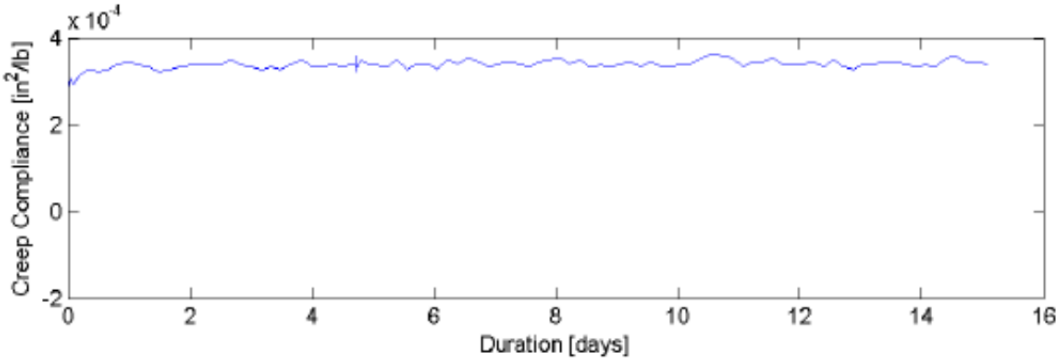

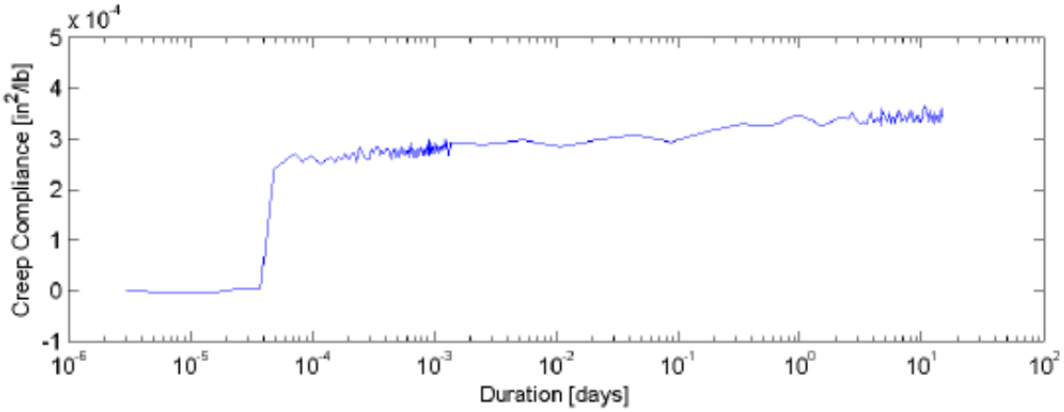

Sample Description:	75%/25% Limerock / Melbourne Milled RAP
Test Date:	8/6/2011
Mold Number:	43
Sample Number:	5
Loading Pressure:	25.0 [lb/ft²] (174.65 [kPa])
Dry Density:	121.4 [lb/ft³] (1944.6 [kg/m³])
Moisture Content:	9.50%
Limerock Bearing Ratio:	128.4
Test Operator:	TJM
Creep Compliance Curve Fit:	D = 1.60e-005*log10(t)+3.26e-004 [in²/lb], R²=0.88
Creep Compliance Rate (0.01d - 7d):	1.85e-005 [in²/lb/day]
Creep Compliance Rate (0.01d - 4d):	1.80e-005 [in²/lb/day]

Figure C-152: Creep vs. Time: 25% MRAP/75% LR Blend 25 psi

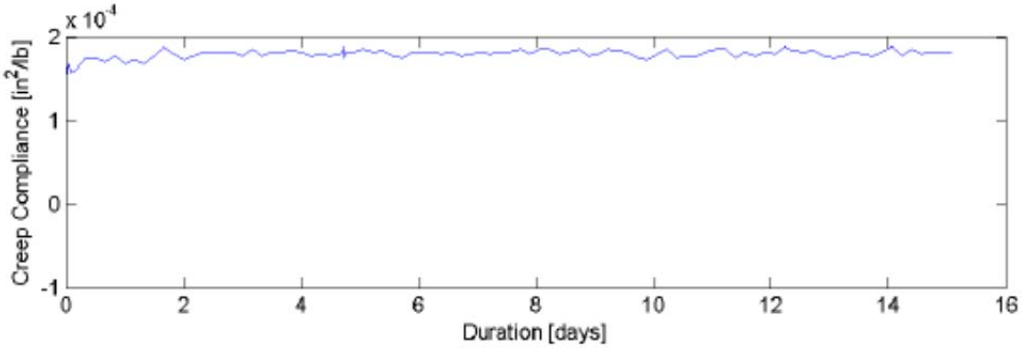

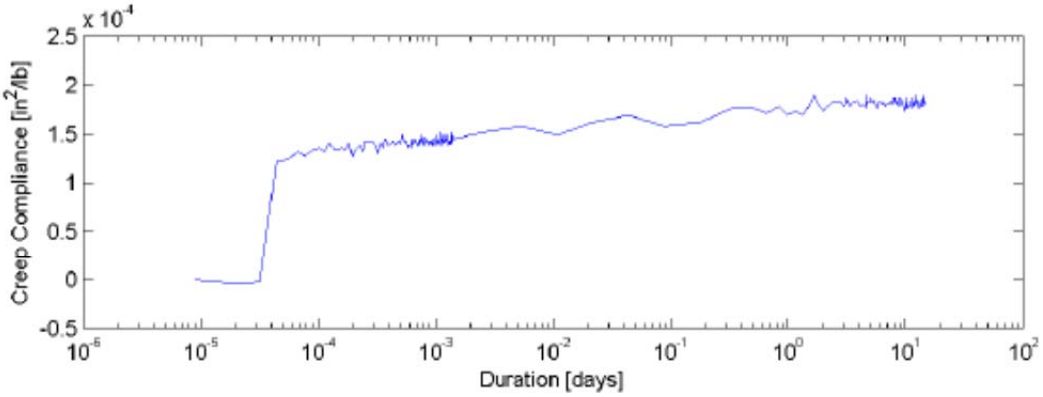

Sample Description:	75%/25% Limerock / Melbourne Milled RAP
Test Date:	8/6/2011
Mold Number:	36
Sample Number:	2
Loading Pressure:	50.0 [lb/ft²] (349.30 [kPa])
Dry Density:	124.6 [lb/ft³] (1995.9 [kg/m³])
Moisture Content:	7.60%
Limerock Bearing Ratio:	178.8
Test Operator:	TJM
Creep Compliance Curve Fit:	D = 8.72e-006*log10(t)+1.74e-004 [in²/lb], R²=0.89
Creep Compliance Rate (0.01d - 7d):	1.09e-005 [in²/lb/day]
Creep Compliance Rate (0.01d - 4d):	1.23e-005 [in²/lb/day]

Figure C-153: Creep vs. Time: 25% MRAP/75% LR Blend 50 psi

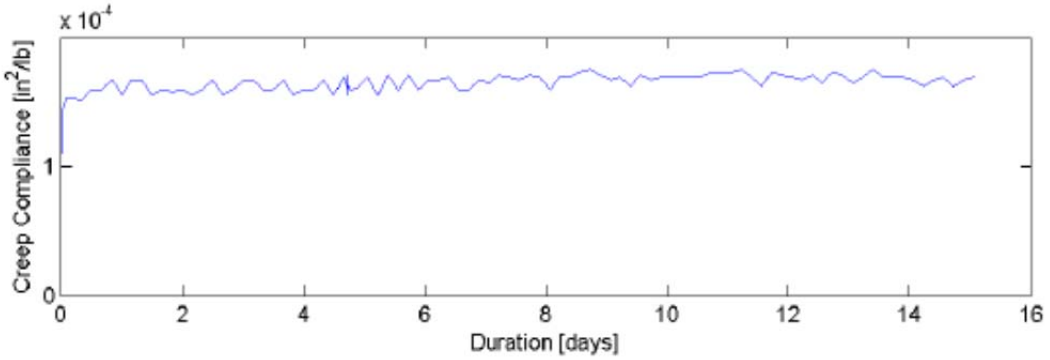

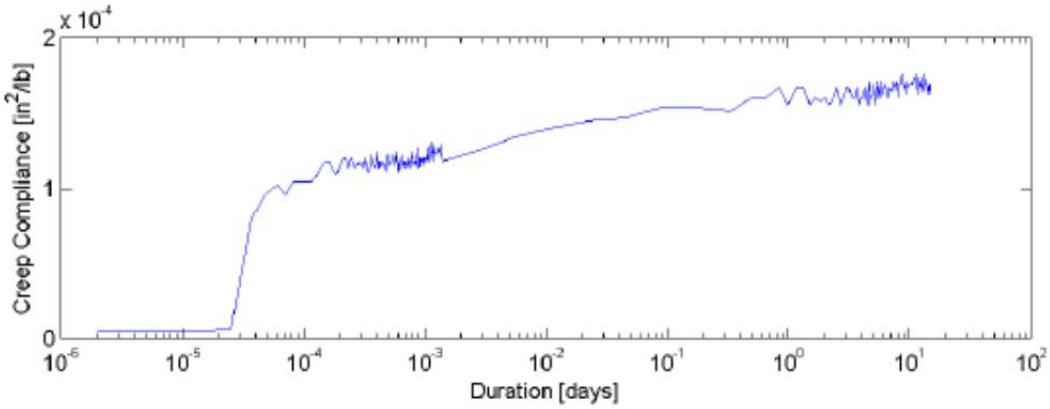

Sample Description:	75%/25% Limerock / Melbourne Milled RAP
Test Date:	8/6/2011
Mold Number:	49
Sample Number:	6
Loading Pressure:	50.0 [lb/ft²] (349.30 [kPa])
Dry Density:	125.6 [lb/ft³] (2011.9 [kg/m³])
Moisture Content:	8.40%
Limerock Bearing Ratio:	188.2
Test Operator:	TJM
Creep Compliance Curve Fit:	D = 1.06e-005*log10(t)+1.57e-004 [in²/lb], R²=0.92
Creep Compliance Rate (0.01d - 7d):	9.24e-006 [in²/lb/day]
Creep Compliance Rate (0.01d - 4d):	8.08e-006 [in²/lb/day]

Figure C-154: Creep vs. Time: 25% MRAP/75% LR Blend 50 psi

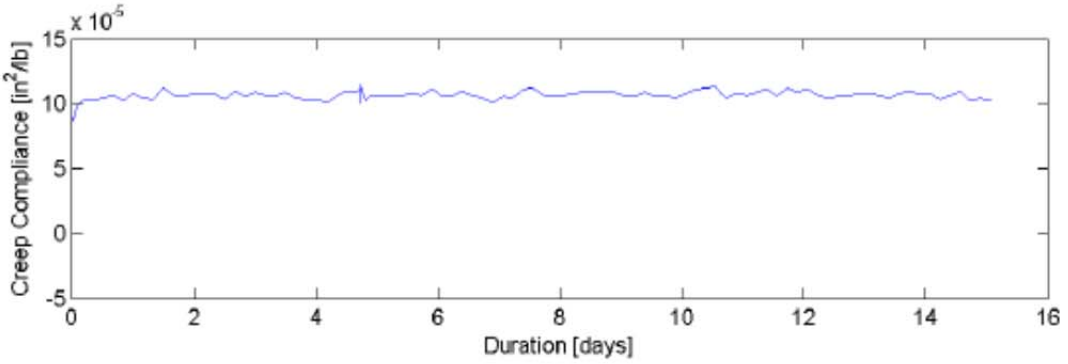

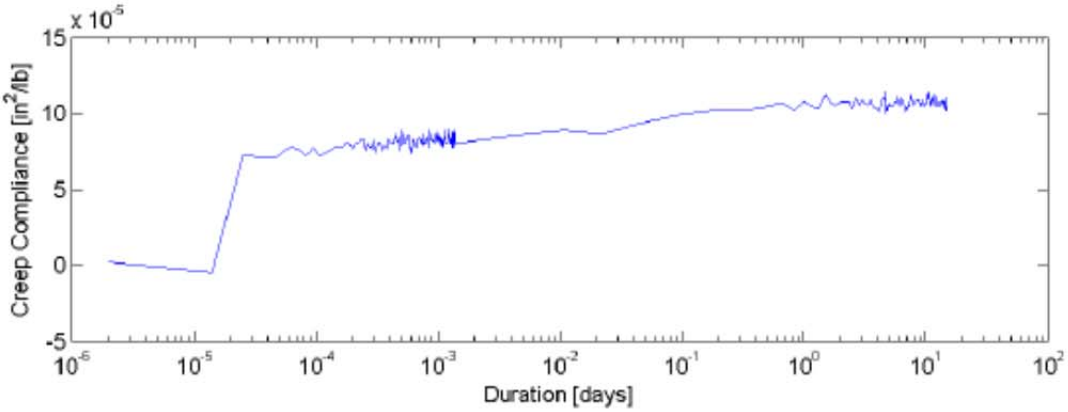

Sample Description:	75%/25% Limerock / Melbourne Milled RAP
Test Date:	8/6/2011
Mold Number:	38
Sample Number:	3
Loading Pressure:	100.0 [lb/ft²] (698.60 [kPa])
Dry Density:	129.0 [lb/ft³] (2066.4 [kg/m³])
Moisture Content:	8.20%
Limerock Bearing Ratio:	194.7
Test Operator:	TJM
Creep Compliance Curve Fit:	D = 6.38e-006*log10(t)+1.03e-004 [in²/lb], R^2=0.85
Creep Compliance Rate (0.01d - 7d):	5.40e-006 [in²/lb/day]
Creep Compliance Rate (0.01d - 4d):	5.68e-006 [in²/lb/day]

Figure C-155: Creep vs. Time: 25% MRAP/75% LR Blend 100 psi

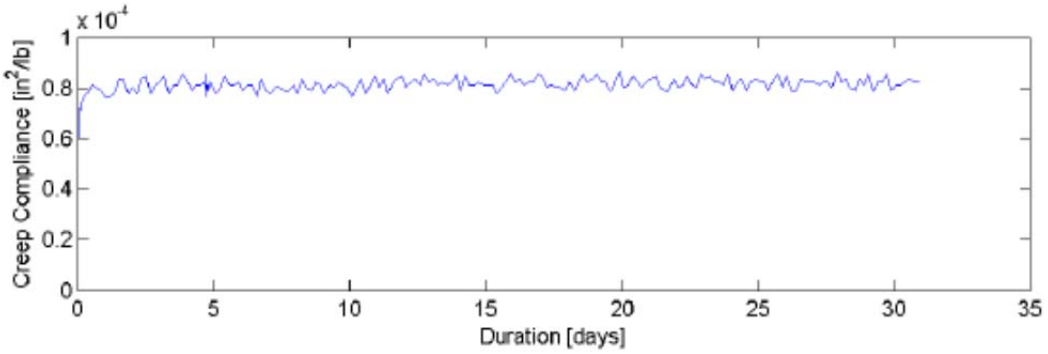

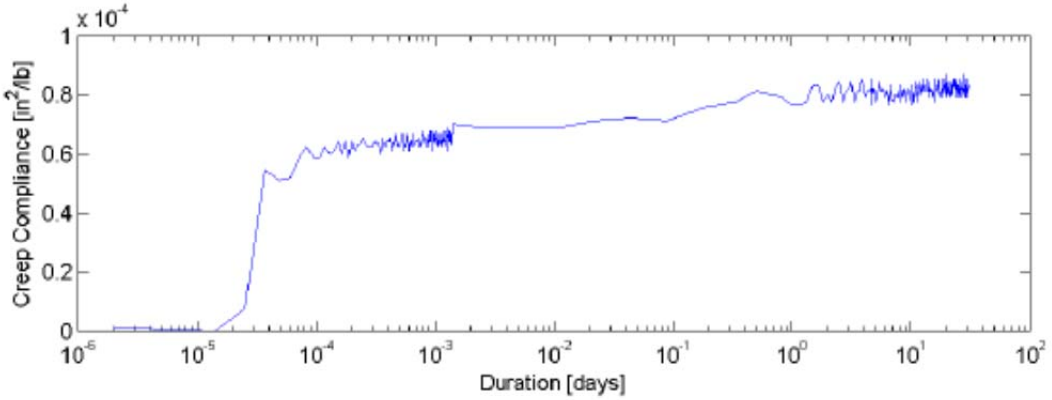

Sample Description:	75%/25% Limerock / Melbourne Milled RAP
Test Date:	8/6/2011
Mold Number:	32
Sample Number:	1
Loading Pressure:	100.0 [lb/ft^2] (698.60 [kPa])
Dry Density:	126.2 [lb/ft^3] (2021.5 [kg/m^3])
Moisture Content:	8.50%
Limerock Bearing Ratio:	218.9
Test Operator:	TJM
Creep Compliance Curve Fit:	D = 3.81e-006*log10(t)+7.78e-005 [in^2/lb], R^2=0.82
Creep Compliance Rate (0.01d - 7d):	3.27e-006 [in^2/lb/day]
Creep Compliance Rate (0.01d - 4d):	5.56e-006 [in^2/lb/day]

Figure C-156: Creep vs. Time: 25% MRAP/75% LR Blend 100 psi

C.3.1.2. 50% MRAP/50% Limerock Blends

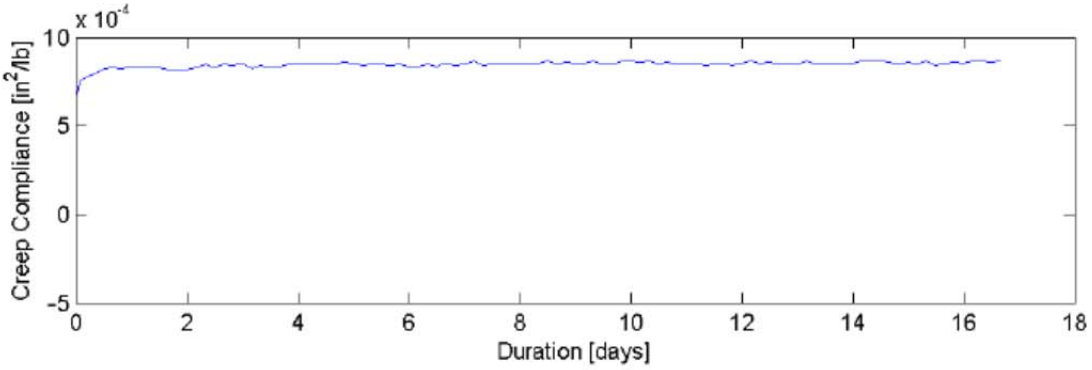

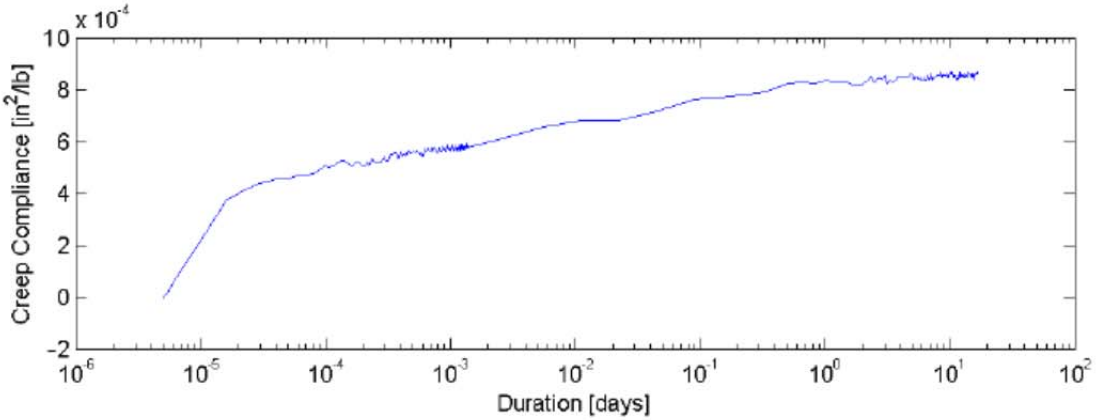

Sample Description:	50/50 Milled Melbourne RAP/Limerock
Test Date:	10/9/2011
Mold Number:	55
Sample Number:	3
Loading Pressure:	25.0 [lb/ft^2] (174.65 [kPa])
Dry Density:	118.9 [lb/ft^3] (1904.6 [kg/m^3])
Moisture Content:	6.30%
Limerock Bearing Ratio:	95.4
Test Operator:	TJM
Creep Compliance Curve Fit:	D = 6.43e-005*log10(t)+7.98e-004 [in^2/lb], R^2=0.95
Creep Compliance Rate (0.01d - 7d):	5.97e-005 [in^2/lb/day]
Creep Compliance Rate (0.01d - 4d):	6.53e-005 [in^2/lb/day]

Figure C-157: Creep vs. Time: 50% MRAP/50% LR Blend 25 psi

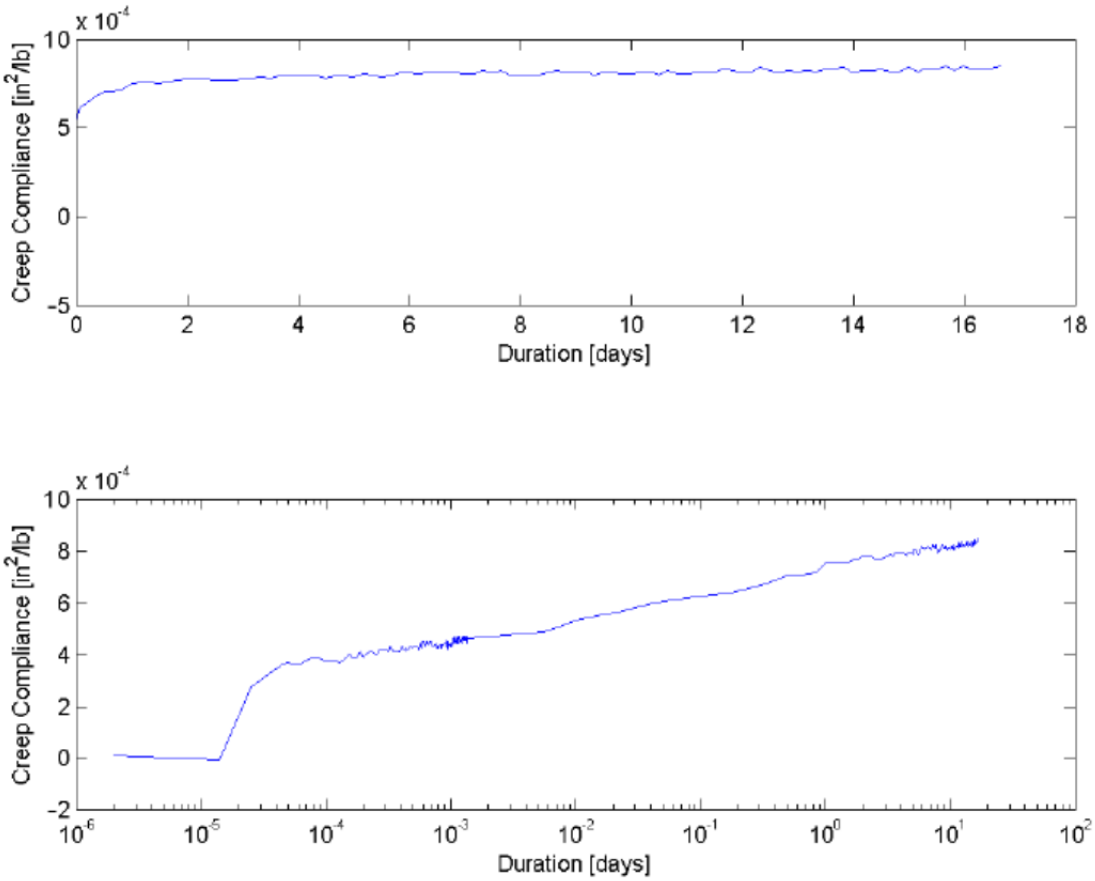

Sample Description:	50/50 Milled Melbourne RAP/Limerock
Test Date:	10/9/2011
Mold Number:	26
Sample Number:	6
Loading Pressure:	25.0 [lb/ft^2] (174.65 [kPa])
Dry Density:	109.7 [lb/ft^3] (1757.2 [kg/m^3])
Moisture Content:	10.80%
Limerock Bearing Ratio:	72.6
Test Operator:	TJM
Creep Compliance Curve Fit:	D = 9.60e-005*log10(t)+7.24e-004 [in^2/lb], R^2=0.99
Creep Compliance Rate (0.01d - 7d):	9.72e-005 [in^2/lb/day]
Creep Compliance Rate (0.01d - 4d):	1.01e-004 [in^2/lb/day]

Figure C-158: Creep vs. Time: 50% MRAP/50% LR Blend 25 psi

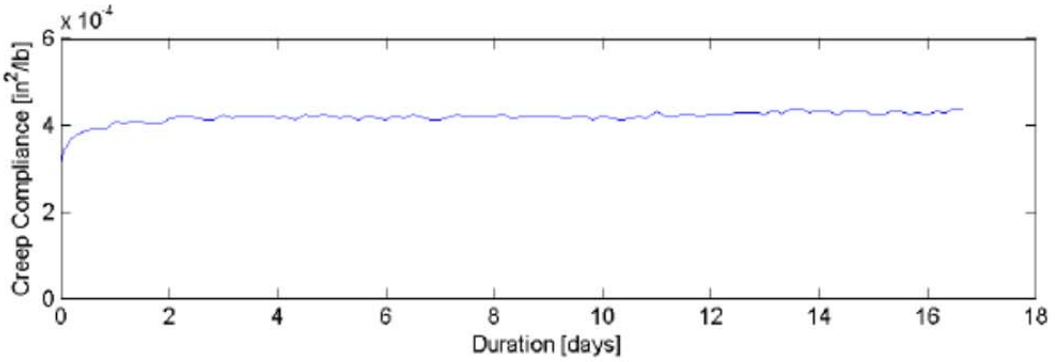

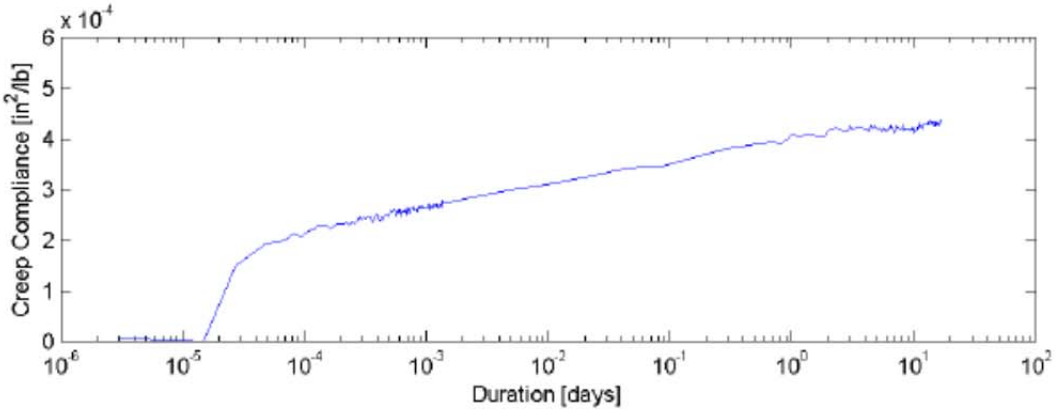

Sample Description:	50%/50% Limerock / Melbourne Milled RAP
Test Date:	10/9/2011
Mold Number:	69
Sample Number:	5
Loading Pressure:	50.0 [lb/ft^2] (349.30 [kPa])
Dry Density:	119.3 [lb/ft^3] (1911.0 [kg/m^3])
Moisture Content:	6.60%
Limerock Bearing Ratio:	134.1
Test Operator:	TJM
Creep Compliance Curve Fit:	D = 3.87e-005*log10(t)+3.91e-004 [in^2/lb], R^2=0.97
Creep Compliance Rate (0.01d - 7d):	3.59e-005 [in^2/lb/day]
Creep Compliance Rate (0.01d - 4d):	4.19e-005 [in^2/lb/day]

Figure C-159: Creep vs. Time: 50% MRAP/50% LR Blend 50 psi

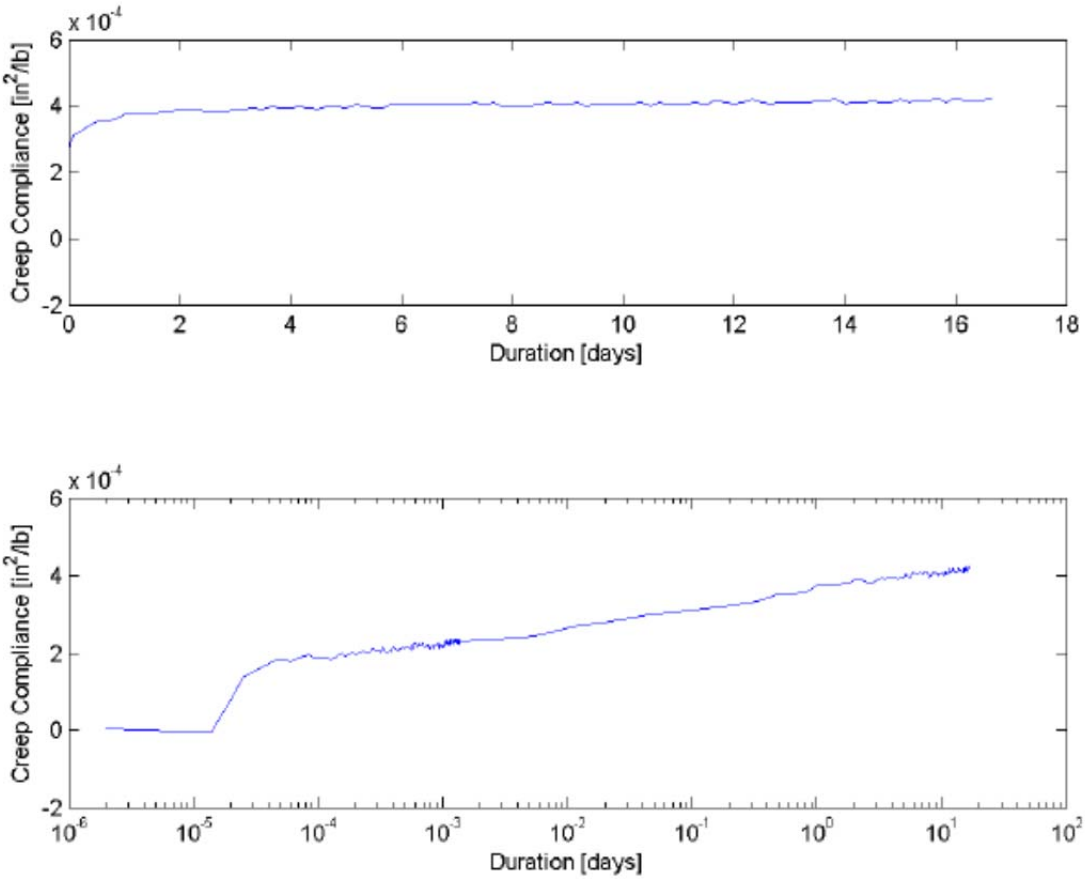

Sample Description:	50%/50% Limerock / Melbourne Milled RAP
Test Date:	10/9/2011
Mold Number:	26
Sample Number:	6
Loading Pressure:	50.0 [lb/ft^2] (349.30 [kPa])
Dry Density:	109.7 [lb/ft^3] (1757.2 [kg/m^3])
Moisture Content:	10.80%
Limerock Bearing Ratio:	72.6
Test Operator:	TJM
Creep Compliance Curve Fit:	D = 4.80e-005*log10(t)+3.62e-004 [in^2/lb], R^2=0.99
Creep Compliance Rate (0.01d - 7d):	4.86e-005 [in^2/lb/day]
Creep Compliance Rate (0.01d - 4d):	5.06e-005 [in^2/lb/day]

Figure C-160: Creep vs. Time: 50% MRAP/50% LR Blend 50 psi

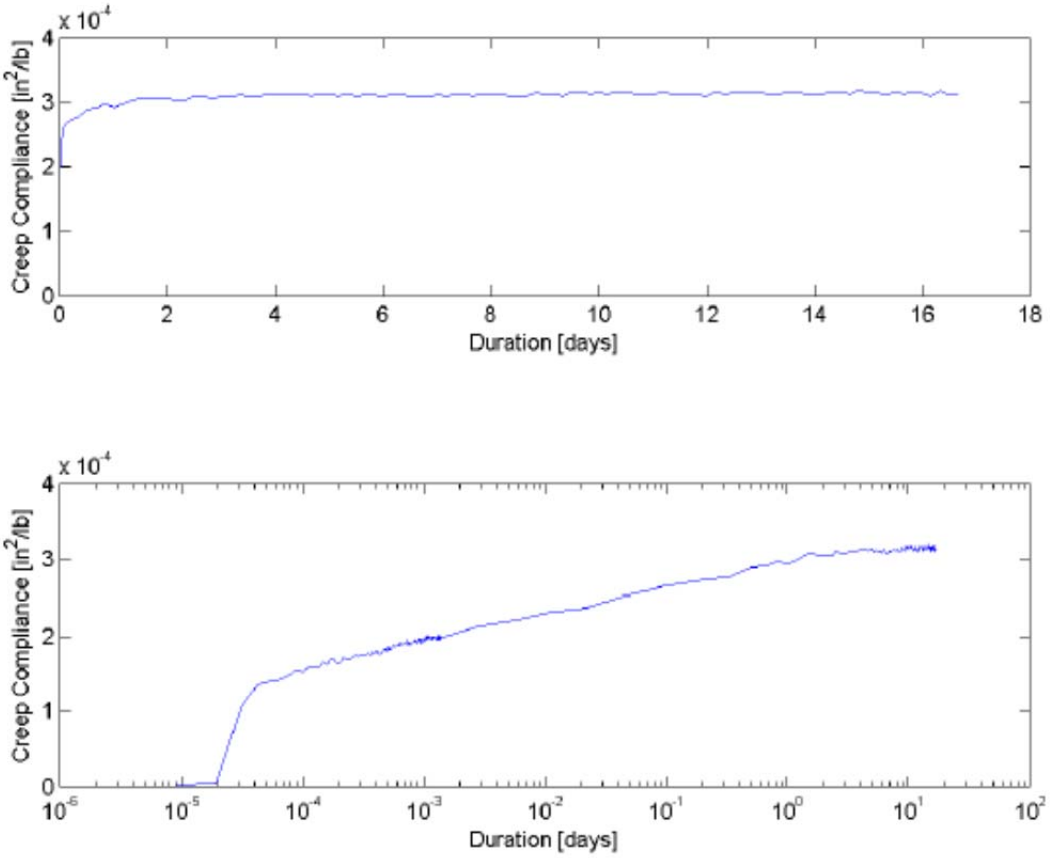

Sample Description:	50%/50% Limerock / Melbourne Milled RAP
Test Date:	10/9/2011
Mold Number:	52
Sample Number:	1
Loading Pressure:	100.0 [lb/ft^2] (698.60 [kPa])
Dry Density:	121.3 [lb/ft^3] (1943.0 [kg/m^3])
Moisture Content:	6.60%
Limerock Bearing Ratio:	142.3
Test Operator:	TJM
Creep Compliance Curve Fit:	D = 2.84e-005*log10(t)+2.89e-004 [in^2/lb], R^2=0.97
Creep Compliance Rate (0.01d - 7d):	2.85e-005 [in^2/lb/day]
Creep Compliance Rate (0.01d - 4d):	3.16e-005 [in^2/lb/day]

Figure C-161: Creep vs. Time: 50% MRAP/50% LR Blend 100 psi

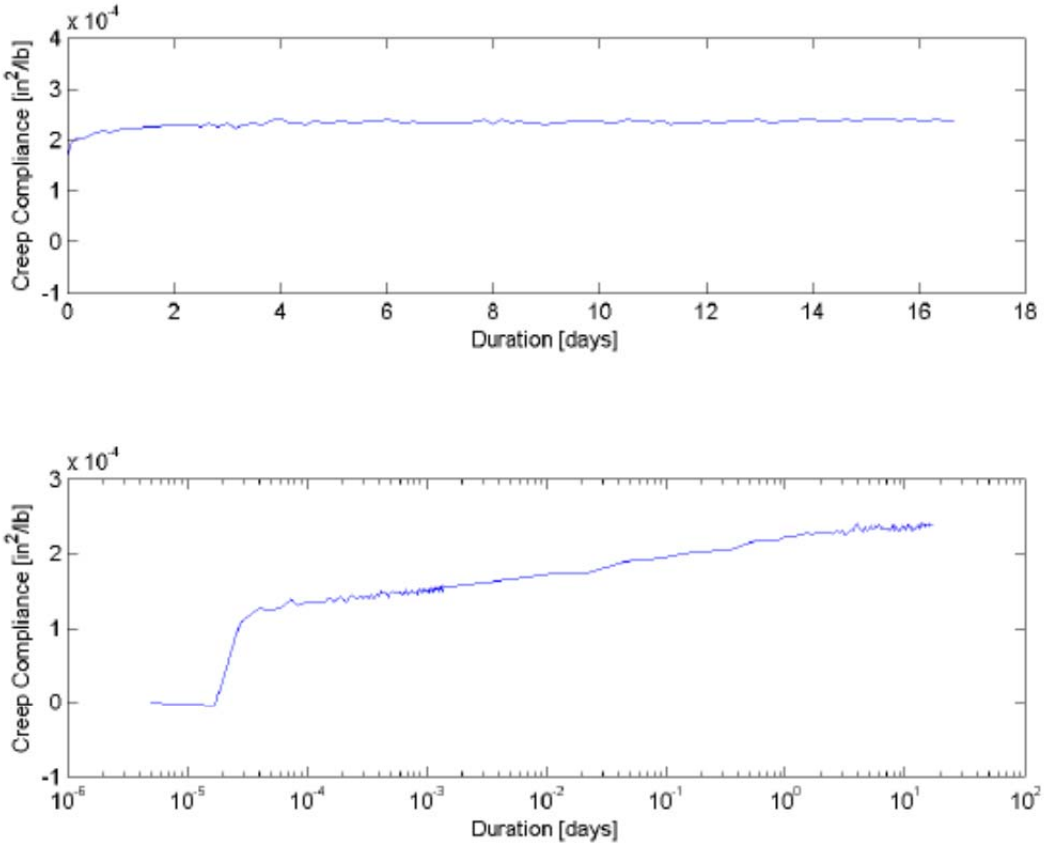

Sample Description:	50%/50% Limerock / Melbourne Milled RAP
Test Date:	10/9/2011
Mold Number:	53
Sample Number:	2
Loading Pressure:	100.0 [lb/ft²] (698.60 [kPa])
Dry Density:	122.6 [lb/ft³] (1963.9 [kg/m³])
Moisture Content:	6.30%
Limerock Bearing Ratio:	174.7
Test Operator:	TJM
Creep Compliance Curve Fit:	D = 2.18e-005*log10(t)+2.16e-004 [in²/lb], R^2=0.97
Creep Compliance Rate (0.01d - 7d):	2.16e-005 [in²/lb/day]
Creep Compliance Rate (0.01d - 4d):	2.70e-005 [in²/lb/day]

Figure C-162: Creep vs. Time: 50% MRAP/50% LR Blend 100 psi

C.3.1.3. 75% MRAP/25% Limerock

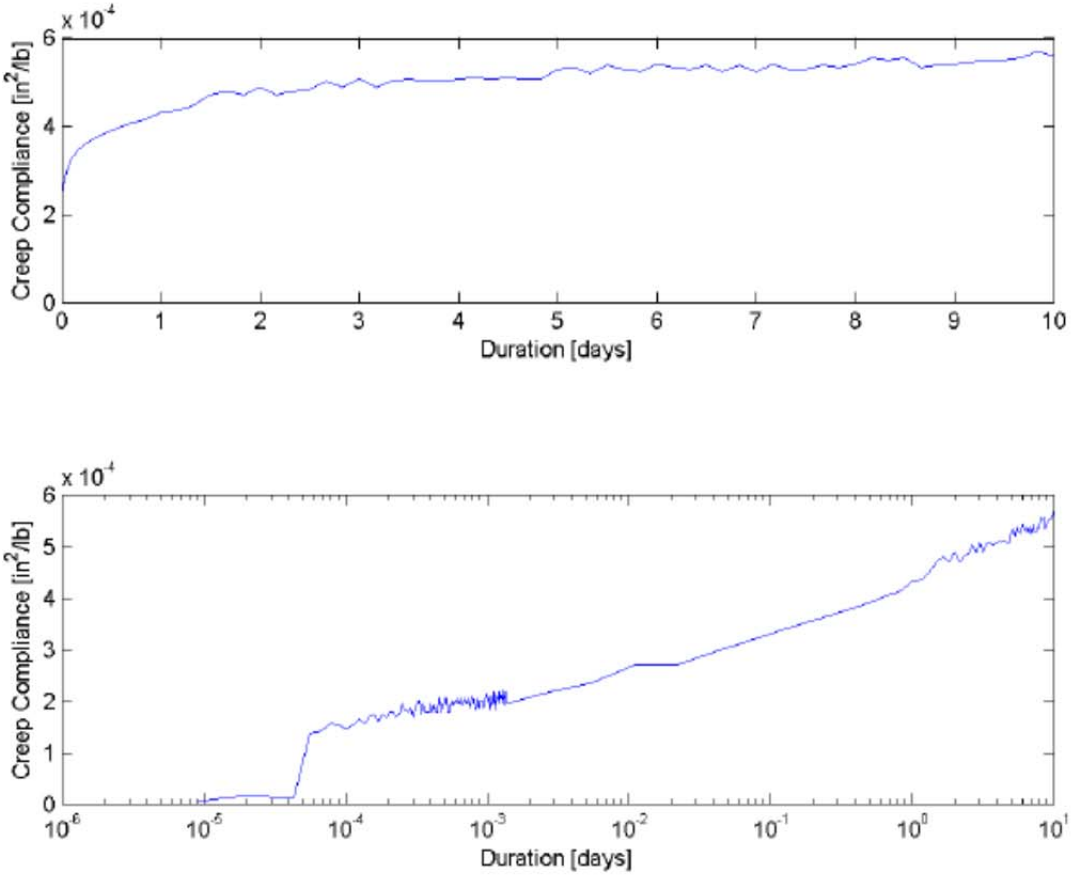

Sample Description:	25%/75% Limerock / Melbourne Milled RAP
Test Date:	10/28/2011
Mold Number:	32
Sample Number:	1
Loading Pressure:	25.0 [lb/ft^2] (174.65 [kPa])
Dry Density:	111.8 [lb/ft^3] (1790.9 [kg/m^3])
Moisture Content:	7.60%
Limerock Bearing Ratio:	64.6
Test Operator:	TJM
Creep Compliance Curve Fit:	D = 9.61e-005*log10(t)+4.50e-004 [in^2/lb], R^2=0.98
Creep Compliance Rate (0.01d - 7d):	9.16e-005 [in^2/lb/day]
Creep Compliance Rate (0.01d - 4d):	9.33e-005 [in^2/lb/day]

Figure C-163: Creep vs. Time: 75% MRAP/25% LR Blend 25 psi

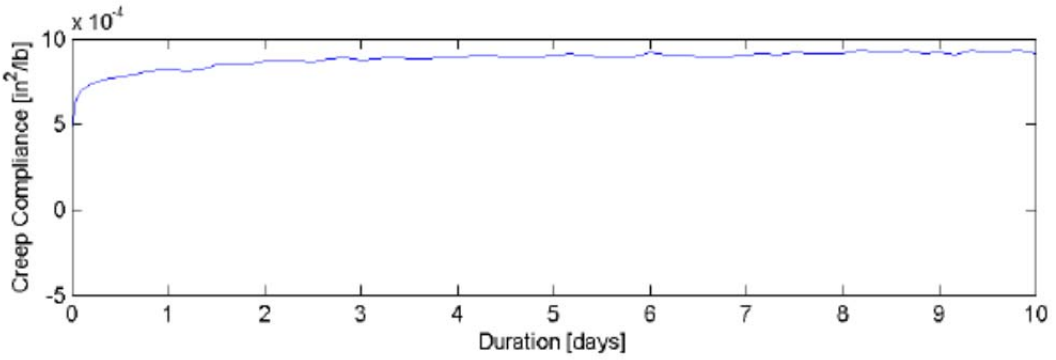

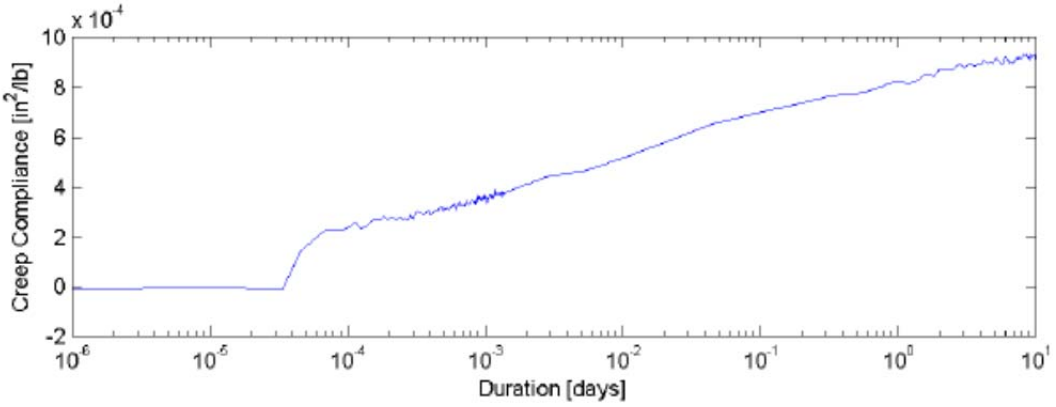

Sample Description:	25%/75% Limerock / Melbourne Milled RAP
Test Date:	10/28/2011
Mold Number:	43
Sample Number:	5
Loading Pressure:	25.0 [lb/ft^2] (174.65 [kPa])
Dry Density:	113.6 [lb/ft^3] (1819.7 [kg/m^3])
Moisture Content:	8.00%
Limerock Bearing Ratio:	92.1
Test Operator:	TJM
Creep Compliance Curve Fit:	D = 1.40e-004*log10(t)+8.06e-004 [in^2/lb], R^2=0.99
Creep Compliance Rate (0.01d - 7d):	1.38e-004 [in^2/lb/day]
Creep Compliance Rate (0.01d - 4d):	1.45e-004 [in^2/lb/day]

Figure C-164: Creep vs. Time: 75% MRAP/25% LR Blend 25 psi

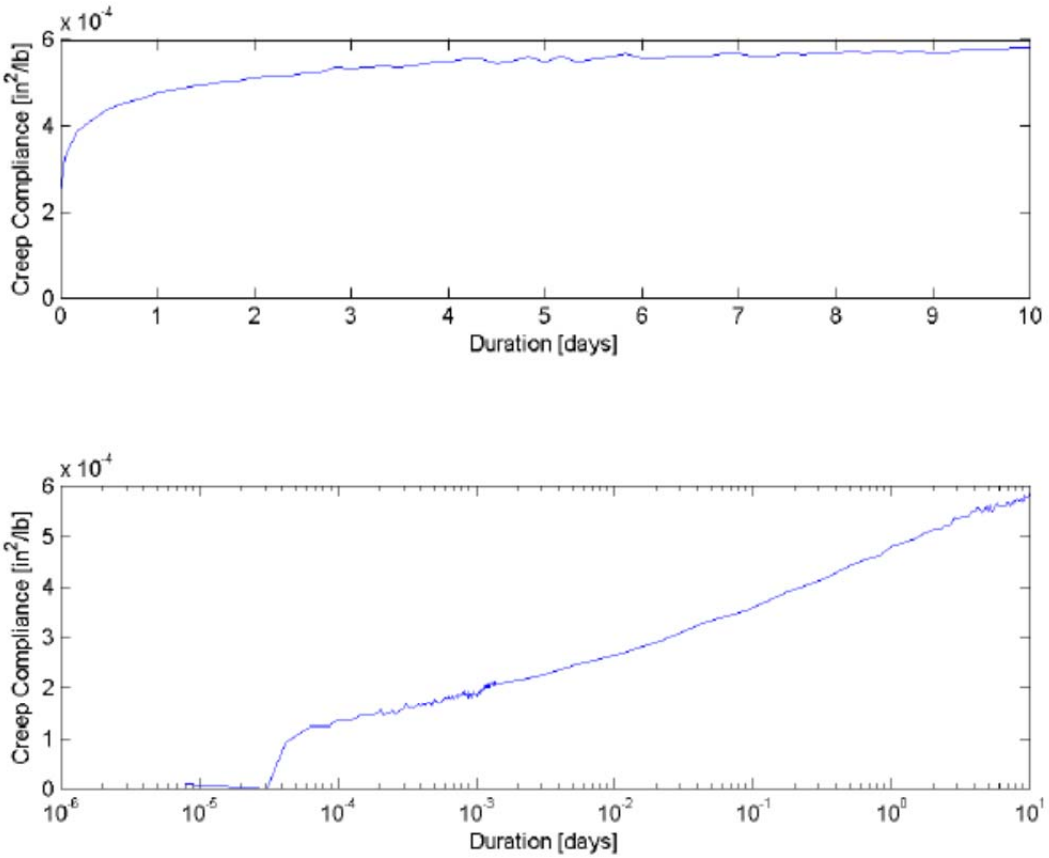

Sample Description:	25%/75% Limerock / Melbourne Milled RAP
Test Date:	10/28/2011
Mold Number:	38
Sample Number:	3
Loading Pressure:	50.0 [lb/ft^2] (349.30 [kPa])
Dry Density:	113.8 [lb/ft^3] (1822.9 [kg/m^3])
Moisture Content:	6.90%
Limerock Bearing Ratio:	78.3
Test Operator:	TJM
Creep Compliance Curve Fit:	D = 1.04e-004*log10(t)+4.77e-004 [in^2/lb], R^2=1.00
Creep Compliance Rate (0.01d - 7d):	1.08e-004 [in^2/lb/day]
Creep Compliance Rate (0.01d - 4d):	1.10e-004 [in^2/lb/day]

Figure C-165: Creep vs. Time: 75% MRAP/25% LR Blend 50 psi

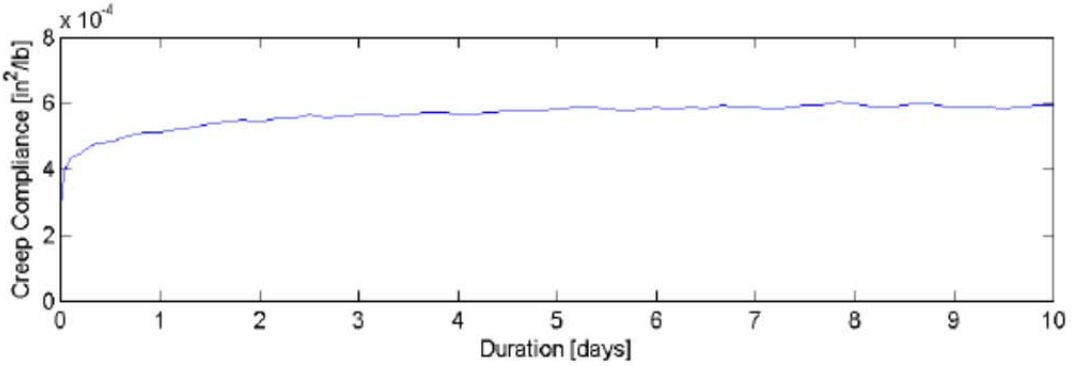

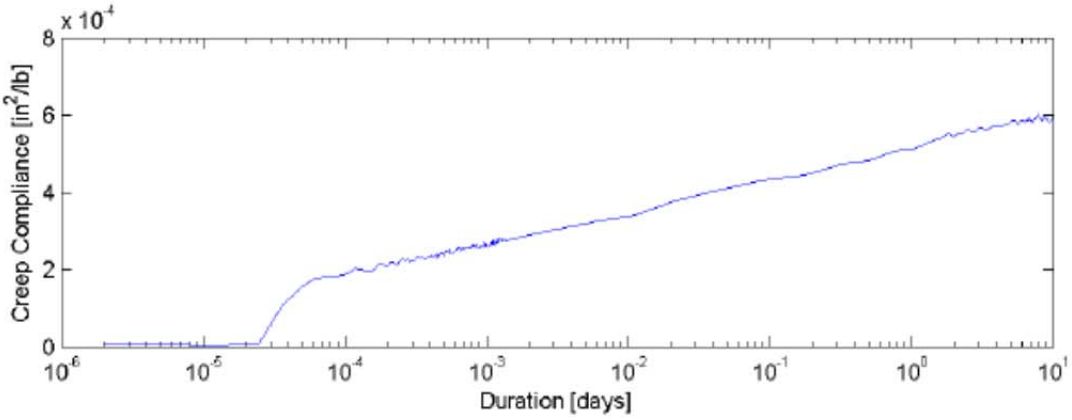

Sample Description:	25%/75% Limerock / Melbourne Milled RAP
Test Date:	10/28/2011
Mold Number:	41
Sample Number:	4
Loading Pressure:	50.0 [lb/ft^2] (349.30 [kPa])
Dry Density:	116.5 [lb/ft^3] (1866.2 [kg/m^3])
Moisture Content:	7.70%
Limerock Bearing Ratio:	108.7
Test Operator:	TJM
Creep Compliance Curve Fit:	D = 8.65e-005*log10(t)+5.18e-004 [in^2/lb], R^2=1.00
Creep Compliance Rate (0.01d - 7d):	8.73e-005 [in^2/lb/day]
Creep Compliance Rate (0.01d - 4d):	8.87e-005 [in^2/lb/day]

Figure C-166: Creep vs. Time: 75% MRAP/25% LR Blend 50 psi

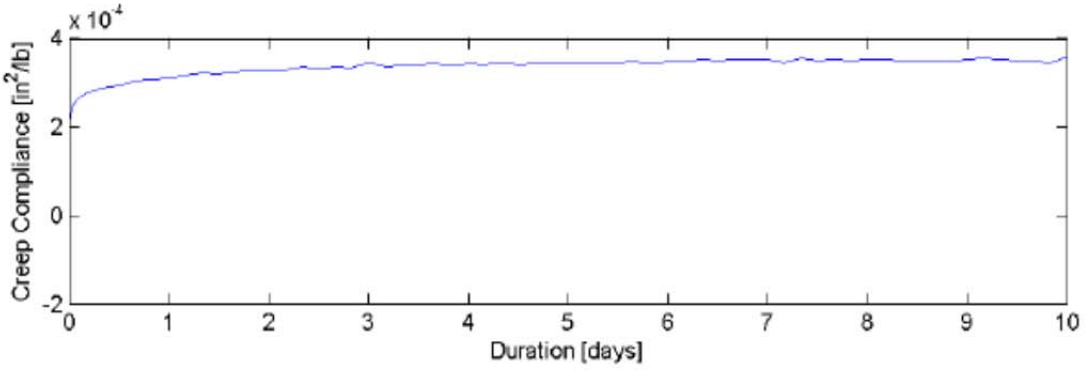

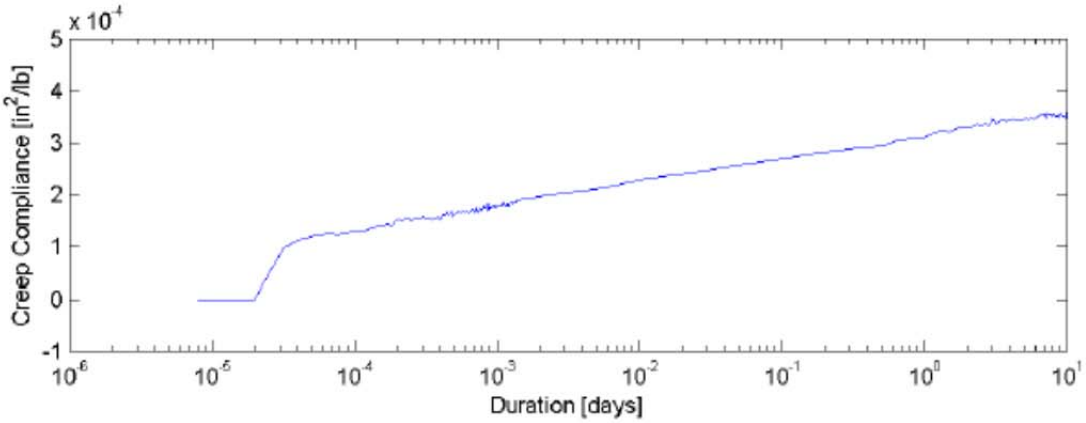

Sample Description:	25%/75% Limerock / Melbourne Milled RAP
Test Date:	10/28/2011
Mold Number:	49
Sample Number:	6
Loading Pressure:	100.0 [lb/ft^2] (698.60 [kPa])
Dry Density:	118.9 [lb/ft^3] (1904.6 [kg/m^3])
Moisture Content:	8.10%
Limerock Bearing Ratio:	129.8
Test Operator:	TJM
Creep Compliance Curve Fit:	D = 4.52e-005*log10(t)+3.13e-004 [in^2/lb], R^2=1.00
Creep Compliance Rate (0.01d - 7d):	4.50e-005 [in^2/lb/day]
Creep Compliance Rate (0.01d - 4d):	4.58e-005 [in^2/lb/day]

Figure C-167: Creep vs. Time: 75% MRAP/25% LR Blend 100 psi

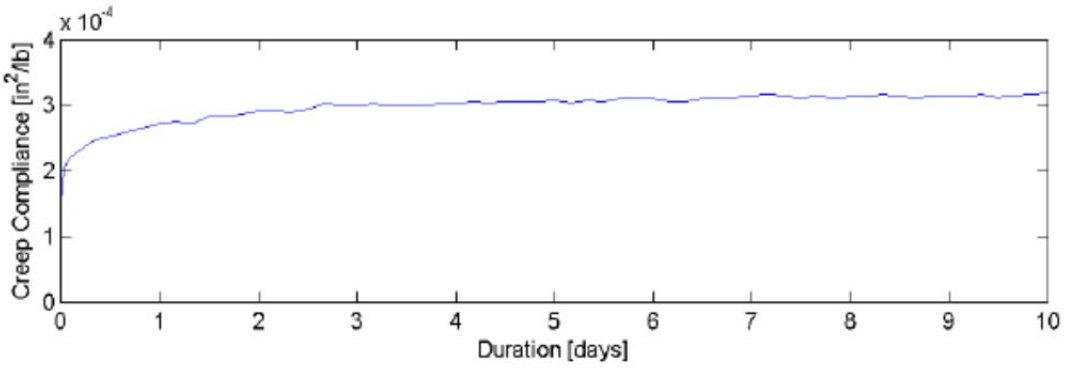

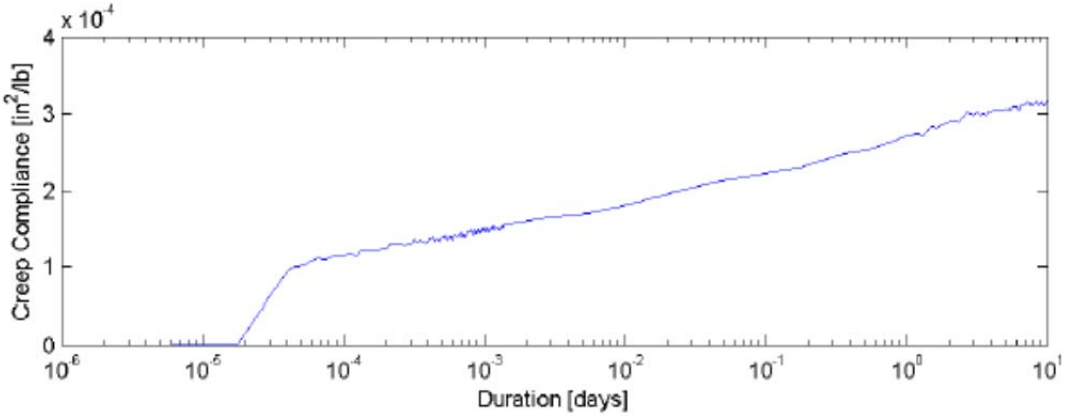

Sample Description:	25%/75% Limerock / Melbourne Milled RAP
Test Date:	10/28/2011
Mold Number:	36
Sample Number:	2
Loading Pressure:	100.0 [lb/ft^2] (698.60 [kPa])
Dry Density:	120.1 [lb/ft^3] (1923.8 [kg/m^3])
Moisture Content:	6.70%
Limerock Bearing Ratio:	133.4
Test Operator:	TJM
Creep Compliance Curve Fit:	D = 4.43e-005*log10(t)+2.74e-004 [in^2/lb], R^2=0.99
Creep Compliance Rate (0.01d - 7d):	4.70e-005 [in^2/lb/day]
Creep Compliance Rate (0.01d - 4d):	4.67e-005 [in^2/lb/day]

Figure C-168: Creep vs. Time: 75% MRAP/25% LR Blend 100 psi

C.3.2. MRAP/Cemented Coquina Blends

C.3.2.1. 25% MRAP/75% Cemented Coquina

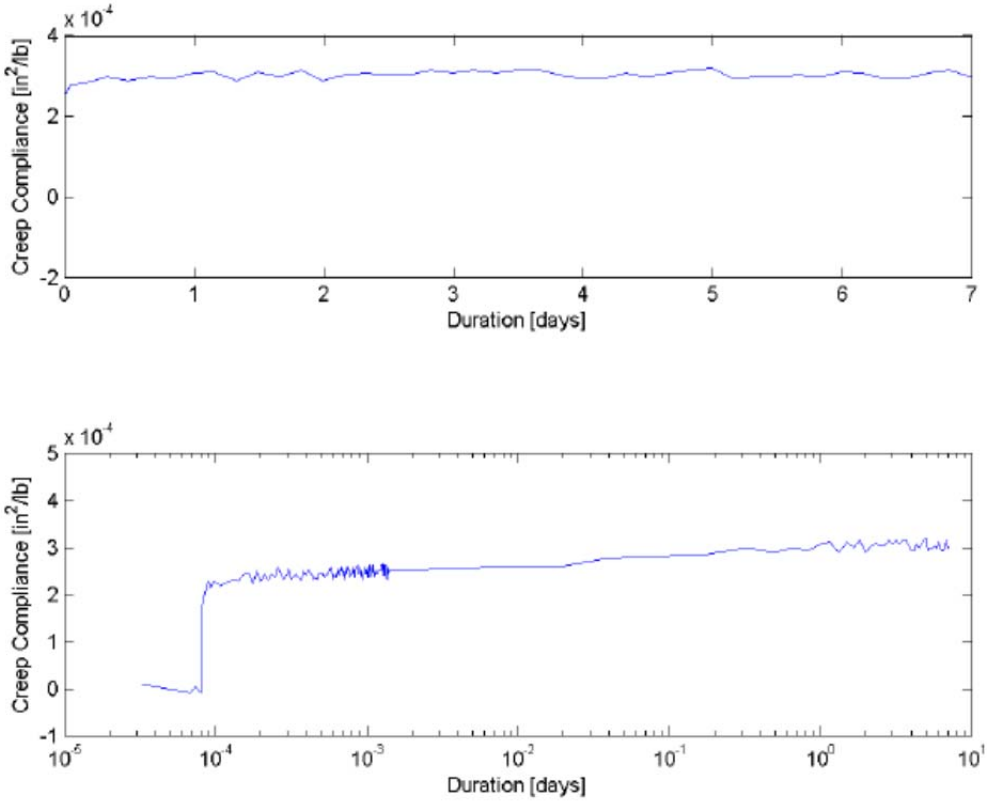

Sample Description:	75%/25% Cemented Coquinia / Melbourne Milled RAP
Test Date:	6/21/2011
Mold Number:	53
Sample Number:	5
Loading Pressure:	25.0 [lb/ft^2] (174.65 [kPa])
Dry Density:	123.5 [lb/ft^3] (1978.3 [kg/m^3])
Moisture Content:	8.20%
Limerock Bearing Ratio:	171.8
Test Operator:	TJM
Creep Compliance Curve Fit:	D = 1.81e-005*log10(t)+2.96e-004 [in^2/lb], R^2=0.89
Creep Compliance Rate (0.01d - 7d)*:	1.77e-005 [in^2/lb/day]
Creep Compliance Rate (0.01d - 4d):	1.37e-005 [in^2/lb/day]

Figure C-169: Creep vs. Time: 25% MRAP/75% CCB Blend 25 psi

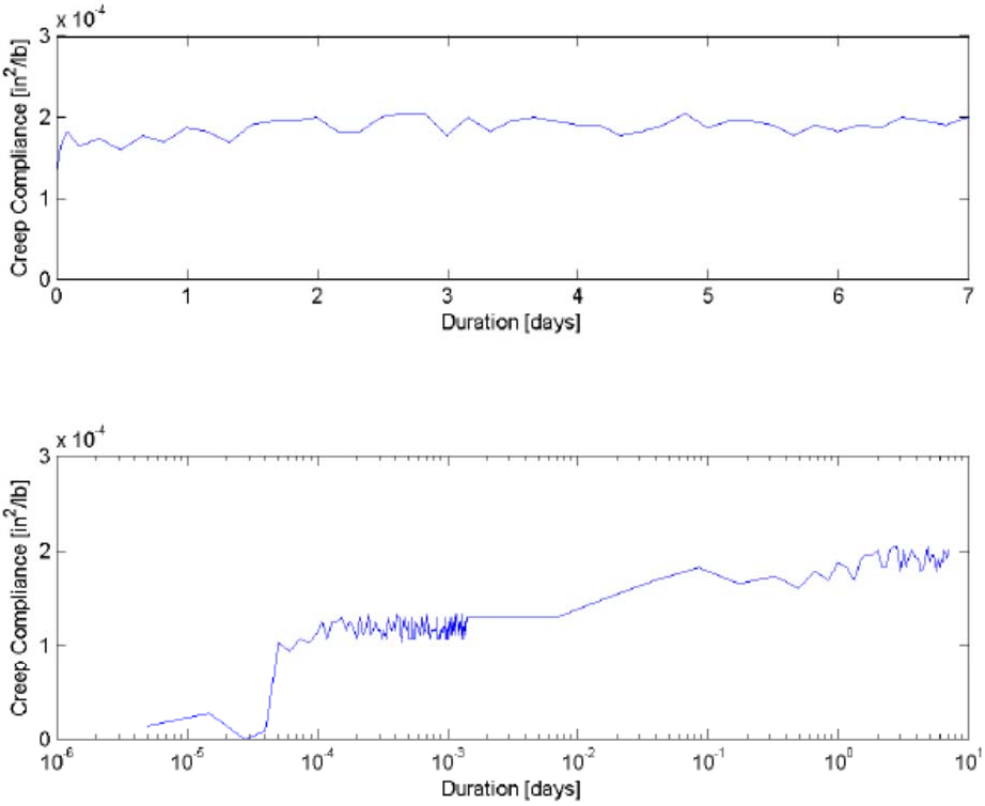

Sample Description:	75%/25% Cemented Coquinia / Melbourne Milled RAP
Test Date:	6/21/2011
Mold Number:	55
Sample Number:	6
Loading Pressure:	25.0 [lb/ft^2] (174.65 [kPa])
Dry Density:	124.8 [lb/ft^3] (1999.1 [kg/m^3])
Moisture Content:	6.20%
Limerock Bearing Ratio:	144.5
Test Operator:	TJM
Creep Compliance Curve Fit:	D = 1.86e-005*log10(t)+1.81e-004 [in^2/lb], R^2=0.84
Creep Compliance Rate (0.01d - 7d)*:	2.10e-005 [in^2/lb/day]
Creep Compliance Rate (0.01d - 4d):	2.15e-005 [in^2/lb/day]

Figure C-170: Creep vs. Time: 25% MRAP/75% CCB Blend 25 psi

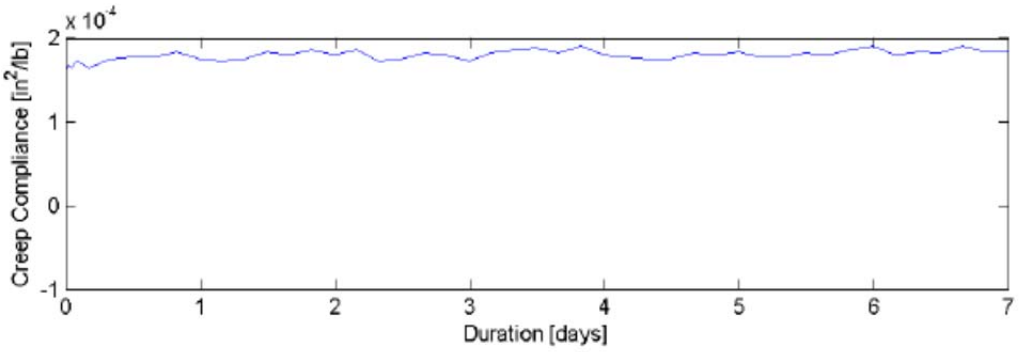

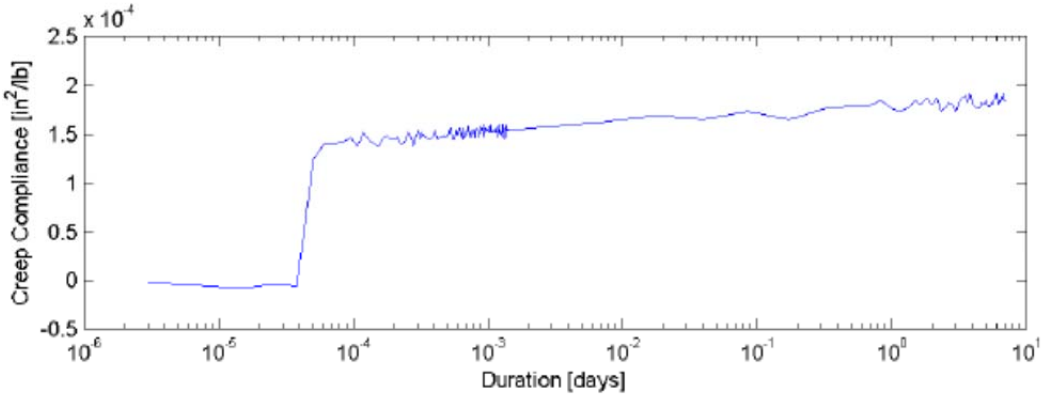

Sample Description:	75%/25% Cemented Coquinia / Melbourne Milled RAP
Test Date:	6/21/2011
Mold Number:	38
Sample Number:	3
Loading Pressure:	50.0 [lb/ft^2] (349.30 [kPa])
Dry Density:	125.9 [lb/ft^3] (2016.7 [kg/m^3])
Moisture Content:	5.70%
Limerock Bearing Ratio:	177.2
Test Operator:	TJM
Creep Compliance Curve Fit:	D = 7.40e-006*log10(t)+1.78e-004 [in^2/lb], R^2=0.84
Creep Compliance Rate (0.01d - 7d)*:	7.15e-006 [in^2/lb/day]
Creep Compliance Rate (0.01d - 4d):	6.07e-006 [in^2/lb/day]

Figure C-171: Creep vs. Time: 25% MRAP/75% CCB Blend 50 psi

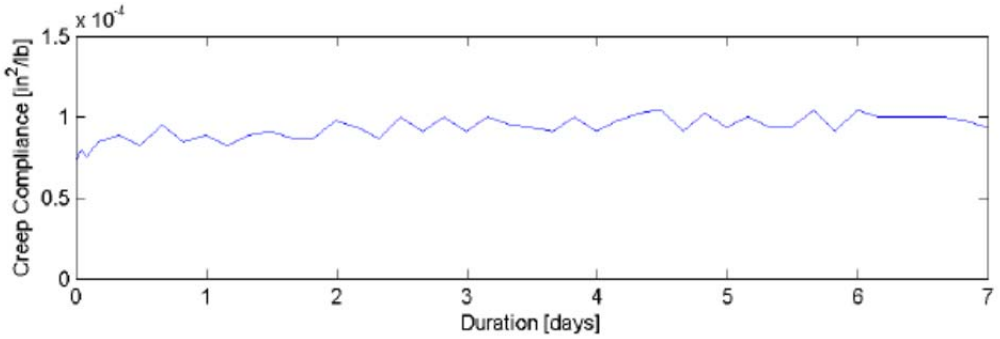

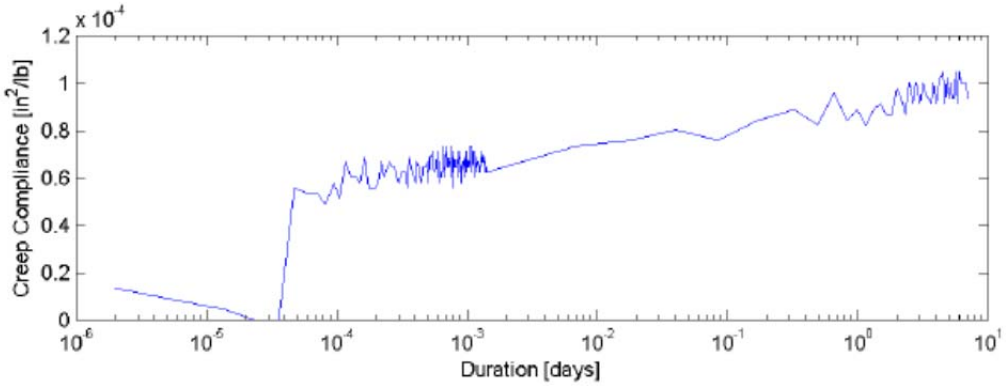

Sample Description:	75%/25% Cemented Coquinia / Melbourne Milled RAP
Test Date:	6/21/2011
Mold Number:	52
Sample Number:	4
Loading Pressure:	50.0 [lb/ft^2] (349.30 [kPa])
Dry Density:	125.5 [lb/ft^3] (2010.3 [kg/m^3])
Moisture Content:	6.70%
Limerock Bearing Ratio:	162.8
Test Operator:	TJM
Creep Compliance Curve Fit:	D = 8.73e-006*log10(t)+9.06e-005 [in^2/lb], R^2=0.87
Creep Compliance Rate (0.01d - 7d)*:	7.73e-006 [in^2/lb/day]
Creep Compliance Rate (0.01d - 4d):	6.67e-006 [in^2/lb/day]

Figure C-172: Creep vs. Time: 25% MRAP/75% CCB Blend 50 psi

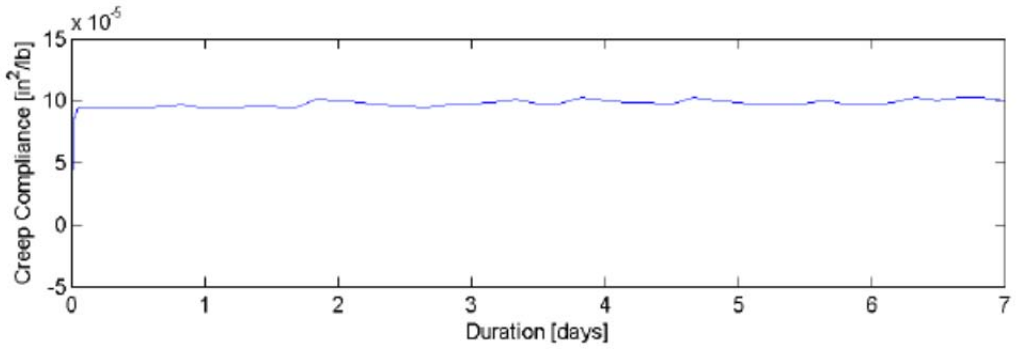

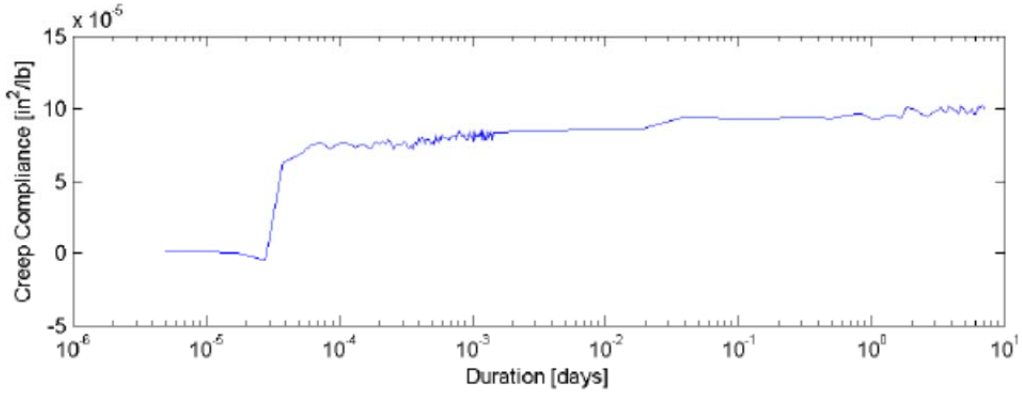

Sample Description:	75%/25% Cemented Coquinia / Melbourne Milled RAP
Test Date:	6/21/2011
Mold Number:	32
Sample Number:	1
Loading Pressure:	100.0 [lb/ft^2] (698.60 [kPa])
Dry Density:	126.1 [lb/ft^3] (2019.9 [kg/m^3])
Moisture Content:	6.10%
Limerock Bearing Ratio:	223.1
Test Operator:	TJM
Creep Compliance Curve Fit:	D = 4.47e-006*log10(t)+9.56e-005 [in^2/lb], R^2=0.89
Creep Compliance Rate (0.01d - 7d)*:	5.54e-006 [in^2/lb/day]
Creep Compliance Rate (0.01d - 4d):	5.55e-006 [in^2/lb/day]

Figure C-173: Creep vs. Time: 25% MRAP/75% CCB Blend 100 psi

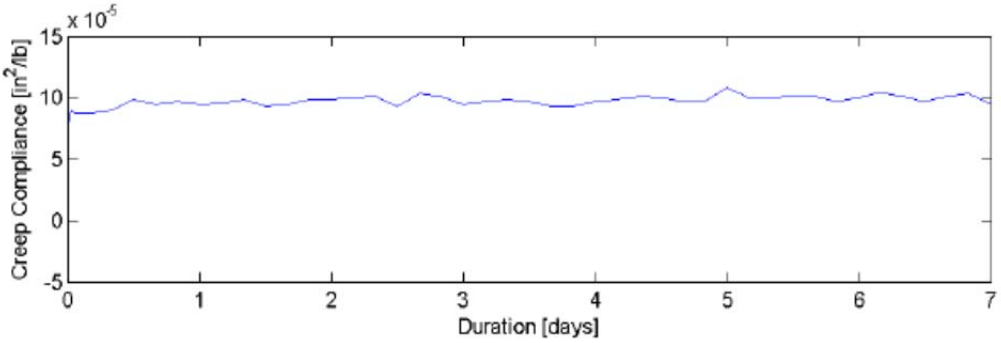

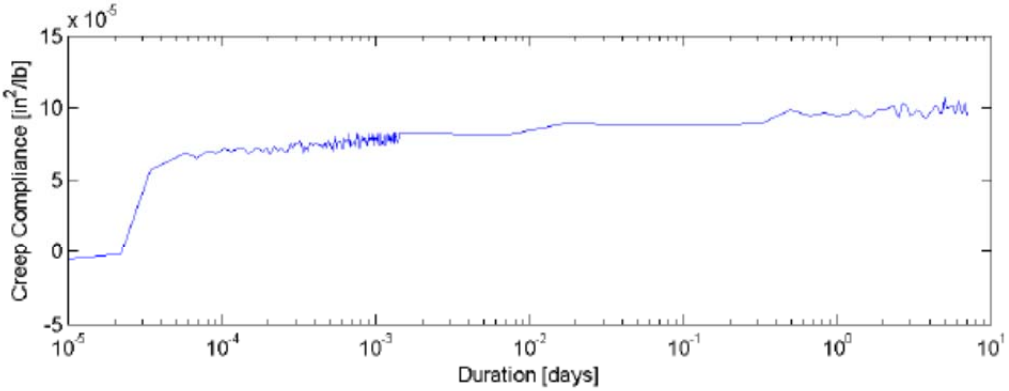

Sample Description:	75%/25% Cemented Coquinia / Melbourne Milled RAP
Test Date:	6/21/2011
Mold Number:	36
Sample Number:	2
Loading Pressure:	100.0 [lb/ft^2] (698.60 [kPa])
Dry Density:	126.5 [lb/ft^3] (2026.3 [kg/m^3])
Moisture Content:	6.50%
Limerock Bearing Ratio:	200.5
Test Operator:	TJM
Creep Compliance Curve Fit:	D = 5.65e-006*log10(t)+9.54e-005 [in^2/lb], R^2=0.85
Creep Compliance Rate (0.01d - 7d)*:	5.76e-006 [in^2/lb/day]
Creep Compliance Rate (0.01d - 4d):	5.03e-006 [in^2/lb/day]

Figure C-174: Creep vs. Time: 25% MRAP/75% CCB Blend 100 psi

C.3.2.2. 50% MRAP/50% Cemented Coquina

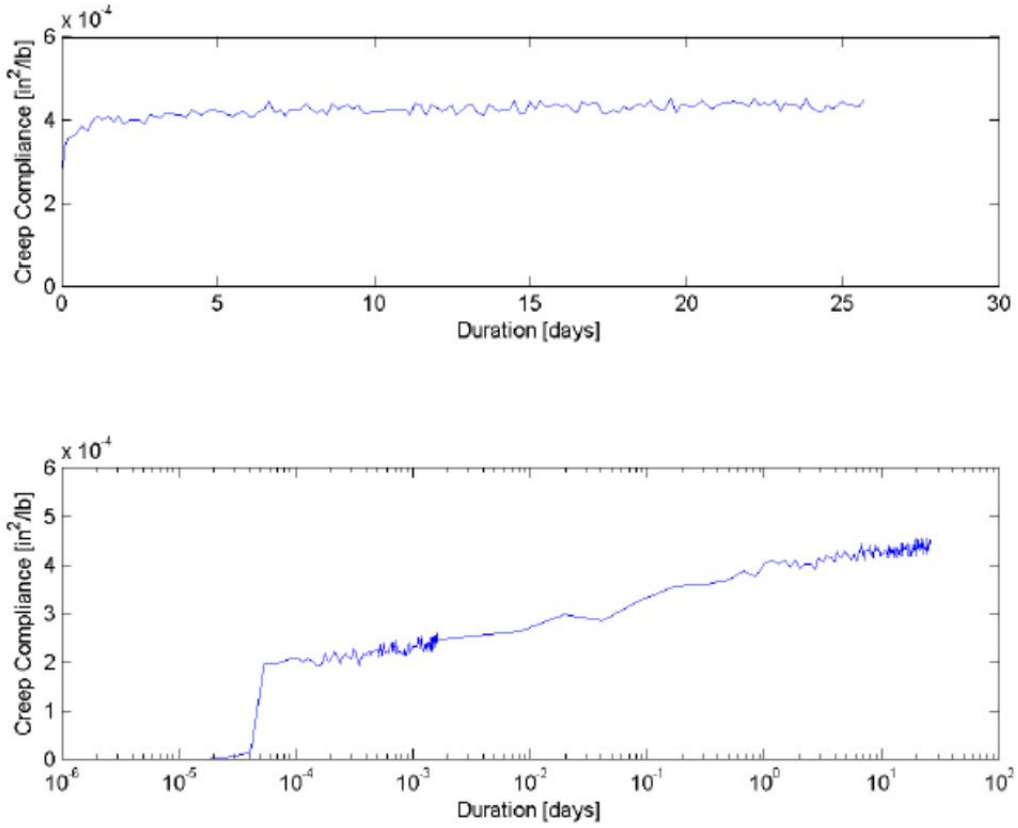

Sample Description:	50%/50% Cemented Coquinia / Melbourne Milled RAP
Test Date:	5/26/2011
Mold Number:	26
Sample Number:	5
Loading Pressure:	25.0 [lb/ft^2] (174.65 [kPa])
Dry Density:	122.2 [lb/ft^3] (1957.5 [kg/m^3])
Moisture Content:	7.40%
Limerock Bearing Ratio:	98.3
Test Operator:	TJM
Creep Compliance Curve Fit:	D = 4.96e-005*log10(t)+3.77e-004 [in^2/lb], R^2=0.97
Creep Compliance Rate (0.01d - 7d):	5.56e-005 [in^2/lb/day]
Creep Compliance Rate (0.01d - 4d):	5.26e-005 [in^2/lb/day]

Figure C-175: Creep vs. Time: 50% MRAP/50% CCB Blend 25 psi

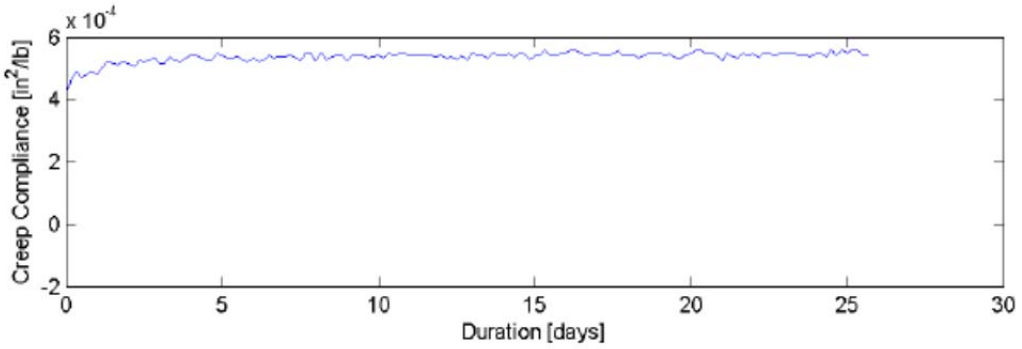

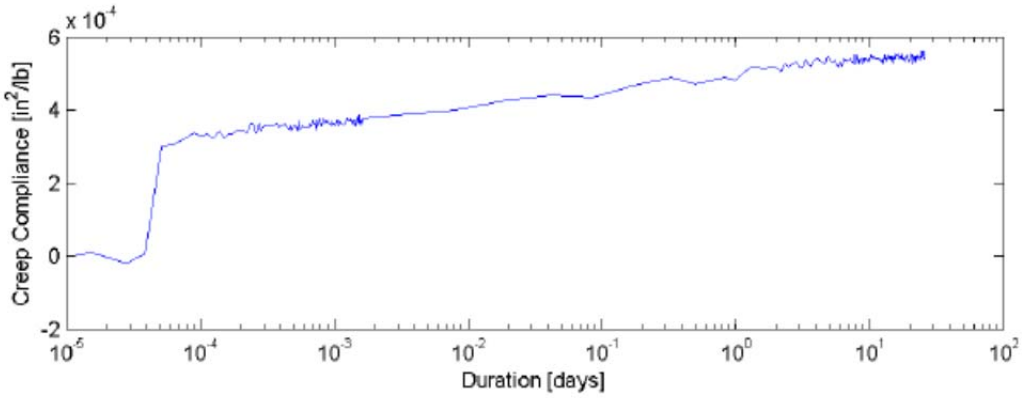

Sample Description:	50%/50% Cemented Coquinia / Melbourne Milled RAP
Test Date:	5/26/2011
Mold Number:	49
Sample Number:	1
Loading Pressure:	25.0 [lb/ft^2] (174.65 [kPa])
Dry Density:	121.9 [lb/ft^3] (1952.7 [kg/m^3])
Moisture Content:	5.10%
Limerock Bearing Ratio:	100.1
Test Operator:	TJM
Creep Compliance Curve Fit:	D = 4.36e-005*log10(t)+4.95e-004 [in^2/lb], R^2=0.97
Creep Compliance Rate (0.01d - 7d):	4.69e-005 [in^2/lb/day]
Creep Compliance Rate (0.01d - 4d):	5.30e-005 [in^2/lb/day]

Figure C-176: Creep vs. Time: 50% MRAP/50% CCB Blend 25 psi

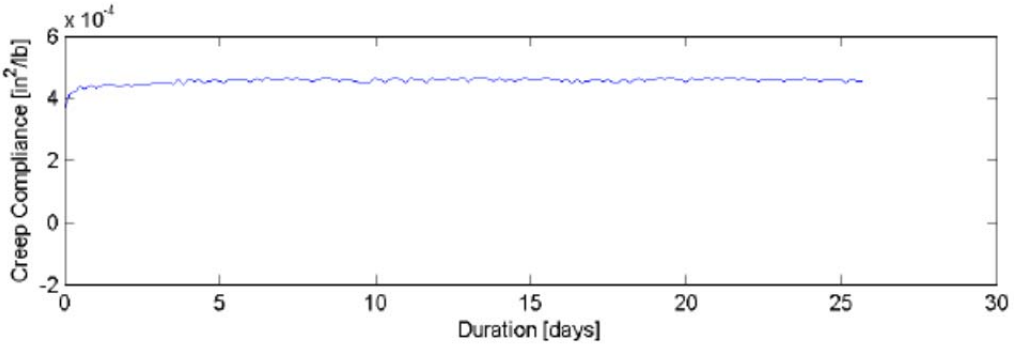

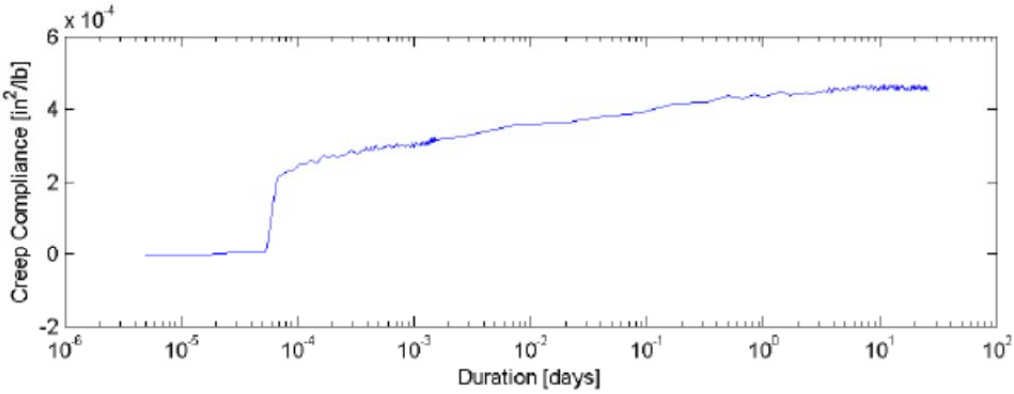

Sample Description:	50%/50% Cemented Coquinia / Melbourne Milled RAP
Test Date:	5/26/2011
Mold Number:	65
Sample Number:	3
Loading Pressure:	50.0 [lb/ft^2] (349.30 [kPa])
Dry Density:	122.3 [lb/ft^3] (1959.1 [kg/m^3])
Moisture Content:	7.60%
Limerock Bearing Ratio:	102.1
Test Operator:	TJM
Creep Compliance Curve Fit:	D = 3.41e-005*log10(t)+4.25e-004 [in^2/lb], R^2=0.94
Creep Compliance Rate (0.01d - 7d):	3.50e-005 [in^2/lb/day]
Creep Compliance Rate (0.01d - 4d):	3.83e-005 [in^2/lb/day]

Figure C-177: Creep vs. Time: 50% MRAP/50% CCB Blend 50 psi

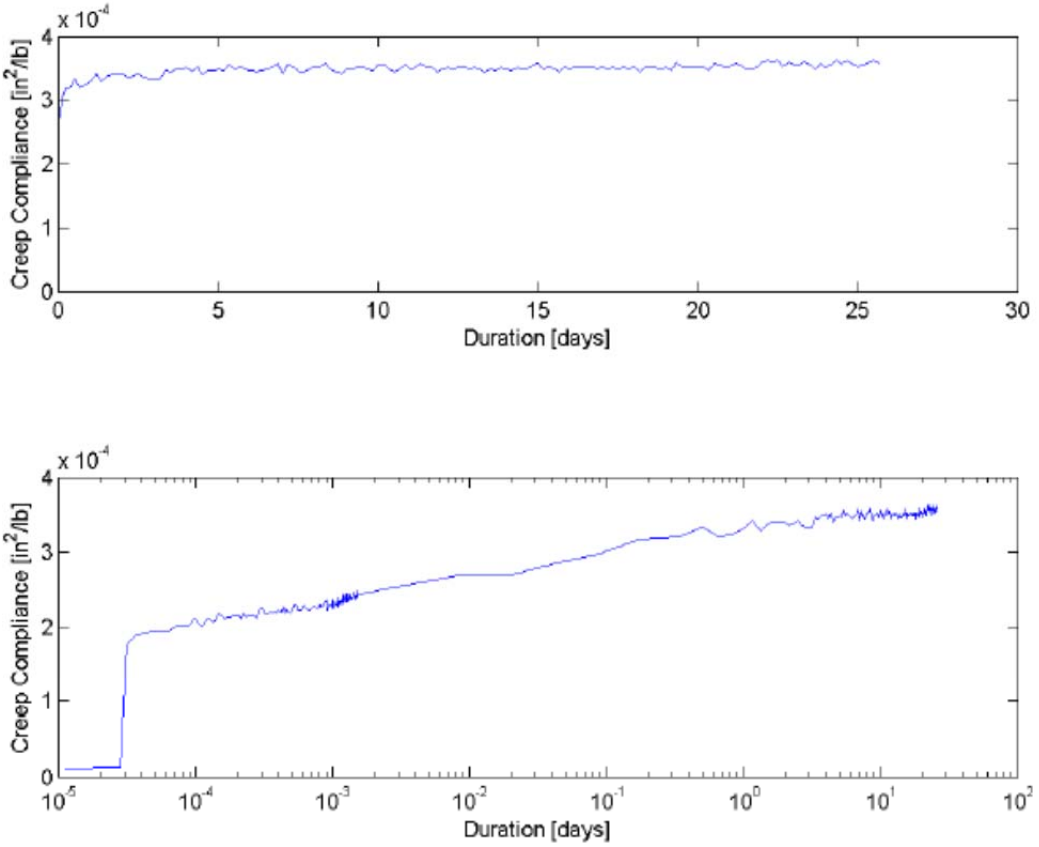

Sample Description:	50%/50% Cemented Coquinia / Melbourne Milled RAP
Test Date:	5/26/2011
Mold Number:	43
Sample Number:	6
Loading Pressure:	50.0 [lb/ft^2] (349.30 [kPa])
Dry Density:	124.0 [lb/ft^3] (1986.3 [kg/m^3])
Moisture Content:	7.40%
Limerock Bearing Ratio:	108.8
Test Operator:	TJM
Creep Compliance Curve Fit:	D = 2.65e-005*log10(t)+3.24e-004 [in^2/lb], R^2=0.96
Creep Compliance Rate (0.01d - 7d):	2.59e-005 [in^2/lb/day]
Creep Compliance Rate (0.01d - 4d):	3.16e-005 [in^2/lb/day]

Figure C-178: Creep vs. Time: 50% MRAP/50% CCB Blend 50 psi

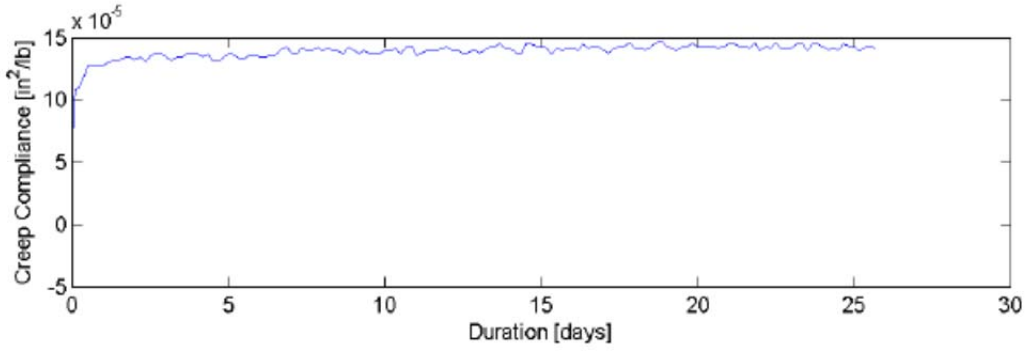

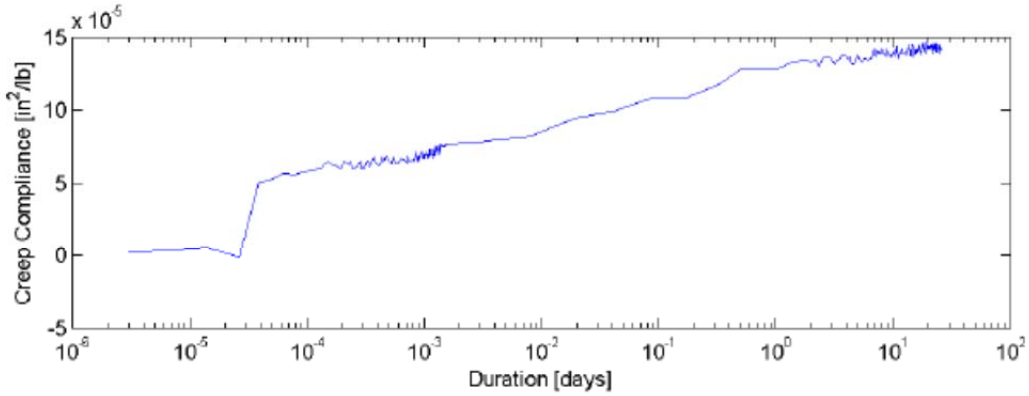

Sample Description:	50%/50% Cemented Coquinia / Melbourne Milled RAP
Test Date:	5/26/2011
Mold Number:	69
Sample Number:	2
Loading Pressure:	100.0 [lb/ft^2] (698.60 [kPa])
Dry Density:	124.3 [lb/ft^3] (1991.1 [kg/m^3])
Moisture Content:	6.90%
Limerock Bearing Ratio:	121.2
Test Operator:	TJM
Creep Compliance Curve Fit:	D = 1.68e-005*log10(t)+1.23e-004 [in^2/lb], R^2=0.97
Creep Compliance Rate (0.01d - 7d):	1.88e-005 [in^2/lb/day]
Creep Compliance Rate (0.01d - 4d):	2.01e-005 [in^2/lb/day]

Figure C-179: Creep vs. Time: 50% MRAP/50% CCB Blend 100 psi

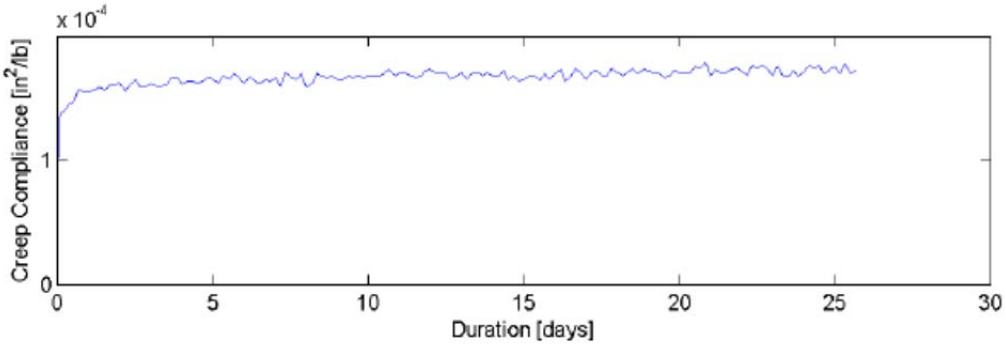

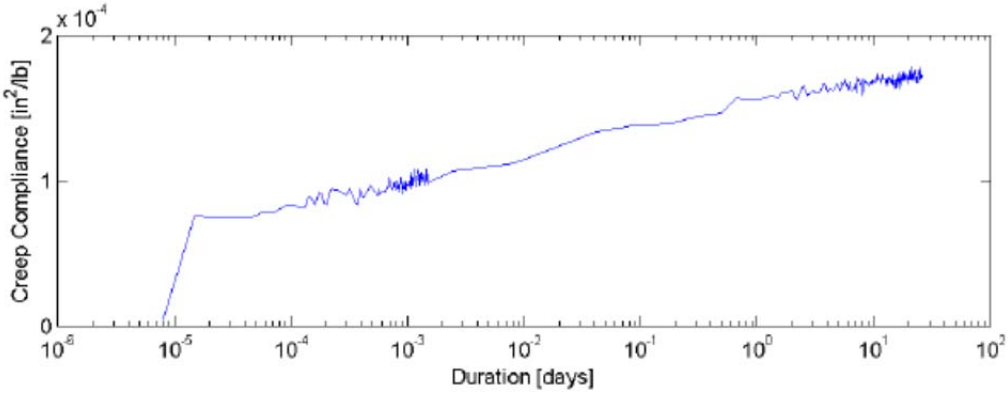

Sample Description:	50%/50% Cemented Coquinia / Melbourne Milled RAP
Test Date:	5/26/2011
Mold Number:	41
Sample Number:	4
Loading Pressure:	100.0 [lb/ft^2] (698.60 [kPa])
Dry Density:	124.3 [lb/ft^3] (1991.1 [kg/m^3])
Moisture Content:	7.70%
Limerock Bearing Ratio:	133.5
Test Operator:	TJM
Creep Compliance Curve Fit:	D = 1.65e-005*log10(t)+1.51e-004 [in^2/lb], R^2=0.97
Creep Compliance Rate (0.01d - 7d):	1.84e-005 [in^2/lb/day]
Creep Compliance Rate (0.01d - 4d):	1.81e-005 [in^2/lb/day]

Figure C-180: Creep vs. Time: 50% MRAP/50% CCB Blend 100 psi

C.3.2.3. 75% MRAP/25% Cemented Coquina

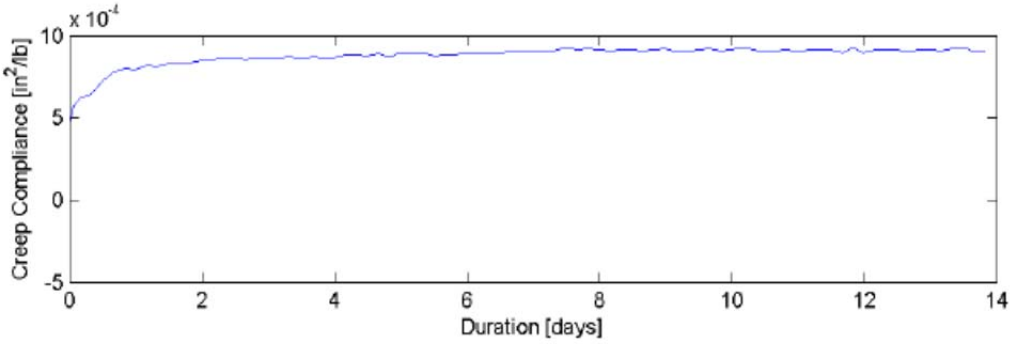

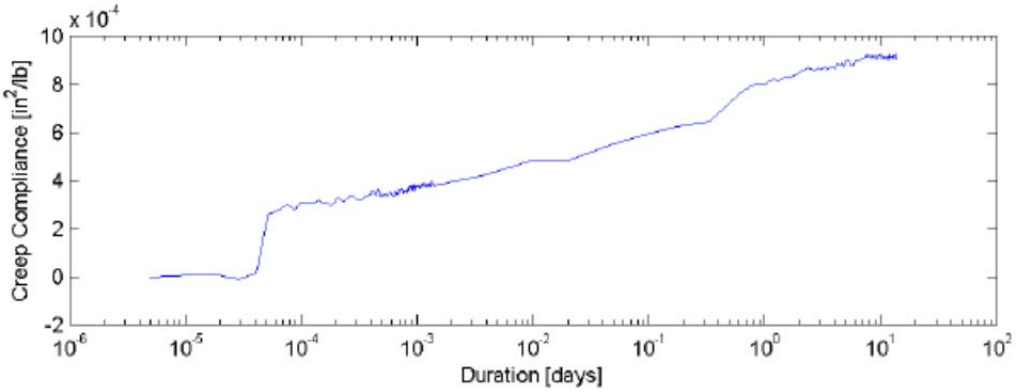

Sample Description:	25%/75% Cemented Coquinia / Melbourne Milled RAP
Test Date:	5/2/2011
Mold Number:	53
Sample Number:	5
Loading Pressure:	25.0 [lb/ft^2] (174.65 [kPa])
Dry Density:	115.2 [lb/ft^3] (1845.3 [kg/m^3])
Moisture Content:	5.60%
Limerock Bearing Ratio:	57.5
Test Operator:	TJM
Creep Compliance Curve Fit:	D = 1.48e-004*log10(t)+7.73e-004 [in^2/lb], R^2=0.98
Creep Compliance Rate (0.01d - 7d):	1.48e-004 [in^2/lb/day]
Creep Compliance Rate (0.01d - 4d):	1.47e-004 [in^2/lb/day]

Figure C-181: Creep vs. Time: 75% MRAP/25% CCB Blend 25 psi

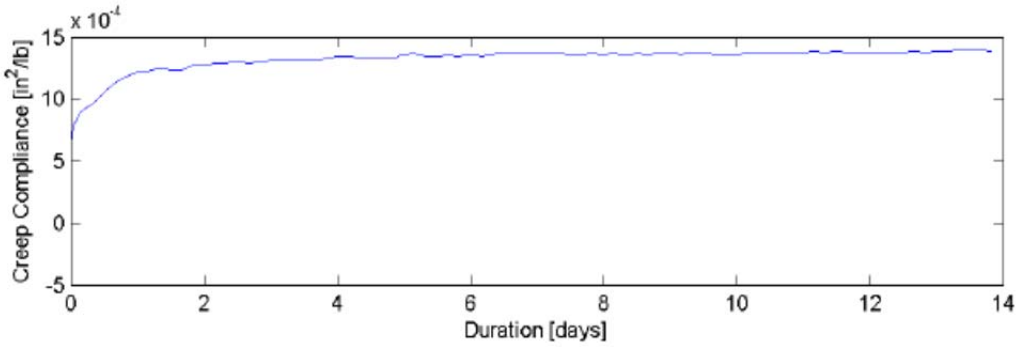

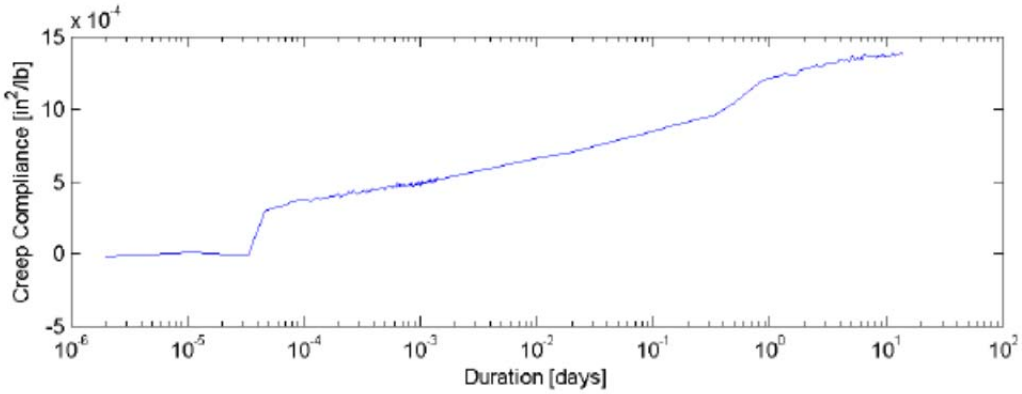

Sample Description:	25%/75% Cemented Coquinia / Melbourne Milled RAP
Test Date:	5/2/2011
Mold Number:	55
Sample Number:	6
Loading Pressure:	25.0 [lb/ft^2] (174.65 [kPa])
Dry Density:	116.4 [lb/ft^3] (1864.5 [kg/m^3])
Moisture Content:	5.70%
Limerock Bearing Ratio:	57.4
Test Operator:	TJM
Creep Compliance Curve Fit:	D = 2.43e-004*log10(t)+1.16e-003 [in^2/lb], R^2=0.98
Creep Compliance Rate (0.01d - 7d):	2.49e-004 [in^2/lb/day]
Creep Compliance Rate (0.01d - 4d):	2.64e-004 [in^2/lb/day]

Figure C-182: Creep vs. Time: 75% MRAP/25% CCB Blend 25 psi

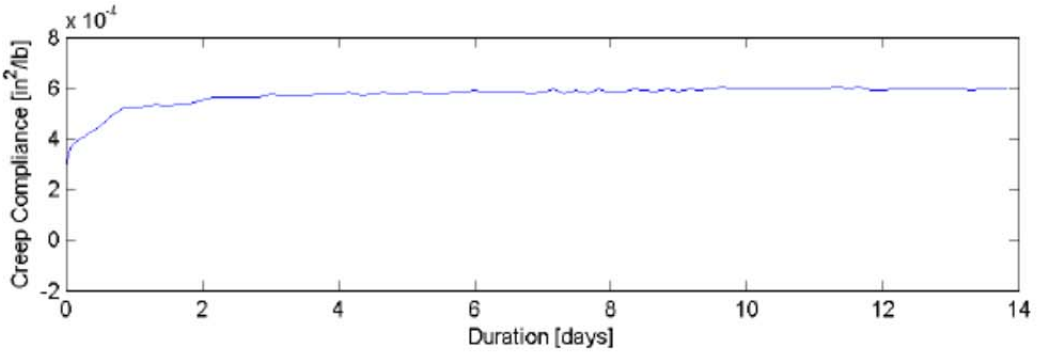

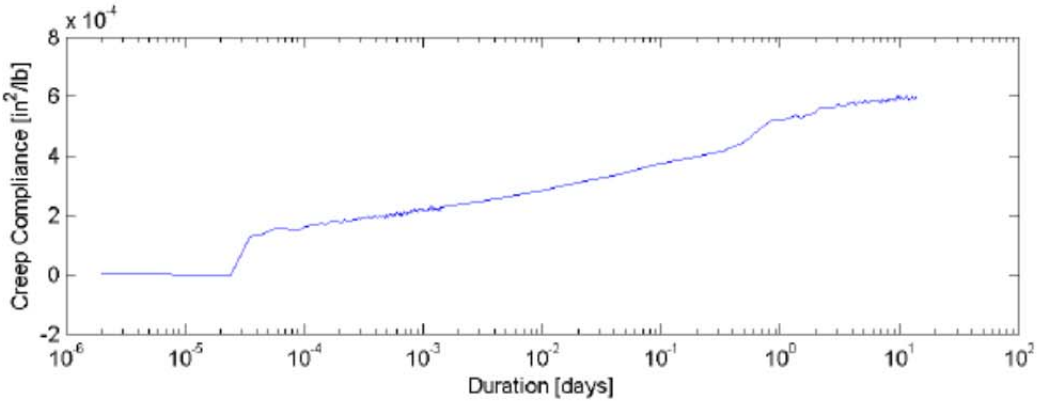

Sample Description:	25%/75% Cemented Coquinia / Melbourne Milled RAP
Test Date:	5/2/2011
Mold Number:	36
Sample Number:	2
Loading Pressure:	50.0 [lb/ft^2] (349.30 [kPa])
Dry Density:	118.7 [lb/ft^3] (1901.4 [kg/m^3])
Moisture Content:	6.90%
Limerock Bearing Ratio:	88.5
Test Operator:	TJM
Creep Compliance Curve Fit:	D = 1.03e-004*log10(t)+4.99e-004 [in^2/lb], R^2=0.98
Creep Compliance Rate (0.01d - 7d):	1.06e-004 [in^2/lb/day]
Creep Compliance Rate (0.01d - 4d):	1.12e-004 [in^2/lb/day]

Figure C-183: Creep vs. Time: 75% MRAP/25% CCB Blend 50 psi

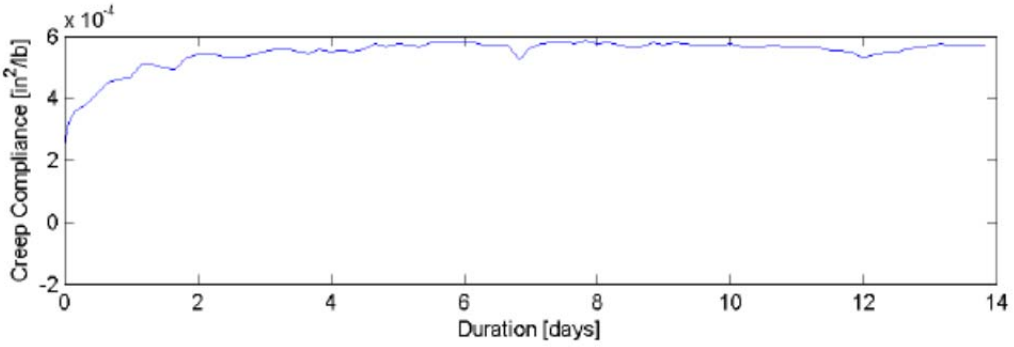

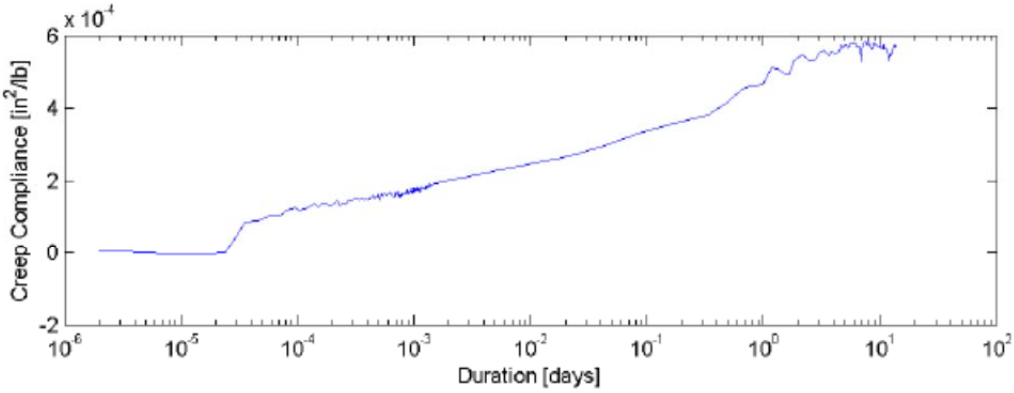

Sample Description:	25%/75% Cemented Coquinia / Melbourne Milled RAP
Test Date:	5/2/2011
Mold Number:	32
Sample Number:	1
Loading Pressure:	50.0 [lb/ft^2] (349.30 [kPa])
Dry Density:	117.8 [lb/ft^3] (1887.0 [kg/m^3])
Moisture Content:	6.00%
Limerock Bearing Ratio:	77.6
Test Operator:	TJM
Creep Compliance Curve Fit:	D = 1.09e-004*log10(t)+4.72e-004 [in^2/lb], R^2=0.97
Creep Compliance Rate (0.01d - 7d):	1.12e-004 [in^2/lb/day]
Creep Compliance Rate (0.01d - 4d):	1.17e-004 [in^2/lb/day]

Figure C-184: Creep vs. Time: 75% MRAP/25% CCB Blend 50 psi

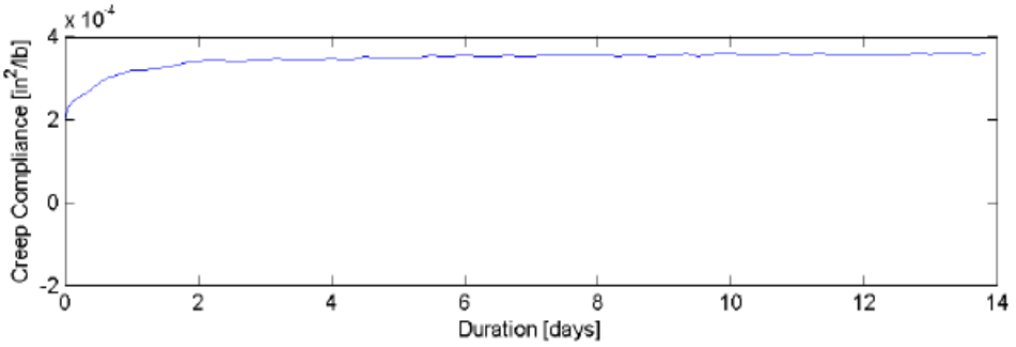

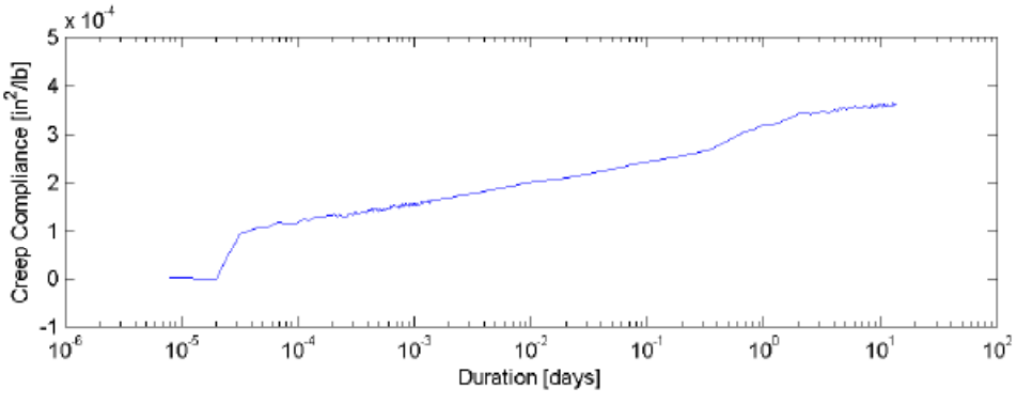

Sample Description:	25%/75% Cemented Coquinia / Melbourne Milled RAP
Test Date:	5/2/2011
Mold Number:	38
Sample Number:	3
Loading Pressure:	100.0 [lb/ft^2] (698.60 [kPa])
Dry Density:	118.8 [lb/ft^3] (1903.0 [kg/m^3])
Moisture Content:	7.20%
Limerock Bearing Ratio:	117.5
Test Operator:	TJM
Creep Compliance Curve Fit:	D = 5.49e-005*log10(t)+3.09e-004 [in^2/lb], R^2=0.98
Creep Compliance Rate (0.01d - 7d):	5.45e-005 [in^2/lb/day]
Creep Compliance Rate (0.01d - 4d):	5.79e-005 [in^2/lb/day]

Figure C-185: Creep vs. Time: 75% MRAP/25% CCB Blend 100 psi

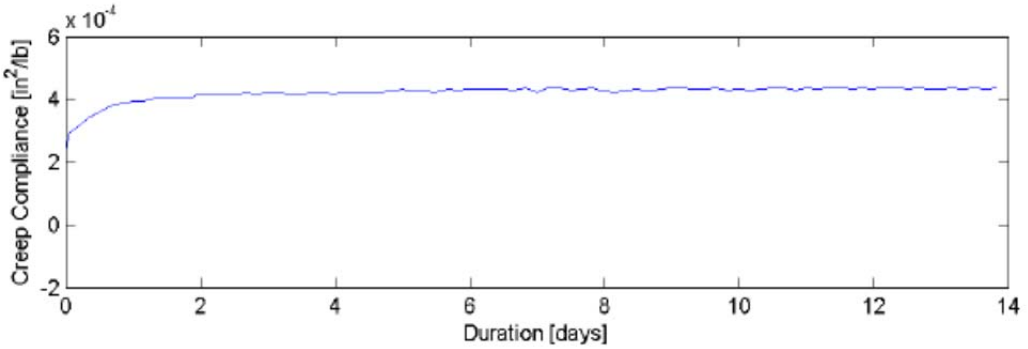

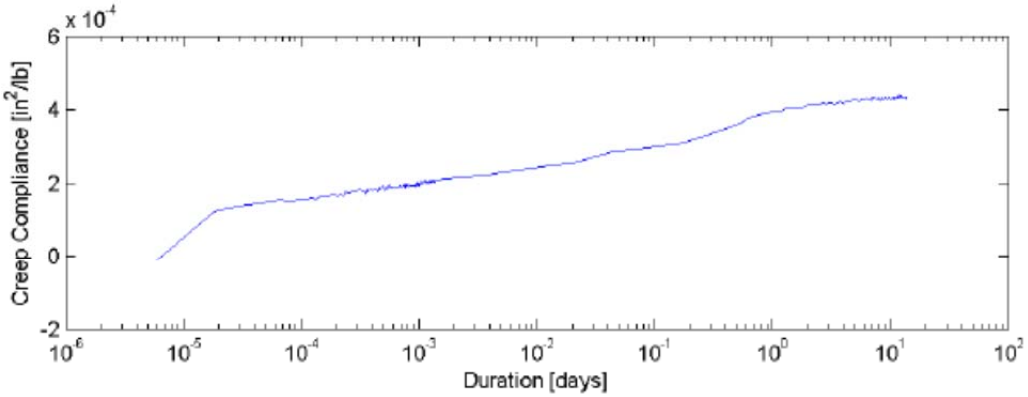

Sample Description:	25%/75% Cemented Coquinia / Melbourne Milled RAP
Test Date:	5/2/2011
Mold Number:	52
Sample Number:	4
Loading Pressure:	100.0 [lb/ft^2] (698.60 [kPa])
Dry Density:	123.2 [lb/ft^3] (1973.5 [kg/m^3])
Moisture Content:	5.40%
Limerock Bearing Ratio:	124.1
Test Operator:	TJM
Creep Compliance Curve Fit:	D = 6.40e-005*log10(t)+3.77e-004 [in^2/lb], R^2=0.98
Creep Compliance Rate (0.01d - 7d):	6.42e-005 [in^2/lb/day]
Creep Compliance Rate (0.01d - 4d):	6.72e-005 [in^2/lb/day]

Figure C-186: Creep vs. Time: 75% MRAP/25% CCB Blend 100 psi

C.3.3. MRAP/Recycled Concrete Blends

C.3.3.1. 25% MRAP/75% Recycled Concrete

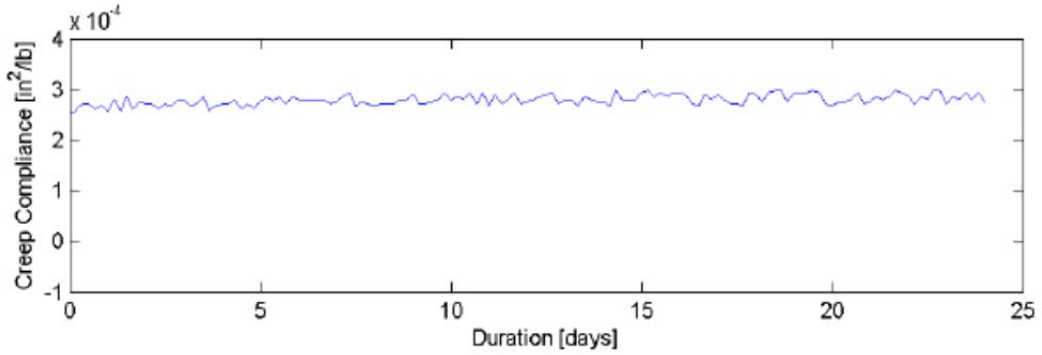

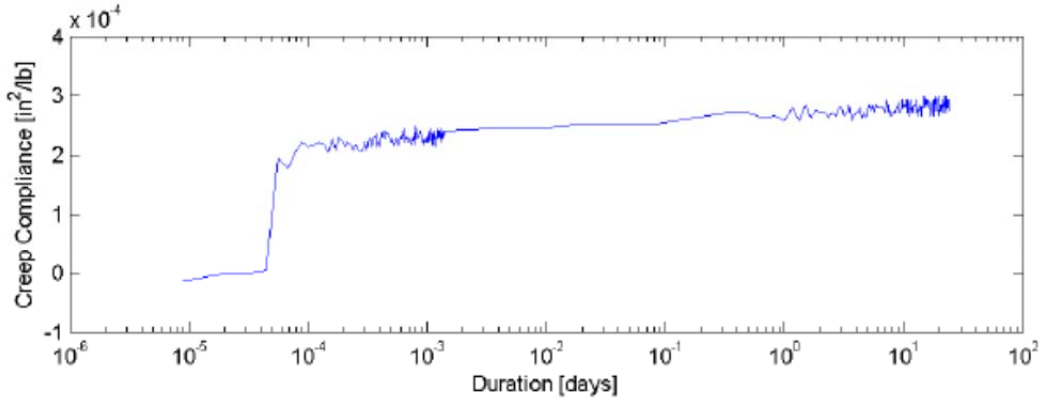

Sample Description:	75%/25% Recycled Concrete / Melbourne Milled RAP
Test Date:	11/22/2011
Mold Number:	26
Sample Number:	1
Loading Pressure:	25.0 [lb/ft^2] (174.65 [kPa])
Dry Density:	107.8 [lb/ft^3] (1726.8 [kg/m^3])
Moisture Content:	8.20%
Limerock Bearing Ratio:	120.8
Test Operator:	TJM
Creep Compliance Curve Fit:	D = 1.10e-005*log10(t)+2.68e-004 [in^2/lb], R^2=0.73
Creep Compliance Rate (0.01d - 7d):	1.07e-005 [in^2/lb/day]
Creep Compliance Rate (0.01d - 4d):	9.93e-006 [in^2/lb/day]

Figure C-187: Creep vs. Time: 25% MRAP/75% RCA Blend 25 psi

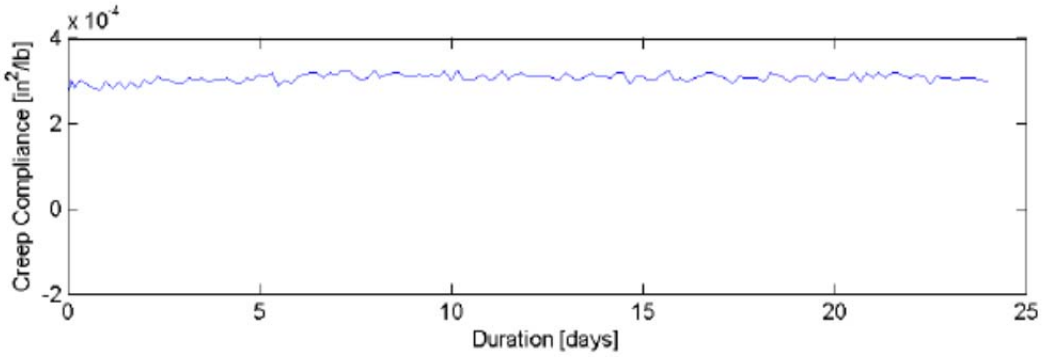

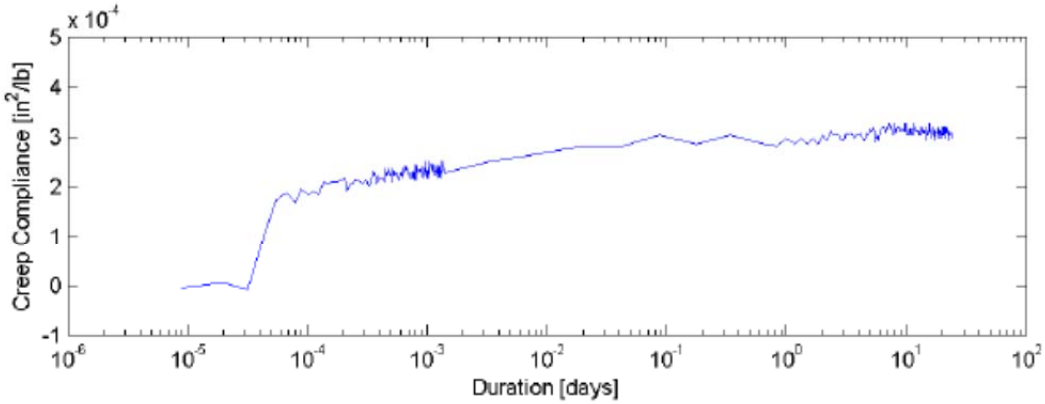

Sample Description:	75%/25% Recycled Concrete / Melbourne Milled RAP
Test Date:	11/22/2011
Mold Number:	52
Sample Number:	2
Loading Pressure:	25.0 [lb/ft^2] (174.65 [kPa])
Dry Density:	107.3 [lb/ft^3] (1718.8 [kg/m^3])
Moisture Content:	9.50%
Limerock Bearing Ratio:	112.9
Test Operator:	TJM
Creep Compliance Curve Fit:	D = 1.56e-005*log10(t)+2.94e-004 [in^2/lb], R^2=0.79
Creep Compliance Rate (0.01d - 7d):	1.68e-005 [in^2/lb/day]
Creep Compliance Rate (0.01d - 4d):	1.32e-005 [in^2/lb/day]

Figure C-188: Creep vs. Time: 25% MRAP/75% RCA Blend 25 psi

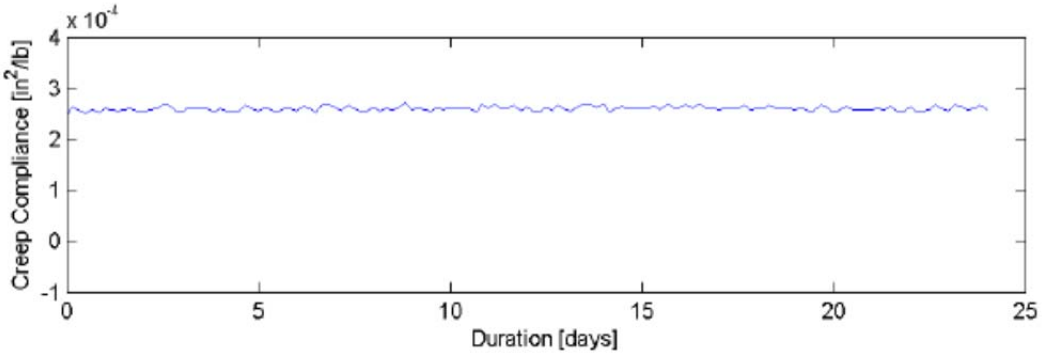

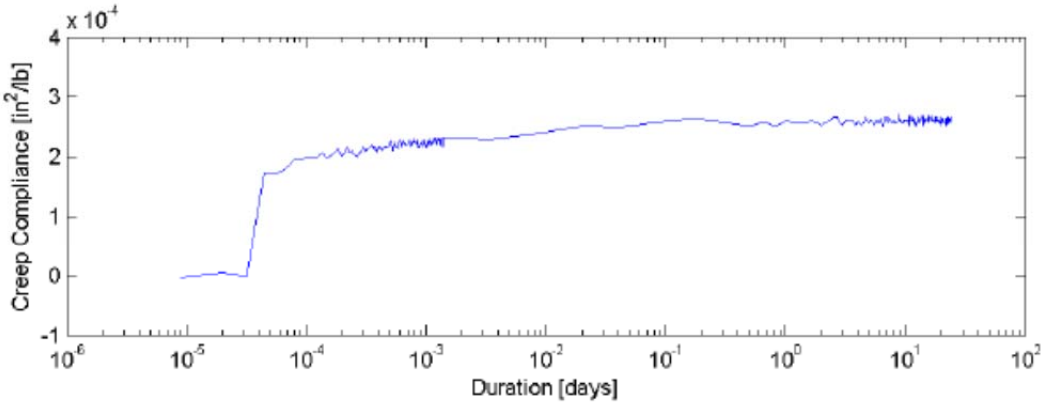

Sample Description:	75%/25% Recycled Concrete / Melbourne Milled RAP
Test Date:	11/22/2011
Mold Number:	55
Sample Number:	4
Loading Pressure:	50.0 [lb/ft^2] (349.30 [kPa])
Dry Density:	105.6 [lb/ft^3] (1691.5 [kg/m^3])
Moisture Content:	9.90%
Limerock Bearing Ratio:	130.8
Test Operator:	TJM
Creep Compliance Curve Fit:	D = 7.01e-006*log10(t)+2.53e-004 [in^2/lb], R^2=0.68
Creep Compliance Rate (0.01d - 7d):	7.39e-006 [in^2/lb/day]
Creep Compliance Rate (0.01d - 4d):	7.24e-006 [in^2/lb/day]

Figure C-189: Creep vs. Time: 25% MRAP/75% RCA Blend 50 psi

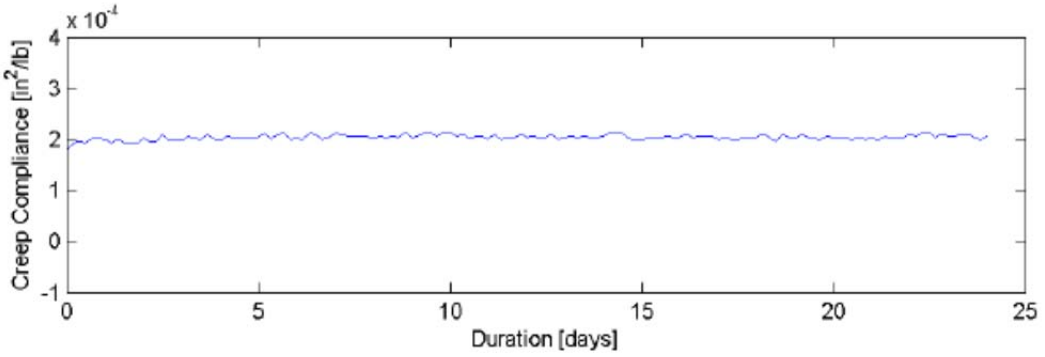

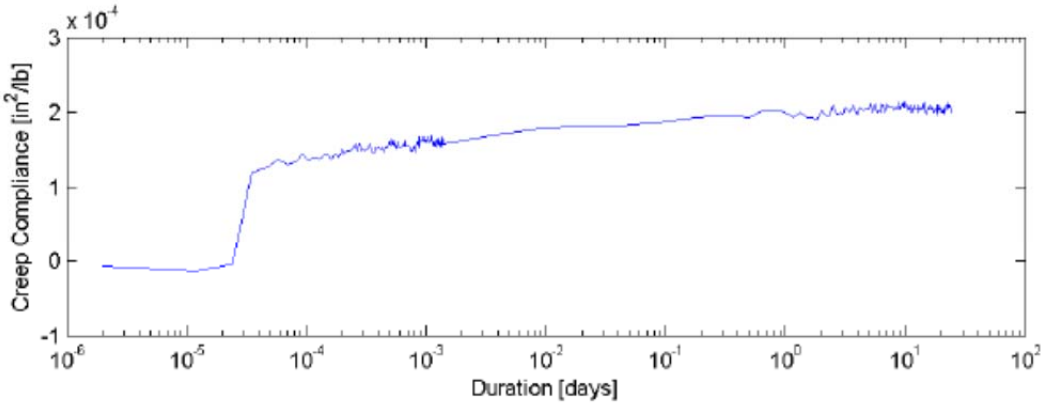

Sample Description:	75%/25% Recycled Concrete / Melbourne Milled RAP
Test Date:	11/22/2011
Mold Number:	69
Sample Number:	6
Loading Pressure:	50.0 [lb/ft^2] (349.30 [kPa])
Dry Density:	106.4 [lb/ft^3] (1704.4 [kg/m^3])
Moisture Content:	9.90%
Limerock Bearing Ratio:	119.4
Test Operator:	TJM
Creep Compliance Curve Fit:	D = 9.68e-006*log10(t)+1.95e-004 [in^2/lb], R^2=0.88
Creep Compliance Rate (0.01d - 7d):	1.16e-005 [in^2/lb/day]
Creep Compliance Rate (0.01d - 4d):	7.57e-006 [in^2/lb/day]

Figure C-190: Creep vs. Time: 25% MRAP/75% RCA Blend 50 psi

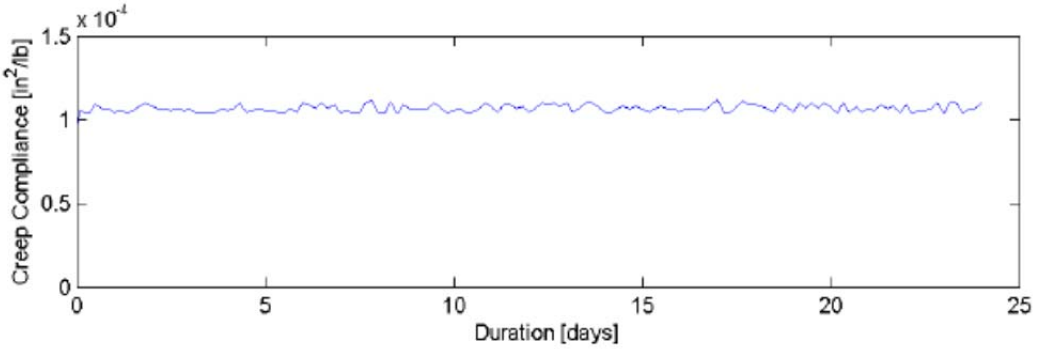

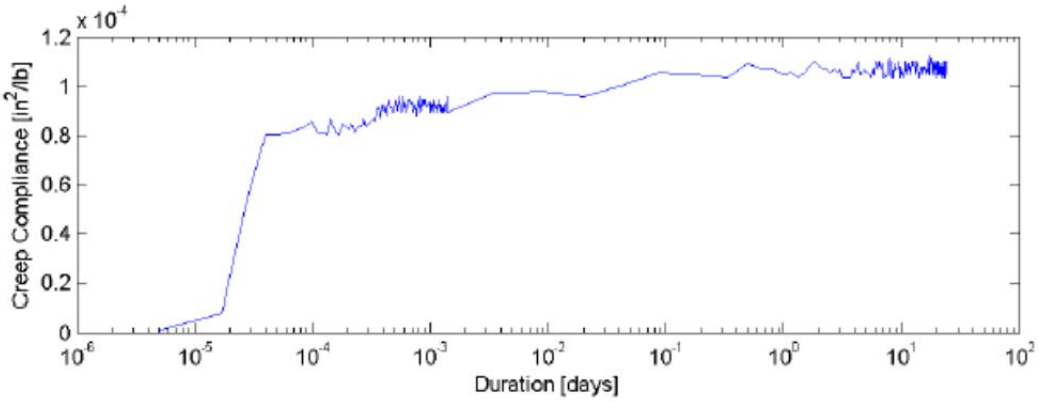

Sample Description:	75%/25% Recycled Concrete / Melbourne Milled RAP
Test Date:	11/22/2011
Mold Number:	53
Sample Number:	3
Loading Pressure:	100.0 [lb/ft^2] (698.60 [kPa])
Dry Density:	109.4 [lb/ft^3] (1752.4 [kg/m^3])
Moisture Content:	8.80%
Limerock Bearing Ratio:	149.4
Test Operator:	TJM
Creep Compliance Curve Fit:	D = 2.76e-006*log10(t)+1.04e-004 [in^2/lb], R^2=0.64
Creep Compliance Rate (0.01d - 7d):	2.04e-006 [in^2/lb/day]
Creep Compliance Rate (0.01d - 4d):	3.08e-006 [in^2/lb/day]

Figure C-191: Creep vs. Time: 25% MRAP/75% RCA Blend 100 psi

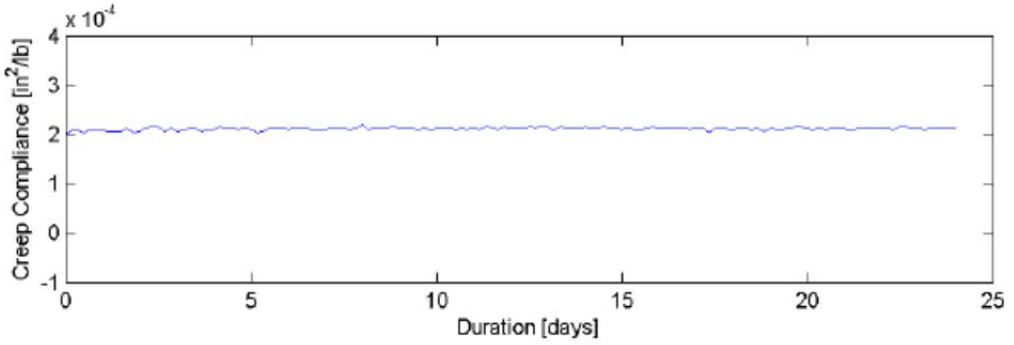

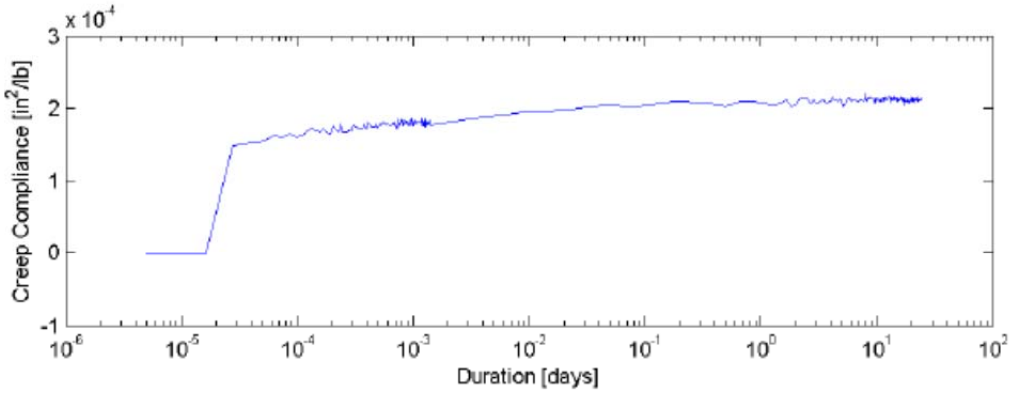

Sample Description:	75%/25% Recycled Concrete / Melbourne Milled RAP
Test Date:	11/22/2011
Mold Number:	65
Sample Number:	5
Loading Pressure:	100.0 [lb/ft^2] (698.60 [kPa])
Dry Density:	105.7 [lb/ft^3] (1693.2 [kg/m^3])
Moisture Content:	9.30%
Limerock Bearing Ratio:	136.6
Test Operator:	TJM
Creep Compliance Curve Fit:	D = 6.44e-006*log10(t)+2.06e-004 [in^2/lb], R^2=0.84
Creep Compliance Rate (0.01d - 7d):	5.41e-006 [in^2/lb/day]
Creep Compliance Rate (0.01d - 4d):	5.93e-006 [in^2/lb/day]

Figure C-192: Creep vs. Time: 25% MRAP/75% RCA Blend 100 psi

C.3.3.2. 50% MRAP/50% Recycled Concrete

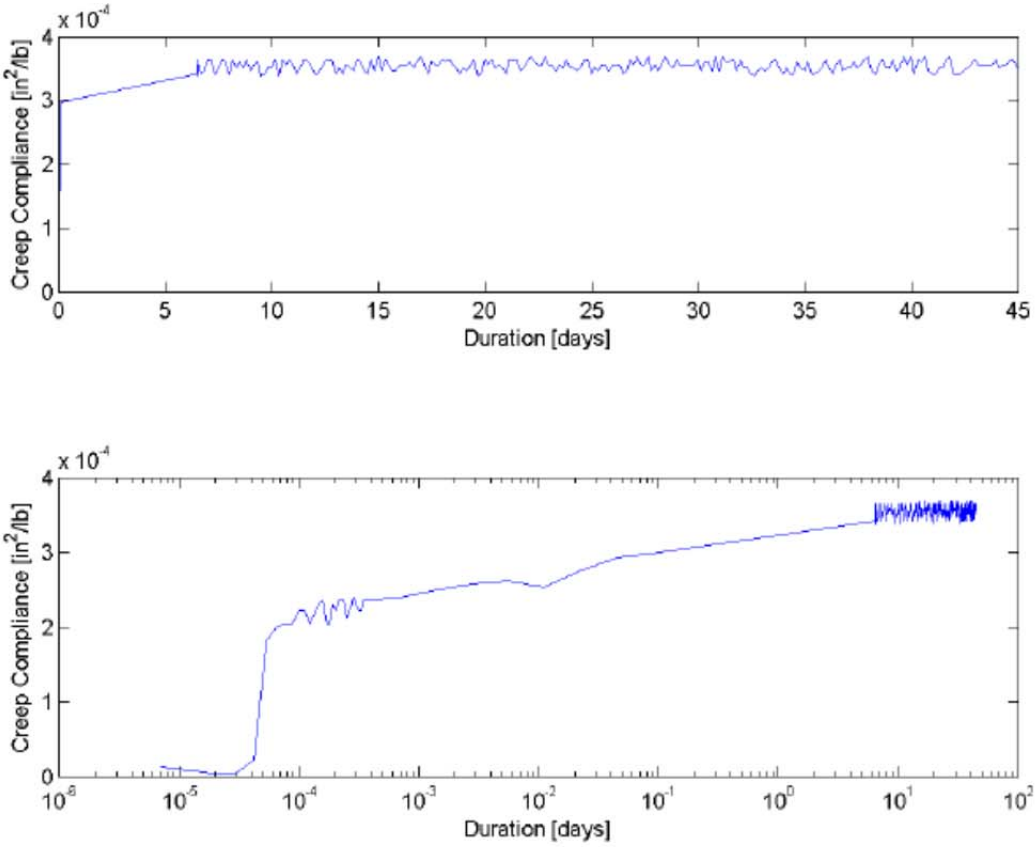

Sample Description:	50%/50% Recycled Concrete / Melbourne Milled RAP
Test Date:	1/11/2012
Mold Number:	38
Sample Number:	3
Loading Pressure:	25.0 [lb/ft^2] (174.65 [kPa])
Dry Density:	104.2 [lb/ft^3] (1669.1 [kg/m^3])
Moisture Content:	16.10%
Limerock Bearing Ratio:	65.6
Test Operator:	TJM
Creep Compliance Curve Fit:	D = 2.61e-005*log10(t)+3.18e-004 [in^2/lb], R^2=0.90
Creep Compliance Rate (0.01d - 7d):	3.84e-005 [in^2/lb/day]
Creep Compliance Rate (0.01d - 4d):	2.69e-005 [in^2/lb/day]

Figure C-193: Creep vs. Time: 50% MRAP/50% RCA Blend 25 psi

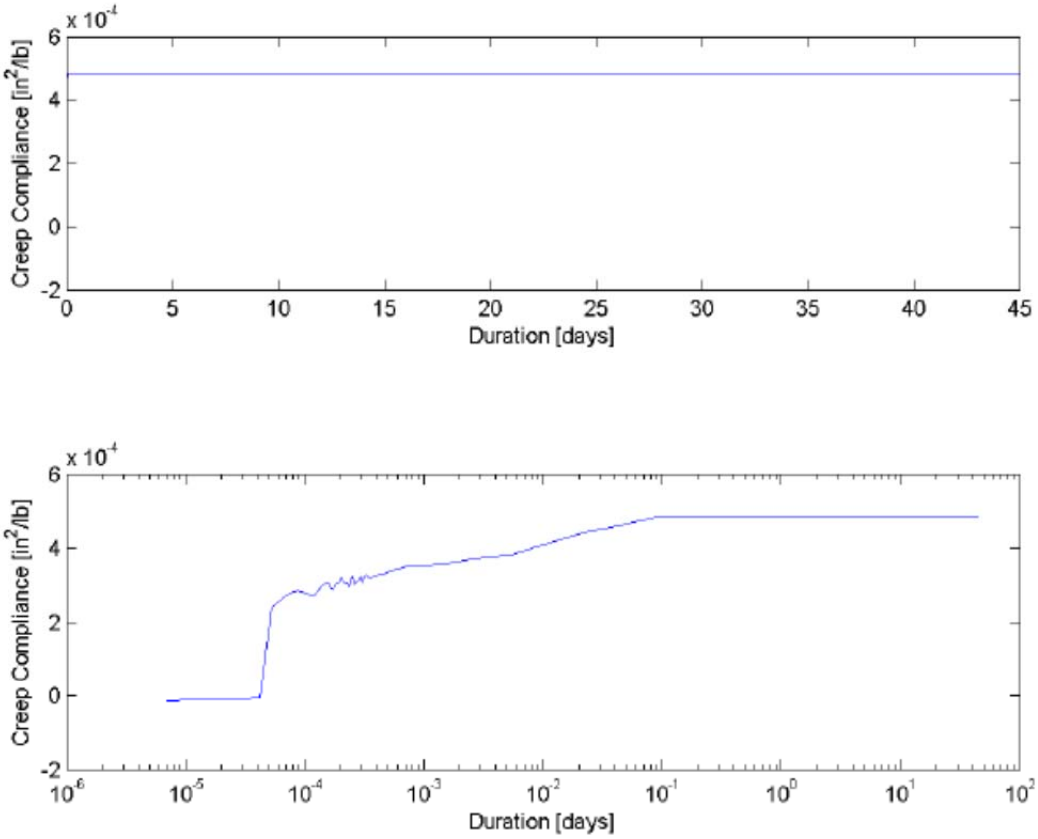

Sample Description:	50%/50% Recycled Concrete / Melbourne Milled RAP
Test Date:	1/11/2012
Mold Number:	41
Sample Number:	4
Loading Pressure:	25.0 [lb/ft^2] (174.65 [kPa])
Dry Density:	108.4 [lb/ft^3] (1736.4 [kg/m^3])
Moisture Content:	9.90%
Limerock Bearing Ratio:	51.3
Test Operator:	TJM
Creep Compliance Curve Fit:	D = 2.02e-005*log10(t)+4.62e-004 [in^2/lb], R^2=0.69
Creep Compliance Rate (0.01d - 7d):	2.72e-005 [in^2/lb/day]
Creep Compliance Rate (0.01d - 4d):	2.97e-005 [in^2/lb/day]

Figure C-194: Creep vs. Time: 50% MRAP/50% RCA Blend 25 psi

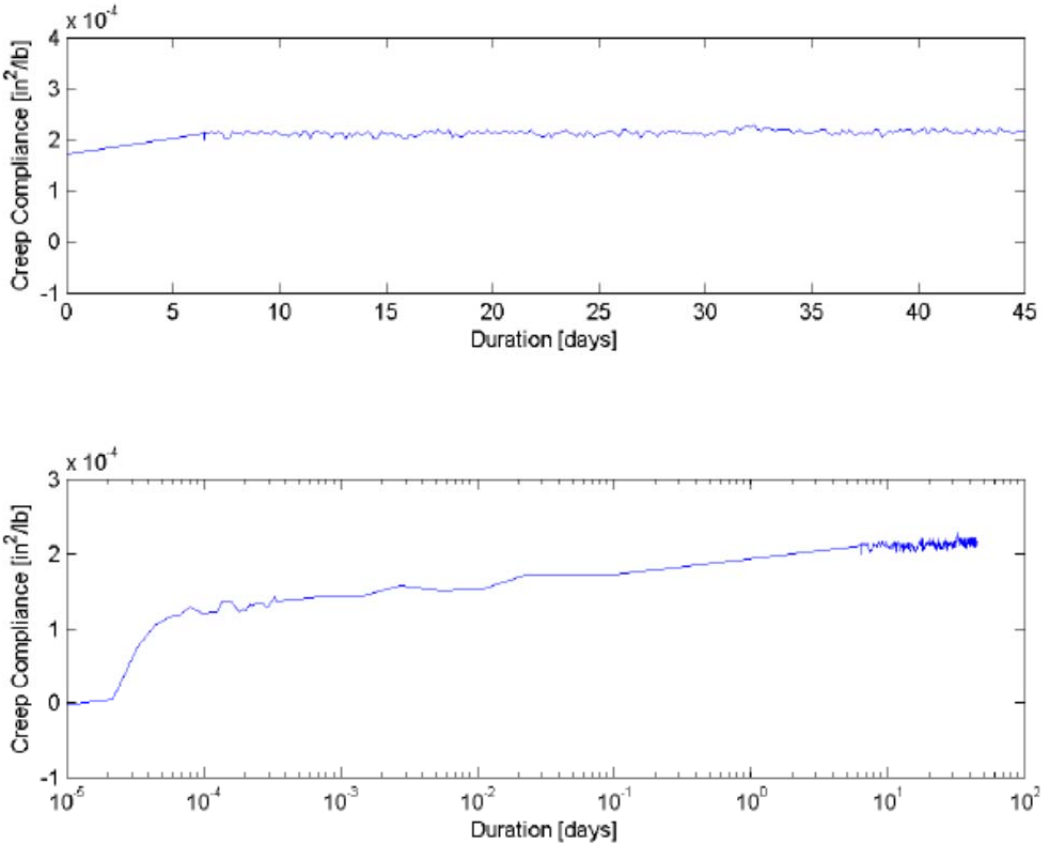

Sample Description:	50%/50% Recycled Concrete / Melbourne Milled RAP
Test Date:	1/11/2012
Mold Number:	49
Sample Number:	6
Loading Pressure:	50.0 [lb/ft^2] (349.30 [kPa])
Dry Density:	110.5 [lb/ft^3] (1770.0 [kg/m^3])
Moisture Content:	12.60%
Limerock Bearing Ratio:	108.2
Test Operator:	TJM
Creep Compliance Curve Fit:	D = 1.66e-005*log10(t)+1.90e-004 [in^2/lb], R^2=0.90
Creep Compliance Rate (0.01d - 7d):	2.08e-005 [in^2/lb/day]
Creep Compliance Rate (0.01d - 4d):	1.64e-005 [in^2/lb/day]

Figure C-195: Creep vs. Time: 50% MRAP/50% RCA Blend 50 psi

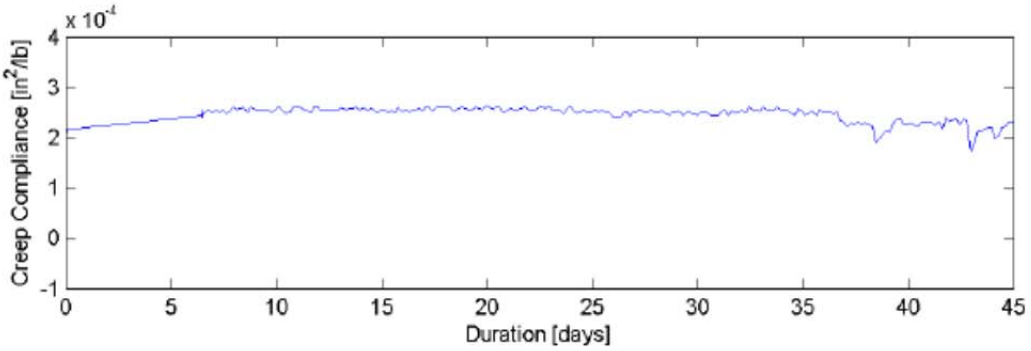

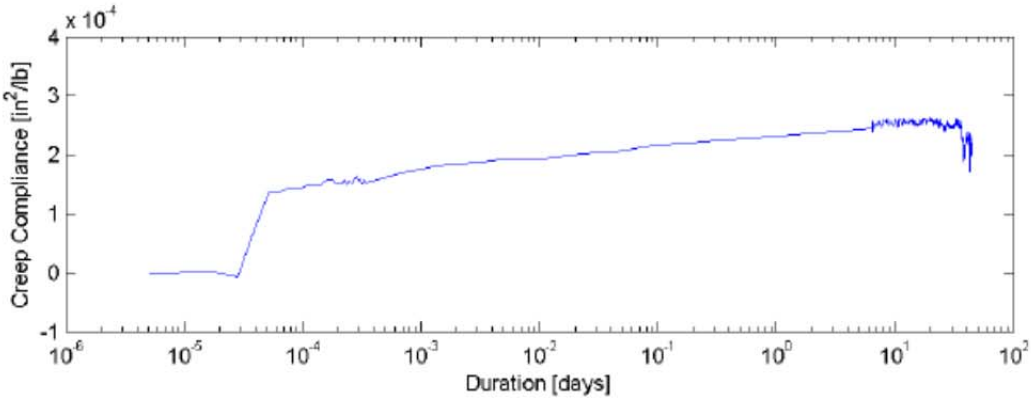

Sample Description:	50%/50% Recycled Concrete / Melbourne Milled RAP
Test Date:	1/11/2012
Mold Number:	32
Sample Number:	1
Loading Pressure:	50.0 [lb/ft^2] (349.30 [kPa])
Dry Density:	109.7 [lb/ft^3] (1757.2 [kg/m^3])
Moisture Content:	12.50%
Limerock Bearing Ratio:	99.5
Test Operator:	TJM
Creep Compliance Curve Fit:	D = 1.42e-005*log10(t)+2.27e-004 [in^2/lb], R^2=0.50
Creep Compliance Rate (0.01d - 7d):	2.00e-005 [in^2/lb/day]
Creep Compliance Rate (0.01d - 4d):	1.53e-005 [in^2/lb/day]

Figure C-196: Creep vs. Time: 50% MRAP/50% RCA Blend 50 psi

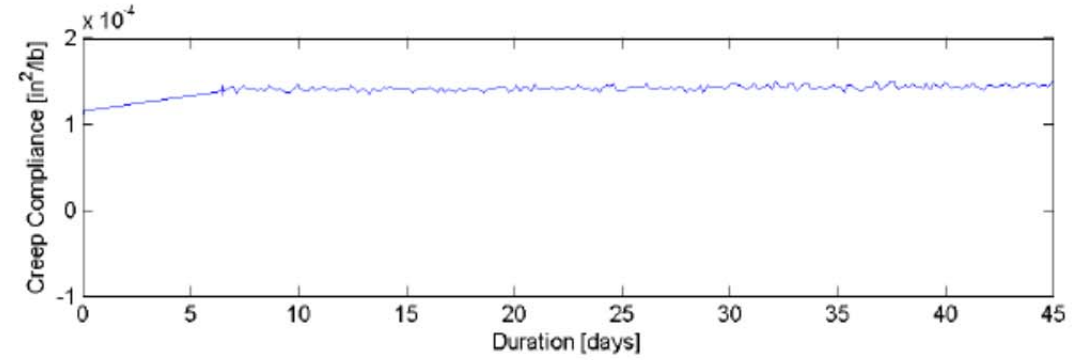

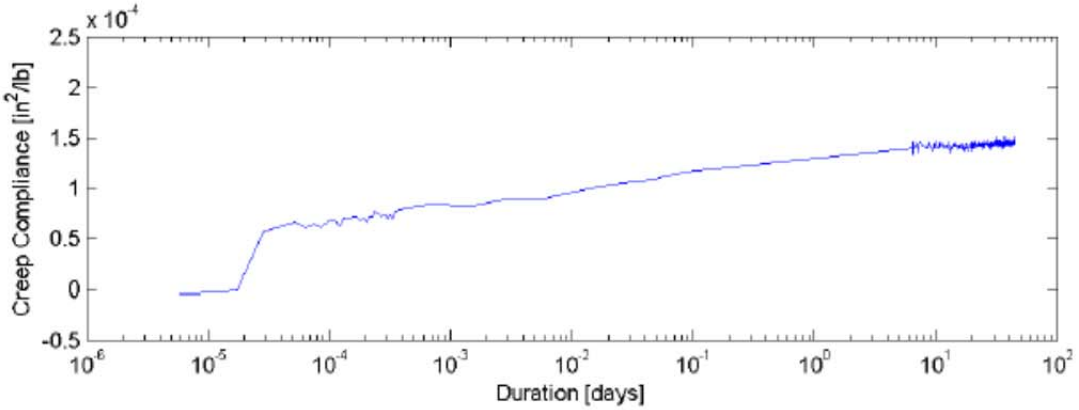

Sample Description:	50%/50% Recycled Concrete / Melbourne Milled RAP
Test Date:	1/11/2012
Mold Number:	43
Sample Number:	5
Loading Pressure:	100.0 [lb/ft^2] (698.60 [kPa])
Dry Density:	112.8 [lb/ft^3] (1806.9 [kg/m^3])
Moisture Content:	11.60%
Limerock Bearing Ratio:	112.5
Test Operator:	TJM
Creep Compliance Curve Fit:	D = 1.39e-005*log10(t)+1.24e-004 [in^2/lb], R^2=0.95
Creep Compliance Rate (0.01d - 7d):	1.68e-005 [in^2/lb/day]
Creep Compliance Rate (0.01d - 4d):	1.34e-005 [in^2/lb/day]

Figure C-197: Creep vs. Time: 50% MRAP/50% RCA Blend 100 psi

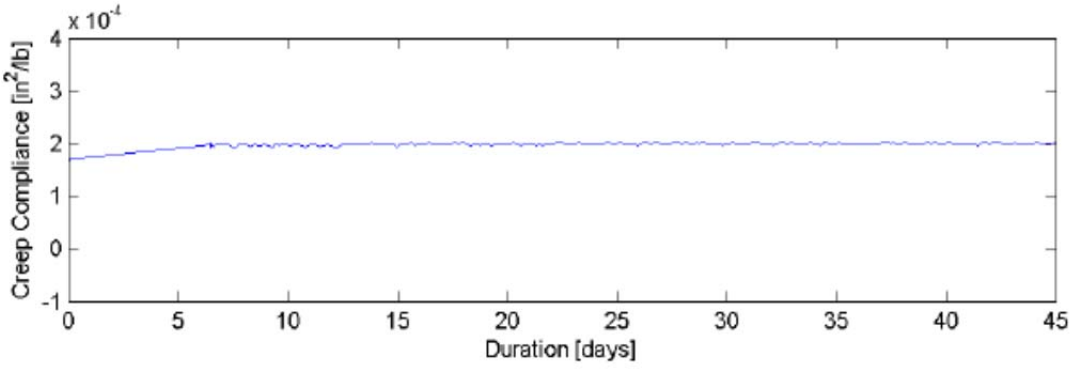

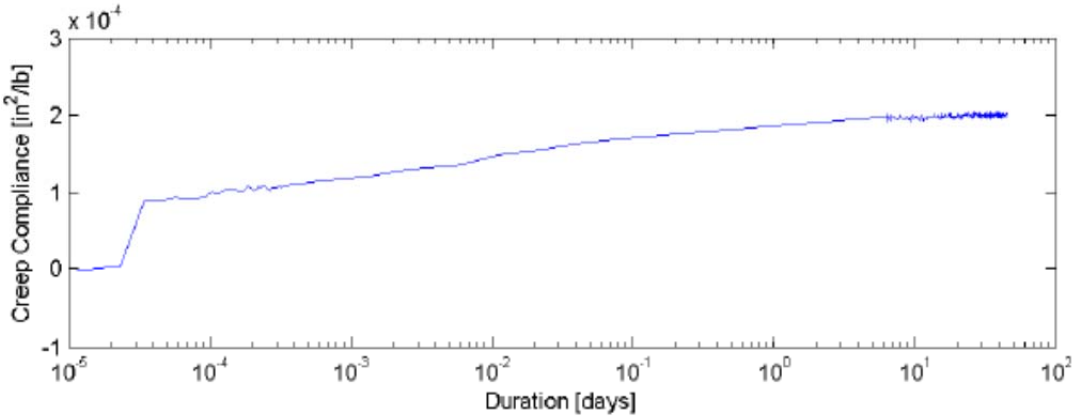

Sample Description:	50%/50% Recycled Concrete / Melbourne Milled RAP
Test Date:	1/11/2012
Mold Number:	36
Sample Number:	2
Loading Pressure:	100.0 [lb/ft^2] (698.60 [kPa])
Dry Density:	111.5 [lb/ft^3] (1786.1 [kg/m^3])
Moisture Content:	11.60%
Limerock Bearing Ratio:	107.9
Test Operator:	TJM
Creep Compliance Curve Fit:	D = 1.63e-005*log10(t)+1.77e-004 [in^2/lb], R^2=0.95
Creep Compliance Rate (0.01d - 7d):	1.85e-005 [in^2/lb/day]
Creep Compliance Rate (0.01d - 4d):	1.61e-005 [in^2/lb/day]

Figure C-198: Creep vs. Time: 50% MRAP/50% RCA Blend 100 psi

C.3.3.3. 75% MRAP/25% Recycled Concrete

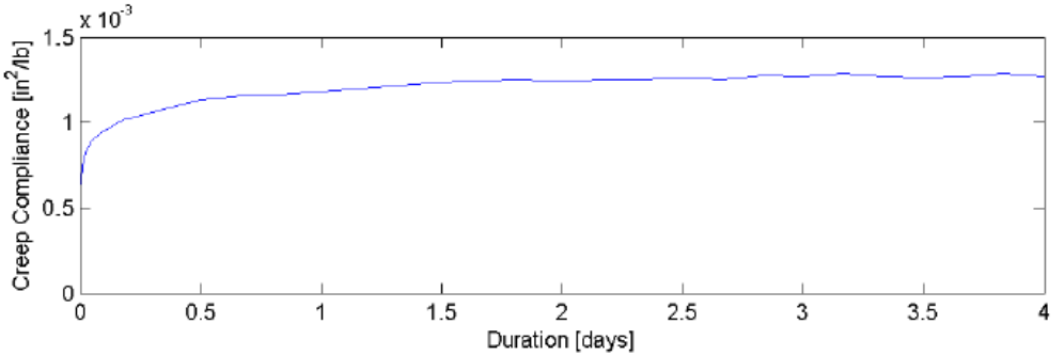

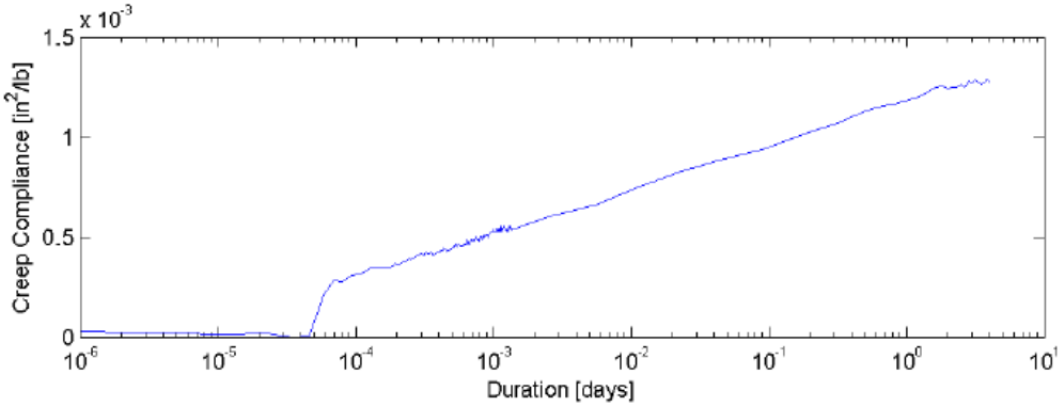

Sample Description:	25/75% RCA/MMRAP
Test Date:	4/2/2012
Mold Number:	36
Sample Number:	2
Loading Pressure:	25.0 [lb/ft^2] (174.65 [kPa])
Dry Density:	107.5 [lb/ft^3] (1722.0 [kg/m^3])
Moisture Content:	6.20%
Limerock Bearing Ratio:	0.0
Test Operator:	TJM
Creep Compliance Curve Fit:	D = 2.22e-004*log10(t)+1.18e-003 [in^2/lb], R^2=1.00
Creep Compliance Rate (0.01d - 7d):	2.13e-004 [in^2/lb/day](0.1-3.9 days)
Creep Compliance Rate (0.01d - 4d):	NaN [in^2/lb/day]

Figure C-199: Creep vs. Time: 75% MRAP/25% RCA Blend 25 psi

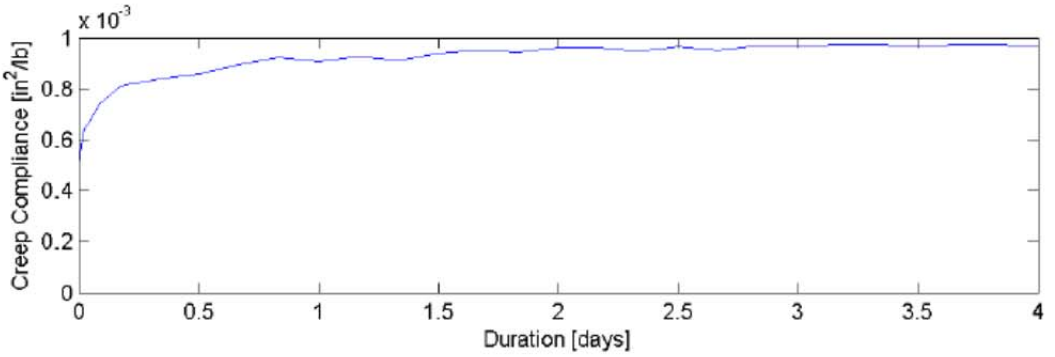

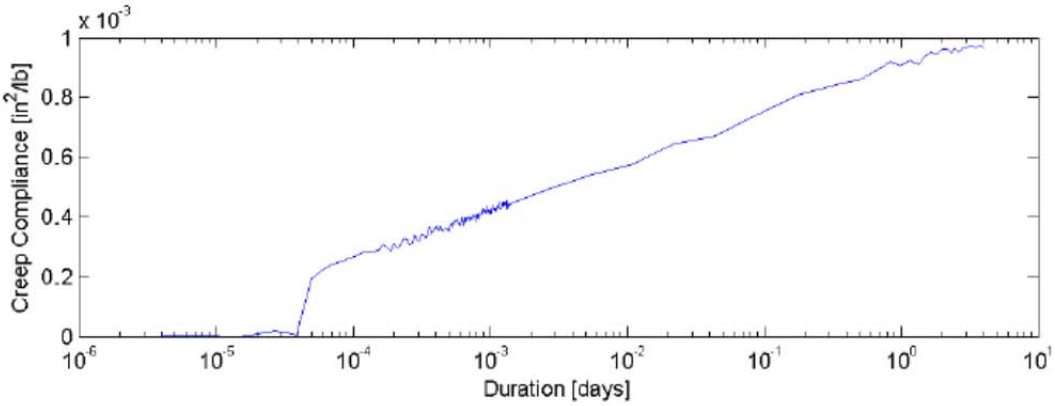

Sample Description:	25/75% RCA/MMRAP
Test Date:	4/2/2012
Mold Number:	43
Sample Number:	5
Loading Pressure:	25.0 [lb/ft^2] (174.65 [kPa])
Dry Density:	108.9 [lb/ft^3] (1744.4 [kg/m^3])
Moisture Content:	6.00%
Limerock Bearing Ratio:	0.0
Test Operator:	TJM
Creep Compliance Curve Fit:	D = 1.62e-004*log10(t)+9.04e-004 [in^2/lb], R^2=1.00
Creep Compliance Rate (0.01d - 7d):	1.54e-004 [in^2/lb/day](0.1-3.9 days)
Creep Compliance Rate (0.01d - 4d):	NaN [in^2/lb/day]

Figure C-200: Creep vs. Time: 75% MRAP/25% RCA Blend 25 psi

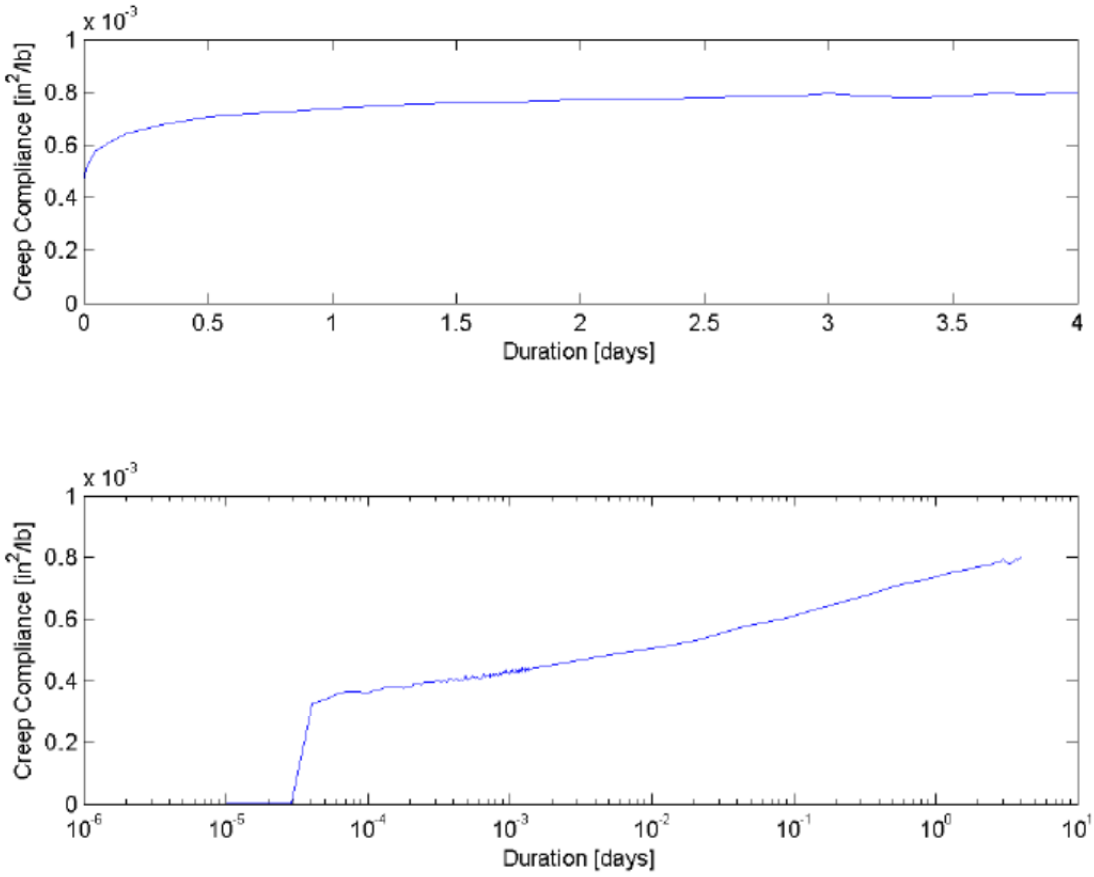

Sample Description:	25/75% RCA/MMRAP
Test Date:	4/2/2012
Mold Number:	49
Sample Number:	6
Loading Pressure:	50.0 [lb/ft^2] (349.30 [kPa])
Dry Density:	109.1 [lb/ft^3] (1747.6 [kg/m^3])
Moisture Content:	6.00%
Limerock Bearing Ratio:	0.0
Test Operator:	TJM
Creep Compliance Curve Fit:	D = 1.09e-004*log10(t)+7.33e-004 [in^2/lb], R^2=0.99
Creep Compliance Rate (0.01d - 7d):	1.12e-004 [in^2/lb/day](0.1-3.9 days)
Creep Compliance Rate (0.01d - 4d):	NaN [in^2/lb/day]

Figure C-201: Creep vs. Time: 75% MRAP/25% RCA Blend 50 psi

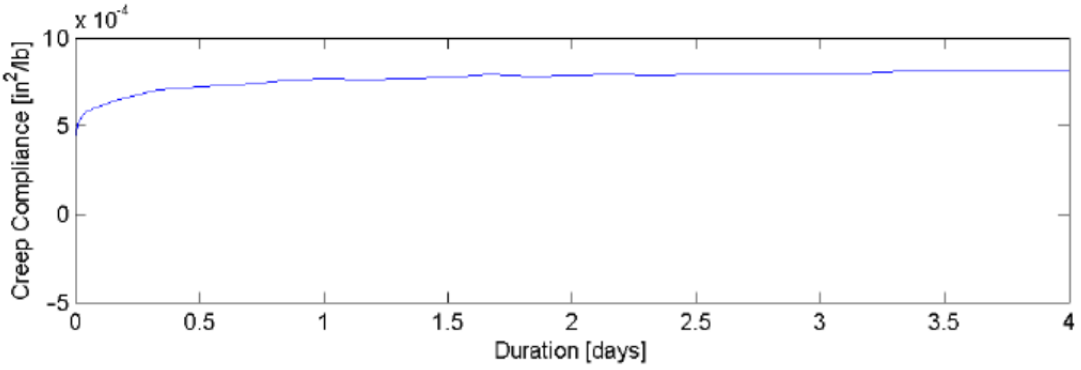

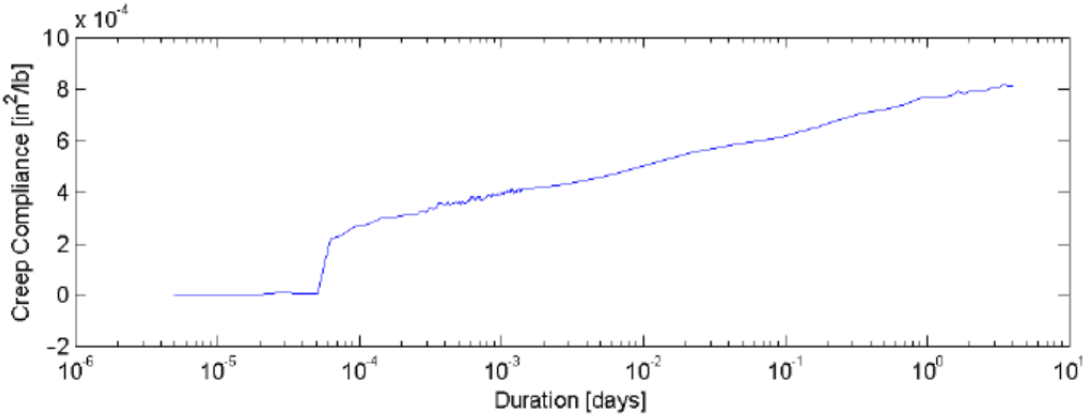

Sample Description:	25/75% RCA/MMRAP
Test Date:	4/2/2012
Mold Number:	41
Sample Number:	4
Loading Pressure:	50.0 [lb/ft^2] (349.30 [kPa])
Dry Density:	109.3 [lb/ft^3] (1750.8 [kg/m^3])
Moisture Content:	6.00%
Limerock Bearing Ratio:	0.0
Test Operator:	TJM
Creep Compliance Curve Fit:	D = 1.24e-004*log10(t)+7.52e-004 [in^2/lb], R^2=1.00
Creep Compliance Rate (0.01d - 7d):	1.20e-004 [in^2/lb/day](0.1-3.9 days)
Creep Compliance Rate (0.01d - 4d):	NaN [in^2/lb/day]

Figure C-202: Creep vs. Time: 75% MRAP/25% RCA Blend 50 psi

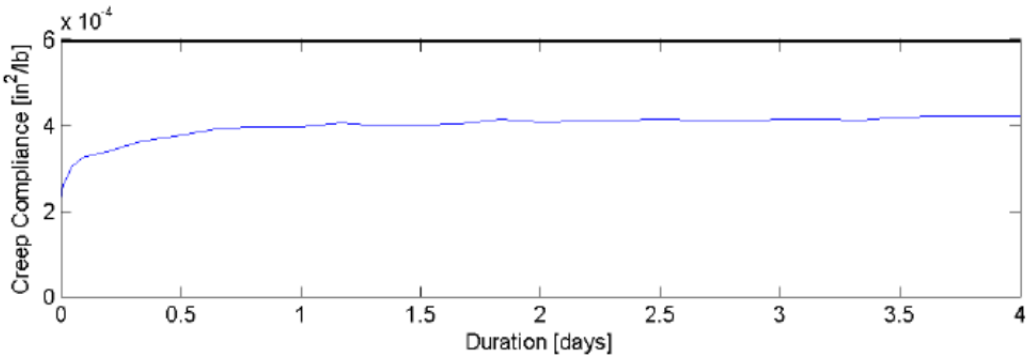

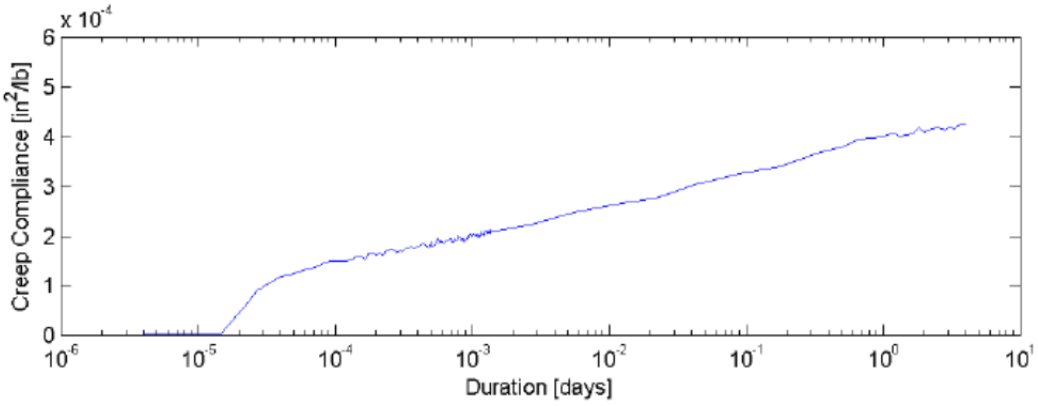

Sample Description:	25/75% RCA/MMRAP
Test Date:	4/2/2012
Mold Number:	38
Sample Number:	3
Loading Pressure:	100.0 [lb/ft^2] (698.60 [kPa])
Dry Density:	111.6 [lb/ft^3] (1787.7 [kg/m^3])
Moisture Content:	6.20%
Limerock Bearing Ratio:	0.0
Test Operator:	TJM
Creep Compliance Curve Fit:	D = 6.50e-005*log10(t)+3.92e-004 [in^2/lb], R^2=1.00
Creep Compliance Rate (0.01d - 7d):	6.30e-005 [in^2/lb/day](0.1-3.9 days)
Creep Compliance Rate (0.01d - 4d):	NaN [in^2/lb/day]

Figure C-203: Creep vs. Time: 75% MRAP/25% RCA Blend 100 psi

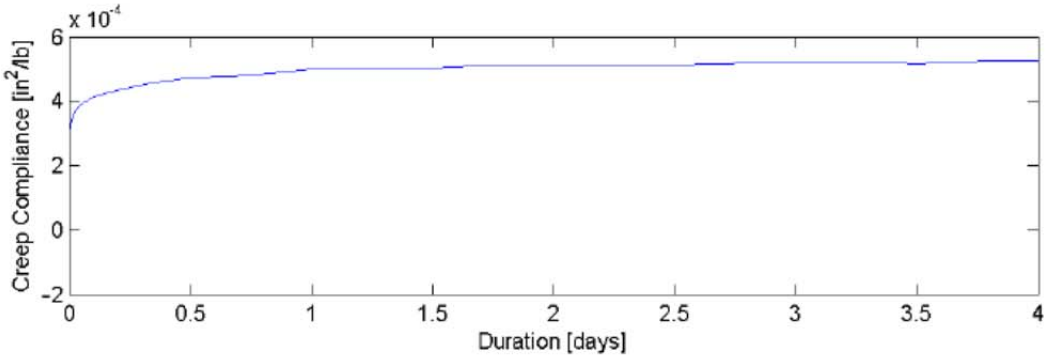

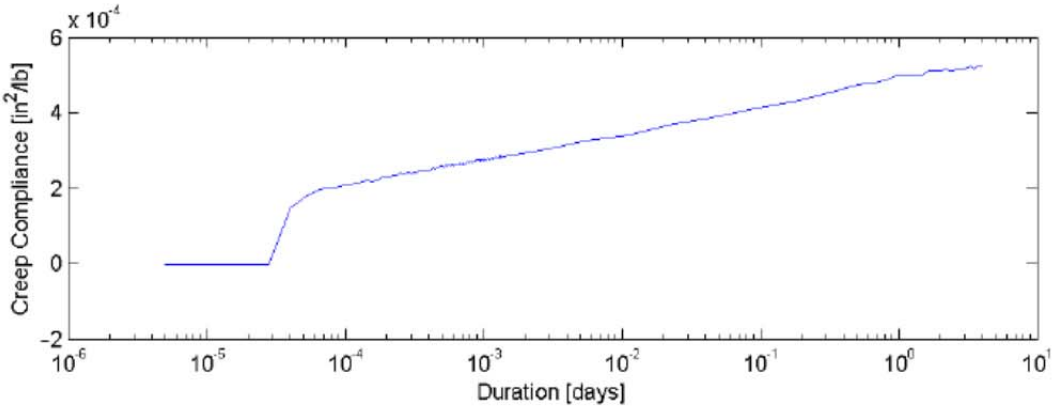

Sample Description:	75/25% RCA/MMRAP
Test Date:	4/2/2012
Mold Number:	32
Sample Number:	1
Loading Pressure:	100.0 [lb/ft^2] (698.60 [kPa])
Dry Density:	110.3 [lb/ft^3] (1766.8 [kg/m^3])
Moisture Content:	5.60%
Limerock Bearing Ratio:	0.0
Test Operator:	TJM
Creep Compliance Curve Fit:	D = 7.34e-005*log10(t)+4.88e-004 [in^2/lb], R^2=1.00
Creep Compliance Rate (0.01d - 7d):	7.18e-005 [in^2/lb/day](0.1-3.9 days)
Creep Compliance Rate (0.01d - 4d):	NaN [in^2/lb/day]

Figure C-204: Creep vs. Time: 75% MRAP/25% RCA Blend 100 psi

C.4. Creep Data MRAP/Limerock with Stabilizing Agent

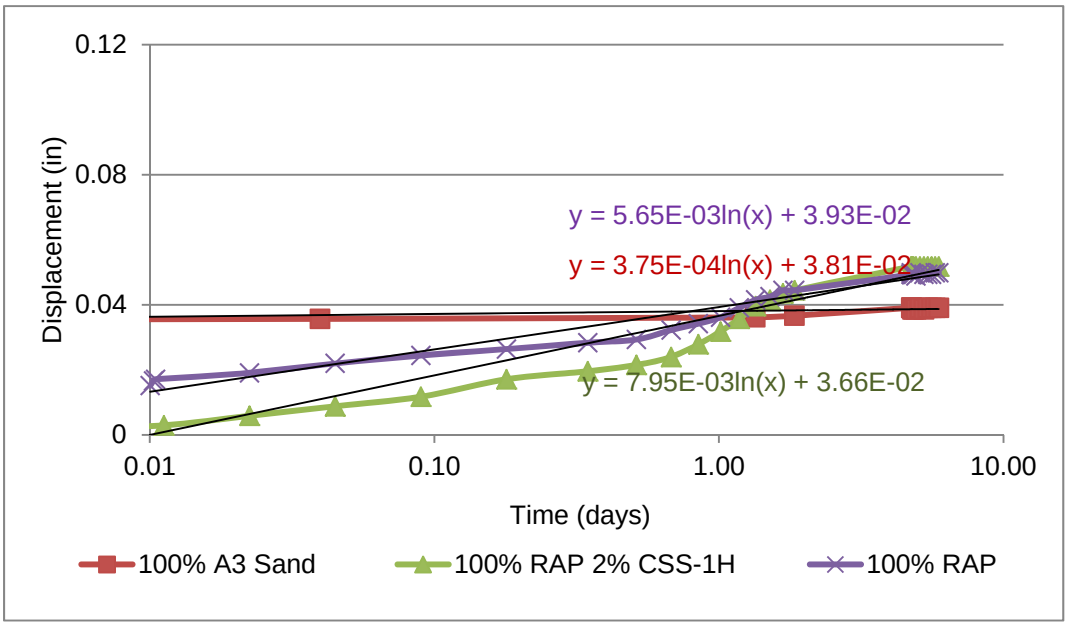

Figure C-205: Trial 1: 100% MRAP 0%, 2% CSS-1H, 100% A-3 Log(time)

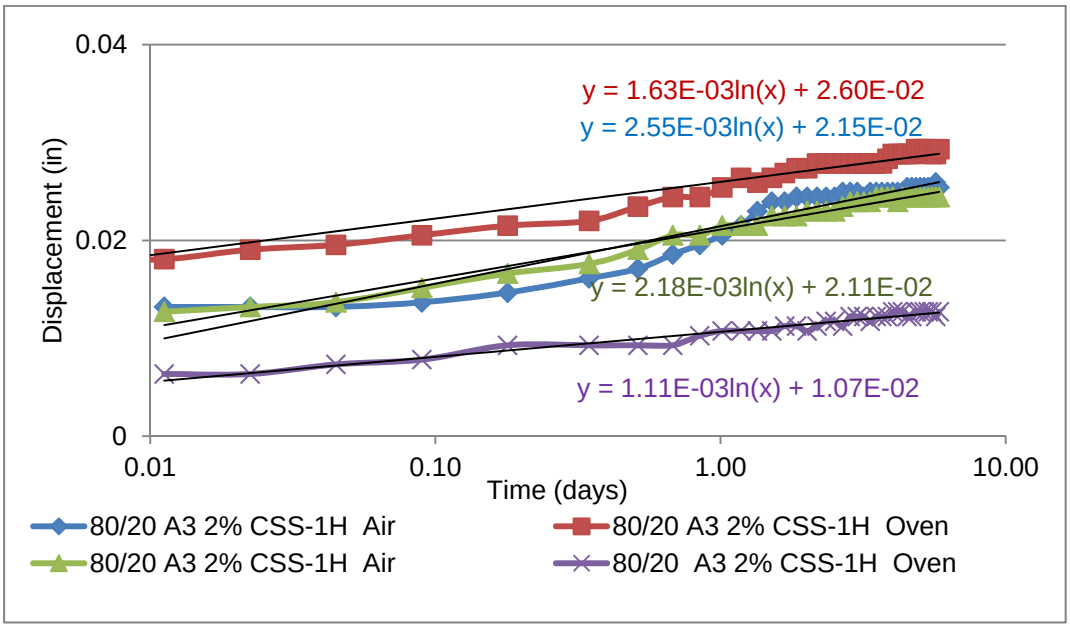

Figure C-206: Trial 2: 20% MRAP/80% A3 2% CSS-1H Air and Oven Cure Log(time)

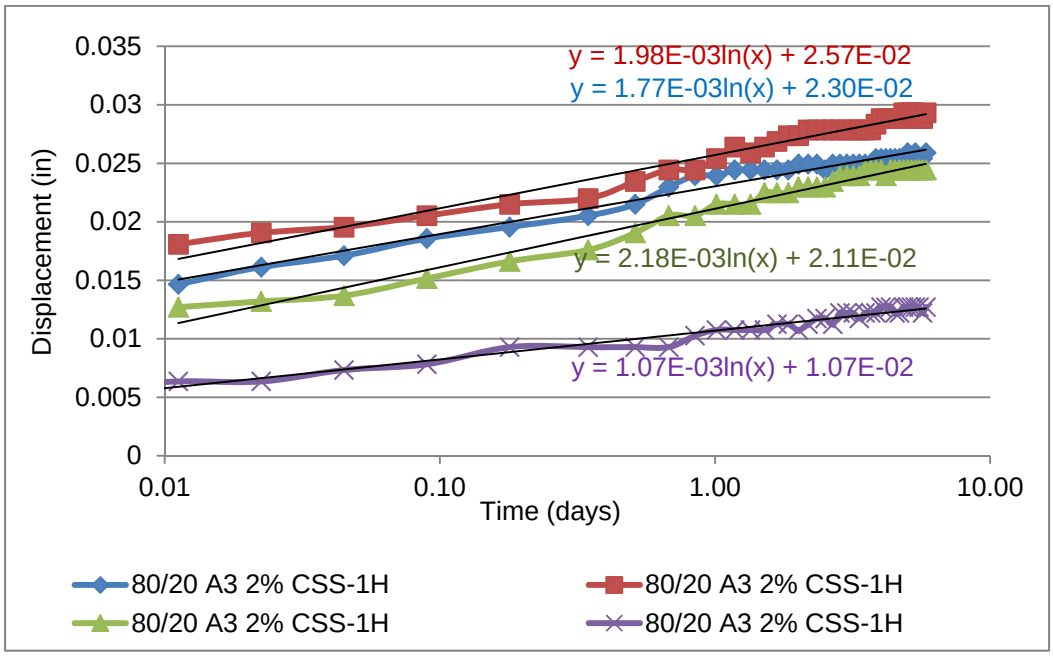

Figure C-207: Trial 3: 20% MRAP/80% A-3 2% CSS-1H Log(time)

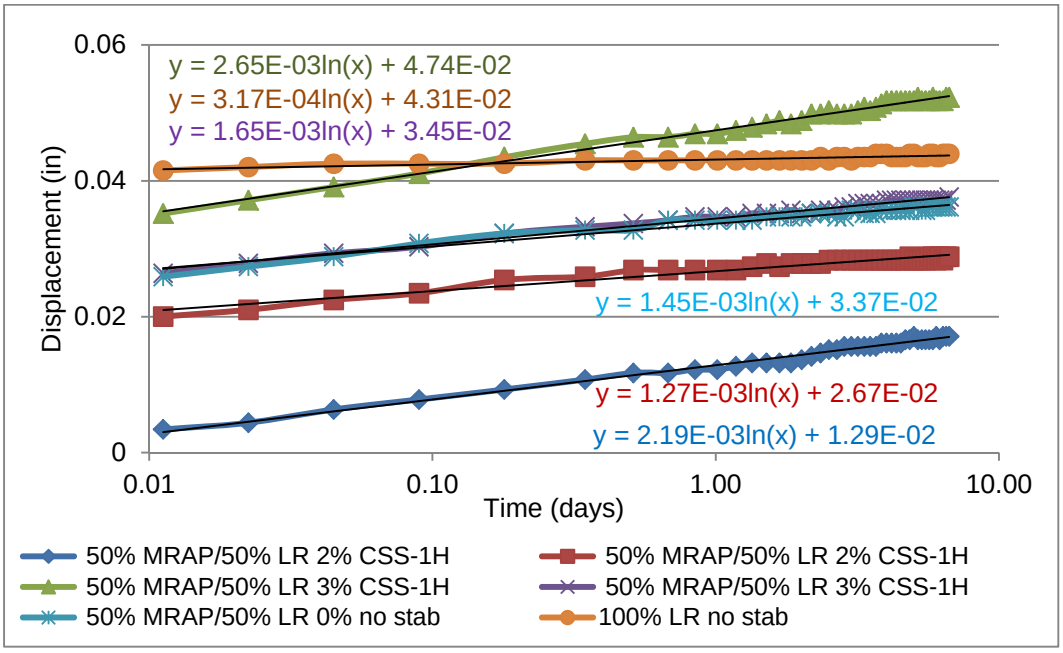

Figure C-208: Trial 4: 50% MRAP/50% LR 0%, 2%, 3% CSS-1H, 100% LR No Stab Log(time)

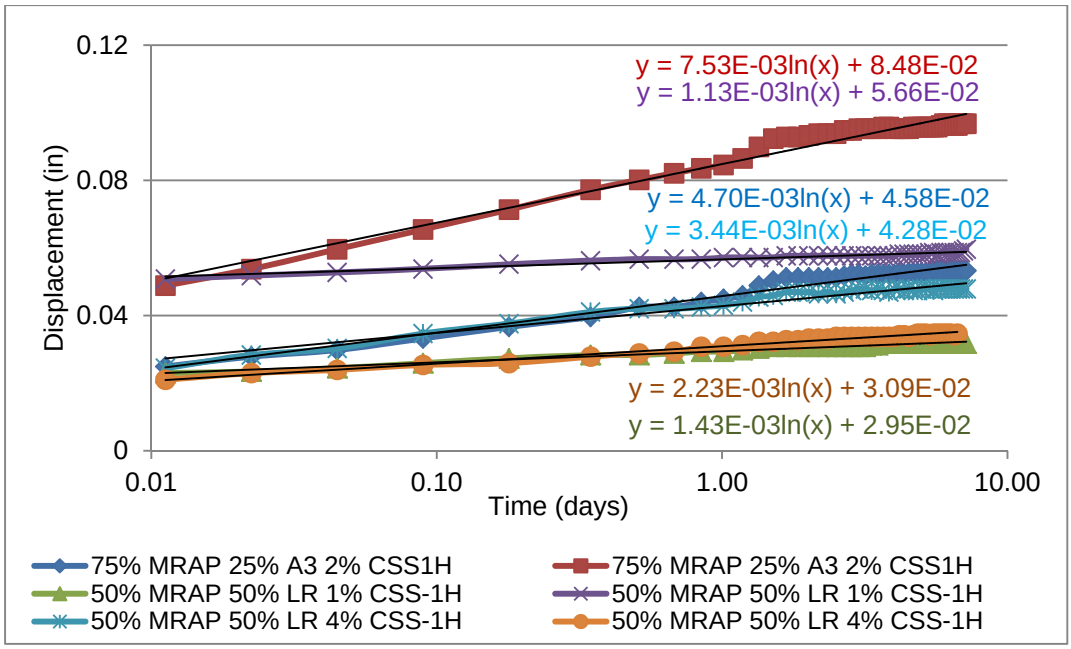

Figure C-209: Trial 5: 75% MRAP/25% A-3 2% CSS-1H, 50% MRAP/50% LR CSS-1H Log(time)

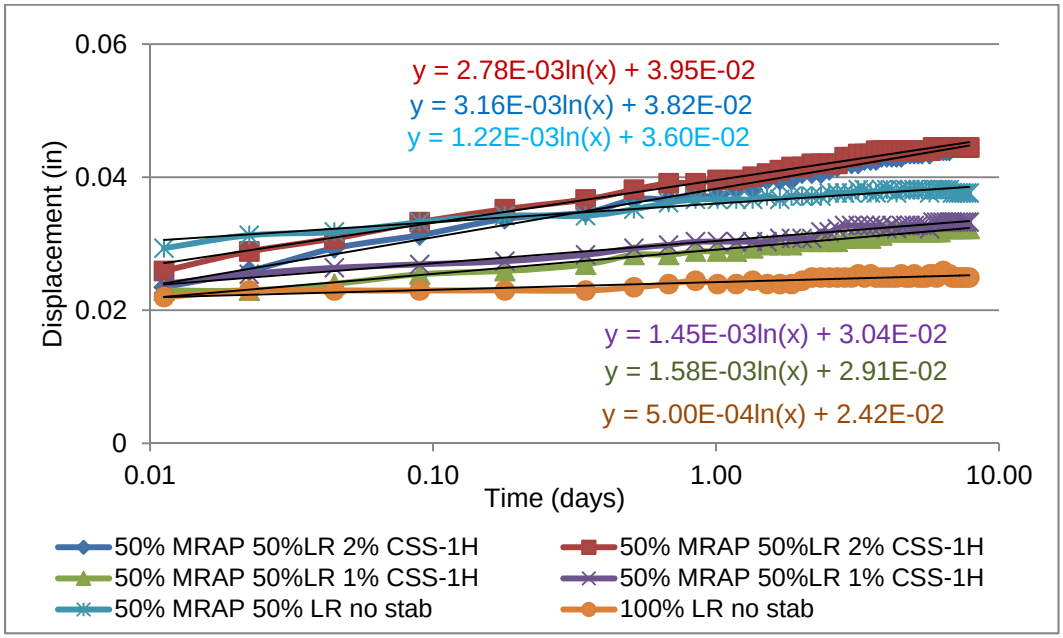

Figure C-210: Trial 7: 50% MRAP/50% LR 0%, 1%, 2% CSS-1H Log(time)

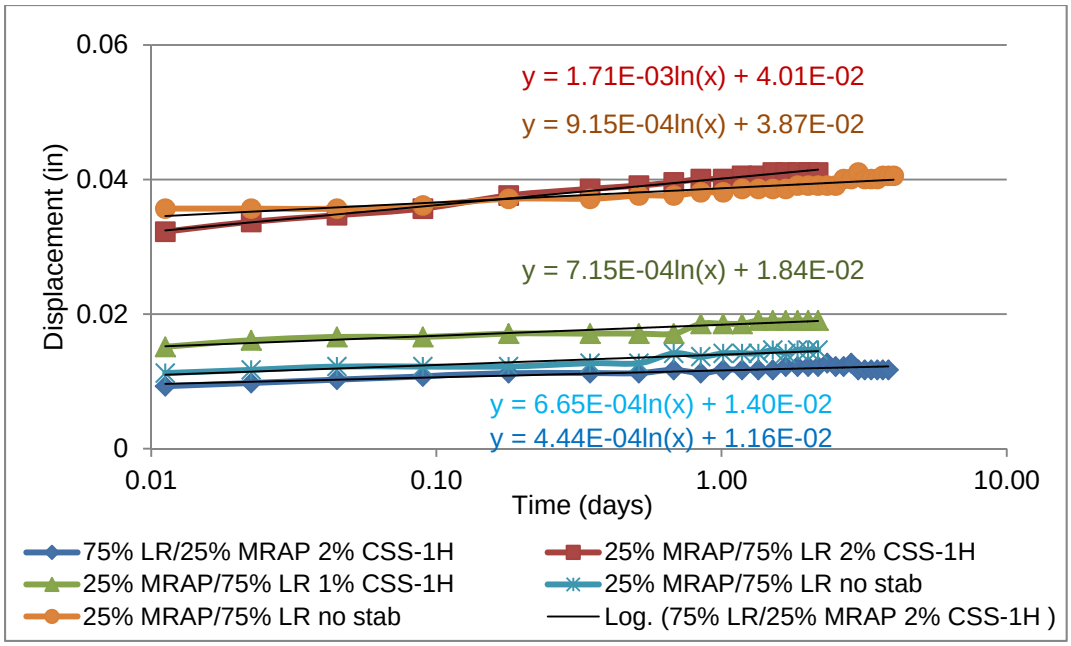

Figure C-211: Trial 8: 25% MRAP/75% Limerock 1%, 2% CSS-1H Log(time)

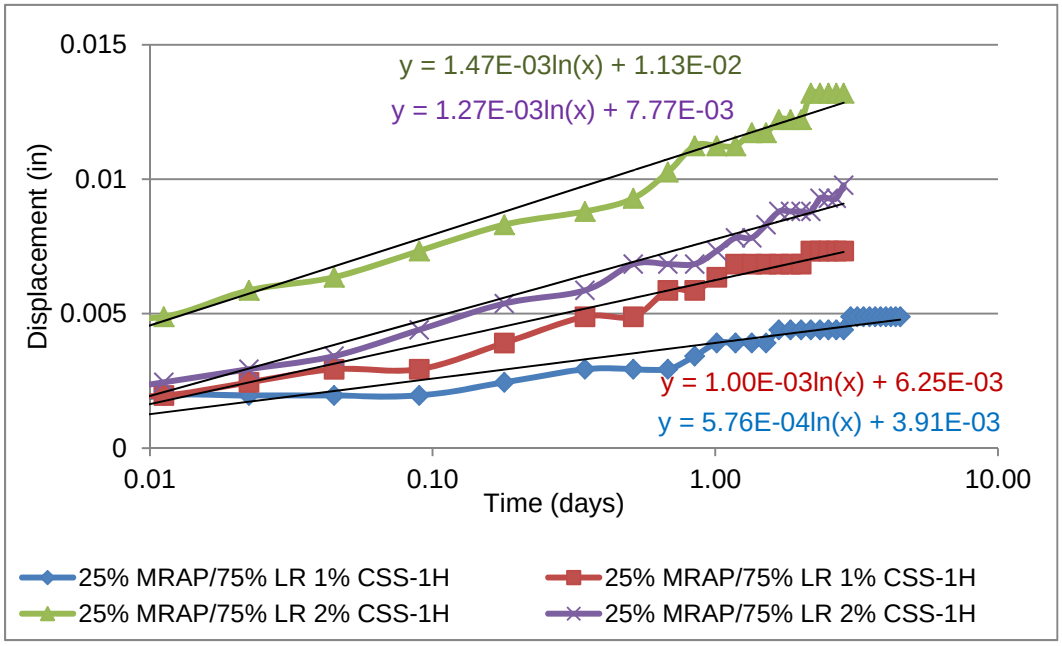

Figure C-212: Trial 9: 25% MRAP/75% Limerock 1%, 2% CSS-1H Log(time)

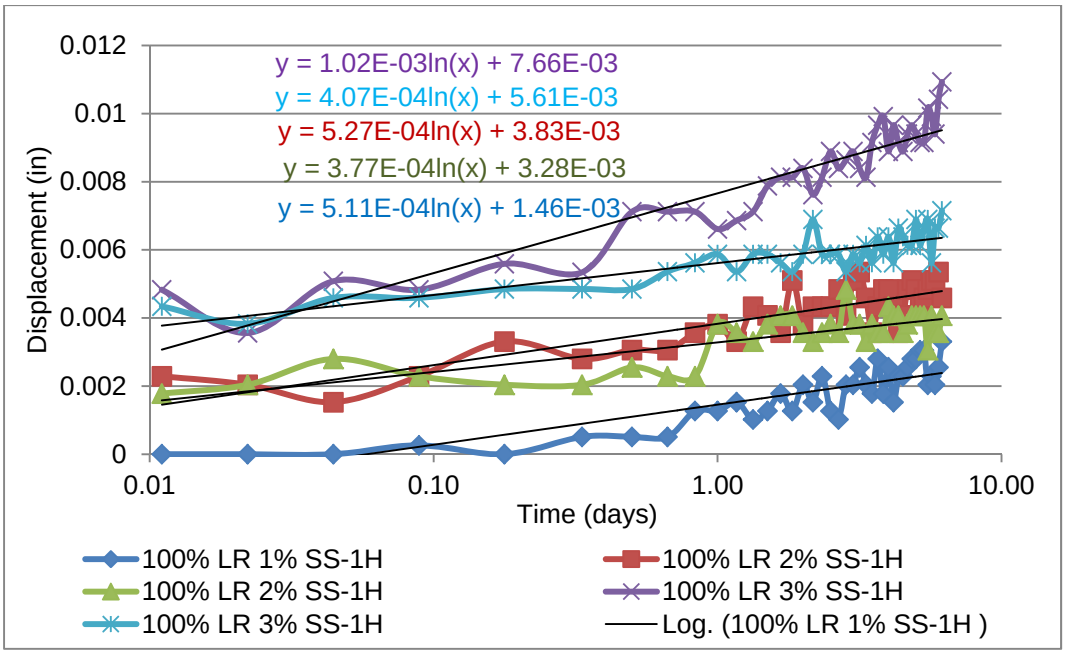

Figure C-213: Trial 10: 100% LR 1%, 2% SS-1H Log(time)

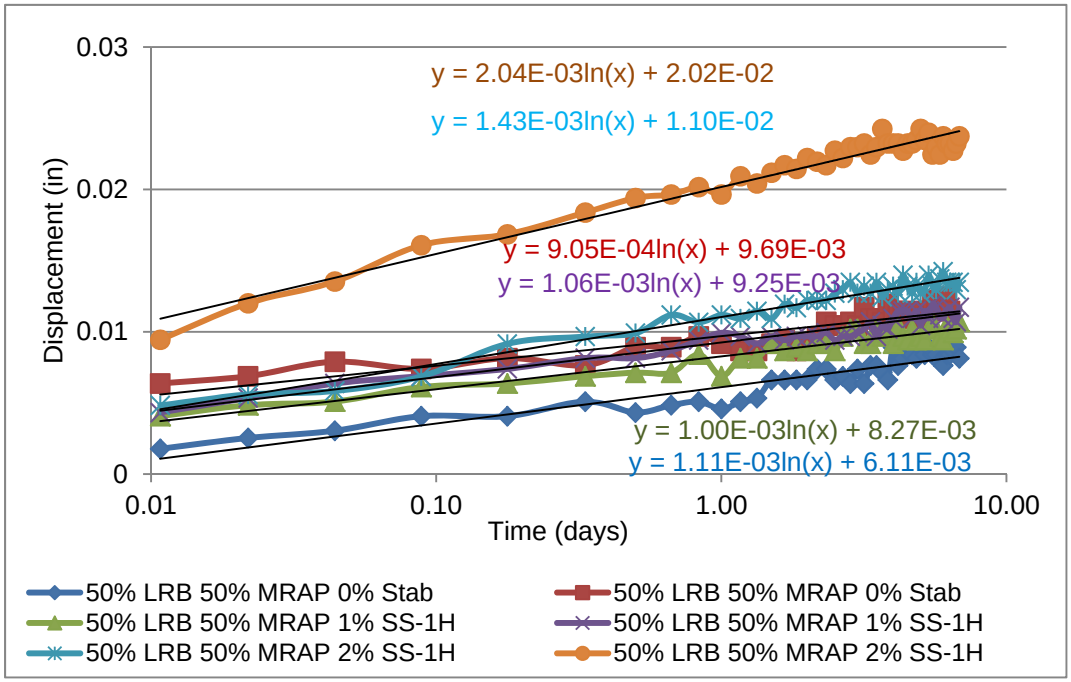

Figure C-214: Trial 11: 50% MRAP/50% LR 0%, 1%, 2% SS-1H Log(time)

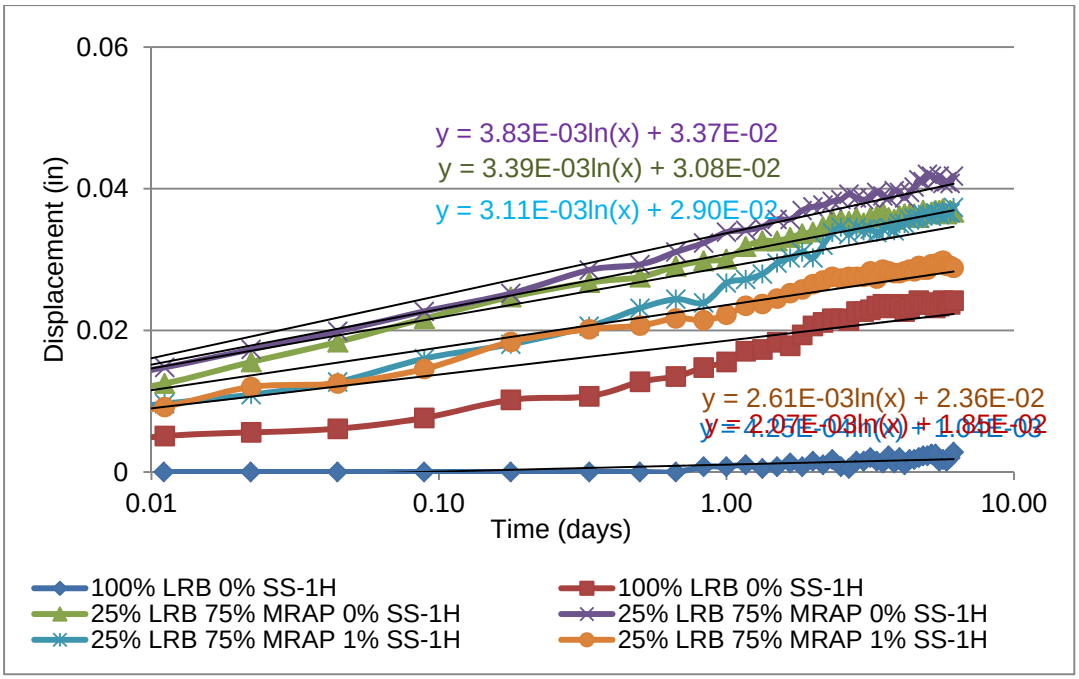

Figure C-215: Trial 12: 75% MRAP/25% LR 0%, 1% SS-1H Log(time)

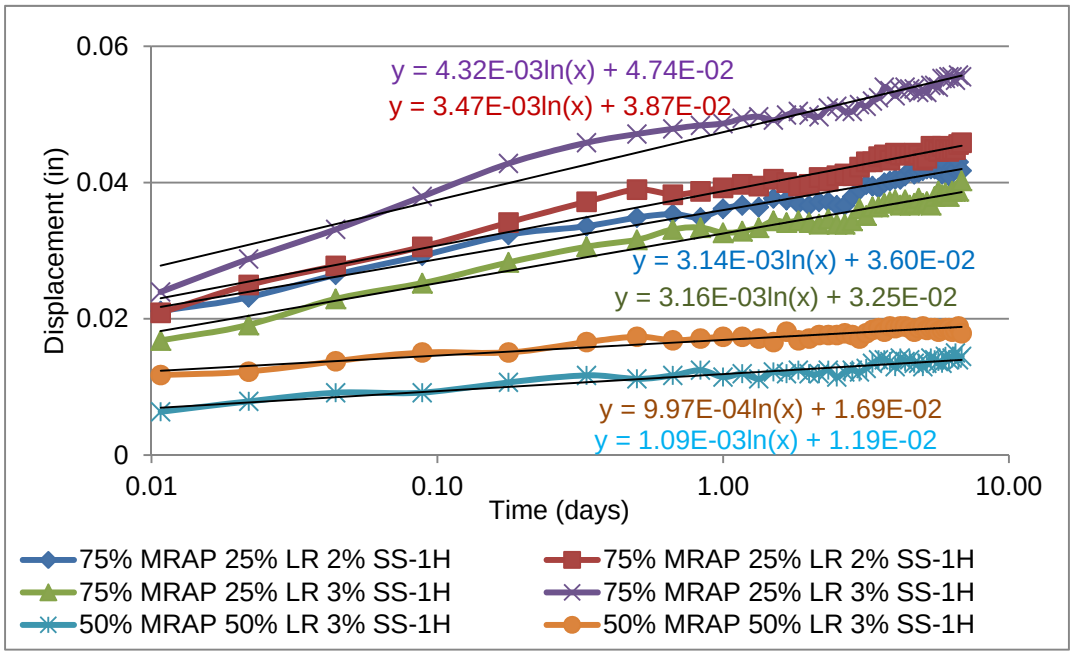

Figure C-216: Trial 13: 75% MRAP/25% LR 2%, 3% SS-1H Log(time)

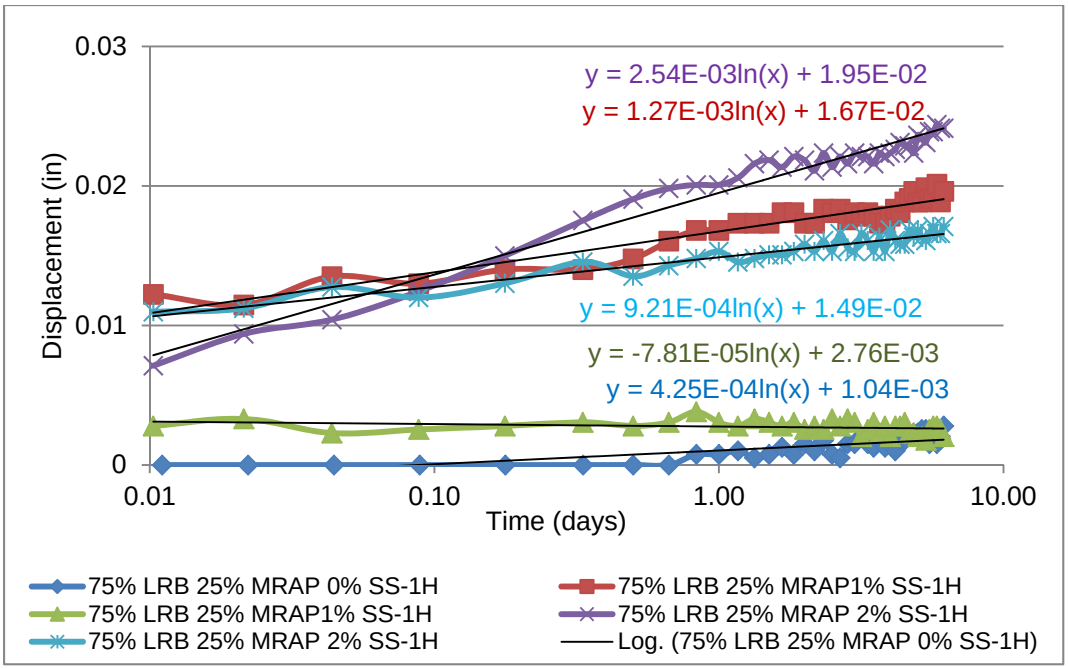

Figure C-217: Trial 14: 75% MRAP/25% LR 0%, 1%, 2% SS-1H Log(time)

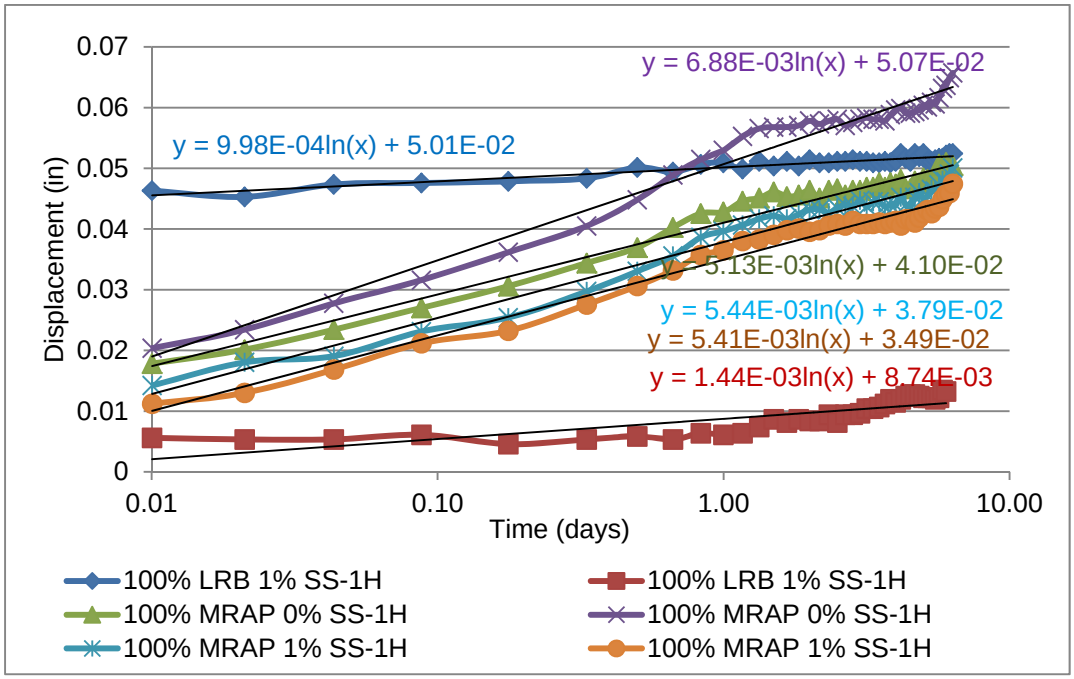

Figure C-218: Trial 15: 100% MRAP and 100% LR 0%, 1%,SS-1H Log(time)

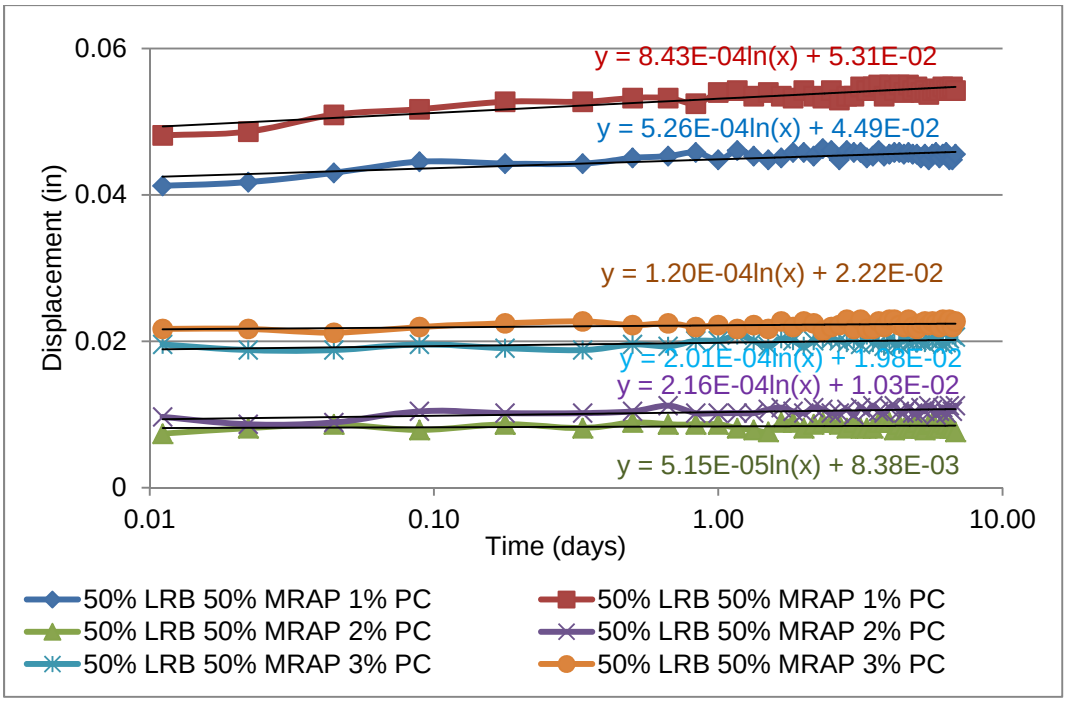

Figure C-219: Trial 16: 50% MRAP/50% Limerock 1%, 2%, 3% Cement Log(time)

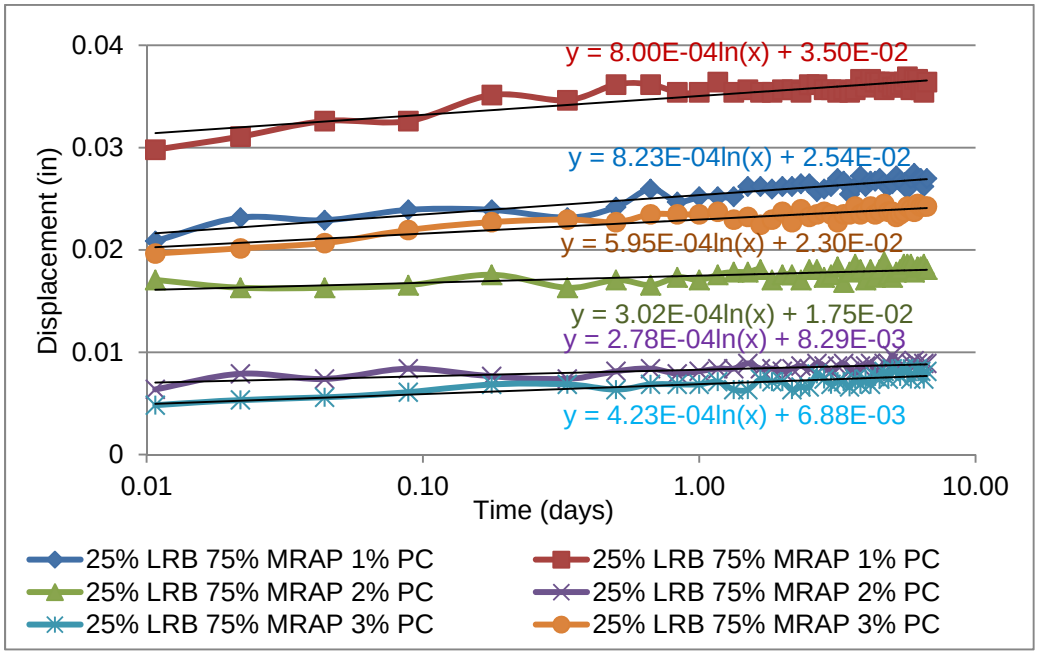

Figure C-220: Trial 17: 75% MRAP/25% Limerock 1%, 2%, 3% Cement Log(time)

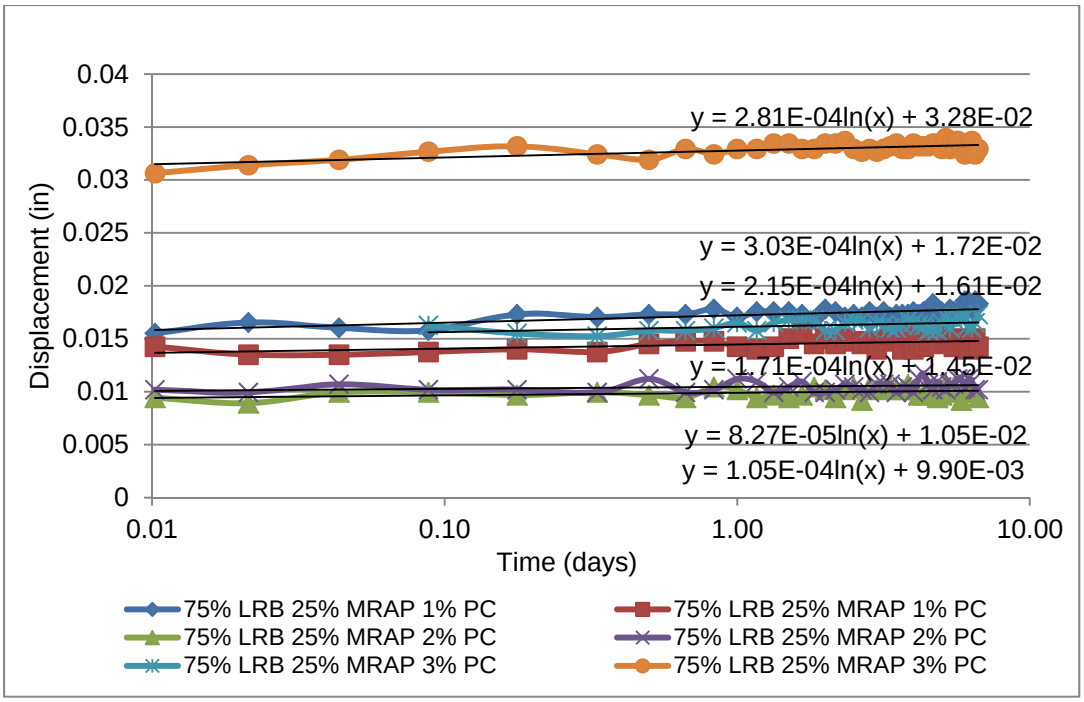

Figure C-221: Trial 18: 25% MRAP/75% Limerock 1%, 2%, 3% Cement Log(time)

Appendix D - Unconfined Creep Data

D.1. Unconfined Creep Tests Tabular Data

Table D-1: Unconfined Creep Test Tabular Data

Trial Set	% MRAP	% Stab	Moisture Content	Dry Density (pcf)	CSR (in/in/ Log (time)	Average CSR
02	100%	0%	7.9%	111.5	4.26×10^{-3}	3.7×10^{-3}
02	100%	0%	7.9%	114.0	3.52×10^{-3}	
02	100%	0%	7.9%	112.4	3.39×10^{-3}	
2G	100%	0%	7.7%	112.5	2.05×10^{-3}	2.2×10^{-3}
2G	100%	0%	7.7%	112.5	2.67×10^{-3}	
2G	100%	0%	7.7%	112.5	1.87×10^{-3}	
10	50%	1% PC	8.2%	124.5	1.00×10^{-4}	7.7×10^{-5}
10	50%	1% PC	8.2%	122.8	3.79×10^{-5}	
10	50%	1% PC	8.2%	124.8	9.24×10^{-5}	
10G	50%	1% PC	8.2%	124.1	1.28×10^{-4}	1.7×10+00
10G	50%	1% PC	8.2%	124.1	1.67×10^{-4}	
10G	50%	1% PC	8.2%	124.1	1.92×10^{-4}	
23	50%	0%	8.3%	125.2	2.73×10^{-4}	2.4×10^{-4}
23	50%	0%	8.3%	125.5	1.83×10^{-4}	
23	50%	0%	8.3%	124.1	2.73×10^{-4}	
23G	50%	0%	6.5%	127.0	1.78×10^{-4}	1.4×10^{-4}
23G	50%	0%	6.5%	127.0	1.57×10^{-4}	
23G	50%	0%	6.5%	127.0	8.99×10^{-5}	
01	0%	0%	7.5%	129.8	7.03×10^{-5}	9.9×10^{-5}
01	0%	0%	7.5%	129.8	5.02×10^{-5}	
01	0%	0%	7.5%	131.2	1.77×10^{-4}	
01G	0%	0%	7.60%	130.1	1.55×10^{-4}	1.1×10^{-4}
01G	0%	0%	7.60%	130.1	9.55×10^{-5}	
01G	0%	0%	7.60%	130.1	6.88×10^{-5}	

D.2. Unconfined Creep Tests Plots

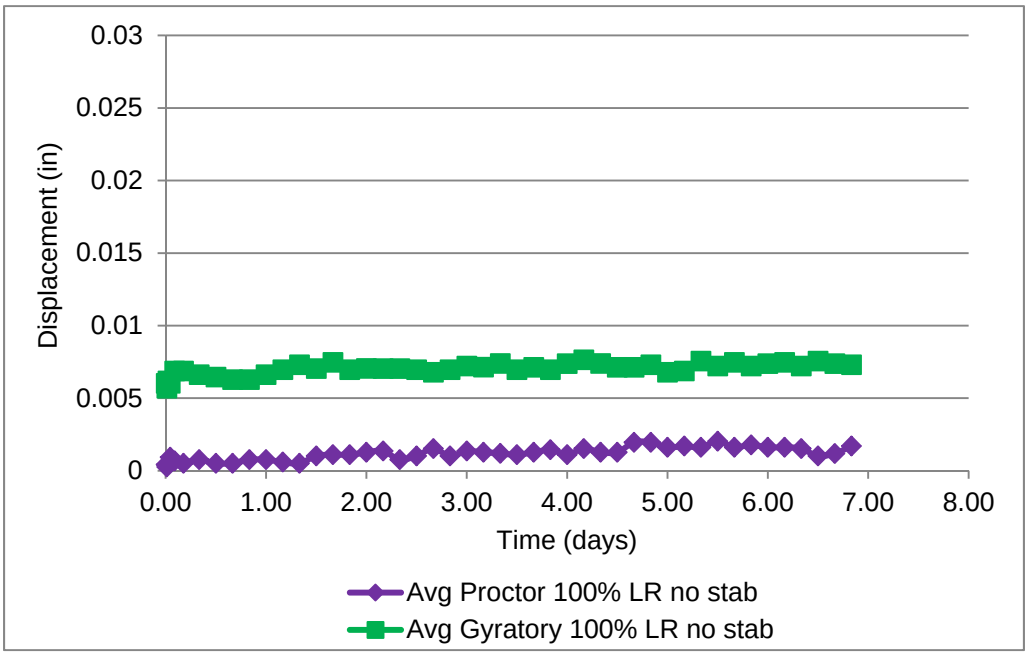

Figure D-1: Unconfined Creep 01: 100% Limerock without Stabilizer Linear Time

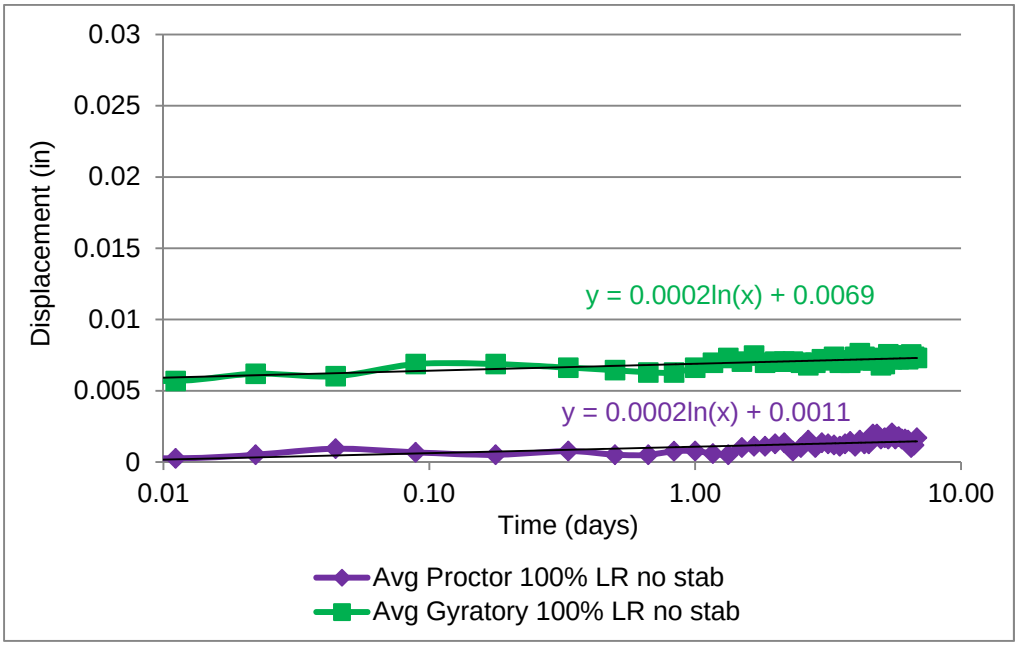

Figure D-2: Unconfined Creep 01: 100% Limerock without Stabilizer Log(time)

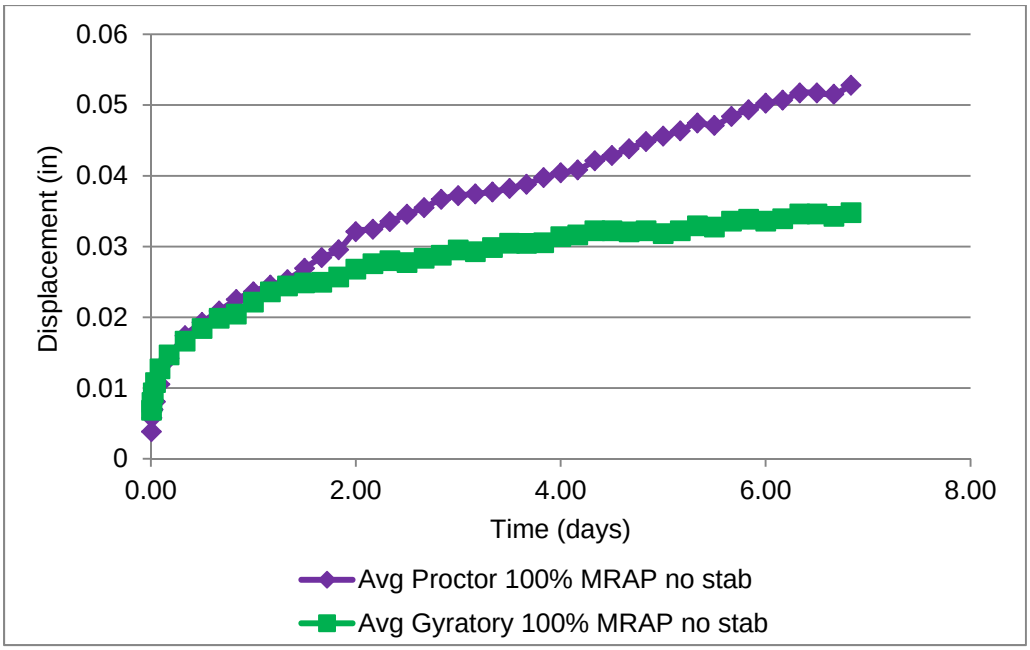

Figure D-3: Unconfined Creep 02 100% MRAP without Stabilizer Linear Time

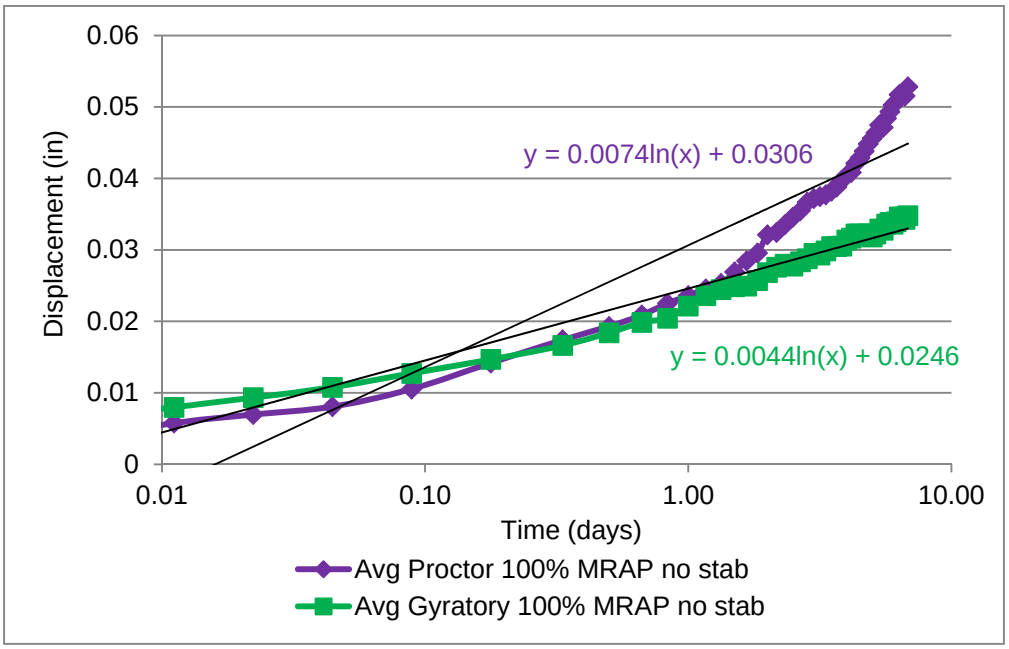

Figure D-4: Unconfined Creep 02: 100% MRAP without Stabilizer Log(time)

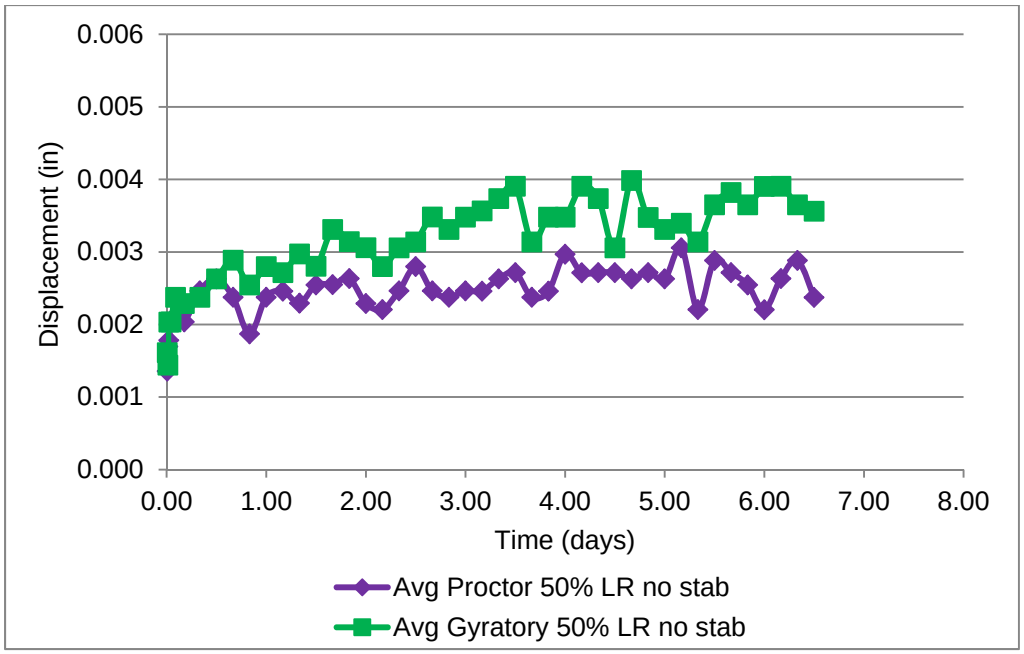

Figure D-5: Unconfined Creep 10: 50% MRAP/50% LR 1% Portland Cement Linear Time

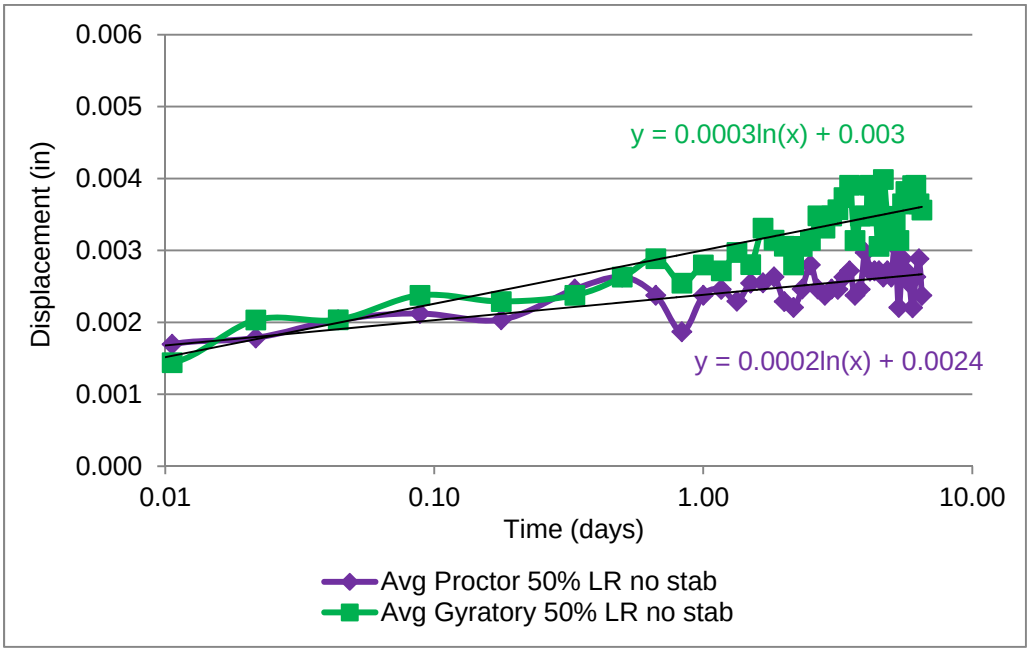

Figure D-6: Unconfined Creep 10: 50% MRAP/50% LR 1% Portland Cement Log(time)

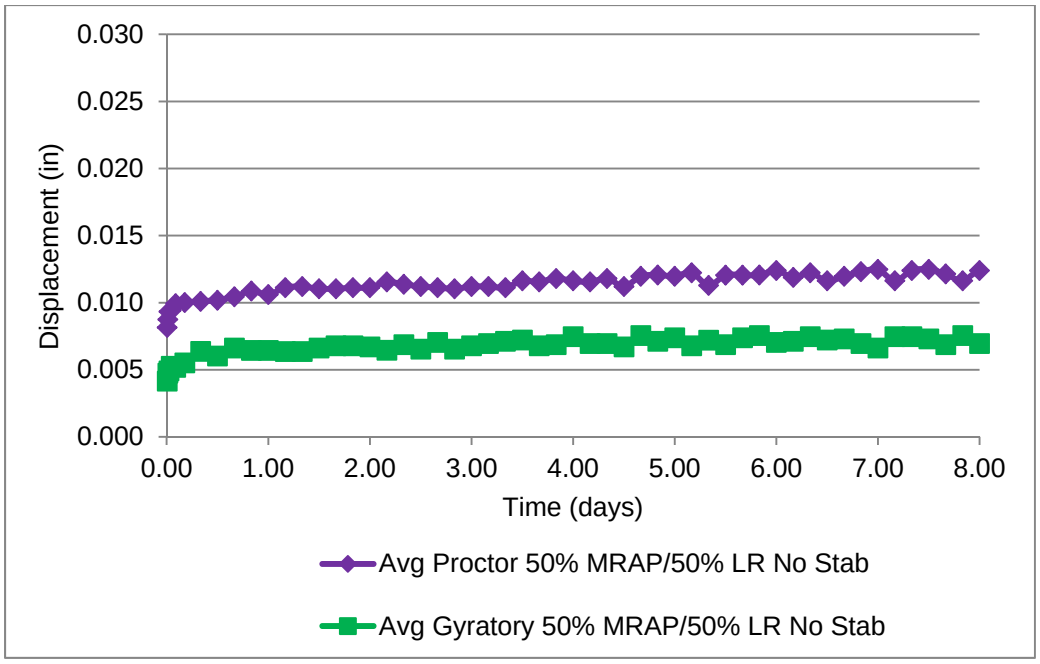

Figure D-7: Unconfined Creep 23: 50% MRAP/50% LR No Stabilizer Linear Time

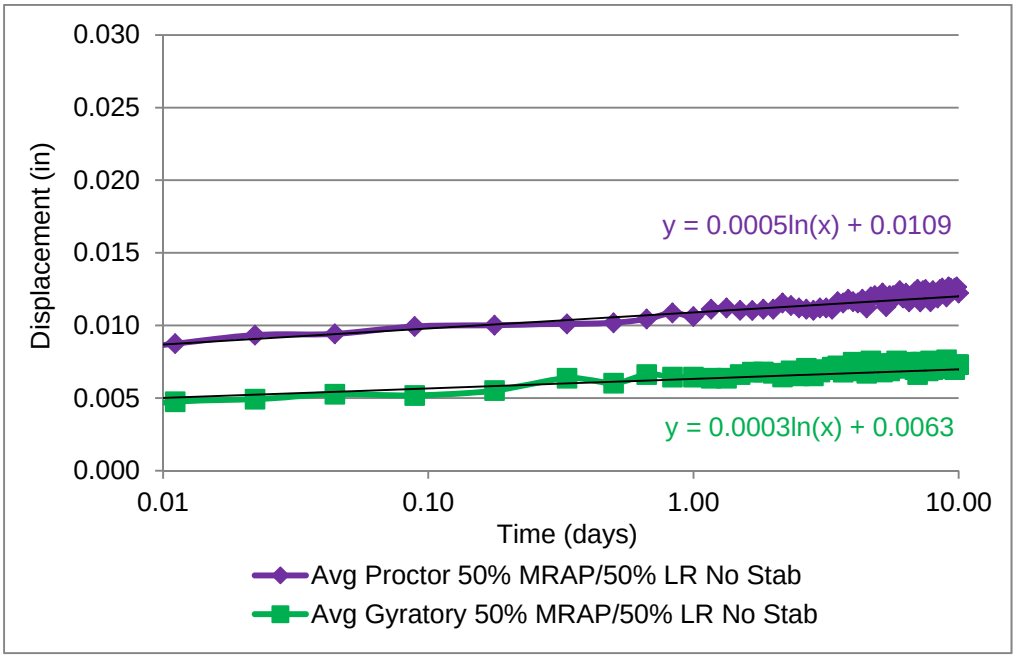

Figure D-8: Unconfined Creep 23: 50% MRAP/50% LR No Stabilizer Log(time)

Appendix E - Marshall Tests MRAP/Limerock

E.1. Marshall Tests MRAP/Limerock No Stabilizer

Note: tabular data for these control samples with no stabilizer is included in the tabular data for each of the stabilizer types following this section.

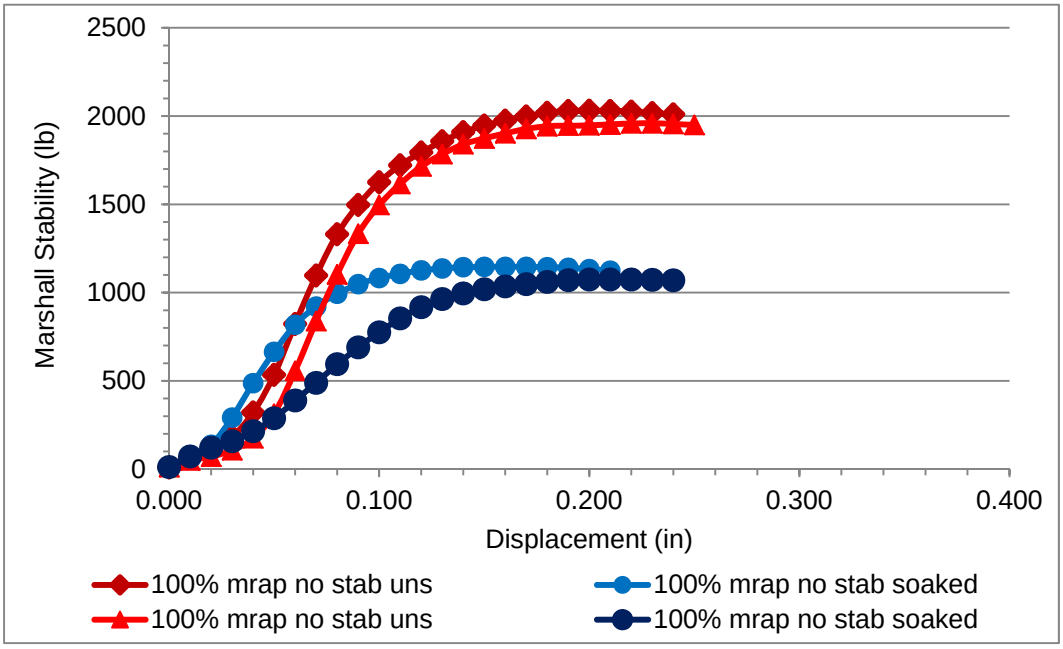

Figure E-1: Marshall Trial 27: 100% MRAP No Stabilizer

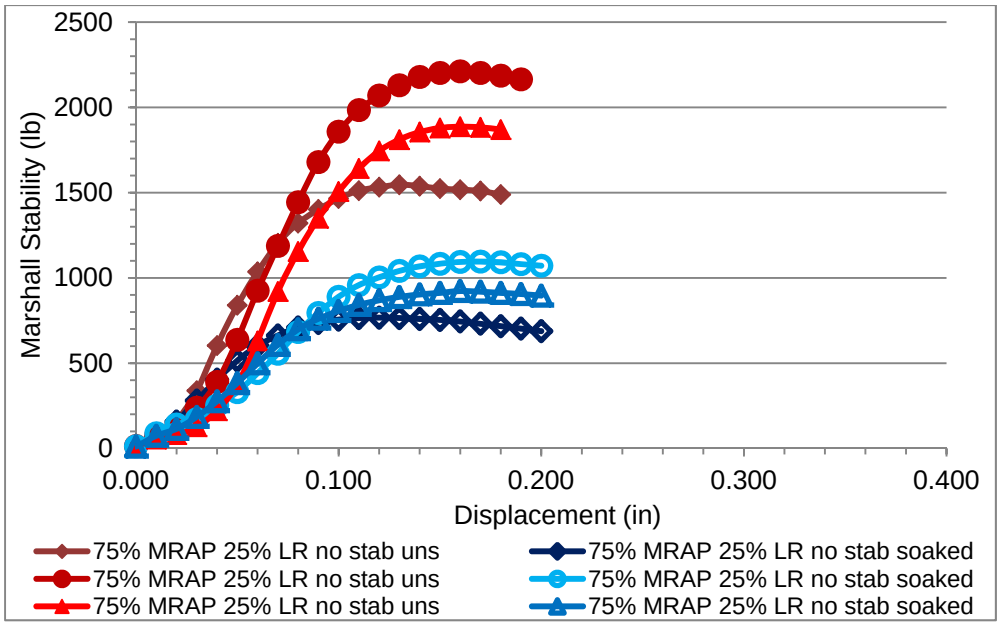

Figure E-2: Marshall Trial 16: 75% MRAP/25% Limerock No Stabilizer

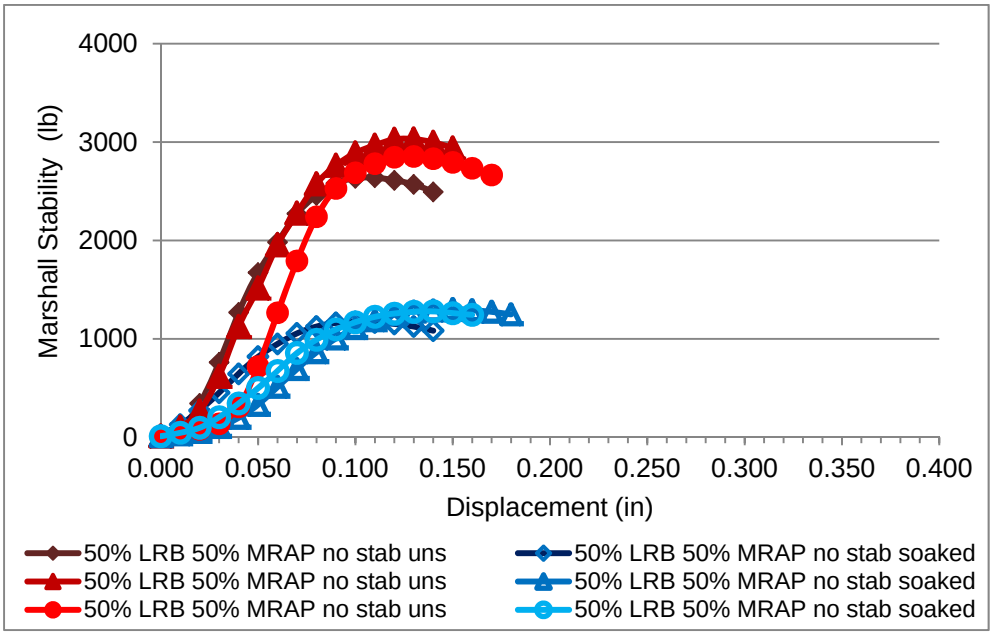

Figure E-3: Marshall Trial 23: 50% MRAP/50% Limerock No Stabilizer

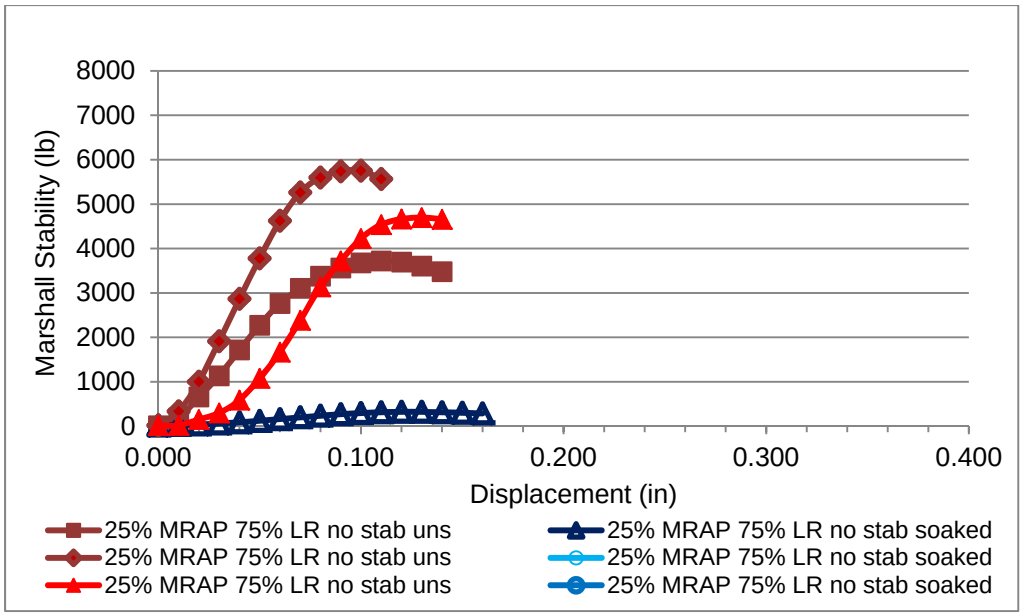

Figure E-4: Marshall Trial 23: 25% MRAP/75% Limerock No Stabilizer

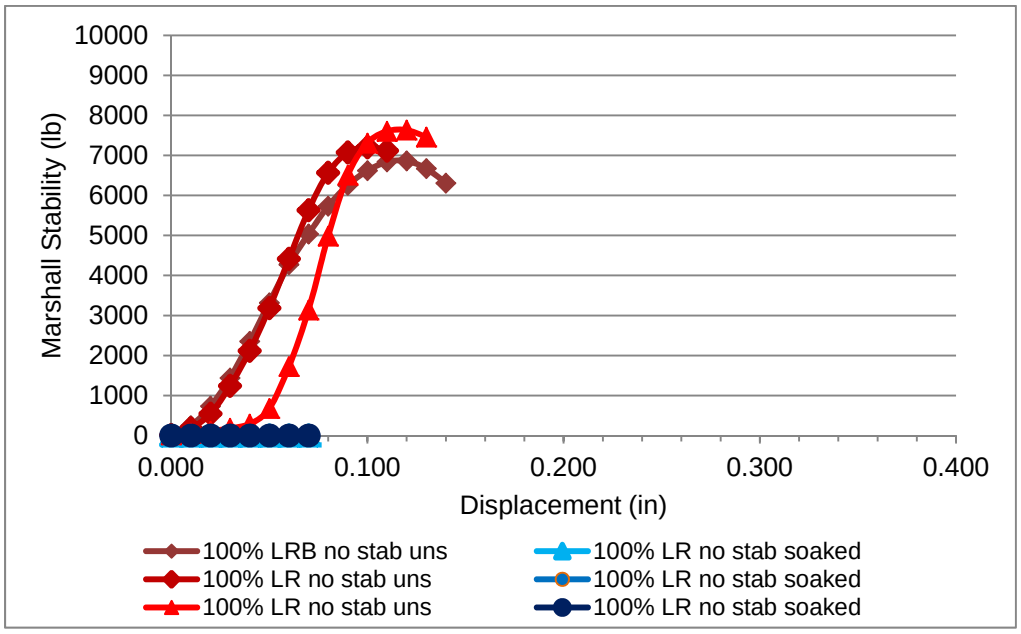

Figure E-5: Marshall Trial 26: 100% Limerock No Stabilizer

E.2. Marshall Tests MRAP/Limerock SS-1H

E.2.1. Marshall MRAP/Limerock SS-1H Compaction Data

Table E-1: Marshall MRAP/Limerock Blends with SS-1H

Trial Set	Soaked/ Unsoaked	MRAP %	% SS-1H	Moisture Content	Dry Density	Marshall Stability (lb)	Marshall Flow (.01 in)
27	Unsoaked	100%	0%	10.2%	107.1	1762	14.3
27	Soaked	100%	0%	10.2%	105.3	1035	15.7
16	Unsoaked	75%	0%	7.3%	111.2	1882	11.0
04	Unsoaked	75%	1%	7.0%	126.5	3123	13.0
05	Unsoaked	75%	2%	7.7%	120.0	2554	14.0
06	Unsoaked	75%	3%	6.3%	118.8	2354	16.0
16	Soaked	75%	0%	7.3%	110.1	928	11.0
04	Soaked	75%	1%	7.0%	124.6	2895	13.0
05	Soaked	75%	2%	7.7%	118.9	2679	14.0
06	Soaked	75%	3%	6.3%	117.9	2377	15.0
23	Unsoaked	50%	0%	7.3%	118.9	2841	9.7
01	Unsoaked	50%	1%	6.8%	120.5	3564	12.2
02	Unsoaked	50%	2%	6.2%	121.5	3272	13.0
03	Unsoaked	50%	3%	5.9%	122.9	2956	10.5
23	Soaked	50%	0%	7.3%	119.1	1252	10.5
01	Soaked	50%	1%	6.8%	120.6	2612	12.5
02	Soaked	50%	2%	6.2%	120.7	2157	11.7
03	Soaked	50%	3%	5.9%	122.4	2581	15.3
24	Unsoaked	25%	0%	8.2%	119.1	4725	10.0
07	Unsoaked	25%	1%	8.2%	124.4	5977	14.3
08	Unsoaked	25%	2%	8.0%	123.8	5154	12.7
09	Unsoaked	25%	3%	7.2%	124.0	4463	15.0
24	Soaked	25%	0%	8.2%	121	107	12.0
07	Soaked	25%	1%	8.1%	124.5	3447	14.0
08	Soaked	25%	2%	7.8%	123.2	3698	15.0
09	Soaked	25%	3%	7.2%	125.2	3593	17.0
26	Unsoaked	0%	0%	9.5%	126.4	6863	10.5
26	Soaked	0%	0%	9.5%	123.4	0	0.0

E.2.2. Marshall MRAP/Limerock SS-1H Plots

E.2.2.1. Marshall 75% MRAP/25% Limerock SS-1H Plots

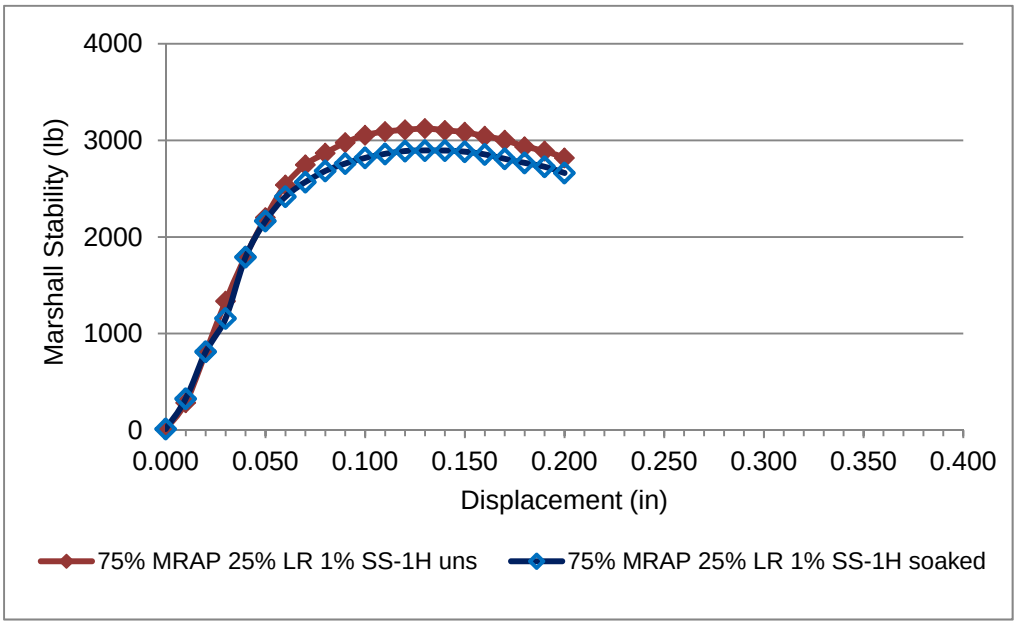

Figure E-6: Marshall Trial 04: 75% MRAP/25% Limerock 1% SS-1H

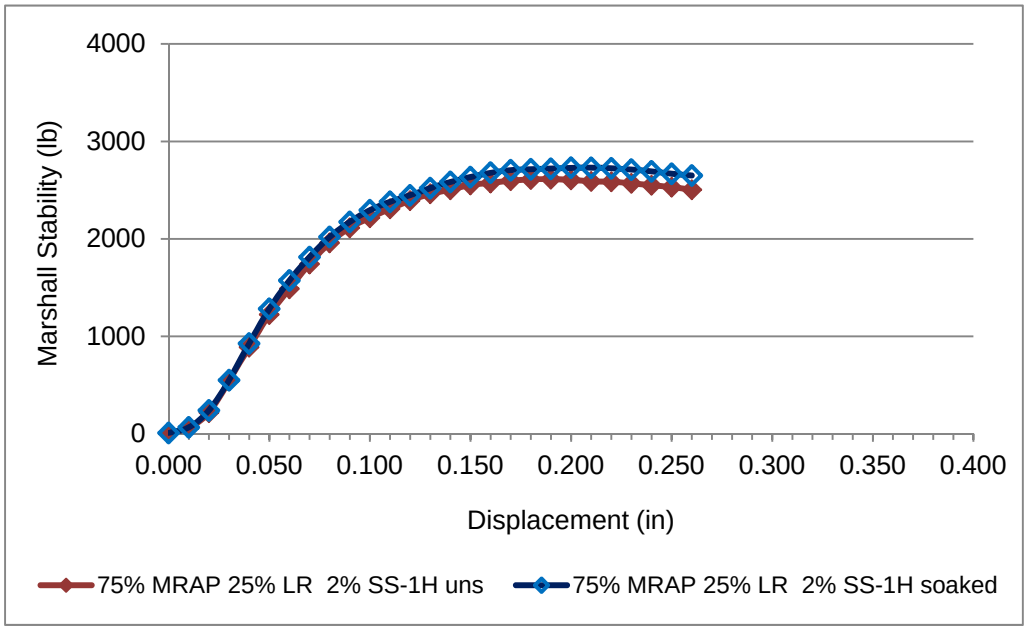

Figure E-7: Marshall Trial 05: 75% MRAP/25% Limerock 2% SS-1H

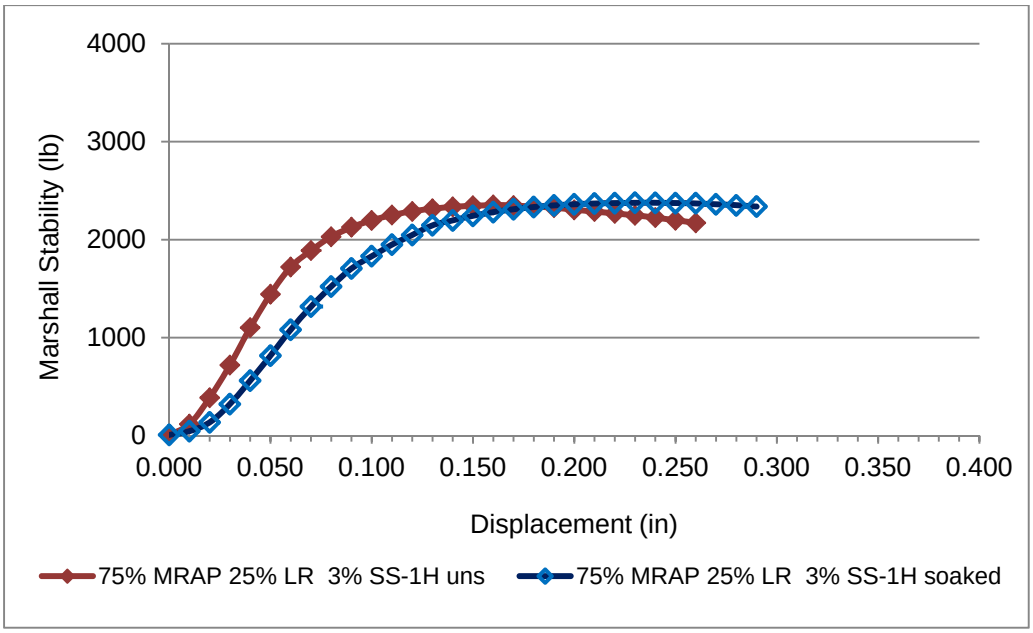

Figure E-8: Marshall Trial 06: 75% MRAP/25% Limerock 3% SS-1H

E.2.2.2. Marshall 50% MRAP/50% Limerock SS-1H Plots

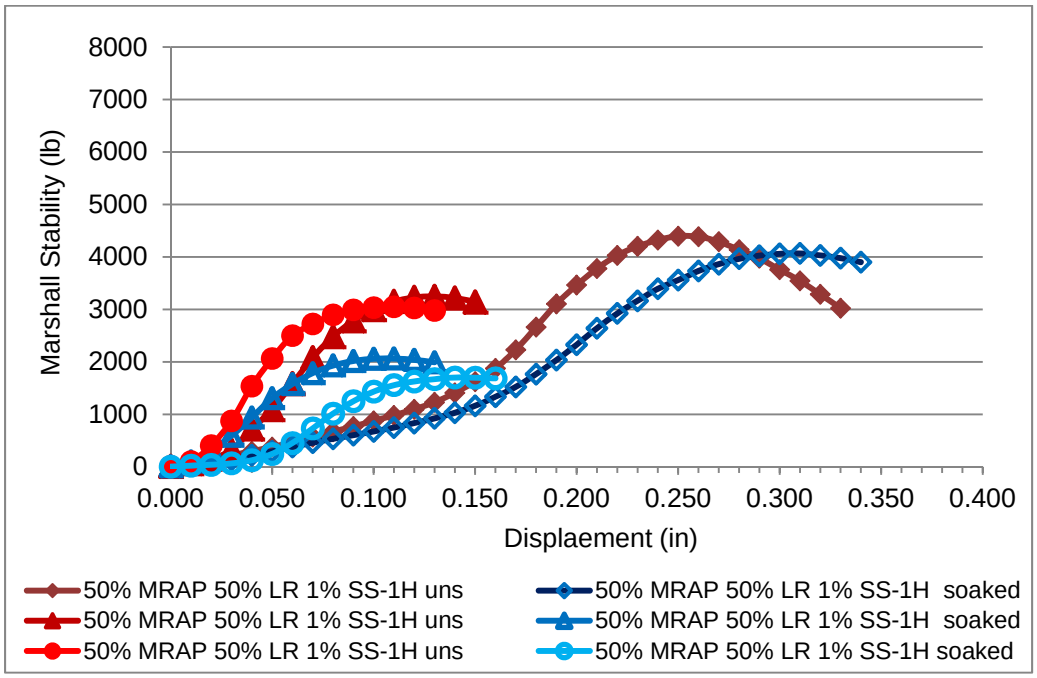

Figure E-9: Marshall Trial 01: 50% MRAP/50% Limerock 1% SS-1H

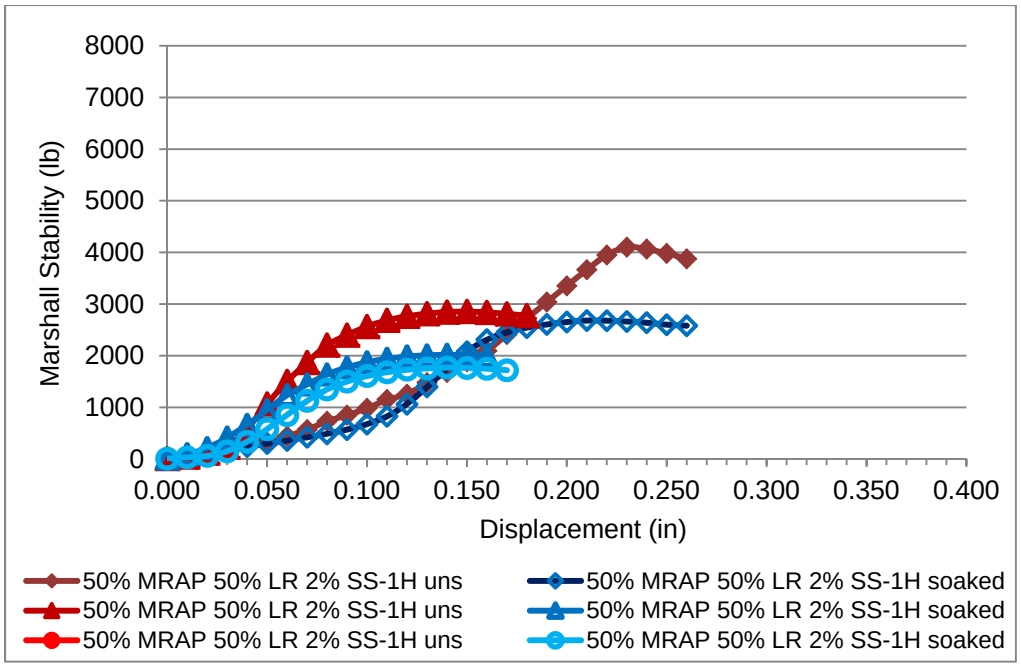

Figure E-10: Marshall Trial 02: 50% MRAP/50% Limerock 2% SS-1H

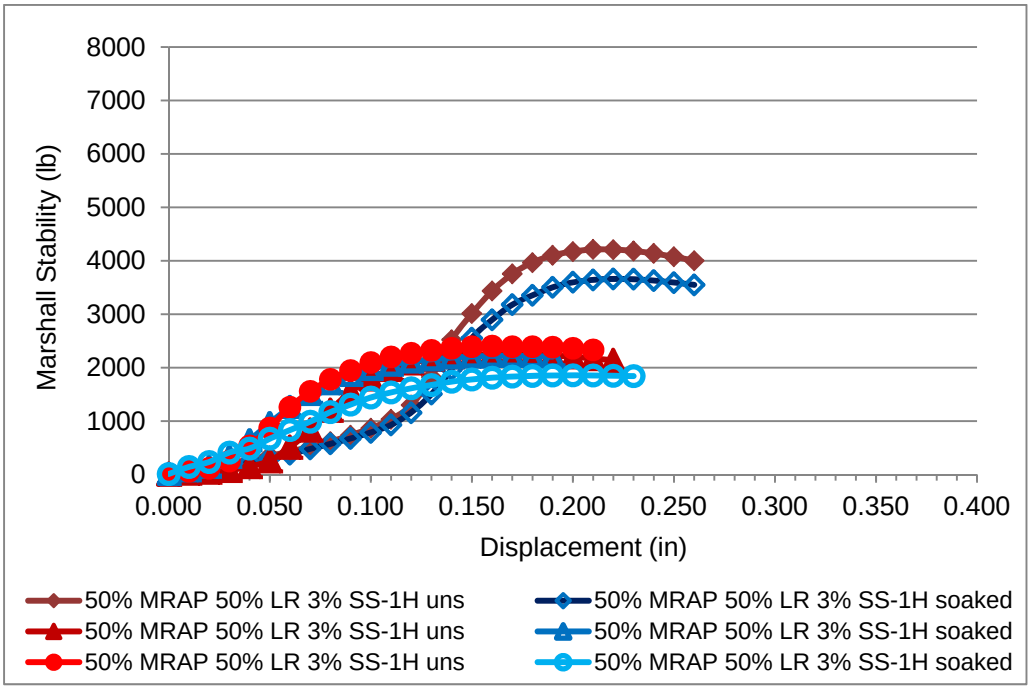

Figure E-11: Marshall Trial 03: 50% MRAP/50% Limerock 3% SS-1H

E.2.2.3. Marshall 25% MRAP/75% LR SS-1H Plots

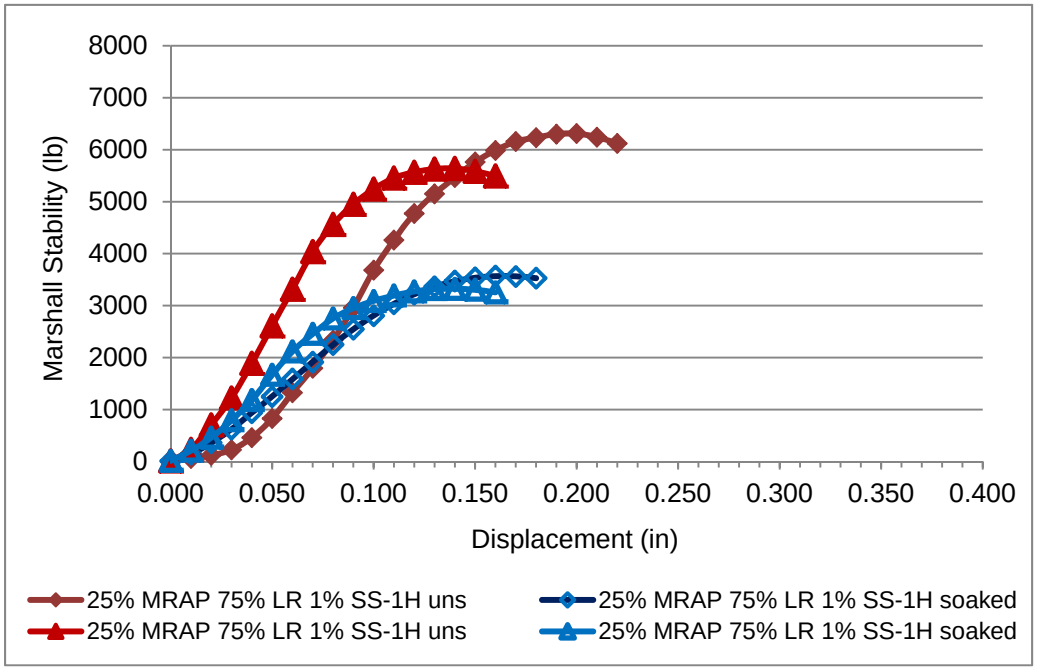

Figure E-12: Marshall Trial 07: 25% MRAP/75% Limerock 1% SS-1H

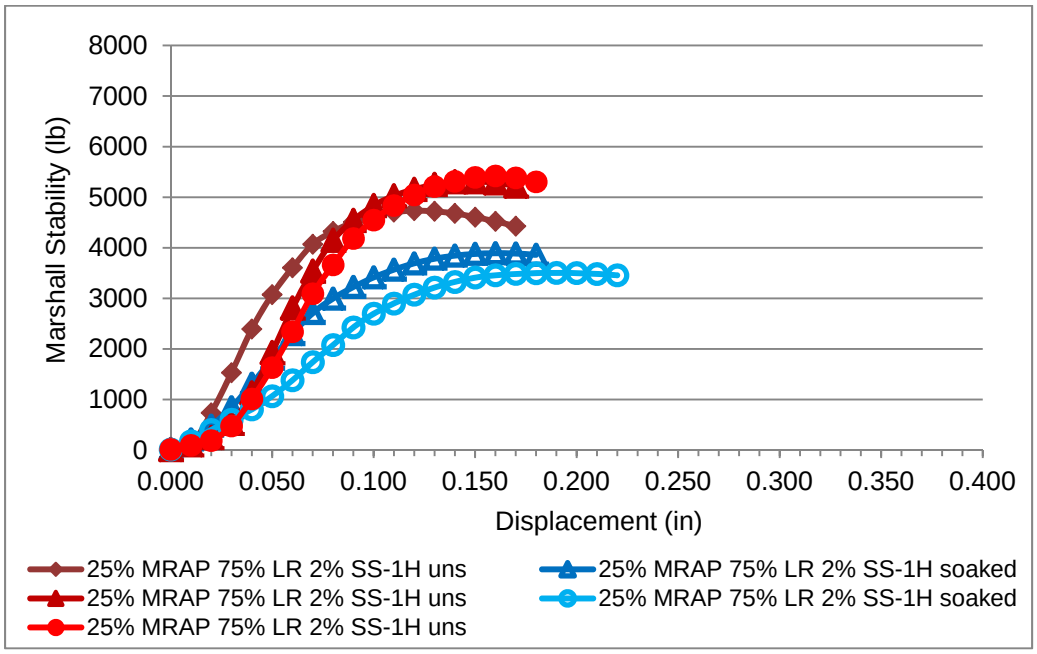

Figure E-13: Marshall Trial 08: 25% MRAP/75% Limerock 2% SS-1H

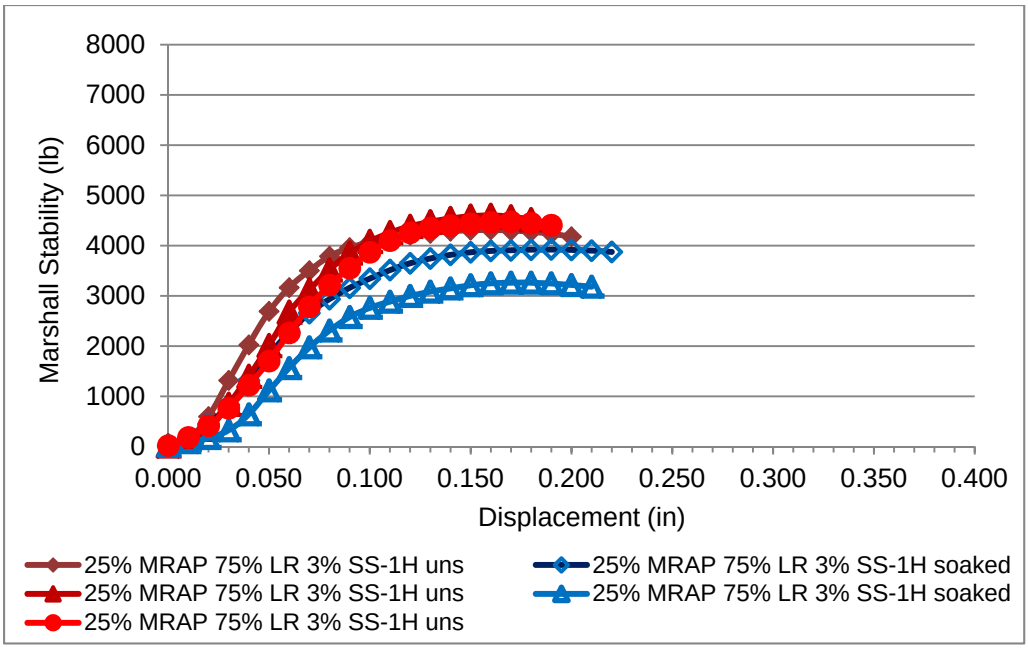

Figure E-14: Marshall Trial 09: 25% MRAP/75% Limerock 3% SS-1H

E.3. Marshall Tests MRAP/Limerock CSS-1H

E.3.1. Marshall MRAP/Limerock CSS-1HF Compaction Data

Trial set	Soaked/ Unsoaked	MRAP %	% CSS-1HF	Moisture Content	Dry Density	Marshall Stability (lb)	Marshall Flow (.01 in)
27	Unsoaked	100%	0%	10.2%	107.1	1762	14.3
32	Unsoaked	100%	1%	10.1%	103.5	1344	19.0
33	Unsoaked	100%	2%	8.3%	107.3	1452	19.0
34	Unsoaked	100%	3%	7.7%	108.0	1657	18.0
27	Soaked	100%	0%	10.2%	105.3	1035	15.7
32	Soaked	100%	1%	10.1%	104.5	1410	15.5
33	Soaked	100%	2%	8.3%	106.6	1422	16.0
34	Soaked	100%	3%	7.7%	105.9	1404	15.0
16	Unsoaked	75%	0%	7.3%	111.2	1882	11.0
13	Unsoaked	75%	1%	7.5%	117.7	2836	14.0
14	Unsoaked	75%	2%	7.2%	112.1	1700	13.0
15	Unsoaked	75%	3%	6.1%	112.6	1457	14.0
16	Soaked	75%	0%	7.3%	110.1	928	11.0
13	Soaked	75%	1%	7.5%	114.8	2334	14.0
14	Soaked	75%	2%	7.2%	109.6	1535	13.0
15	Soaked	75%	3%	6.1%	110.0	1448	15.5
23	Unsoaked	50%	0%	7.3%	118.9	2841	9.7
17	Unsoaked	50%	1%	6.2%	118.2	3230	11.8
18	Unsoaked	50%	2%	6.1%	119.8	3586	15.5
19	Unsoaked	50%	3%	6.8%	116.4	2928	16.7
23	Soaked	50%	0%	7.3%	119.1	1252	10.5
17	Soaked	50%	1%	6.2%	116.6	2130	12.0
18	Soaked	50%	2%	6.1%	120.1	3037	16.3
19	Soaked	50%	3%	6.8%	117.2	2529	16.3
24	Unsoaked	25%	0%	8.2%	119.1	3723	10.0
20	Unsoaked	25%	1%	7.5%	123.3	5505	13.0
21	Unsoaked	25%	2%	7.5%	122.4	4697	12.0

Trial set	Soaked/ Unsoaked	MRAP %	% CSS-1HF	Moisture Content	Dry Density	Marshall Stability (lb)	Marshall Flow (.01 in)
22	Unsoaked	25%	3%	7.4%	118.9	3685	15.3
24	Soaked	25%	0%	8.2%	121.0	322	12.0
20	Soaked	25%	1%	7.5%	121.7	3435	12.0
21	Soaked	25%	2%	7.5%	120.8	3196	13.0
22	Soaked	25%	3%	7.4%	118.7	2948	14.7
26	Unsoaked	0%	0%	9.50%	126.4	6863	10.5
29	Unsoaked	0%	1%	8.00%	125.1	6426	11.5
30	Unsoaked	0%	2%	8.10%	128.1	6144	11.0
31	Unsoaked	0%	3%	8.40%	125.8	5120	11.5
26	Soaked	0%	0%	9.50%	123.4	0	N/A
29	Soaked	0%	1%	8.00%	127.9	3610	9.0
30	Soaked	0%	2%	8.10%	128.5	4012	11.0
31	Soaked	0%	3%	8.40%	123.9	3188	10.0

E.3.2. Marshall MRAP/Limerock CSS-1HF Plots

E.3.2.1. Marshall MRAP/Limerock CSS-1HF Plots 75%/25%

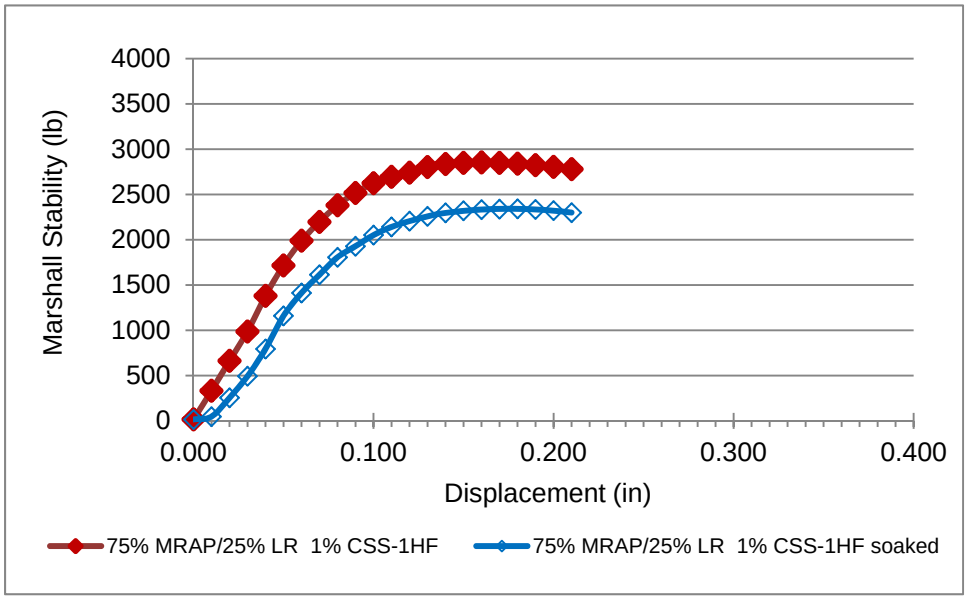

Figure E-15: Marshall Trial 13: 75% MRAP/25% Limerock 1% CSS-1HF

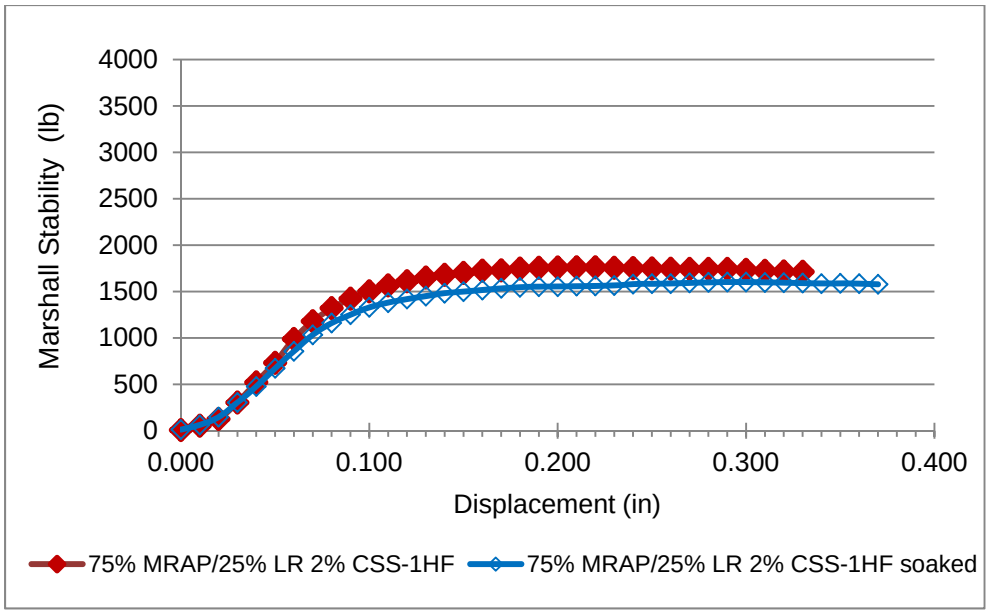

Figure E-16: Marshall Trial 14: 75% MRAP/25% Limerock 2% CSS-1HF

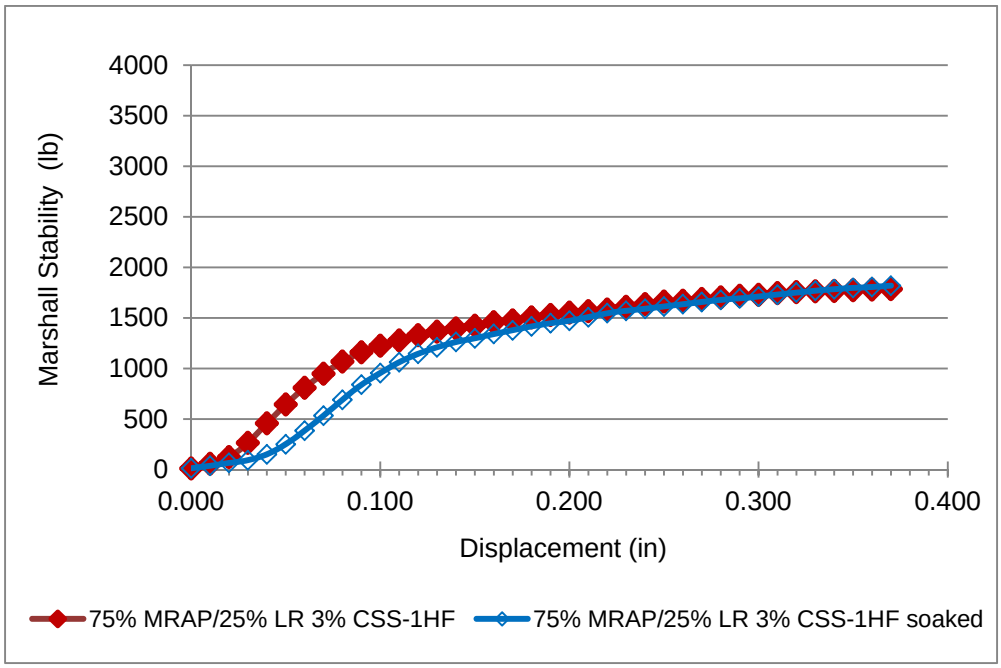

Figure E-17: Marshall Trial 15: 75% MRAP/25% Limerock 3% CSS-1HF

E.3.2.2. Marshall MRAP/Limerock CSS-1HF Plots 50%/50%

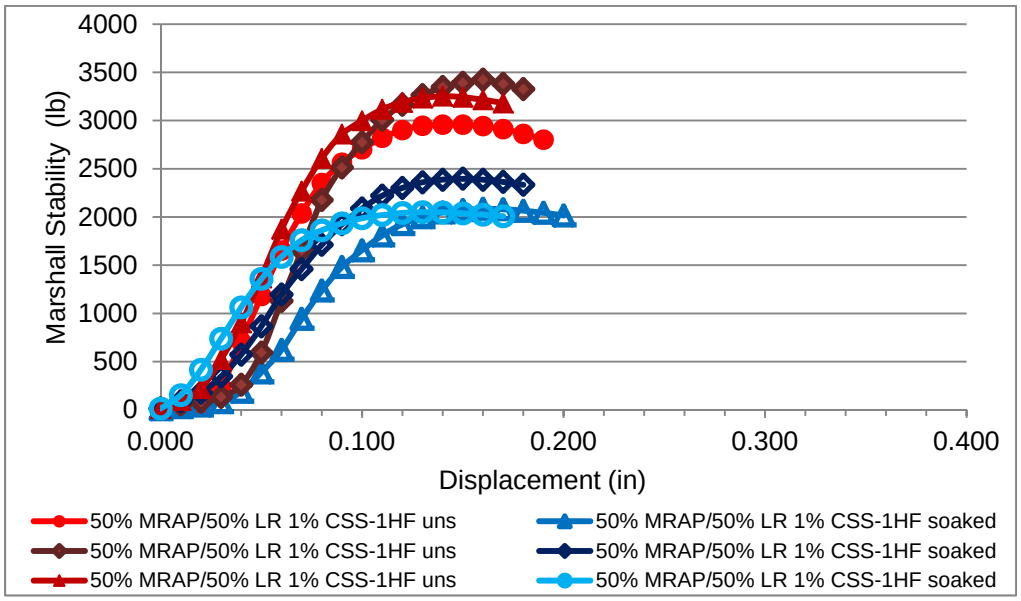

Figure E-18: Marshall Trial 17: 50% MRAP/50% LR 1% CSS-1HF

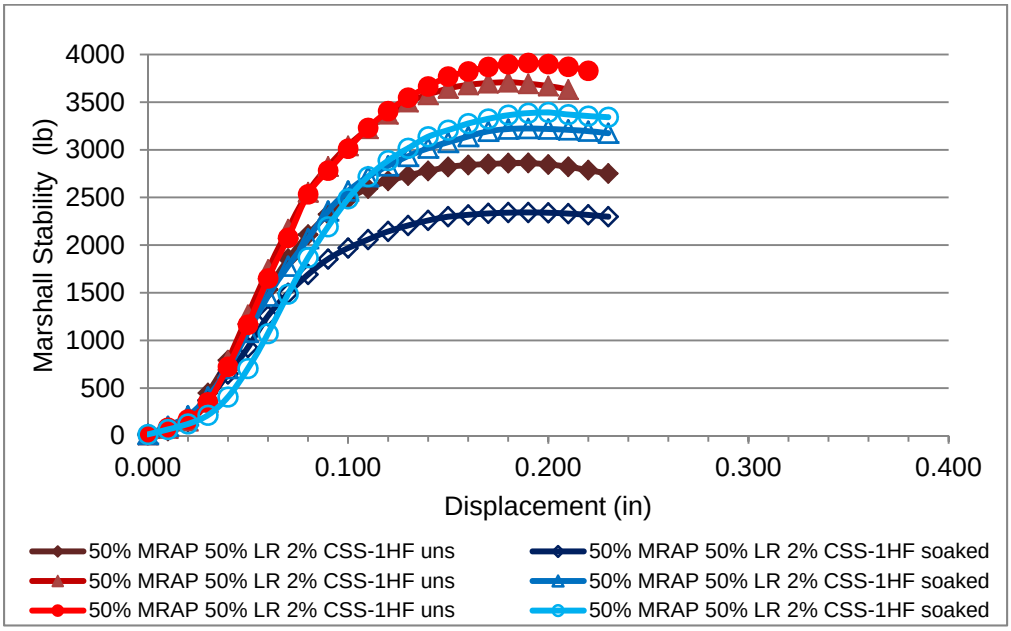

Figure E-19: Marshall Trial 18: 50% MRAP/50% LR 2% CSS-1HF

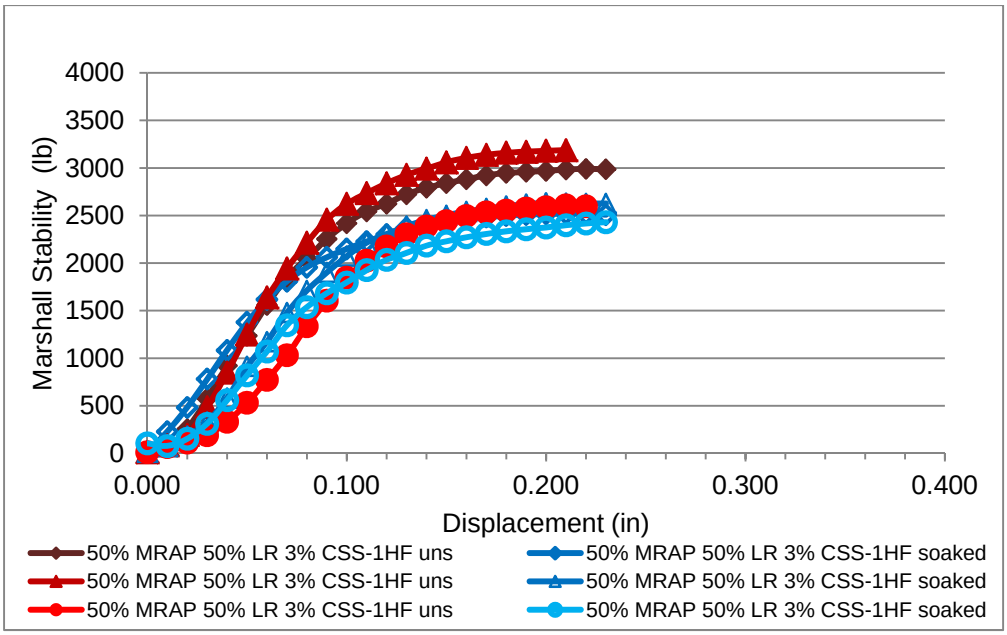

Figure E-20: Marshall Trial 19: 50% MRAP/50% LR 3% CSS-1HF

E.3.2.3. Marshall 25% MRAP/75% Limerock CSS-1HF Plots

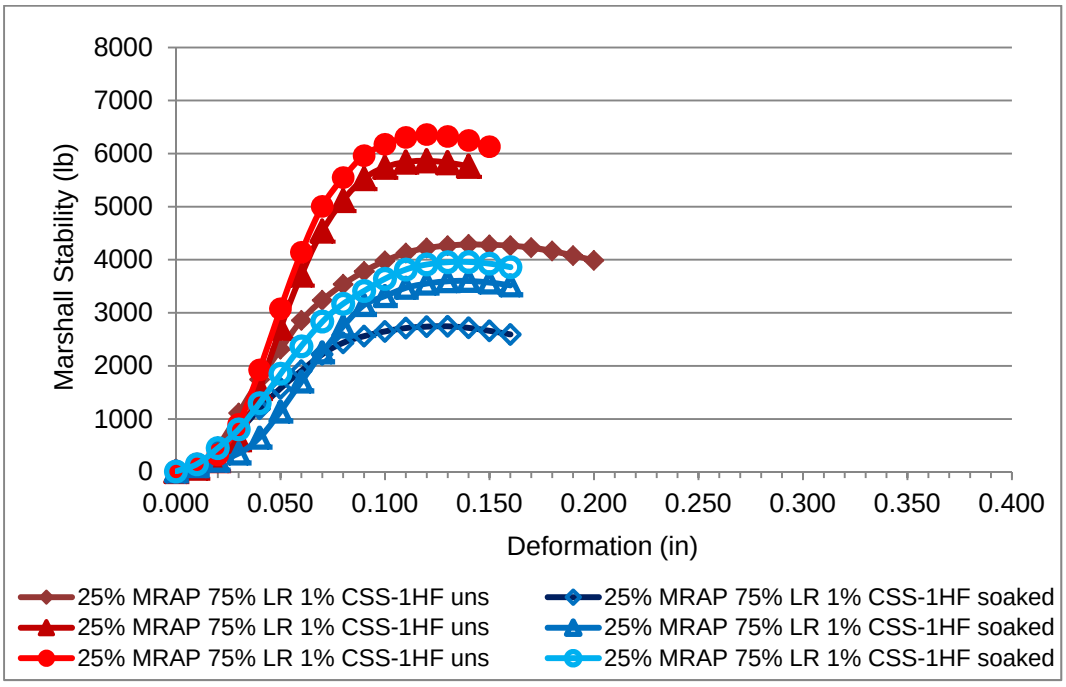

Figure E-21: Marshall Trial 20: 25% MRAP/75% Limerock 1% CSS-1HF

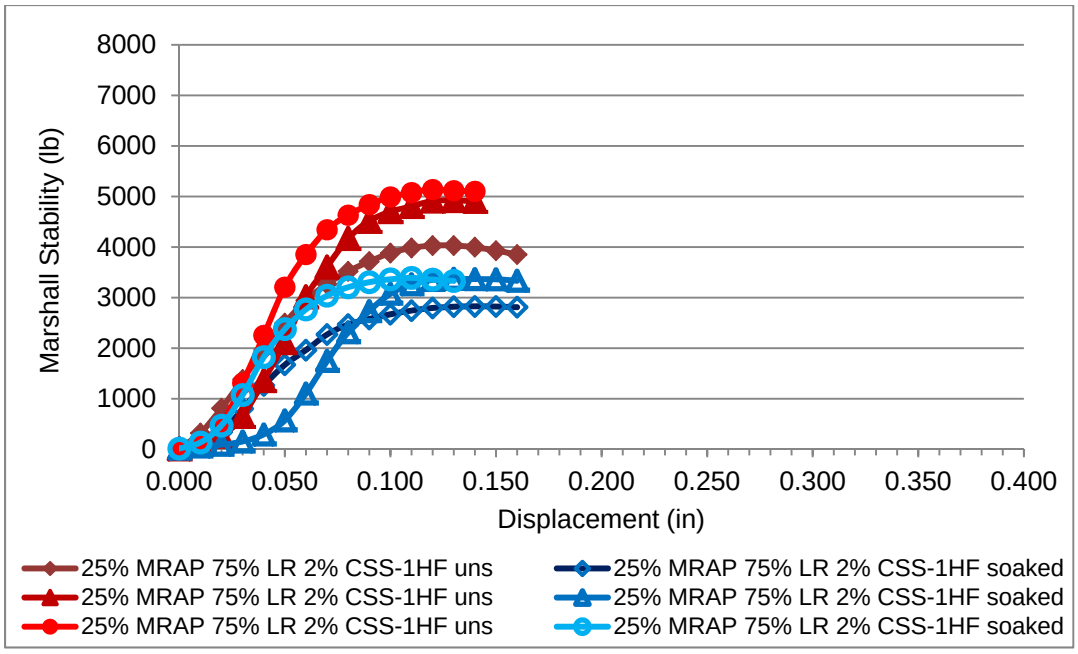

Figure E-22: Marshall Trial 21: 25% MRAP/75% Limerock 2% CSS-1HF

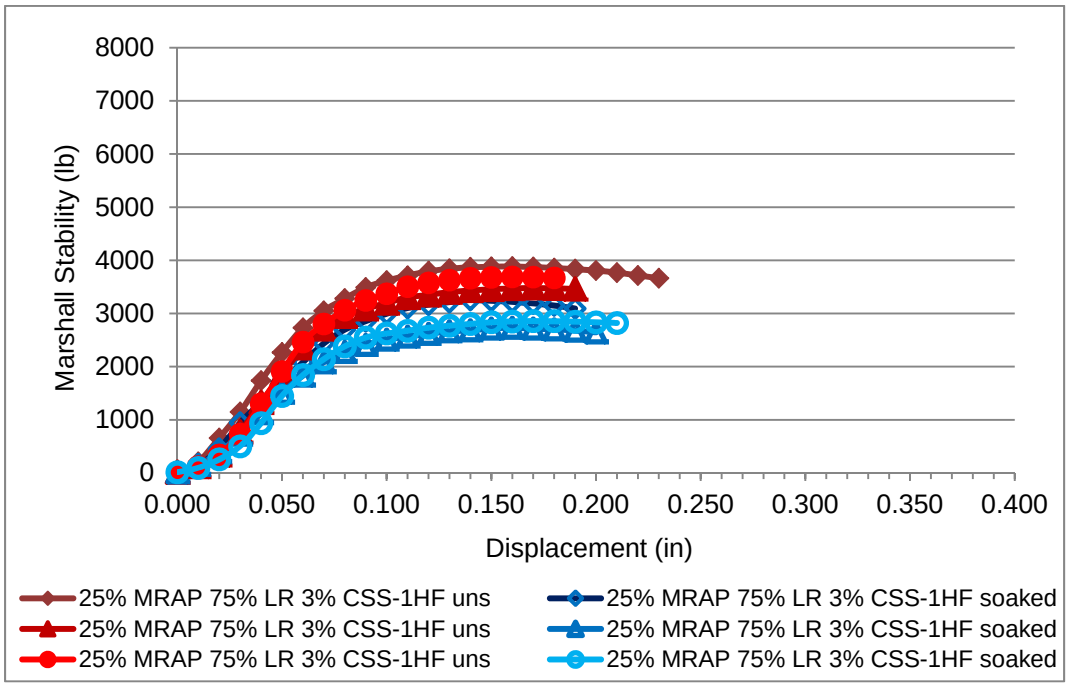

Figure E-23: Marshall Trial 22: 25% MRAP/75% Limerock 3% CSS-1HF

E.4. Marshall Tests MRAP/Limerock Portland Cement

E.4.1. Marshall MRAP/Limerock Cement Compaction Data

Table E-2: Marshall MRAP/Limerock Blends with Portland Cement

Trial Set	Soaked/ Unsoaked	MRAP %	% PC	Moisture Content	Dry Density	Marshall Stability (lb)	Marshall Flow (.01 in)
27	Unsoaked	100%	0%	10.2%	107.1	1,762	14.3
38	Unsoaked	100%	1%	8.10%	112.7	1,067	19.0
39	Unsoaked	100%	2%	9.10%	111.4	1,539	15.0
40	Unsoaked	100%	3%	8.00%	118.9	2,520	15.0
27	Soaked	100%	0%	10.2%	105.3	1,035	15.7
38	Soaked	100%	1%	8.10%	110.7	882	17.0
39	Soaked	100%	2%	9.10%	109.8	1,468	15.0
40	Soaked	100%	3%	8.00%	115.5	2,456	14.0
16	Unsoaked	75%	0%	7.3%	114.0	1,882	12.5
42	Unsoaked	75%	1%	7.6%	120.1	2,783	15.0
43	Unsoaked	75%	2%	7.8%	119.3	4,290	14.5
44	Unsoaked	75%	3%	7.7%	120.4	5,986	12.0
16	Soaked	75%	0%	7.3%	111.3	929	13.3
42	Soaked	75%	1%	7.6%	118.4	1,689	16.0
43	Soaked	75%	2%	7.8%	119.4	3,243	12.5
44	Soaked	75%	3%	7.7%	119.7	4,470	9.0
23	Unsoaked	50%	0%	7.3%	118.9	2,841	9.7
10	Unsoaked	50%	1%	7.00%	122.2	3,824	11.8
11	Unsoaked	50%	2%	6.80%	122.6	6,216	10.0
12	Unsoaked	50%	3%	5.87%	123.1	6,991	10.0
23	Soaked	50%	0%	7.3%	119.1	1,252	11.5
10	Soaked	50%	1%	7.00%	121.1	2,469	12.8
11	Soaked	50%	2%	6.80%	123.3	4,658	12.0
12	Soaked	50%	3%	5.87%	121.7	5,599	8.5
24	Unsoaked	25%	0%	8.2%	119.1	4,725	9.2

Trial Set	Soaked/ Unsoaked	MRAP %	% PC	Moisture Content	Dry Density	Marshall Stability (lb)	Marshall Flow (.01 in)
45	Unsoaked	25%	1%	6.6%	128.2	8,412	9.0
46	Unsoaked	25%	2%	6.5%	128.9	10,946	8.3
47	Unsoaked	25%	3%	7.10%	129.1	12,235	10.0
24	Soaked	25%	0%	8.2%	121.0	107	12.0
45	Soaked	25%	1%	6.6%	128.2	4,815	11.3
46	Soaked	25%	2%	6.5%	127.7	7,808	9.0
47	Soaked	25%	3%	7.10%	129.1	10,823	9.8
26	Unsoaked	0%	0%	9.50%	126.4	7,233	8.7
48	Unsoaked	0%	1%	8.80%	129.2	8,886	7.0
49	Unsoaked	0%	2%	9.10%	130.3	12,942	6.0
50	Unsoaked	0%	3%	8.60%	128.8	16,742	6.0
26	Soaked	0%	0%	9.50%	123.4	0	N/A
48	Soaked	0%	1%	8.80%	129.4	5,947	7.0
49	Soaked	0%	2%	9.10%	130.1	11,587	6.5
50	Soaked	0%	3%	8.60%	128.8	14,442	6.5

E.4.2. Marshall MRAP/Limerock Portland Cement Plots

E.4.2.1. Marshall 100% MRAP Cement Plots

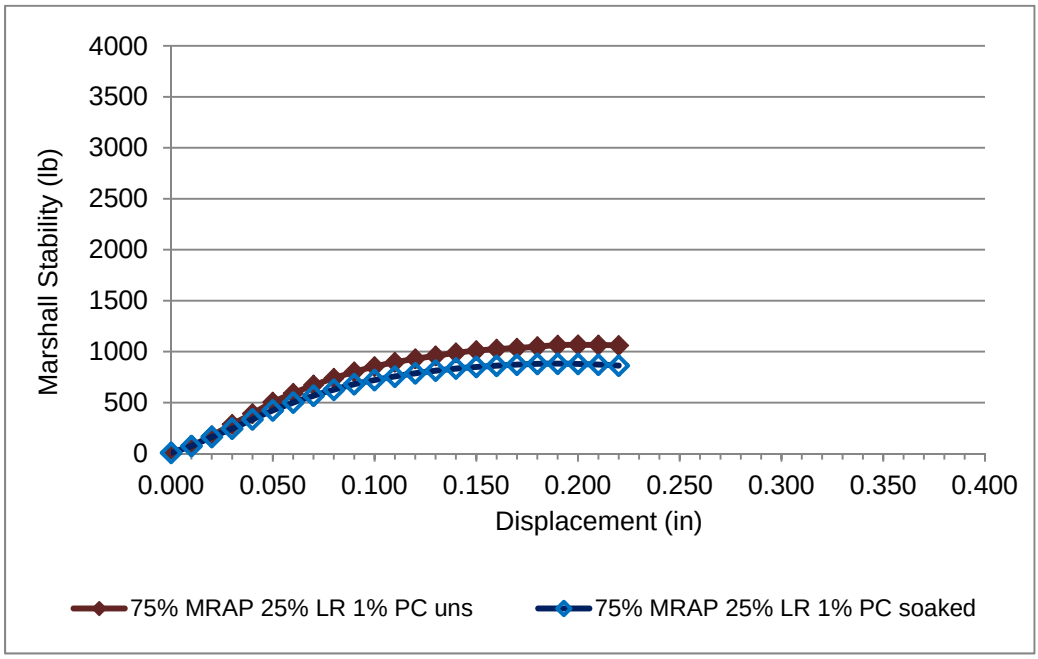

Figure E-24: Marshall Trial 38: 100% MRAP 1% PC

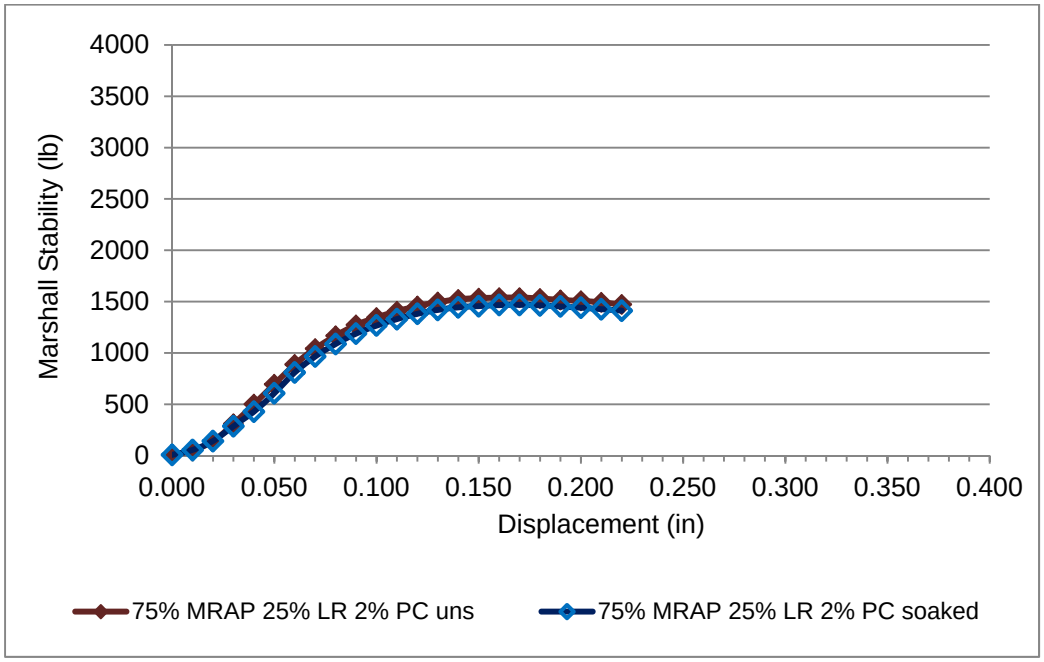

Figure E-25: Marshall Trial 39: 100% MRAP 2% PC

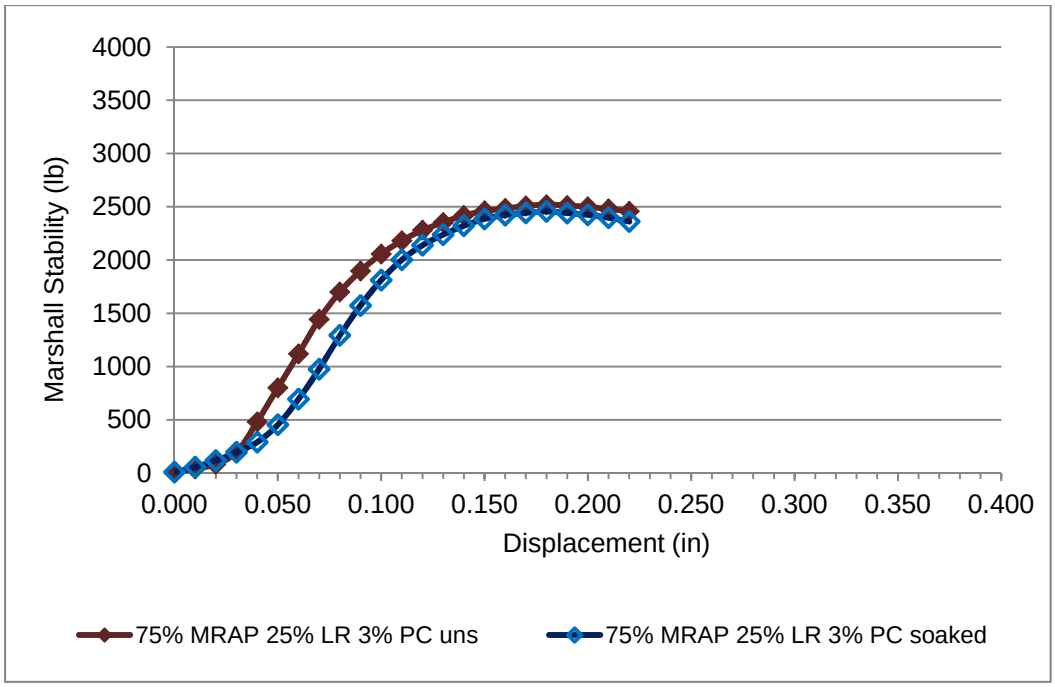

Figure E-26: Marshall Trial 40: 100% MRAP 3% PC

E.4.2.2. Marshall 75% MRAP/25% LR Cement Plots

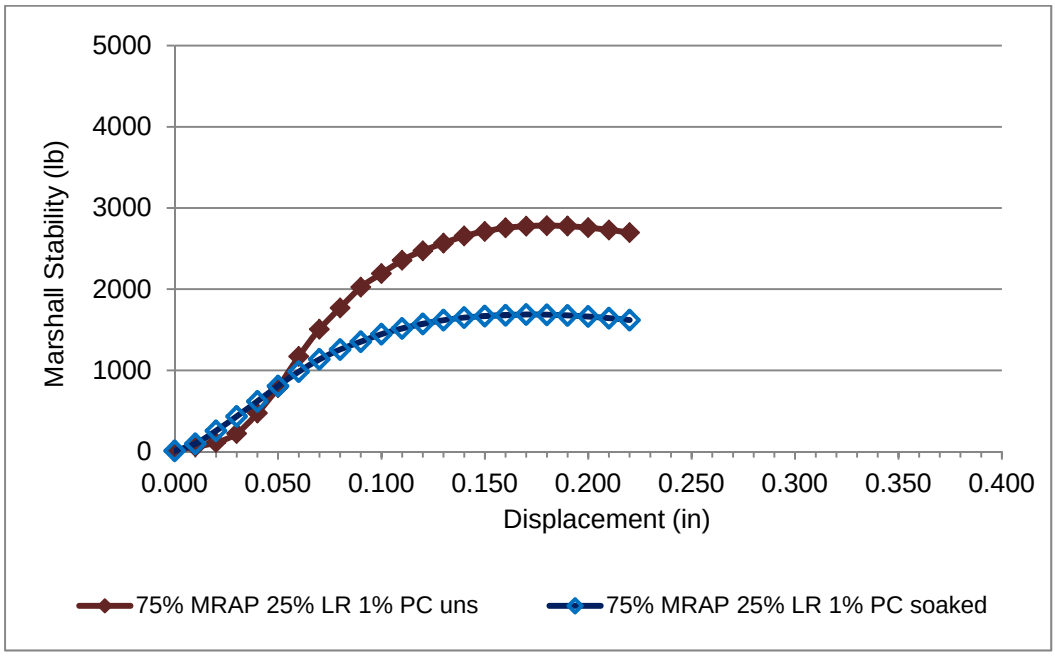

Figure E-27: Marshall Trial 42: 75% MRAP/25% LR 1% PC

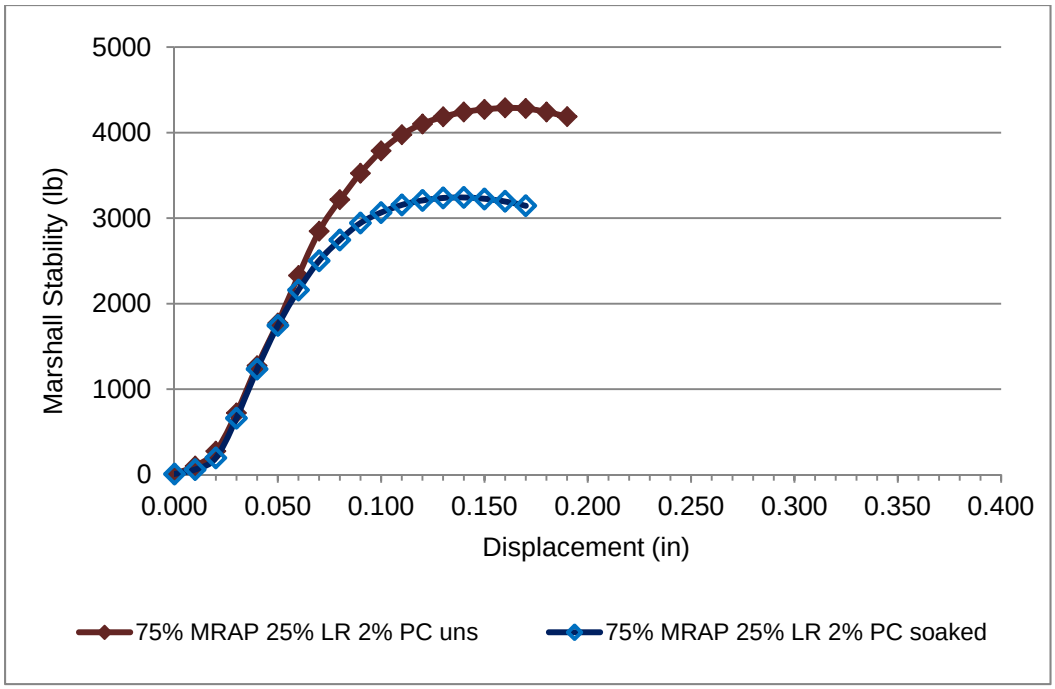

Figure E-28: Marshall Trial 43: 75% MRAP/25% LR 2% PC

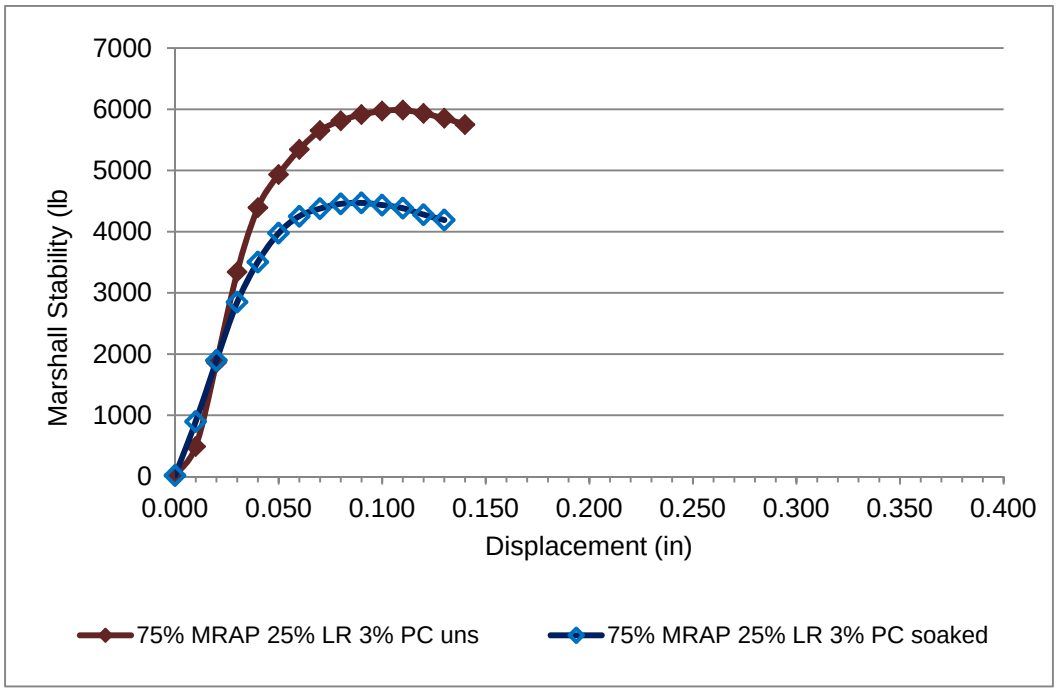

Figure E-29: Marshall Trial 44: 75% MRAP/25% LR 3% PC

E.4.2.3. Marshall 50% MRAP/50% LR Cement Plots

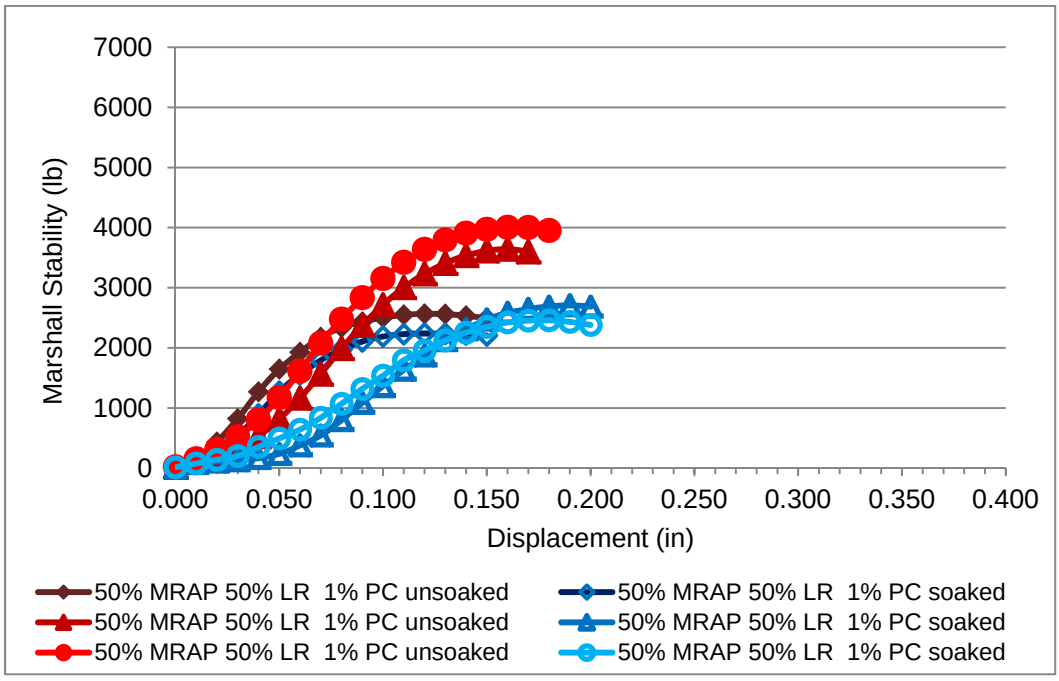

Figure E-30: Marshall Trial 10: 50% MRAP/50% LR 1% PC

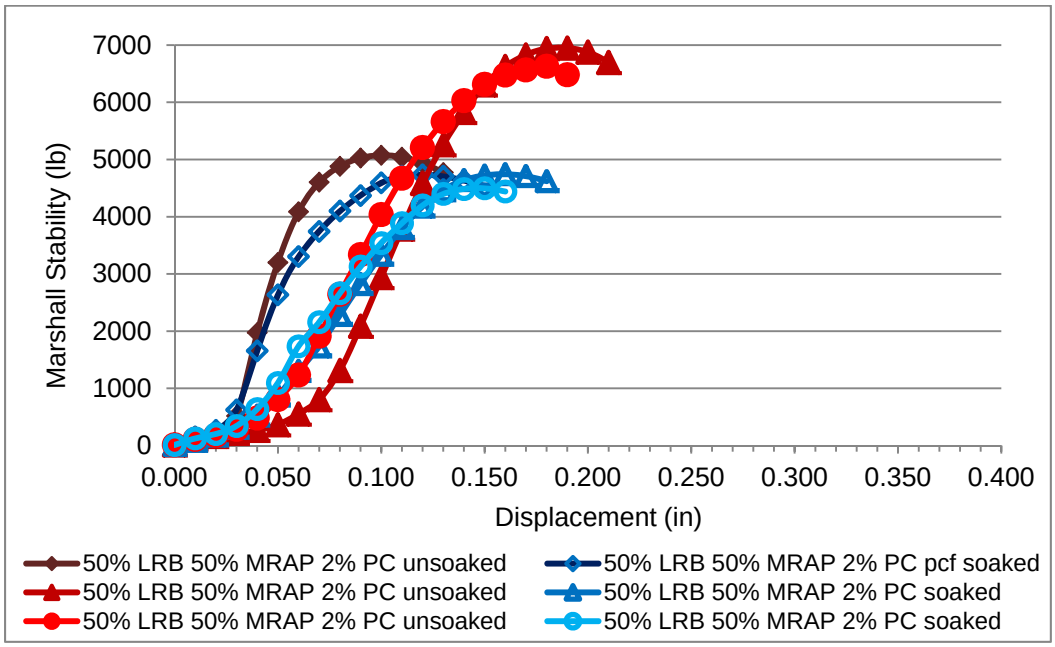

Figure E-31: Marshall Trial 11: 50% MRAP/50% LR 2% PC

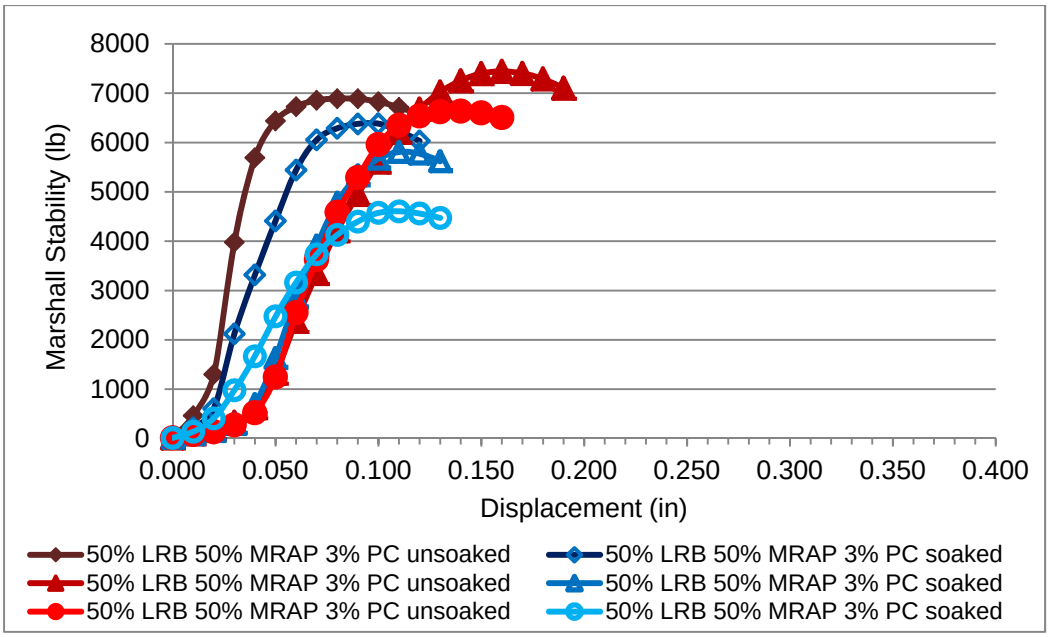

Figure E-32: Marshall Trial 12: 50% MRAP/50% LR 3% PC

E.4.2.4. Marshall 25% MRAP/75%LR Cement Plots

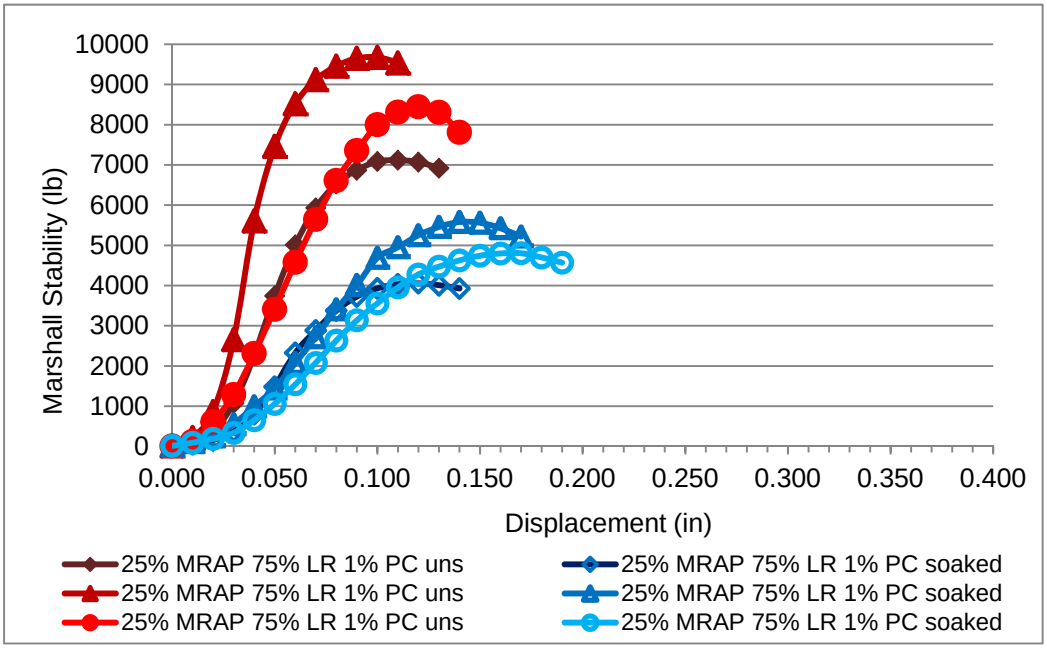

Figure E-33: Marshall Trial 45: 25% MRAP/75% LR 1% PC

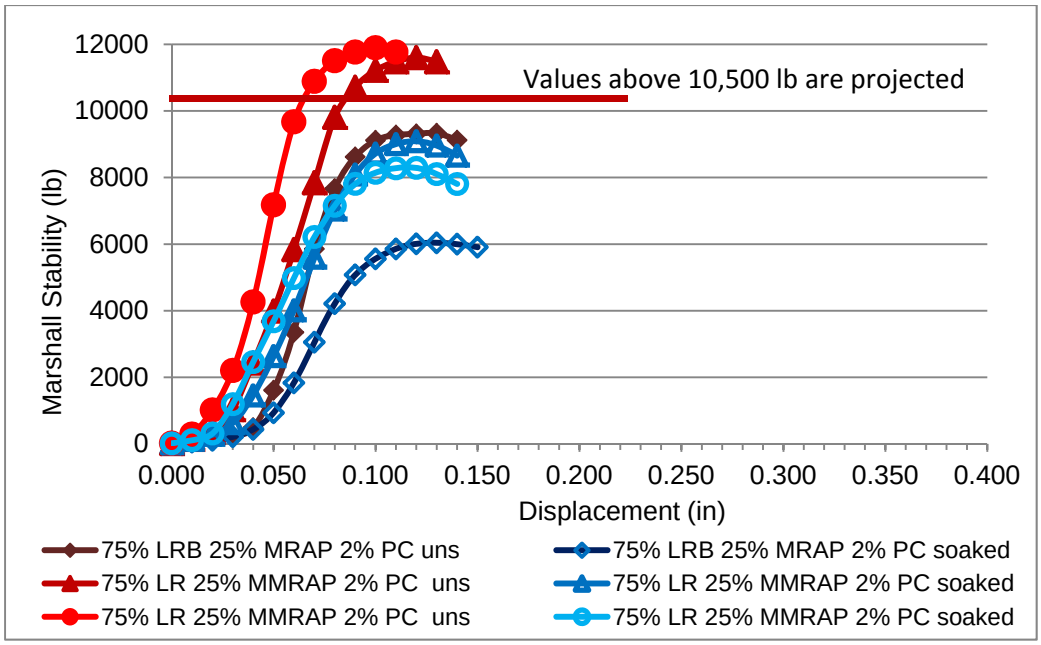

Figure E-34: Marshall Trial 46: 25% MRAP/75% LR 2% PC

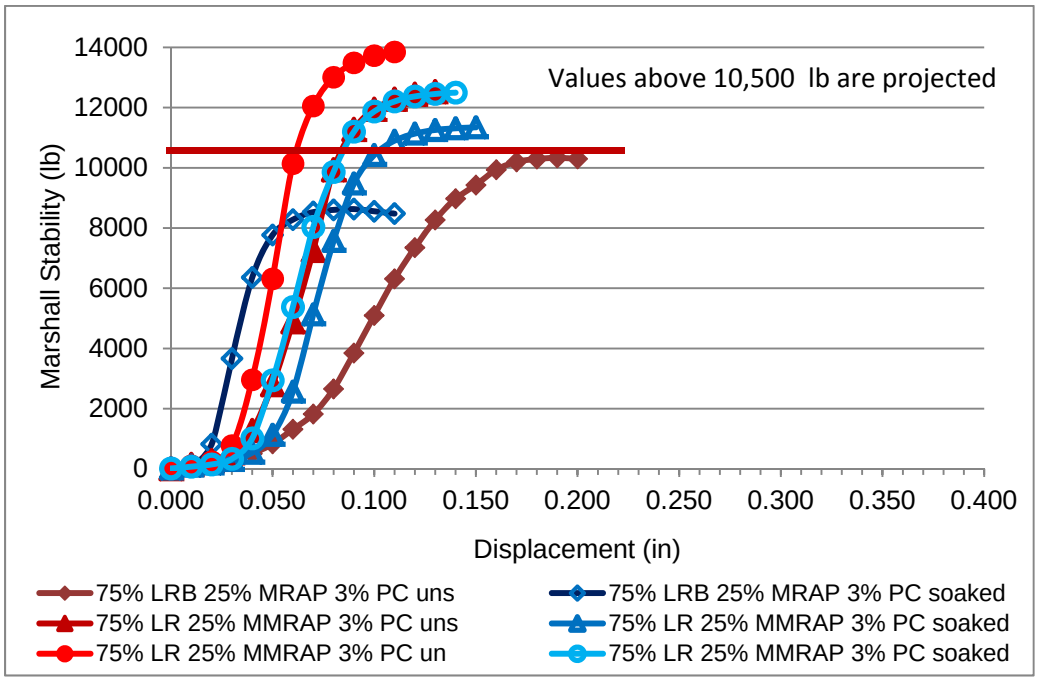

Figure E-35: Marshall Trial 47: 25% MRAP/75% LR 3% PC

E.4.3. Marshall 100% Limerock Cement Plots

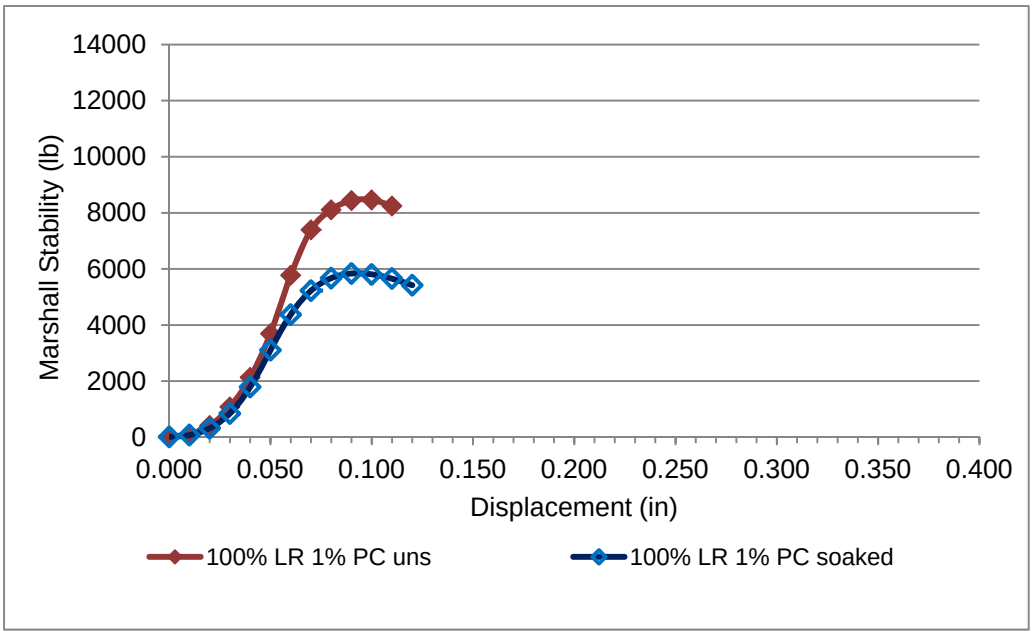

Figure E-36: Marshall Trial 48: 100% LR 1% PC

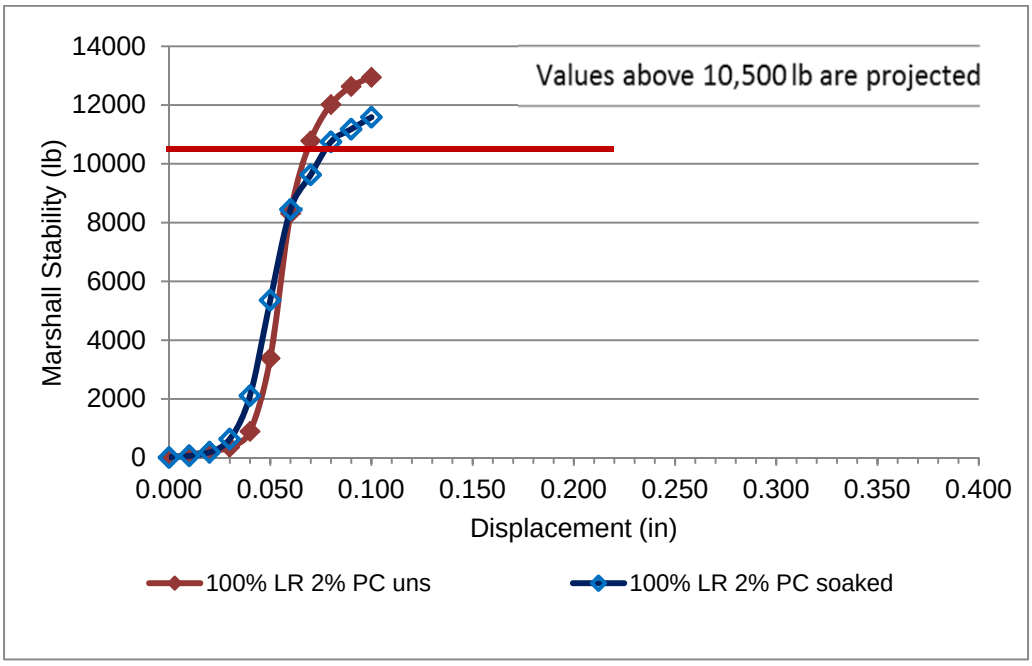

Figure E-37: Marshall Trial 49 100% LR 2% PC

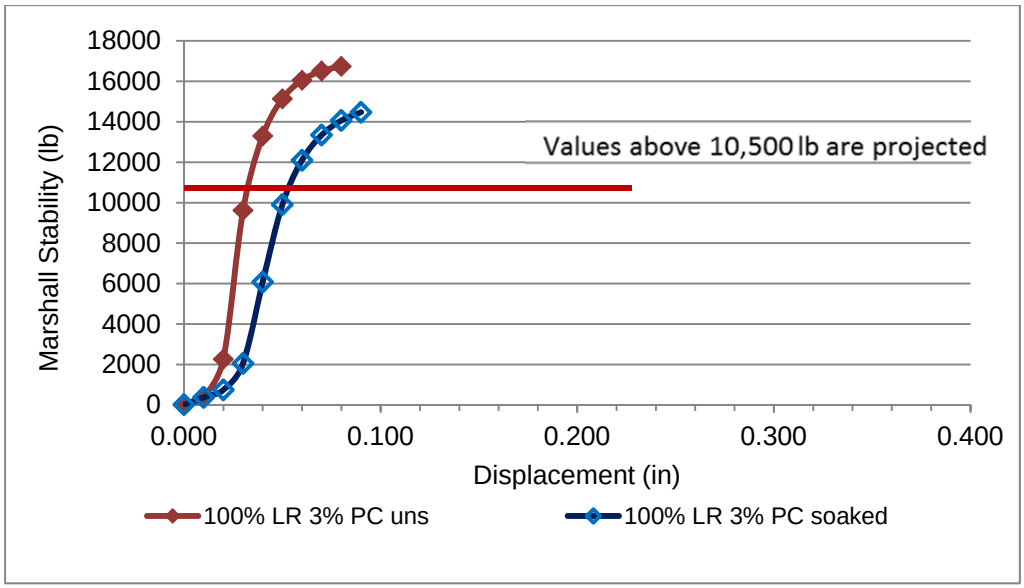

Figure E-38: Marshall Trial 50: 100% LR 3% PC

E.5. Marshall MRAP/Limerock Lime

E.5.1. Marshall MRAP/Limerock Compaction Data

Table E-3: Marshall MRAP/Limerock Compaction with Lime

Trial Set	Soaked/ Unsoaked	MRAP %	% Lime	Moisture Content	Dry Density	Marshall Stability (lb)	Marshall Flow (.01 in)
27	Unsoaked	100%	0%	7.5%	104.6	1,191	18.0
27	Soaked	100%	0%	7.5%	105.2	779	18.0
16	Unsoaked	75%	0%	7.8%	111.7	1,547	11.0
16	Soaked	75%	0%	7.8%	110.1	767	11.0
23	Unsoaked	50%	0%	7.4%	117.6	2,638	10.0
35	Unsoaked	50%	1%	7.6%	118.5	3,023	13.0
36	Unsoaked	50%	2%	7.1%	118.7	2,904	10.5
37	Unsoaked	50%	3%	7.5%	121.2	2,530	8.5
23	Soaked	50%	0%	7.4%	117.9	1,173	10.0
35	Soaked	50%	1%	7.6%	118.7	2,619	12.5
36	Soaked	50%	2%	7.1%	120.1	2,204	11.0
37	Soaked	50%	3%	7.5%	121.6	1,627	8.5
24	Unsoaked	25%	0%	8.2%	119.1	3,723	10.0
24	Soaked	25%	0%	8.2%	121.0	322	13.0
26	Unsoaked	0%	0%	9.5%	126.4	6,438	10.5
26	Soaked	0%	0%	9.5%	123.4	0	N/A

E.5.2. Marshall MRAP/Limerock Lime Compaction Plots

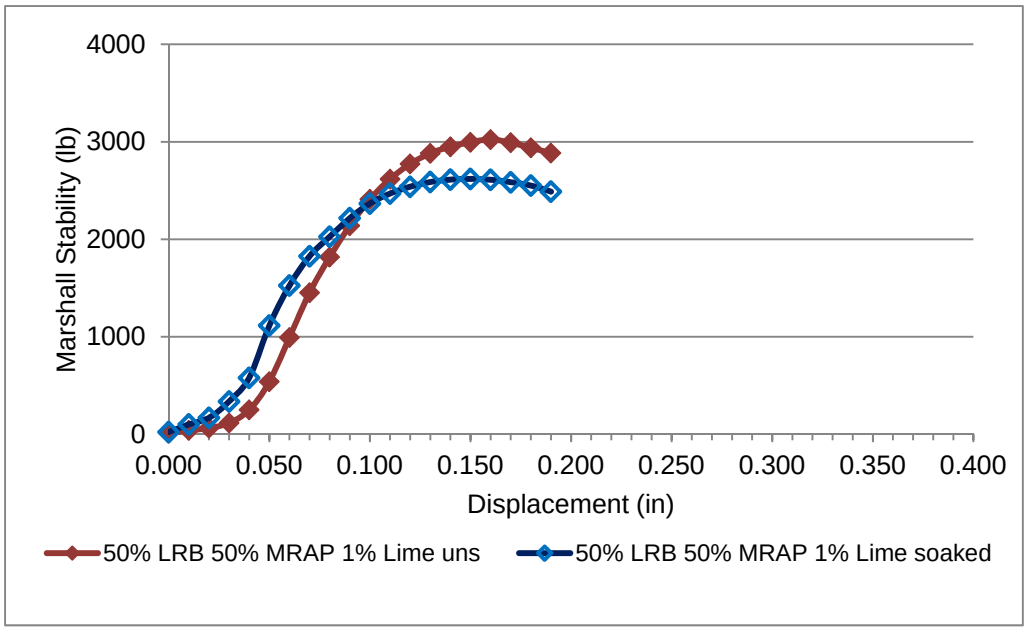

Figure E-39: Marshall Trial 36: 50% MRAP/50% LR 1% Lime

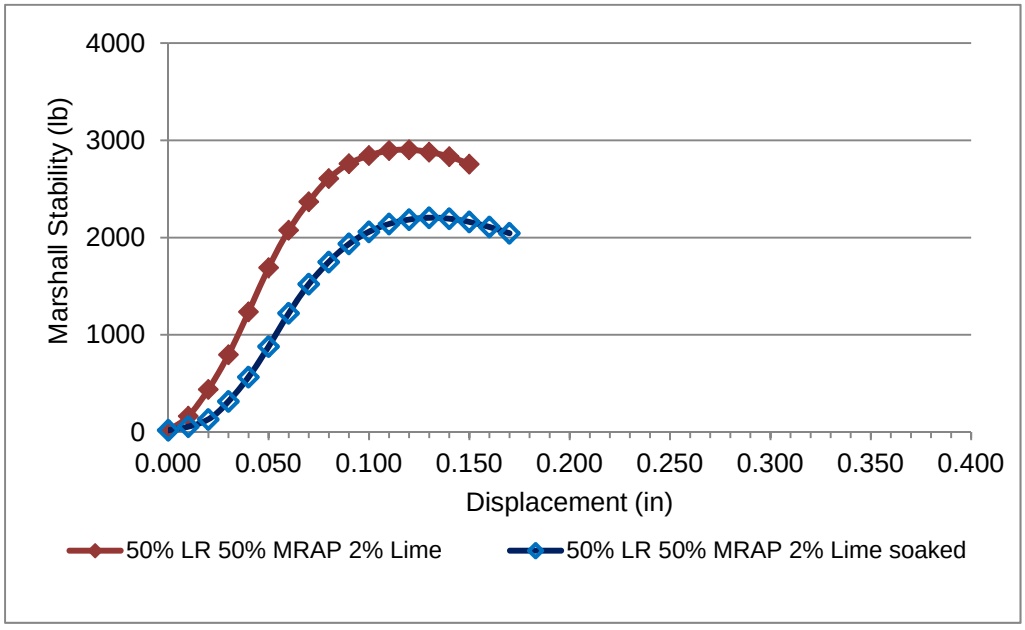

Figure E-40: Marshall Trial 36: 50% MRAP/50% LR 2% Lime

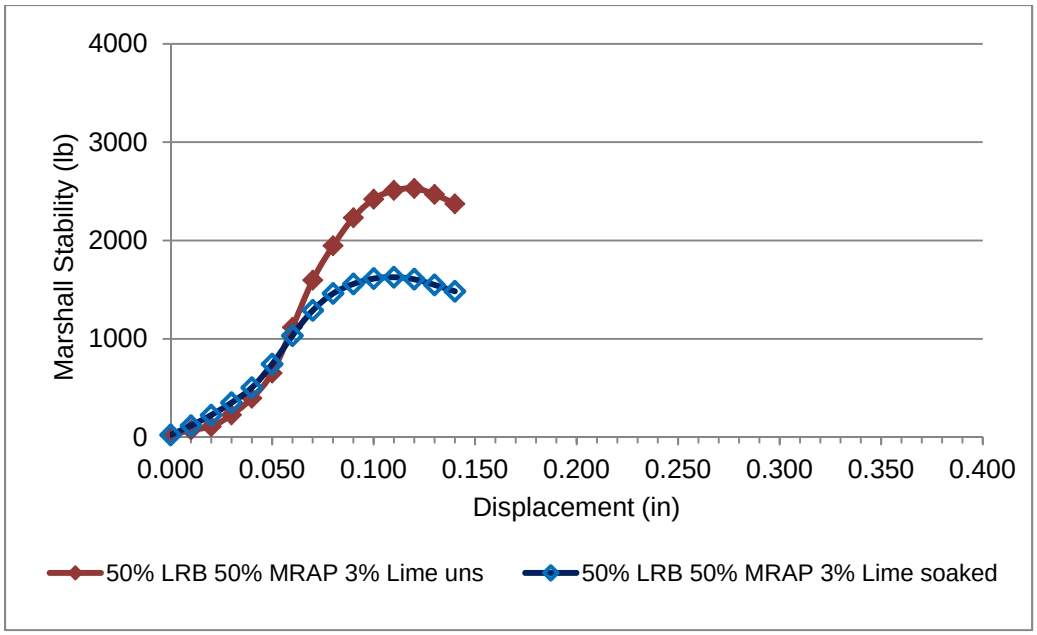

Figure E-41: Marshall Trial 37: 50% MRAP/50% LR 3% Lime

Appendix F - Unconfined Compression Tests

F.1. Unconfined Compression Tests MRAP/Limerock No Stabilizer

Note: tabular data for these control samples with no stabilizer is included in the tabular data for each of the stabilizer types following this section.

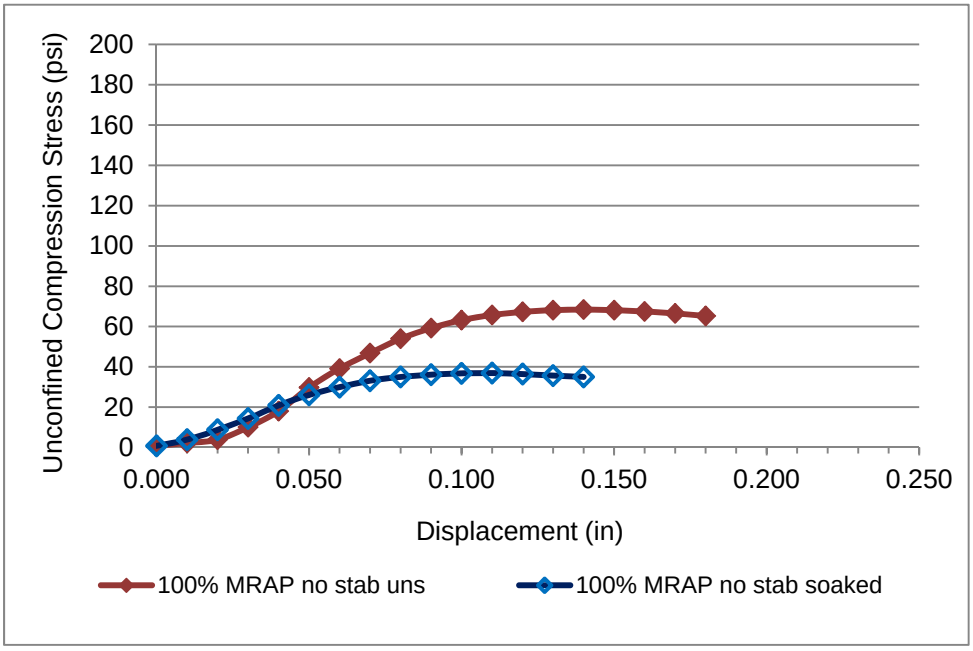

Figure F-1: Unconfined Compression Trial 27: 100% MRAP No Stabilizer

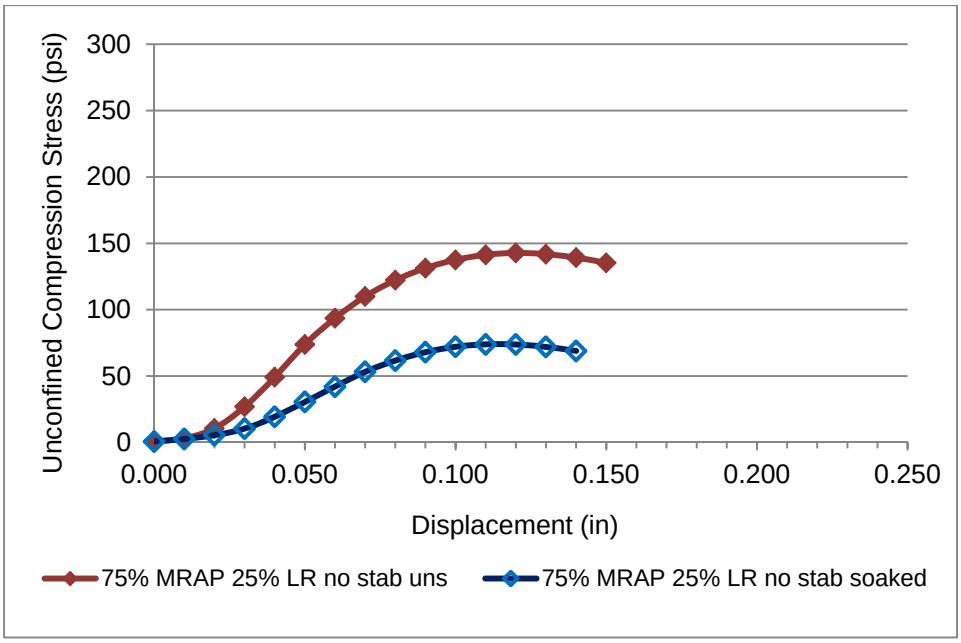

Figure F-2: Unconfined Compression Trial 16: 75% MRAP/25% LR No Stabilizer

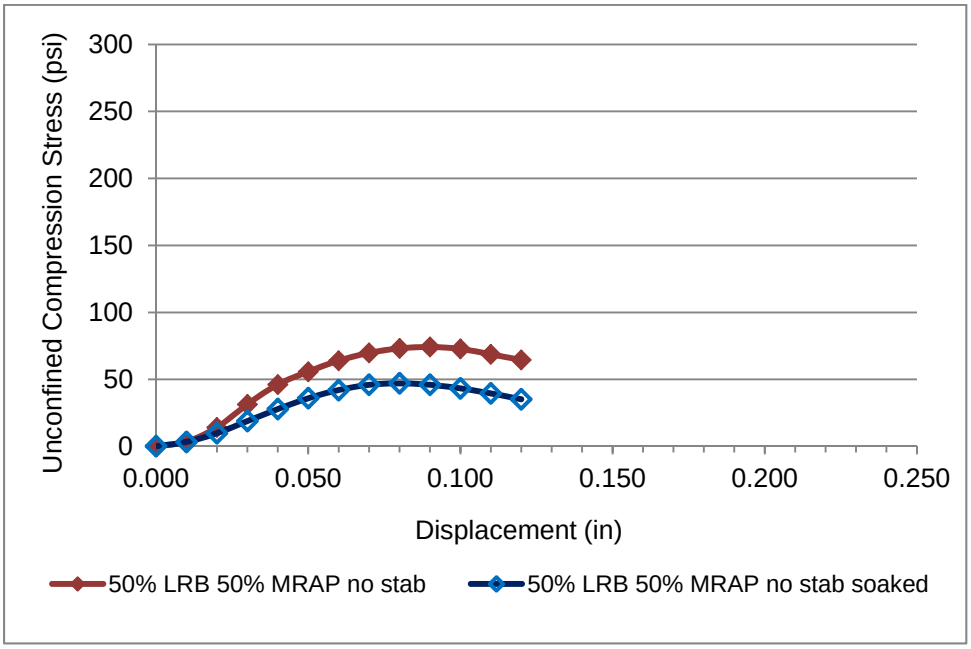

Figure F-3: Unconfined Compression Trial 23: 50% MRAP/50% LR No Stabilizer

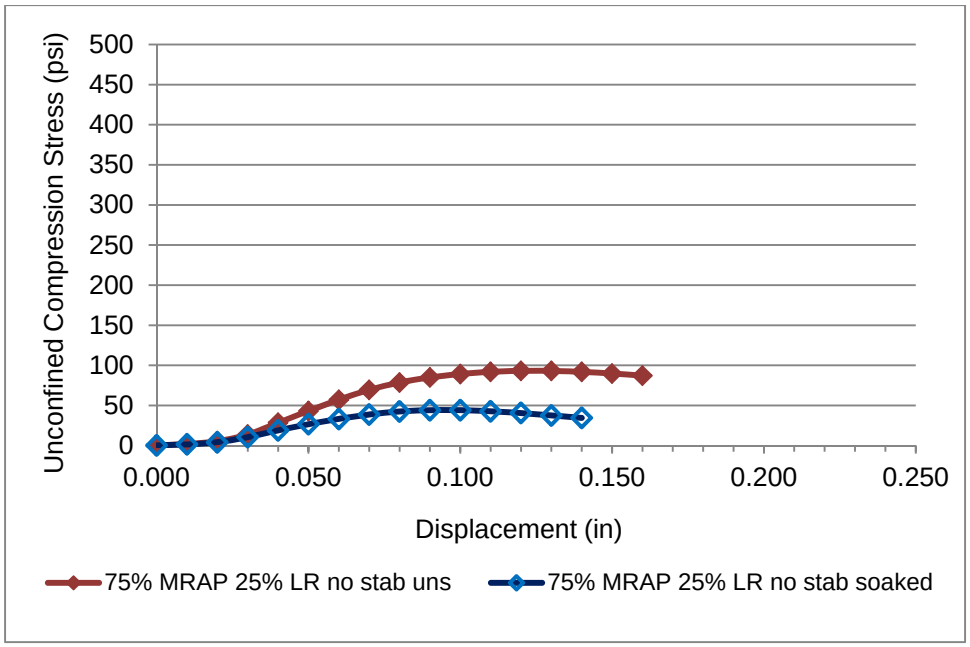

Figure F-4: Unconfined Compression Trial 24: 25% MRAP/75% LR No Stabilizer

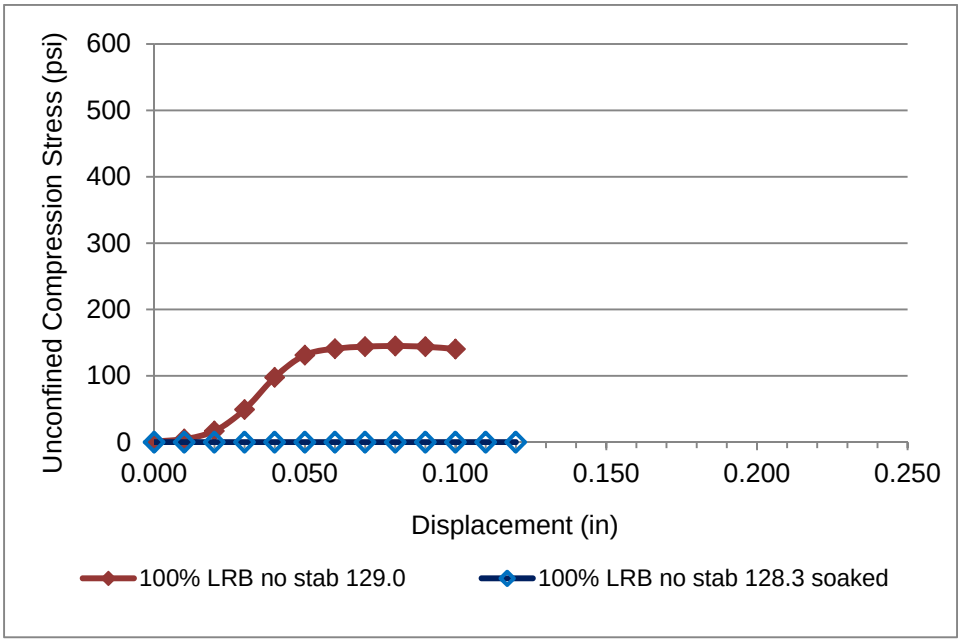

Figure F-5: Unconfined Compression Trial 26: 100% LR No Stabilizer

F.2. Unconfined Compression Tests MRAP/Limerock SS-1H

F.2.1. Unconfined Compression MRAP/Limerock SS-1H Compaction Data

Table F-1: Unconfined Compression MRAP/LR Blends with

Trial	Soaked/ Unsoaked	MRAP %	% SS-1H	Moisture Content	Dry Density	Peak Strength (psi)	Peak Displace (in)
27	Unsoaked	100%	0%	8.0%	104.9	68.0	0.120
27	Soaked	100%	0%	8.0%	105.2	37.0	0.115
16	Unsoaked	75%	0%	7.8%	113.1	93.3	0.120
13	Unsoaked	75%	1%	7.5%	118.6	160.0	0.160
14	Unsoaked	75%	2%	7.2%	114.3	150.0	0.120
15	Unsoaked	75%	3%	6.1%	112.8	121.0	0.170
16	Soaked	75%	0%	7.8%	112.3	44.2	0.090
13	Soaked	75%	1%	7.5%	118.0	145.0	0.150
14	Soaked	75%	2%	7.2%	114.1	107.0	0.120
15	Soaked	75%	3%	6.1%	112.8	110.0	0.180
23	Unsoaked	50%	0%	7.0%	119.0	74.0	0.080
01	Unsoaked	50%	1%	6.4%	119.5	173.0	0.095
02	Unsoaked	50%	2%	6.2%	118.3	198.0	0.110
03	Unsoaked	50%	3%	5.6%	122.2	258.0	0.100
23	Soaked	50%	0%	7.0%	118.7	47.0	0.080
01	Soaked	50%	1%	6.4%	118.7	158.0	0.110
02	Soaked	50%	2%	6.2%	119.4	107.0	0.140
03	Soaked	50%	3%	5.6%	123.6	172.0	0.110
24	Unsoaked	25%	0%	8.2%	123.1	131.9	0.080
07	Unsoaked	25%	1%	8.3%	127.1	167.1	0.100
08	Unsoaked	25%	2%	9.3%	124.0	134.0	0.105
09	Unsoaked	25%	3%	7.5%	126.8	193.9	0.110
24	Soaked	25%	0%	8.2%	121.7	27.1	0.080
07	Soaked	25%	1%	8.3%	125.9	69.4	0.130
08	Soaked	25%	2%	9.3%	126.1	110.8	0.120
09	Soaked	25%	3%	7.5%	126.1	137.4	0.130
26	Unsoaked	0%	0%	9.5%	129.0	145.0	0.085
26	Soaked	0%	0%	9.5%	128.3	0.0	0.000

F.2.2. Unconfined Compression MRAP/Limerock SS-1H Plots

F.2.2.1. Unconfined Compression 75% MRAP/25% Limerock SS-1H Plots

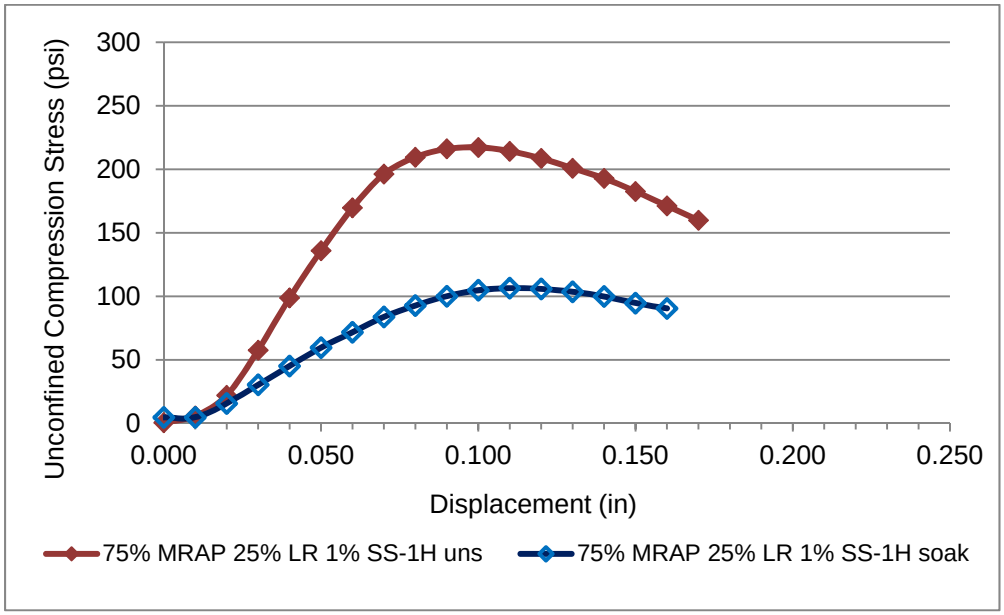

Figure F-6: Unconfined Compression Trial 04: 75% MRAP/25% LR 1% SS-1H

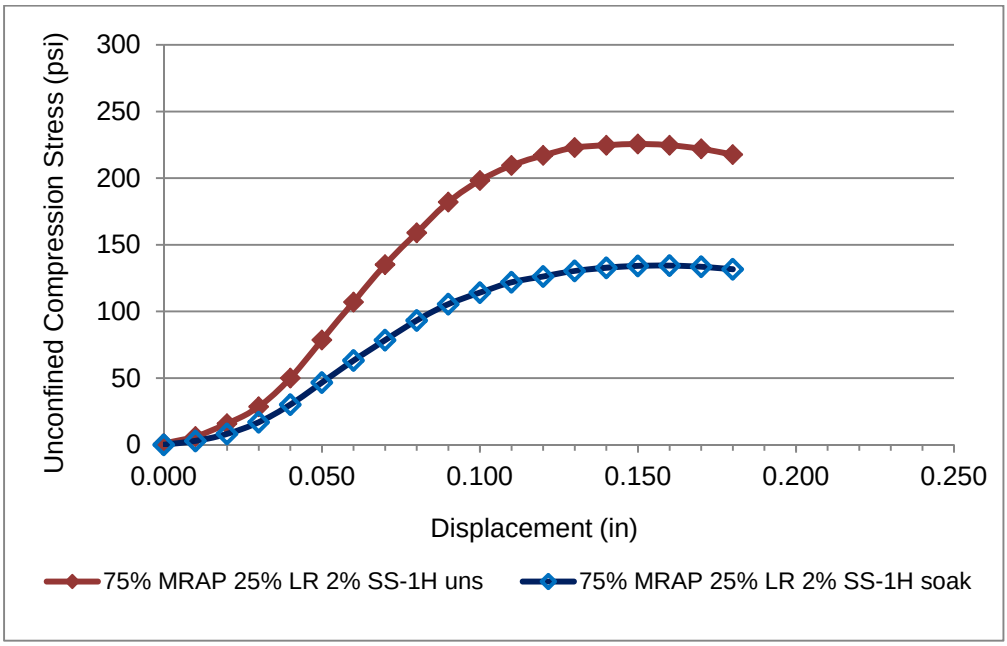

Figure F-7: Unconfined Compression Trial 05: 75% MRAP/25% LR 2% SS-1H

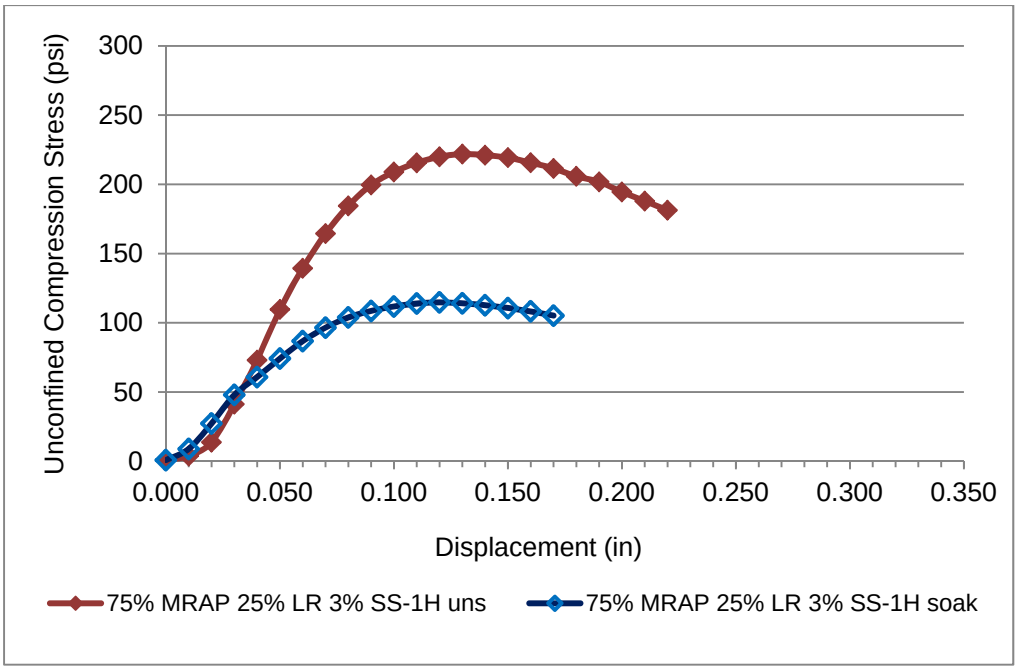

Figure F-8: Unconfined Compression Trial 06: 75% MRAP/25% LR 3% SS-1H

F.2.2.2. Unconfined Compression 50% MRAP/50% Limerock SS-1H Plots

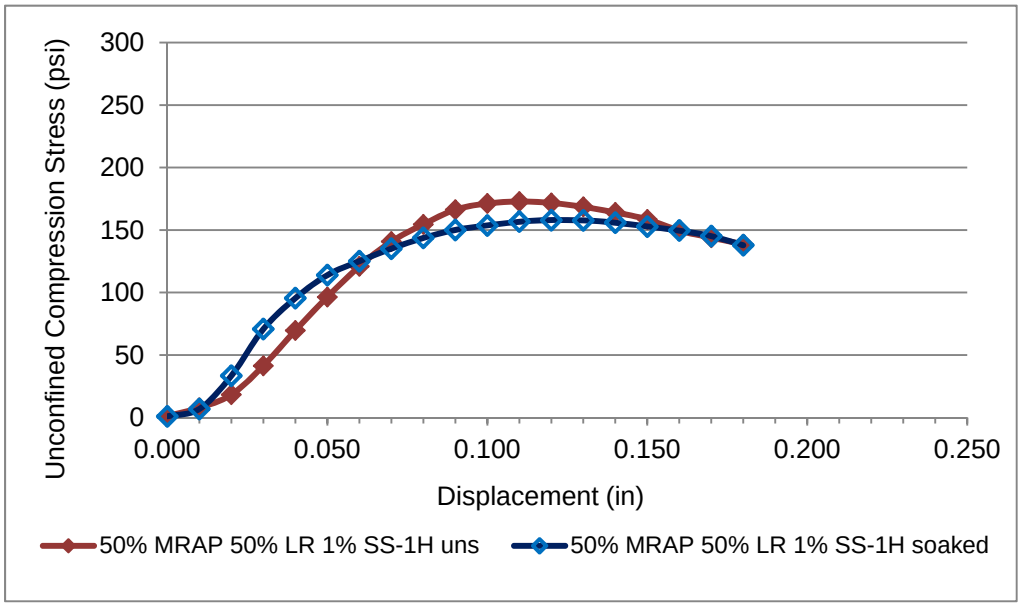

Figure F-9: Unconfined Compression Trial 01: 50% MRAP/50% LR 1% SS-1H

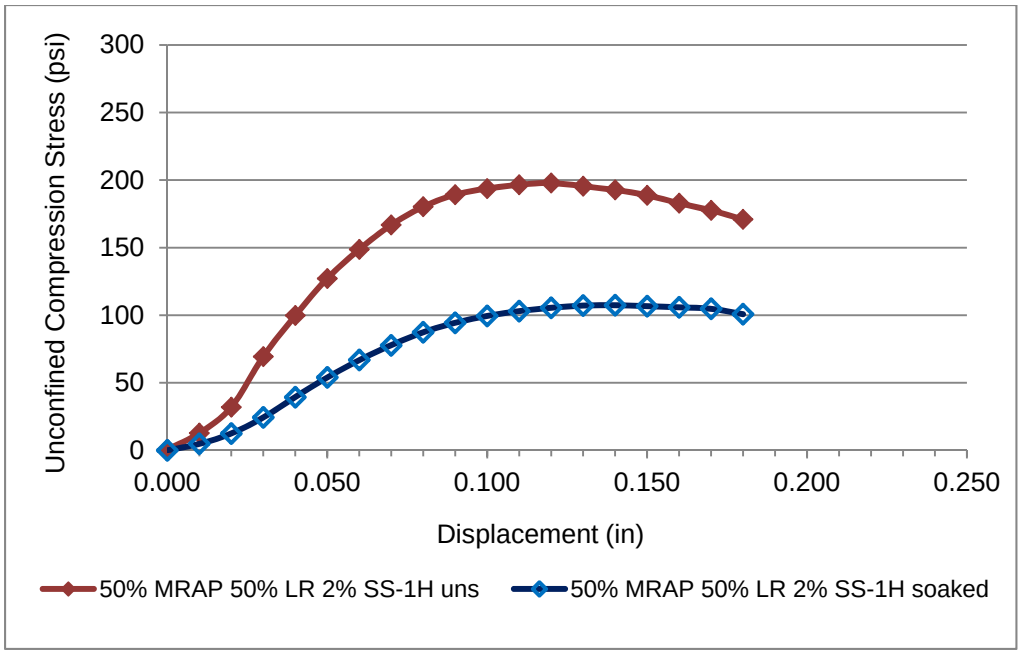

Figure F-10: Unconfined Compression Trial 02: 50% MRAP/50% LR 2% SS-1H

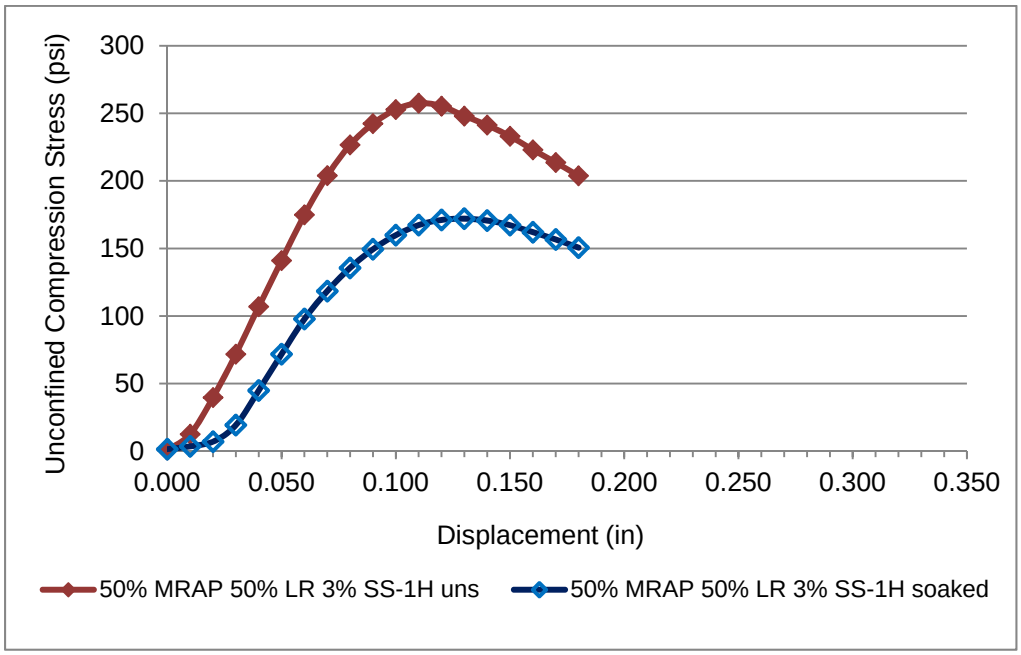

Figure F-11: Unconfined Compression Trial 03: 50% MRAP/50% LR 3% SS-1H

F.2.2.3. Unconfined Compression 25% MRAP/75% Limerock SS-1H Plots

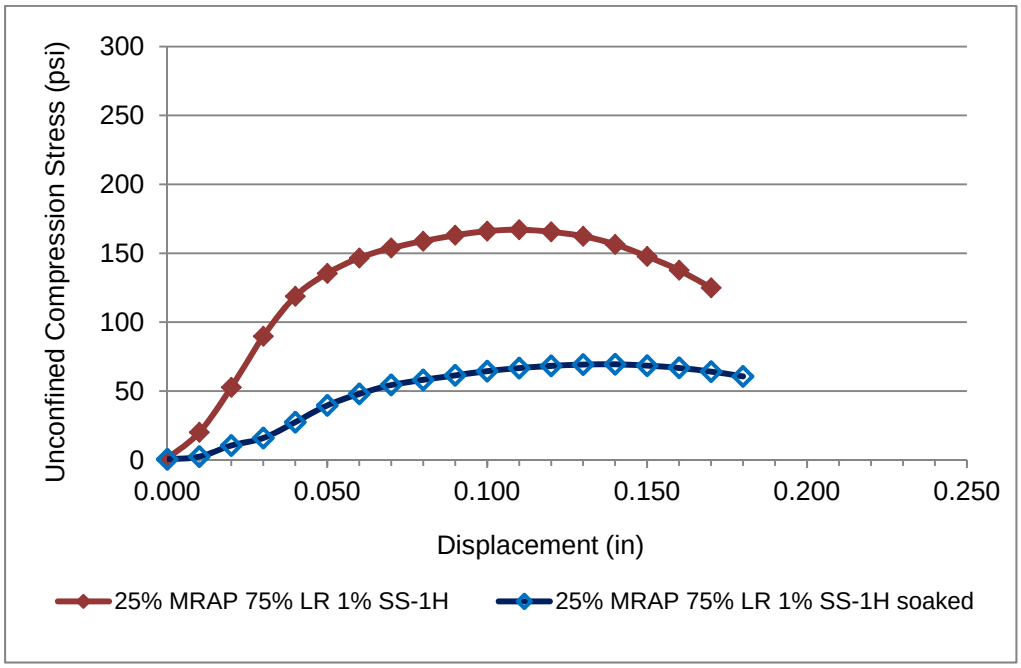

Figure F-12: Unconfined Compression Trial 07: 25% MRAP/75% LR 1% SS-1H

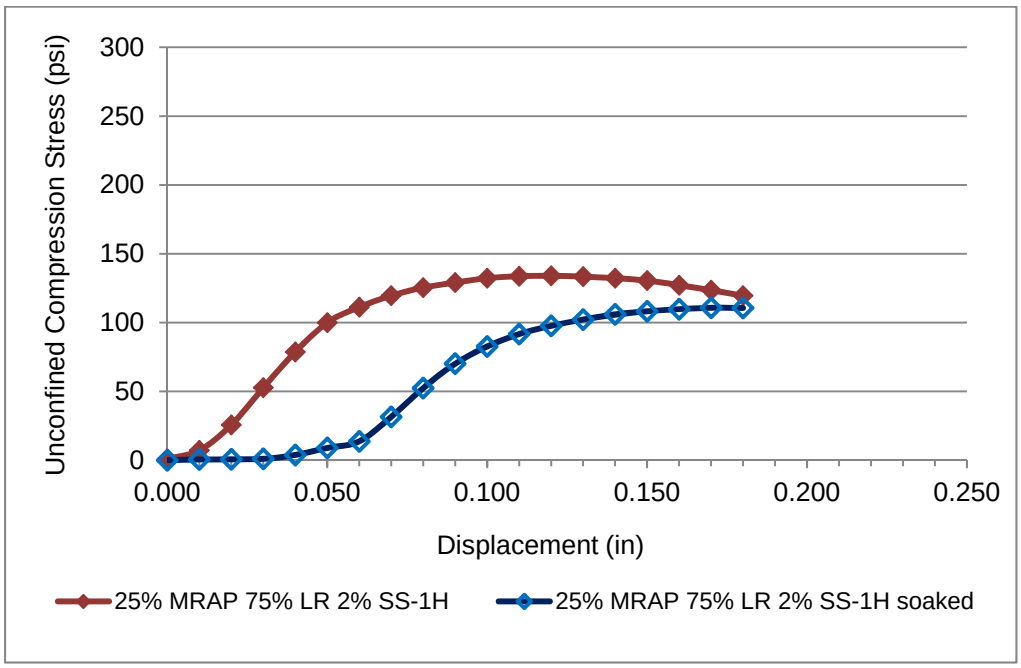

Figure F-13: Unconfined Compression Trial 08: 25% MRAP/75% LR 2% SS-1H

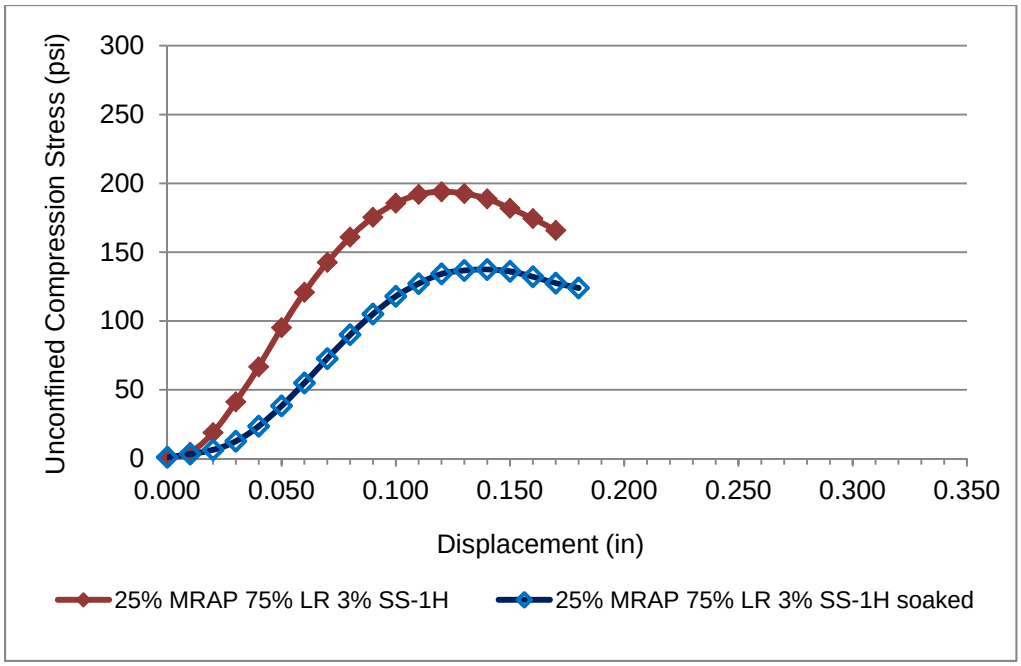

Figure F-14: Unconfined Compression Trial 09: 25% MRAP/75% LR 3% SS-1H

F.3. Unconfined Compression Tests MRAP/Limerock CSS-1HF

F.3.1. Unconfined Compression MRAP/Limerock CSS-1HF Compaction Data

Table F-2: Unconfined Compression MRAP/LR Blends with CSS-1HG

Trial Set	Soaked/ Unsoaked	MRAP %	% CSS-1HF	Moisture Content	Dry Density	Peak Strength (psi)	Max Displ (in)
27	Unsoaked	100%	0%	8.0%	104.9	68.4	0.14
32	Unsoaked	100%	1%	10.1%	106.6	101.1	0.18
33	Unsoaked	100%	2%	8.3%	108.2	NP	NP
34	Unsoaked	100%	3%	7.7%	108.3	107.1	0.34
27	Soaked	100%	0%	8.0%	105.2	36.9	0.11
32	Soaked	100%	1%	10.1%	108.9	105.4	0.23
33	Soaked	100%	2%	8.3%	107.2	NP	NP
34	Soaked	100%	3%	7.7%	108.5	NP	NP
16	Unsoaked	75%	0%	7.8%	113.1	93.3	0.12
13	Unsoaked	75%	1%	7.5%	118.6	160.3	0.16
14	Unsoaked	75%	2%	7.2%	114.3	149.9	0.12
15	Unsoaked	75%	3%	6.1%	123.7	121.0	0.17
16	Soaked	75%	0%	7.8%	112.3	44.2	0.09
13	Soaked	75%	1%	7.5%	118.0	144.7	0.15
14	Soaked	75%	2%	7.2%	114.1	106.6	0.12
15	Soaked	75%	3%	6.1%	125.1	110.3	0.18
23	Unsoaked	50%	0%	7.0%	119.0	74.2	0.09
17	Unsoaked	50%	1%	6.7%	119.0	157.2	0.11
18	Unsoaked	50%	2%	7.0%	119.6	152.5	0.14
19	Unsoaked	50%	3%	7.9%	119.2	128.0	0.14
23	Soaked	50%	0%	7.0%	118.7	47.1	0.08
17	Soaked	50%	1%	6.7%	119.6	99.9	0.10
18	Soaked	50%	2%	7.0%	119.4	114.6	0.11
19	Soaked	50%	3%	7.9%	122.0	120.3	0.14
24	Unsoaked	25%	0%	8.2%	123.1	131.9	0.08
20	Unsoaked	25%	1%	7.3%	123.3	163.1	0.08

Trial Set	Soaked/ Unsoaked	MRAP %	% CSS-1HF	Moisture Content	Dry Density	Peak Strength (psi)	Max Displ (in)
21	Unsoaked	25%	2%	7.6%	123.6	149.8	0.10
22	Unsoaked	25%	3%	7.3%	123.6	166.5	0.10
24	Soaked	25%	0%	8.2%	121.7	27.1	0.08
20	Soaked	25%	1%	7.3%	122.5	93.6	0.08
21	Soaked	25%	2%	7.5%	123.5	87.9	0.09
22	Soaked	25%	3%	7.3%	121.9	137.2	0.10
26	Unsoaked	0%	0%	9.5%	129.0	145.0	0.08
29	Unsoaked	0%	1%	8.0%	128.8	202.1	0.11
30	Unsoaked	0%	2%	8.1%	128.9	189.1	0.10
31	Unsoaked	0%	3%	8.4%	125.6	167.1	0.10
26	Soaked	0%	0%	9.5%	128.3	0.0	
29	Soaked	0%	1%	8.0%	127.5	96.3	0.08
30	Soaked	0%	2%	8.1%	128.1	117.8	0.90
31	Soaked	0%	3%	8.4%	125.5	121.8	0.12

F.3.2. Unconfined Compression MRAP/Limerock CSS-1HF Plots

F.3.2.1. 100% MRAP CSS-1HF

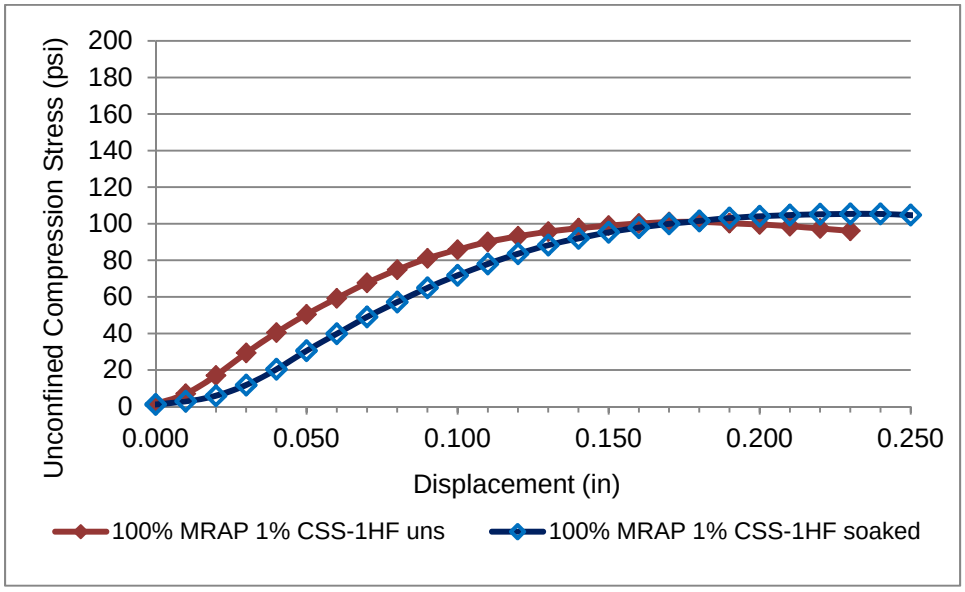

Figure F-15: Unconfined Compression Trial 32: 100% MRAP 1% CSS-1HF

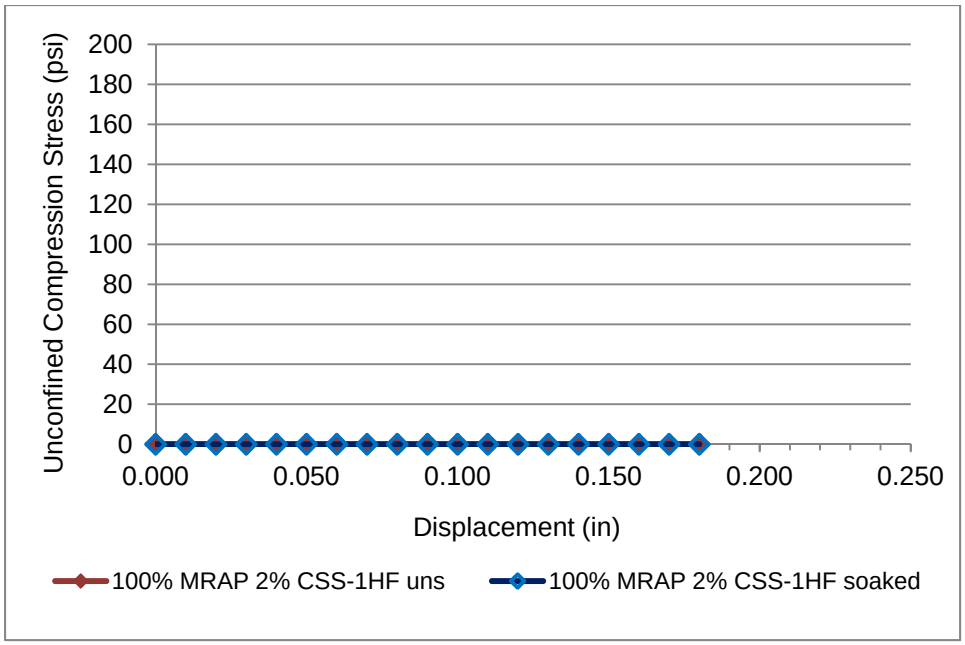

Figure F-16: Unconfined Compression Trial 33: 100% MRAP 2% CSS-1HF (blends were unstable)

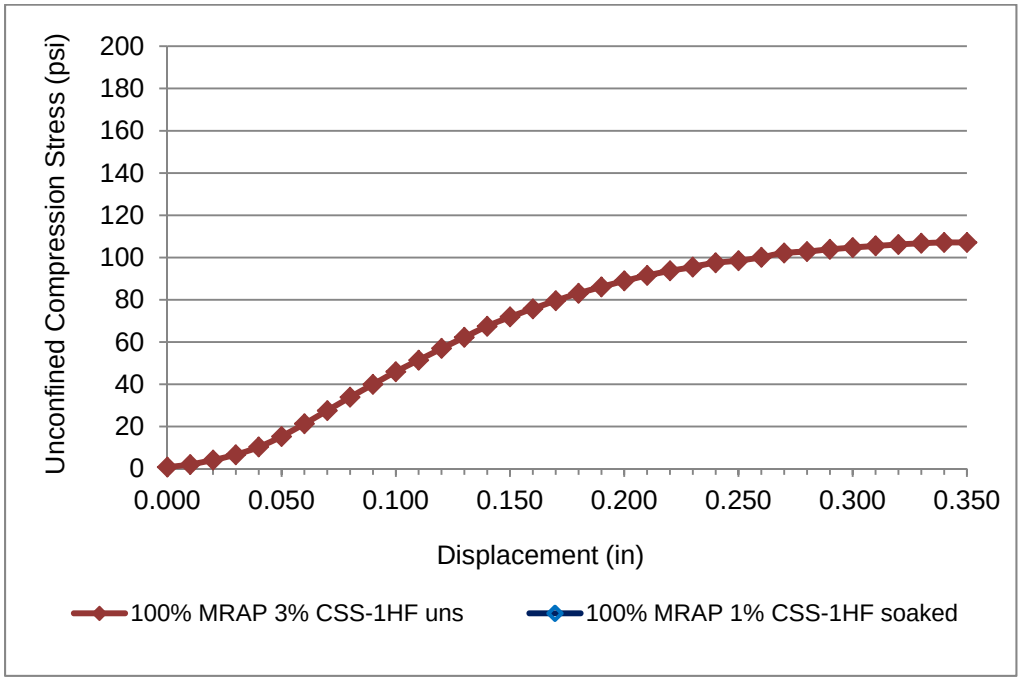

Figure F-17: Unconfined Compression Trial 34: 100% MRAP 3% CSS-1HF (one blend was unstable)

F.3.2.2. Unconfined Compression 75% MRAP/25% Limerock CSS-1HF

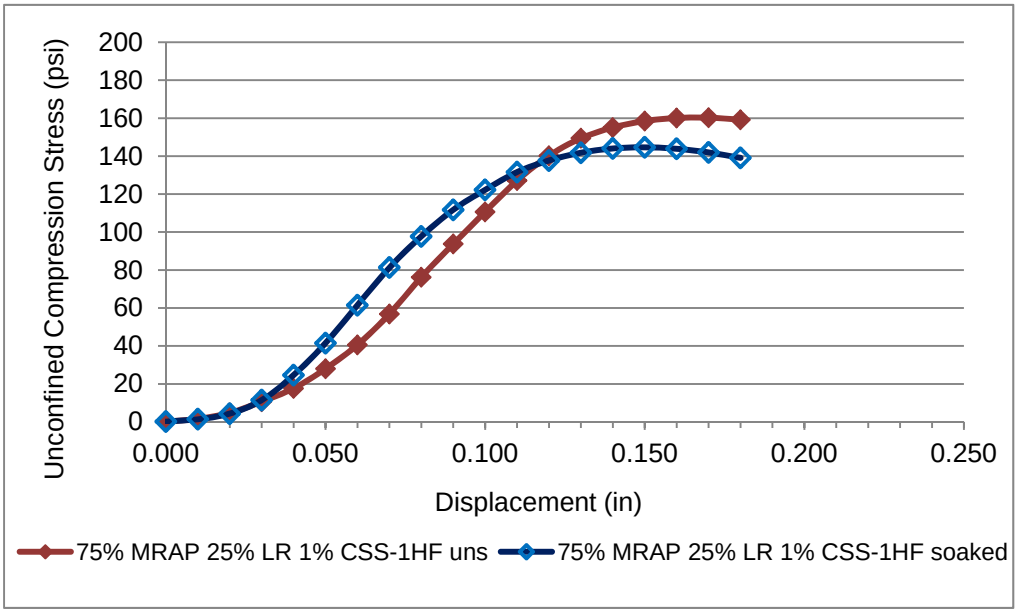

Figure F-18: Unconfined Compression Trial 13: 75% MRAP 25% LR 1% CSS-1HF

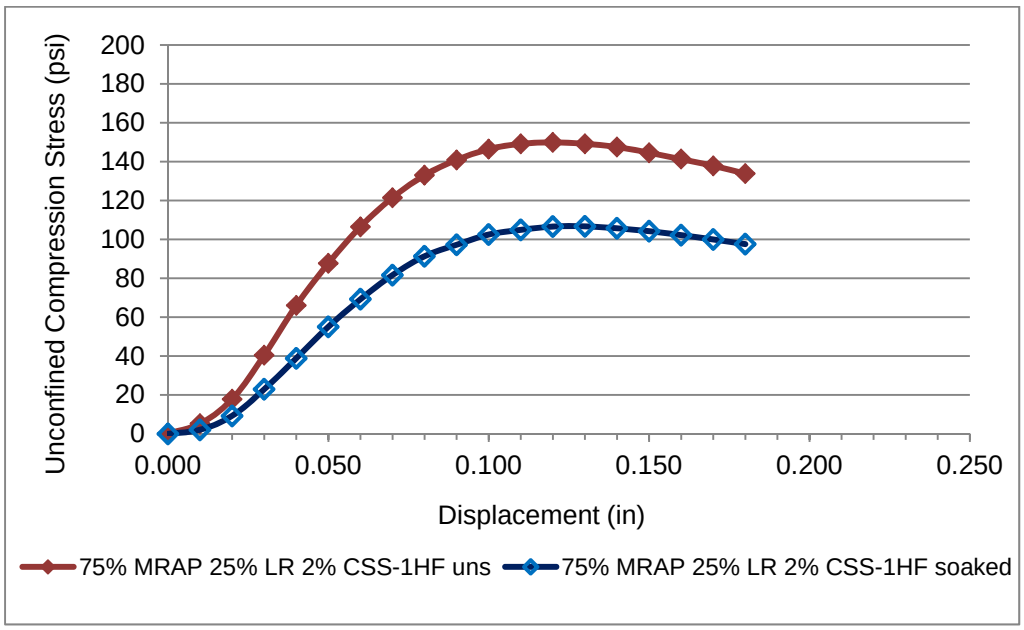

Figure F-19: Unconfined Compression Trial 14: 75% MRAP 25% LR 2% CSS-1HF

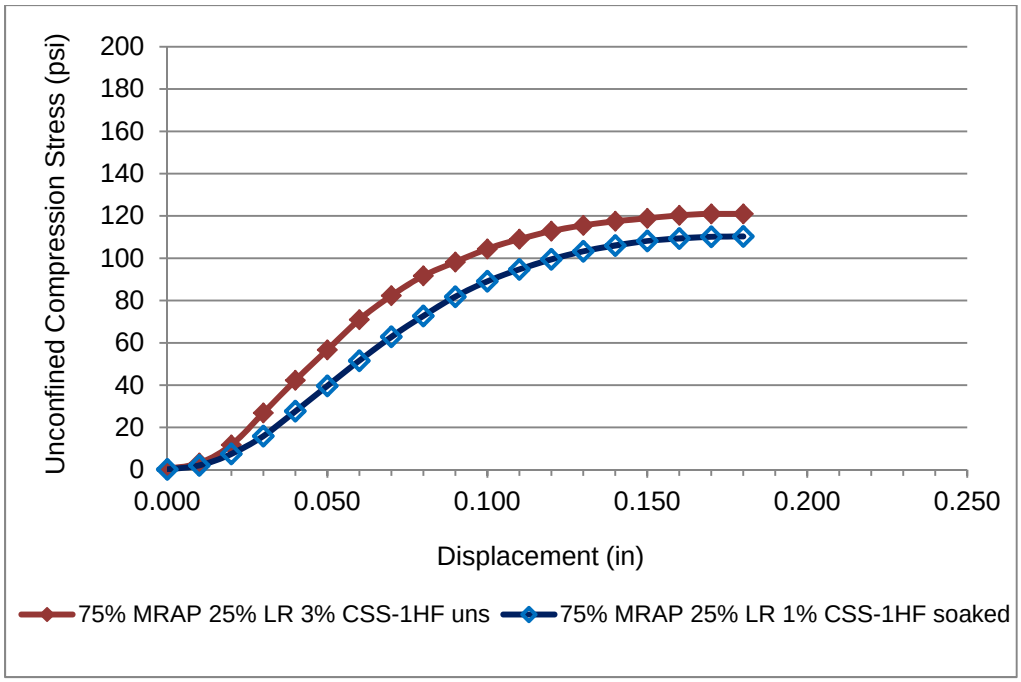

Figure F-20: Unconfined Compression Trial 15: 75% MRAP 25% LR 3% CSS-1HF

F.3.2.3. Unconfined Compression 50% MRAP/50% Limerock CSS-1HF

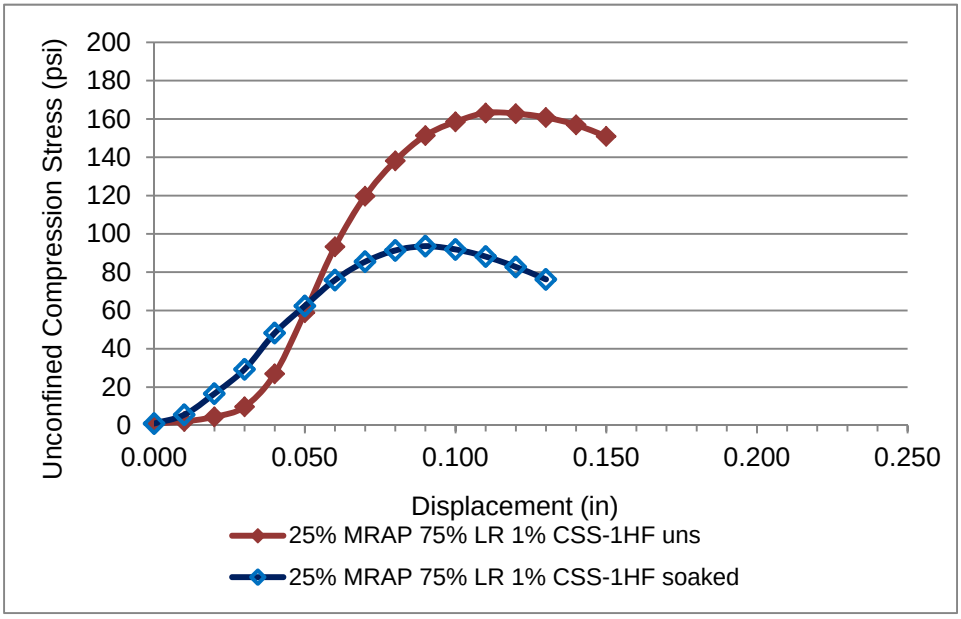

Figure F-21: Unconfined Compression Trial 17: 50% MRAP 50% LR 1% CSS-1HF

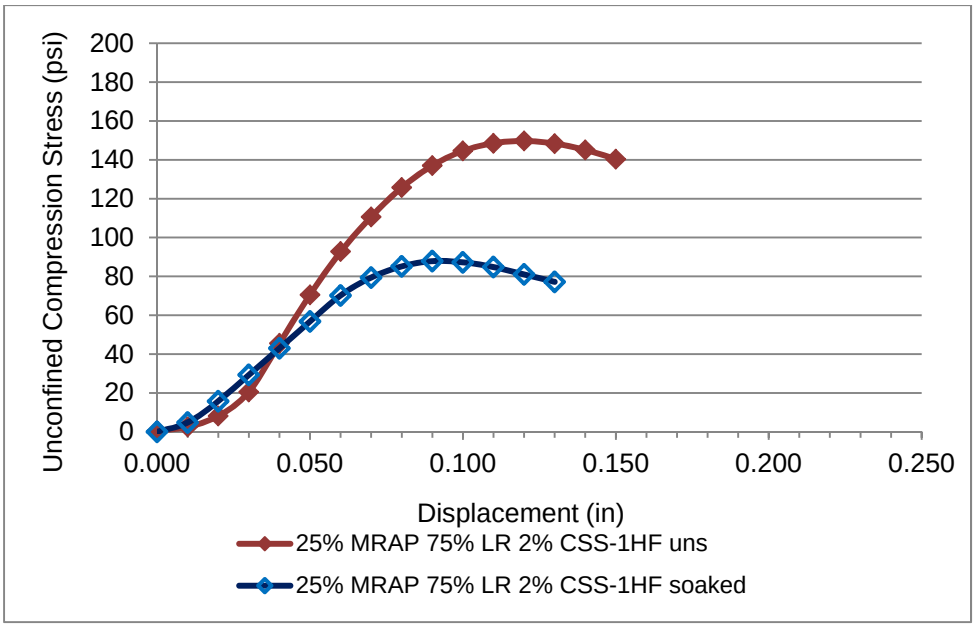

Figure F-22: Unconfined Compression Trial 18: 50% MRAP 50% LR 2% CSS-1HF

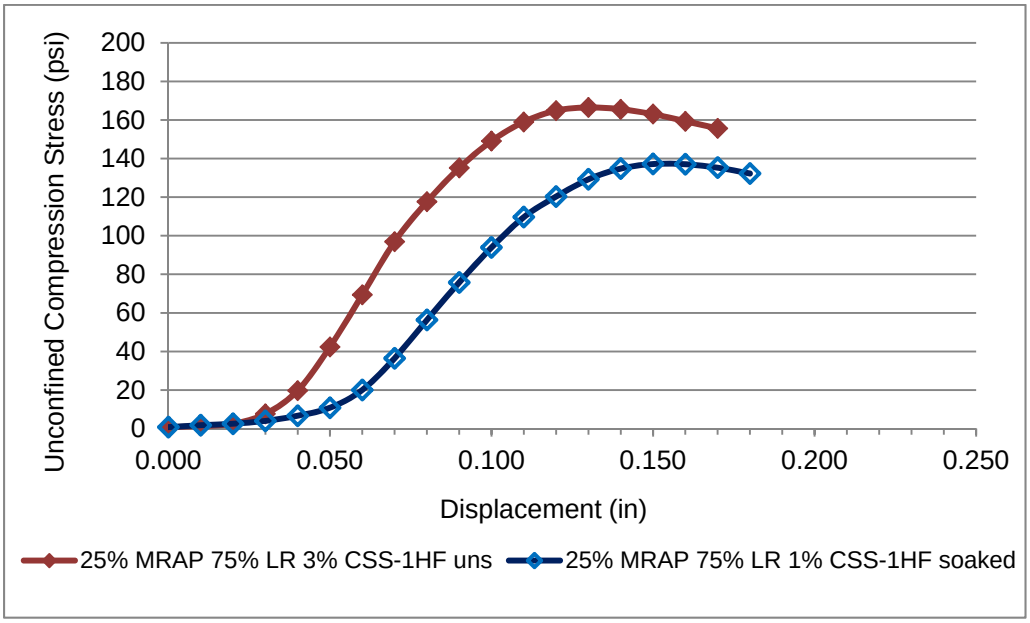

Figure F-23: Unconfined Compression Trial 19: 50% MRAP 50% LR 3% CSS-1HF

F.3.2.4. 25%/75%

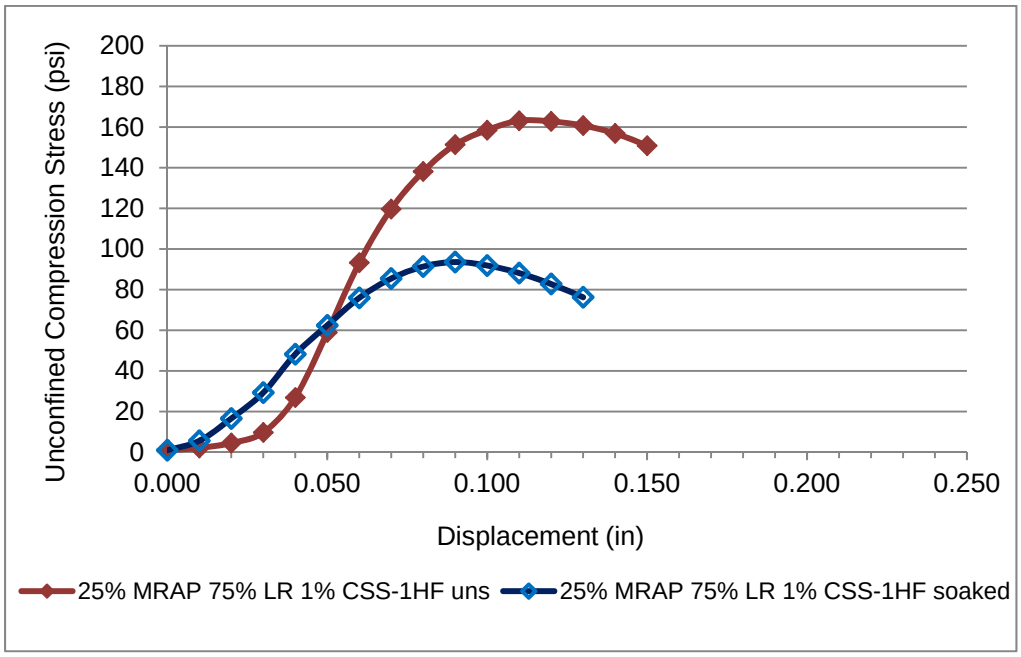

Figure F-24 Unconfined Compression Trial 20: 25% MRAP 75% LR 1% CSS-1HF

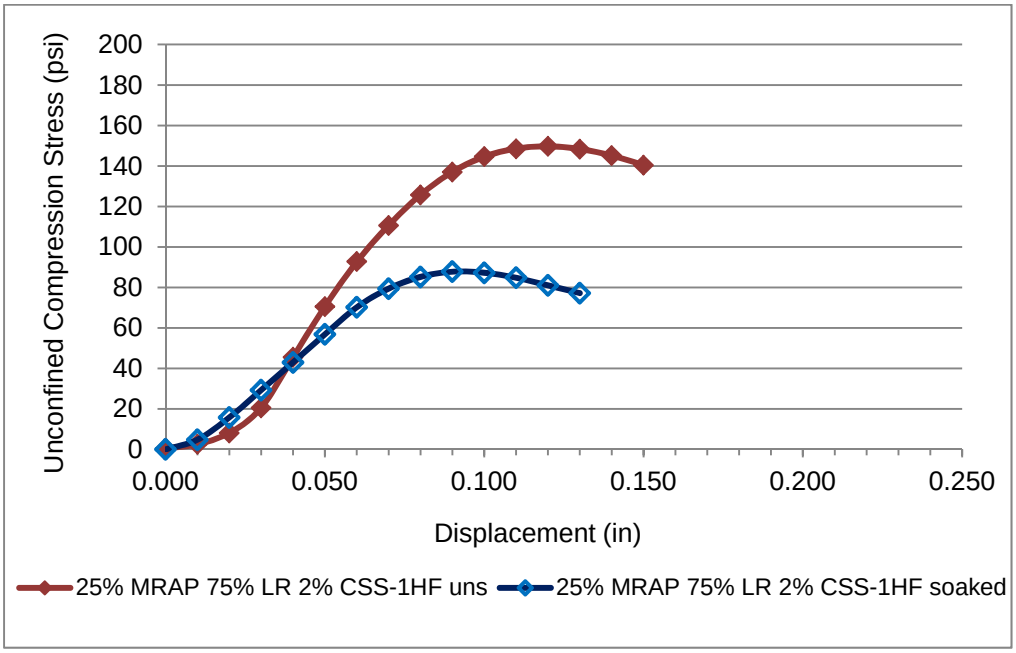

Figure F-25 Unconfined Compression Trial 21: 25% MRAP 75% LR 2% CSS-1HF

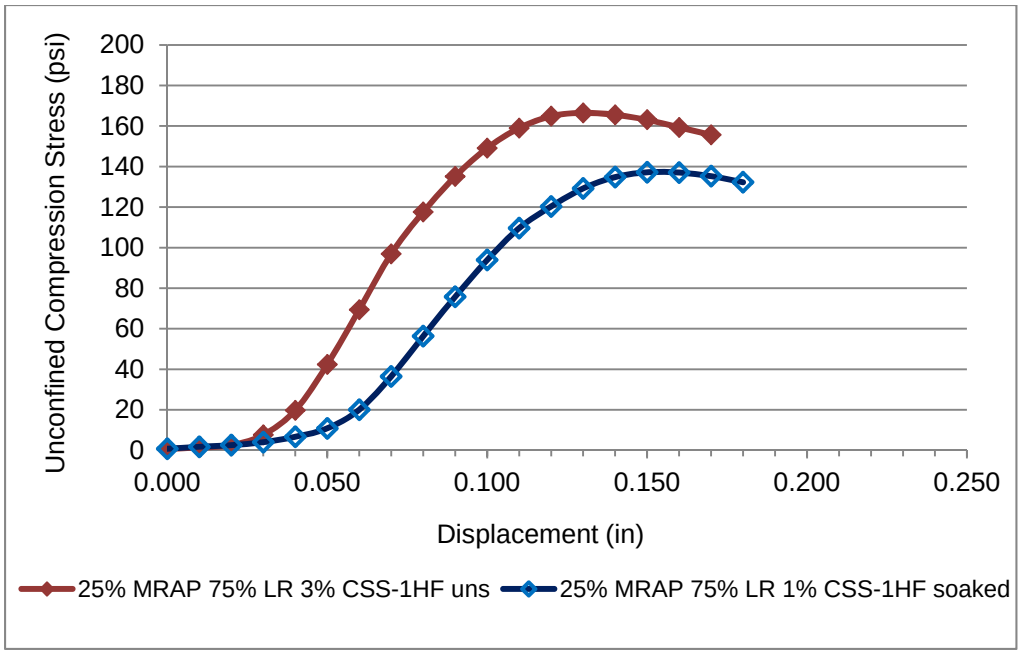

Figure F-26: Unconfined Compression Trial 22: 25% MRAP 75% LR 3% CSS-1HF

F.3.2.5. Unconfined Compression 100% Limerock CSS-1HF

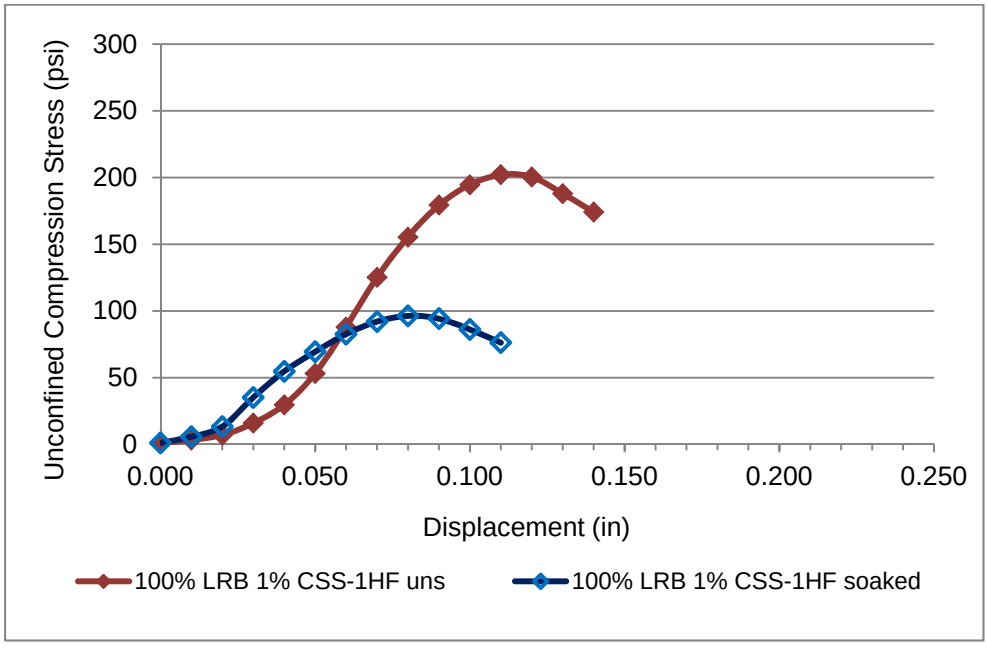

Figure F-27: Unconfined Compression Trial 29: 100% Limerock 1% CSS-1HF

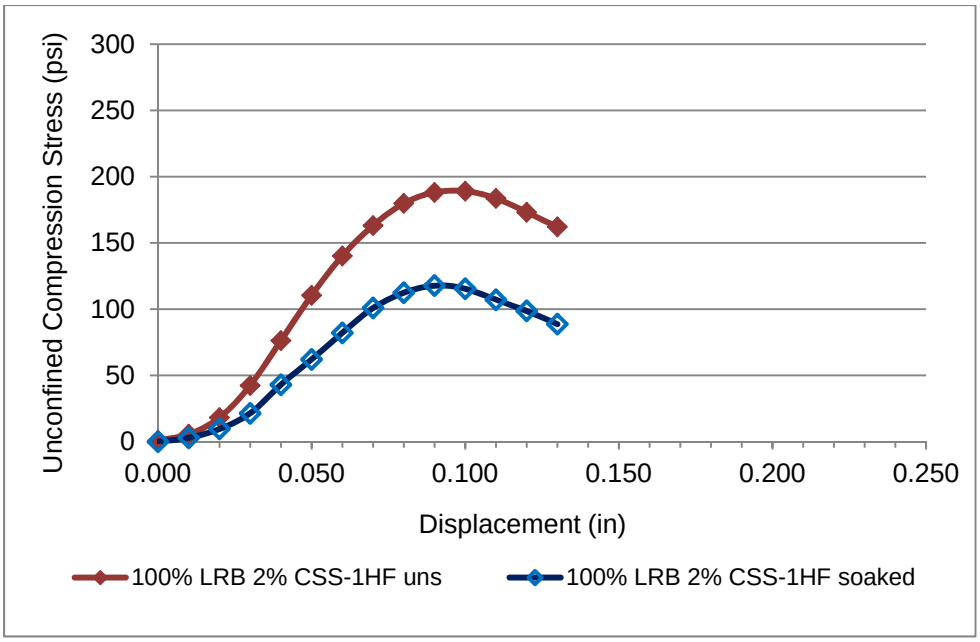

Figure F-28: Unconfined Compression Trial 30: 100% Limerock 2% CSS-1HF

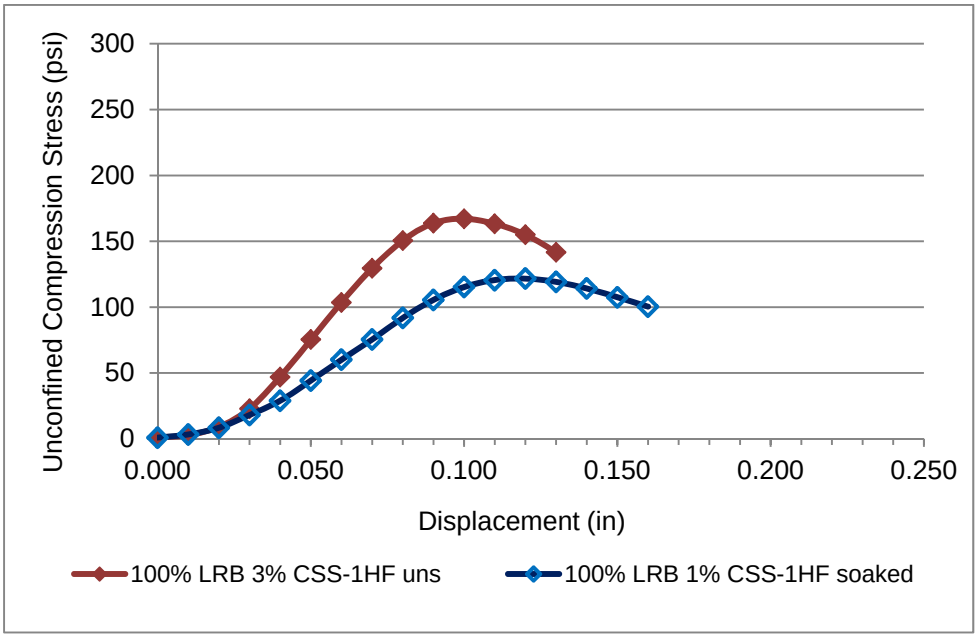

Figure F-29: Unconfined Compression Trial 31: 100% Limerock 3% CSS-1HF

F.4. Unconfined Compression Tests MRAP/Limerock Portland Cement

F.4.1. Unconfined Compression MRAP/Limerock Portland Cement Compaction Data

Table F-3: Unconfined Compression MRAP/LR Blends with Portland Cement

Trial Set	Soaked/ Unsoaked	MRAP %	% Cement	Moisture Content	Dry Density	Peak Strength (psi)	Max Displ (in)
27	Unsoaked	100%	0%	8.0%	104.9	68.4	0.110
38	Unsoaked	100%	1%	8.1%	114.9	63.5	0.110
39	Unsoaked	100%	2%	9.1%	112.6	108.2	0.100
40	Unsoaked	100%	3%	8.0%	119.1	154.1	0.120
27	Soaked	100%	0%	8.0%	105.2	36.9	0.110
38	Soaked	100%	1%	8.1%	113.0	47.0	0.100
39	Soaked	100%	2%	9.1%	112.3	94.1	0.090
40	Soaked	100%	3%	8.0%	117.0	138.3	0.100
16	Unsoaked	75%	0%	8.7%	113.1	93.3	0.100
42	Unsoaked	75%	1%	8.1%	118.6	89.0	0.090
43	Unsoaked	75%	2%	7.8%	114.3	156.0	0.100
44	Unsoaked	75%	3%	8.0%	112.8	245.0	0.095
16	Soaked	75%	0%	8.7%	112.3	44.2	0.090
42	Soaked	75%	1%	8.1%	118.0	63.0	0.100
43	Soaked	75%	2%	7.8%	114.1	109.0	0.080
44	Soaked	75%	3%	8.0%	112.8	210.0	0.095
23	Unsoaked	50%	0%	7.0%	119.0	74.2	0.080
10	Unsoaked	50%	1%	7.6%	124.0	102.0	0.090
11	Unsoaked	50%	2%	7.3%	125.4	208.8	0.080
12	Unsoaked	50%	3%	7.6%	126.7	291.9	0.070
23	Soaked	50%	0%	7.0%	118.7	47.1	0.070
10	Soaked	50%	1%	7.6%	123.8	94.4	0.090
11	Soaked	50%	2%	7.3%	124.1	200.2	0.080
12	Soaked	50%	3%	7.5%	126.3	276.5	0.090
24	Unsoaked	25%	0%	8.2%	123.1	131.9	0.080
45	Unsoaked	25%	1%	7.8%	129.2	185.7	0.100
46	Unsoaked	25%	2%	7.4%	129.7	362.6	0.080
47	Unsoaked	25%	3%	7.7%	130.0	432.4	0.090
24	Soaked	25%	0%	8.2%	121.7	27.1	0.090

Trial Set	Soaked/ Unsoaked	MRAP %	% Cement	Moisture Content	Dry Density	Peak Strength (psi)	Max Displ (in)
45	Soaked	25%	1%	7.8%	127.4	118.6	0.090
46	Soaked	25%	2%	7.4%	120.0	227.1	0.070
47	Soaked	25%	3%	7.7%	128.8	323.1	0.080
26	Unsoaked	0%	0%	9.5%	129.0	145.0	0.060
48	Unsoaked	0%	1%	8.1%	131.3	244.0	0.100
49	Unsoaked	0%	2%	8.1%	132.7	413.0	0.070
50	Unsoaked	0%	3%	8.3%	132.2	529.5	0.070
26	Soaked	0%	0%	9.5%	128.3	0.0	N/A
48	Soaked	0%	1%	8.1%	129.3	146.1	0.070
49	Soaked	0%	2%	8.1%	130.6	254.8	0.060
50	Soaked	0%	3%	8.3%	131.4	408.6	0.090

F.4.2. Unconfined Compression MRAP/Limerock Portland Cement Plots

F.4.2.1. Unconfined Compression 100% MRAP Portland Cement

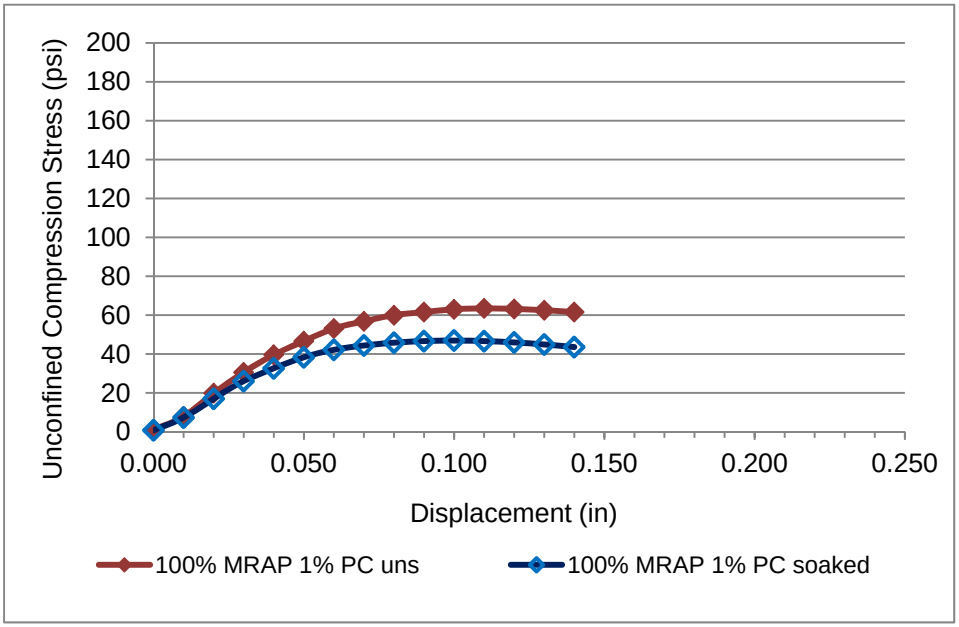

Figure F-30: Unconfined Compression: 100% MRAP 1% Cement

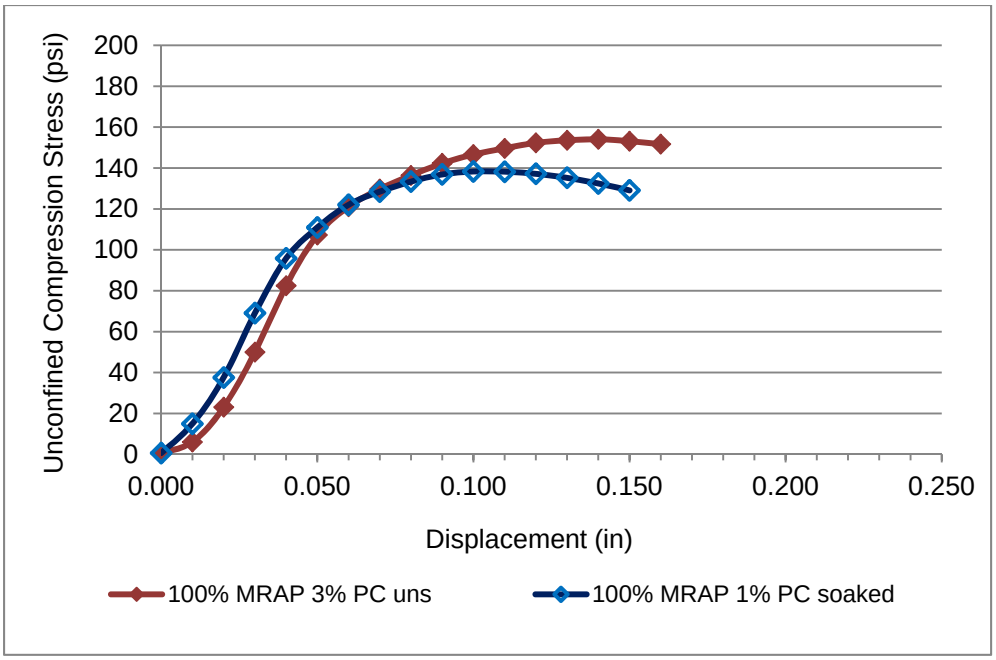

Figure F-31: Unconfined Compression: 100% MRAP 2% Cement

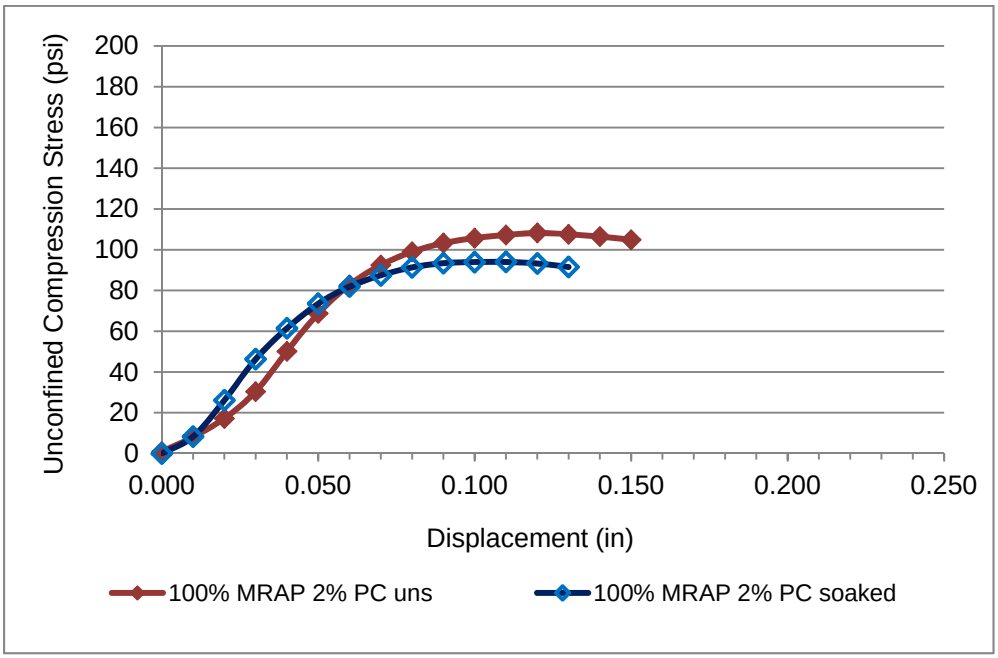

Figure F-32: Unconfined Compression: 100% MRAP 3% Cement

F.4.2.2. Unconfined Compression 75% MRAP/25% Limerock Portland Cement

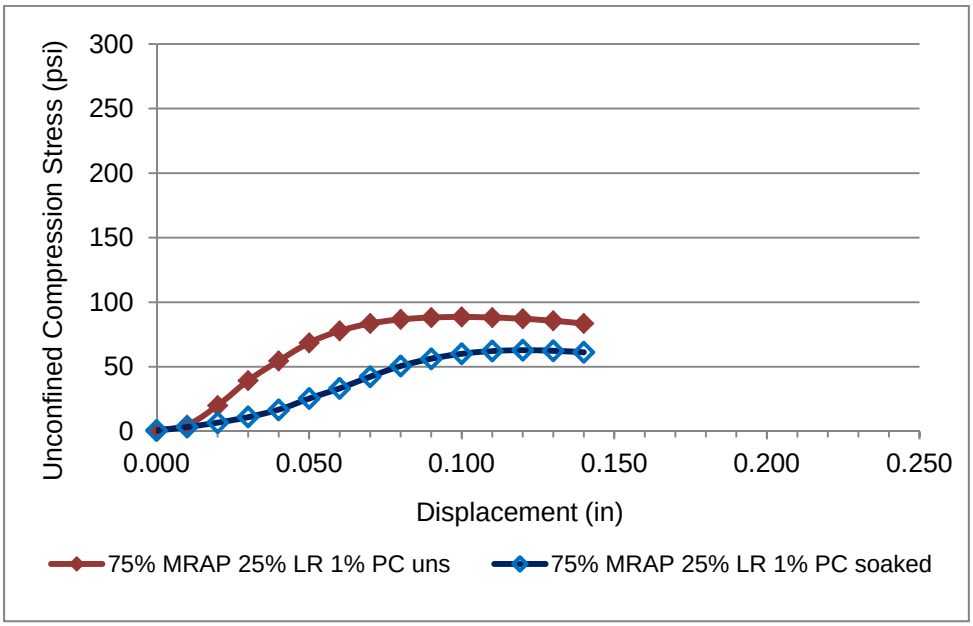

Figure F-33: Unconfined Compression: 75% MRAP/25% LR 1% Cement

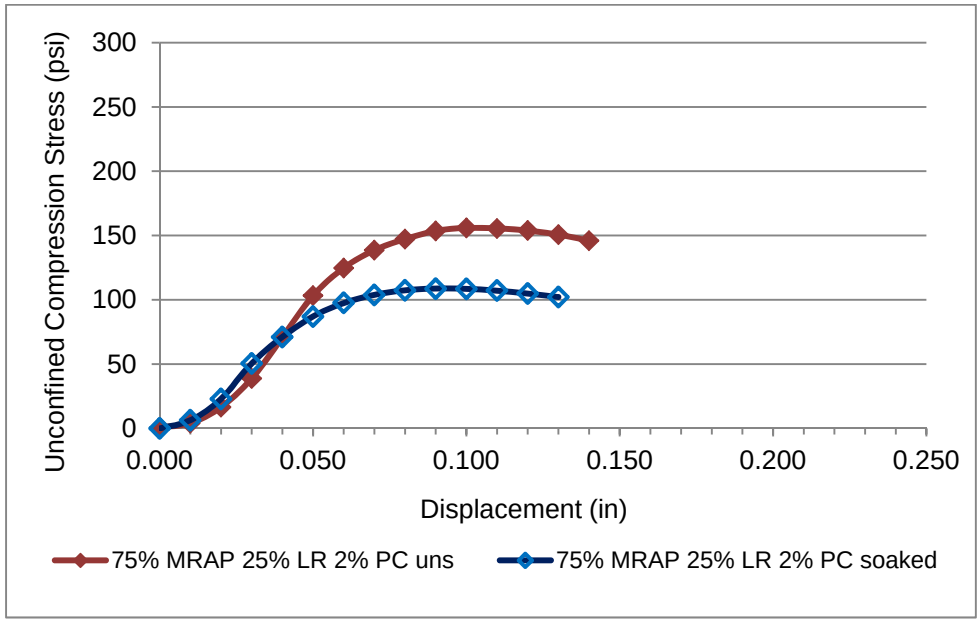

Figure F-34: Unconfined Compression: 75% MRAP/25% LR 2% Cement

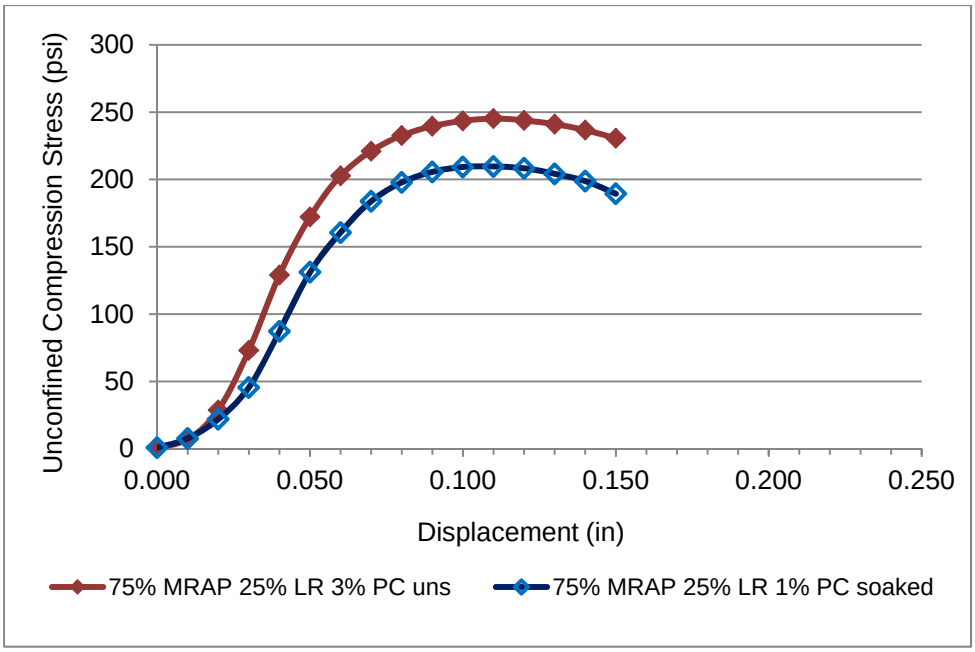

Figure F-35: Unconfined Compression: 75% MRAP/25% LR 3% Cement

F.4.2.3. Unconfined Compression 50% MRAP/50% Limerock Portland Cement

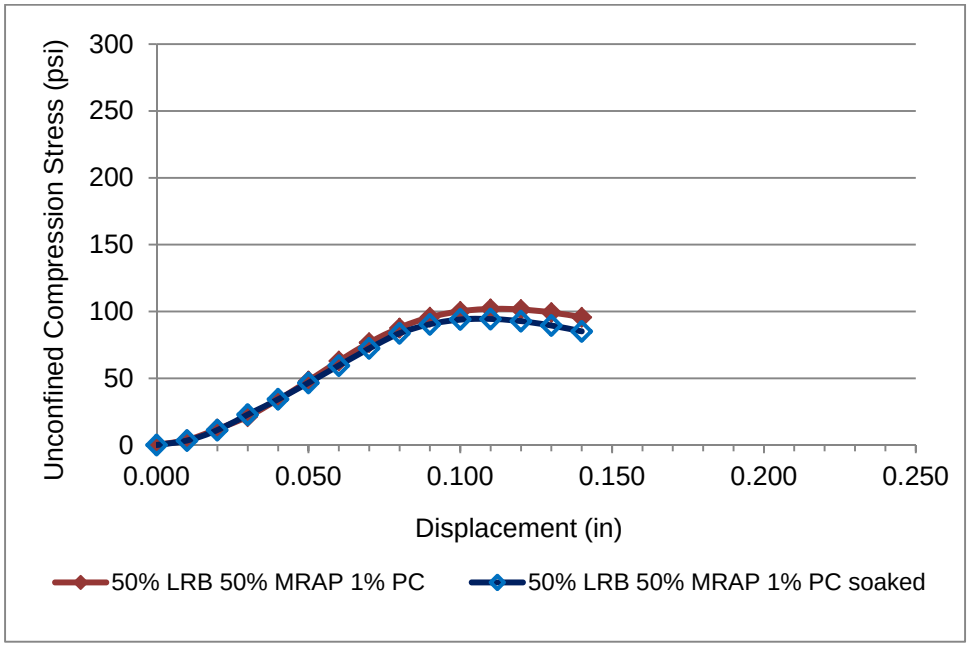

Figure F-36: Unconfined Compression: 50% MRAP/50% LR 1% Cement

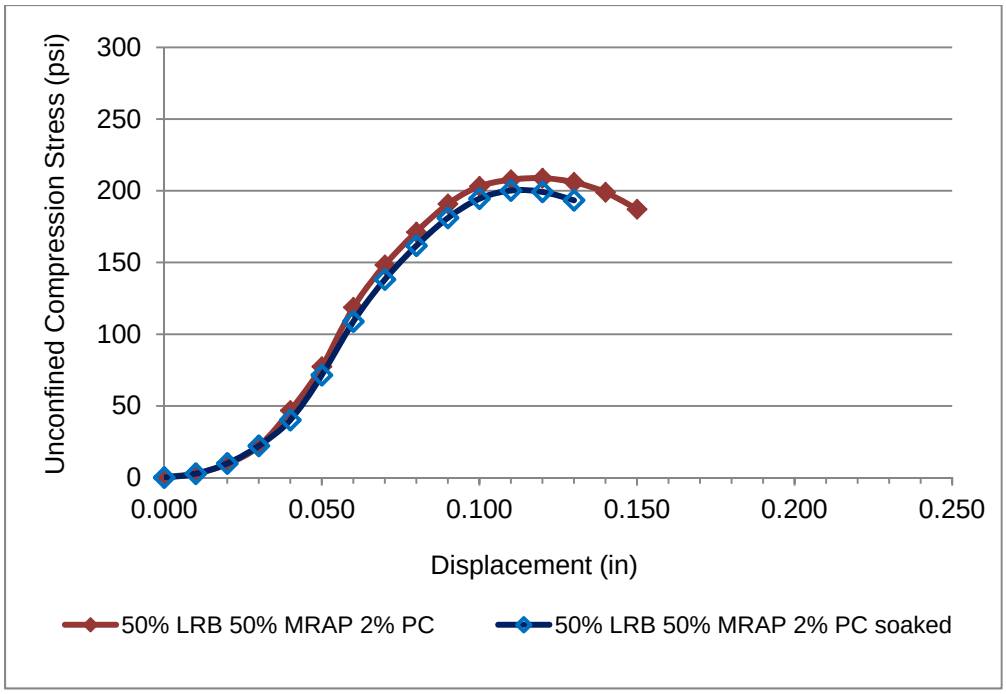

Figure F-37: Unconfined Compression: 50% MRAP/50% LR 2% Cement

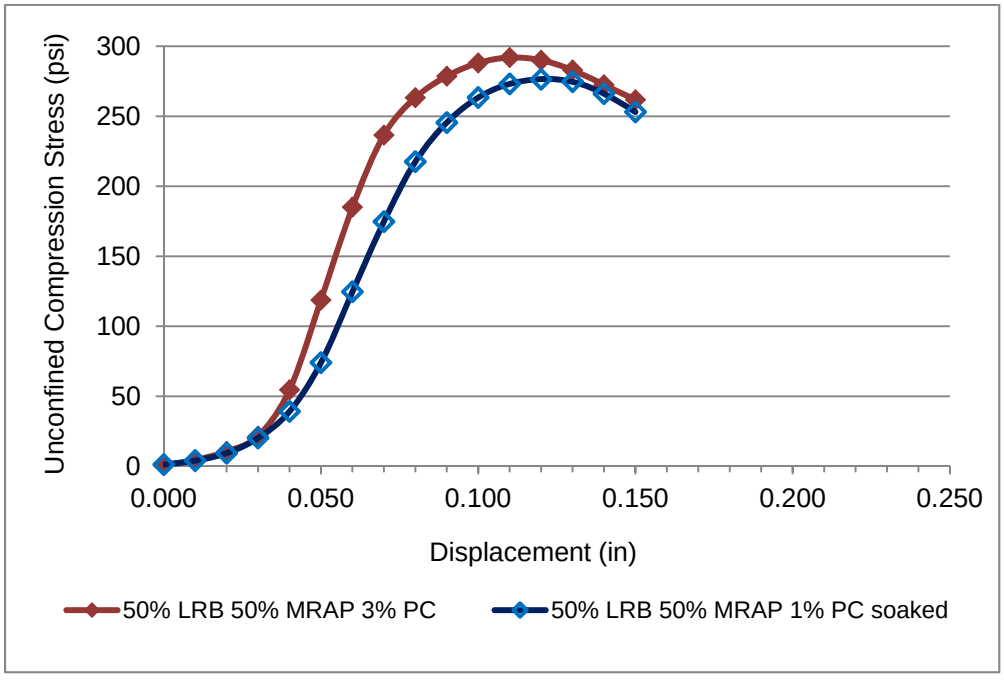

Figure F-38: Unconfined Compression: 50% MRAP/50% LR 3% Cement

F.4.2.4. Unconfined Compression 25% MRAP/75% Limerock Portland Cement

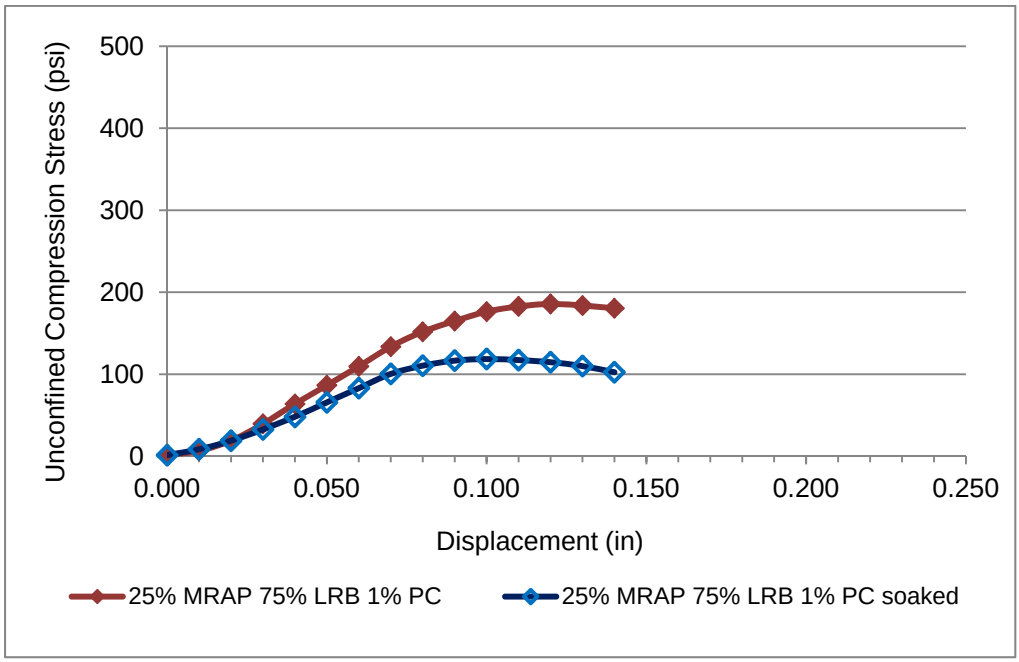

Figure F-39: Unconfined Compression Trial 45: 25% MRAP/75% LR 1% Cement

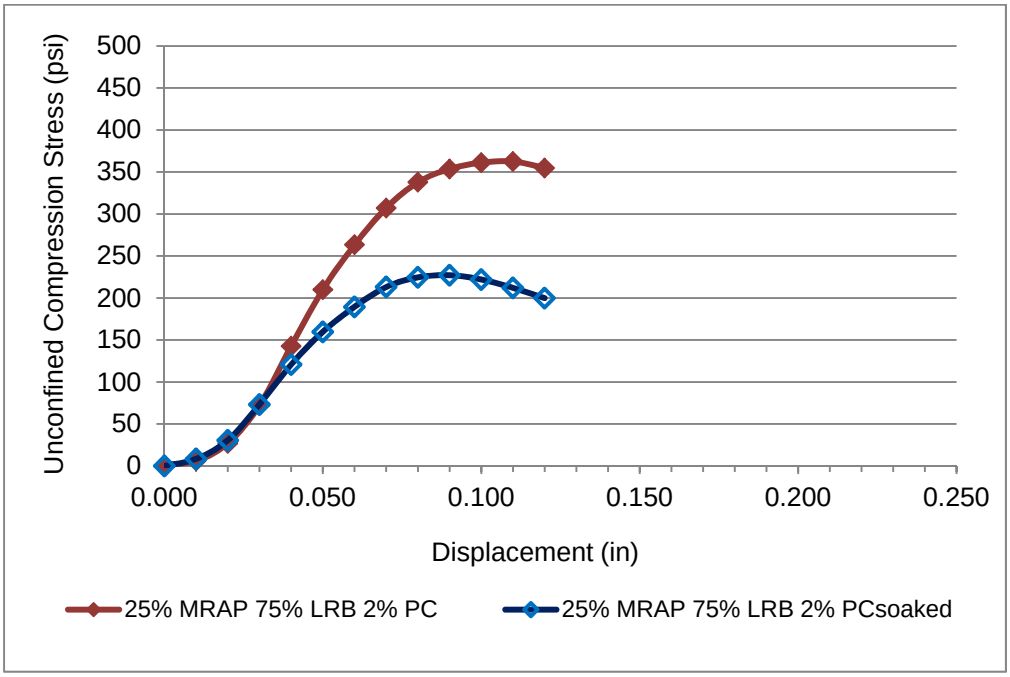

Figure F-40: Unconfined Compression Trial 46: 25% MRAP/75% LR 2% Cement

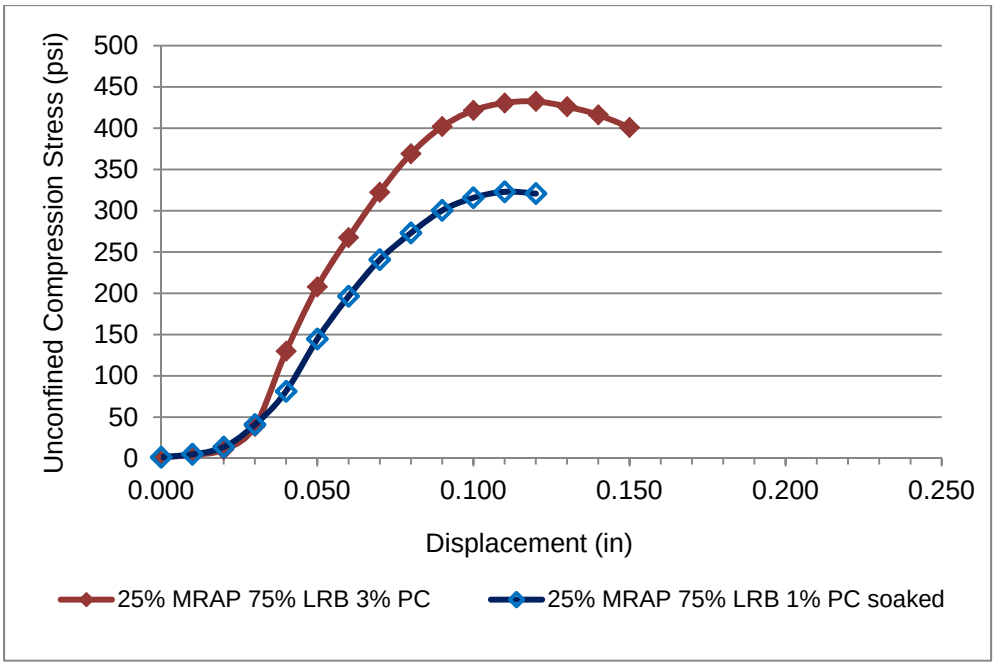

Figure F-41: Unconfined Compression Trial 47: 25% MRAP/75% LR 3% Cement

F.4.2.5. Unconfined Compression 100% Limerock Portland Cement

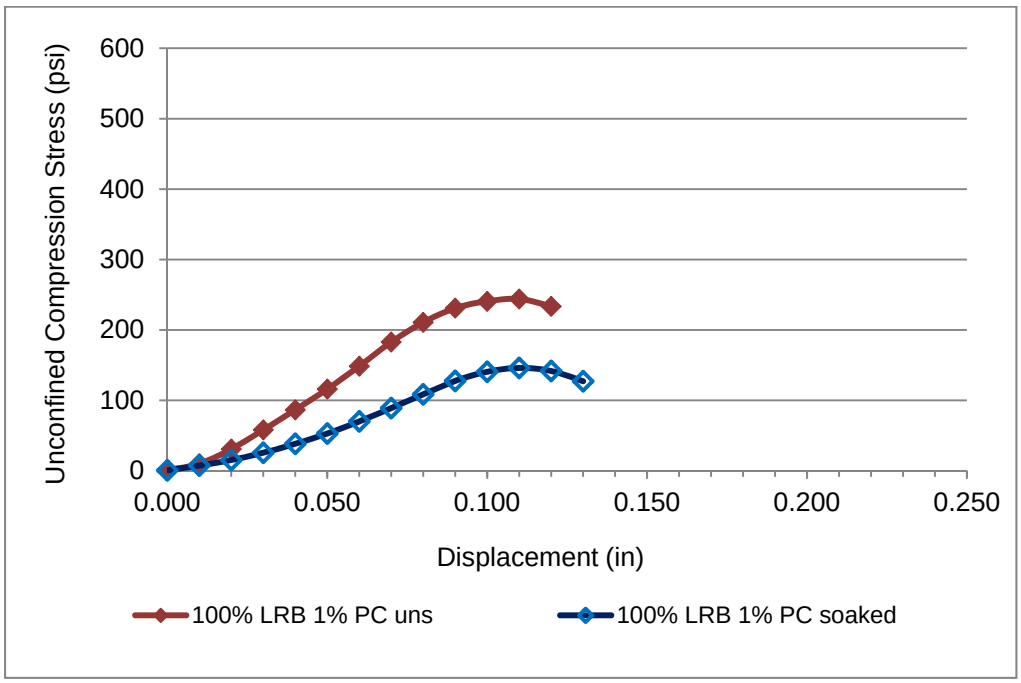

Figure F-42: Unconfined Compression Trial 50: 100% LR 1% Portland Cement

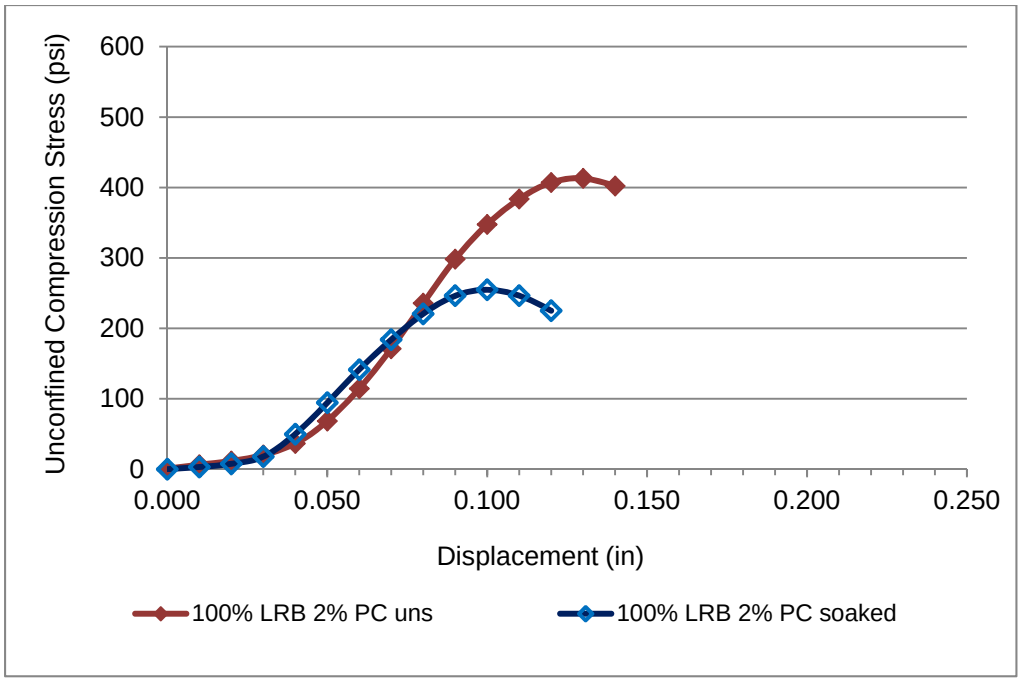

Figure F-43: Unconfined Compression Trial 50: 100% LR 2% Portland Cement

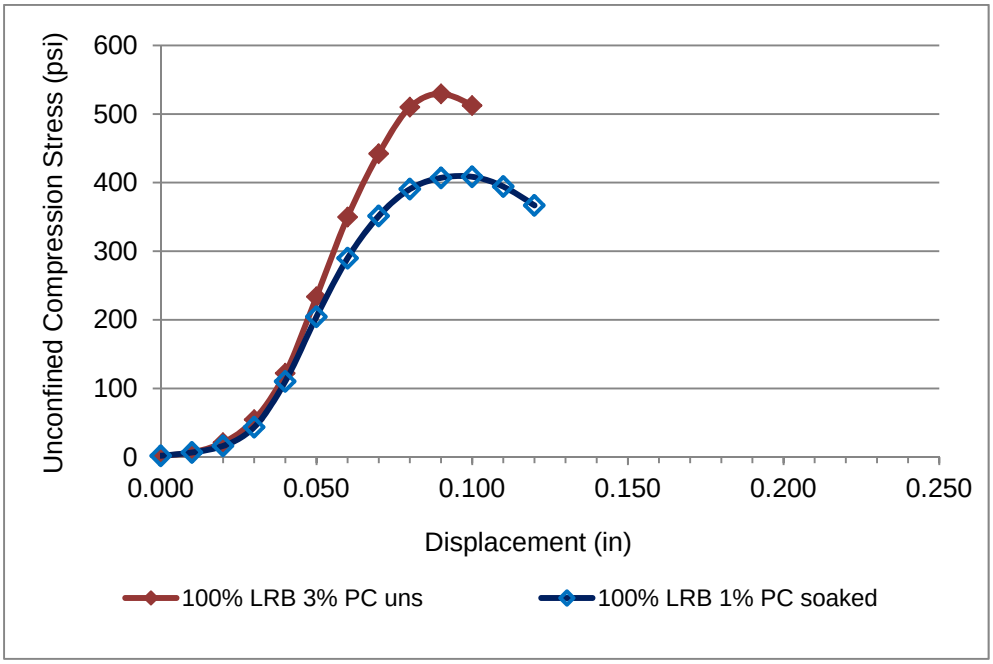

Figure F-44: Unconfined Compression Trial 50: 100% LR 3% Portland Cement

F.5. Unconfined Compression Tests MRAP/Limerock Lime

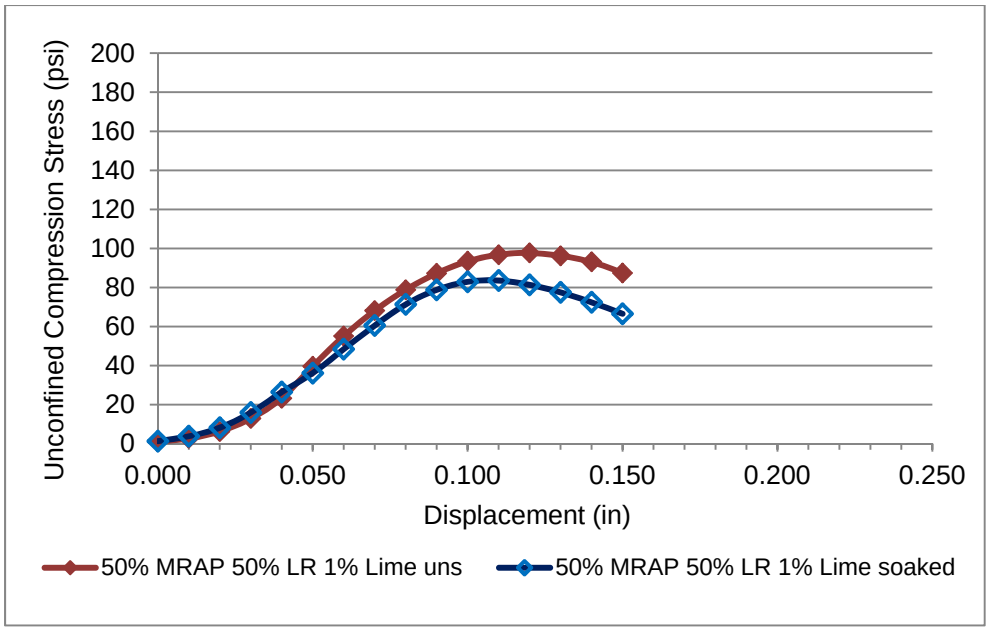

Figure F-45: Unconfined Compression Trial 35: 50% MRAP/50% LR 1% Lime

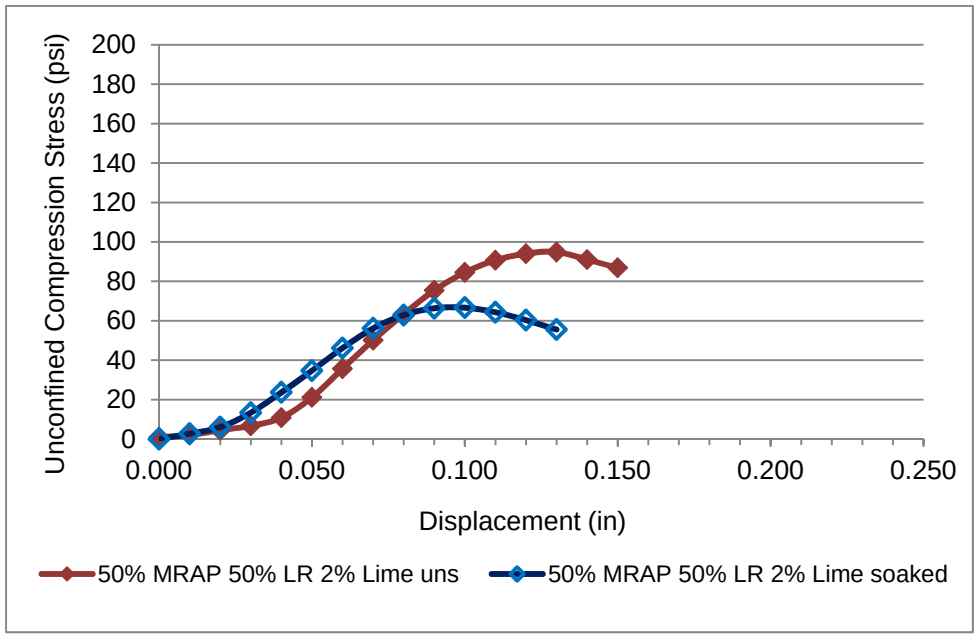

Figure F-46: Unconfined Compression Trial 36: 50% MRAP/50% LR 2% Lime

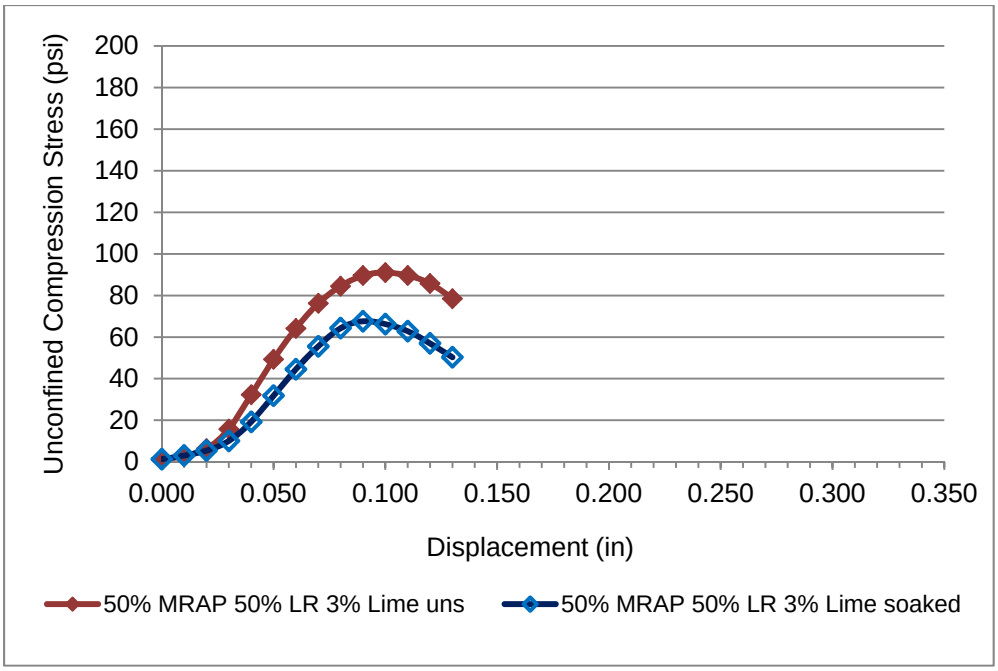

Figure F-47: Unconfined Compression Trial 37: 50% MRAP/50% LR 3% Lime

Appendix G - Soaked LBR Tests

G.1. Soaked LBR Tests FDOT Data 2011

Florida Department of Transportation

Aggregate Analysis System

Print Date: 1/11/2012 3:42:43 PM

Mine ID: 87090
Terminal ID:
Material ID: B01
Process: 1

Statistical Data
1/1/2011 to 1/11/2012
Sample Type: 03 (QC-Producer at Source)

Total Samples: 21

Geological Type:
Limerock

FSTM FM5-515 LBR

	Samples Found	Mean	Std. Dev.	Min	Max	Est. of Compliance	Z-Value	Lower Limit	Upper Limit	Target
Limerock bearing ratio	21	184.3	24.69	149	239	OK-NFP		100		
Maximum Density	21	128.5	1.40	126.0	131.0					
Percent Moisture	21	8.2	0.62	7.0	9.0					
Percent Pass 3.5" Sieve	21	100.0	0.00	100	100	OK		97	100	
Percent Pass No.4 Sieve	21	51.0	3.29	43	58					

G.2. Soaked LBR Tests Tabular Data

Table G-1: Soaked LBR Tests Tabular Data

Trial Set	Soaked/ Unsoaked	% MRAP	% Stabilizer	Agent	Moisture Content	Average Dry Density	Average LBR
S01	Soaked	50%	0%	No stab	6.6%	126.6	53.0
S06	Soaked	50%	1%	SS-1H	7.3%	123.5	106.0
S07	Soaked	50%	2%	SS-1H	7.4%	123.0	103.0
S08	Soaked	50%	3%	SS-1H	7.7%	121.6	100.0
S10	Soaked	50%	1%	CSS-1H	7.4%	122.2	127.0
S11	Soaked	50%	2%	CSS-1H	7.4%	122.4	105.0
S12	Soaked	50%	3%	CSS-1H	8.3%	123.0	107.0
S02	Soaked	50%	1%	PC	8.9%	121.1	175.0
S03	Soaked	50%	2%	PC	8.1%	121.0	288.0
S04	Soaked	50%	3%	PC	7.3%	129.3	396.0
S14	Soaked	25%	0%	No stab	7.7%	128.5	98.7
S13	Soaked	0%	0%	No stab	8.6%	130.0	162.0

G.3. Soaked LBR Tests Plots

G.3.1. Blends with No Stabilizer

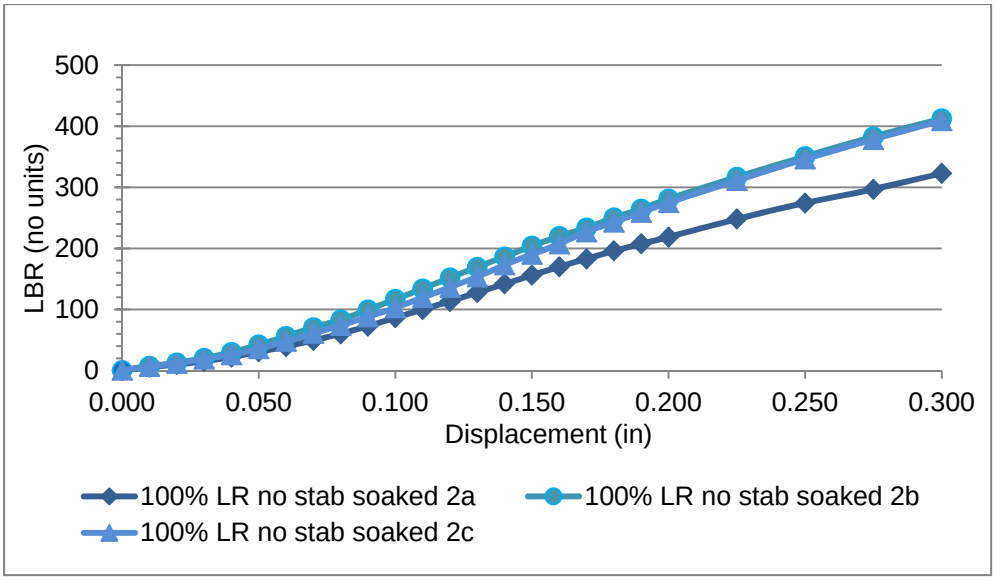

Figure G-1: Soaked LBR 100% Limerock without Stabilizer

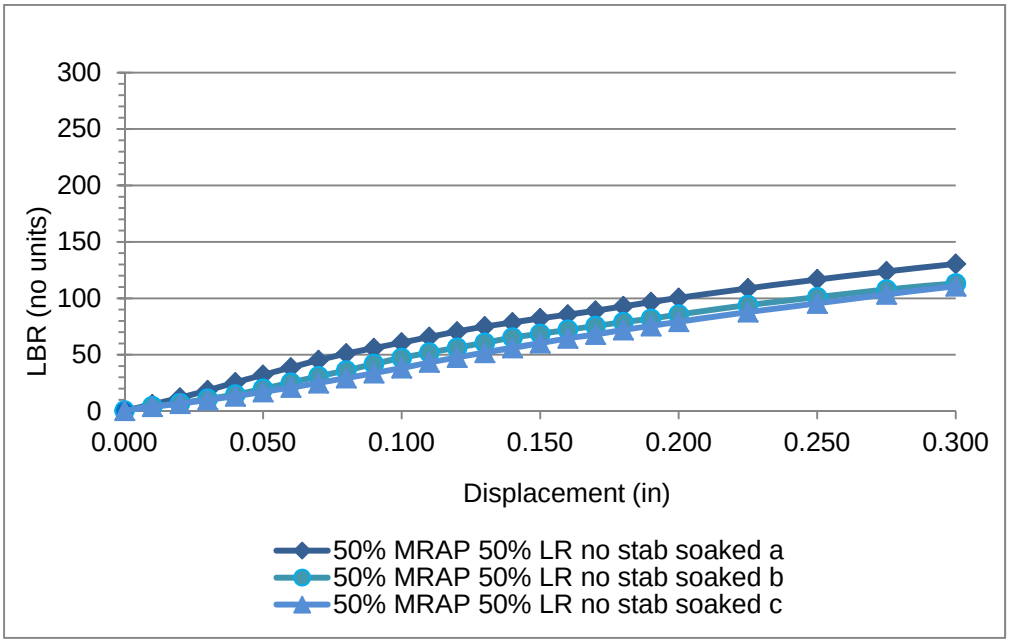

Figure G-2: Soaked LBR 50% MRAP/50% Limerock without Stabilizer

G.3.2. Soaked LBR 50% MRAP/50% LR SS-1H

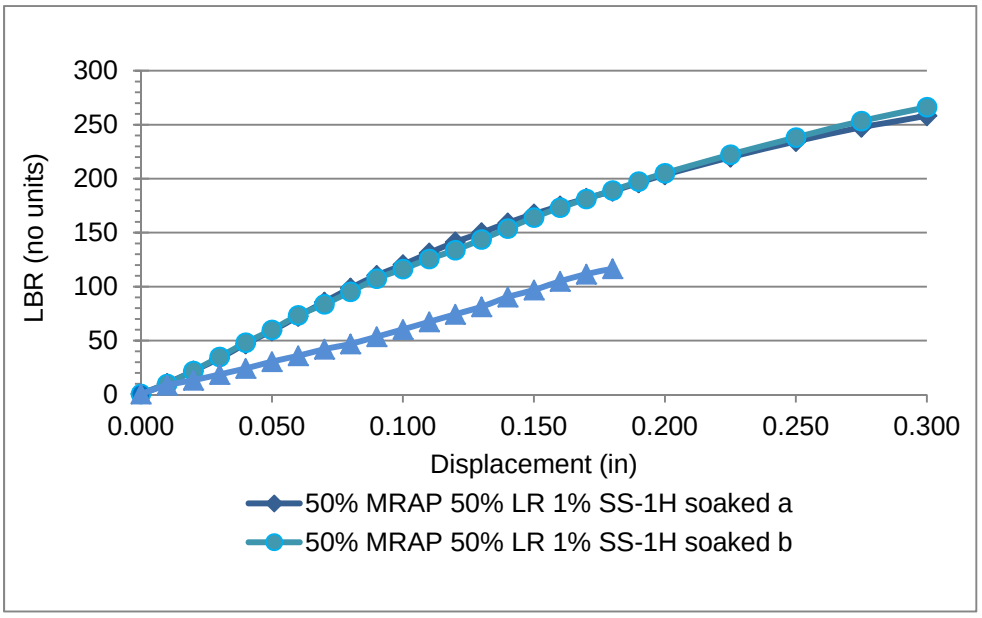

Figure G-3: Soaked LBR 50% MRAP/50% Limerock with 1% SS-1H

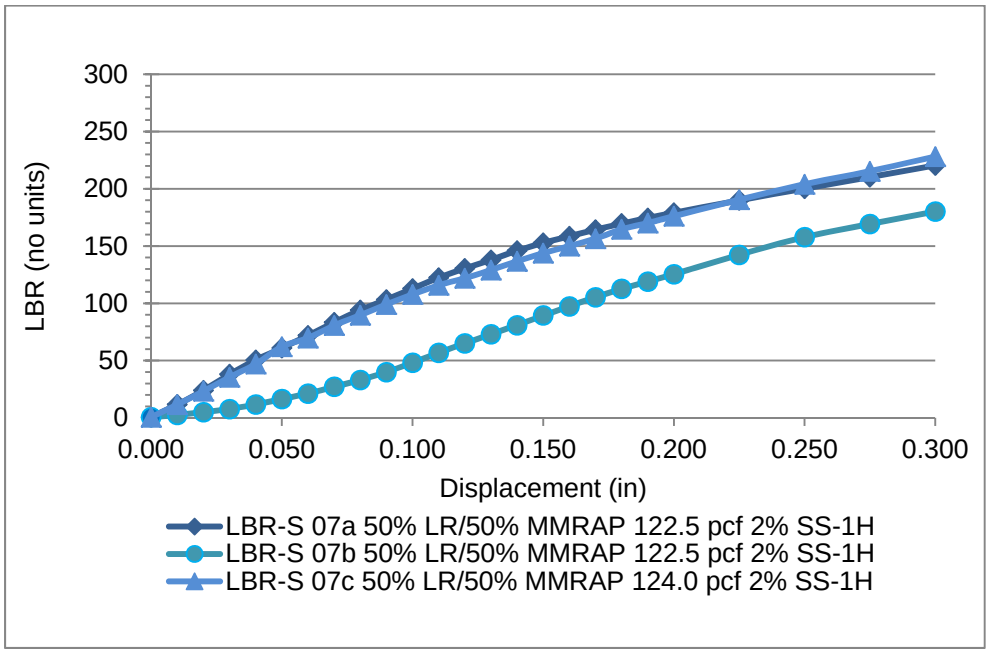

Figure G-4: Soaked LBR 50% MRAP/50% Limerock with 2% SS-1H

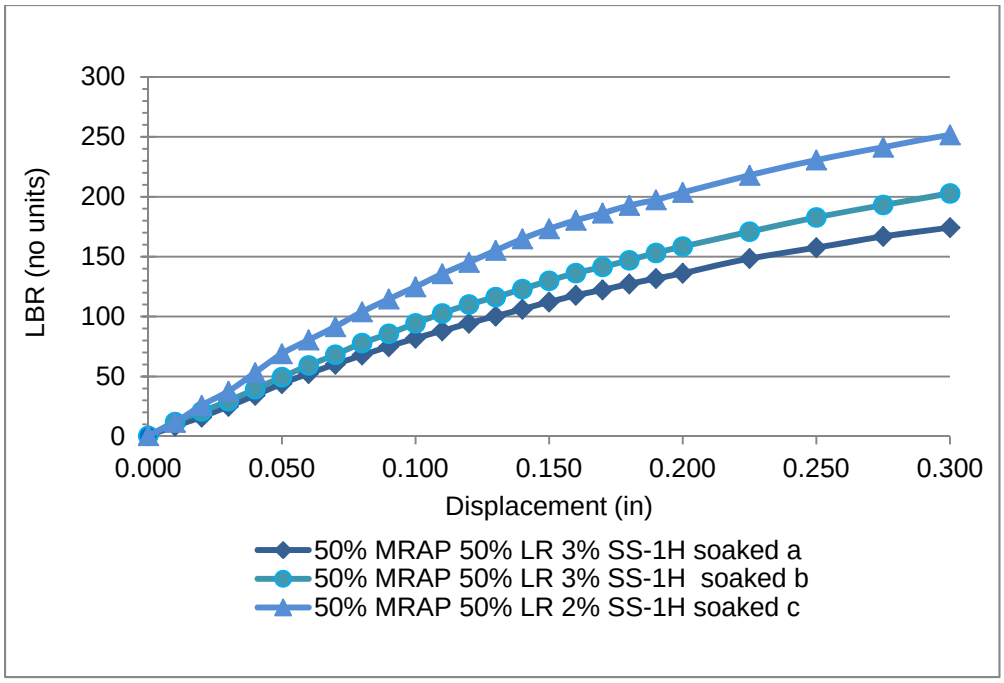

Figure G-5: Soaked LBR 50% MRAP/50% Limerock with 3% SS-1H

G.3.3. Soaked LBR 50% MRAP/50% LR CSS-1H

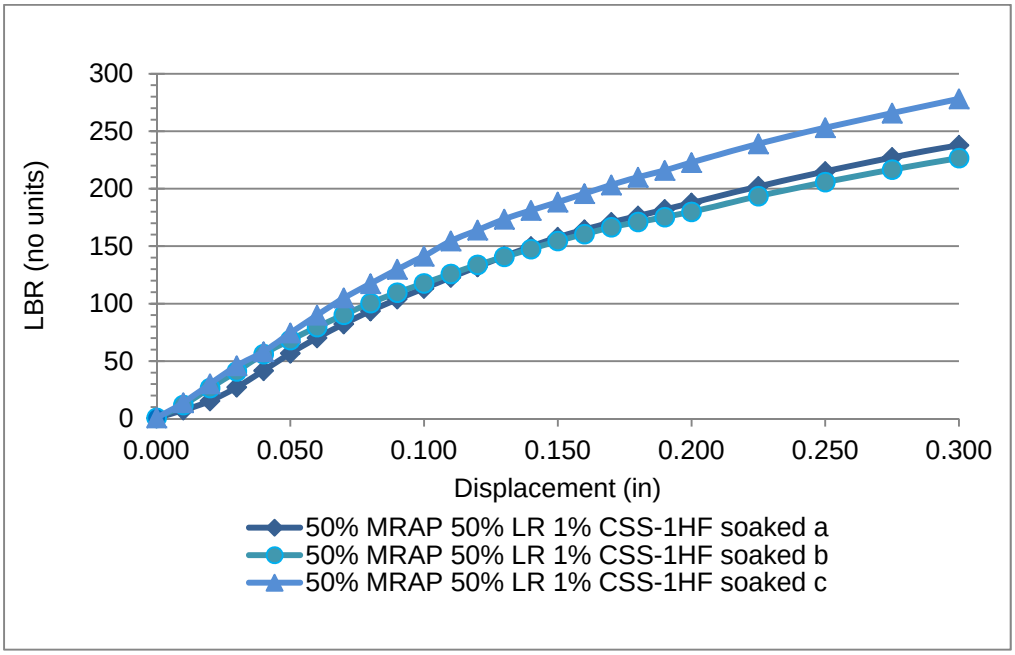

Figure G-6: Soaked LBR 50% MRAP/50% Limerock with 1% CSS-1H

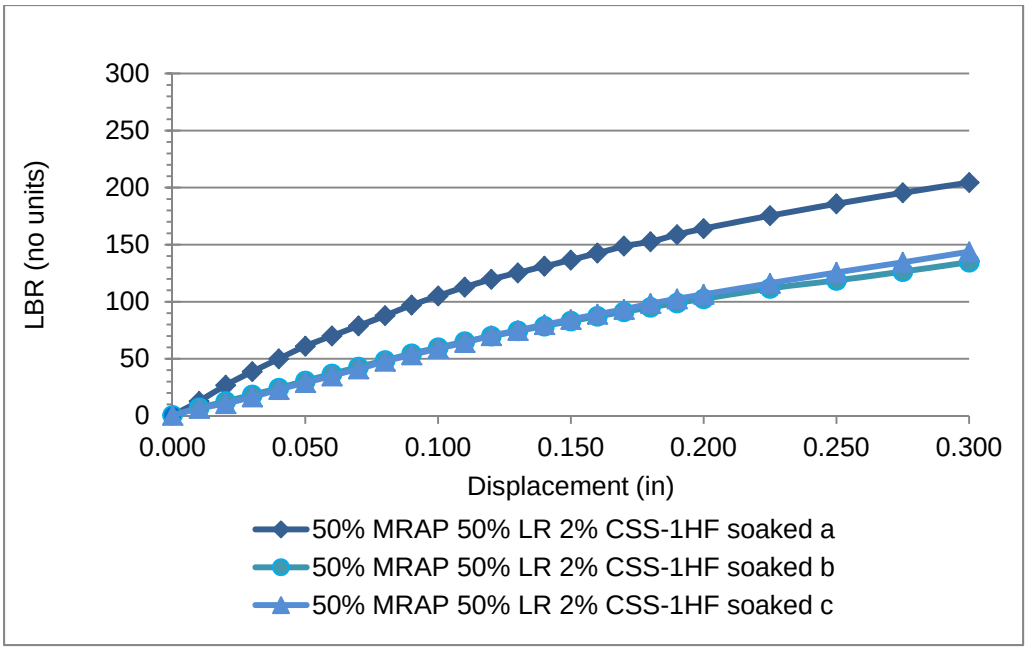

Figure G-7: Soaked LBR 50% MRAP/50% Limerock with 2% CSS-1H

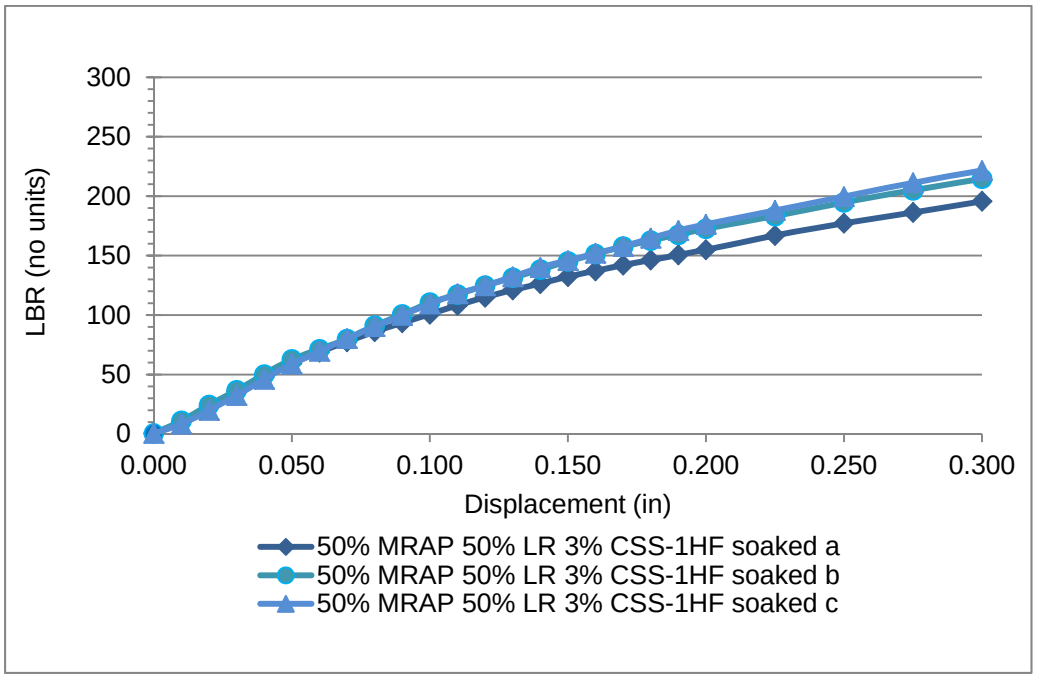

Figure G-8: Soaked LBR 50% MRAP/50% Limerock with 3% SS-1H

G.3.4. Soaked LBR 50% MRAP/50% LR Portland Cement

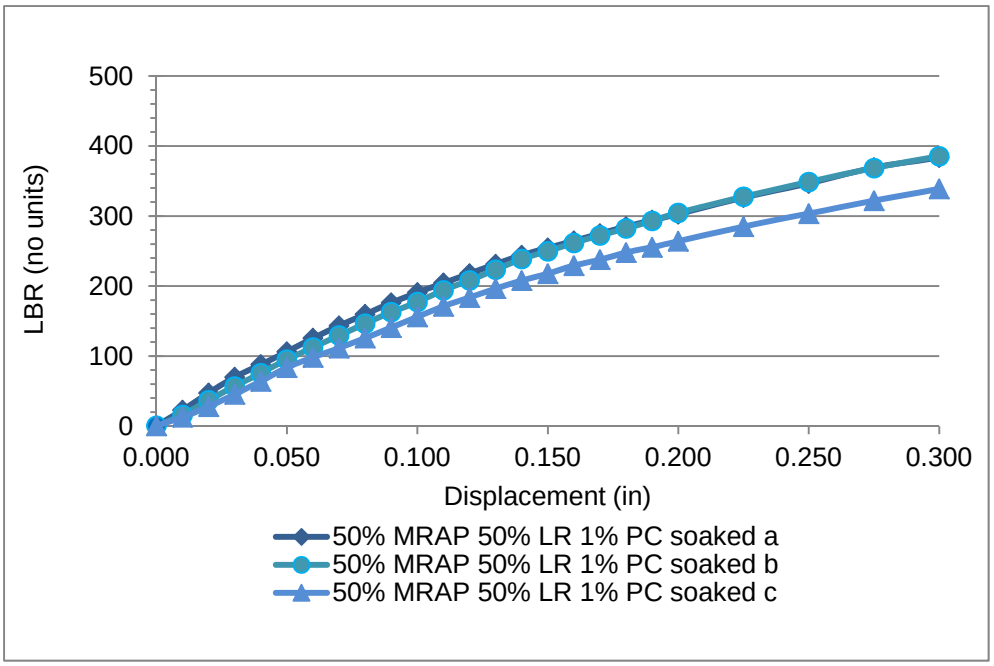

Figure G-9: Soaked LBR 50% MRAP/50% Limerock with 1% Cement

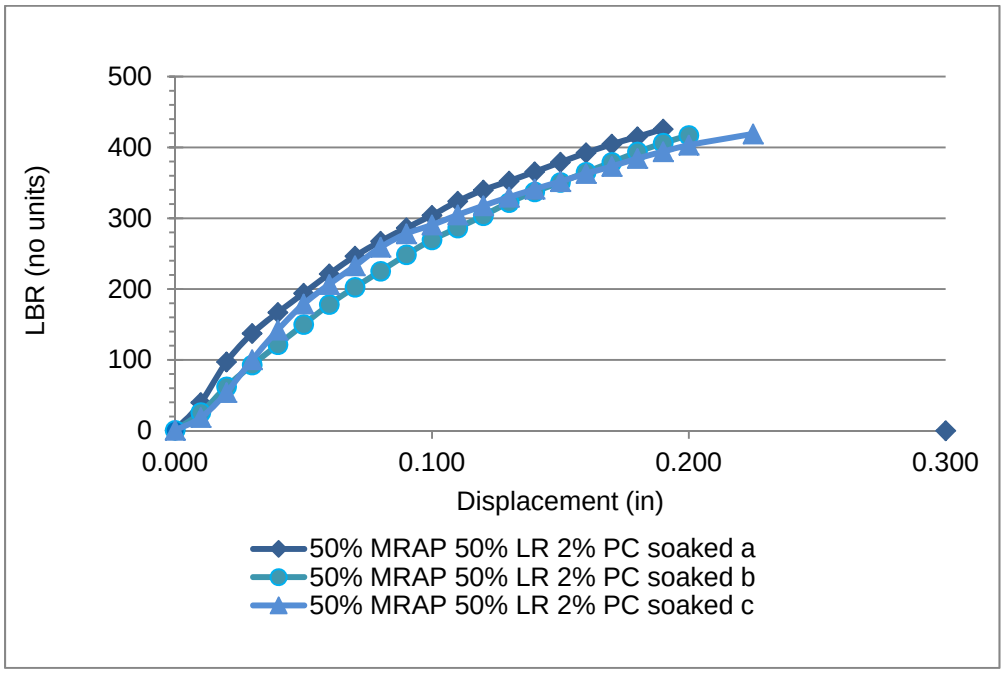

Figure G-10: Soaked LBR 50% MRAP/50% Limerock with 2% Cement

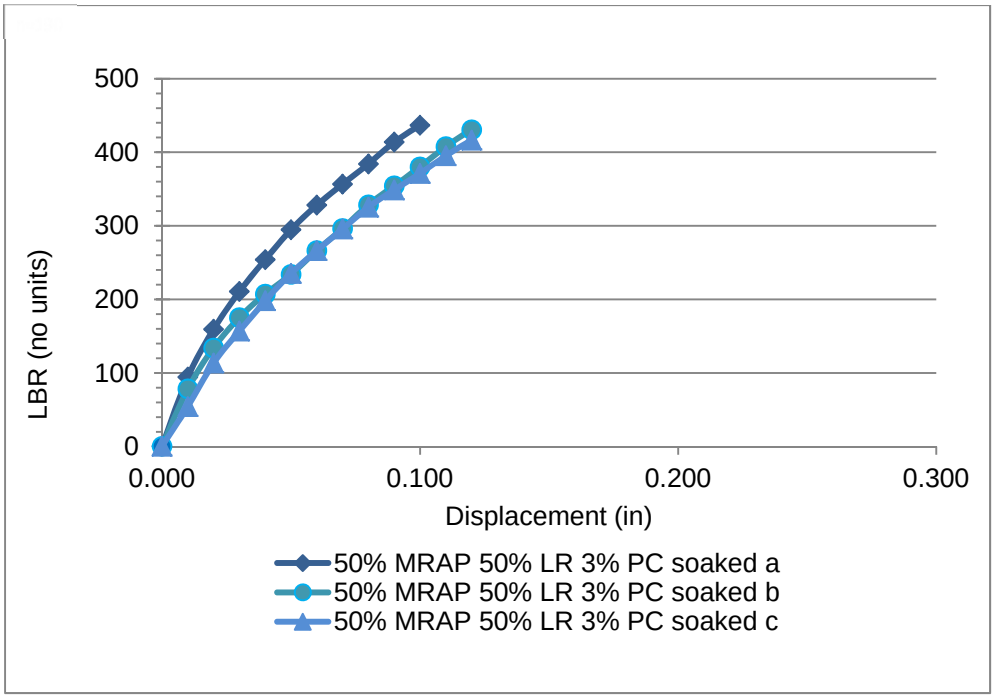

Figure G-11: Soaked LBR 50% MRAP/50% Limerock with 3% Cement

Appendix H - Indirect Tensile Tests

H.1. Indirect Tensile Tests Tabular Data

Table H-1: Indirect Tensile Test Tabular Data

Trial Set	Soak/ Uns	MRAP %	% Stab	Agent	Moist Cont	Avg Density	Avg Stress	Avg Deform
1	Uns	100%	0%	no stab	6.9%	115.9	9.2	0.080
1G	Uns	100%	0%	no stab	8.3%	112.0	23.5	0.080
1	Soak	100%	0%	no stab	7.0%	114.2	5.0	0.060
1G	Soak	100%	0%	no stab	8.7%	112.4	7.8	0.060
2	Uns	50%	0%	no stab	7.9%	121.5	11.7	0.050
2G	Uns	50%	0%	no stab	8.0%	121.5	19.7	0.070
7	Uns	50%	1%	SS-1H	8.2%	124.1	14.0	0.073
7G	Uns	50%	1%	SS-1H	7.8%	121.2	19.1	0.110
10	Uns	50%	1%	CSS-1H	7.7%	122.2	13.5	0.063
10G	Uns	50%	1%	CSS-1H	7.8%	122.2	24.4	0.080
19	Uns	50%	1%	PC	7.8%	122.7	12.5	0.060
19G	Uns	50%	1%	PC	8.2%	122.4	16.8	0.067
2	Soak	50%	0%	no stab	7.9%	120.2	2.2	0.040
2G	Soak	50%	0%	no stab	8.0%	120.4	5.0	1.568
7	Soak	50%	1%	SS-1H	8.2%	124.0	9.2	0.073
7G	Soak	50%	1%	SS-1H	7.8%	125.2	8.2	0.087
10	Soak	50%	1%	CSS-1H	7.7%	122.8	12.7	0.073
10G	Soak	50%	1%	CSS-1H	7.8%	122.1	16.0	0.083
19	Soak	50%	1%	PC	7.8%	123.9	6.2	0.055
19G	Soak	50%	1%	PC	8.2%	123.1	12.3	0.070
4	Uns	0%	0%	no stab	8.8%	128.2	0.4	0.023
4G	Uns	0%	0%	no stab	8.9%	130.0	0.6	0.027

H.2. Indirect Tensile Tests Plots

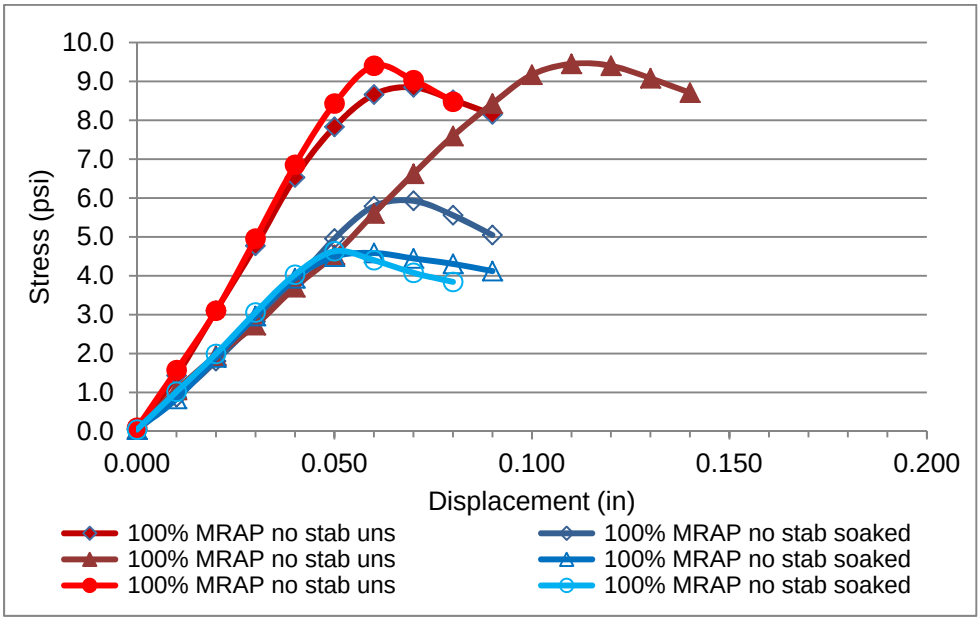

Figure H-1: IDT Trial 01 Mod Proctor 100% MRAP No Stabilizer

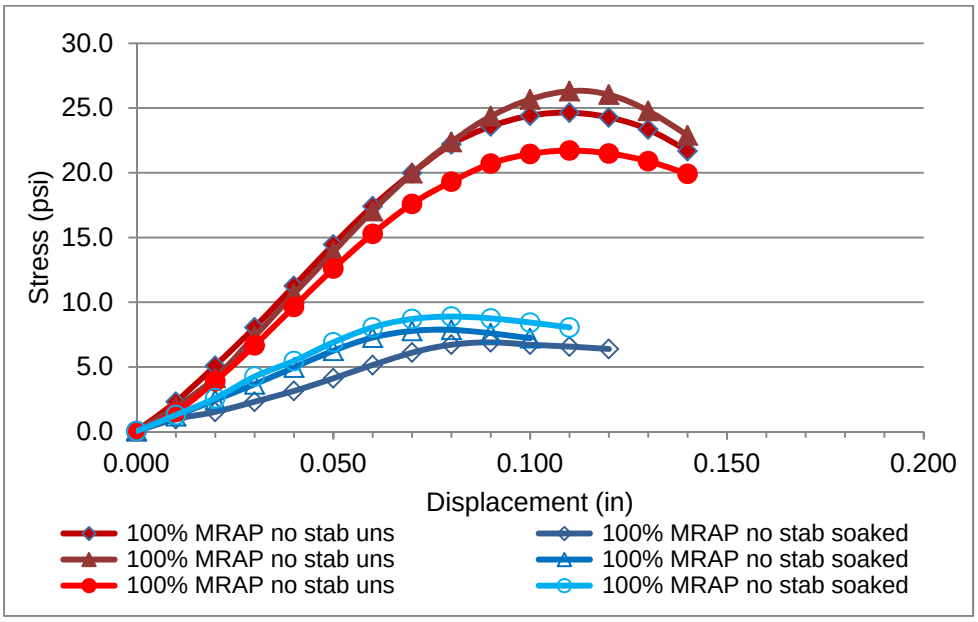

Figure H-2: IDT Trial 01G Gyratory 100% MRAP No Stabilizer

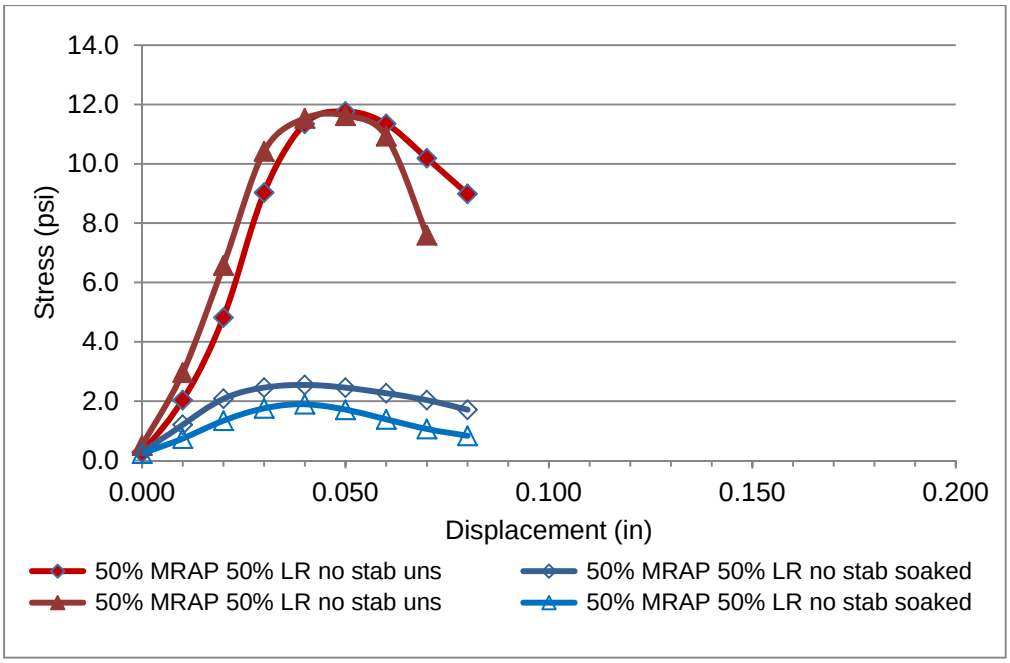

Figure H-3: IDT Trial 02 Mod Proctor 50% MRAP 50% LR No Stabilizer

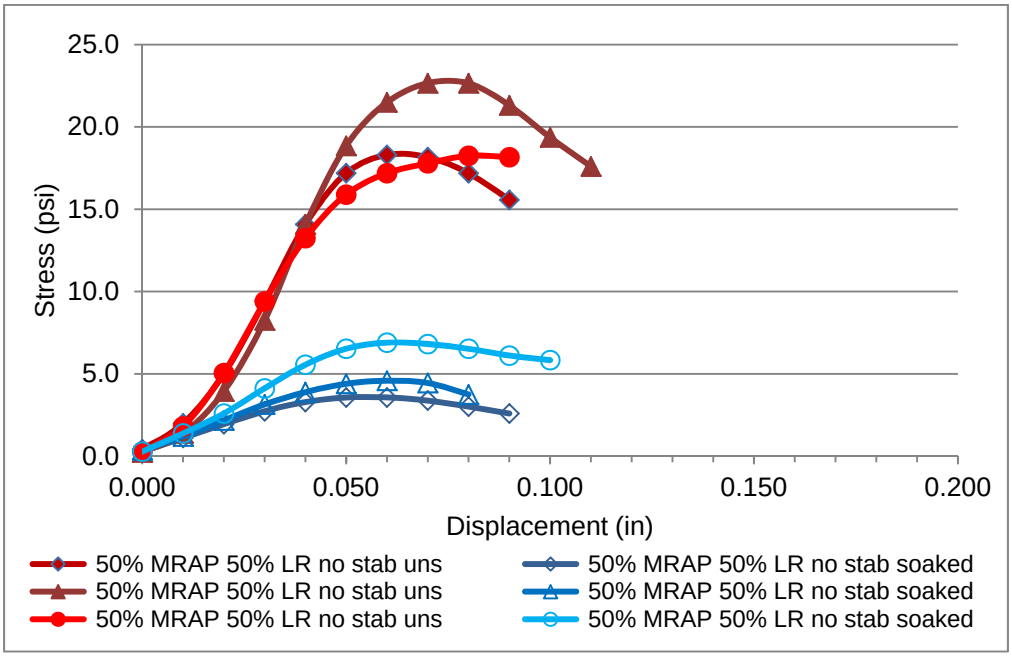

Figure H-4: IDT Trial 02G Gyratory 50% MRAP 50% LR No Stabilizer

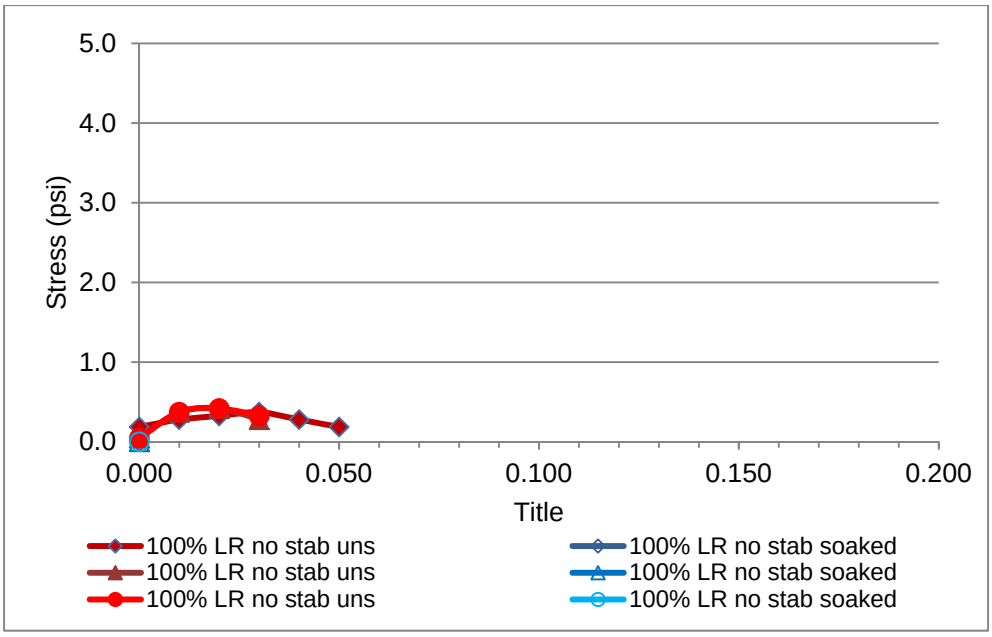

Figure H-5: IDT Trial 04 Mod Proctor 100% Limerock No Stabilizer

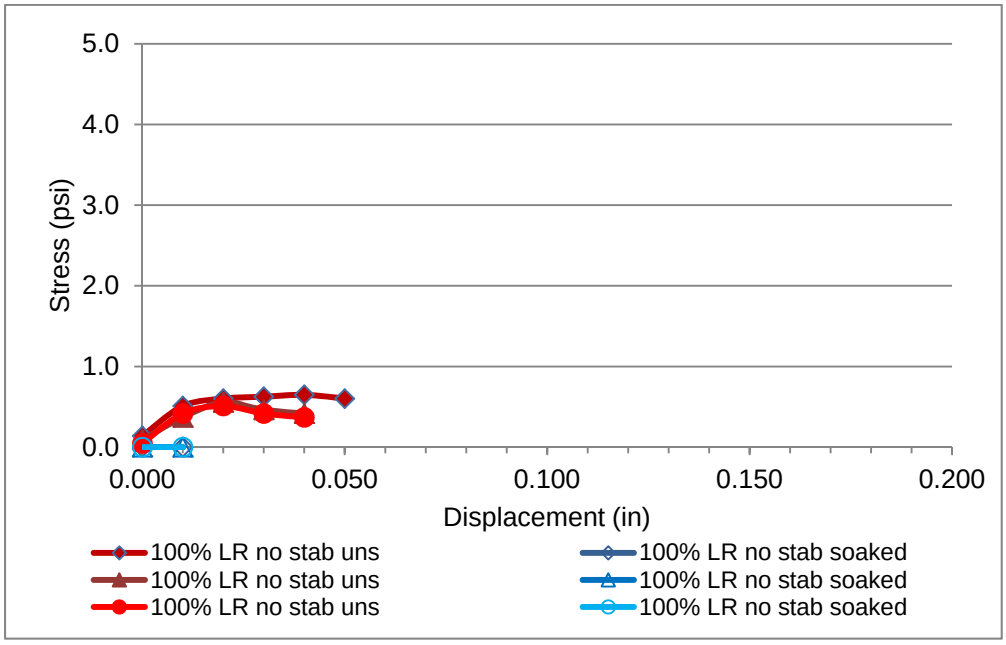

Figure H-6: IDT Trial 04G Gyratory 100% Limerock No Stabilizer

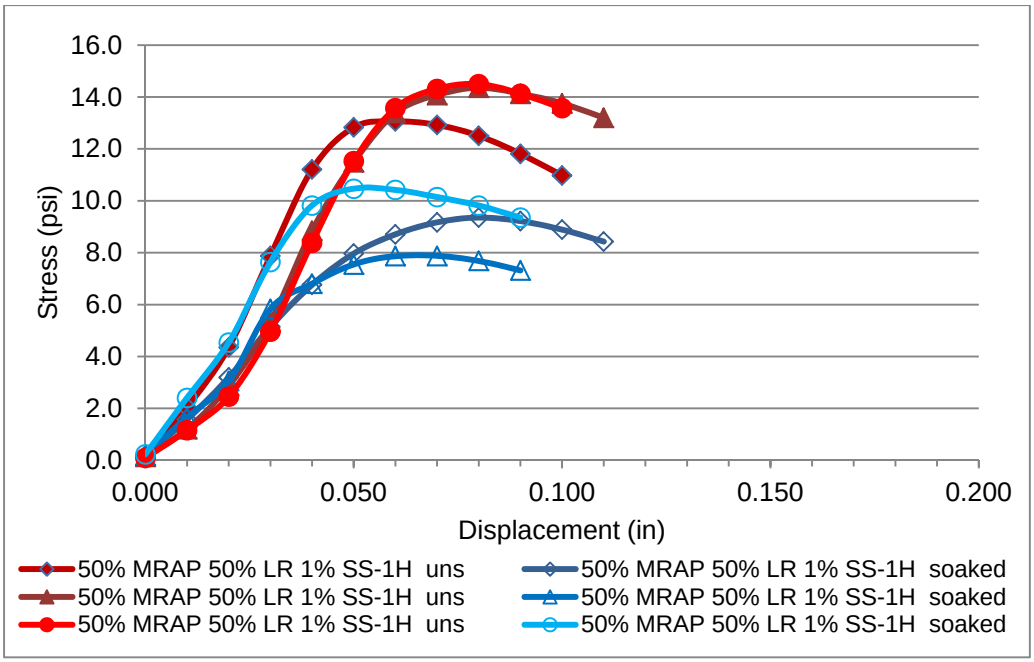

Figure H-7: IDT Trial 07 Mod Proctor 50% MRAP/50% Limerock 1% SS-1H

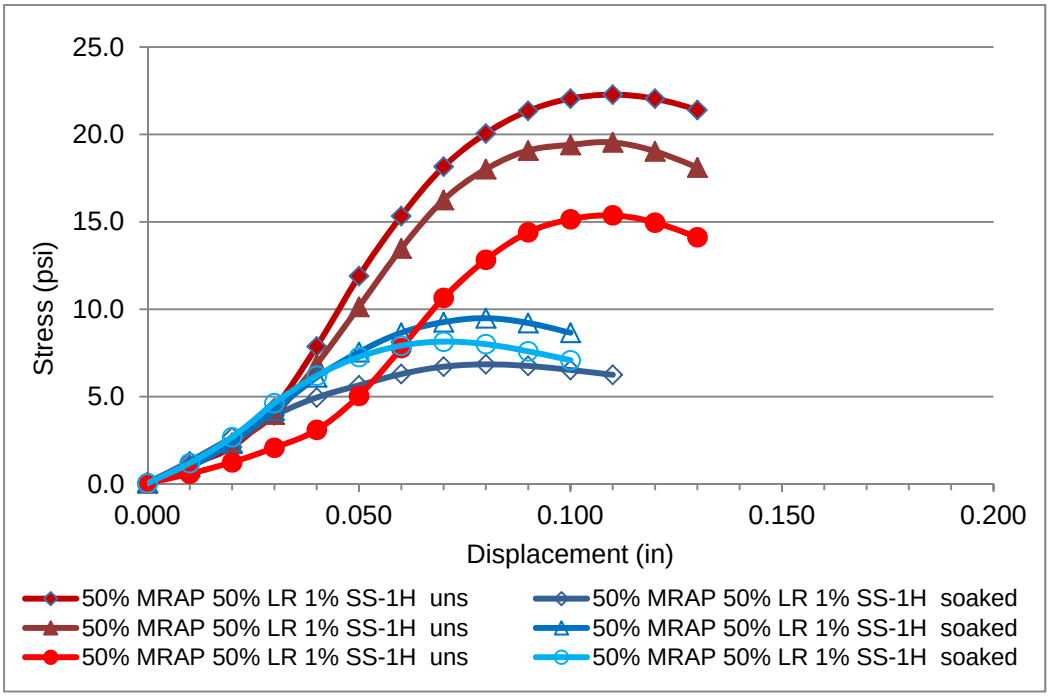

Figure H-8: IDT Trial 07G Gyratory 50% MRAP/50% Limerock 1% SS-1H

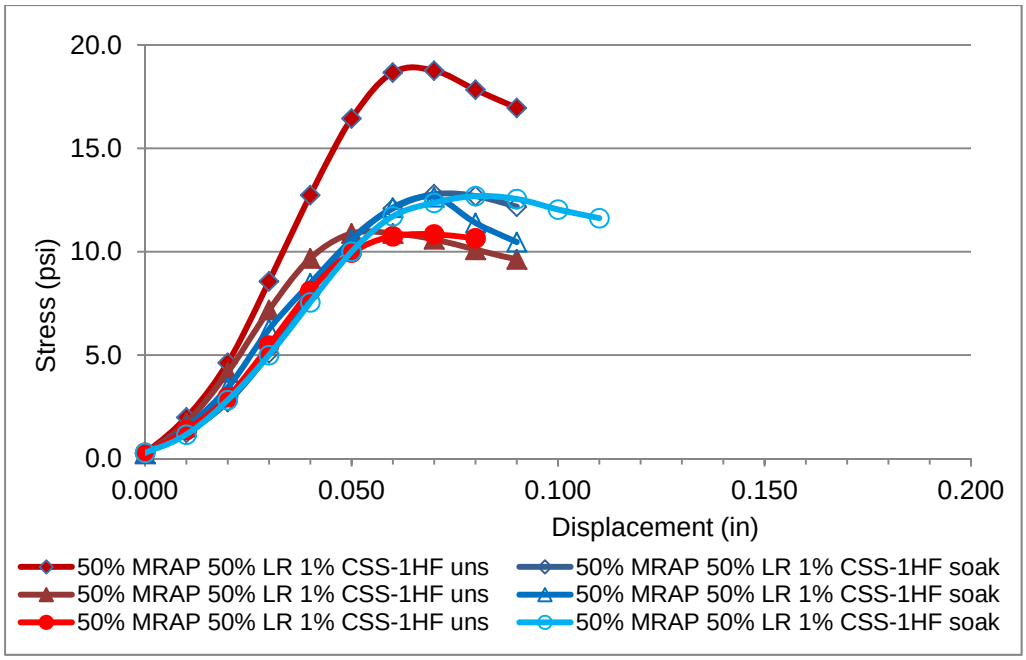

Figure H-9: IDT Trial 10 Mod Proctor 50% MRAP/50% Limerock 1% CSS-1HF

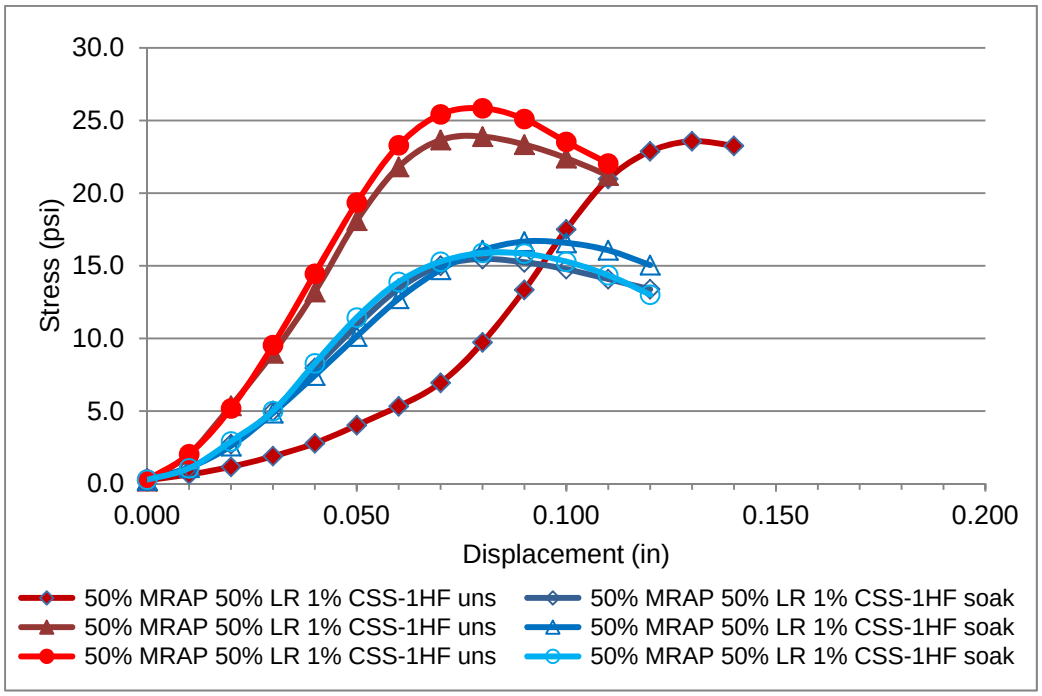

Figure H-10: IDT Trial 10G Gyratory 50% MRAP/50% Limerock 1% CSS-1HF

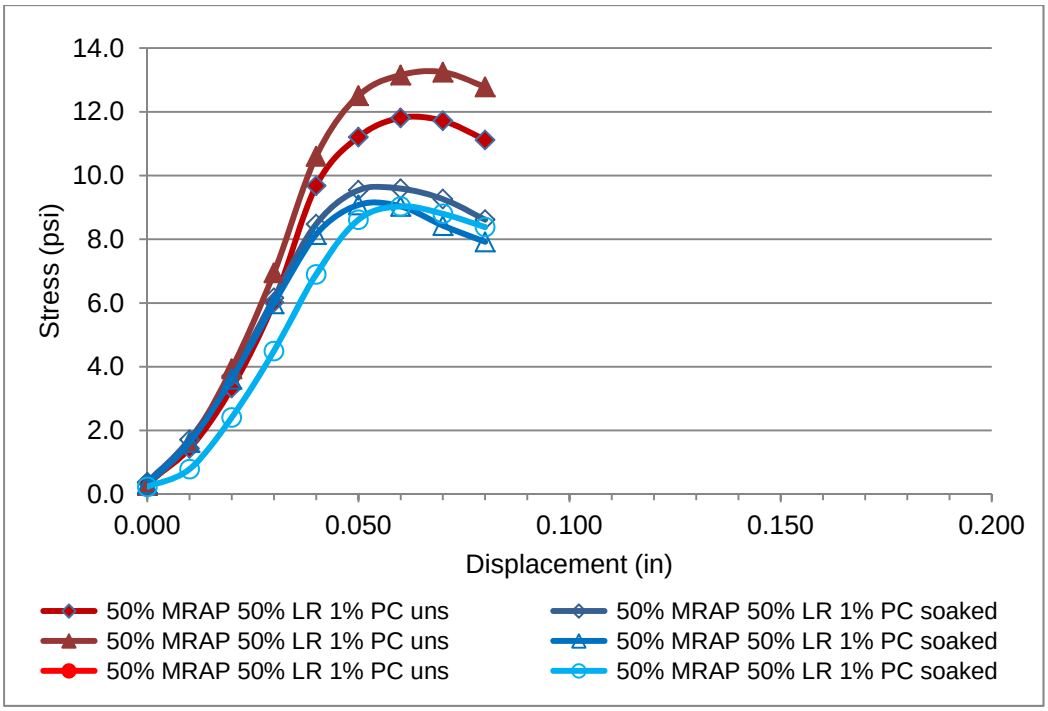

Figure H-11: IDT Trial 19 Mod Proctor 50% MRAP/50% Limerock 1% Cement

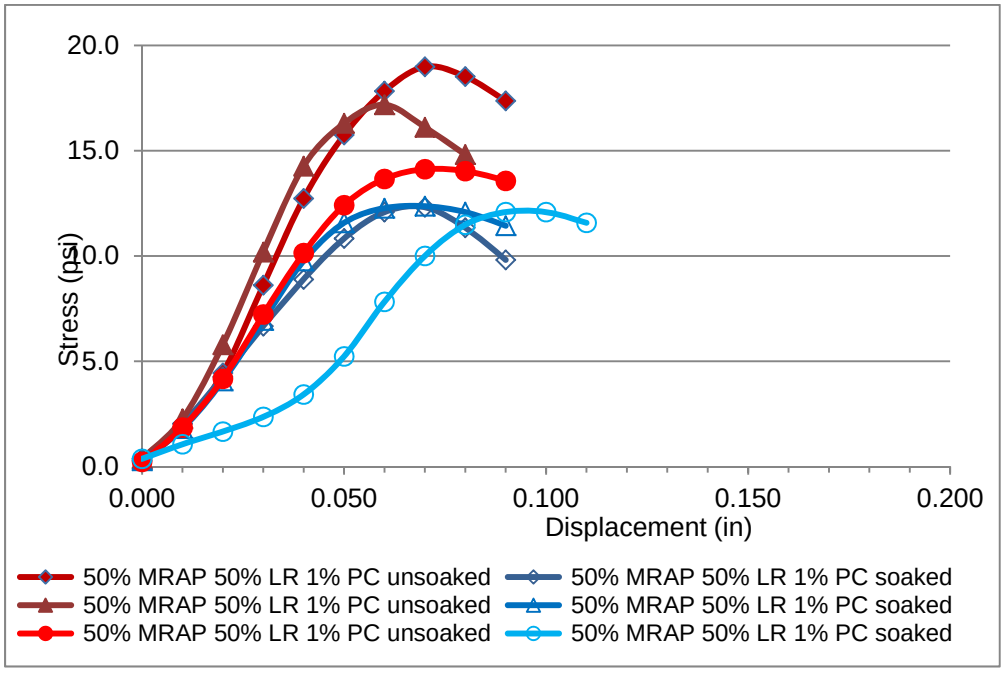

Figure H-12: IDT Trial 19G Gyratory 50% MRAP/50% Limerock 1% Cement

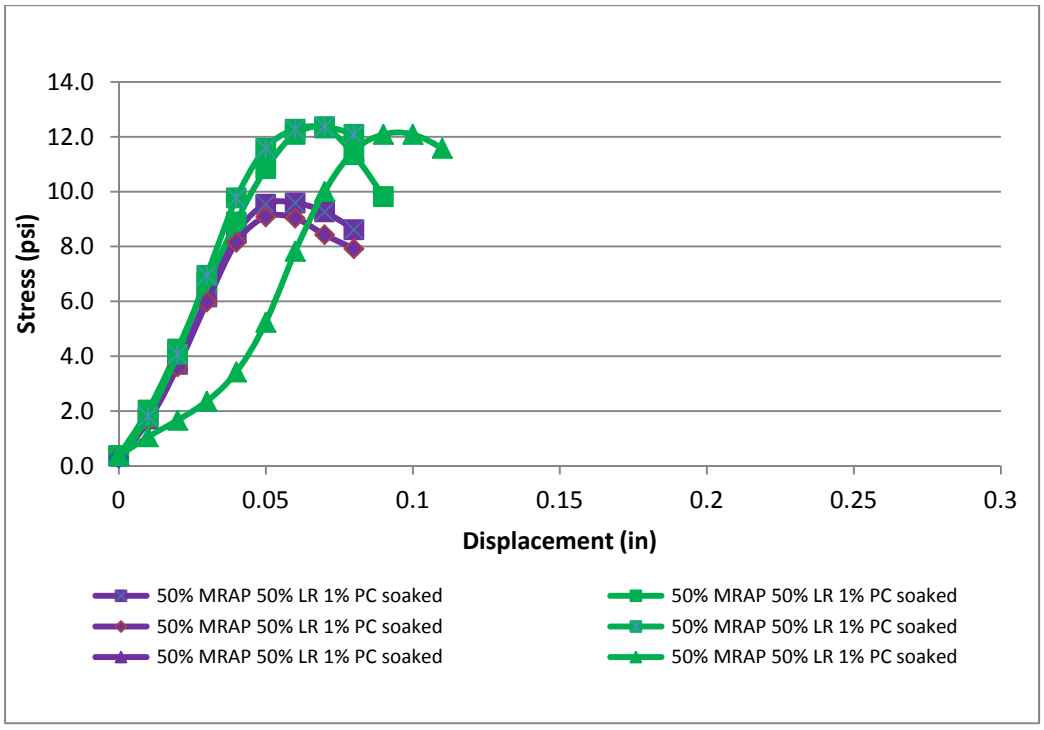

Figure H-13: IDT 19/19G Mod Proctor and Gyratory 50% MRAP/50% LR Soaked

Appendix I - Creep Modeling

I.1. Model Parameters for 100% MRAP

Table I-1: Experimental Data to Determine A and α Coefficients 100% MRAP (Dikova, 2006)

Stress Level D (psi)	1 Day	
	Strain (in/in)	Strain Rate (%/min)
6	$2.47E^{-2}$	$1.69E^{-3}$
12	$2.72E^{-2}$	$1.86E^{-3}$
18	$4.03E^{-2}$	$2.76E^{-3}$

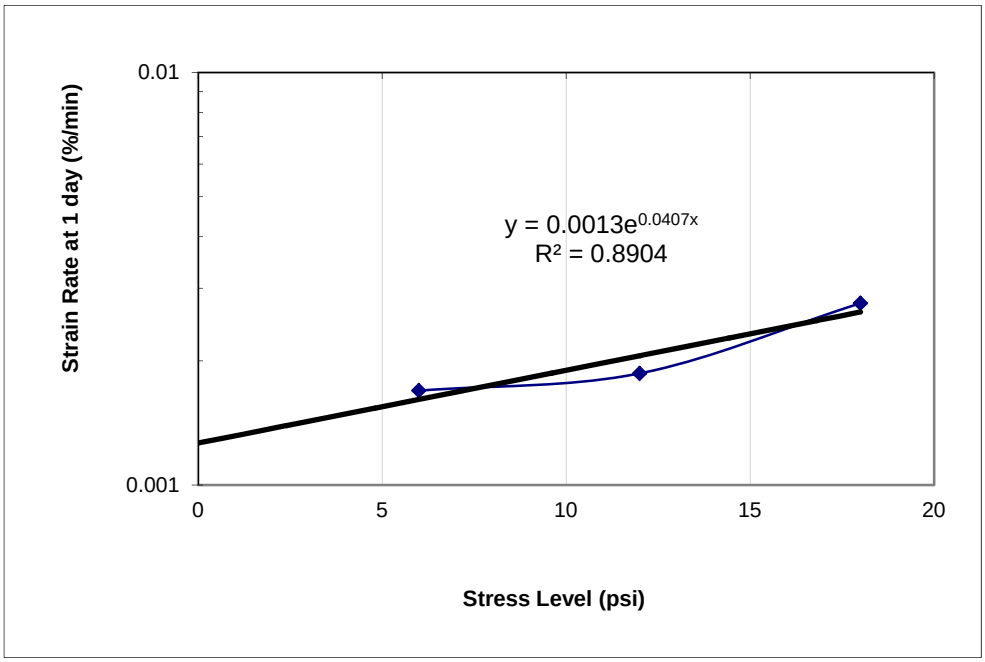

Figure I-1: Logarithm of Strain Rate vs. Stress for 100% RAP (Dikova, 2006)

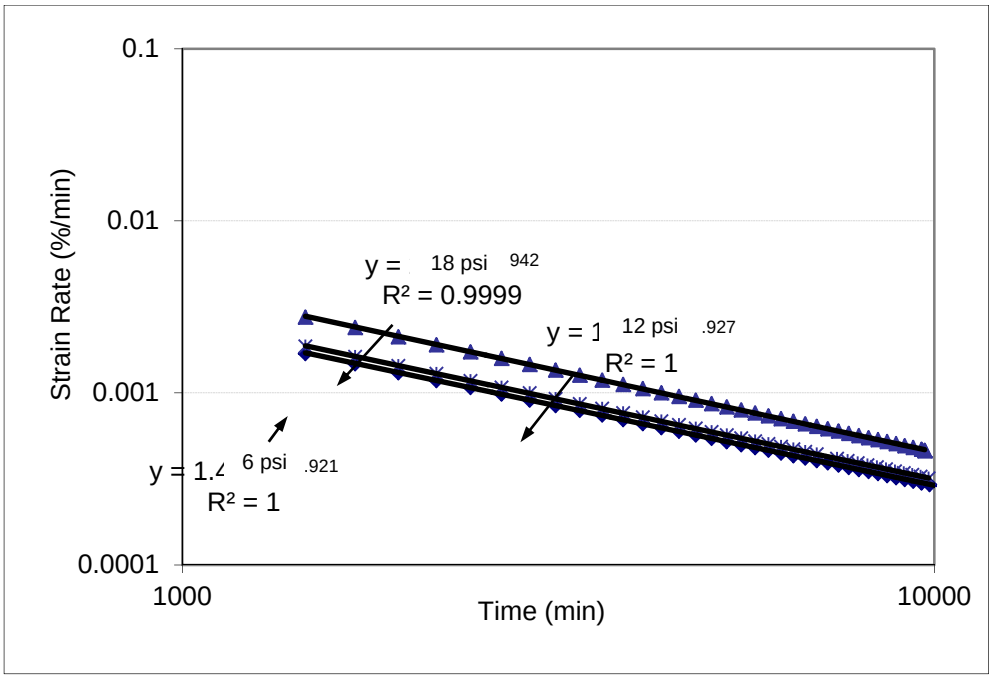

Figure I-2: Logarithm of Strain Rate vs. Logarithm of Time for 100% RAP (Dikova, 2006)

Table I-2: Singh and Mitchell m Coefficient 100% MRAP (Dikova, 2006)

Stress Level D (psi)	Slope m
6	0.9209
12	0.9273
18	0.9423
Average m =	0.93017

I.2. Model Parameters for 100% Limerock

Table I-3: Experimental Data to Determine A and α Coefficients 100% Limerock

Stress Level D (psi)	1 Day	
	Strain (in/in)	Strain Rate (%/min)
12	3.25×10^{-3}	2.33×10^{-4}
25	7.25×10^{-3}	4.69×10^{-4}

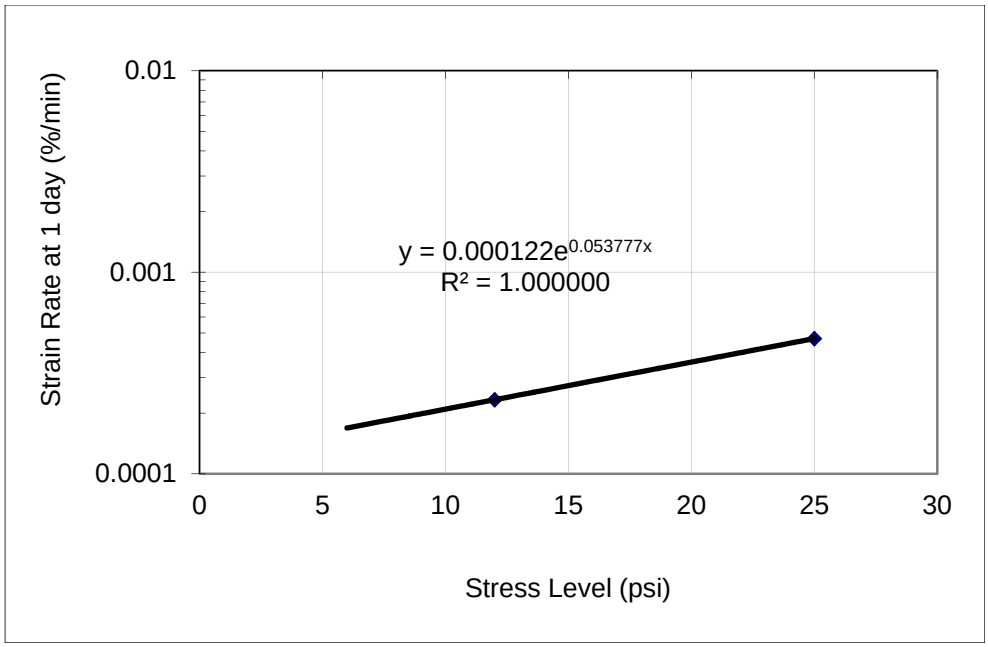

Figure I-3 Logarithm of Strain Rate vs. Stress for 100% Limerock

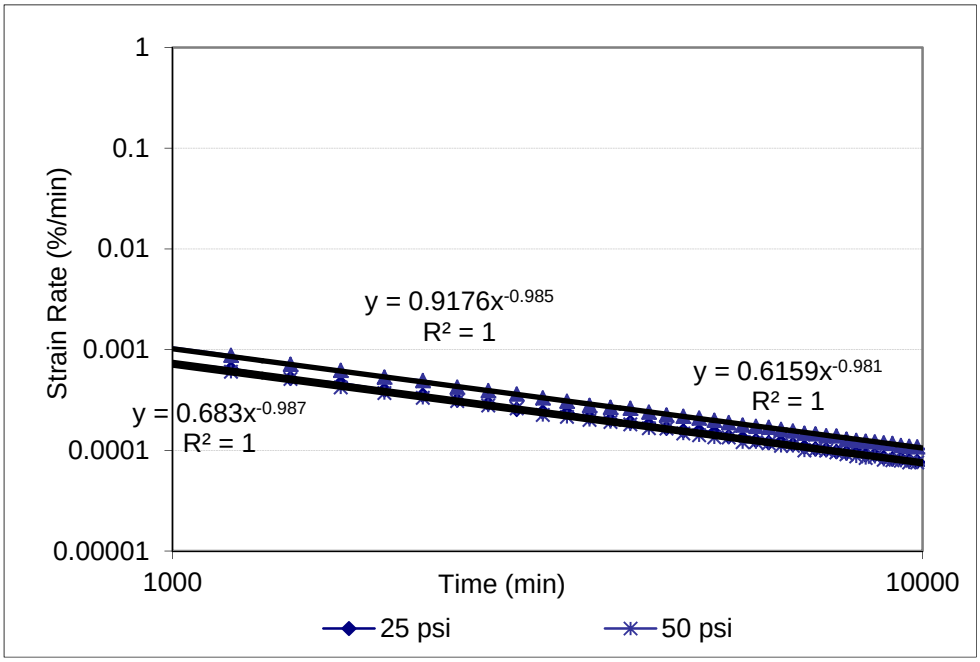

Figure I-4: Logarithm of Strain Rate vs. Logarithm of Time for 100% Limerock

Table I-4: Singh and Mitchell m Coefficient 100% Limerock

Stress Level D (psi)	Slope m
25	0.9870
50	0.9810
100	0.9850
Average m =	0.9843

I.3. Model Parameters for 50% MRAP/50% Limerock Blend without Stabilizer

Table I-5 Experimental Data to Determine A and α Coefficients 50% MRAP/50% Limerock without Stabilizer

Stress Level D (psi)	1 Day	
	Strain (in/in)	Strain Rate (%/min)
12	1.47×10^{-3}	1.09×10^{-4}
25	2.01×10^{-2}	1.40×10^{-3}

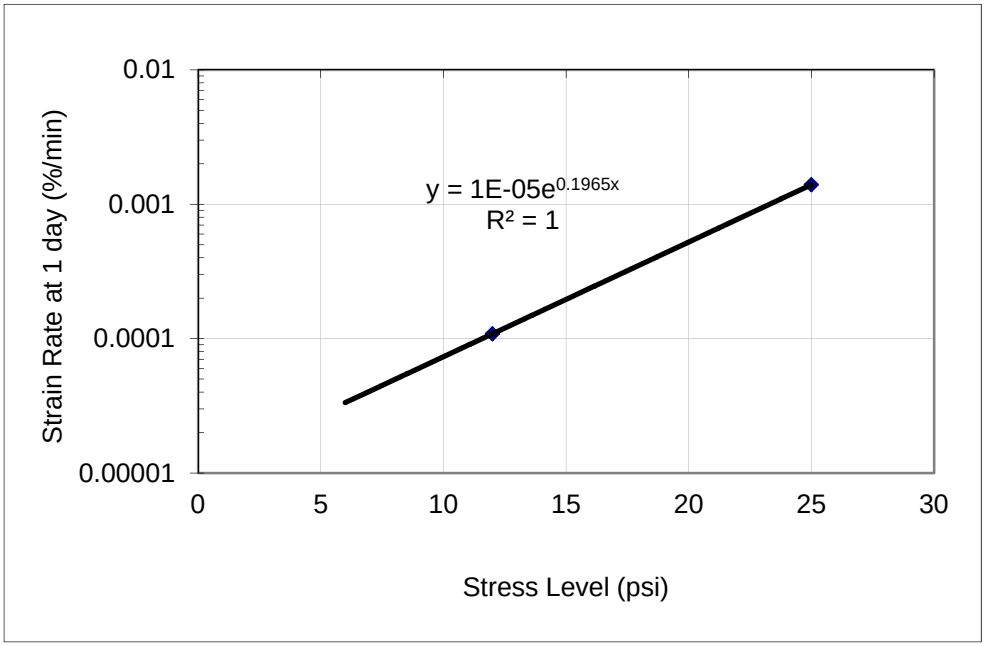

Figure I-5: Logarithm of Strain Rate vs. Stress for 50% MRAP without Stabilizer

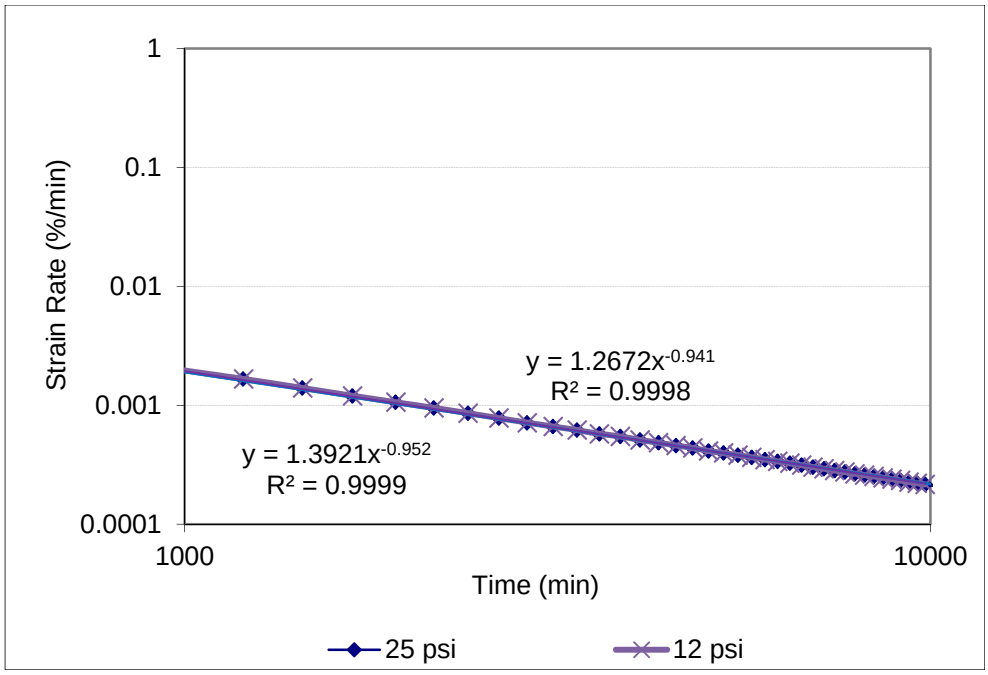

Figure I-6: Logarithm of Strain Rate vs. Logarithm of Time for 50% MRAP/50% Limerock without Stabilizer

Table I-6: Singh and Mitchell m Coefficient 50% MRAP/50% Limerock without Stabilizer

Stress Level D (psi)	Slope m
12	0.9520
25	0.9410
Average m =	0.9465

I.4. Model Parameters for 50% MRAP/50% Limerock Blend with 1% Portland Cement Stabilizer

Table I-7 Experimental Data to Determine A and α Coefficients 50% MRAP/50% LR with 1% Portland Cement Stabilizer

Stress Level D (psi)	1 Day	
	Strain (in/in)	Strain Rate (%/min)
12	1.08×10^{-2}	7.48×10^{-4}
25	7.50×10^{-3}	5.21×10^{-4}

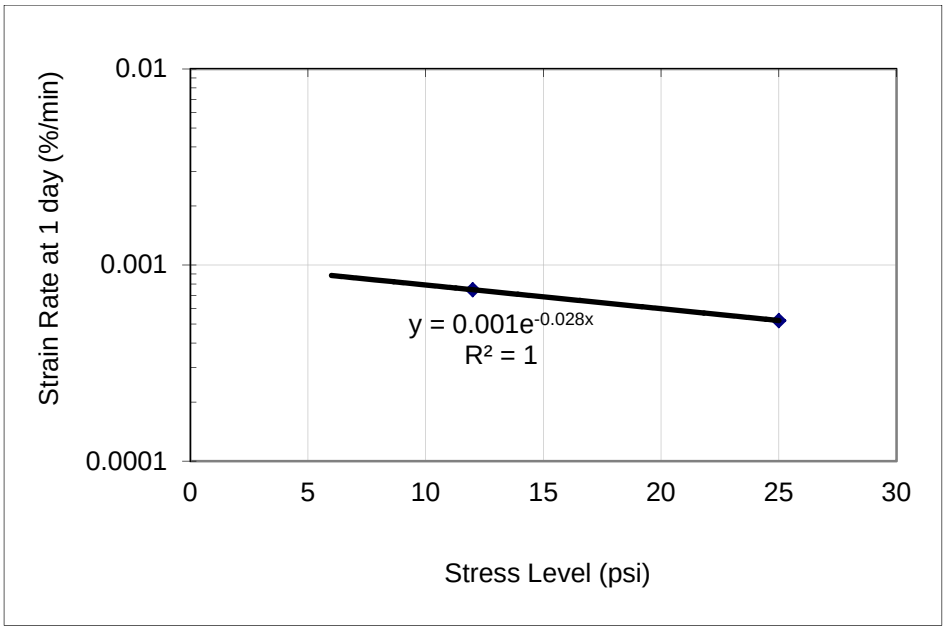

Figure I-7: Logarithm of Strain Rate vs. Stress for 50% MRAP with 1% Portland Cement Stabilizer

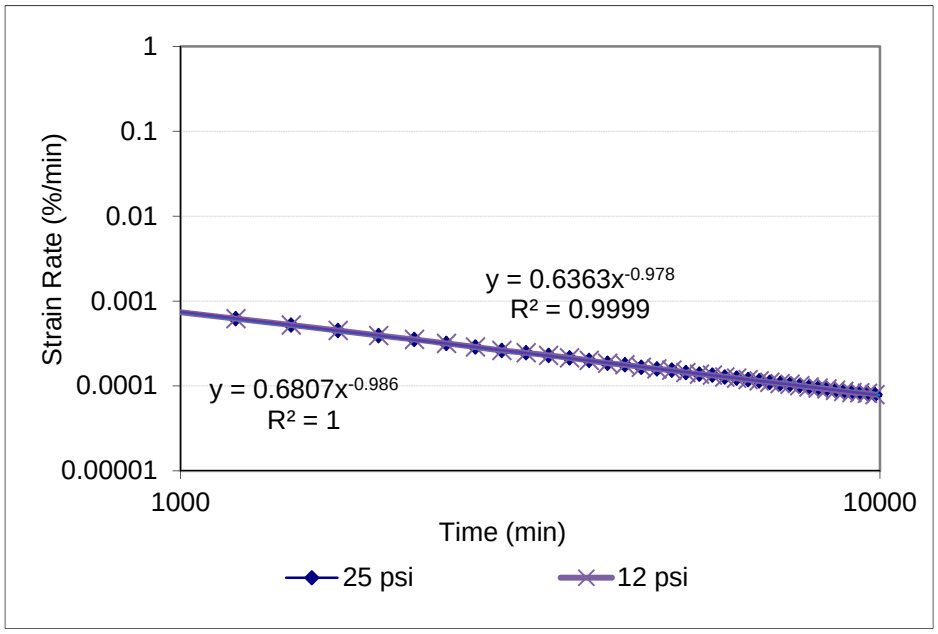

Figure I-8: Logarithm of Strain Rate vs. Logarithm of Time for 50% MRAP/50% Limerock with 1% PC Stabilizer

Table I-8: Singh and Mitchell m Coefficient 50% MRAP/50% Limerock with 1% Portland Cement Stabilizer

Stress Level D (psi)	Slope m
12	0.9780
25	0.9860
Average m =	0.9820

Appendix J - Asphalt Content and Specific Gravity Data

Table J-1: Crushed APAC Melbourne RAP

	F.I.T. Sample No.	1	2	3	4	5	6	7
	F.D.O.T. Lab No.	19830	19831	19832	19833	19834	19835	19836
Sieve Sizes	1"	100.00	100.00	100.00	100.00	100.00	100.00	100.00
	3/4"	100.00	100.00	100.00	100.00	100.00	100.00	100.00
	1/2"	76.66	100.00	100.00	100.00	100.00	100.00	97.60
	3/8"	33.72	99.59	100.00	100.00	100.00	100.00	93.30
	No.4	18.40	33.54	99.47	100.00	100.00	100.00	76.07
	No.8	15.15	19.96	42.55	99.98	99.99	99.46	58.85
	No. 16	13.59	18.22	23.94	80.43	99.97	98.58	49.03
	No. 30	12.30	16.85	21.78	60.17	99.94	98.04	42.19
	No. 50	9.75	14.06	18.13	33.84	99.77	97.63	30.77
	No. 100	5.75	9.06	11.27	18.18	41.42	97.36	16.62
	No. 200	3.11	5.62	6.36	10.80	13.26	96.28	9.04
	% Asphalt Binder	2.63	2.22	4.74	6.33	6.19	12.79	5.06

Table J-2: Milled APAC Melbourne RAP

	F.I.T. Sample No.	A	B	C	D	E	F	G	H	I
	F.D.O.T. Lab No.	19837	19838	19839	19840	19841	19842	19843	19844	19845
Sieve Sizes	1"	100.00	100.00	100.00	100.00	100.00	100.00	100.00	100.00	100.00
	3/4"	100.00	100.00	100.00	100.00	100.00	100.00	100.00	100.00	100.00
	1/2"	100.00	98.87	97.82	100.00	100.00	100.00	100.00	100.00	99.42
	3/8"	98.11	95.26	83.09	100.00	100.00	100.00	100.00	100.00	98.46
	No. 4	77.40	75.97	60.04	61.92	99.61	100.00	100.00	100.00	85.43
	No. 8	58.76	57.91	45.54	41.12	58.35	99.95	100.00	100.00	65.24
	No. 16	44.94	45.14	35.27	32.06	36.11	80.06	100.00	100.00	48.19
	No. 30	36.65	37.21	28.83	26.64	30.41	58.14	99.93	100.00	38.08
	No. 50	27.08	27.86	21.57	20.46	23.87	37.38	99.65	100.00	28.75
	No. 100	14.04	14.80	12.01	11.97	14.57	22.74	48.00	99.93	17.35
	No. 200	6.82	7.01	6.68	6.89	8.83	15.17	18.01	99.41	10.64
	% Asphalt Binder	7.07	6.84	5.51	5.09	5.81	7.21	6.02	6.83	5.55

Table J-3: Fractionated RAP

		Crushed APAC Jacksonville		Milled Whitehurst Gainesville		Crushed APAC Melbourne		Milled APAC Melbourne	
		% AC	G_{sb}	% AC	G_{sb}	% AC	G_{sb}	% AC	G_{sb}
Fraction	(+) No. 4	3.11	2.658	5.18	2.515	5.16	2.555	4.29	2.561
	(-) No. 4	4.58	2.612	6.04	2.524	6.22	2.53	5.79	2.498
	(+) No. 8	3.43	2.661	6.40	2.550	5.33	2.548	4.31	2.545
	(-) No. 8	5.13	2.549	6.77	2.514	5.48	2.508	5.65	2.491
	(+) No. 40	4.22	2.634	6.04	2.524	5.94	2.527	4.77	2.527
	(-) No. 40	4.45	2.515	7.34	2.507	6.12	2.504	5.17	2.499
	Non-Fractionated	4.03	2.604	4.18	2.576	5.42	2.524	4.41	2.508

Appendix K - Modified Proctor Compaction Data

Table K-1: Modified Proctor Compaction for APAC Melbourne, Crushed

Test #	Moisture Content %	Dry Density (pcf)	LBR	UCC (psi)	ITS (psi)
AMC-1	2.94	113.56	16.5		
AMC-2	4.63	112.36	14.2		
AMC-3	4.63	112.50	15.1		
AMC-4	6.64	119.38	16.8		
AMC-5	10.92	117.42	16.9		
AMC-6	4.02	112.9	17.5		
AMC-7	5.48	115.38	18.0		
AMC-8	8.11	118.40	23.6		
AMC-9	8.82	119.4	23.2		
AMC-39	7.52	120.5		27	
AMC-40	3.97	118.0		21	
AMC-41	5.76	117.7		22	
AMC-49	4.19	117.1			0.28
AMC-50	6.29	115.0			0.00
AMC-51	4.04	116.1			0.18
AMC-52	3.51	118.6			0.28

Table K-2: Modified Proctor Compaction for APAC Melbourne, Milled

Test #	Moisture Content %	Dry Density (pcf)	LBR
AMM-1	2.33	108.30	11.5
AMM-2	3.92	107.40	10.2
AMM-3	6.18	106.30	8.4
AMM-4	6.89	108.50	10.0
AMM-5	8.08	110.90	8.0
AMM-6	9.72	107.18	11.8
AMM-7	6.82	107.10	10.4
AMM-8	10.81	105.13	5.2

Table K-3: Modified Proctor Compaction for Whitehurst, Milled

Test #	Moisture Content %	Dry Density (pcf)	LBR
WHM-1	2.86	117.40	16.2
WHM-2	3.49	116.10	13.5
WHM-3	5.04	117.50	11.1
WHM-4	7.10	118.50	12.6
WHM-5	8.64	121.20	12.2
WHM-6	9.60	117.50	15.7
WHM-7	10.28	118.70	16.5

Table K-4: Modified Proctor Compaction for Jacksonville, Crushed

Test #	Moisture Content %	Dry Density (pcf)	LBR	UCC (psi)
AJC-1	3.37	122.00	15.6	
AJC-2	4.01	124.30	18.8	
AJC-3	4.98	123.80	20.4	
AJC-4	1.76	121.20	16.5	
AJC-5	5.96	125.30	17.2	
AJC-6	6.48	125.10	19.5	
AJC-7	7.37	123.00	20.9	
AJC-8	8.01	123.90	22.5	
AJC-9	10.69	121.30	23.1	
AJC-38	5.61	120.5		21
AJC-39	5.03	119.9		21
AJC-40	4.71	120.1		19
AJC-42	8.29	122.7		15
AJC-43	5.95	121.9		21

Appendix L - Vibratory Compaction Data

Table L-1: Vibratory Compaction for APAC Melbourne, Crushed

Test #	Moisture Content %	Moist Density (pcf)	Dry Density (pcf)	LBR	Vibration Time	Compactive Effort ft-lbs/ft^3
AMC-15	3.94	108.2	104.1	11.4	8	28,583
AMC-16	6.14	113.8	107.3	11.4	8	29,424
AMC-17	8.6	131.8	121.3	21.3	8	29,982
AMC-18	7.14	117.3	109.5	14.4	8	25,267
AMC-19	7.79	121.6	112.8	15.4	8	26,575
AMC-20	8.17	121.9	112.7	11.6	8	26,928
AMC-21	4.73	113.4	108.2	17.2	12	39,144
AMC-22	5.42	112.1	106.3	12.4	12	39,962
AMC-23	4.3	112.5	107.9	17.9	16	53,944
AMC-24	4.51	114	109.1	20.2	16	56,701

Table L-2: Vibratory Compaction for APAC Melbourne, Milled

Test #	Moisture Content %	Moist Density (pcf)	Dry Density (pcf)	LBR	Vibration Time	Compactive Effort ft-lbs/ft^3
AMM-9	6.1	106.2	100.1	7.5	8	28,610
AMM-10	6.93	118.3	110.7	6.9	8	33,909
AMM-11	5.47	103.9	98.5	9.3	12	55,066
AMM-12	9.28	109.9	100.6	8	12	63,290
AMM-13	3.44	98.9	95.6	8	8	32,169
AMM-14	4.58	116.7	111.6	19.7	16	63,252
AMM-15	7.17	114.7	107.1	17.9	16	54,832
AMM-24	0	108.9	108.5	17.8	8	23,448
AMM-25	0	108.7	108.5	21.3	8	27,362

Table L-3: Vibratory Compaction for Whitehurst, Milled

Test #	Moisture Content %	Moist Density (pcf)	Dry Density (pcf)	LBR	Vibration Time	Compactive Effort ft-lbs/ft^3
WHM-8	5.58	112.1	111.47	-	8	31,964
WHM-9	4.8	115.8	110.49	10	8	34,300
WHM-10	5.05	117.1	111.4	13.7	12	45,813
WHM-11	4.89	117.8	112.3	12.2	12	41,472
WHM-12	4.81	114.8	109.6	12	8	28,219
WHM-13	5.41	115.2	109.3	14.9	16	49,111
WHM-14	4.93	118.2	112.7	13.2	16	56,284
WHM-15	2.48	111.8	109.1	12.4	8	23,728
WHM-16	1.72	113.8	111.9	13.8	8	30,508
WHM-33b	0.95	103.3	102.3	13.5	8	25,940
WHM-34	1.15	106.9	105.7	-	8	28,462
WHM-35	8.33	112.3	103.6	6.6	8	28,351
WHM-36	7.09	105.6	98.6	7.0	8	25,759

Table L-4: Vibratory Compaction for APAC Jacksonville Crushed

Test #	Moisture Content %	Moist Density (pcf)	Dry Density (pcf)	LBR	Vibration Time	Compactive Effort ft-lbs/ft^3
AJC-10	5.48	125.00	118.50	12.2	8	30,189
AJC-11	6.29	126.50	119.00	11.1	8	34,820
AJC-12	2.05	114.90	112.60	12.1	8	31,960
AJC-13	4.46	121.70	116.30	13.3	12	46,317
AJC-14	5.32	124.00	117.70	12.7	12	43,649
AJC-15	5.52	125.70	119.10	14.6	16	64,600
AJC-16	6.51	126.30	118.60	13.1	16	67,308
AJC-48	0.39	113.90	113.5	-	8	27,716

Appendix M - Gyratory Compaction Data

Table M-1: Gyratory Compaction Summary for APAC Melbourne, Crushed

Test #	Moisture Content (%)	Dry Density (pcf)	LBR	UCC (psi)	IDTS (psi)	Number of Gyrations	Initial Height (mm)
AMC-25	3.4	121.2	72.1			75	129.0
AMC-26	3.29	121.1	68.9			75	134.1
MC-27	6.04	120.1	61.7			75	130.2
AMC-28	5.38	120.4	70.4			75	129.6
AMC-29	11.19	117.8	67.8			75	137.3
AMC-30	7.18	120.5	63.9			75	142.0
AMC-31	3.21	121.7	80.5			100	129.3
AMC-32	3.83	118	51.7			100	134.7
AMC-33	3.5	122.4	82.9			100	131.5
AMC-34	4.24	124.2	100.0			150	129.5
AMC-35	4.24	124.4	100.0			150	131.6
AMC-36	4.42	124.8	106.0			150	128.7
AMC-37	6.03	123.2		110		75	129.0
AMC-38	5.56	122.5		106		75	136.3
AMC-42	5.44	116.7		54		19	130.0
AMC-43	4.72	117.5		64		29	133.3
AMC-44	5.89	115.5		58		26	133.3
AMC-45	4.95	120.0		90		50	134.4
AMC-46	4.87	123.8			1.3	75	130
AMC-47	5.91	122.6			1.75	75	134.3
AMC-48	4.88	122.1			1.15	75	134.5
AMC-53	4.17	115.6			0.65	16	129.4
AMC-54	4.41	115.4			0.6	31	135.6
AMC-55	3.78	116.10			0.75	32	135.2

Table M-2: Gyratory Compaction Summary for APAC Melbourne, Milled

Test #	Moisture Content (%)	Dry Density (pcf)	LBR	UCC (psi)	IDTS (psi)	Number of Gyrations	Initial Height (mm)
AMM-16	3.2	113.4	54.7			75	140.2
AMM-17	3.15	113.0	57.3			75	143.1
AMM-18	3.02	114.0	54.5			75	141.6
AMM-19	7.07	121.1	63.4			75	120.1
AMM-20	5.52	121.7	85.3			75	124.2
AMM-21	5.45	120.7	82.4			75	124.3
AMM-22	7.25	120.3	74.8			75	134.8
AMM-23	3.8	121.4	95.1			150	133.3
AMM-26	6.72	104.3	23.8			8	130.9
AMM-27	7.49	103.9	36			22	140.2
AMM-28	6.46	109.3	48.8			28	133.8
AMM-29	5.07	110.8	46.3			31	133.4

Table M-3: Gyratory Compaction Summary for Whitehurst, Milled

Test #	Moisture Content (%)	Dry Density (pcf)	LBR	UCC (psi)	IDTS (psi)	Number of Gyrations	Initial Height (mm)
WHM-18	4.24	121.6	83			75	136.0
WHM-19	3	121.6	88.1			75	136.1
WHM-20	6.72	119.3	74.2			75	136.4
WHM-21	5.26	120.5	82.3			75	139.9
WHM-22	7.42	121.1	84.9			75	127.2
WHM-23	7.65	119.8	66.5			75	129.8
WHM-24	3.03	123.5	84.4			100	124.9
WHM-25	3.15	123.6	84.7			100	125.6
WHM-26	3.32	124.6	81.5			100	125.2
WHM-27	3.3	125.1	86.7			150	126.1
WHM-28	3.27	124.5	92.1			150	130.7
WHM-30	4.11	124.9	92.5			150	127.7
WHM-31	4.55	125.4	105.5			150	125.9
WHM-32	4.44	122.2	84.1			100	133.9

Table M-4: Gyratory Compaction Summary for APAC Jacksonville, Crushed

Test #	Moisture Content (%)	Dry Density (pcf)	LBR	UCC (psi)	IDTS (psi)	Number of Gyrations	Initial Height (mm)
AJC-17	3.37	123.7	72.7			75	125.1
AJC-18	2.58	125.2	78.2			75	123.9
AJC-19	5.91	125.7	68.3			75	133.4
AJC-20	5.97	124.2	66.3			75	136.2
AJC-21	8.8	122.1	65.1			75	144.8
AJC-22	9.44	121.8	66.4			75	137.4
AJC-23	3.31	122.3	85.3			100	124.3
AJC-24	2.86	123.7	82			100	123.8
AJC-25	3.77	127.3	97.5			150	126.5
AJC-26	3.77	121.3	60.1			150	132.1
AJC-27	3.72	128.6	102.6			150	128.3
AJC-28	3.72	128.9	95.2			150	130.0
AJC-29	3.91	125.7	84.3			100	127.1
AJC-30	3.48	127.5	77.6			100	129.5
AJC-31	4.54	119.9	47.3			32	118.7
AJC-32	6.15	117.8	33.5			17	120.7
AJC-33	6.1	125.3	66.3			90	121.2
AJC-34	5.18	126	70.6			90	121.2
AJC-35	4.31	124.2		118		75	128.3
AJC-36	4.09	124		114		75	129.4
AJC-37	3.76	124		106		75	128.7
AJC-44	6.39	112.9		31		8	122.2
AJC-45	6.06	119.7		67		32	133.5
AJC-46	5.51	119.5		66		29	130.9
AJC-47	3.78	122.7		82		44	129.7

Appendix N - Linear Regression Data

N.1. LBR vs. Percent Passing Difference between Talbot Curve and Gradation Curves

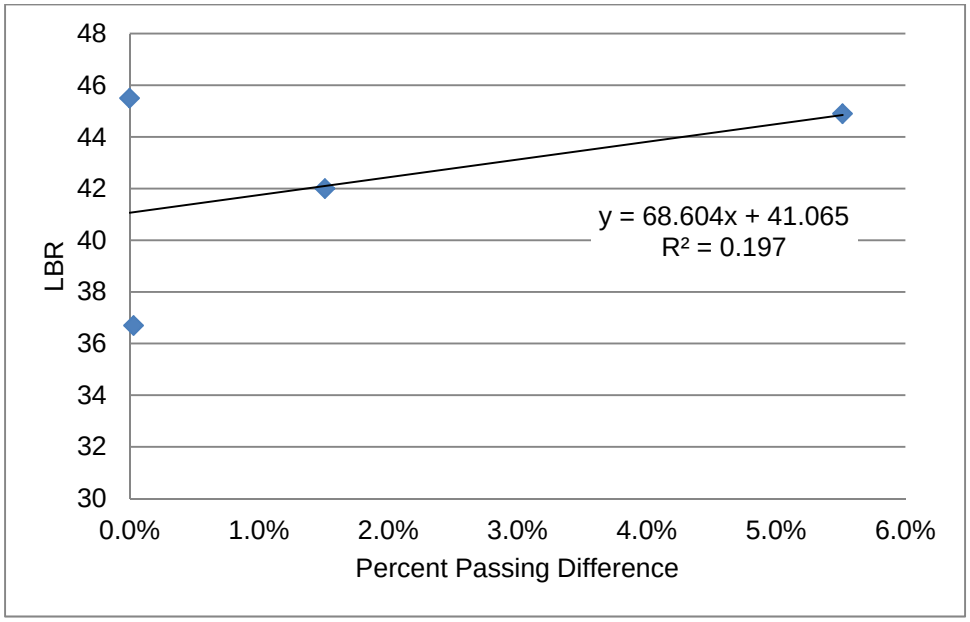

Figure N-1: LBR vs. Percent Passing Difference at Sieve ¾”

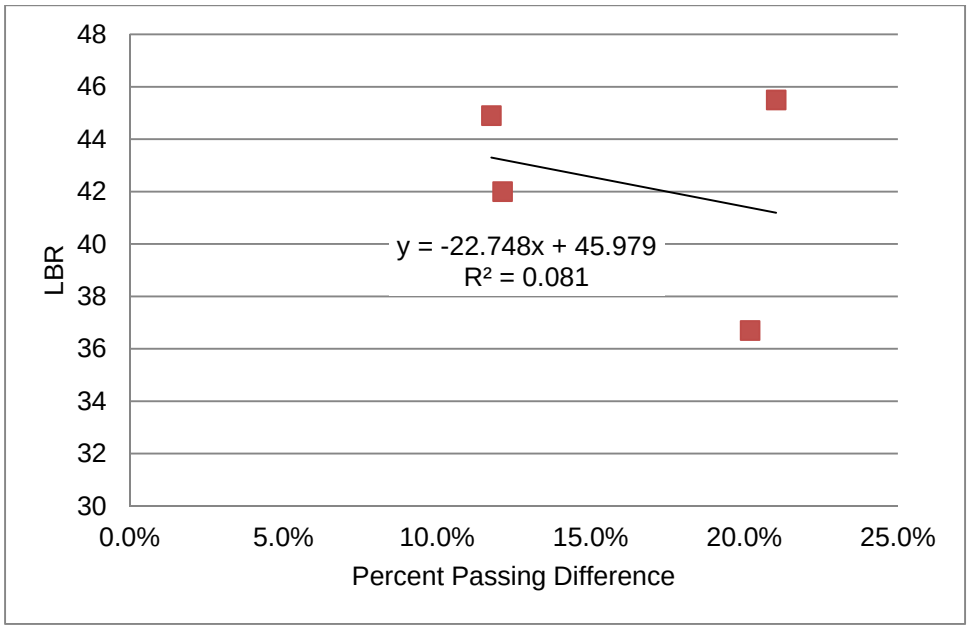

Figure N-2: LBR vs. Percent Passing Difference at Sieve 3/8”

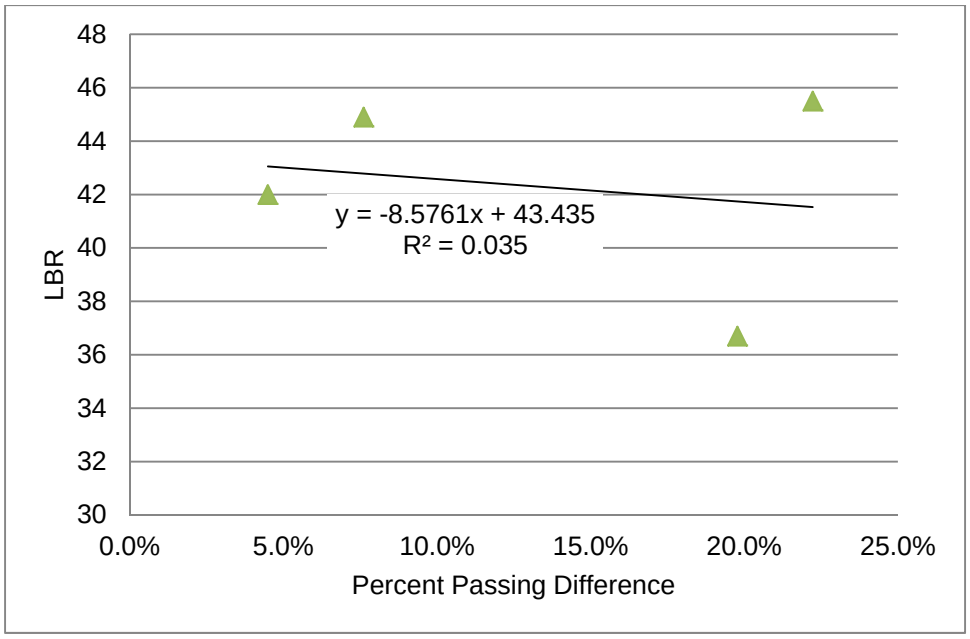

Figure N-3: LBR vs. Percent Passing Difference at Sieve #4

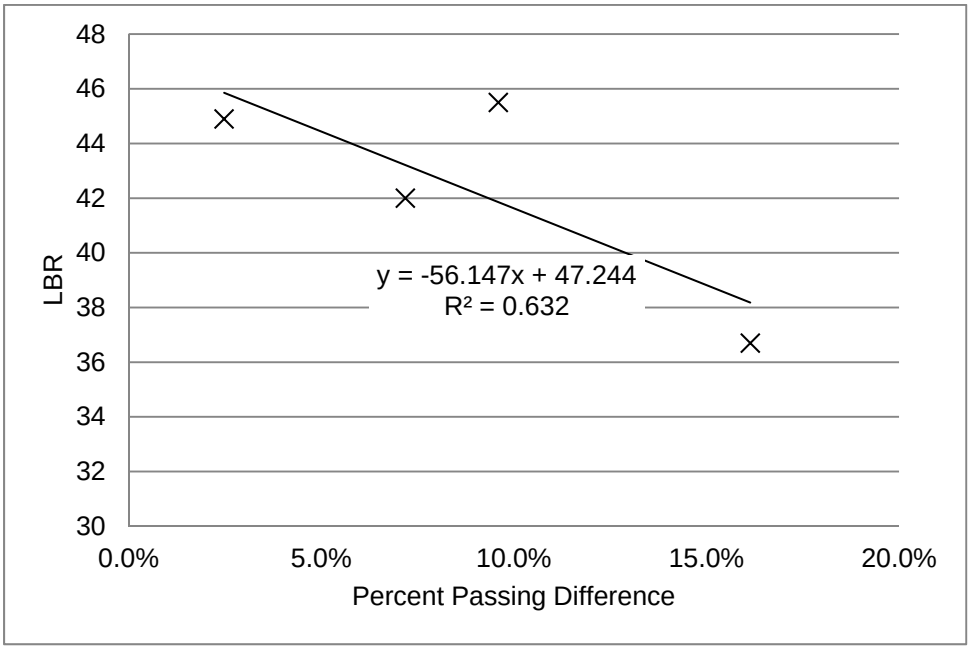

Figure N-4: LBR vs. Percent Passing Difference at Sieve #10

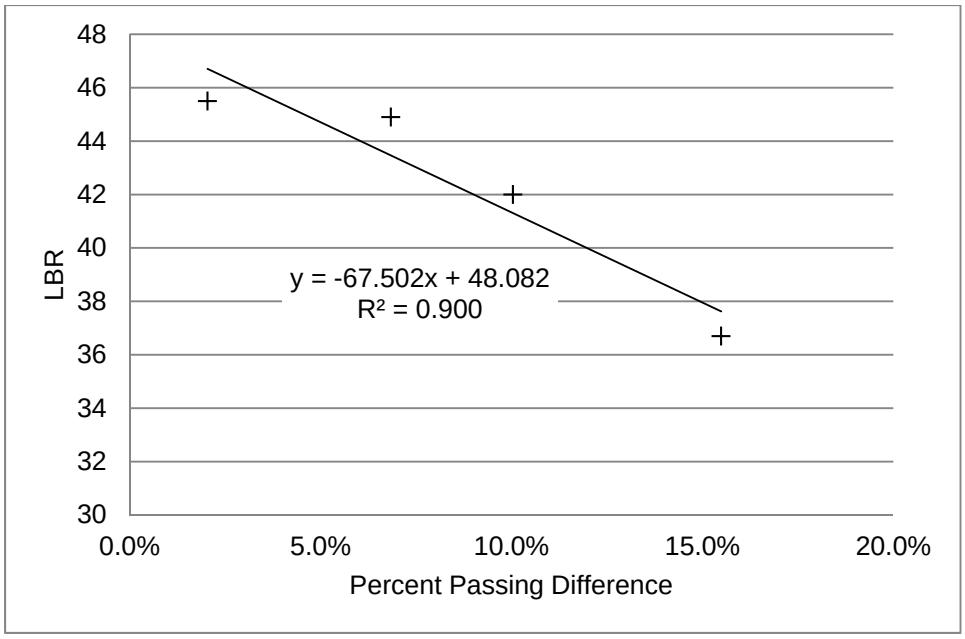

Figure N-5: LBR vs. Percent Passing Difference at Sieve #30

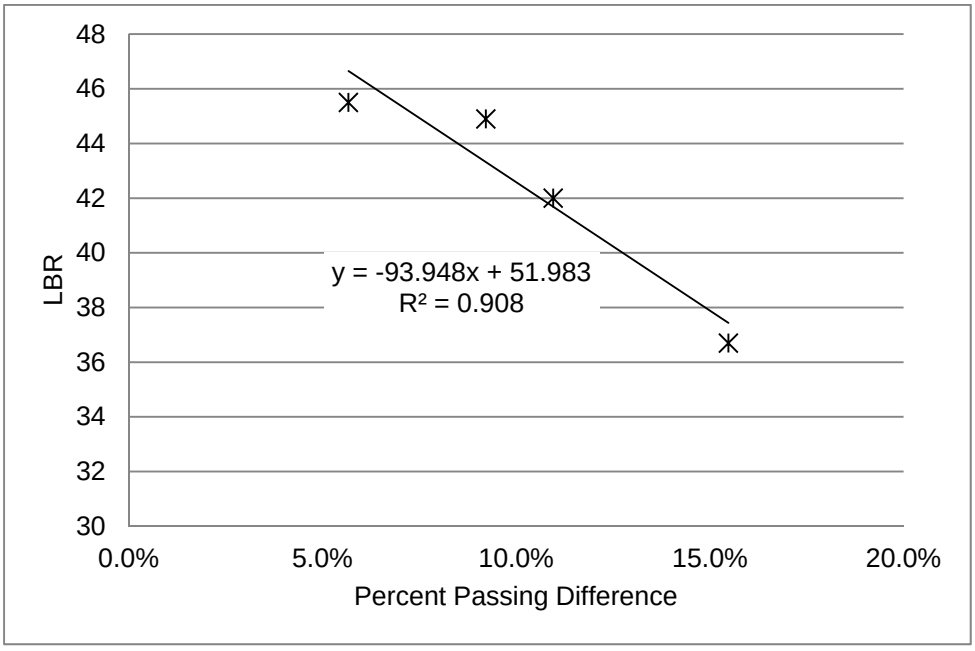

Figure N-6: LBR vs. Percent Passing Difference at Sieve #50

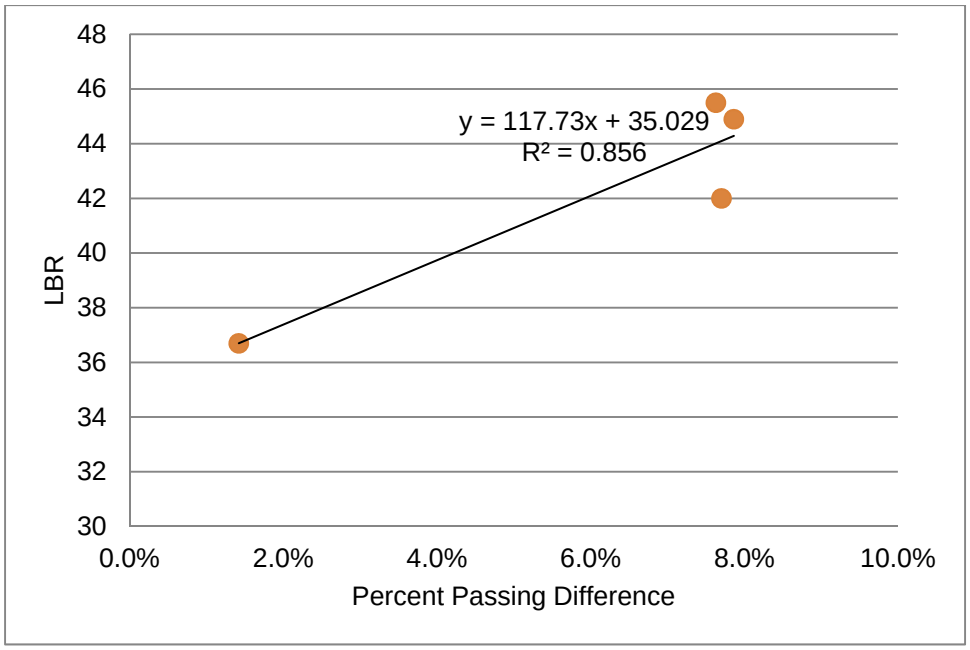

Figure N-7: LBR vs. Percent Passing Difference at Sieve #200

N.2. Creep Strain Rate vs. Percent Passing Difference between Talbot Curve and Gradation Curves

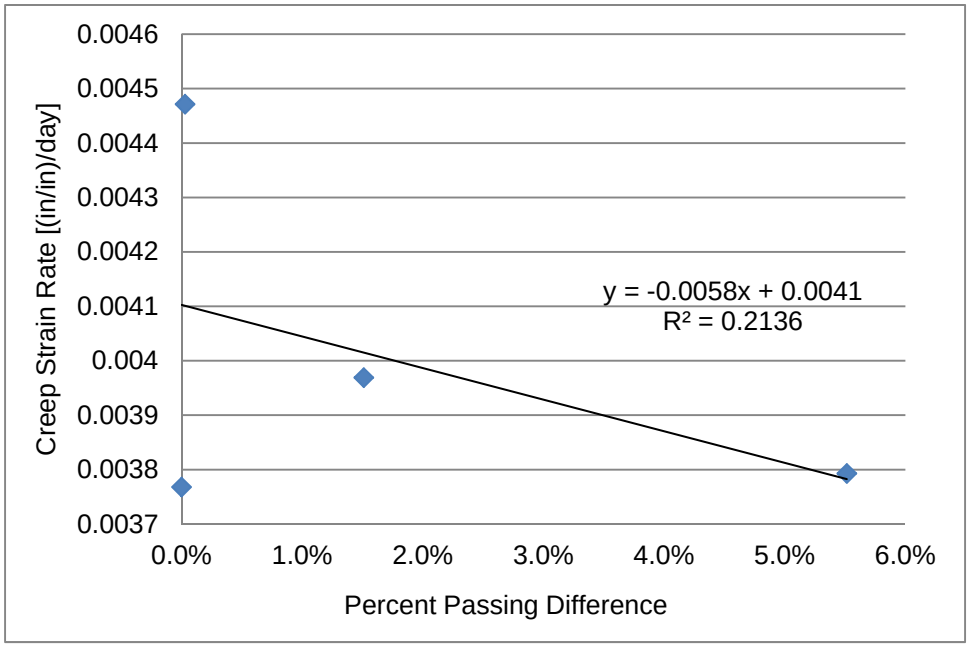

Figure N-8: Creep Strain Rate vs. Percent Passing Difference at Sieve ¾”

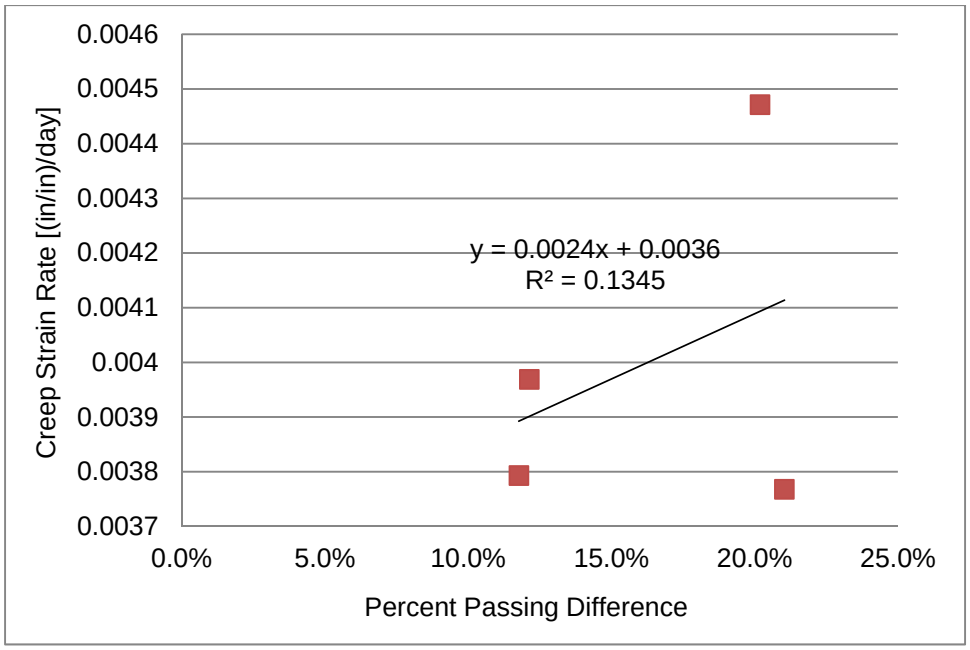

Figure N-9: Creep Strain Rate vs. Percent Passing Difference at Sieve 3/8”

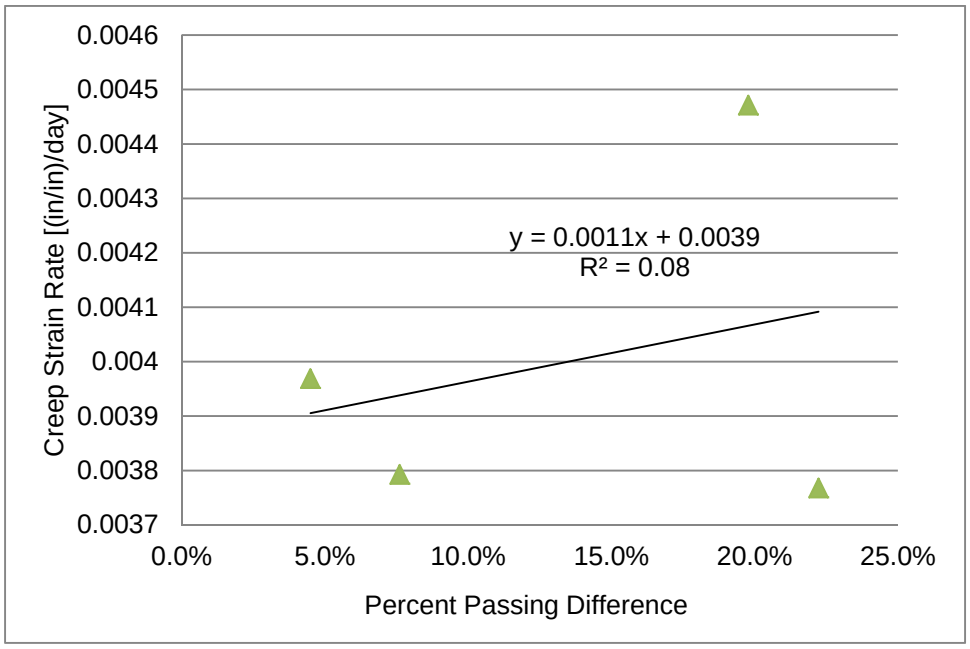

Figure N-10: Creep Strain Rate vs. Percent Passing Difference at Sieve #4

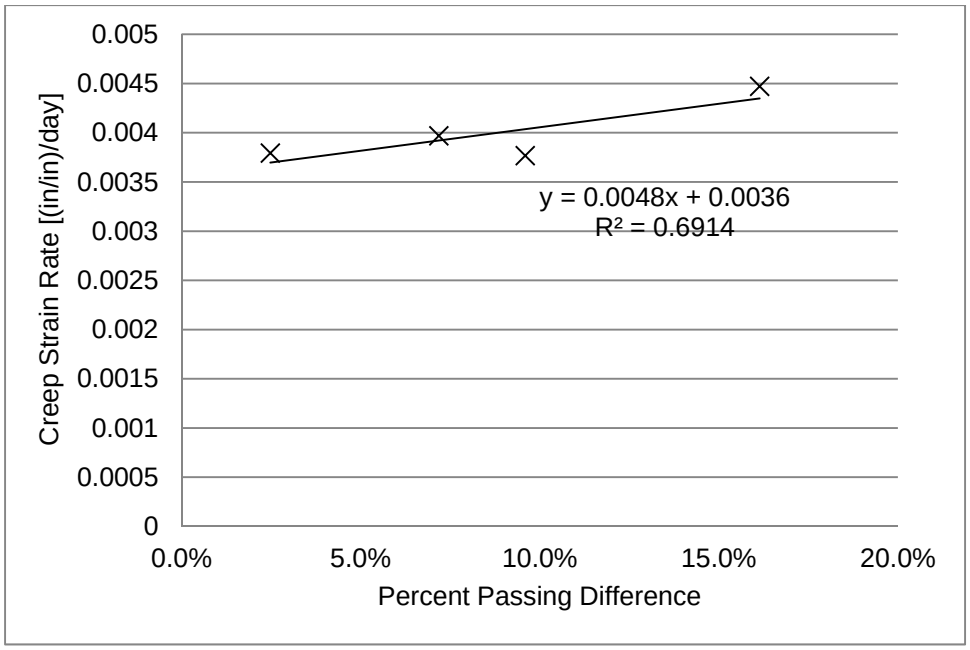

Figure N-11: Creep Strain Rate vs. Percent Passing Difference at Sieve #10

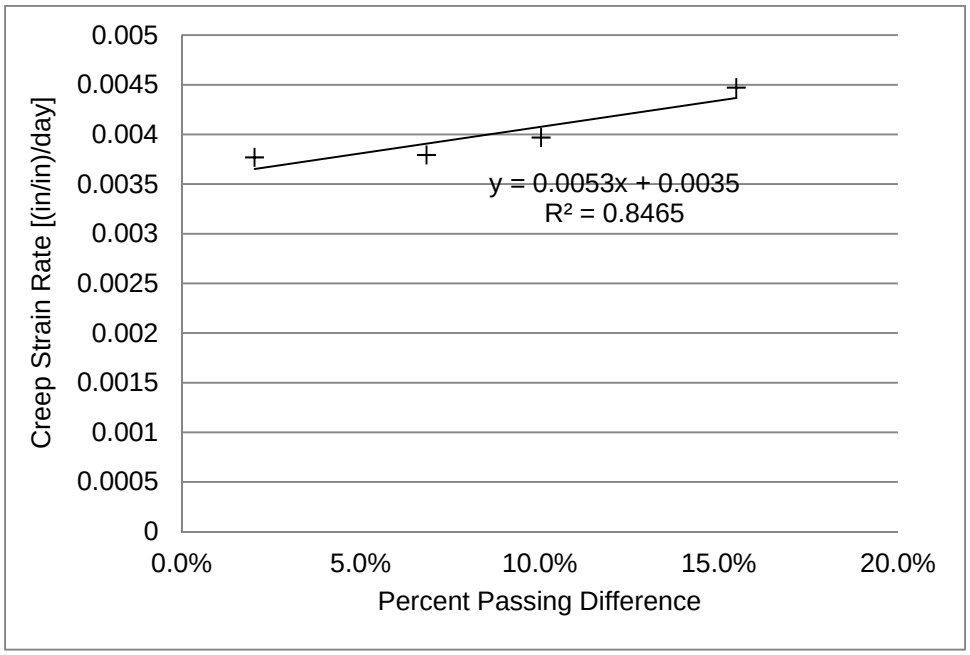

Figure N-12: Creep Strain Rate vs. Percent Passing Difference at Sieve #30

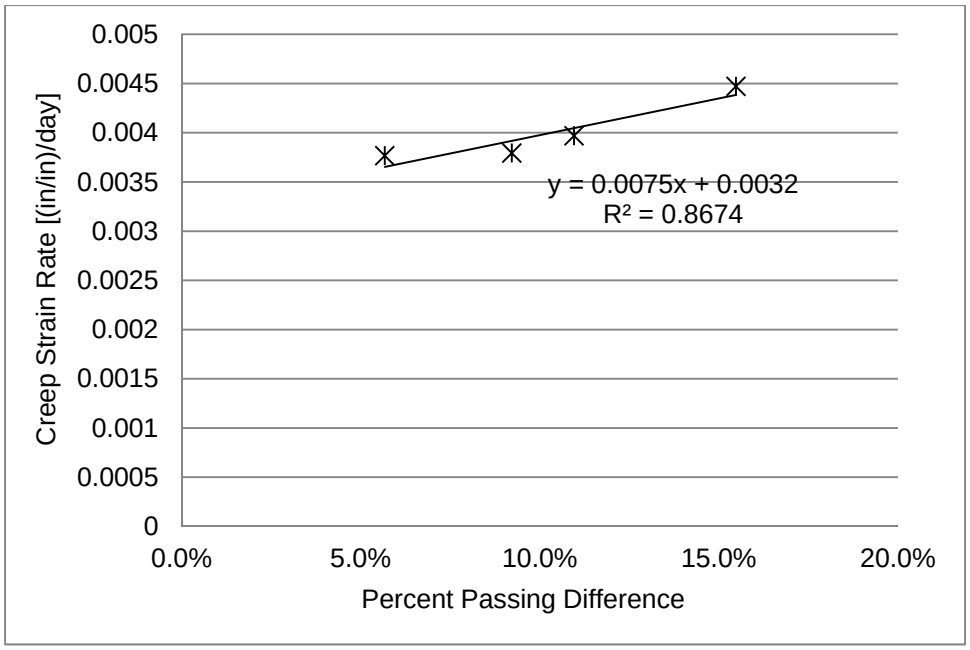

Figure N-13: Creep Strain Rate vs. Percent Passing Difference at Sieve #50

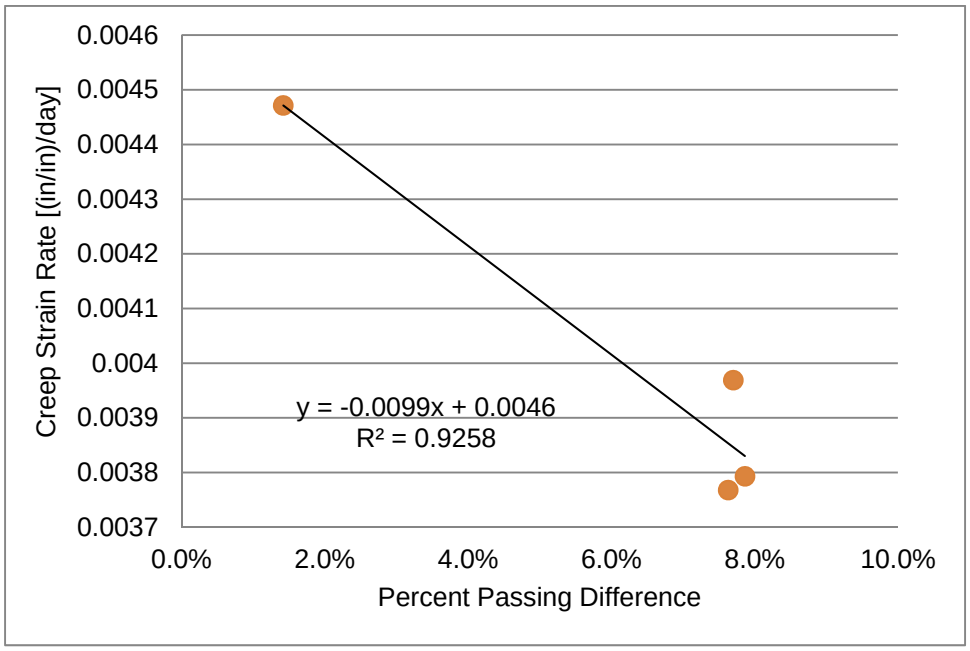

Figure N-14: Creep Strain Rate vs. Percent Passing Difference at Sieve #200